

TESTING AND EVALUATION
OF
DAMAGED JACKET BRACES

FINAL REPORT

CONFIDENTIAL

Confidentiality ends December 31, 1994

by

PMB Engineering Inc

and

Texas A & M University

May, 1990

TABLE OF CONTENTS

EXECUTIVE SUMMARY	Page
1.0 INTRODUCTION	1-1
1.1 Objective	1-1
1.2 Background	1-2
1.3 Participants and Representatives	1-4
2.0 SCOPE OF WORK	2-1
2.1 Testing	2-2
2.2 Analysis	2-3
3.0 EXPERIMENTAL TEST PROGRAM	3-1
3.1 Introduction	3-1
3.2 Specimen Collection	3-1
3.3 Catalog Condition	3-1
3.4 Specimen Description	3-3
3.5 Instrument Component	3-6
3.6 Full Scale Testing	3-7
3.7 Ultrasonic Testing	3-11
3.8 Tensile Coupon Tests	3-11
3.9 Ring Tests	3-12
3.10 Test Results	3-14
3.11 Summary of Specimen Behavior	3-21
3.12 Comparison of Experimental Ultimate Capacities to Predicted Capacities	3-22
3.13 Evaluation of Ultrasonic Measurements	3-33
4.0 ANALYSIS	4-1
4.1 Procedure	4-1
4.2 Software Documentation	4-5
4.3 Results	4-19
5.0 COMPARISON OF RESULTS	5-1
6.0 SUMMARY AND CONCLUSIONS	6-1

REFERENCE LIST

Figures are located at the end of their respective sections.

APPENDIX A - SPECIMEN TEST RESULTS

APPENDIX B - COMPUTER CODE FOR "DISPLACE" PROGRAM

APPENDIX C - DERIVATION OF FORMULATION FOR COMPUTED STRAIN AND DISPLACEMENT FROM MEASURED STRAIN AND DISPLACEMENT DATA

APPENDIX D - APPLIED LOAD ECCENTRICITY AS COMPUTED FROM END MOMENTS

APPENDIX E - FORMULATION FOR COMPUTING FULL SCALE EFFECTIVE WALL THICKNESS

APPENDIX F - DOCUMENTATION OF INFORMATION PRESENTED ON COMPUTER DISKS

APPENDIX G - DOCUMENTATION FOR SLIDE PRESENTATION

LIST OF FIGURES & TABLES

SECTION 3

- | | |
|---------------|---|
| Figure 3 - 1 | Full Scale Test Specimen Orientation And Coordinate System |
| Figure 3 - 2 | Severity Of Corrosion |
| Figure 3 - 3 | Damage Summary Specimen No. 17 |
| Figure 3 - 4 | Out-of Straightness Measurements For 17 |
| Figure 3 - 5 | Dent Cross Section |
| Figure 3 - 6 | Placement of Strain Gages |
| Figure 3 - 7 | Test Frame |
| Figure 3 - 8 | End Conditions |
| Figure 3 - 9 | Strain Gage Locations On Load Frame |
| Figure 3 - 10 | Location Of Dial Gages |
| Figure 3 - 11 | Horizontal And Vertical Displacements |
| Figure 3 - 12 | Tensile Coupon Specimen |
| Figure 3 - 13 | Effective Length and Load Deflection vs. Load Step Specimen 17 |
| Figure 3 - 14 | Load vs. Chord Shortening Specimen 17 |
| Figure 3 - 15 | Horizontal Displacements Specimen 17 |
| Figure 3 - 16 | Vertical Displacements Specimen 17 |
| Figure 3 - 17 | Load & Eccentricity vs. Load Step Specimen 17:
(x Eccentricities From Inflection Points) |
| Figure 3 - 18 | Load & Eccentricity vs. Load Step Specimen 17:
(y Eccentricities) From Inflection Points |
| Figure 3 - 19 | Load & Eccentricity vs. Load Step Specimen 17:
(x Eccentricities) From End Moments |
| Figure 3 - 20 | Load & Eccentricity vs. Load Step Specimen 17:
(y Eccentricities) From End Moments |
| Figure 3 - 21 | Specimen No 17 - Full Scale Test Computed Wall |

Thickness

Figure 3 - 22	Specimen 17: Wall Thickness
Figure 3 - 23	Tensile Specimen 17 - 2; Stress vs. Strain
Figure 3 - 24	Tensile Coupon Test Specimen 17 - 2
Figure 3 - 25	Examples Of Observed Failure Modes
Figure 3 - 26	Actual vs. Predicted Capacity; AISC Allowable Stress Design
Figure 3 - 27	Actual vs. Predicted Capacity; Cox (1987) - Tubular Member Mean Column Curve And Nominal Wall Thickness
Figure 3 - 28	Actual vs. Predicted Capacity; CSA Limit States Design And Nominal Wall Thickness
Figure 3 - 29	Actual vs. Predicted Capacity; AISC Allowable Stress Design And Effective Wall Thickness
Figure 3 - 30	Actual vs. Predicted Capacity; Cox (1987) - Tubular Member Mean Column Curve And Effective Wall Thickness
Figure 3 - 31	Actual vs. Predicted Capacity; CSA Limit States Design And Effective Wall Thickness
Figure 3 - 32	Actual vs. Predicted Capacity; Specimens With Observed Local Failure
Figure 3 - 33	Full Scale Effective vs. Ultrasonic Wall Thickness
Table 3 - 1	Specimen Description
Table 3 - 2	Type Of Damage For Each Specimen
Table 3 - 3	Magnitude Of Initial Damage
Table 3 - 4	Summary Of Full Scale Tests
Table 3 - 5	Summary Of Wall Thickness Determination.
Table 3 - 6	Summary Of Specimen Material Properties.
Table 3 - 7	Specimen Geometric Properties
Table 3 - 8	Observed Specimen Failure Modes
Table 3 - 9	Specimen Properties Used In Ultimate Capacity Formulae
Table 3 - 10	Specimen Slenderness Ratios and Parameters

Table 3 - 11	Ultimate Capacity Of Specimens Using Nominal Wall Thickness
Table 3 - 12	Ratio Of Measured To Predicted Ultimate Loads Using Nominal Wall Thickness
Table 3 - 13	Ultimate Capacity Of Specimens Using Effective Wall Thickness
Table 3 - 14	Ratio Of Measured To Predicted Ultimate Loads Using Effective Wall Thickness
Table 3 - 15	Ultimate Capacity Of Specimens Experiencing Local Failure
Table 3 - 16	Radius Of Kern Circle And Eccentricities
Table 3 - 17	Evaluation Of Ultrasonic Data
Table 3 - 18	Comparison Of Wall Thickness Measurements

SECTION 4

Figure 4 - 1	Seastar Beam - Column Model
Figure 4 - 2	Variable Spring Stiffness Specimen #2
Figure 4 - 3	Specimen 16 Beam - Column Model Data
Figure 4 - 4	Wall Thickness Ratios - Full Scale Test
Figure 4 - 5	Specimen Axial Capacity Summary
Figure 4 - 6	Specimen Data Used In Computer Analysis
Figure 4 - 7	Damage Summary, Specimen #1
Figure 4 - 8	Program Damage, Specimen #1
Figure 4 - 9	Compression Capacity vs. Slenderness
Figure 4 - 10	Specimen #1 Axial Load vs. Axial Deformation
Figure 4 - 11	Damage Summary, Specimen #2
Figure 4 - 12	Compression Capacity vs. Slenderness, Specimen #2
Figure 4 - 13	Specimen #2, Axial Load vs. Axial Deformation
Figure 4 - 14	Damage Summary, Specimen #3
Figure 4 - 15	Compression Capacity vs. Slenderness, Specimen #3

Figure 4 - 16 Specimen #3, Axial Load vs. Axial Deformation
Figure 4 - 17 Damage Summary, Specimen #4
Figure 4 - 18 Program Damage, Specimen #4
Figure 4 - 19 Compression Capacity vs. Slenderness, Specimen #4
Figure 4 - 20 Specimen #4, Axial Load vs. Axial Deformation
Figure 4 - 21 Damage Summary, Specimen #5
Figure 4 - 22 Program Damage, Specimen #5
Figure 4 - 23 Compression Capacity vs. Slenderness, Specimen #5
Figure 4 - 24 Specimen #5, Axial Load vs. Axial Deformation
Figure 4 - 25 Damage Summary, Specimen #6
Figure 4 - 26 Program Damage, Specimen #6
Figure 4 - 27 Compression Capacity vs. Slenderness, Specimen #6
Figure 4 - 28 Specimen #6, Axial Load vs. Axial Deformation
Figure 4 - 29 Damage Summary, Specimen #7
Figure 4 - 30 Program Damage, Specimen #7
Figure 4 - 31 Compression Capacity vs. Slenderness, Specimen #7
Figure 4 - 32 Specimen #7, Axial Load vs. Axial Deformation
Figure 4 - 33 Damage Summary, Specimen #8
Figure 4 - 34 Program Damage, Specimen #8
Figure 4 - 35 Compression Capacity vs. Slenderness, Specimen #8
Figure 4 - 36 Specimen # 8, Axial Load vs. Axial Displacement
Figure 4 - 37 Damage Summary, Specimen #9
Figure 4 - 38 Compression Capacity vs. Slenderness, Specimen #9
Figure 4 - 39 Specimen #9, Axial Load vs. Axial Deformation
Figure 4 - 40 Damage Summary, Specimen #10
Figure 4 - 41 Compression Capacity vs. Slenderness, Specimen #10
Figure 4 - 42 Specimen #10, Axial Load vs. Axial Deformation

Figure 4 - 43 Damage Summary, Specimen #11
Figure 4 - 44 Compression Capacity vs. Slenderness, Specimen #11
Figure 4 - 45 Specimen #11, Axial Load vs. Axial Deformation
Figure 4 - 46 Damage Summary, Specimen #12
Figure 4 - 47 Program Damage, Specimen #12
Figure 4 - 48 Compression Capacity vs. Slenderness, Specimen #12
Figure 4 - 49 Axial Load vs. Axial Deformation, Specimen #12
Figure 4 - 50 Damage Summary, Specimen #13
Figure 4 - 51 Program Damage, Specimen #13
Figure 4 - 52 Compression Capacity vs. Slenderness, Specimen #13
Figure 4 - 53 Specimen #13, Axial Load vs. Axial Deformation
Figure 4 - 54 Damage Summary, Specimen #14
Figure 4 - 55 Program Damage, Specimen #14
Figure 4 - 56 Compression Capacity vs. Slenderness, Specimen #14
Figure 4 - 57 Specimen #14, Axial Load vs. Axial Deformation
Figure 4 - 58 Damage Summary, Specimen #16
Figure 4 - 59 Program Damage, Specimen #16
Figure 4 - 60 Compression Capacity vs. Slenderness, Specimen #16
Figure 4 - 61 Specimen #16, Axial Load vs. Axial Deformation
Figure 4 - 62 Damage Summary, Specimen #17
Figure 4 - 63 Program Damage, Specimen #17
Figure 4 - 64 Compression Capacity vs. Slenderness, Specimen #17
Figure 4 - 65 Specimen #17, Axial Load vs. Axial Deformation
Figure 4 - 66 Damage Summary, Specimen #18
Figure 4 - 67 Program Damage, Specimen #18
Figure 4 - 68 Compression Capacity vs. Slenderness, Specimen #18
Figure 4 - 69 Specimen #18, Axial Load vs. Axial Deformation

Figure 4 - 70 Damage Summary, Specimen #19
Figure 4 - 71 Compression Capacity vs. Slenderness, Specimen #19
Figure 4 - 72 Specimen #19, Axial Load vs. Axial Deformation
Figure 4 - 73 Damage Summary, Specimen #20
Figure 4 - 74 Compression Capacity vs. Slenderness, Specimen #20
Figure 4 - 75 Specimen #20, Axial Load vs. Axial Deformation
Figure 4 - 76 Damage Summary, Specimen #21
Figure 4 - 77 Program Damage, Specimen #21
Figure 4 - 78 Compression Capacity vs. Slenderness, Specimen #21
Figure 4 - 79 Specimen #21, Axial Load vs. Axial Deformation

EXECUTIVE SUMMARY

This report documents the work performed and the results of the joint industry project, "Testing and Evaluation of Damaged Jacket Braces". The project was funded by nine industry participants and conducted by PMB Engineering with testing performed by Texas A&M University.

The purpose of the project was to determine the reduction in load carrying capacity that occurs to tubular members because of in-service damage. This was carried out by testing twenty salvaged braces and comparing the resulting ultimate and residual capacities to the values calculated using finite element beam column models of the damaged braces.

The first task of testing the braces was performed at Texas A&M. The braces were examined for damage, catalogued, equipped with strain gages and mounted in the test frame. Then they were loaded with increasing axial load until failure occurred. Failure was generally located in areas of obvious damage. Results of the tests were then compiled and compared against the response which was calculated by PMB.

PMB performed the second of the two primary tasks, that is the formulation of an analysis method and computer modeling technique to predict the response of the individual braces to axial load. This task resulted in two PC programs. The first was a simple prediction method for peak load in a damaged member. The other was a program to determine damaged member characteristics for use in generating a finite element beam column model. The FEA model was then used to predict the full response of the member including peak load and the nonlinear response or residual capacity of the member.

The results of the test program and the analysis predictions were compared. In general the predictions exceeded the actual capacities by an average of around 20%. Variations ranged from under predictions of 25% to over predictions of as much as 76%. Agreement is not as good as that shown by other investigations. This may be due to the use of new or artificially damaged samples in other programs.

The response of members with multiple forms of damage were generally dominated by one damage state. Yielding in areas of reduced wall thickness was a common failure mode in members with significant corrosion. This usually occurred at levels less than would be predicted by the beam column method.

The project has provided valuable information on the response of damaged tubular braces and the ability to predict damage dominated responses. Additionally, it has shown that further work is justified in more completely understanding this problem area or in developing remedial actions to account for the limitations of the present understanding.

1.0 INTRODUCTION

This report documents the results of a joint industry study to test and evaluate damaged jacket braces. The work was performed by PMB Engineering Inc. with the testing portion of the project subcontracted to Texas A & M University. Funding for the project was from a joint industry effort with nine participants.

1.1 Objective

The objective of the study was to observe the buckling and post buckling behavior of full scale, damaged jacket braces and to compare this with analytical predictions. This was achieved by the use of testing to determine the ultimate capacity of tubular members which had been subjected to different types of in-service damage. The study addressed corroded and damaged member capacities by testing members that had been removed from the participants' salvaged platforms. Thus, the test specimens were full scale and exhibited characteristics of members that have been in service for varying periods of time. The results obtained from the testing program were therefore representative of components that are currently in service.

The test results contributed to an improved understanding of the loss of strength due to corrosion and damage in two ways:

The observed capacity of the tested members gave information about the strength that could be expected from similar, *in situ*, members.

The comparison of test data to analytical procedures that were developed for the project and to the Denta II program provide a basis for future analytical evaluation of in-service members.

1.2 Background

A major source of uncertainty in the computed reliability of offshore structures is the extent to which the structure's strength degrades with time in service. This uncertainty not only affects the design of new structures, but also is a key factor in determining if an existing facility will survive its design life, whether damaged members must be fully restored to their original strength and whether a salvaged structure can safely be reused at a new site. Thus, in addition to being a significant safety issue, the matter can have major economic consequences for the offshore industry.

Visual inspection (for dents and corrosion holes) and ultrasonic measurements (to quantify losses due to corrosion and indicate material cracks) are two methods for determining the physical deterioration of a structure. Even after these observations have been made, though, there is little historical evidence to indicate how much this deterioration reduces the structure's strength. In the past, some information has been obtained from the results of tests on small-scale, artificially damaged members. It has been difficult, however, to extrapolate these scale model results to the full scale components. Few comparisons of small scale to full scale test data are available in the literature.

In one full scale study (1) two dented specimens were tested in compression. The specimens had diameters of 40 and 60 inches and were approximately 80 to 90 inches long. They were new, non-corroded specimens which had been artificially dented. The damaged members exhibited very little loss of strength due to denting, but this was largely attributed to the test's fixed end conditions and the relative shortness of the members. These tests did not include any corrosion effects. The results were not very helpful for predicting the behavior of more slender members.

The study which most closely approximated this study involved the testing of four members which had been salvaged from a structure after 12 years of service in the North Sea (2). These specimens were approximately 25 feet long and had diameters of 12 and 16 inches. They were "in good condition as

regards to straightness, circularity, thickness, and freedom from corrosion and denting." One of the specimens was artificially bent before axial testing and another was artificially dented. The results obtained were in good agreement with the results of: a) prior tests of virgin full scale specimens, b) small-scale tests of virgin and damaged specimens and c) strength prediction curves in the API and DNV design recommendations. Although these limited results seemed to suggest that present models may be adequate for some bent or dented members with little or no corrosion, they gave no information on the magnitude of corrosion effects, or on the interaction of corrosion effects with denting or bending effects. In addition, artificially induced damage may not adequately represent damage that occurs in service.

1.3 Participants and Representatives

This project was funded by nine companies representing oil & gas operators, contractors, and regulators. Each of these organizations has been represented by very capable and consciencious individuals. Their input to the project is greatly appreciated.

The following is the list of participants and their representatives;

CHEVRON USA

Mr. Bill Krieger
c/o Chevron Corp.
Bishop Ranch 6, Bldg. K., Rm.
1082
2400 Camino Ramon
San Ramon, CA 94583
415-842-8135

EXXON PRODUCTION RESEARCH

Dr. Jim Loh
2 Greenway Plaza
Suite 800
Houston, Tx 77027
713-940-4608

MARATHON OIL COMPANY

Mr. Jim Saunders
P.O. Box 3128
Houston, Tx 77253
713-629-6600

MINERALS MANAGEMENT SERVICE

Mr. Charles Smith
318 Elden St., M.S. 647
Herndon, Va 22070-4817
703-787-1559

MOBIL OIL E & P

Dr. Damodarin Nair
c/o Mobil Research & Develop-
ment
13777 Midway Rd.
Dallas, Texas 75244
214-851-8308

NIPPON STEEL CORPORATION

Mr. T. Tabira
Planning & Design Dept.
Marine Engineering Division
2-6-3 Otemachi, Chiyoda-Ku
Tokyo 100 Japan
81-3-275-6244

OXY USA

Mr. Win Thornton
1980 Post Oak Blvd
Houston, TX 77227-2189
713-840-7100

PHILLIPS PETROLEUM

Mr. Roger Thomas
1390 Plaza Office Bldg.
Bartlesville, OK 74004
918-661-5875

SHELL OIL COMPANY

Mr. Kris Digre
200 North Dairy Ashford
Houston, TX 77079
713-870-4104

PMB ENGINEERING INC

Mr. David A. Stewart
24 Greenway Plaza, Suite 1303
Houston, TX 77046
713-529-1500

TEXAS A&M UNIVERSITY

Dr. Terry Kohutek
Civil Engineering Dept
CE/TTI Building, Rm 705J
College Station, TX 77843-3136
409-845-1967

2.0 SCOPE OF WORK

The two primary tasks of the project were the testing to failure of damaged tubular braces by application of axial load and the independent calculation of the ultimate capacity of each of the damaged braces. Comparisons of the results were performed to indicate how well the calculated capacity and test data correlated.

Twenty-one tubular bracing members were selected and removed from the participants' salvaged jacket structures for use in the test program. The specimens were selected by PMB or the participant's representative once the jackets had arrived at their respective onshore sites. Members were selected in order to have a sampling of damage including holes, dents and corrosion. Where possible, varying lengths and diameters were chosen to get samples of various L/r and D/t values. After selection, the members were transported to the Structural Testing Laboratory of Texas A & M University.

2.1 Testing

In the laboratory, visual and ultrasonic inspection methods were used to quantify the types and the extent of apparent damage in each member. After this inspection was completed, each member was loaded to failure in compression in a 1.8 million pound load frame designed and fabricated for the project. The stroke of the loading device was approximately two feet, so displacements that caused a 5% shortening of the members could be applied. This allowed accurate observation of the post-buckling residual strength of each member, as well as the maximum load to which the component could be subjected.

The components used in this study were tested as closely as possible to an "as is" condition. The only significant preparation (detailed in Section 3.0) included: readying the ends for attachment in the load fixture, cleaning some surfaces for the application of strain gauges and removing welded attachments by flame cutting. Twenty members were tested and included the following:

1. Seven members which exhibited some corrosion but no dents, holes or out-of-straightness, and
2. Thirteen members which exhibited varying degrees of denting, corrosion, corrosion holes and out-of-straightness.

No members were larger than 20 inches in diameter with a 0.5 inch effective wall thickness. The smallest member was 10.75 inch diameter with 0.264 inch effective wall thickness. The L/r varied from 35.5 to 108.5 and D/t from 30.2 to 66.7.

2.2 Analysis

An analytical model of each member was developed and analyzed to predict the compression behavior in the buckling stages. Various modeling approaches based on phenomenological models were employed. The buckling load, residual load, and slope of the unloading curve were determined for comparison with the test results. The intent was to determine the differences that exist between the damage-influenced prediction and the test results.

To facilitate the modelling and prediction capabilities of the project, two PC Fortran 77 programs were written. The first, DAMAGE, was a formulation of previous work on the ultimate capacity of damaged members. It gives an estimate of the peak capacity of a member with specific properties and damage. The other, EQUIV, was written to calculate the material characteristics for both the damaged and undamaged sections of the members for the subsequent computer model.

The properties calculated by EQUIV were input to the FEA beam column model of the individual braces. Axial loads were incrementally applied and the response of the member was determined. The response calculations were carried out as far as practical on the unloading curve to obtain the residual load capacity of each brace.

Additionally, Shell Oil Company provided the project with similar results from their DENTA II analysis of the twenty damaged braces. Following these independent analyses, the two sets of beam column results were compared against those obtained from the testing program. The two analysis approaches showed reasonable agreement to each other for all of the cases. The test results varied widely from those of the predicted results.

3.0 EXPERIMENTAL TEST PROGRAM

3.1 Introduction

The experimental program was conducted to evaluate the ultimate and post-ultimate behavior of twenty damaged tubular braces. The data obtained from this phase of the project were used to verify the analytical models described in Chapter 4. This phase of the project consisted of eight major tasks. These tasks were: 1) specimen collection, 2) specimen inspection and damage documentation, 3) specimen instrumentation, 4) full scale compression testing, 5) ultrasonic testing to determine wall thickness, 6) tensile coupon testing to determine material properties, 7) ring testing to determine effective wall thickness, and 8) data reduction and evaluation. Each of these tasks is described in greater detail in the subsequent sections.

3.2 Specimen Collection

The specimens tested were removed from jacket-type platforms that were being salvaged after having been in service for approximately 5-20 years. The specimens collected had varying types and degrees of damage. All damage found was typical of platforms with 5-20 years of service. The types of damage that occurred in the components included dents, observable cracks, initial out-of-straightness, corrosion, and corrosion holes. Specimen lengths varied from 17 feet to approximately 40 feet while diameters varied from 10.75 inches to 20 inches. Nominal wall thicknesses varied from 0.375 to 0.500 inches.

3.3 Catalog Condition

All specimens were numbered and their ends marked A and B for specimen identification and orientation. The A and B labels correspond to ends of the load frame as shown in Figure 3-1. Figure 3-1 also shows the coordinate system used in the reduction of the full scale test data. Each specimen was visually inspected to determine its usable length and overall condition. Observable dents, holes, or other damages were documented with respect to size, distance from end B, and circumferential distance from a reference chalk line. This chalk line was located at the top of the specimen (corresponding

to the +y axis) and extended the full length of the specimen. Photographic records of all damage and the overall condition of the specimens were also taken.

Dent damage was documented by recording the longitudinal location from end B and by measuring the depth of the dent at known circumferential locations from the reference chalk line. Measurements of dent depth were made perpendicular to the circumference on the specimen by using a light-gage tin strap and a ruler. The strap was wrapped tightly around the specimen such that the strap represented the undamaged circumference of the tube. The perpendicular distance between the specimen and the strap was then measured and recorded at every inch along the circumference in the dented region. These measurements were used to determine the cross-section profile of the dented area. By making successive measurements longitudinally along the pipe, a series of dent profiles for a dented region were produced.

Initial out-of-straightness of the specimen was also measured. Clamps were attached to the specimen at its ends, and a string was pulled taut then tied to each clamp at the same height above the surface at the ends of the specimen. Perpendicular measurements were made between the string and the member surface at one foot intervals along the specimen and at locations where the out-of-straightness appeared to be a maximum. The measurements were subtracted from the height of the string at the ends to obtain the magnitude of the initial out-of straightness. For specimens with out-of-straightness in two directions, additional clamps were placed on the ends of the specimens 90 degrees from the first clamps. The same measurements previously described were made to determine the out-of-straightness in the second direction.

Any attachments welded to the member were removed as close to the specimen surface as possible by flame cutting. Although it is unlikely that these features affected the behavior of the specimen, their location and size were documented with the other damage.

Whenever necessary, as much loose corrosion as possible was removed (with a hammer) from the outside surface of the specimens. This was done in order to evaluate the surface of the specimen and to facilitate the installation of

strain gages. The location of any localized heavy corrosion was recorded along with the location of corrosion holes. From visual inspection of the specimens, the severity of corrosion was rated as low, medium, or high, and the extent of corrosion was classified as local or overall. Photos of corroded specimens can be found in Figure 3-2a), 3-2b), and 3-2c) which represent low, medium, and high corrosion. Corrosion which occurred over a limited region of a specimen was classified as local corrosion while overall corrosion indicated that corrosion occurred along the entire specimen. Also shown in Figure 3-2d) is an example of overall medium corrosion with local high corrosion.

All damage was documented and presented in a damage summary for each specimen. In addition, photographs were taken of each damage location to provide a visual record.

3.4 Specimen Description

A brief description of each of the specimens tested is presented in this section. In addition, Table 3-1 contains a summary of the relevant geometric properties for each specimen including length, diameter, nominal wall thickness, diameter-to-thickness (D/t) ratio, and length-to-radius of gyration (L/r). The specimens were also identified as rolled fabricated pipe or manufactured seamless pipe as shown in Table 3-1. The type and magnitude of initial damage present on the test specimens are presented in Tables 3-2 and 3-3. Table 3-2 presents the type of damage present on each specimen while Table 3-3 further details the initial damage by listing the amount and extent of corrosion for each specimen, and the magnitude of initial denting and bending damage. For specimens with more than one dent or initial out-of-straightness, the largest dent depth or out-of-straightness is given. An example of the detailed damage summary prepared for each specimen is shown in Figure 3-3. Figures 3-4 and 3-5 are examples of initial out-of-straightness and dent profile documentation, respectively. Complete descriptions of all specimens can be found in Appendix A. Given below are brief descriptions of each specimen.

Specimen 01: Specimen 01 was 19.6 feet in length, 18.00 inches in diameter, and had a nominal wall thickness of 0.375 inches. The specimen was initially straight with an 8 inch diameter and 0.50 inch deep dent, located 3'-2" from end B. In addition, the specimen was highly corroded.

Specimen 02: Specimen 02 had a length of 22.13 feet, an outside diameter of 18.00 inches, and a nominal wall thickness of 0.438 inches. The specimen had no dents or initial out-of-straightness, but it did have medium corrosion along its entire length and a localized region of high corrosion.

Specimen 03: Specimen 03 was 24.20 feet long with an outside diameter of 18.00 inches and a nominal wall thickness of 0.375 inches. Overall medium corrosion and localized high corrosion were the only kinds of damage for this specimen.

Specimen 04: Specimen 04 had a length of 34.73 feet, an outside diameter of 12.75 inches, and a nominal wall thickness of 0.375 inches. The specimen was not dented, but was initially bent 1.31 inches in the vertical (y-z) plane. The overall corrosion along the specimen was low with a region of medium corrosion.

Specimen 05: Specimen 05 was 18.52 feet in length and 18.00 inches in diameter with a nominal wall thickness was 0.375 inches. This specimen was initially straight with high corrosion over its entire length. It had a small corrosion hole near end B, and a 9 inch diameter, 0.50 inch deep dent located 5'-7" from end B.

Specimen 06: Specimen 06 had a length of 39.5 feet, an outside diameter of 20.00 inches, and a nominal wall thickness of 0.500 inches. This specimen had no visible damage.

Specimen 07: Specimen 07 was 39.46 feet in length with an outside diameter of 12.75 inches and a nominal wall thickness of 0.375 inches. The specimen was initially straight with low corrosion and had an 8 inch diameter, 1.5 inch deep dent located near its midspan.

Specimen 08: Specimen 08 was 26.63 feet long, 10.75 inches in diameter, and had a nominal wall thickness of 0.375 inches. It was initially straight, but had a 5 inch diameter, 0.25 inch deep dent, 3'-8" from end B. The specimen had medium corrosion over its entire length and a localized region of high corrosion.

Specimen 09: Specimen 09 had a length of 22.04 feet with an outside diameter of 14.00 inches and a nominal wall thickness of 0.500 inches. There was low corrosion on the specimen and no dents or initial out-of-straightness.

Specimen 10: Specimen 10 was 31.60 feet in length and 14.00 inches in diameter with a nominal wall thickness of 0.500 inches. The specimen was initially straight with no dents. The amount of corrosion was low, and there were three small torch holes in the wall of the specimen 26 feet from end B.

Specimen 11: Specimen 11 was 28.96 feet in length with an outside diameter of 10.75 inches and a nominal wall thickness of 0.375 inches. The specimen was initially straight with no dents and had low corrosion.

Specimen 12: Specimen 12 had a length of 39.48 feet, an outside diameter of 12.75 inches, and a nominal wall thickness of 0.375 inches. The specimen was initially straight but was highly corroded. In addition, there were two holes with some denting and a third dent with no hole. The largest dent depth on the specimen was 3 inches.

Specimen 13: Specimen 13 was 24.13 feet in length with a 12.75 inch outside diameter and a nominal wall thickness of 0.375 inches. This specimen was initially bent in both the vertical (y-z) and (x-z) horizontal planes. The largest out-of-straightness was 8.13 inches in the y-z plane. There were also four large dents on the specimen and high overall corrosion.

Specimen 14: Specimen 14 had a length of 16.75 feet and was the shortest specimen tested. The outside diameter was 12.75 inches with a nominal wall thickness of 0.375 inches. This specimen was initially bent in both the vertical (y-z) and horizontal (x-z) planes with the largest initial deflection being 2.88 inches in the y-z plane. There were three dents located near end B and heavy corrosion over the entire length. Two small corrosion holes and an area in which the wall was very thin were located at 4'-9" from end B. In addition, the overall corrosion along the specimen was very high.

Specimen 16: Specimen 16 was 28.77 feet in length and 12.75 inches in diameter with a nominal wall thickness of 0.375 inches. This specimen was also bent in both the vertical (y-z) and (x-z) horizontal planes with a maximum out-of-straightness of 6.63 inches in the y-z plane. There were four small dents along the specimen with a maximum dent depth of 0.25 inches. This specimen was composed of two pipe segments with the same outside diameter but different wall thicknesses. The two segments were connected by a collar welded to both pipes. Corrosion was low over the entire specimen.

Specimen 17: Specimen 17 had a length of 31.17 feet, an outside diameter of 12.75 inches, and a nominal wall thickness of 0.375 inches. The specimen was initially bent in the vertical (y-z) plane. In addition, there was a dent along the top of the specimen located 19 feet from end B. The maximum out-of-straightness was 4.75 inches, and the dent was 8 inches wide and 1.375 inches deep. There was low corrosion on the specimen.

Specimen 18: Specimen 18 had a length of 17.08 feet, an outside diameter of 10.75 inches, and a nominal wall thickness of 0.375 inches. This specimen was initially out-of-straight 0.88 inches in the vertical (y-z) plane and had medium corrosion over the entire length of the specimen with a localized high corrosion region. In addition, there were seven small dents on the specimen. The largest of these dents was located 5 feet 4 inches from end B and was 8 inches wide and 0.375 inches deep.

Specimen 19: Specimen 19 was 37.27 feet in length with an outside diameter of 16.00 inches with a nominal wall thickness of 0.375 inches. The specimen was initially straight with no dents. There was medium overall corrosion and a 70 inch crack in a longitudinal welded seam near end A.

Specimen 20: Specimen 20 had a length of 34.67 feet, an outside diameter of 12.75 inches, and a nominal wall thickness of 0.375 inches. The specimen was initially straight with high corrosion and no denting.

Specimen 21: Specimen 21 had a length of 22.33 feet, an outside diameter of 16.00 inches, and a nominal wall thickness of 0.375 inches. This specimen was initially straight with no denting. There was a medium amount of corrosion over the entire specimen, and there was a corrosion hole near end A. There was also a 95 inch long longitudinal crack through the wall of the specimen near end A.

3.5 Instrument component

Each test specimen was instrumented with thirty electric resistance, 350 ohm, foil strain gages. Six strain gages were mounted, equally spaced, around the circumference at five locations along the specimen. Whenever possible, the first and last ring of strain gages were placed three specimen diameters from each end. The remaining three rings of gages were equally spaced between the first and last rings as shown in Figure 3-6. For short specimens, with large diameters, an end spacing of three diameters was greater than the resulting

equal spacing between the interior rings. For these specimens all the rings were equally spaced along the specimen. Finally, if a ring was to be located at a damaged area it was moved to the nearest undamaged location on the specimen.

The location of all thirty strain gages was carefully documented for later use in the data reduction. The longitudinal distance from end B of the specimen to each strain gage was recorded as well as the circumferential distance from the reference chalk line. With these measurements, the x, y, and z coordinates of the each strain gage was determined.

3.6 Full Scale Testing

3.6.1 Load Frame. The full scale specimen testing was carried out in a 1.8 million pound load frame specifically designed and built for this experimental study. The load frame, shown in Figure 3-7, consists of three - 58 feet long, W24 x 104 members which serve as the tension legs of the load frame. The legs are held in position by a fixed headstock and fixed tailstock. Three 300 ton capacity, four foot stroke, jacks are attached to the fixed headstock, and positioned so that the resultant load acts through the centroid of the headstock. The jacks apply load to the specimens through a movable headstock which, along with the fixed tailstock, serve to hold the specimen in position. The movable headstock corresponds to end A of the test specimens while end B corresponds to the fixed tailstock.

3.6.2 Specimen Preparation. After mounting the strain gages, the specimen was prepared for testing. The ends of the specimen were ground smooth to provide good contact between them and the load frame. After the ends were ground, the specimen was placed horizontally in the load frame and positioned so that its centroid coincided with the line of action of the resultant load of the jacks. The specimen was held in place at each end by three clip angles located 120 degrees around the circumference of the specimen as shown in Figure 3-8. These angles provided restraint against end translation but provided no restraint against end rotation. Further discussion of the end conditions is presented in Section 3.12.3.

With the specimen in the load frame, six hooks were welded on the specimen to attach the instrumentation for measuring the horizontal and vertical displacements. The strain gages were then soldered to the lead wires of the data acquisition equipment.

Although every effort was made to grind the ends of the specimens smooth, it was very difficult to get them to fit flush with the headstock and/or tailstock. For specimens with initial bending, it was impractical to attempt to grind the ends such that they were flush with the tailstock and headstock of the load frame. As a result, the ends of the specimens were shimmed with thin pieces of steel in order to ensure uniform contact between the load frame and the specimen. This significantly reduced the eccentricity of the applied load prior to the ultimate or buckling load. It should be noted that the first two specimens tested, specimens 06 and 12, were not shimmed.

3.6.3 Instrumentation. As mentioned earlier, the specimen was instrumented with thirty strain gages to measure normal strains in the specimen. Strain gages were also mounted on the load frame to measure the applied load. Pairs of strain gages were mounted on the three legs near the midspan of the load frame as shown in Figure 3-9. The gages on each leg were mounted on diagonally opposite flanges at equal distances from the flange edges. During data reduction, the readings from the two diagonal gages (40 and 42, 43 and 45, 46 and 48) were added to negate any strain induced from incidental bending in the leg. The average of the two strains is then the average axial strain in the leg. The sum of the axial strains in the three legs is then used to compute the total load in the frame, and thus, the total compressive load in the specimen.

The chord shortening of the specimen was measured with three wire displacement transducers (hereafter called stringpots) placed between the tailstock and the movable headstock. These displacement transducers were placed one hundred twenty (120) degrees apart on the movable headstock at equal distances from the centerline of the headstock. The resultant chord shortening was determined by averaging the three stringpot readings.

Past the peak load, it was possible for the specimen end to rotate away from the headstock or tailstock. To measure this rotation, two dial gages with magnetic bases were attached 180 degrees apart at the specimen ends as shown in Figure 3-10. The dial gages were read at each load step and appropriate corrections were made to the chord shortening measurements taken from the stringpots.

Finally, the horizontal and vertical displacements of the specimen were measured at the first and last rings of strain gages and midway between these two rings. These measurements were taken by displacement transducers attached to the load frame and hooks welded on the specimen.

3.6.4 Testing. The specimen was tested in axial compression. Load was applied by advancing the movable headstock at timed increments. The load was allowed to stabilize and three sets of load, lateral displacement, chord shortening, and strain data were taken at each load step. The dial gages used to monitor the specimen end rotation were also read at each load step. The specimen was subjected to increasing axial deformation until one of the following occurred: 1) the specimen contacted the load frame or ground or 2) the safety of further testing was in doubt.

3.6.5 Data Acquisition. Load, displacement, and strain data measured during the full scale compression test was collected and recorded using the FASTBOX. The FASTBOX is a high-speed data acquisition system designed for Texas A&M University. At each data step, the FASTBOX sampled and read the forty-nine channels of data, saved the data on a standard 5-1/4 inch floppy disk, and generated a printout of the data. The four dial gages on the specimen were manually read and recorded at each load step.

3.6.6 Results. The full scale compression tests provided information on the buckling and post-buckling behavior of damaged tubular members. The ultimate strength, chord shortening, and lateral displacement were obtained by simple reduction and/or correction of the raw data. The effective length and wall thickness of the specimen as well as the eccentricity of the applied load was determined from a more rigorous reduction and analysis of the data.

The measured chord shortening, load, and horizontal and vertical displacement data were reduced by means of the computer program, DISPLAC, written specifically for this test program. A listing of this program can be found in Appendix B. The load at any step was calculated by multiplying the sum of the average axial strain in each leg of the load frame by the modulus of elasticity (29,500 ksi) and cross-sectional area of a W24 X 104. The chord shortening was computed as the average of the three chord shortening measurements with the appropriate dial gage corrections applied for end rotation. The resolution of the horizontal and vertical measurements to the actual horizontal and vertical displacements was not as simple. Due to the large deformations involved, the measurements provided by the displacement transducers (Δx and Δy) were not actual horizontal or vertical displacements. Instead each reading was a combination of these two displacements as shown in Figure 3-11. At each location, two quadratic equations can be written that relate the measured to the actual horizontal and vertical displacements (δ_h and δ_v). These two equations were solved simultaneously to determine the actual displacements.

The least-squares error analysis algorithm, CURVE, was written that produces the best-fit curvature and displacement for the thirty channels of measured strain gage data and the six channels of measured lateral displacement data. The derivation of this formulation and a listing of the computer code can be found in Appendix C. The curvature, the displaced shape, and the effective length of the member, in the pre-buckling and post-buckling regions, were determined from the analysis. In addition, the eccentricity of the applied load was computed based on 1) the lateral displacement at the points of inflection and 2) the moments at the end of the member.

Since the inflection point is a location of zero moment, the resultant load must pass through the centroid of the cross-section at that point. Thus, the eccentricity of the resultant load was determined by computing the lateral deflection of the member at the location of the inflection points in the program CURVE. In addition, the end moments were computed at each data step by multiplying the member curvature at each end by the modulus of elasticity and moment of inertia of the specimen. The end moment was then divided by the

measured load to compute the eccentricity of the load. A summary of these formulations and a listing of the computer program, ECC, used to compute the eccentricities from the calculated end moments can be found in Appendix D.

The overall effective wall thickness was computed for each specimen using the results from the CURVE program. At each load step, the axial strain component, ϵ , from the least-squares fit of the measured strain data was used with the measured load data and the modulus of elasticity to compute an effective wall thickness. Appendix E contains a description of this calculation. The average of the computed wall thicknesses from the initial to the ultimate (buckling) load, was defined as the overall effective wall thickness.

3.7 Ultrasonic Testing

The wall thickness of the tubular specimens was determined by taking ultrasonic measurements at the thirty strain gage locations. Additional wall thickness measurements were taken on some specimens in areas of heavy corrosion and in regions of local buckling. A SONIC FTS Mark I instrument with a 220 Thickness Adapter was used with a Panametrics 0.5 inch diameter, 2.5 MHz, longitudinal transducer on all specimens. Ordinary lightweight grease was used for couplant.

3.8 Tensile Coupon Tests

3.8.1 Specimen Collection and Preparation. Upon completion of the full scale compression test, two coupons were taken from an unyielded region of each specimen. Each coupon, approximately 10 inches by 3 inches, was removed by flame cutting so that the long axis of the coupon was parallel to the longitudinal (z) axis of the specimen.

The specimens were then machined to the final configuration specified by ASTM E8-88 as shown in Figure 3-12. Both faces of the coupon were machined so that the 2-1/4 inch throat area had a constant cross-sectional thickness free from corrosion and pitting. The dimensions of the throat cross-section were accurately measured and recorded for use in the data reduction.

3.8.2 Testing Equipment and Procedure. Each coupon was placed in a 20 kip, MTS Axial Test machine and loaded in uniaxial tension. The tests were conducted according to the procedures in SSRC Technical Memorandum No. 7. The specimens were loaded in a stroke control mode at an approximate strain rate of 0.01/minute. The load was measured using a calibrated 20 kip, MTS load cell while the strains were measured using a model 632.11B-20 MTS Extensometer with a 20% maximum strain range.

Stress and strain data were recorded at 1 second intervals throughout the entire test. To obtain the static yield stress, the test was paused for five minutes at three specified strains beyond the yield strain (approximately 0.005, 0.010, and 0.015). During this time, the strain was held almost constant as the load drops slightly. Strain data were recorded until the extensometer reached its maximum range of approximately 20% (well beyond the yield strain for all specimens). The extensometer was removed, the test continued, and load data were taken until the specimen ruptured. Each test took approximately 45 minutes to complete.

3.8.3 Results. Stress-strain plots were generated for each coupon tested. Yield stress, ultimate stress, and modulus of elasticity were determined from the average values from the two tensile coupon tests. Both static and dynamic yield stress were determined for seventeen of the twenty specimens tested. The modulus of elasticity was determined using a spreadsheet linear regression analysis on the stress-strain data for each specimen, but due to the sensitivity of the extensometer used to measure strains, these values are questionable.

3.9 Ring Tests

3.9.1 Specimen Preparation. After completion of the full scale compression tests, a cross-sectional ring, two or three diameters long, was flame cut from the specimen. The ring was removed from a straight, unyielded area that was somewhat representative of the overall damage of the specimen. The ring was then taken to a machine shop to have its ends turned to ensure that the ring would make full contact with the platens of the load fixture. The length of the specimen was then accurately measured and recorded.

3.9.2 Testing Equipment and Procedure. The ring was placed in a 500 kip MTS universal testing machine and loaded in uniaxial compression. The load was applied in increments of 25 kips until the load capacity of the MTS machine was reached. At each load step, the deformation of the ring was measured by four (0.0001 inch increment, 0.5000 inch stroke) dial gages symmetrically located (90 degrees) around the ring. The axial deformation of the ring was determined by taking the average of the four dial gage readings.

3.9.3 Results. The basic result desired from the ring tests was the effective wall thickness of the specimen. It was assumed that the effective wall thickness of the specimen could be determined by testing a representative ring from the specimen. The modulus of elasticity ($E = 29,500$ ksi), the length of the ring, and the slope of the load-displacement curve from the ring test were used to compute the effective area and wall thickness of the ring.

3.9.4 Discontinuation of Ring Tests. As previously stated, the primary purpose of the ring tests was to compute an effective wall thickness for the full scale specimen. This wall thickness was to be compared with the wall thickness as determined by ultrasonic testing and later used in the analytical models to predict the behavior of the member.

The ring tests were conducted on the first eight specimens to determine effective wall thicknesses. As previously mentioned, the effective wall thickness was also determined from the full scale compression tests. Comparison of these wall thickness values showed that the full scale values were typically smaller than those obtained from the ring test. The reason for this is simple. The wall thickness determined from the full scale tests was based on data taken over the entire length of the specimen, including all damaged regions. The wall thicknesses determined from the ring tests was based on data from a significantly shorter specimen that, proportionally, contained less damage. It became apparent that the location from which the ring was removed greatly influenced the effective wall thickness as computed from the ring tests. Thus, it would be impossible to obtain a ring specimen that was truly representative of the full scale specimen. After the eight tests it was decided that the full scale data provided a more accurate value of wall thickness, and the ring tests were discontinued.

3.10 Test Results

3.10.1 General. The data collected during the tests described in the previous sections were analyzed, and summarized in graphical and tabular form. A complete presentation of the results for all specimens is included in Appendix A. A brief summary of these results and a detailed description of the results for a typical specimen are presented in the subsequent sections.

3.10.2 Full Scale Tests. The full scale axial compression tests provided all the data on the ultimate and post-ultimate behavior of the damaged tubular members. The results obtained from these tests included peak axial load, chord shortening, and specimen effective length. Additional information concerning the displaced shape, load eccentricity, and effective wall thickness was also determined.

3.10.3 Ultrasonic Tests. An average wall thickness for the specimen was computed from 30 individual ultrasonic wall thickness measurements. In addition, wall thickness measurements were also taken in regions of local failure.

3.10.4 Tensile Coupon Tests. The tensile coupon tests were conducted to determine the material properties for each full scale specimen. The following results were obtained from the uniaxial tension tests:

- (a) Modulus of elasticity
- (b) Static yield stress
- (c) Dynamic yield stress
- (e) Ultimate strength.

All properties were obtained by averaging the individual values obtained from the two tensile coupon tests conducted for each specimen.

3.10.5 Ring Tests. The purpose of the ring tests was to determine an effective wall thickness for the specimen. The load-axial deformation data from the tests were used with the modulus of elasticity and the length of the specimen to compute an effective wall thickness.

3.10.6 Presentation of Results. The results obtained from the full scale compression tests, ultrasonic tests, tensile coupon tests, and ring tests are presented in thirteen graphs for each specimen. These graphs include:

- (1) Effective Length vs Load Step
- (2) Load and Normalized Deflection vs Load Step
- (3) Load vs Chord Shortening
- (4) Horizontal Displacements
- (5) Vertical Displacements
- (6) x - Eccentricities based on Inflection Points
- (7) y - Eccentricities based on Inflection Points
- (8) x - Eccentricities based on End Moments
- (9) y - Eccentricities based on End Moments
- (10) Computed Wall Thickness based on Full Scale Test Data
- (11) Summary of Effective Wall Thickness Results
- (12) Stress-Strain Curve for Tensile Coupon 1
- (13) Stress-Strain Curve for Tensile Coupon 2

These graphs are presented for each specimen in Appendix A.

The effective length graphs are one of the results from the least-squares error analysis of the full scale strain and displacement test data. The effective length, "k", of a specimen is a function of the end conditions and is one of the key parameters used to compute the critical global buckling load of an axially loaded member. The (L_{eff}/L) or "k" values obtained from the curve-fit analysis were highly dependent on the initial condition, and the behavior of the specimen during the full scale test. For some of the specimens with severe local corrosion, failure was observed to occur by local yielding of the reduced cross-section as opposed to failure by global buckling. In such cases the effective length has little or no meaning.

The values of effective length were also dependent upon the initial out-of-straightness of the specimen. For straight specimens there was no lateral displacement prior to buckling (or ultimate) load. Thus, there was no curvature, and again the effective length had little meaning. For initially bent specimens, lateral displacements occurred and thus curvature existed prior to peak load. Therefore, it was possible to obtain a relevant effective length value prior to peak load for these specimens.

It should be further noted, that for some specimens, the deformations became large in the post-buckling region. For these specimens the ends tended to rotate away from the tailstock and movable headstock platens. This resulted in decreased end restraint and an apparent increase in effective length near the end of the test.

The load and normalized deflection graph was intended to be used in conjunction with the effective length graph. The peak load and the resultant displacement at the center of the specimen, normalized with respect to the length of the specimen, were plotted at each load step. This graph was used to define the load step at which "buckling" of the member occurred so the proper (L_{eff}/L) value at buckling could be determined.

The load versus chord shortening graph was perhaps the most important result of the experimental program. This graph shows the axial deformation of the tubular members in the pre- and post-ultimate range with respect to applied axial load.

The horizontal and vertical displacements were measured at three locations on the specimen during the full scale tests. The results of these measurements were plotted in the horizontal and vertical displacements graphs.

Graphs six through nine show the computed eccentricity of the axial load at each end. The eccentricities were computed from two different methods and, in general, produce similar results for most specimens. The computed eccentricities indicate the point of application of the applied resultant axial load. The eccentricity of the applied load was calculated for each end of the specimen and plotted for each load step along with the average of the two end eccentricities. For most initially straight specimens, the eccentricities were nearly zero until buckling occurred. At large lateral displacements, the location of the applied load began to move in the direction of the displacement as the ends of the specimens tended to rotate off the headstock and tailstock of the load fixture. However, this behavior generally occurred well beyond the measured peak load.

Due to the corrosion of the specimens, it was necessary to determine an effective wall thickness to be used in the analytical models discussed in Chapter 4. Three methods were used to determine the wall thickness. The results of all the wall thickness measurements and calculations were plotted for each specimen. On this graph, the individual values of wall thickness as determined from ultrasonic testing were plotted along with the average of the ultrasonic results. In addition, the effective wall thickness computed from the full scale tests (see Appendix E) and the ring tests (if applicable) were also plotted.

The final two plots for each specimen are the stress-strain curves for the tensile coupons. These graphs were used to determine the specimen material properties.

Several tables were also prepared which summarized the major findings of the experimental program. Table 3-4 provides a summary of the full scale compression tests. Included in this table are the peak axial load, deflections at peak load, and the computed effective length.

The results of the measured and computed wall thicknesses are presented in Table 3-5. The average wall thickness as computed from full scale and ring tests and as measured in the ultrasonic tests are reported along with the nominal wall thickness.

The material properties presented in Table 3-6 are the modulus of elasticity, static and dynamic yield strengths, and ultimate strength. It should be noted that the values given for modulus of elasticity are dubious at best due to the sensitivity of the extensometer. An accepted value of the modulus of elasticity ($E = 29,500$ ksi) for steel was used for all data reduction calculations in the experimental portion of the test program.

Finally, Table 3-7 presents the diameter-to-thickness ratios and length-to-radius of gyration ratios for the specimens tested. In this table, the effective wall thicknesses as determined from the full scale tests are used to compute the ratios. The values in this table can be compared with the values that are based on nominal wall thickness as presented in Table 3-1.

3.10.7 Typical Results for a Test Specimen. This section presents a detailed description of the test results for Specimen 17. Specimen 17 was 31.17 feet long with an outside diameter of 12.75 inches and a nominal wall thickness of 0.500 inches. The specimen was initially bent in the vertical (y) direction and was dented near midspan. The specimen was tested in axial compression and attained an ultimate load of 420 kips. The effective buckling length for this specimen was calculated as 0.52. The wall thickness was determined to be 0.496 inches based on ultrasonic testing and 0.422 inches using the data from the full scale tests. The static yield strength was 49.2 ksi, the dynamic yield strength was 51.4 ksi, and the ultimate strength was 64.0 ksi.

The effective length, load, and normalized resultant deflections of Specimen 17 were plotted versus load step and are shown in Figure 3-13. The normalized resultant deflection computed as the resultant deflection at midspan divided by the specimen length was also computed and plotted at each load step. A normalized resultant deflection of 0.007 was used for all specimens to define the load step at which buckling of the specimen occurred. Using the lower graph of Figure 3-13, a horizontal line was drawn from a normalized deflection of 0.007 to determine that buckling occurred at load step 35. The (L_{eff}/L) at buckling was then determined by constructing a vertical line at the corresponding load step (35) on the upper graph of Figure 3-13 and reading the vertical scale at the intersection of the two lines. Using this procedure, the effective length for specimen 17 was determined to be 0.52.

Figure 3-14 is the load versus chord shortening relationship for Specimen 17. This graph is used to characterize the ultimate and post-ultimate axial deformation of the specimen. The curve shown in Figure 3-14 consists of two distinct regions: 1) the pre-buckling region and 2) the post-buckling region. The maximum value of axial load is considered the peak load. The portion of the curve prior to peak load is the loading curve and is generally linear. After the peak load is attained, the specimen undergoes significant axial deflection while the load decreases. This is called the post-buckling or unloading portion of the curve. The behavior shown in Figure 3-14 is typical for members loaded in axial compression.

The horizontal displacements at the three measured locations are plotted in Figure 3-15. Location 1 refers to the measurements taken at the first ring of strain gages near end A while location 3 corresponds to the measurements taken at the ring of strain gages near end B. Location 2 refers to the measurements taken near midspan.

The horizontal displacements, as shown in Figure 3-15, were extremely small until the peak load was reached and the specimen began to deflect. As shown, the maximum horizontal deflection of -1.17 inches occurred near midspan while the deflection near the ends remained small. The horizontal displacements, at all locations were relatively small when compared to the vertical displacements.

Figure 3-16 is a plot of the vertical displacements for Specimen 17. The locations at which the measurements were taken are the same as those for the horizontal displacements. The specimen deflected vertically at the onset of loading since it was initially bent in the y - direction. These deflections became quite large in the post-buckling region. As expected, the measured deflections at midspan were significantly larger than the deflections measured near the ends. The maximum vertical displacement was -11.2 inches near the midspan of the member and occurred at the end of the test.

The eccentricity of the applied axial load as computed from the displacements at the inflection points of the specimen are shown in Figures 3-17 and 3-18. Figure 3-17 contains the eccentricities in the x direction, while Figure 3-18 contains the eccentricities in the y direction. These graphs indicate that the load remained centric throughout the test in the x direction but not in the y direction past the peak load. This behavior was caused by the large vertical displacements that occurred in the post-buckling region. As the load was applied, the specimen deflected downward causing the ends to rotate from the headstock and tailstock of the load frame. This results in the line of action of the resultant load being located below the centroid of the cross section (-y direction).

Figures 3-19 and 3-20 are plots of the eccentricity of the axial load as computed from the calculated end moments. These end moments were computed

from the curvature at the ends of the specimen as determined by the curve fit algorithm. The results shown in these plots, when compared to Figures 3-17 and 3-18, show that the two methods of computing eccentricities produced similar results.

An effective wall thickness was computed for each load step from the data measurements taken during the full scale tests. These values were calculated based on the average axial strain component, C , as determined by the curve fit algorithm (see Appendices C and E) and are shown in Figure 3-21. Prior to the ultimate load, the computed wall thickness remained essentially constant. The effective wall thickness was computed by taking the average of these values prior to peak load. After the peak load, bending produces the dominant strains so that the effective wall thickness based on axial strains is meaningless.

The results of all the methods used to measure and compute specimen wall thickness were graphed as shown in Figure 3-22. The individual ultrasonic measurements were plotted along with an ultrasonic average. For Specimen 17, the individual ultrasonic readings exhibited little scatter since the specimen did not contain significant corrosion damage. For other members with severe widespread corrosion, the ultrasonic data had significantly more scatter. Also plotted on Figure 3-22 were the average wall thicknesses computed from the full scale tests and, when applicable, the ring tests.

Finally, the stress-strain curves for the tensile coupon tests were plotted as shown in Figures 3-23 and 3-24. The dynamic yield strength was determined by the standard 0.2% offset method. As mentioned previously, all test and data reduction procedures were performed according to SSRC Technical Memorandum No. 7. The tests were stopped three times (5 minutes each time) at specified strains beyond the yield strain. During these stops, the strain was held relatively constant while the load was allowed to stabilize. This was done so that the static yield strength of the specimen could be determined. These stops result in the three dips shown in the stress-strain curves of Figures 3-23 and 3-24. To determine the static yield stress, a line is drawn through the three dips. The stress at which this line intersects the 0.2%

offset line is defined as the static yield strength. Both yield strength values are shown in Figure 3-24.

3.11 Summary of Specimen Behavior - Full Scale Tests

For each specimen tested, the location and type of failure were recorded. There were three distinct failure modes observed during the full scale tests: 1) global buckling, 2) local failure, and 3) crack opening. Shown in Figure 3-25 are examples of each failure mode. Specimens with high slenderness ratios typically failed by global buckling while short specimens with large (D/t) ratios exhibited a more localized failure at ultimate load. The localized failure was generally caused by material yielding in highly corroded regions with reduced wall thickness. Only two specimens failed by crack opening. Both of these specimens had a visible through-thickness crack in a welded seam prior to testing.

A summary of the failure type and location is presented in Table 3-8. In addition, a brief description of the behavior of each specimen is included in this section.

Specimen 01: Local failure occurred 3'-0" from end B in a region of high corrosion. The wall thickness in this area was determined to be 0.265 in. using ultrasonic measurements compared to an overall effective wall thickness of 0.270 in. determined from the full scale test data.

Specimen 02: This specimen experienced local failure near a circumferential weld located 3'-3" from end B. Ultrasonic wall thickness measurements in the failure region indicated that the wall thickness in the failed region was 0.284 in. while the overall effective wall thickness was calculated as 0.346 in. Due to the reduced wall thickness, material yielding caused the local failure.

Specimen 03: Local failure occurred 2'-4" from end B for this specimen. The specimen wall thickness was determined to be 0.247 in. in the failed region while the overall effective wall thickness was calculated to be 0.305 in. The local failure was caused by material yielding due to the reduced wall thickness.

Specimen 04: Specimen 04 was initially bent in one direction with no other damage. The specimen failed by overall buckling with the location of failure 15'- 6 1/2" from end B. As expected, the location of failure was near the location of maximum initial out-of-straightness.

Specimen 05: This specimen failed initially due to the opening of an 8 in. long through-thickness crack in welded seam located 24 in. from end B. Shortly after this failure occurred, the specimen began to experience localized failure 4'- 10" from end B.

Specimen 06: Specimen 06 was an undamaged pipe with no corrosion and failed by global buckling. Beyond the buckling load, a hinge point formed 17'- 6 1/2" from end B. This failure location was near the midspan of the specimen.

Specimen 07: The major damage on this specimen was a single dent located 19'- 1 1/2" from end B. Specimen failure by global buckling occurred with the hinge point at this location. During the test, a longitudinal tear formed in the wall of the specimen just above the dent.

Specimen 08: This specimen failed by global buckling. The post-buckling hinge point formed 19'- 9" from end B. The only damage on this specimen was a small dent 3'- 8" from end B which did not affect the behavior of the specimen.

Specimen 09: Specimen 09 was an undamaged specimen which experienced global buckling failure. A hinge point located 12'- 8" from end B formed beyond the buckling load.

Specimen 10: Specimen 10 was an undamaged specimen which experienced global buckling failure. The post-buckling hinge point was located 16'- 6" from end B.

Specimen 11: Specimen 11 was an undamaged specimen which experienced global buckling failure. The post-buckling hinge point was located 14'- 5 1/2" from end B.

Specimen 12: This specimen was highly corroded and heavily damaged. Damaged include three major regions with holes and/or denting. The specimen failed by global buckling with the hinge point located at a damaged region 14'- 5 1/2" from end B. The other damage regions did not affect the overall specimen behavior.

Specimen 13: Specimen 13 was initially bent in both the vertical and horizontal planes and had four dented regions. The location of the deepest dent corresponded to the location of the largest initial out-of-straightness

in the vertical plane. This location was 8'- 3" from end B and was also the point of hinging for the specimen. Failure occurred due to global buckling, and the other dent damage did not affect the behavior of the specimen.

Specimen 14: This specimen had initial out-of-straightness and denting damage as well as a region of heavy corrosion. The corroded region was identified prior to testing due to two visible corrosion holes. Local failure due to material yielding occurred in the highly corroded region 4'- 9" from end B. The wall thickness in this yielded region was determined to be 0.219 in. using ultrasonic measurements compared to an overall effective wall thickness of 0.295 inches as determined from the full-scale tests.

Specimen 16: Specimen 16 failed due to global buckling. The location of the post-buckling hinge was 13'- 1" from end B which corresponded to the location of maximum initial out-of-straightness for this specimen. Four small dents on the specimen did not seem to affect the overall specimen behavior.

Specimen 17: This specimen was initially bent in one direction. In addition, there was a single dent on the specimen located at the point of maximum initial out-of-straightness. This specimen failed by global buckling with the post-buckling hinge point corresponding to the dent location of 19'- 1" from end B.

Specimen 18: Specimen 18 had seven small dents, was initially bent, and had a localized region of high corrosion. Local failure due to material yielding occurred in a region that was highly corroded 2'- 11" from end B. The wall thickness in this region was 0.261 inches as determined by ultrasonic testing. The dents did not affect the overall behavior of the specimen.

Specimen 19: This specimen experienced local failure in a region of local heavy corrosion 29'- 11" from end B. The wall thickness was determined to be 0.279 inches in this region compared to an overall effective wall thickness of 0.338 inches as determined from the full-scale tests. Prior to testing, there was a crack near end A which appeared to be a result of corrosion in a welded longitudinal seam. This crack was only through about half the wall thickness and did not affect the overall behavior of the specimen.

Specimen 20: This specimen had only corrosion damage and failed by global buckling. The post-buckling hinge point was located 18'- 1" from end B.

Specimen 21: Specimen 21 had a series of cracks along a longitudinal welded seam. Some of these cracks were through-thickness cracks while others were not. Failure was caused by the opening of a through-thickness crack located

19'-8" from end B. The other through-thickness crack did not open significantly. It was observed that crack growth was arrested by a circumferential girth weld located 19'- 11 1/4" from end B. It should also be noted that a highly corroded region 20'- 3" from end B containing a 1 inch diameter corrosion hole did not affect the specimen failure.

3.12 Comparison of Experimental Ultimate Capacities to Predicted Capacities

In order to evaluate the reduction in strength of the tested specimens, the measured ultimate loads were compared to analytical predictions for the ultimate load of members with the same physical and material properties but without damage. The predicted ultimate loads were computed using the design equations for compression members as presented in the literature and in applicable design codes. The design equations for compression members as presented in the American Institute of Steel Construction, Manual of Steel Construction, Allowable Stress Design, 9th Edition (1989) and the Canadian Standards Association, Steel Structures for Buildings - Limit States Design by Prion (1987) were used without the safety or resistance factors in order to predict member ultimate loads. It should be noted that the American Petroleum Institute design equations (API RP 2A, 1989) are the same as the AISC equations. In addition, a mean value curve for predicting the ultimate strength of tubular members (Cox, 1987) was also used for comparison purposes.

The physical and material properties needed to calculate the ultimate capacity of the undamaged members include length, diameter, wall thickness, yield strength, effective length, and modulus of elasticity. The modulus of elasticity, E, was taken as 29,500 ksi and the static yield strength was used for all calculations. The remainder of the parameters were reported in Tables 3-1, 3-5, and 3-6 and are summarized in Tables 3-9 and 3-10.

3.12.1 Discussion of Design Equations. Design codes provide design equations for typical structural members. These equations generally contain factors which account for the various uncertainties involved in the analysis and design of structures. Load and resistance factors are used in limit state design while safety factors are used in working stress design. In the formulations used for computing ultimate loads in this research, these factors

were removed to obtain the predicted ultimate capacity of the undamaged members.

The allowable axial stress for a compression member is given by the AISC Manual of Steel Construction, Allowable Stress Design (1989) as:

$$F_a = \frac{\left[1 - \frac{(kL/r)^2}{2C_c^2} \right] * F_y}{\frac{5}{3} + \frac{3(kL/r)}{8C_c} - \frac{(kL/r)^3}{8C_c^3}} \quad (3-1)$$

for $(kL/r) < C_c$ and

$$F_a = \frac{12\pi^2 E}{23 (kL/r)^2} \quad (3-2)$$

for $(kL/r) > C_c$.

where: F_a = allowable axial stress

k = effective length factor of member

L = length of member

r = radius of gyration

F_y = yield stress

C_c = slenderness ratio corresponding to the Euler buckling stress of

$$0.5 F_y$$

$$= [2\pi^2 E / F_y]^{1/2}$$

E = modulus of elasticity.

As shown in Table 3-10 for all specimens tested in this research,

$(kL/r) < C_c$ so that only Eq. 3-1 is applicable. To compute the predicted ultimate capacity, the safety factor (denominator) of Eq. 3-1 should be 1.0 so that:

$$F_u = \left[1 - \frac{(kL/r)^2}{2C_c^2} \right] * F_y \quad (3-3)$$

where F_u is the ultimate axial stress.

The ultimate load is then computed as:

$$P_{ult} = F_u A \quad (3-4)$$

where A is the cross-sectional area of the member. As previously mentioned, the American Petroleum Institute (API RP 2A, 1989) uses the same equation to predict the ultimate capacity of undamaged tubular members.

The Canadian Standards Association buildings code presents the buckling resistance, P_r , of members subjected to axial compression as follows (Prion, 1987):

$$P_r = \phi A F_y \quad \text{for } 0 \leq \lambda \leq 0.15 \quad (3-5)$$

$$P_r = \phi A F_y (0.990 + 0.122\lambda - 0.367\lambda^2) \quad (3-6)$$

$$\text{for } 0.15 < \lambda \leq 1.2$$

$$P_r = \phi A F_y (0.051 + 0.801\lambda^{-2}) \quad (3-7)$$

$$\text{for } 1.2 < \lambda \leq 1.8$$

$$P_r = \phi A F_y (0.008 + 0.942\lambda^{-2}) \quad (3-8)$$

$$\text{for } 1.8 < \lambda \leq 2.8$$

$$P_r = \phi A F_y \lambda^{-2} \quad \text{for } 2.8 > \lambda \quad (3-9)$$

where: ϕ = resistance factor

$$\lambda = \frac{kL}{r} \sqrt{\frac{F_y}{\pi^2 E}} \quad (3-10)$$

As can be seen from Table 3-10, Eq. 3-6 is applicable for all specimens tested in this research. The resistance factor, ϕ , was taken as 1.0 in all cases so that the predicted ultimate capacity was calculated.

Strength equations for load and resistance factor design were presented by Cox (1987). A column curve was obtained by determining the best fit for previously reported compressive strength data for undamaged tubular members. The mean value column curve strength for fabricated tubular members was determined to be:

$$P_{ult} = (1.03 - 0.24\lambda^2) P_y, \text{ for } 0 < \lambda < 1.7 \quad (3-11)$$

where: $P_y = F_y A$

and F_y , A are as previously defined.

As can be seen from Table 3-10, λ varied from 0.20 to 0.78 so that Eq. 3-11 is valid for all specimens tested in this research.

3.12.2 Evaluation of Results The calculated ultimate loads based on the three formulas just described are presented with the experimentally measured ultimate loads, P_{meas} , in Table 3-11. The analytical values, P_{an} , were computed using the nominal wall thickness values. The yield load, P_{yld} , was computed by multiplying the specimen's cross-sectional area based on nominal wall thickness values by the measured static yield strength.

A ratio of the ultimate measured axial load to the predicted ultimate load, P_{meas}/P_{an} , using the nominal wall thickness values is presented in Table 3-12. From this table, it was noted that the measured and predicted values for the undamaged specimen, specimen 06, were nearly identical. For the heavily damaged specimens such as 12, 13, 14 and 16, the measured capacities were only 25 to 40% of the predicted ultimate capacity. For the remaining slightly and moderately damaged specimens, the measured capacities ranged from about 50 to 80% of predicted capacity.

Figures 3-26, 3-27, and 3-28 are plots of the measured capacities, P_{meas} , (hereafter called the actual capacities) versus the predicted capacities, P_{an} , listed in Table 3-11. The specimens are numbered and have been separated by damage types. A line for $P_{an} = P_{meas}$ is plotted to aid in the comparison. It should be noted that all specimens, except specimen 06, have corrosion damage. As indicated by these figures all specimens, except specimen 06, have a measured capacity less than the predicted capacity. The greatest differences in strength occurred in the most severely damaged members. Members with large out-of-straightness (OOS) damage, members 13, 14, and 16, exhibited the largest reduction in capacity. Members with only corrosion damage or corrosion and single dent damage, exhibited the smallest reduction in capacity.

Table 3-13 presents the ultimate capacities of the specimens predicted using the effective wall thickness values as determined from the full scale tests. Table 3-14 contains the ratios of the measured capacities, P_{meas} , to the predicted capacities, P_{an} . Table 3-14 again indicates that the measured and predicted capacities of specimen 06 are nearly the same. Heavily damaged specimens 12, 13, 14 and 16 had measured capacities that were 29 to 48% of the predicted ultimate capacities. This is only a slight increase over the values obtained using the nominal wall thickness values. For the remaining less damaged specimens, the measured capacities were 56 to 95% of the predicted capacities.

Figures 3-29, 3-30, and 3-31 are plots of actual measured capacities, P_{meas} , versus the predicted capacities, P_{an} , listed in Table 3-13. Once again, the specimens have been numbered and separated by damage types. All specimens had corrosion damage except specimen 06. In these three figures, only the specimens which failed due to global buckling or crack opening are plotted. Specimens which experienced local failure were evaluated separately and are discussed below. Figures 3-29, 3-30, and 3-31 indicate that the specimens which were undamaged or corroded only, had ultimate measured loads slightly less than the predicted ultimate loads. Again, severely damaged specimens, that is specimens with large out-of-straightness (OOS) damage and/or multiple damage, exhibited the greatest difference in measured and predicted ultimate load. All specimens, with the exception of specimen 06, had measured ultimate loads less than predicted ultimate loads.

The ultimate capacities of the specimens which experienced local failure were calculated by multiplying the yield strength or critical local buckling stress by the minimum cross-sectional area of the specimen. The minimum cross-sectional area was determined after the full scale test by taking ultrasonic wall thickness measurements in the region of local failure. In general, the wall thickness in these regions were found to be significantly less than the overall effective wall thickness. In some specimens, the reduced wall thickness resulted in D/t ratios greater than 60. For these specimens, the yield stress was reduced according to the procedure given by API RP 2A (1989)

to account for possible local buckling effects. According to API RP 2A the local buckling stress, F_{xc} is given by:

$$F_{xc} = F_y [1.64 - 0.23 (D/t)^{0.25}] \leq F_{xe} \quad (3-12)$$

$$F_{xc} = F_y \text{ for } D/t \leq 60 \quad (3-13)$$

where: F_{xe} = critical elastic local buckling stress

= $2 C E t/D$ for $t \geq 0.25$ and $D/t < 300$

C = critical elastic buckling coefficient

= 0.3

Table 3-15 presents the ultimate capacities predicted for specimens experiencing local failure and the ratio of measured to predicted capacities. Figure 3-32 is a plot of the measured capacities versus the predicted capacities of the specimens experiencing local failure. It should be noted that all specimens in this figure had corrosion damage. It should be further noted that the measured ultimate load was less than the predicted ultimate load for all specimens. One possible reason for this behavior is the presence of small corrosion pits in yielded regions that were not detected by ultrasonic testing. These localized forms of damage would cause very localized stress concentrations and an overall reduction in member capacity.

A brief summary of the comparison between the measured and the predicted ultimate capacity follows for each specimen. First, the measured capacities for all specimens are compared to predicted capacities using the nominal wall thickness. If the specimen failed by global buckling, the measured capacity is compared to the predicted capacity using the effective wall thickness. However, if the specimen experienced a local failure, the capacity is compared to the predicted yield load using the minimum wall thickness (in the region of local yielding).

Specimen 01: Specimen 01 had a measured ultimate load that was 57% of the predicted nominal ultimate capacity. The measured load was 82% of the yield load. This specimen had initial damage in the form of a dent.

Specimen 02: Specimen 02 had a measured ultimate load that was 57% of the predicted nominal ultimate capacity. The actual ultimate capacity was 88% of the predicted yield load. The only type of damage on this specimen was corrosion.

Specimen 03: Specimen 03 had a measured ultimate load that was 58% of the predicted nominal ultimate capacity. The measured ultimate load was 89% of the predicted yield load. Corrosion was the only damage for this specimen.

Specimen 04: The measured ultimate capacity of this specimen was 57% of the predicted nominal ultimate capacity. The specimen failed by global buckling in the direction the specimen was initially bent. The measured capacity was 68% of the buckling capacity predicted using the effective wall thickness.

Specimen 05: Specimen 05 had a measured ultimate capacity that was 62% of the predicted nominal ultimate capacity. The measured capacity was 76% of the predicted yield load. This specimen was corroded and had one dented region.

Specimen 06: This specimen was undamaged and failed by global buckling. It had a measured ultimate load that was 3% greater than the predicted nominal capacity. The measured capacity was 2% greater than the predicted ultimate capacity using the effective wall thickness.

Specimen 07: Specimen 07 had a measured load that was 84% of the predicted nominal capacity. The specimen buckled globally with the location of the post-buckling hinge coinciding with the location of the single dent. The measured capacity was 78% of the capacity predicted using the effective wall thickness.

Specimen 08: Specimen 08 had a measured load that was 57% of the predicted nominal capacity. The measured ultimate load was 89% of the predicted ultimate load using the effective wall thickness. This specimen had a single dent and corrosion damage.

Specimen 09: The measured ultimate load was 67% of the predicted nominal ultimate load for this specimen and 93% of the ultimate capacity predicted using the effective wall thickness. Corrosion was the only damage for this specimen.

Specimen 10: Specimen 10 had a measured ultimate load that was 81% of the predicted nominal capacity. The measured load was 95% of the ultimate capacity predicted using the effective wall thickness. The only damage present was corrosion.

Specimen 11: This was also a specimen with only corrosion damage. The specimen had a measured ultimate load that was 83% of the predicted nominal ultimate capacity. The measured load was 89% of the predicted ultimate capacity using the effective wall thickness.

Specimen 12: Specimen 12 had a measured ultimate capacity that was 40% of the predicted nominal ultimate capacity. The measured capacity was 42% of the predicted capacity using the effective wall thickness. This specimen was corroded and had several holes and dents.

Specimen 13: This specimen was initially bent in both the vertical (y) and horizontal (x) directions. In addition, the specimen was dented in several locations and was highly corroded. It had a measured ultimate load that was 25% of the predicted nominal capacity. The measured capacity was 29% of the predicted ultimate capacity using the effective wall thickness.

Specimen 14: Specimen 14 had a measured load that was 38% of the predicted nominal capacity. The specimen was initially bent in two directions, dented, and heavily corroded. The measured capacity was 64% of the predicted yield load.

Specimen 16: Specimen 16 had a measured load that was 33% of the predicted nominal capacity. The measured ultimate load was 38% of the predicted ultimate load using the effective wall thickness. This specimen had initial out-of-straightness in two directions and dent damage.

Specimen 17: The measured ultimate load was 47% of the predicted nominal ultimate load for this specimen and 56% of the ultimate capacity predicted using the effective wall thickness. This specimen was initially bent in one direction with a single dent.

Specimen 18: Specimen 18 had a measured load that was 63% of the predicted nominal capacity. The measured load was 88% of the predicted yield load. This specimen had denting and initial out-of-straightness damage.

Specimen 19: The specimen had a measured ultimate load that was 60% of the predicted nominal ultimate capacity. The measured load was 75% of the predicted yield load. The only damage on this specimen was corrosion.

Specimen 20: The measured ultimate load was 72% of the predicted nominal ultimate load for this specimen and 82% of the ultimate capacity predicted using the effective wall thickness. This specimen was undamaged except for corrosion.

Specimen 21: Specimen 21 had a measured load that was 58% of the predicted nominal capacity. The measured load was 78% of the ultimate capacity predicted using the effective wall thickness. The specimen had a through-thickness crack which was the initiation site for local failure.

3.12.3 Discussion of End Conditions and Effective Length From Eq. 3-3, 3-6, 3-10, and 3-11, it can be seen that the effective length factor, k , is one of the principal parameters used to determine the ultimate capacity of a compressive member. For straight, undamaged members, this factor is a function of the restraint at the ends of the member. Theoretical values for k , k_{theo} , range from 0.50 to 1.00 for members with their ends restrained against lateral translation. If the ends of these members are fully restrained against rotation (fixed), then: $k_{\text{theo}} = 0.5$. However, if the ends are fully unrestrained against rotation (pinned), then: $k_{\text{theo}} = 1.0$. When performing compression tests on members in the laboratory, it is very difficult to design and fabricate end fixtures which achieve either of these ideal conditions so that: $0.5 < k_{\text{exp}} < 1.0$. Thus, the "fixity" of the ends must always be evaluated if the experimental results are to be compared with analytical or design formulae such as Eq. 3-3, 3-6, and 3-11.

As previously mentioned, all specimens tested were held in place at each end by three clip angles located 120 degrees around the circumference of the member as shown in Figure 3-8. These angles provided full restraint against end translation. The specimen ends were not attached in any other manner to the tailstock and headstock platens so that there was no physical attachment which would provide restraint against rotation.

The fixity of the ends, and thus the effective length factor, $k_{\text{exp}} = L_{\text{eff}}/L$, were evaluated for all specimens using the algorithm in the program, CURVE, described in Appendix C. It should be noted that limits for k were set between 0.32 and 2.00 in the program CURVE in order to exceed the range of theoretical values for k . Thus, the theoretical limits of k were not automatically imposed on k_{exp} in the CURVE algorithm.

Effective length factors ($k_{\text{exp}} = L_{\text{eff}}/L$) are presented in Table 3-4 for the eleven specimens which failed in a global buckling mode. Values are not

reported for specimens which yielded locally prior to buckling since the effective length is meaningless for members which fail in this mode.

The values found in Table 3-4 show that nine of the eleven specimens which failed by global buckling had effective length factors equal to or very nearly equal to 0.50. This indicates that nearly ideal fixed end conditions were achieved with the end supports used for the full scale tests. Since the ends were not physically restrained against rotation, one would expect the value for k to be approximately 1.0 rather than 0.5. However, the rotation at the ends of the specimens were closely monitored using dial indicators during all full scale tests. It was determined that, prior to ultimate load, the ends of all specimens remained in full contact with the headstock and tailstock platens of the load frame. Thus, there was essentially no end rotation between the member and the platens prior to buckling.

The fact that the member ends did not rotate away from the platens of the load frame prior to buckling can be explained by considering the line of action of the applied load. If the member is subjected to an eccentric compressive load, the resultant stress in the outer fibers of the member cannot be tensile unless the load is applied outside the kern area of the cross-section. Thus, the ends of the member cannot rotate away from the load frame platens if the load is applied within the kern area. Shown in Table 3-16 are the computed radius of the kern area and the maximum computed resultant eccentricity for each specimen. Note, that with three exceptions, the maximum eccentricity prior to peak load was less than the radius of the kern circle. Thus, the ends of the specimens could not rotate off the platens prior to peak load, and the specimens behaved as though there were fixed end conditions up to this point. It should be noted that specimen 06 had eccentricities inside the kern area at peak load and an effective length of 0.86. However, this specimen was not shimmed, and as a result, the applied load may not have been uniformly distributed over the ends of the specimen causing the ends to rotate.

3.13 Evaluation of Ultrasonic Measurements

For each specimen tested, 30 ultrasonic wall thickness measurements were taken at locations corresponding to the strain gage locations. In Table 3-17, the

average of the wall thickness measurements is listed for each specimen along with the standard deviation, and coefficient of variation. Table 3-18 presents the ultrasonic wall thickness, full scale effective wall thickness (see Appendix E), and a ratio of the full scale to ultrasonic wall thicknesses. Shown in Figure 3-33 is a graph comparing the two methods used to determine the wall thickness. Note the specimens are numbered for identification purposes.

The values presented in Tables 3-17 and 3-18 indicate the difficulty in trying to predict the type of specimen in which the ultrasonic wall thickness is an accurate measurement of the effective (full scale) wall thickness. It was originally thought that there would be significant scatter and thus, a large coefficient of variation, in the ultrasonic data for specimens with locally severe corrosion and pitting. Further, it was thought that these specimens would have significantly different full scale and ultrasonic wall thickness values. However, this was not the case. For instance, both specimens 09 and 10 had an effective full scale wall thickness that was 95% of the thickness as determined by ultrasound. However, the ultrasonic wall thickness measurements for specimen 09 had a coefficient of variation of 19.8% while those for specimen 10 had a coefficient of variation of only 3.8%. As another example, the ultrasonic thickness measurements of both specimens 08 and 09 had a coefficient of variation of approximately 20%. However, the full scale effective wall thickness of specimen 08 was only 76% of the ultrasonic wall thickness while the effective wall thickness of specimen 09 was 95% of the ultrasonic wall thickness.

Based on these observations, it was decided that the coefficient of variation was not a good parameter to use in determining the type of specimen in which ultrasonics provides an accurate measurement of the effective wall thickness. The data presented in Table 3-17, Table 3-18, and Figure 3-33, further indicates there is no obvious relationship between the two wall thickness determinations. With the amount of ultrasonic data taken during the test program, it would be dubious at best to formulate a relationship between full scale effective wall thickness and the wall thickness determined by ultrasonic testing.

The average and standard deviation for the full scale wall thickness to ultrasonic wall thickness ratios presented in Table 3-18 are 0.93 and 0.076, respectively. Based on the data from the twenty specimens tested in this program, it appears that a lower bound full scale to ultrasonic wall thickness ratio would be approximately 0.80. It should be noted that this lower bound value is valid only if: 1) the members are approximately the same size as those tested, 2) the members have similar types and magnitude of damage as those tested, and 3) a minimum of 30 ultrasonic measurements are taken along each member.

It should be further noted that regions of greatly reduced cross section were not obvious by visual inspection and were not located until after the full scale tests were completed and the local failure regions were evident. It is likely that these areas would be even more difficult to detect under in-service conditions. Sound engineering judgement and experience should be exercised when evaluating any ultrasonic wall thickness data for damaged tubular members.

FULL SCALE TEST SPECIMEN ORIENTATION AND COORDINATE SYSTEM

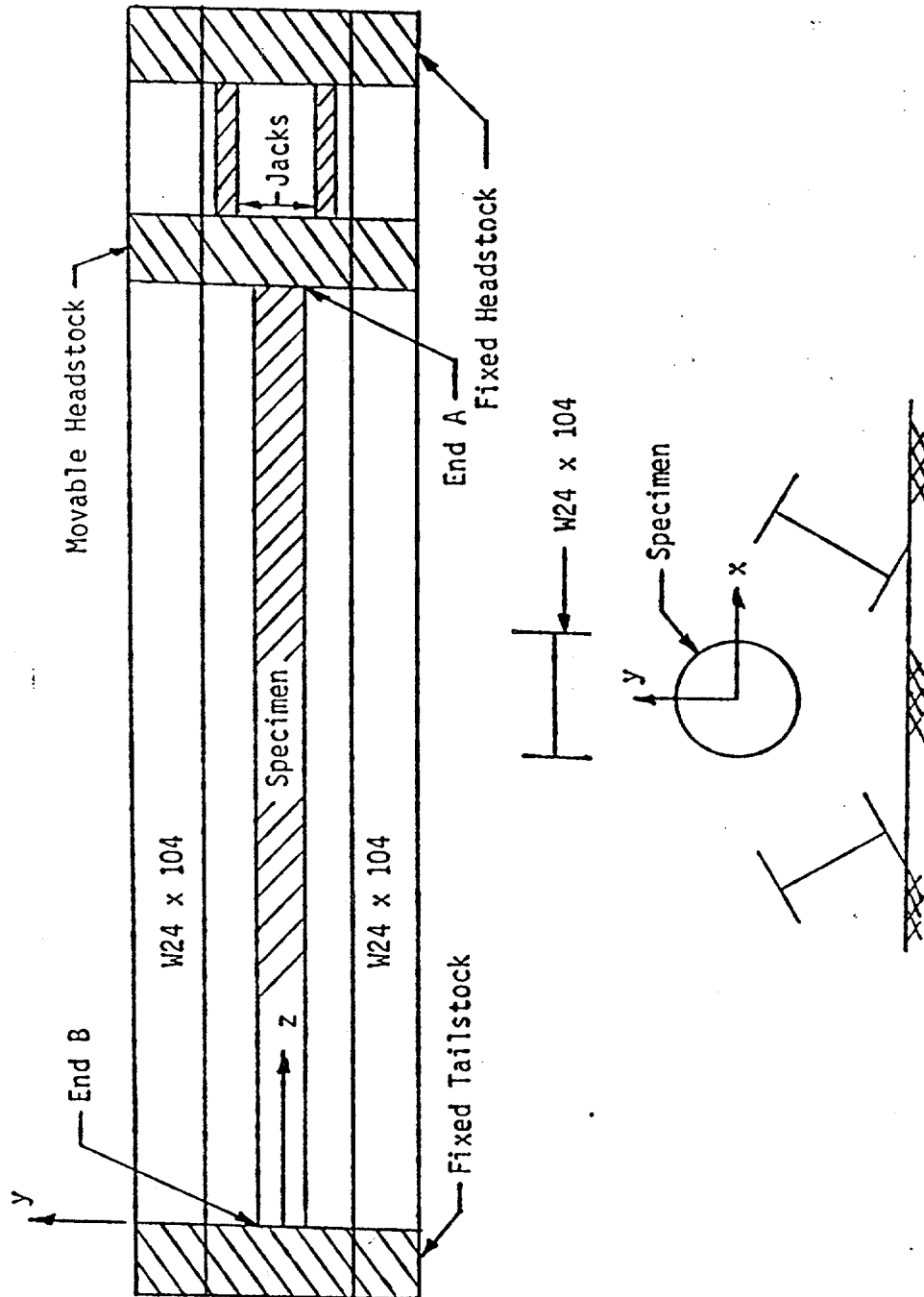
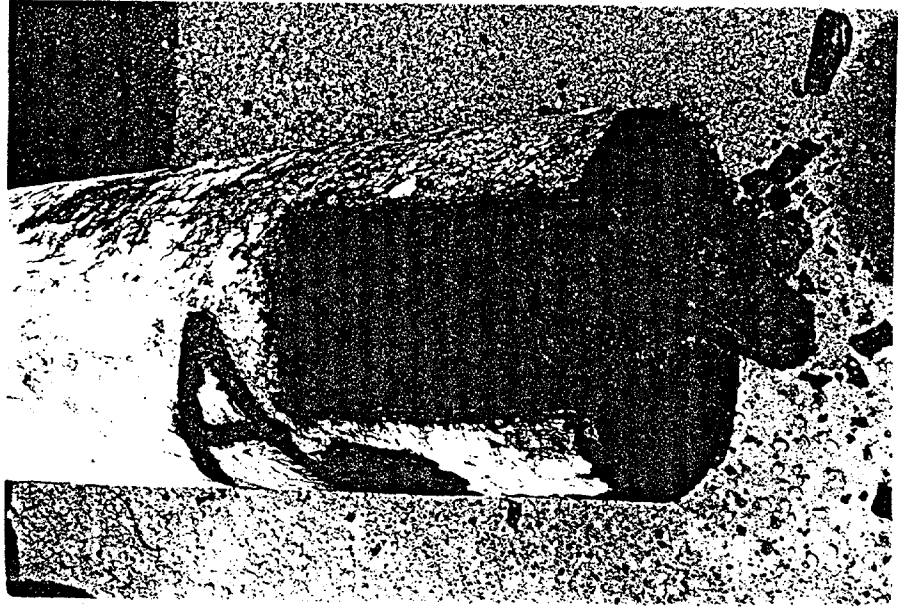
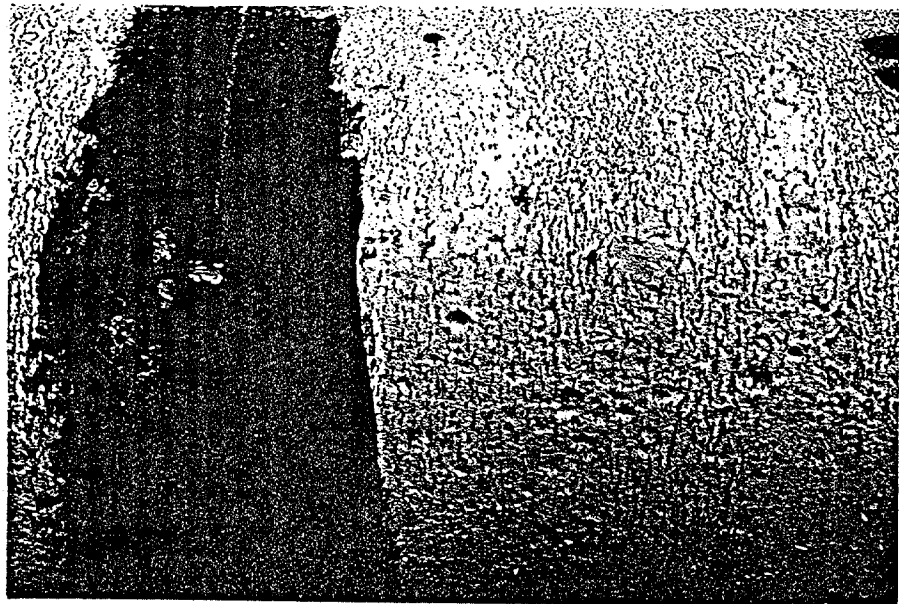


Figure 3-1

SEVERITY OF CORROSION



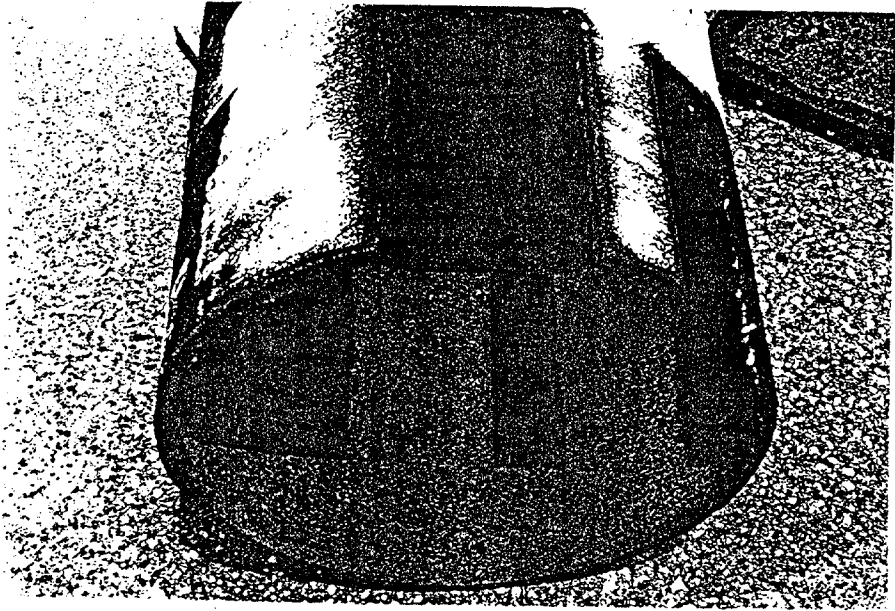
a) High Corrosion



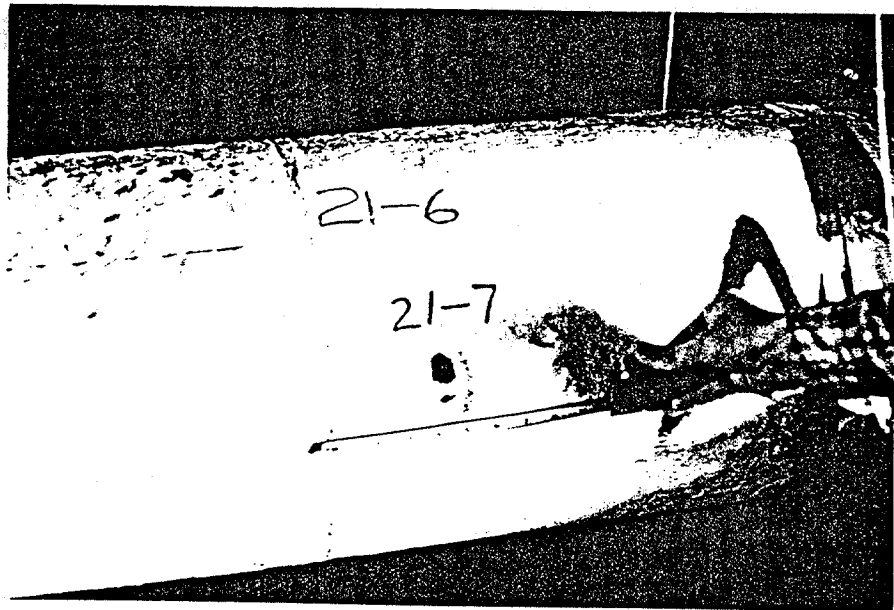
b) Medium Corrosion

Figure 3-2

SEVERITY OF CORROSION (cont.)



c) Low Corrosion



d) Overall Medium Corrosion with Local High Corrosion

Figure 3-2 (cont.)

DAMAGE SUMMARY

Specimen No. 17

DISTANCE FROM END "B"	*DISTANCE FROM CHALK LINE		DESCRIPTION OF DAMAGE
	LEFT	RIGHT	
1. 4'-8 3/4"			3/4" circumferential butt weld
2. 19'-1"		2" (center)	8" diameter dent (Round) (See additional pages for cross sections)

The specimen is curved. See additional page for initial out-of-straightness information.

*Looking from end "A" towards end "B"

Figure 3-3

**Out-of-Straightness Measurements
for Specimen 17**

The specimen was initially curved in the yz-plane and straight in the xz-plane. The following measurements are in the y-direction.

	Distance from End B (ft)	Distance from stringline to top of pipe (in)	Out-of- straightness in y direction (in)
	0	3.875	0
	1	4	-0.125
	2	4.25	-0.375
	3	4.5	-0.625
	4	4.75	-0.875
	5	5	-1.125
	6	5.1875	-1.3125
	7	5.375	-1.5
	8	5.5	-1.625
	9	5.6875	-1.8125
	10	5.875	-2
	11	6.0625	-2.1875
	12	6.25	-2.375
	13	6.4375	-2.5625
	14	6.625	-2.75
	15	6.75	-2.875
	16	6.9375	-3.0625
	17	7.125	-3.25
	18	7.375	-3.5
Begin dent	18.583	7.625	-3.75
	19	8.5	-4.625
Dent center	19.083	8.625	-4.75
End dent	19.5	7.625	-3.75
	20	7.375	-3.5
	21	6.875	-3
	22	6.5	-2.625
	23	6.25	-2.375
	24	5.9375	-2.0625
	25	5.625	-1.75
	26	5.3125	-1.4375
	27	4.9375	-1.0625
	28	4.625	-0.75
	29	4.375	-0.5
	30	4	-0.125
	31	3.875	0
	31.167	3.875	0

Figure 3-4

DENT CROSS SECTION

Specimen No. 17

Damage No. 2

Distance from End B 19'-1"

Scale 1"=3"

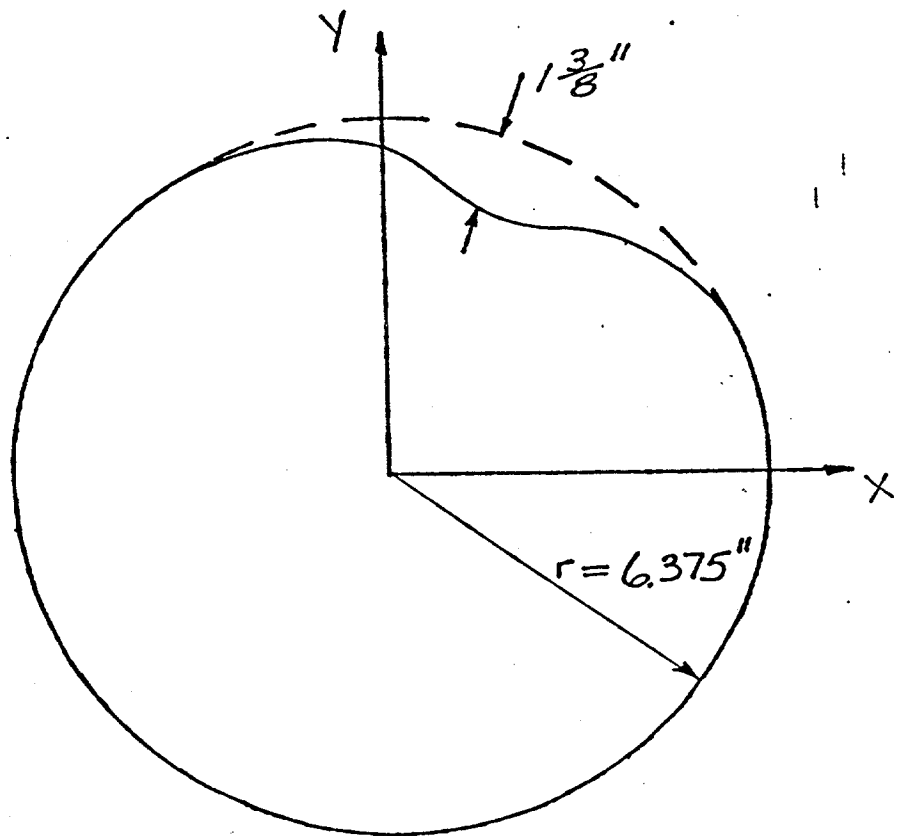


Figure 3-5

PLACEMENT OF STRAIN GAGES

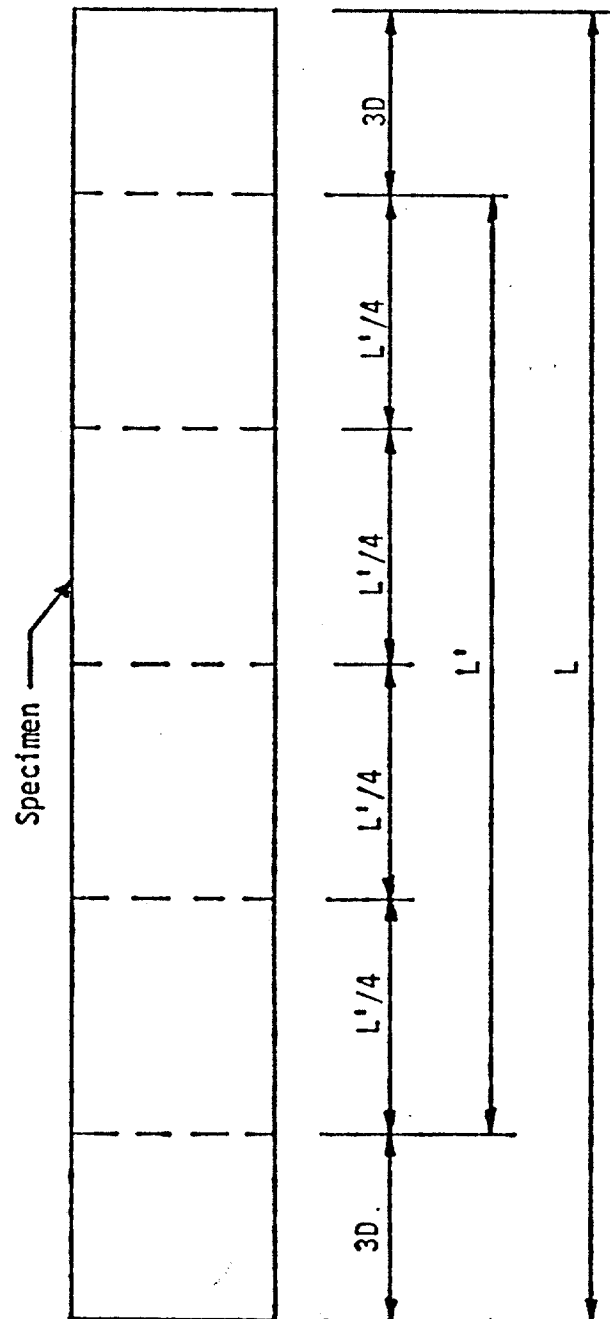


Figure 3-6

TEST FRAME

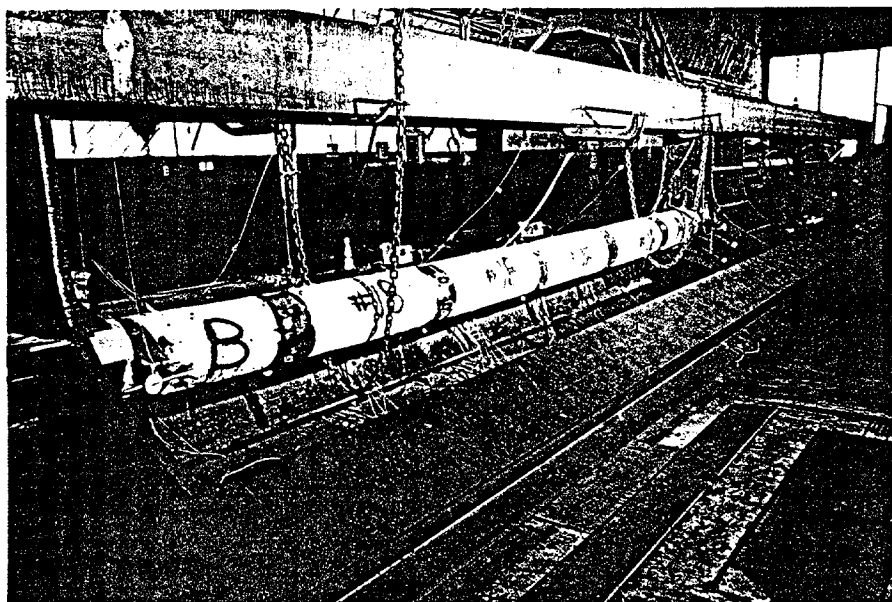


Figure 3-7

END CONDITIONS

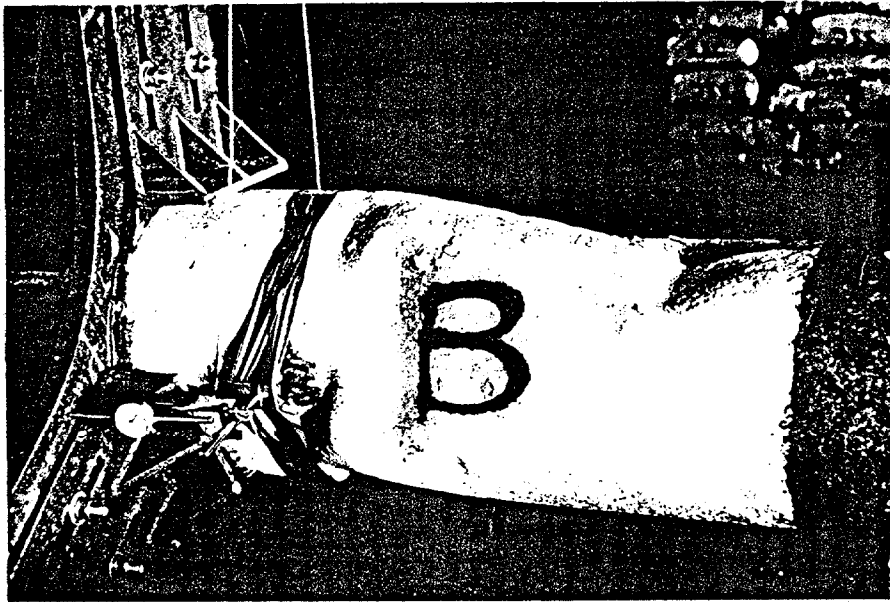


Figure 3-8

STRAIN GAGE LOCATIONS ON LOAD FRAME

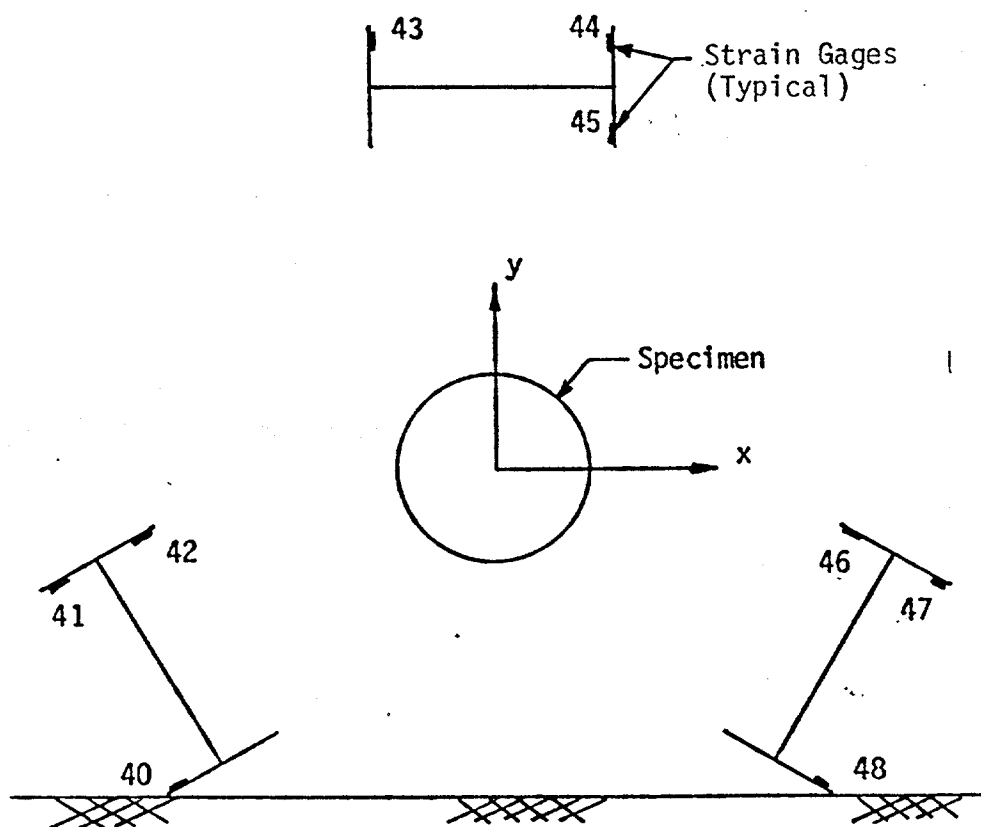


Figure 3-9

LOCATION OF DIAL GAGES

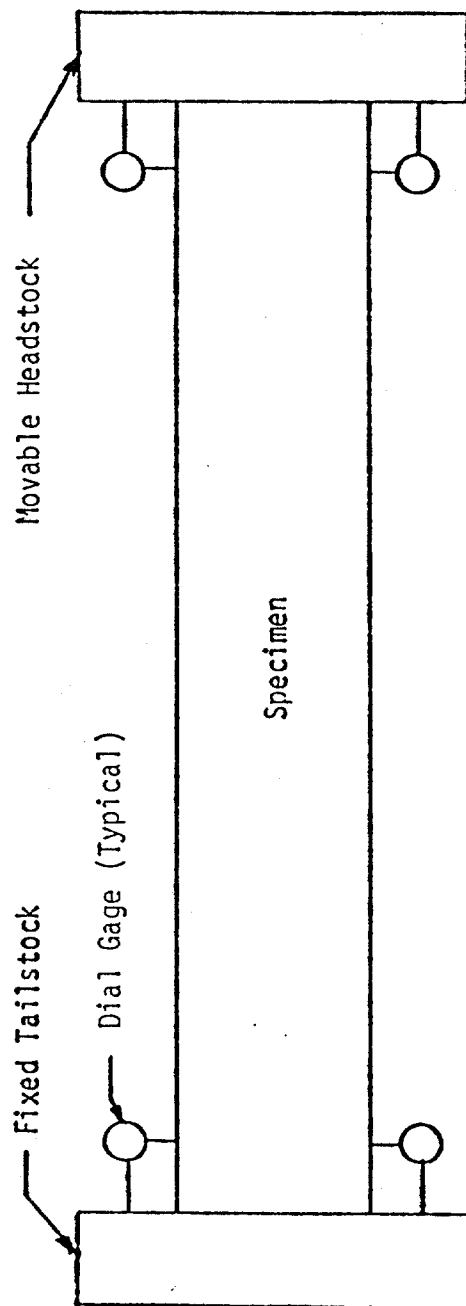


Figure 3-10

HORIZONTAL AND VERTICAL DISPLACEMENTS

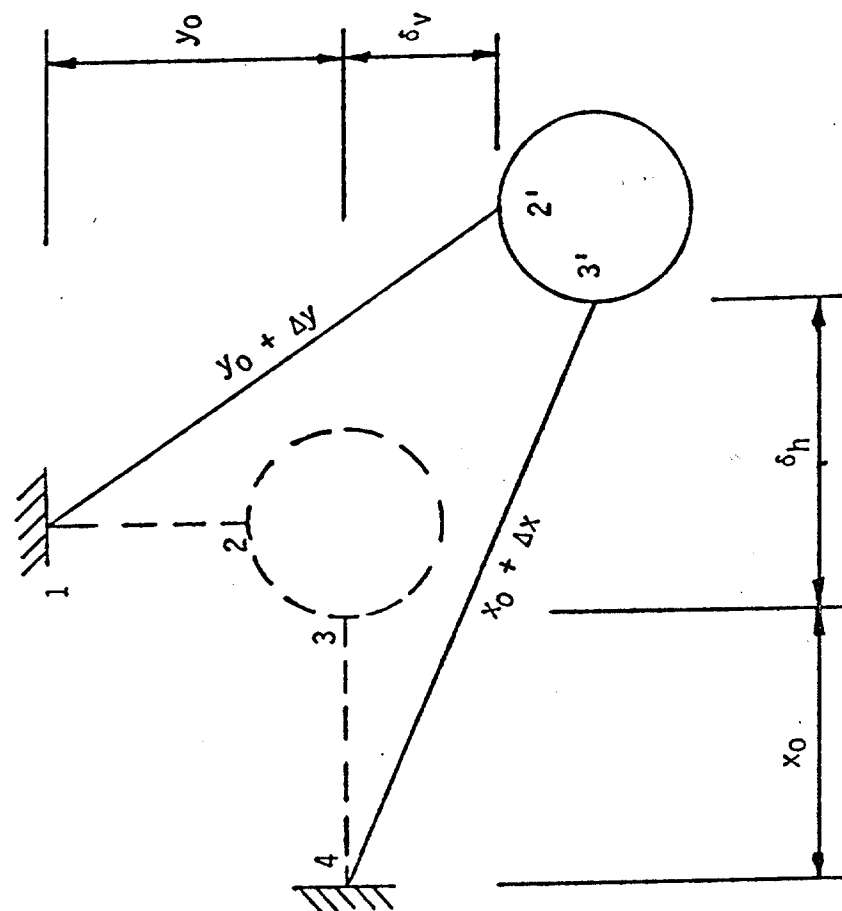


Figure 3-11

TENSILE COUPON SPECIMEN

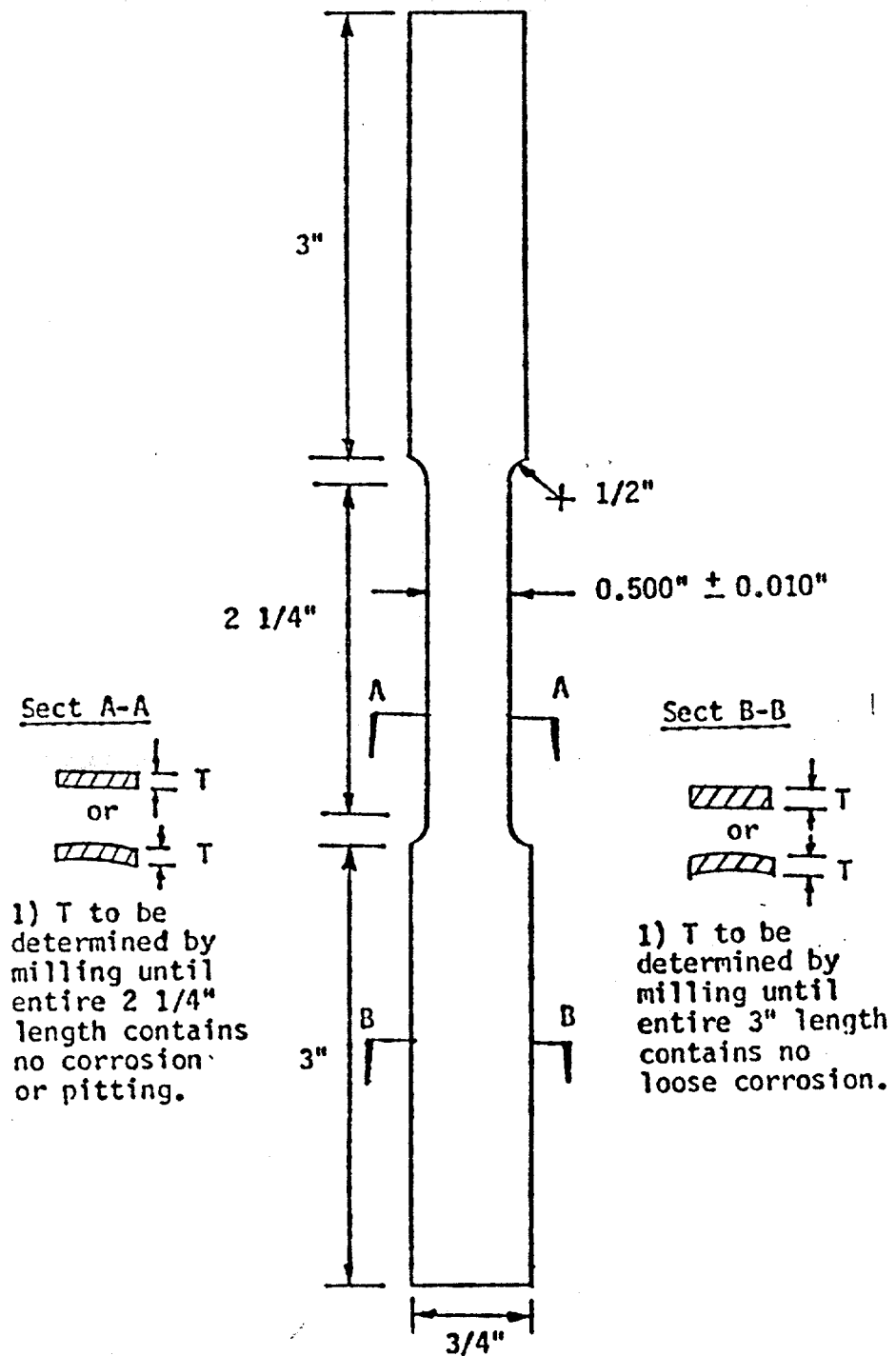
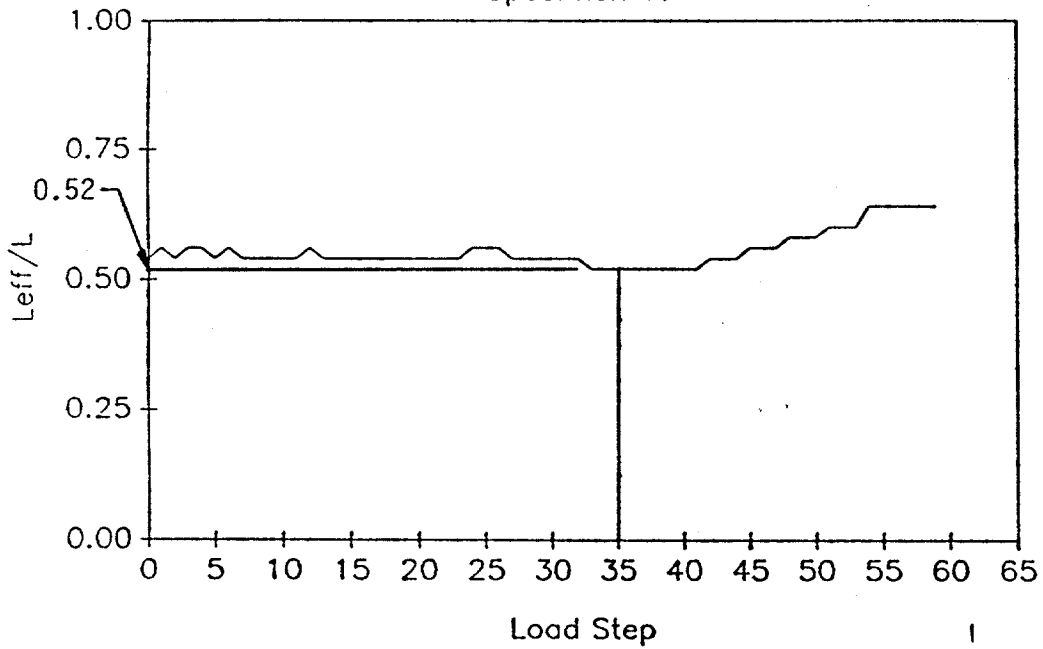


Figure 3-12

EFFECTIVE LENGTH vs LOAD STEP

Specimen 17



LOAD AND DEFLECTION vs LOAD STEP

Specimen 17

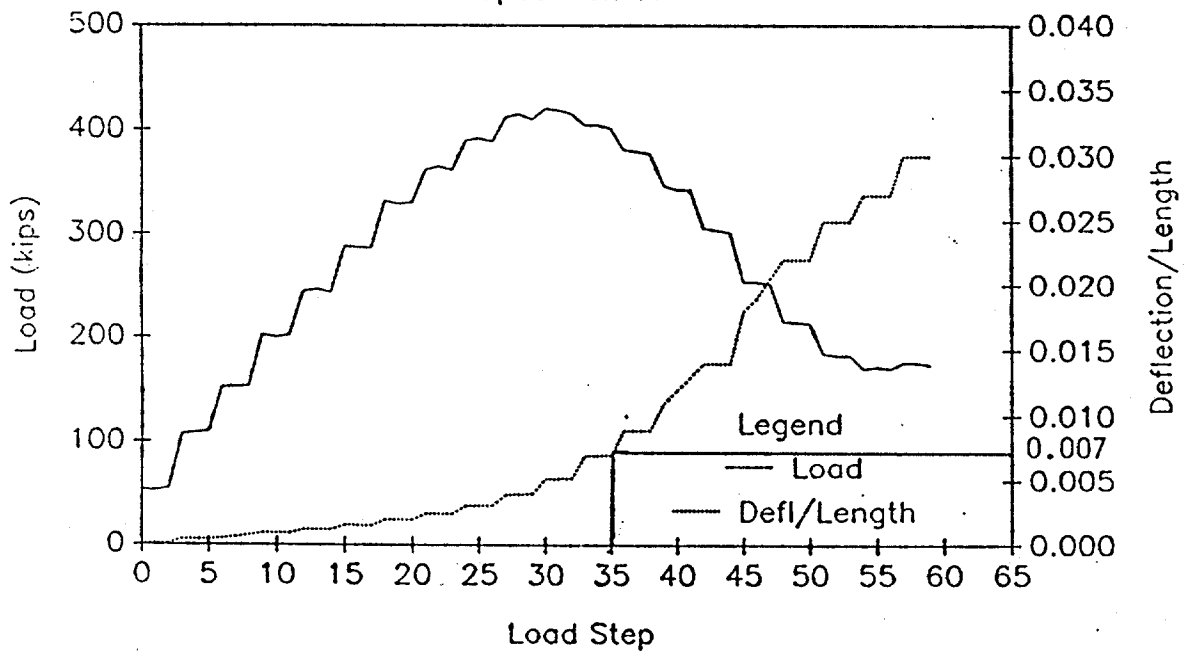


Figure 3-13

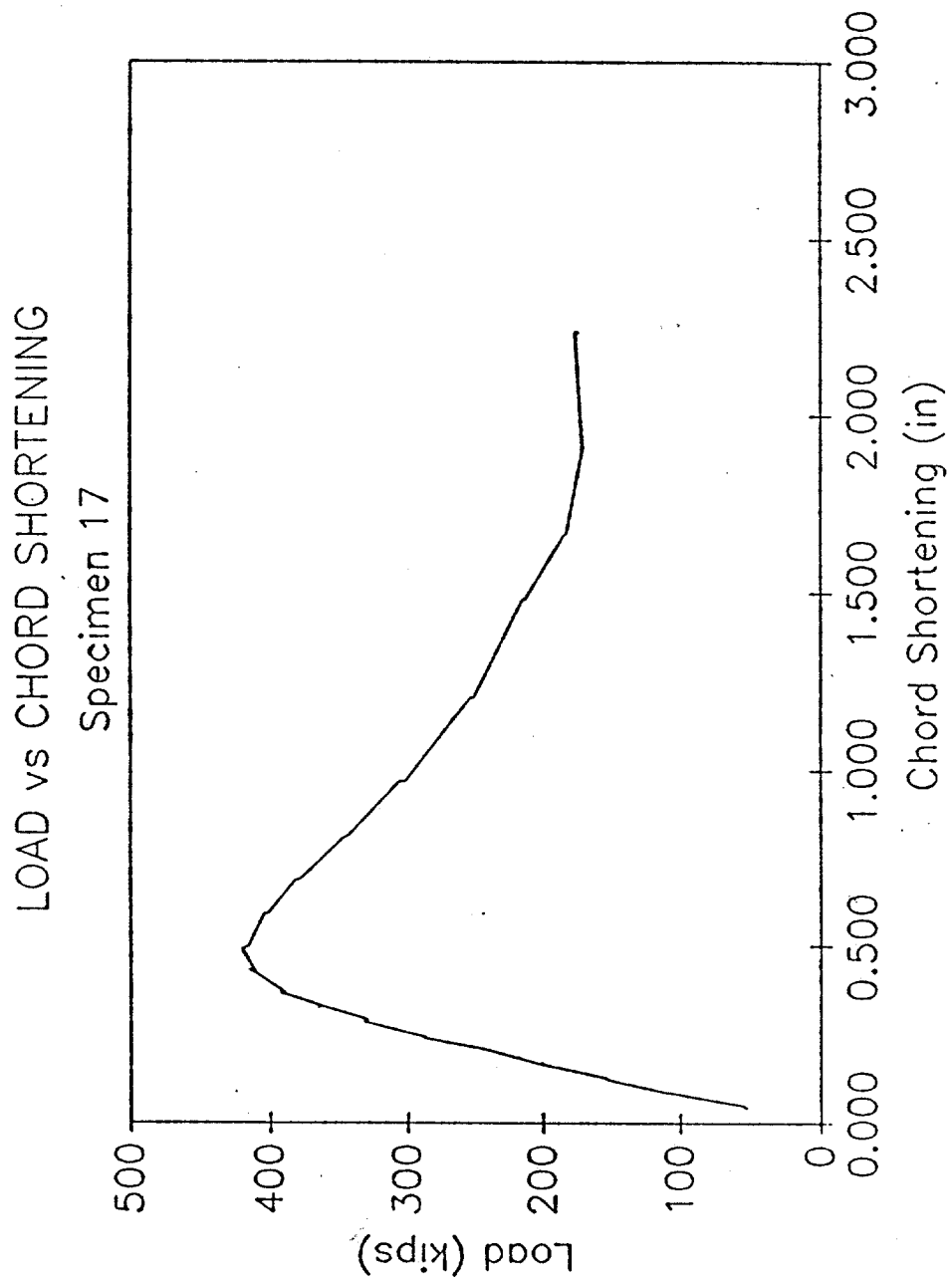


Figure 3-14

HORIZONTAL DISPLACEMENTS

Specimen 17

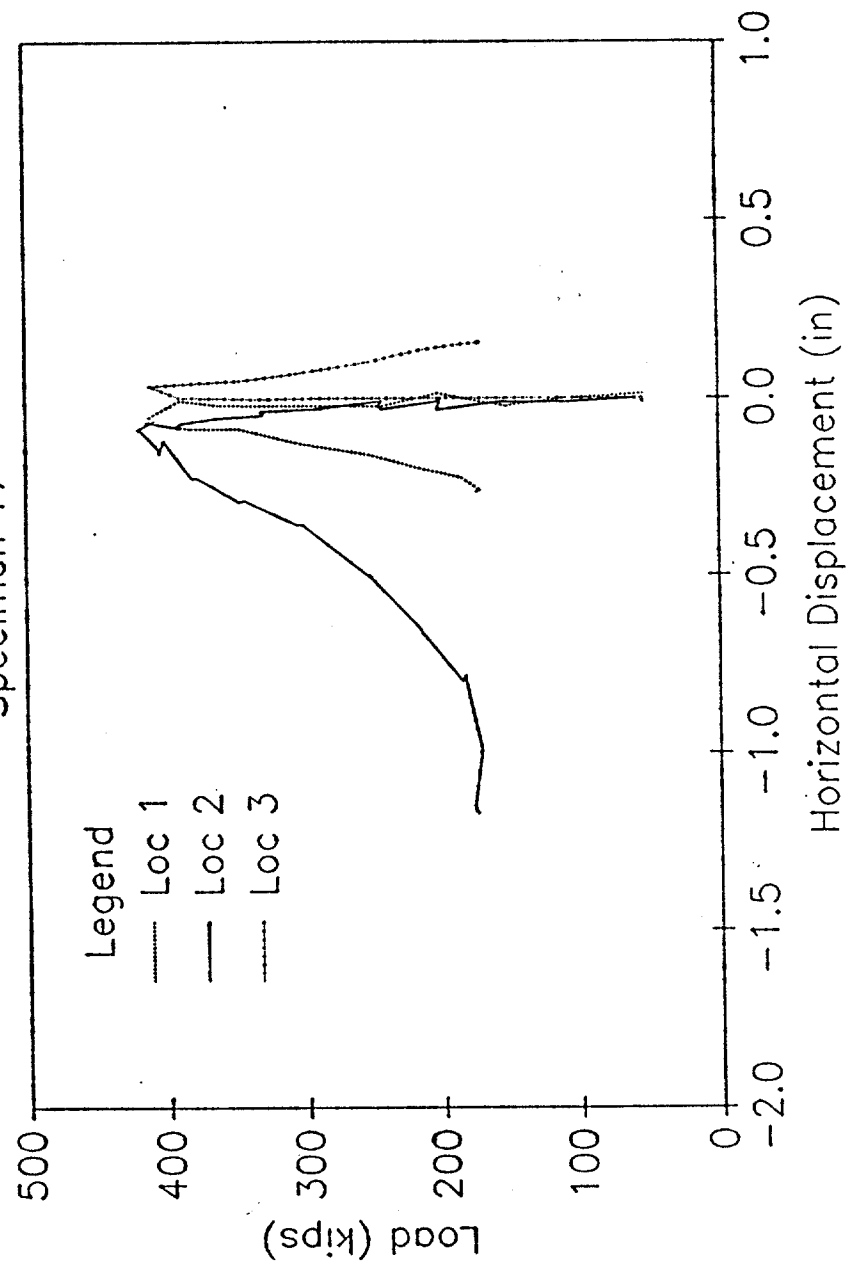


Figure 3-15

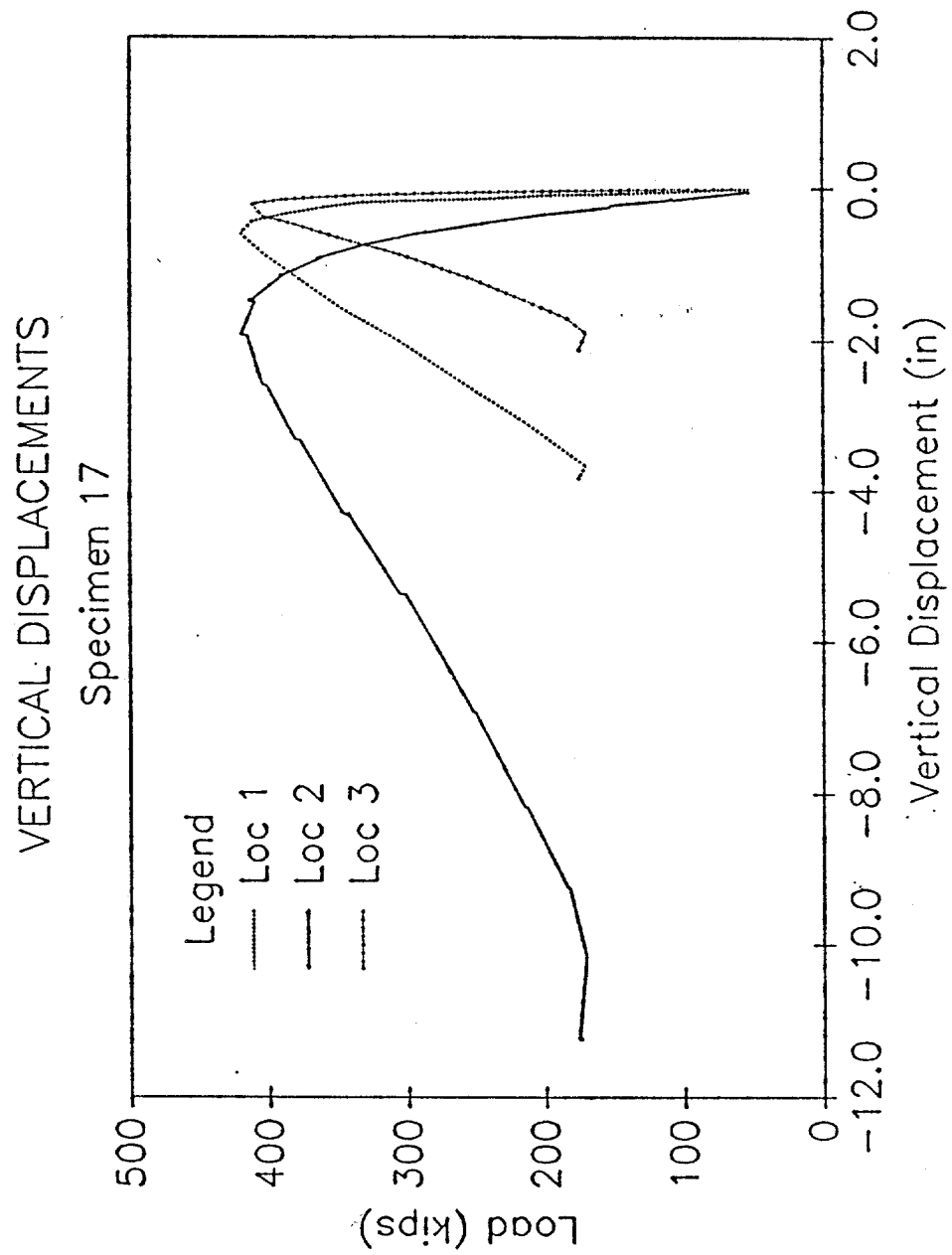


Figure 3-16

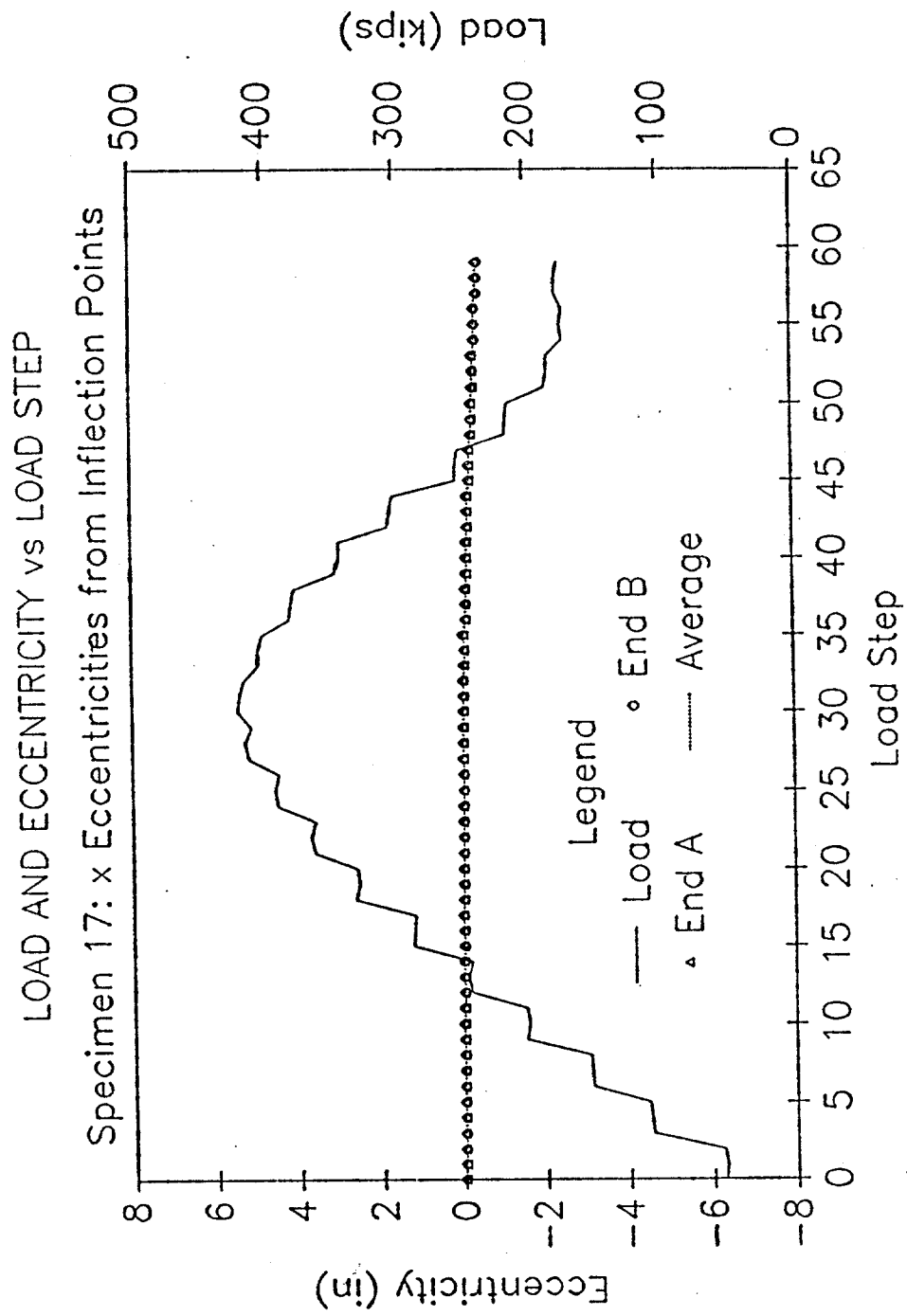


Figure 3-17

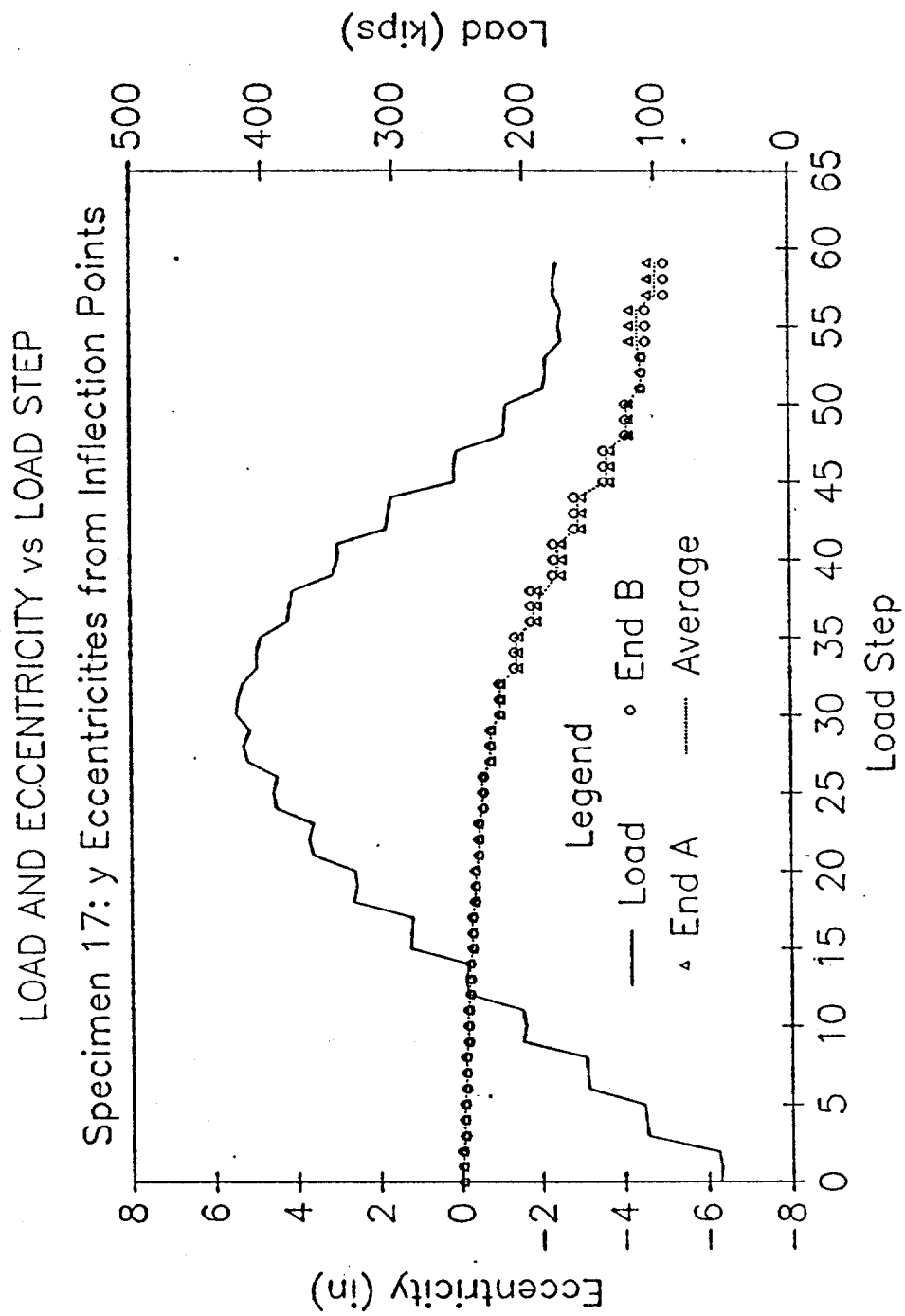


Figure 3-18

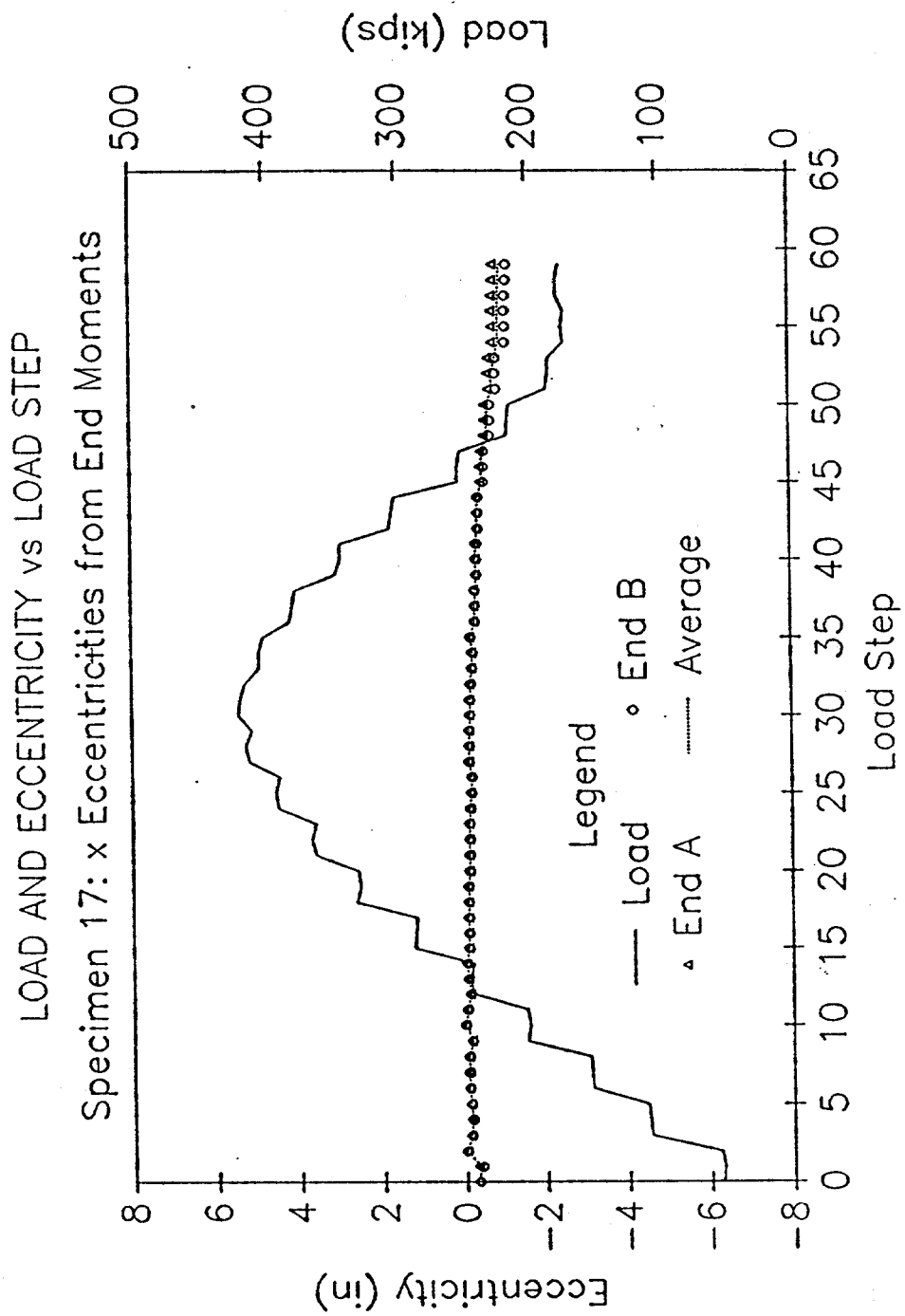


Figure 3-19

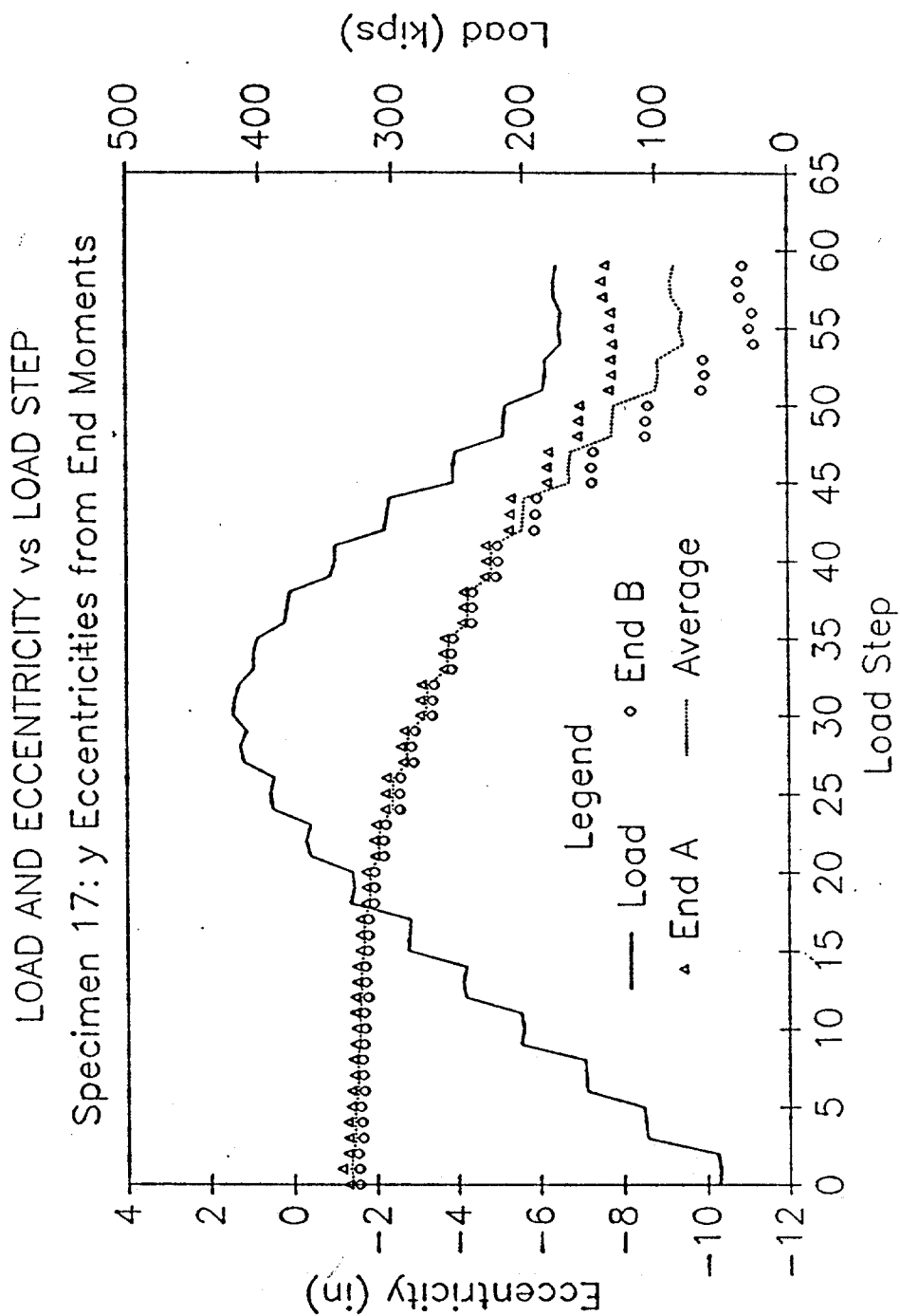


Figure 3-20

SPECIMEN NO 17-FULL SCALE TEST

COMPUTED WALL THICKNESS

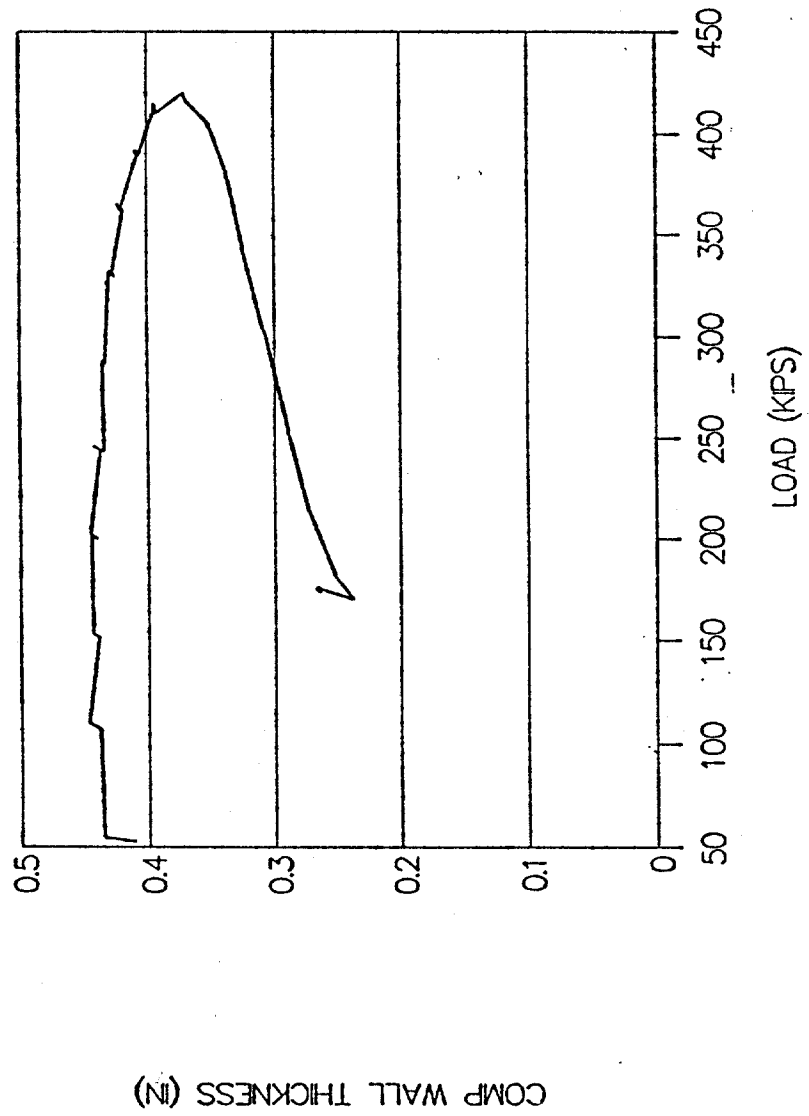


Figure 3-21

SPECIMEN 17: WALL THICKNESS

Nominal Wall Thickness = 0.500 in

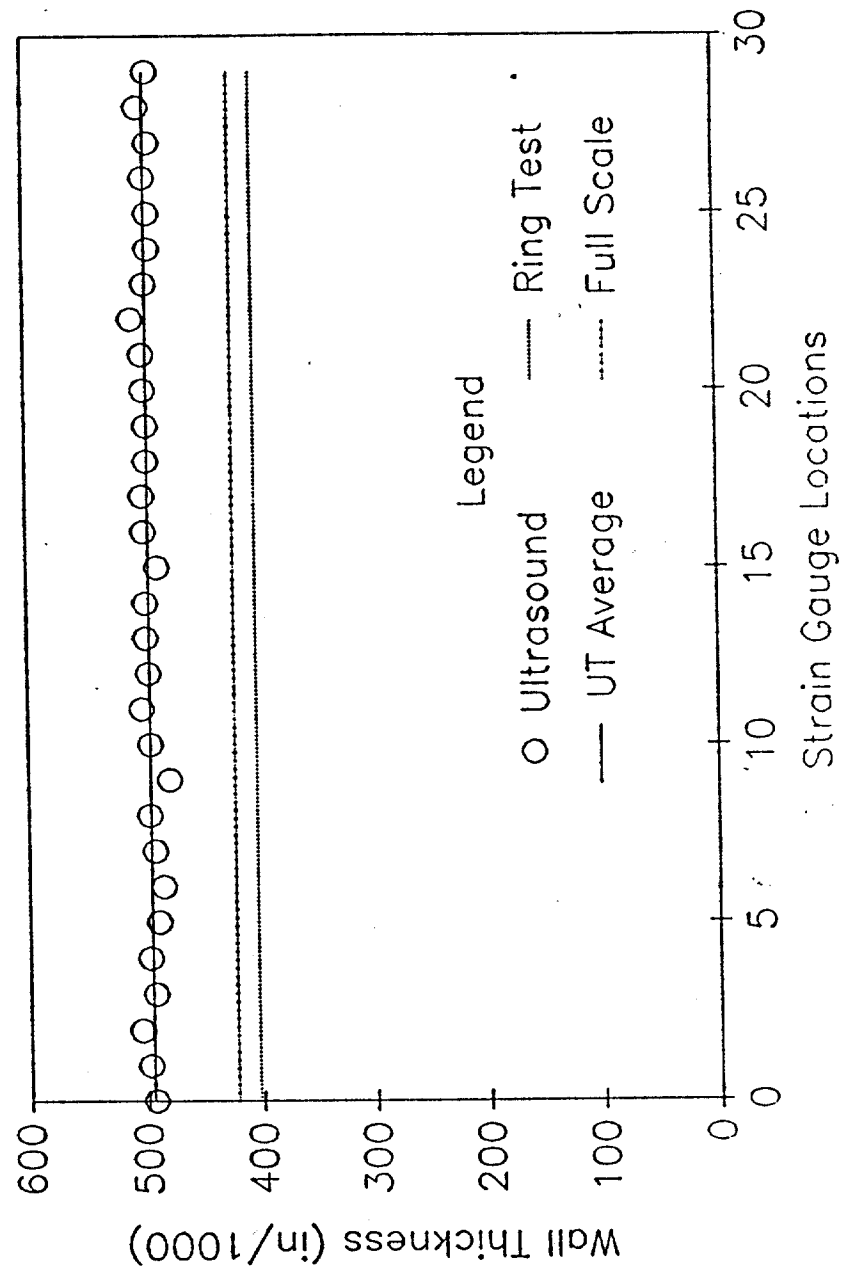


Figure 3-22

TENSILE SPECIMEN 17-2

Stress vs-Strain

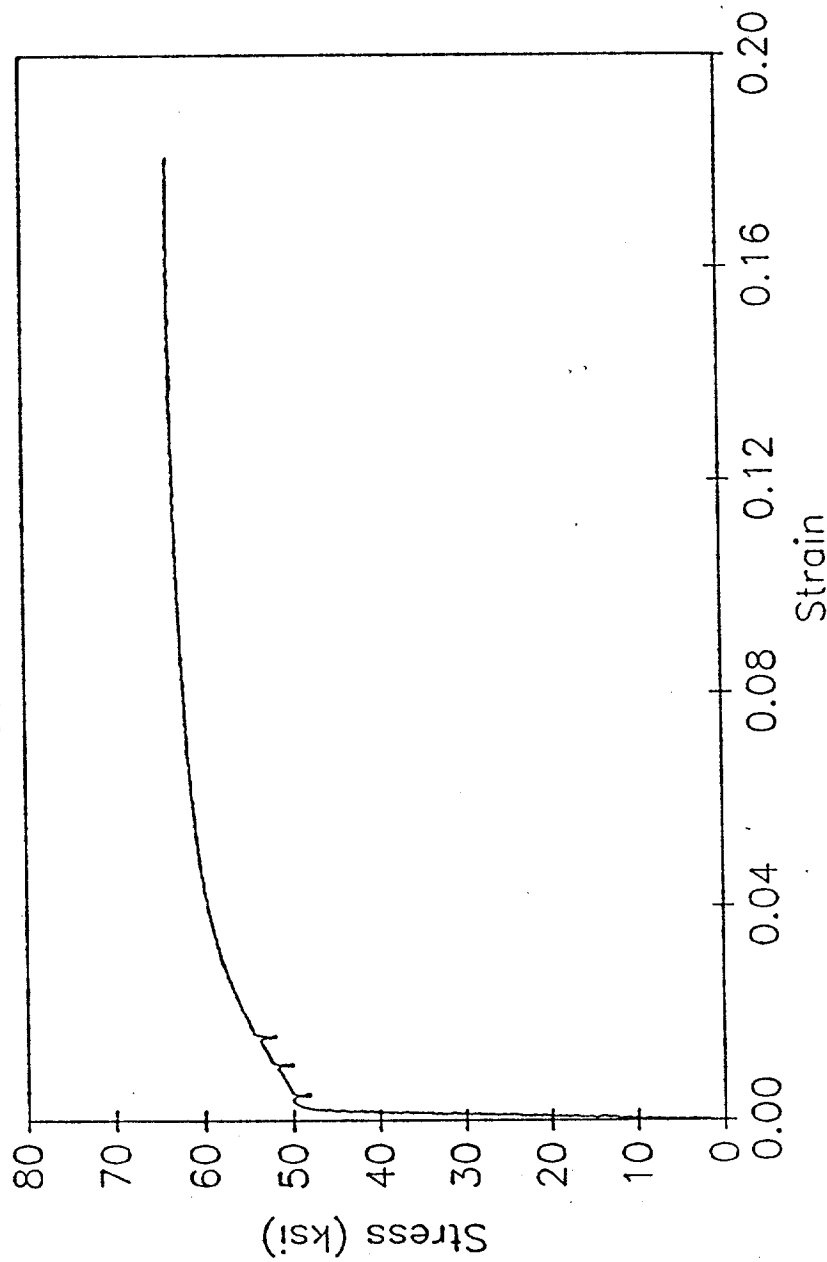


Figure 3-23

TENSILE COUPON TEST
Specimen 17-2

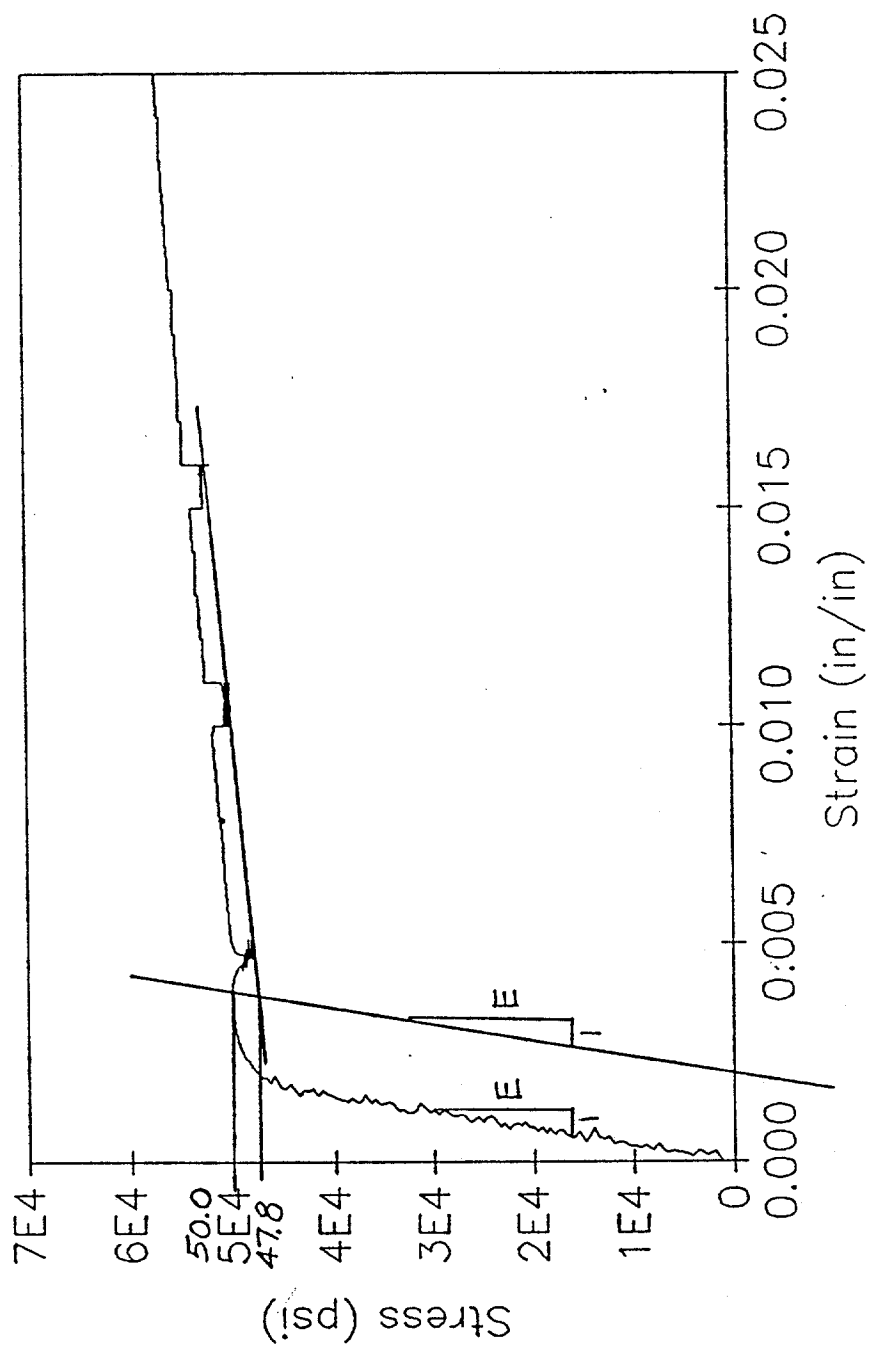
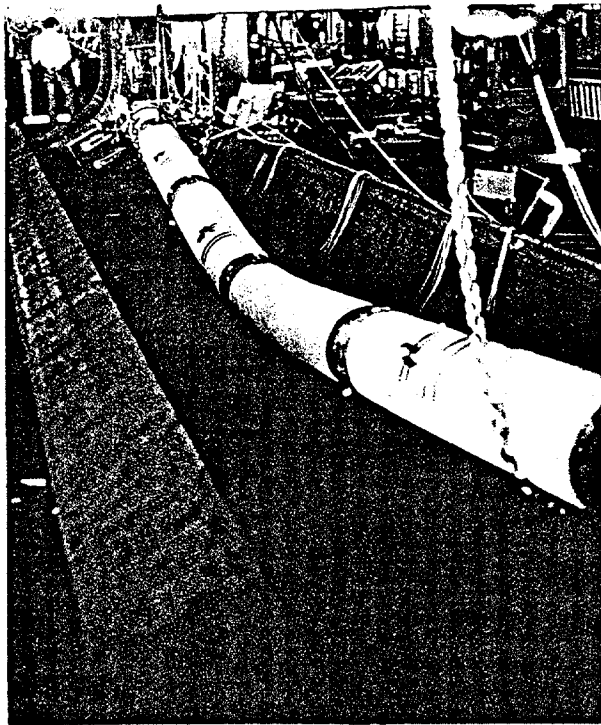
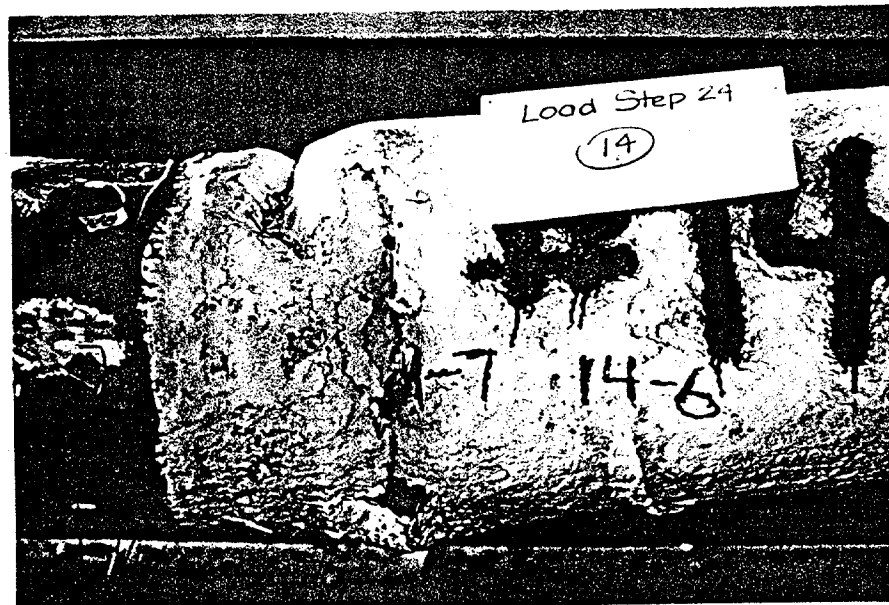


Figure 3-24

EXAMPLES OF OBSERVED FAILURE MODES

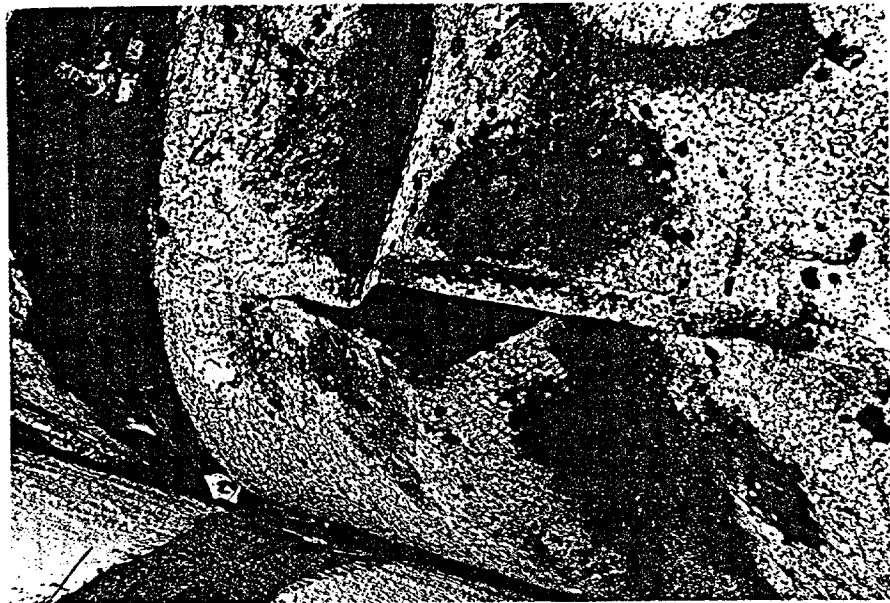


a) Global Buckling



b) Local Failure

EXAMPLES OF OBSERVED FAILURE MODES (cont.)



c) Crack Opening

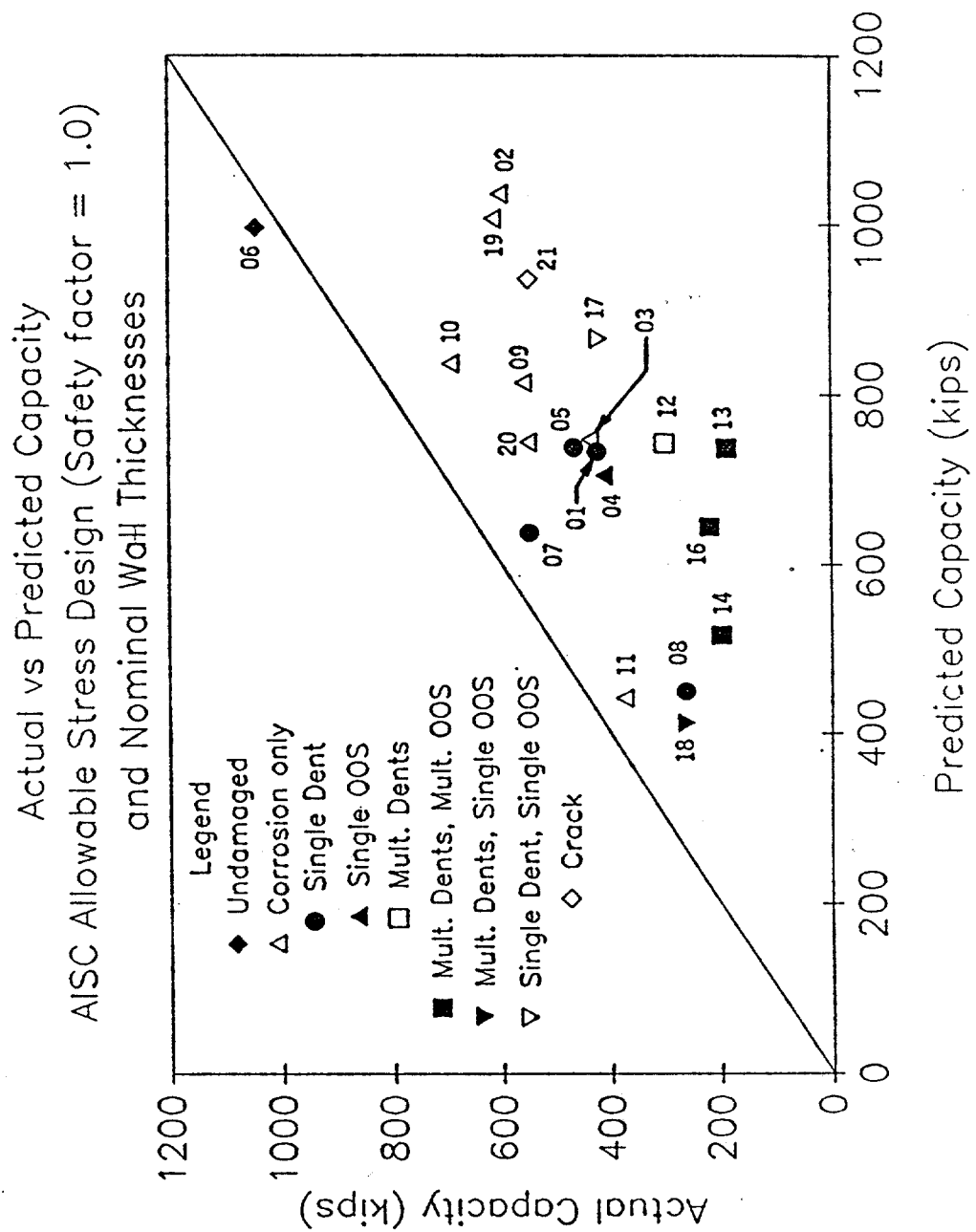


Figure 3-26

Actual vs Predicted Capacity
Cox (1987) – Tubular Member Mean Column Curve
and Nominal Wall Thicknesses

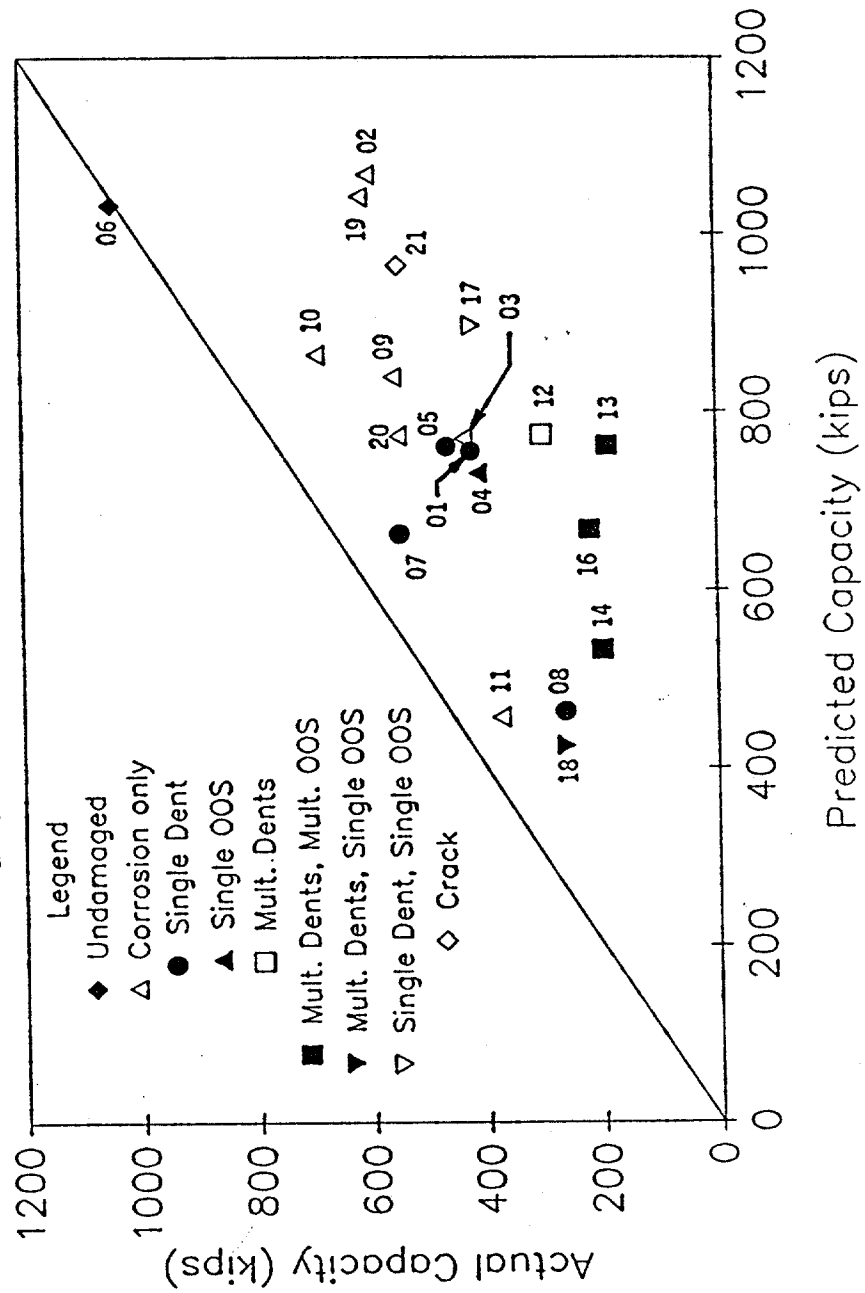


Figure 3-27

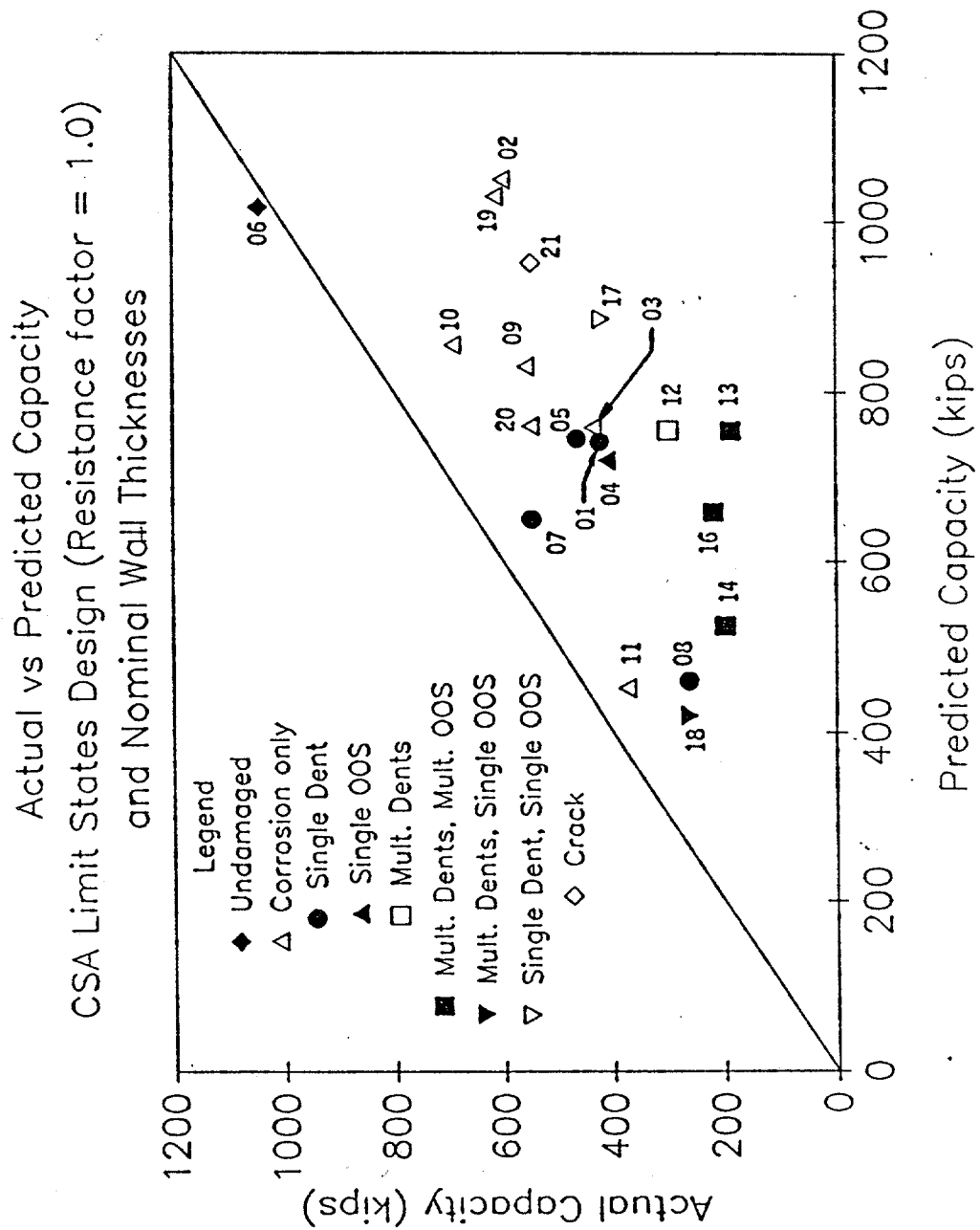


Figure 3-28

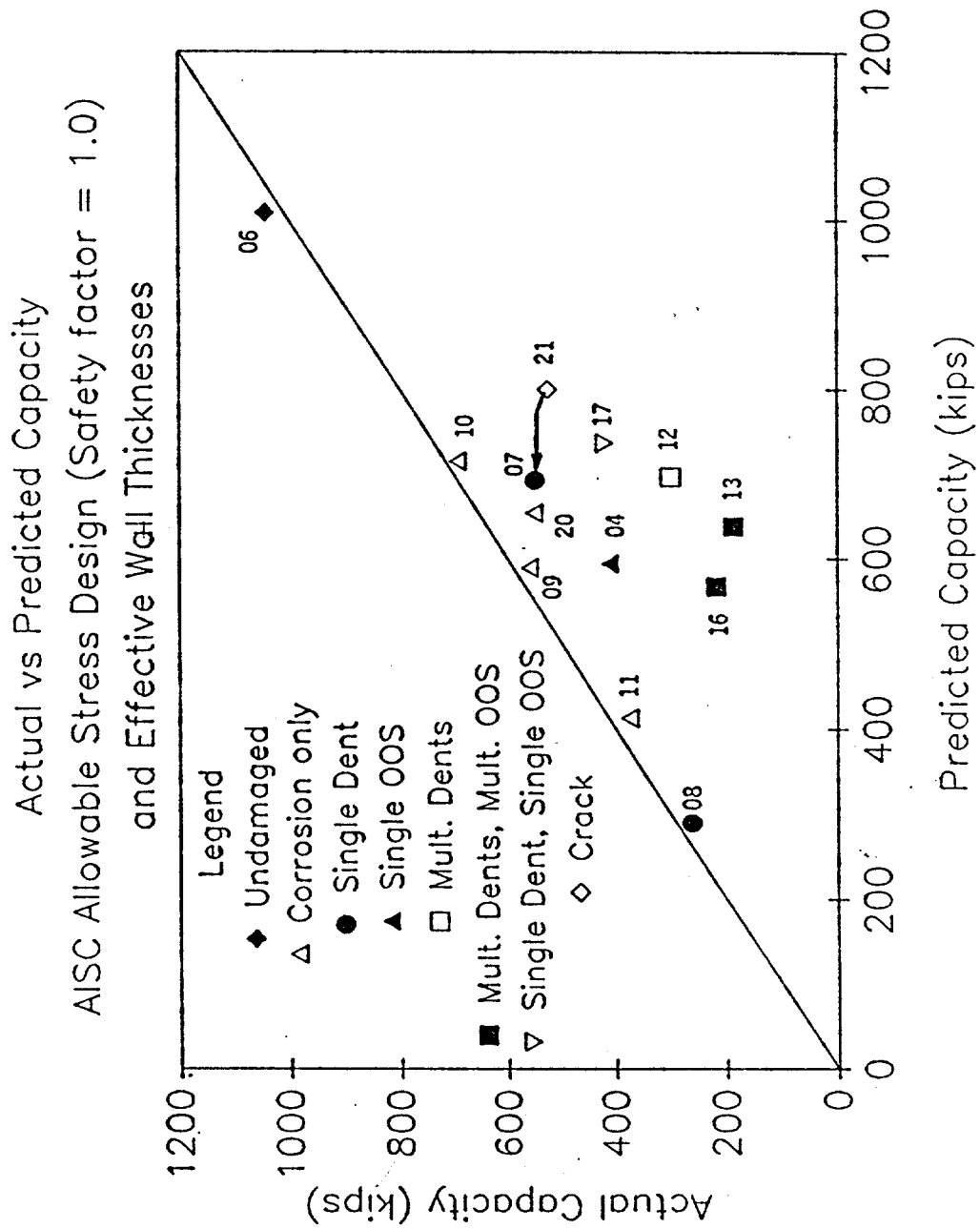


Figure 3-29

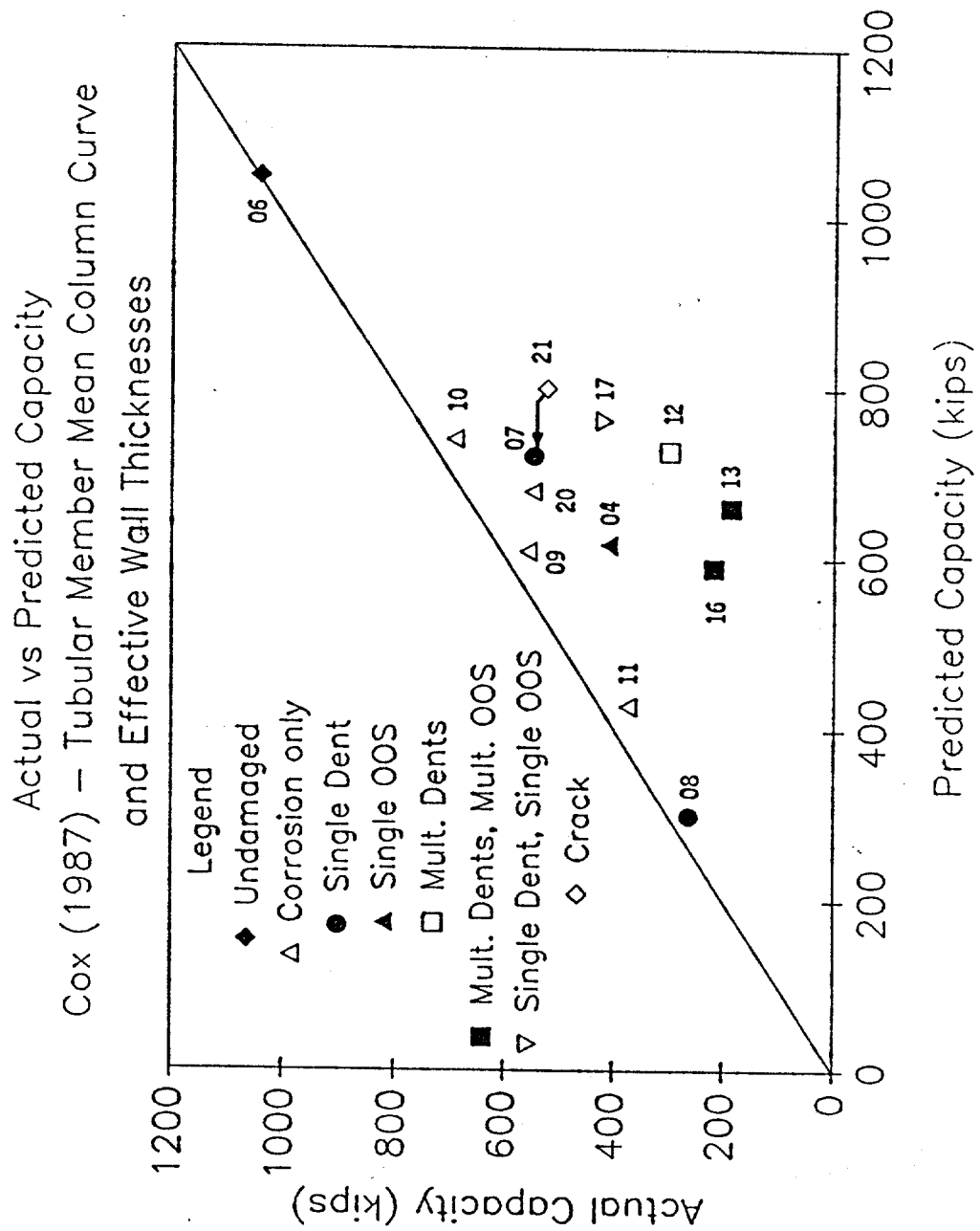


Figure 3-30

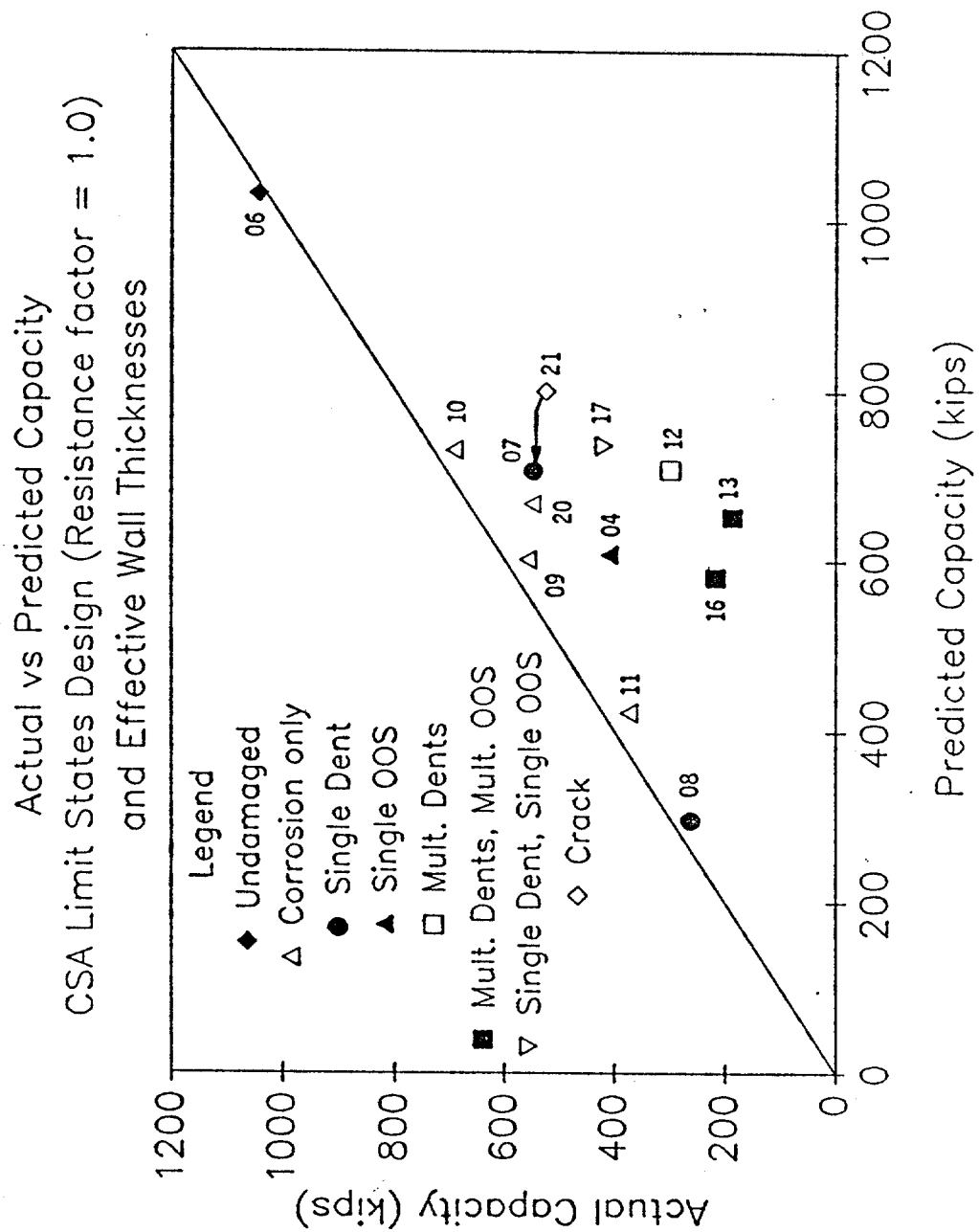


Figure 3-31

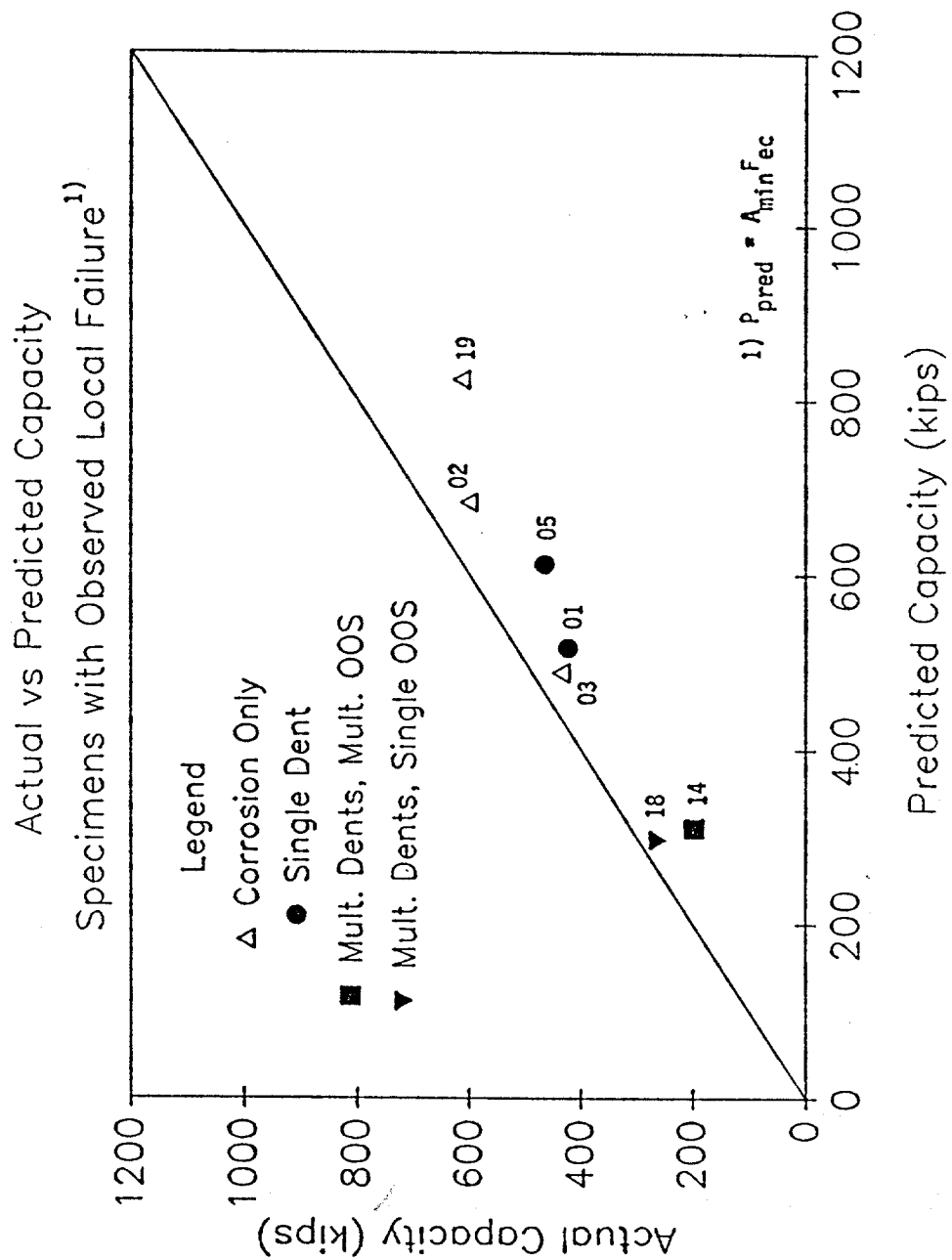


Figure 3-32

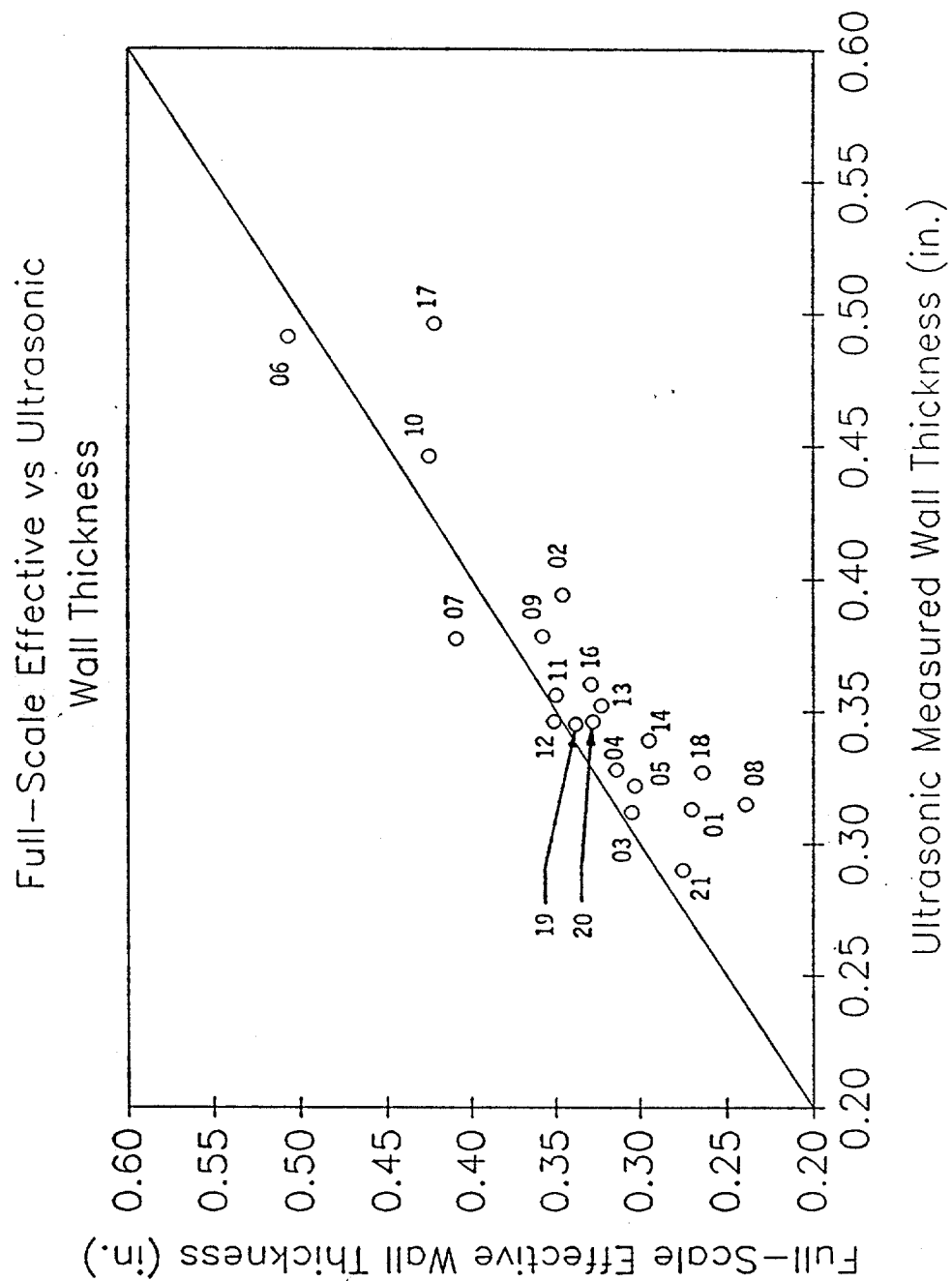


Figure 3-33

SPECIMEN DESCRIPTION

Specimen No	Type of Pipe ¹⁾	Length (ft)	Nominal Diameter (in)	Nominal Wall Thickness (in)	D/t ratio (nominal)	L/r ratio (nominal)
01	F	19.60	18.00	0.375	48.00	37.74
02	F	22.13	18.00	0.438	41.10	42.76
03	F	24.20	18.00	0.375	48.00	46.59
04	S	34.73	12.75	0.375	34.00	95.21
05	F	18.52	18.00	0.375	48.00	35.66
06	S	39.50	20.00	0.500	40.00	68.73
07	S	39.46	12.75	0.375	34.00	108.18
08	S	26.63	10.75	0.375	28.67	87.06
09	S	22.04	14.00	0.500	28.00	55.37
10	S	31.60	14.00	0.500	28.00	79.39
11	S	28.96	10.75	0.375	28.67	94.68
12	S	39.48	12.75	0.375	34.00	108.23

Table 3-1

SPECIMEN DESCRIPTION - (cont.)

Specimen No	Type of pipe ¹⁾	Length (ft)	Nominal Diameter (in)	Nominal Wall Thickness (in)	D/t ratio (nominal)	L/r ratio (nominal)
13	S	24.13	12.75	0.375	34.00	66.15
14	S	16.75	12.75	0.375	34.00	45.92
16	S	28.77	12.75	0.375	34.00	78.87
17	S	31.17	12.75	0.500	25.50	86.29
18	S	17.08	10.75	0.375	28.67	55.84
19	F	37.27	16.00	0.375	42.67	80.94
20	S	34.67	12.75	0.375	34.00	95.05
21	F	22.33	16.00	0.375	42.67	48.49

1) F denotes fabricated pipe and S denotes seamless/continuous seam pipe.

Table 3-1 (cont.)

TYPE OF DAMAGE FOR EACH SPECIMEN

Specimen No	Corrosion	Single Dent	Multiple Dents	Single Out-of-Straightness	Multiple Out-of-Straightness	Cracks	Holes
01	X	X					X ¹⁾
02	X						X ¹⁾
03	X						
04	X			X			
05	X	X				X	X ¹⁾
06							
07	X	X					
08	X	X					
09	X						
10	X						X ¹⁾
11	X						
12	X		X				X

Table 3-2

TYPE OF DAMAGE FOR EACH SPECIMEN (cont.)

Specimen No	Corrosion	Single Dent	Multiple Dents	Single Out-of-Straightness	Multiple Out-of-Straightness	Cracks	Holes
13	X		X		X		X ¹⁾
14	X		X		X		X ¹⁾
16	X		X		X		X ¹⁾
17	X	X		X			
18	X		X	X			
19 ²⁾	X						
20	X						
21	X					X	X

Notes: 1) Specimen had small corrosion or torch holes which did not affect overall specimen behavior.

2) Specimen 19 had a split in a longitudinal weld near one end. This split was not completely through the wall of the specimen.

Table 3-2 (cont.)

MAGNITUDE OF INITIAL DAMAGE

Specimen No	Severity of Corrosion ¹⁾	Extent of Corrosion ²⁾	Maximum Dent Depth ³⁾ (in)	Maximum Initial Out-of-Straightness ⁴⁾ (in)
01	H	O	0.50	0.00
02	M H	O Lo	0.00	0.00
03	M H	O Lo	0.00	0.00
04	L M	O Lo	0.00	1.31
05	H	O	0.50	0.00
06	None	O	0.00	0.00
07	L	O	1.50	0.00
08	M H	O Lo	0.25	0.00
09	L	O	0.00	0.00

Table 3-3

MAGNITUDE OF INITIAL DAMAGE (cont.)

Specimen No	Severity of Corrosion ¹⁾	Extent of Corrosion ²⁾	Maximum Dent Depth ³⁾ (in)	Maximum Initial Out-of-Straightness ⁴⁾ (in)
10	L	O	0.00	0.00
11	L	O	0.00	0.00
12	H	O	3.00	0.00
13	H	O	1.75	8.13
14	H	O	0.50	2.88
16	L	O	0.25	6.63
17	L	O	1.38	4.75
18	M H	O Lo	0.38	0.88
19	M H	O Lo	0.00	0.00

Table 3-3 (cont.)

MAGNITUDE OF INITIAL DAMAGE (cont.)

Specimen No	Severity of Corrosion ¹⁾	Extent of Corrosion ²⁾	Maximum Dent Depth ³⁾ (in)	Maximum Initial Out-of-Straightness ⁴⁾ (in)
20	H	O	0.00	0.00
21	M	O	0.00	0.00

- 1) L - low corrosion, M - medium corrosion, H - high corrosion.
- 2) O - overall corrosion, Lo - local corrosion.
- 3) For specimens with multiple dents, the maximum value of dent depth is given.
- 4) For specimens with initial out-of-straightness in two directions, the maximum out-of-straightness is given.

Table 3-3 (cont.)

SUMMARY OF FULL SCALE TESTS

Specimen No.	Length (ft)	Diameter (in)	P_{max} (kips)	Chord Shortening at P_{max} (in)	Midspan Deflections at P_{max} (in)		L_{eff}/L at Point of Buckling
					Vertical	Horizontal	
01	19.60	18.00	424	0.49	-0.18	0.06	ND ¹⁾
02	22.13	18.00	601	0.60	0.12	0.13	ND ¹⁾
03	24.20	18.00	436	0.36	-0.14	-0.03	ND ¹⁾
04	34.73	12.75	410	0.70	-1.90	-0.29	0.50
05	18.52	18.00	465	0.44	0.16	0.08	ND ¹⁾
06	39.50	20.00	1043	1.09	0.26	0.35	0.86
07	39.46	12.75	548	0.66	1.87	0.41	0.50
08	26.63	10.75	263	0.64	0.43	-0.15	ND ¹⁾
09	22.04	14.00	558	0.59	0.15	0.59	0.54
10	31.60	14.00	692	0.47	0.39	-0.31	0.52
11	28.96	10.75	374	0.40	-0.52	-0.10	0.50

Table 3-4

SUMMARY OF FULL SCALE TESTS (cont.)

Specimen No.	Length (ft)	Diameter (in)	P_{max} (kips)	Chord Shortening at P_{max} (in)	Midspan Deflections at P_{max} (in)		L_{eff}/L at Point of Buckling
					Vertical	Horizontal	
12	39.48	12.75	299	1.03	1.60	2.00	0.50
13	24.13	12.75	187	0.39	-1.31	0.53	0.54
14	16.75	12.75	198	0.13	0.24	0.18	ND ¹⁾
16	28.77	12.75	218	0.59	-1.60	0.06	0.62
17	31.17	12.75	420	0.49	-1.92	-0.09	0.52
18	17.08	10.75	262	0.42	-0.44	-0.27	ND ¹⁾
19	37.27	16.00	614	0.18	-0.25	0.45	ND ¹⁾
20	34.67	12.75	550	0.31	-0.40	-0.24	0.50
21	22.33	16.00	549	0.50	-0.01	0.08	ND ²⁾

1) Not determined since specimen locally yielded prior to buckling.

2) Not determined since specimen did not buckle.

Table 3-4 (cont.)

SUMMARY OF WALL THICKNESS DETERMINATION

Specimen No	Nominal Wall Thickness (in.)	Ring Test Effective Wall Thickness (in.)	UT Average Wall Thickness (in.)	Full Scale Effective Wall Thickness (in.)
01	0.375	NT ¹⁾	0.313 ²⁾	0.270
02	0.438	NT	0.394 ³⁾	0.346
03	0.375	NT	0.312 ⁴⁾	0.305
04	0.375	0.282	0.328	0.314
05	0.375	NT	0.322 ⁵⁾	0.303
06	0.500	0.507	0.491	0.507
07	0.375	0.376	0.377	0.409
08	0.375	NT	0.315 ⁶⁾	0.239
09	0.500	NT	0.378	0.358
10	0.500	0.384	0.446	0.425
11	0.375	NT	0.356	0.350
12	0.375	0.279	0.346	0.351
12 UT and ring retest		0.294	0.300	
13	0.375	NT	0.352	0.323
14	0.375	NT	0.339 ⁷⁾	0.295
16	0.375	NT	0.360	0.329
17	0.500	0.403	0.496	0.422
18	0.375	NT	0.327 ⁸⁾	0.264
19	0.375	0.312	0.345 ⁹⁾	0.338

Table 3-5

SUMMARY OF WALL THICKNESS DETERMINATION (cont.)

Specimen No	Nominal Wall Thickness (in.)	Ring Test Effective Wall Thickness (in.)	UT Average Wall Thickness (in.)	Full Scale Effective Wall Thickness (in.)
20	0.375	0.327	0.346	0.328
21	0.375	NT	0.290	0.275

1) NT - No test conducted.

2) t_{eff} = 0.265 in. in region of local yielding located 3 ft. 6 in. from end B. This effective wall thickness was determined using UT.

3) t_{eff} = 0.284 in. in region of local yielding located 3 ft. 3 in. from end B. This effective wall thickness was determined using UT.

4) t_{eff} = 0.247 in. in region of local yielding located 2 ft. 4 in. from end B. This effective wall thickness was determined using UT.

5) t_{eff} = 0.307 in. in region of local yielding located 4 ft. 10 in. from end B. This effective wall thickness was determined using UT.

6) t_{eff} = 0.262 in. in region of local yielding located 19 ft. 9 in. from end B. This effective wall thickness was determined using UT.

7) t_{eff} = 0.219 in. in region of local yielding located 4 ft. 9 in. from end B. This effective wall thickness was determined using UT.

8) t_{eff} = 0.261 in. in region of local yielding located 2 ft. 11 in. from end B. This effective wall thickness was determined using UT.

9) t_{eff} = 0.279 in. in region of local yielding located 29 ft. 11 in. from end B. This effective wall thickness was determined using UT.

Table 3-5 (cont.)

SUMMARY OF SPECIMEN MATERIAL PROPERTIES

Specimen No	Modulus of Elasticity (ksi)	Yield Strength ¹⁾		Ultimate Strength (ksi)
		Static (ksi)	Dynamic (ksi)	
01	25,800	35.7	38.6	56.5
02	27,400	43.6	47.3	67.2
03	26,200	36.6	40.9	66.7
04	28,000	54.0	57.0	68.5
05	26,300	35.9	38.9	59.5
06	28,300	ND ²⁾	36.5	64.4
07	29,200	ND	50.0	67.1
08	29,400	39.2	44.7	72.9
09	29,600	39.6	43.5	72.8
10	25,900	42.0	45.0	73.4
11	27,300	39.0	41.9	65.8
12	28,600	ND	60.0	78.0
13	30,000	53.7	56.7	70.7
14	29,300	36.0	39.6	74.0
16a ³⁾	29,000	49.1	51.6	77.3
16b	26,100	52.7	55.4	71.2
17	25,000	49.2	51.4	64.0
18	24,900	34.5	38.2	66.8
19	27,700	59.7	62.2	74.2

Table 3-6

SUMMARY OF SPECIMEN MATERIAL PROPERTIES (cont.)

Specimen No	Modulus of Elasticity (ksi)	Yield Strength ¹⁾		Ultimate Strength (ksi)
		Static (ksi)	Dynamic (ksi)	
20	28,000	57.4	60.0	70.9
21	25,900	52.2	55.2	68.3

1) Nominal yield strength is 35 ksi for all specimens.

2) ND - Not determined.

3) Two different material types in Specimen No. 16.

Table 3-6 (cont.)

SPECIMEN GEOMETRIC PROPERTIES

Specimen No	Length (ft)	Diameter (in)	Effective ¹⁾ Wall Thickness (in)	D/t ratio (effective)	L/r ratio (effective)
01	19.60	18.00	0.270	66.67	37.52
02	22.13	18.00	0.346	52.02	42.54
03	24.20	18.00	0.305	59.02	46.41
04	34.73	12.75	0.314	40.61	94.76
05	18.52	18.00	0.303	59.41	35.51
06	39.50	20.00	0.507	39.45	68.75
07	39.46	12.75	0.409	31.17	108.47
08	26.63	10.75	0.239	44.98	85.97
09	22.04	14.00	0.358	39.11	54.82
10	31.60	14.00	0.425	32.94	78.97

Table 3-7

SPECIMEN GEOMETRIC PROPERTIES (cont.)

Specimen No	Length (ft)	Diameter (in)	Effective ¹⁾ Wall Thickness (in)	D/t ratio (effective)	L/r ratio (effective)
11	28.96	10.75	0.350	30.71	94.46
12	39.48	12.75	0.351	36.32	108.03
13	24.13	12.75	0.323	39.47	65.88
14	16.75	12.75	0.295	43.22	45.63
16	28.77	12.75	0.329	38.75	78.59
17	31.17	12.75	0.422	30.21	85.77
18	17.08	10.75	0.264	40.72	55.27
19	37.27	16.00	0.338	47.34	80.75
20	34.67	12.75	0.328	38.87	94.70
21	22.33	16.00	0.275	58.18	48.19

1) Effective wall thickness computed from full scale tests.

Table 3-7 (cont.)

OBSERVED SPECIMEN FAILURE MODES

Specimen No	Location of Failure from End B	Failure Mode
01	3'- 0"	Local Failure
02	3'- 3"	Local Failure ¹⁾
03	2'- 4"	Local Failure
04	15'- 6 1/2"	Global Buckling
05	4'- 10"	Crack Opening ²⁾
06	17'- 6 1/2"	Global Buckling
07	19'- 1 1/2"	Global Buckling ³⁾
08	19'- 9"	Global Buckling
09	12'- 8"	Global Buckling
10	16'- 6"	Global Buckling
11	14'- 5 1/2"	Global Buckling
12	14'- 5 1/2"	Global Buckling ⁴⁾
13	8'- 3"	Global Buckling ⁵⁾
14	4'- 9"	Local Failure ⁶⁾
16	13'- 1"	Global Buckling
17	19'- 1"	Global Buckling ⁷⁾
18	2'- 11"	Local Failure
19	29'- 11"	Local Failure

Table 3-8

OBSERVED SPECIMEN FAILURE MODES (cont.)

Specimen No	Location of Failure from End B	Failure Mode
20	18'- 1"	Global Buckling
21	19'- 8"	Crack Opening ⁸⁾

- 1) Local failure in region of circumferential weld.
- 2) Failure at thru-thickness crack in a longitudinal welded seam 24 inches from end B. Crack began to open but not propagate prior to ultimate load.
- 3) Failure initiated in dented region. A longitudinal split formed near the dented region after ultimate load.
- 4) Failure initiated in region with large dent and hole. Other large holes did not have a significant role in failure.
- 5) Specimen failed at location of deepest dent and maximum initial out-of-straightness.
- 6) Local failure initiated in a region which had experienced a high degree of observable local corrosion.
- 7) Specimen failed at location of dent and maximum initial out-of-straightness.
- 8) Failure occurred due to the opening of a thru-thickness crack at the welded longitudinal seam. Crack propagation was arrested by girth weld near end A.

Table 3-8 (cont.)

SPECIMEN PROPERTIES USED IN ULTIMATE CAPACITY FORMULAE

Specimen No.	Length (in)	Diameter (in)	Nominal Wall Thickness ¹⁾ (in)	Effective Wall Thickness ²⁾ (in)	Yield Strength ³⁾ (ksi)	Effective Length
01	19.60	18.00	0.375	0.270	35.7	0.50 ⁴⁾
02	22.13	18.00	0.438	0.346	43.6	0.50 ⁴⁾
03	24.20	18.00	0.375	0.305	36.6	0.50 ⁴⁾
04	34.73	12.75	0.375	0.314	54.0	0.50
05	18.52	18.00	0.375	0.303	35.9	0.50 ⁴⁾
06	39.50	20.00	0.500	0.507	36.5	0.86
07	39.46	12.75	0.375	0.409	50.0	0.50
08	26.63	10.75	0.375	0.239	39.2	0.50 ⁴⁾
09	22.04	14.00	0.500	0.358	39.6	0.54
10	31.60	14.00	0.500	0.425	42.0	0.52
11	28.96	10.75	0.375	0.350	39.0	0.50
12	39.48	12.75	0.375	0.351	60.0	0.50

Table 3-9

SPECIMEN PROPERTIES USED IN ULTIMATE CAPACITY FORMULAE (cont.)

Specimen No.	Length (in)	Diameter (in)	Nominal Wall Thickness ¹⁾ (in)	Effective Wall Thickness ²⁾ (in)	Yield Strength ³⁾ (ksi)	Effective Length
13	24.13	12.75	0.375	0.323	53.7	0.54
14	16.75	12.75	0.375	0.295	36.0	0.50 ⁴⁾
16	28.77	12.75	0.375	0.329	49.1	0.62
17	31.17	12.75	0.500	0.422	49.2	0.52
18	17.08	10.75	0.375	0.264	34.5	0.50 ⁴⁾
19	37.27	16.00	0.375	0.338	59.7	0.50 ⁴⁾
20	34.67	12.75	0.375	0.328	57.4	0.50
21	22.33	16.00	0.375	0.275	52.2	0.50 ⁵⁾

1) Determined by measurements at the ends of the specimens.

2) Determined from full-scale tests.

3) Static yield strength used for all specimens but 06, 07, and 12.

4) Local yielding occurred prior to buckling.

5) Specimen did not buckle.

Table 3-9 (cont.)

SPECIMEN SLENDERNESS RATIOS AND PARAMETERS

Specimen No	C_c	$(kL/r)_{nom}$	$(kL/r)_{eff}$	λ_{nom}	λ_{eff}
01	127.71	18.87	18.76	0.21	0.21
02	115.57	21.38	21.27	0.26	0.26
03	126.13	23.30	23.21	0.26	0.26
04	103.84	47.61	47.38	0.65	0.65
05	127.36	17.83	17.76	0.20	0.20
06	126.31	59.11	59.13	0.66	0.66
07	107.92	54.09	54.23	0.71	0.71
08	121.88	43.53	42.98	0.51	0.50
09	121.26	29.90	29.60	0.35	0.35
10	117.75	41.28	41.06	0.50	0.49
11	122.19	47.34	47.23	0.55	0.55
12	98.51	54.12	54.01	0.78	0.78
13	104.13	35.72	35.58	0.49	0.48
14	127.18	22.96	22.82	0.26	0.25
16	108.90	48.90	48.72	0.64	0.63
17	108.79	44.87	44.60	0.58	0.58
18	129.92	27.92	27.63	0.30	0.30
19	98.76	40.47	40.37	0.58	0.58
20	100.72	47.52	47.35	0.67	0.66
21	105.62	24.25	24.10	0.32	0.32

Table 3-10

ULTIMATE CAPACITY OF SPECIMENS USING
NOMINAL WALL THICKNESS¹⁾

Specimen No	P _{meas} (kips)	P _{yld} F _y A (kips)	P _{an} AISC ²⁾ (kips)	P _{an} COX ³⁾ (kips)	P _{an} CSA ⁴⁾ (kips)
01	424	741	733	756	741
02	601	1054	1036	1068	1050
03	436	760	747	770	758
04	410	787	705	731	720
05	465	745	738	761	745
06	1043	1118	996	1034	1017
07	548	729	637	663	650
08	263	479	449	464	459
09	558	840	814	840	830
10	692	891	836	865	855
11	374	477	441	457	451
12	299	875	743	774	755
13	187	783	737	762	754
14	198	525	516	532	523
16	218	716	644	668	658
17	420	947	866	898	886
18	262	422	412	425	419

Table 3-11

ULTIMATE CAPACITY OF SPECIMENS USING
NOMINAL WALL THICKNESS¹⁾ (cont.)

Specimen No	P _{meas} (kips)	P _{yld} F _y A (kips)	P _{an} AISC ²⁾ (kips)	P _{an} COX ³⁾ (kips)	P _{an} CSA ⁴⁾ (kips)
19	614	1099	1007	1043	1030
20	550	837	744	773	760
21	549	961	936	965	952

- 1) The nominal specimen wall thickness was used in all calculations for predicted ultimate capacity.
- 2) Ultimate capacity based on the AISC - ASD column equation, 9th Edition, 1989.
- 3) Ultimate capacity based the mean value column strength curve presented by Cox, 1987.
- 4) Ultimate capacity based on CSA Steel Structures for Buildings - Limit States Design column equation as presented in Prion, 1987.

Table 3-11 (cont.)

RATIO OF MEASURED TO PREDICTED ULTIMATE
LOADS USING NOMINAL WALL THICKNESS¹⁾

Specimen No	$P_{\text{meas}}/P_{\text{yld}}$	$P_{\text{meas}}/P_{\text{an}}$ AISC ²⁾	$P_{\text{meas}}/P_{\text{an}}$ COX ³⁾	$P_{\text{meas}}/P_{\text{an}}$ CSA ⁴⁾
01	0.57	0.58	0.56	0.57
02	0.57	0.58	0.56	0.57
03	0.57	0.58	0.57	0.58
04	0.52	0.58	0.56	0.57
05	0.62	0.63	0.61	0.62
06	0.93	1.05	1.01	1.03
07	0.75	0.86	0.83	0.84
08	0.55	0.59	0.57	0.57
09	0.66	0.69	0.66	0.67
10	0.78	0.83	0.80	0.81
11	0.78	0.85	0.82	0.83
12	0.34	0.40	0.39	0.40
13	0.24	0.25	0.25	0.25
14	0.38	0.38	0.37	0.38
16	0.30	0.34	0.33	0.33
17	0.44	0.49	0.47	0.47
18	0.62	0.64	0.62	0.63

Table 3-12

RATIO OF MEASURED TO PREDICTED ULTIMATE
LOADS USING NOMINAL WALL THICKNESS¹⁾ (cont.)

Specimen No	$P_{\text{meas}}/P_{\text{yld}}$	$P_{\text{meas}}/P_{\text{an}}$ AISC ²⁾	$P_{\text{meas}}/P_{\text{an}}$ COX ³⁾	$P_{\text{meas}}/P_{\text{an}}$ CSA ⁴⁾
19	0.56	0.61	0.59	0.60
20	0.66	0.74	0.71	0.72
21	0.57	0.59	0.57	0.58

- 1) The nominal specimen wall thickness was used in all calculations for predicted ultimate capacity.
- 2) Ultimate capacity based on the AISC - ASD column equation, 9th Edition, 1989.
- 3) Ultimate capacity based the mean value column strength curve presented by Cox, 1987.
- 4) Ultimate capacity based on CSA Steel Structures for Buildings - Limit States Design column equation as presented in Prion, 1987.

Table 3-12 (cont.)

ULTIMATE CAPACITY OF SPECIMENS USING
EFFECTIVE WALL THICKNESS¹⁾

Specimen No	P _{meas} (kips)	P _{yld} F _y A (kips)	P _{an} AISC ²⁾ (kips)	P _{an} COX ³⁾ (kips)	P _{an} CSA ⁴⁾ (kips)
01	424	537	531	547	537
02	601	837	823	848	834
03	436	621	610	629	619
04	410	662	594	616	607
05	465	605	599	617	605
06	1043	1133	1009	1048	1031
07	548	793	693	721	707
08	263	309	290	300	297
09	558	608	589	608	601
10	692	761	715	740	731
11	374	446	413	427	422
12	299	820	697	727	709
13	187	677	638	660	652
14	198	416	409	422	414
16	218	630	567	589	580
17	420	804	737	763	754
18	262	300	293	303	298

Table 3-13

ULTIMATE CAPACITY OF SPECIMENS USING
EFFECTIVE WALL THICKNESS¹⁾ (cont.)

Specimen No	P _{meas} (kips)	P _{yld} F _y A (kips)	P _{an} AISC ²⁾ (kips)	P _{an} COX ³⁾ (kips)	P _{an} CSA ⁴⁾ (kips)
19	614	993	910	943	931
20	550	735	654	679	668
21	549	709	691	713	703

Notes: 1) The effective specimen wall thickness as determined from the full-scale test data was used in all calculations for predicted ultimate capacity.

2) Ultimate capacity based on the AISC - ASD column equation, 9th Edition, 1989.

3) Ultimate capacity based the mean value column strength curve presented by Cox, 1987.

4) Ultimate capacity based on CSA Steel Structures for Buildings - Limit States Design column equation as presented in Prion, 1987.

Table 3-13 (cont.)

RATIO OF MEASURED TO PREDICTED ULTIMATE LOADS
USING EFFECTIVE WALL THICKNESS¹⁾

Specimen No	$P_{\text{meas}}/P_{\text{yld}}$	$P_{\text{meas}}/P_{\text{an}}$ AISC ²⁾	$P_{\text{meas}}/P_{\text{an}}$ COX ³⁾	$P_{\text{meas}}/P_{\text{an}}$ CSA ⁴⁾
01	0.79	0.80	0.78	0.79
02	0.72	0.73	0.71	0.72
03	0.70	0.71	0.69	0.70
04	0.62	0.69	0.67	0.68
05	0.77	0.78	0.75	0.77
06	0.92	1.03	1.00	1.01
07	0.69	0.79	0.76	0.78
08	0.85	0.91	0.88	0.89
09	0.92	0.95	0.92	0.93
10	0.91	0.97	0.94	0.95
11	0.84	0.91	0.88	0.89
12	0.36	0.43	0.41	0.42
13	0.28	0.29	0.28	0.29
14	0.48	0.48	0.47	0.48
16	0.35	0.38	0.37	0.38
17	0.52	0.57	0.55	0.56
18	0.87	0.89	0.86	0.88

Table 3-14

RATIO OF MEASURED TO PREDICTED ULTIMATE LOADS
USING EFFECTIVE WALL THICKNESS¹⁾ (cont.)

Specimen No	P_{meas}/P_{yld}	P_{meas}/P_{an} AISC ²⁾	P_{meas}/P_{an} COX ³⁾	P_{meas}/P_{an} CSA ⁴⁾
19	0.62	0.67	0.65	0.66
20	0.75	0.84	0.81	0.82
21	0.77	0.79	0.77	0.78

- Notes: 1) The effective specimen wall thickness as determined from the full-scale test data was used in all calculations for predicted ultimate capacity.
- 2) Ultimate capacity based on the AISC - ASD column equation, 9th Edition, 1989.
- 3) Ultimate capacity based the mean value column strength curve presented by Cox, 1987.
- 4) Ultimate capacity based on CSA Steel Structures for Buildings - Limit States Design column equation as presented in Prion, 1987.

Table 3-14 (cont.)

ULTIMATE CAPACITY OF SPECIMENS EXPERIENCING LOCAL FAILURE

Specimen No	Diameter (in)	Minimum Wall Thickness ¹⁾ (in)	D/t ratio	F _Y ²⁾ (ksi)	F _{XC} ³⁾ (ksi)	P _{Yld} ⁴⁾ (kips)	P _{meas} (kips)	P _{meas} /P _{Yld}
01	18.00	0.265	67.92	35.7	35.0	516	424	0.82
02	18.00	0.284	63.38	43.6	43.2	683	601	0.88
03	18.00	0.247	72.87	36.6	35.4	488	436	0.89
05	18.00	0.307	58.63	35.9	35.9	612	465	0.76
14	12.75	0.219	58.22	36.0	36.0	310	198	0.64
18	10.75	0.261	41.19	34.5	34.5	297	262	0.88
19	16.00	0.279	50.18	59.7	59.7	823	614	0.75

1) Determined from ultrasonic wall thickness measurements in region of local failure.

2) Static yield stress determined from tensile coupon tests.

3) Reduced yield stress in accordance with API RP 2A for specimens with D/t greater than 60.

4) $P_{Yld} = F_{XC} * \text{cross-sectional area}$.

RADIUS OF KERN CIRCLE AND ECCENTRICITIES

Specimen No	Outside Diameter (in.)	Effective Wall Thickness ¹⁾ (in.)	Radius of Kern circle ²⁾ (in.)	e _{ip} ³⁾ (in.)	e _{em} ⁴⁾ (in.)
01	18.00	0.270	4.37	0.17	1.16
02	18.00	0.346	4.33	0.32	0.62
03	18.00	0.305	4.35	2.14	0.54
04	12.75	0.314	3.03	1.02	2.18
05	18.00	0.303	4.35	1.57	1.32
06	20.00	0.507	4.75	0.10	2.13
07	12.75	0.409	2.99	1.28	1.39
08	10.75	0.239	2.57	3.75	1.03
09	14.00	0.358	3.33	0.46	0.46
10	14.00	0.425	3.29	0.22	0.53
11	10.75	0.350	2.52	0.28	0.51
12	12.75	0.351	3.02	2.38	1.61
13	12.75	0.323	3.03	0.90	2.68
14	12.75	0.295	3.04	0.28	1.21
16	12.75	0.329	3.03	0.68	4.00
17	12.75	0.422	2.98	1.00	3.51
18	10.75	0.264	2.56	1.78	1.18

Table 3-16

RADIUS OF KERN CIRCLE AND ECCENTRICITIES (cont.)

Specimen No	Outside Diameter (in.)	Effective Wall Thickness ¹⁾ (in.)	Radius of Kern Circle ²⁾ (in.)	e _{ip} ³⁾ (in.)	e _{em} ⁴⁾ (in.)
19	16.00	0.338	3.83	0.17	0.64
20	12.75	0.328	3.03	0.35	1.28
21	16.00	0.275	3.86	0.72	0.75

1) Based on reduced data of full scale compression tests.

2) Radius of kern circle = e

$$e = (OD^2 - 2*OD*t + 2*t^2) / (4*OD)$$

where: OD = outside diameter
t = wall thickness

3) Largest resultant eccentricity, computed from inflection points, that occurred prior to the maximum load.

4) Largest resultant eccentricity, computed from end moments, that occurred prior to the maximum load.

Table 3-16 (cont.)

EVALUATION OF ULTRASONIC DATA

Specimen No	Average ¹⁾ (in)	Standard Deviation (in)	Coefficient of Variation, (%)
01	0.313	0.0469	15.0
02	0.394	0.0306	7.8
03	0.312	0.0213	6.8
04	0.328	0.0233	7.1
05	0.322	0.0226	7.0
06	0.491	0.0168	3.4
07	0.377	0.0146	3.9
08	0.315	0.0643	20.4
09	0.378	0.0748	19.8
10	0.446	0.0171	3.8
11	0.356	0.0106	3.0
12	0.346	0.0461	13.3
13	0.352	0.0210	6.0
14	0.339	0.0646	19.1
16	0.360	0.0758	21.1
17	0.496	0.0056	1.1
18	0.327	0.0439	13.4
19	0.345	0.0407	11.8
20	0.346	0.0152	4.4
21	0.290	0.0255	8.8

Note: 1) Average of 30 ultrasonic wall thickness measurements.

Table 3-17

COMPARISON OF WALL THICKNESS MEASUREMENTS

Specimen No	Ultrasonic Wall Thickness (in)	Full Scale Wall Thickness (in)	Full Scale <u>Ultrasonic</u>
01	0.313	0.270	0.86
02	0.394	0.346	0.88
03	0.312	0.305	0.98
04	0.328	0.314	0.96
05	0.322	0.303	0.94
06	0.491	0.507	1.03
07	0.377	0.409	1.08
08	0.315	0.239	0.76
09	0.378	0.358	0.95
10	0.446	0.425	0.95
11	0.356	0.350	0.98
12	0.346	0.351	1.01
13	0.352	0.323	0.92
14	0.339	0.295	0.87
16	0.360	0.329	0.91
17	0.496	0.422	0.85
18	0.327	0.264	0.81
19	0.345	0.338	0.98
20	0.346	0.328	0.95
21	0.290	0.275	0.95

Table 3-18

4.0 ANALYSIS

The goal of this phase of the study was to develop a method of analyzing damaged braces and to determine what differences exist between the predictions of damaged member capacity and the test results. The twenty members were analytically modelled and studied using finite element analysis methods. The modelling techniques were based on phenomenological models found in the literature.

4.1 Procedure

After a review of relevant literature, two basic methods were deemed suitable for estimating member axial load behavior for this project. The first was a simplified method to give a quick estimate of the peak axial capacity of a damaged member. It took the form of a PC Fortran 77 program called DAMAGE (documented in Section 4.2). The second, a beam-column finite element analysis, involved a complete computer model of the member (including damage and end conditions) to predict the complete cycle of behavior from the beginning of loading up to and beyond the point of buckling.

Two major problems were evident in the use of the beam-column finite element method. The first was determining the modelling characteristics of the damaged sections. The second was defining the end conditions to adequately mimic the actual testing facilities. The former was solved by investigating relevant literature and formulating a method (which became the PC Fortran 77 program, EQUIV) to determine the reduction in capacity of a cross section which has been damaged by a dent or a hole. It is documented in the following section on software. The latter was solved by a modelling scheme which seeks to apply the load to the specimen in much the same way as in the actual test and is described below.

During the early stages of the project, the specimens were modelled with either fixed or pinned ends. It soon became apparent that this method did not adequately model the end conditions which existed during the physical tests. As the members buckled in the testing apparatus their ends tended to lift off

the headstock and tailstock creating an eccentric end load. Also, the simplified end conditions used in the models did not allow any adjustment to be made for an effective length factor.

These problems led to the development of the "spoke" model (Figure 4-1). Imagine the specimen as the axle of a wagon. At each end, eight members (modelled as practically rigid) radiate from the "axle" much like the spokes of a wagon wheel. Each spoke is the length of the member's radius so together they recreate the ends of the member in size and shape. The outer ends of the spokes (those not connected to the member) are connected to springs which are modelled to carry load only in compression. Initially they are all in compression, but as the member buckles and the ends rotate some of the springs go into tension and the load shifts to those springs still in compression. With this model the "lift off" seen in the tests can be recreated and with it, the eccentric load.

The compressive stiffness of the springs was set at 5000 kips/in. for all the specimens analyzed. This was chosen so the possibility of the springs yielding would be remote. Tests were performed with other spring stiffnesses (both greater and less than 5000 kips/in.) and Figure 4-2 shows the results. The analyses were, for all practical purposes, identical for the three different stiffnesses used and the original 5000 kips/in. stiffness was used throughout the study.

Accurate modelling of the load eccentricity wasn't the only reason for adopting this "spoke-ended" scheme. Because the end conditions are explicitly modelled in this manner, the k-factor need not be input directly for each member. The end stiffness is accounted for automatically as the eccentric load and the member rotation interact during the analysis.

The model for each specimen was made up of a series of beam-column elements representing the damaged (containing dents or holes) and undamaged (no dents or holes) sections of the member. An example of which can be seen in Figure 4-3. The following is a description of the modelling routine:

1. The member description was taken from Texas A&M. Meaningful factors were member length, OD, thickness, yield stress and Young's modulus. (The effective wall thickness calculated from the full scale test was used in the models and in the data reduction. It was felt that this was a better measure of the specimen's actual thickness than the average value of a series of ultrasound measurements taken on each specimen. When compared, the two measures are actually quite close (on average only a 7% difference) as shown in Figure 4-4). Damage, in the form of dents, holes or out-of-straightness, was taken from the Texas A&M report.
2. If dents or holes were present, separate elements were designed for each damage state using EQUIV. The length used for each was either that measured by Texas A&M or that calculated by the EQUIV program whichever was longer. These damaged elements were placed in the position described in the damage report and the undamaged portions around them (with characteristics defined by EQUIV) were split up into elements as was convenient. If there were no dents or holes present, the member was divided into ten elements of equal length, each with the same characteristics as determined by the EQUIV program.
3. The characteristics of the damaged and undamaged elements were then put into the model. The end spokes and their springs were added. If out-of-straightness was present, it was explicitly modelled by positioning the nodes in their deformed position.
4. With the model then complete, the analysis consisted of a series of load steps applied axially to one end of the member. The load was applied until an axial deformation of about four inches was reached. For members with dents, holes or out-of-straightness, two models were analyzed, one containing all of the damage and one containing only corrosion damage (the effects of which were accounted for by using the effective wall thickness), if any, for comparison.

All of the specimens were analyzed using this same basic scheme with the following exceptions:

1. Specimens with no damage (i.e. no dents, holes or out-of-straightness) had small amounts (about 0.4" maximum at the center of the beam) of symmetric out-of-straightness introduced to the model to induce buckling. Mathematically, no buckling will occur to a member which is perfectly straight and has a perfectly axial load.
2. Specimens with only one damaged section near the end of the member were rotated axially so that the eccentricity of the damage was oriented along either the y- or z-axis. The members were allowed to displace laterally only in that direction. This produced a more stable solution.
3. Specimen 16 was comprised of two sections with different wall thicknesses connected by a 24 inch sleeve. Instead of using the effective wall thickness as determined by Texas A&M the nominal wall thickness for each section was used to differentiate between them. However, in the calculation of D/t and other factors for the data reduction the effective wall thickness was used for specimen 16 as it was for the other specimens.
4. It should be noted that specimens 19 and 21 had a longitudinal cracks which were not considered in the analysis. There was no methodology developed to account for damage of this type. The failure of specimen 19 was independent of the crack (it experienced local yielding in an uncracked section) while specimen 21 failed as the cracked expanded during the test.

4.2 Software Documentation

Two PC Fortran 77 programs were written in support of this project. The first, DAMAGE, was a formulation of research on the effect of a damaged cross section on the peak axial capacity of a tubular member. It was used as the simplified method of analysis mentioned earlier. The second, EQUIV, computes the capacity characteristics of a section (with or without damage) for use in the beam-column finite element analysis. Both are documented in this section.

DAMAGE Program

The DAMAGE program is an interactive PC Fortran 77 computer program written by PMB Engineering, Inc. The program is based on work by C.P. Ellinas (3) and was developed for use in assessing the reduction in capacity of damaged braces being tested as part this study. Reference (3) addresses dents and out-of-straightness and also provides a method for considering these damage types in a combined damage state. The equations have been extended by PMB for predicting the reduced capacity of braces with holes or holes in combination with out-of-straightness. The original formulation has no explicit reference to a k-factor. The current version of DAMAGE has been modified to allow the user to input k.

The equations presented in Reference (3) were developed assuming:

1. Stresses resulting from a small axial load are resisted in the dented zone mainly as bending stress which leads to the rapid formation of a plastic hinge.
2. Once the dent zone plastification stress level is reached, the damaged part of the tubular cross-section carries no additional load.
3. The bending stiffness of the tubular is mainly controlled by the undamaged cross-sectional area.
4. The properties at the damaged cross-section are assumed for the member along its entire length.

Reference (3) addresses three types of brace damage: out-of-straightness, dents, and a combination of a dent and out-of-straightness. For members with no specified out-of-straightness, an imperfection parameter α is defined which includes a tolerance limit lateral displacement. Another equation for α is proposed when the bending deformation exceeds the tolerance limit displacement of 1.5 percent of the member length. Thus some imperfection is

always included accounting for construction tolerances, residual stresses, etc. If the bending damage exceeds the default tolerance limit, the tolerance limit is ignored in favor of the larger deformation.

For braces having dents, the method assumes the member carries the entire axial load as uniform stress until the stress level reaches the plastification stress. At this load level further load is assumed to be resisted by uniform compression and bending stress over the undamaged area of the damaged cross-section. The line of action of the additional axial load is assumed to act through the neutral axis of the undamaged portion of the cross-section. The axial load times its eccentricity ($e = \text{lateral displacement} + \text{damaged brace eccentricity}$) is resisted by the damaged cross-section moment capacity.

The DAMAGE program equation for the imperfection parameter α does not differentiate in the calculation of α based on a tolerance limit value of the lateral displacement. Rather, unless a specific value of lateral displacement is input, the lateral displacement is assumed to be zero. The imperfection parameter adopted for use in the program is:

$$\alpha = 1.414\delta_0 - 0.000954 + 0.875 \frac{F_y}{E}$$

where δ_0 is the lateral displacement divided by the brace length. This equation is different than that shown in Reference (3). Reference (4) was consulted to determine the sign of the second term in the equation. The current version of the program has been benchmarked against some documented results to verify the signs in the α equation.

The original version of the program was enhanced for estimating the reduction in capacity due to holes. In this case a dent depth is defined internally which encompasses the same arc length as the specified hole diameter. The plastification stress is then set equal to zero. All other calculations are performed as for dents.

The basic equation for the axial capacity includes a term involving the imperfection parameter α . When out-of-straightness is not specified, α is small. If residual bending deformations are present, the imperfection parameter includes this damage via the δ_0 term. In this manner the combined effect of out-of-straightness and a hole or dent can be evaluated.

The following is a brief description of the input/output from the program.

REQUIRED INPUT:

Outside diameter
 Wall thickness
 Brace length
 k-factor
 Yield stress
 Young's modulus
 Dent depth
 Hole diameter
 Lateral displacement

OUTPUT:

Dent/hole angle	= 2π - angle (radians) of damaged portion of the cross-section
Axial eccentricity	= distance between undamaged section center and neutral axis of damaged section
Reduced radius of gyration	= radius of gyration of damaged section
Reduced section modulus	= section modulus of damaged section of brace
Plastification stress (P_s)	= maximum stress which can be sustained by the dented portion of the cross-section
Average squash stress	= $(P_s A_d + F_y A_{ud})/A$
Imperfection parameter	= $1.414\delta_0 - 0.000954 + 0.875 \frac{F_y}{E}$

Slenderness ratio

$$= k \left(\frac{L}{r} - 0.2\pi \sqrt{\frac{E}{F_y}} \right)$$

Undamaged slenderness
ratio

$$= \frac{kL}{\pi r} \sqrt{\frac{F_y}{E}}$$

PROGRAM DAMAGE

```

C*****
C  WRITTEN BY R.FIGGERS FOR JIP
C
C  PROGRAM TO CALCULATE THE AXIAL CAPACITY OF DAMAGED MEMBERS
C*****
C
  CHARACTER*60 TITLE,FILOT
  WRITE(*,10)
  WRITE(*,*)' *****'
  WRITE(*,*)' *                PROGRAM DAMAGE                *'
  WRITE(*,*)' *'
  WRITE(*,*)' *  Program to estimate the axial capacity of    *'
  WRITE(*,*)' *  dented members with or without residual      *'
  WRITE(*,*)' *  bending deformations. Axial capacities of    *'
  WRITE(*,*)' *  members with holes may also be estimated.    *'
  WRITE(*,*)' *'
  WRITE(*,*)' *  Ref: "Ultimate Strength of Damaged Tubular    *'
  WRITE(*,*)' *        Bracing Members", C.P. Ellinas,        *'
  WRITE(*,*)' *        ASCE, J.Structural Division 110,        *'
  WRITE(*,*)' *        Feb 1984.                                *'
  WRITE(*,*)' *'
  WRITE(*,*)' *  Written by R Figgers                          10/25/88 *'
  WRITE(*,*)' *  Modified by R Figgers for all                  *'
  WRITE(*,*)' *        values of k                             1/16/89 *'
  WRITE(*,*)' *  Modified by R Figgers - Alpha 0                *'
  WRITE(*,*)' *        calculation revised                     2/02/89 *'
  WRITE(*,*)' *****'

C
  NT2=2
  WRITE(*,2)
2  FORMAT(/,' ENTER OUTPUT FILE NAME:')
  READ(*,'(A)')FILOT
  OPEN(NT2,FILE=FILOT,STATUS='NEW')

C
  WRITE(NT2,*)' *****'
  WRITE(NT2,*)' *'
  WRITE(NT2,*)' *                Program DAMAGE                *'
  WRITE(NT2,*)' *'
  WRITE(NT2,*)' *****'

C
  WRITE(*,890)
890  FORMAT(/,' TITLE:',$)
  READ(*,'(A)')TITLE
  WRITE(NT2,891)TITLE
891  FORMAT(/,' TITLE: ',A)
  WRITE(*,900)
  READ(*,'(F10.0)')D
  WRITE(NT2,901)D
901  FORMAT(/,' INPUT:',//,
        ' OUTSIDE DIAMETER (in) = ',F7.3)
  DO = D
  WRITE(*,910)
  READ(*,'(F10.0)')T
  WRITE(NT2,911)T
911  FORMAT(' THICKNESS (in) = ',F7.3)
  D=D-T
  WRITE(*,950)
  READ(*,'(F10.0)')XL
  WRITE(NT2,951)XL

```



```

951  FORMAT(      '    LENGTH (ft)                = ',F7.3)
      XL=XL*12.
      WRITE(*,962)
      READ(*,'(F10.0)')XK
      IF(XK.EQ.0.0)XK=1.0
      WRITE(NT2,963)XK
963  FORMAT(      '    EFF. LENGTH FACTOR          = ',F7.2)
      WRITE(*,930)
      READ(*,'(F10.0)')FY
      IF(FY.EQ.0.0)FY=36.
      WRITE(NT2,931)FY
931  FORMAT(/,    '    YIELD STRESS (ksi)          = ',F7.2)
      WRITE(*,940)
      READ(*,'(F10.0)')E
      IF(E.EQ.0.0)E=29000.
      WRITE(NT2,941)E
941  FORMAT(      '    YOUNGS MODULUS (ksi)         = ',F7.1)
      WRITE(*,920)
      READ(*,'(F10.0)')DD
      WRITE(NT2,921)DD
921  FORMAT(/,    '    DENT DEPTH (in)              = ',F7.3)
      WRITE(*,972)
      READ(*,'(F10.0)')HOLE
      WRITE(NT2,973)HOLE
      WRITE(*,960)
      READ(*,'(F10.0)')DELL
      WRITE(NT2,961)DELL
961  FORMAT(      '    LAT. DISPL. (in)             = ',F7.2)
973  FORMAT(      '    HOLE DIAMETER (in)           = ',F7.3)
10   FORMAT(////)
900  FORMAT(/,    '    MEMBER DIAMETER (in)         = ',,$)
910  FORMAT(      '    MEMBER THICKNESS (in)        = ',,$)
920  FORMAT(/,    '    DENT DEPTH (in)              = ',,$)
930  FORMAT(/,    '    YIELD STRESS (def=36 ksi)    = ',,$)
940  FORMAT(      '    YOUNGS MODULUS (def=29000 ksi) = ',,$)
950  FORMAT(      '    MEMBER LENGTH (ft)           = ',,$)
960  FORMAT(      '    LATERAL DISPLACEMENT (in)    = ',,$)
962  FORMAT(      '    k FACTOR ( def=1.0 )         = ',,$)
972  FORMAT(      '    HOLE DIAMETER (in)           = ',,$)
C
C      CALCULATE REQUIRED PARAMETERS
C
C      DEFORMATION TO LENGTH RATIO
C
      DELO = DELL/XL
C
C      AREA
C
      PI = 4.0*ATAN(1.0)
      AREA = PI*D*T
      WRITE(*,2000)AREA
      WRITE(NT2,2000)AREA
C
C      DENT ANGLE
C
      DELD = DD/D
      THETA = 2.*PI-2.*ASIN(2.*SQRT(DELD*(1.-DELD)))
      IF(DELD.LT.0.2)THETA = 2.*PI-4.*SQRT(DELD)
      IF(HOLE.NE.0.0)THETA=2.*PI-2.*ASIN(HOLE/D)
      WRITE(*,2100)THETA

```

WRITE(NT2,2100)THETA

REDUCED CROSS-SECTIONAL AREA

AD = .5*D*T*THETA

ECCENTRICITY

ED = D*SIN(THETA/2.)/THETA

WRITE(*,2300)ED

WRITE(NT2,2300)ED

REDUCED RADIUS OF GYRATION

RID = D/2.*SQRT(.5*(1.+SIN(THETA)/THETA-8.*(SIN(THETA/2.))**2
/THETA**2))

IF(HOLE.EQ.0.0)GO TO 46

XI = .125*D**3*T*(THETA/2.+.5*SIN(THETA))-ED*D**2*T*SIN(THETA/2.)
+D*T*ED**2*THETA/2.

RID=SQRT(XI/AD)

CONTINUE

WRITE(*,2200)RID

WRITE(NT2,2200)RID

REDUCED ELASTIC SECTION MODULUS

UP = THETA+SIN(THETA)-8.*(SIN(THETA/2.))**2/THETA

DOWN = 1.-2.*DELD+2.*ED/D

ZD = .125*D**2*T*(UP/DOWN)

IF(HOLE.EQ.0.0)GO TO 63

YBAR1=D/2.-ED

YBAR2=ED-D/2.*COS(THETA/2.)

YBAR=MAX(YBAR1,YBAR2)

ZD=XI/YBAR

CONTINUE

WRITE(*,2500)ZD

WRITE(NT2,2500)ZD

SIGMA PD

SPD = FY*D/T*(SQRT(16.*DELD**2/9.+(T/D)**2)-4./3.*DELD)

IF(HOLE.NE.0.0)SPD=0.0

WRITE(*,2600)SPD

WRITE(NT2,2600)SPD

AVERAGE SQUASH LOAD

SL = (FY-SPD)*AD/AREA + SPD

WRITE(*,2700)SL

WRITE(NT2,2700)SL

ALPHA 0

ALPHA0 = 1.4142*DELO - .000954 + 0.875*FY/E

IF(ALPHA0.LT.0.0)ALPHA0=0.

WRITE(*,2800)ALPHA0

WRITE(NT2,2800)ALPHA0

SLENDERNES

```

AMBD = XK*(XL/RID - 0.2*PI*SQRT(E/FY))
WRITE(*,2900)AMBD
WRITE(NT2,2900)AMBD

```

EULER BUCKLING STRESS

```

XI = PI*(D0**4-(D0-2.*T)**4)/64.
RI = SQRT(XI/AREA)
SXKE = PI**2*E*RI**2/(XL*XK)**2
WRITE(*,2910)SXKE
WRITE(NT2,2910)SXKE

```

DAMAGED MEMBER ULTIMATE STRENGTH

```

B = -(1.+ALPHA0*AMBD+AD*ED/ZD+SL/SXKE)
A = 1./SXKE
C = SL+SPD*AD*ED/ZD
SDCE1 = (-B+SQRT(B**2-4.*A*C))/(2.*A)
SDCE2 = (-B-SQRT(B**2-4.*A*C))/(2.*A)

```

```

WRITE(*,970)SDCE1,SDCE2
WRITE(NT2,970)SDCE1,SDCE2

```

```

IF(SDCE1.GT.FY)SDCE1=0.0
IF(SDCE2.GT.FY)SDCE2=0.0
IF(SDCE1.LT.0.0)SDCE1=0.0
IF(SDCE2.LT.0.0)SDCE2=0.0
AXCAP=SDCE2
IF(SDCE1.LT.SDCE2)AXCAP=SDCE1
IF(AXCAP.GT.FY)AXCAP=FY
SLEND=XK*XL*SQRT(FY/E)/RI/PI
SRAT=AXCAP/FY
WRITE(*,980)AXCAP,SRAT
WRITE(NT2,980)AXCAP,SRAT
WRITE(*,982)SLEND
WRITE(NT2,982)SLEND
WRITE(NT2,993)
WRITE(NT2,994)
WRITE(NT2,995)

```

```

980  FORMAT(/,'  DAMAGED MEMBER AXIAL CAPACITY (ksi) = ',F10.3,/,
      '      DAMAGED/UNDAMAGED STRESS RATIO      = ',F10.5)
982  FORMAT('  UNDAMAGED SLENDERNESS RATIO      = ',F10.5)
2000 FORMAT(/,'  RESULTS:',/,

```

```

      '      CROSS-SECTIONAL AREA (sq.in)          = ',F10.2)
2100 FORMAT('  DENT/HOLE ANGLE (rad)              = ',F10.5)
2200 FORMAT('  REDUCED RAD. OF GYRATION (cu.in)     = ',F10.3)
2300 FORMAT('  AXIAL ECCENTRICITY (in)              = ',F10.4)
2500 FORMAT('  REDUCED ELAS. SECTION MOD. (cu.in)   = ',F10.3)
2600 FORMAT('  PLASTIFICATION STRESS (ksi)         = ',F10.3)
2700 FORMAT('  AVG. SQUASH STRESS (ksi)            = ',F10.3)
2800 FORMAT('  IMPERFECTION PARAMETER              = ',F10.5)
2900 FORMAT('  SLENDERNESS RATIO                  = ',F10.5)
2910 FORMAT('  EULER BUCKLING STRESS (ksi)         = ',F10.4)
970  FORMAT('  SOLUTION ROOTS (SDCE1,SDCE2) (ksi)   = ',2F10.3)
993  FORMAT(/,'  Notes:',/,

```

```

      (1) Hole diameter and dent depth should be measure
      .d w/r the',/,
      tubular mid-wall diameter.')
994  FORMAT('  (2) For dented members it is assumed that the maxi
      .mum stress',/,

```

	.	'	the dented region can sustain is equal to the
	.plastification',/,	'	stress. This stress is set equal to zero for
	.hole damage.')		
995	.ge.')		
	FORMAT(' (3)		Dent and hole damage must be evaluated separat
	.ely. Either',/,		can be assessed in conjunction with bending da
	.mage.')		
	STOP		
	END		

```

*****
*
*           Program DAMAGE
*
*****

```

TITLE: Example Analysis

INPUT:

```

OUTSIDE DIAMETER (in) = 30.000
THICKNESS (in)       = .500
LENGTH (ft)         = 50.000
EFF. LENGTH FACTOR   = .80

YIELD STRESS (ksi)   = 50.00
YOUNGS MODULUS (ksi) = 29000.0

DENT DEPTH (in)       = 3.000
HOLE DIAMETER (in)    = .000
LAT. DISPL. (in)      = 3.00

```

RESULTS:

```

CROSS-SECTIONAL AREA (sq.in) = 46.34
DENT/HOLE ANGLE (rad)         = 5.00760
AXIAL ECCENTRICITY (in)       = 3.5077
REDUCED RAD. OF GYRATION (cu.in) = 8.700
REDUCED ELAS. SECTION MOD. (cu.in) = 183.217
PLASTIFICATION STRESS (ksi)   = 3.113
AVG. SQUASH STRESS (ksi)     = 40.481
IMPERFECTION PARAMETER       = .00763
SLENDERNESS RATIO            = 43.06542
EULER BUCKLING STRESS (ksi)   = 135.1743
SOLUTION ROOTS (SDCE1,SDCE2) (ksi) = 296.138      19.483

DAMAGED MEMBER AXIAL CAPACITY (ksi) = 19.483
DAMAGED/UNDAMAGED STRESS RATIO      = .38965
UNDAMAGED SLENDERNESS RATIO          = .60819

```

Notes:

- (1) Hole diameter and dent depth should be measured w/r the tubular mid-wall diameter.
- (2) For dented members it is assumed that the maximum stress the dented region can sustain is equal to the plastification stress. This stress is set equal to zero for hole damage.
- (3) Dent and hole damage must be evaluated separately. Either can be assessed in conjunction with bending damage.

EQUIV Program

EQUIV is an interactive PC Fortran 77 program developed to generate damaged tubular member data for this study's computer analyses. The program calculates reduced axial and moment capacities for members having holes or dents. In addition, moment-curvature and axial force-moment interaction data is developed for a damaged or an undamaged cross-section. A damaged section is one with a hole or a dent while an undamaged one contains neither. This data can then be used in conjunction with the element length to develop axial force-deformation, moment-rotation, and axial force-moment yield surface data for input to the SEASTAR program.

The program calculates the cross-sectional properties of damaged and undamaged thin-walled tubes. Damage can assume the form of either a hole or a dent. The program also calculates the eccentricity of the damaged section and the reduction factors to be applied to the undamaged section axial force and moment capacities to obtain the damaged section capacities. The undamaged section yield moment, plastic moment, maximum axial load and yield curvature are reported with the program geometric data output. The eccentricity is determined as the difference between the undamaged section geometric center and the center of gravity of the undamaged arc of the cross-section. The damaged arc of the cross-section is not considered in determining the center of gravity, the plastic moment or the maximum axial capacity. If the plastification stress is included in the property calculation then the maximum stress the dented region can sustain is included in the moment and axial capacity.

Several damaged section properties are calculated and printed. The plastic moment and maximum axial load, the cross-sectional area of the hole or dented region, the maximum load which can be sustained by the dented region of the cross-section and the dent zone plastification stress are output. Also reported are equivalent linear properties which can be included in an analysis to represent the damaged section stiffness. An estimated dent length based upon the dent depth and member diameter is also calculated and reported.

Two tables are developed and printed. The first table in the output file provides moment and curvature data from which a moment-curvature or moment-rotation plot (provided the member length is known) can be constructed. The second table lists discrete points on the damaged section axial force-moment (P-M) interaction surface. This surface is different in form from that of an undamaged section. It can be input to SEASTAR as a type 4 yield surface having the exponential powers of α_1 and α_2 . For the Damaged Brace JIP, the α exponents were selected by trial and error. The procedure involved programming the type 4 yield surface equation in a spreadsheet format. Various combinations of α exponents were tried until a best fit graphically was obtained with the generated damaged section yield surface.

At execution, the user is asked if he wants to include the plastification stress of the dented region of the cross-section in the calculation of the section axial capacity and plastic moment. For dent sizes which significantly affect brace capacity, including this stress provides little additional capacity and can be conservatively neglected. This stress is determined using the same equations as employed in the DAMAGE program.

The following is a list of the input/output from the EQUIV program.

REQUIRED INPUT:

- Outside Diameter
- Wall Thickness
- Material yield stress
- Young's modulus of elasticity
- Dent depth
- Hole diameter

OUTPUT:

Eccentricity due to damage
Moment-curvature data
P-M interaction surface data
Undamaged Section Properties:

Yield Moment
Plastic Moment
Axial Capacity
Yield Curvature

Damaged Section Properties:

Plastic Moment
Axial Capacity
Plastification Stress
Max Dent Load
Yield Curvature
Yield Strain
Dented Length

Most of the equations used in the EQUIV program to determine the member cross-sectional properties are discussed below. An attempt has been made to provide these equations in the order in which they occur in the program.

The parameter α is the angle corresponding to half of the cross-section damaged arc for dent damage and half of the angle subtended by the hole diameter for hole damage:

$$\alpha = \cos^{-1} \left(1 - \frac{d_d}{R} \right)$$

where

R = mid-wall thickness radius

d_d = dent depth or "equivalent" hole diameter

Another damage parameter, δ_d is the ratio of the dent depth to the member diameter:

$$\delta_d = \frac{d_d}{D}$$

where

D = member diameter

If the plastification stress is to be included in the determination of the axial and moment capacity of the dented member, this stress is calculated as:

$$\sigma_p = F_y \frac{D}{t} \left(\sqrt{1.778 \delta_d^2 + \frac{t^2}{D^2}} - 1.333 \delta_d \right)$$

where

F_y = material yield stress

t = member wall thickness

The cross-sectional area of the dented cross-section is determined as:

$$A_d = 2tR \sin \alpha$$

The eccentricity due to a dent or hole of comparable dent depth is determined by:

$$e = -R \frac{\sin \alpha}{\pi - \alpha}$$

The damaged section axial and bending capacities are calculated by defining a reduction factor to be applied to the undamaged section properties. The factors h_m and h_p are the moment and axial capacity reduction factors respectively. They are determined using the following equations:

$$h_m = \cos \frac{\alpha}{2} - \frac{\sin \alpha}{2}$$

$$h_p = \frac{\pi - \alpha}{\pi}$$

These reduction factors are applied to the undamaged axial and bending properties to determine the damaged section capacities. The undamaged cross-sectional properties are tabulated below:

The undamaged plastic moment:

$$M_p = 4R^2 t F_y$$

The undamaged axial capacity:

$$P_p = 2\pi R t F_y$$

The undamaged yield moment:

$$M_y = \pi R^2 t F_y$$

The undamaged yield curvature:

$$\phi_y = \frac{F_y}{R E}$$

where

E = Young's modulus of elasticity

The damaged section properties are as follows: (The plastification stress terms are included for completeness.)

The damaged plastic moment (about the damaged cross-section neutral axis):

$$M_{pd} = h_m M_p + \sigma_p A_d (R - d_d - e)$$

The damaged cross-section axial capacity:

$$P_{pd} = h_p P_p + \sigma_p A_d$$

An estimate of the damaged length is provided for a dented member via the following equation. If the member has a hole, the damaged length is assumed to be equal to the hole diameter.

$$L_d = 2\sqrt{2} R \alpha$$

The above equations form the basis for the uncoupled axial and moment capacities. The capacity of a member having both axial and bending stresses is defined by a 2-D yield surface. The axes of this surface represent pure stress states of axial or bending stress. Any point not on an axis is a combined stress state. To determine the points on the yield surface, combinations of axial load and bending moment were substituted in the following equations on a trial and error basis. Those combinations of stress satisfying the yield surface equation (value of zero) define the yield surface. In these equations the eccentricity due to the damage is included in the yield surface formulation. Thus, the denominators of the ratios in the equations are undamaged section properties.

$$\gamma = \left(\frac{\pi - \alpha}{2} \right) - \pi \frac{P}{2P_p}$$

$$\left(\frac{M}{M_p} \right) - \left(\frac{\pi d_d}{2R} \right) \left(\frac{P}{P_p} \right) - \sin \gamma + \sin \frac{\alpha}{2} = 0$$

The beam-column element in the SEASTAR program requires that the force-deformation data as well as the axial-bending interaction characteristics be input for each nonlinear element. It is assumed that the force-axial deformation characteristics are linear up to the section yield stress. Beyond this axial deformation the element is assumed to have a minimal amount of strain hardening for larger values of strain. The element moment-rotation input is assumed to be trilinear which requires three stiffness and four moment input values. This data is obtained by imposing curvatures on the cross-section about the damaged section neutral axis and calculating the resulting moment and rotation. Determining the rotation requires that the element length be known.

A multi-step process is required to determine the cross-section moment-curvature characteristics. The first step is to determine the yield curvature which will just cause material yielding at the member extreme fiber strains are as follows:

$$\gamma = \frac{\pi}{2} - \alpha$$

$$\epsilon_y = \frac{\sigma_y}{E}$$

$$\epsilon_c = \phi(R \sin \gamma - e) < \epsilon_y$$

$$\epsilon_t = \phi(-R - e) < \epsilon_y$$

where

ϵ_y = material yield strain

ϵ_c = compression fiber strain

ϵ_t = tension fiber strain

ϕ = curvature

e = damaged section eccentricity

Using the above strain calculations as reference, the stress state of the extreme fibers of the member can be evaluated. Three stress states can occur: 1) both tension and compression fiber stresses are less than σ_y , 2) the compression stress has reached yield and the tension side has remained elastic or 3) both extreme fiber stresses have reached the material yield stress.

The general procedure is to assume a cross-section curvature and determine the corresponding moment. The curvature is then increased and the associated moment determined. The curvature is continually increased until the cross-section plastic moment is reached or the curvature is beyond practical limits. As the curvature is increased, the stress distribution about the neutral axis

progresses from elastic to plastic corresponding to the three states described above. If both extreme fiber strains are less than the yield strain then the cross-sectional elastic moment is determined as:

$$M_e = 2ERt\phi(e^2\theta|_{-\frac{\pi}{2}}^{\gamma} + R^2\left(\frac{\theta}{2} - \frac{\sin 2\theta}{4}\right)|_{-\frac{\pi}{2}}^{\gamma} + 2Re\cos\theta|_{-\frac{\pi}{2}}^{\gamma})$$

The equation for the elastic moment is the result of integrating the stress distribution over the depth of the member. This equation must be evaluated with θ taking on the upper and lower values on the vertical bar.

When the compression side of the member has reached yield but the tension side remains elastic, the moment is defined using the following equations:

$$\theta_1 = \sin^{-1}\left(\frac{\sigma_y}{\phi RE} + \frac{e}{R}\right)$$

$$M_1 = -2\sigma_y R^2 t (\cos \gamma - \cos \theta_1) - 2\sigma_y R t e (\gamma - \theta_1)$$

$$M_2 = 2E\phi R t [e^2\theta|_{-\frac{\pi}{2}}^{\theta_1} + R^2\left(\frac{\theta}{2} - \frac{\sin 2\theta}{4}\right)|_{-\frac{\pi}{2}}^{\theta_1} + 2Re\cos\theta|_{-\frac{\pi}{2}}^{\theta_1}]$$

$$M = M_1 + M_2$$

When both sides have reached the material yield strain the cross-sectional moment is determined by:

$$\theta_2 = \sin^{-1}\left(\frac{-\epsilon_y}{\phi R} + \frac{e}{R}\right)$$

$$M_3 = 2\sigma_y R^2 t \left(\cos \theta_2 - \cos\left(-\frac{\pi}{2}\right) \right) + 2\sigma_y R t e \left(\theta_2 + \frac{\pi}{2} \right)$$

$$M = M_1 + M_2 + M_3$$

The methods outlined above describe the basic equations and methods employed in the EQUIV program to determine the cross-sectional capacities, the force-deformation characteristics and the axial force-moment interaction for intact

and damaged members. These equations were extracted from the work of Van Aanhold and Taby and the program was verified against known results. A detailed explanation for the computation of the plastic capacities and the yield surface for undamaged and damaged sections can be found in Reference 5.

```

PROGRAM EQUIV
CHARACTER*60 FILOT,TITLE
CHARACTER*1 Y1,Y2,INPL
Y1 = 'Y'
Y2 = 'y'

```

Program to develop equivalent properties for damaged sections of tubular members. The program excludes any contribution of the damaged region of a dented member, therefore, the generated properties also apply for holes.

Ref: "Analysis of Structures with Damaged Structural Members",
J.E. van Aanhold and J. Taby
Veritas Technical Report STFA83002
Oct. 1983

READ INPUT DATA

```

WRITE(*,1)
1  FORMAT(//,' TITLE:')
  READ(*,'(A)')TITLE
  WRITE(*,2)
2  FORMAT(//,' ENTER OUTPUT FILE NAME:')
  READ(*,'(A)')FILOT
  OPEN(1,FILE=FILOT,STATUS='NEW')
  WRITE(1,4)
4  FORMAT(//,'                                PROGRAM EQUIV')
  WRITE(1,3)TITLE
3  FORMAT(//,' TITLE: ',A)
  WRITE(*,5)
5  FORMAT(///,' ENTER MEMBER OUTSIDE DIAMETER (in)')
  READ(*,'(F10.0)')DIA
10  FORMAT(/)
  WRITE(*,*)' ENTER MEMBER WALL THICKNESS (in)'
  READ(*,'(F10.0)')T
  WRITE(*,*)' ENTER MATERIAL YIELD STRESS (ksi)'
  READ(*,'(F10.0)')FY
  WRITE(*,*)' ENTER MODULUS OF ELASTICITY (ksi)'
  READ(*,'(F10.0)')YMOD
  WRITE(*,*)' ENTER DENT DEPTH (in)'
  READ(*,'(F10.0)')DD
  WRITE(*,*)' ENTER HOLE DIAMETER (in)'
  READ(*,'(F10.0)')HOLE
  IF(DD.NE.0.0)
  .WRITE(*,*)' INCLUDE PLASTIFICATION STRESS (Y/N)?'
  IF(DD.NE.0.0)
  .READ(*,'(A)')INPL
  DIA = DIA - T
  R = DIA / 2.0
  PI = 4.0 * ATAN (1.0)

```

Plastification Stress and Dent Area Load

```

DELD = 0.0
SPL = 0.0
DAREA = 0.0
PLLOAD = 0.0

```

```

ALPH = ACOS(1-DD/R)
IF(DD.EQ.0.0)GO TO 8
IF(INPL.NE.Y1.AND.INPL.NE.Y2)GO TO 8
DELD = DD/DIA
SPL = FY*DIA/T*(SQRT(16./9.*DELD**2+(T/DIA)**2)-4./3.*DELD)
DAREA = T*R*2.0*SIN(ALPH)
PLLOAD = DAREA*SPL
CONTINUE

```

Geometric parameters

```

IF(HOLE.NE.0.0)ALPH = ASIN((HOLE/2.0)/R)
ECC = -R * (SIN(ALPH))/(PI - ALPH)
HM = COS(ALPH/2.0)-0.5*SIN(ALPH)
HP = (PI-ALPH)/PI
AREA = 2.0 * PI * R * T * (1.0 - (2.0 * ALPH)/(2.0 * PI ))

```

Undamaged plastic moment and axial load

```

XMP = 4.0 * R**2 * T * FY
PP = 2.0 * PI * R * T * FY

```

Undamaged Yield Moment

```

XMY = PI*R**2*T*FY

```

Undamaged Yield Curvature

```

PHIYUN=FY/(YMOD*R)

```

Damaged section plastic moment and axial load

```

EQMP = HM * XMP + PLLOAD*(R-DD-ECC)
HMM = EQMP/XMP
EQAX = HP * PP + PLLOAD
HPP = EQAX/PP
EQR = R * HMM/ HPP
EQT = T * HPP**2 / HMM
EQD = DIA * (2.0 * EQR + EQT)/(2.0 * R + T)
DAML = 2.82843 * R * ALPH
IF(HOLE.NE.0.0)DAML = HOLE

```

Print data

```

WRITE(*,50)DIA,T,FY,YMOD,DD,HOLE,AREA
WRITE(1,50)DIA,T,FY,YMOD,DD,HOLE,AREA
50  FORMAT(//,' INPUT DATA:',/,

```

```

.      '      MEMBER DIAMETER (in)      = ',F8.3,/,
.      '      MEMBER THICKNESS (in)     = ',F8.4,/,
.      '      MEMBER YIELD STRESS (ksi)  = ',F8.3,/,
.      '      MODULUS OF ELASTICITY (ksi) = ',F8.1,/,
.      '      DENT DEPTH (in)            = ',F8.4,/,
.      '      HOLE DIAMETER (in)         = ',F8.4,/,
.      '      UNDAMAGED SECTION AREA (in^2) = ',F8.3)

```

```

READ(*,'(I1)')IDUM

```

```

WRITE(*,60)ALPH,ECC,HMM,HPP,XMY,XMP,PP,PHIYUN
WRITE(1,60)ALPH,ECC,HMM,HPP,XMY,XMP,PP,PHIYUN

```

```

60  FORMAT(//,' GEOMETRIC DATA:',/,

```

```

.      '      DAMAGE ANGLE (rad) = ',F8.6,/,
.      '      ECCENTRICITY (in)   = ',F8.4,/,

```



```

      '      HMM      = ',F8.4,/,
      '      HPP      = ',F8.4,/,
      '      UNDAMAGED YIELD MOMENT (k-in) = ',F8.1,/,
      '      UNDAMAGED PLASTIC MOMENT (k-in) = ',F8.1,/,
      '      UNDAMAGED PLASTIC AXIAL LOAD (k) = ',F8.2,/,
      '      UNDAMAGED YIELD CURVATURE = ',E12.6)

```

```

READ(*,'(I1)')IDUM
WRITE(*,70)EQMP,EQAX,DAREA,SPL,PLLOAD,EQR,EQT,EQD,DAML
WRITE(1,70)EQMP,EQAX,DAREA,SPL,PLLOAD,EQR,EQT,EQD,DAML

```

```

70  FORMAT(//,' EQUIVALENT DAMAGED SECTION PROPERTIES:',/,
      '      PLASTIC MOMENT (k-in)      = ',F8.2,/,
      '      PLASTIC AXIAL LOAD (k)     = ',F8.2,/,
      '      DENT AREA (in^2)           = ',F8.3,/,
      '      PLASTIFICATION STRESS (ksi) = ',F8.2,/,
      '      MAX DENT LOAD (k)           = ',F8.2,/,
      '      MEMBER RADIUS (in)          = ',F8.3,/,
      '      MEMBER THICKNESS (in)       = ',F8.4,/,
      '      MEMBER DIAMETER (in)       = ',F8.4,/,
      '      DAMAGED LENGTH (in)        = ',F8.2)

```

```

READ(*,'(I1)')IDUM

```

```

      Generate Moment - Curvature data for damaged section

```

```

PHI = 0.
GAMMA = PI/2.0 - ALPH
PHIYLD = FY/(R*YMOD*(SIN(GAMMA) -(ECC/R)))
DELPHI = PHIYUN/5.0001
YLDST = FY/YMOD

```

```

WRITE(*,80)GAMMA,PHIYLD,YLDST
WRITE(1,80)GAMMA,PHIYLD,YLDST

```

```

80  FORMAT(//,' DAMAGED SECTION MOMENT-CURVATURE DATA:',/,
      '      UNDAMAGED ANGLE (rad) = ',F8.6,/,
      '      YIELD CURVATURE (rad) = ',E13.6,/,
      '      YIELD STRAIN (in/in) = ',E13.6,/)

```

```

WRITE(*,*)
.'      Comp      Ten      Curv-      Moment      Phi/      Mom/'
WRITE(*,*)
.'      Strn      Strn      ature      (k-in)      Phiy      Momy'
WRITE(*,*)' '
WRITE(1,*)
.'      Comp      Ten      Curv-      Moment      Phi/      Mom/'
WRITE(1,*)
.'      Strn      Strn      ature      (k-in)      Phiy      Momy'
WRITE(1,*)' '

```

```

100 CONTINUE
CSTR = PHI*(R*SIN(GAMMA)-ECC)
TSTR = PHI*(-R-ECC)
CS = CSTR*YMOD
DLOAD = CS*DAREA
IF(CS.GT.SPL)DLOAD = SPL*DAREA
IF(CSTR.GT.YLDST.OR.TSTR.LT.-YLDST)GO TO 110

```

```

      Elastic moment

```

```

XM = 2.0*YMOD*PHI*R*T*(ECC**2*(GAMMA+PI/2.)+R**2*(.5*GAMMA-
      .25*SIN(2.*GAMMA)-.5*(-PI/2.)+.25*SIN(-PI))+2.0*R*ECC*
      (COS(GAMMA)-COS(-PI/2.))) + DLOAD*(R-DD-ECC)
RPHI=PHI/PHIYUN
RMOM = XM/XMY
WRITE(*,101)CSTR,TSTR,PHI,XM,RPHI,RMOM

```

```

WRITE(1,101) CSTR,TSTR,PHI,XM,RPHI,RMOM
PHI = PHI + DELPHI
GO TO 100
CONTINUE

```

110
C
C
C

Compression Yield

```

PHI = PHI - DELPHI
DELPHI=DELPHI/1.
PHI = PHI +DELPHI
115 CONTINUE
TH1 = ASIN(FY/(PHI*R*YMOD)+ECC/R)
TSTR = PHI*(-R-ECC)
CSTR = PHI*(R*SIN(GAMMA)-ECC)
CS = CSTR*YMOD
DLOAD = CS*DAREA
IF(CS.GT.SPL) DLOAD = SPL*DAREA
IF(CSTR.GT.YLDST.AND.TSTR.LT.-YLDST) GO TO 120
XM1 = -2.0*FY*R**2*T*(COS(GAMMA)-COS(TH1))-2.0*FY*R*T*ECC*
      (GAMMA-TH1)
XM2 = 2.0*PHI*YMOD*R*T*(ECC**2*(TH1+PI/2.)+R**2*(.5*TH1-.25*
      SIN(2.*TH1)-.5*(-PI/2.))+.25*SIN(-PI))+2.*R*ECC*
      (COS(TH1)-COS(-PI/2.)))
XM = XM1+XM2+DLOAD*(R-DD-ECC)
RPHI = PHI/PHIYUN
RMOM=XM/XMY
WRITE(*,101) CSTR,TSTR,PHI,XM,RPHI,RMOM
WRITE(1,101) CSTR,TSTR,PHI,XM,RPHI,RMOM
PHI = PHI + DELPHI
GO TO 115

```

C
C
C

Compression and tension yield

```

120 CONTINUE
PHI = PHI-DELPHI
DELPHI = DELPHI/1.0
PHI = PHI + DELPHI
125 CONTINUE
IF(PHI.GT.5.0*PHIYUN) GO TO 130
TH1 = ASIN(FY/(PHI*R*YMOD)+ECC/R)
TH2 = ASIN(-FY/(PHI*R*YMOD)+ECC/R)
TSTR = PHI*(-R-ECC)
CSTR = PHI*(R*SIN(GAMMA)-ECC)
CS = CSTR*YMOD
DLOAD = CS*DAREA
IF(CS.GT.SPL) DLOAD = SPL*DAREA
XM1 = -2.0*FY*R**2*T*(COS(GAMMA)-COS(TH1))-2.0*FY*R*T*ECC*
      (GAMMA-TH1)
XM2 = 2.0*PHI*YMOD*R*T*(ECC**2*(TH1-TH2)+R**2*(.5*TH1-.25*
      SIN(2.*TH1)-.5*(TH2)+.25*SIN(2.*TH2))+2.*R*ECC*
      (COS(TH1)-COS(TH2)))
XM3 = 2.0*FY*R**2*T*(COS(TH2)-COS(-PI/2.))+2.0*FY*R*T*ECC*
      (TH2+PI/2.)
XM = XM1+XM2+XM3+DLOAD*(R-DD-ECC)
RPHI = PHI/PHIYUN
RMOM = XM/XMY
WRITE(*,101) CSTR,TSTR,PHI,XM,RPHI,RMOM
WRITE(1,101) CSTR,TSTR,PHI,XM,RPHI,RMOM
PHI = PHI + DELPHI
GO TO 125

```

```

130  CONTINUE
101  FORMAT(2X,3F10.7,3X,F10.2,1X,2F10.4)
    READ(*,'(I1)')IDUM
C
C      Generate P-M Interaction Surface
C
    PRATIO=0.0
    IDEL = 10
    DELP = HP/IDEL
    IDEL = IDEL+1
    WRITE(*,140)
    WRITE(1,140)
140  FORMAT(,////, '   DAMAGED SECTION P-M INTERACTION SURFACE')
    WRITE(*,142)
    WRITE(1,142)
142  FORMAT(/,
    . '      P/Pp      M/Mp      PRAT      MRAT      P(k)  M(k-in)',/)

150  CONTINUE
    DO 165 I=1, IDEL
    RATIO=PI*ECC*PRATIO/2./R -SIN((PI-ALPH)/2.-PI*PRATIO/2.)+
    .5*SIN(ALPH)
    RATIO = -RATIO
    AX = PRATIO*PP*HPP/HP
    XM = RATIO*XMP*HMM/HM
    PRATIP = PRATIO*HPP/HP
    RATIO = RATIO*HMM/HM
    RAT1 = PRATIP/HPP
    RAT2 = RATIO/HMM
    WRITE(*,155) PRATIP, RATIO, RAT1, RAT2, AX, XM
    WRITE(1,155) PRATIP, RATIO, RAT1, RAT2, AX, XM
    PRATIO=PRATIO+DELP
165  CONTINUE
155  FORMAT(1X,4F9.5,2F9.1)
    STOP
    END

```

PROGRAM EQUIV

TITLE: Documentation for EQUIV Program

INPUT DATA:

MEMBER DIAMETER (in) = 29.500
 MEMBER THICKNESS (in) = .5000

 MEMBER YIELD STRESS (ksi) = 42.000
 MODULUS OF ELASTICITY (ksi) = 29000.0

 DENT DEPTH (in) = 6.0000
 HOLE DIAMETER (in) = .0000
 UNDAMAGED SECTION AREA (in²) = 32.536

GEOMETRIC DATA:

DAMAGE ANGLE (rad) = .935743
 ECCENTRICITY (in) = -5.3831
 HMM = .5021
 HPP = .7101

 UNDAMAGED YIELD MOMENT (k-in) = 14353.3
 UNDAMAGED PLASTIC MOMENT (k-in) = 18275.3
 UNDAMAGED PLASTIC AXIAL LOAD (k) = 1946.22
 UNDAMAGED YIELD CURVATURE = .981882E-04

EQUIVALENT DAMAGED SECTION PROPERTIES:

PLASTIC MOMENT (k-in) = 9175.11
 PLASTIC AXIAL LOAD (k) = 1382.09
 DENT AREA (in²) = 11.874
 PLASTIFICATION STRESS (ksi) = 1.31
 MAX DENT LOAD (k) = 15.57

 MEMBER RADIUS (in) = 10.428
 MEMBER THICKNESS (in) = .5022
 MEMBER DIAMETER (in) = 21.0019
 DAMAGED LENGTH (in) = 39.04

DAMAGED SECTION MOMENT-CURVATURE DATA:

UNDAMAGED ANGLE (rad) = .635053
 YIELD CURVATURE (rad) = .102474E-03
 YIELD STRAIN (in/in) = .144828E-02

Comp Strn	Ten Strn	Curv- ature	Moment (k-in)	Phi/ Phiy	Mom/ Momy
.0000000	.0000000	.0000000	.00	.0000	.0000
.0002775	-.0001839	.0000196	1262.34	.2000	.0879
.0005551	-.0003679	.0000393	2304.62	.4000	.1606
.0008326	-.0005518	.0000589	3346.90	.6000	.2332
.0011101	-.0007358	.0000785	4389.19	.8000	.3058
.0013877	-.0009197	.0000982	5431.47	1.0000	.3784

.0016652	-.0011036	.0001178	6379.68	1.2000	.4445
.0019427	-.0012876	.0001375	7125.00	1.4000	.4964
.0022203	-.0014715	.0001571	7755.75	1.6000	.5403
.0024978	-.0016555	.0001767	8128.60	1.8000	.5663
.0027754	-.0018394	.0001964	8365.08	2.0000	.5828
.0030529	-.0020233	.0002160	8530.67	2.2000	.5943
.0033304	-.0022073	.0002356	8652.45	2.4000	.6028
.0036080	-.0023912	.0002553	8745.08	2.5999	.6093
.0038855	-.0025752	.0002749	8817.38	2.7999	.6143
.0041630	-.0027591	.0002946	8874.98	2.9999	.6183
.0044406	-.0029430	.0003142	8921.67	3.1999	.6216
.0047181	-.0031270	.0003338	8960.07	3.3999	.6242
.0049956	-.0033109	.0003535	8992.05	3.5999	.6265
.0052732	-.0034949	.0003731	9018.98	3.7999	.6284
.0055507	-.0036788	.0003927	9041.87	3.9999	.6299
.0058282	-.0038627	.0004124	9061.50	4.1999	.6313
.0061058	-.0040467	.0004320	9078.46	4.3999	.6325
.0063833	-.0042306	.0004517	9093.21	4.5999	.6335
.0066609	-.0044146	.0004713	9106.14	4.7999	.6344
.0069384	-.0045985	.0004909	9117.52	4.9999	.6352

DAMAGED SECTION P-M INTERACTION SURFACE

P/Pp	M/Mp	PRAT	MRAT	P(k)	M(k-in)
.00000	.50205	.00000	1.00000	.0	9175.1
.07101	.48688	.10000	.96977	138.2	8897.8
.14203	.46127	.20000	.91878	276.4	8429.9
.21304	.42606	.30000	.84863	414.6	7786.3
.28406	.38216	.40000	.76119	552.8	6984.0
.35507	.33060	.50000	.65850	691.0	6041.8
.42609	.27253	.60000	.54282	829.3	4980.5
.49710	.20913	.70000	.41656	967.5	3822.0
.56812	.14169	.80000	.28223	1105.7	2589.5
.63913	.07153	.90000	.14248	1243.9	1307.3
.71014	.00000	1.00000	.00000	1382.1	.0

4.3 Results

After completing the various analyses for the twenty specimens the data was reduced to graphs and tables. These are presented in Figures 4-5 to 4-79. The following section details the format of these results.

Figure 4-5 is a summary of the specimen peak axial capacities from the full scale test, the DAMAGE program, the beam-column finite element analysis (FEA) and the DENTA-2 analysis (provided by Shell). Only members with holes or dents have entries in the DAMAGE column. Predominate types of member damage along with the ratios of FEA to test capacity and DENTA to test capacity are listed for quick reference.

Figure 4-6 lists the specimen data used in the computer analyses. The k-factor was calculated by Texas A&M from the full scale test except as noted in the figure. The yield stress (F_y) is the static yield stress calculated from the coupon test; Young's modulus (E) also comes from this test. The diameter and length were measured at the test site. The thickness is the effective wall thickness calculated from the full scale test. All analyses and data reduction were performed using these numbers unless otherwise indicated.

The remainder of the results are broken down into sections by specimen number. Each section contains the following:

1. Damage Summary.

This is a description of the damage which was included in the beam-column finite element model. Each dent or hole is identified by the number given it in the damage descriptions provided by Texas A&M. The other information given describes how it was modelled for the analysis. The dent depth or hole diameter, model segment length, distance from the loaded end of the member to the center of the damage and the angle of the damage from vertical are all provided to

show exactly where the damage was modelled on each member. The maximum out-of-straightness, if any, in either direction is also detailed.

2. DAMAGE Program Results.

The output contains several quantities defined by the geometry and the extent of the damage. The most pertinent of which is the damaged member axial capacity, shown as a maximum stress. Only a single dent or a single hole can be input as damage along with an out-of-straightness. Therefore, for members with multiple dents or holes, the damage which caused the lowest axial capacity was presented. The DAMAGE program wasn't run for members without holes, dents or out-of-straightness.

3. Compression Capacity vs. Slenderness Curve.

This graph compares the axial capacities from the full scale test, the Beam-Column FEA and the DAMAGE program (where applicable) to the capacities predicted by four different theories of buckling. Member slenderness is defined as:

$$\frac{kL}{\pi r} \sqrt{\left(\frac{F_y}{E}\right)}$$

where

k = effective length factor

L = member length

F_y = yield stress

E = Young's Modulus of Elasticity

r = radius of gyration

The four theoretical curves include the Euler buckling curve (constant over a range of slenderness and then controlled by elastic buckling), the AISC LRFD curve (calculated from the AISC Load and Resistance Factor Design equation), the AISC WS curve (representing the AISC Working Stress design equations without the factor of safety and the same as the API LRFD equations) and the W/R curve (from the Wolford-Rebholz column capacity equation). These curves don't account for dents, holes or out-of-straightness. Therefore, they give an indication of how much the capacity is reduced in members which have those types of damage. The vertical line on the graph was drawn at the corresponding slenderness for the given specimen. The capacities from the full scale test and the analyses were then plotted on this line to compare to each other and to the theoretical curves.

4. Axial Load vs. Axial Deformation Curve.

This plot shows a direct comparison between the force-deformation behavior predicted by the beam-column FEA and demonstrated by the full scale test. For members with dents, holes or out-of-straightness another curve is provided showing the predicted behavior for the member if only the corrosion were present. Also, the force-deformation behavior predicted by the DENTA-2 program is shown. In five cases the DENTA-2 program was not able to complete the analysis. Instead it displayed an error message which was thought (by Shell who provided the data) to indicate a local yielding problem. No DENTA results are shown for these cases. The design ultimate load, represented by a horizontal line on the graph, is provided as an indication of the capacity a designer might expect from the member if it were new. It was calculated using the AISC WS equations without the factor of safety. Nominal values for the wall thickness were used as were nominal values of the yield stress (36 ksi) and Young's modulus (29500 ksi). This is intended to mimic the design approach. In cases where the specimen didn't buckle or yielded locally prior to buckling, the fact is noted on these curves.

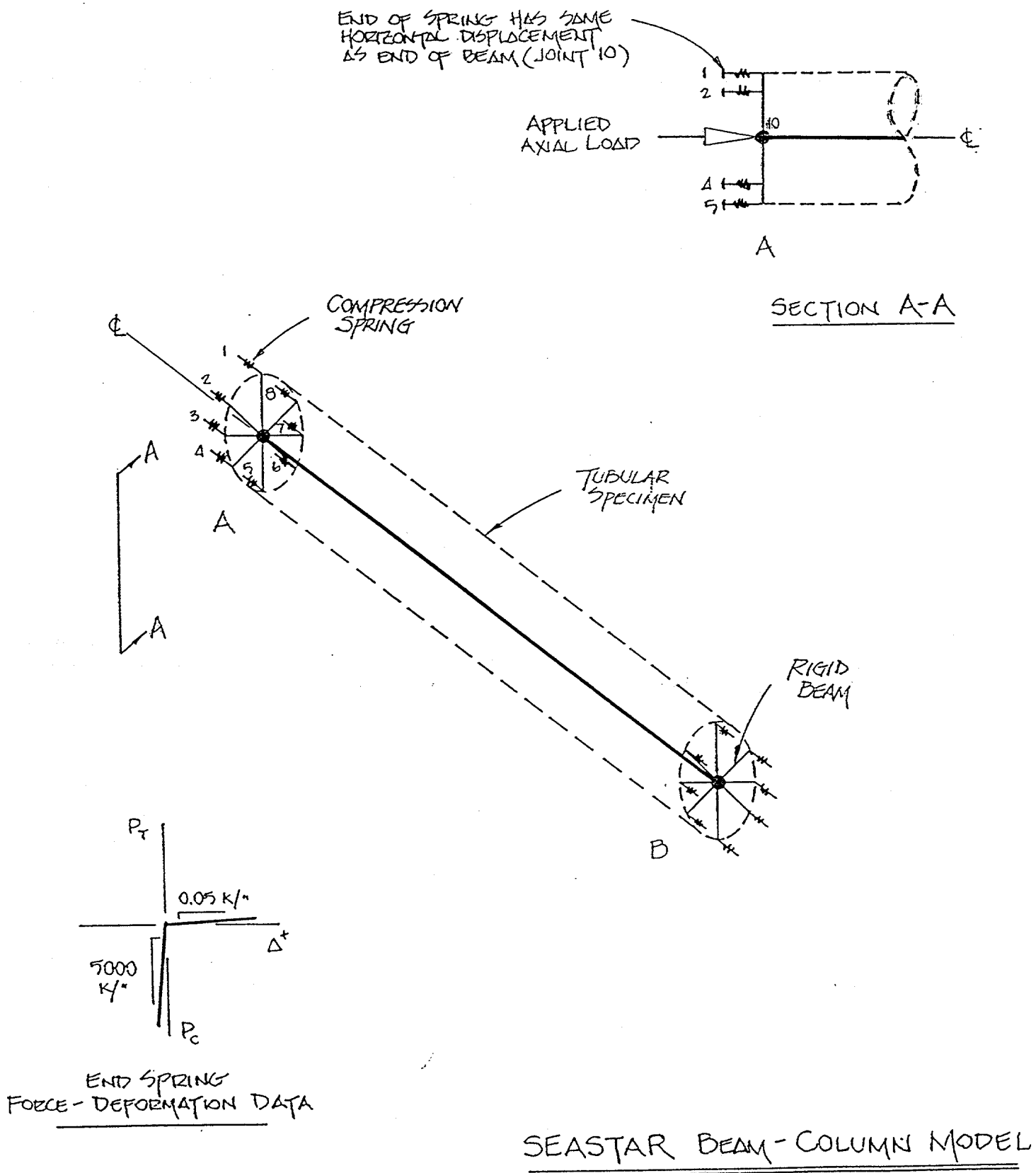


Figure 4-1

Variable Spring Stiffness

Specimen #2

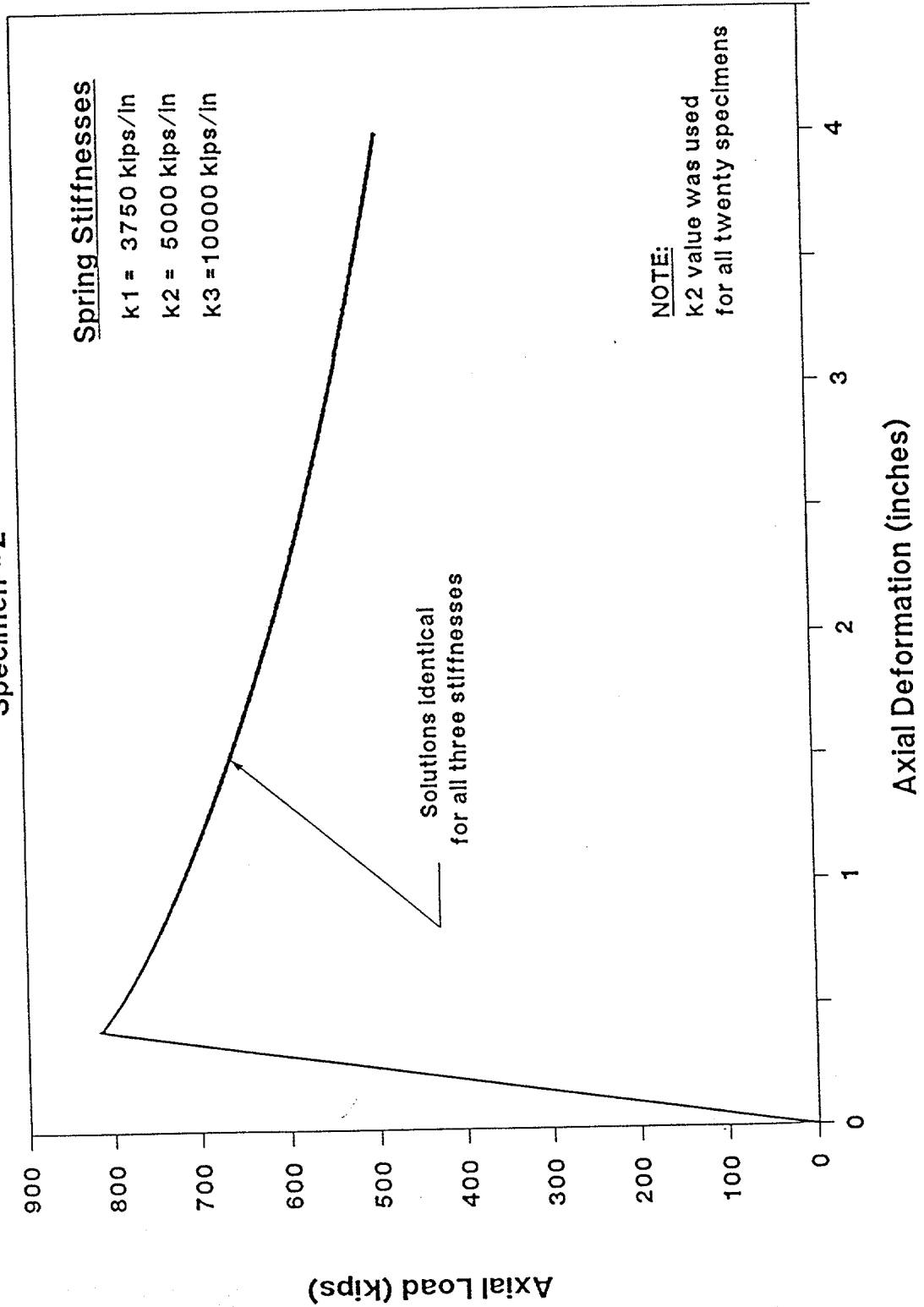


Figure 4-2

UNDAMAGED

0

-

716

2820

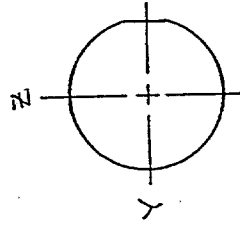
$d = 0.125"$

0.4209

4.0

670

2523



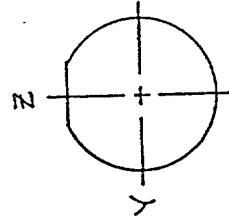
$d = 0.25"$

0.6095

8.0

651

2394



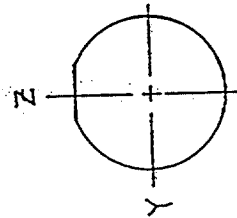
$d = 0.25"$

0.6095

6.0

651

2394



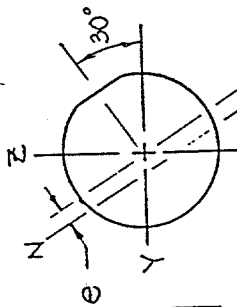
$d = 0.25"$

0.6095

5.0

651

2394



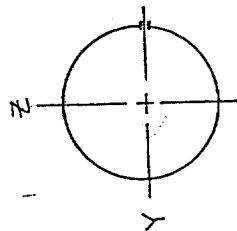
$\eta = 1.0"$

0.1034

2.0

697

2703



DAMAGE

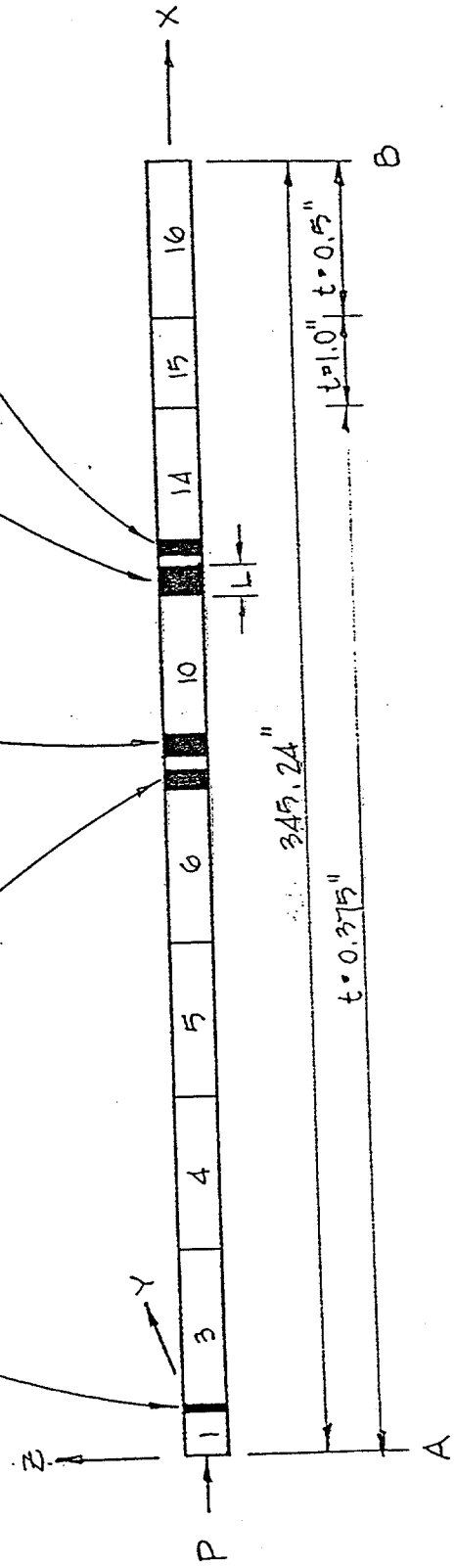
e (IN)

L' (IN)

P_p (K)

M_p (K-IN)

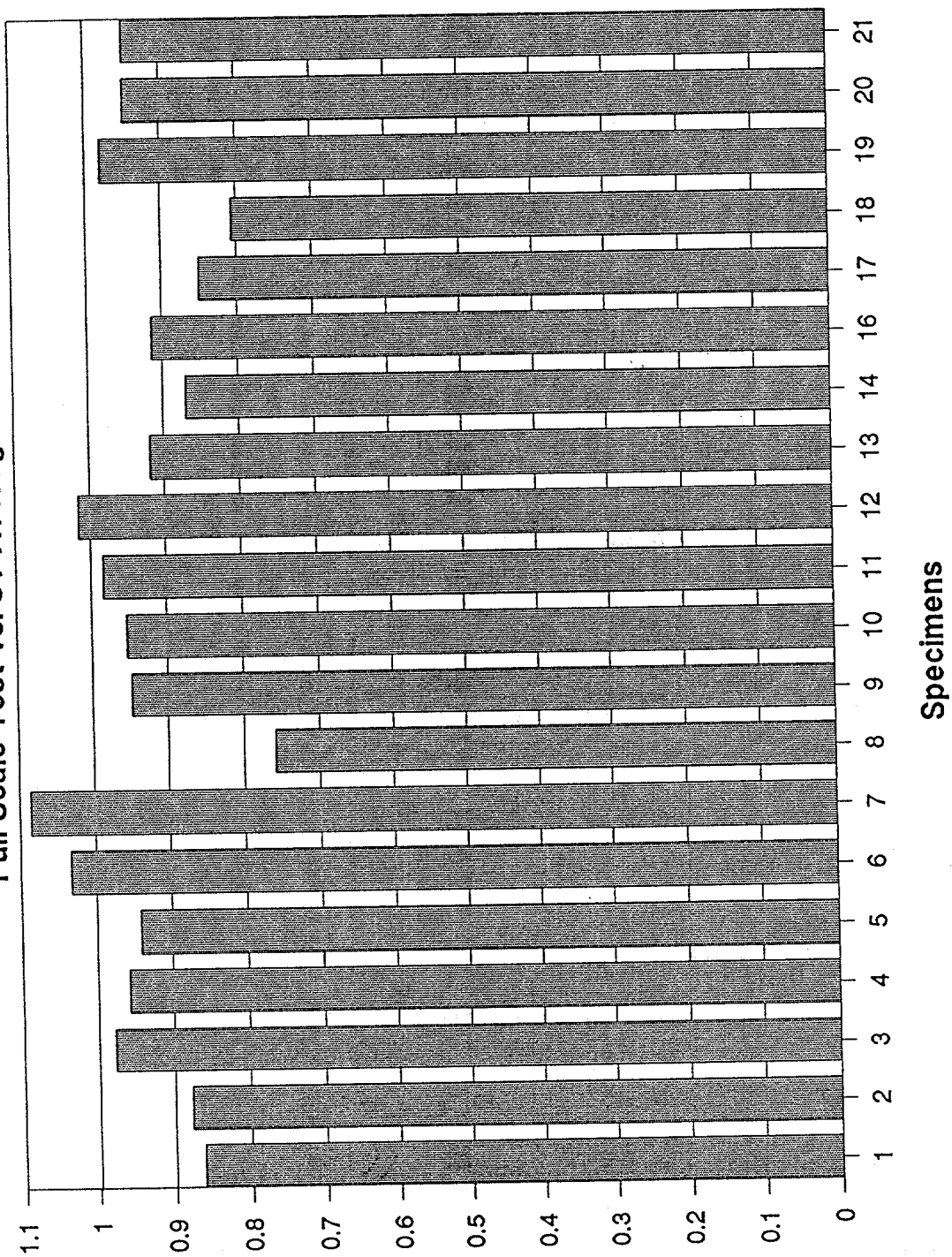
Figure 4-3



SPECIMEN 16 BEAM - COLUMN MODEL DATA

Wall Thickness Ratios

Full Scale Test vs. UT Average



Eff. t / UT t

Figure 4-4

Specimen Axial Capacity Summary

Specimen	Test	DAMAGE Program	FEA	DENTA-2	FEA/Test	DENTA/Test	Type of Damage ⁽¹⁾
1	424	401	438	493	1.03	1.16	Dent
2	601	-	816	839	1.36	1.40	None
3	436	-	609	623	1.40	1.42	None
4	410	504	553	549	1.35	1.33	OoS
5	465	456	496	555	1.07	1.19	Dent
6	1043	1118	1084	1068	1.04	1.02	None
7	548	345	410	518	0.75	0.95	Dent
8	236	241	273	370	1.16	1.56	Dent
9	558	-	586	595	1.05	1.07	None
10	692	-	718	749	1.04	1.08	None
11	374	-	424	437	1.13	1.17	None
12	299	192	319	370	1.07	1.22	Holes, Dent
13	187	162	263	256	1.41	1.37	Dents, OoS
14	198	235	329	319	1.66	1.61	Dents, OoS
16	218	287	384	324	1.76	1.48	Dents, OoS ⁽³⁾
17	420	255	368	398	0.88	0.93	Dent, OoS
18	262	199	231	269	0.88	1.02	Dents, OoS
19	614	-	940	976	1.53	1.59	Long. Crack ⁽²⁾
20	550	-	686	718	1.25	1.30	None
21	549	566	659	667	1.20	1.21	Hole, Crack ⁽²⁾

Notes:

- (1) OoS denotes out-of-straightness
- (2) Longitudinal crack not modeled in beam-column analyses or included in DAMAGE program results
- (3) Specimen has collar and different wall thicknesses to either side of collar. Nominal wall thicknesses used in the analysis.

Figure 4-5

Specimen Data Used in Computer Analyses

Specimen	k	Fy (ksi)	D (")	t (")	E(ksi)	L(")
1	0.50	35.7	18.00	0.270	25800	235.20
2	0.50	43.6	18.00	0.346	27400	265.56
3	0.50	36.6	18.00	0.305	26200	290.40
4	0.50	54.0	12.75	0.314	28000	416.75
5	0.50	35.9	18.00	0.303	26300	222.24
6	0.86	36.5	20.00	0.500	28300	474.00
7	0.50	50.0	12.75	0.409	29200	473.50
8	0.50	39.2	10.75	0.293	29400	319.56
9	0.54	39.6	14.00	0.358	29600	264.48
10	0.52	42.0	14.00	0.425	25900	379.25
11	0.50	39.0	10.75	0.350	27300	347.52
12	0.50	60.0	12.75	0.351	28600	474.00
13	0.54	53.7	12.75	0.323	30000	289.56
14	0.50	36.0	12.75	0.295	29300	201.00
16	0.62	49.1	12.75	0.375	29000	345.24
17	0.52	49.2	12.75	0.422	25000	374.04
18	0.50	34.5	10.75	0.264	24900	204.96
19	0.50	59.7	16.00	0.338	27700	447.25
20	0.50	57.4	12.75	0.328	28000	416.00
21	0.50	52.2	16.00	0.275	25900	267.96

Note: The data shown above was used in all the computer analyses and data reduction for this study. Unless otherwise noted, when these characteristics are referred to (in the text or on plots and tables) these are the values indicated

For specimens 1, 2, 3, 5, 8, 14, 18, 19 and 21 the effective length wasn't calculated do to local yielding prior to buckling or the fact that the member never buckled. A factor of 0.5 was used for these specimens.

Figure 4-6

SPECIMEN #1

Damage Summary
Specimen #1

A&M Damage Number

Damage Description

2

Dent:

Depth = 0.5"

Model Segment Length = 8"

Distance from loaded end = 197.20"

Angle from vertical = 127°

*Angle from vertical is clockwise from +Z axis
looking from the loaded end toward the opposite end
of the member

Compression Capacity vs Slenderness

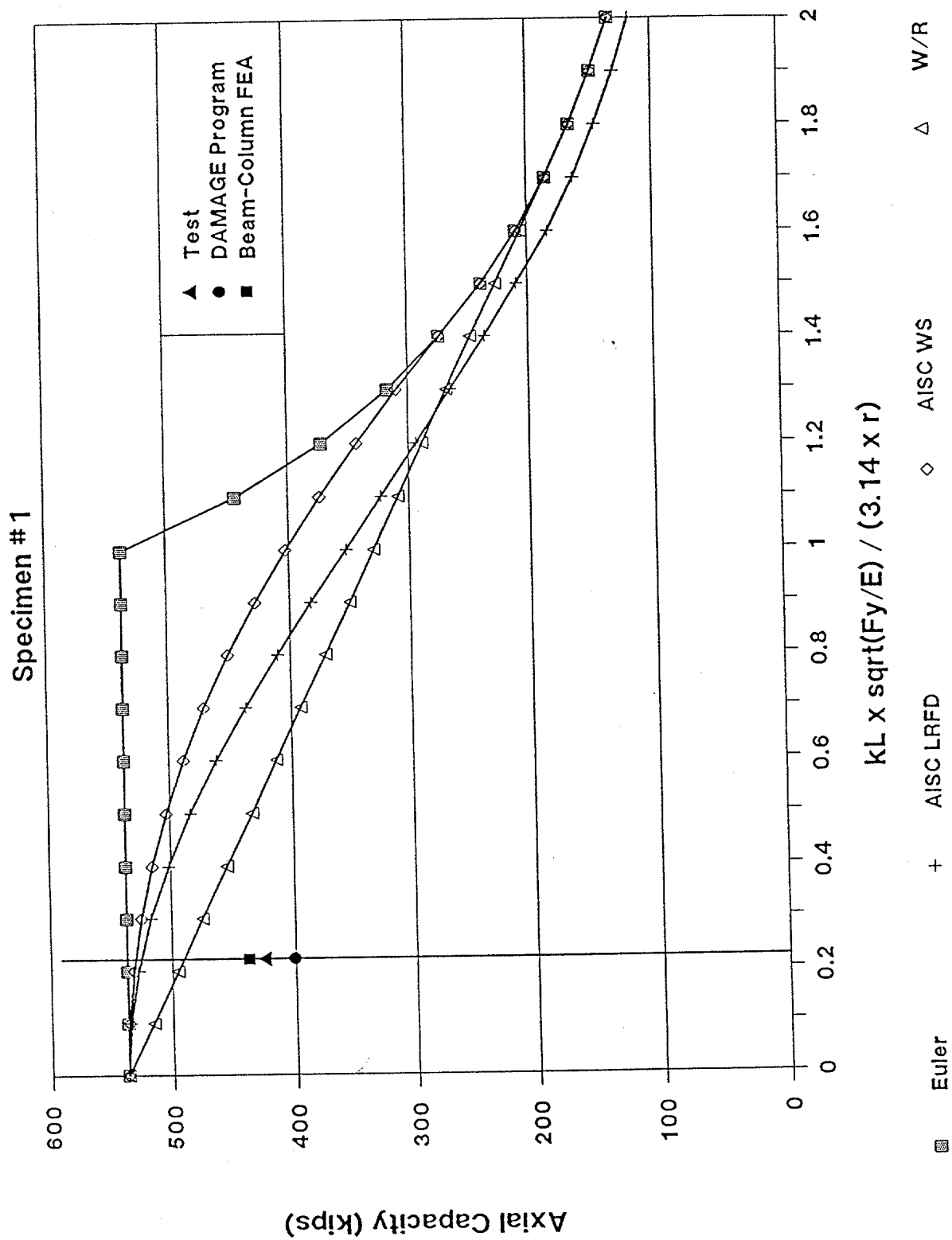


Figure 4-9

Specimen #1

Axial Load vs. Axial Deformation

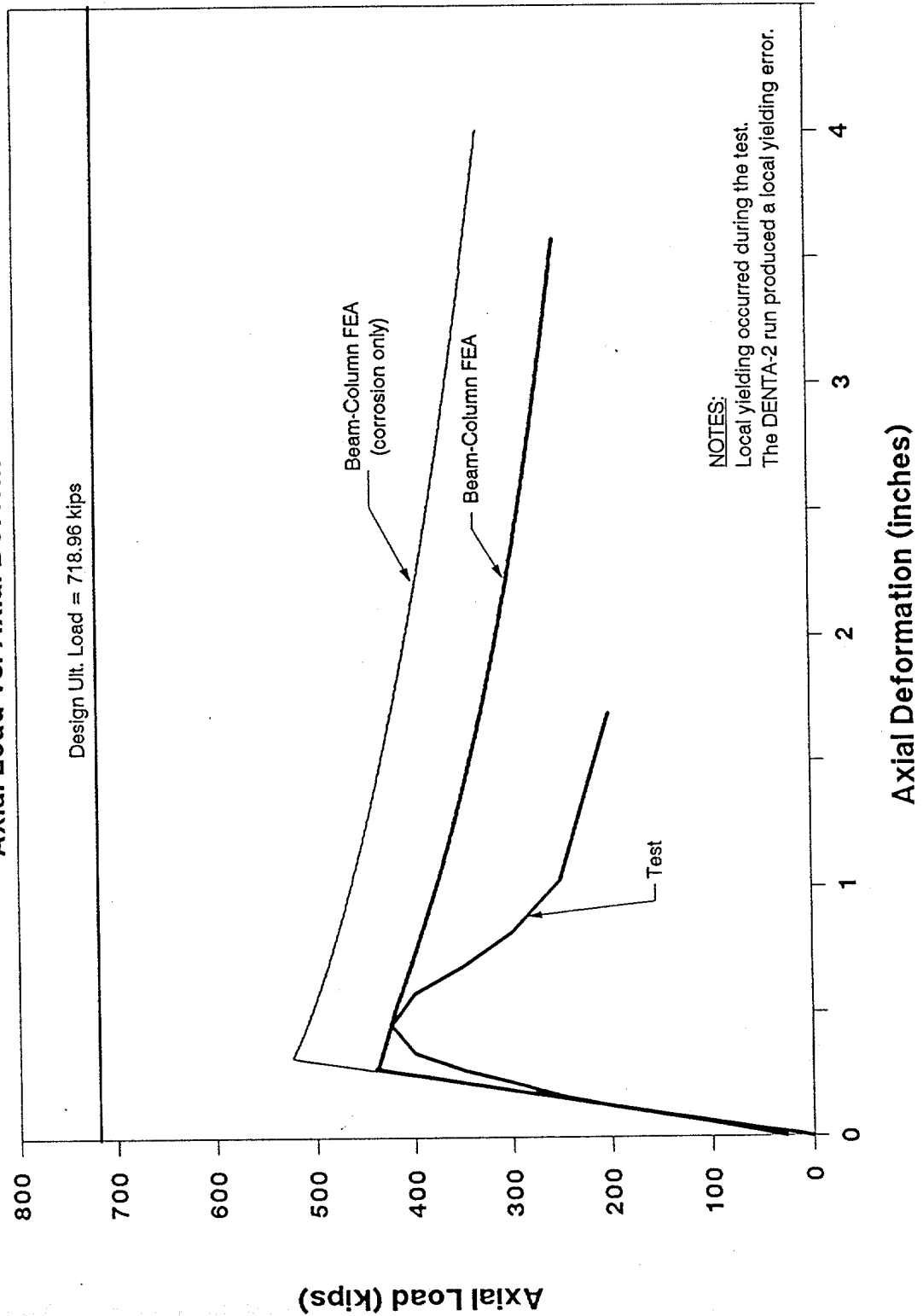


Figure 4-10

SPECIMEN #2

Damage Summary
Specimen #2

A&M Damage Number

Damage Description

No Damage

Compression Capacity vs Slenderness

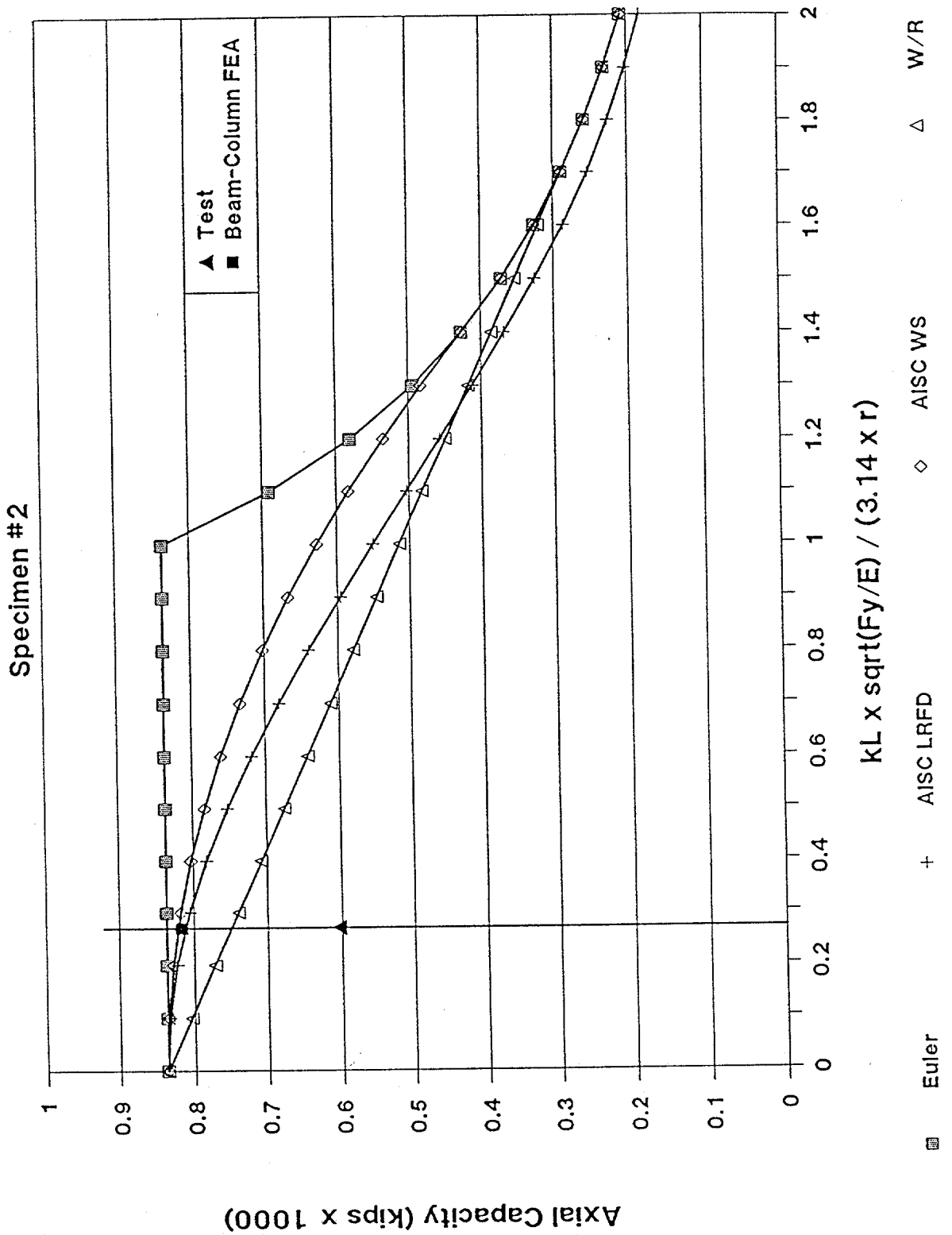


Figure 4-12

Specimen #2

Axial Load vs. Axial Deformation

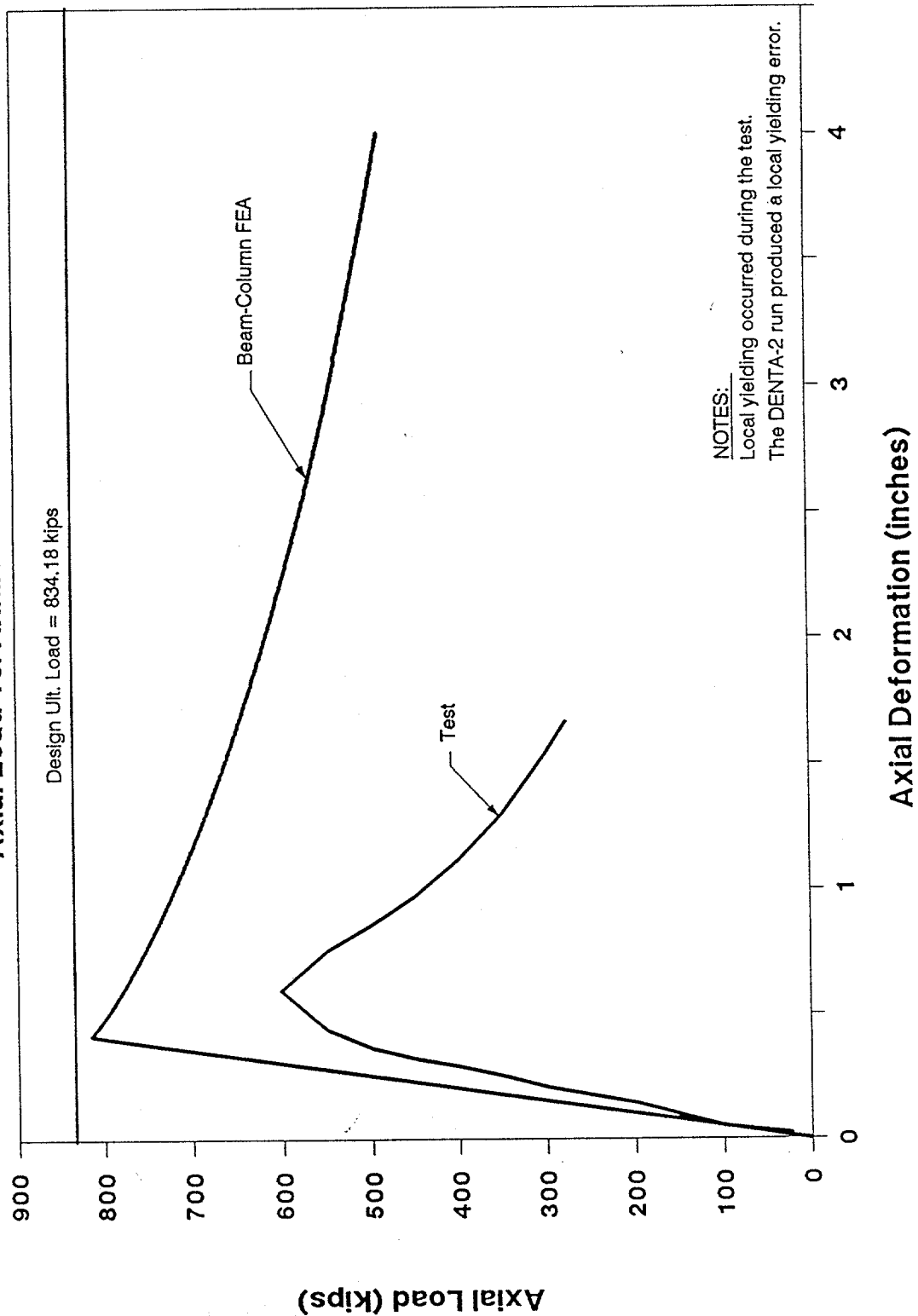


Figure 4-13

SPECIMEN . 3

Damage Summary
Specimen #3

A&M Damage Number

Damage Description

No Damage

Compression Capacity vs Slenderness

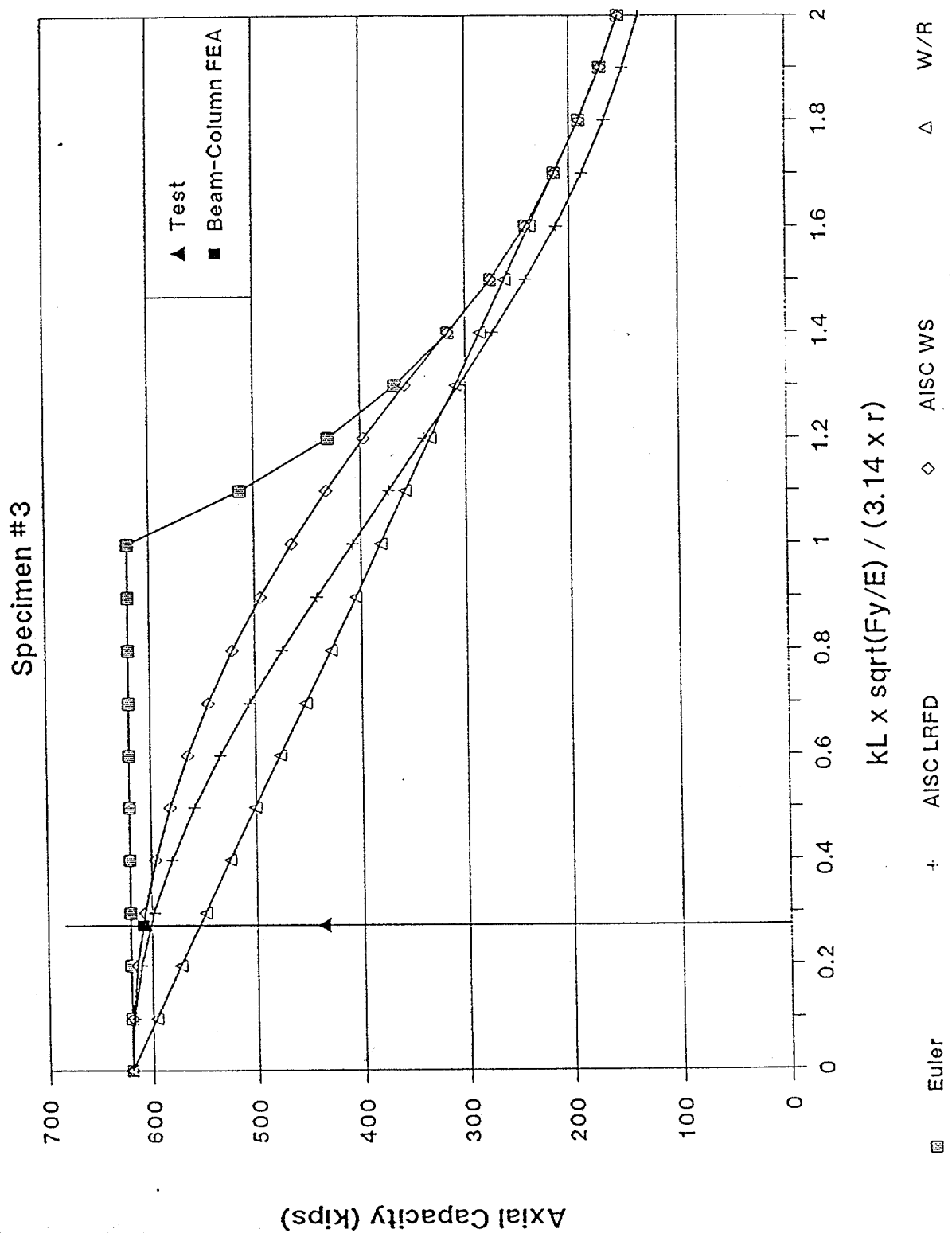


Figure 4-15

Specimen #3

Axial Load vs. Axial Deformation

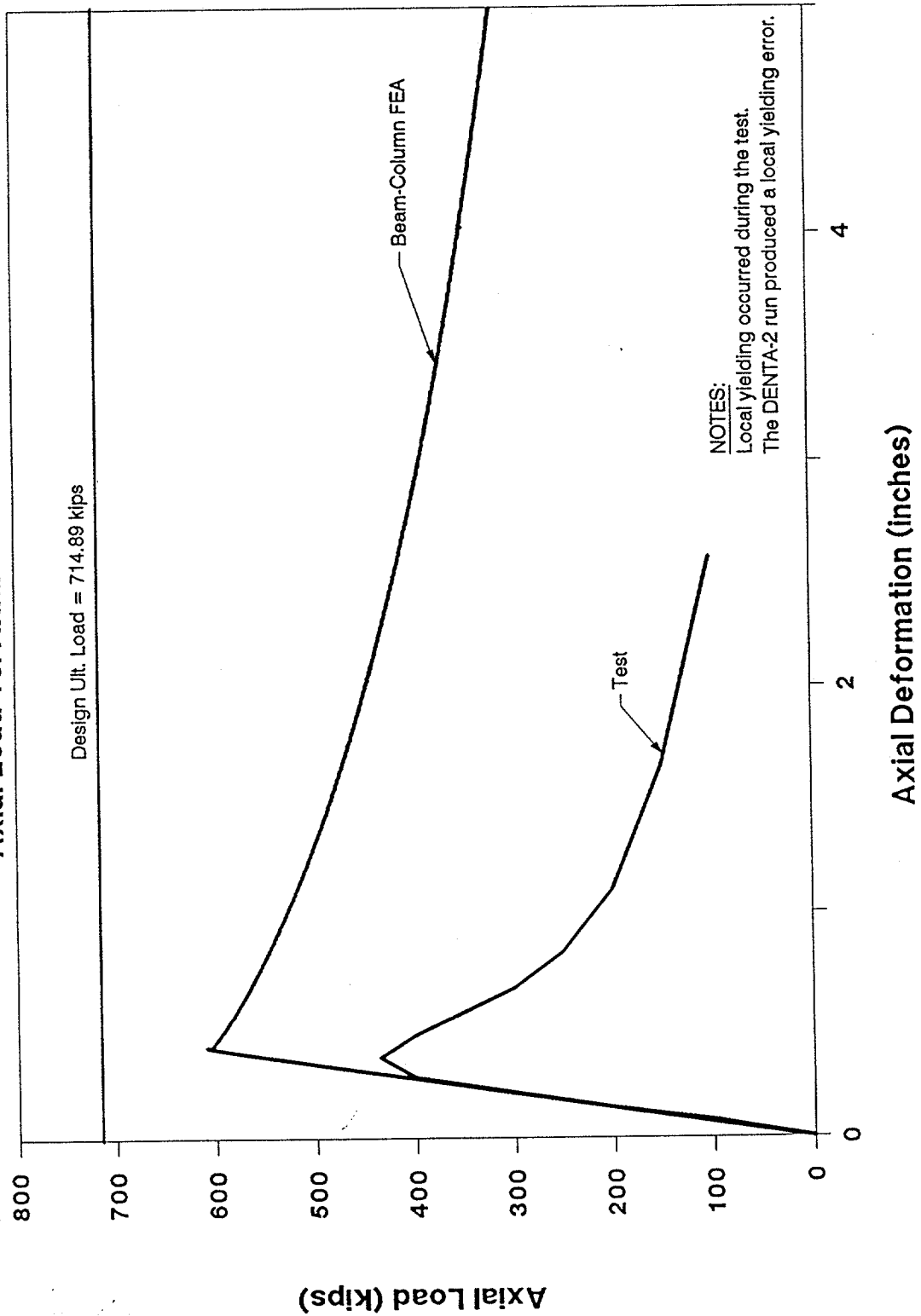


Figure 4-16

SPECIMEN 4

Damage Summary
Specimen #4

A&M Damage Number

Damage Description

None

Out of Straightness:

Direction: -Z

Maximum Deflection = 1.3125"

```

*****
*                                     *
*               Program DAMAGE       *
*                                     *
*****

```

TITLE: SPECIMEN #4

INPUT:

```

OUTSIDE DIAMETER (in) = 12.750
THICKNESS (in)       = .314
LENGTH (ft)         = 34.730
EFF. LENGTH FACTOR   = .50

YIELD STRESS (ksi)   = 54.00
YOUNGS MODULUS (ksi) = 28000.0

DENT DEPTH (in)      = .000
HOLE DIAMETER (in)   = .000
LAT. DISPL. (in)     = 1.31

```

RESULTS:

```

CROSS-SECTIONAL AREA (sq.in) = 12.27
DENT/HOLE ANGLE (rad)         = 6.28319
AXIAL ECCENTRICITY (in)       = .0000
REDUCED RAD. OF GYRATION (cu.in) = 4.397
REDUCED ELAS. SECTION MOD. (cu.in) = 38.140
PLASTIFICATION STRESS (ksi)    = 54.000
AVG. SQUASH STRESS (ksi)      = 54.000
IMPERFECTION PARAMETER        = .00519
SLENDERNESS RATIO             = 40.23994
EULER BUCKLING STRESS (ksi)    = 123.1102
SOLUTION ROOTS (SDCE1,SDCE2) (ksi) = 161.693 41.115

DAMAGED MEMBER AXIAL CAPACITY (ksi) = 41.115
DAMAGED/UNDAMAGED STRESS RATIO      = .76138
UNDAMAGED SLENDERNESS RATIO         = .66229

```

Notes:

- (1) Hole diameter and dent depth should be measured w/r the tubular mid-wall diameter.
- (2) For dented members it is assumed that the maximum stress the dented region can sustain is equal to the plastification stress. This stress is set equal to zero for hole damage.
- (3) Dent and hole damage must be evaluated separately. Either can be assessed in conjunction with bending damage.

Compression Capacity vs Slenderness

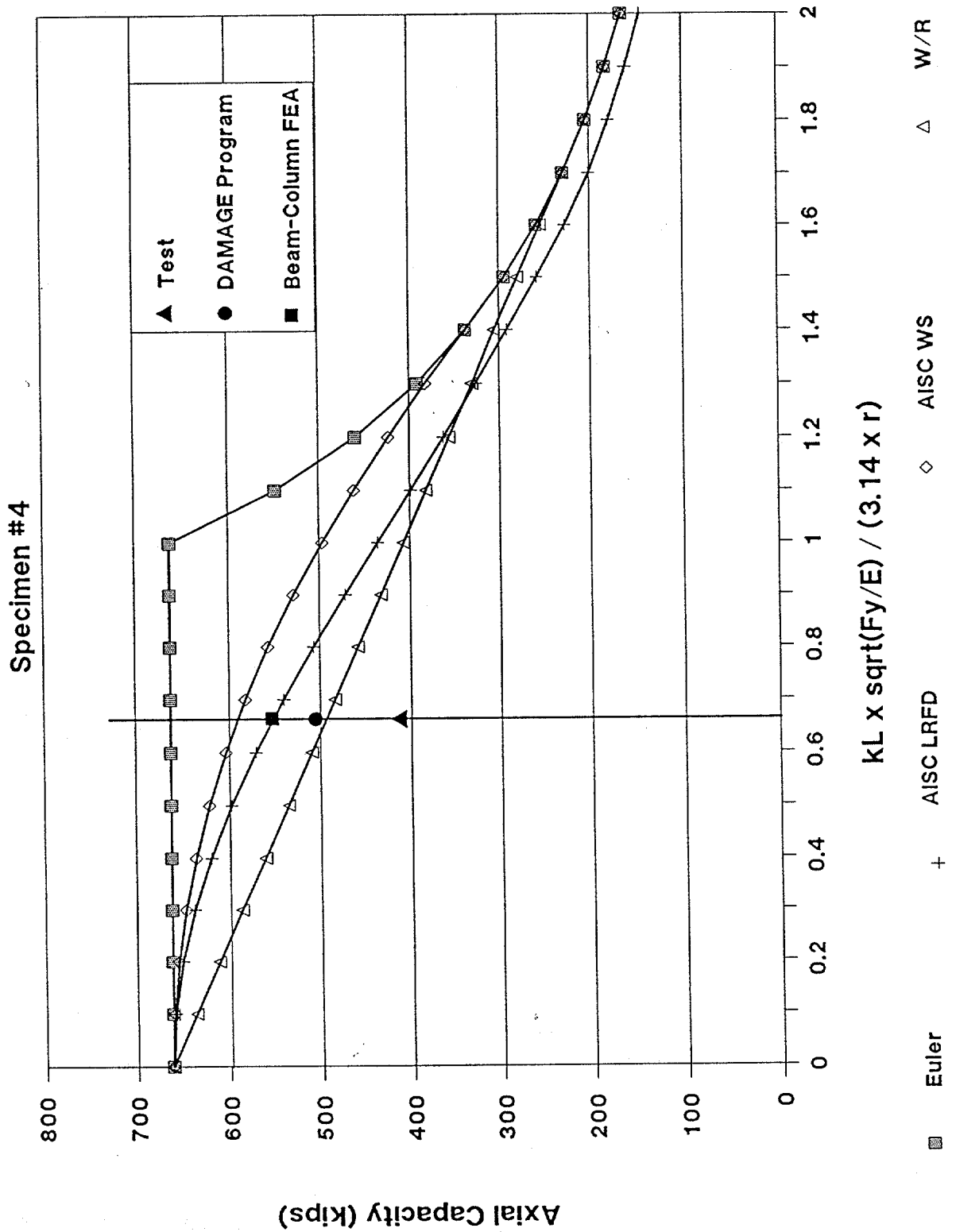


Figure 4-19

Specimen #4

Axial Load vs. Axial Deformation

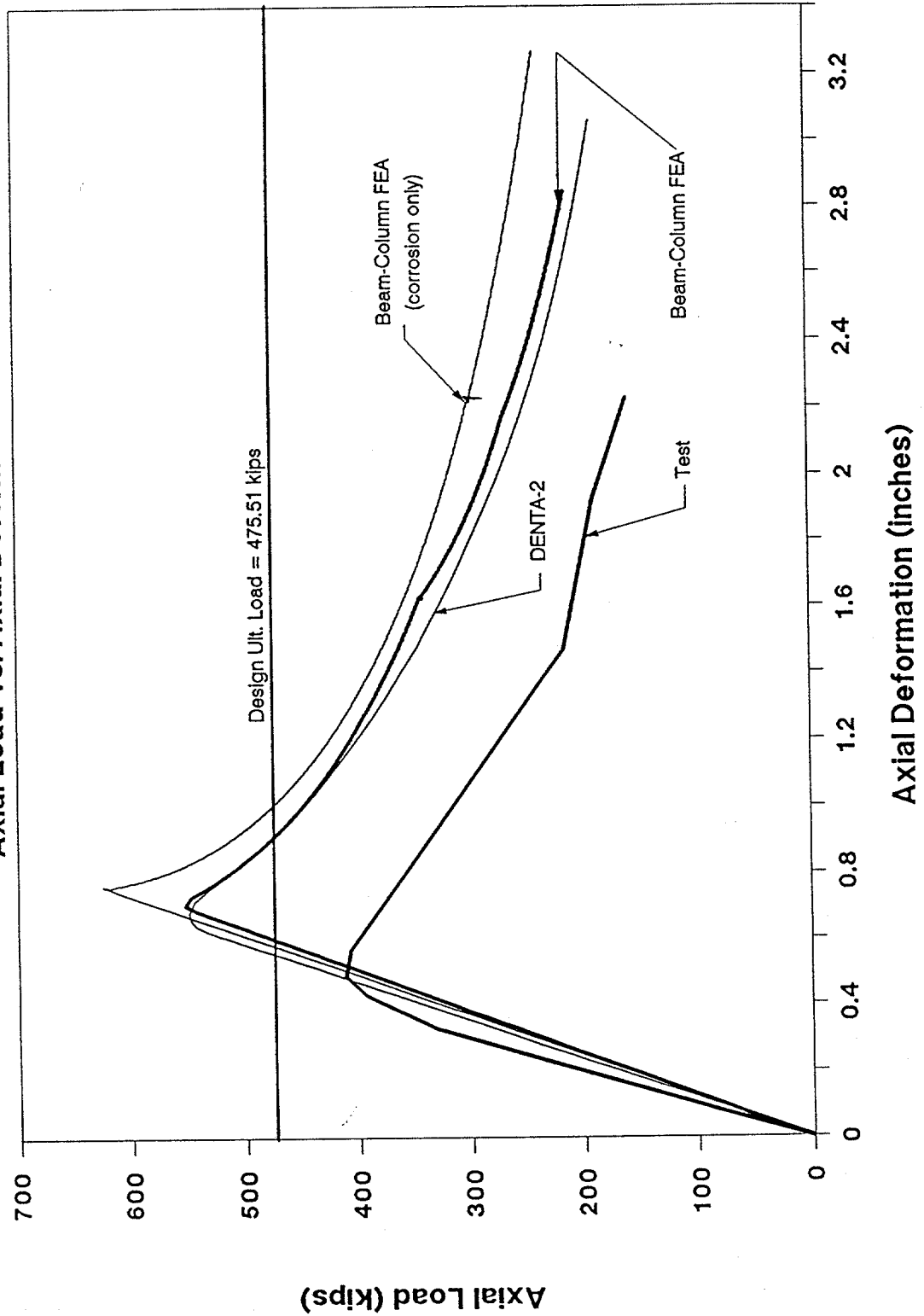


Figure 4-20

SPECIMEN #5

Damage Summary
Specimen #5

A&M Damage Number

Damage Description

10

Dent:

Depth = 0.5"

Model Segment Length = 8.5"

Distance from loaded end = 154.87"

Angle from vertical = 180°

*Angle from vertical is clockwise from +Z axis
looking from the loaded end toward the opposite end
of the member

```

*****
*
*           Program DAMAGE
*
*
*****

```

TITLE: Specimen #5

INPUT:

```

OUTSIDE DIAMETER (in) = 18.000
THICKNESS (in)       =  .303
LENGTH (ft)         = 18.520
EFF. LENGTH FACTOR   =  .50

YIELD STRESS (ksi)   =  35.90
YOUNGS MODULUS (ksi) = 26300.0

DENT DEPTH (in)      =  .500
HOLE DIAMETER (in)   =  .000
LAT. DISPL. (in)     =  .00

```

RESULTS:

```

CROSS-SECTIONAL AREA (sq.in) = 16.85
DENT/HOLE ANGLE (rad)        = 5.61084
AXIAL ECCENTRICITY (in)      = 1.0405
REDUCED RAD. OF GYRATION (cu.in) = 5.807
REDUCED ELAS. SECTION MOD. (cu.in) = 54.027
PLASTIFICATION STRESS (ksi)   = 7.776
AVG. SQUASH STRESS (ksi)     = 32.890
IMPERFECTION PARAMETER      = .00024
SLENDERNESS RATIO           = 10.63276
EULER BUCKLING STRESS (ksi)   = 823.2053
SOLUTION ROOTS (SDCE1,SDCE2) (ksi) = 1069.641 27.046

DAMAGED MEMBER AXIAL CAPACITY (ksi) = 27.046
DAMAGED/UNDAMAGED STRESS RATIO      = .75338
UNDAMAGED SLENDERNESS RATIO         = .20883

```

Notes:

- (1) Hole diameter and dent depth should be measured w/r the tubular mid-wall diameter.
- (2) For dented members it is assumed that the maximum stress the dented region can sustain is equal to the plastification stress. This stress is set equal to zero for hole damage.
- (3) Dent and hole damage must be evaluated separately. Either can be assessed in conjunction with bending damage.

Compression Capacity vs Slenderness

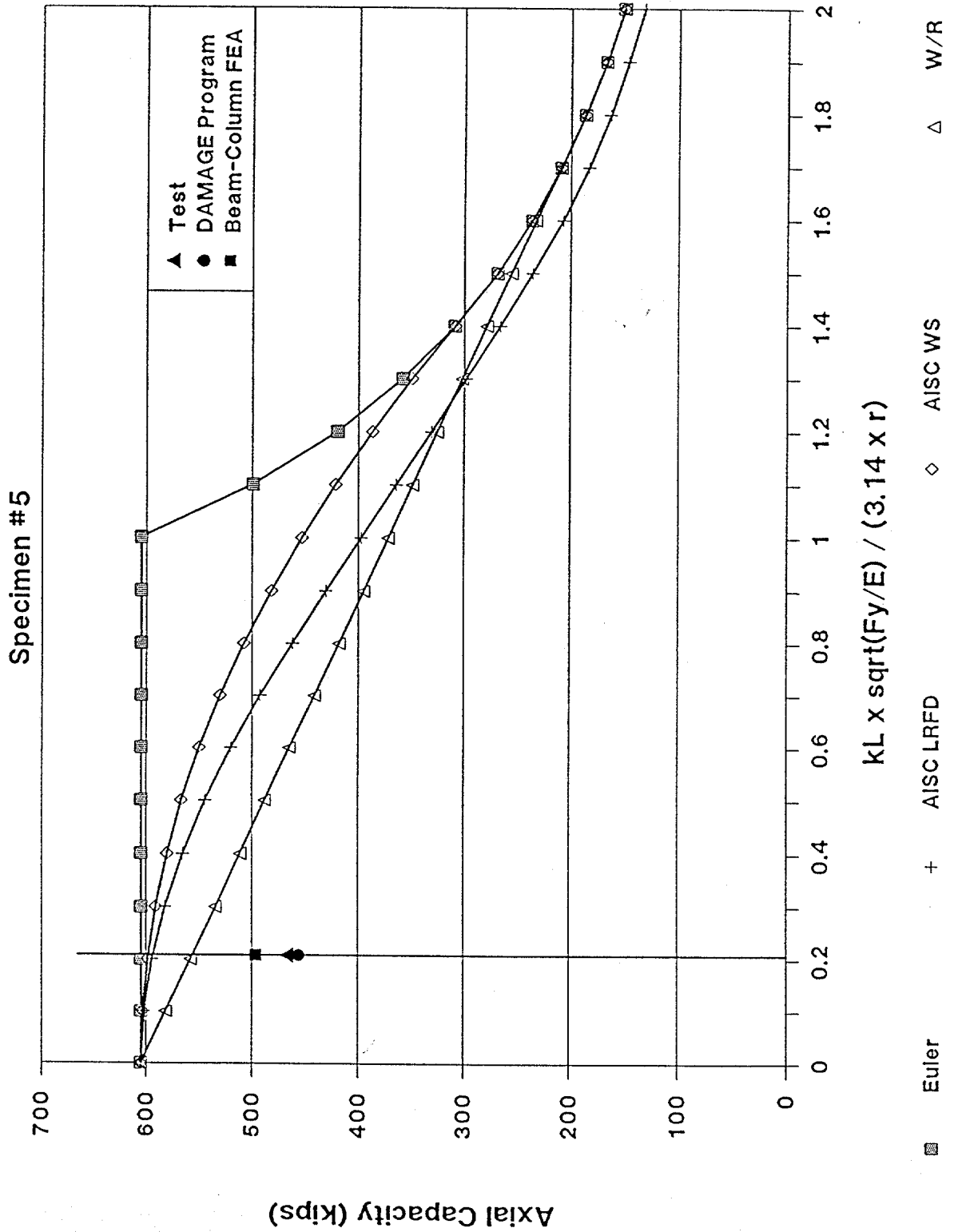


Figure 4-23

Specimen #5

Axial Load vs. Axial Deformation

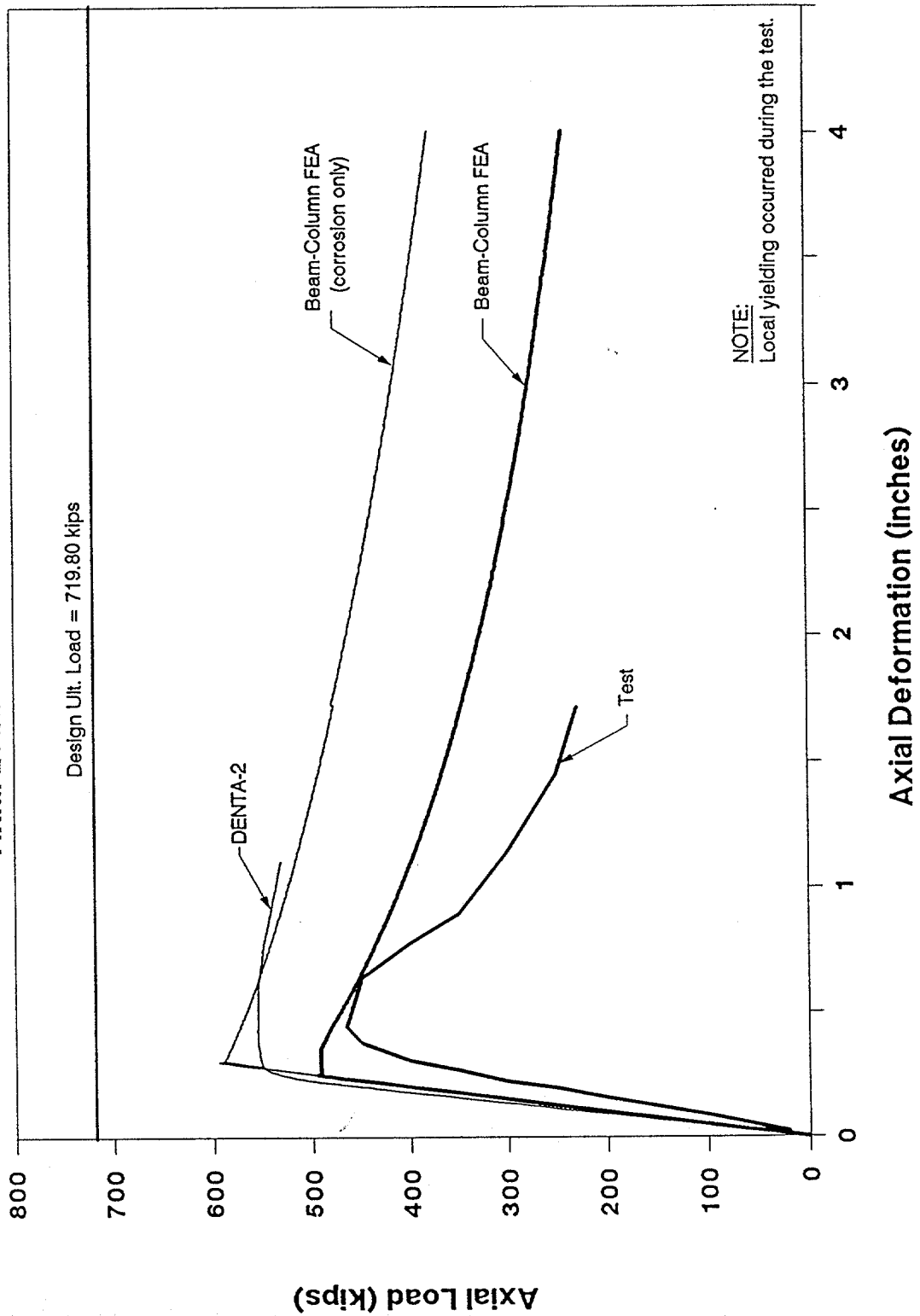


Figure 4-24

SPECIMEN 6

Damage Summary
Specimen #6

A&M Damage Number

Damage Description

No Damage

```

*****
*                                     *
*               Program DAMAGE       *
*                                     *
*****

```

TITLE: SPECIMEN #6

INPUT:

OUTSIDE DIAMETER (in) = 20.000
 THICKNESS (in) = .507
 LENGTH (ft) = 39.500
 EFF. LENGTH FACTOR = .86

YIELD STRESS (ksi) = 36.50
 YOUNGS MODULUS (ksi) = 28300.0

DENT DEPTH (in) = .000
 HOLE DIAMETER (in) = .000
 LAT. DISPL. (in) = .00

RESULTS:

CROSS-SECTIONAL AREA (sq.in) = 31.05
 DENT/HOLE ANGLE (rad) = 6.28319
 AXIAL ECCENTRICITY (in) = .0000
 REDUCED RAD. OF GYRATION (cu.in) = 6.892
 REDUCED ELAS. SECTION MOD. (cu.in) = 151.306
 PLASTIFICATION STRESS (ksi) = 36.500
 AVG. SQUASH STRESS (ksi) = 36.500
 IMPERFECTION PARAMETER = .00017
 SLENDERNESS RATIO = 44.10228
 EULER BUCKLING STRESS (ksi) = 79.8902
 SOLUTION ROOTS (SDCE1,SDCE2) (ksi) = 81.009 35.996

 DAMAGED MEMBER AXIAL CAPACITY (ksi) = 35.996
 DAMAGED/UNDAMAGED STRESS RATIO = .98618
 UNDAMAGED SLENDERNESS RATIO = .67593

Notes:

- (1) Hole diameter and dent depth should be measured w/r the tubular mid-wall diameter.
- (2) For dented members it is assumed that the maximum stress the dented region can sustain is equal to the plastification stress. This stress is set equal to zero for hole damage.
- (3) Dent and hole damage must be evaluated separately. Either can be assessed in conjunction with bending damage.

Compression Capacity vs Slenderness

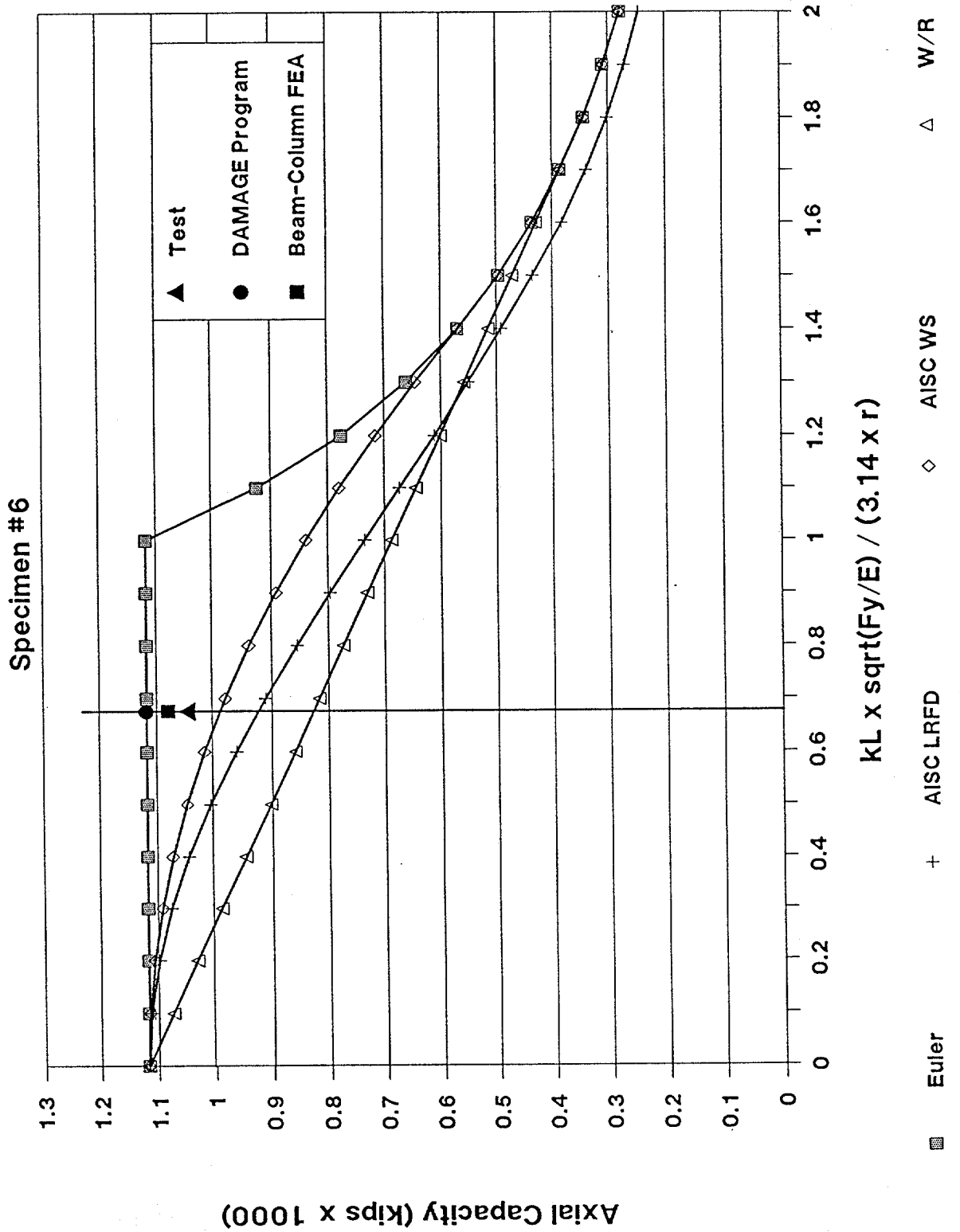


Figure 4-27

Specimen #6

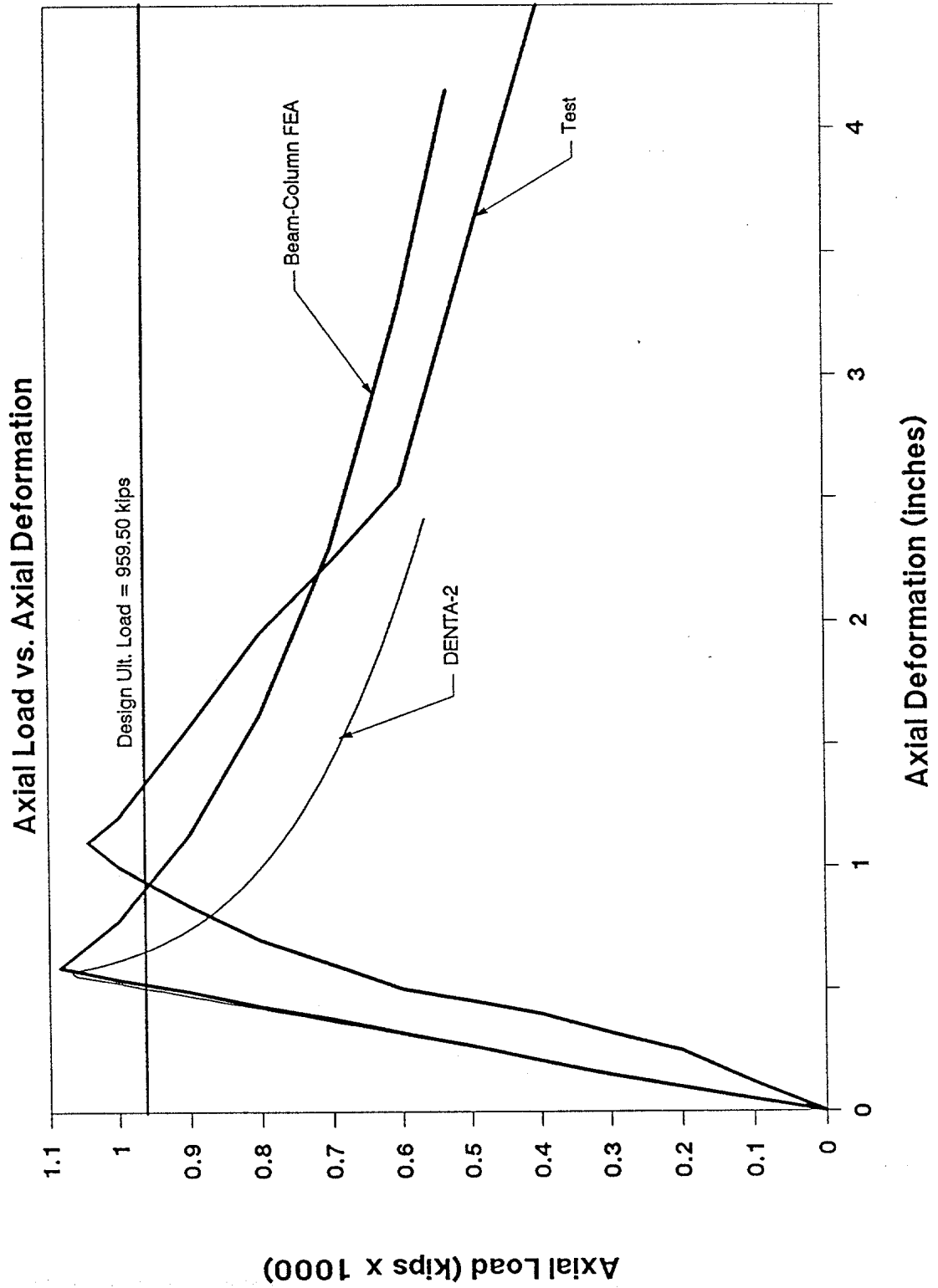


Figure 4-28

SPECIMEN 7

Damage Summary
Specimen #7

A&M Damage Number

Damage Description

6

Dent:

Depth = 1.5"

Model Segment Length = 15"

Distance from loaded end = 243.75"

Angle from vertical = 81°

*Angle from vertical is clockwise from +Z axis
looking from the loaded end toward the opposite end
of the member

```

*****
*                                     *
*               Program DAMAGE       *
*                                     *
*****

```

TITLE: SPECIMEN #7

INPUT:

OUTSIDE DIAMETER (in) = 12.750
 THICKNESS (in) = .409
 LENGTH (ft) = 39.460
 EFF. LENGTH FACTOR = .50

YIELD STRESS (ksi) = 50.00
 YOUNGS MODULUS (ksi) = 29200.0

DENT DEPTH (in) = 1.500
 HOLE DIAMETER (in) = .000
 LAT. DISPL. (in) = .00

RESULTS:

CROSS-SECTIONAL AREA (sq.in)	=	15.86	
DENT/HOLE ANGLE (rad)	=	4.88865	
AXIAL ECCENTRICITY (in)	=	1.6210	
REDUCED RAD. OF GYRATION (cu.in)	=	3.546	
REDUCED ELAS. SECTION MOD. (cu.in)	=	24.662	
PLASTIFICATION STRESS (ksi)	=	5.060	
AVG. SQUASH STRESS (ksi)	=	40.026	
IMPERFECTION PARAMETER	=	.00054	
SLENDERNES RATIO	=	59.17118	
EULER BUCKLING STRESS (ksi)	=	97.9836	
SOLUTION ROOTS (SDCE1,SDCE2) (ksi)	=	198.884	21.741
DAMAGED MEMBER AXIAL CAPACITY (ksi)	=	21.741	
DAMAGED/UNDAMAGED STRESS RATIO	=	.43482	
UNDAMAGED SLENDERNES RATIO	=	.71435	

Notes:

- (1) Hole diameter and dent depth should be measured w/r the tubular mid-wall diameter.
- (2) For dented members it is assumed that the maximum stress the dented region can sustain is equal to the plastification stress. This stress is set equal to zero for hole damage.
- (3) Dent and hole damage must be evaluated separately. Either can be assessed in conjunction with bending damage.

Compression Capacity vs Slenderness

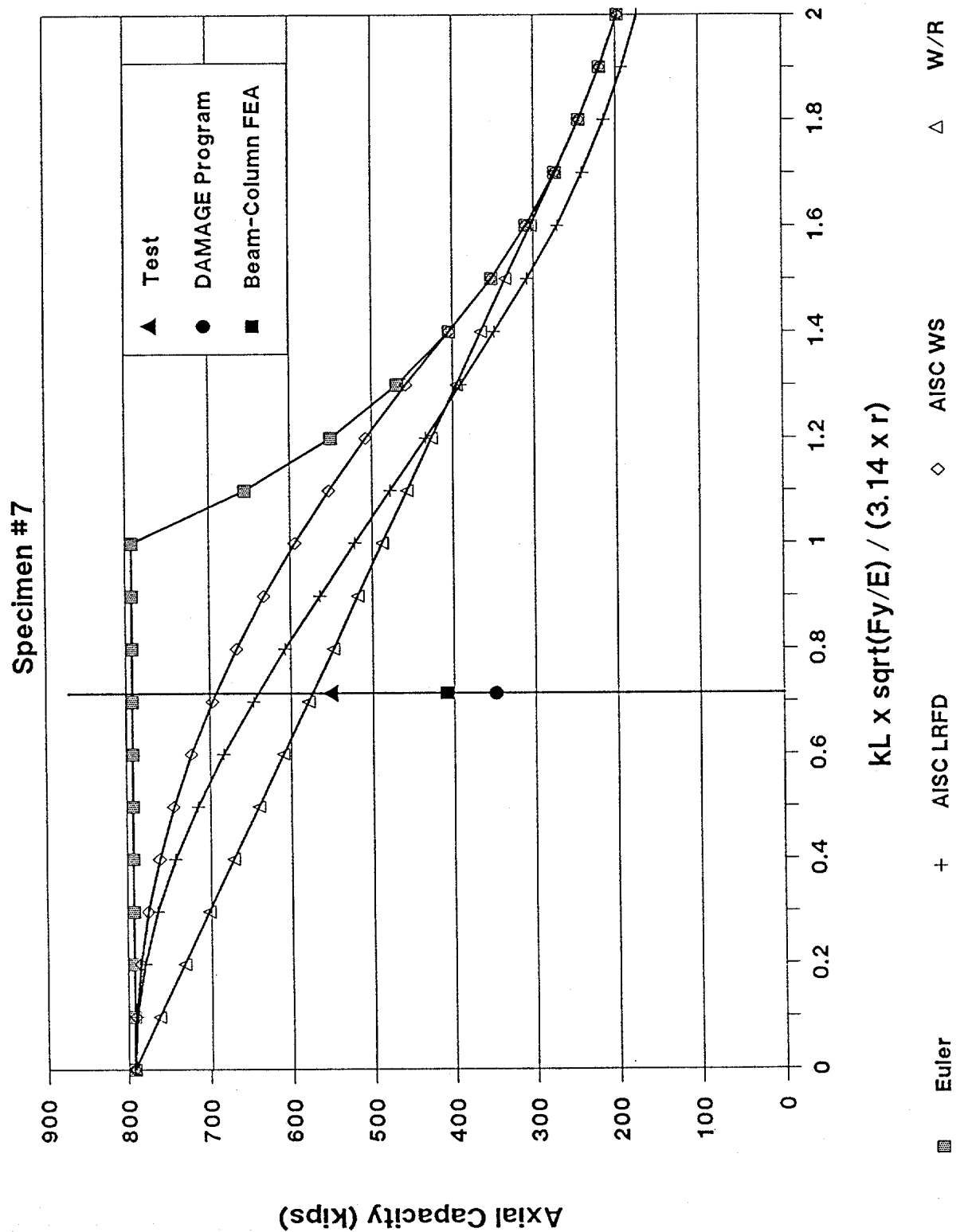


Figure 4-31

Specimen #7

Axial Load vs. Axial Deformation

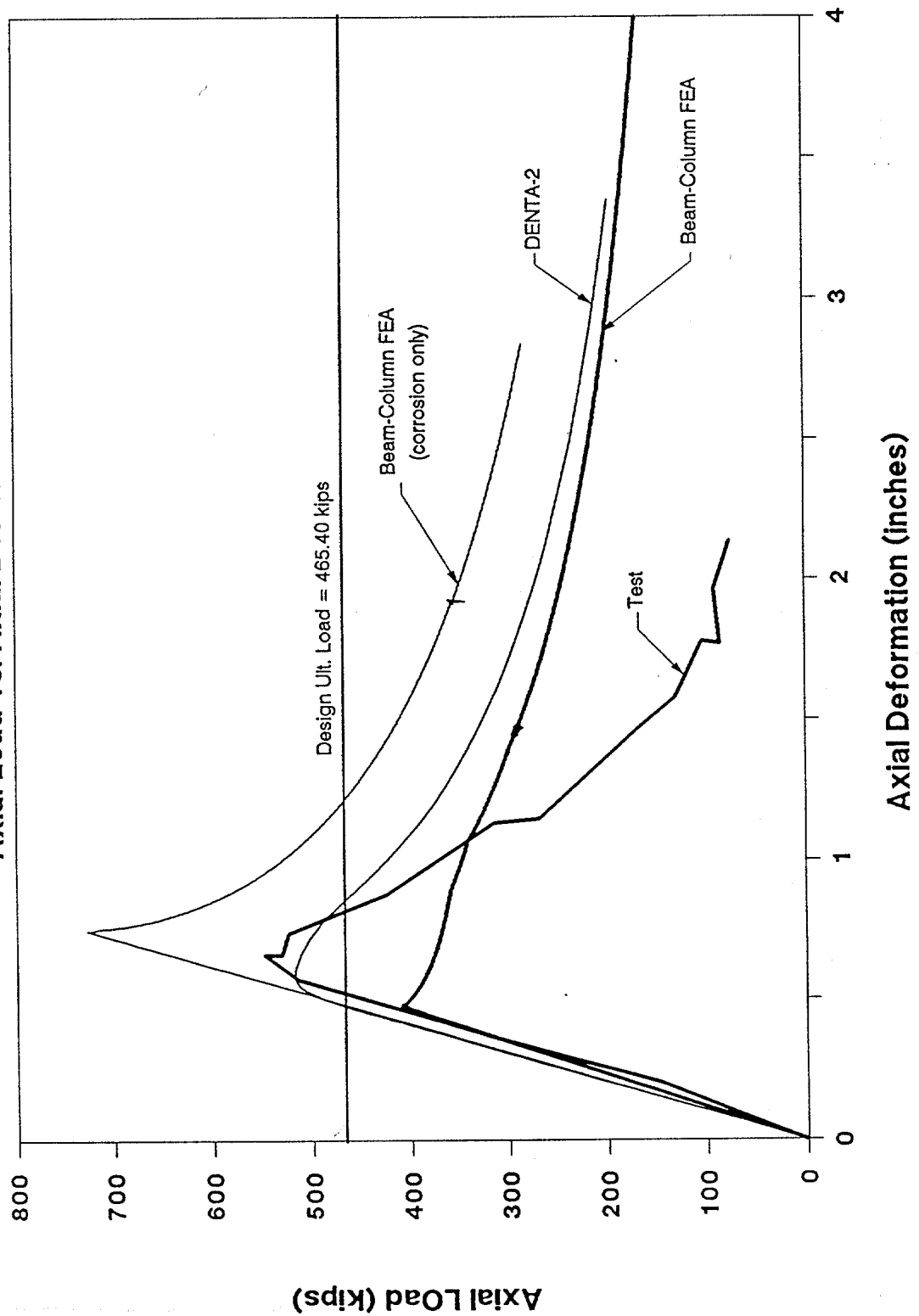


Figure 4-32

SPECIMEN 8

Damage Summary
Specimen #8

A&M Damage Number

Damage Description

2

Dent:

Depth = 0.25"

Model Segment Length = 5"

Distance from loaded end = 275.57"

Angle from vertical = 64°

*Angle from vertical is clockwise from +Z axis
looking from the loaded end toward the opposite end
of the member


```

*****
*
*                               Program DAMAGE
*
*****

```

TITLE: Specimen #8 - Damage #2

INPUT:

OUTSIDE DIAMETER (in) = 10.750
 THICKNESS (in) = .239
 LENGTH (ft) = 26.630
 EFF. LENGTH FACTOR = .50

YIELD STRESS (ksi) = 39.20
 YOUNGS MODULUS (ksi) = 29400.0

DENT DEPTH (in) = .250
 HOLE DIAMETER (in) = .000
 LAT. DISPL. (in) = .00

RESULTS:

CROSS-SECTIONAL AREA (sq.in)	=	7.89	
DENT/HOLE ANGLE (rad)	=	5.66630	
AXIAL ECCENTRICITY (in)	=	.5631	
REDUCED RAD. OF GYRATION (cu.in)	=	3.476	
REDUCED ELAS. SECTION MOD. (cu.in)	=	15.443	
PLASTIFICATION STRESS (ksi)	=	12.601	
AVG. SQUASH STRESS (ksi)	=	36.588	
IMPERFECTION PARAMETER	=	.00021	
SLENDERNESS RATIO	=	37.36209	
EULER BUCKLING STRESS (ksi)	=	157.0452	
SOLUTION ROOTS (SDCE1,SDCE2) (ksi)	=	205.123	30.517
DAMAGED MEMBER AXIAL CAPACITY (ksi)	=	30.517	
DAMAGED/UNDAMAGED STRESS RATIO	=	.77848	
UNDAMAGED SLENDERNESS RATIO	=	.49961	

Notes:

- (1) Hole diameter and dent depth should be measured w/r the tubular mid-wall diameter.
- (2) For dented members it is assumed that the maximum stress the dented region can sustain is equal to the plastification stress. This stress is set equal to zero for hole damage.
- (3) Dent and hole damage must be evaluated separately. Either can be assessed in conjunction with bending damage.

Compression Capacity vs Slenderness

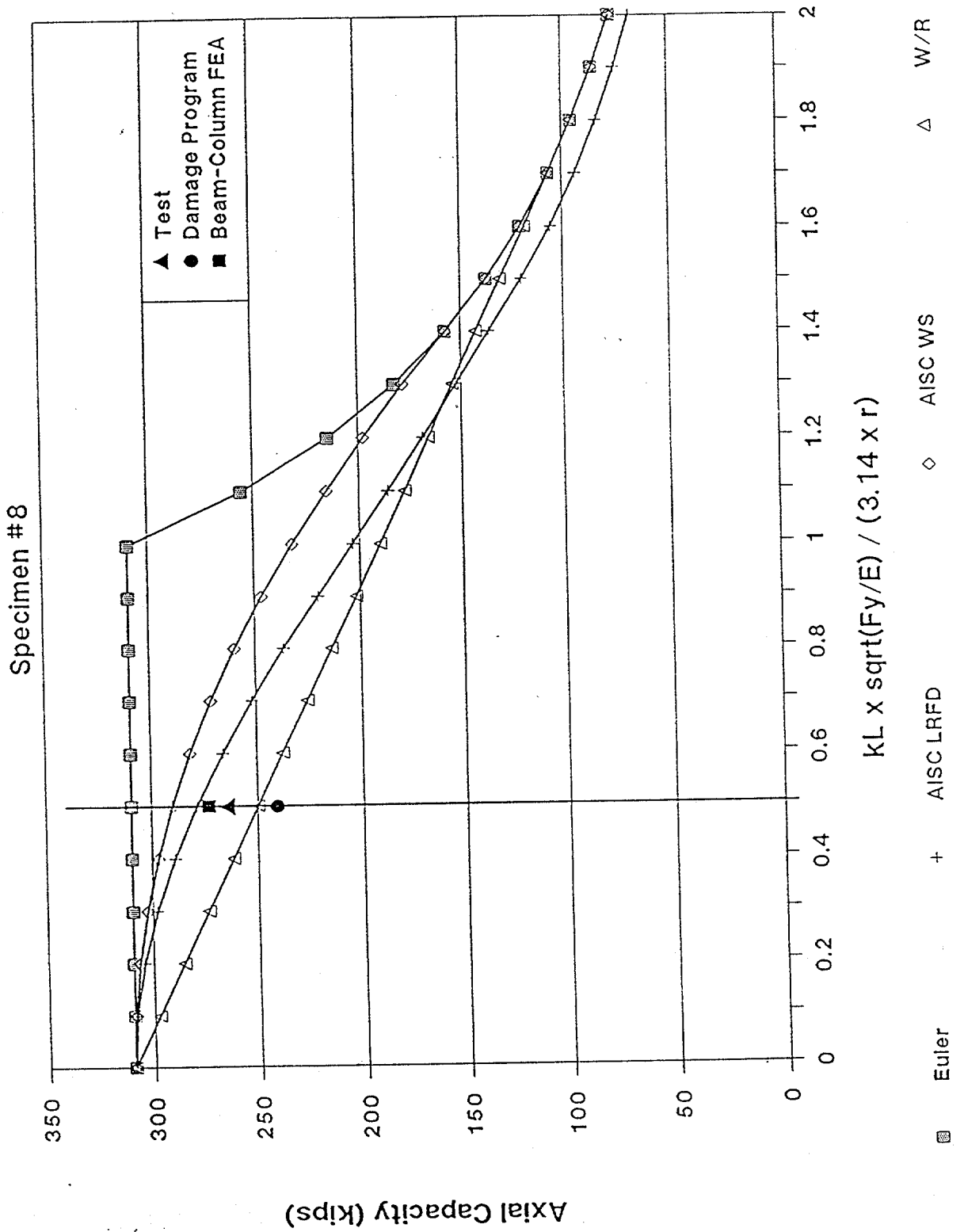


Figure 4-35

Specimen #8

Axial Load vs. Axial Displacement

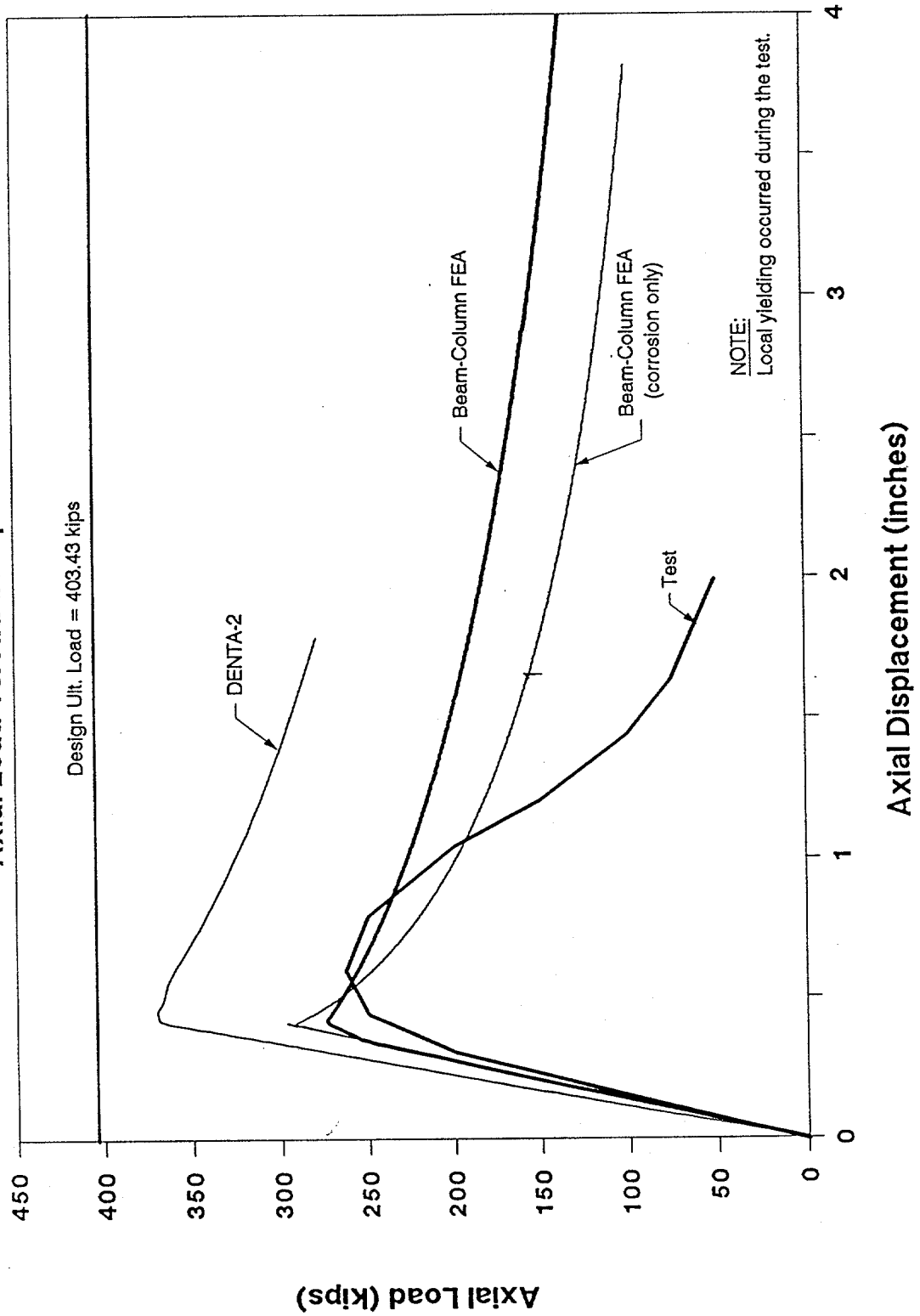


Figure 4-36

SPECIMEN . 9

Damage Summary
Specimen #9

A&M Damage Number

Damage Description

No Damage

Compression Capacity vs Slenderness

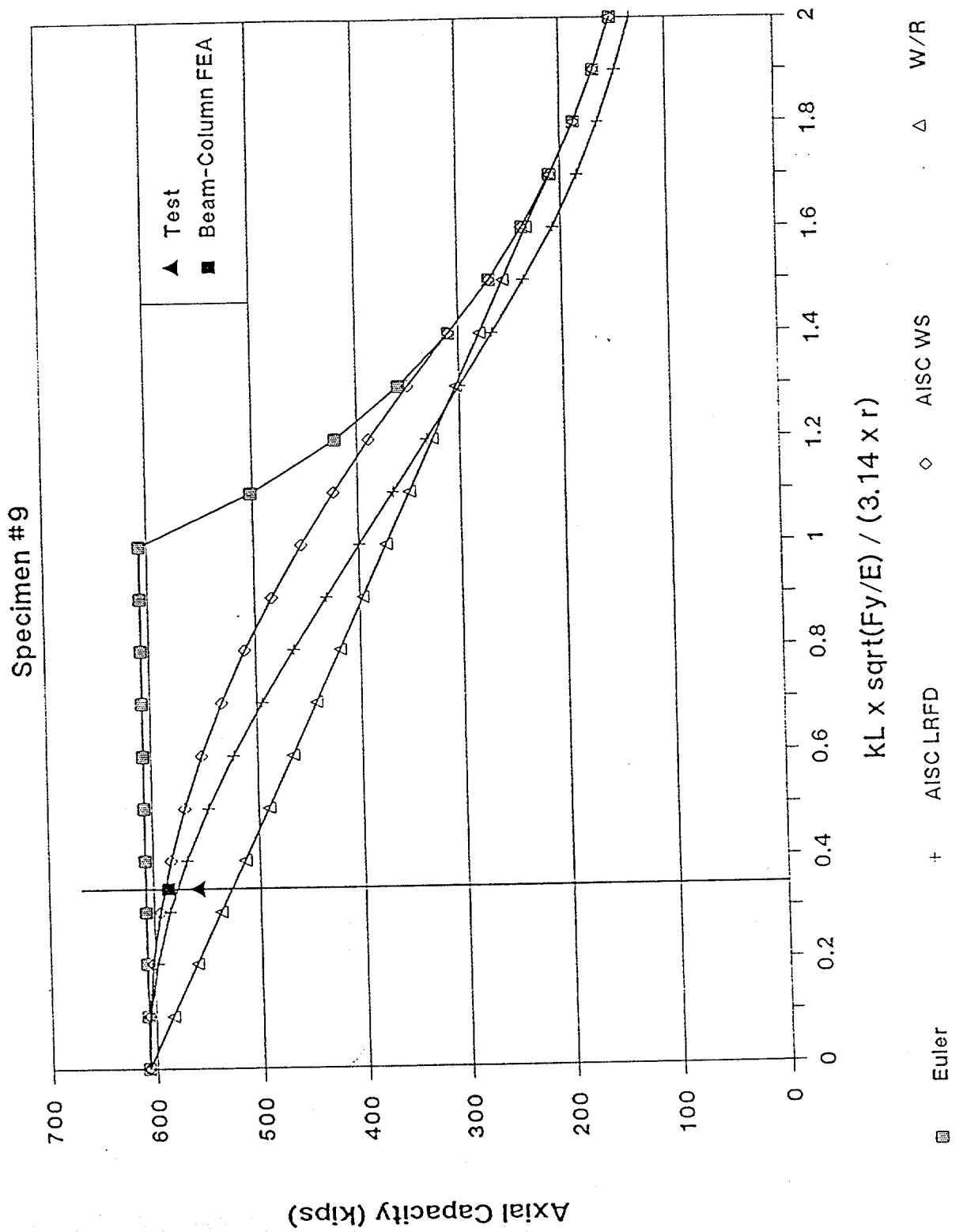


Figure 4-38

Specimen #9

Axial Load vs. Axial Deformation

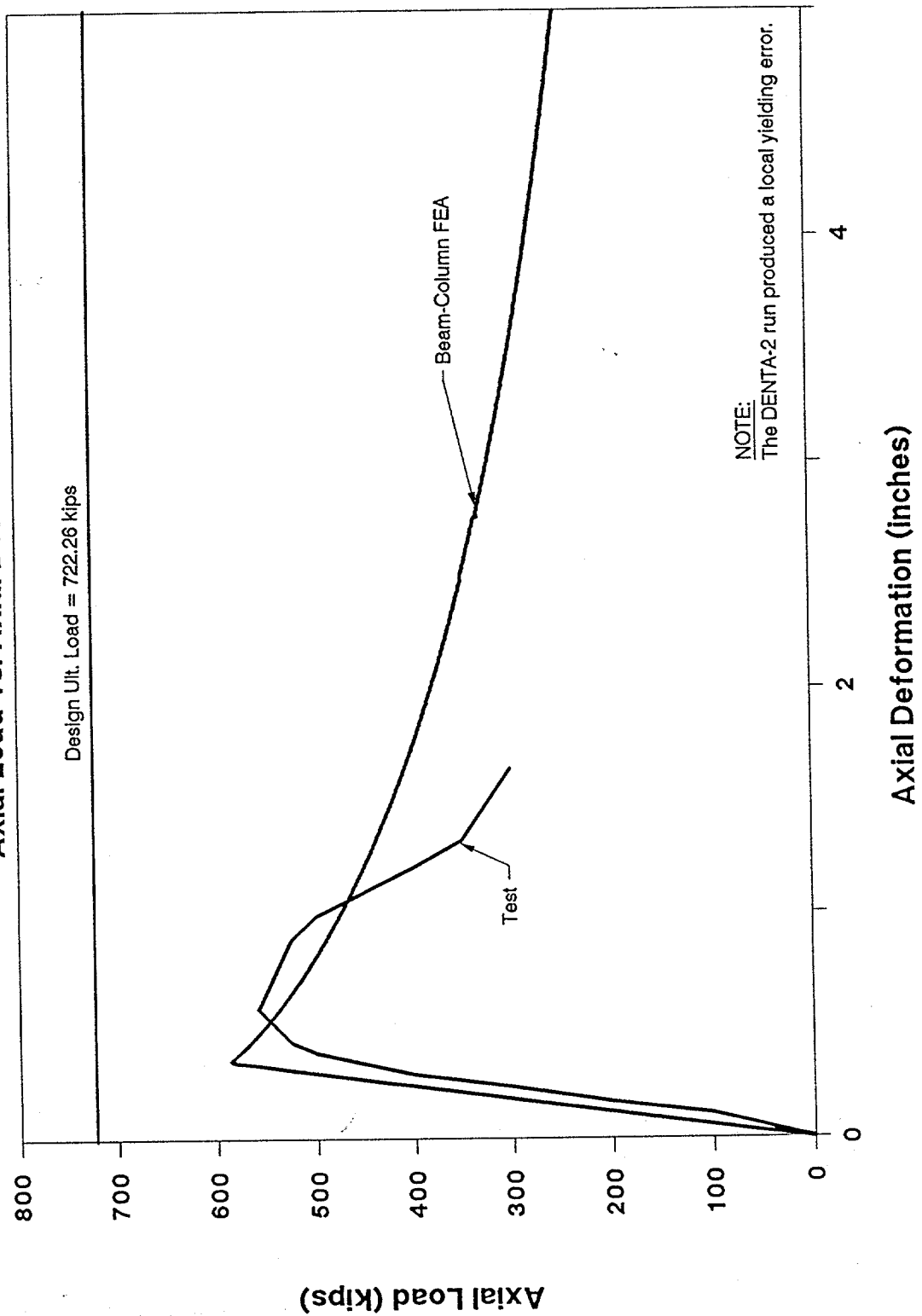


Figure 4-39

SPECIMEN 10

Damage Summary
Specimen #10

A&M Damage Number

Damage Description

No Damage

Compression Capacity vs Slenderness

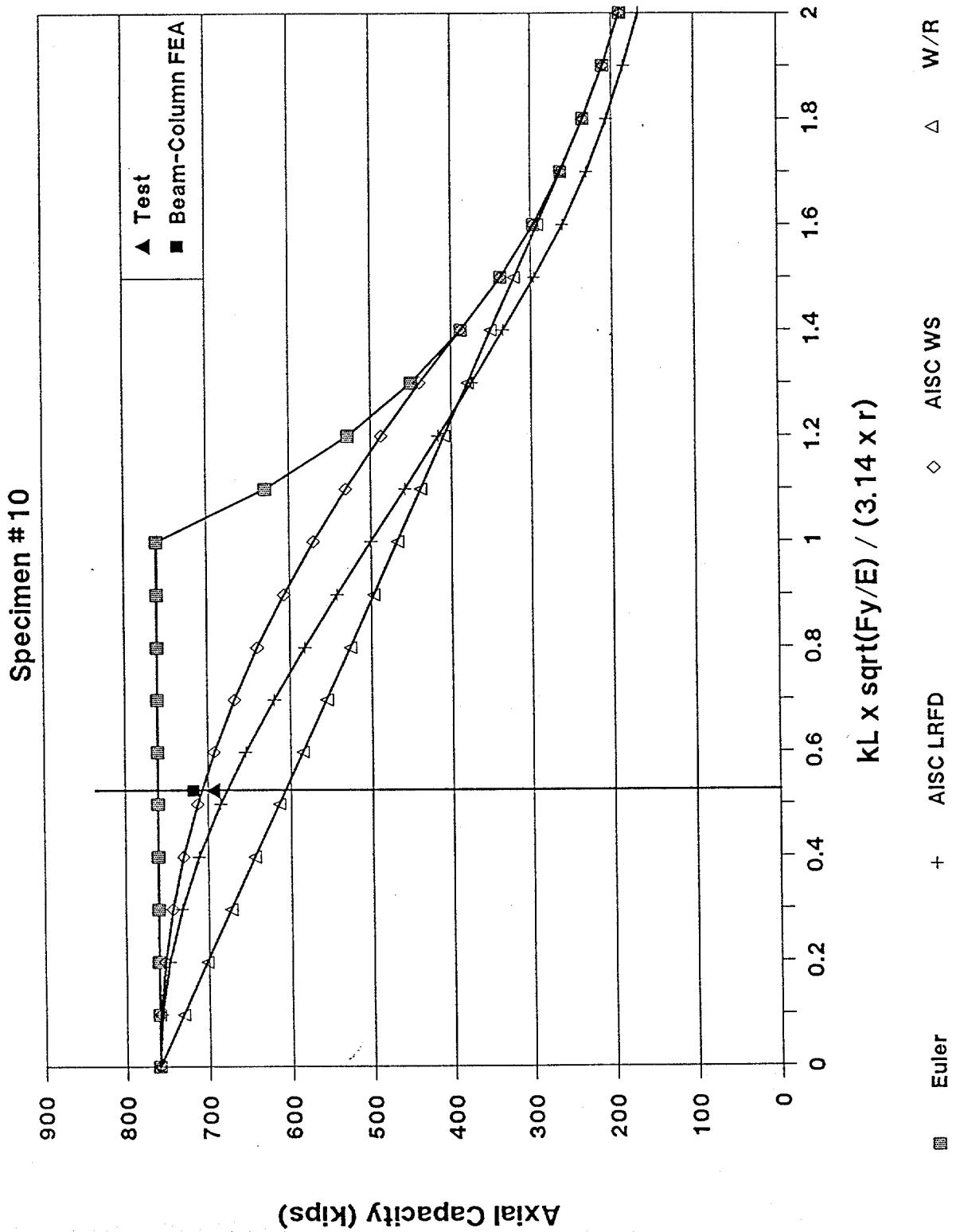


Figure 4-41

Specimen #10

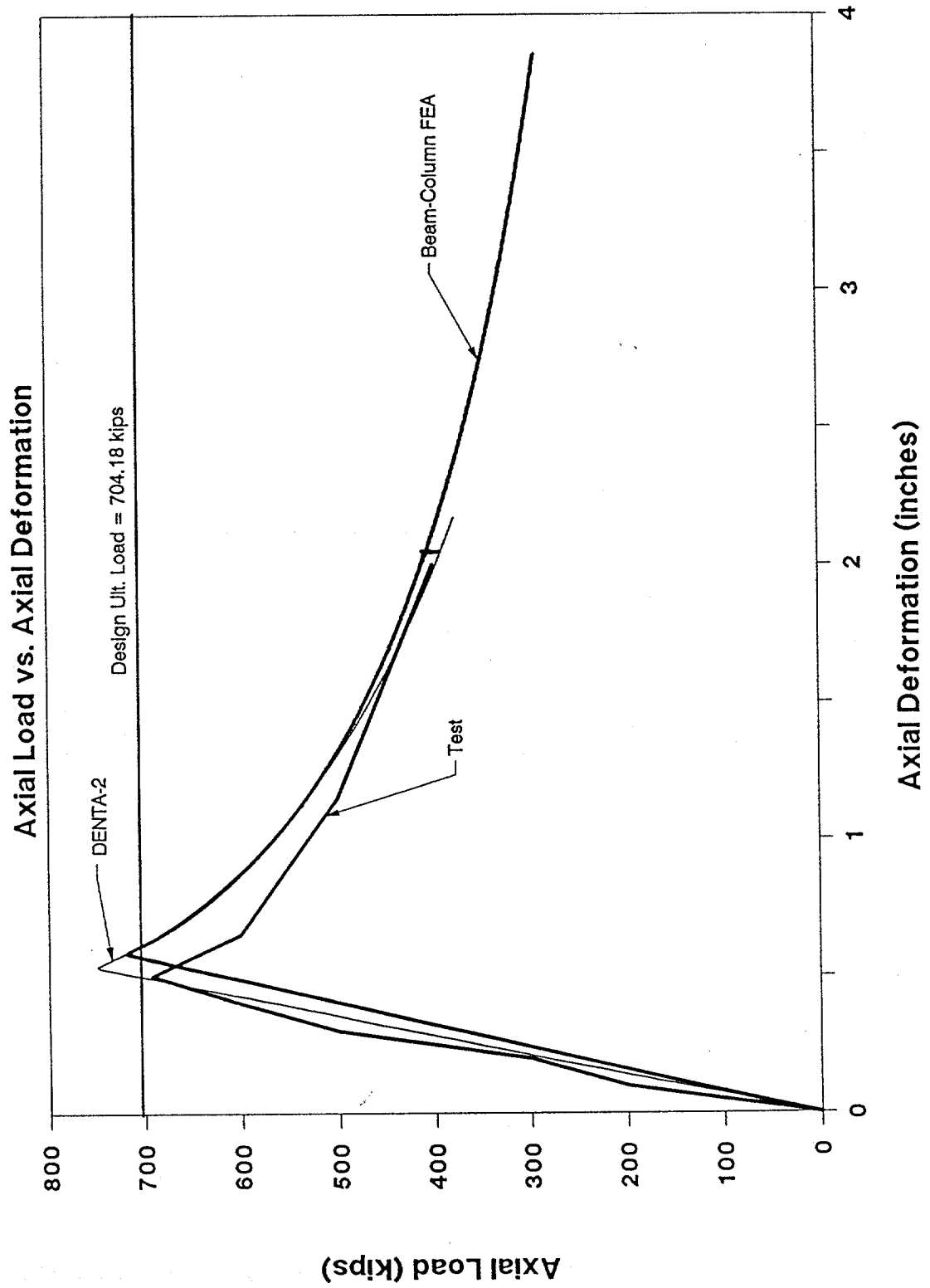


Figure 4-42

SPECIMEN 11

Damage Summary
Specimen #11

A&M Damage Number

Damage Description

No Damage

Compression Capacity vs Slenderness

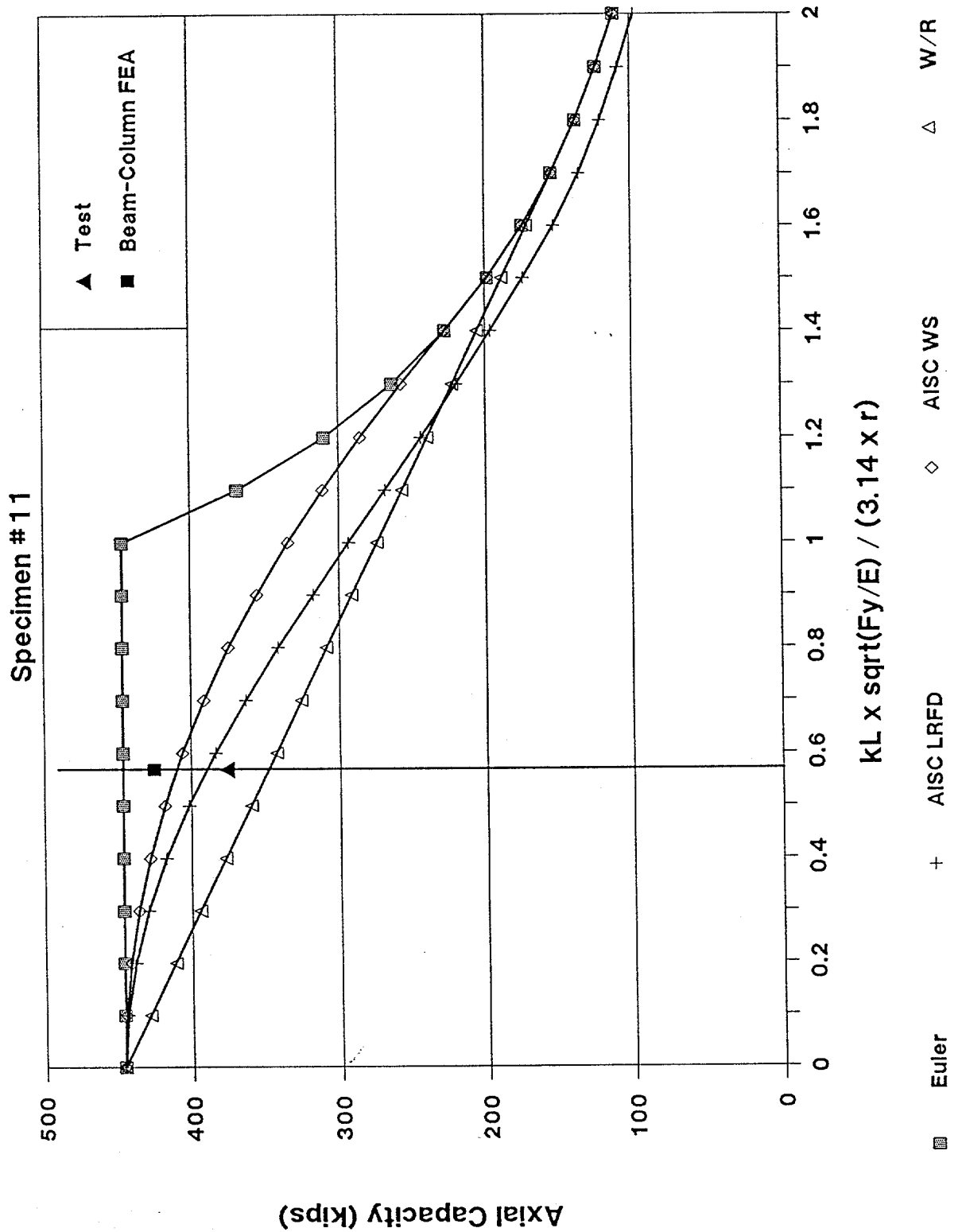


Figure 4-44

Specimen #11

Axial Load vs. Axial Deformation

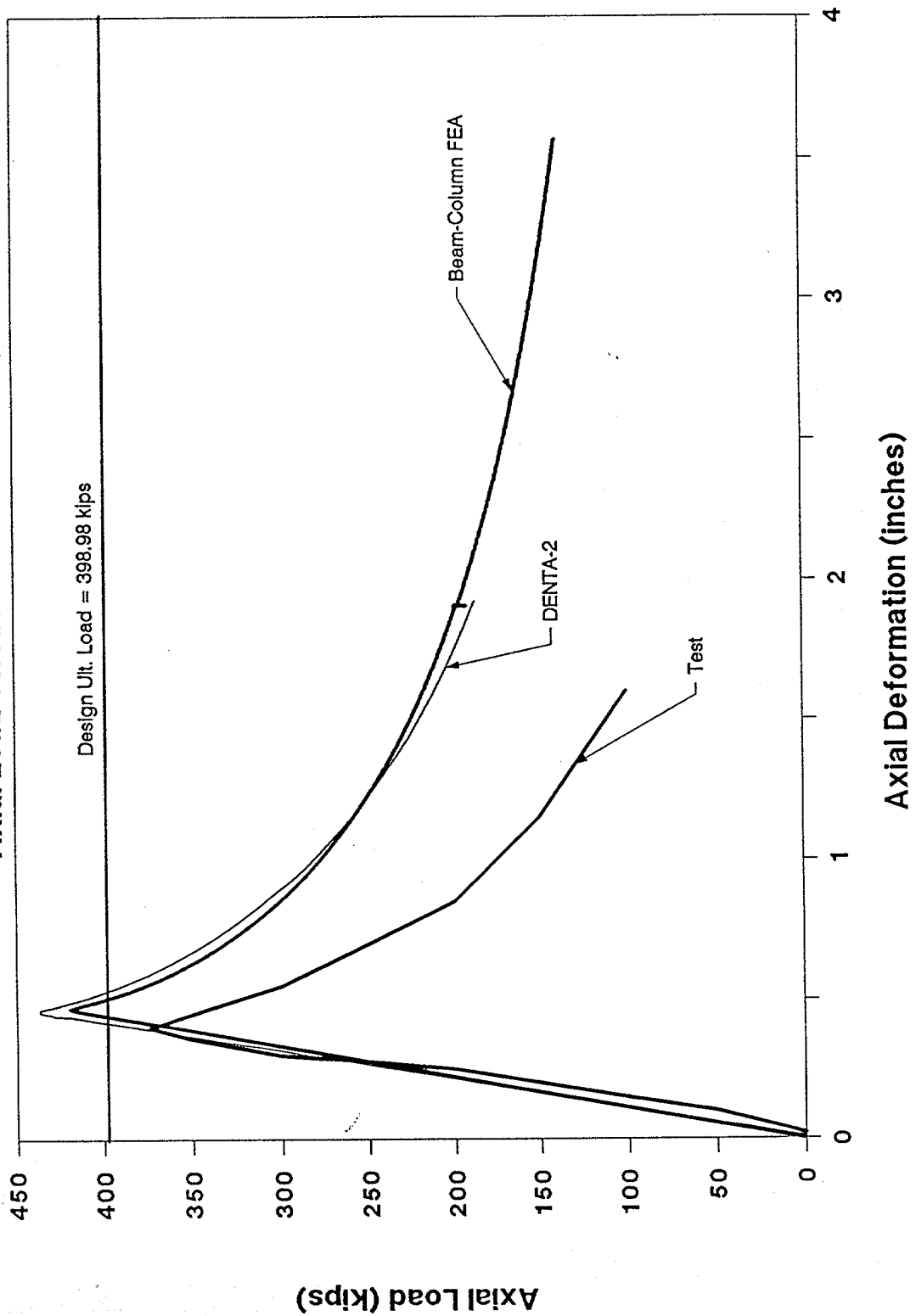


Figure 4-45

SPECIMEN 12

Damage Summary
Specimen #12

<u>A&M Damage Number</u>	<u>Damage Description</u>
9	Dent: Depth = 3" Model Segment Length = 14" Distance from loaded end = 251" Angle from vertical = 135°
12	Hole: Diameter = 7.5" Model Segment Length = 15" Distance from loaded end = 265.5" Angle from vertical = 60°
13	Hole: Diameter = 10.5" Model Segment Length = 12" Distance from loaded end = 301" Angle from vertical = 202°

*Angle from vertical is clockwise from +Z axis
looking from the loaded end toward the opposite end
of the member

```

*****
*                                     *
*               Program DAMAGE       *
*                                     *
*****

```

TITLE: SPECIMEN #12

INPUT:

```

OUTSIDE DIAMETER (in) = 12.750
THICKNESS (in)       = .351
LENGTH (ft)          = 39.480
EFF. LENGTH FACTOR   = .50

YIELD STRESS (ksi)   = 60.00
YOUNGS MODULUS (ksi) = 28600.0

DENT DEPTH (in)       = .000
HOLE DIAMETER (in)    = 10.500
LAT. DISPL. (in)      = .00

```

RESULTS:

```

CROSS-SECTIONAL AREA (sq.in) = 13.67
DENT/HOLE ANGLE (rad)         = 4.26315
AXIAL ECCENTRICITY (in)       = 2.4630
REDUCED RAD. OF GYRATION (cu.in) = 3.015
REDUCED ELAS. SECTION MOD. (cu.in) = 14.640
PLASTIFICATION STRESS (ksi)   = .000
AVG. SQUASH STRESS (ksi)     = 40.710
IMPERFECTION PARAMETER       = .00088
SLENDERNESS RATIO            = 71.70803
EULER BUCKLING STRESS (ksi)   = 96.7476
SOLUTION ROOTS (SDCE1,SDCE2) (ksi) = 280.527 14.040

DAMAGED MEMBER AXIAL CAPACITY (ksi) = 14.040
DAMAGED/UNDAMAGED STRESS RATIO      = .23400
UNDAMAGED SLENDERNESS RATIO          = .78751

```

Notes:

- (1) Hole diameter and dent depth should be measured w/r the tubular mid-wall diameter.
- (2) For dented members it is assumed that the maximum stress the dented region can sustain is equal to the plastification stress. This stress is set equal to zero for hole damage.
- (3) Dent and hole damage must be evaluated separately. Either can be assessed in conjunction with bending damage.

Compression Capacity vs Slenderness

Specimen #12

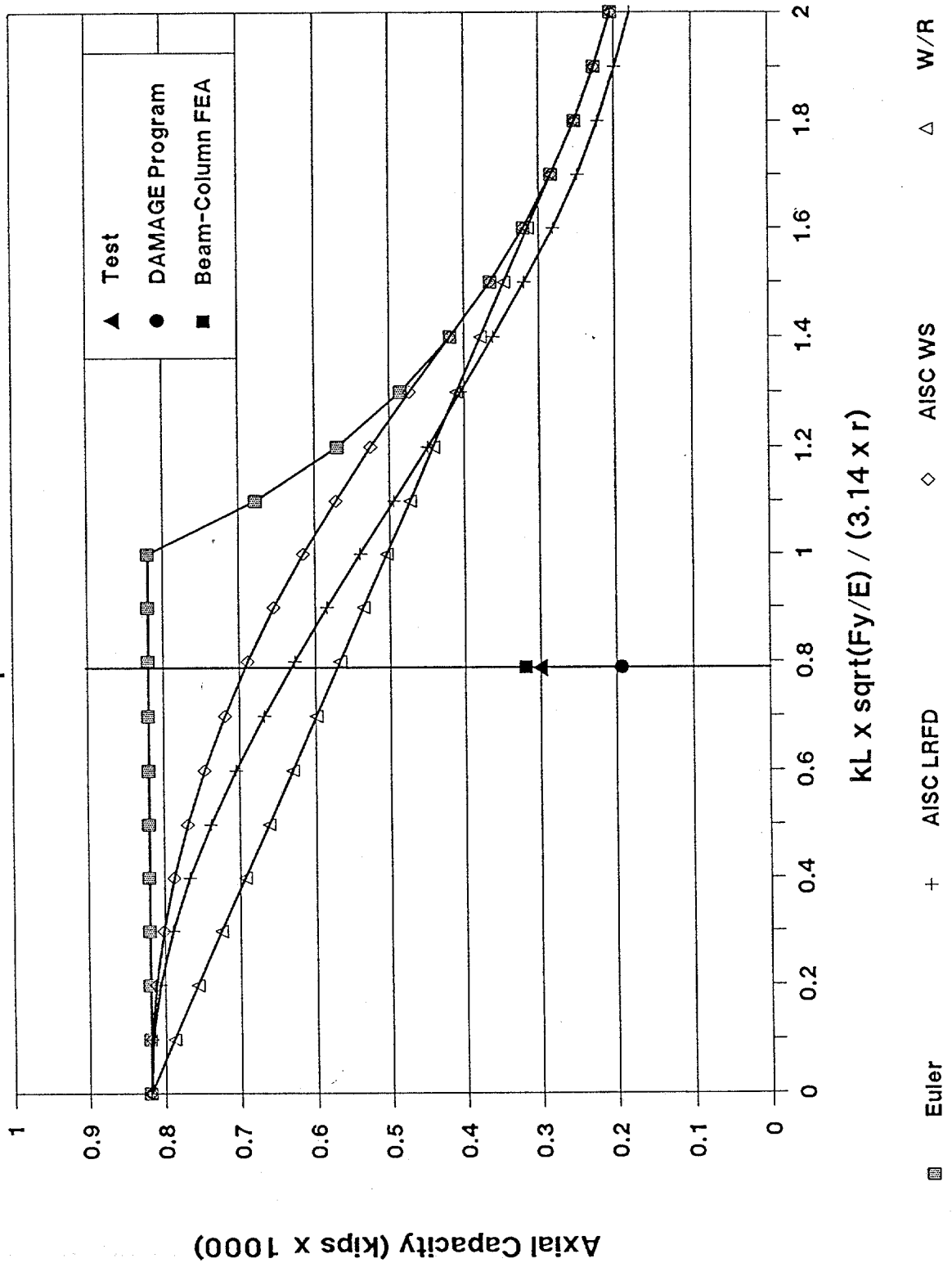


Figure 4-48

Specimen #12

Axial Load vs. Axial Deformation

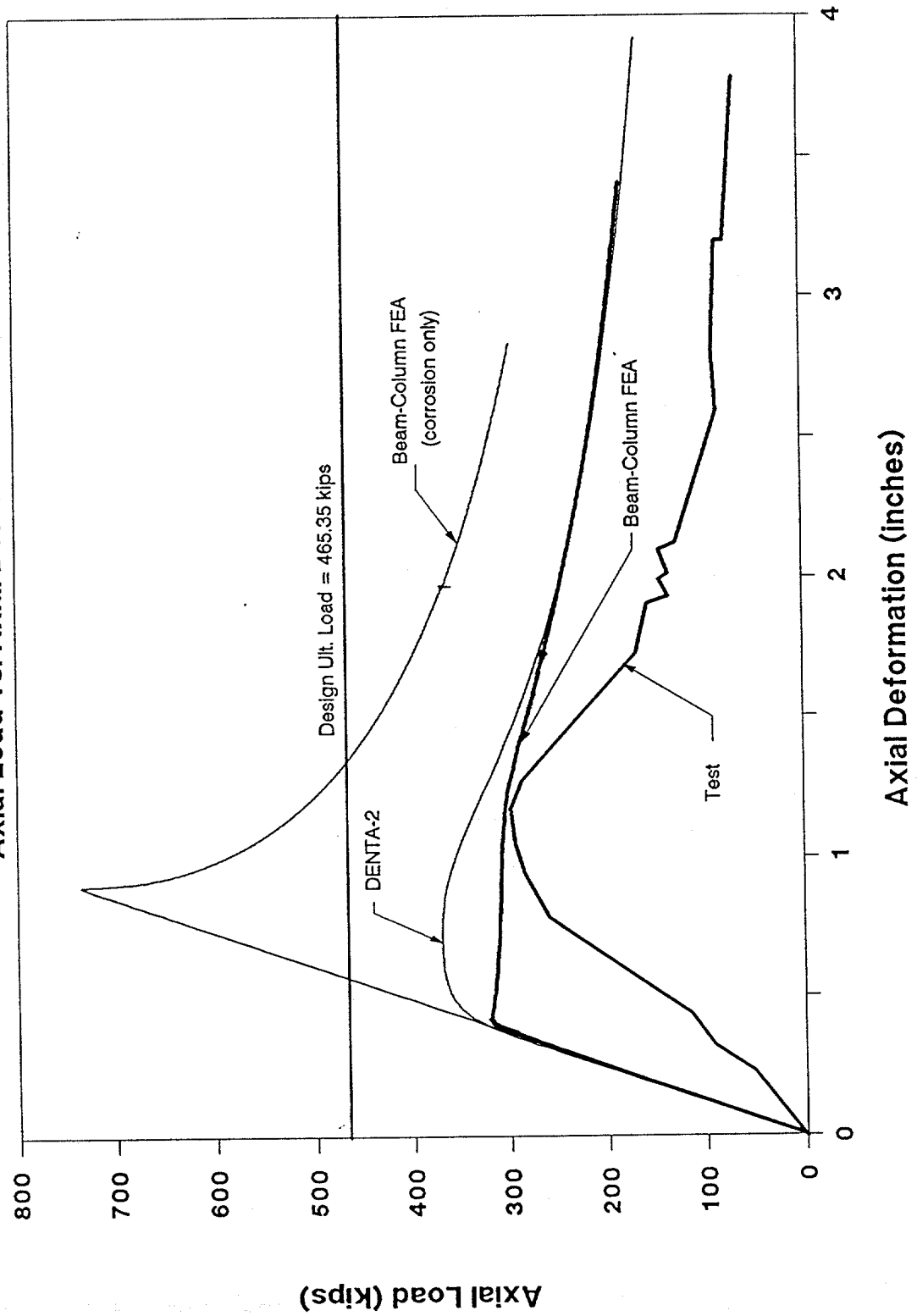


Figure 4-49

SPECIMEN 13

Damage Summary
Specimen #13

A&M Damage Number

Damage Description

1	Dent: Depth = 0.625" Model Segment Length = 8" Distance from loaded end = 197.56" Angle from vertical = 306°
2	Dent: Depth = 1.75" Model Segment Length = 14" Distance from loaded end = 185.56" Angle from vertical = 9°
3	Dent: Depth = 0.75" Model Segment Length = 9" Distance from loaded end = 160.56" Angle from vertical = 324°
4	Dent: Depth = 1.75" Model Segment Length = 14" Distance from loaded end = 77.56" Angle from vertical = 302°
None	Out of Straightness: Direction: -Z Maximum Deflection = 8.125"
None	Out of Straightness: Direction: -Y Maximum Deflection = 2.25"

*Angle from vertical is clockwise from +Z axis
looking from the loaded end toward the opposite end
of the member

```

*****
*
*               Program DAMAGE
*
*
*****

```

TITLE: Specimen #13 - Damage #2,4

INPUT:

OUTSIDE DIAMETER (in) = 12.750
 THICKNESS (in) = .323
 LENGTH (ft) = 24.130
 EFF. LENGTH FACTOR = .54

YIELD STRESS (ksi) = 53.70
 YOUNGS MODULUS (ksi) = 30000.0

DENT DEPTH (in) = 1.750
 HOLE DIAMETER (in) = .000
 LAT. DISPL. (in) = 8.13

RESULTS:

CROSS-SECTIONAL AREA (sq.in)	=	12.61	
DENT/HOLE ANGLE (rad)	=	4.78213	
AXIAL ECCENTRICITY (in)	=	1.7723	
REDUCED RAD. OF GYRATION (cu.in)	=	3.484	
REDUCED ELAS. SECTION MOD. (cu.in)	=	18.678	
PLASTIFICATION STRESS (ksi)	=	3.699	
AVG. SQUASH STRESS (ksi)	=	41.755	
IMPERFECTION PARAMETER	=	.04029	
SLENDERNESS RATIO	=	36.86516	
EULER BUCKLING STRESS (ksi)	=	233.9334	
SOLUTION ROOTS (SDCE1,SDCE2) (ksi)	=	823.407	12.820
DAMAGED MEMBER AXIAL CAPACITY (ksi)	=	12.820	
DAMAGED/UNDAMAGED STRESS RATIO	=	.23873	
UNDAMAGED SLENDERNESS RATIO	=	.47912	

Notes:

- (1) Hole diameter and dent depth should be measured w/r the tubular mid-wall diameter.
- (2) For dented members it is assumed that the maximum stress the dented region can sustain is equal to the plastification stress. This stress is set equal to zero for hole damage.
- (3) Dent and hole damage must be evaluated separately. Either can be assessed in conjunction with bending damage.

Compression Capacity vs Slenderness

Specimen #13

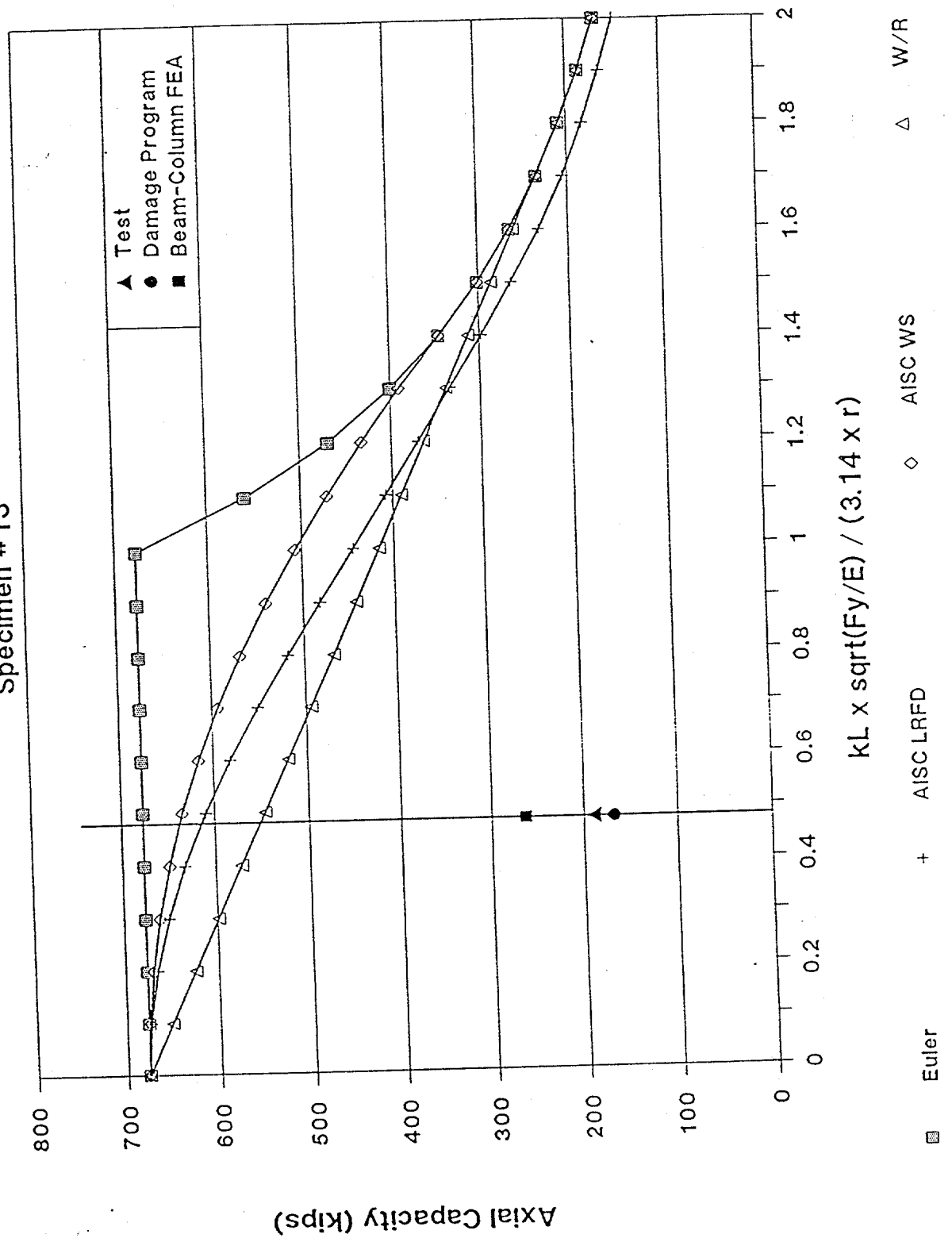


Figure 4-52

Specimen #13

Axial Load vs. Axial Deformation

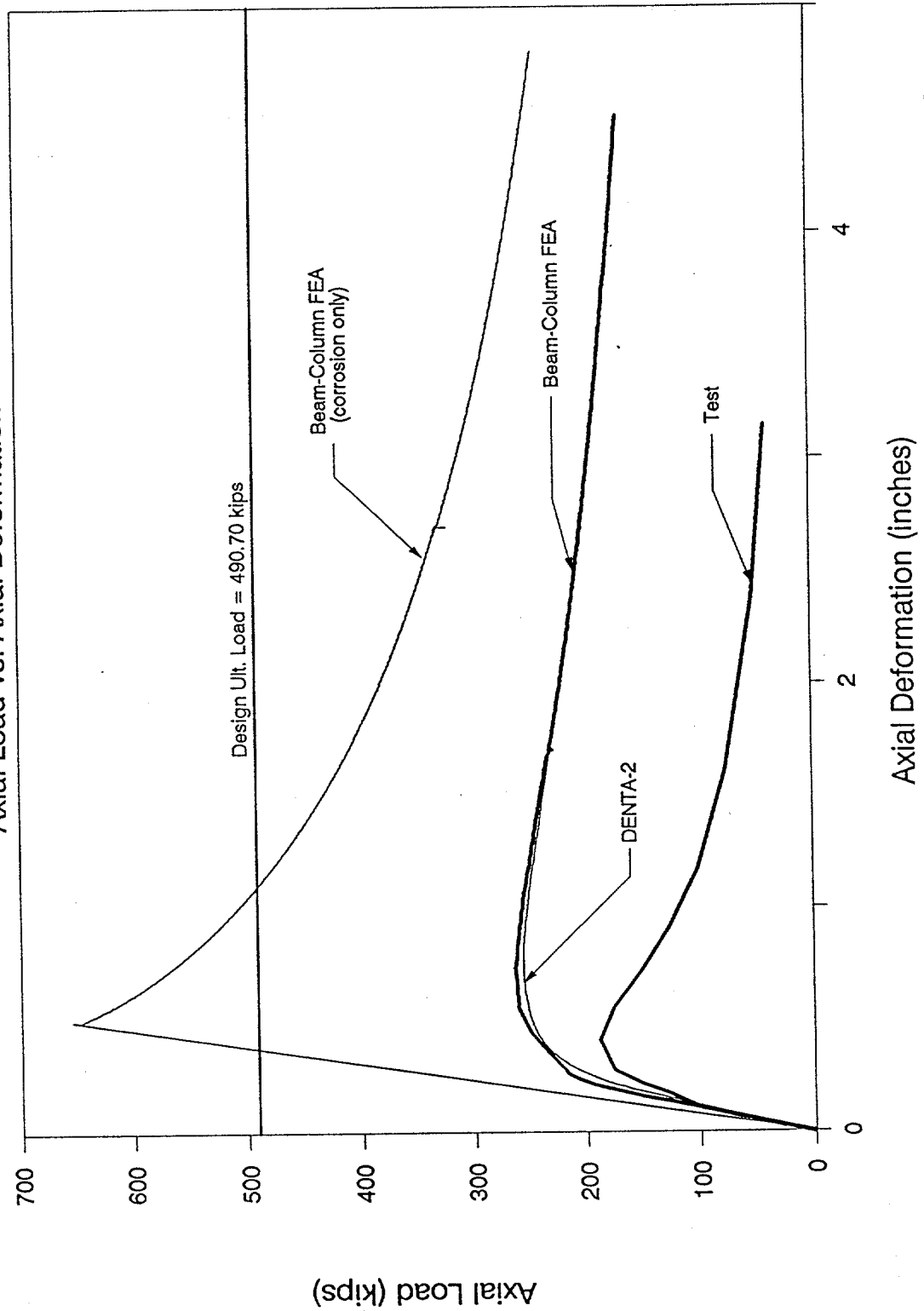


Figure 4-53

SPECIMEN #14

Damage Summary
Specimen #14

A&M Damage Number

Damage Description

2,3⁺

Dent:

Depth = 0.375" and 0.500" respectively
Model Segment Length = 9"
Distance from loaded end = 184.5"
Angle from vertical = 27°

4

Dent:

Depth = 0.25"
Model Segment Length = 5"
Distance from loaded end = 177.5"
Angle from vertical = 342°

None

Out of Straightness:

Direction: -Z
Maximum Deflection = 3.0"

None

Out of Straightness:

Direction: Y
Maximum Deflection = 0.50"

*Angle from vertical is clockwise from +Z axis
looking from the loaded end toward the opposite end
of the member

⁺Both dents occur at the same cross section. The
properties were obtained for a dent with a depth
equal to the summation of the two dent depths. The
angle is the resultant of the two angles.

```

*****
*
*           Program DAMAGE
*
*****

```

TITLE: Specimen #14

INPUT:

```

OUTSIDE DIAMETER (in) = 12.750
THICKNESS (in)       = .295
LENGTH (ft)          = 16.750
EFF. LENGTH FACTOR   = .50

YIELD STRESS (ksi)    = 36.00
YOUNGS MODULUS (ksi)  = 29300.0

DENT DEPTH (in)       = .500
HOLE DIAMETER (in)    = .000
LAT. DISPL. (in)      = 3.00

```

RESULTS:

```

CROSS-SECTIONAL AREA (sq.in) = 11.54
DENT/HOLE ANGLE (rad)         = 5.48174
AXIAL ECCENTRICITY (in)       = .8863
REDUCED RAD. OF GYRATION (cu.in) = 4.008
REDUCED ELAS. SECTION MOD. (cu.in) = 24.460
PLASTIFICATION STRESS (ksi)    = 7.609
AVG. SQUASH STRESS (ksi)      = 32.379
IMPERFECTION PARAMETER        = .02123
SLENDERNESS RATIO             = 16.11214
EULER BUCKLING STRESS (ksi)    = 555.4902
SOLUTION ROOTS (SDCE1,SDCE2) (ksi) = 960.228    20.337

DAMAGED MEMBER AXIAL CAPACITY (ksi) = 20.337
DAMAGED/UNDAMAGED STRESS RATIO      = .56492
UNDAMAGED SLENDERNESS RATIO          = .25457

```

Notes:

- (1) Hole diameter and dent depth should be measured w/r the tubular mid-wall diameter.
- (2) For dented members it is assumed that the maximum stress the dented region can sustain is equal to the plastification stress. This stress is set equal to zero for hole damage.
- (3) Dent and hole damage must be evaluated separately. Either can be assessed in conjunction with bending damage.

Compression Capacity vs Slenderness

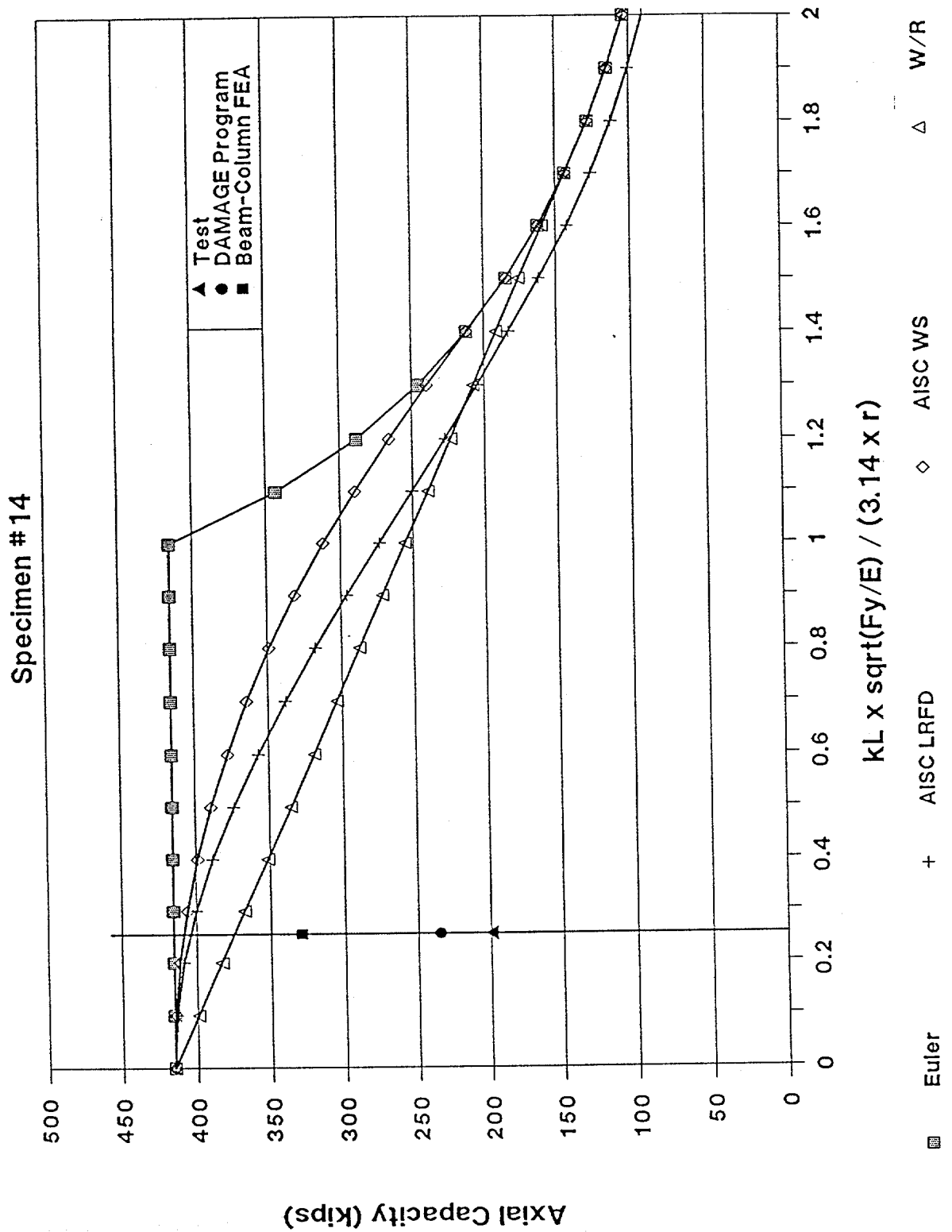


Figure 4-56

Specimen #14

Axial Load vs. Axial Deformation

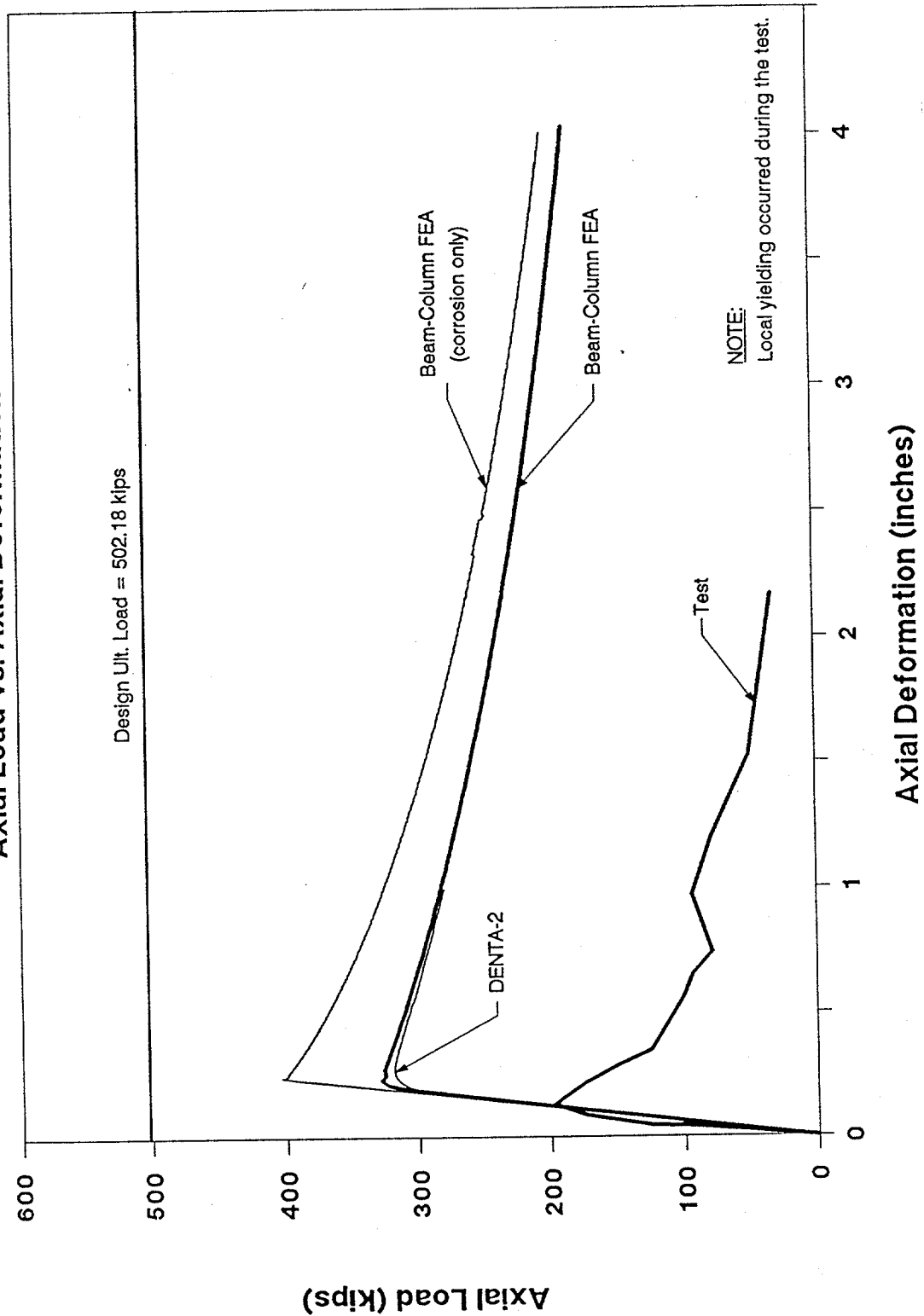


Figure 4-57

SPECIMEN 16

Damage Summary
Specimen #16

A&M Damage Number

Damage Description

6	Dent: Depth = 0.125" Model Segment Length = 4" Distance from loaded end = 241.24" Angle from vertical = 90°
7	Dent: Depth = 0.25" Model Segment Length = 8" Distance from loaded end = 232.24" Angle from vertical = 0°
8	Dent: Depth = 0.25" Model Segment Length = 6" Distance from loaded end = 188.24" Angle from vertical = 0°
9	Dent: Depth = 0.25" Model Segment Length = 5" Distance from loaded end = 179.24" Angle from vertical = 60°
13	Hole: Diameter = 1" Model Segment Length = 2" Distance from loaded end = 12.24" Angle from vertical = 90°
None	Out of Straightness: Direction: -Z Maximum Deflection = 6.625"
None	Out of Straightness: Direction: +Y Maximum Deflection = 1.875"

*Angle from vertical is clockwise from +Z axis
looking from the loaded end toward the opposite end
of the member


```

*****
*                                     *
*               Program DAMAGE       *
*                                     *
*****

```

TITLE: SPECIMEN #16

INPUT:

OUTSIDE DIAMETER (in) = 12.750
 THICKNESS (in) = .375
 LENGTH (ft) = 28.770
 EFF. LENGTH FACTOR = .62

YIELD STRESS (ksi) = 49.10
 YOUNGS MODULUS (ksi) = 29000.0

DENT DEPTH (in) = .000
 HOLE DIAMETER (in) = .000
 LAT. DISPL. (in) = 6.63

RESULTS:

CROSS-SECTIONAL AREA (sq.in) = 14.58
 DENT/HOLE ANGLE (rad) = 6.28319
 AXIAL ECCENTRICITY (in) = .0000
 REDUCED RAD. OF GYRATION (cu.in) = 4.375
 REDUCED ELAS. SECTION MOD. (cu.in) = 45.104
 PLASTIFICATION STRESS (ksi) = 49.100
 AVG. SQUASH STRESS (ksi) = 49.100
 IMPERFECTION PARAMETER = .02767
 SLENDERNESS RATIO = 39.45556
 EULER BUCKLING STRESS (ksi) = 119.6937
 SOLUTION ROOTS (SDCE1,SDCE2) (ksi) = 278.330 21.115

 DAMAGED MEMBER AXIAL CAPACITY (ksi) = 21.115
 DAMAGED/UNDAMAGED STRESS RATIO = .43004
 UNDAMAGED SLENDERNESS RATIO = .64048

Notes:

- (1) Hole diameter and dent depth should be measured w/r the tubular mid-wall diameter.
- (2) For dented members it is assumed that the maximum stress the dented region can sustain is equal to the plastification stress. This stress is set equal to zero for hole damage.
- (3) Dent and hole damage must be evaluated separately. Either can be assessed in conjunction with bending damage.

Compression Capacity vs Slenderness

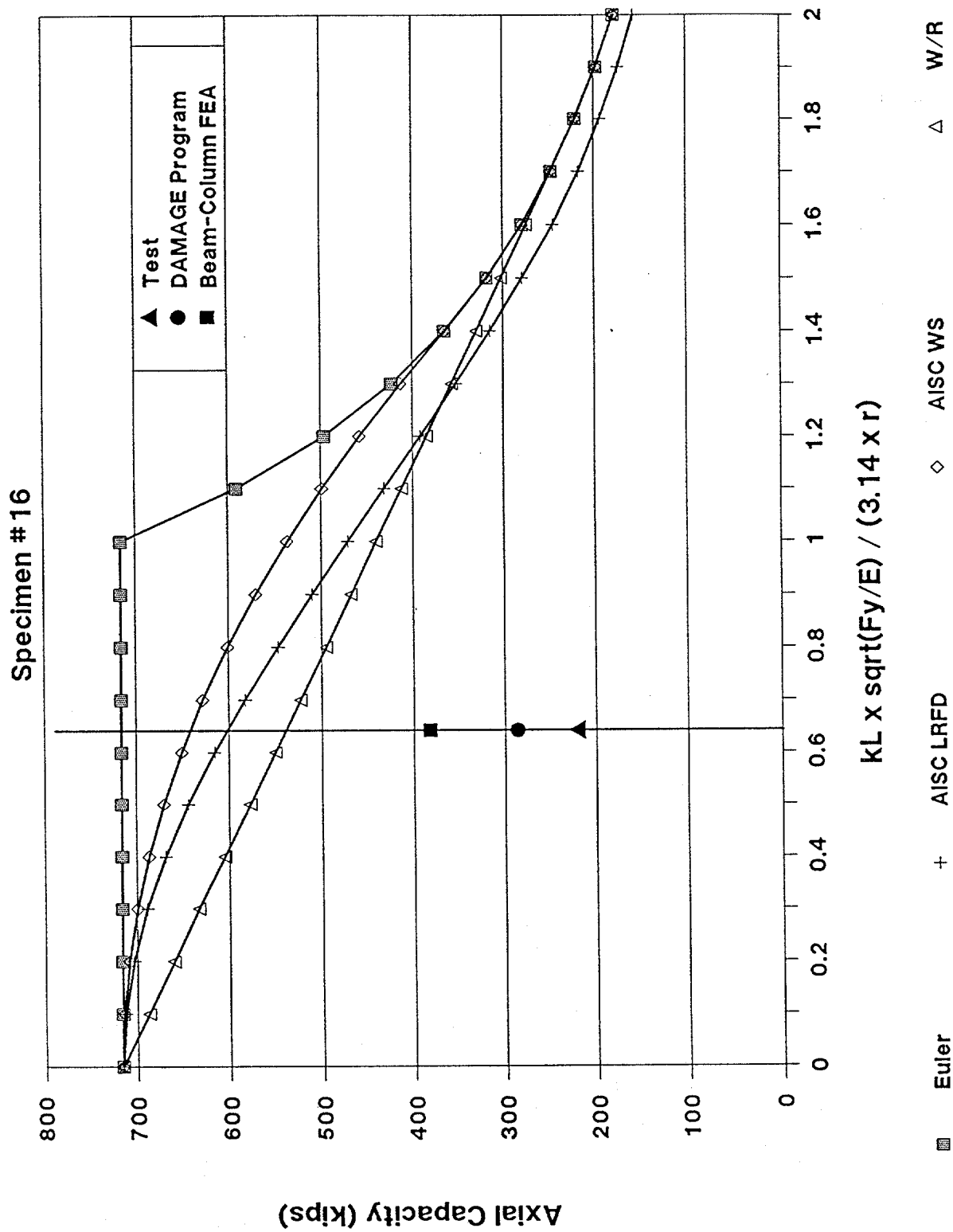


Figure 4-60

Specimen #16

Axial Load vs. Axial Deformation

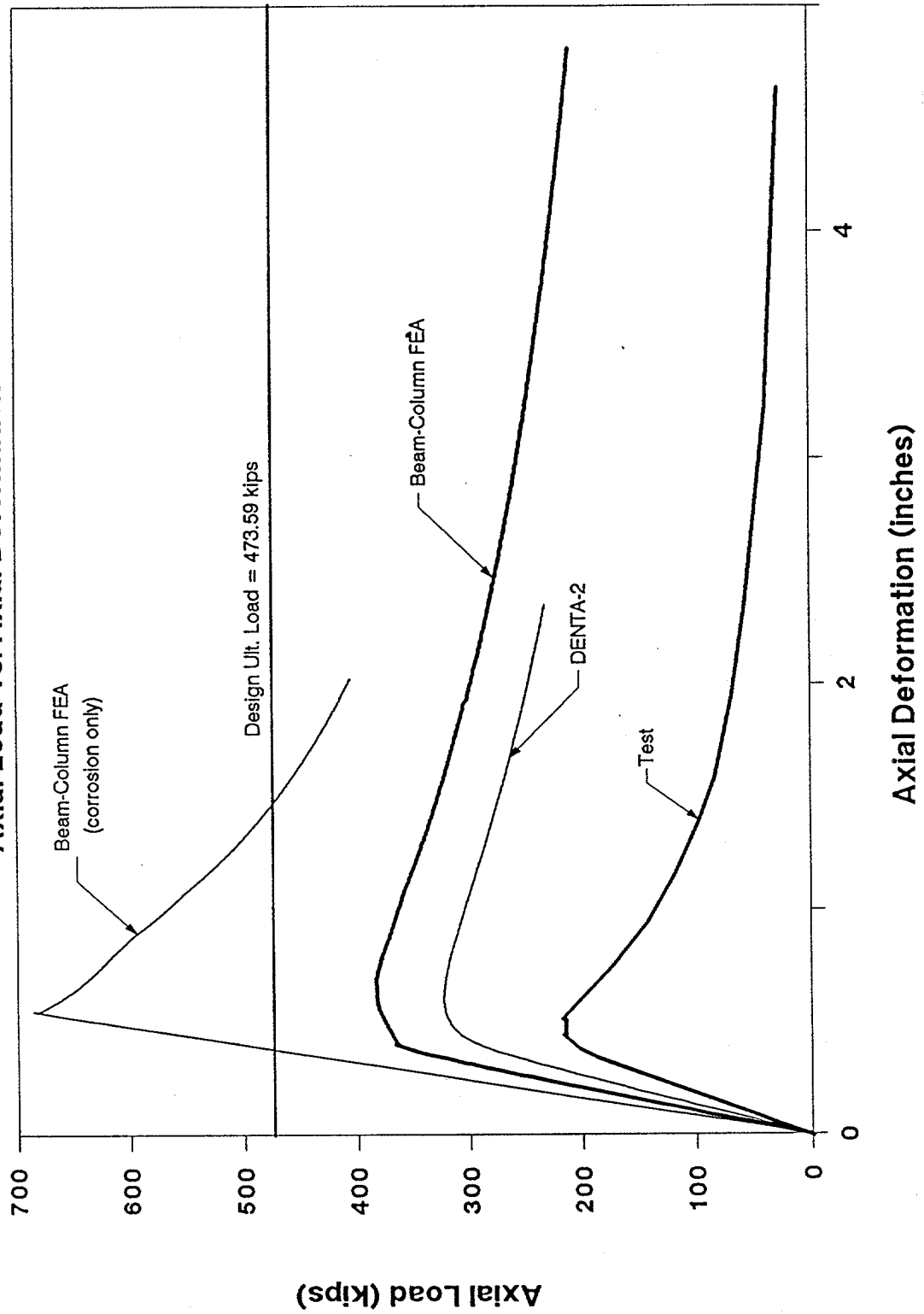


Figure 4-61

SPECIMEN 17

Damage Summary
Specimen #17

A&M Damage Number

Damage Description

2

Dent:

Depth = 1.375"

Model Segment Length = 12"

Distance from loaded end = 145.04"

Angle from vertical = 18°

None

Out of Straightness:

Direction: -Z

Maximum Deflection = 4.75"

*Angle from vertical is clockwise from +Z axis
looking from the loaded end toward the opposite end
of the member

```

*****
*                                     *
*                               Program DAMAGE                               *
*                                     *
*****

```

TITLE: SPECIMEN #17

INPUT:

OUTSIDE DIAMETER (in) = 12.750
 THICKNESS (in) = .422
 LENGTH (ft) = 31.170
 EFF. LENGTH FACTOR = .52

YIELD STRESS (ksi) = 49.20
 YOUNGS MODULUS (ksi) = 25000.0

DENT DEPTH (in) = 1.375
 HOLE DIAMETER (in) = .000
 LAT. DISPL. (in) = .00

RESULTS:

CROSS-SECTIONAL AREA (sq.in) = 16.34
 DENT/HOLE ANGLE (rad) = 4.94731
 AXIAL ECCENTRICITY (in) = 1.5434
 REDUCED RAD. OF GYRATION (cu.in) = 3.589
 REDUCED ELAS. SECTION MOD. (cu.in) = 26.177
 PLASTIFICATION STRESS (ksi) = 5.589
 AVG. SQUASH STRESS (ksi) = 39.928
 IMPERFECTION PARAMETER = .00077
 SLENDERNESS RATIO = 46.82853
 EULER BUCKLING STRESS (ksi) = 124.0512
 SOLUTION ROOTS (SDCE1,SDCE2) (ksi) = 239.704 22.858

 DAMAGED MEMBER AXIAL CAPACITY (ksi) = 22.858
 DAMAGED/UNDAMAGED STRESS RATIO = .46460
 UNDAMAGED SLENDERNESS RATIO = .62977

Notes:

- (1) Hole diameter and dent depth should be measured w/r the tubular mid-wall diameter.
- (2) For dented members it is assumed that the maximum stress the dented region can sustain is equal to the plastification stress. This stress is set equal to zero for hole damage.
- (3) Dent and hole damage must be evaluated separately. Either can be assessed in conjunction with bending damage.

Compression Capacity vs Slenderness

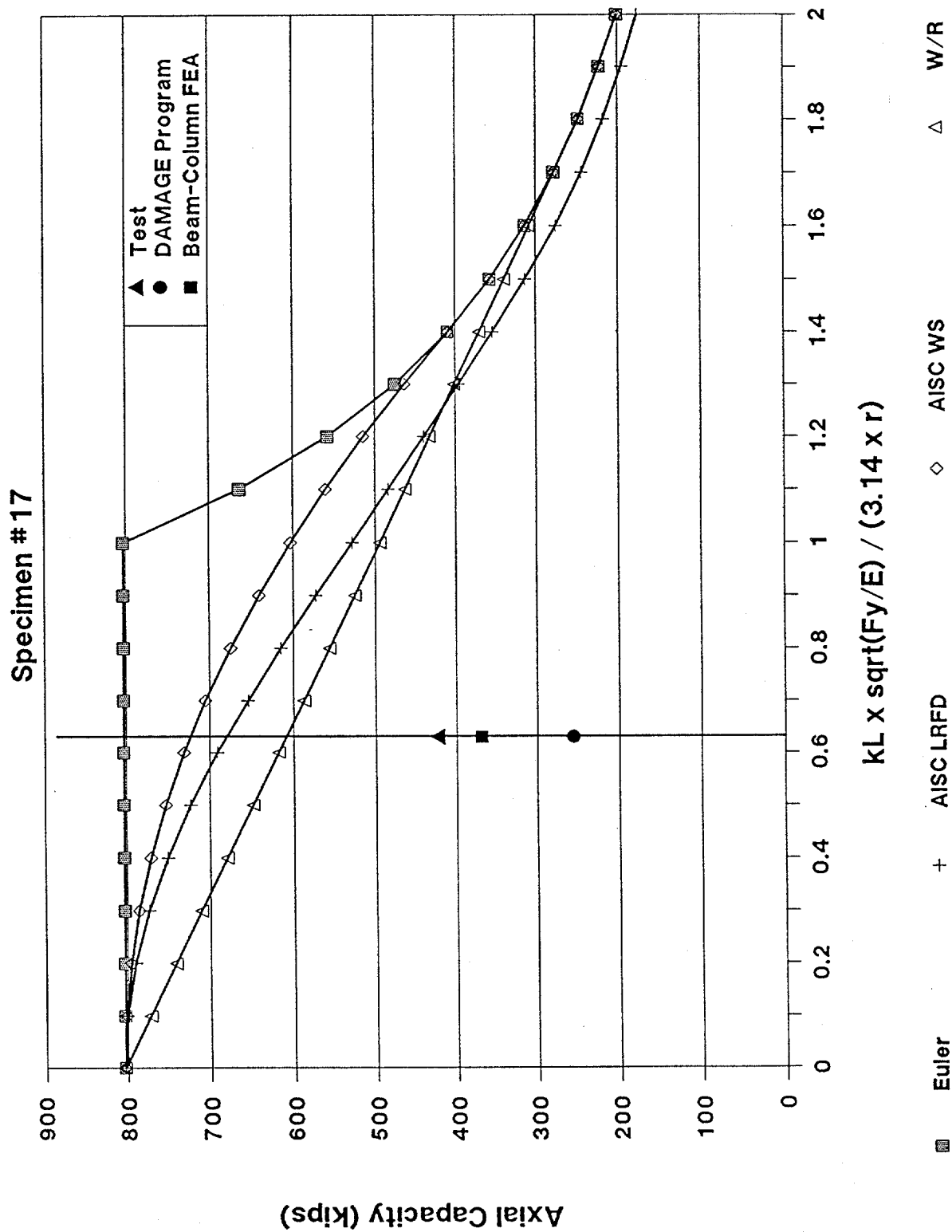


Figure 4-64

Specimen #17

Axial Load vs. Axial Deformation

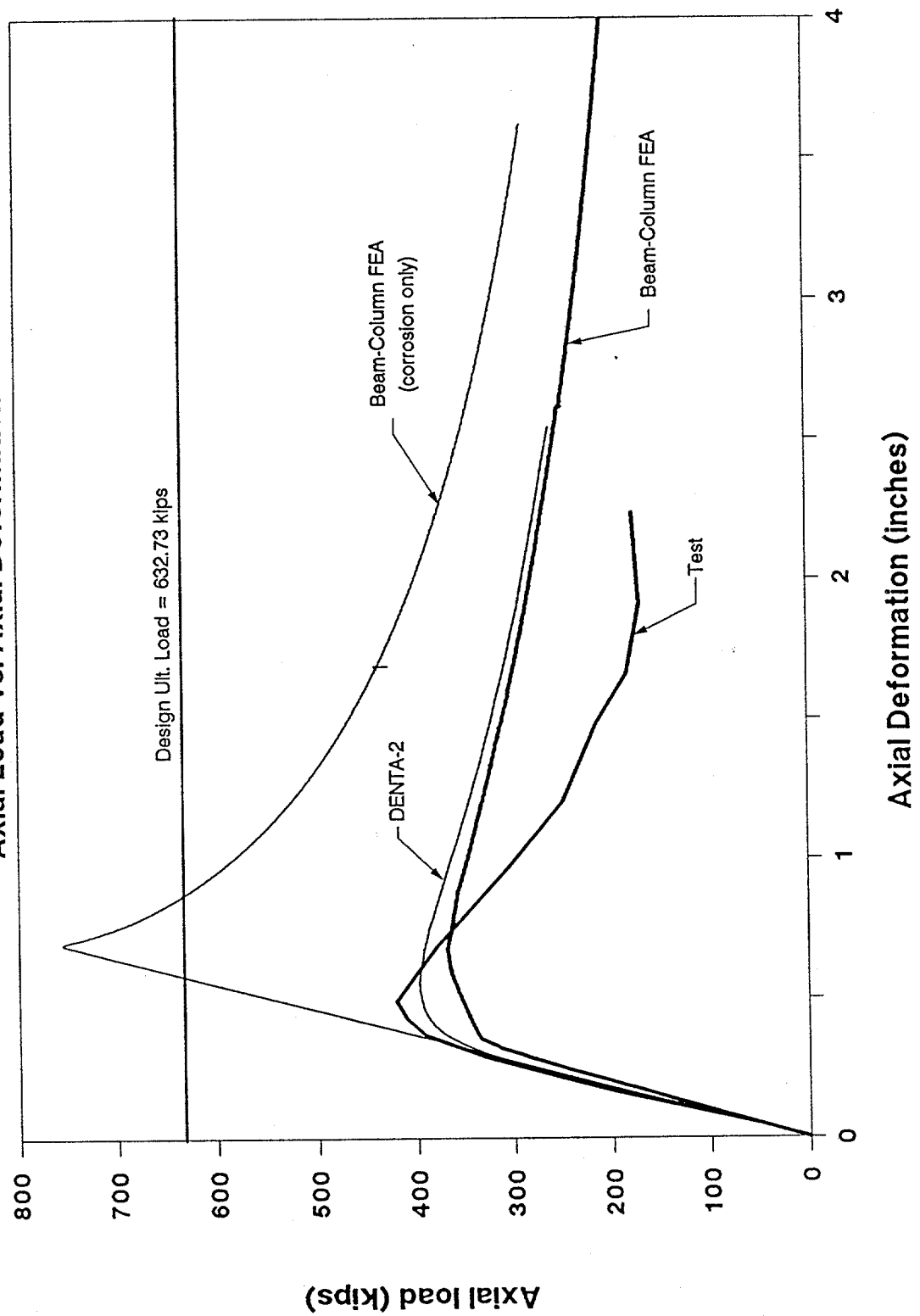


Figure 4-65

SPECIMEN #18

Damage Summary
Specimen #18

A&M Damage Number

Damage Description

2	Dent: Depth = 0.375" Model Segment Length = 8" Distance from loaded end = 140.46" Angle from vertical = 53.3°
3	Dent: Depth = 0.125" Model Segment Length = 4" Distance from loaded end = 85.96" Angle from vertical = 328°
4	Dent: Depth = 0.25" Model Segment Length = 6" Distance from loaded end = 70.96" Angle from vertical = 42.6°
6	Dent: Depth = 0.25" Model Segment Length = 6" Distance from loaded end = 50.46" Angle from vertical = 349.3°
7	Dent: Depth = 0.125" Model Segment Length = 4" Distance from loaded end = 62.96" Angle from vertical = 53.3°
None	Out of Straightness: Direction: -Z Maximum Deflection = 0.875"

*Angle from vertical is clockwise from +Z axis
looking from the loaded end toward the opposite end
of the member

```

*****
*
*           Program DAMAGE
*
*****

```

TITLE: Specimen #18

INPUT:

OUTSIDE DIAMETER (in) = 10.750
 THICKNESS (in) = .264
 LENGTH (ft) = 17.080
 EFF. LENGTH FACTOR = .50

YIELD STRESS (ksi) = 34.50
 YOUNGS MODULUS (ksi) = 24900.0

DENT DEPTH (in) = .375
 HOLE DIAMETER (in) = .000
 LAT. DISPL. (in) = .88

RESULTS:

CROSS-SECTIONAL AREA (sq.in)	=	8.70	
DENT/HOLE ANGLE (rad)	=	5.52675	
AXIAL ECCENTRICITY (in)	=	.7006	
REDUCED RAD. OF GYRATION (cu.in)	=	3.398	
REDUCED ELAS. SECTION MOD. (cu.in)	=	15.862	
PLASTIFICATION STRESS (ksi)	=	8.549	
AVG. SQUASH STRESS (ksi)	=	31.376	
IMPERFECTION PARAMETER	=	.00630	
SLENDERNESS RATIO	=	21.71841	
EULER BUCKLING STRESS (ksi)	=	321.8294	
SOLUTION ROOTS (SDCE1,SDCE2) (ksi)	=	483.125	22.825
DAMAGED MEMBER AXIAL CAPACITY (ksi)	=	22.825	
DAMAGED/UNDAMAGED STRESS RATIO	=	.66159	
UNDAMAGED SLENDERNESS RATIO	=	.32741	

Notes:

- (1) Hole diameter and dent depth should be measured w/r the tubular mid-wall diameter.
- (2) For dented members it is assumed that the maximum stress the dented region can sustain is equal to the plastification stress. This stress is set equal to zero for hole damage.
- (3) Dent and hole damage must be evaluated separately. Either can be assessed in conjunction with bending damage.

Compression Capacity vs Slenderness

Specimen #18

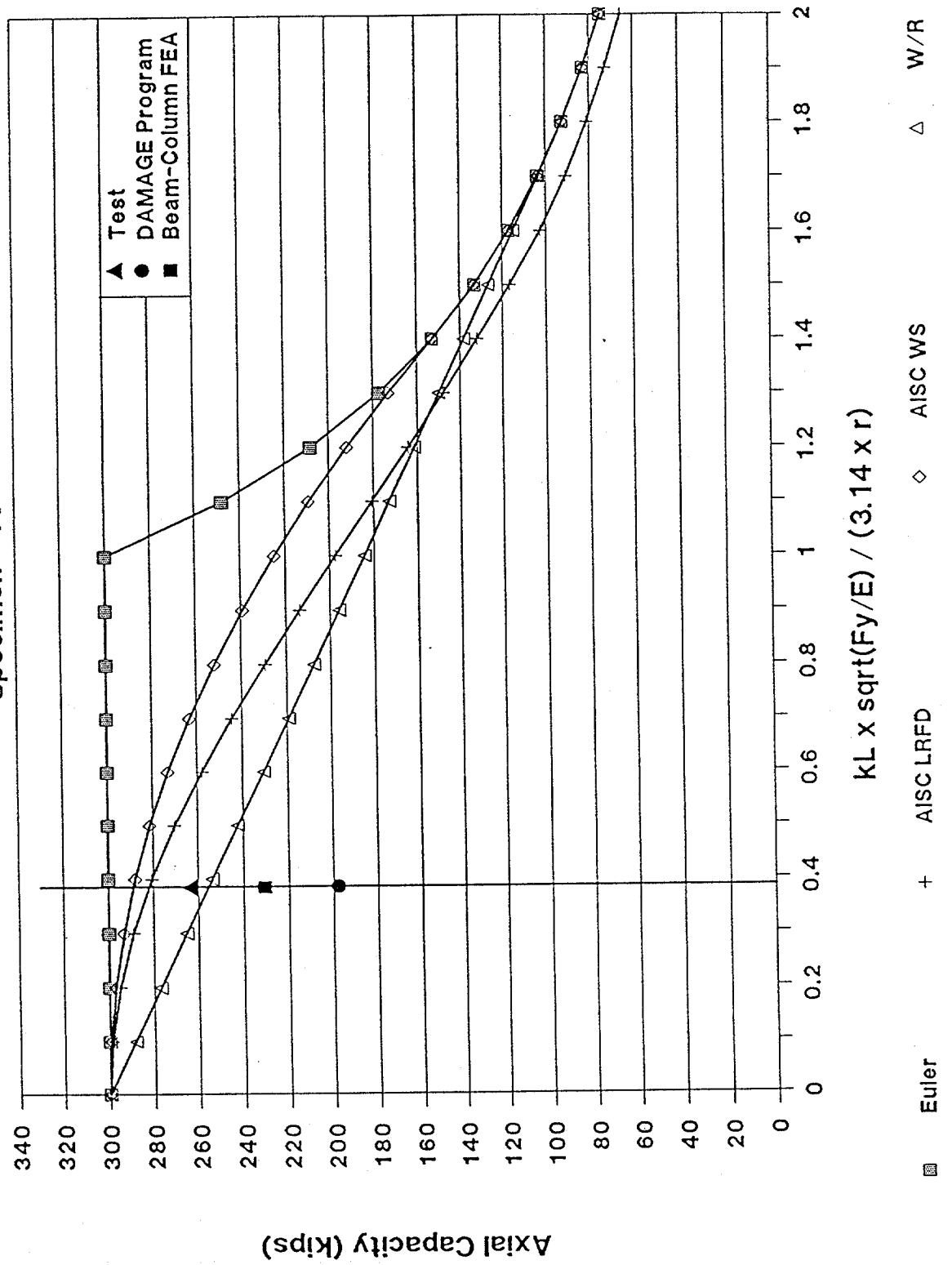


Figure 4-68

Specimen #18

Axial Load vs. Axial Deformation

Design Ult. Load = 417.77 kips

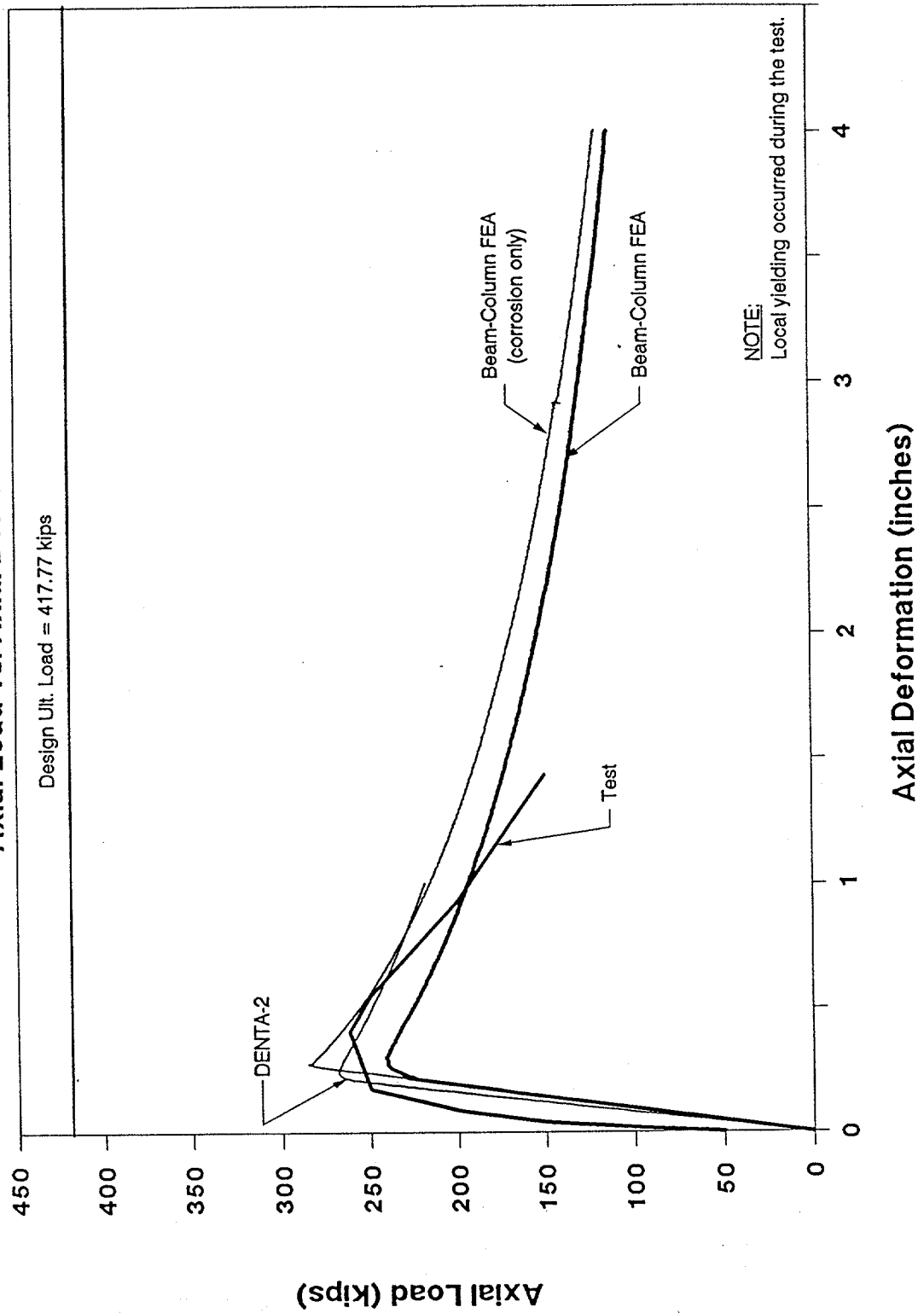


Figure 4-69

SPECIMEN 19

Damage Summary
Specimen #19

A&M Damage Number

Damage Description

No Damage

Compression Capacity vs Slenderness

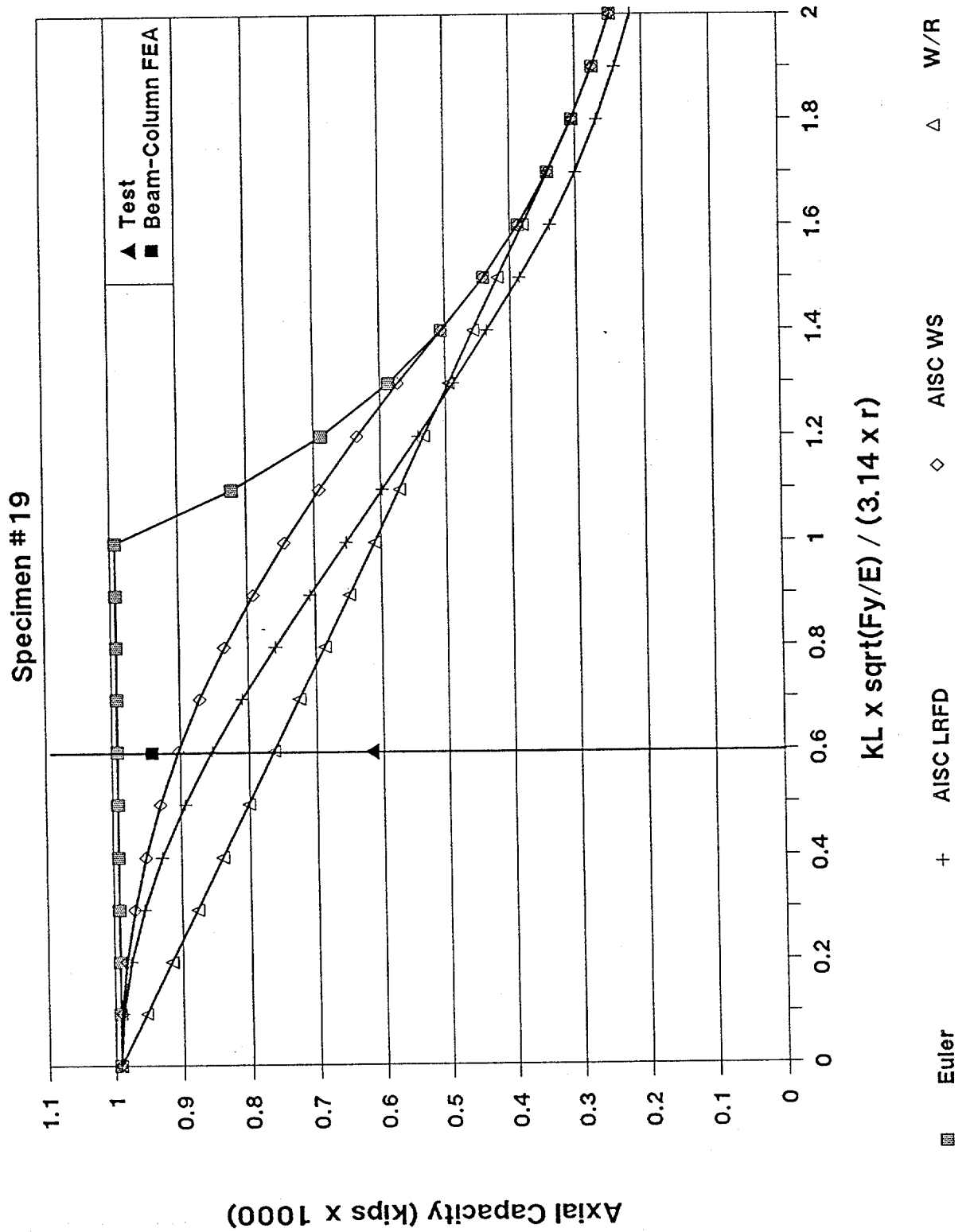


Figure 4-71

Specimen #19

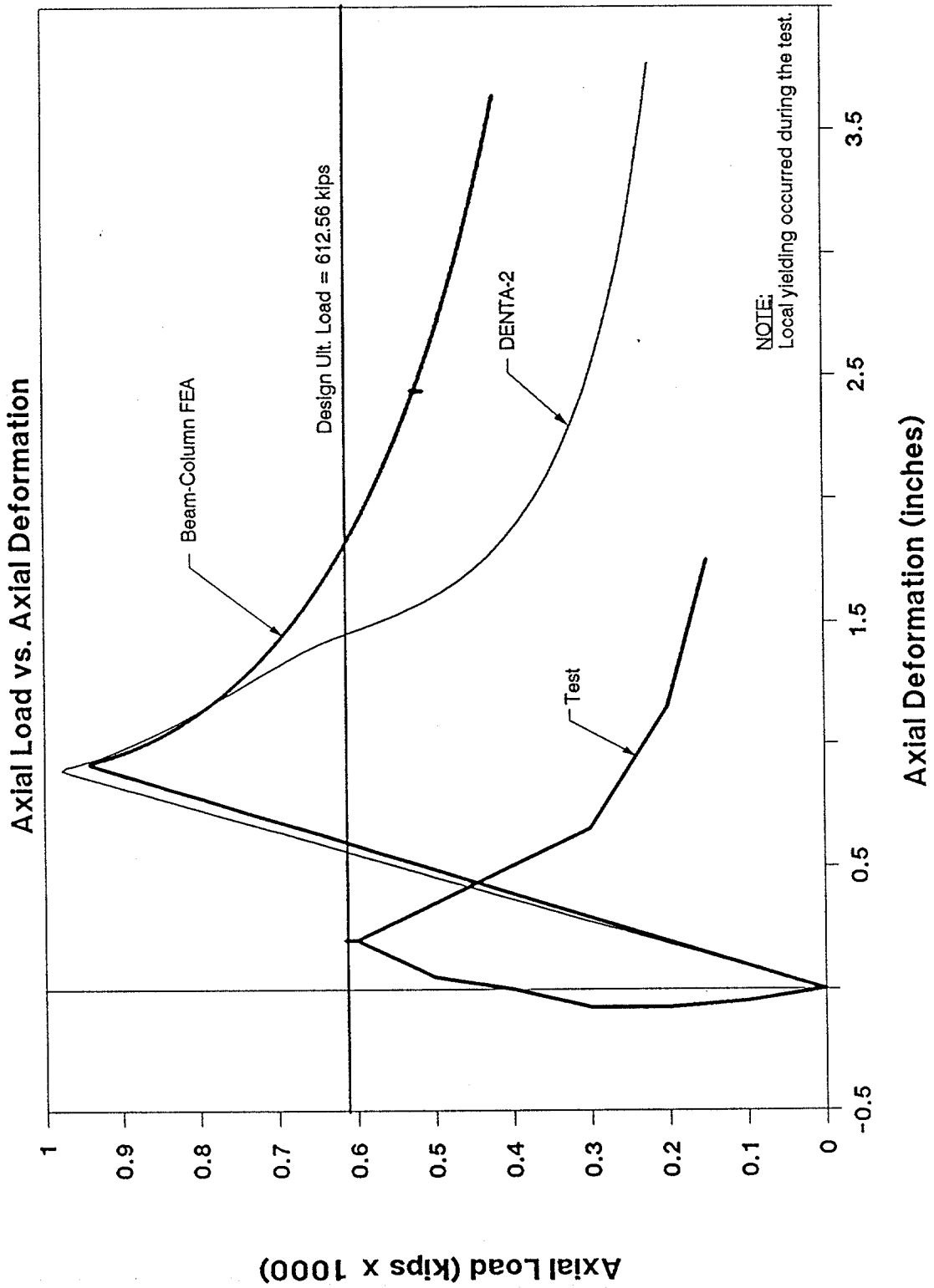


Figure 4-72

SPECIMEN 20

Damage Summary
Specimen #20

A&M Damage Number

Damage Description

No Damage

Compression Capacity vs Slenderness

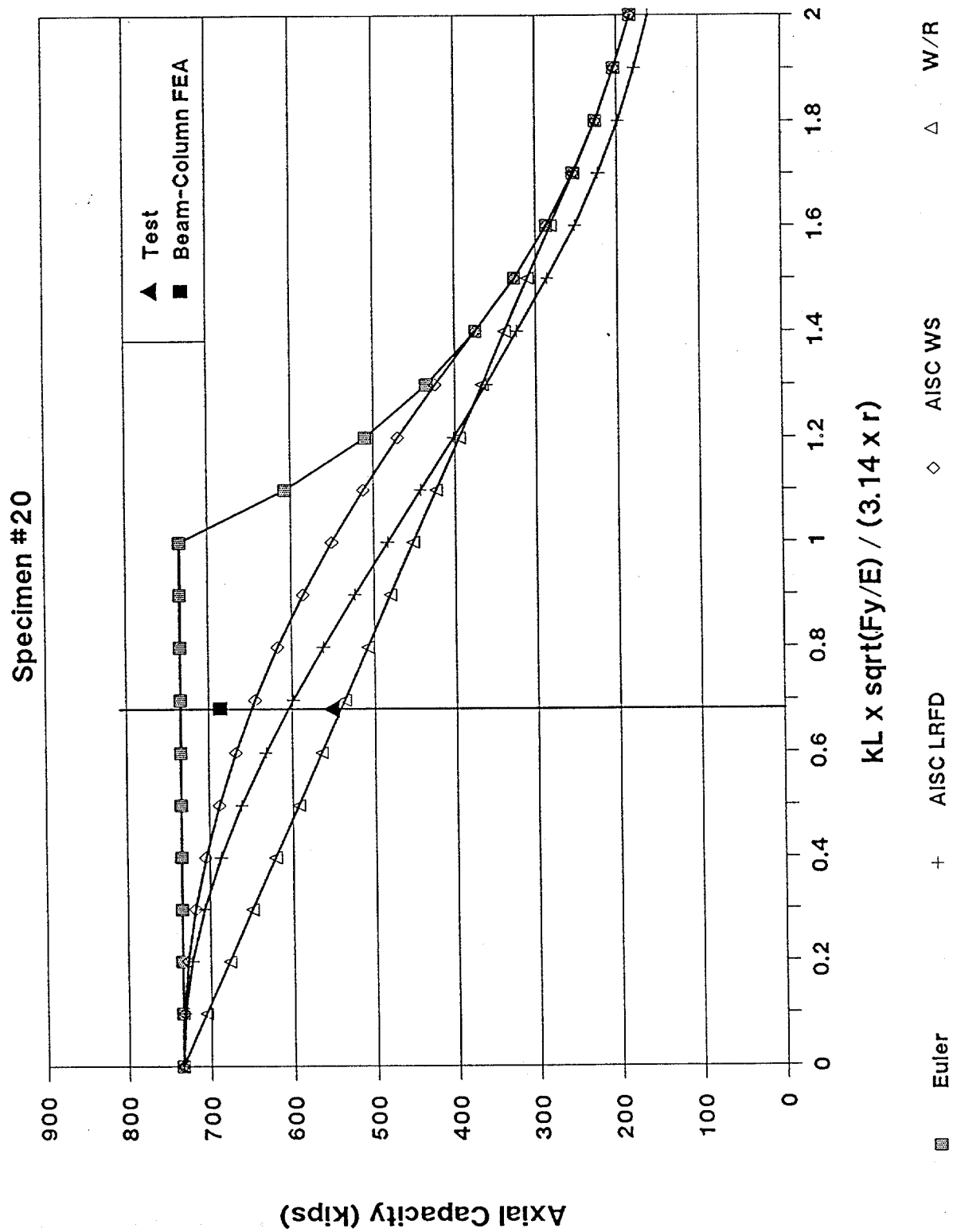


Figure 4-74

Specimen #20

Axial Load vs. Axial Deformation

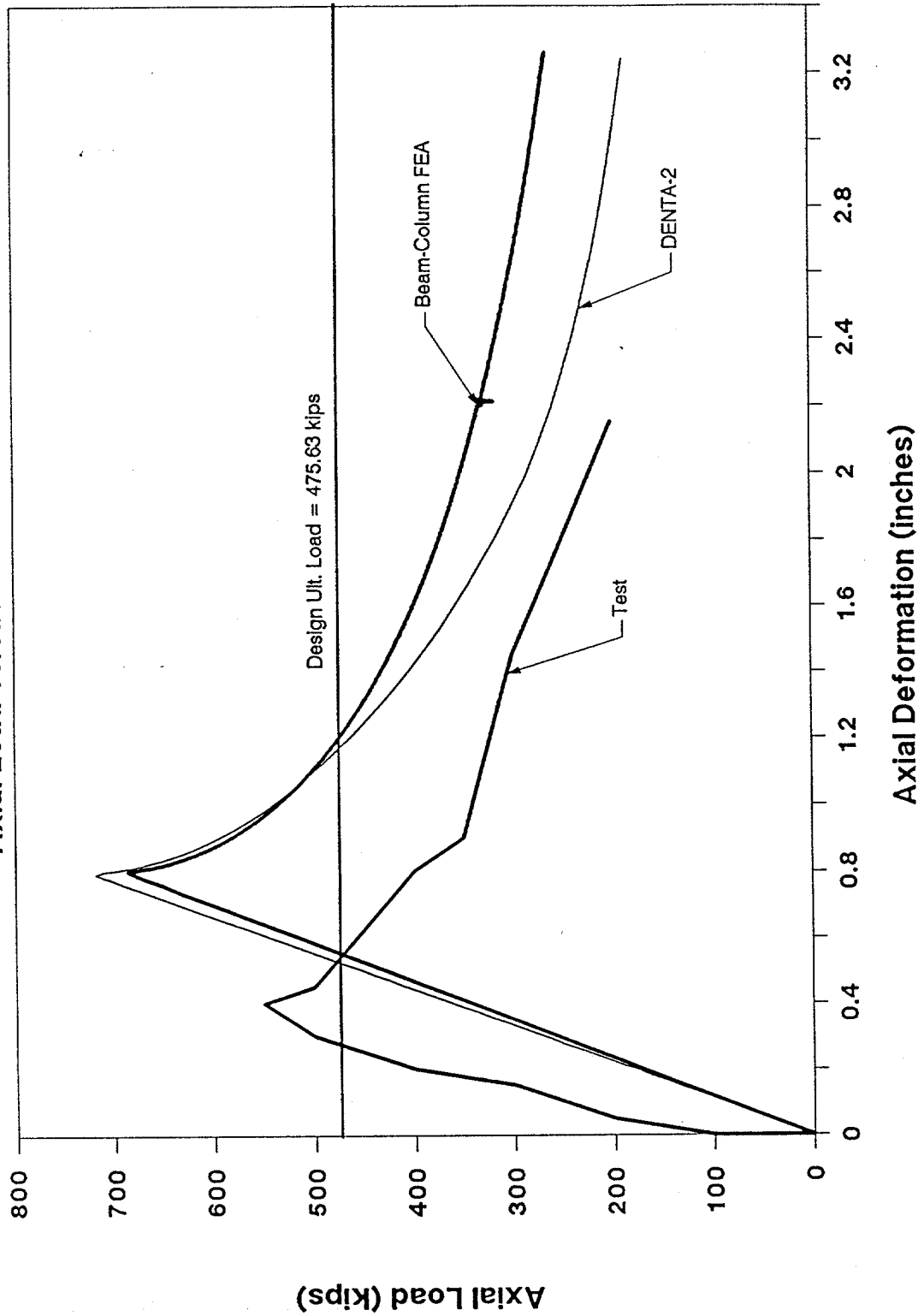


Figure 4-75

SPECIMEN 21

Damage Summary
Specimen #21

A&M Damage Number

Damage Description

7

Hole:

Diameter = 3"

Model Segment Length = 3"

Distance from loaded end = 24.96"

Angle from vertical = 288.4°

*Angle from vertical is clockwise from +Z axis
looking from the loaded end toward the opposite end
of the member

```

*****
*
*           Program DAMAGE
*
*
*****

```

TITLE: Specimen #21 - Damage #7

INPUT:

```

OUTSIDE DIAMETER (in) = 16.000
THICKNESS (in)       = .275
LENGTH (ft)          = 22.330
EFF. LENGTH FACTOR   = .50

YIELD STRESS (ksi)   = 52.20
YOUNGS MODULUS (ksi) = 25900.0

DENT DEPTH (in)       = .000
HOLE DIAMETER (in)    = 3.000
LAT. DISPL. (in)      = .00

```

RESULTS:

```

CROSS-SECTIONAL AREA (sq.in) = 13.59
DENT/HOLE ANGLE (rad)         = 5.89927
AXIAL ECCENTRICITY (in)       = .5085
REDUCED RAD. OF GYRATION (cu.in) = 5.356
REDUCED ELAS. SECTION MOD. (cu.in) = 44.481
PLASTIFICATION STRESS (ksi)   = .000
AVG. SQUASH STRESS (ksi)     = 49.011
IMPERFECTION PARAMETER       = .00081
SLENDERNESS RATIO            = 18.01637
EULER BUCKLING STRESS (ksi)   = 440.2952
SOLUTION ROOTS (SDCE1,SDCE2) (ksi) = 518.300      41.634

DAMAGED MEMBER AXIAL CAPACITY (ksi) = 41.634
DAMAGED/UNDAMAGED STRESS RATIO      = .79759
UNDAMAGED SLENDERNESS RATIO          = .34432

```

Notes:

- (1) Hole diameter and dent depth should be measured w/r the tubular mid-wall diameter.
- (2) For dented members it is assumed that the maximum stress the dented region can sustain is equal to the plastification stress. This stress is set equal to zero for hole damage.
- (3) Dent and hole damage must be evaluated separately. Either can be assessed in conjunction with bending damage.

Compression Capacity vs Slenderness

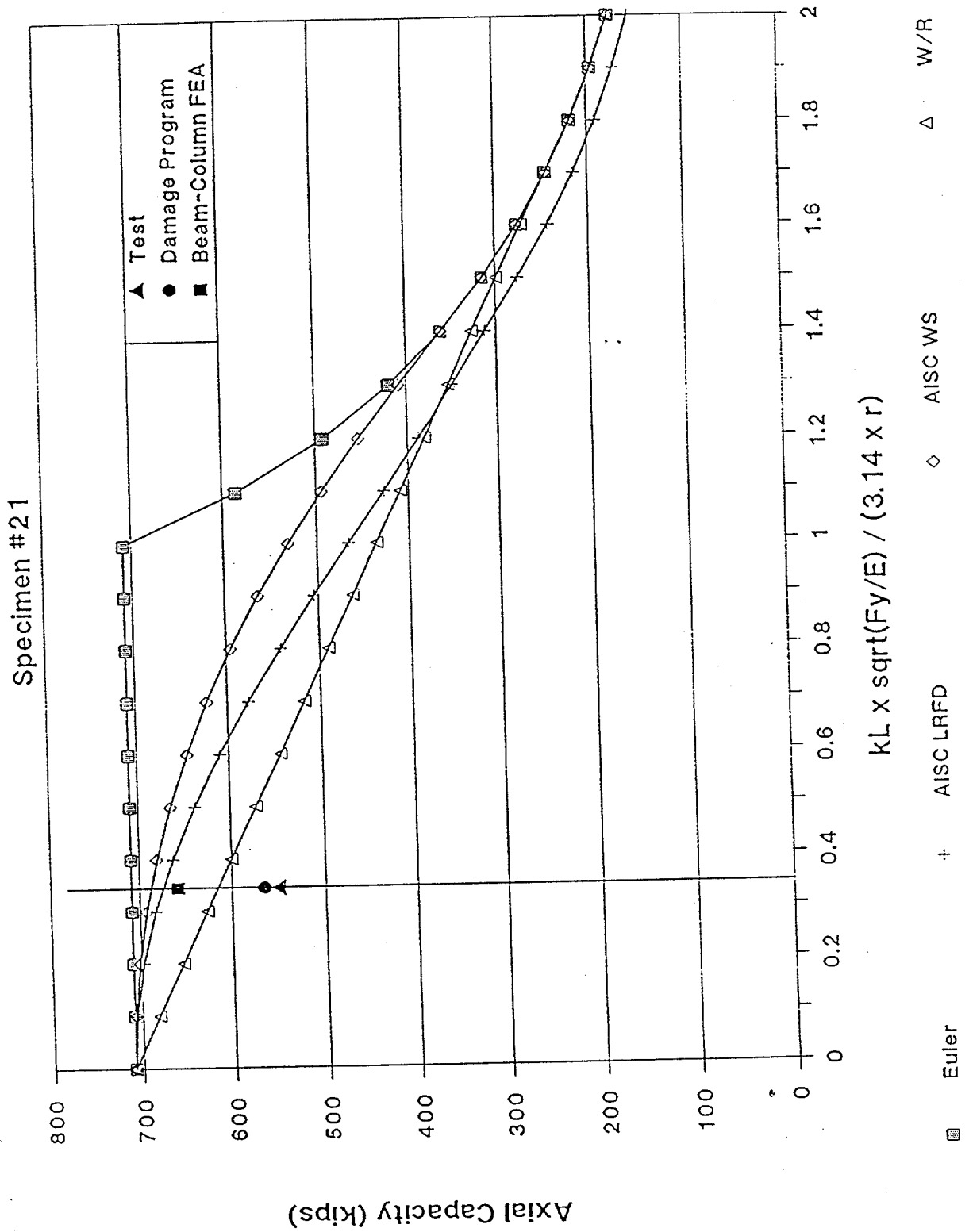


Figure 4-78

Specimen #21

Axial Load vs. Axial Deformation

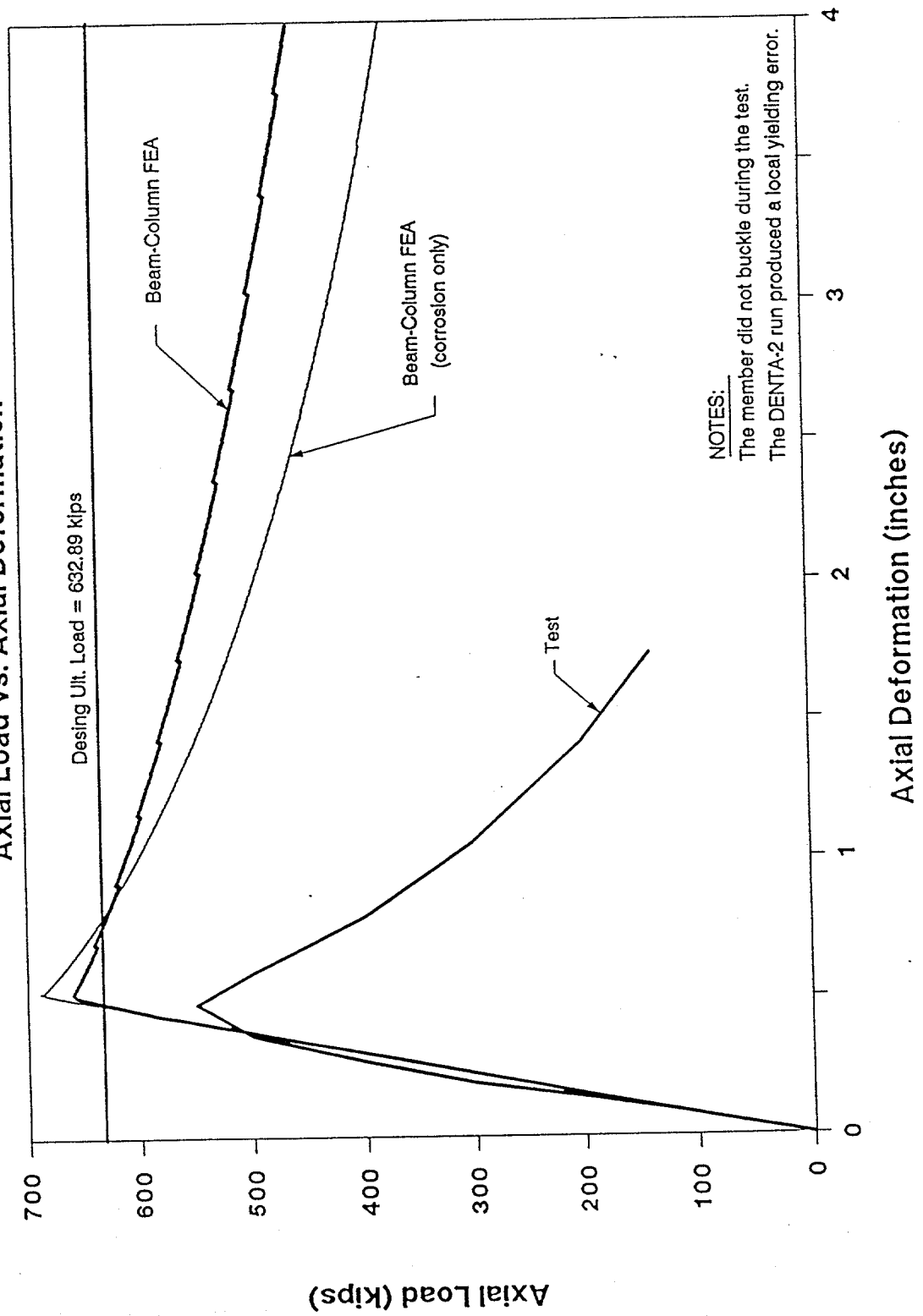


Figure 4-79

5.0 COMPARISON OF RESULTS

There are several factors affecting the analysis which should be considered when comparing these results to the full scale tests. Some of the more important ones are related to the limitations of the beam-column element used in the finite element analysis (FEA). These include:

1. Absence of damage growth.

Once numerically defined in the model, the damaged section properties remain constant. In actuality, a dent or a hole can become more severe as the bending increases, thereby reducing the overall strength of the member more than initially assumed. A Norwegian Institute of Technology report (5) found this factor to be especially significant in the post-buckling region.

2. Assumption of a single dent shape.

Though the dents in this study came in all shapes and sizes, for modelling purposes, they were treated the same with only depth and orientation changing.

Other idealizations include: using the effective wall thickness for the entire member, neglecting local properties and ignoring longitudinal cracks and other types of damage. Though necessary to achieve a workable analysis, these idealizations contribute, in varying amounts, to discrepancies between the predicted and the actual responses.

A question was raised during the study regarding the use of the modulus of elasticity (E) calculated by Texas A&M. In all of the computer analyses this calculated E was used. Texas A&M, in its data reduction used a nominal value of 29500 ksi for E. It is not believed that this difference is significant in the results. To demonstrate this, the DENTA-2 results were recalculated by Shell using 29500 ksi for E instead of the calculated E (which ranged from

24900 ksi to 30000 ksi). The peak capacities were identical or nearly identical in every case and the overall force-deformation relationships were practically the same. These results are shown graphically in Figures 5-1 and 5-2 which are representative of the results for all the specimens.

The basic yardstick by which the analyses and the tests were compared was the force-deformation curve. When looking at the two curves the important features are the initial stiffness, the peak capacity (buckling load) and the post-buckling region. In most cases, the initial stiffnesses agreed but the post-buckling curves seldom compared favorably. In all but three of the tests, the peak capacity was overestimated. The difference ranged from 3% to 76%. The three specimens which underpredicted the capacity did so by an average of 23%.

The following is a brief description of the results for each specimen and how the two tests compared:

- | | |
|------------|--|
| Specimen 1 | Damage included some locally heavy corrosion as well as one significant dent. The peak capacities compared well (predicted was 3% greater than actual) though the post-buckling slopes did not. In the full scale test, the member experienced local yielding prior to buckling. |
| Specimen 2 | Aside from some moderate corrosion there was no significant damage. The peak capacities didn't compare well (the predicted was 36% greater than the test) nor did the post-buckling slope. The specimen did not buckle until after local yielding occurred in the full scale test. |
| Specimen 3 | This specimen was described as highly corroded by the Texas A&M report but no significant dents or holes were present. The predicted capacity exceeded the actual capacity by 40% in this case. The |

post-buckling slopes weren't well correlated. The member yielded locally prior to buckling in the full scale test.

Specimen 4 The member was bent in one lateral direction but was otherwise undamaged. The peak capacities differed by 35% (the predicted capacity was higher). The post-buckling slopes had relatively the same shape for this specimen.

Specimen 5 The damage here was limited to a single dent near one end. Only a 7% difference was found in the capacities (with the analytical prediction the greater of the two). The analytical post-buckling slope was relatively flat compared to that of the test. During the full scale test, the specimen experienced local yielding prior to buckling.

Specimen 6 This specimen was not visibly damaged. The predicted capacity exceeded the test capacity by only 4%. Also, the post-buckling slopes compared well.

Specimen 7 A single dent and light corrosion were the extent of the damage to the specimen. The analysis under-predicted the test results by 25%. The post-buckling slopes didn't compare well.

Specimen 8 The damage to this specimen consisted of a dent close to the end. A fair correlation was found between the two peak capacity values. The prediction exceeded the actual value by 16%. The post-buckling slope was considerably flatter for the analytical method than for the physical test. Local yielding occurred prior to buckling in the full scale test.

- Specimen 9 Widespread corrosion was visible on the specimen. Good correlation (only a 5% difference) was found for the peak capacities. The post-buckling slopes didn't match well.
- Specimen 10 There was no significant damage to the member aside from corrosion. The predicted capacity was only 4% greater than the test value. The post-buckling slopes in both cases agreed quite well.
- Specimen 11 This specimen had only corrosion damage. A 13% difference separated the predicted capacity and the actual capacity. The post-buckling slope from the analysis didn't fall off as quickly as that of the full scale test.
- Specimen 12 Two holes and a dent were the extent of the damage to the member. The two capacities compared well (only differing by 7%). The post-buckling slopes didn't match well.
- Specimen 13 This specimen was damaged by several dents and widespread corrosion. The predicted capacity was 41% greater than the actual capacity. The two post-buckling slopes did not correlate well.
- Specimen 14 Widespread, heavy corrosion as well as dents and out-of-straightness damaged this member. The peak capacity was over-predicted by 66%. The two post-buckling slopes did not match well. There was evidence of local yielding before the buckling load was reached in the full scale test.

- Specimen 16 This specimen had several dents and was bent in both lateral directions. Also, it consisted of two sections of different thicknesses connected by a collar. The predicted results didn't compare well to the test results (+76%). The shape of the post-buckling curves correlates somewhat better.
- Specimen 17 A single dent and some out-of-straightness comprise the damage to this member. The two capacities didn't compare well (-22%). The post-buckling regions aren't well related.
- Specimen 18 This specimen showed heavy to moderate corrosion along its entire length as well as denting and bending. The capacity was under-predicted by 22%. The predicted post-buckling slope is somewhat flatter than that shown by the physical test. The member yielded locally before buckling in the full scale test.
- Specimen 19 A longitudinal crack was present in the specimen but was not modelled. Widespread corrosion was also present. The prediction was in error by 53% on the high side. The post-buckling slopes showed better correlation than the capacities. The specimen experienced local yielding prior to buckling in the full scale test.
- Specimen 20 No dents or holes were found on the specimen. The analysis predicted a 25% higher peak capacity than the test results showed. The post-buckling regions correlated fairly well.

Specimen 21

A hole was the only damage present in the member. A longitudinal crack was present but was not modelled. The predicted capacity was 20% higher than the test capacity. The post-buckling slopes did not compare well. The specimen didn't buckle in the full scale test.

A graphical comparison of these results is shown in Figures 5-3 and 5-4. The first plot shows the peak capacity predicted by the finite element analysis against the peak capacity from the full scale test. The diagonal line on the plot represents where the points would fall if the prediction matched the test exactly. On average, the peak is overpredicted by 20.1% with a standard deviation of 25.68%.

Buckling was the assumed mode of failure for the analysis but nine of the twenty specimens yielded locally so the results are somewhat skewed. To clarify the results, the specimens which buckled were separated from those which didn't. When only specimens which buckled are compared, the overprediction drops to 15.73% (standard deviation = 26.34%). The overprediction rises to 25.44% (standard deviation = 23.79%) when only the non-buckling specimens are considered.

Figure 5-4 shows, in bar chart format, a comparison of several different ratios. The finite element analysis (FEA) peak capacity over the full scale test peak capacity, the DENTA-2 capacity over the test capacity and the FEA capacity over the DENTA capacity are the three ratios presented. As shown by this chart, the best correlation is between the two computer methods. This is not surprising since their solution schemes are somewhat similar. The average values for the three ratios are also shown on the chart. All specimens are included here regardless of the mode of failure.

To try to find some pattern to the results obtained in this study, the specimens were divided into groups based on several factors: amount of damage, D/t , L/r , dent depth over diameter (D_d/D) and whether local yielding occurred. Figure 5-5 is a table of the results separated according to these categories.

Sorting the specimens in this manner does not show any obvious trends. Sometimes, members with similar damage, D/t and L/r had similar ratios of FEA capacity to test capacity, at other times they did not. In general, too few samples from any given category were present to identify a trend.

To extend this idea of relating predicted results and geometric properties to actual results to discover a trend, a regression analysis was performed. Using the full scale test capacity as the dependent variable and the beam-column finite element analysis capacity, the diameter to effective thickness ratio and the length to radius of gyration ratio (also calculated with the effective wall thickness) as the independent variables, three formulae were created for estimating the peak capacity. The first is illustrated in Figure 5-6 and includes all the specimens used in the study regardless of the specimen's mode of failure. The second (Figure 5-7) includes only those members that buckled during the full scale test. Figure 5-8 shows the last regression line, created with data from the specimens where buckling wasn't the primary mode of failure.

The first regression line has the following formula:

$$P_{est}(kips) = 168.83 + 0.815(FEA) - 2.874(D/t) - 0.315(L/r)$$

where

P_{est} = Estimated Peak Axial Compressive Load

FEA = Peak Axial Compressive Load from Beam-Column FEA

D/t = Diameter to Effective Wall Thickness Ratio

L/r = Length to Radius of Gyration Ratio

The estimated capacity from this formula exceeds the test capacity by an average of 4.75% with a standard deviation of 23.76%. Statistically, this average is valid only for this specific set of twenty specimens. To calculate the true mean, an infinite number of specimens would have to be tested. But,

if a normal distribution is assumed for the results, one can estimate the range in which the true mean would fall. Given these twenty known results and a normal distribution, there is a 95% probability (100% being certain) that the true mean for the estimated to actual capacity ratio would fall somewhere between a 5.66% underprediction and a 15.16% overprediction. This is called the confidence interval for the mean.

The other two regression lines are shown to demonstrate the better predictive ability evident if one knows the actual mode of failure for the member. For the members which buckled during the full scale test the regression line formula is as follows:

$$P_{est}(kips) = 365.61 + 1.039(FEA) - 12.62(D/t) + 0.249(L/r)$$

The average overestimate for these eleven specimens was 2.77% with a standard deviation of 22.5%. The 95% confidence interval for the mean falls between -10.56% (negative indicating a lower-than-actual value) and 16.09%.

For those members that yielded prior to buckling or didn't buckle during the full scale test, the regression line formula is:

$$P_{est}(kips) = -85.95 + 0.538(FEA) + 4.121(D/t) + 0.151(L/r)$$

This line overestimates the results for nine specimens by an average of 1.65% (standard deviation 15.5%). The 95% confidence interval for the mean is from -9.11% to 12.42%. Because determining the mode of failure of a member prior to testing is difficult, these last two formulae are presented here merely for comparison.

Modulus Comparison

Axial Load vs. Axial Deformation

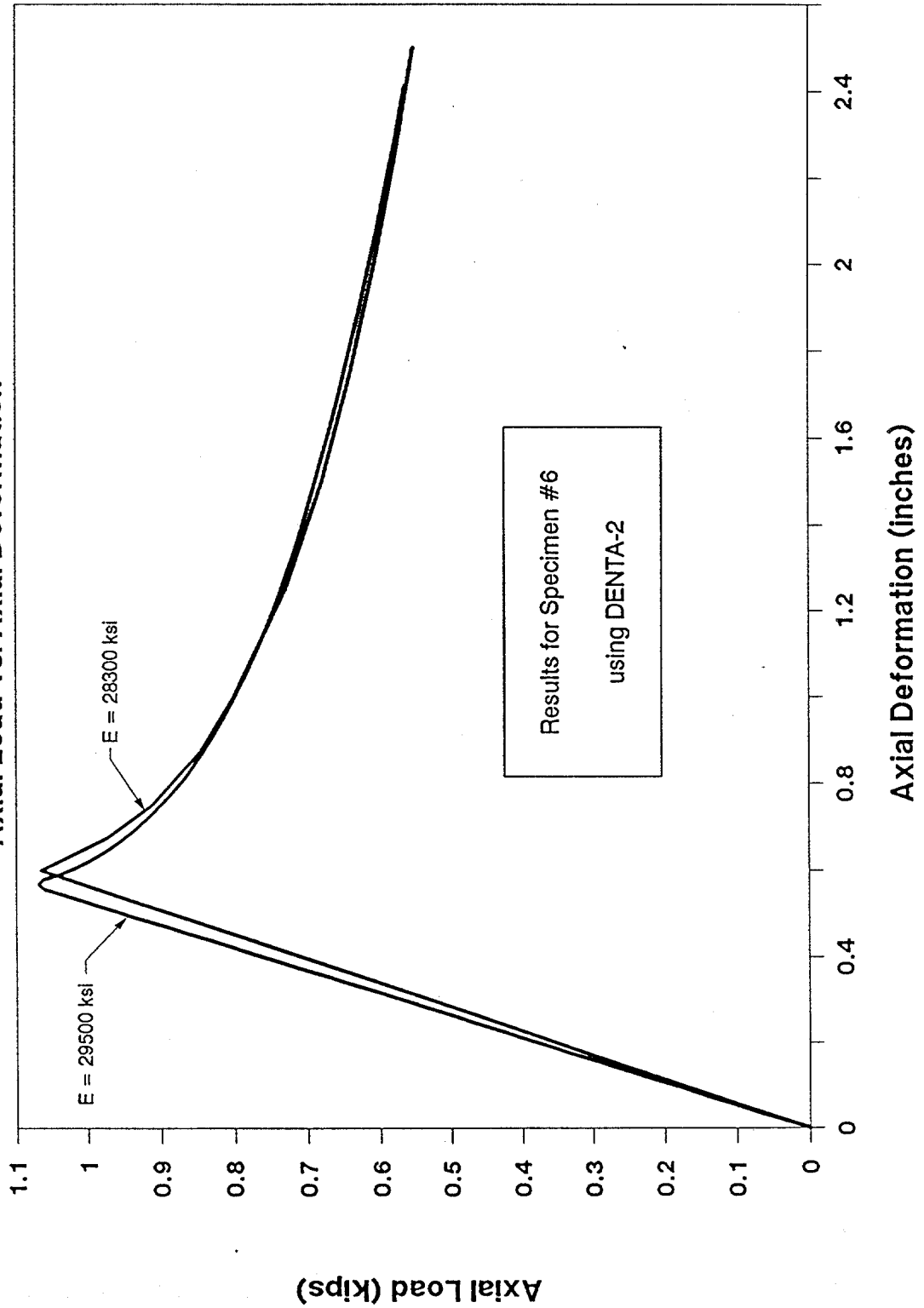


Figure 5-1

Modulus Comparison

Axial Load vs. Axial Deformation

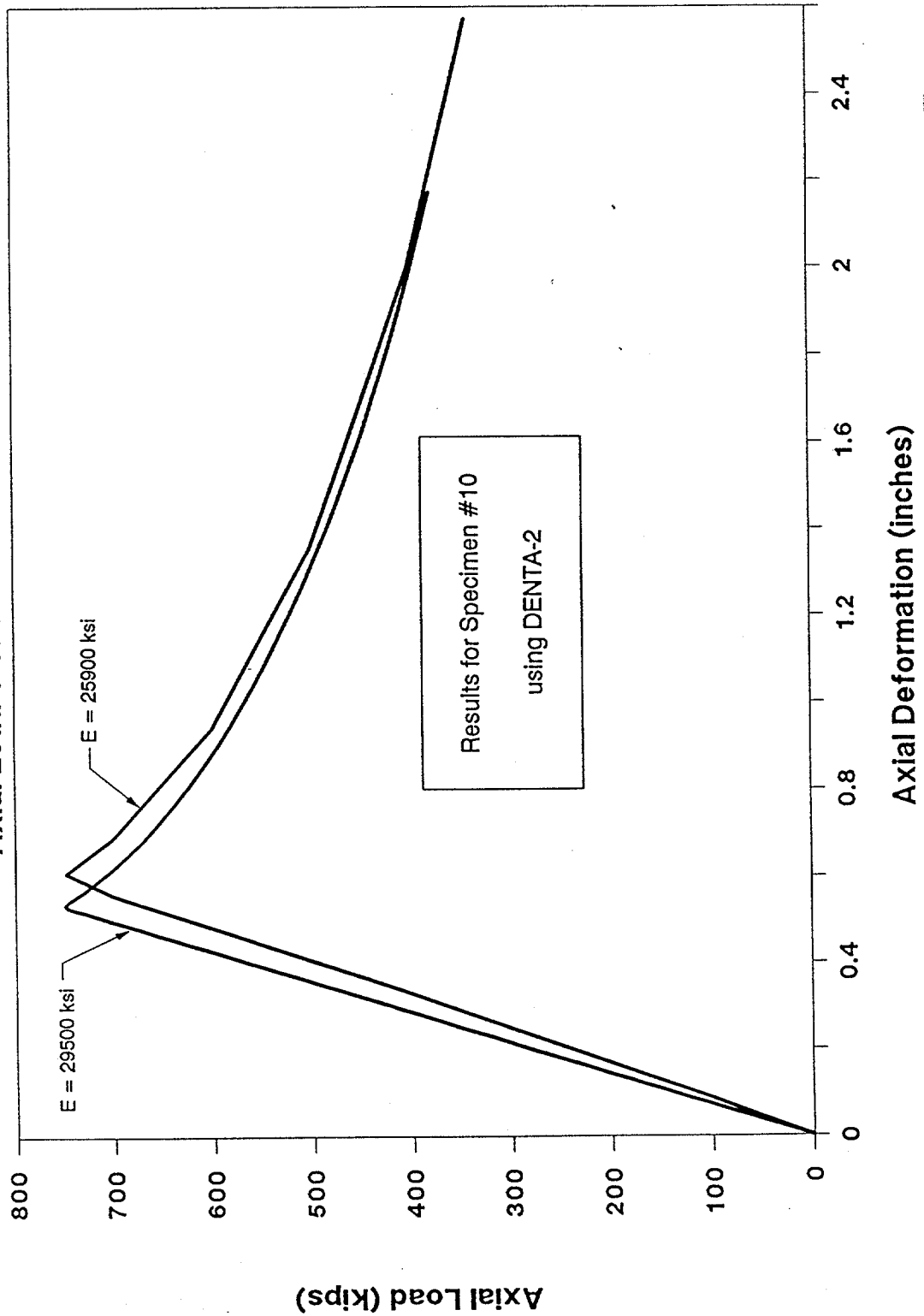


Figure 5-2

Capacity Comparison

Beam-Column FEA vs. Full Scale Test

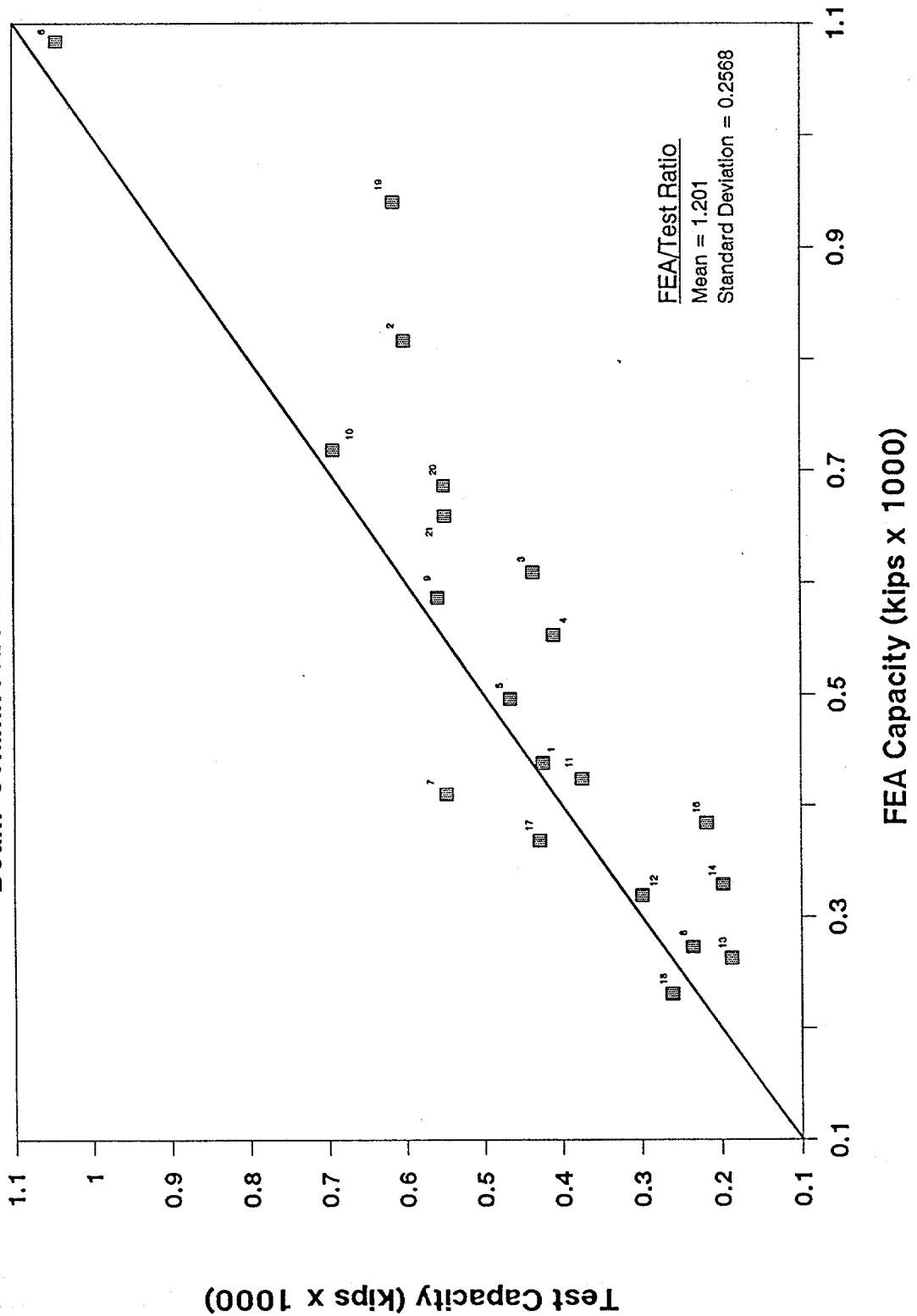


Figure 5-3

Axial Capacity Comparison

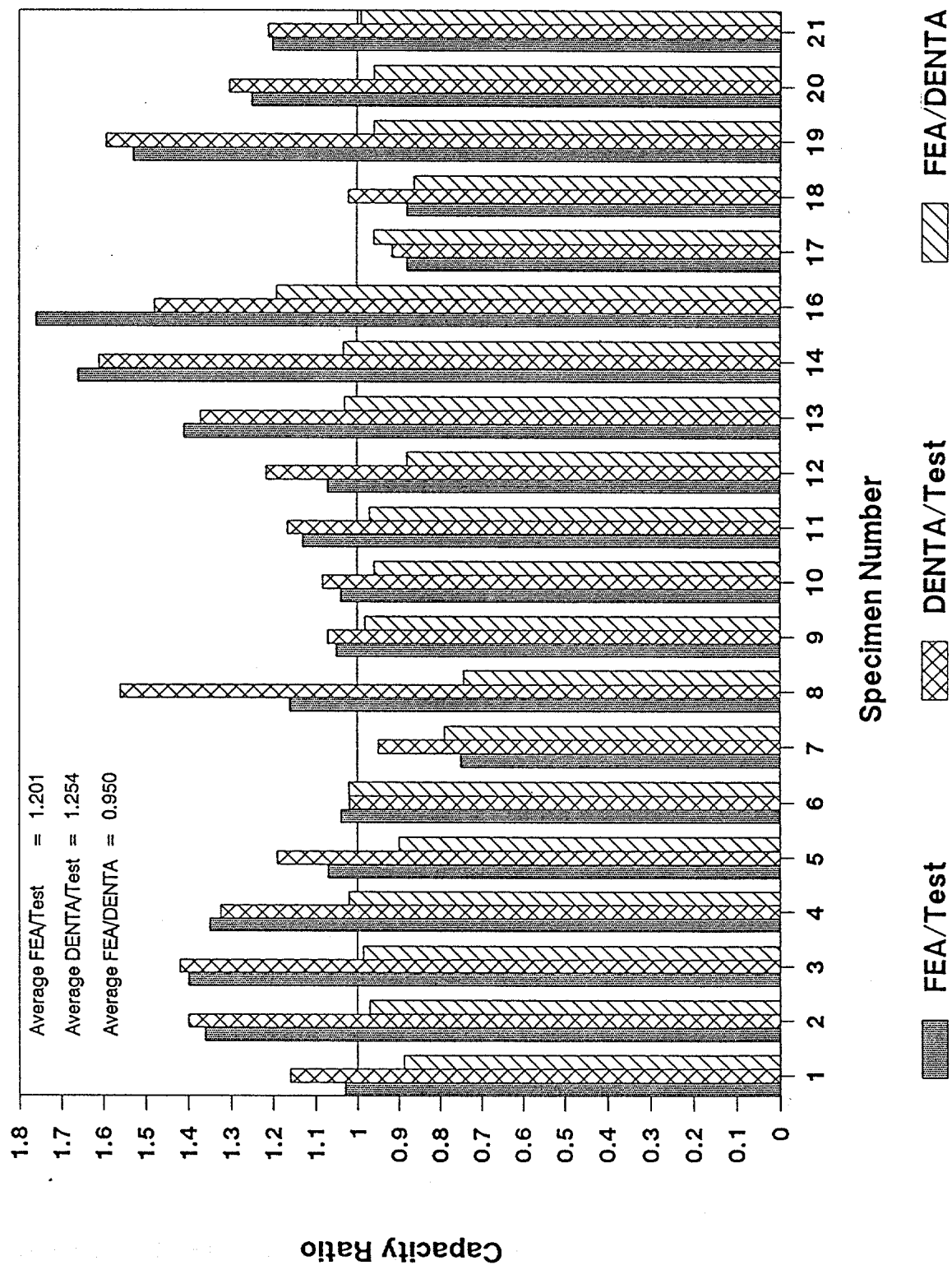


Figure 5-4

Capacity Comparison Summary

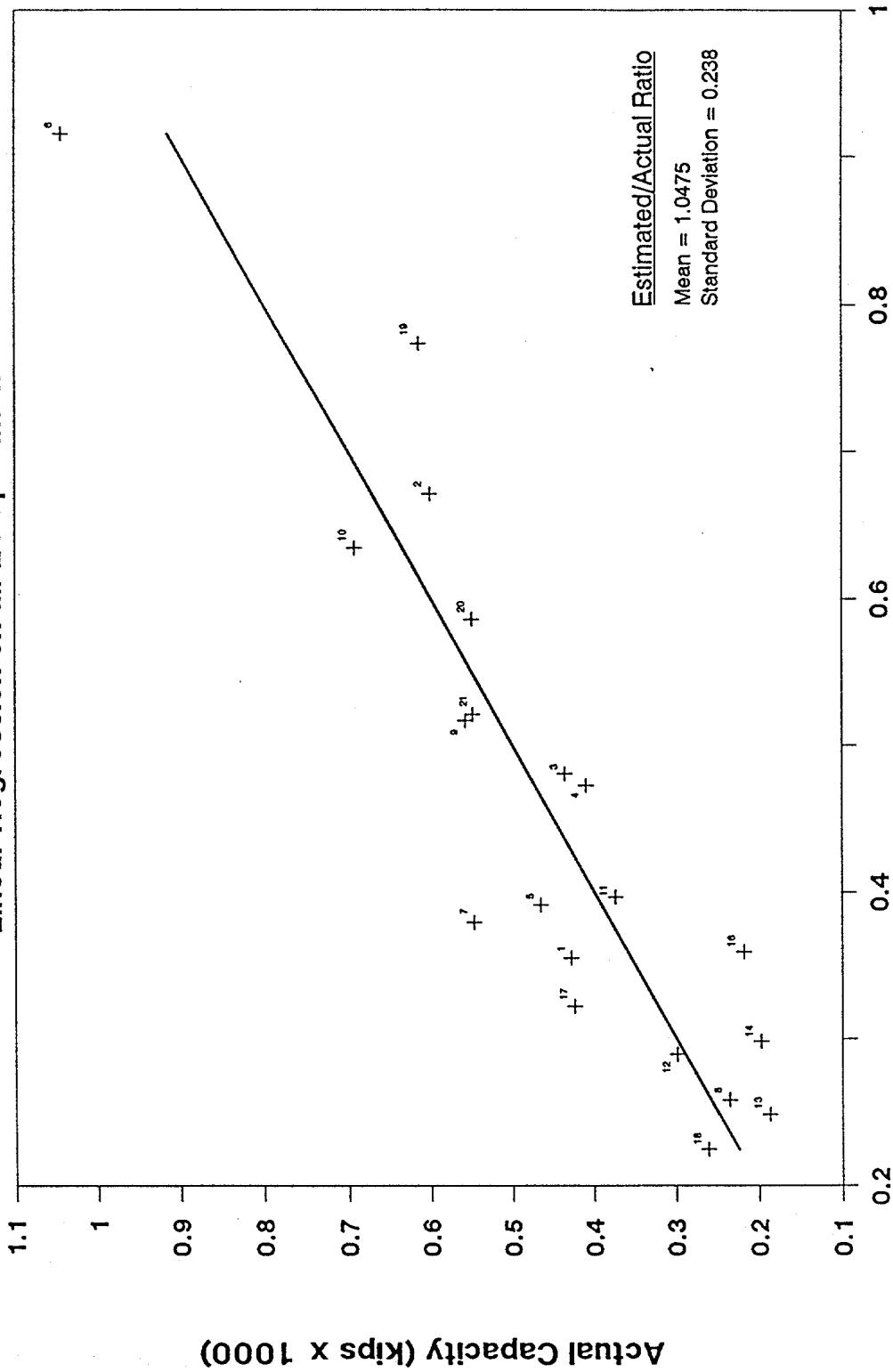
Specimen	Test	FEA	FEA/Test	D/t	L/r	D _d /D
<u>No dents or holes</u>						
10	692	718	1.04	32.9	79.0	-
6	1043	1084	1.04	40.0	68.8	-
9	558	586	1.05	39.1	54.8	-
11	374	424	1.13	30.7	94.5	-
20	550	686	1.25	38.9	94.7	-
4	410	553	1.35	40.6	94.8	-
2*	601	816	1.36	52.0	42.6	-
3*	436	609	1.40	59.0	46.4	-
19*	614	940	1.53	47.3	80.8	-
<u>One dent or hole</u>						
7	548	410	0.75	31.2	108.5	.098
17	420	368	0.88	30.2	85.8	.108
1*	424	438	1.03	66.7	37.5	.028
5*	465	496	1.07	59.4	35.5	.028
8*	236	273	1.16	36.7	86.4	.023
21*	549	659	1.20	58.2	55.3	-
<u>Multiple dents and/or holes</u>						
12	299	319	1.07	36.3	108.1	-
13	187	263	1.41	39.5	65.9	-
16	218	384	1.76	34.0	78.9	-
18*	262	231	0.88	40.7	48.2	-
14*	198	329	1.66	43.2	45.7	-

Note: * denotes members which experienced local yielding and/or didn't buckle.

Figure 5-5

Estimated vs. Actual Capacity

Linear Regression on all 20 Specimens



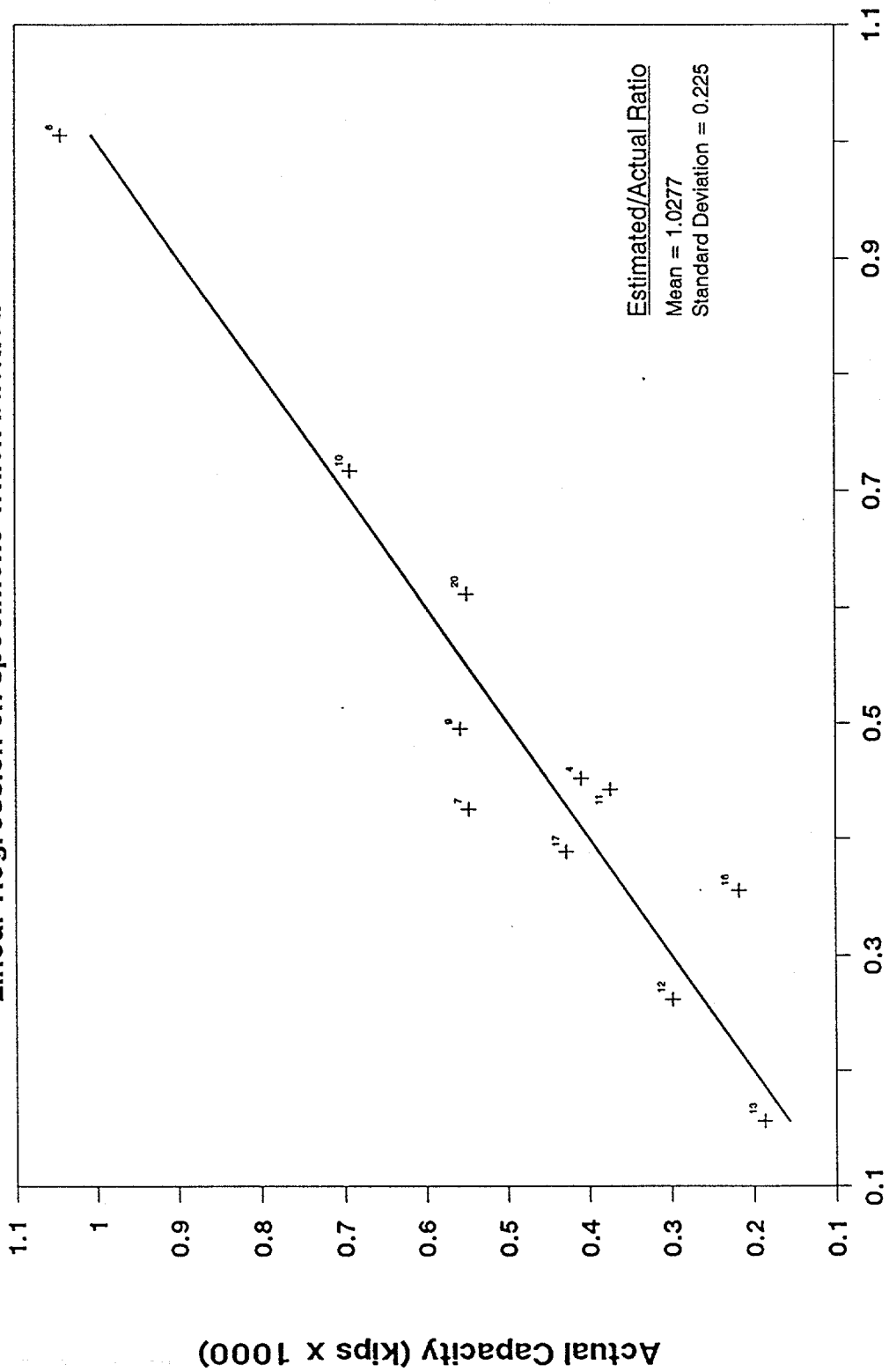
Estimated Capacity (kips x 1000)

$$\text{Estimated Capacity} = 168.83 + 0.815 (\text{FEA}) - 2.874 (D/t) - 0.315 (L/r)$$

Figure 5-6

Estimated vs. Actual Capacity

Linear Regression on specimens which buckled



Estimated Capacity (kips x 1000)

$$\text{Estimated Capacity} = 365.61 + 1.039 (\text{FEA}) - 12.62 (D/t) + 0.249 (L/r)$$

Figure 5-7

Estimated vs. Actual Capacity

Linear Regression on members which did not buckle

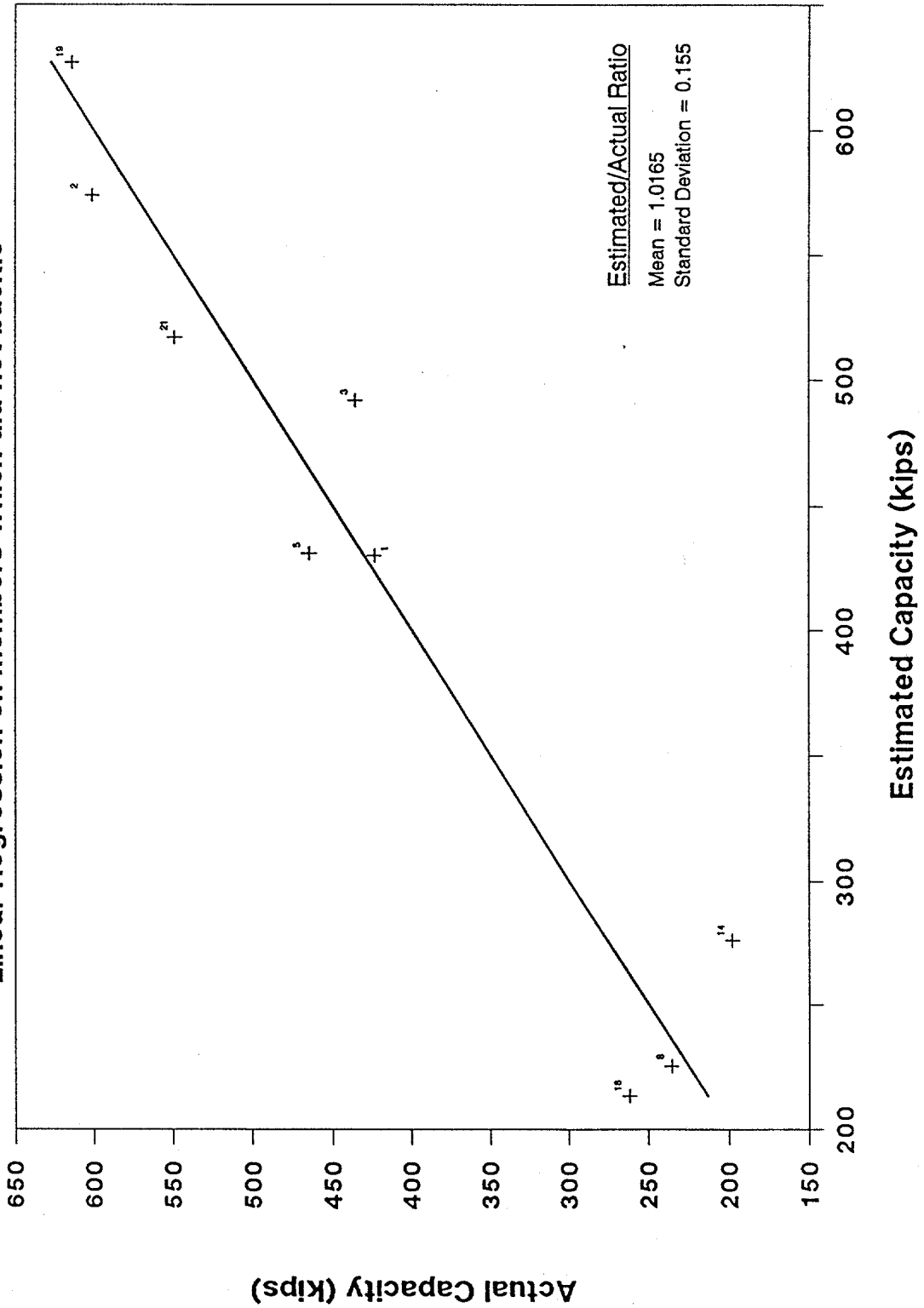


Figure 5-8

6.0 Summary and Conclusions

During the course of this project, full scale, axial compression tests were performed on salvaged, damaged tubular members. A procedure was developed for the analysis of the effects of in-service damage on tubular member capacity using both simplified and beam-column finite element (FE) analyses of the members.

The data from the full scale tests were directly compared with the FEA predictions and showed scattered results. For the twenty specimens tested, the predicted capacity exceeded the actual capacity by an average of 20.1%. Also, the predicted post-buckling capacity usually exceeded the capacity recorded during the full scale test. This may be in part due to the lack of dent growth capability in the beam column element.

When a regression analysis was performed on the specimens using the FEA results, the D/t ratios and the L/r ratios as the independent variables; a reasonable estimate of the actual capacity was formulated. This provided an equation that over predicted the peak capacity by an average of 4.75% with a standard deviation of about 24%.

In studies similar to this one (mentioned in the introduction), the predicted response of the specimens to axial loading matched well with the actual (test) response. The members used were new and their characteristics were easily identifiable. Even the damage, when present, was carefully controlled.

Results from this joint industry project do not show the same agreement between FEA predictions and actual response. The methods used in this project were based on and verified by valid studies which achieved good results. When compared to those studies, there are several major differences. These include the presence of corrosion, multiple damage areas on a single member and irregular rather than controlled damage shape and condition.

The scattered results were probably not the result of the irregular damage shape. A study by C.S. Smith (6) showed that the reduction in strength of a tubular member due to a dent was insensitive to the shape of the dent.

Multiple damage on a single member does not appear to be a likely cause of the discrepancies either. When re-analysed with only the most significant damage modelled, Specimen #12 showed the same response as the model which included all of the damage (see Figure 6-1). Also, the DENTA-2 results, which matched the FEA results very well, allow only a single damage condition to be modelled. This indicates that, despite multiple damage states, a member can be modelled as a single damage specimen without dramatically sacrificing results.

Another significant factor was corrosion. Corrosion was evident on most of the members and was the cause of many of the local problems encountered during the tests. Eight of the twenty members experienced local yielding prior to buckling. Most of these members had significantly reduced wall thicknesses (as measured by ultrasonic testing after testing) in the area of the local yielding. In some cases, the reduction in wall thickness caused the local D/t ratio to rise above the API (7) limit for local buckling considerations (see Figure 6-2). The corrosion lends a large degree of uncertainty to the properties of the entire member and significantly increases the likelihood of local anomalies.

Despite the problems with quantifying the corrosion damage reasonably, the regression estimates show good correlation with the test results. With a larger sample of data points and more accurate computer predictions, this estimate could be improved. Even so, the confidence interval (defined in the previous section) for the mean spans a fairly small range, only about 20%. This means that using the regression line formula created for all twenty specimens within reasonable bounds of D/t and L/r (about 30-70 and 35-110 respectively) can yield reasonable results. It is important to consider that these results were obtained from member information not readily available from present offshore inspection techniques. The effective wall thickness and the actual yield stress of the material used in this study are more exact quantities than a designer usually has at his disposal.

As a result of the experimental program the following specific observations and conclusions can be made:

1. The behavior of members with multiple forms of damage were generally dominated by one damage site. The origin of the failure mode was generally located at the dominate damage site.
2. Five specimens (Specimens 04, 13, 14, 16, and 17) had significant out-of-straightness damage. This damage dominated the behavior and the ultimate capacity of these members.
3. Two specimens (Specimens 05 & 21) had large through thickness cracks at a welded longitudinal seam. The behavior and ultimate capacity of these members were dominated by this damage.
4. Holes did not dominate the behavior or the ultimate strength of the specimens tested. Only one specimen (Specimen 12) of the nine specimens with holes, failed at the location of the hole. In the case of Specimen 12, the hole was actually a 4 x 7.5 inch tear located next to a 6 x 10 x 1.75 inch dent.
5. Seven of the twenty specimens failed by yielding in a region of reduced cross section caused by severe corrosion damage. The failure region for six of these seven specimens was not located until after the full scale tests were performed.
6. The most severe corrosion can occur on the inside surface of the member. Thus, it is can be extremely difficult to locate and evaluate the most severely corroded areas using only visual and ultrasonic testing. The primary indication of this possible condition would be a hole in the member.
7. Ultrasonic wall thickness measurements tend to over predict the overall effective wall thickness (as determined from the full scale test data) of members with corrosion damage. Thirty ultrasonic measurements were taken

on each of the specimens. For these twenty specimens, the average effective wall thickness to ultrasonic wall thickness ratio, $(t_{eff}/t_{ut})_{avg}$, was 0.93. Further, the data indicates that a lower bound for t_{eff}/t_{ut} would be approximately 0.80.

8. Seven of the specimens tested failed by yielding in a severely corroded region. Additional ultrasonic measurements were taken in these regions to obtain the net cross sectional area so that an ultimate load based on yielding, P_{yld} , could be computed. The measured ultimate loads were less than the computed yield loads for all of these specimens. The P_{meas}/P_{yld} ratios ranged from 0.75 to 0.89.
9. The experimental, ultimate capacities were compared with three formulae for ultimate compressive strength as presented by AISC (API), CSA, and Cox. For the undamaged member (Specimen 06) the measured and computed capacities were nearly equal. The measured, ultimate capacities for all damaged members were less than the capacities computed by the referenced formulae. The most significant reduction in strength occurred in members with large initial out-of-straightness damage.

Some future work which might prove useful in developing a more accurate methodology for assessing damage conditions and determining damaged member strengths include the following:

Large scale members that have been damaged and subsequently repaired by should be experimentally tested and analytically modelled. These members may be artificially dented and/or bent, but it is recommended that in-service corrosion damage also be evaluated.

The development of a PC based analytical tool which would be more flexible than the present program DENTA-2 should be considered. The tool could be developed to handle multiple damage states, more varied end conditions and repaired members.

The methods currently used to inspect and assess damaged members should be further evaluated with emphasis on corrosion. A study which would seek to develop a rational, consistent system to qualitatively and quantitatively measure the amount of corrosion on a member and determine how it affects the overall strength of a member. This would be most useful if it could be based on present inspection techniques.

The members in offshore platforms are subject to axial and lateral loadings caused by the dynamic forces of wind and waves. Damaged or repaired members should be evaluated based on more complex loadings such as combined axial compression and bending. Further studies could also include complex dynamic combined loadings and load histories.

A study on the effect of holes on strength could be beneficial. The methods used in this study were an extension of previous work on dents since little literature existed during this study specific to hole damage. A recent paper (8) was presented at the ASCE Structures Congress dealing with hole effects which should prove useful.

Single vs. Multiple Damage

Specimen #12

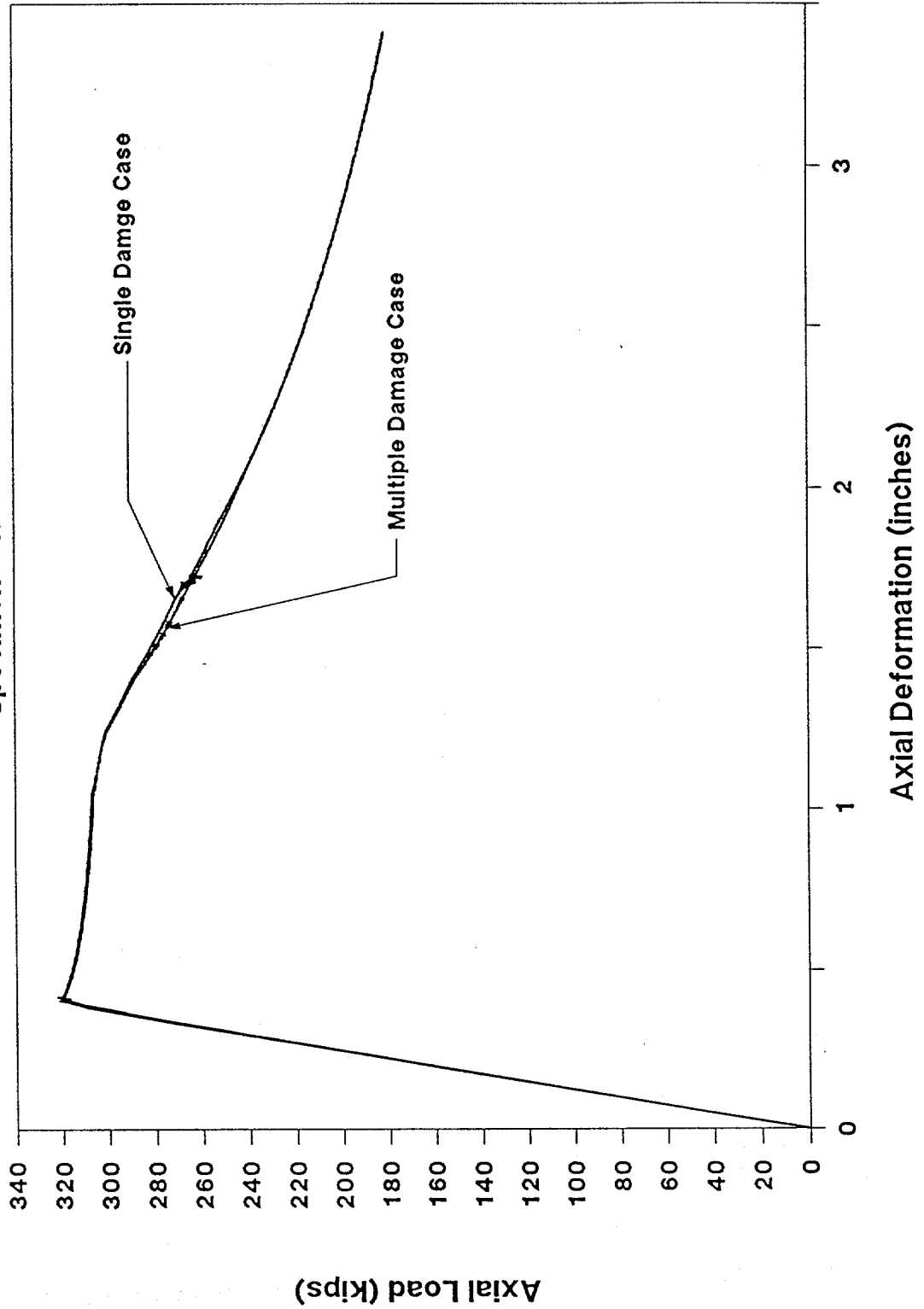


Figure 6-1

Local Buckling Effects

<u>Specimen</u>	<u>Diam.</u> (in.)	<u>Effective t</u> (in.)	<u>Reduced t</u> (in.)	<u>D/t_e</u>	<u>D/t_r</u>
1	18.00	0.270	0.265	66.67	67.92
2	18.00	0.346	0.284	52.02	63.38
3	18.00	0.305	0.247	59.02	72.87
5	18.00	0.303	0.307	59.41	58.63
8	10.75	0.239	0.262	44.98	41.03
14	12.75	0.295	0.219	43.22	58.22
18	10.75	0.264	0.261	40.72	40.72
19	16.00	0.338	0.279	47.34	57.35

The specimens listed above yielded locally during the full scale test. The reduced thickness was measured at the point of yielding after the test using ultrasound. The first three have D/t ratios greater than 60, the maximum allowable value (API RP2A 3.2.2a). This indicates a tendency for local buckling to occur. The following shows the predicted capacity reduction for these members according the API procedures.

<u>Specimen</u>	<u>Normal</u> <u>Yld. Str.</u> (ksi)	<u>Reduced</u> <u>Yld. Str.</u> (ksi)	<u>Capacity</u> <u>(col. buckling)</u> (kips)	<u>Capacity</u> <u>(local buckling)</u> (kips)
1	35.7	35.0	530.27	510.52
2	43.6	43.2	821.42	670.59
3	36.6	35.4	608.73	478.74

The column buckling capacity was calculated with the effective thickness and the normal yield stress. The local buckling capacity was calculated with the reduced thickness and yield stress. The AISC Working Stress equations without the factor of safety were used to calculate capacity. API RP2A equation 3.2.2-4 was used to calculate the reduced yield stress.

Figure 6-2

REFERENCES

Final Report

Testing and Evaluation of Damaged Jacket Braces

This reference list contains those references cited in the body of this document.

SECTION 1.2

1. J.A. Padula and A. Ostapenko, "Indentation Behavior and Axial Tests of Two Tubular Columns", OTC Paper No. 5438, 1987.
2. C.S. Smith, W.L. Somerville and J.W. Swan, "Residual Strength and Stiffness of Damaged Steel Bracing Members", OTC Paper No. 3981, 1981.

SECTION 3.0

American Institute of Steel Construction, Manual of Steel Construction, Allowable Stress Design, 9th Edition, Chicago, IL., 1989

American Petroleum Institute, Recommended Practice for Planning, Designing, and Constructing Fixed Offshore Platforms, API RP 2A, 18th Edition, Washington, D.C., October, 1989

American Society for Testing and Materials, "Standard Test Methods of Tension Testing of Metallic Materials", ASTM E8-88, Part 3, ASTM Annual Standards, Philadelphia, Pa., 1988.

"B.7: SSCR Technical Memorandum No. 7: Tension Testing", Guide to Stability Design Criteria for Metal Structures, 4th Edition, Ed. T.V. Galambos, John Wiley & Sons, New York, 1988, pp. 744-749.

Cox, J.W., "Tubular Member Strength Equations for LRFD", Final Report, February, 1987.

Prion, G.G.L., "Beam-Column Behavior of Unstiffened Fabricated Steel-Tubes", Dissertation, University of Toronto, Department of Civil Engineering, 1897.

SECTION 4.2

3. C.P. Ellinas, "Ultimate Strength of Damaged Tubular Bracing Members", ASCE Structural Journal, Vol. 110, No. 2, Feb. 1984, pp. 245-259.
4. Buckling of Offshore Structures, prepared for the U.K. Department of Energy by J.P. Kenny and Partners, Ltd., London, Gulf Publishing Co., 1984.
5. J.E. Van Aanhold and J. Taby, "Analysis of Structures with Damaged Structural Members", U.S. Department of Commerce, National Technical Information Service, 15 October 1983.

SECTION 5.0

6. Ultimate and Post-Ultimate Strength of Dented Tubular Members, J. Taby, Division of Marine Structures, Report UR-86-50, The Norwegian Institute of Technology, Trondheim, October 1986.

SECTION 6.0

7. American Petroleum Institute, "Recommended Practice for Planning, Design and Constructing Fixed Offshore Platforms", API RP2A (18th Edition), September 1, 1989.
8. Hsu, Teh-Min and William F. Krieger, "Residual Strength of Tubular Members with Holes", ASCE Structures Congress, Baltimore, MD, 1990.

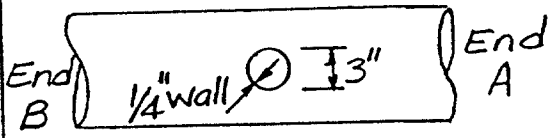
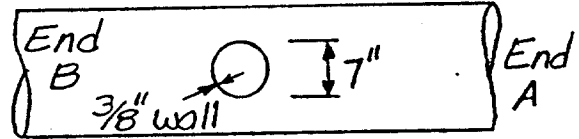
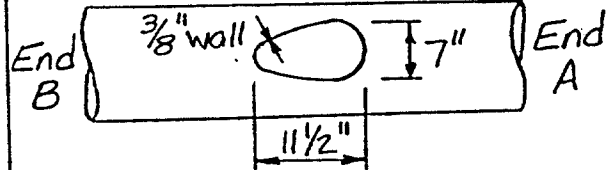
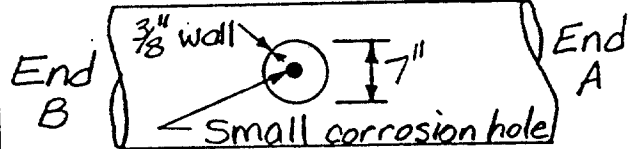
APPENDIX A

SPECIMEN TEST RESULTS

SPECIMEN 01

DAMAGE SUMMARY

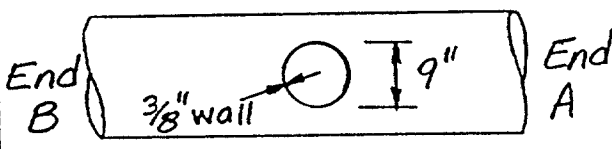
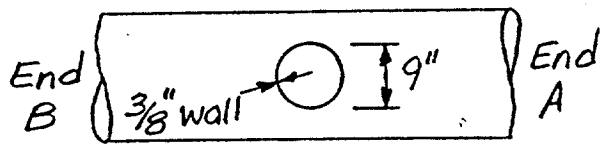
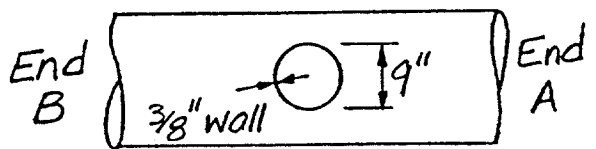
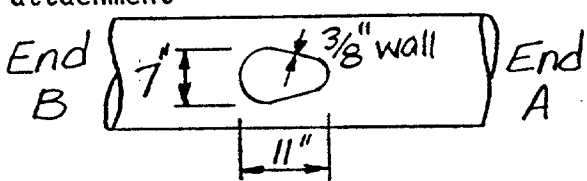
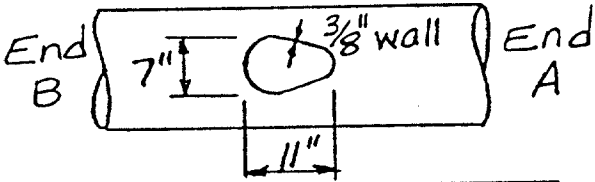
Specimen No. 1
2-14-90

DISTANCE FROM END "B"	*DISTANCE FROM CHALK LINE		DESCRIPTION OF DAMAGE
	LEFT	RIGHT	
1. From 0' to 5'-0 1/4"		8"	3/4" longitudinal weld
2. 3'-2"		20"	8" round dent (See additional sheets)
3. 4'-7"	10 1/2"		Cut-off, round welded attachment 3" diameter 
4. 5'-0"	14"		Cut-off, round welded attachment 7" diameter 
5. 5'-0 3/4"			3/4" circumferential butt weld
6. 6'-5 1/2"	22"		Cut-off, oblong welded attachment 
7. 7'-3"	1/2"		Cut-off, round welded attachment 7" diameter with heavy corrosion (and small hole) 

*Looking from end "A" towards end "B"

DAMAGE SUMMARY

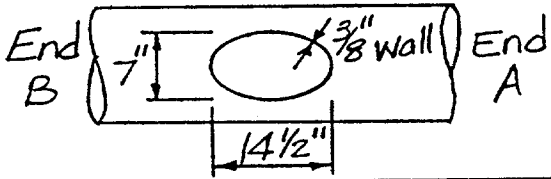
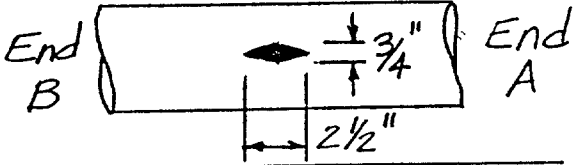
Specimen No. 1 (continued)

DISTANCE FROM END "B"	*DISTANCE FROM CHALK LINE		DESCRIPTION OF DAMAGE
	LEFT	RIGHT	
8. 7'-10	22 1/2"		<p>Cut-off, round welded attachment 9" diameter</p> 
9. 7'-10"	8"		<p>Cut-off, round welded attachment 9" diameter</p> 
10. 7'-10"		6 1/2"	<p>Cut-off, round welded attachment 9" diameter</p> 
11. 8'-11"	22"		<p>Cut-off, oblong welded attachment</p> 
12. 8'-11"	8"		<p>Cut-off, oblong welded attachment</p> 

*Looking from end "A" towards end "B"

DAMAGE SUMMARY

Specimen No. 1 (continued)

DISTANCE FROM END "B"	*DISTANCE FROM CHALK LINE		DESCRIPTION OF DAMAGE
	LEFT	RIGHT	
13. 9'-2"	3/4"		Cut-off, oblong welded attachment 
14. 9'-9 1/4"	9 1/4"		Torch hole 2 1/2" long by 3/4" wide (at widest point) 
15. From 5'-1" to 17'-0 1/4"	20 3/4"		3/4" longitudinal weld
16. 15'-2 1/2"	13 1/2"		Cut-off, 1/2" square welded attachment
17. 17'-0 5/8"			3/4" circumferential butt weld
18. From 17'-1" to 19'-7 1/4"		15 1/2"	3/4" longitudinal weld

*Looking from end "A" towards end "B"

SOME LOCALIZED HEAVY CORROSION. END B APPEARS THIN ($\approx .25$ in.)

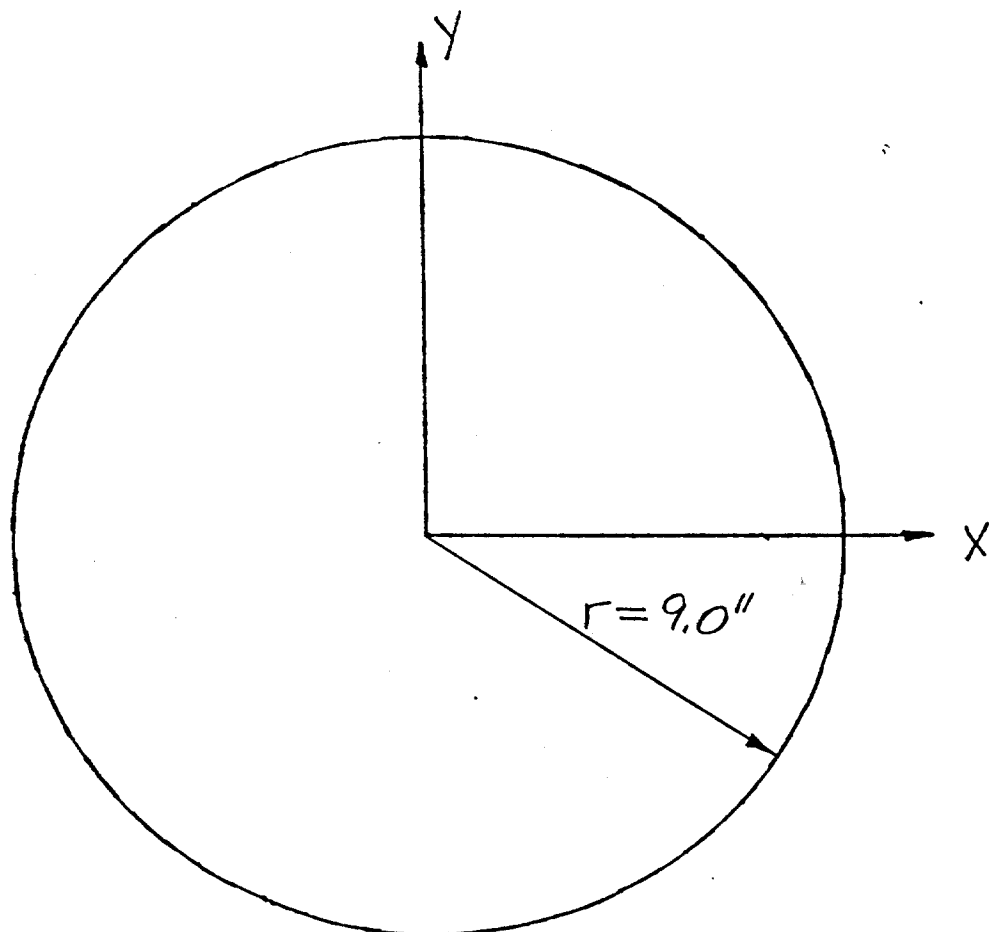
DENT CROSS SECTION

Specimen No. 1

Damage No. 2

Distance from End B 2'-10"

Scale 1" = 4.24"



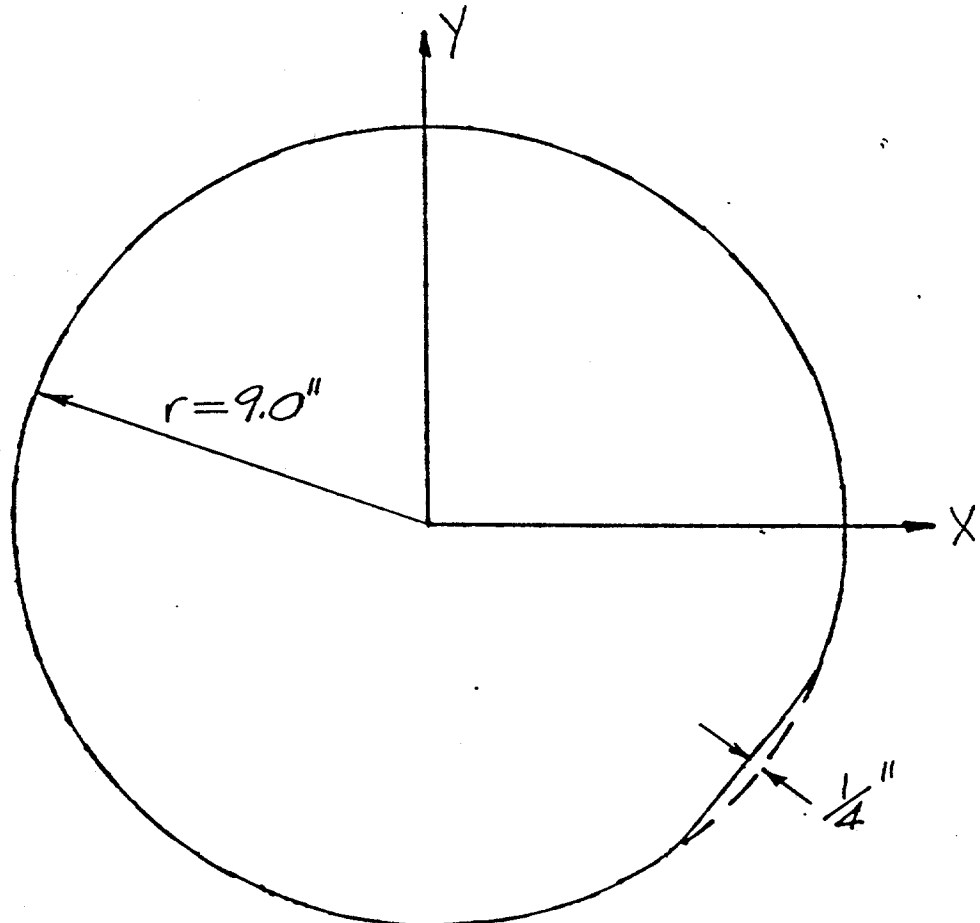
DENT CROSS SECTION

Specimen No. 1

Damage No. 2

Distance from End B 3'-0"

Scale 1" = 4.24"



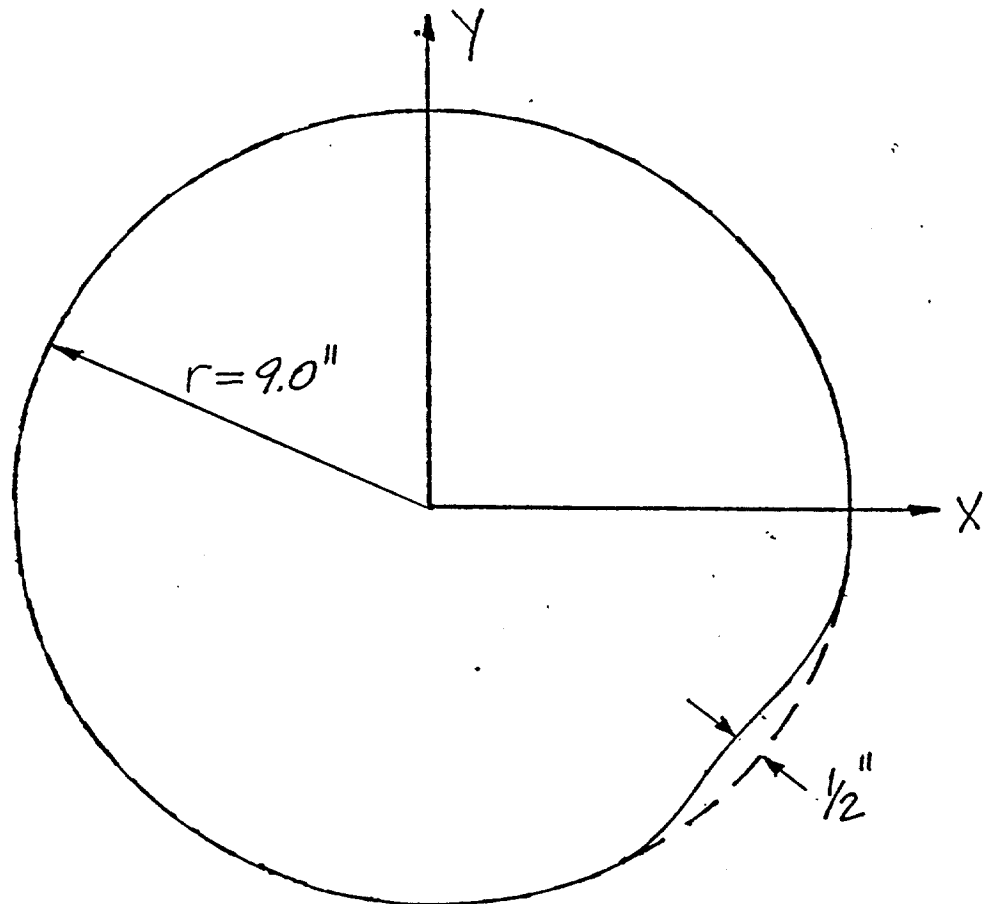
DENT CROSS SECTION

Specimen No. 1

Damage No. 2

Distance from End B 3'-2"

Scale 1" = 4.24"



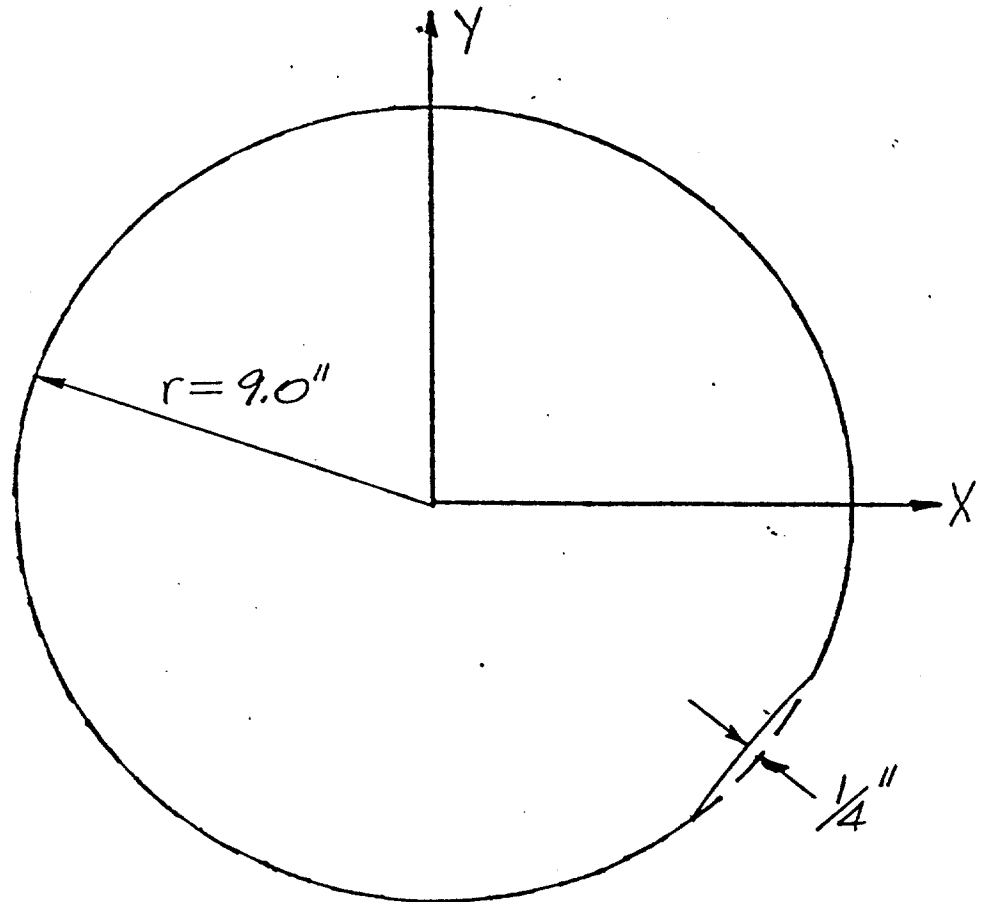
DENT CROSS SECTION

Specimen No. 1

Damage No. 2

Distance from End B 3'-4"

Scale 1" = 4.24"



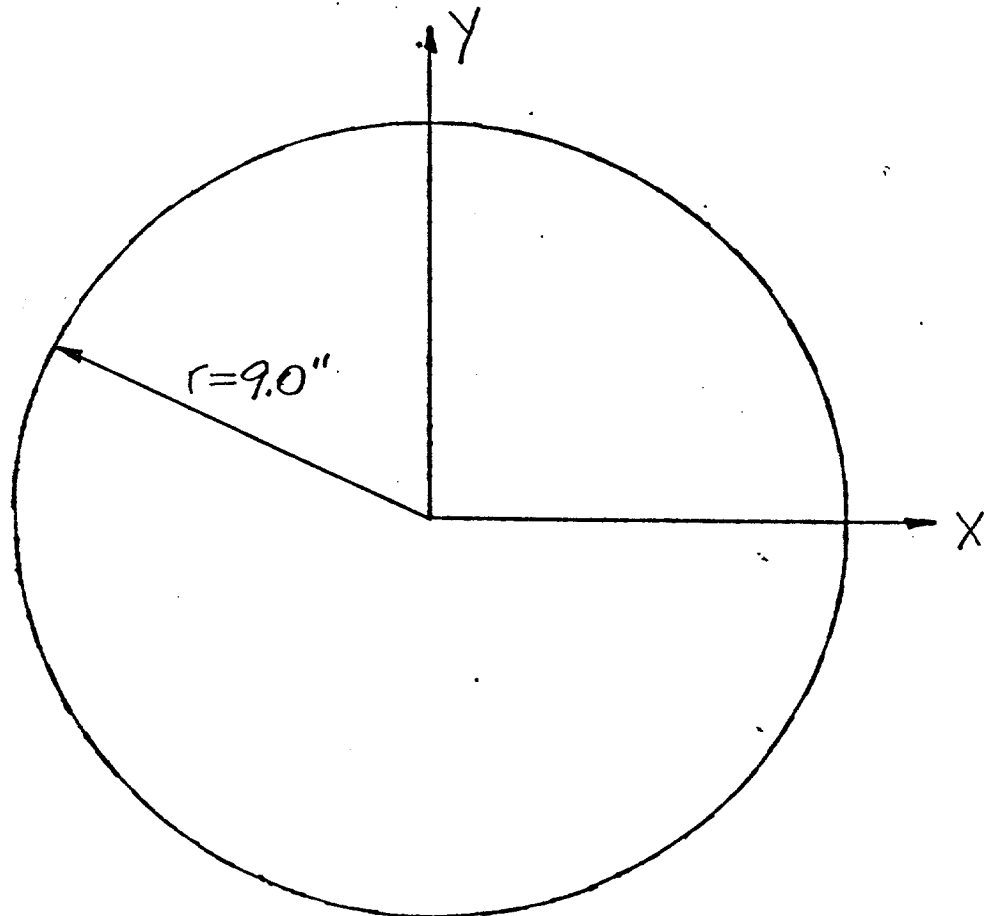
DENT CROSS SECTION

Specimen No. 1

Damage No. 2

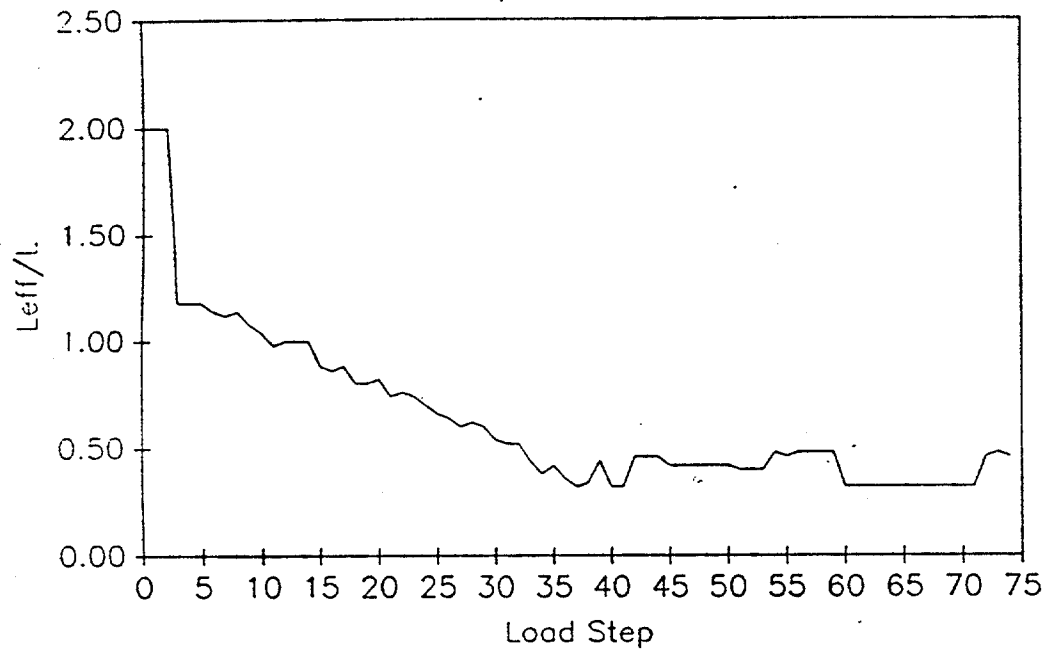
Distance from End B 3'-6"

Scale 1"=4.24"



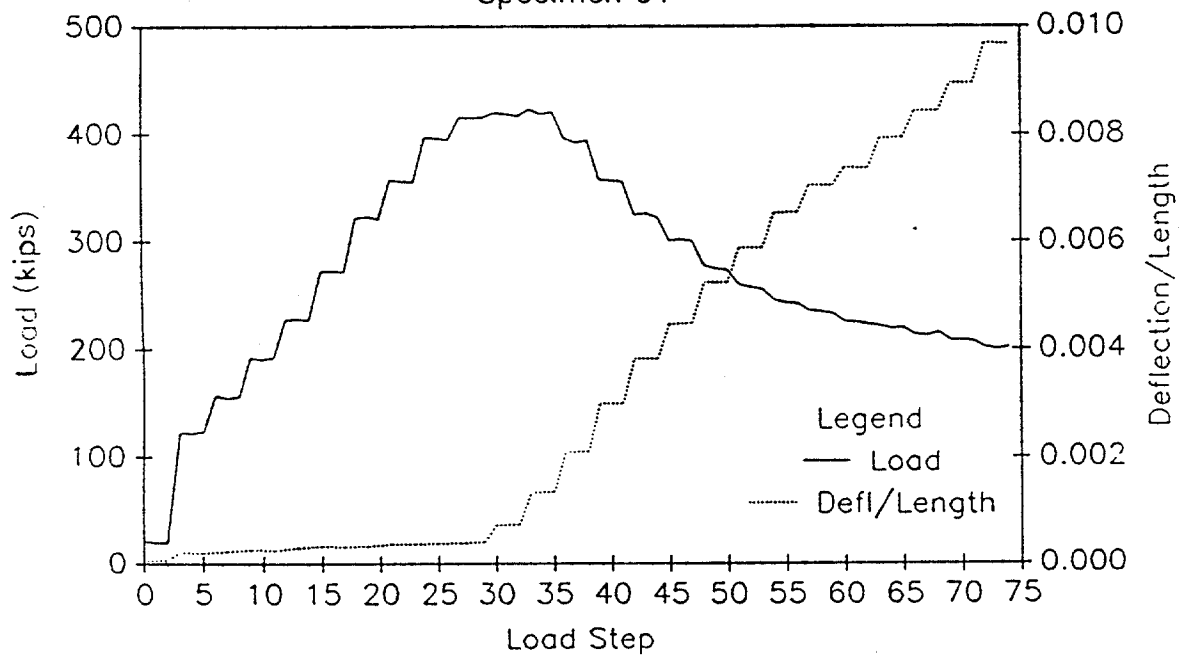
EFFECTIVE LENGTH vs LOAD STEP

Specimen 01

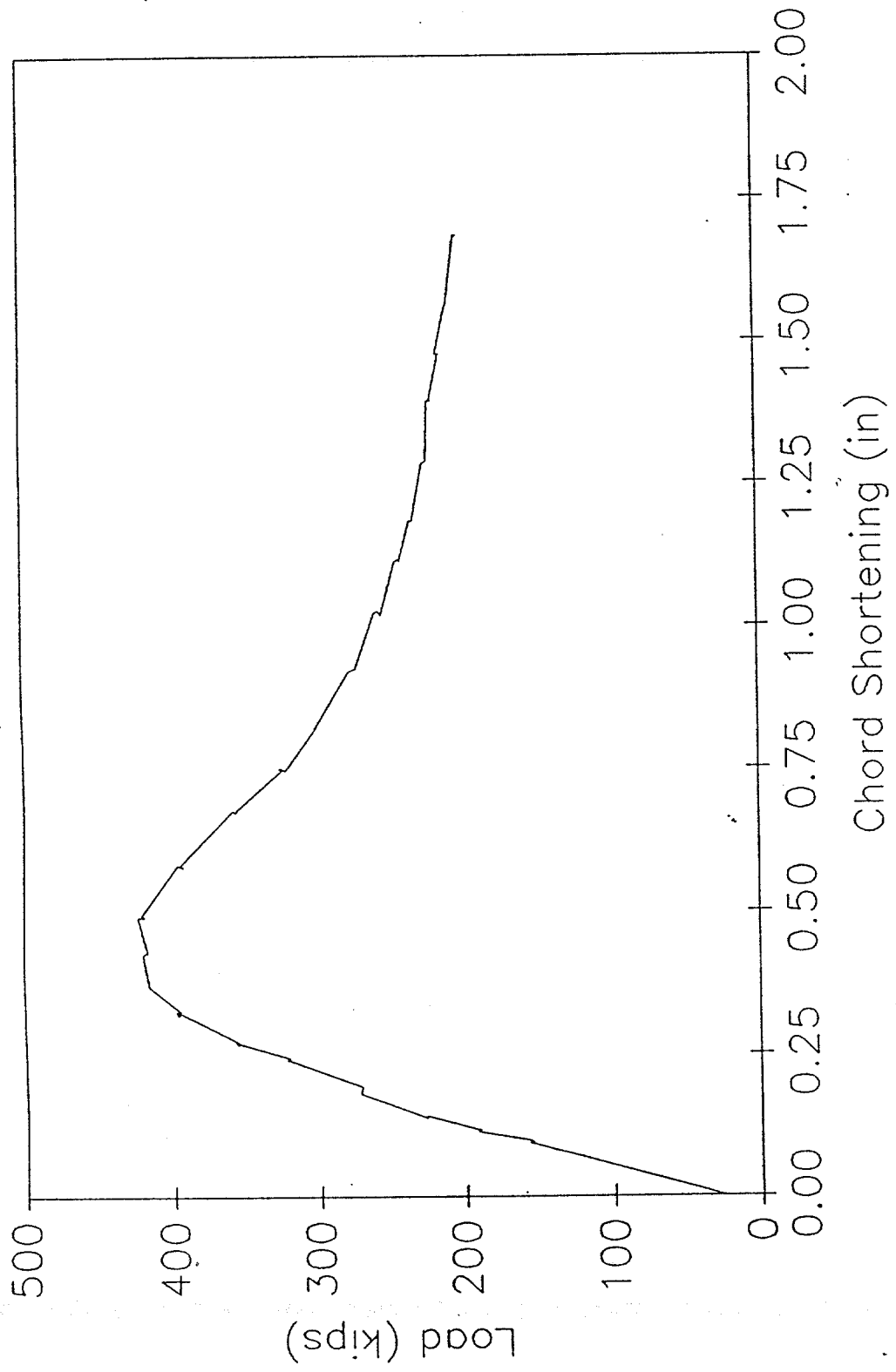


LOAD AND DEFLECTION vs LOAD STEP

Specimen 01

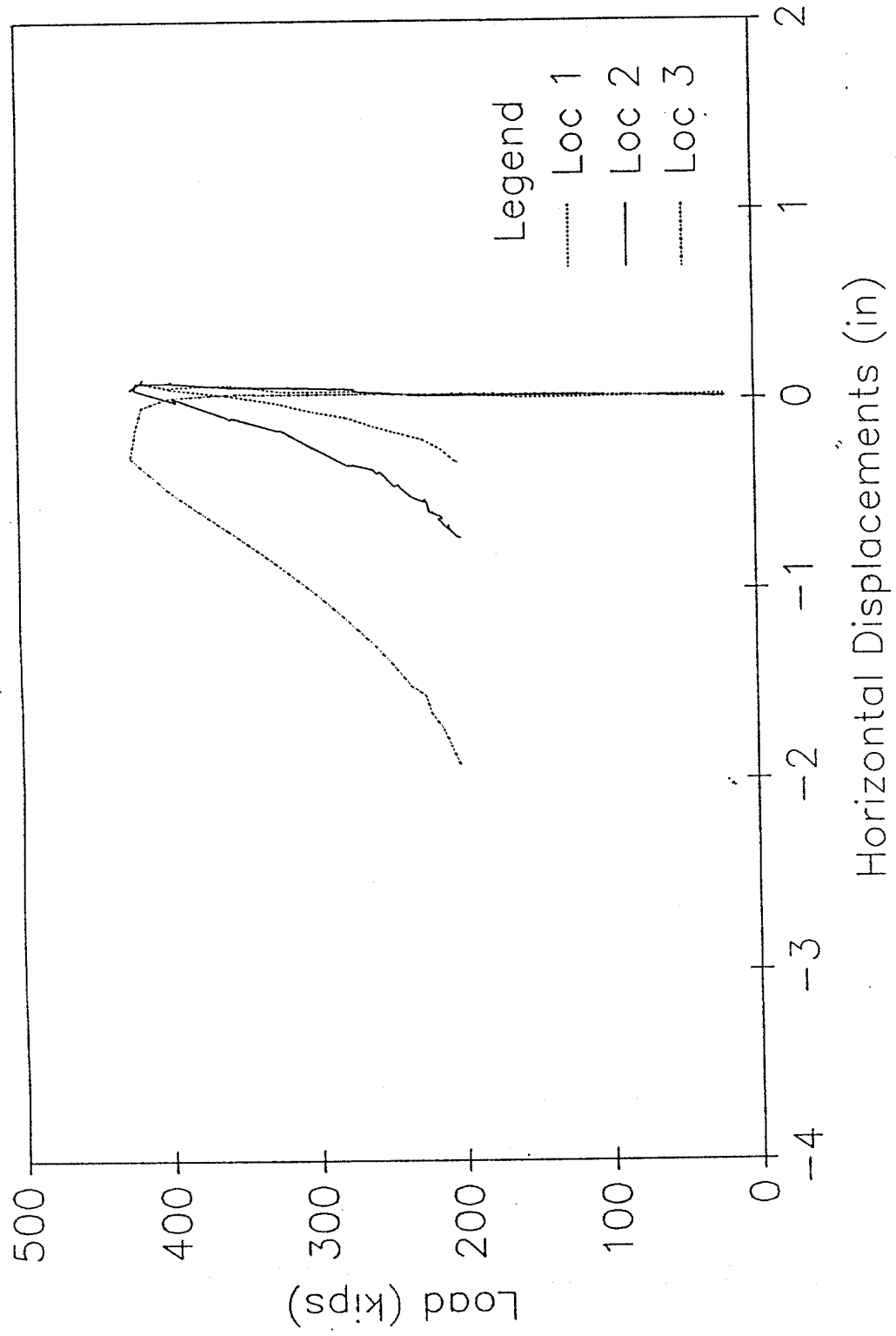


LOAD vs CHORD SHORTENING
Specimen 01



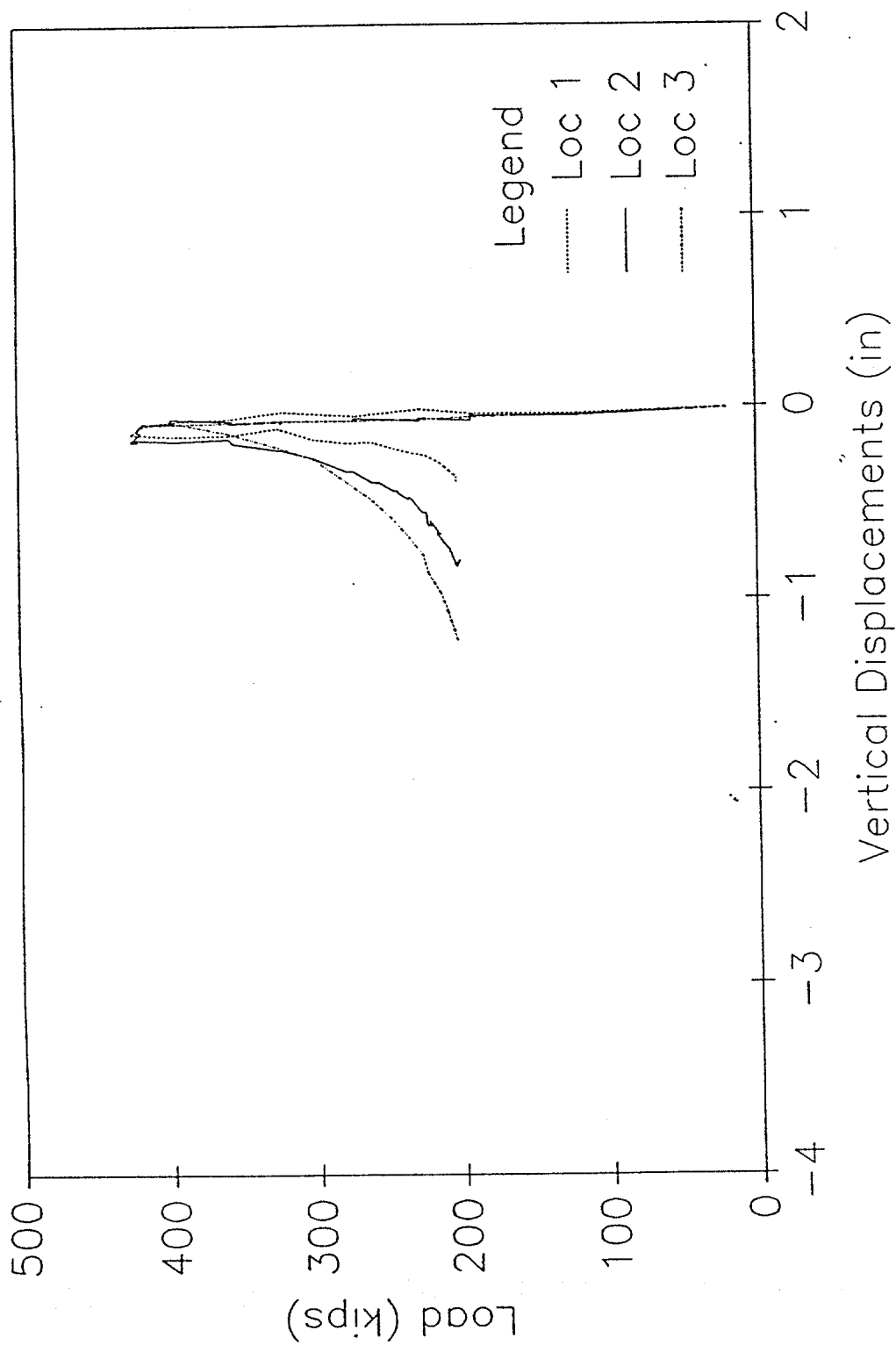
HORIZONTAL DISPLACEMENTS

Specimen 01



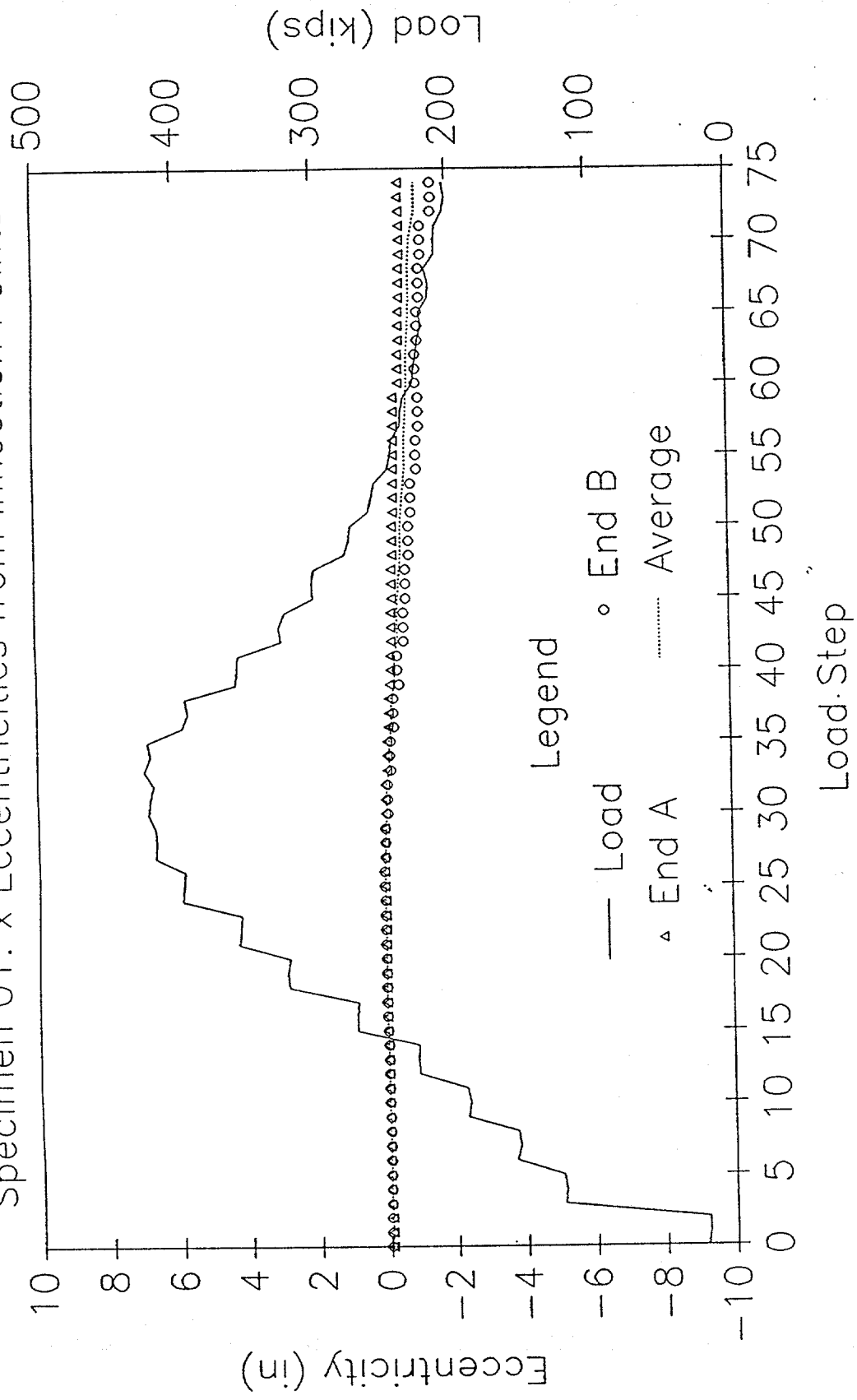
VERTICAL DISPLACEMENTS

Specimen 01



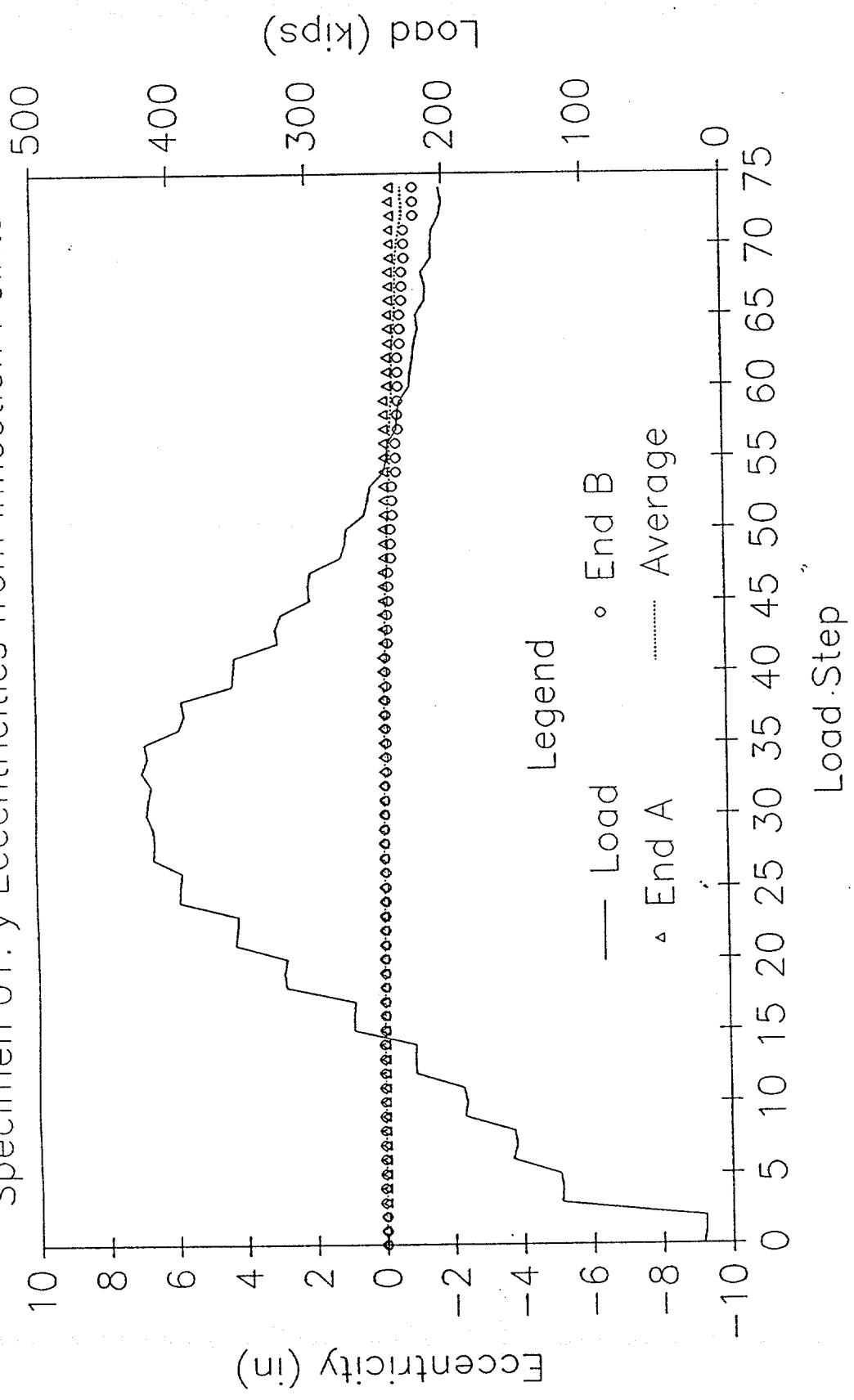
LOAD AND ECCENTRICITY vs LOAD STEP

Specimen 01: x Eccentricities from Inflection Points



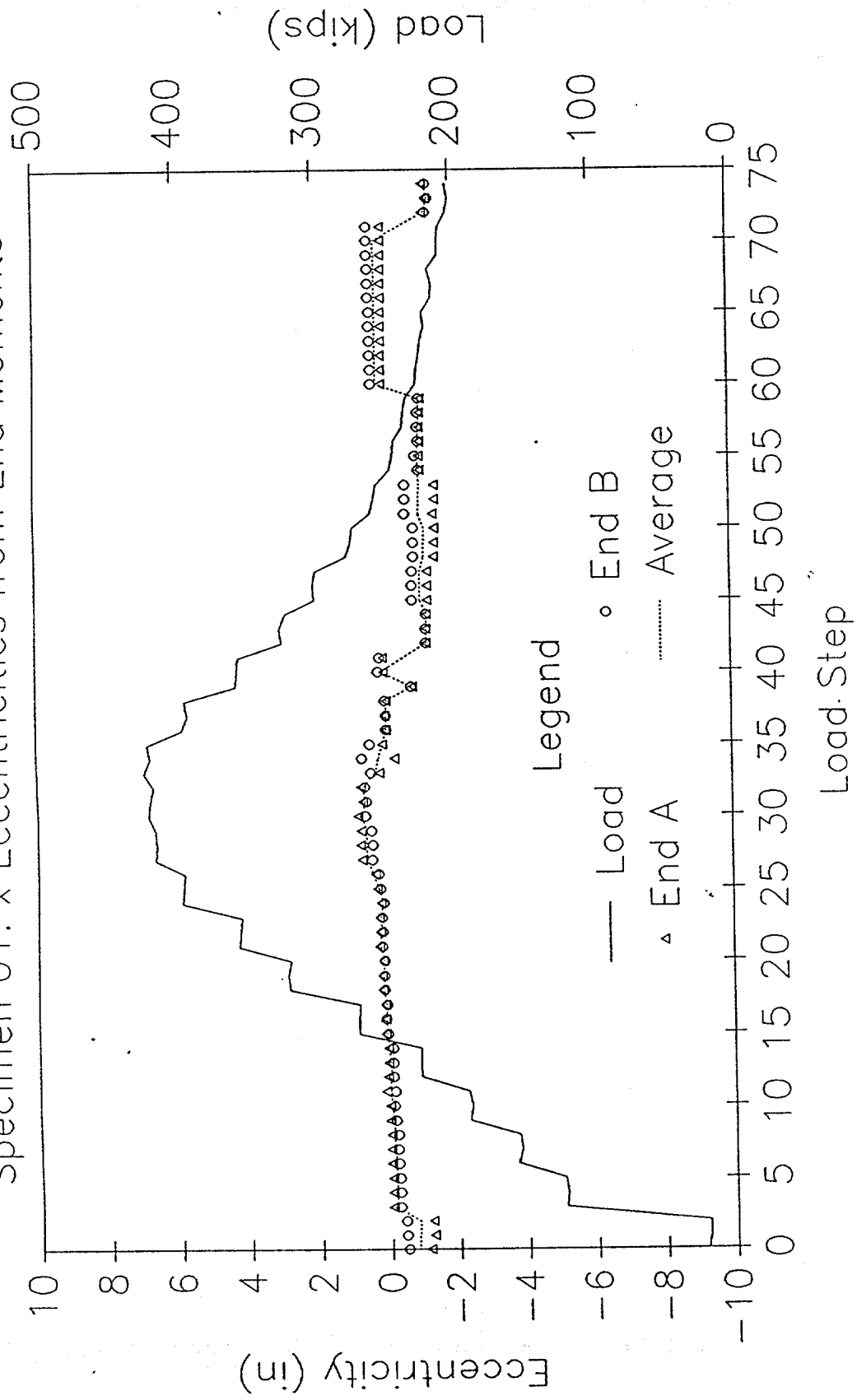
LOAD AND ECCENTRICITY vs LOAD STEP

Specimen 01: y Eccentricities from Inflection Points



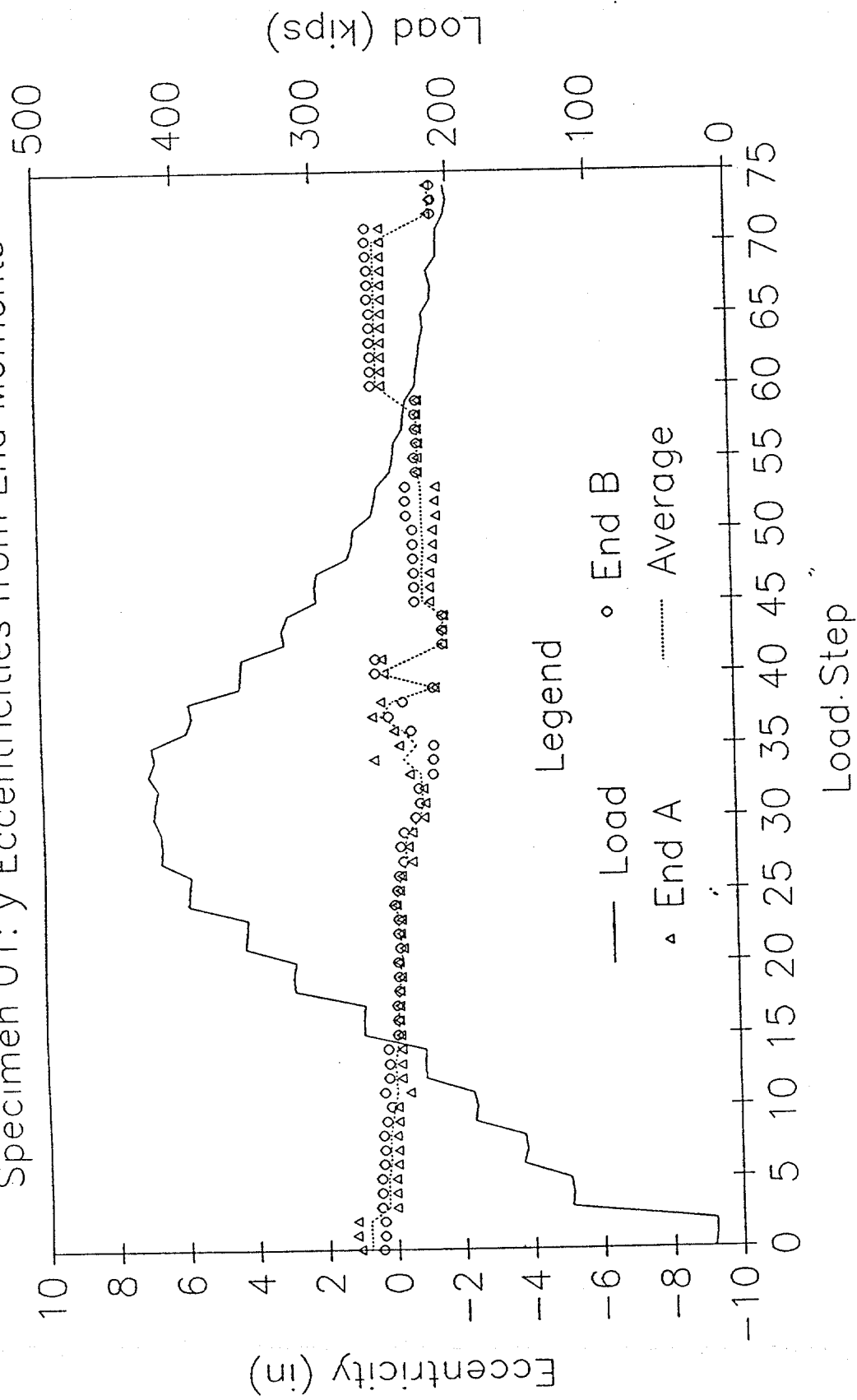
LOAD AND ECCENTRICITY vs LOAD STEP

Specimen 01: x Eccentricities from End Moments



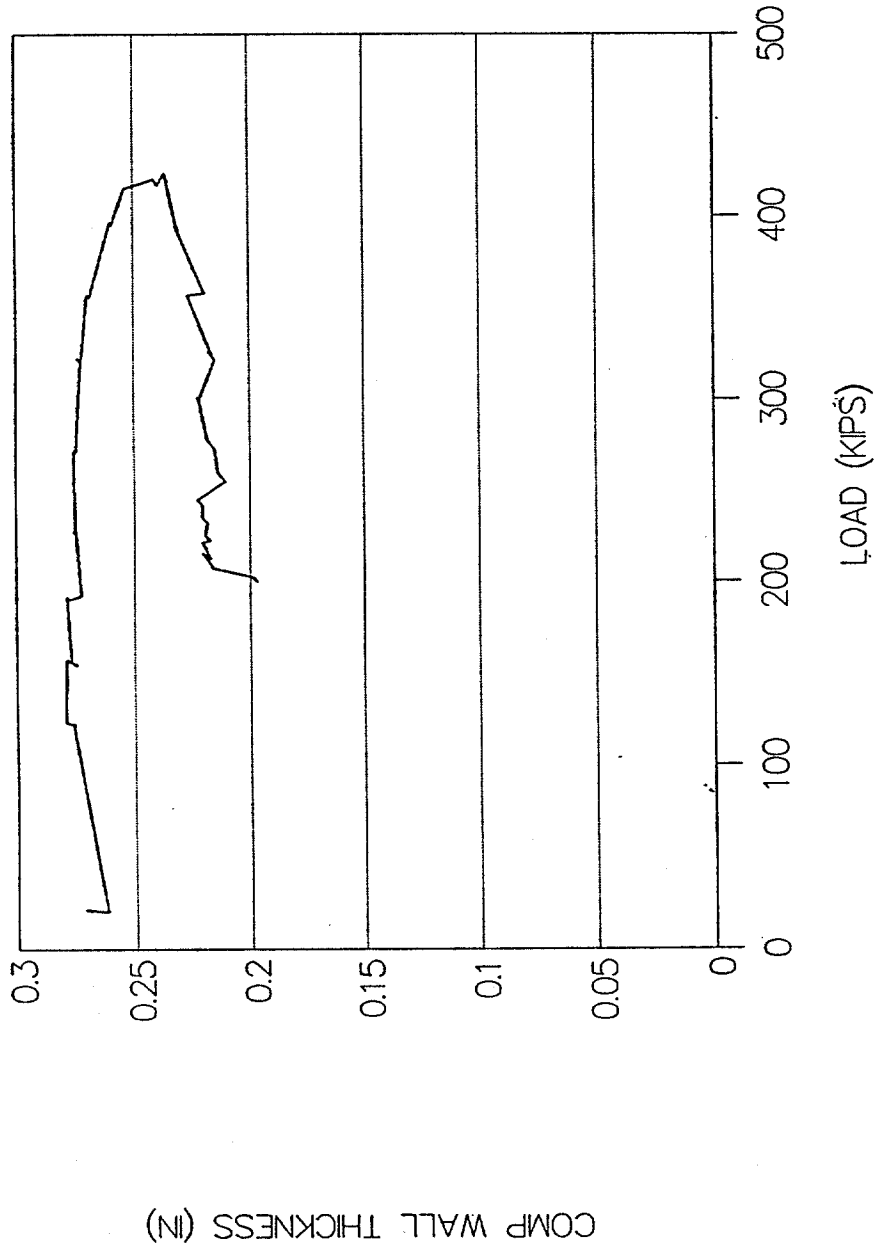
LOAD AND ECCENTRICITY vs LOAD STEP

Specimen 01: y Eccentricities from End Moments



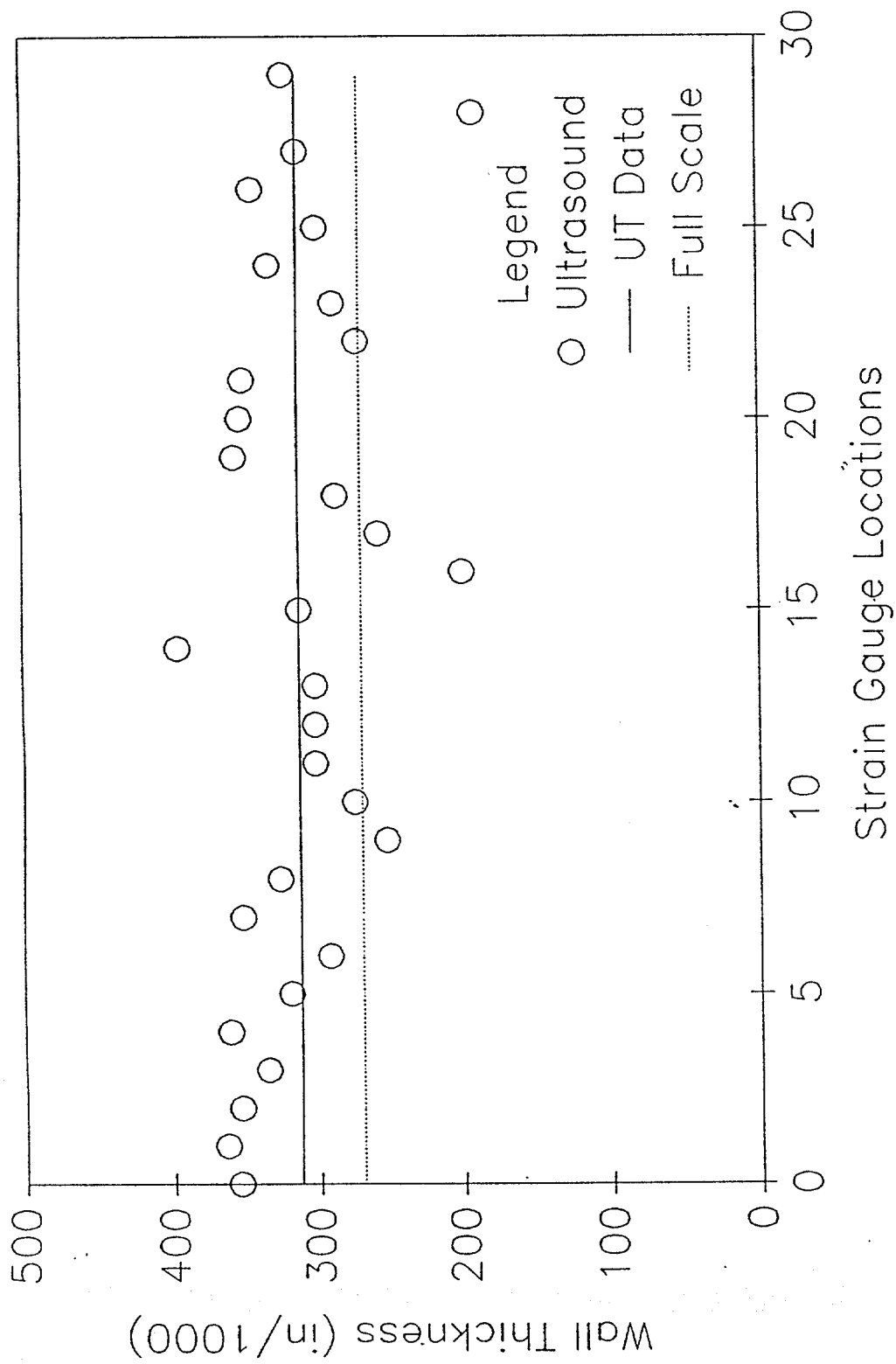
SPECIMEN 01-FULL SCALE TEST

COMPUTED WALL THICKNESS



SPECIMEN 01: WALL THICKNESS

Nominal Wall Thickness = 0.375 in



Ultrasound Data for Specimen 1
(All values in inches)

Gauge No.	UT Thickness	UT Average
0	0.355	
1	0.364	
2	0.354	
3	0.336	
4	0.362	
5	0.320	0.348
6	0.293	
7	0.353	
8	0.327	
9	0.253	
10	0.275	
11	0.302	0.300
12	0.302	
13	0.302	
14	0.396	
15	0.313	
16	0.200	
17	0.258	0.295
18	0.287	
19	0.357	
20	0.353	
21	0.351	
22	0.272	
23	0.288	0.318
24	0.333	
25	0.300	
26	0.344	
27	0.313	
28	0.191	
29	0.322	0.301

Overall Average = 0.313

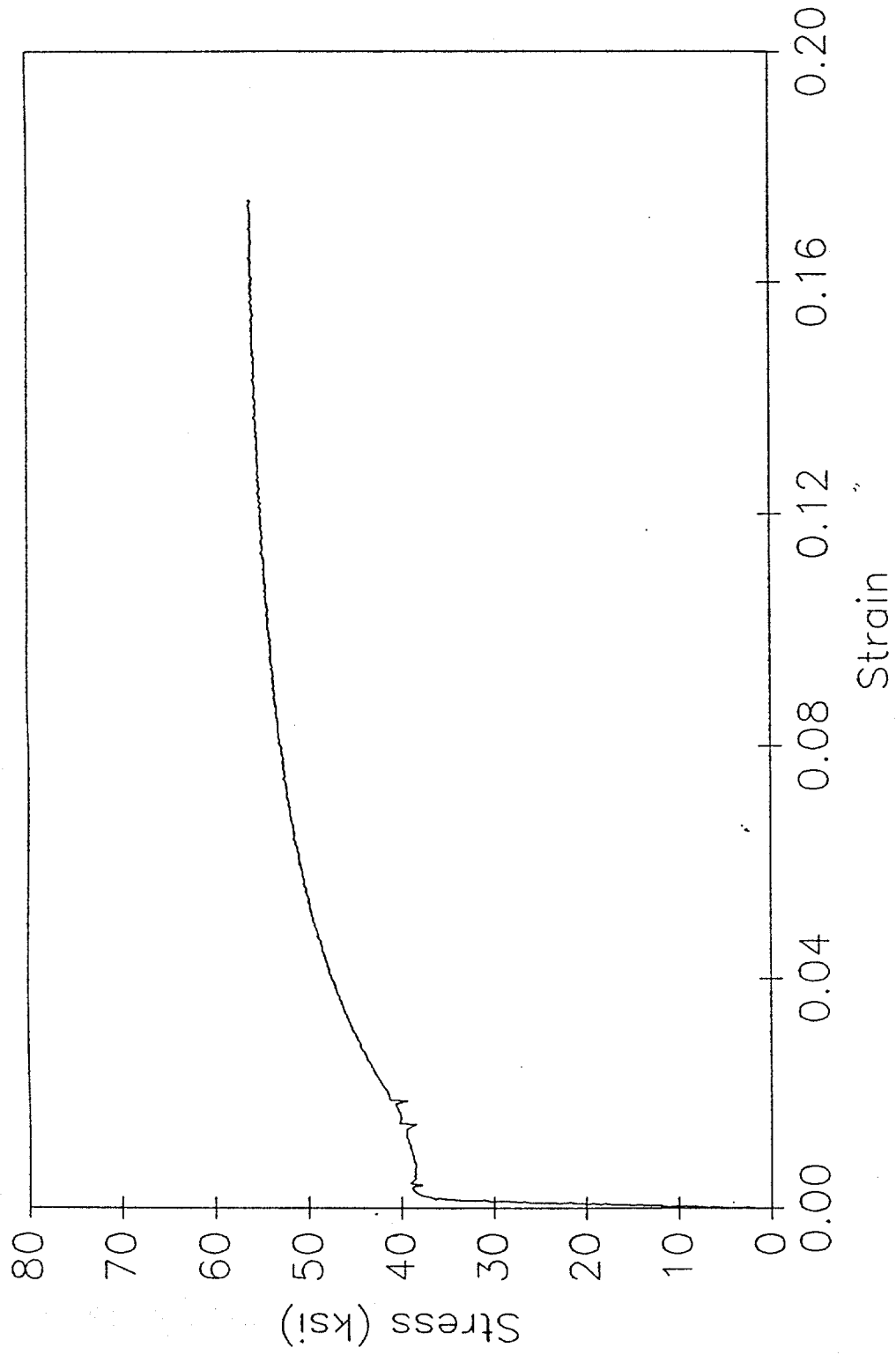
Random Readings near Buckling Point

No.	Reading
1	0.282
2	0.261
3	0.225
4	0.292
5	0.237
6	0.292

Random Average = 0.265

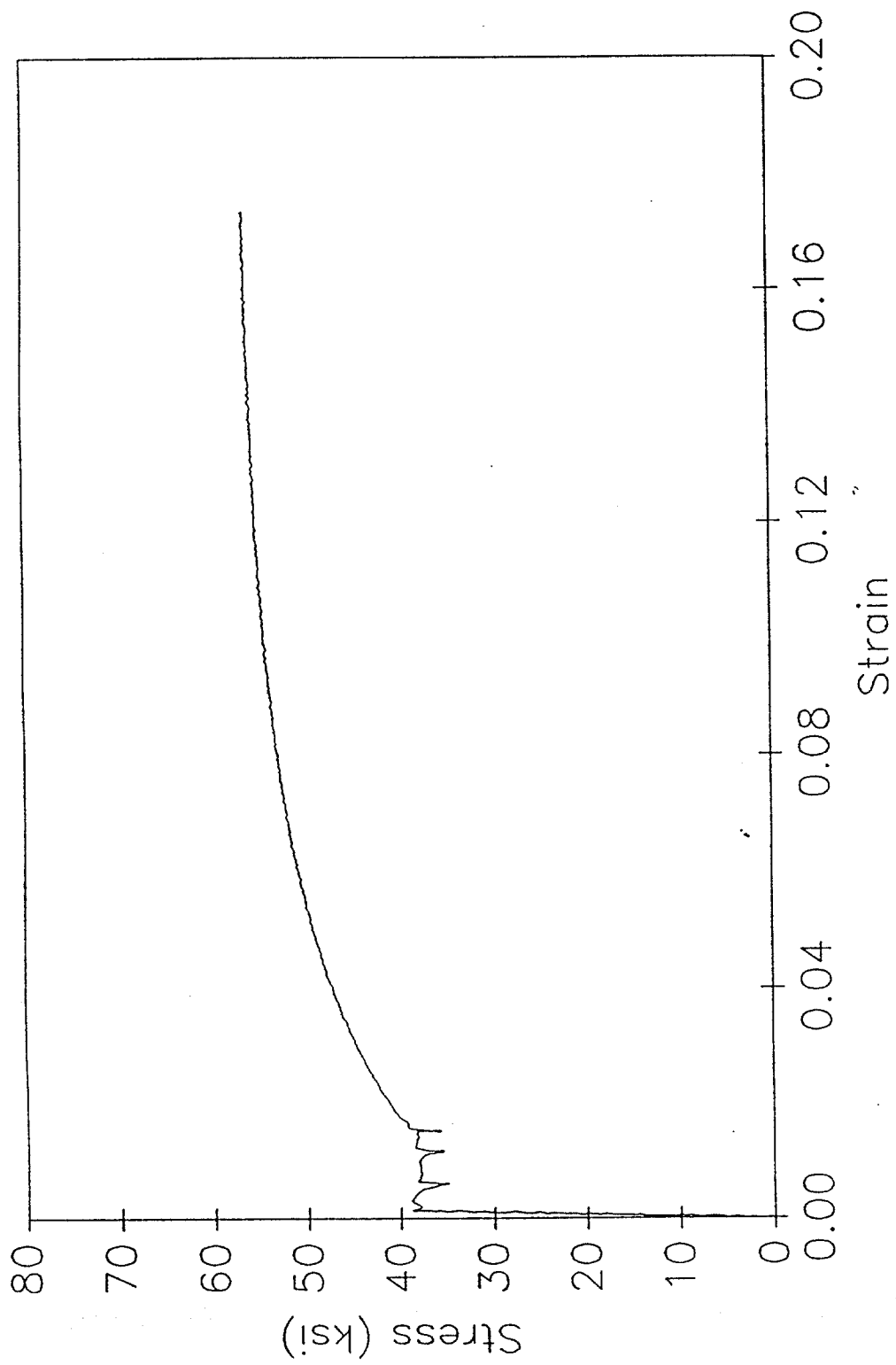
TENSILE SPECIMEN 1-1

Stress vs Strain



TENSILE SPECIMEN 1-2

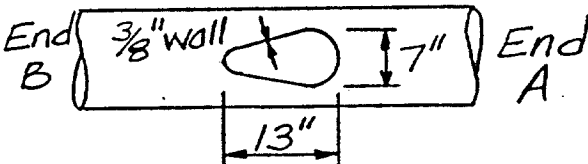
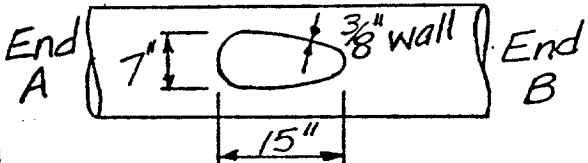
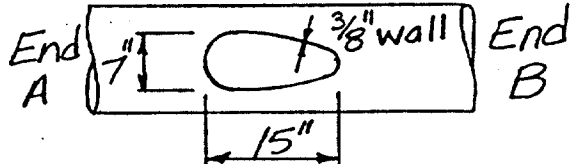
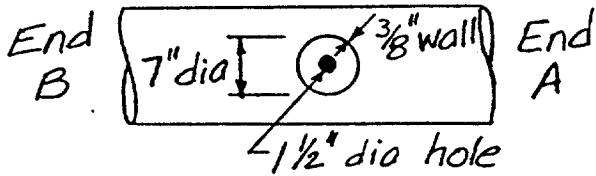
Stress vs Strain



SPECIMEN 02

DAMAGE SUMMARY

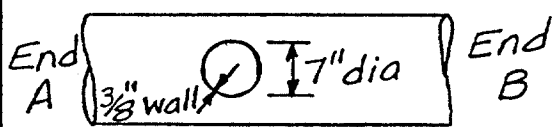
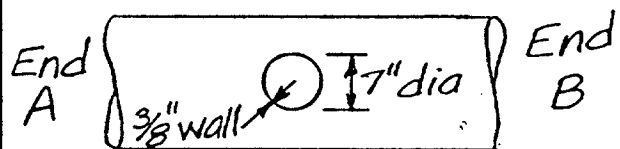

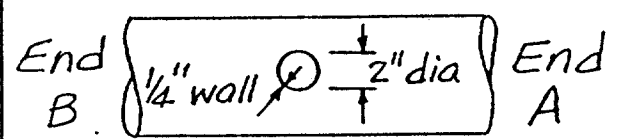
Specimen No. 2
2-2-90

DISTANCE FROM END "B"	*DISTANCE FROM CHALK LINE		DESCRIPTION OF DAMAGE
	LEFT	RIGHT	
1. 3'-4 3/8"			3/4" circumferential butt weld
2. From 3'-4 3/4" to 12'-1"	4"		3/4" longitudinal weld
3. 6'-1"	15"		Cut-off, oblong welded attachment 
4. 5'-10"		26"	Cut-off, oblong welded attachment 
5. 6'-2"		12 3/4"	Cut-off, oblong welded attachment 
6. 6'-11"	15"		Cut-off, round welded attachment with 1 1/2" corrosion hole in center 

*Looking from end "A" towards end "B"

DAMAGE SUMMARY

Specimen No. 2 (continued)

DISTANCE FROM END "B"	*DISTANCE FROM CHALK LINE		DESCRIPTION OF DAMAGE
	LEFT	RIGHT	
7. 7'-1"		27"	Cut-off, round welded attachment 
8. 7'-3"		13"	Cut-off, round welded attachment 
9. 7'-9"	4"		Cut-off, round welded attachment 
10. 12'-1 3/8"			3/4" circumferential butt weld
11. From 12'-1 3/4" to 20'-3 1/4"		24"	3/4" longitudinal weld
12. 15'-0"	10"		Cut-off, round welded attachment 
13. 20'-3 5/8"			3/4" circumferential butt weld

*Looking from end "A" towards end "B"

DAMAGE SUMMARY

Specimen No. 2 (continued)

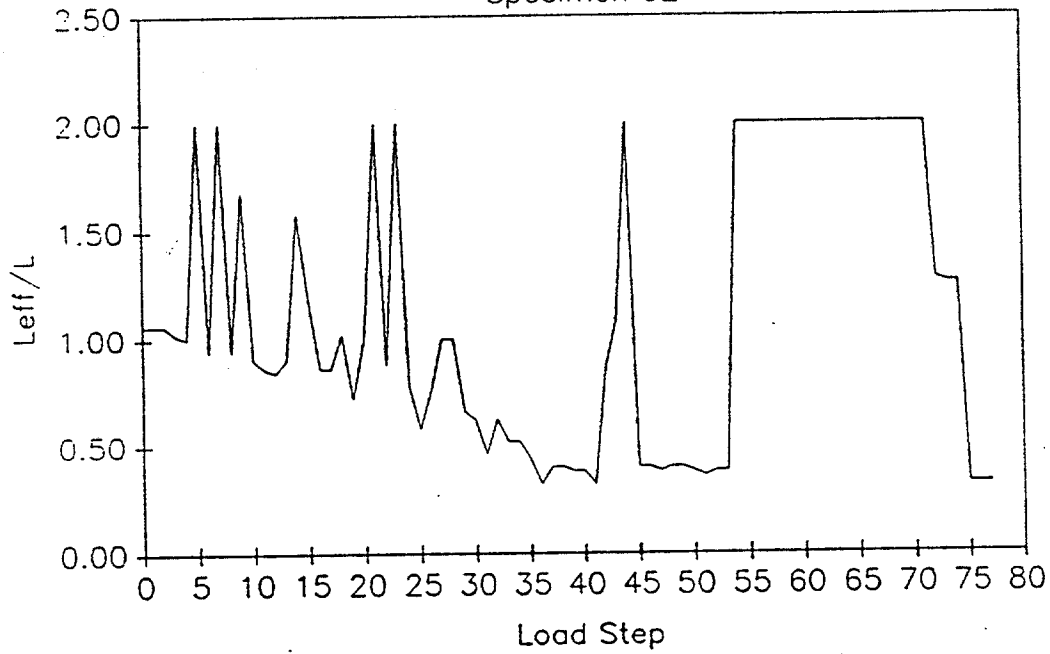
DISTANCE FROM END "B" \\ \\ \\ \\	*DISTANCE FROM CHALK LINE		DESCRIPTION OF DAMAGE \\ \\ \\ \\ \\ \\ \\ \\ \\ \\ \\ \\ \\ \\
	LEFT	RIGHT	
14. From 20'-4" to 22'-1 1/2"	5"		3/4" longitudinal weld
15. From 0' to 3'-4"	26"		3/4" longitudinal weld

*Looking from end "A" towards end "B"

MODERATE CORROSION

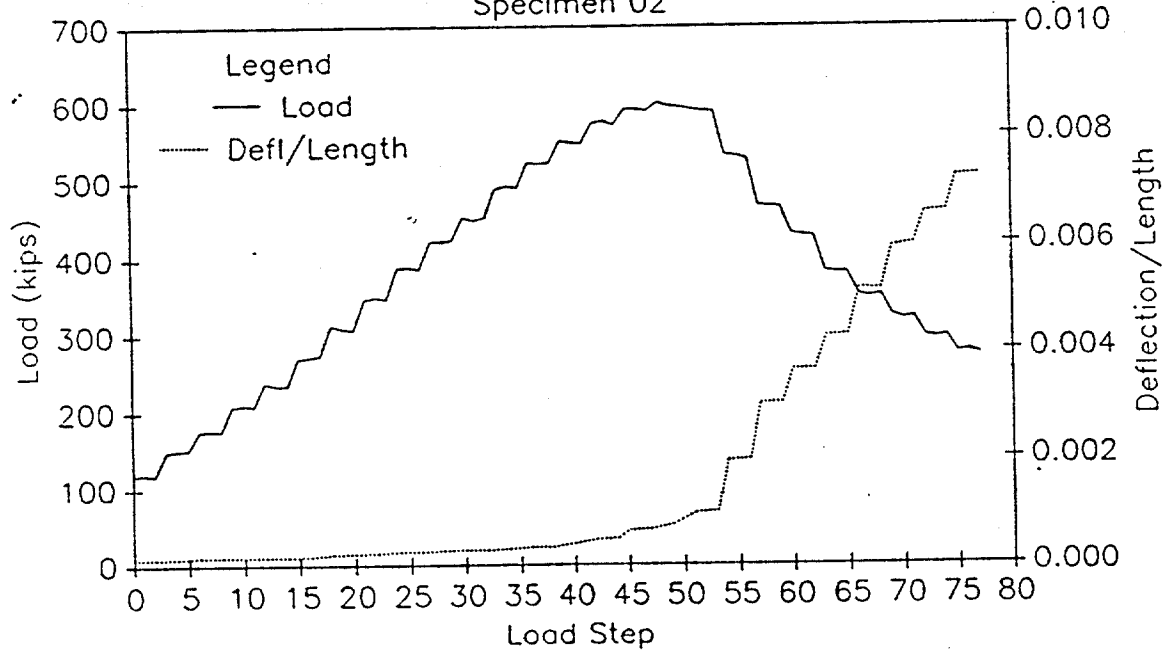
EFFECTIVE LENGTH vs LOAD STEP

Specimen 02



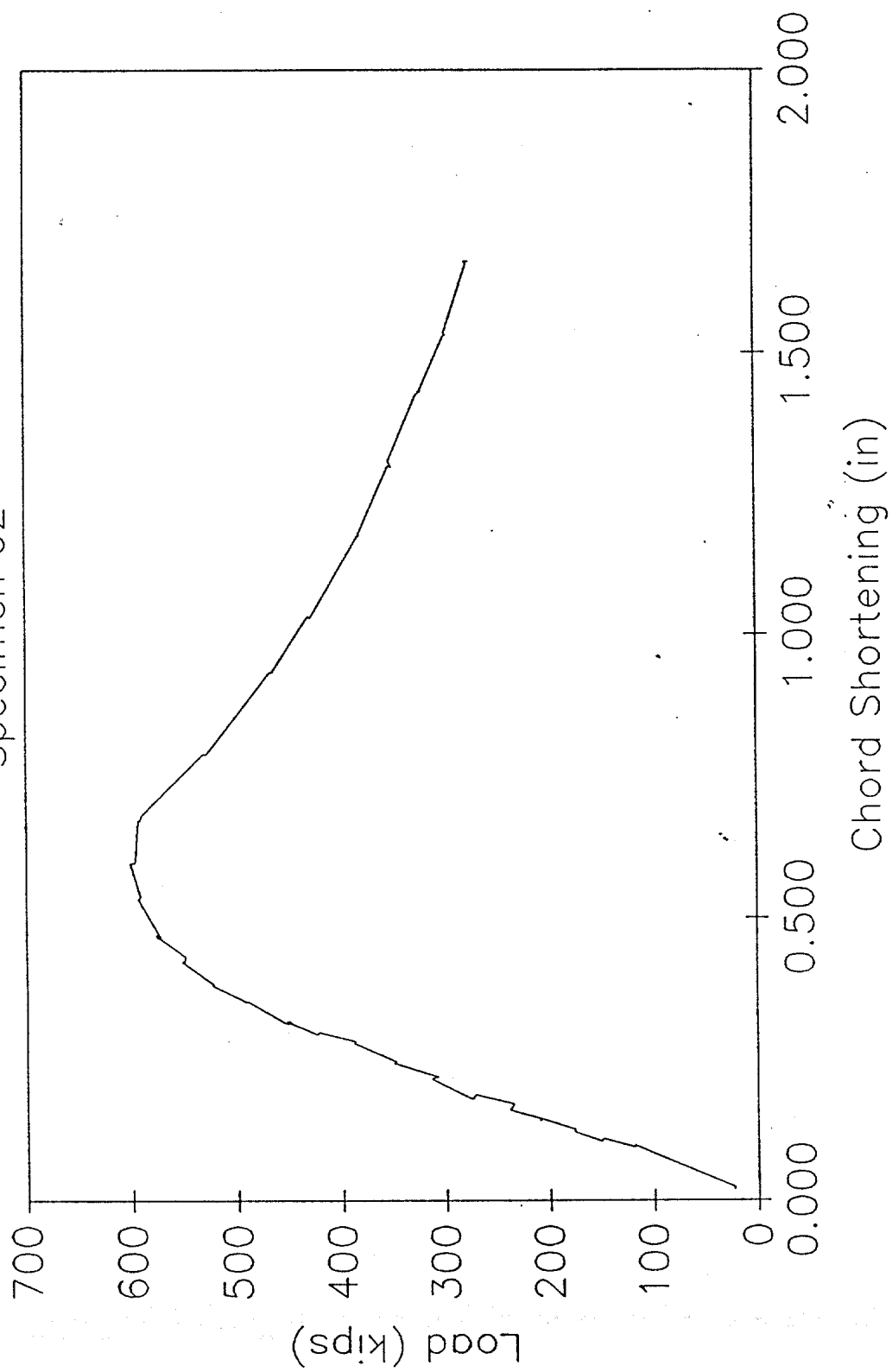
LOAD AND DEFLECTION vs LOAD STEP

Specimen 02



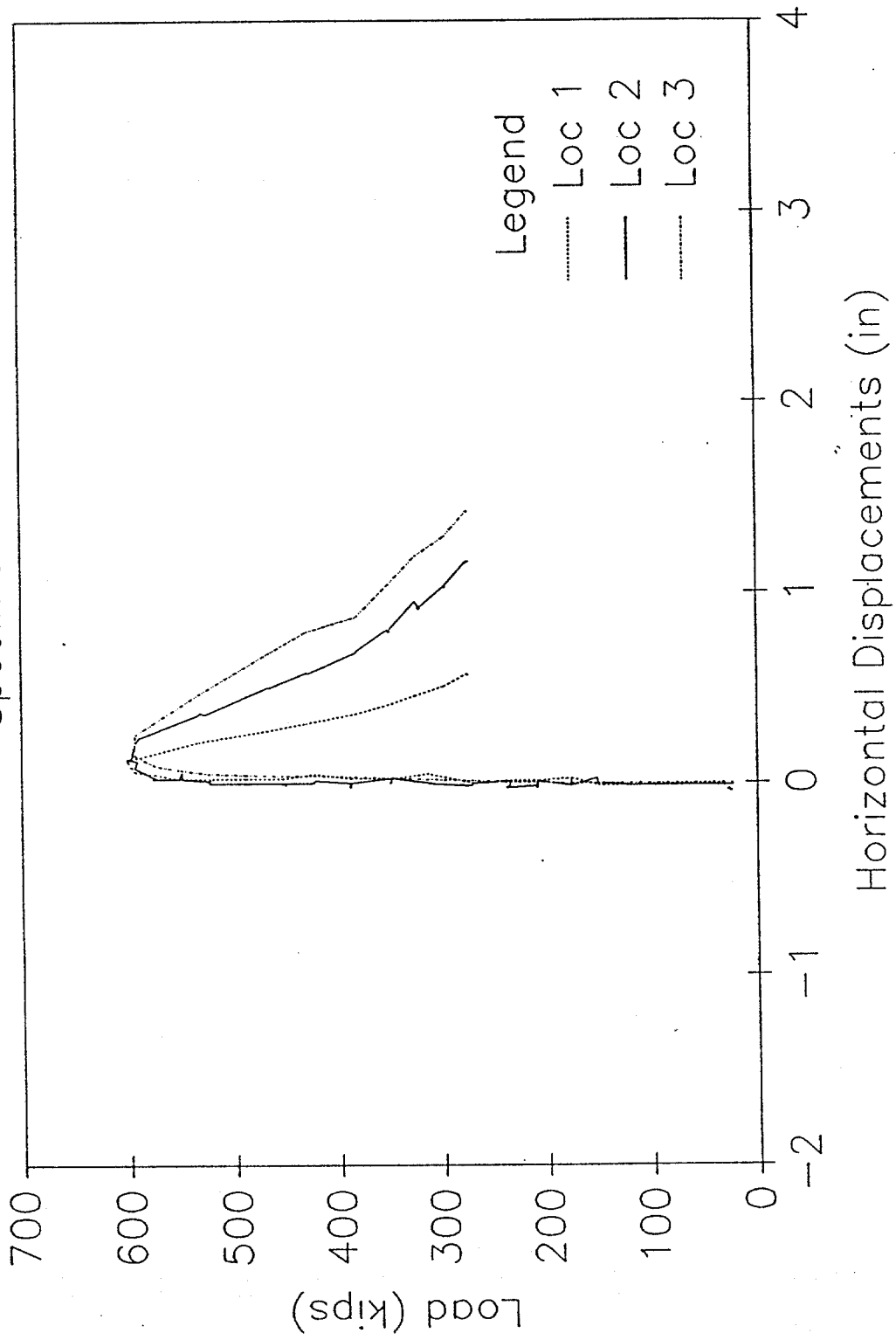
LOAD vs CHORD SHORTENING

Specimen 02



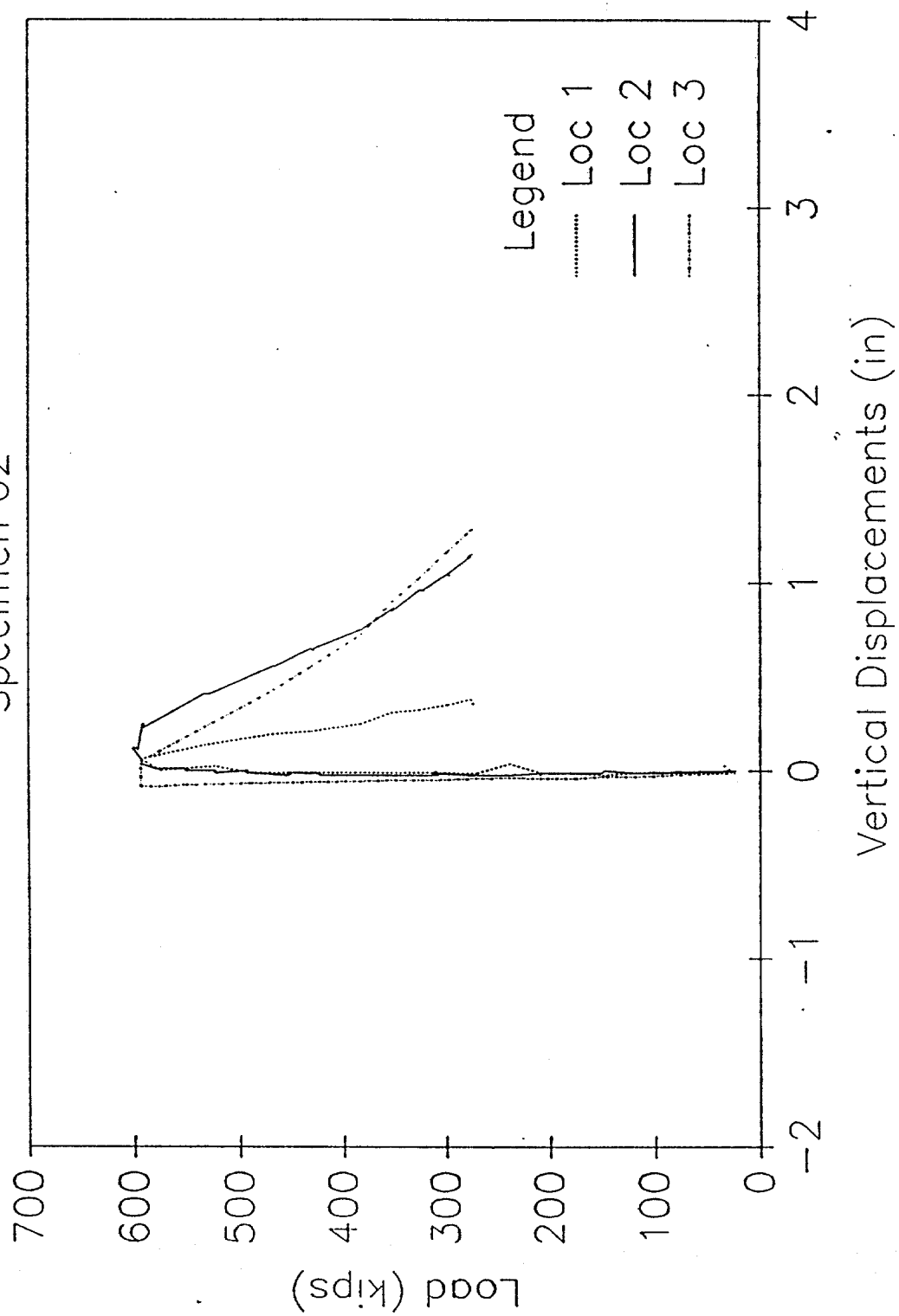
HORIZONTAL DISPLACEMENTS

Specimen 02



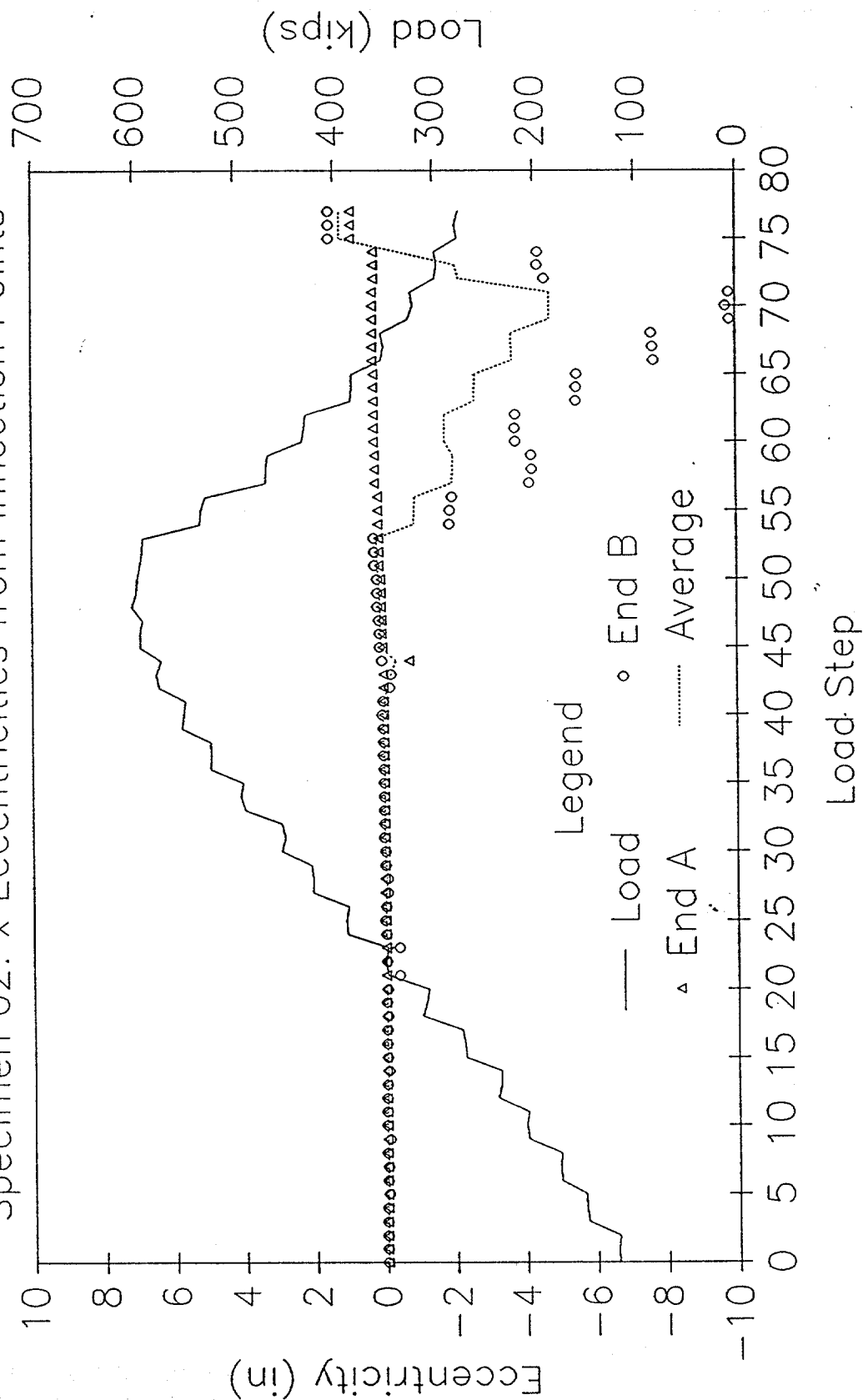
VERTICAL DISPLACEMENTS

Specimen 02



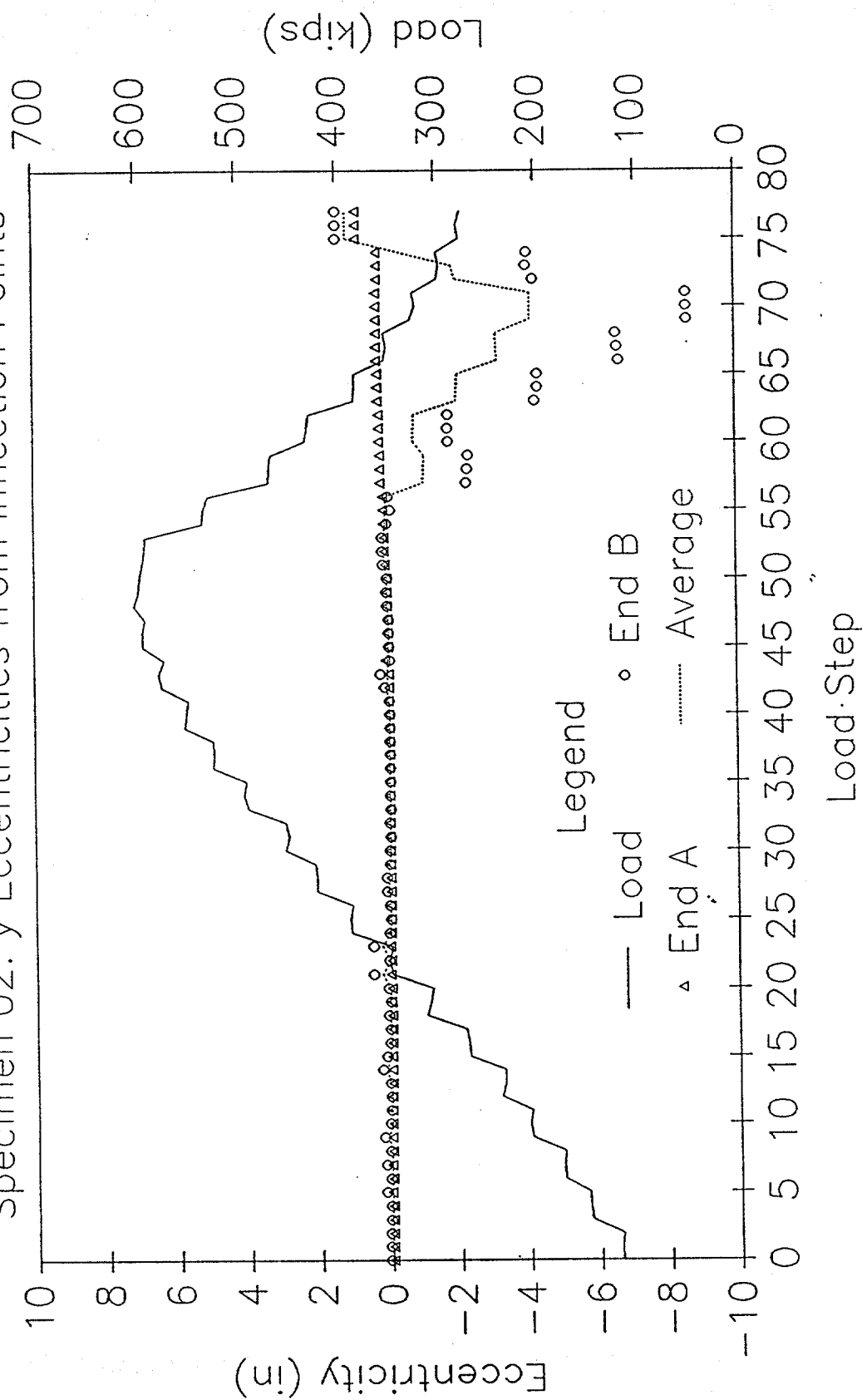
LOAD AND ECCENTRICITY vs LOAD STEP

Specimen 02: x Eccentricities from Inflection Points



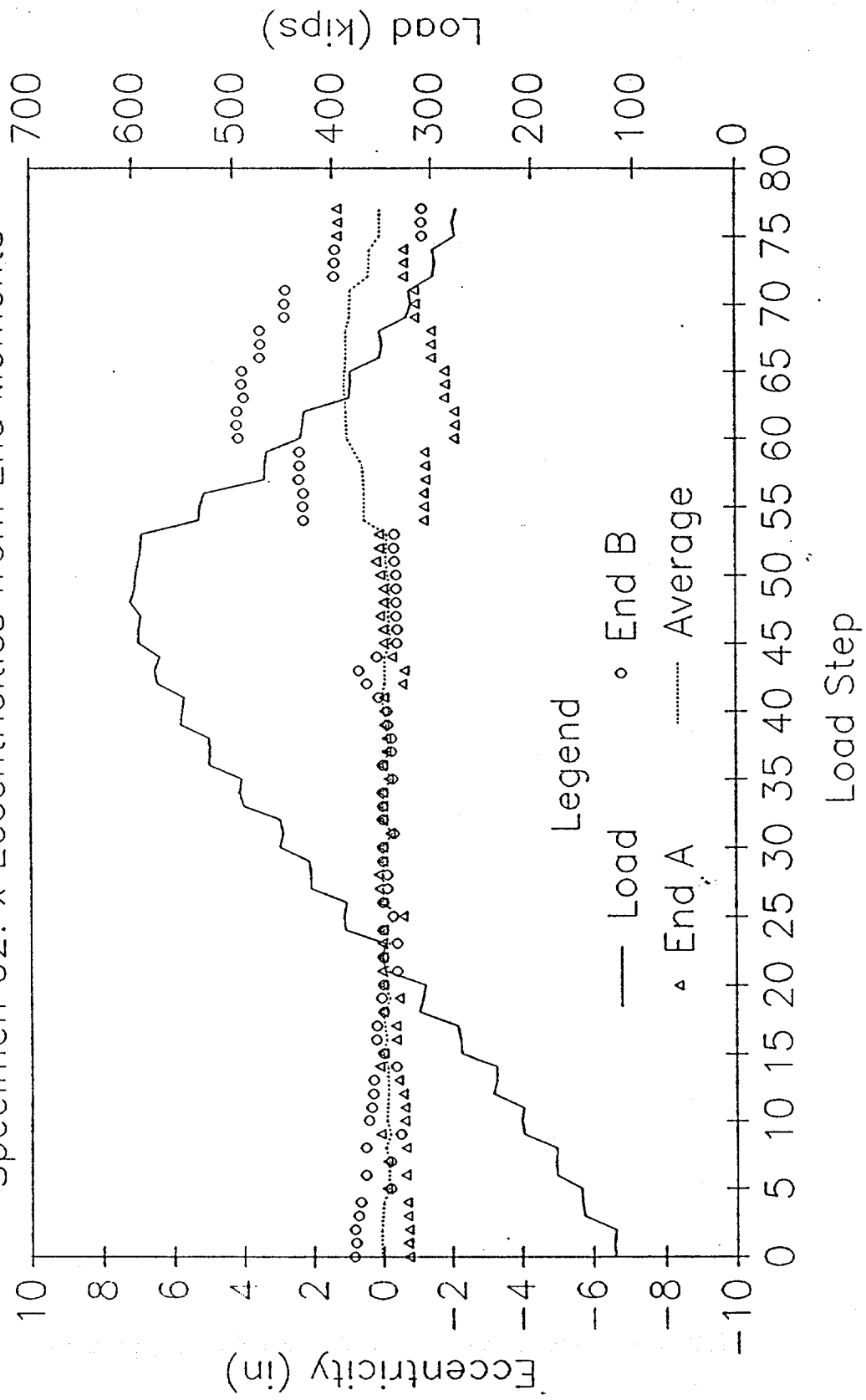
LOAD AND ECCENTRICITY vs LOAD STEP

Specimen 02: y Eccentricities from Inflection Points

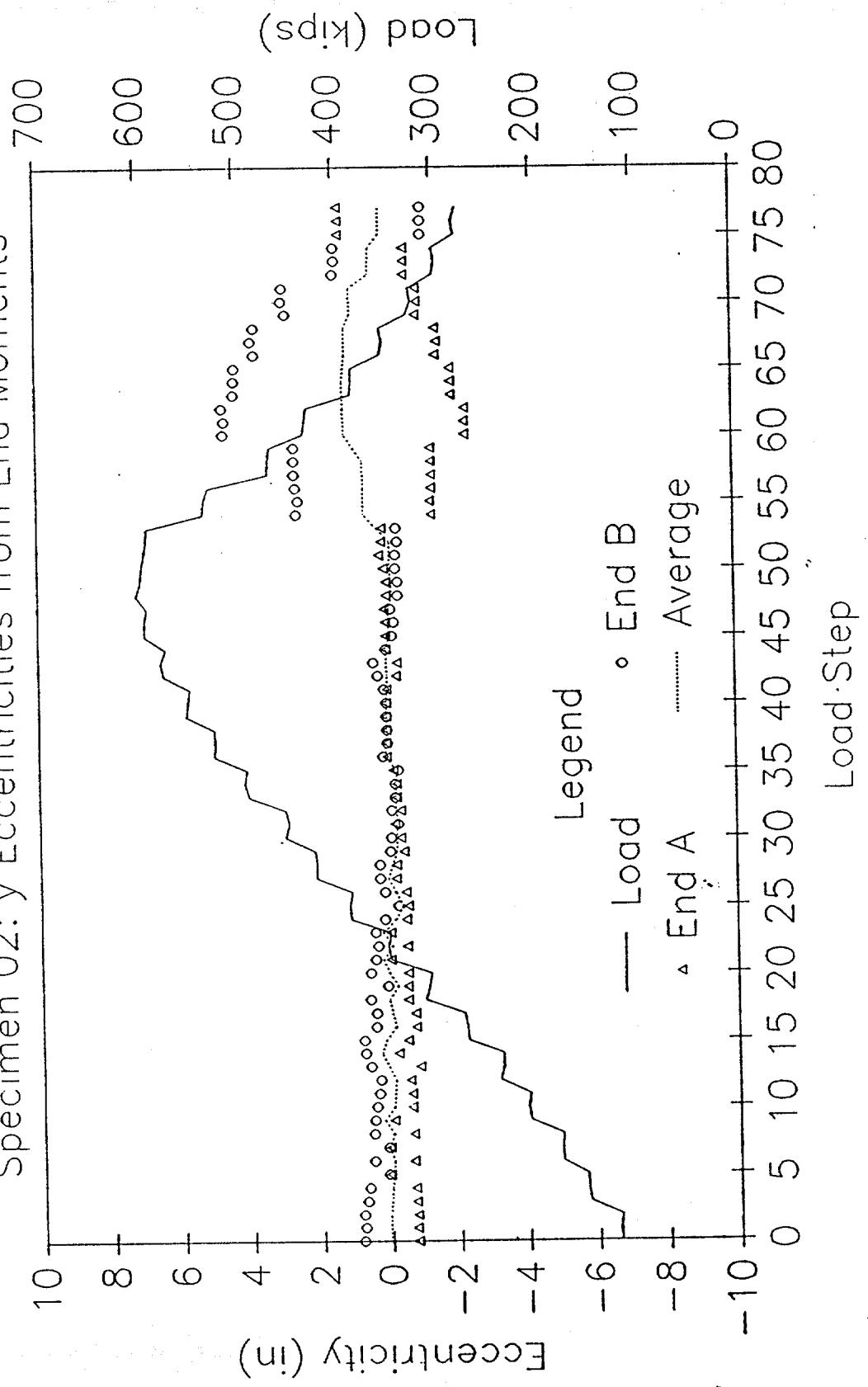


LOAD AND ECCENTRICITY vs LOAD STEP

Specimen 02: x Eccentricities from End Moments

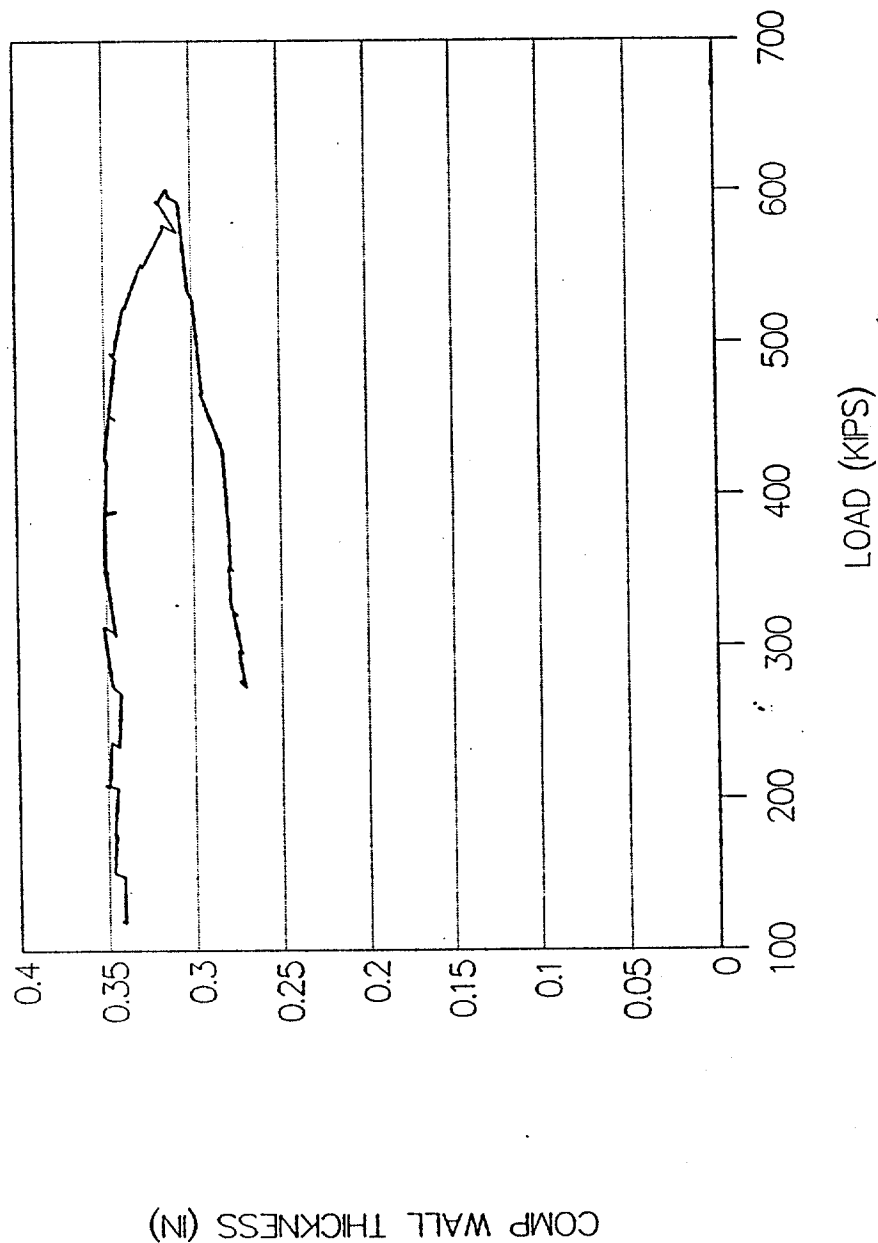


LOAD AND ECCENTRICITY vs LOAD STEP
Specimen 02: y Eccentricities from End Moments



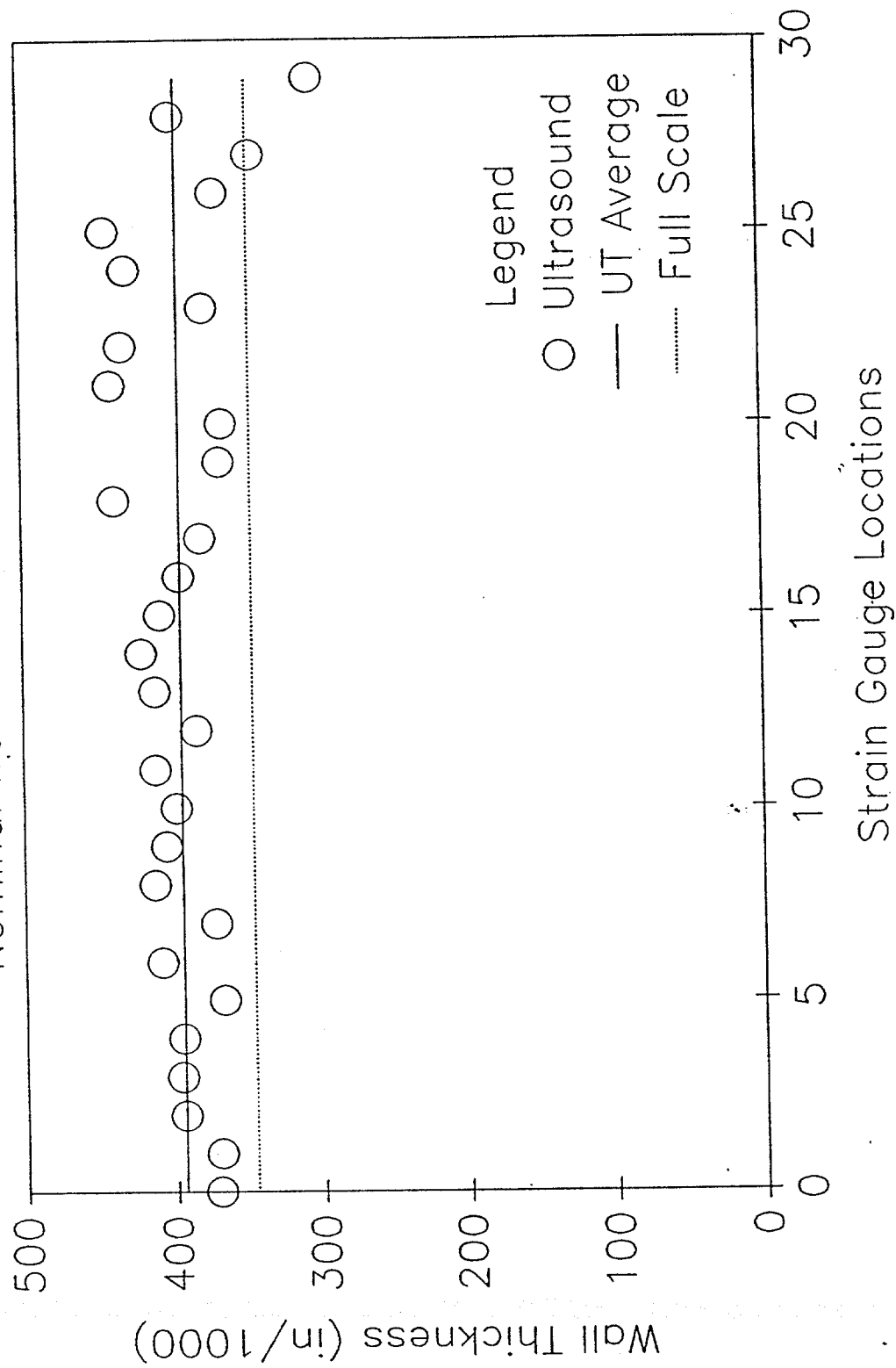
SPECIMEN 02—FULL SCALE TEST

COMPUTED WALL THICKNESS



SPECIMEN 02: WALL THICKNESS

Nominal Wall Thickness = 0.438 in



Ultrasound Data for Specimen 2
(All values in inches)

Gauge No.	UT Thickness	UT Average
0	0.371	
1	0.370	
2	0.394	
3	0.396	
4	0.395	
5	0.367	0.382
6	0.409	
7	0.372	
8	0.413	
9	0.405	
10	0.398	
11	0.412	0.401
12	0.384	
13	0.412	
14	0.421	
15	0.408	
16	0.395	
17	0.380	0.400
18	0.438	
19	0.367	
20	0.365	
21	0.440	
22	0.432	
23	0.377	0.403
24	0.429	
25	0.443	
26	0.369	
27	0.344	
28	0.398	
29	0.304	0.381

Overall Average = 0.394

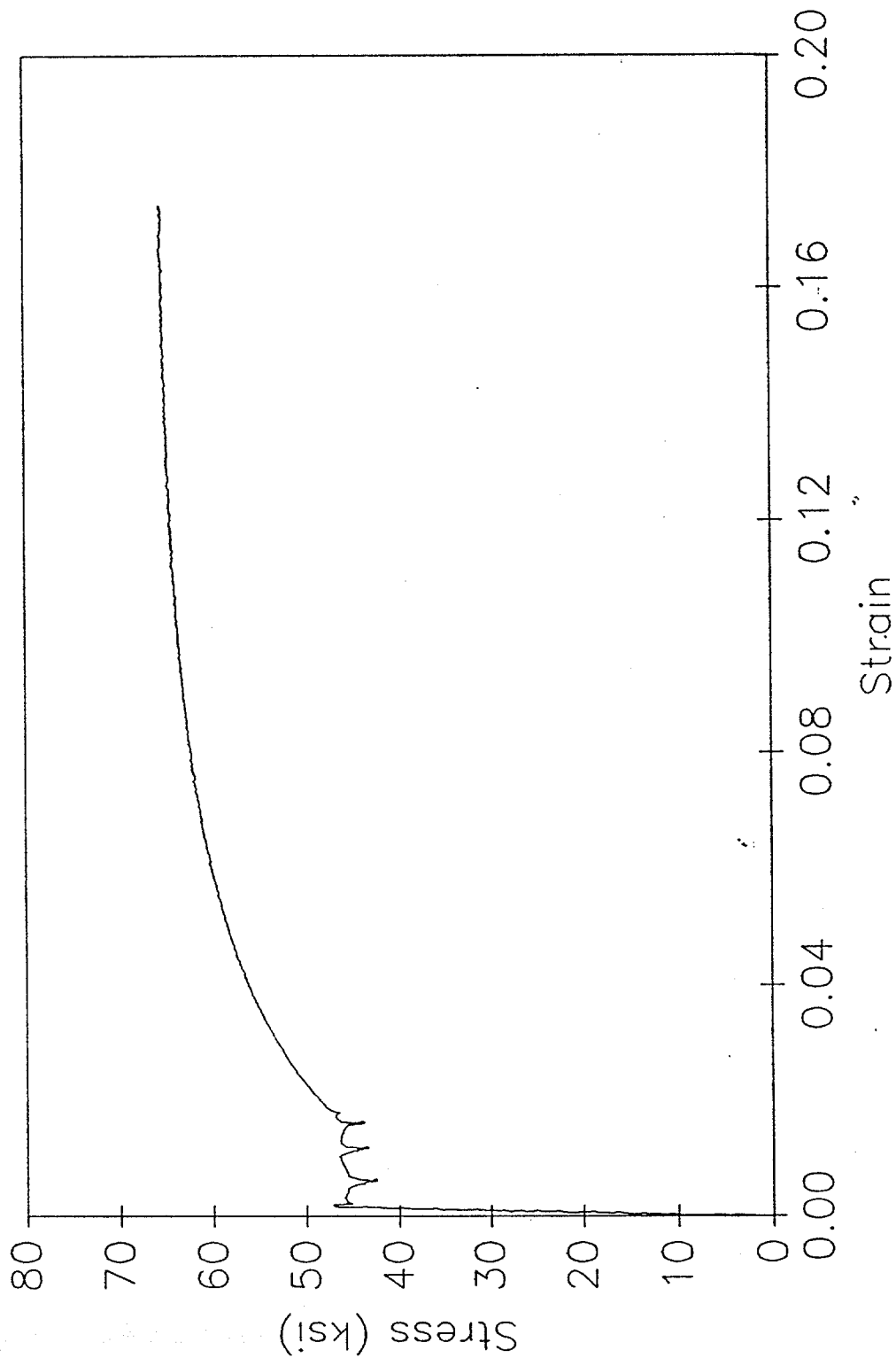
Random Readings near Buckling Point

No.	Reading
1	0.340
2	0.250
3	0.242
4	0.253
5	0.324
6	0.300
7	0.281

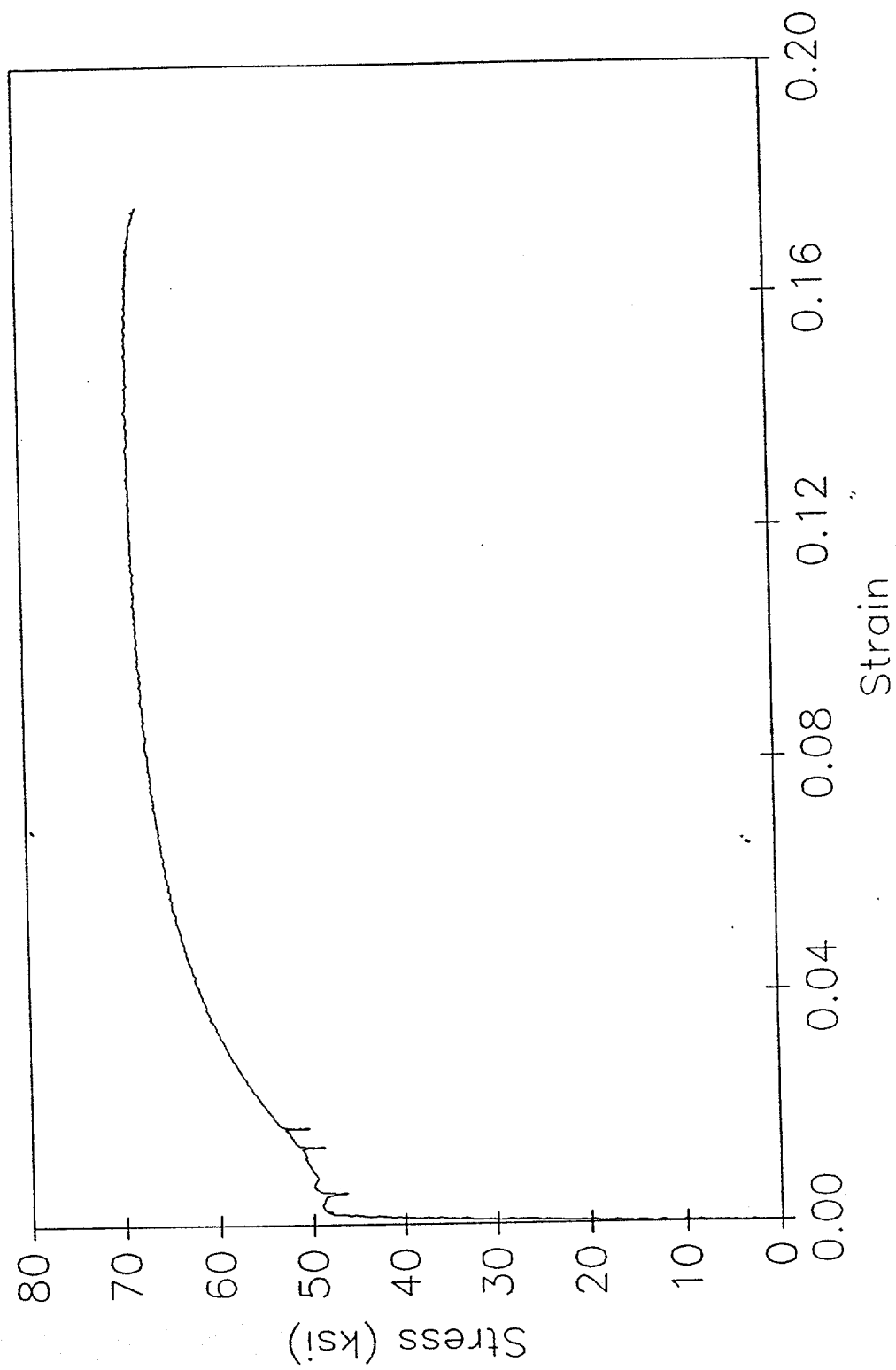
Random Average = 0.284

TENSILE SPECIMEN 2-1

Stress vs Strain



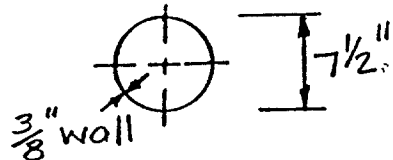
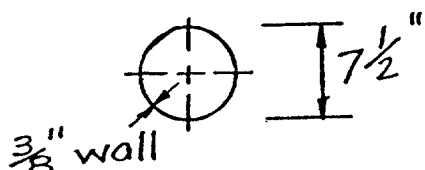
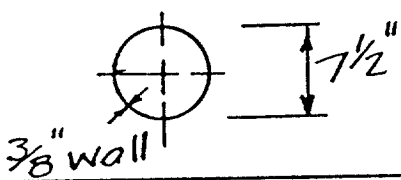
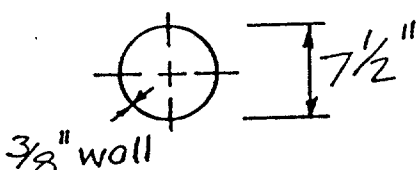
TENSILE SPECIMEN 2-2
Stress vs Strain



SPECIMEN 03

DAMAGE SUMMARY

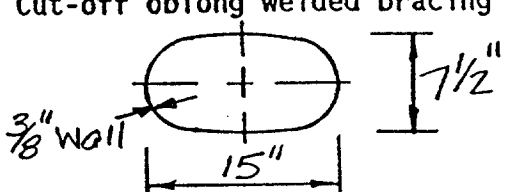
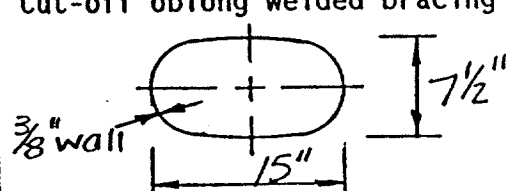
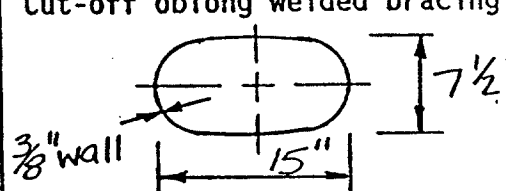
Specimen No. 3

DISTANCE FROM END "B"	*DISTANCE FROM CHALK LINE		DESCRIPTION OF DAMAGE
	LEFT	RIGHT	
1. From 0' to 4'-2 1/2"	3/4"		1/2" longitudinal weld (4'-2 1/2" long)
2. 4'-2 1/2"			1/2" circumferential butt weld
3. From 4'-2 1/2" to 12'-4 1/2"		26 1/2"	1/2" longitudinal weld (8'-2")
4. 9"-5"	23"		Cut-off round welded bracing attachment 7 1/2" diameter 
5. 10'-3"		4"	Cut-off round welded bracing attachment 7 1/2" diameter 
6. 10'-3"	11"		Cut-off round welded bracing attachment 7 1/2" diameter 
7. 10'-3"		19"	Cut-off round welded bracing attachment 7 1/2" diameter 

*Looking from end "A" towards end "B"

DAMAGE SUMMARY

Specimen No. 3 (continued)

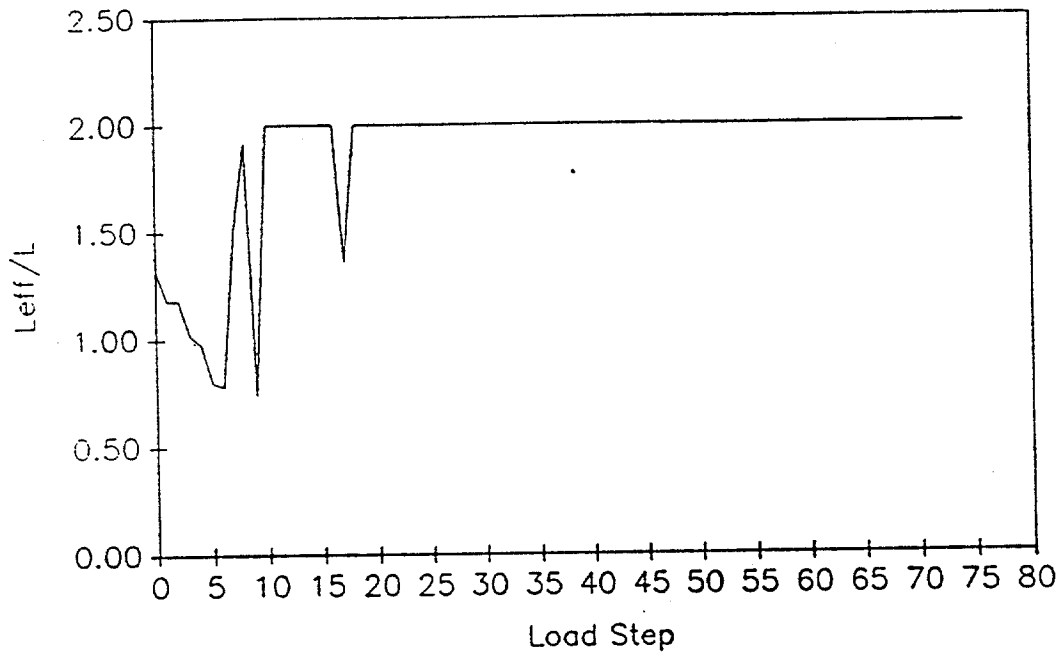
DISTANCE FROM END "B"	*DISTANCE FROM CHALK LINE		DESCRIPTION OF DAMAGE
	LEFT	RIGHT	
8. 11'-8"		4"	Cut-off oblong welded bracing 
9. 11'-8"	11"		Cut-off oblong welded bracing 
10. 11'-8"		18"	Cut-off oblong welded bracing 
11. 12'-4 1/2"			1/2" circumferential butt weld
12. From 12'-4 1/2" to 20'-6 1/2"	5 1/2"		1/2" longitudinal weld (8'-2")
13. 20'-6 1/2"			1/2" circumferential butt weld
14. From 20'-6 1/2" to 24'-2 3/8"		22"	1/2" longitudinal weld (3'-7 7/8")

SPECIMEN IS VERY CORRODED!

*Looking from end "A" towards end "B"

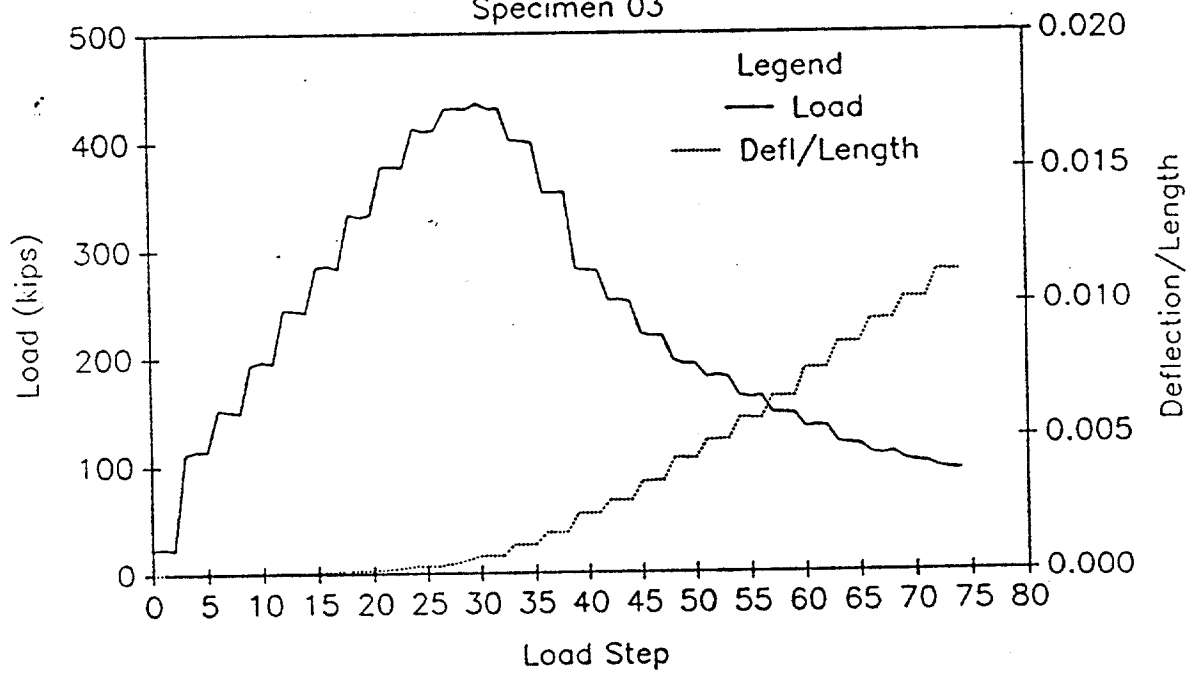
EFFECTIVE LENGTH vs LOAD STEP

Specimen 03



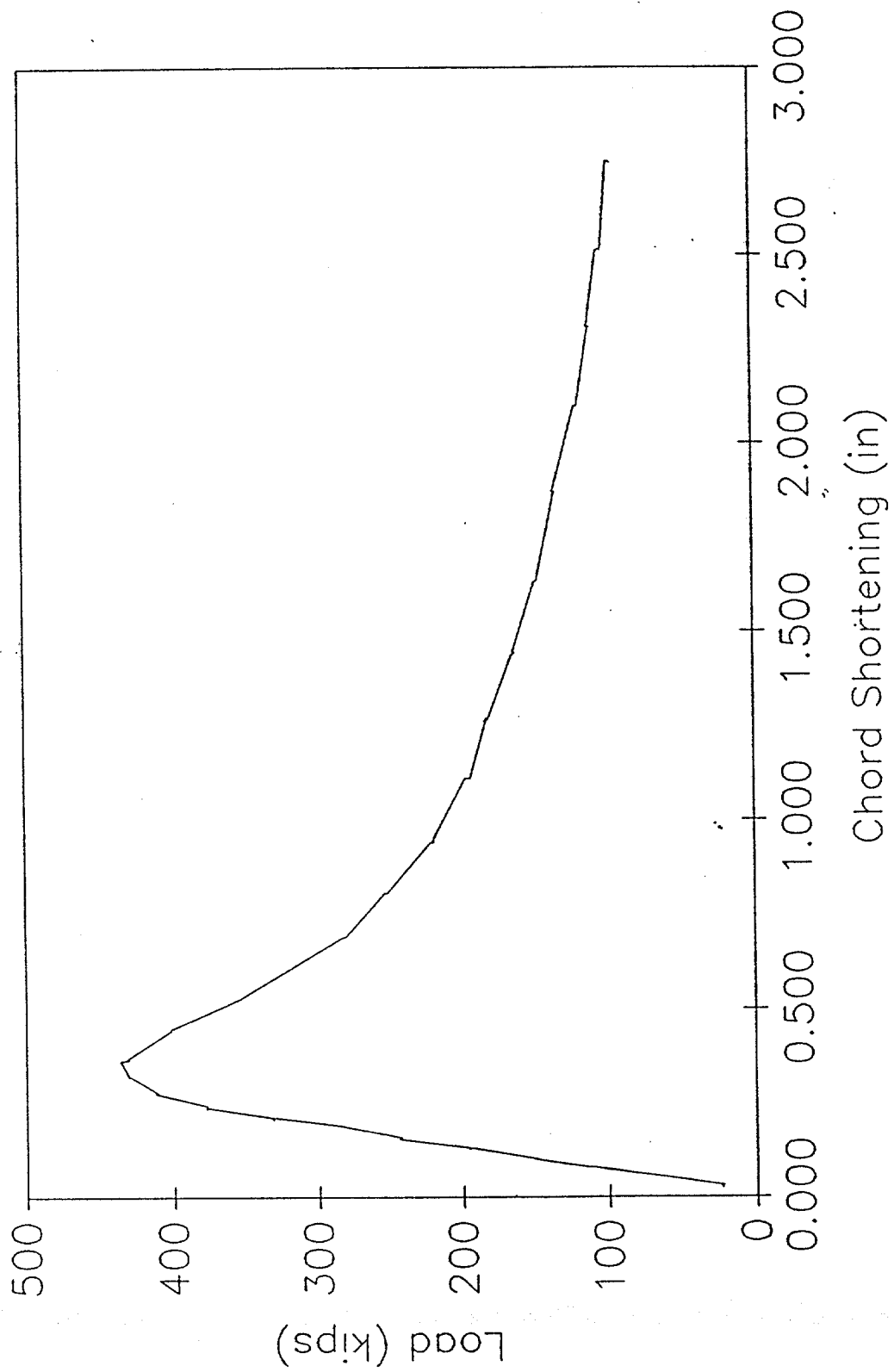
LOAD AND DEFLECTION vs LOAD STEP

Specimen 03



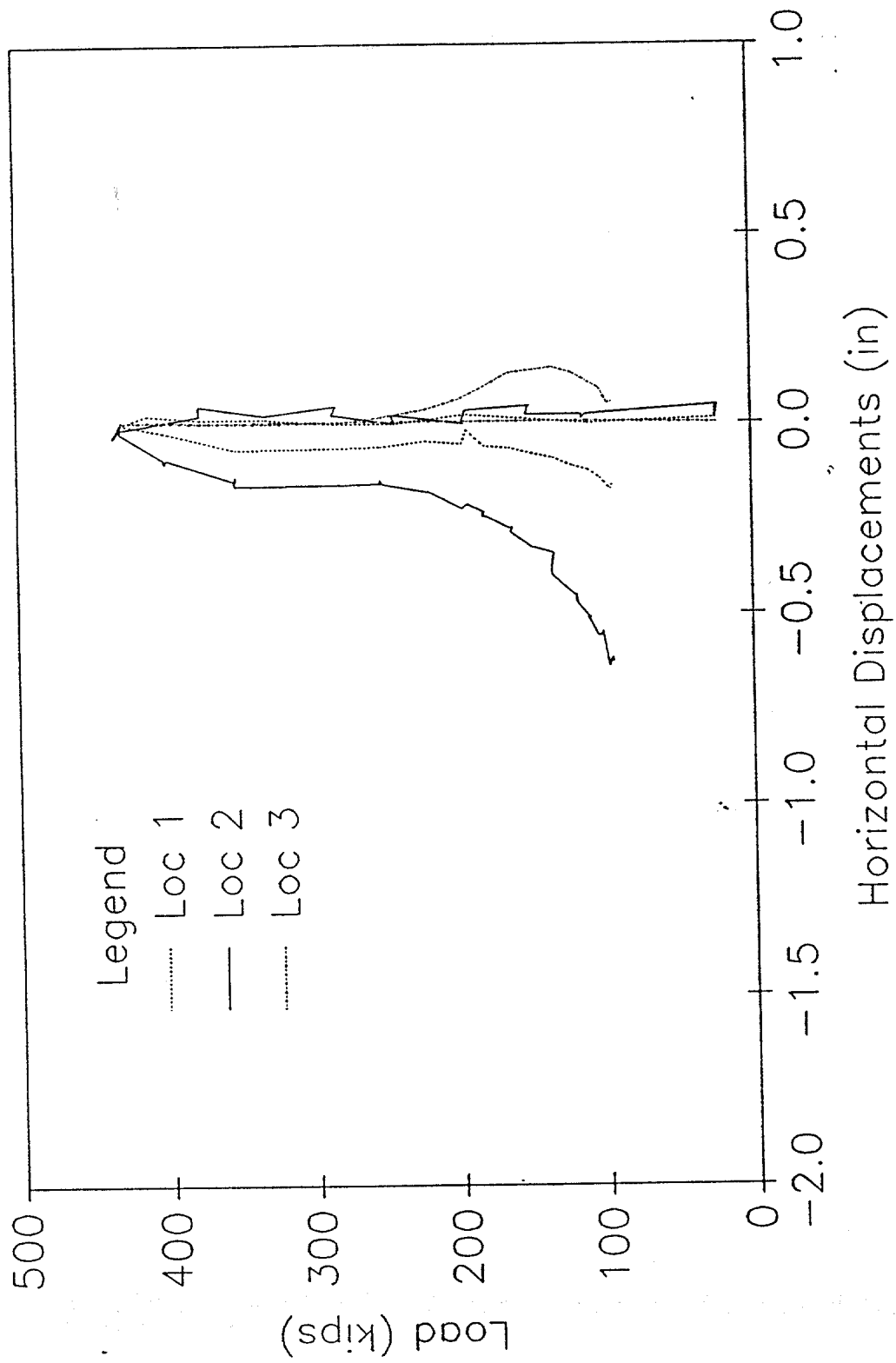
LOAD vs CHORD SHORTENING

Specimen 03



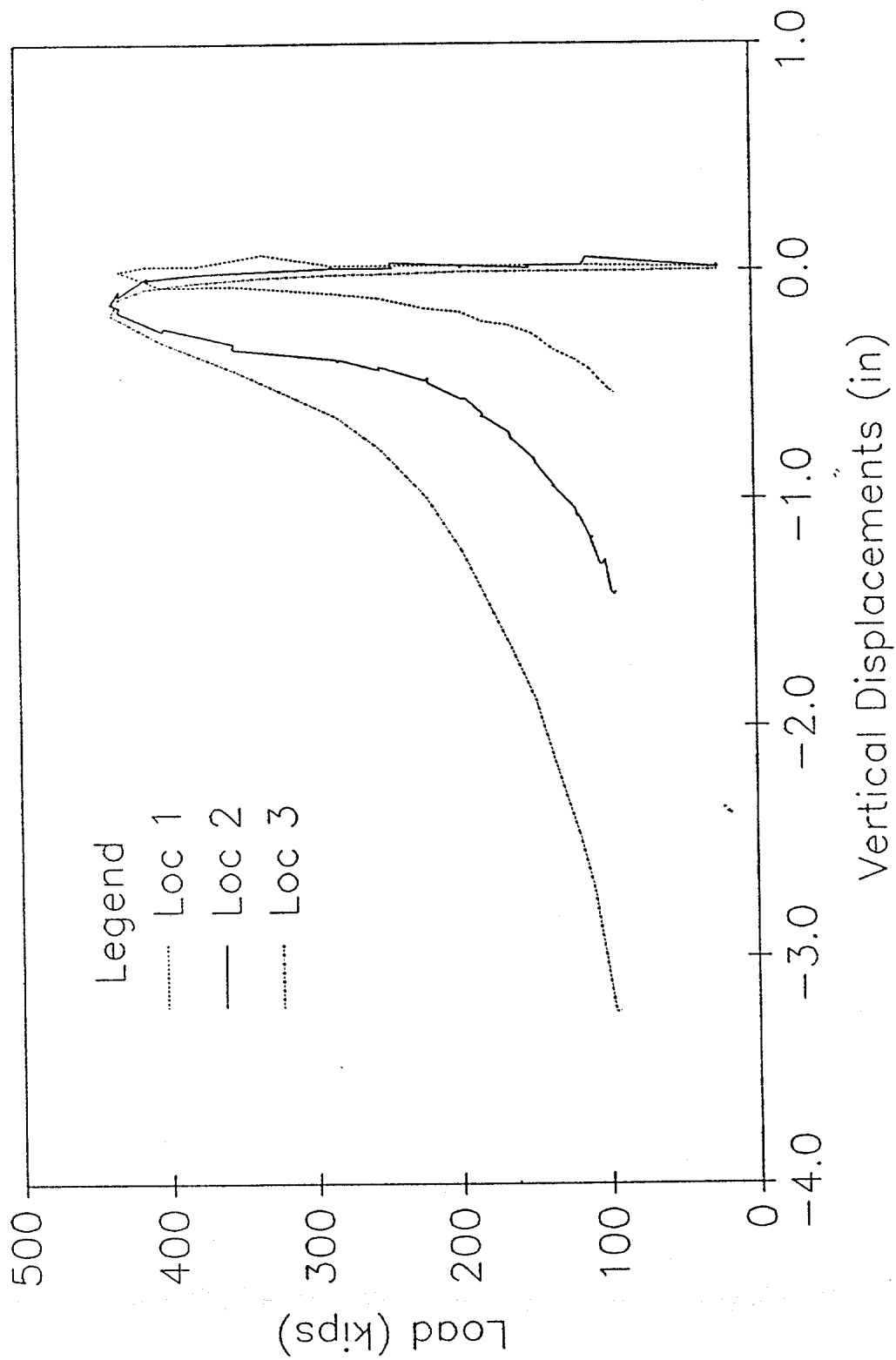
HORIZONTAL DISPLACEMENTS

Specimen 03



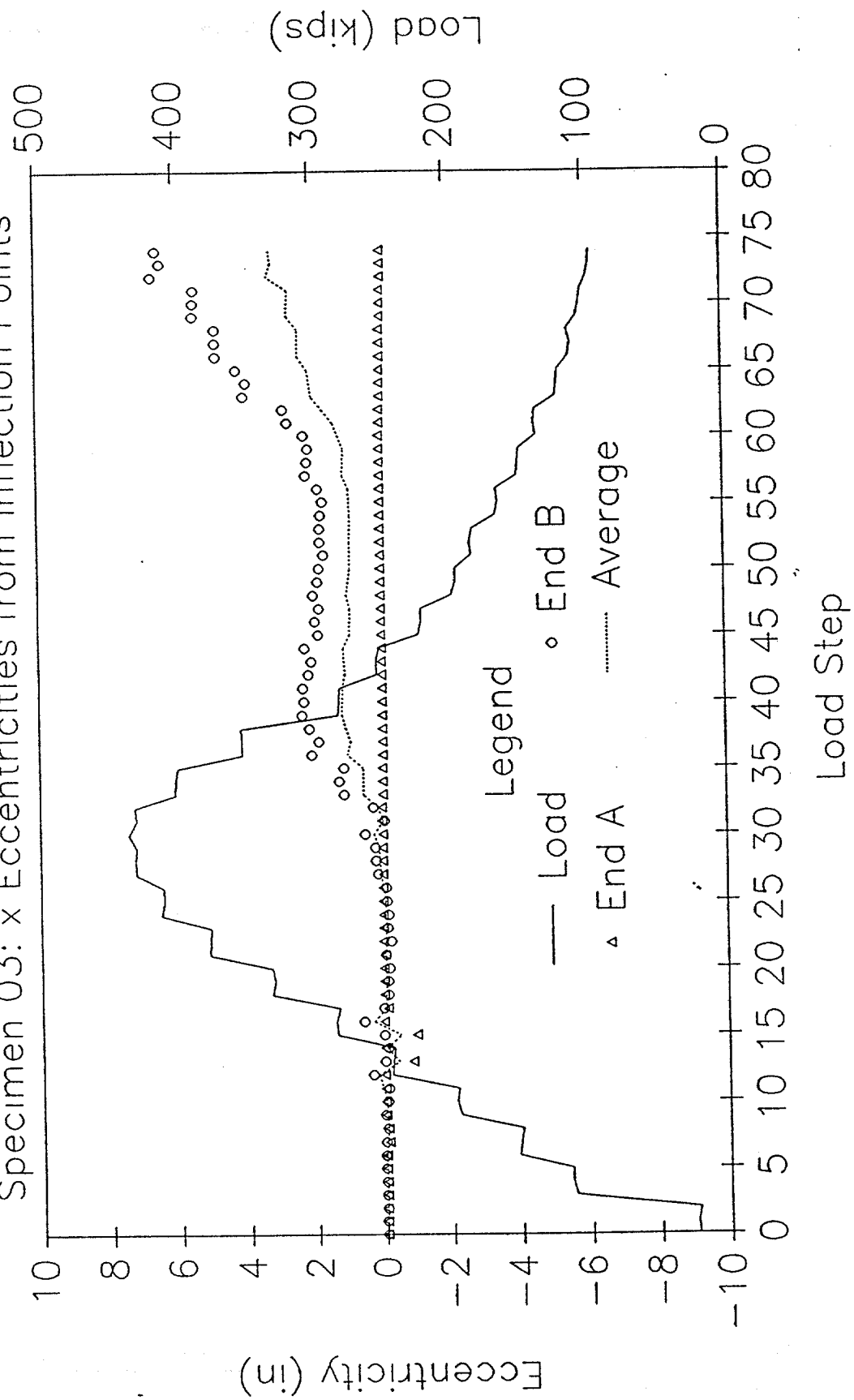
VERTICAL DISPLACEMENTS

Specimen 03



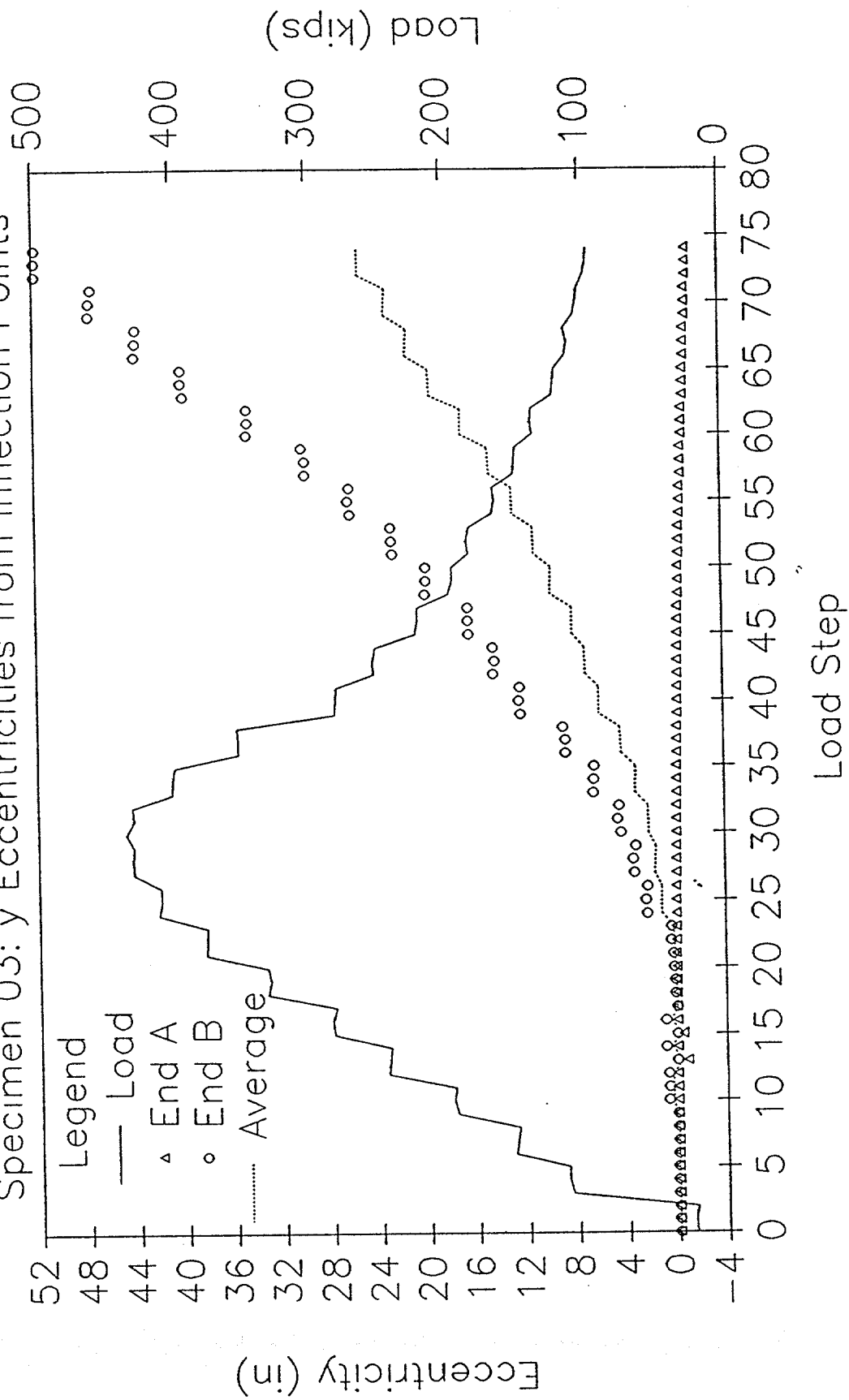
LOAD AND ECCENTRICITY vs LOAD STEP

Specimen 03: x Eccentricities from Inflection Points



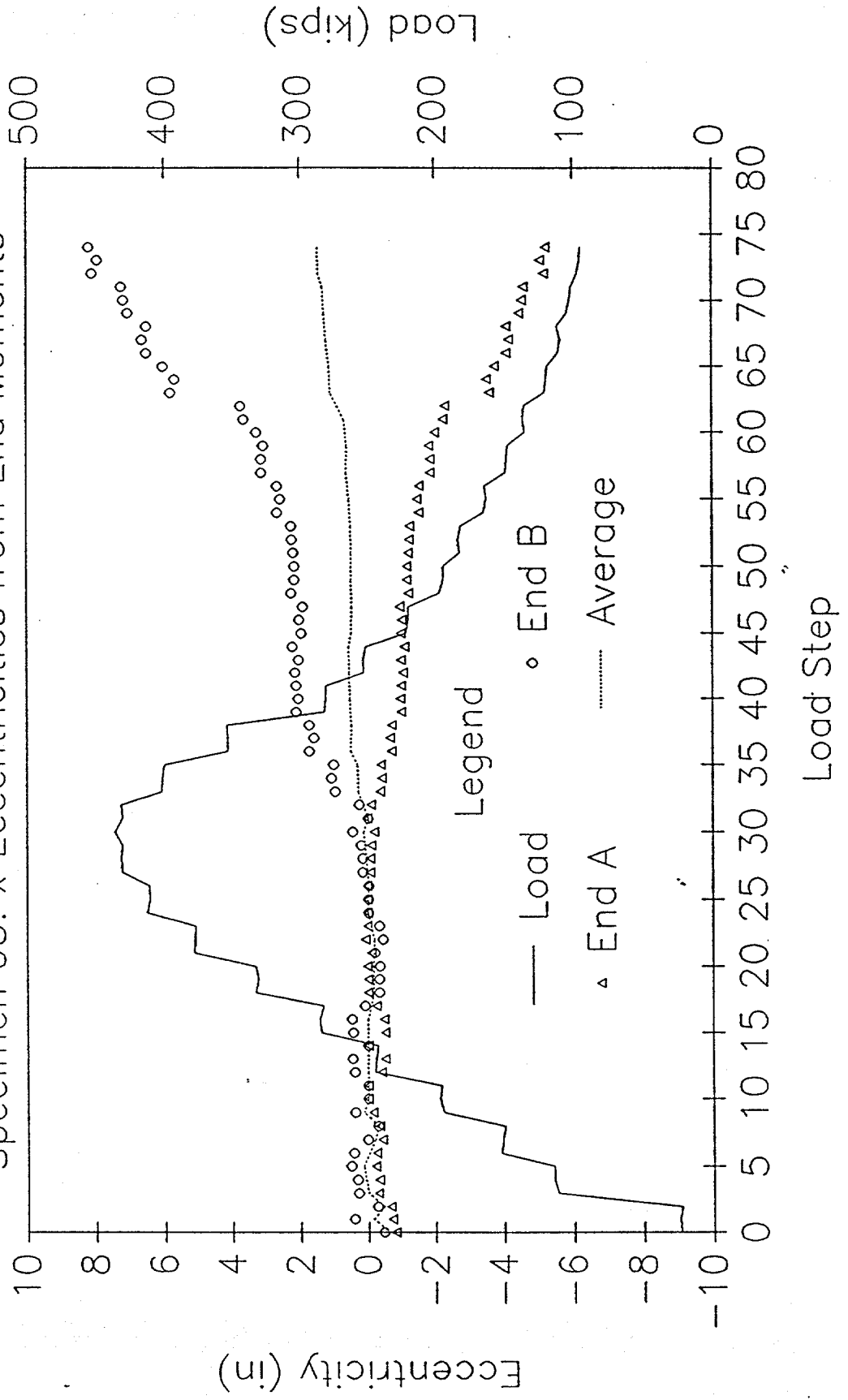
LOAD AND ECCENTRICITY vs LOAD STEP

Specimen 03: y Eccentricities from Inflection Points



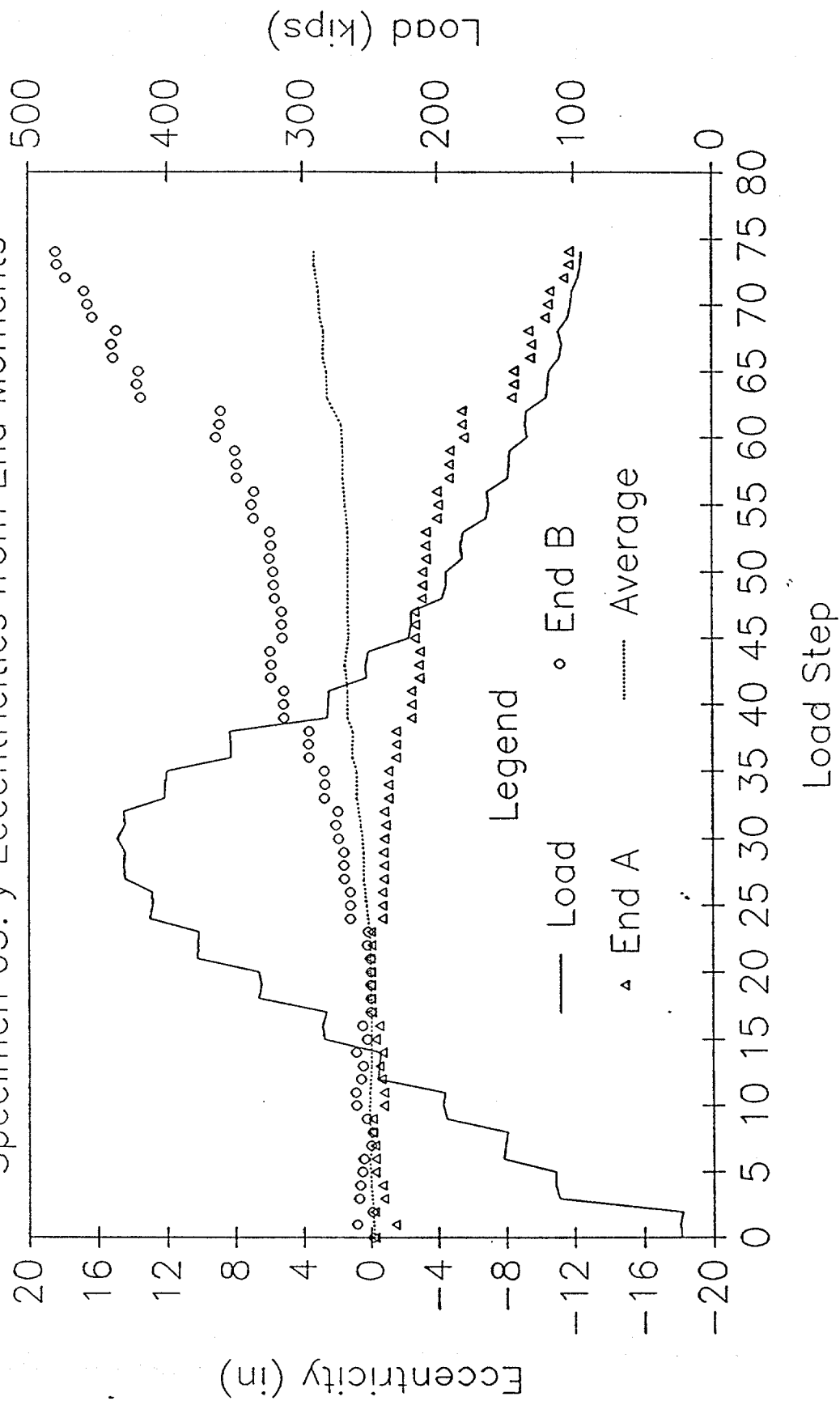
LOAD AND ECCENTRICITY vs LOAD STEP

Specimen 03: x Eccentricities from End Moments



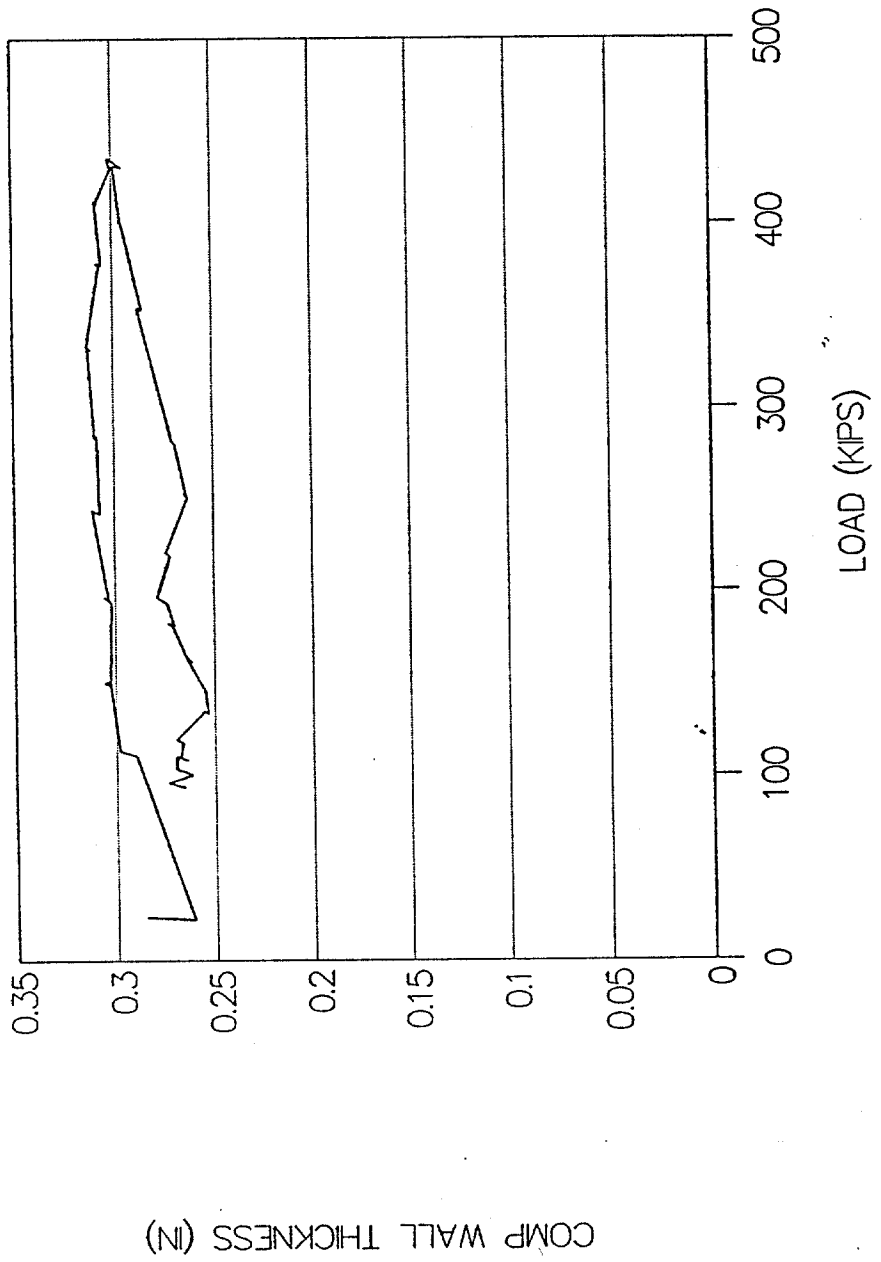
LOAD AND ECCENTRICITY vs LOAD STEP

Specimen 03: y Eccentricities from End Moments



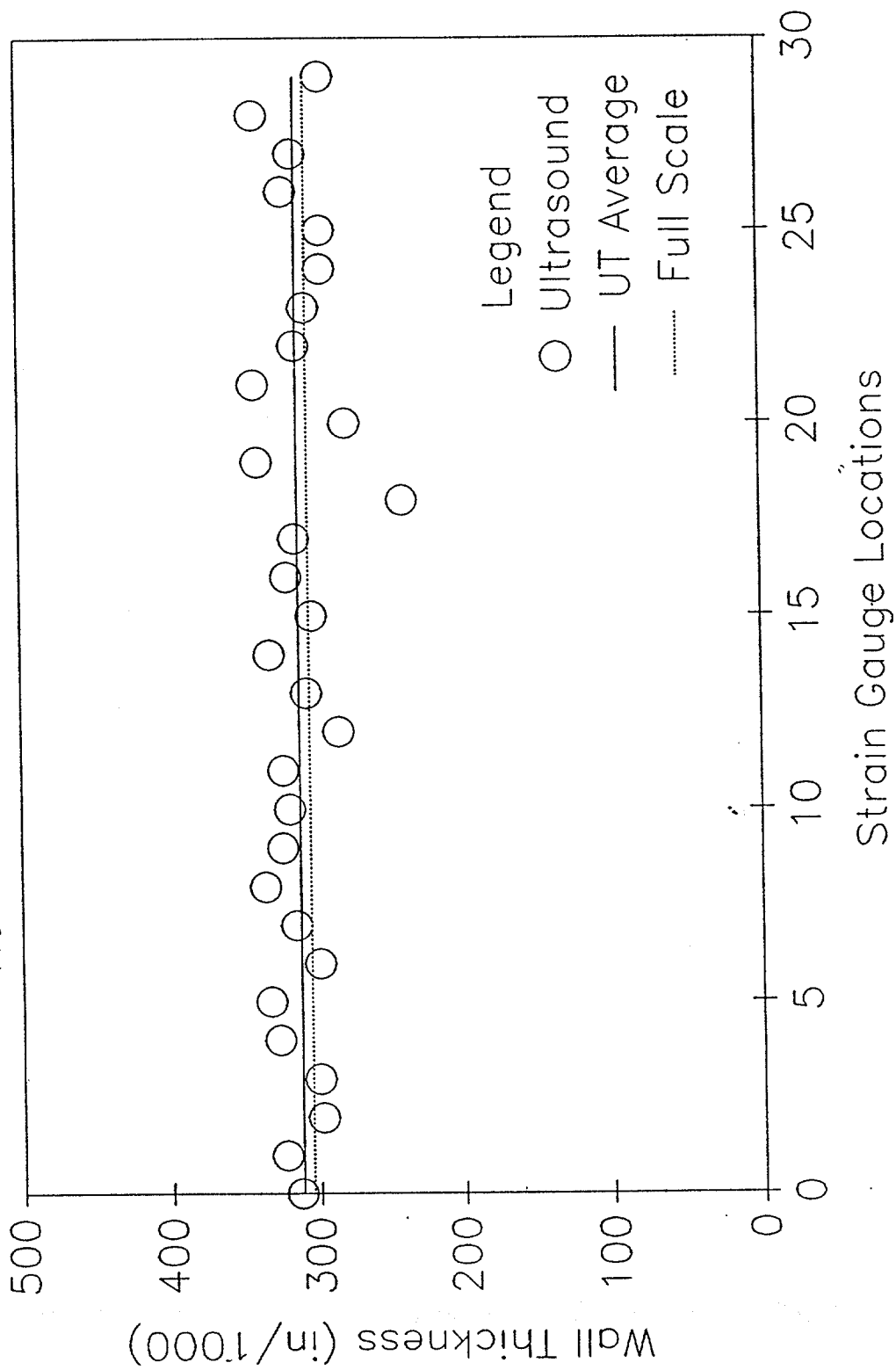
SPECIMEN 03--FULL SCALE TEST

COMPUTED WALL THICKNESS



SPECIMEN 03: WALL THICKNESS

Nominal Wall Thickness = 0.375 in



Ultrasound Data for Specimen 3
(All values in inches)

Gauge No.	UT Thickness	UT Average
0	0.313	
1	0.323	
2	0.298	
3	0.300	
4	0.327	
5	0.333	0.316
6	0.299	
7	0.315	
8	0.336	
9	0.324	
10	0.319	
11	0.323	0.319
12	0.285	
13	0.307	
14	0.332	
15	0.303	
16	0.320	
17	0.314	0.310
18	0.240	
19	0.339	
20	0.279	
21	0.341	
22	0.313	
23	0.306	0.303
24	0.295	
25	0.295	
26	0.321	
27	0.314	
28	0.340	
29	0.295	0.310

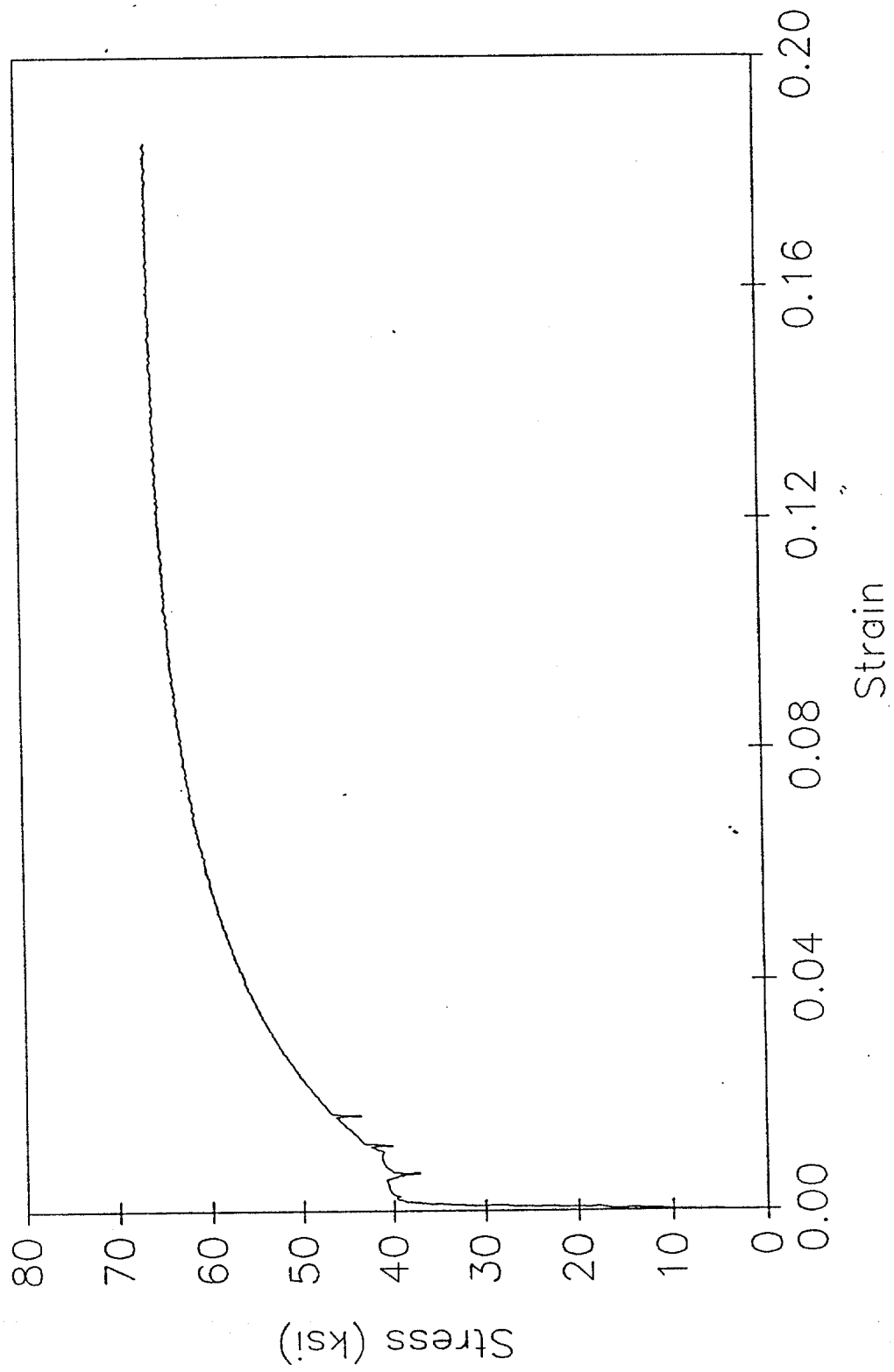
Overall Average = 0.312

Random Readings near Buckling Point

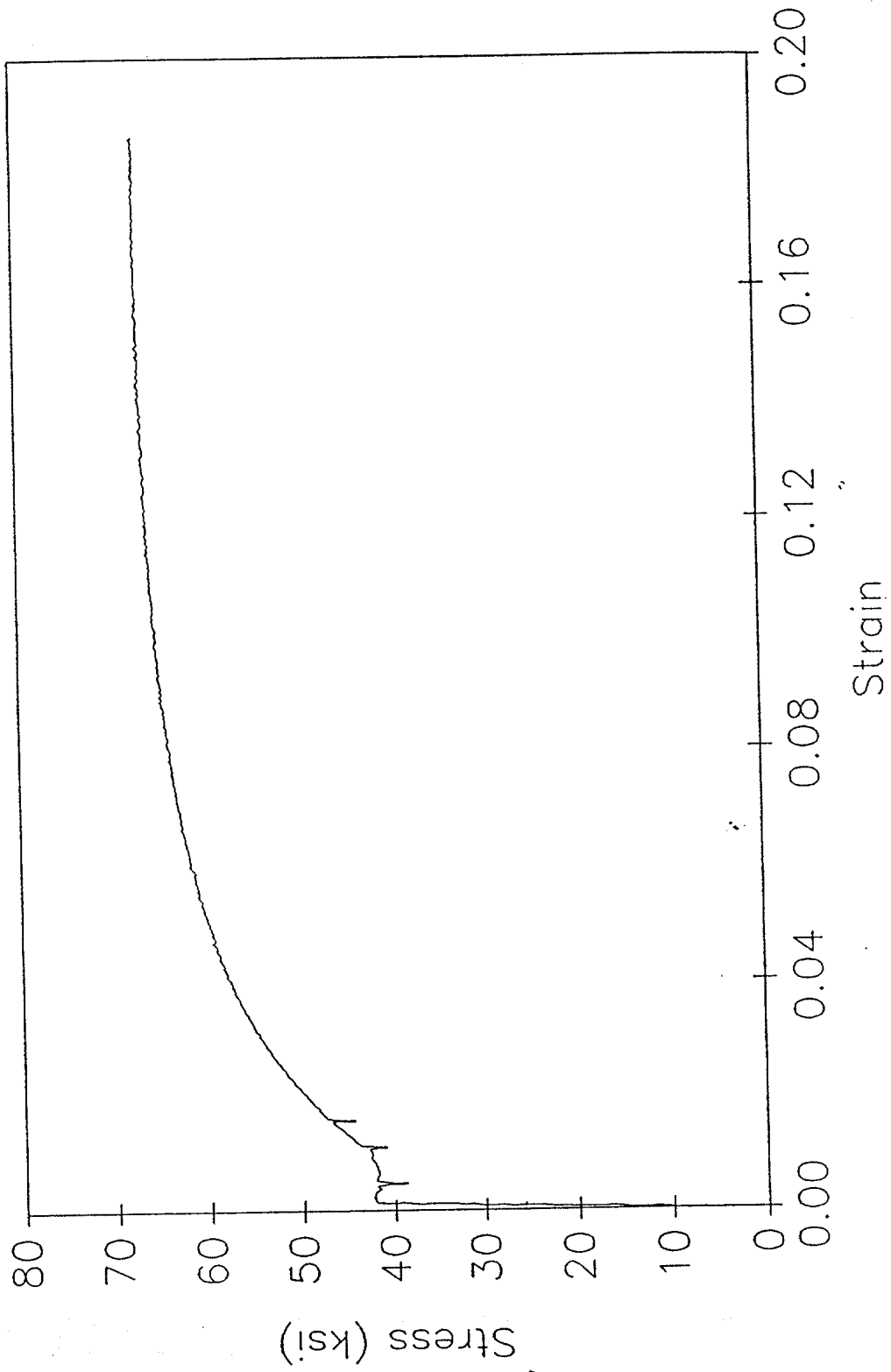
No.	Reading
1	0.239
2	0.245
3	0.259
4	0.262
5	0.240
6	0.249
7	0.234
8	0.290
9	0.264
10	0.241
11	0.192

Random Average = 0.247

TENSILE SPECIMEN 3-1
Stress vs Strain



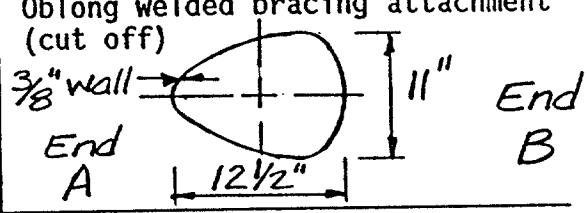
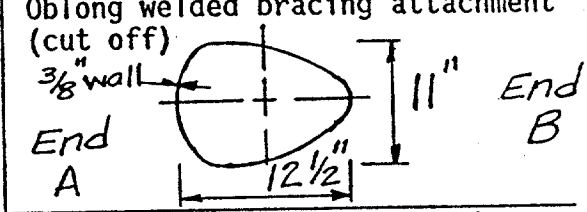
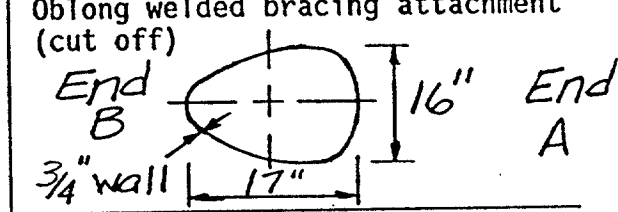
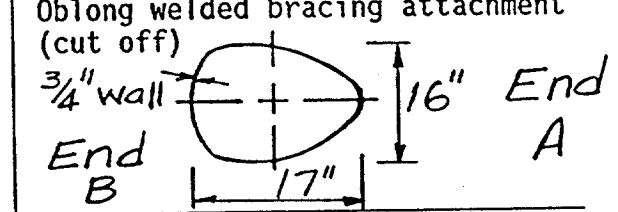
TENSILE SPECIMEN 3-2
Stress vs Strain



SPECIMEN 04

DAMAGE SUMMARY

Specimen No. 4

DISTANCE FROM END "B"	*DISTANCE FROM CHALK LINE		DESCRIPTION OF DAMAGE
	LEFT	RIGHT	
1. 18'-5"		7 1/2"	Oblong welded bracing attachment (cut off) 
2. 17'-3"		7 1/2"	Oblong welded bracing attachment (cut off) 
3. 17'-10"		10 3/4"	Welded in torch cut 5 1/4" long X 5/8" wide (circumferential)
4. 17'-0"	3 3/4"		Oblong welded bracing attachment (cut off) 
5. 18'-9"	3 3/4"		Oblong welded bracing attachment (cut off) 
6. 3'-9 1/2"		17 1/2"	5 1/2" long X 1/2" wide circumferential weld

The specimen is curved. See additional page for initial out-of-straightness information.

*Looking from end "A" towards end "B"

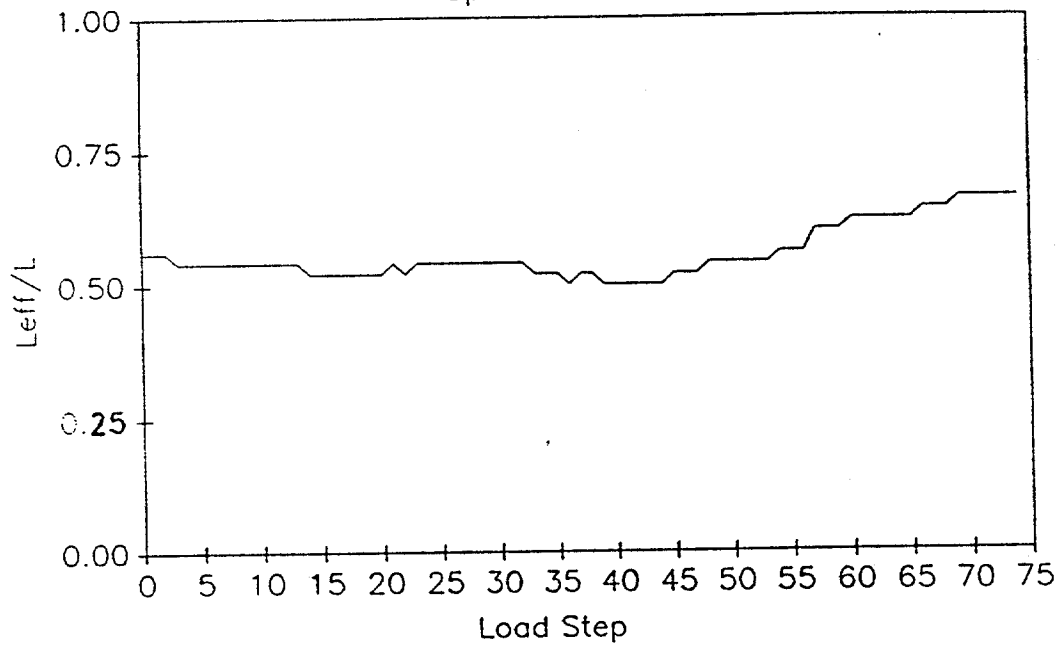
Out-of-Straightness Measurements
for Specimen 04

The specimen was initially curved in the yz-plane and straight in the xz-plane. The following measurements are in the y-direction.

Distance from End B (ft)	Distance from stringline to top of pipe (in)	Out -of straightness in y direction (in)
0	3.375	0
1	3.375	0
2	3.4375	-0.0625
3	3.5	-0.125
4	3.5625	-0.1875
5	3.625	-0.25
6	3.6875	-0.3125
7	3.8125	-0.4375
8	3.875	-0.5
9	3.9375	-0.5625
10	4	-0.625
11	4.125	-0.75
12	4.1875	-0.8125
13	4.25	-0.875
14	4.375	-1
15	4.4375	-1.0625
16	4.625	-1.25
17	4.6875	-1.3125
18	4.6875	-1.3125
19	4.6875	-1.3125
20	4.625	-1.25
21	4.5	-1.125
22	4.375	-1
23	4.3125	-0.9375
24	4.25	-0.875
25	4.125	-0.75
26	4.0625	-0.6875
27	4	-0.625
28	3.875	-0.5
29	3.75	-0.375
30	3.6875	-0.3125
31	3.625	-0.25
32	3.5625	-0.1875
33	3.4375	-0.0625
34	3.375	0
34.75	3.375	0

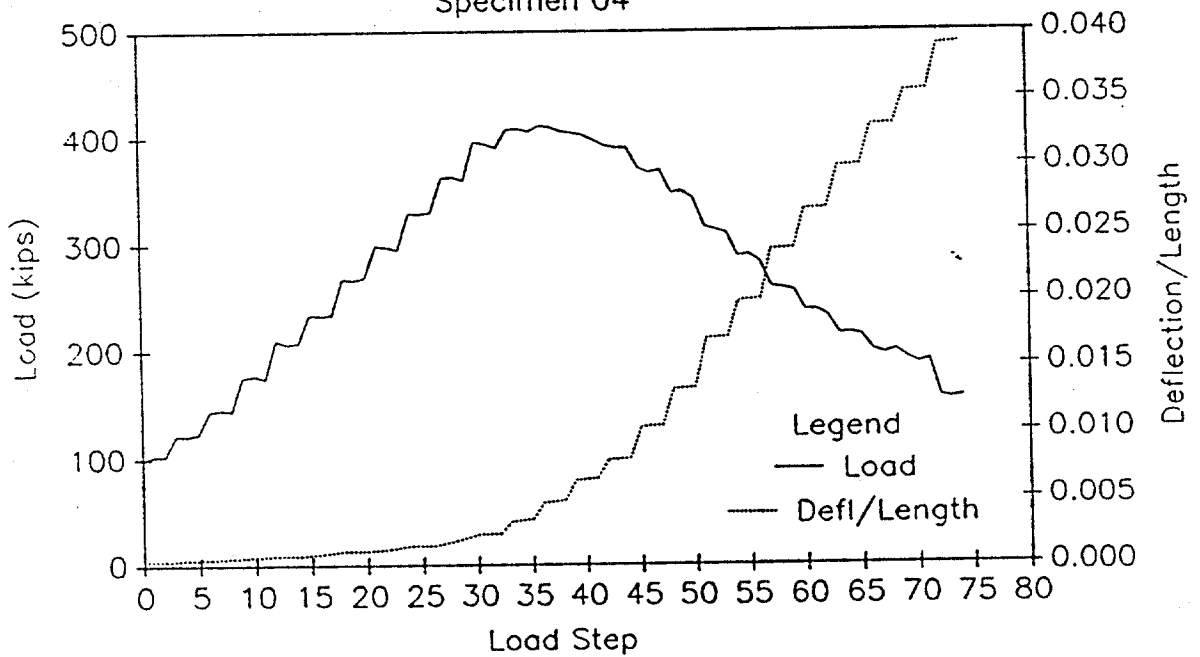
EFFECTIVE LENGTH vs LOAD STEP

Specimen 04

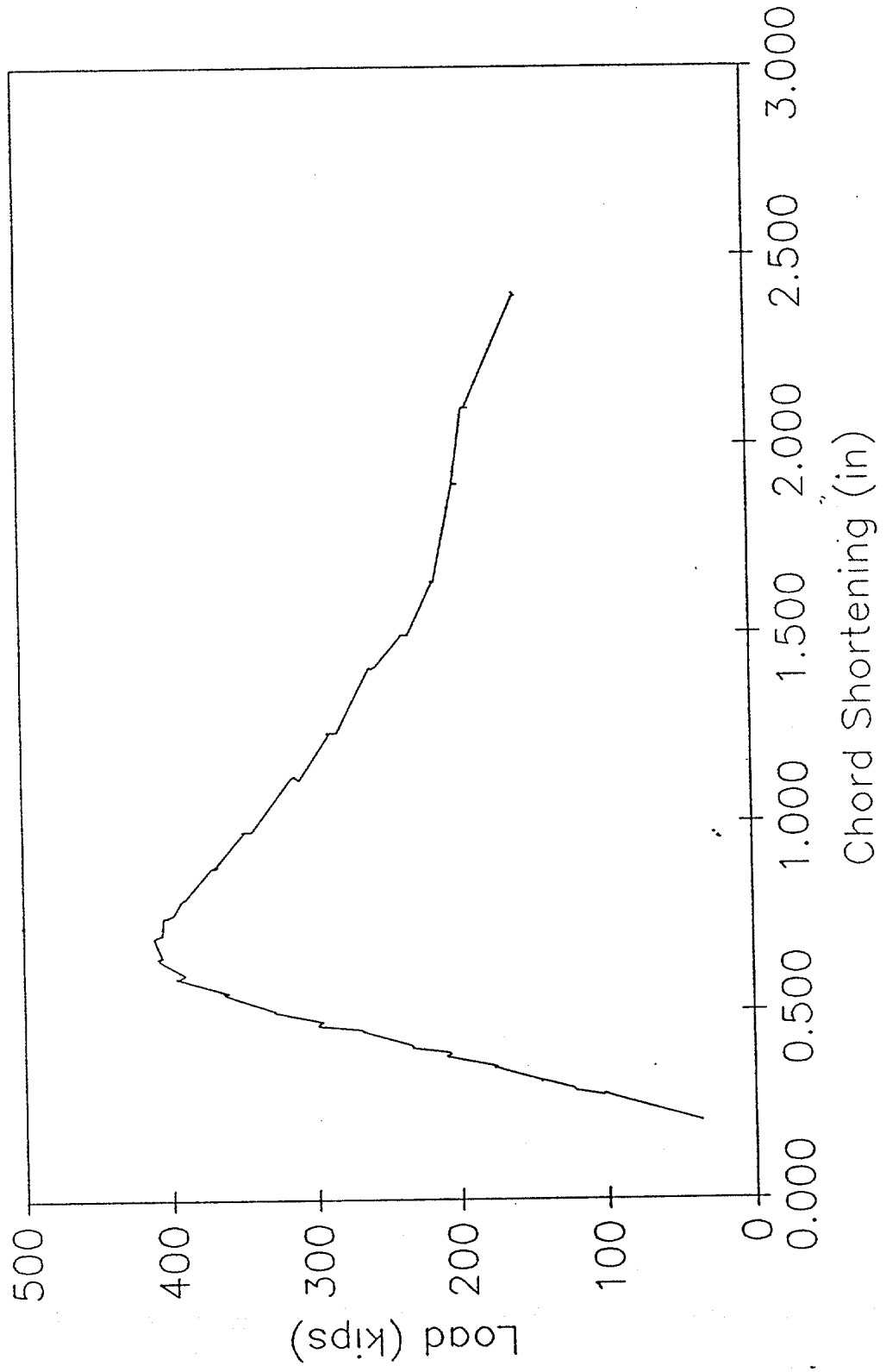


LOAD AND DEFLECTION vs LOAD STEP

Specimen 04

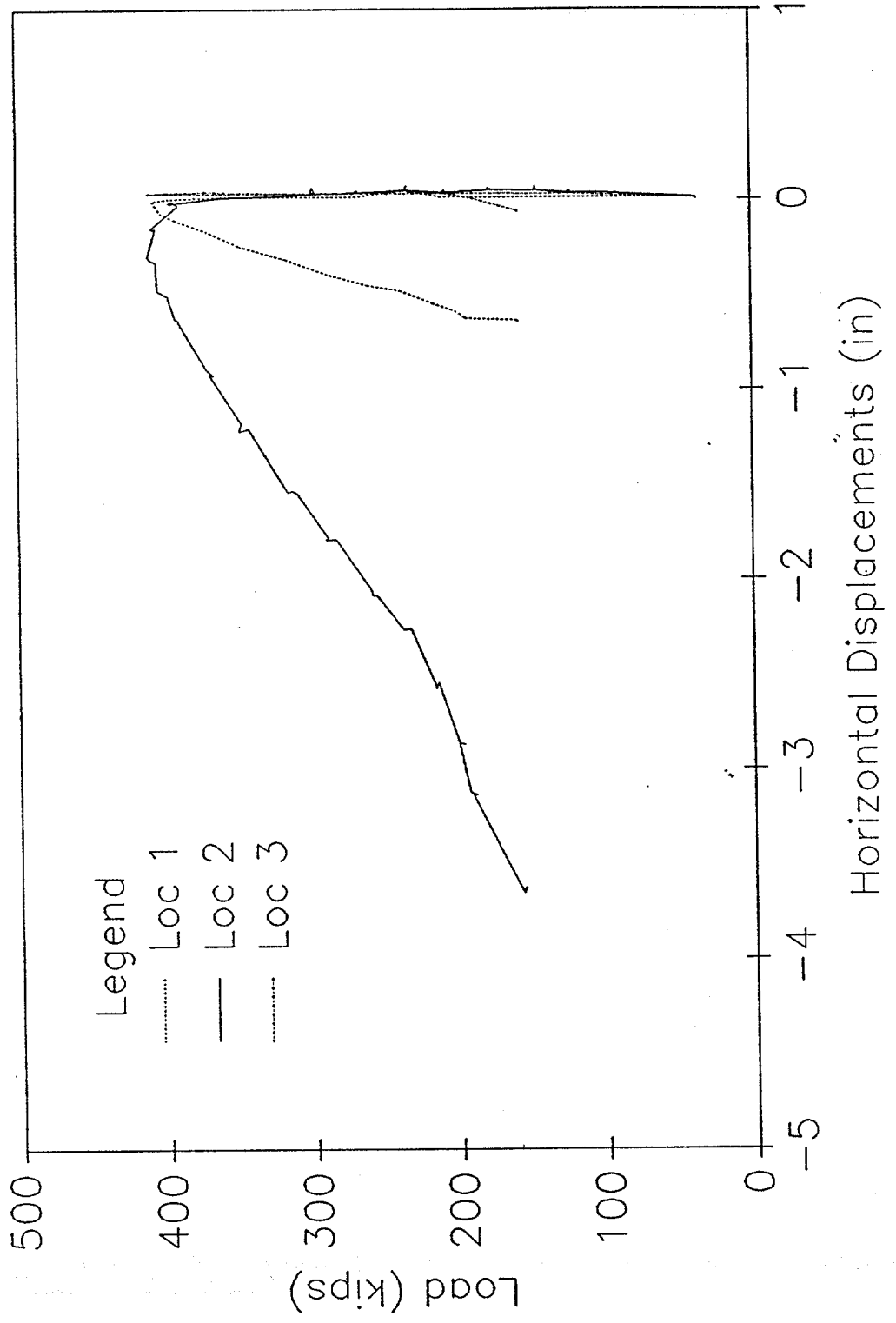


LOAD vs CHORD SHORTENING
Specimen 04



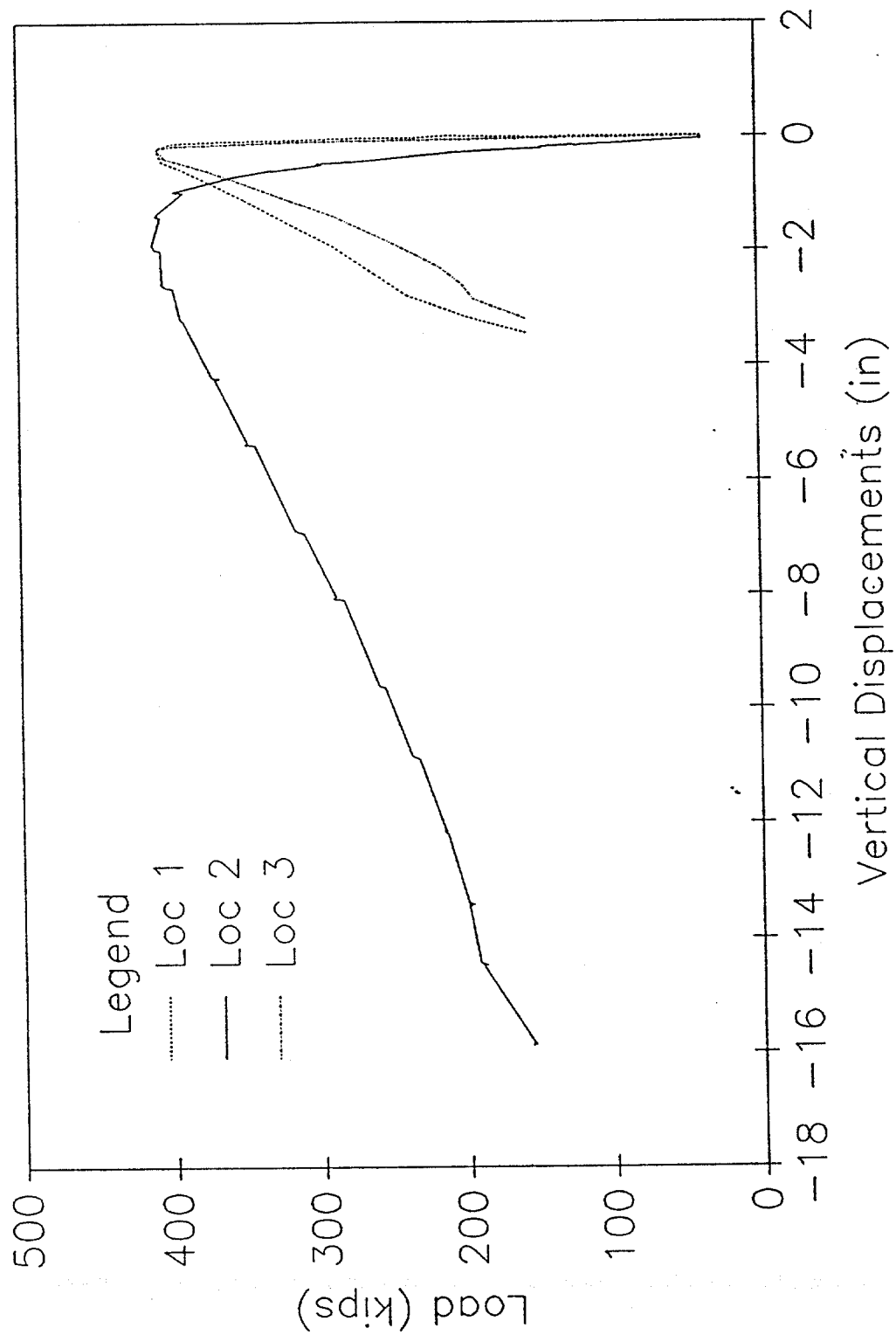
HORIZONTAL DISPLACEMENTS

Specimen 04



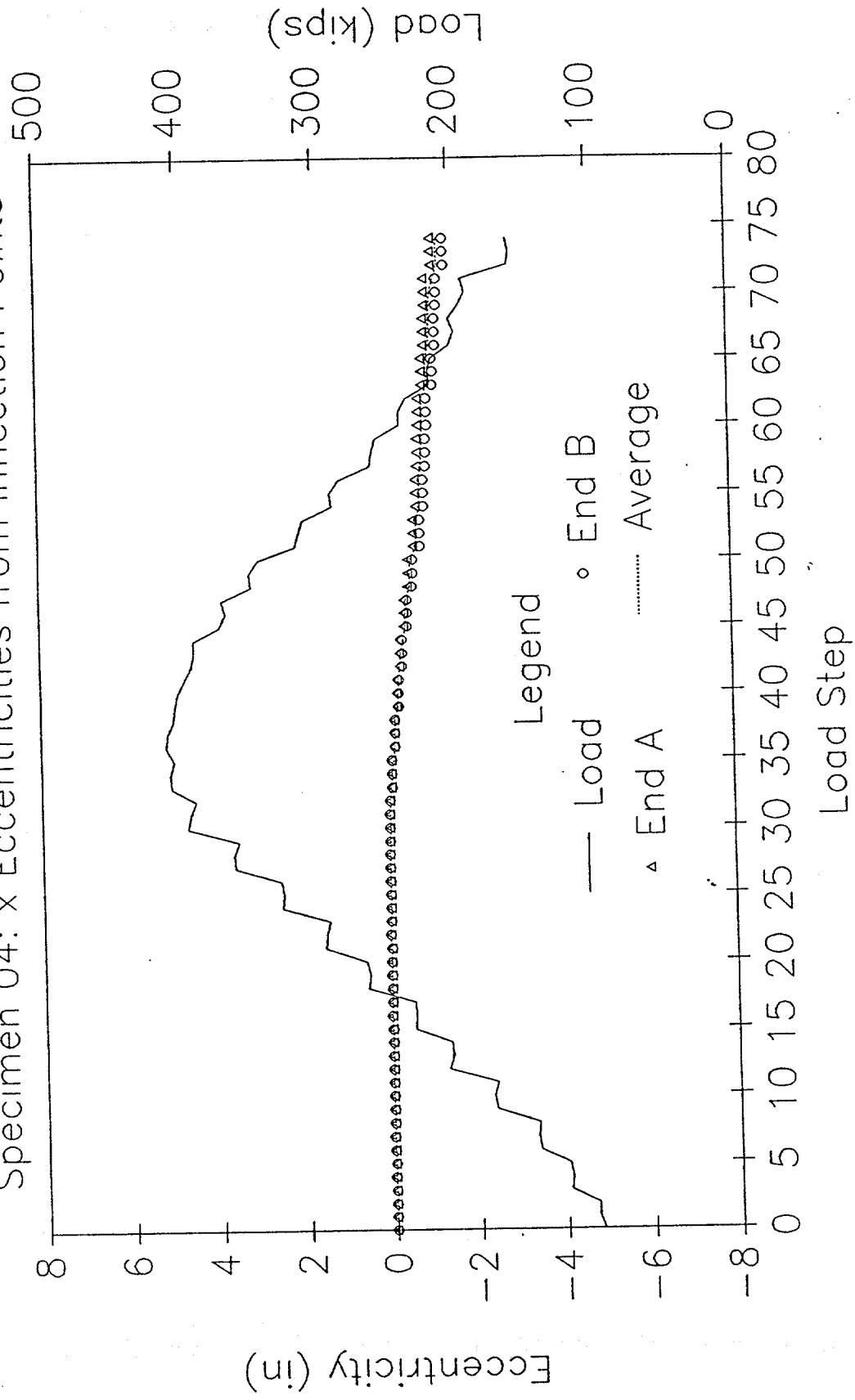
VERTICAL DISPLACEMENTS

Specimen 04



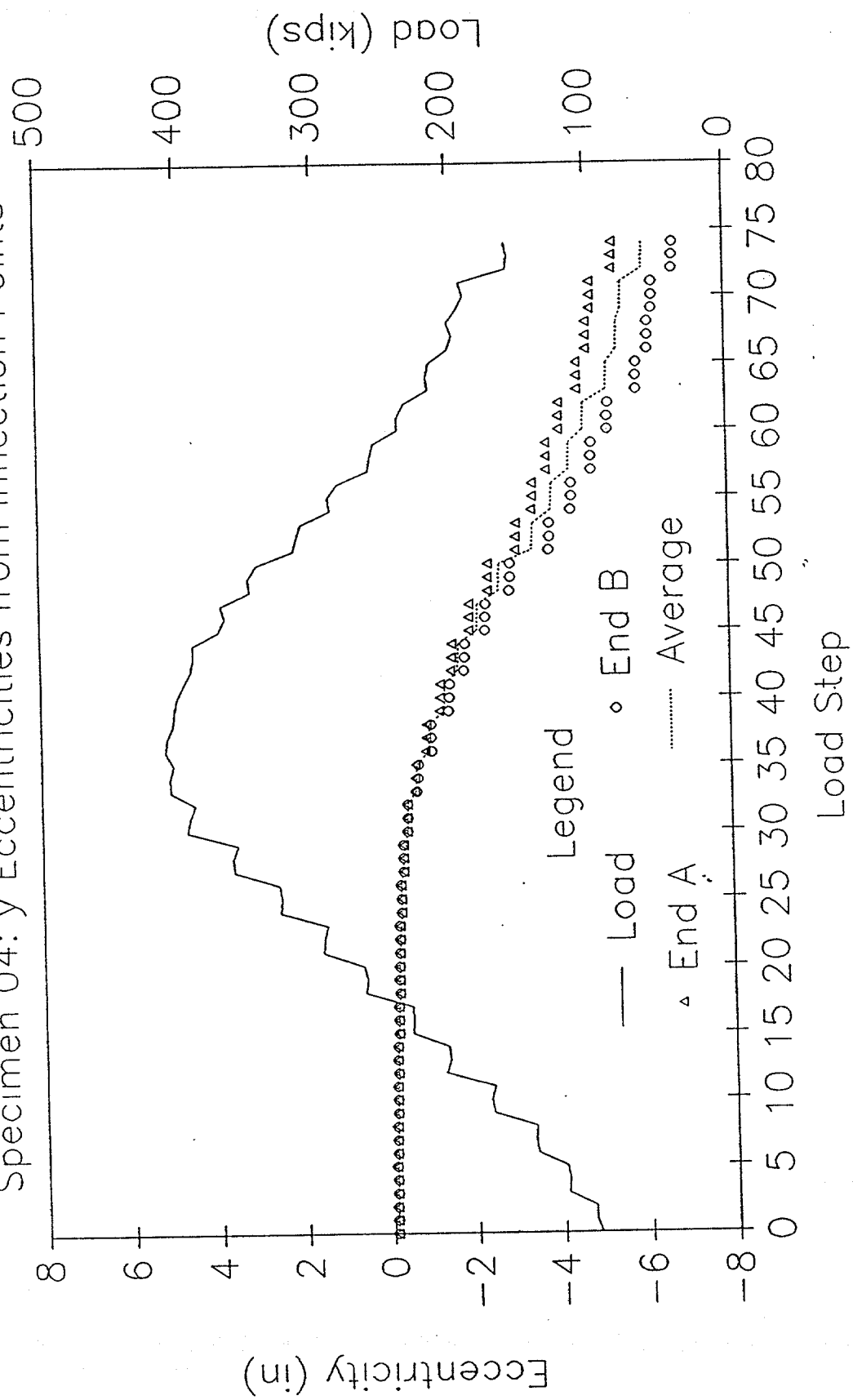
LOAD AND ECCENTRICITY vs LOAD STEP

Specimen 04: x Eccentricities from Inflection Points



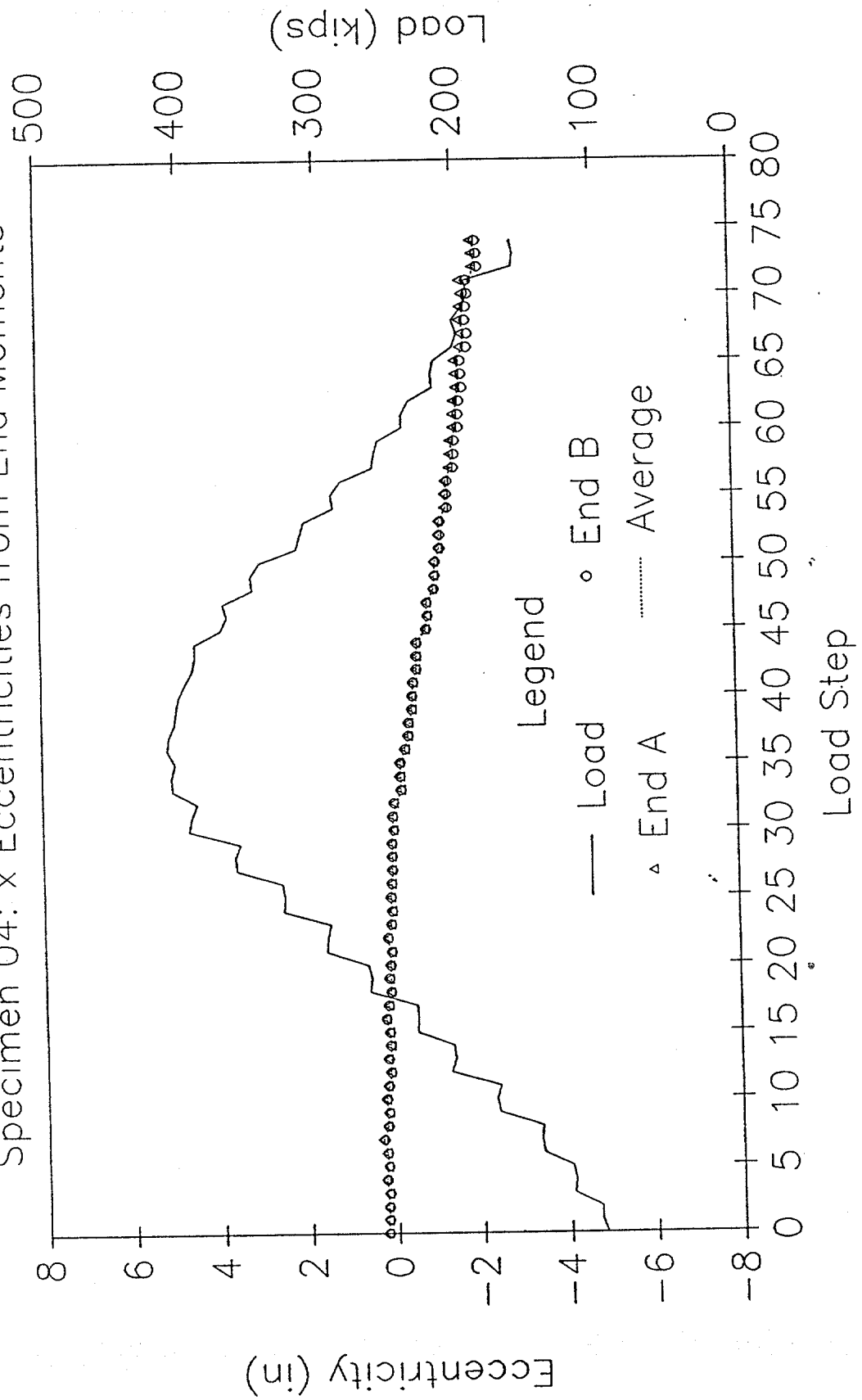
LOAD AND ECCENTRICITY vs LOAD STEP

Specimen 04: y Eccentricities from Inflection Points



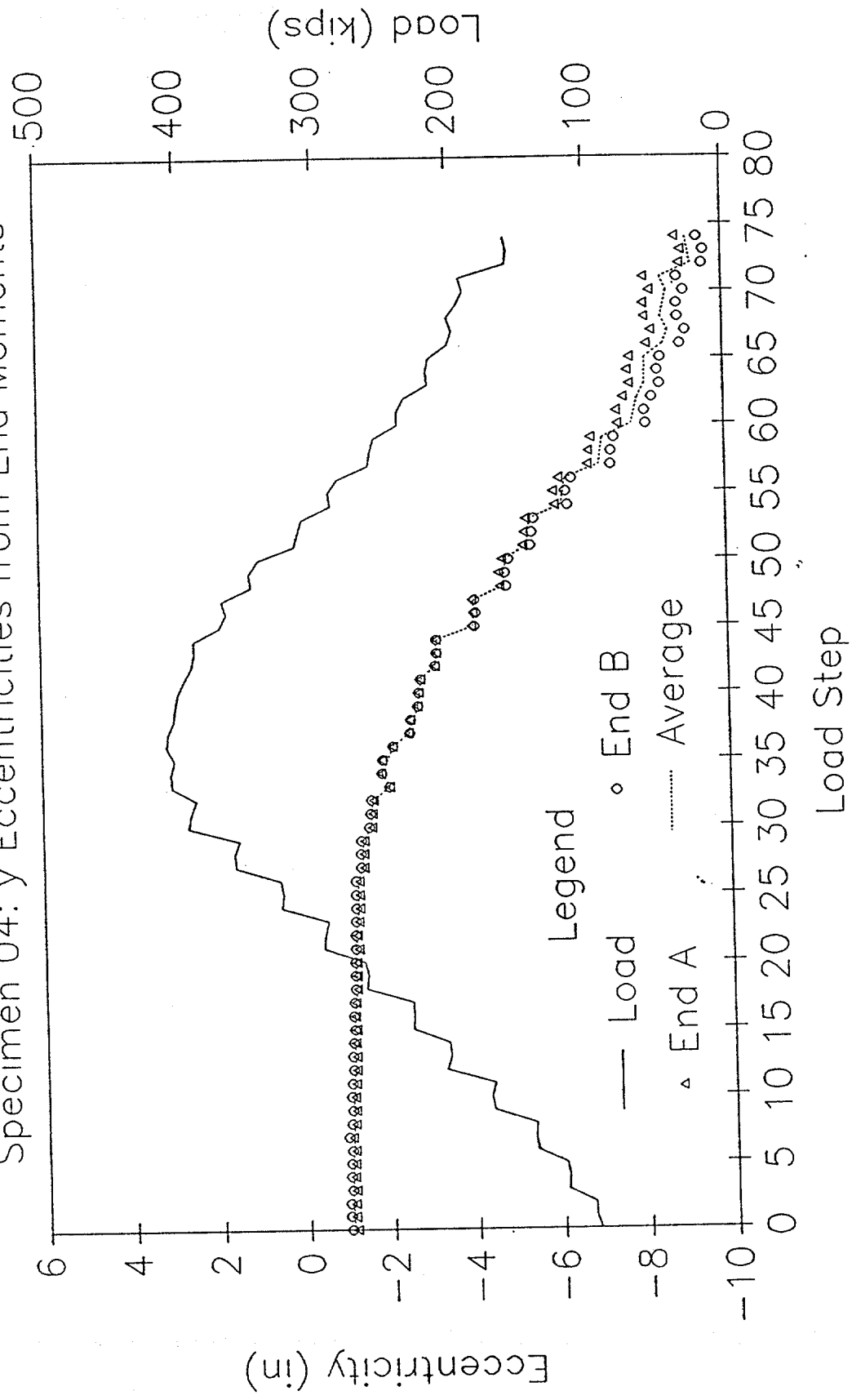
LOAD AND ECCENTRICITY vs LOAD STEP

Specimen 04: x Eccentricities from End Moments



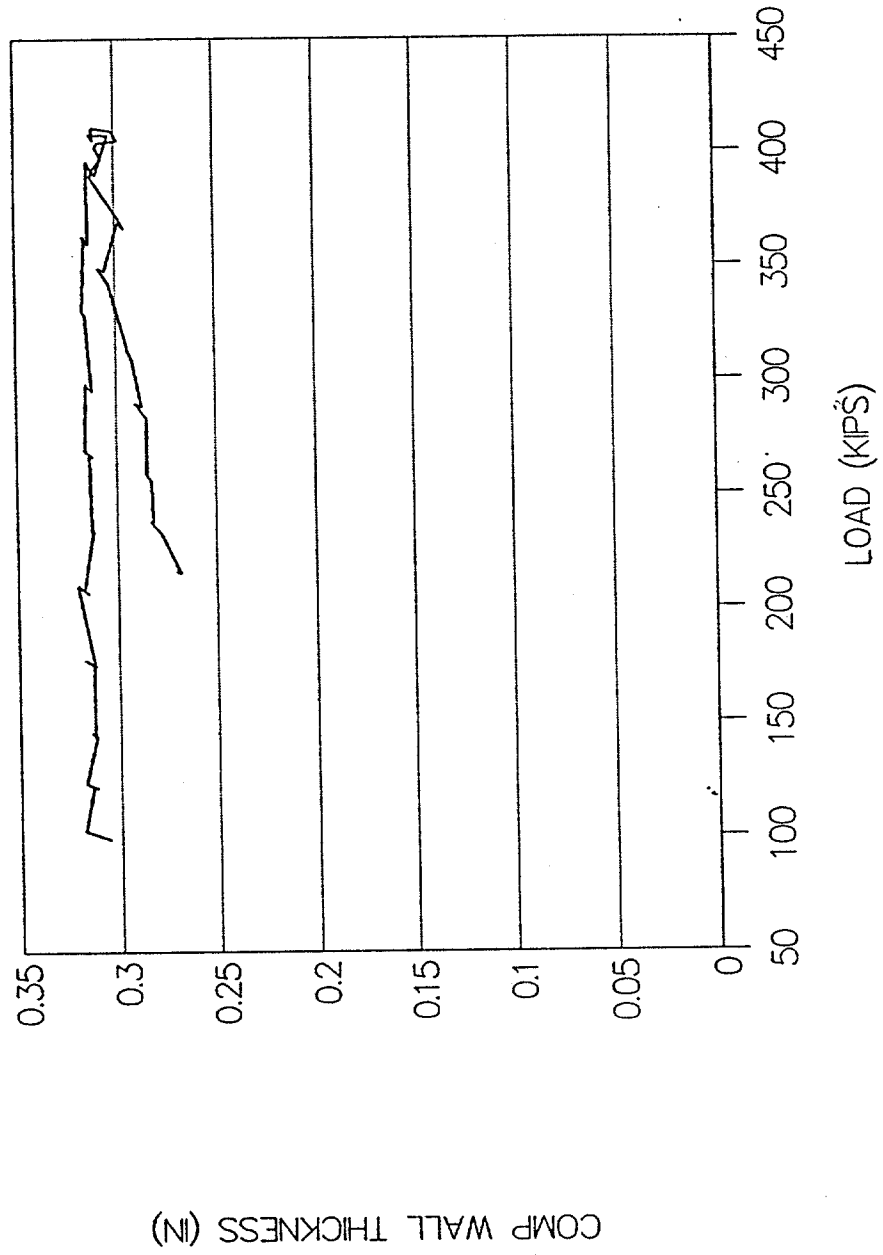
LOAD AND ECCENTRICITY vs LOAD STEP

Specimen 04: y Eccentricities from End Moments



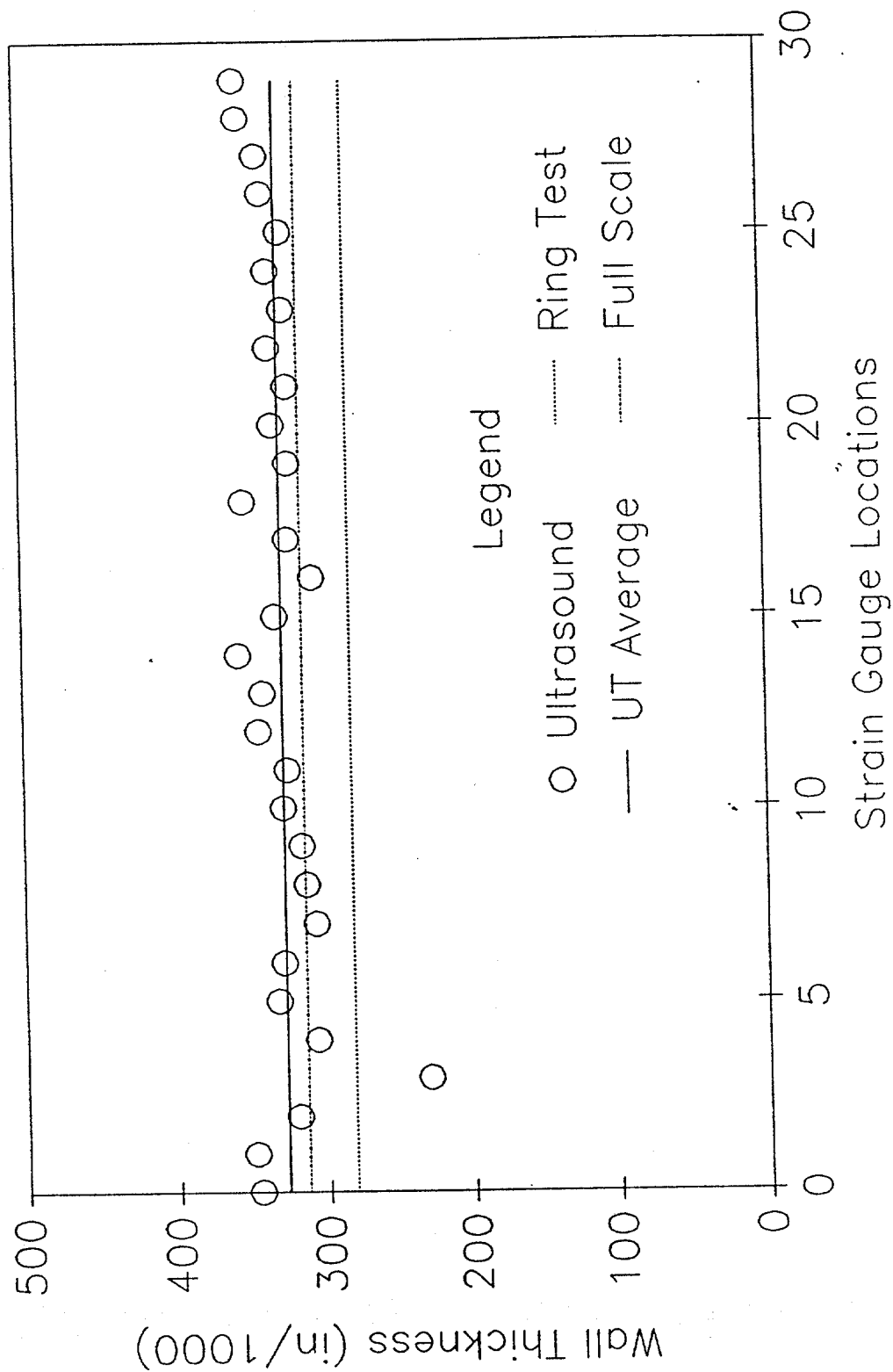
SPECIMEN 04--FULL SCALE TEST

COMPUTED WALL THICKNESS



SPECIMEN 04: WALL THICKNESS

Nominal Wall Thickness = 0.375 in



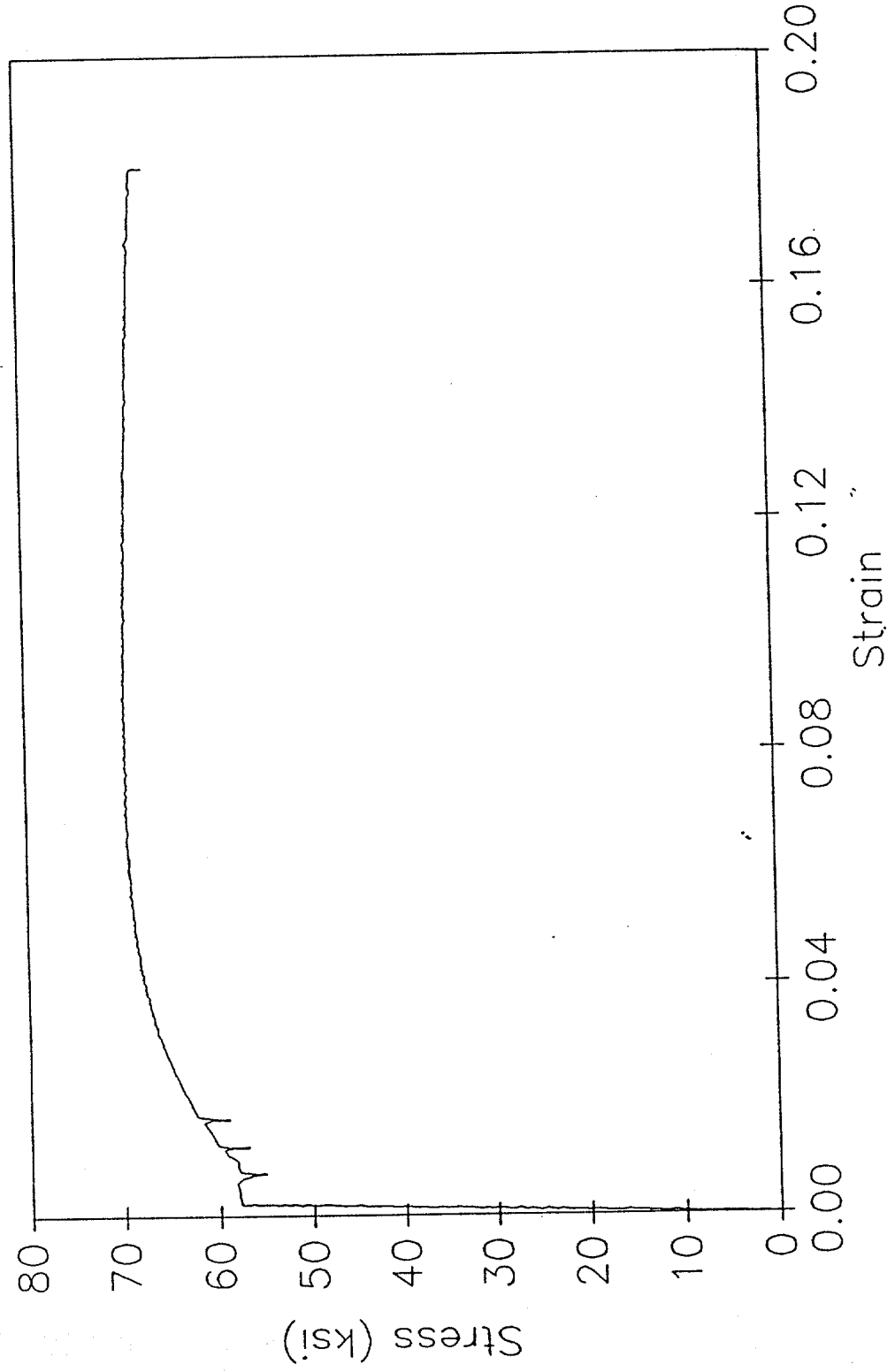
Ultrasound Data for Specimen 4

Gauge No.	UT Thickness	UT Average
0	0.346	
1	0.349	
2	0.320	
3	0.230	
4	0.307	
5	0.333	0.314
6	0.329	
7	0.307	
8	0.313	
9	0.316	
10	0.328	
11	0.325	0.320
12	0.344	
13	0.341	
14	0.357	
15	0.332	
16	0.307	
17	0.323	0.334
18	0.352	
19	0.322	
20	0.332	
21	0.322	
22	0.334	
23	0.324	0.331
24	0.334	
25	0.325	
26	0.337	
27	0.340	
28	0.352	
29	0.354	0.340

Overall Average = 0.328

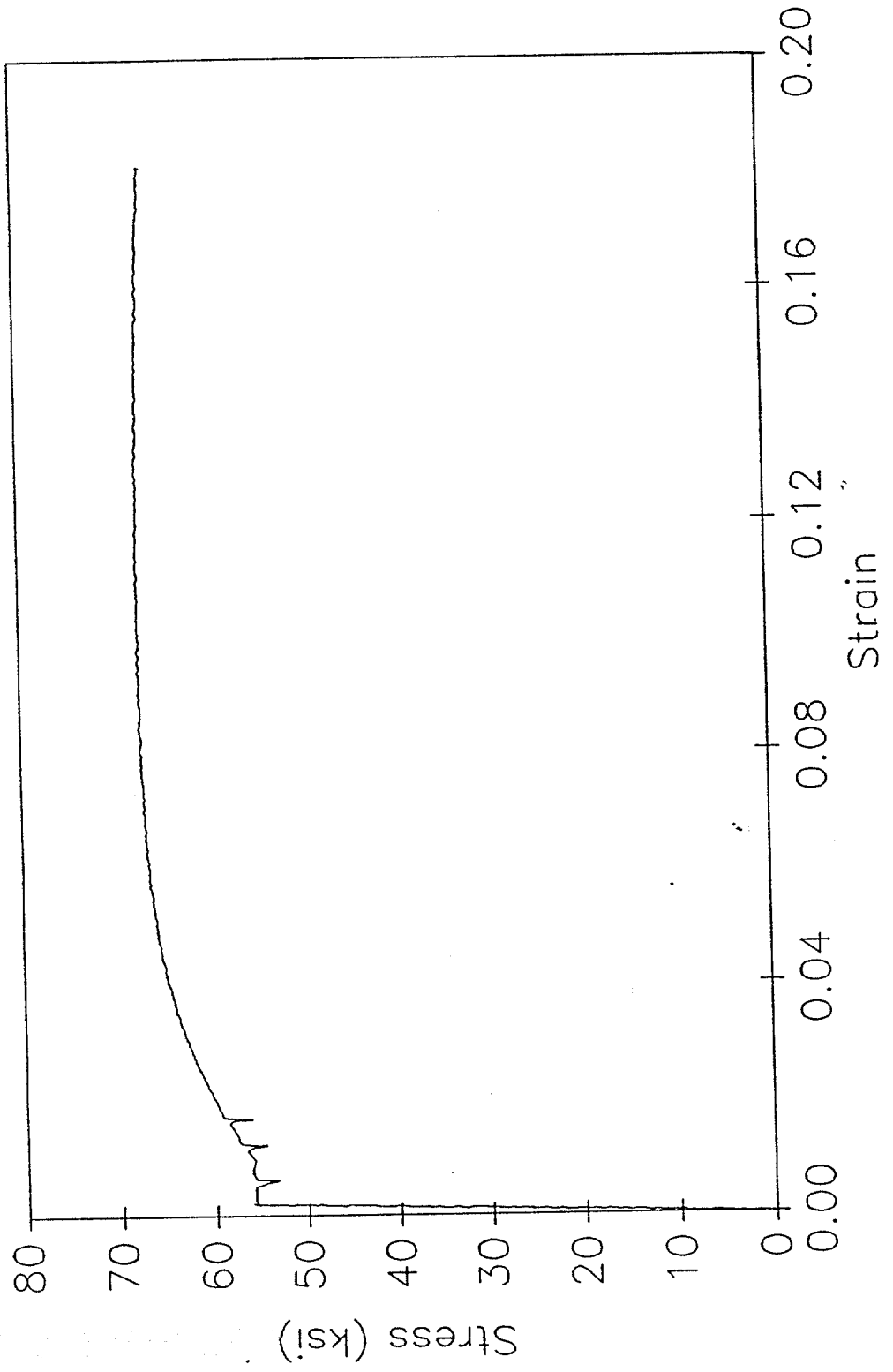
TENSILE SPECIMEN 4-1

Stress vs Strain



TENSILE SPECIMEN 4-2

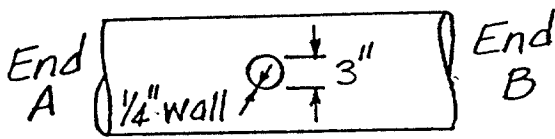
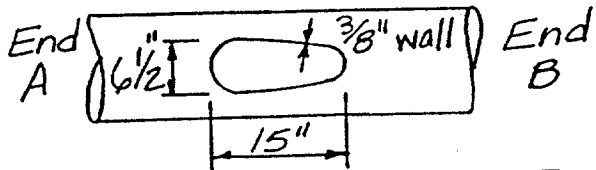
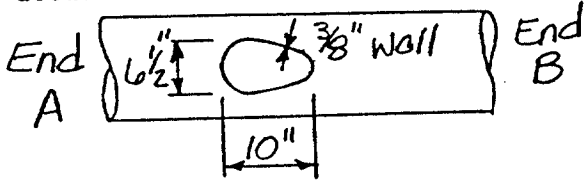
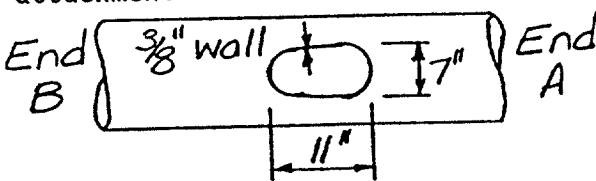
Stress vs Strain



SPECIMEN 05

DAMAGE SUMMARY

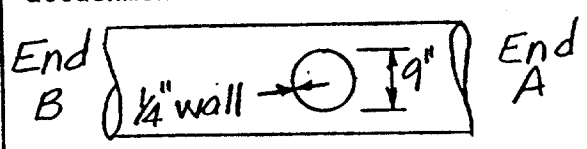
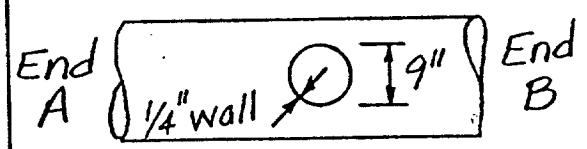
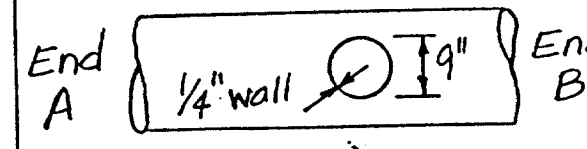
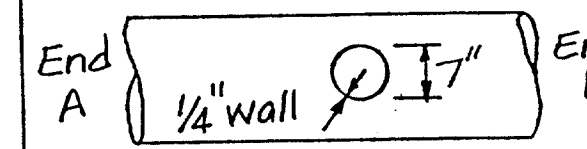
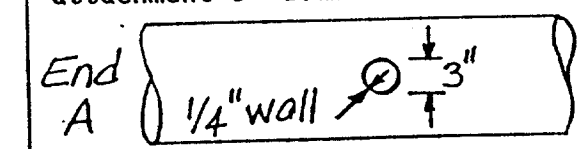
Specimen No. 5
2-21-90

DISTANCE FROM END "B"	*DISTANCE FROM CHALK LINE		DESCRIPTION OF DAMAGE
	LEFT	RIGHT	
1. From 0' to 2'-9 1/4"	2 3/4"		1/2" longitudinal weld From 1'-8" to 2'-4" the seam is split
2. 2"-9 1/2"			1/2" circumferential butt weld
3. 2'-9"	9 3/4"		Small corrosion hole
4. 1'-4 1/2"		16 1/2"	Cut-off, round welded attachment, 3" diameter 
5. 4'-1"		7"	Cut-off, oblong welded attachment 
6. 4'-5 1/2"		13 1/2"	Cut-off, oblong welded attachment 
7. 4'-6"	1 1/2"		Cut-off, oblong welded attachment 

*Looking from end "A" towards end "B"

DAMAGE SUMMARY

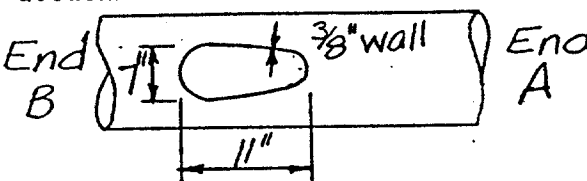
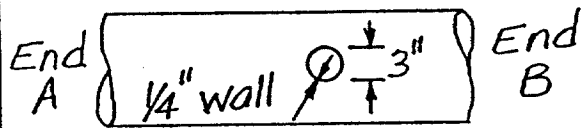
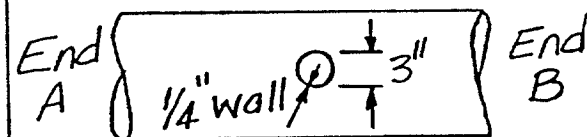
Specimen No. 5 (continued)

DISTANCE FROM END "B"	*DISTANCE FROM CHALK LINE LEFT	RIGHT	DESCRIPTION OF DAMAGE
8. 5'-7 1/4"	1 1/2"		Cut-off, round welded attachment 9" diameter End B  End A
9. 5'-7 1/4"		13"	Cut-off, round welded attachment 9" diameter End A  End B
10. 5'-7 1/4"		28"	Cut-off, round welded attachment 9" diameter with additional denting (See additional sheets) End A  End B
11. 6'-2 1/2"		5 3/4"	Cut-off, round welded attachment 7" diameter End A  End B
12. 6'-6"		16 3/4"	Cut-off, round welded attachment 3" diameter End A  End B

*Looking from end "A" towards end "B"

DAMAGE SUMMARY

Specimen No. 5 (continued)

DISTANCE FROM END "B"	*DISTANCE FROM CHALK LINE		DESCRIPTION OF DAMAGE
	LEFT	RIGHT	
13. 6'-11"	1 1/2"		Cut-off, oblong welded attachment 
14. From 2'-9 3/4" to 14'-9 1/2"		17"	1/2" longitudinal weld
15. 12'-8 1/4"		17"	Cut-off, round welded attachment 3" diameter 
16. 14'-9 3/4"			1/2" circumferential butt weld
17. From 14'-10" to 18'-6 1/4"	11 1/2"		1/2" longitudinal weld
18. 17'-9 1/2"		16 3/4"	Cut-off, round welded attachment 3" diameter 

* Looking from end "A" towards end "B"

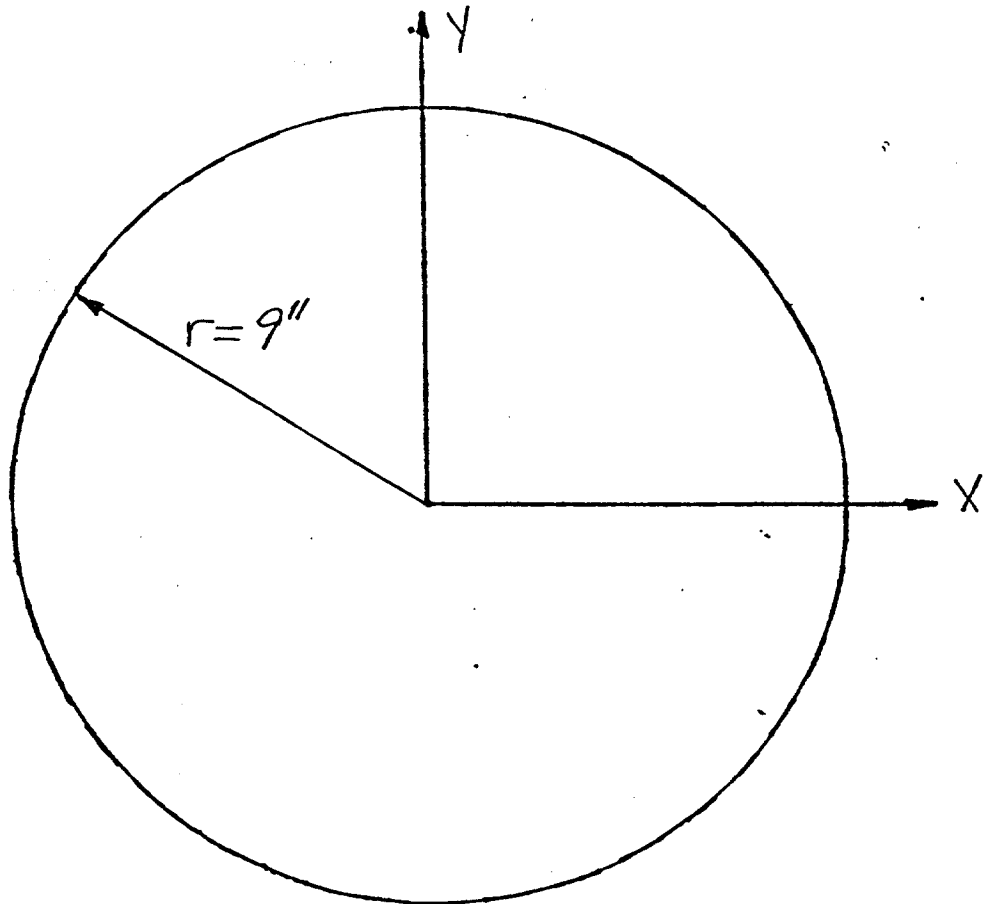
DENT CROSS SECTION

Specimen No. 5

Damage No. 10

Distance from End B 5'-2"

Scale 1"=4.24"



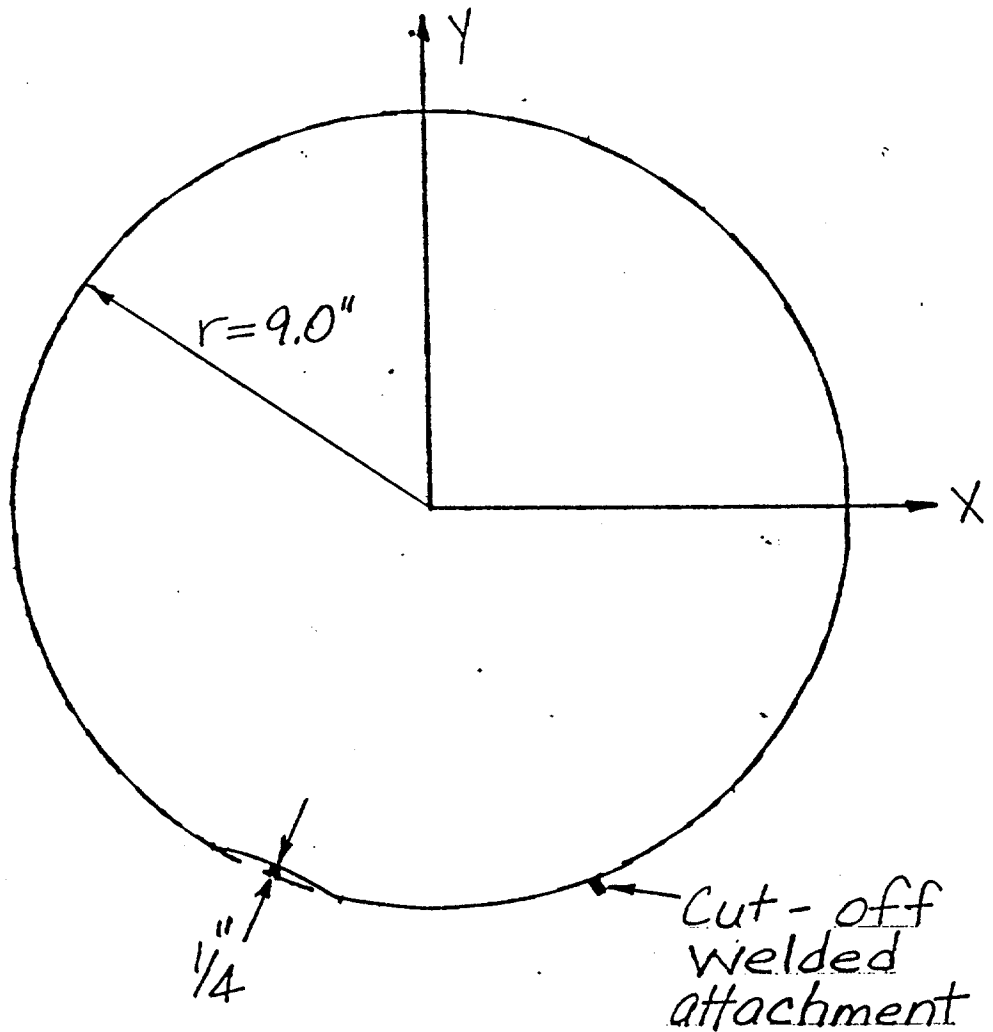
DENT CROSS SECTION

Specimen No. 5

Damage No. 10

Distance from End B 5'-4"

Scale 1" = 4.24"



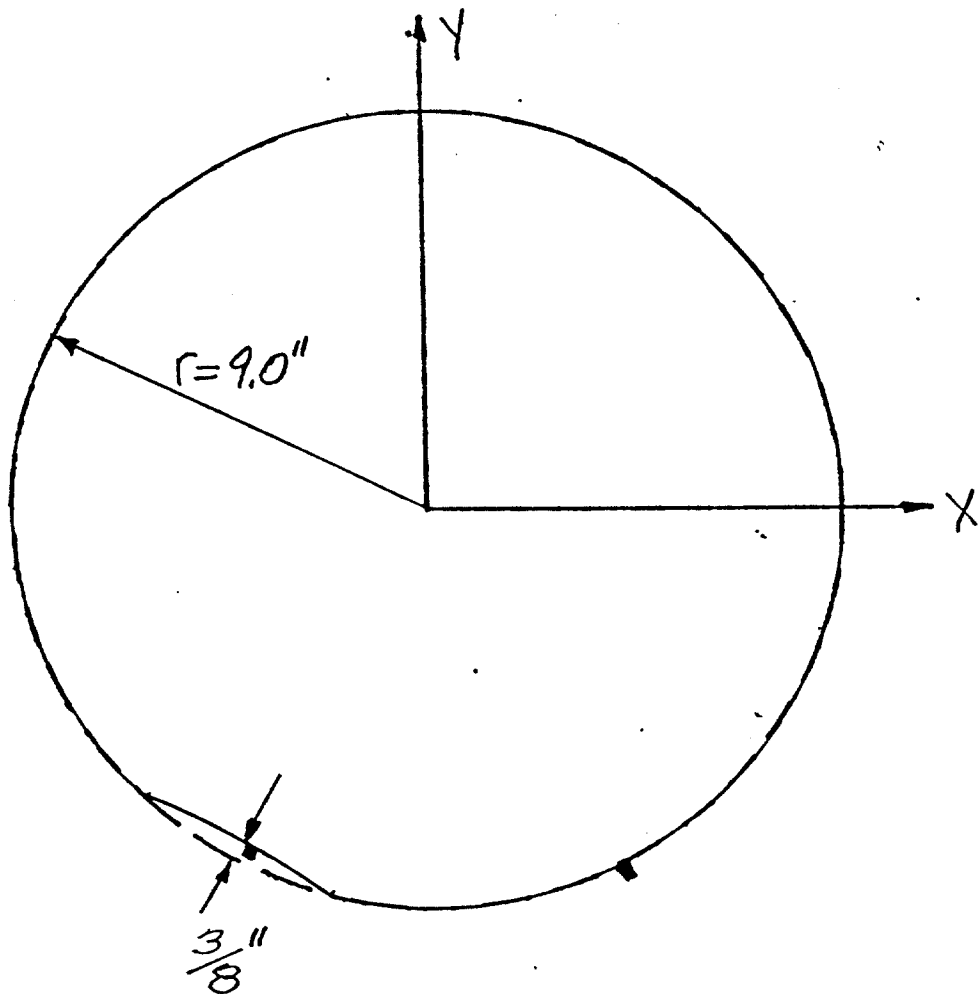
DENT CROSS SECTION

Specimen No. 5

Damage No. 10

Distance from End B 5'-6"

Scale 1" = 4.24"



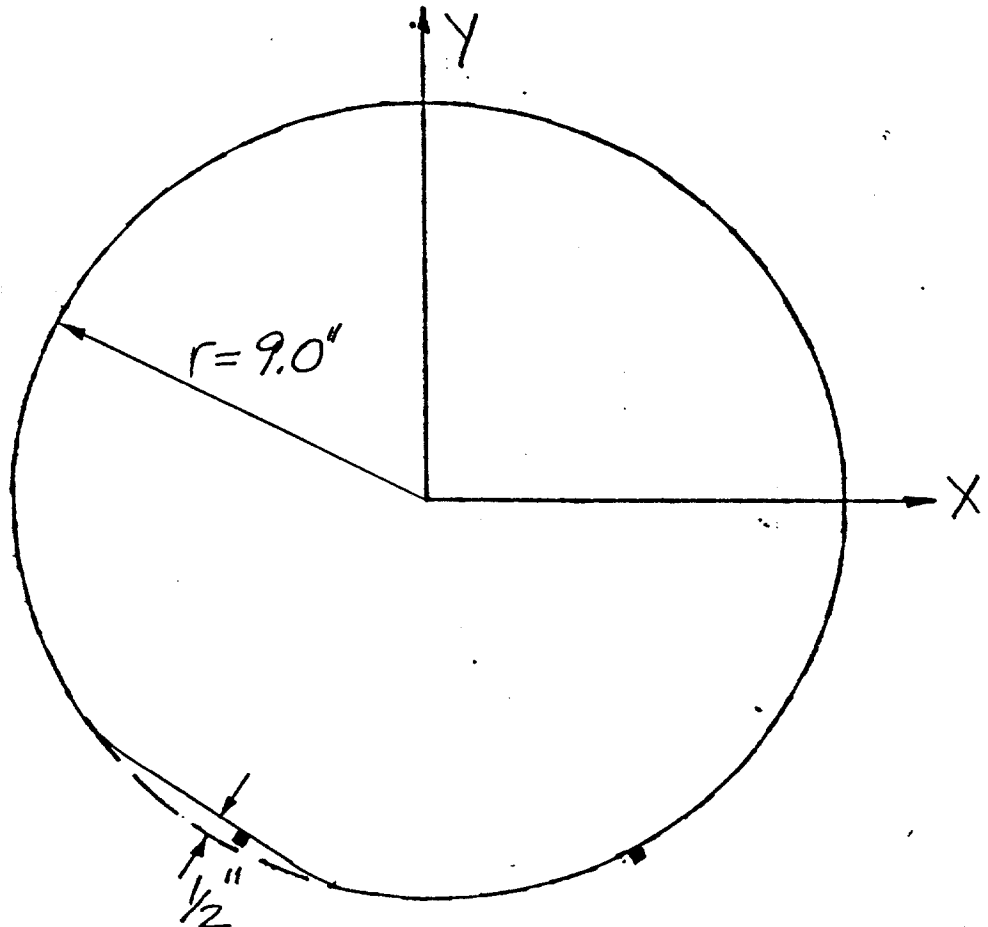
DENT CROSS SECTION

Specimen No. 5

Damage No. 10

Distance from End B 5'-7"

Scale 1"=4.24"



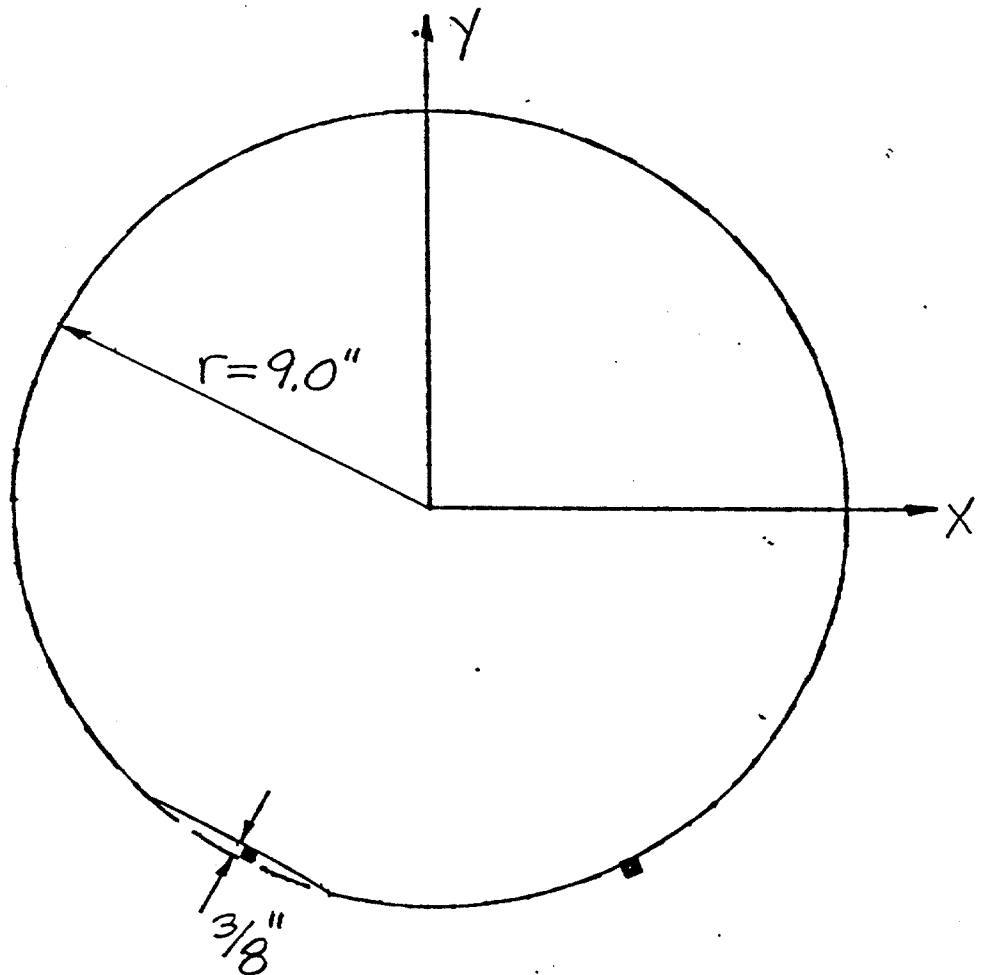
DENT CROSS SECTION

Specimen No. 5

Damage No. 10

Distance from End B 5'-8"

Scale 1" = 4.24"



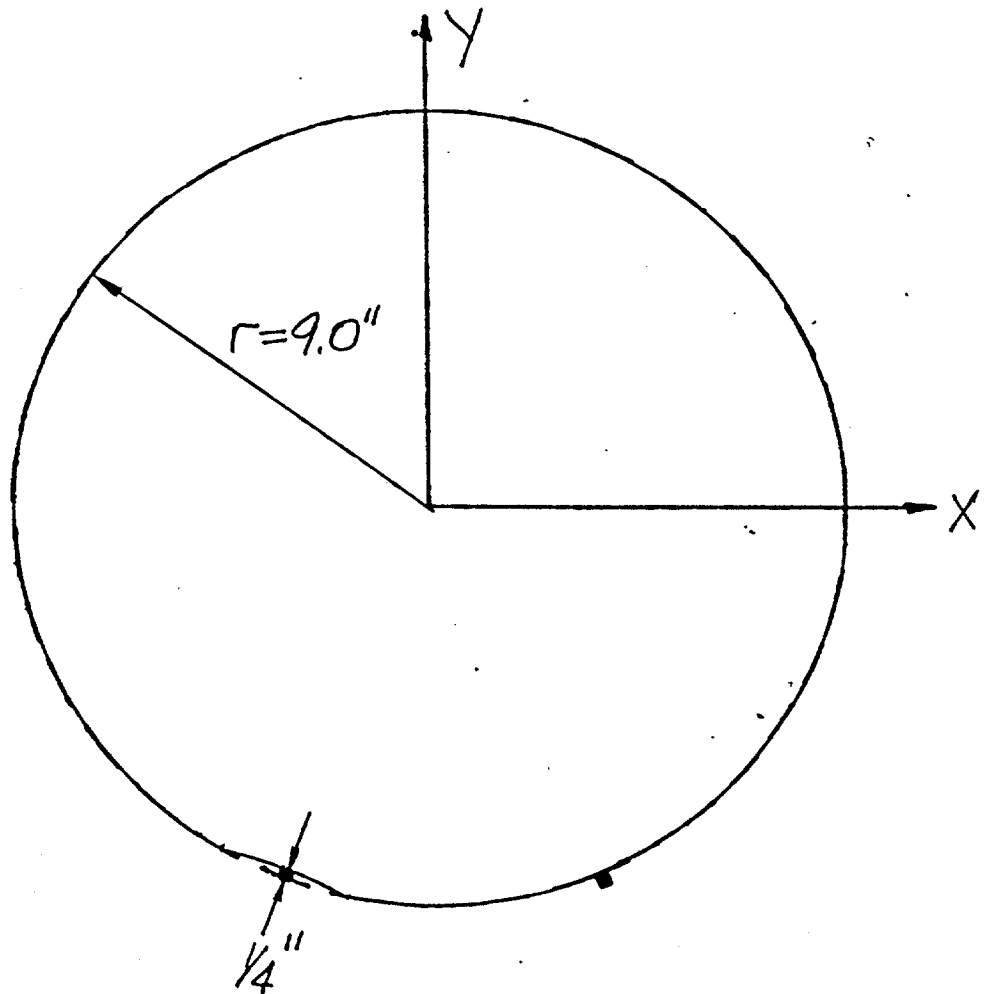
DENT CROSS SECTION

Specimen No. 5

Damage No. 10

Distance from End B 5'-10"

Scale 1" = 4.24"



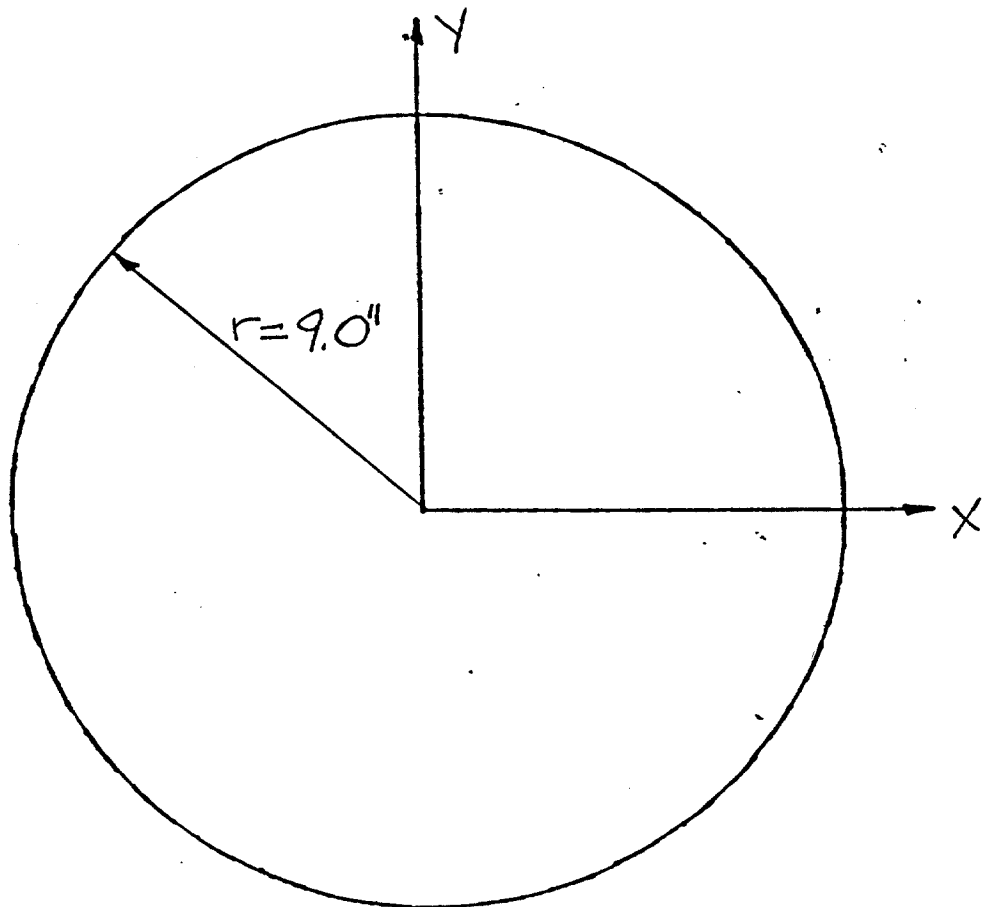
DENT CROSS SECTION

Specimen No. 5

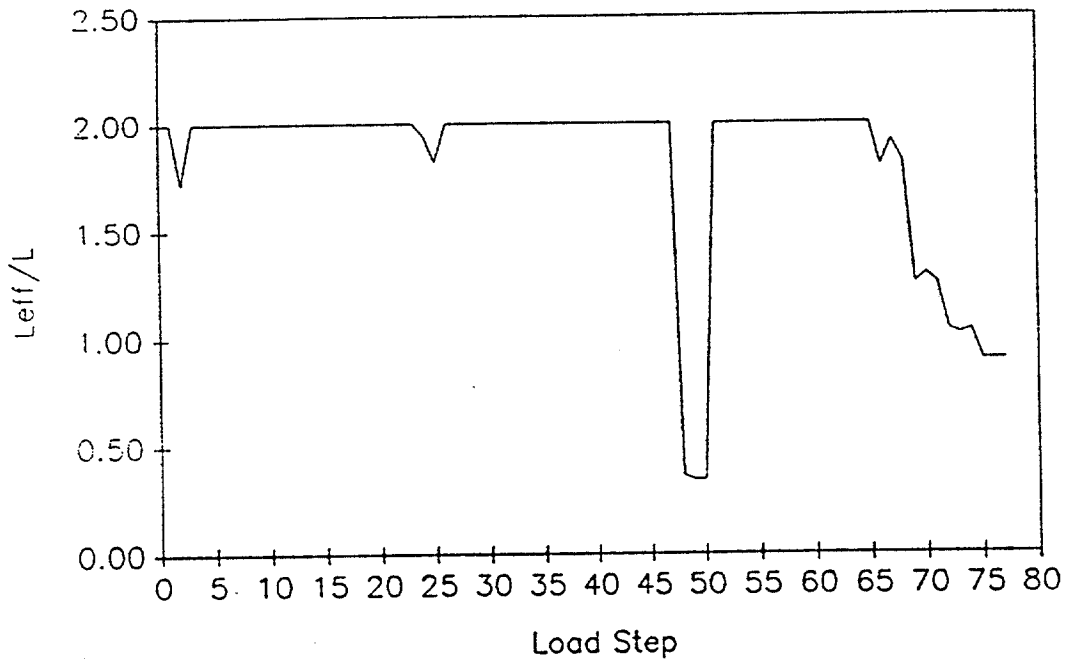
Damage No. 10

Distance from End B 6'-0"

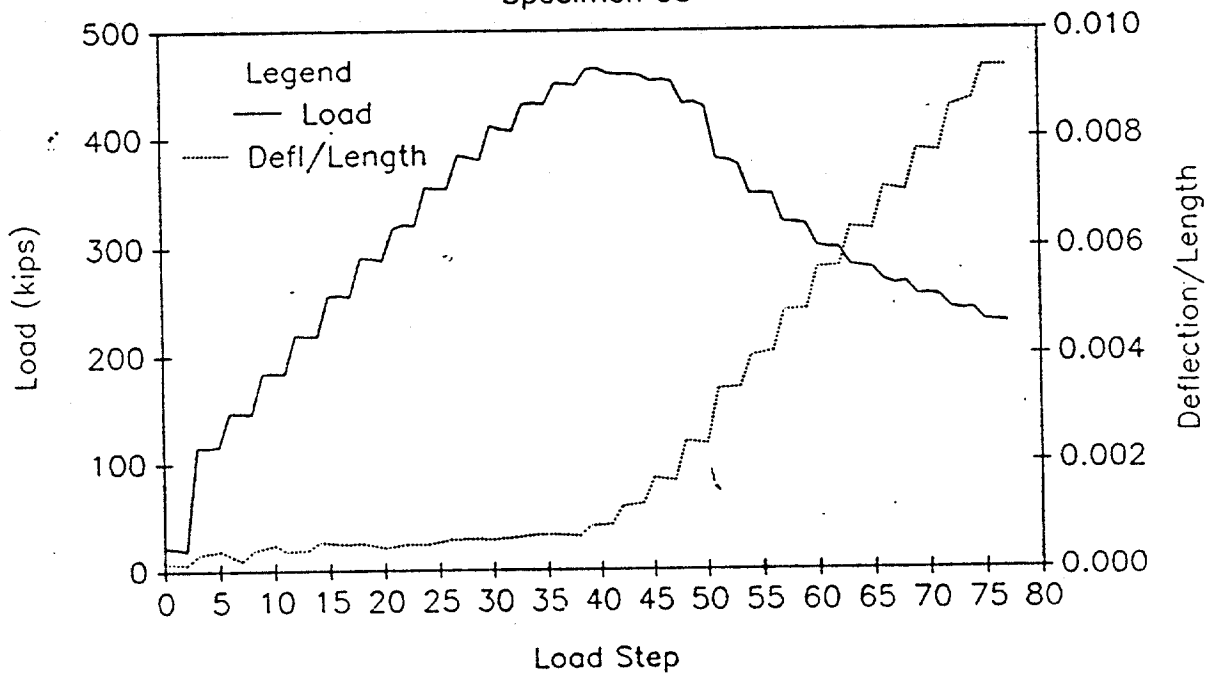
Scale 1"=4.24"



EFFECTIVE LENGTH vs LOAD STEP
Specimen 05

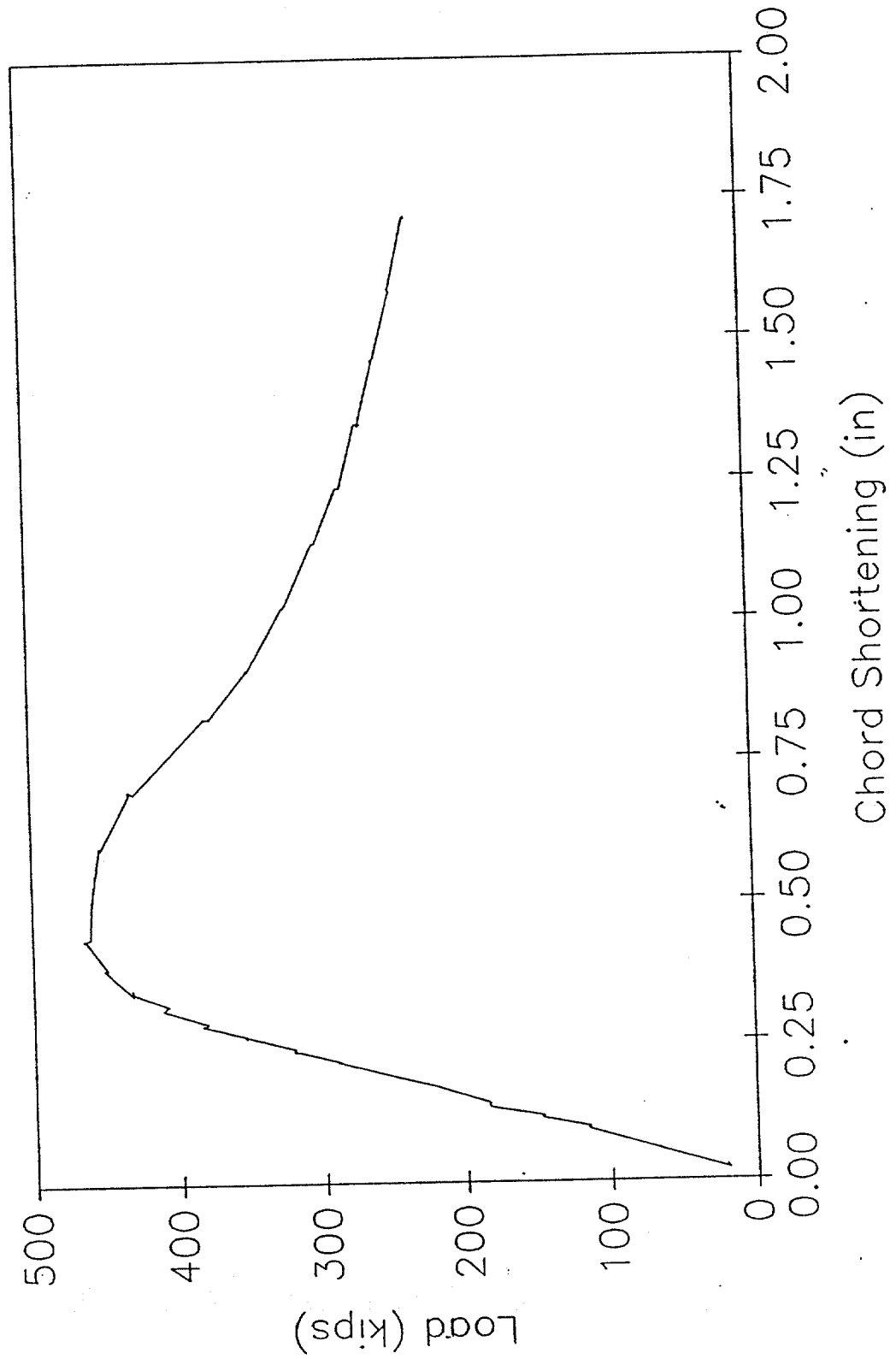


LOAD AND DEFLECTION vs LOAD STEP
Specimen 05



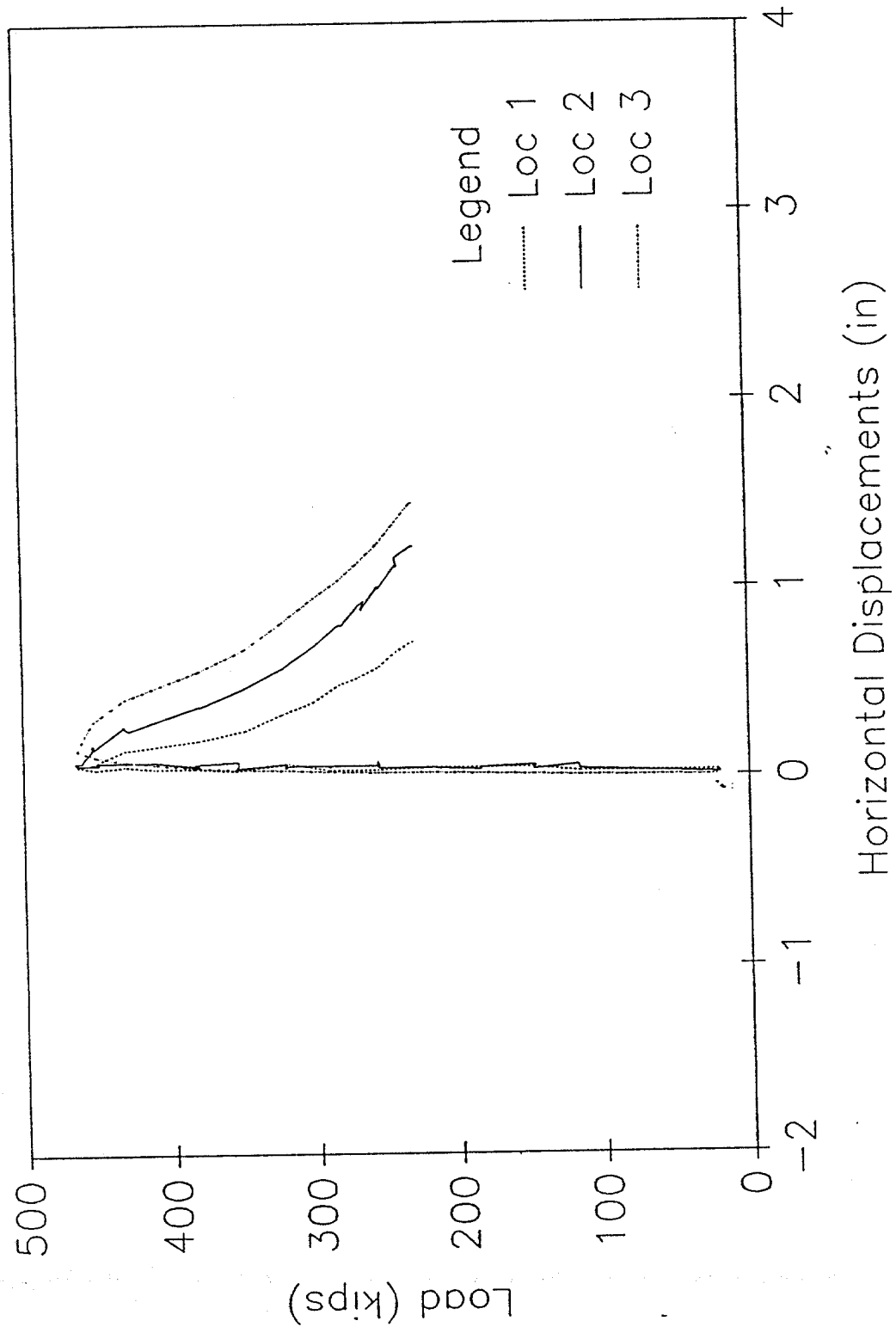
LOAD vs CHORD SHORTENING

Specimen 05



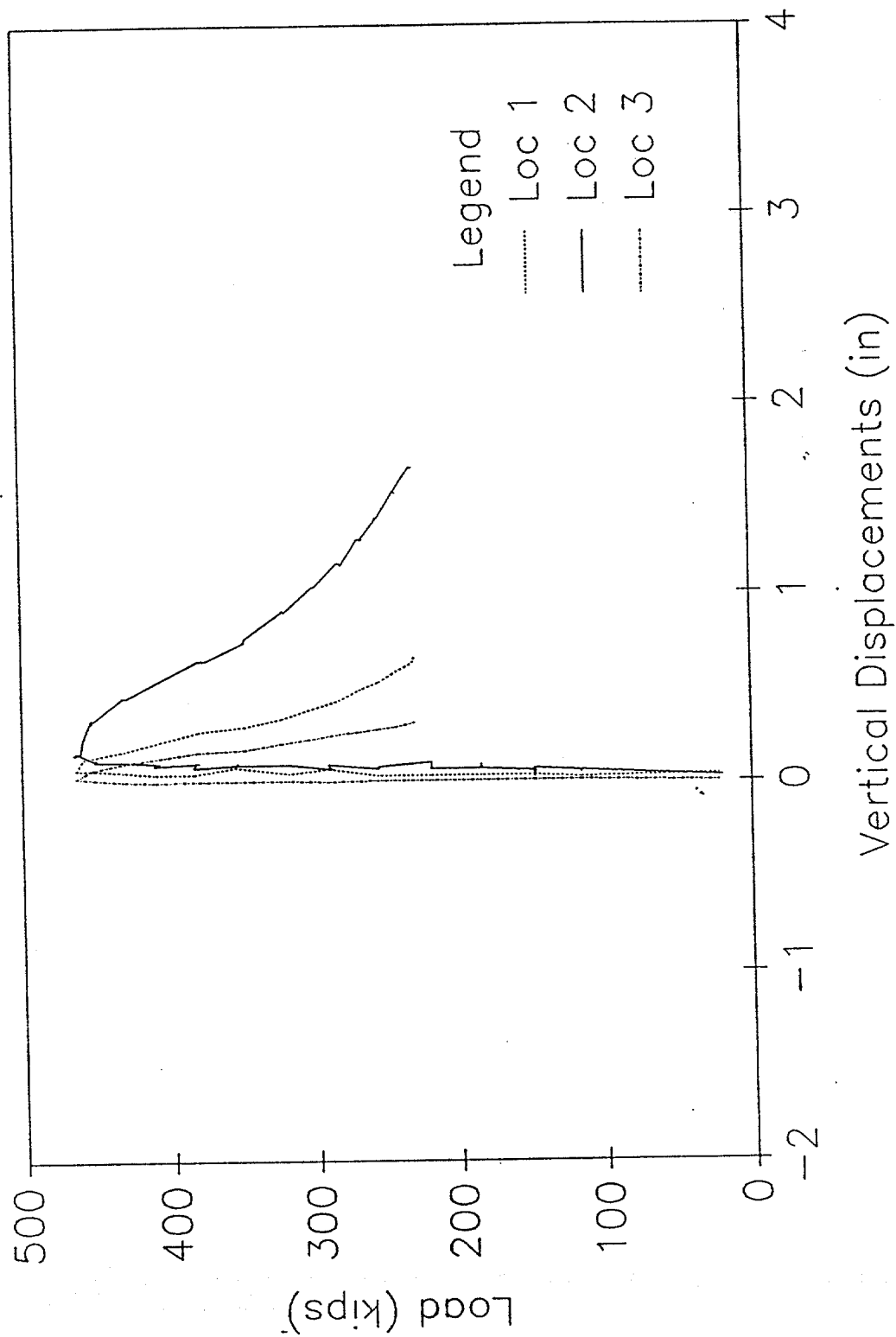
HORIZONTAL DISPLACEMENTS

Specimen 05



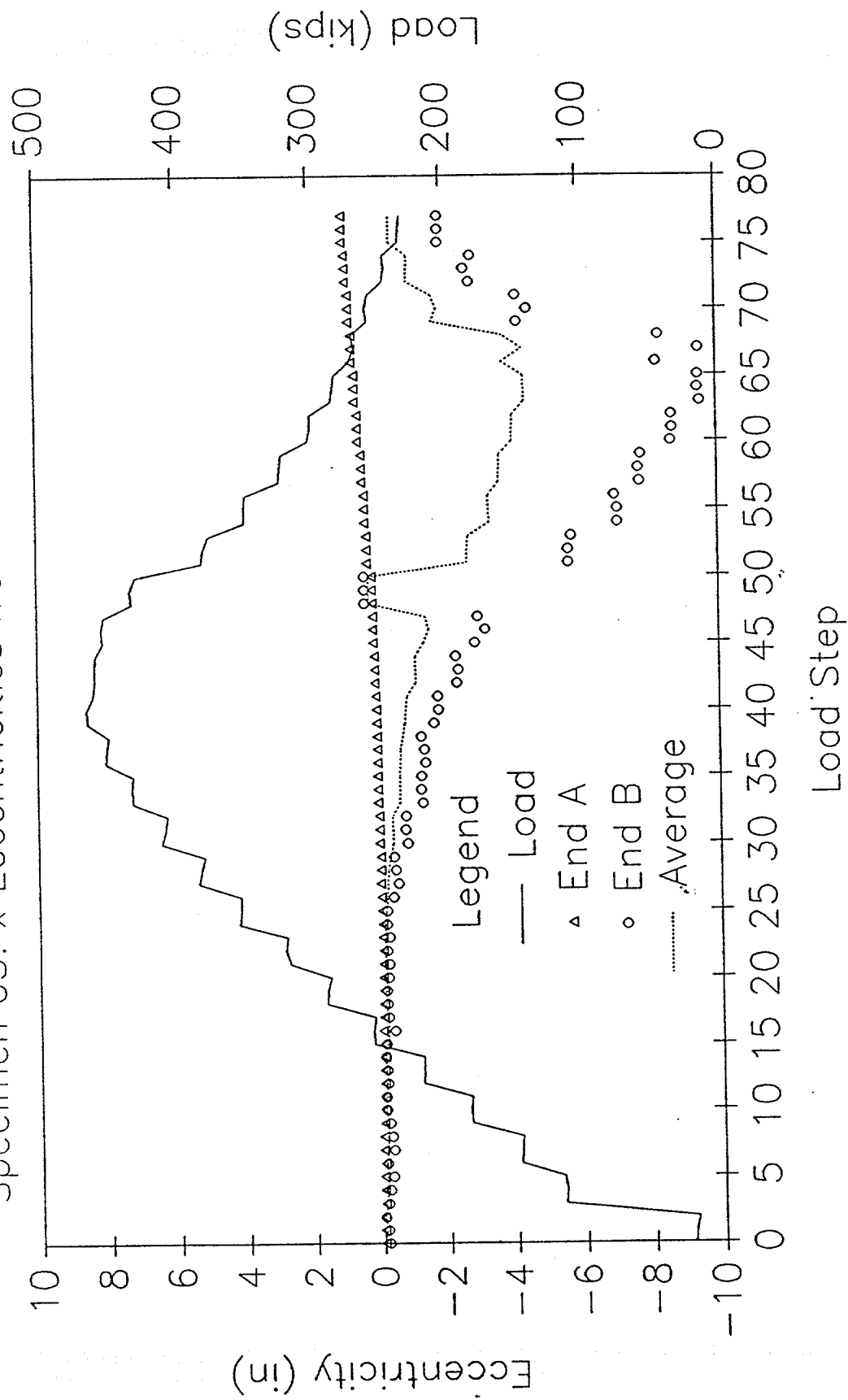
VERTICAL DISPLACEMENTS

Specimen 05



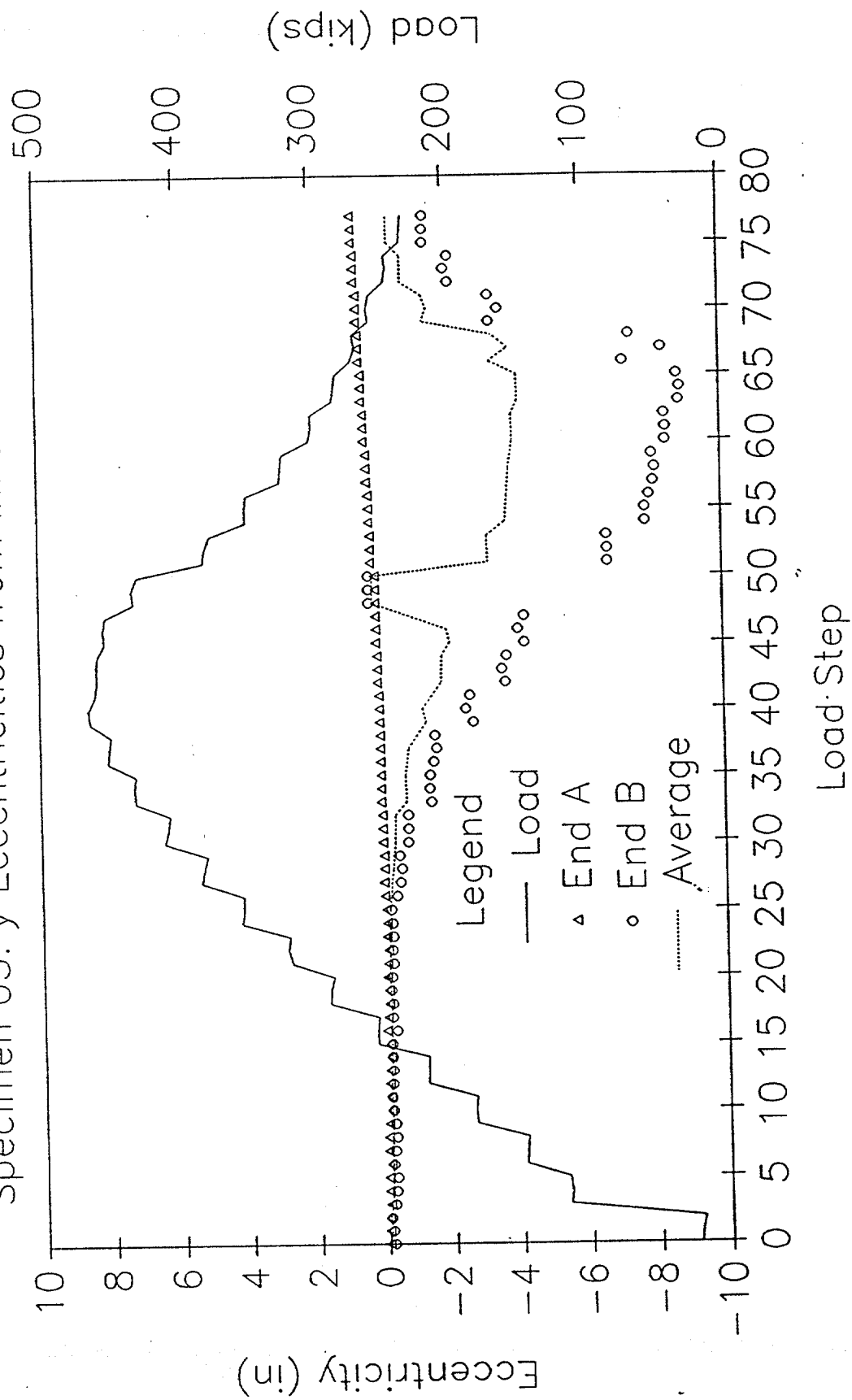
LOAD AND ECCENTRICITY vs LOAD STEP

Specimen 05: x Eccentricities from Inflection Points



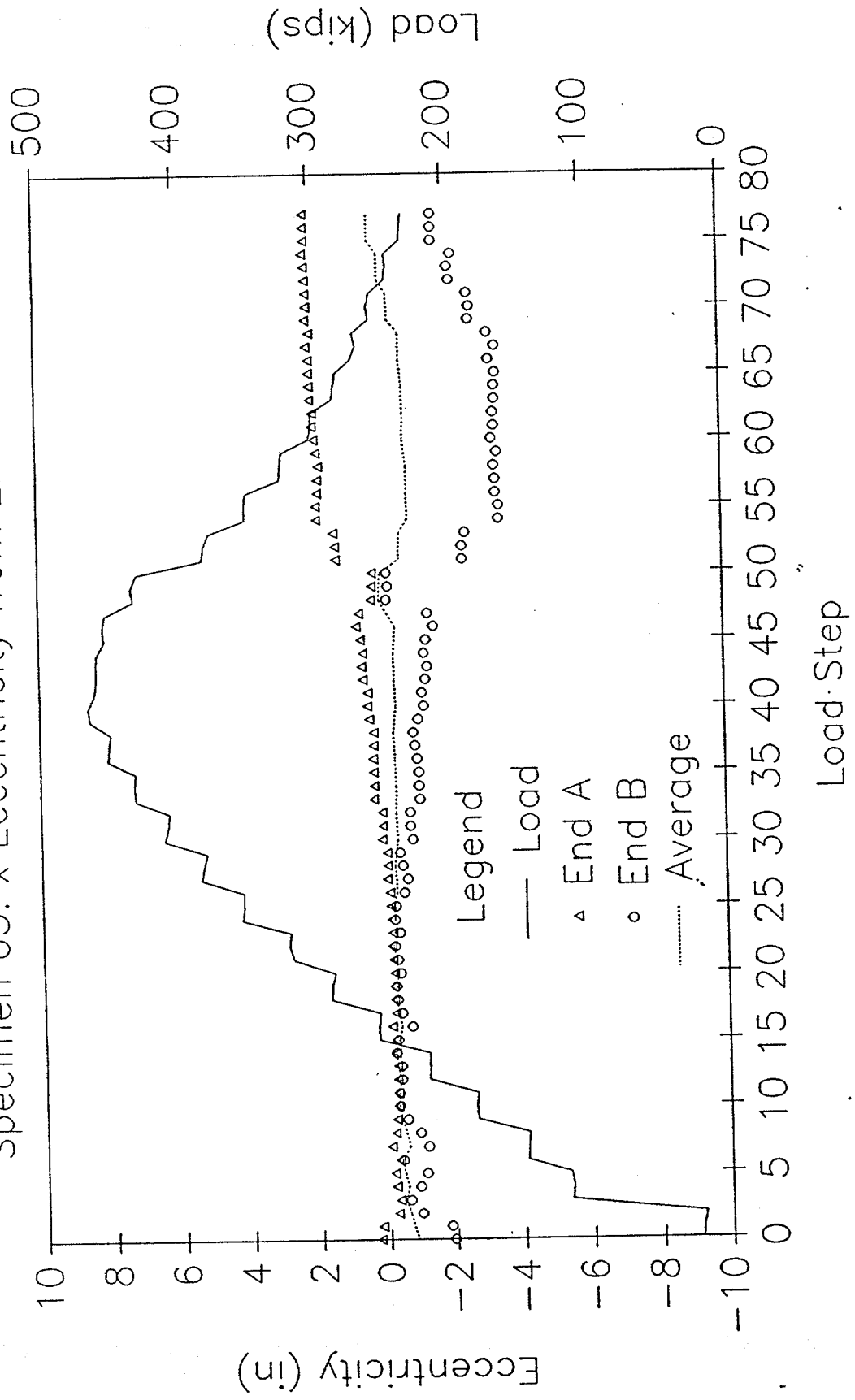
LOAD AND ECCENTRICITY vs LOAD STEP

Specimen 05: y Eccentricities from Inflection Points



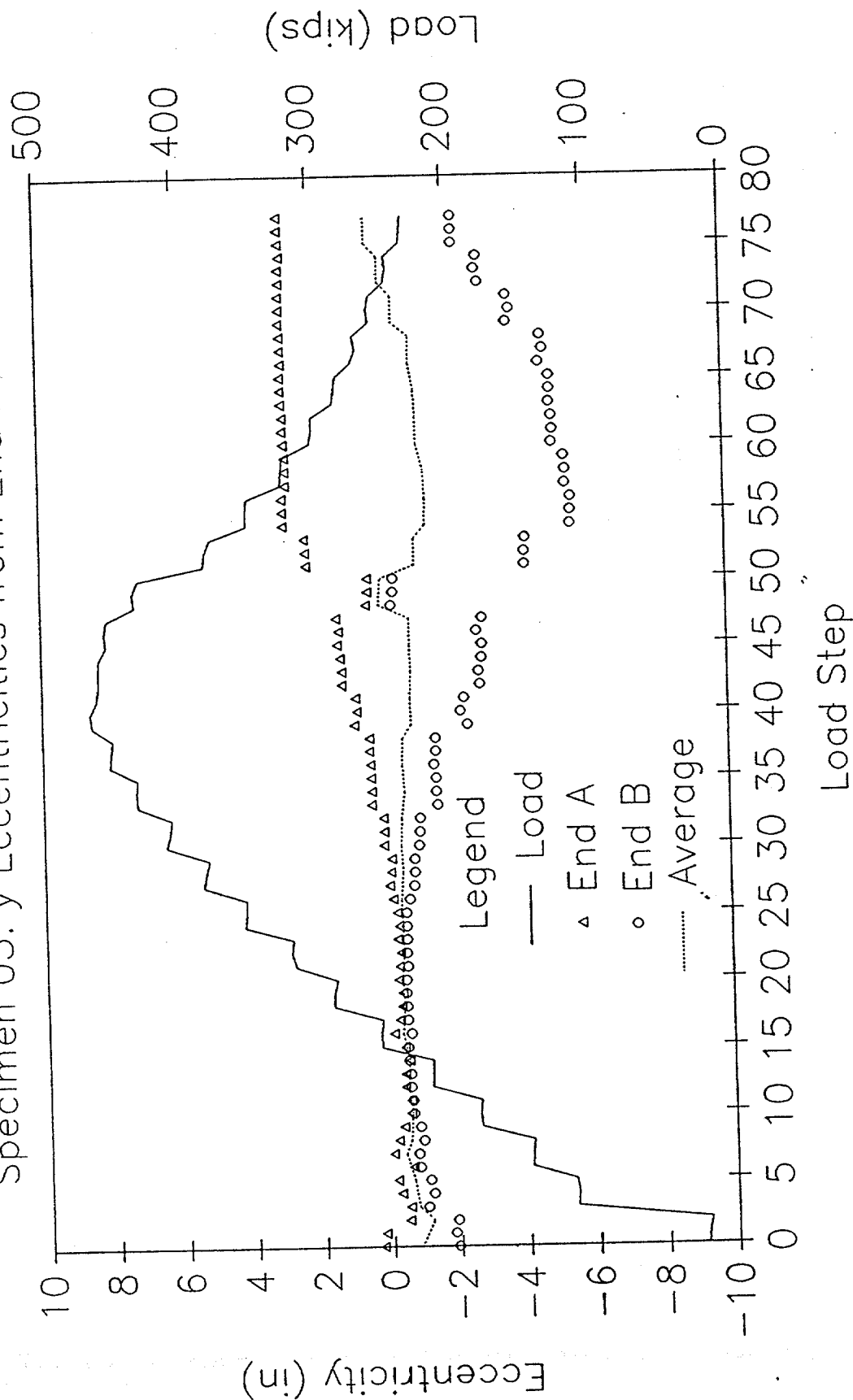
LOAD AND ECCENTRICITY vs LOAD STEP

Specimen 05: x Eccentricity from End Moments



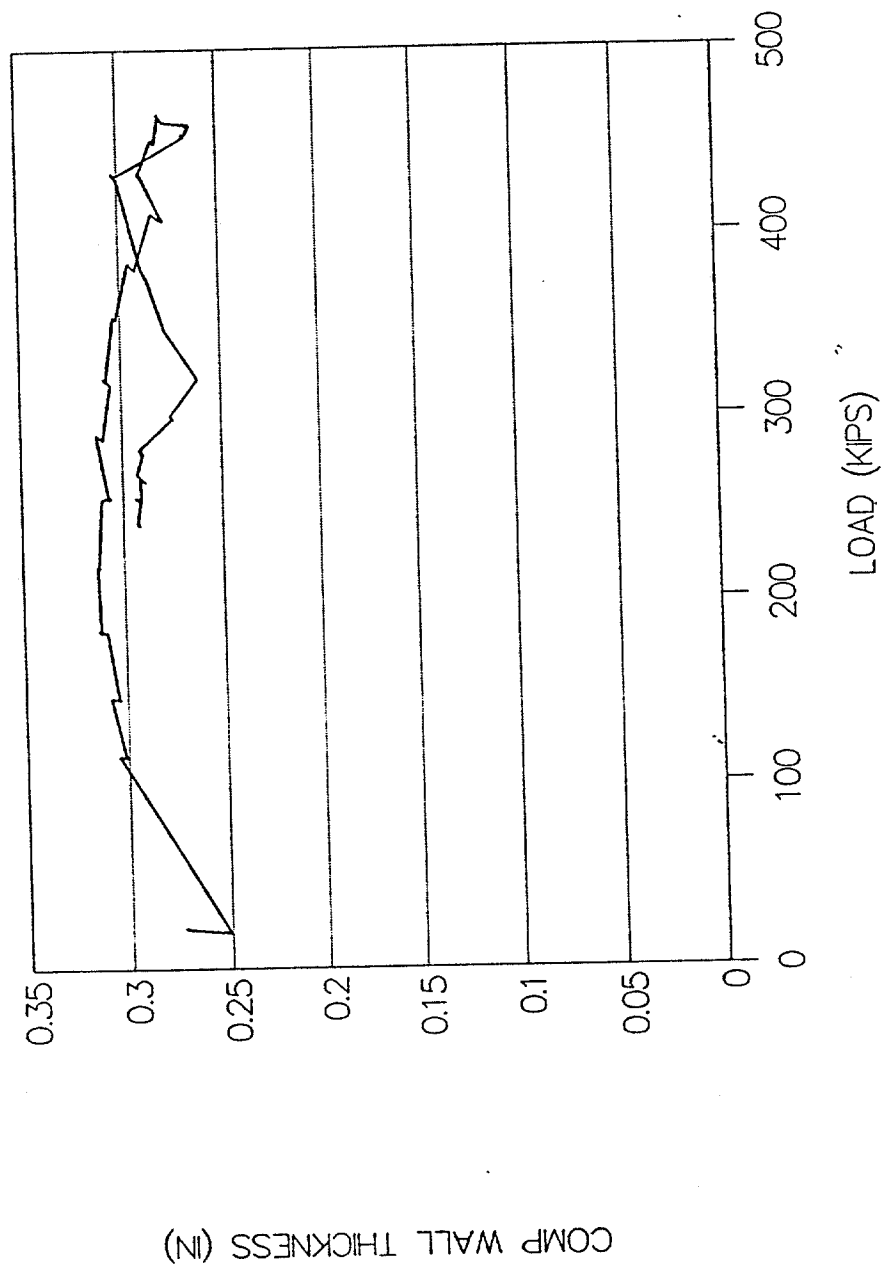
LOAD AND ECCENTRICITY vs LOAD STEP

Specimen 05: y Eccentricities from End Moments



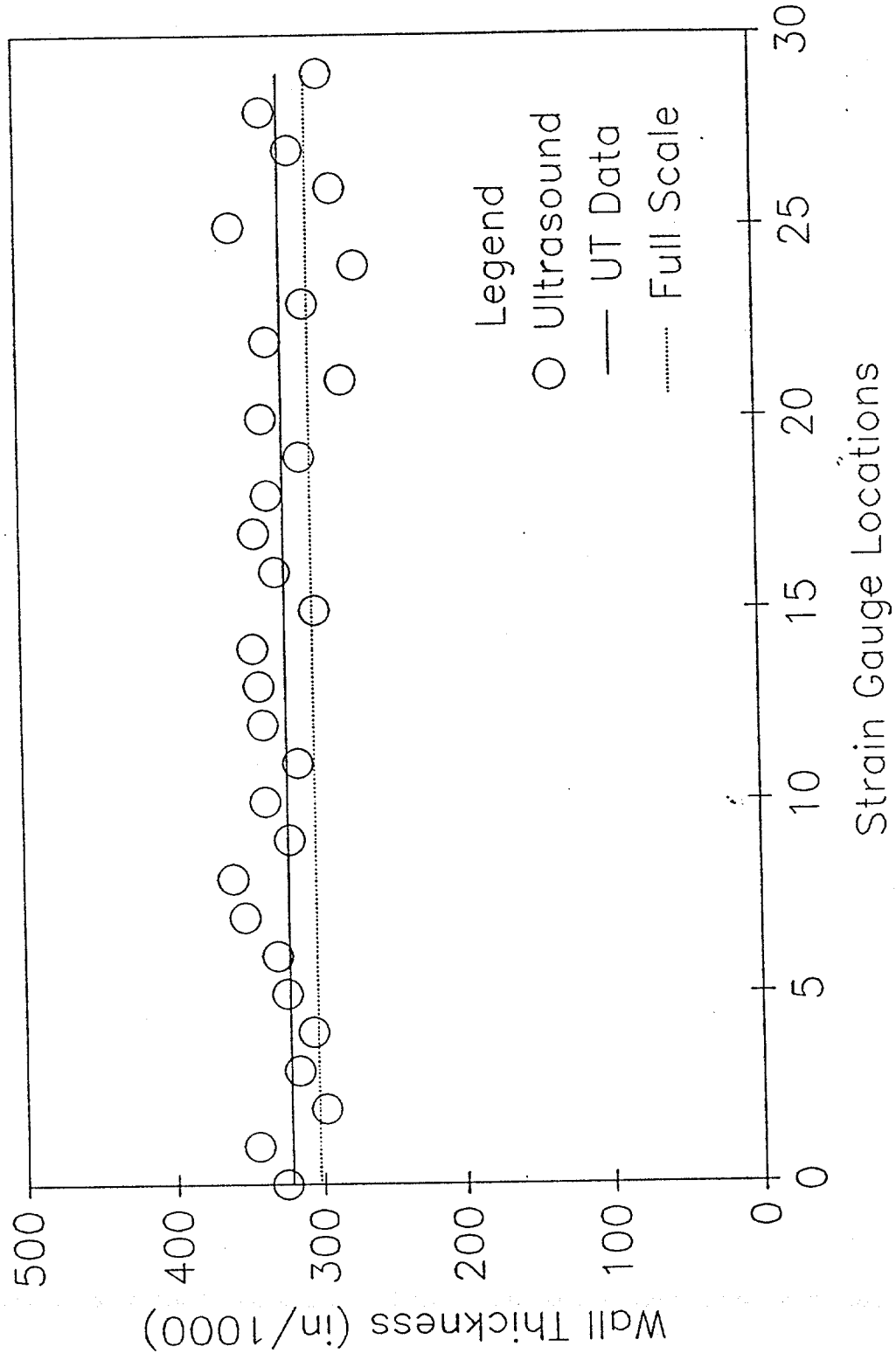
SPECIMEN 05--FULL SCALE TEST

COMPUTED WALL THICKNESS



SPECIMEN 05: WALL THICKNESS

Nominal Wall Thickness = 0.375 in



Ultrasound Data for Specimen 5
(All values in inches)

Gauge No.	UT Thickness	UT Average
0	0.326	
1	0.345	
2	0.298	
3	0.316	
4	0.306	
5	0.324	0.319
6	0.330	
7	0.352	
8	0.360	
9	0.321	
10	0.337	
11	0.314	0.336
12	0.338	
13	0.340	
14	0.344	
15	0.301	
16	0.328	
17	0.342	0.332
18	0.333	
19	0.310	
20	0.336	
21	0.280	
22	0.332	
23	0.306	0.316
24	0.270	
25	0.356	
26	0.286	
27	0.315	
28	0.334	
29	0.294	0.309

Overall Average = 0.322

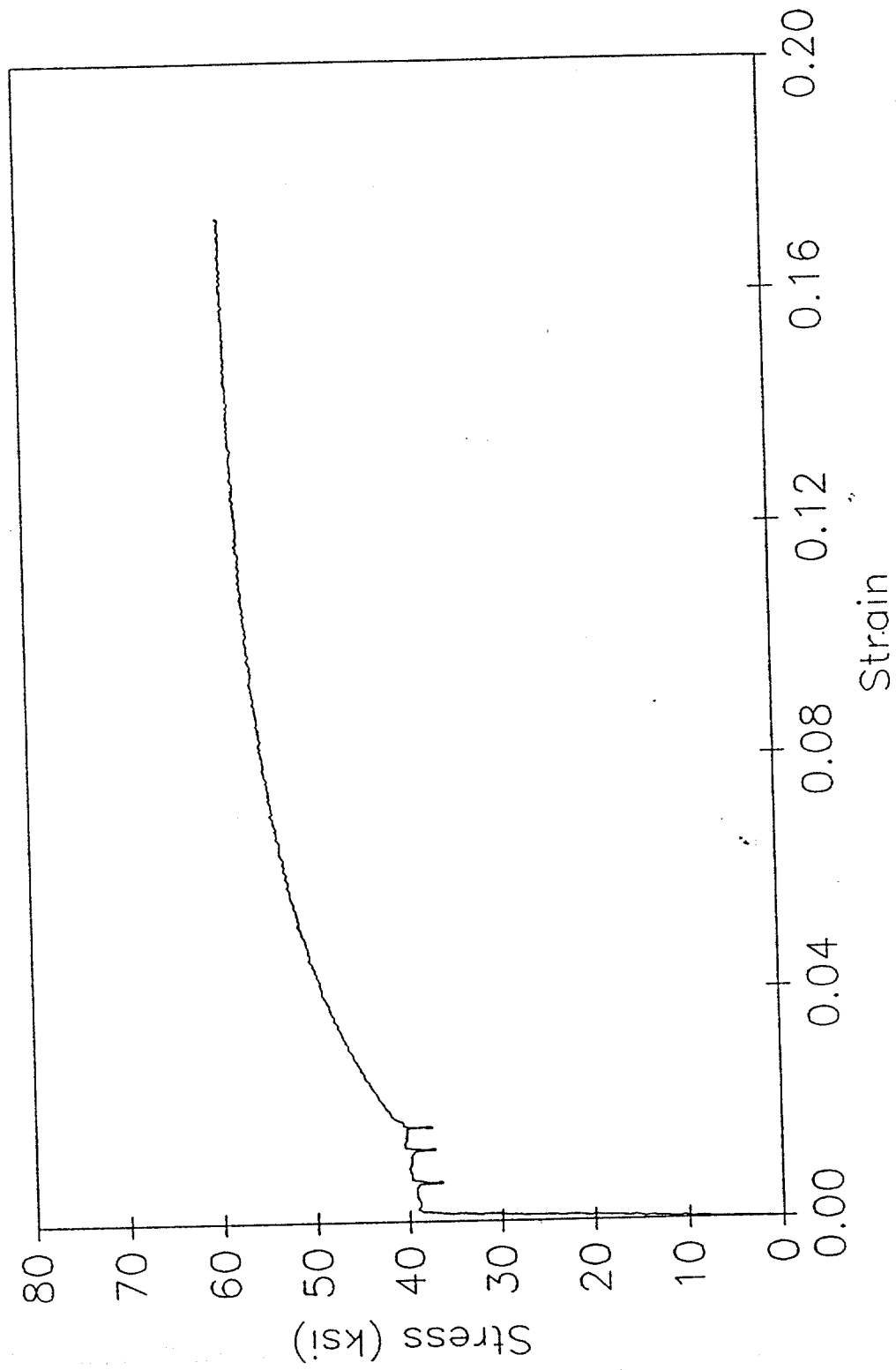
Random Readings near Buckling Point

No.	Reading
1	0.302
2	0.316
3	0.318
4	0.330
5	0.251
6	0.259
7	0.338
8	0.338

Random Average = 0.306

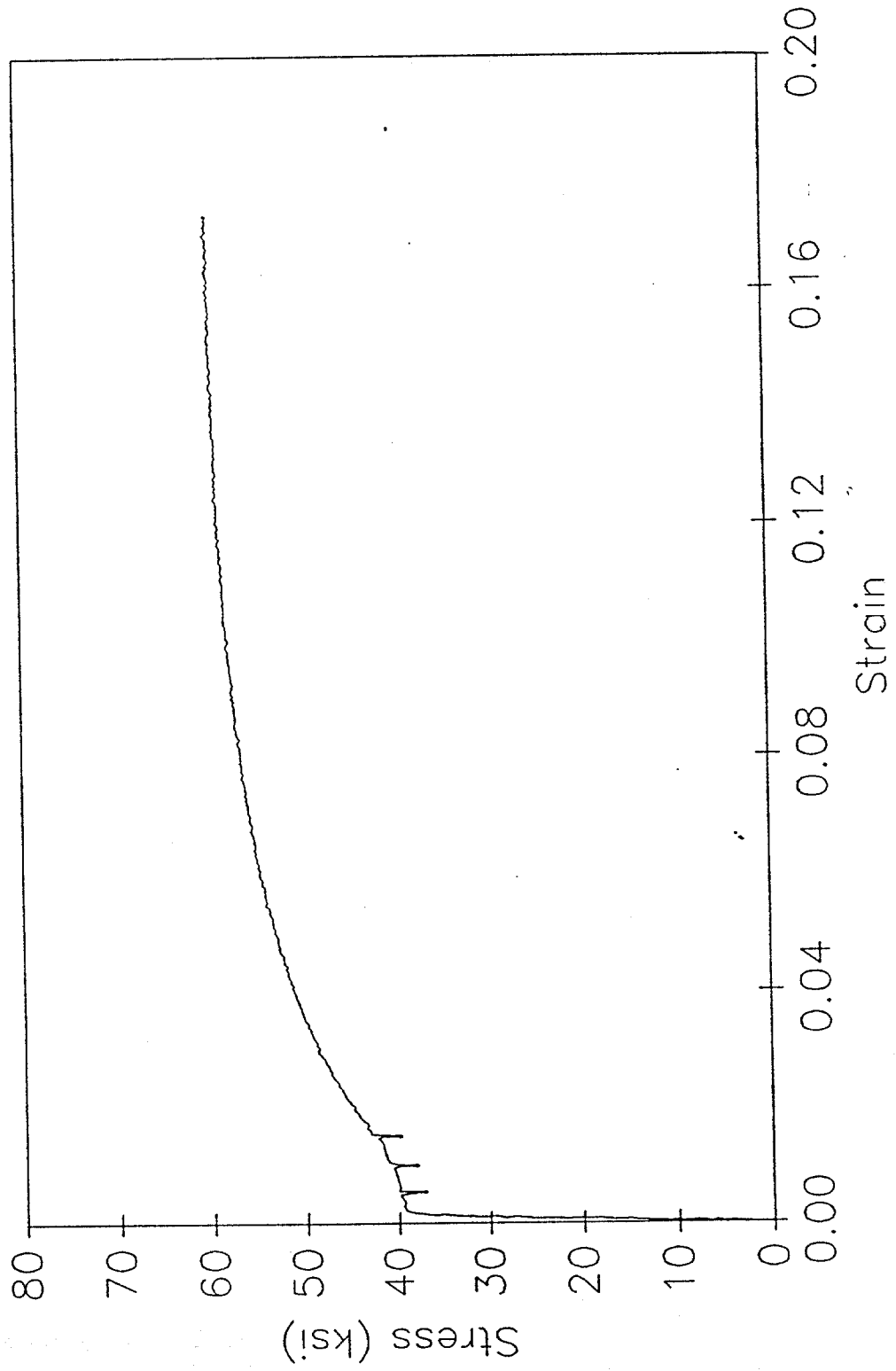
TENSILE SPECIMEN 5-1

Stress vs Strain



TENSILE SPECIMEN 5-2

Stress vs Strain



SPECIMEN 06

DAMAGE SUMMARY

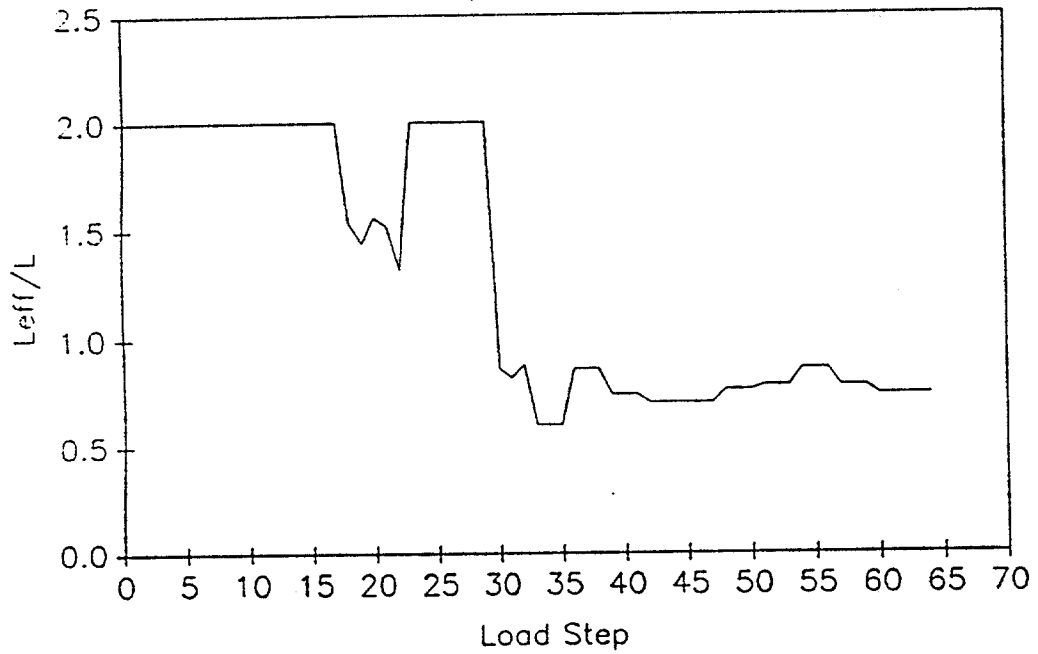
Specimen No. 6

DISTANCE FROM END "A"	*DISTANCE FROM CHALK LINE		DESCRIPTION OF DAMAGE
	LEFT	RIGHT	
	NO VISIBLE EXTERNAL DAMAGE!		
	Some minor corrosion pitting on inside wall surface of ring test specimen.		

*Looking from end "A" towards end "B"

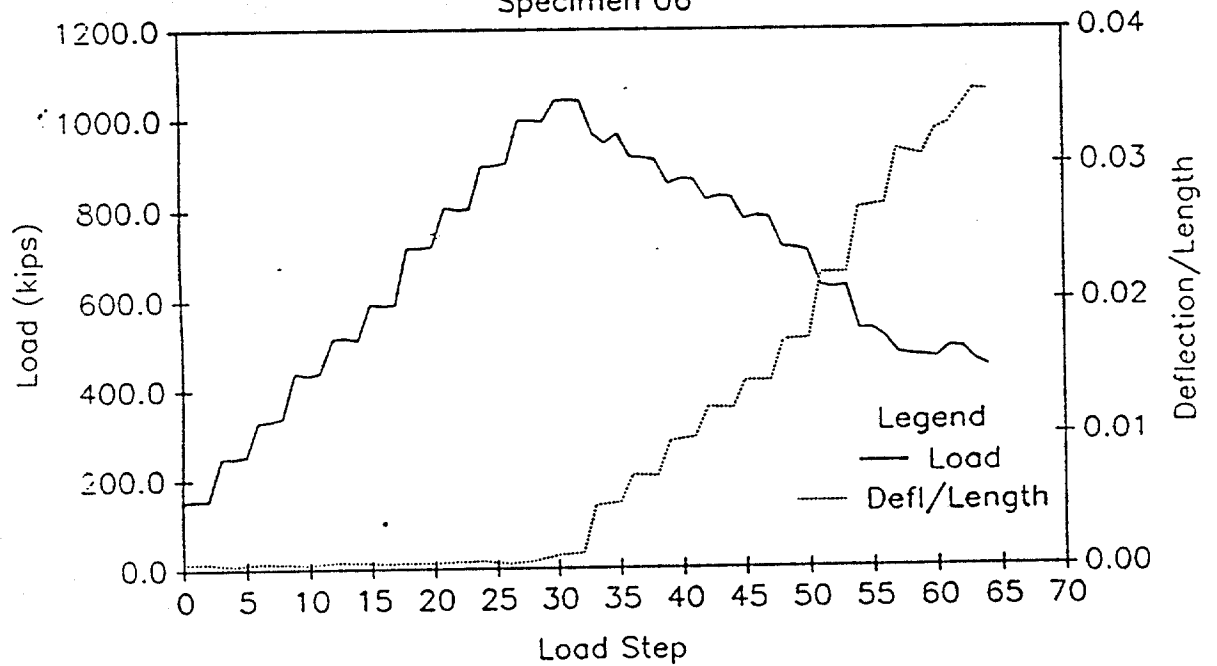
EFFECTIVE LENGTH vs LOAD STEP

Specimen 06



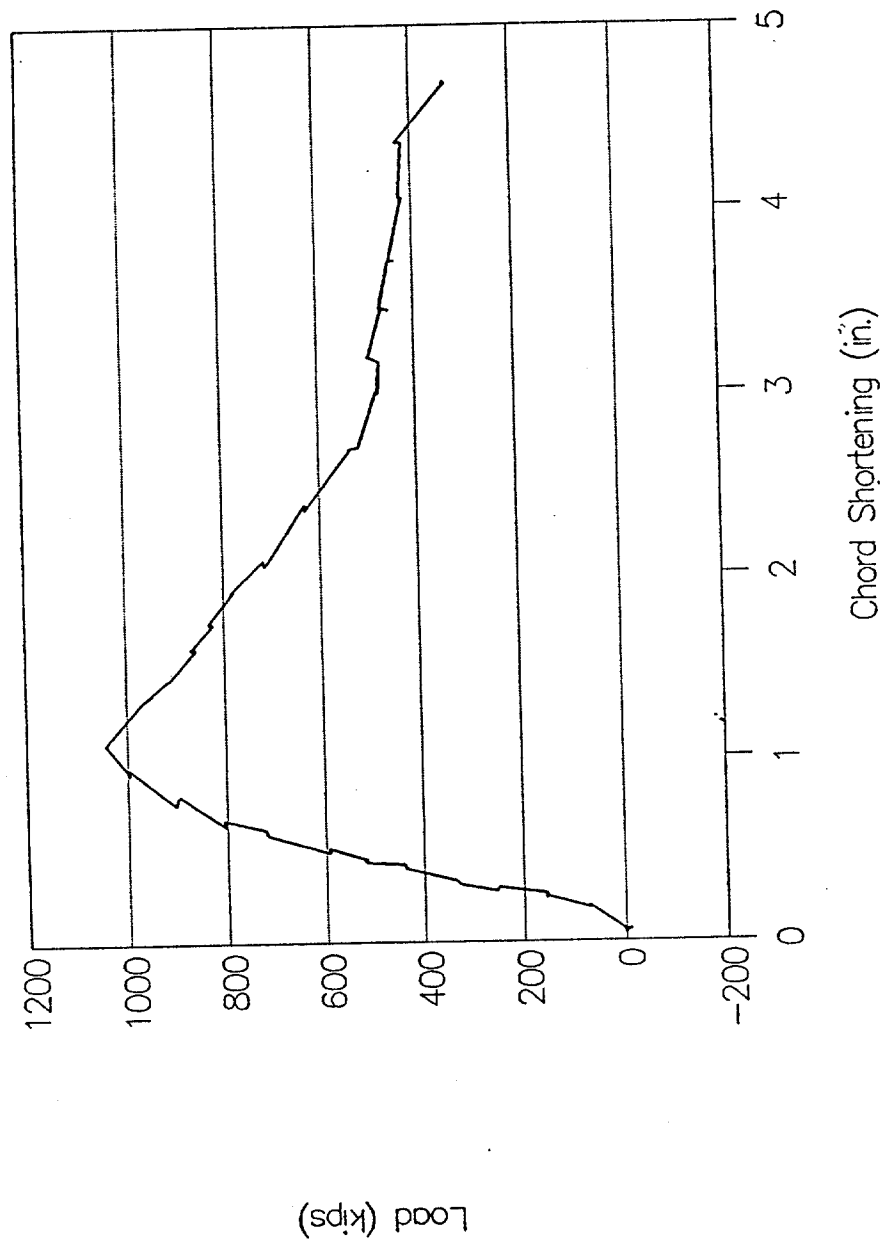
LOAD AND DEFLECTION vs LOAD STEP

Specimen 06

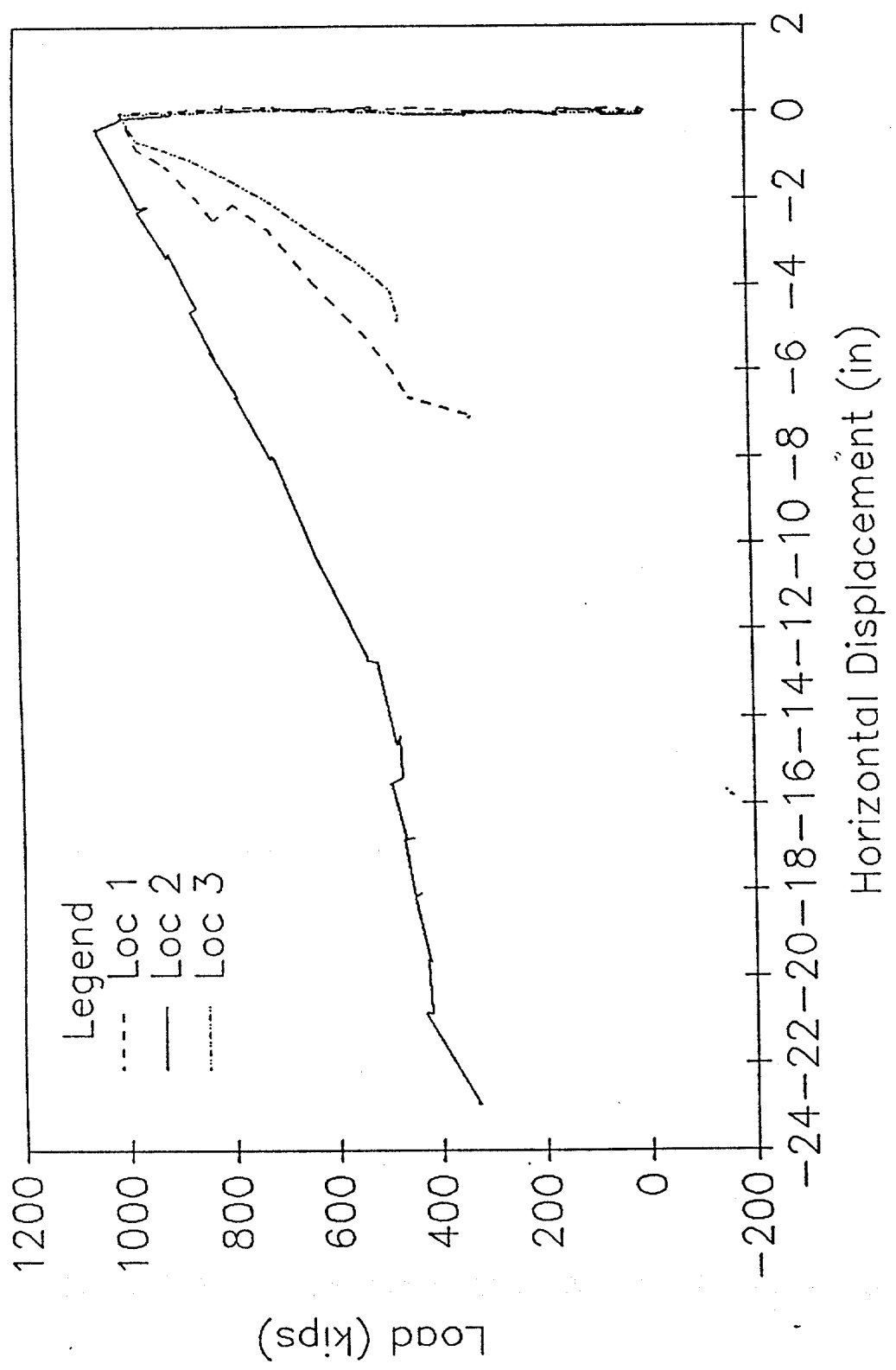


Chord Shortening

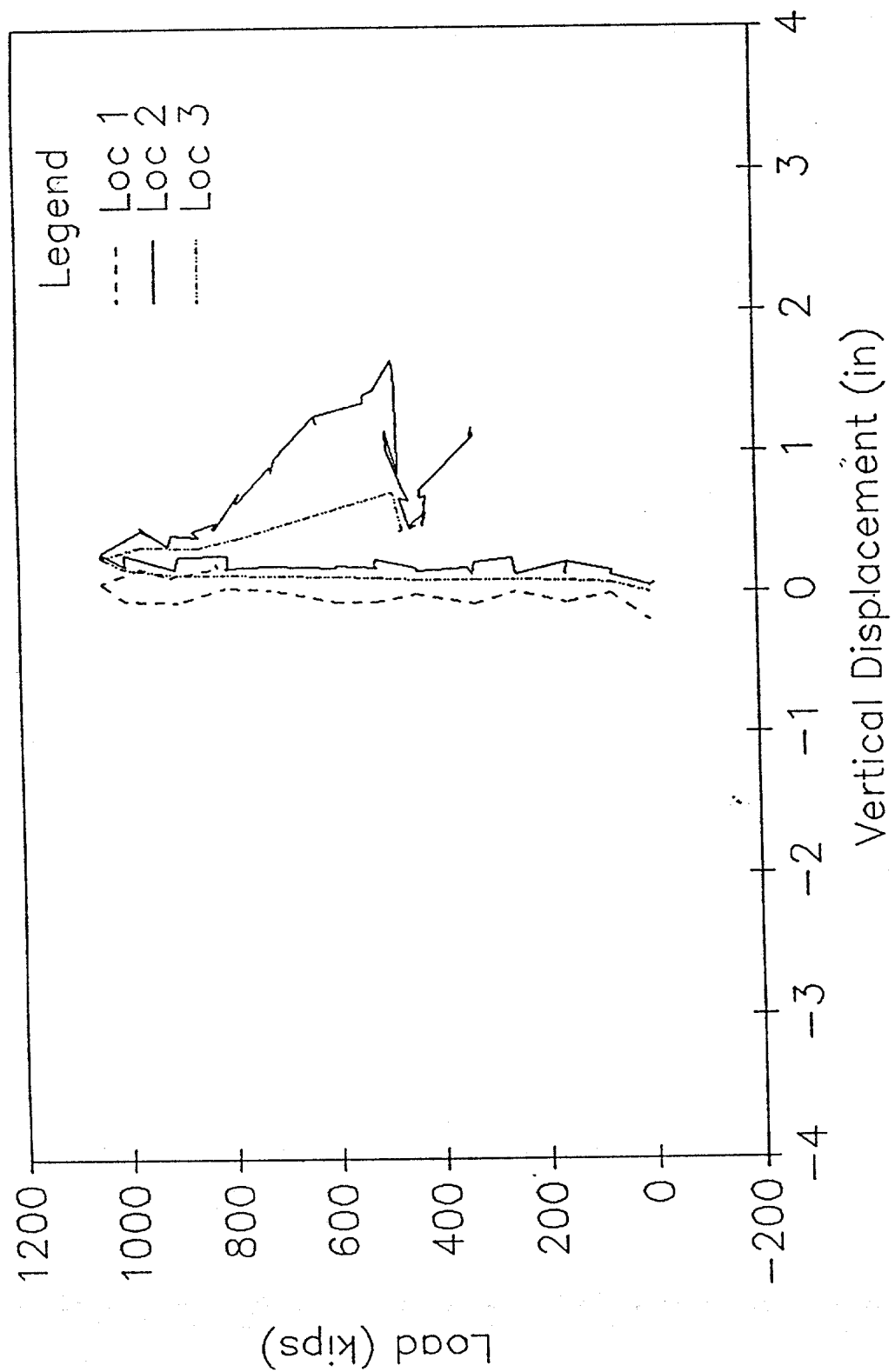
Specimen 06



Horizontal Displacements Specimen 06

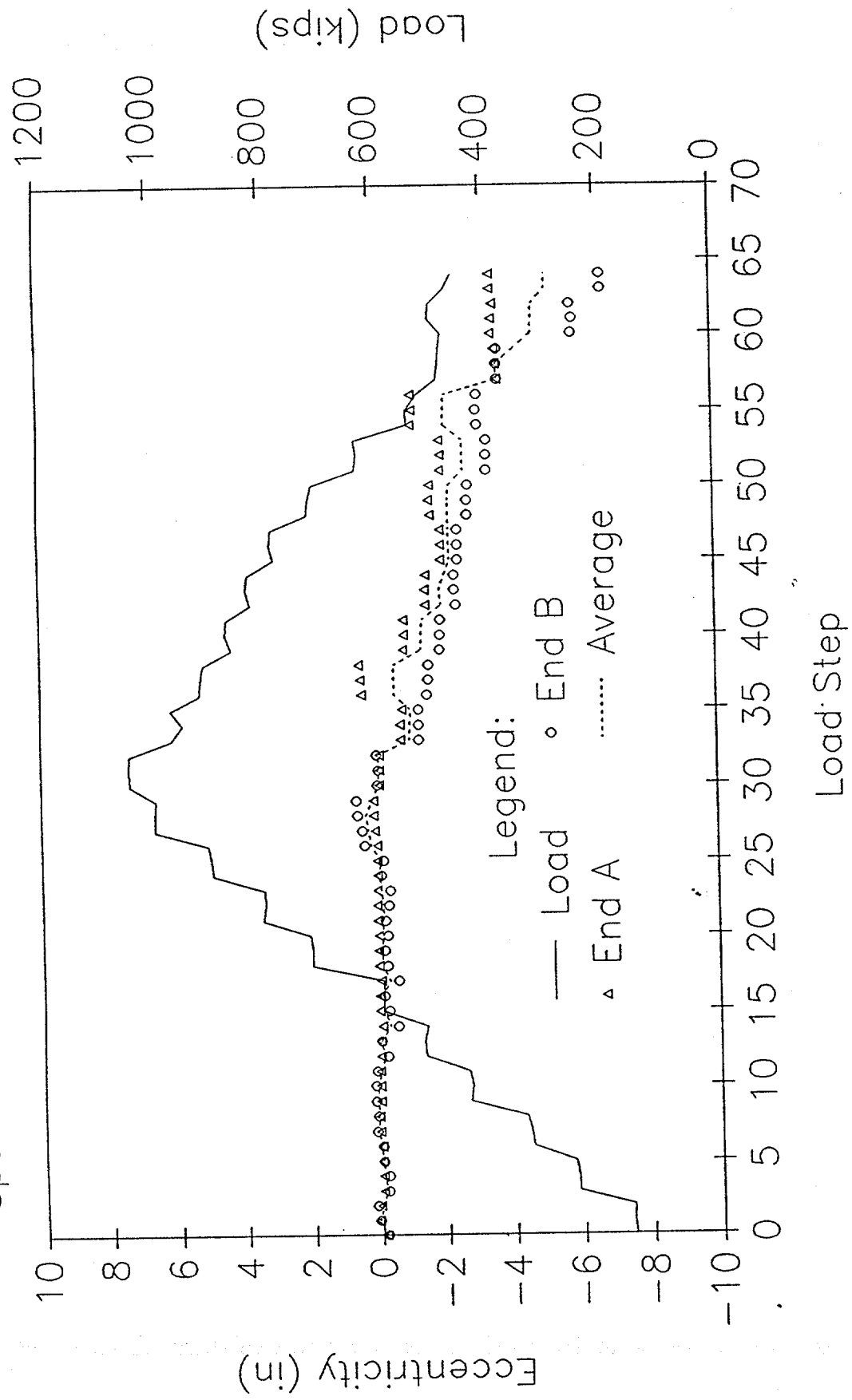


Vertical Displacements Specimen 06



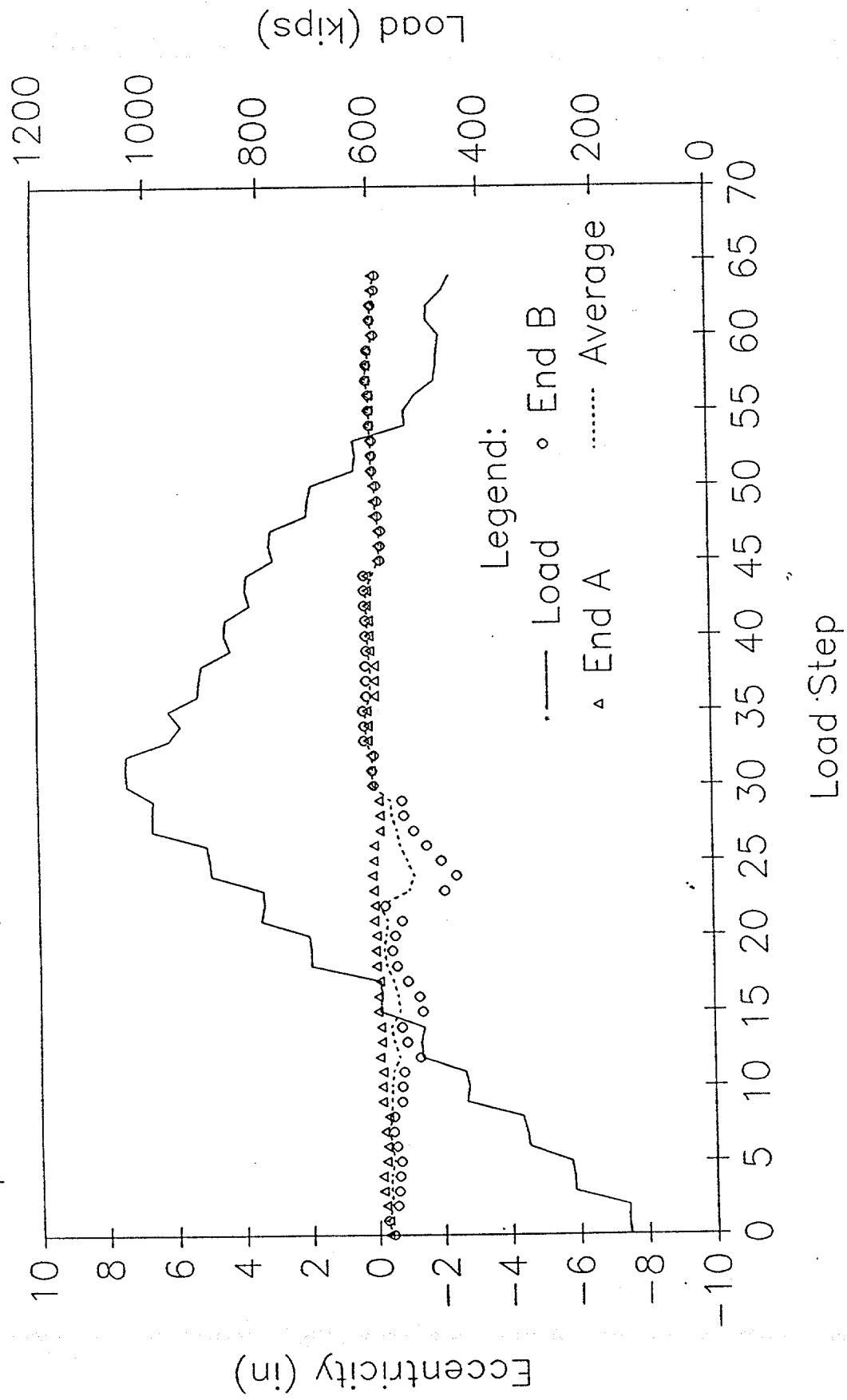
LOAD AND ECCENTRICITY VS LOAD STEP

Specimen 06: x Eccentricities from Inflection Points



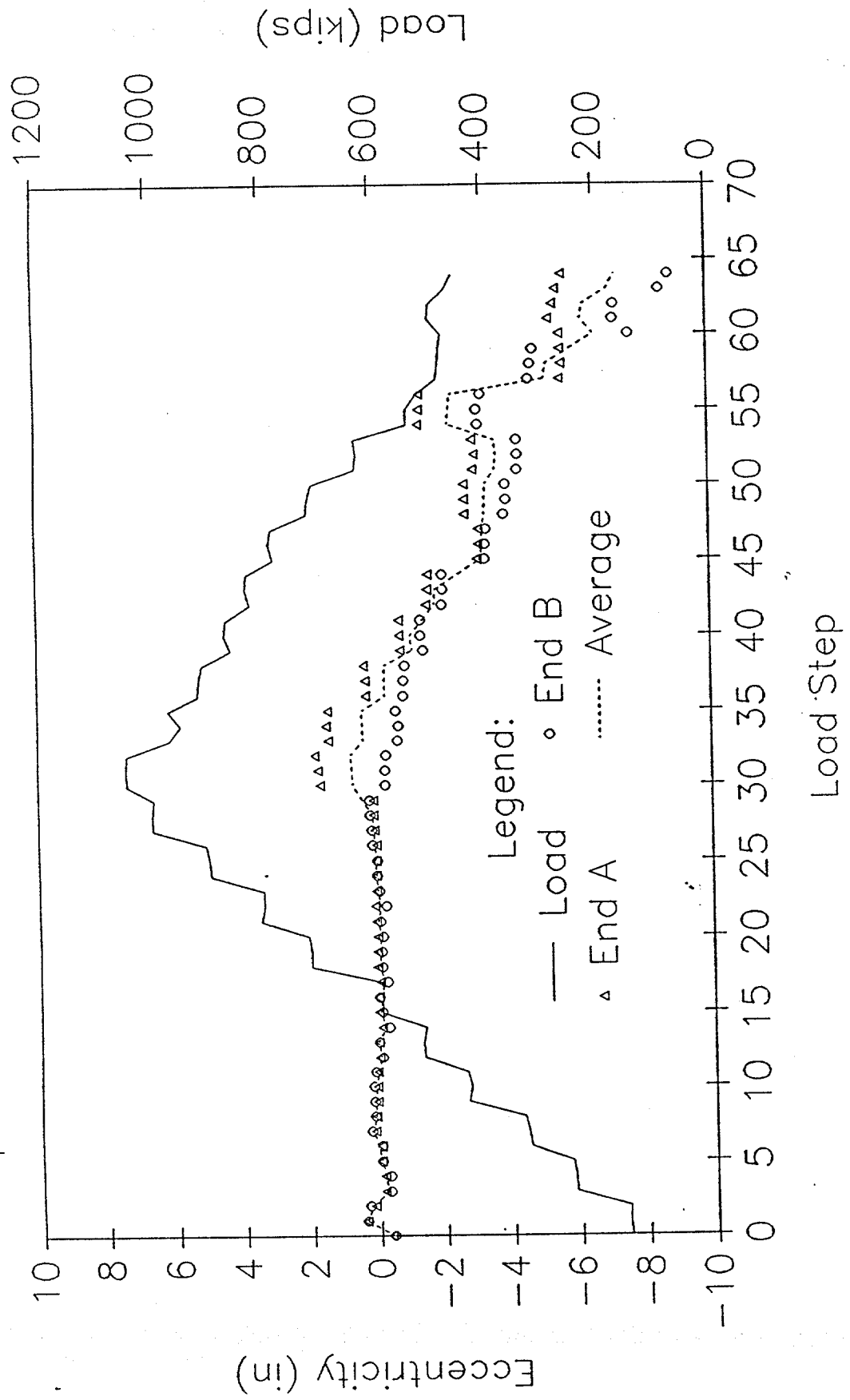
LOAD AND ECCENTRICITY VS LOAD STEP

Specimen 06: y Eccentricities from Inflection Points



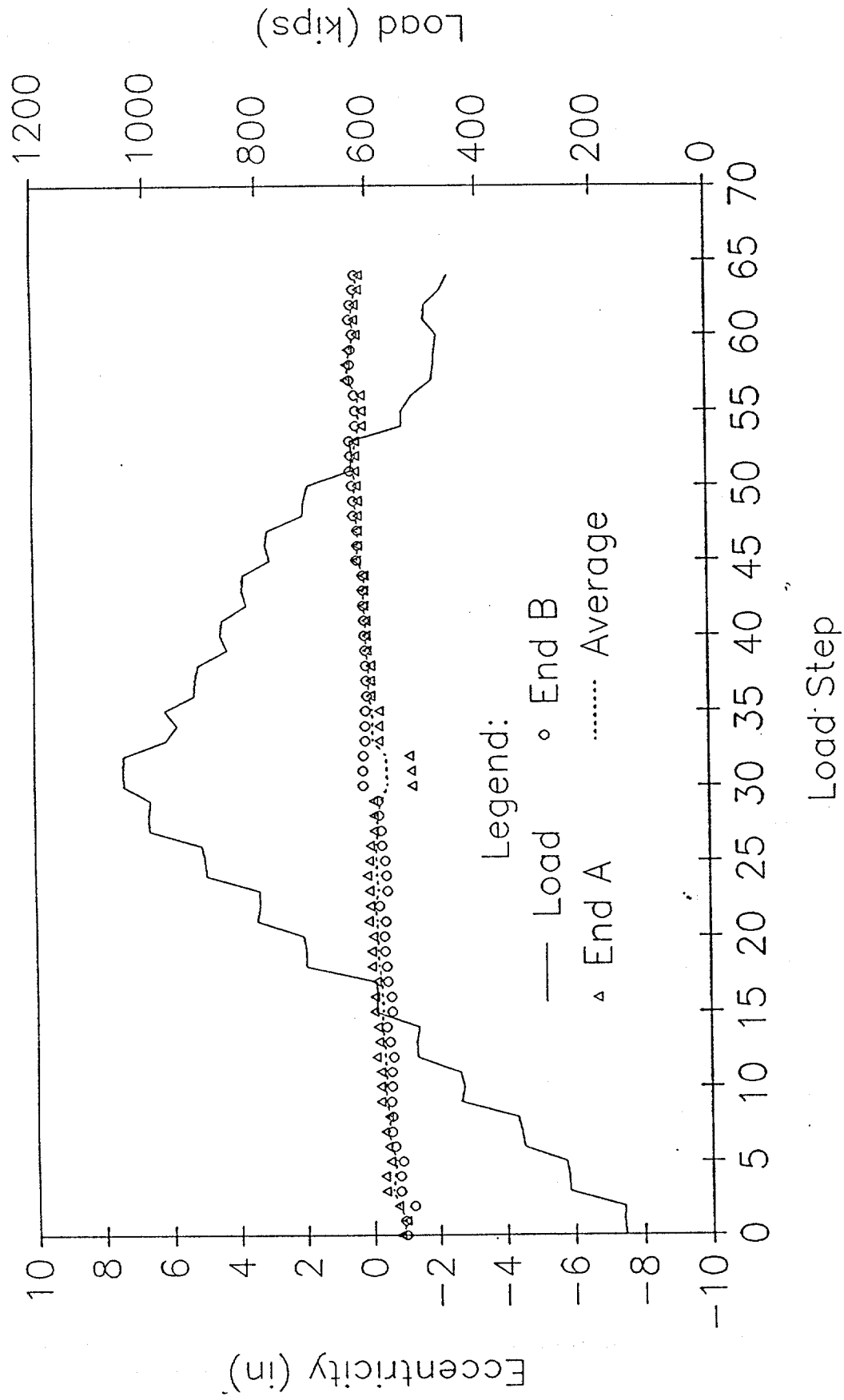
LOAD AND ECCENTRICITY vs LOAD STEP

Specimen 06: x Eccentricities from End Moments



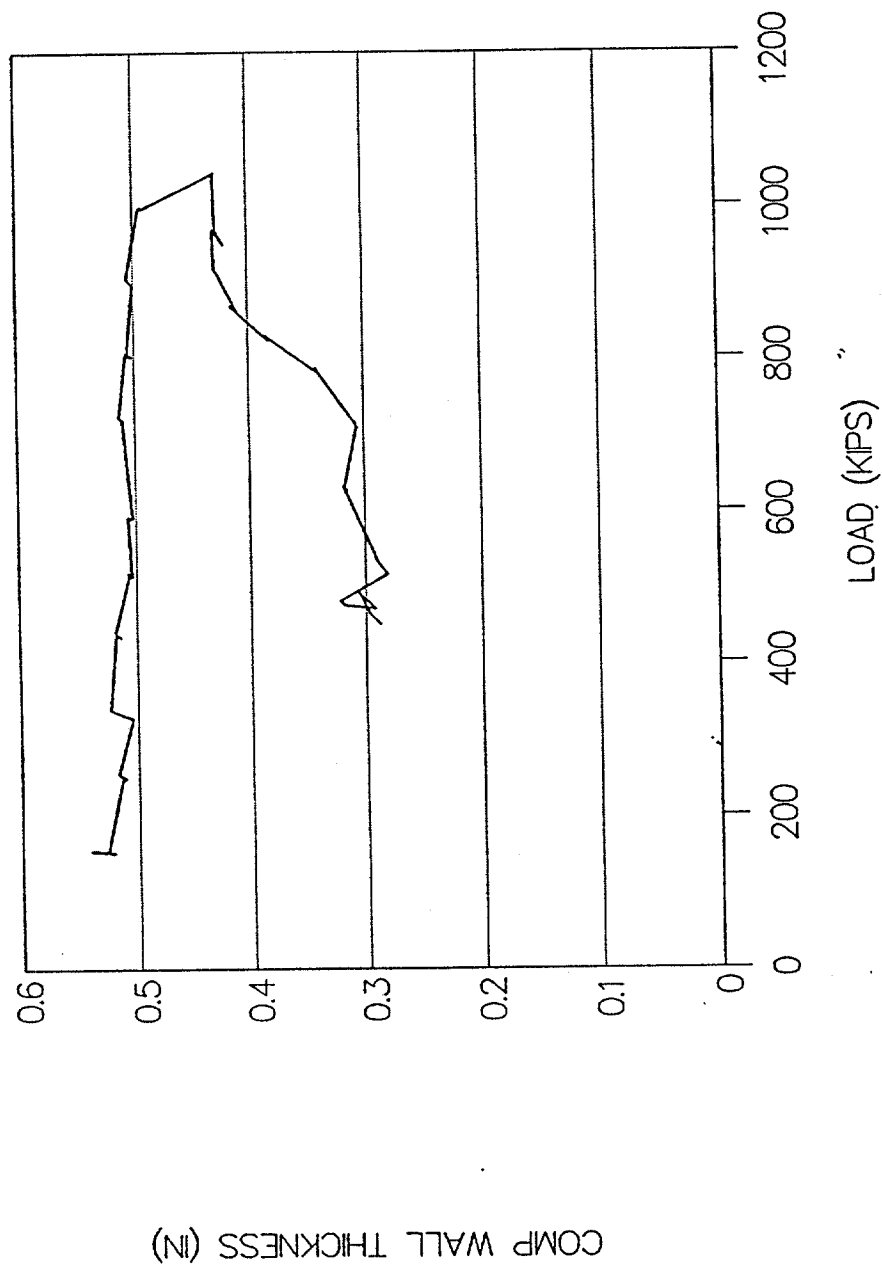
LOAD AND ECCENTRICITY vs LOAD STEP

Specimen 06: y Eccentricities from End Moments



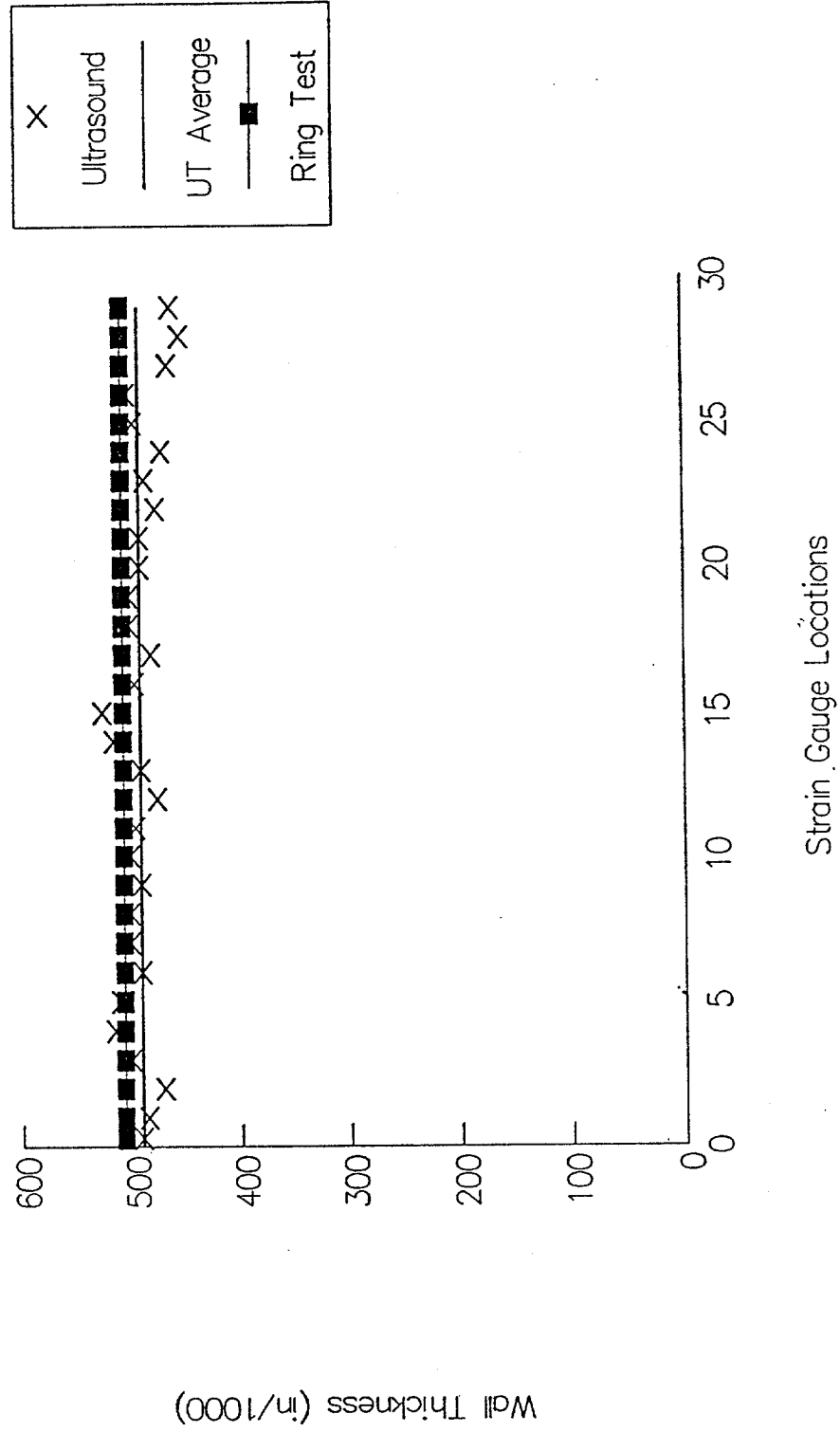
SPECIMEN 06—FULL SCALE TEST

COMPUTED WALL THICKNESS



Specimen 06: Wall Thickness

Nominal Thickness = 0.500 in



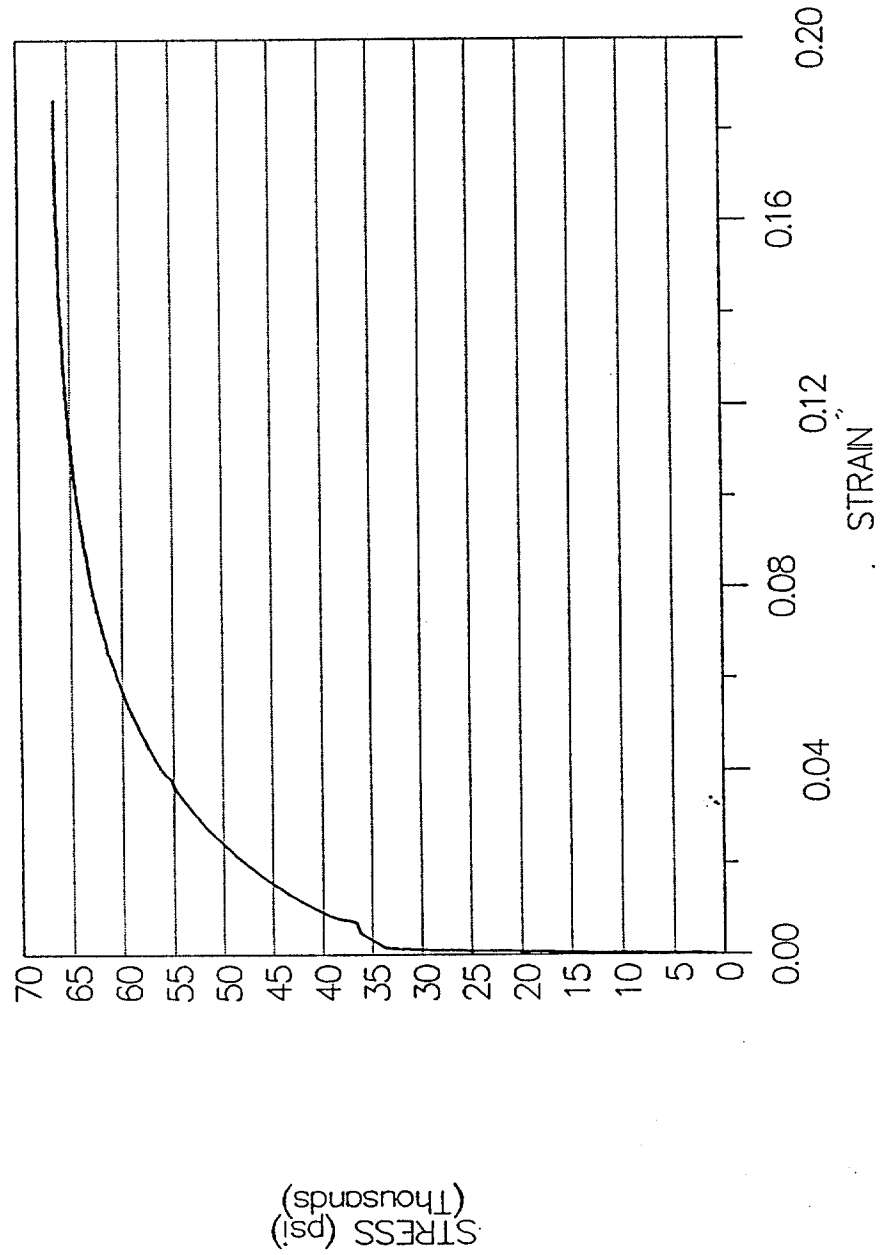
Ultrasound Data for Specimen 6
(All values in inches)

Gauge No.	UT Thickness	UT Average
0	0.491	
1	0.486	
2	0.471	
3	0.501	
4	0.516	
5	0.511	0.496
6	0.491	
7	0.501	
8	0.501	
9	0.491	
10	0.501	
11	0.496	0.497
12	0.476	
13	0.491	
14	0.516	
15	0.526	
16	0.496	
17	0.481	0.498
18	0.501	
19	0.501	
20	0.491	
21	0.491	
22	0.476	
23	0.486	0.491
24	0.464	
25	0.502	
26	0.496	
27	0.470	
28	0.461	
29	0.453	0.474

Overall Average = 0.491

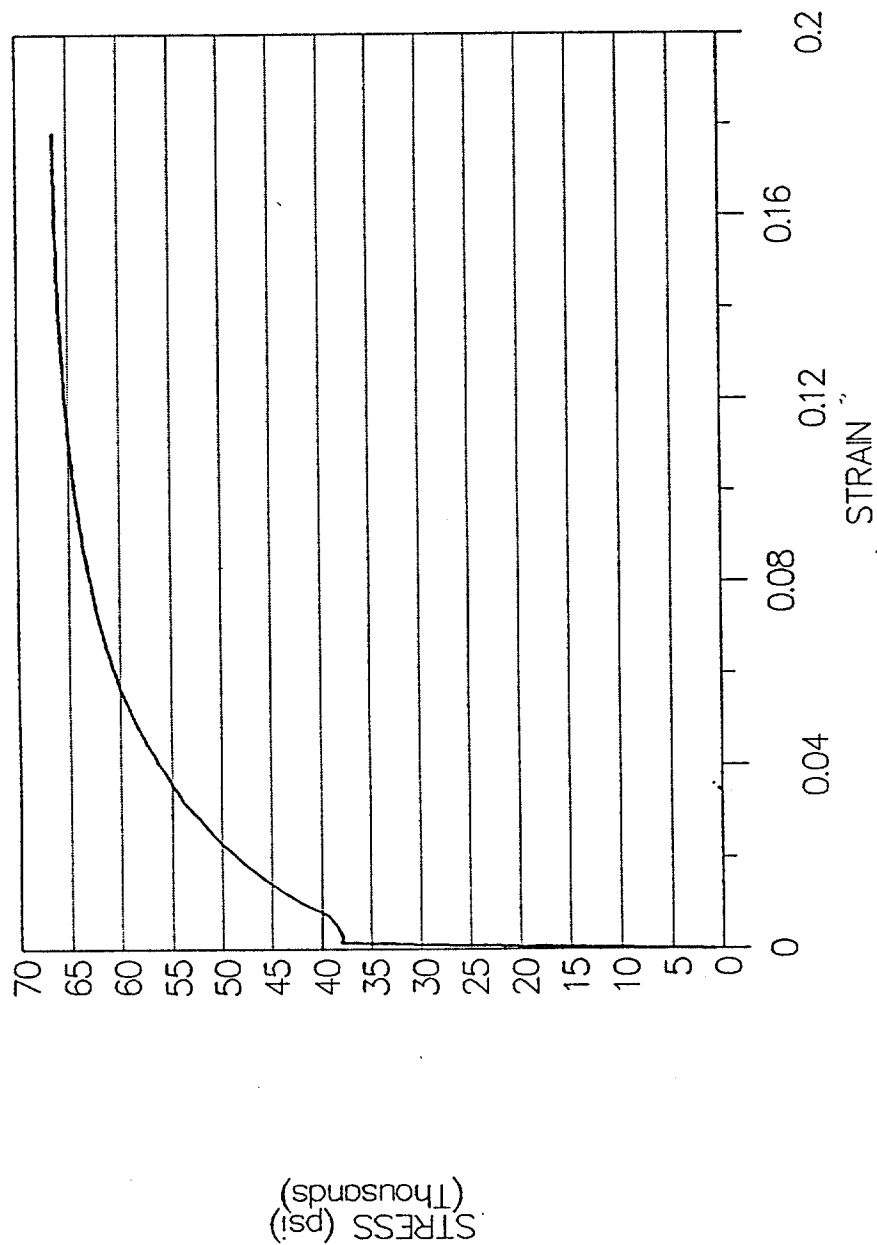
TENSILE SPECIMEN 6-3

Stress vs Strain



TENSILE SPECIMEN 6-4

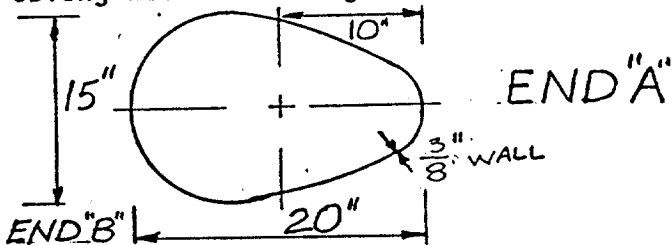
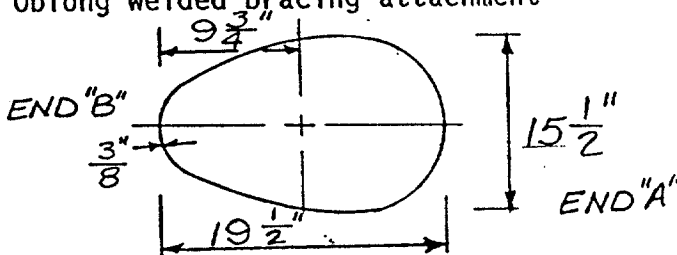
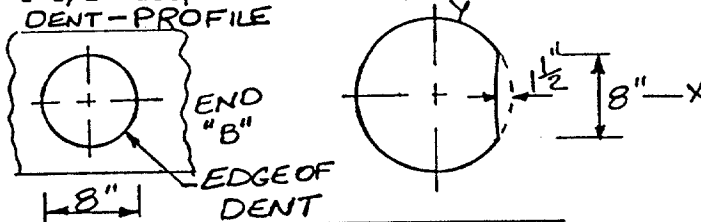
Stress vs Strain



SPECIMEN 07

DAMAGE SUMMARY

Specimen No. 7

DISTANCE FROM END "A"	*DISTANCE FROM CHALK LINE		DESCRIPTION OF DAMAGE
	LEFT	RIGHT	
1. 5'-10"		12 1/4"	C-section welded to pipe (rectangular) 6" X 3"
2. 11'-0"		10 3/4"	C-section welded to pipe (rectangular) 6" X 3"
3. 18'-3 3/4"			3/4" circumferential butt weld
4. 18'-2 3/4"	10"		Oblong welded bracing attachment 
5. 20'-0"	9 5/8"		Oblong welded bracing attachment 
6. 20'-3 3/4"		9"	Dent - 8" circular, CROSS-SECTION 1 1/2" deep at center AT C. OF DENT DENT-PROFILE 
7. 30'-1"		11 5/8"	C-section welded to pipe (rectangular) 6" X 3"

*Looking from end "A" towards end "B"

DAMAGE SUMMARY

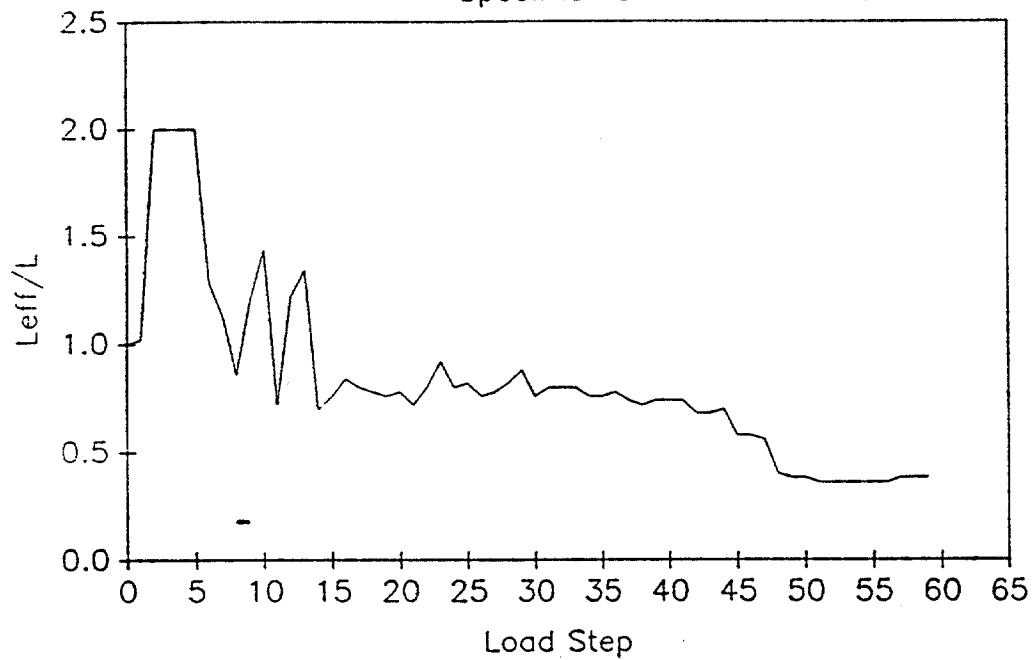
Specimen No. 7

DISTANCE FROM END "A"	*DISTANCE FROM CHALK LINE		DESCRIPTION OF DAMAGE
	LEFT	RIGHT	
8. 35'-2"		11 3/8"	C-section welded to pipe (rectangular) 6" X 3"
9. 19'-2"	21"		6 1/2" diameter circular round bracing connection, 1/4" wall thick
	LIGHT CORROSION		

*Looking from end "A" towards end "B"

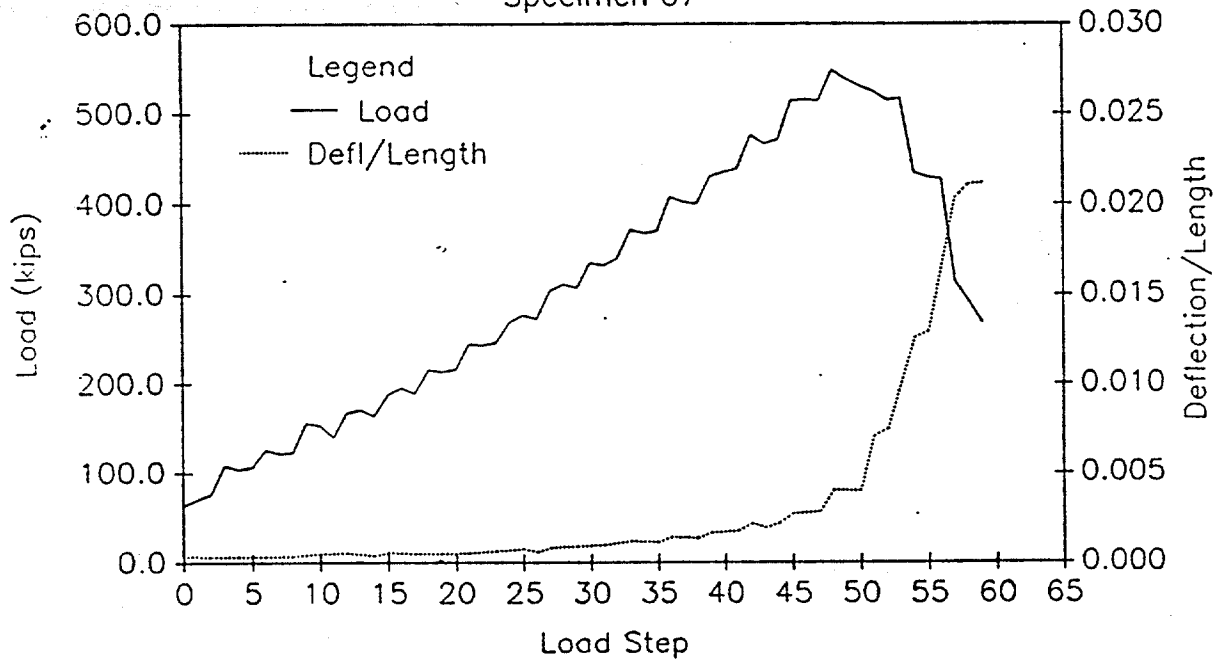
EFFECTIVE LENGTH vs LOAD STEP

Specimen 07



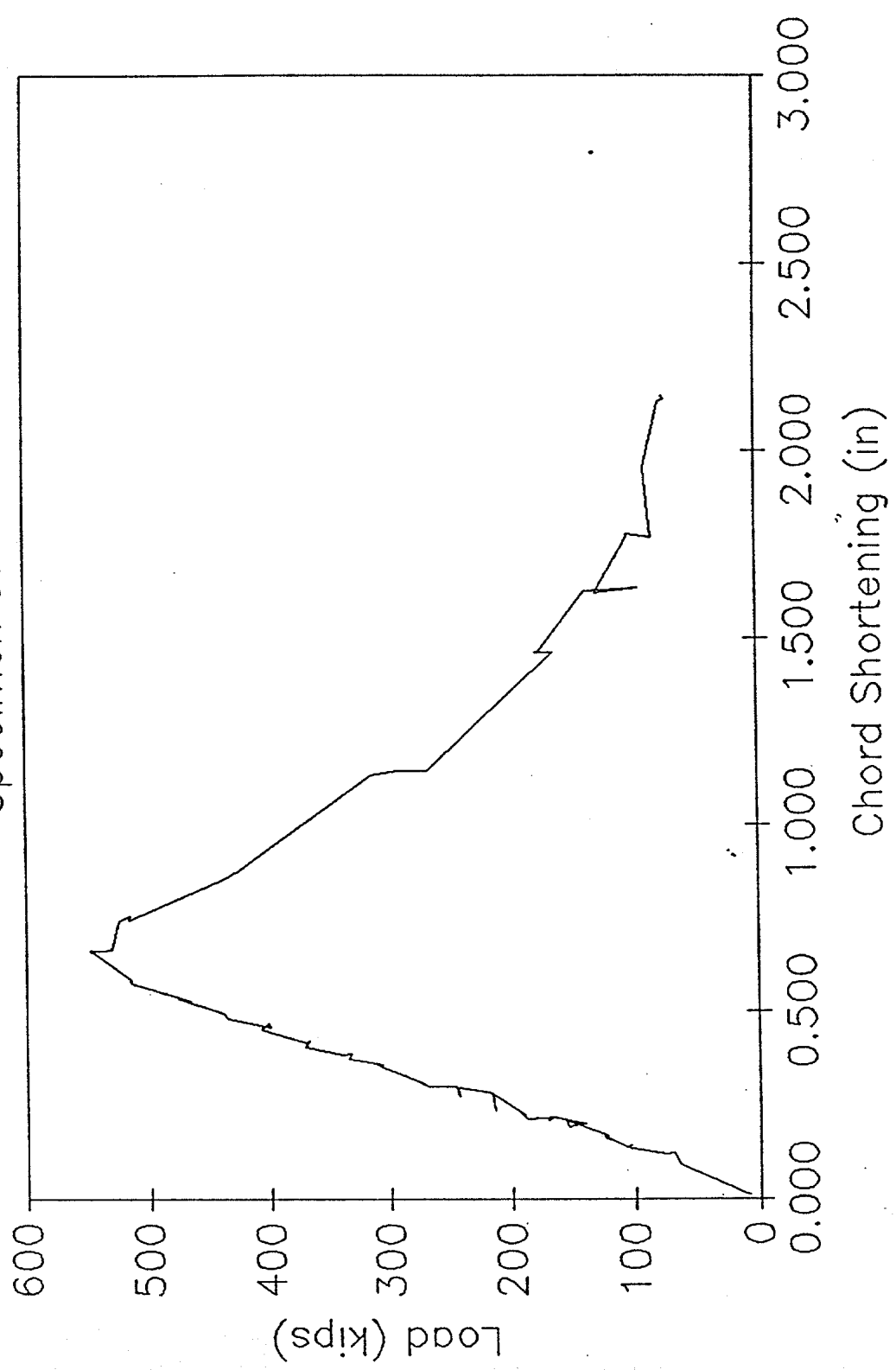
LOAD AND DEFLECTION vs LOAD STEP

Specimen 07



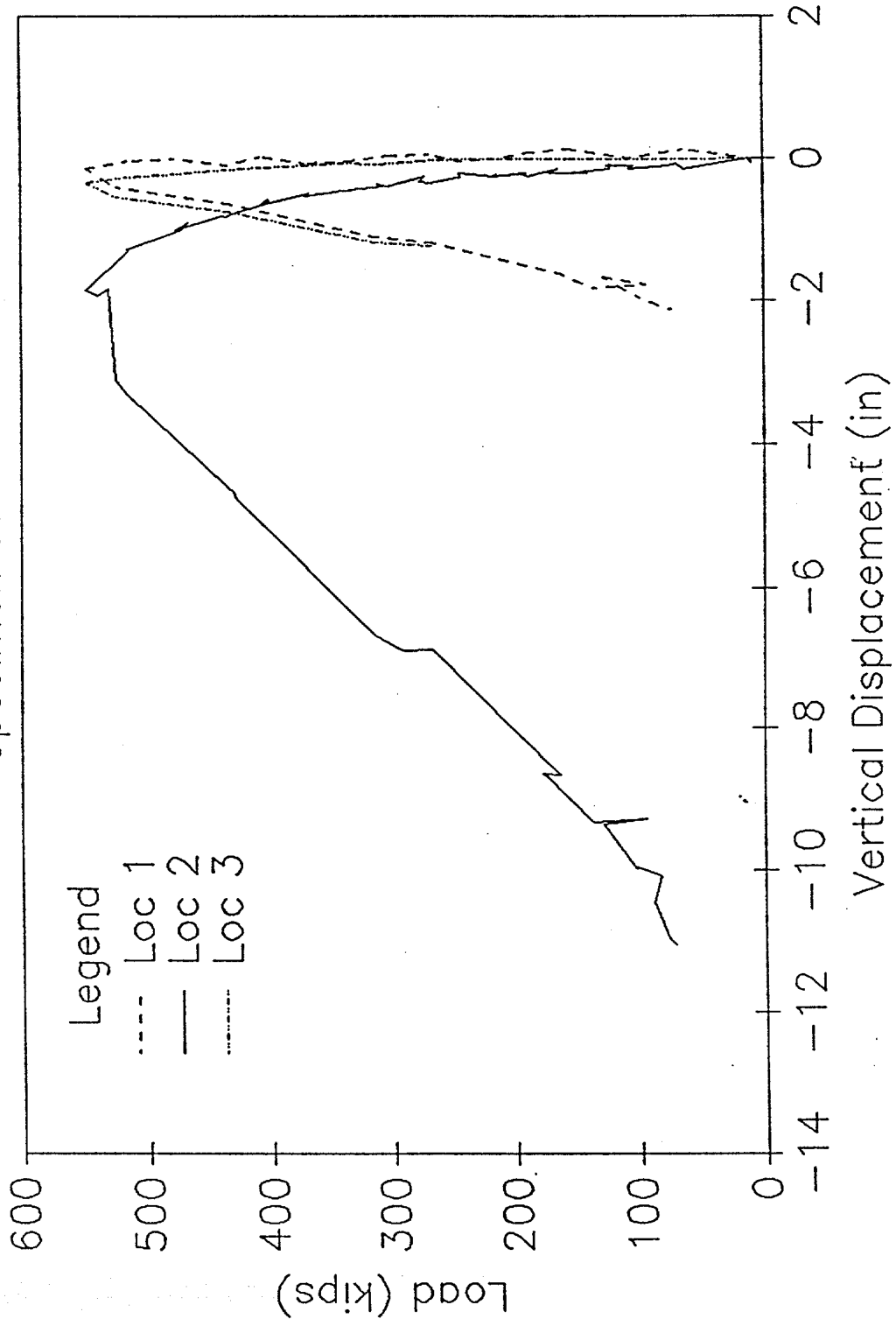
LOAD vs CHORD SHORTENING

Specimen 07



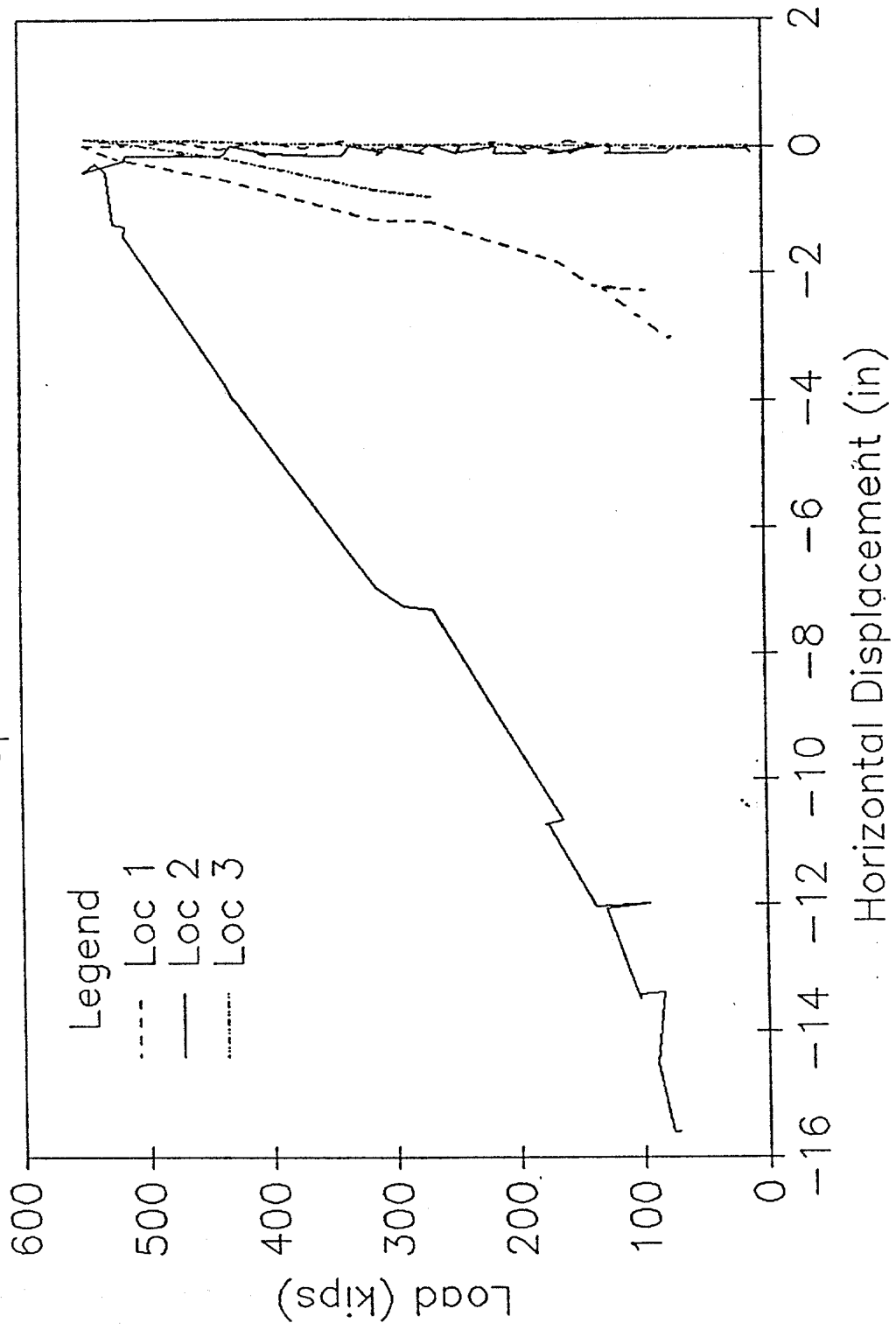
VERTICAL DISPLACEMENTS

Specimen 07

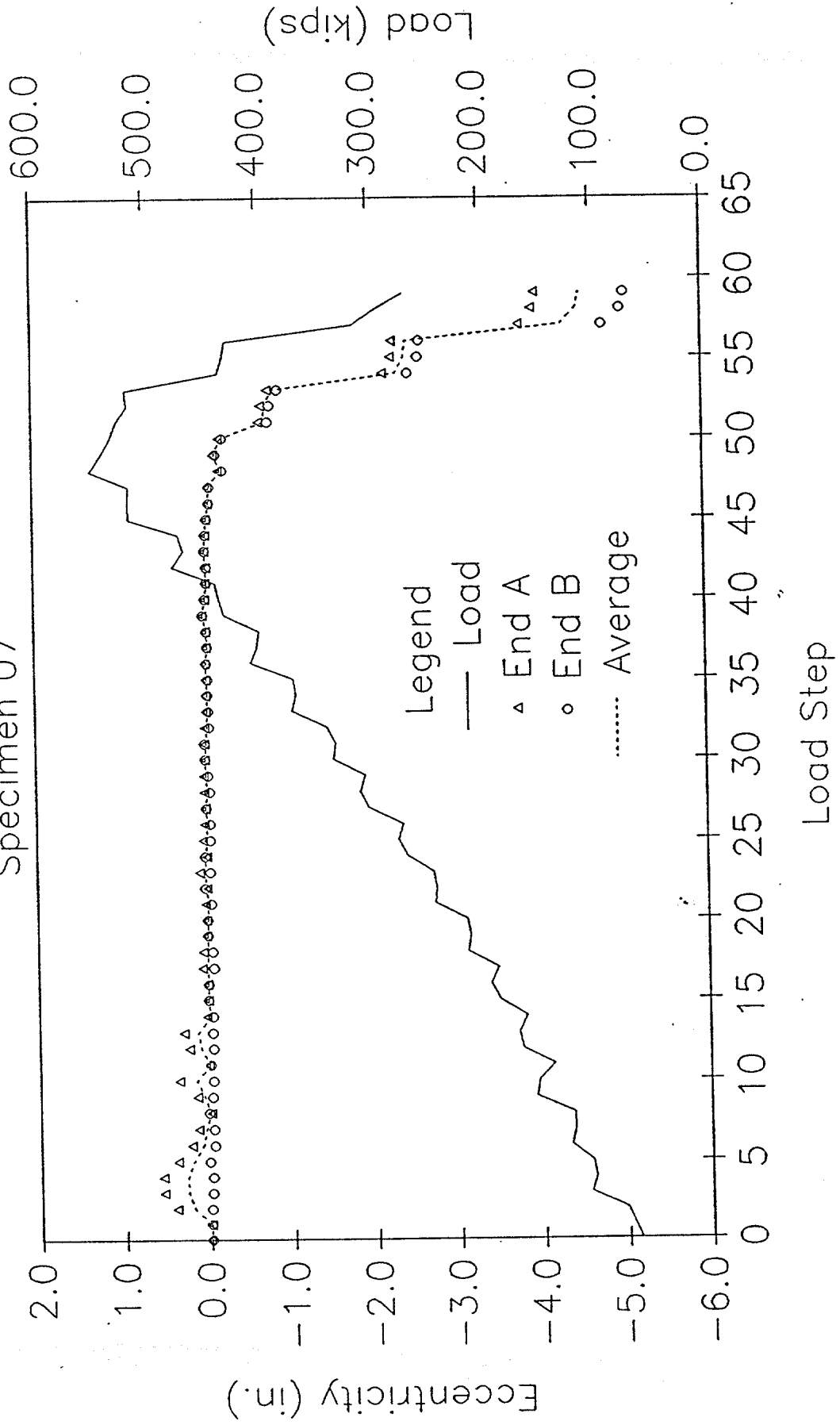


HORIZONTAL DISPLACEMENTS

Specimen 07



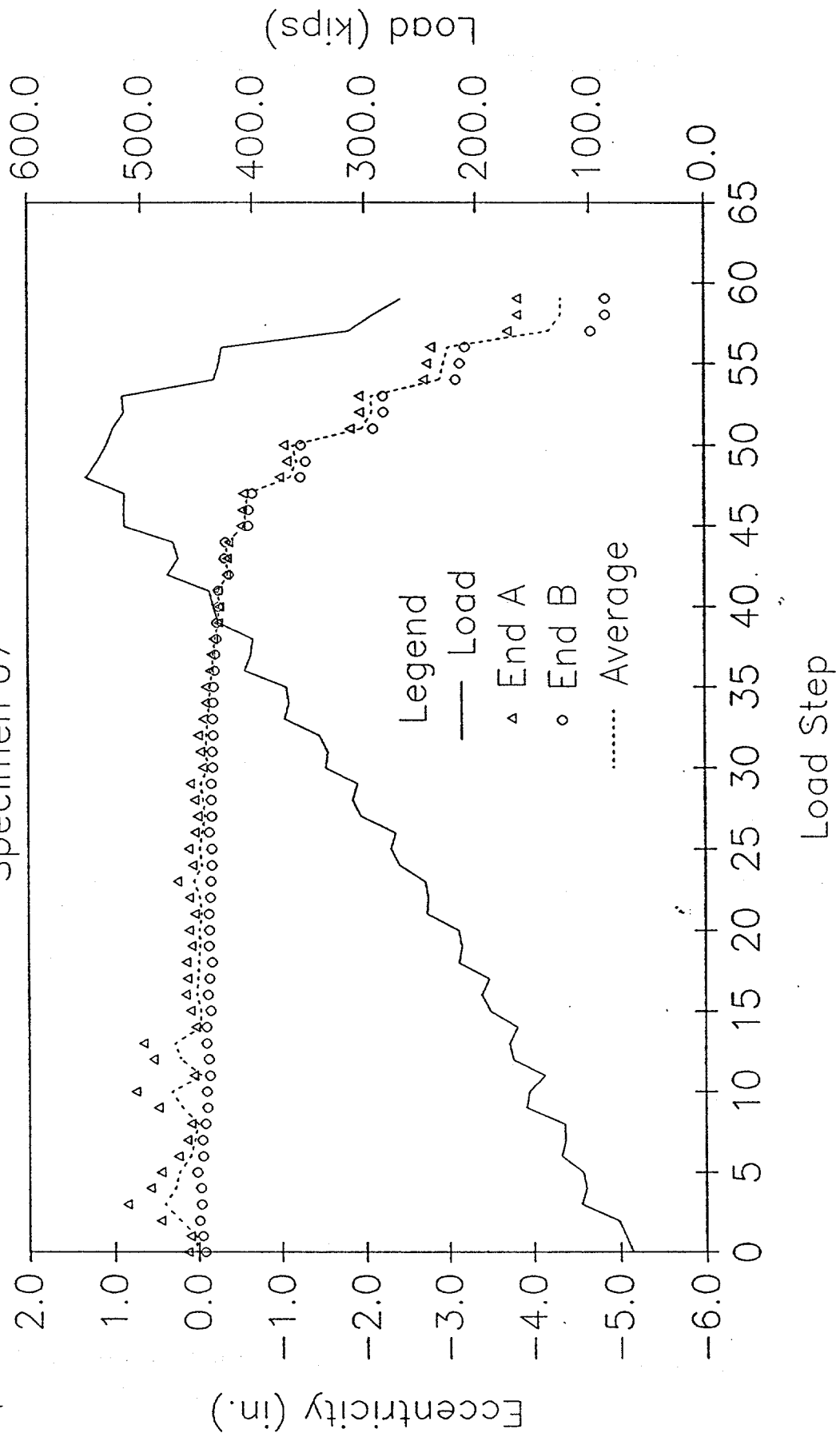
LOAD AND ECCENTRICITY vs LOAD STEP
x Eccentricities from Inflection Points
Specimen 07



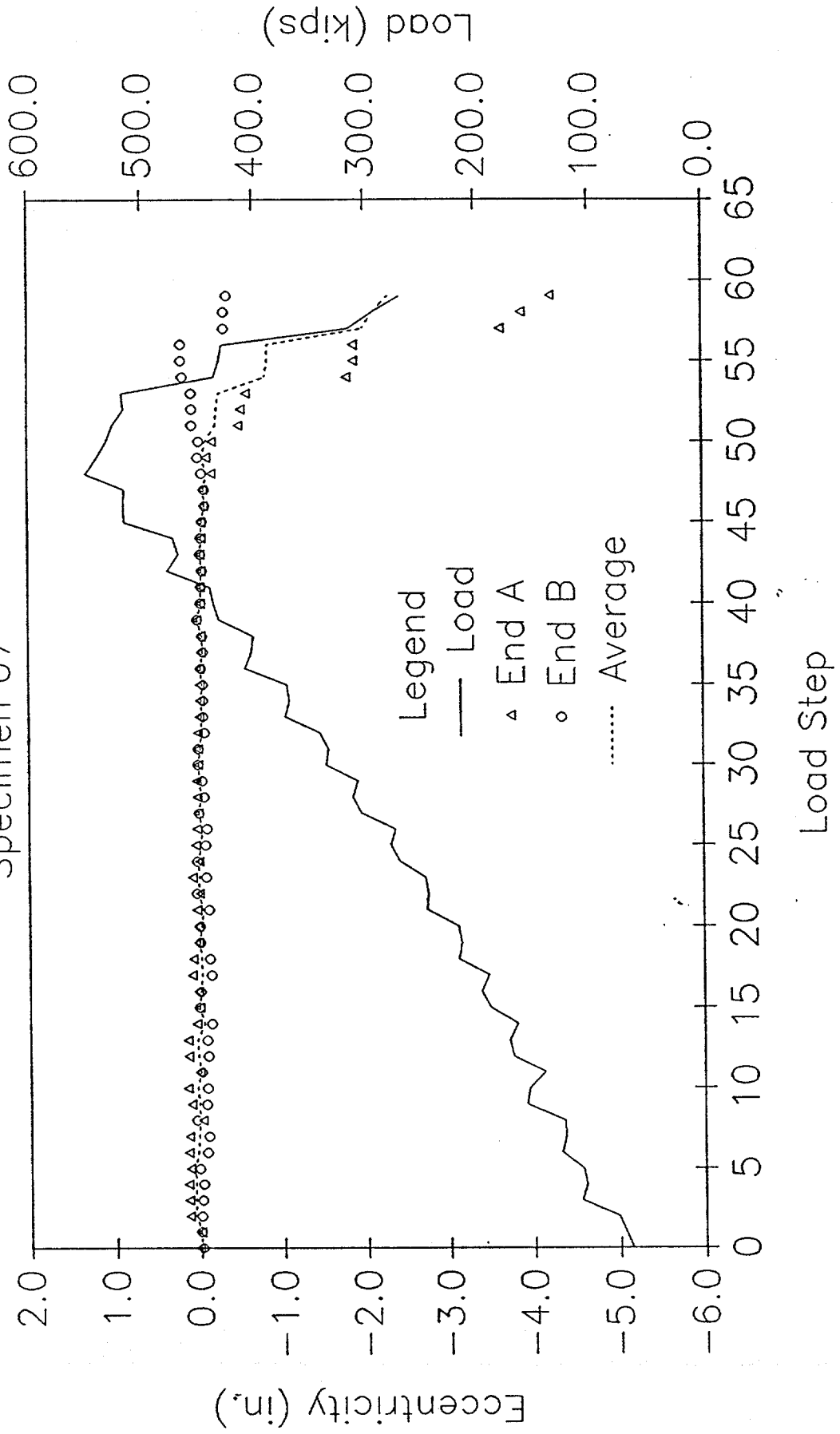
LOAD AND ECCENTRICITY vs LOAD STEP

y Eccentricities from Inflection Points

Specimen 07



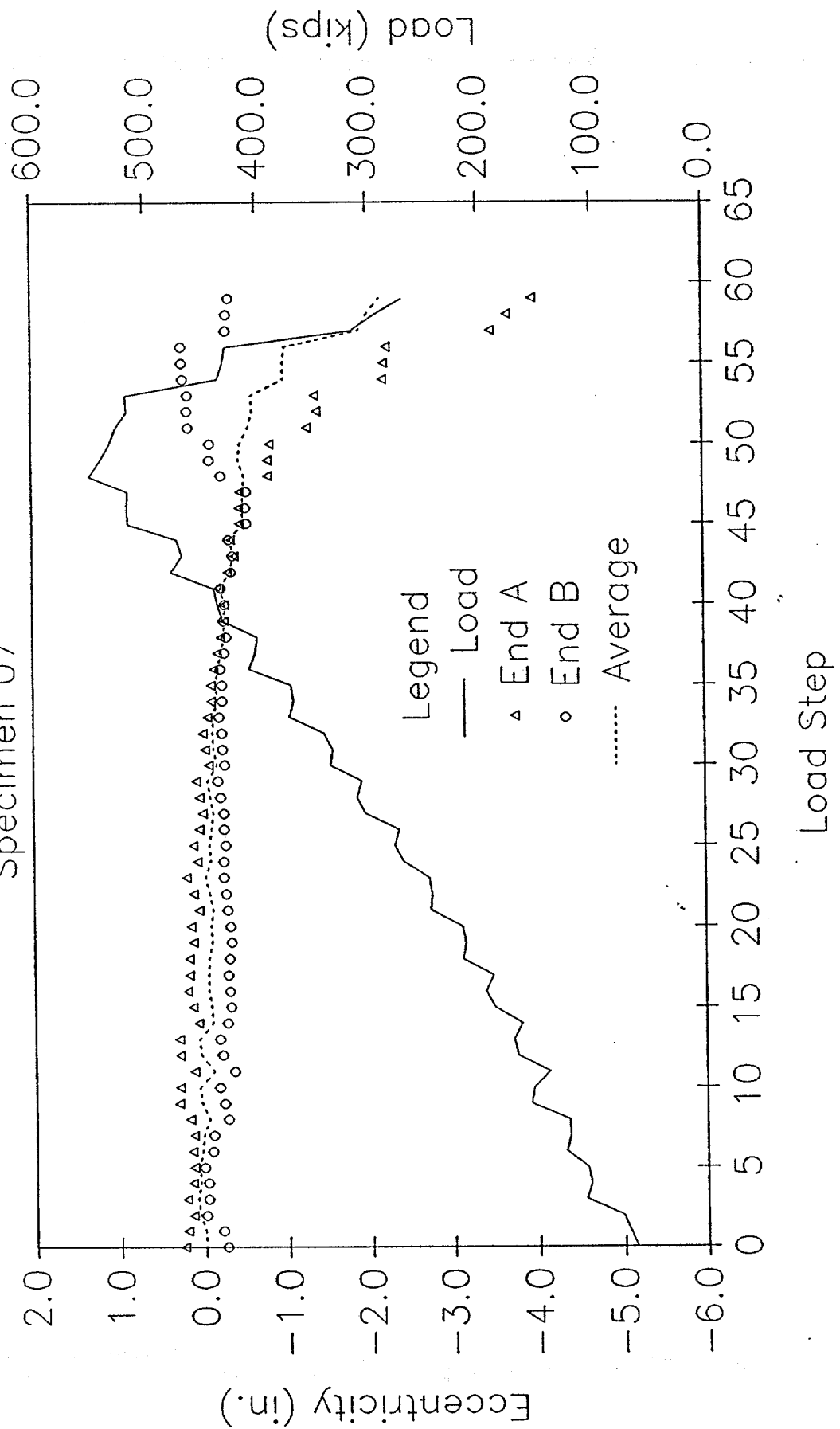
LOAD AND ECCENTRICITY vs LOAD STEP x Eccentricities from End Moments Specimen 07



LOAD AND ECCENTRICITY vs LOAD STEP

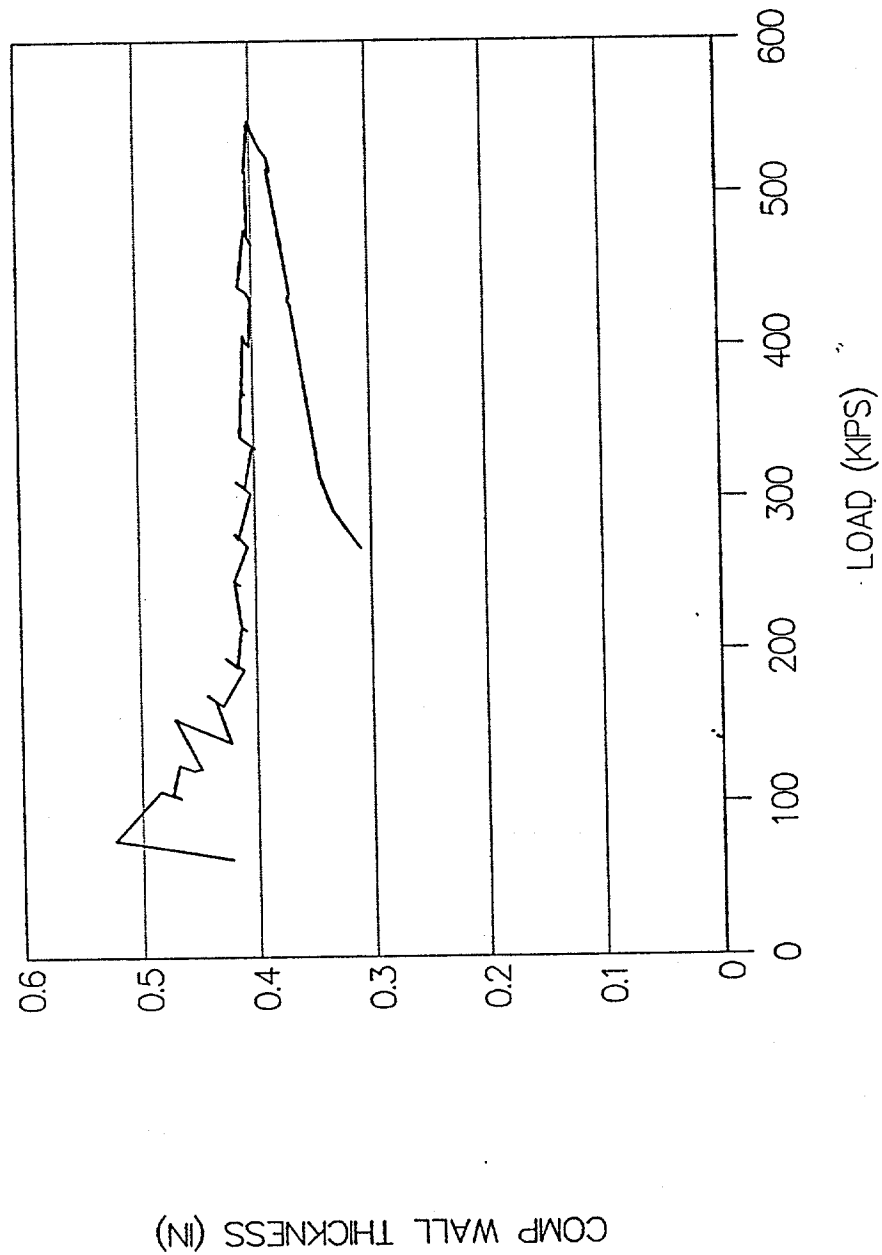
y Eccentricities from End Moments

Specimen 07

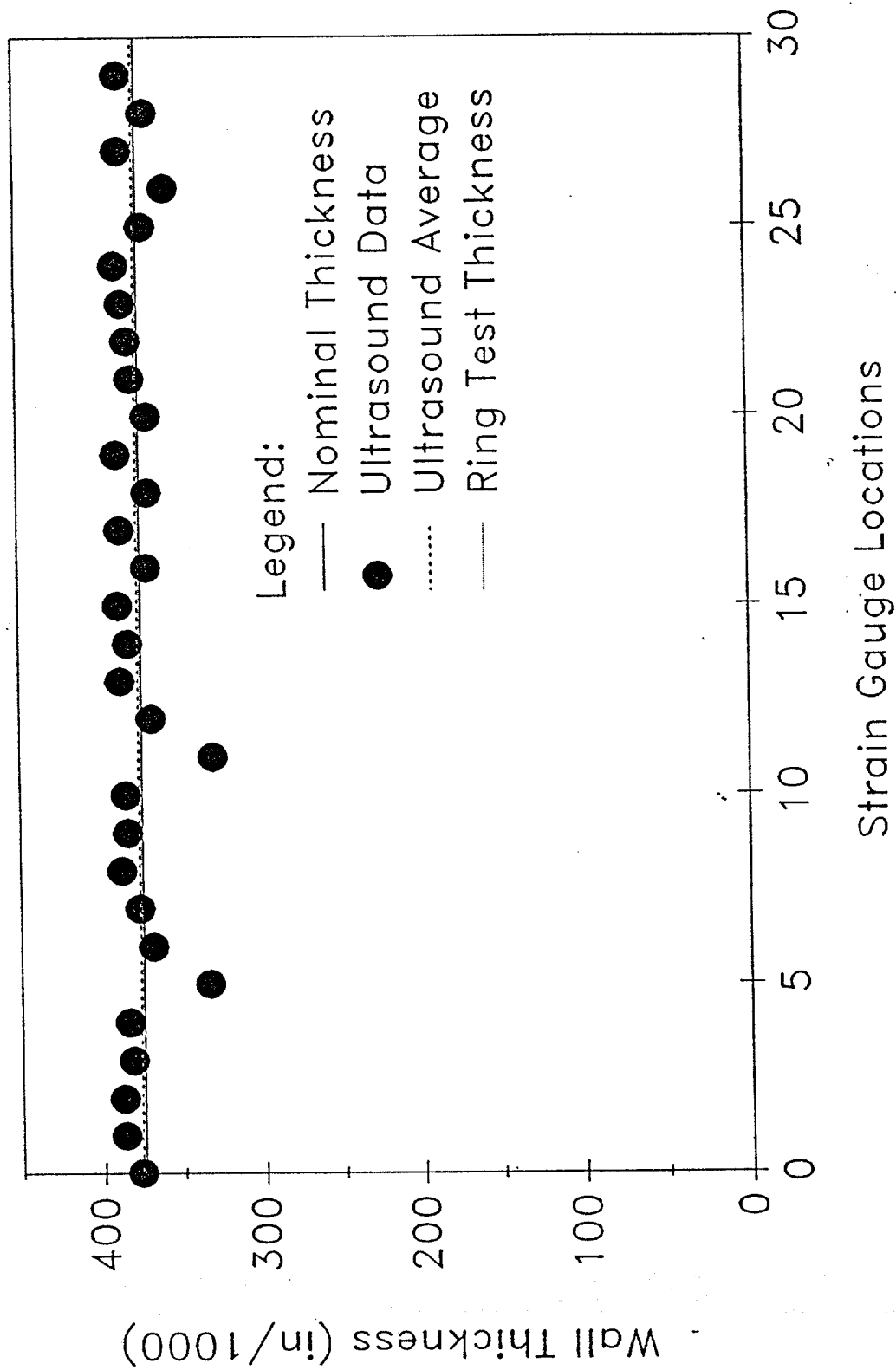


SPECIMEN 07-FULL SCALE TEST

COMPUTED WALL THICKNESS



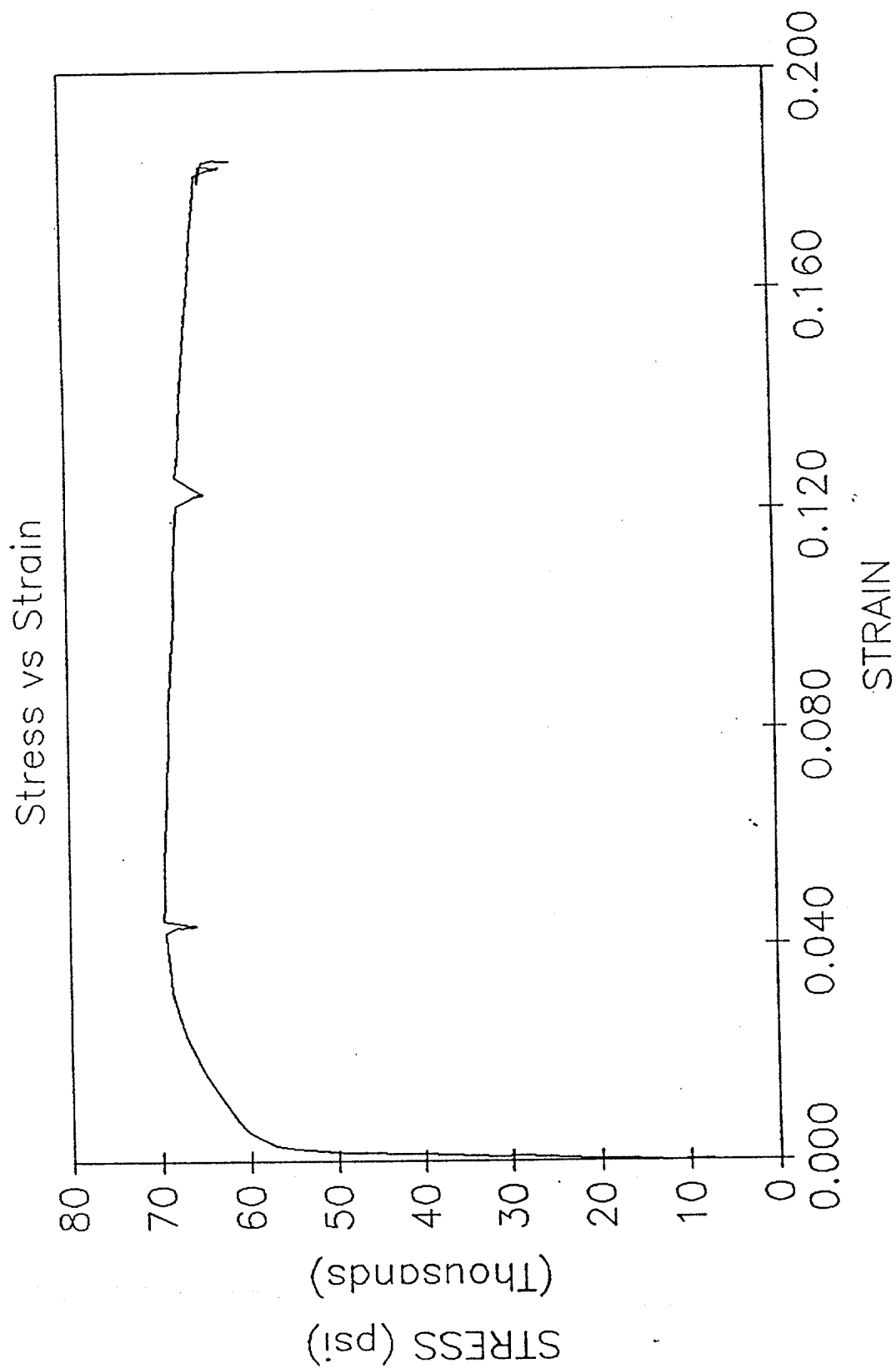
Specimen 07: Wall Thickness
Nominal Thickness = 0.375 in



Ultrasound Data for Specimen 7
(All data in inches)

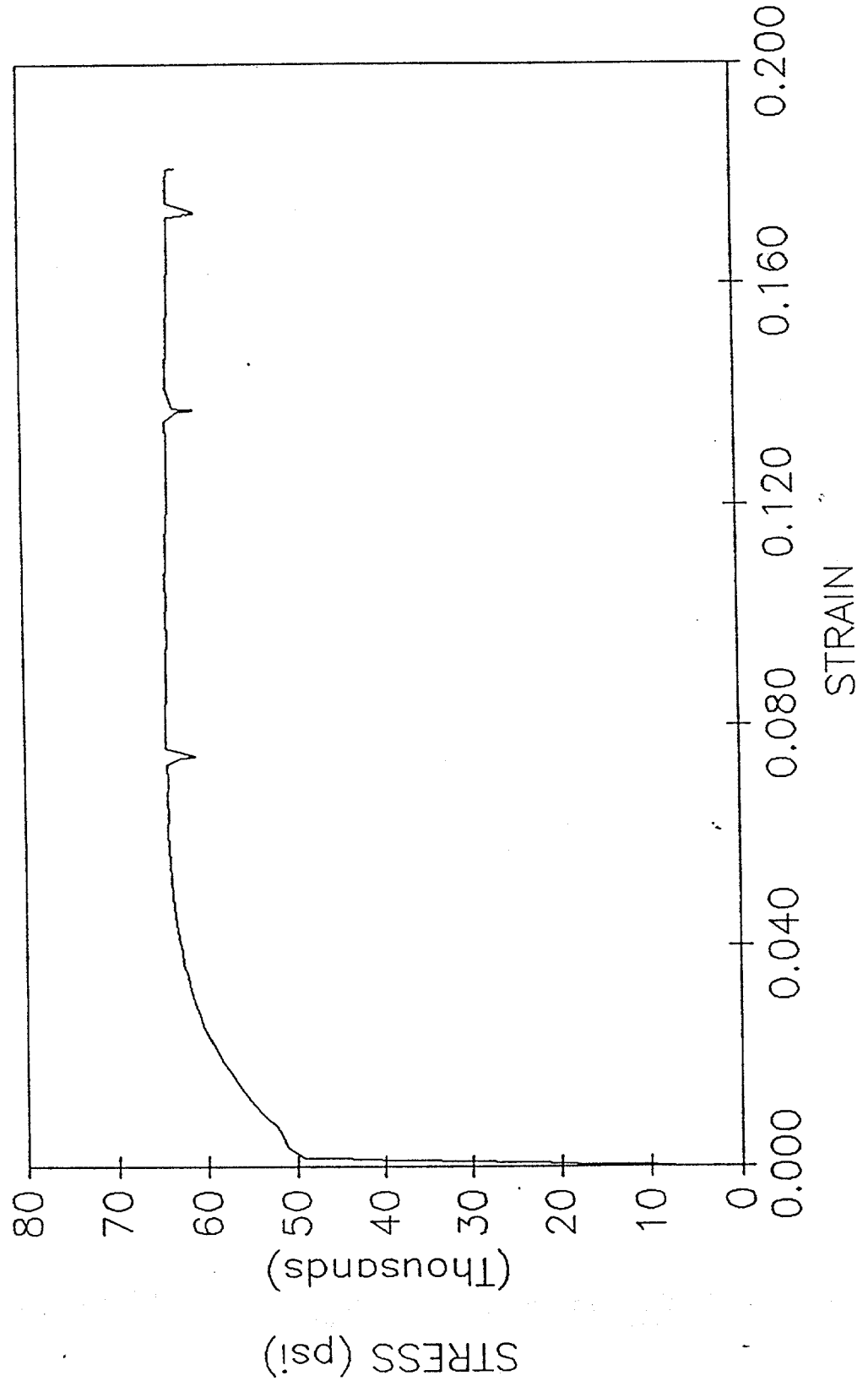
Gauge No.	UT Thickness	UT Average
0	0.377	
1	0.387	
2	0.388	
3	0.382	
4	0.384	
5	0.334	0.375
6	0.369	
7	0.377	
8	0.388	
9	0.384	
10	0.385	
11	0.331	0.372
12	0.369	
13	0.388	
14	0.383	
15	0.389	
16	0.371	
17	0.387	0.381
18	0.370	
19	0.389	
20	0.370	
21	0.380	
22	0.382	
23	0.385	0.379
24	0.389	
25	0.372	
26	0.358	
27	0.386	
28	0.370	
29	0.386	0.377
Overall Average =		0.377

TENSILE SPECIMEN 7-1



TENSILE SPECIMEN 7-2

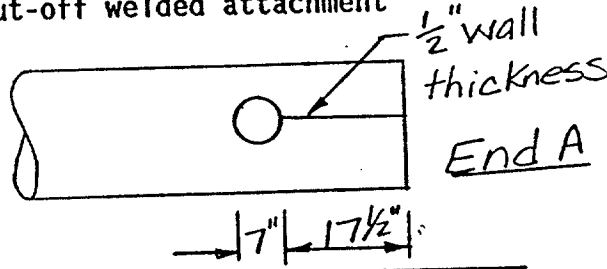
Stress vs Strain



SPECIMEN 08

DAMAGE SUMMARY

Specimen No. 8

DISTANCE FROM END "B"	*DISTANCE FROM CHALK LINE		DESCRIPTION OF DAMAGE
	LEFT	RIGHT	
1. 7 1/2"			3/4" circumferential butt weld
2. 3'-8"		6"	Dent - 5" diameter with 1/4" deflection at center (See additional sheets)
3. See drawing for location	6 1/2"		Cut-off welded attachment 

* Looking from end "A" towards end "B"

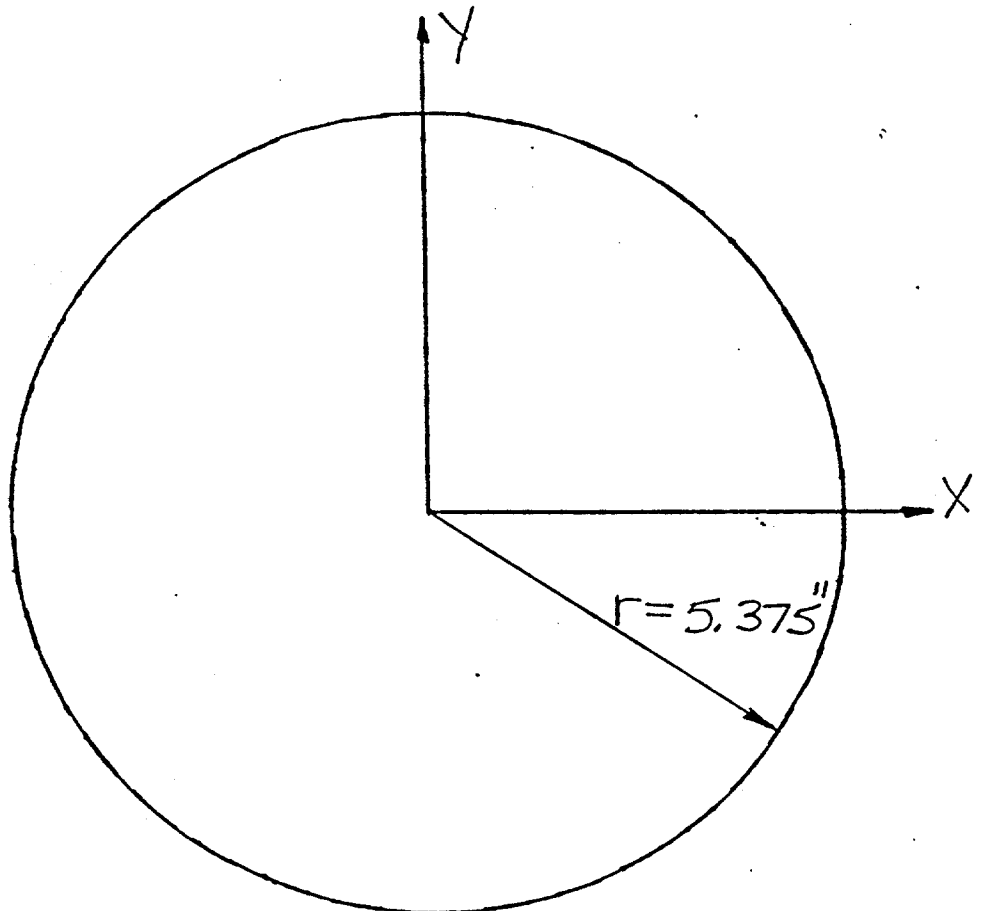
DENT CROSS SECTION

Specimen No. 8

Damage No. 2

Distance from End B 3'-5"

Scale 1" = 2.53"



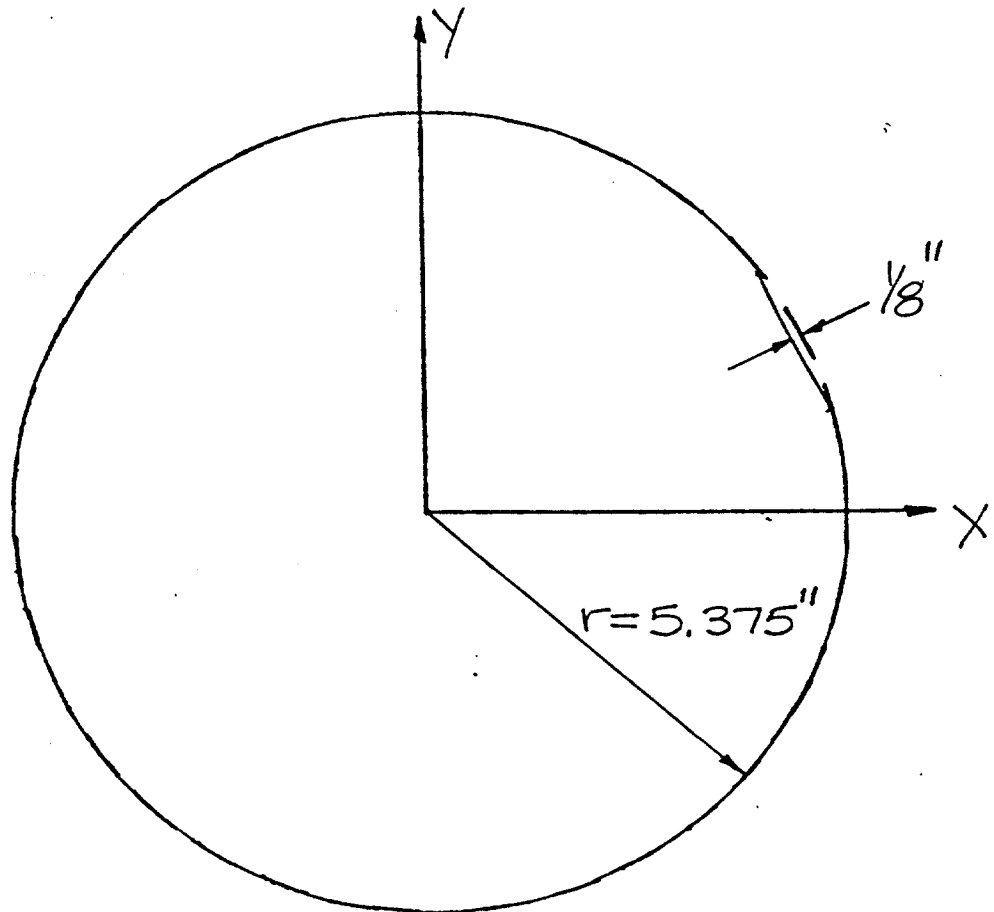
DENT CROSS SECTION

Specimen No. 8

Damage No. 2

Distance from End B 3'-6"

Scale 1" = 2.53"



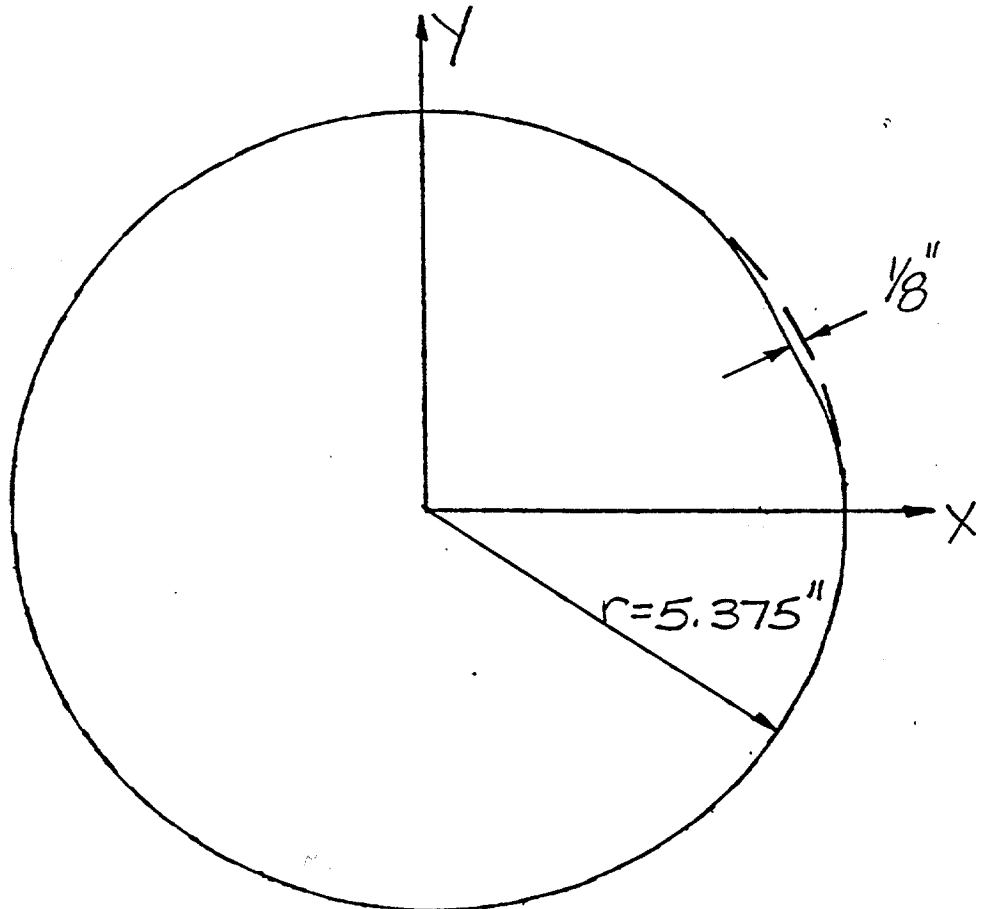
DENT CROSS SECTION

Specimen No. 8

Damage No. 2

Distance from End B 3'-7"

Scale 1" = 2.53"



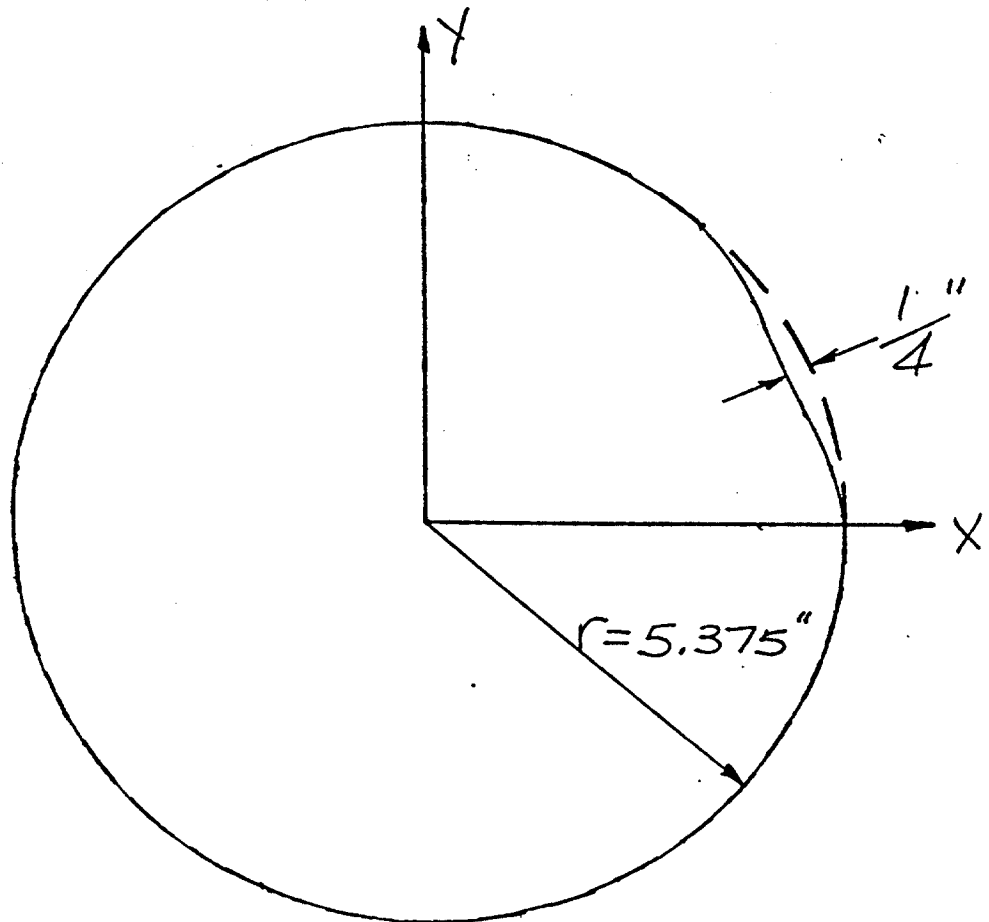
DENT CROSS SECTION

Specimen No. 8

Damage No. 2

Distance from End B 3'-8"

Scale 1" = 2.53"



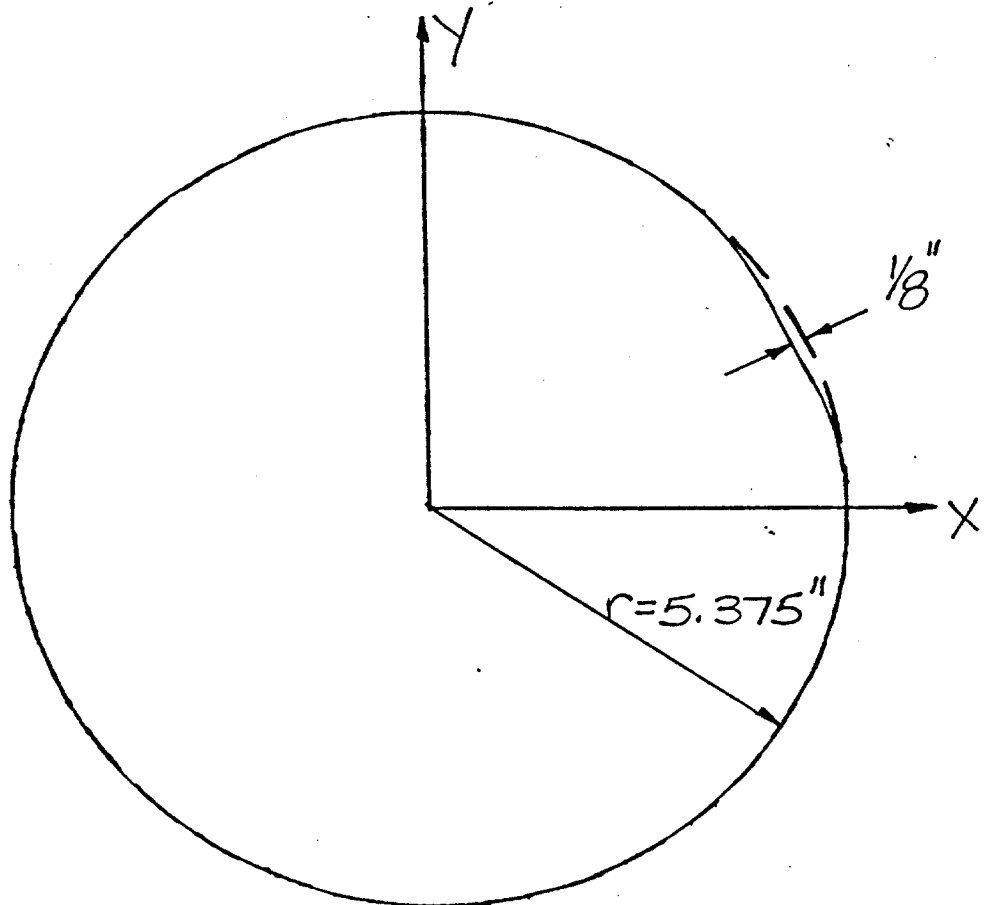
DENT CROSS SECTION

Specimen No. 8

Damage No. 2

Distance from End B 3'-9"

Scale 1" = 2.53"



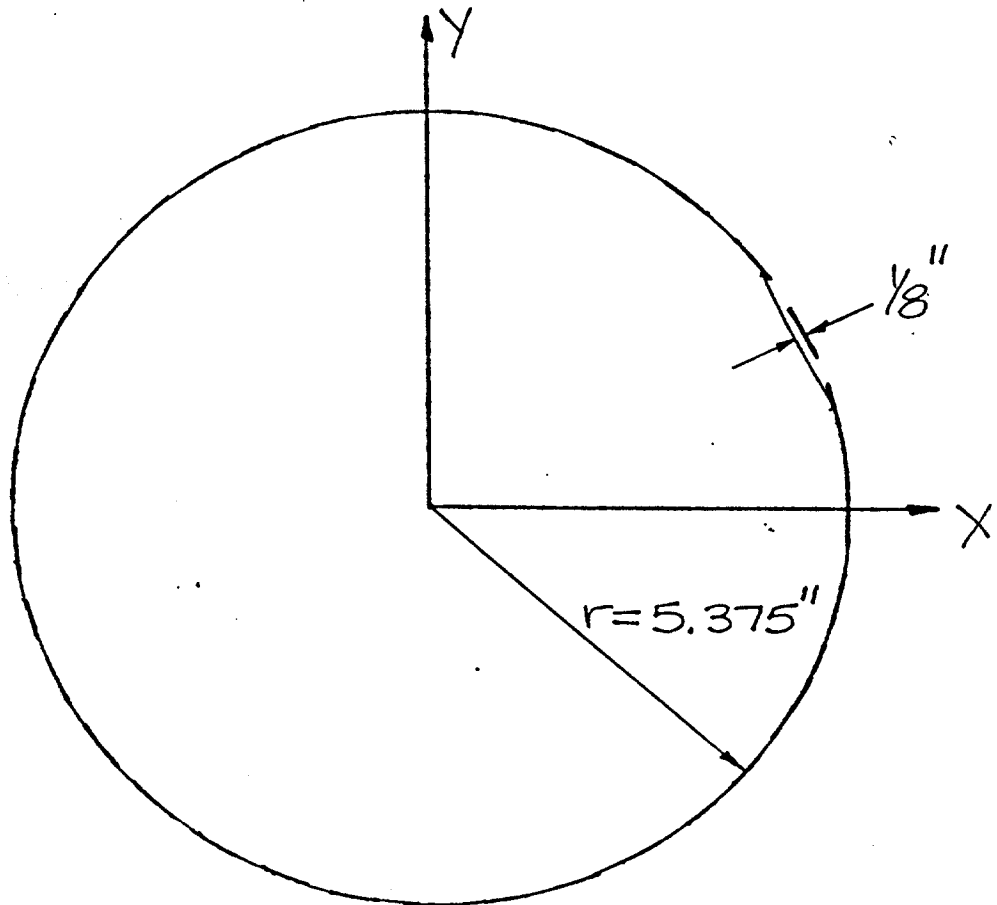
DENT CROSS SECTION

Specimen No. 8

Damage No. 2

Distance from End B 3'-10"

Scale 1" = 2.53"



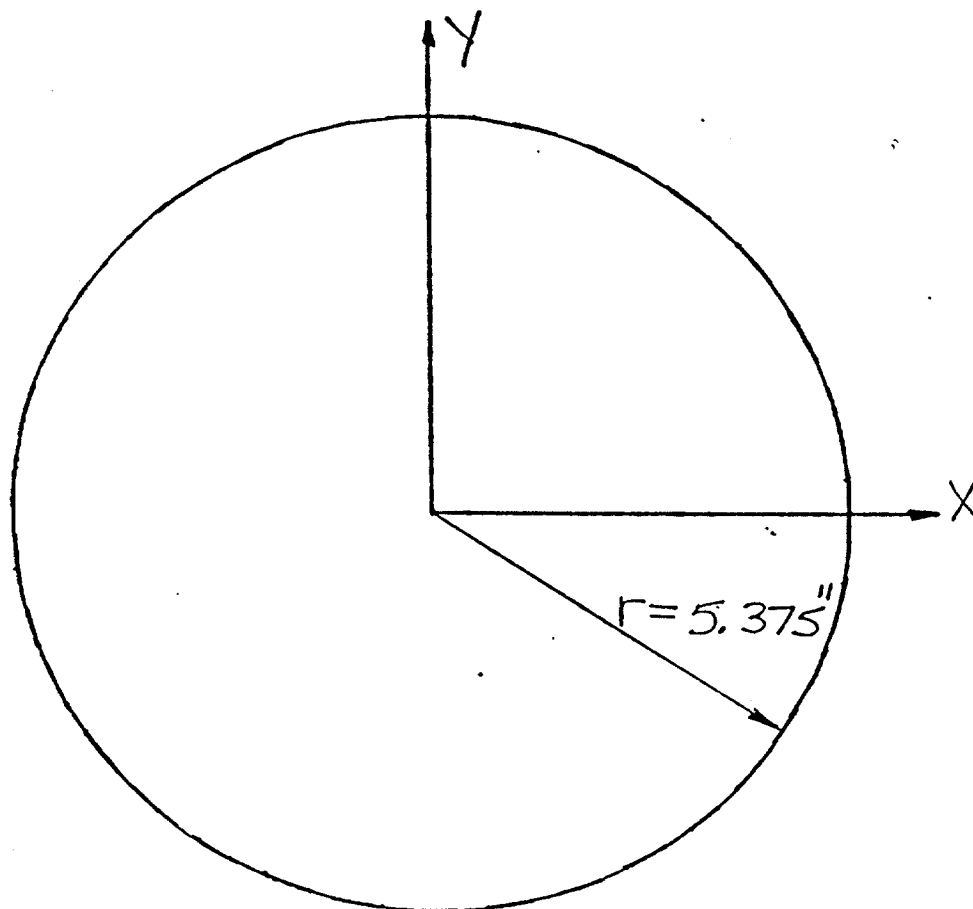
DENT CROSS SECTION

Specimen No. 8

Damage No. 2

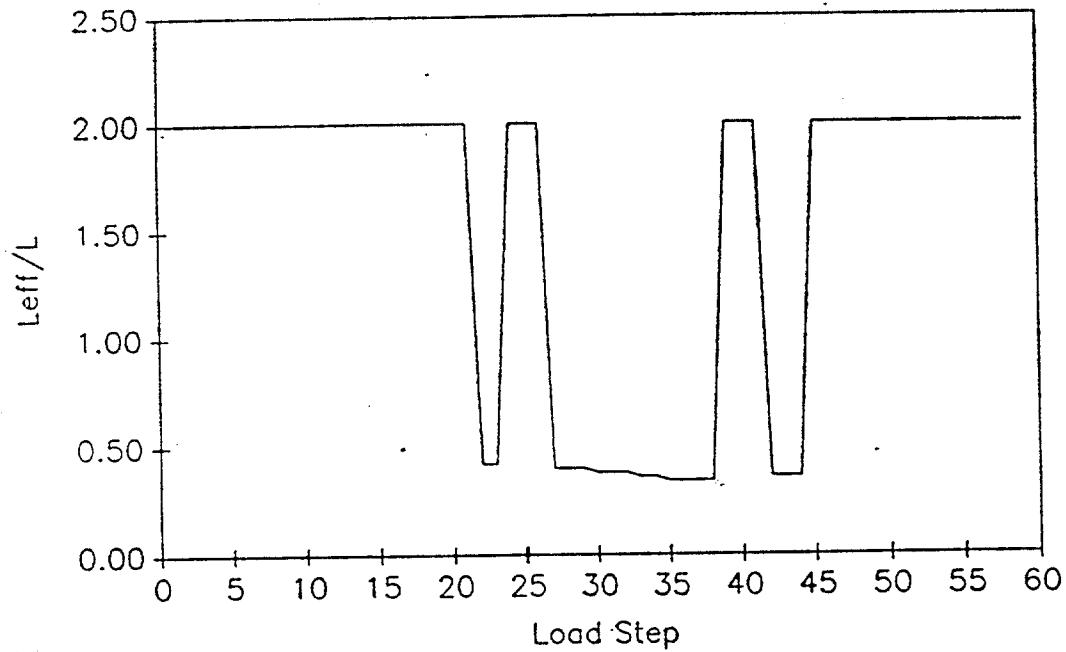
Distance from End B 3'-11"

Scale 1" = 2.53"



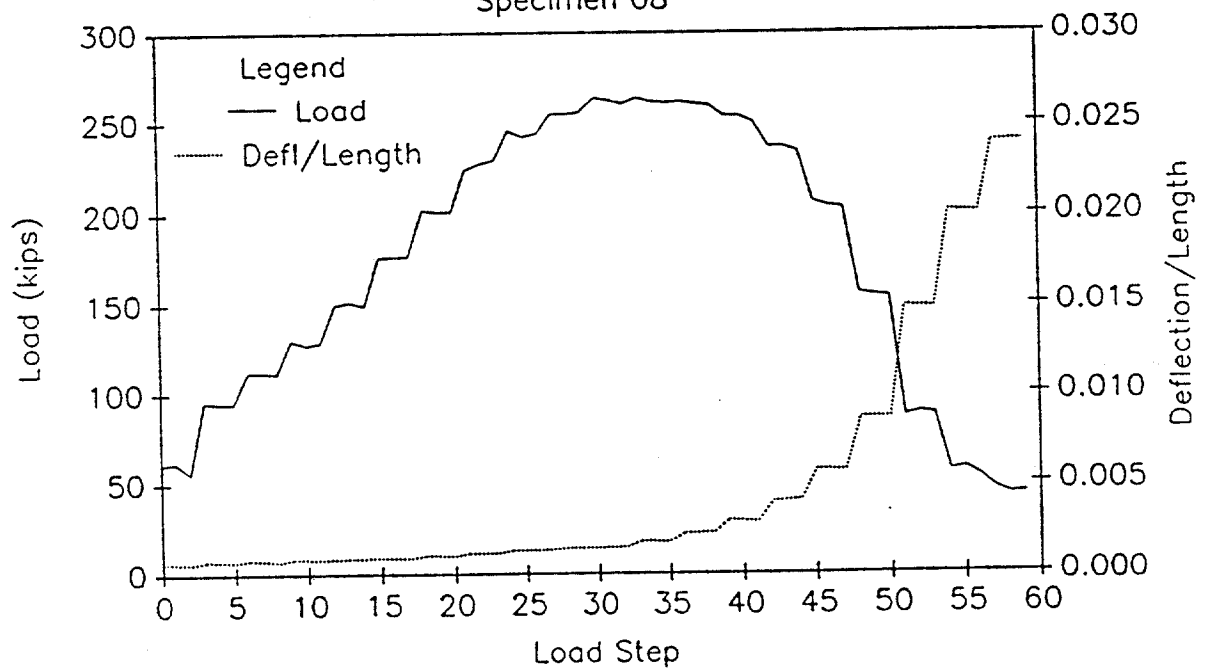
EFFECTIVE LENGTH vs LOAD STEP

Specimen 08



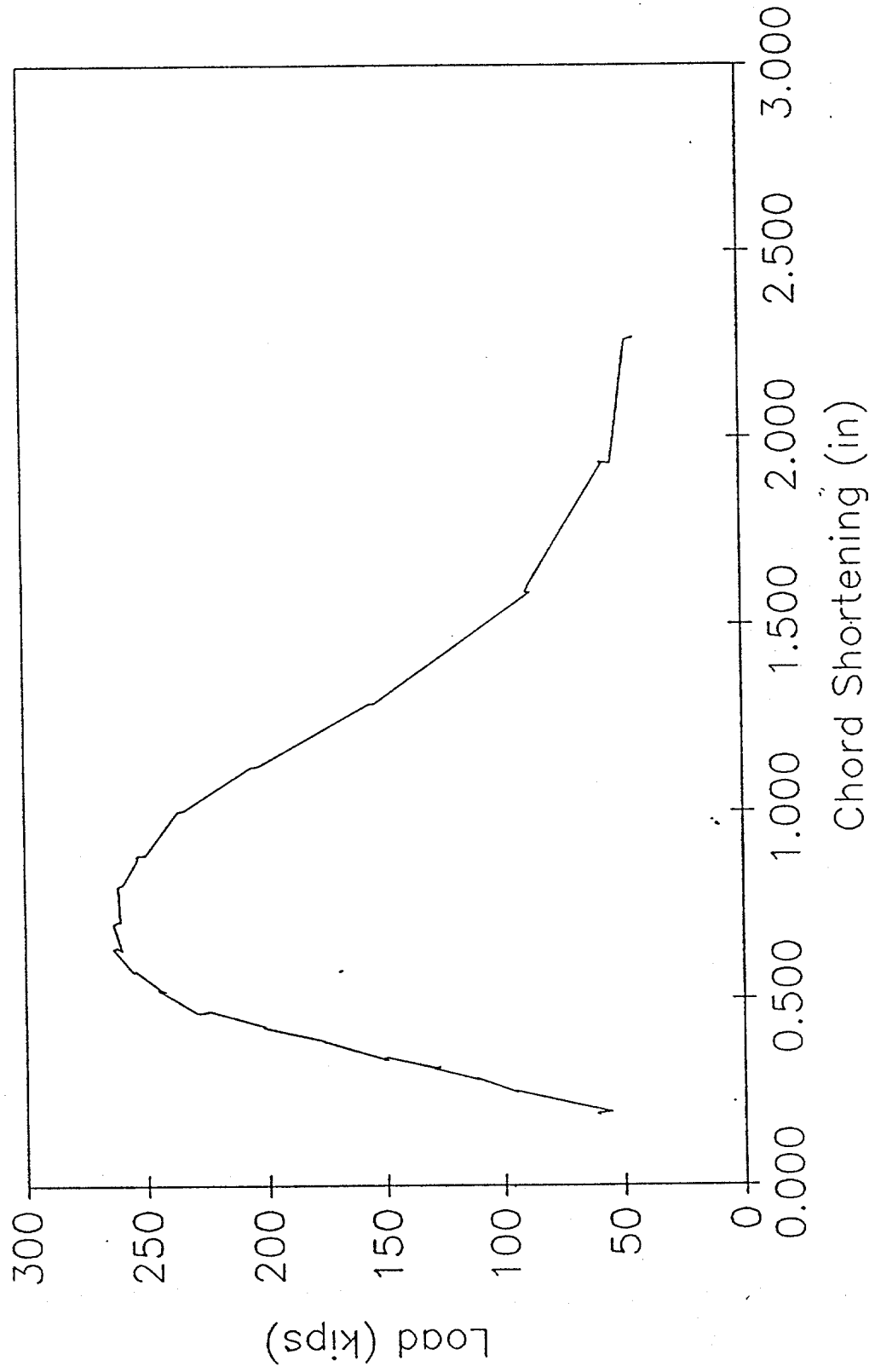
LOAD AND DEFLECTION vs LOAD STEP

Specimen 08



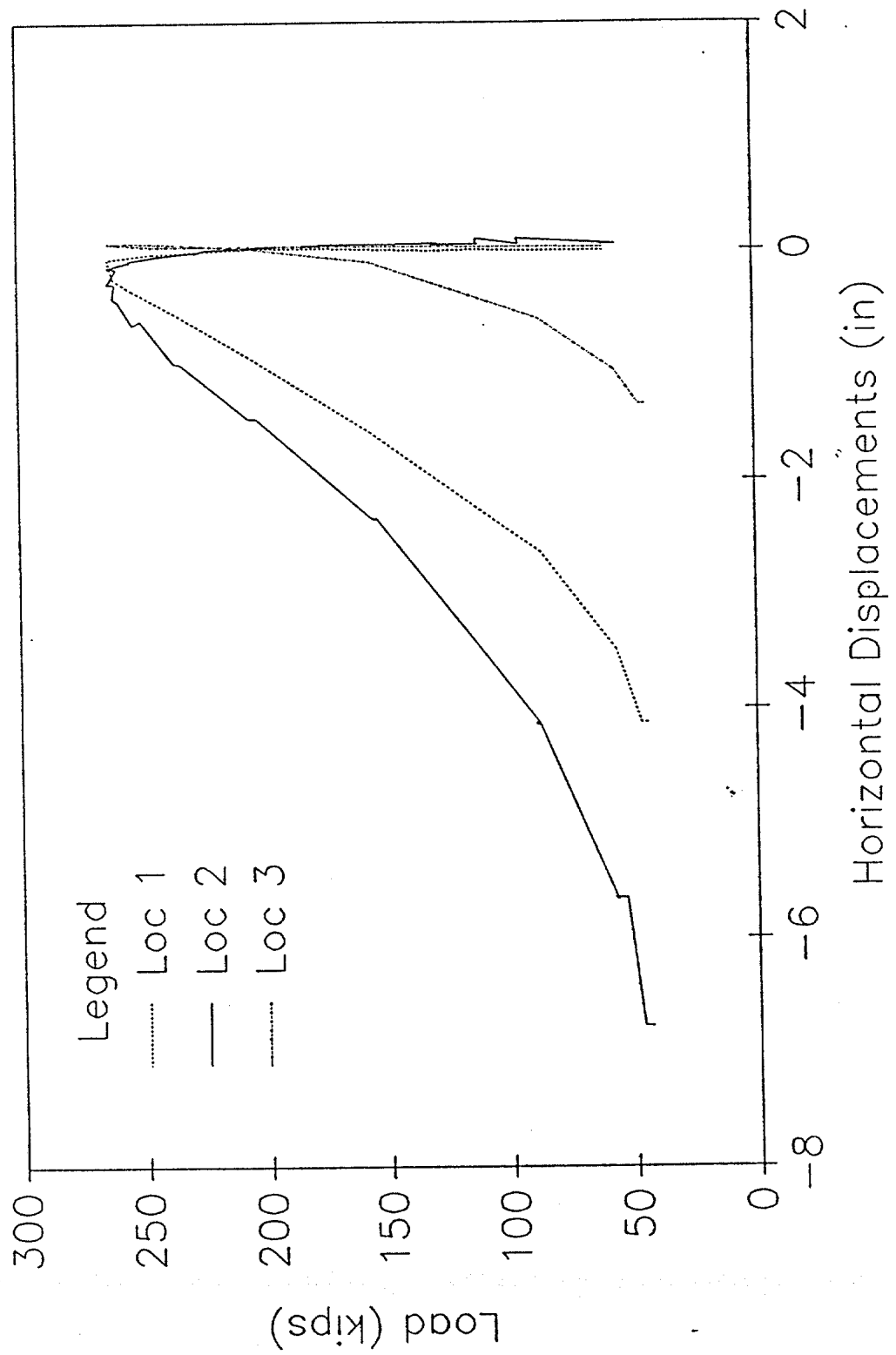
LOAD vs CHORD SHORTENING

Specimen 08



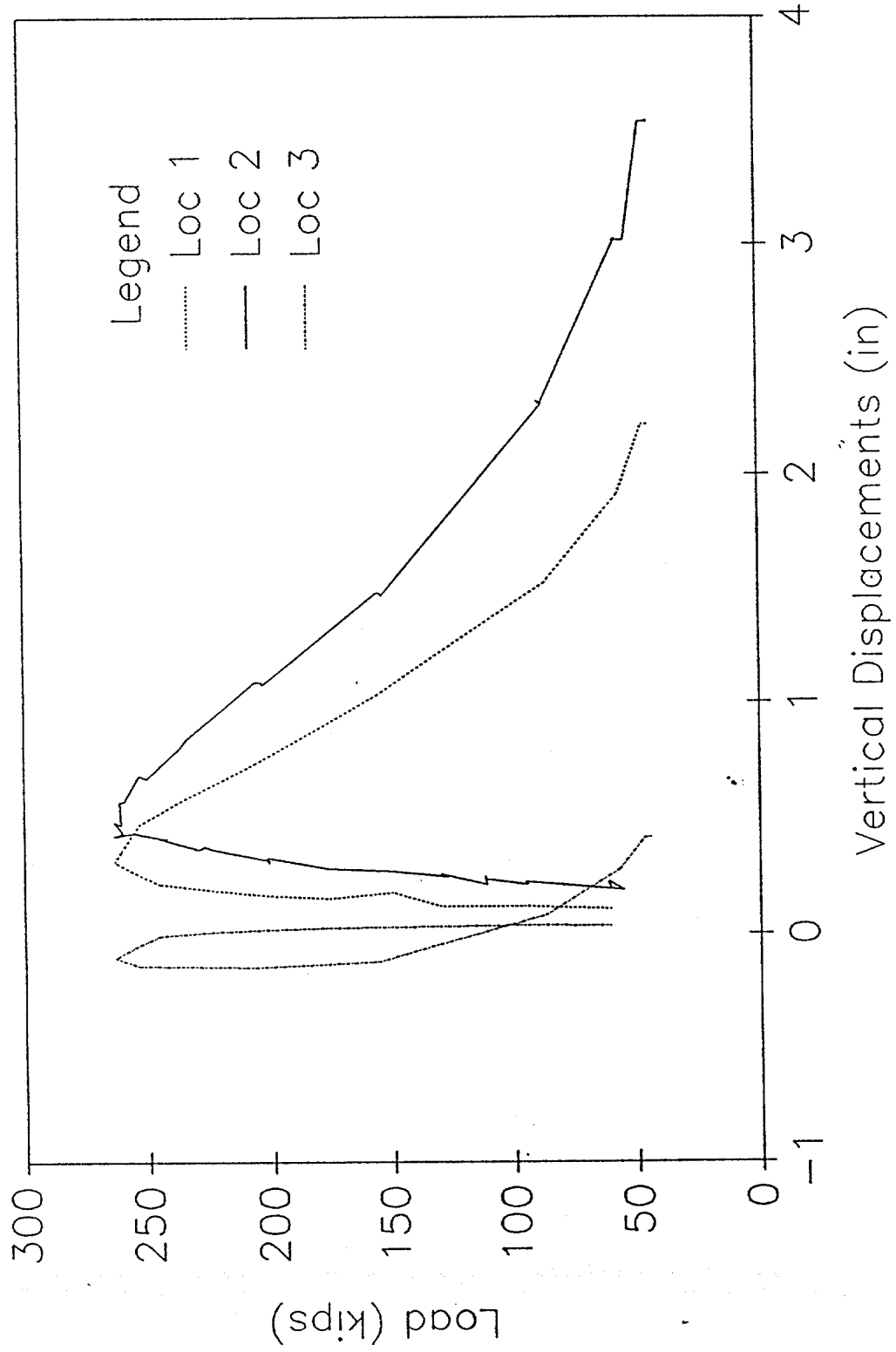
HORIZONTAL DISPLACEMENTS

Specimen 08



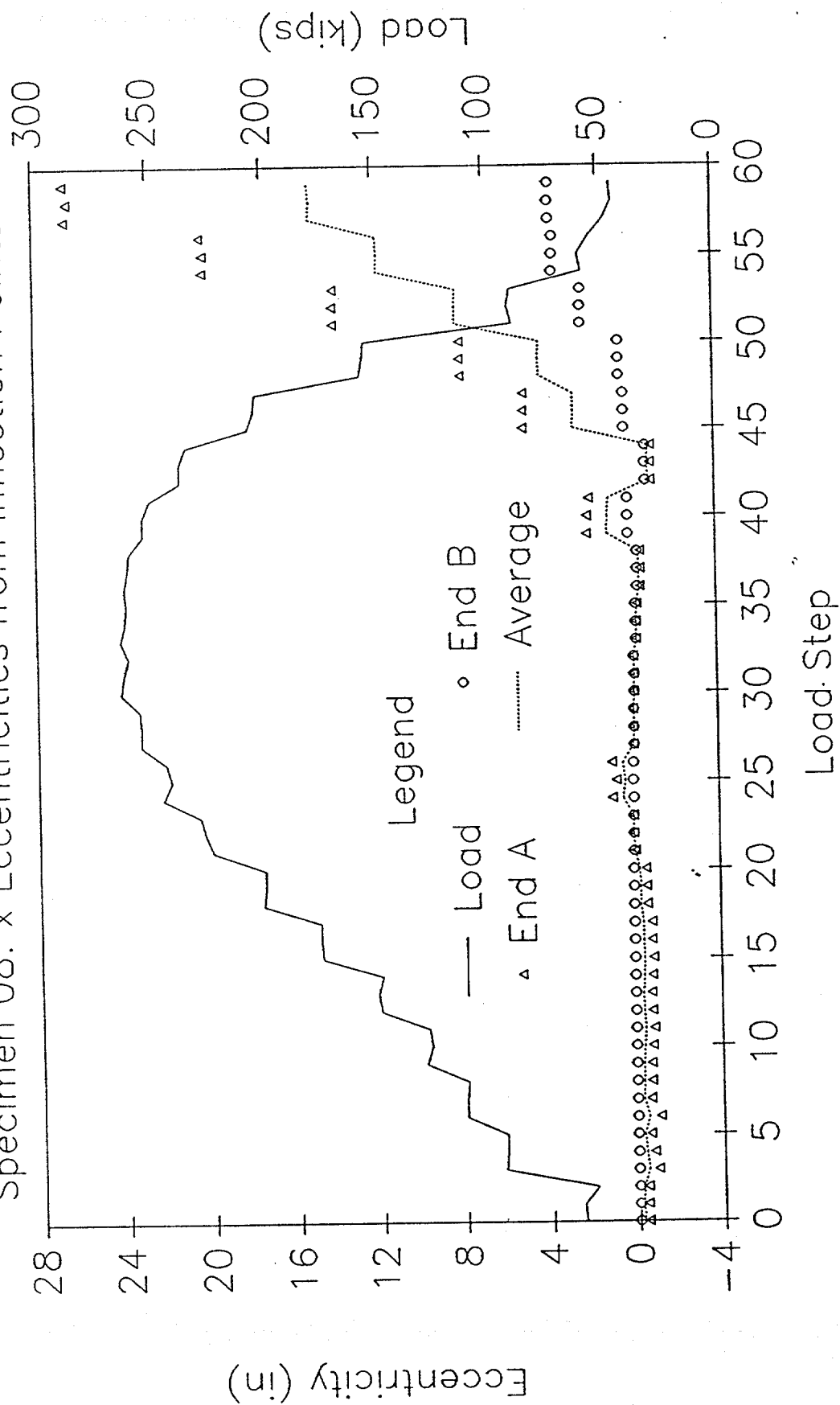
VERTICAL DISPLACEMENTS

Specimen 08



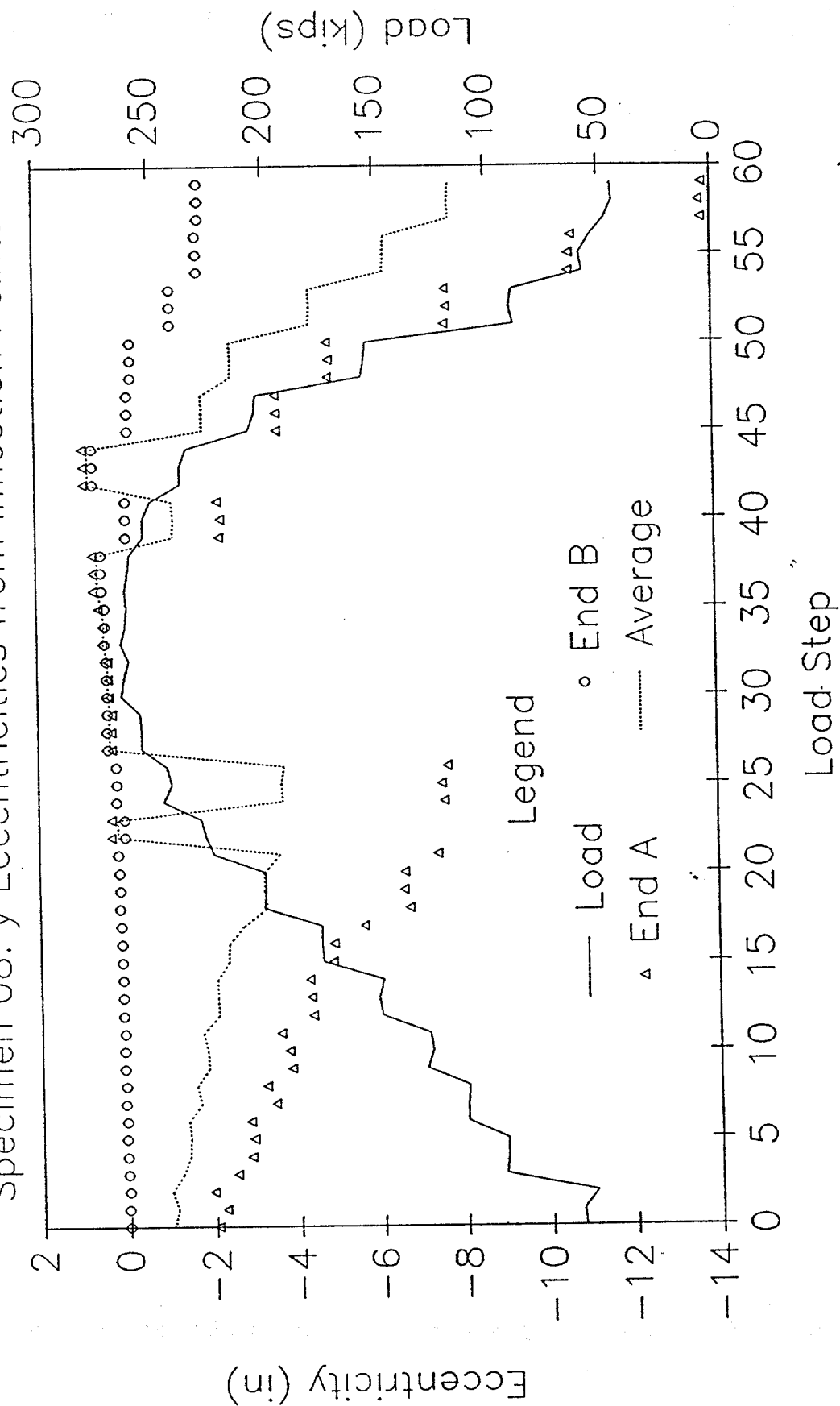
LOAD AND ECCENTRICITY vs LOAD STEP

Specimen 08: x Eccentricities from Inflection Points



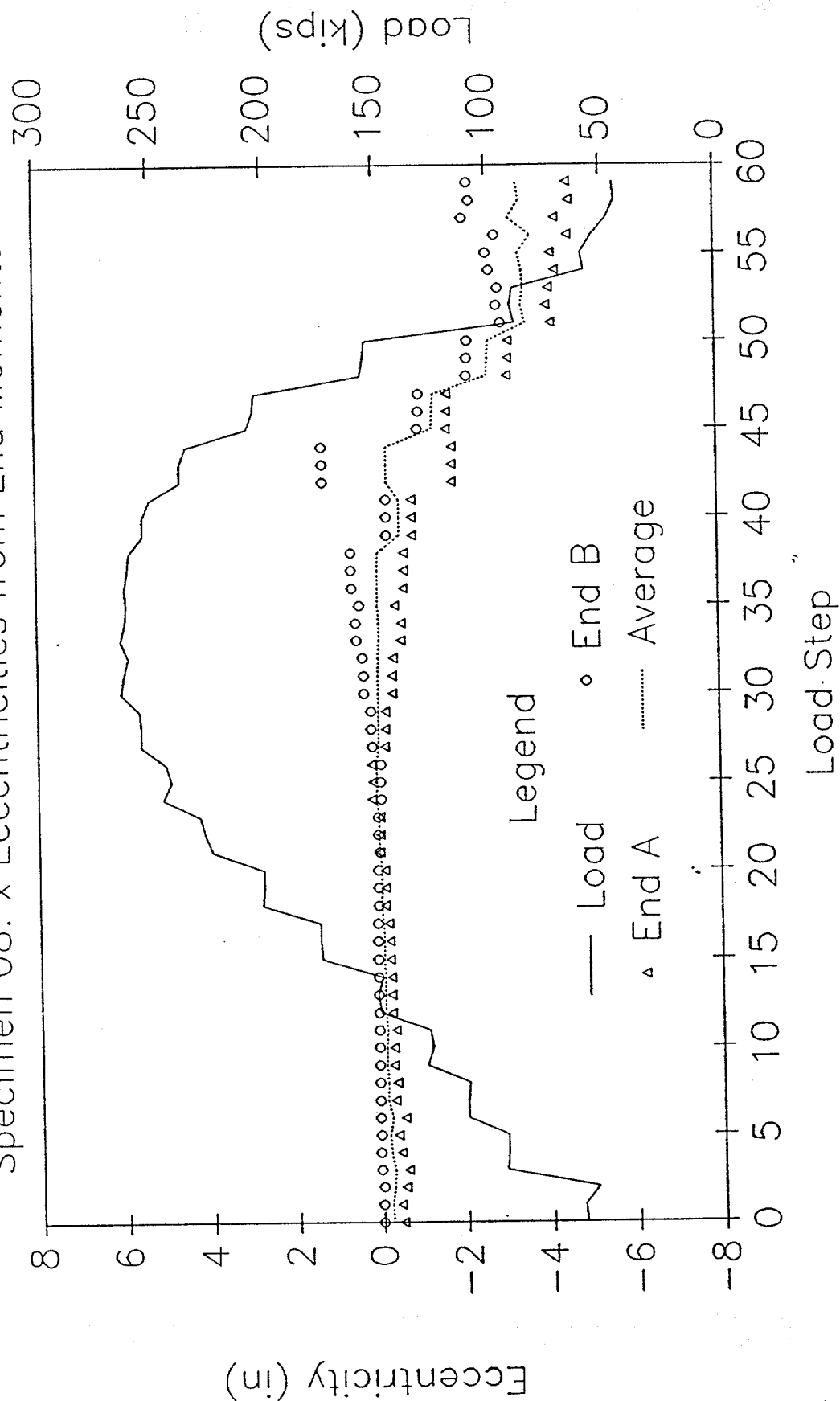
LOAD AND ECCENTRICITY vs LOAD STEP

Specimen 08: y Eccentricities from Inflection Points



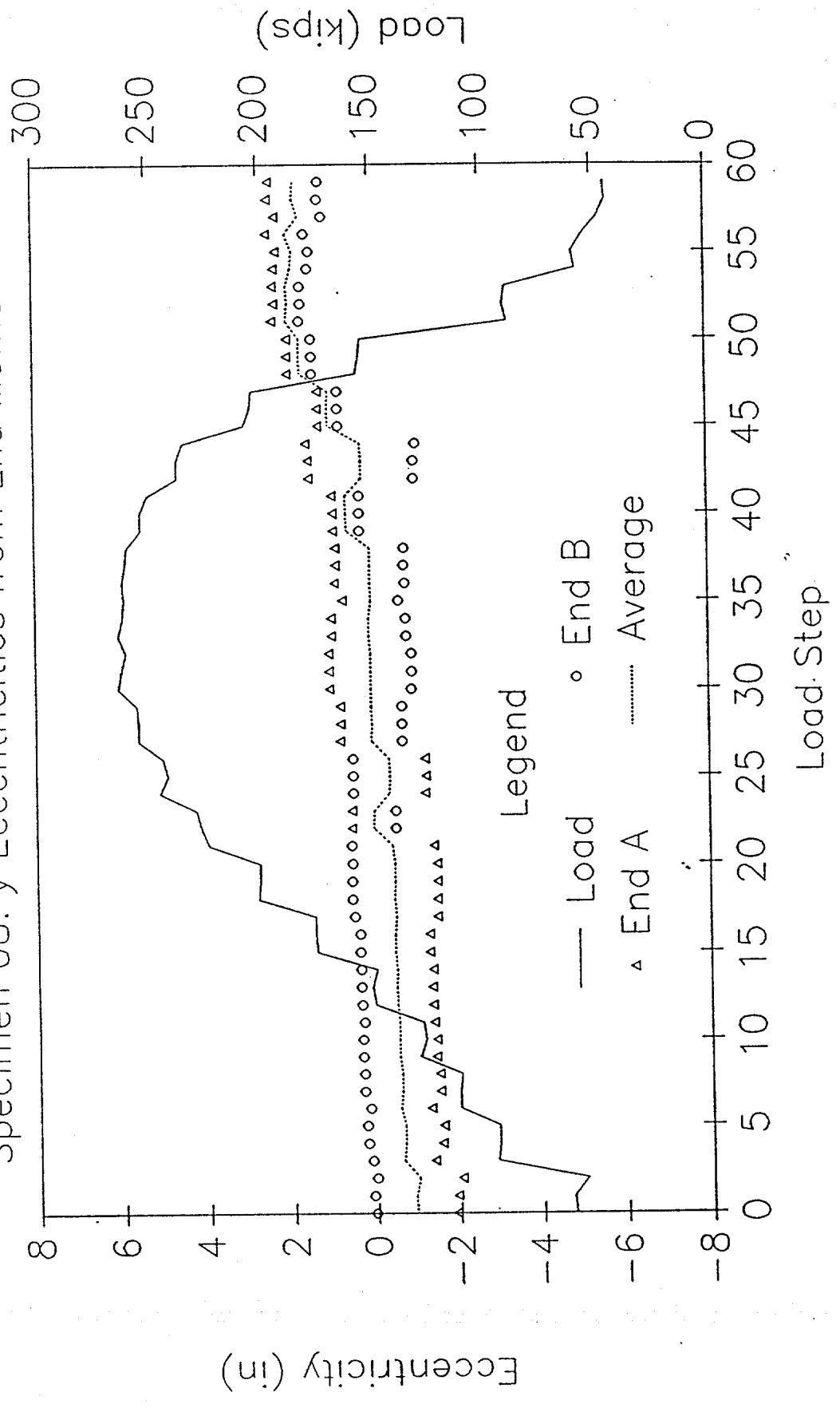
LOAD AND ECCENTRICITY vs LOAD STEP

Specimen 08: x Eccentricities from End Moments



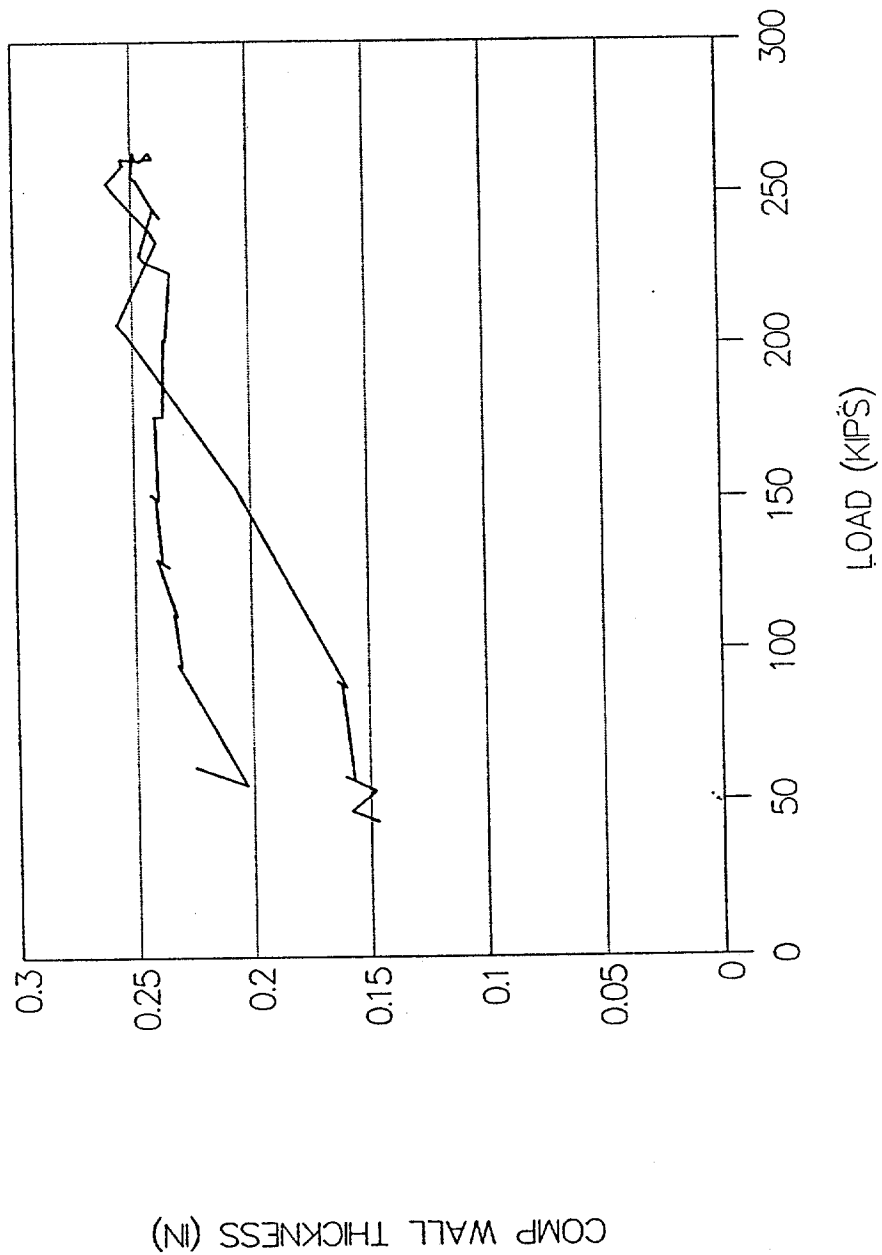
LOAD AND ECCENTRICITY vs LOAD STEP

Specimen 08: y Eccentricities from End Moments



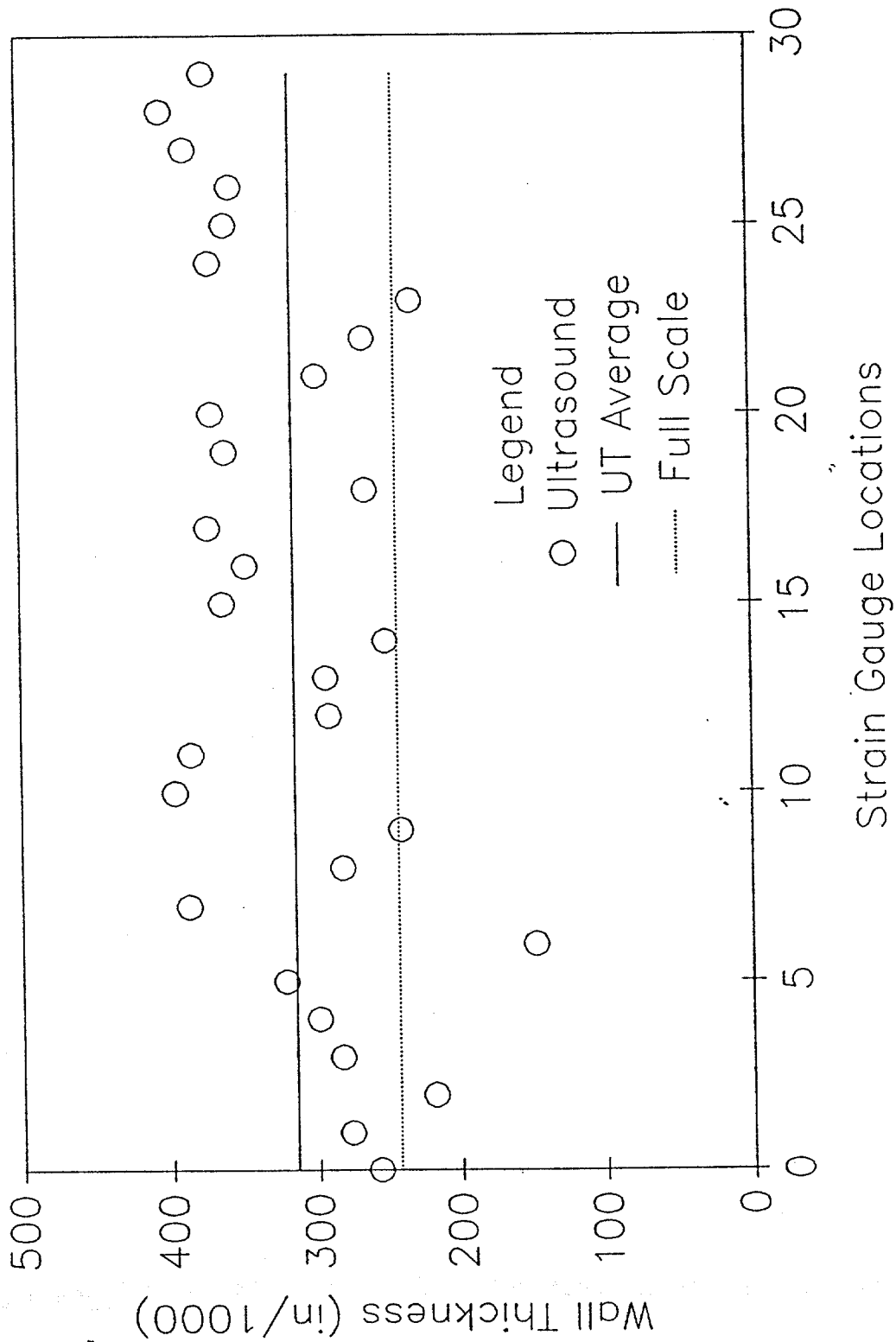
SPECIMEN 08—FULL SCALE TEST

COMPUTED WALL THICKNESS



SPECIMEN 08: WALL THICKNESS

Nominal Wall Thickness = 0.375 in



Ultrasound Data for Specimen 8
(All values in inches)

Gauge No.	UT Thickness	UT Average
0	0.257	
1	0.277	
2	0.218	
3	0.283	
4	0.299	
5	0.322	0.276
6	0.148	
7	0.388	
8	0.282	
9	0.241	
10	0.397	
11	0.386	0.307
12	0.291	
13	0.293	
14	0.251	
15	0.364	
16	0.348	
17	0.373	0.320
18	0.264	
19	0.361	
20	0.370	
21	0.298	
22	0.265	
23	0.231	0.298
24	0.371	
25	0.360	
26	0.356	
27	0.387	
28	0.403	
29	0.374	0.375

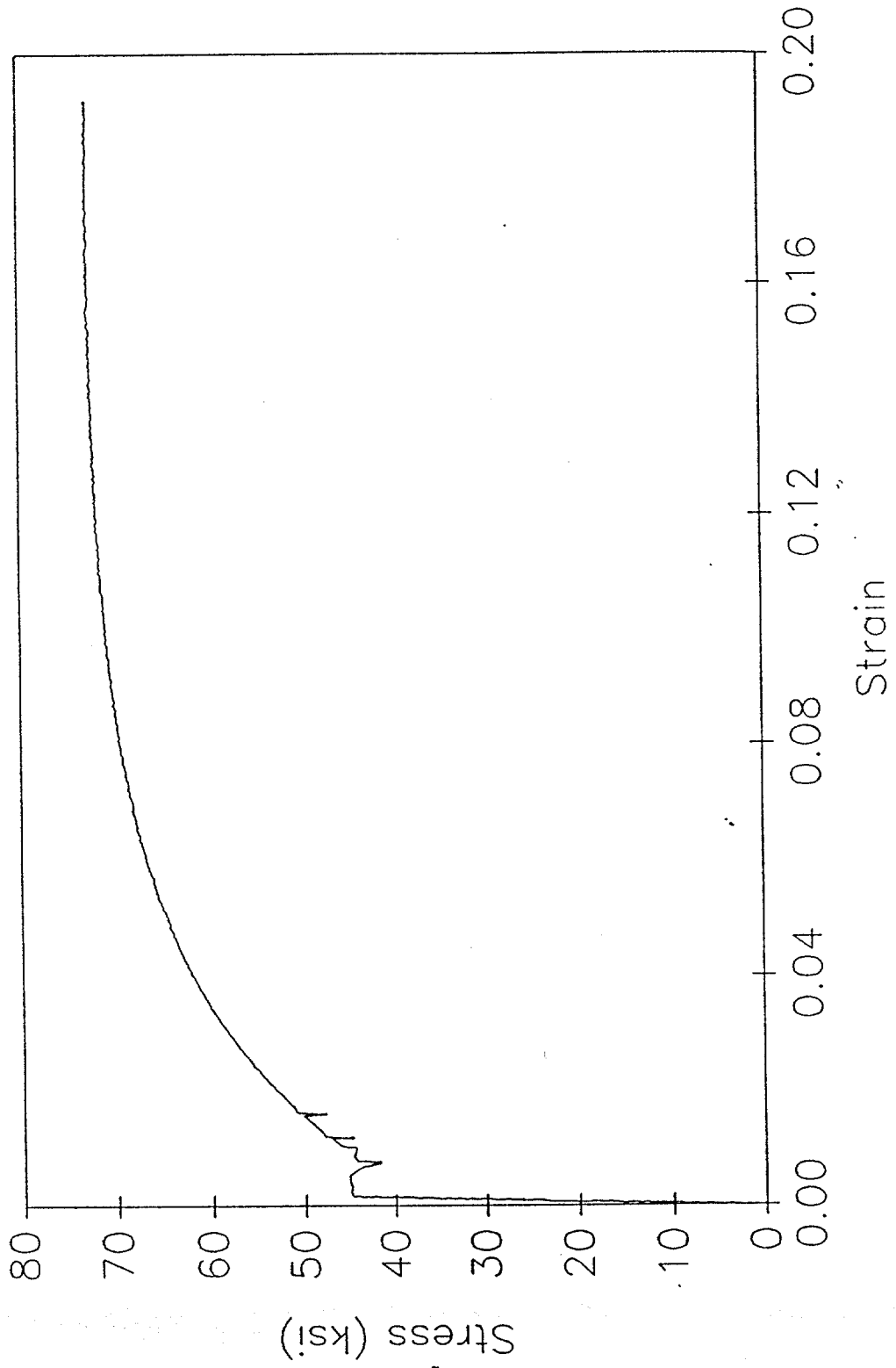
Overall Average = 0.315

Random Readings near Buckling Point

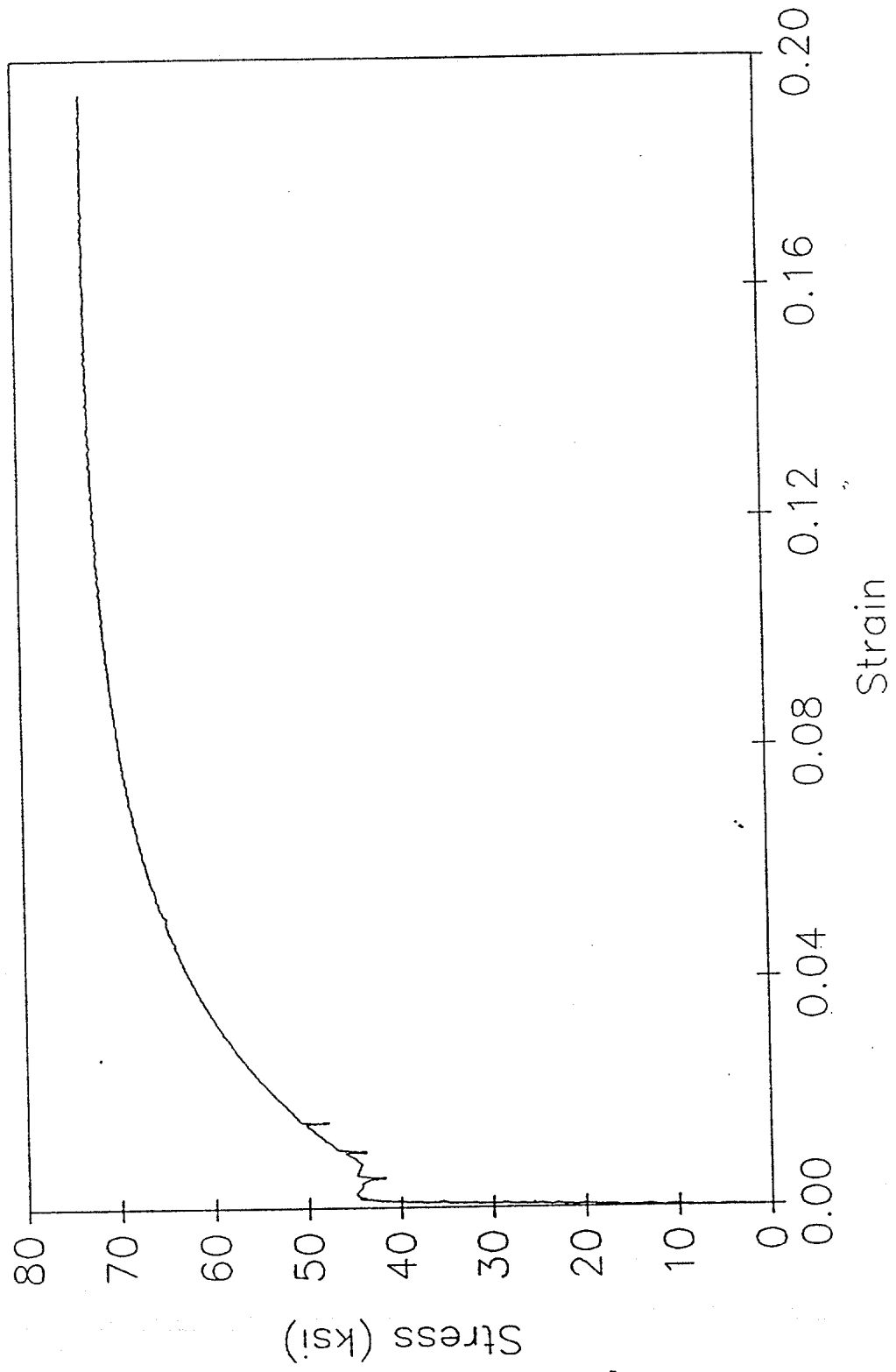
No.	Reading
1	0.212
2	0.280
3	0.213
4	0.277
5	0.224
6	0.292
7	0.294
8	0.249
9	0.208
10	0.100
11	0.335
12	0.268
13	0.289
14	0.366
15	0.327

Random Average = 0.262

TENSILE SPECIMEN 8-1
Stress vs Strain



TENSILE SPECIMEN 8-2
Stress vs Strain



SPECIMEN 09

DAMAGE SUMMARY

Specimen No. 9

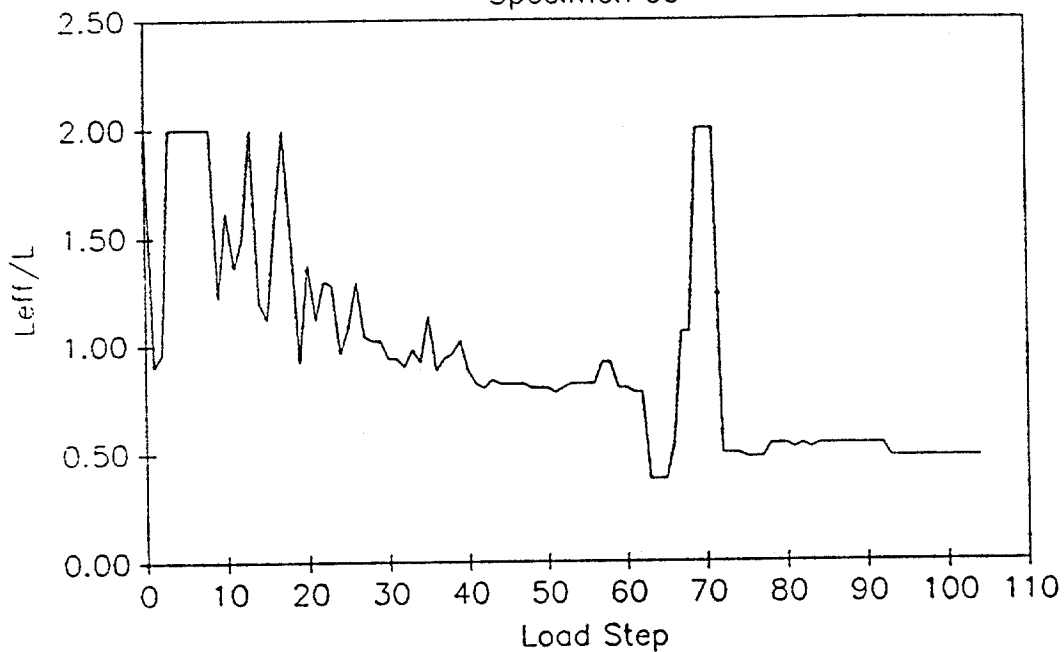
DISTANCE FROM END "B"	*DISTANCE FROM CHALK LINE		DESCRIPTION OF DAMAGE
	LEFT	RIGHT	
1. 14'-0 3/8"			3/4" circumferential butt weld

WIDESPREAD CORROSION ON SPECIMEN!

*Looking from end "A" towards end "B"

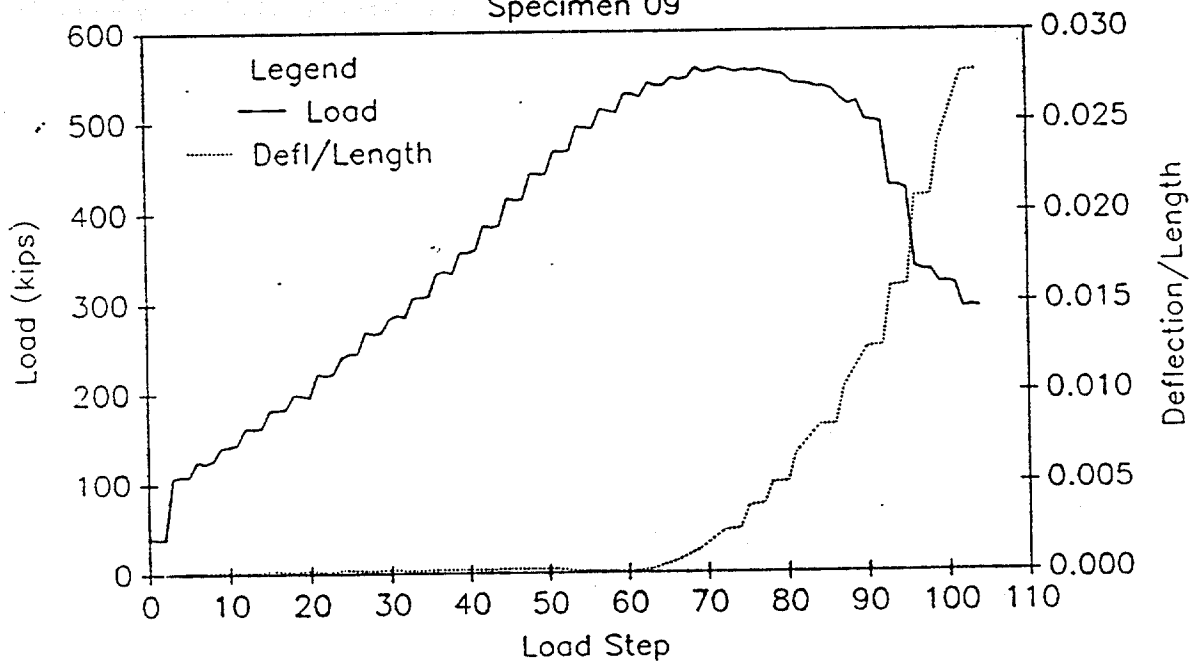
EFFECTIVE LENGTH vs LOAD STEP

Specimen 09



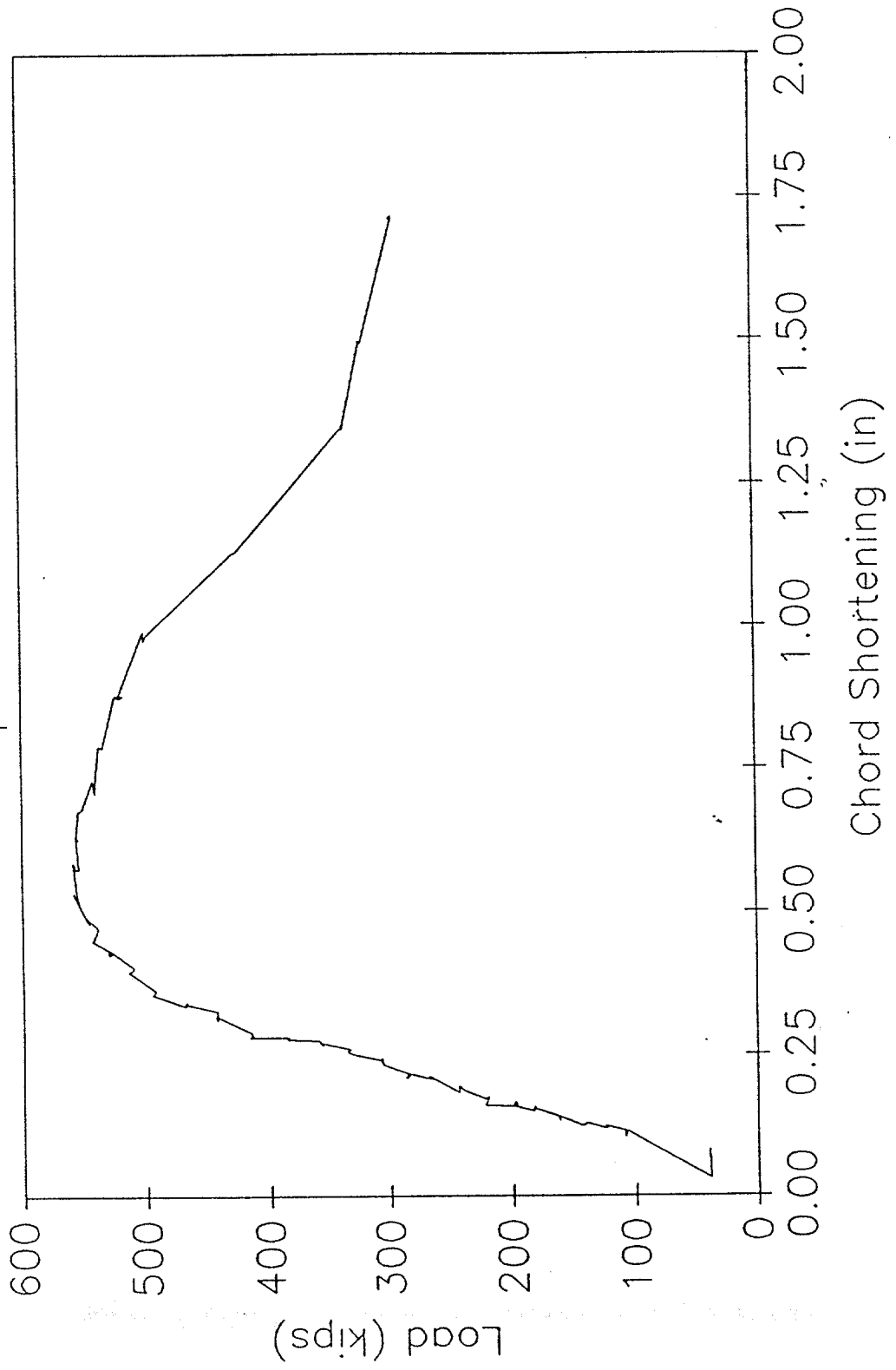
LOAD AND DEFLECTION vs LOAD STEP

Specimen 09



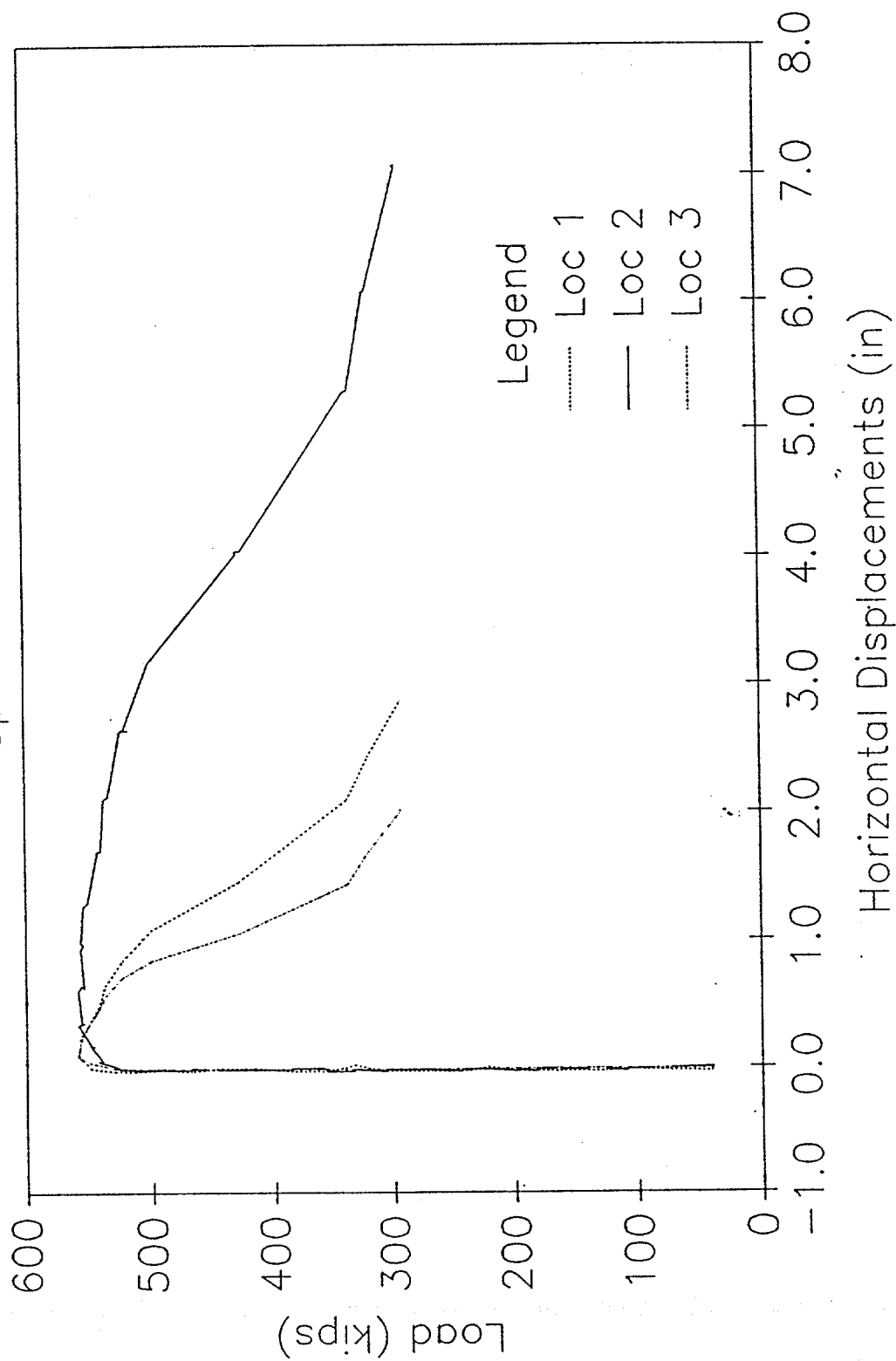
LOAD vs CHORD SHORTENING

Specimen 09



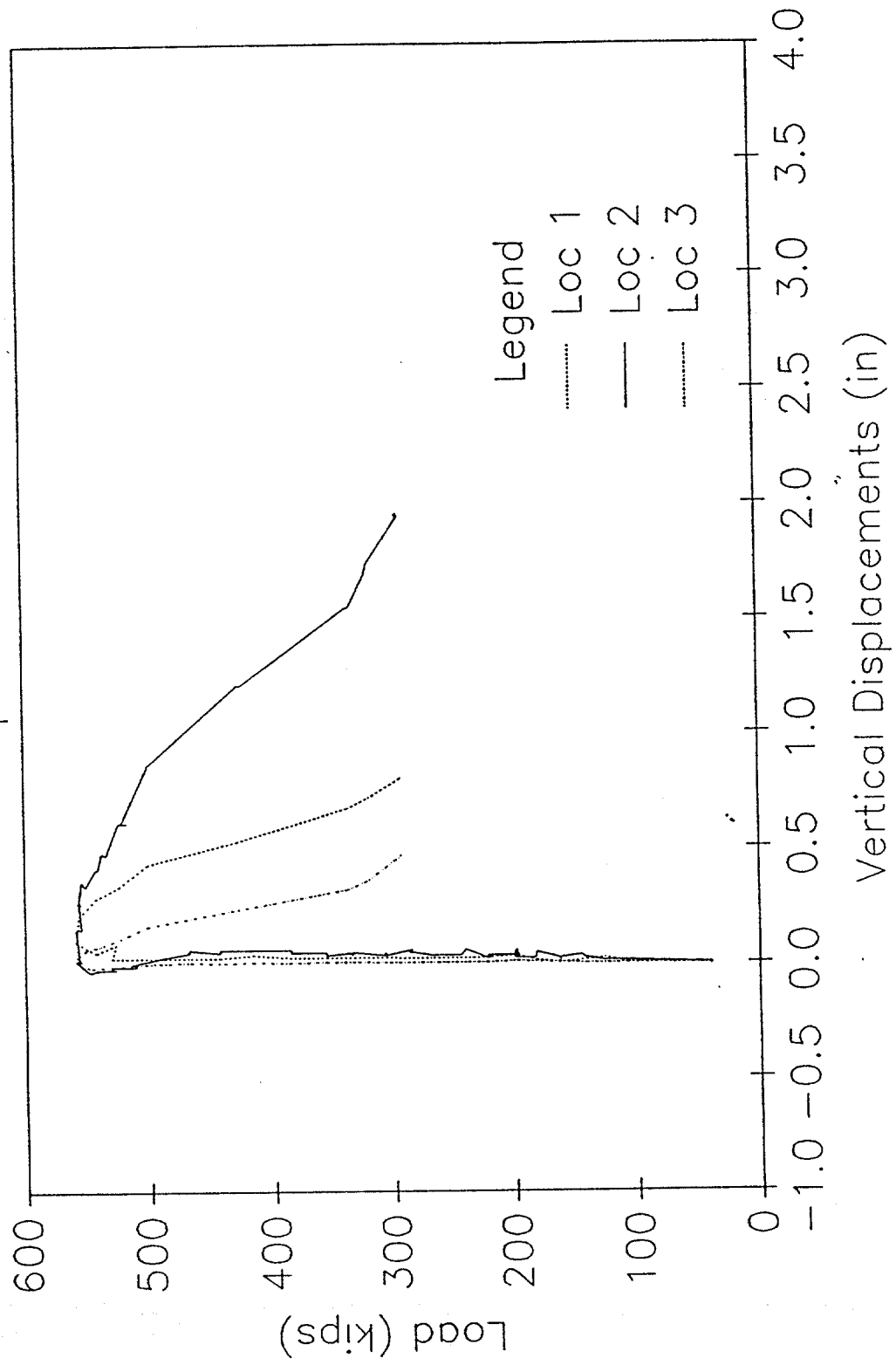
HORIZONTAL DISPLACEMENTS

Specimen 09



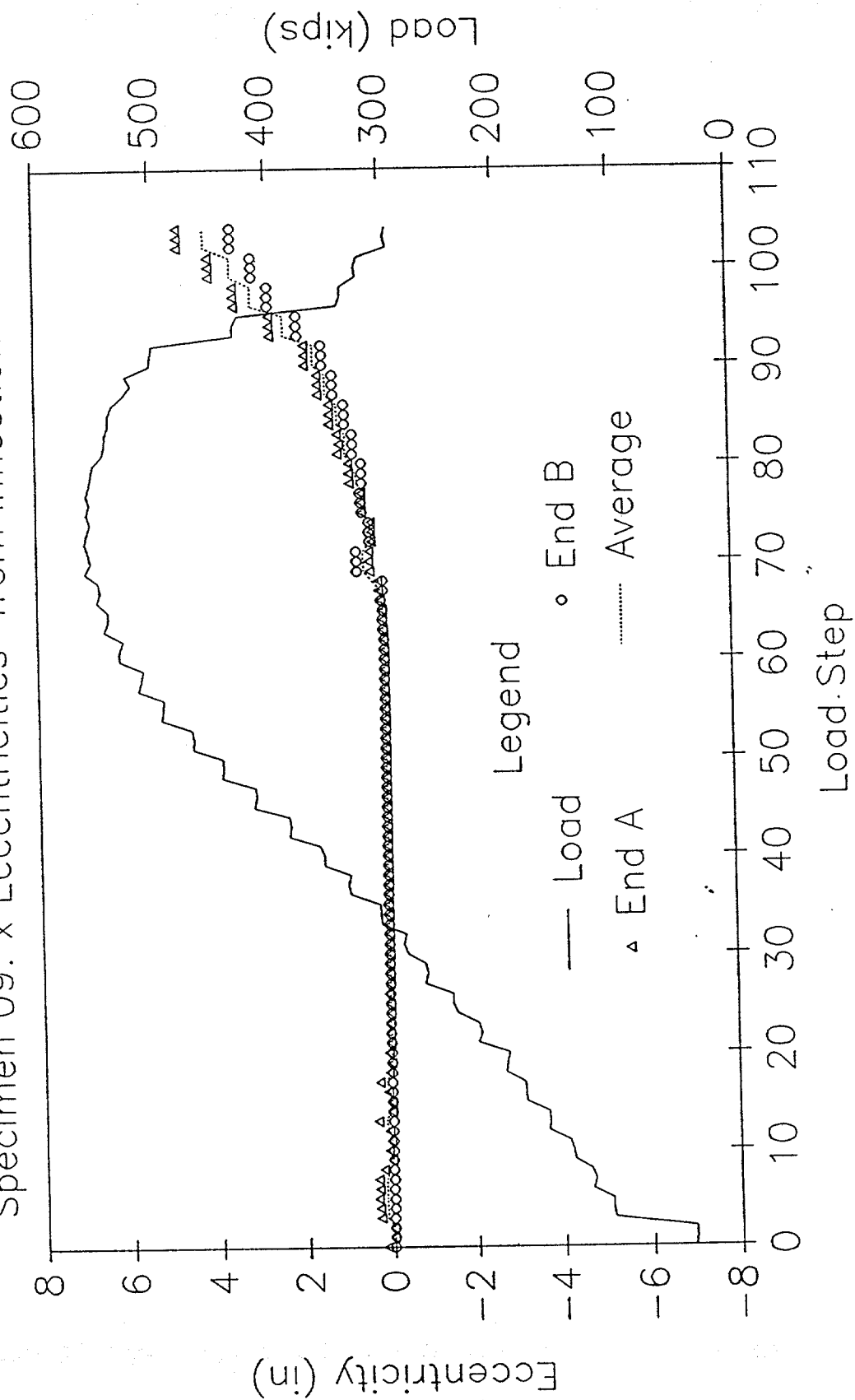
VERTICAL DISPLACEMENTS

Specimen 09



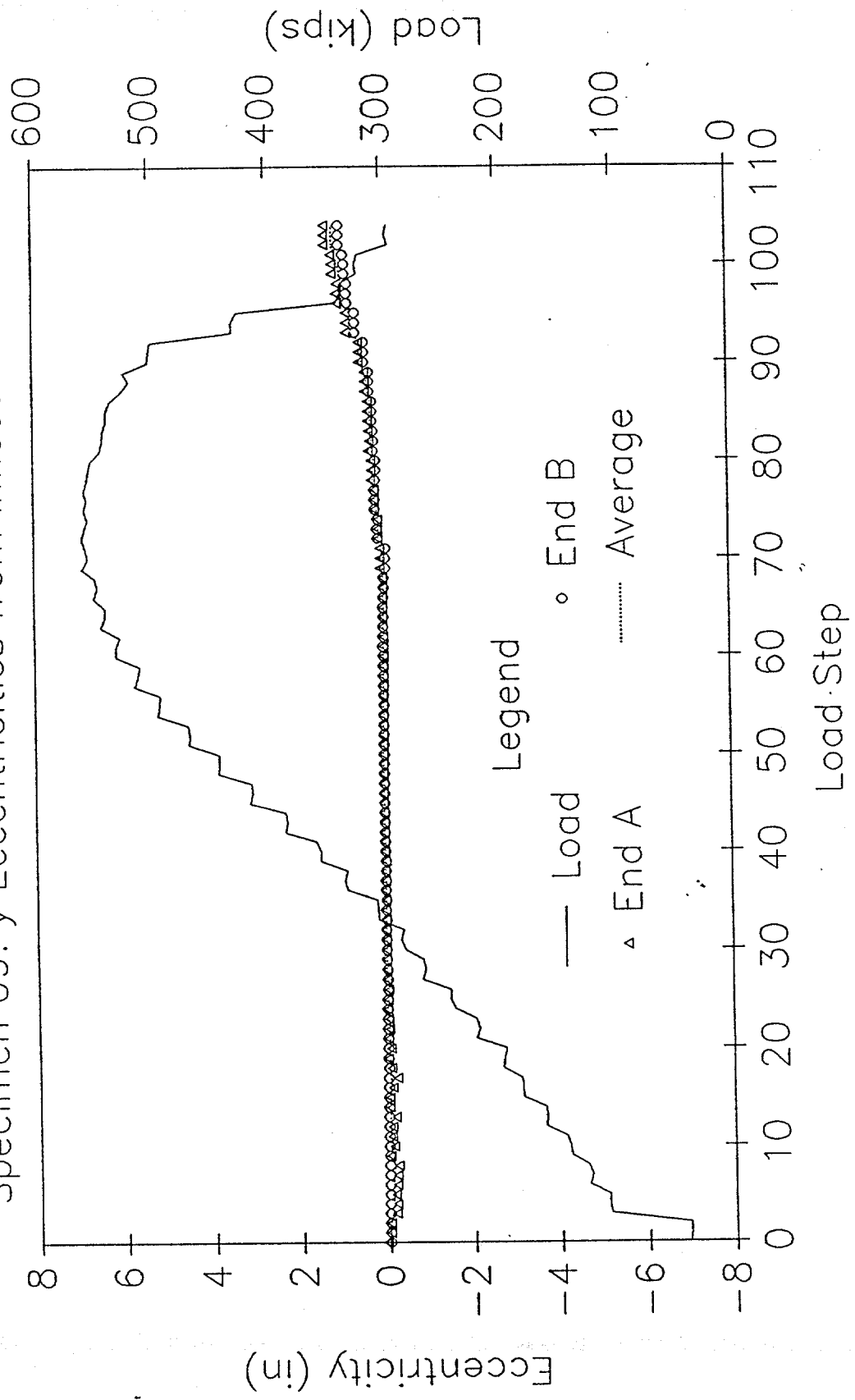
LOAD AND ECCENTRICITY vs LOAD STEP

Specimen 09: x Eccentricities from Inflection Points



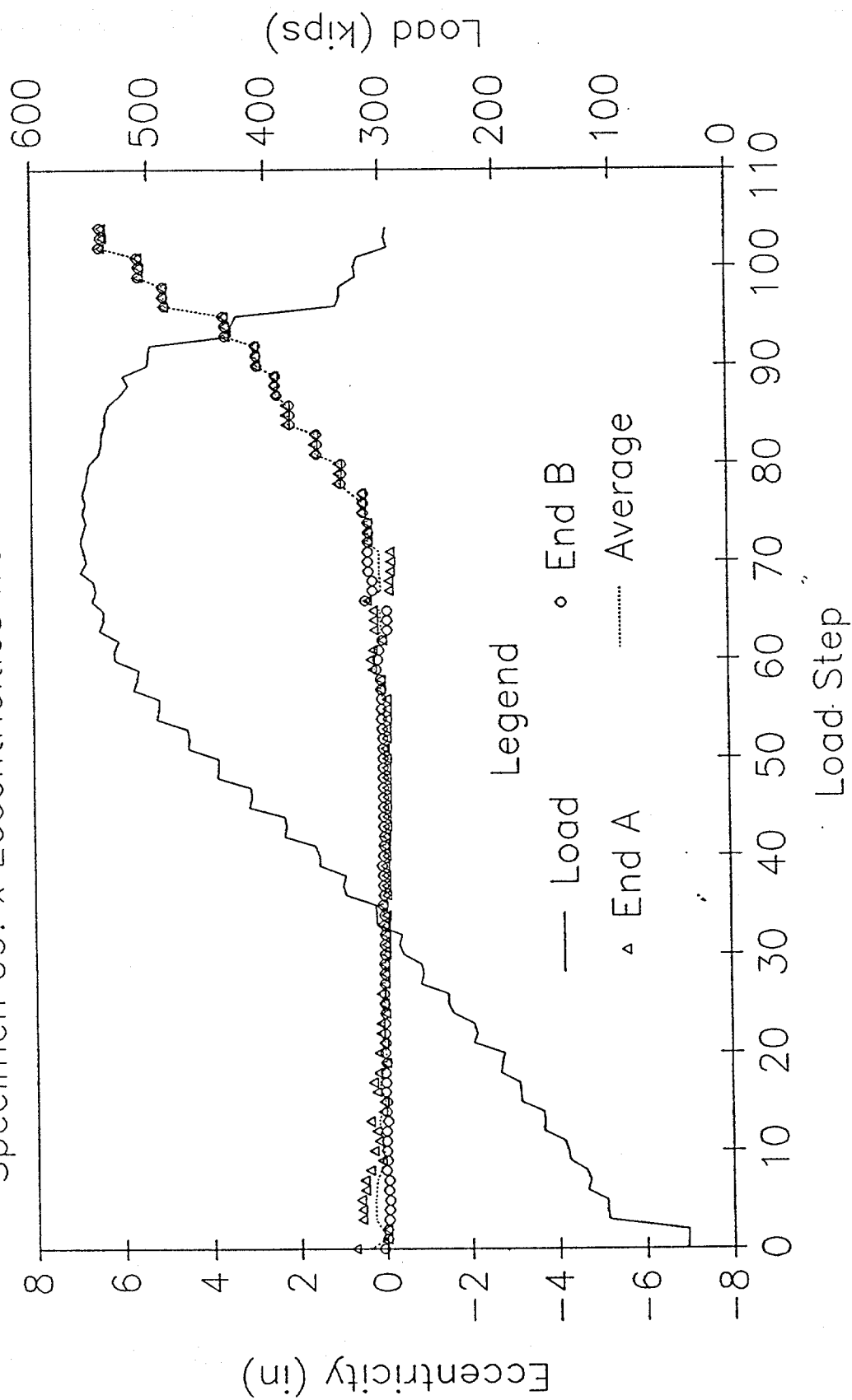
LOAD AND ECCENTRICITY vs LOAD STEP

Specimen 09: y Eccentricities from Inflection Points



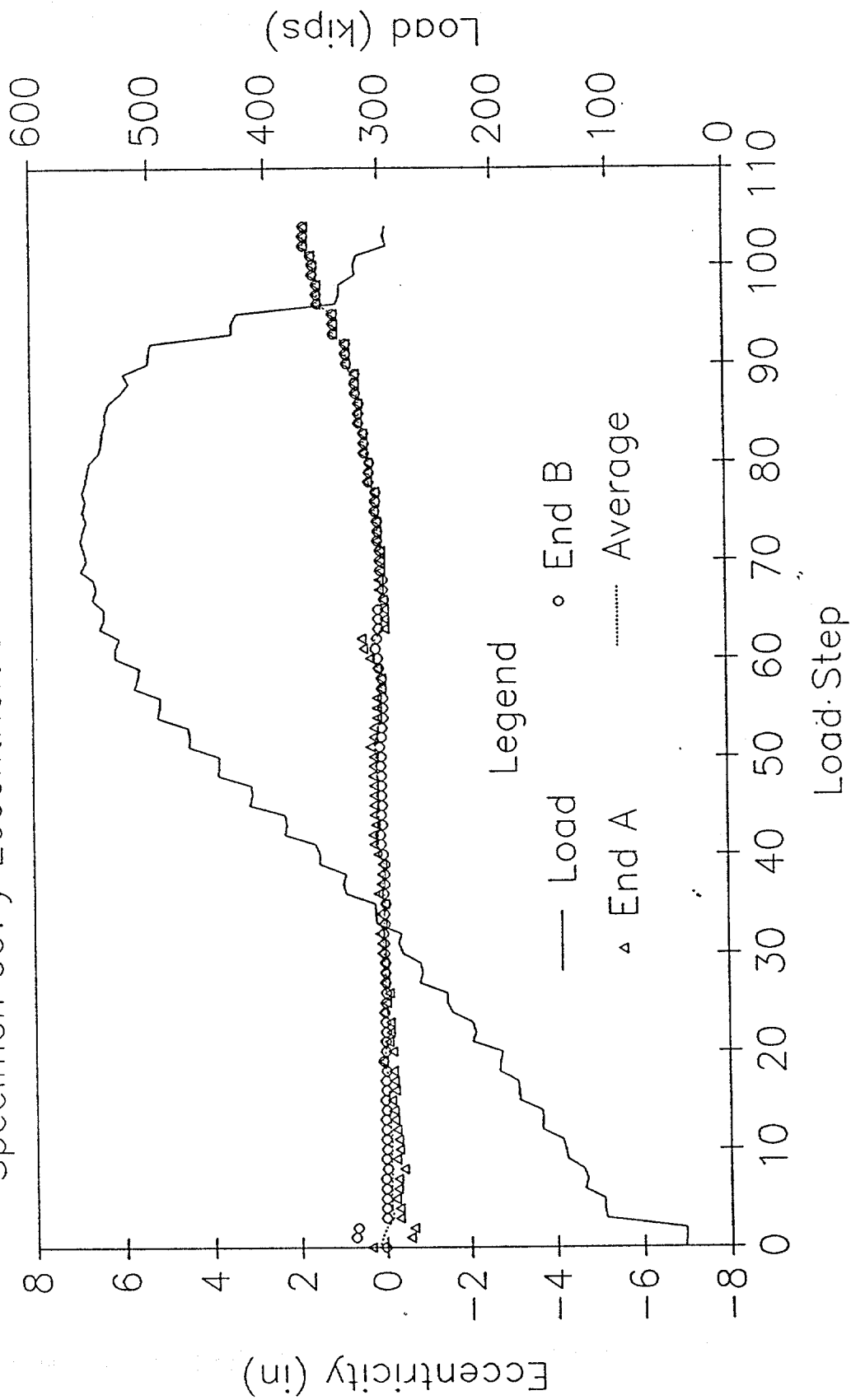
LOAD AND ECCENTRICITY vs LOAD STEP

Specimen 09: x Eccentricities from End Moments



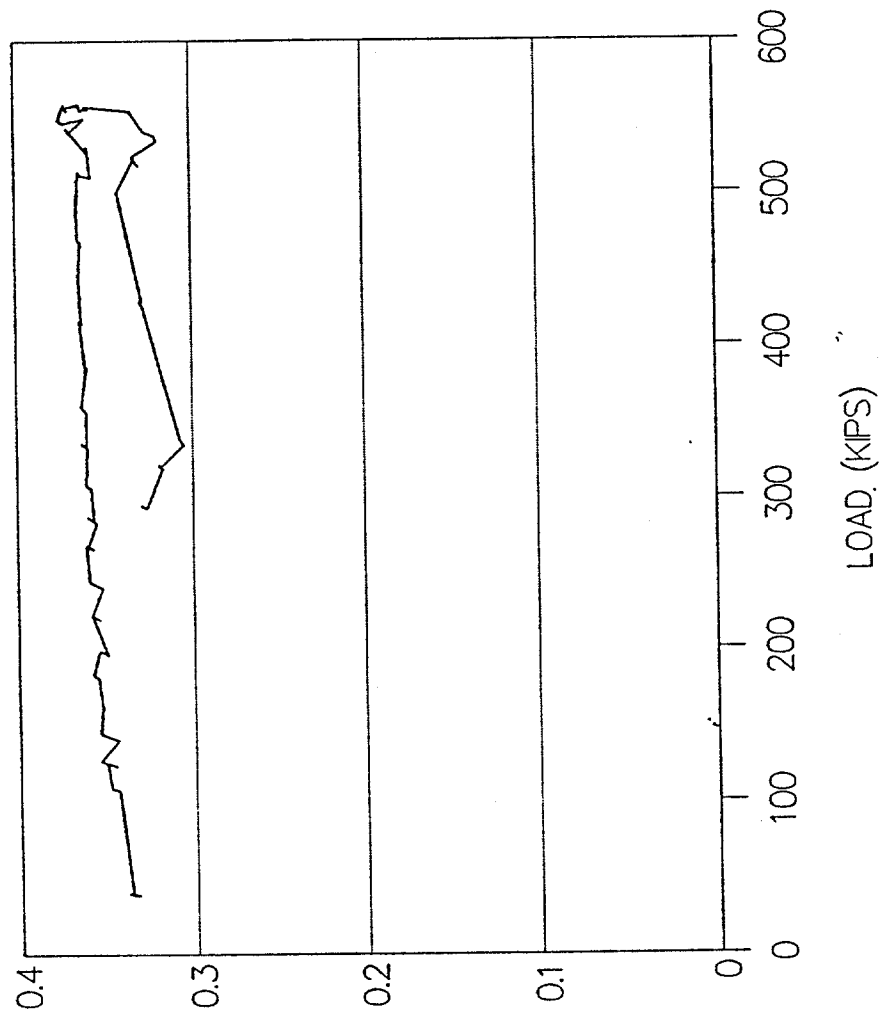
LOAD AND ECCENTRICITY vs LOAD STEP

Specimen 09: y Eccentricities from End Moments



SPECIMEN 09--FULL SCALE TEST

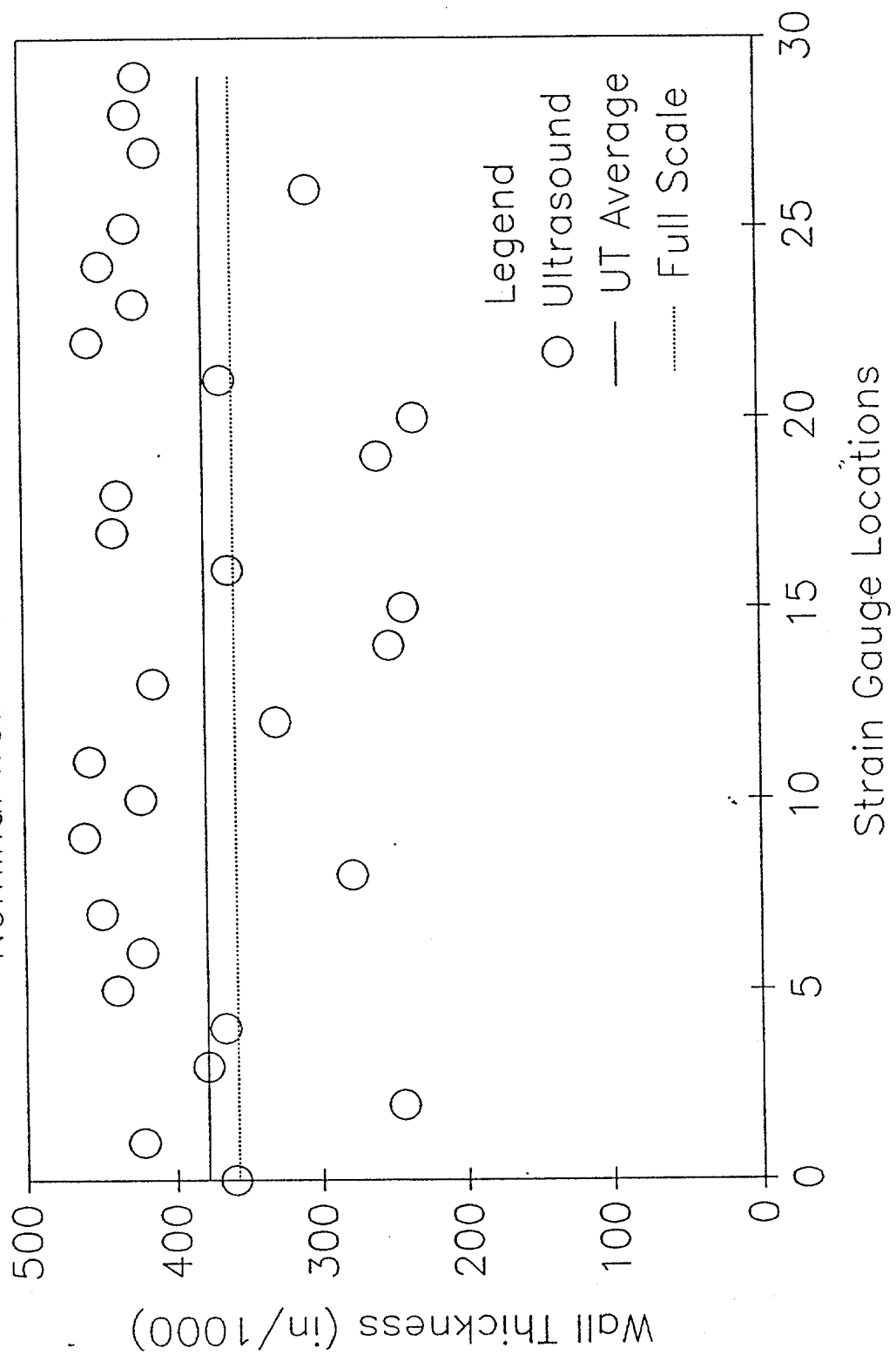
COMPUTED WALL THICKNESS



COMP WALL THICKNESS (IN)

SPECIMEN 09: WALL THICKNESS

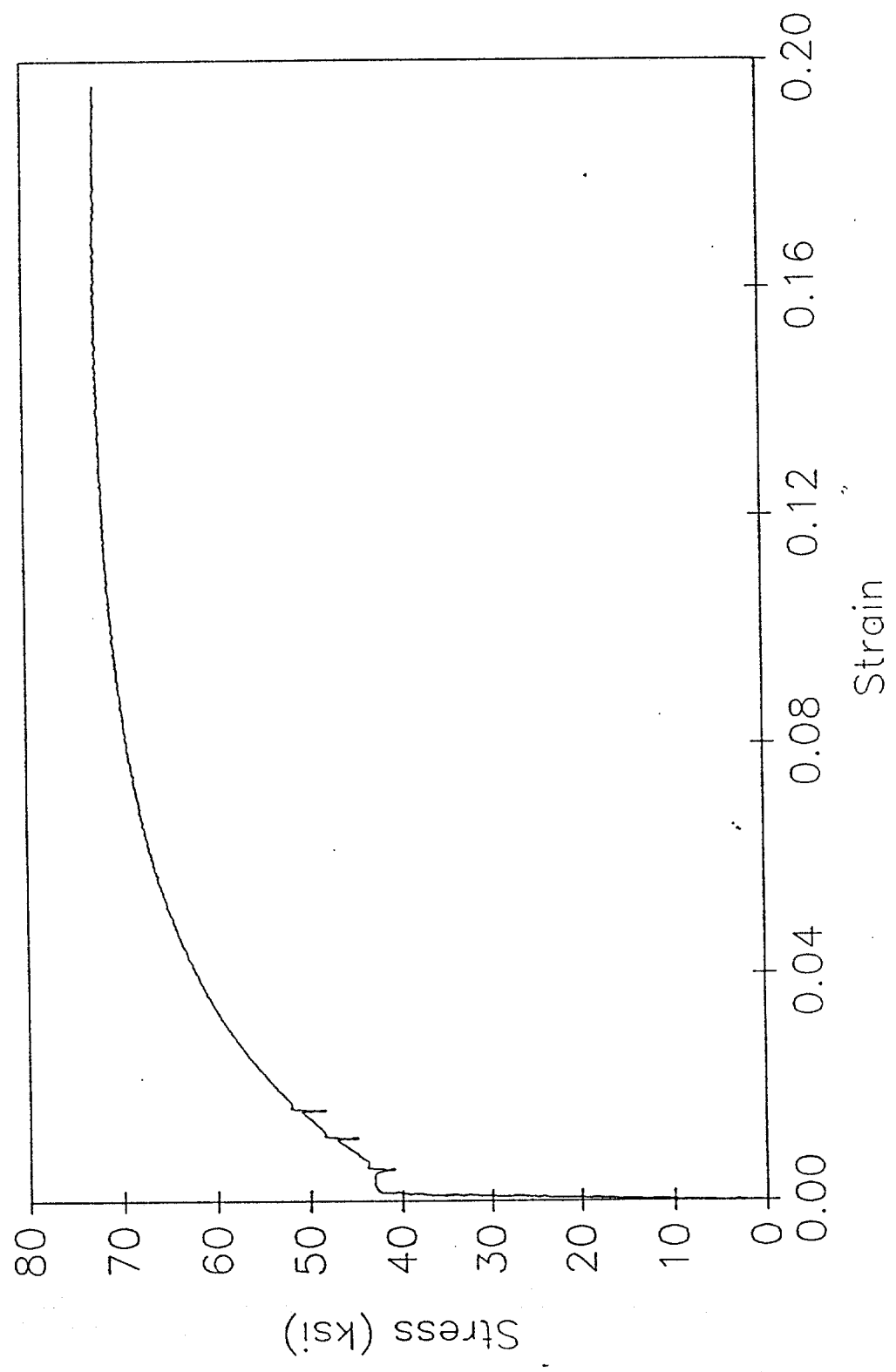
Nominal Wall Thickness = 0.500 in



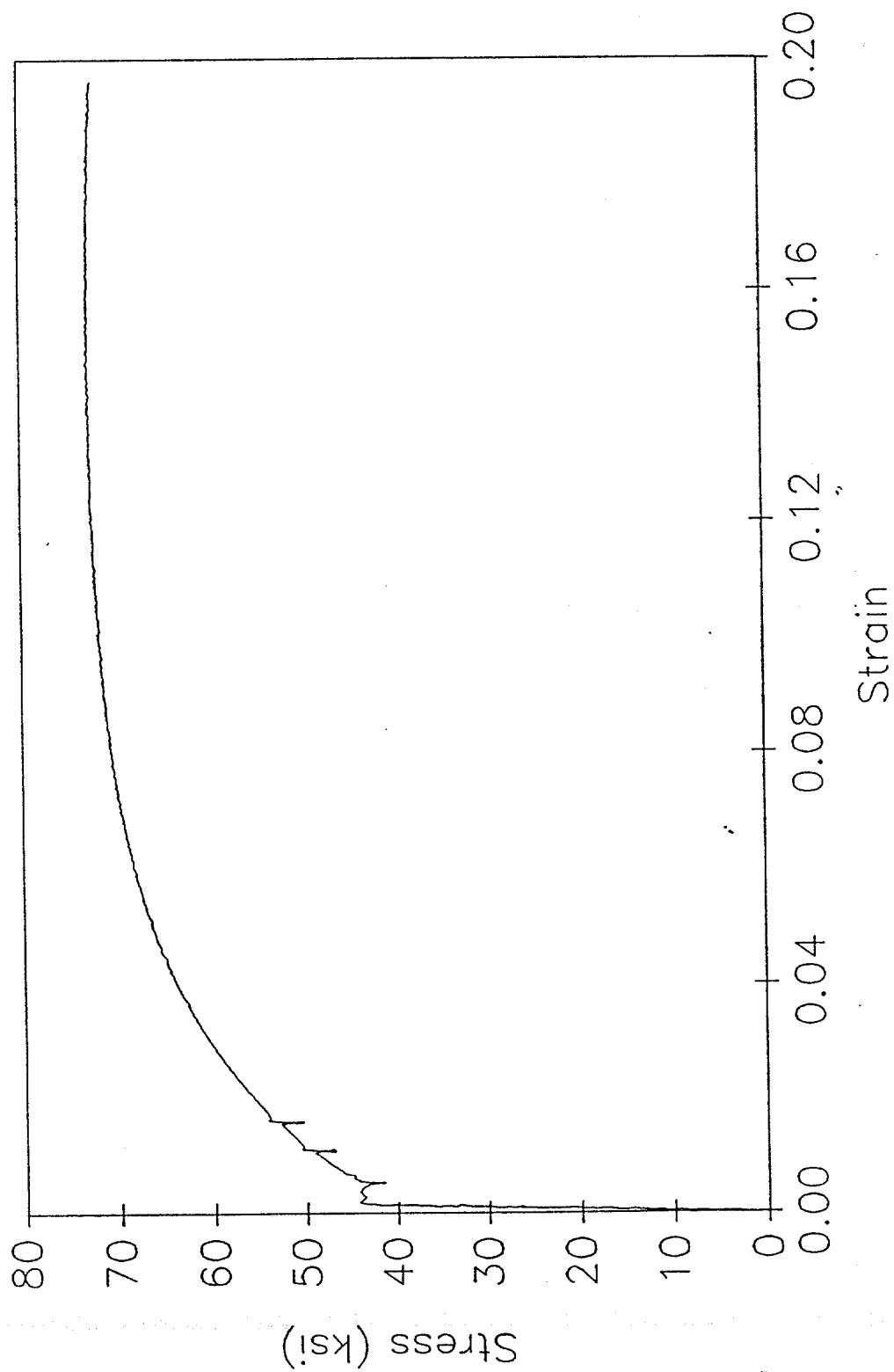
Ultrasound Data for Specimen 9
(All values in inches)

Gauge No.	UT Thickness	UT Average
0	0.360	
1	0.422	
2	0.244	
3	0.378	
4	0.366	
5	0.439	0.368
6	0.422	
7	0.449	
8	0.278	
9	0.460	
10	0.422	
11	0.456	0.415
12	0.330	
13	0.413	
14	0.252	
15	0.242	
16	0.362	
17	0.439	0.340
18	0.436	
19	0.259	
20	0.234	
21	0.366	
22	0.455	
23	0.424	0.362
24	0.447	
25	0.429	
26	0.306	
27	0.415	
28	0.428	
29	0.421	0.408
Overall Average =		0.378

TENSILE SPECIMEN 9-1
Stress vs Strain



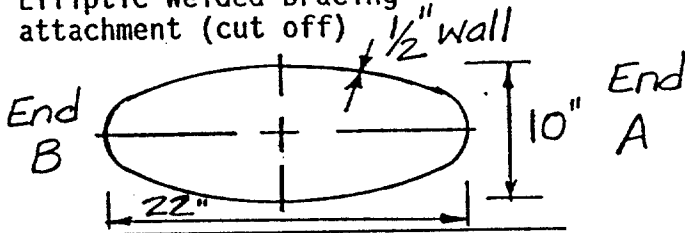
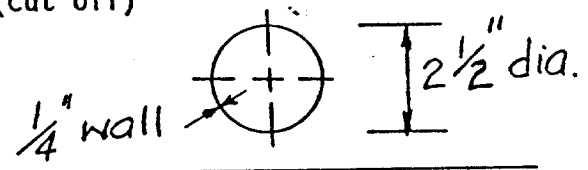
TENSILE SPECIMEN 9-2
Stress vs Strain



SPECIMEN 10

DAMAGE SUMMARY

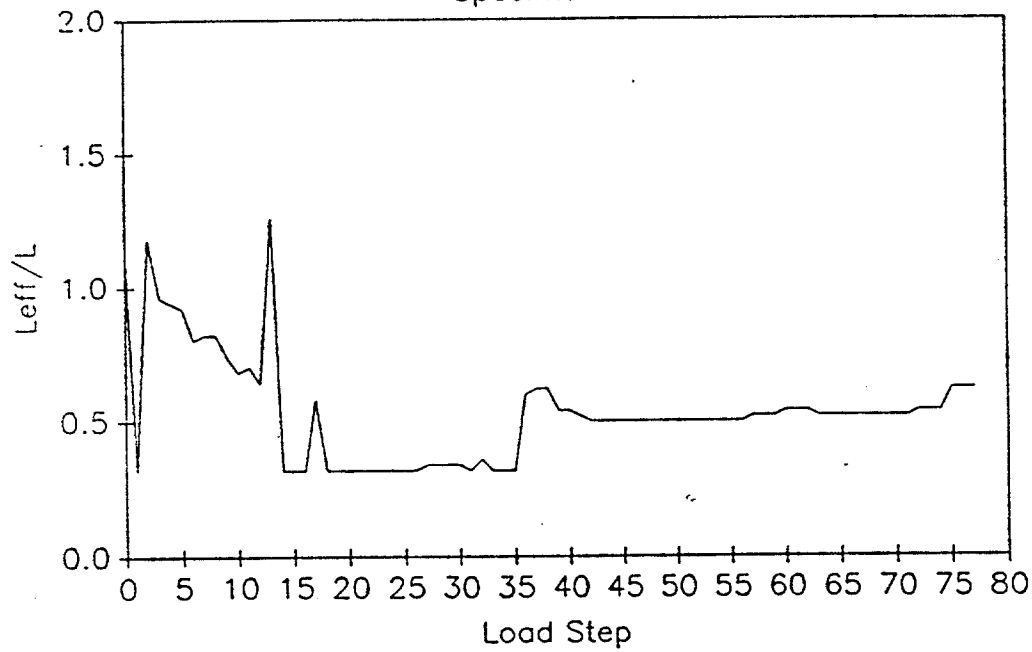
Specimen No. 10

DISTANCE FROM END "B"	*DISTANCE FROM CHALK LINE		DESCRIPTION OF DAMAGE
	LEFT	RIGHT	
1. 24'-1/2"			3/4" circumferential butt weld
2. 30'-3 1/2"		12"	Welded up torch cuts 1) 3" long X 3/4" wide 2) 4 1/2" long X 1" wide
3. 26'-1"	7 3/4"		Small torch gouge (long.) 1" long X 1/4" wide X 1/4" deep
4. 26'-6 1/4"	9"		Small torch gouge (circum.) 7/8" long X 1/4" wide X 1/4" deep
5. 21'-1"	8 1/2"		2 pits - round 1/2" diameter X 1/4" deep
6. 15'-10"	21 1/2" (to center)		Elliptic welded bracing attachment (cut off) 
7. 5'-6"	20 7/8"		Round welded bracing attachment (cut off) 
8. 21'-5 1/2"	7 1/4"		Small torch gouge 1 1/4" long X 1/4" wide X 1/4" deep

*Looking from end "A" towards end "B"

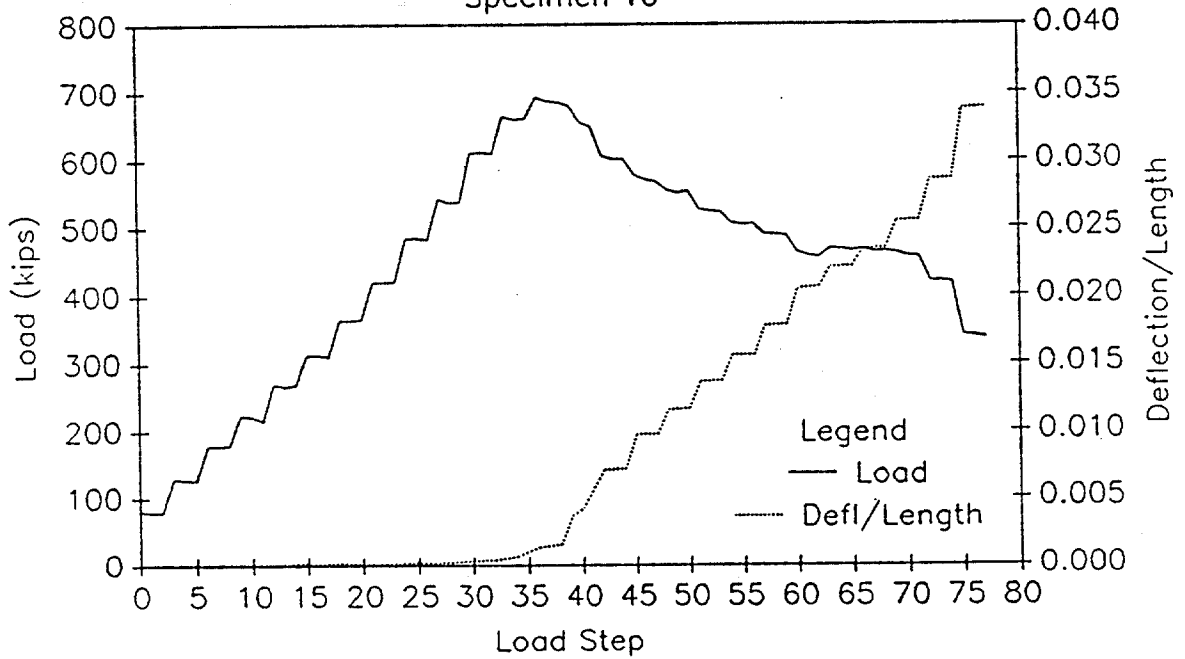
EFFECTIVE LENGTH vs LOAD STEP

Specimen 10

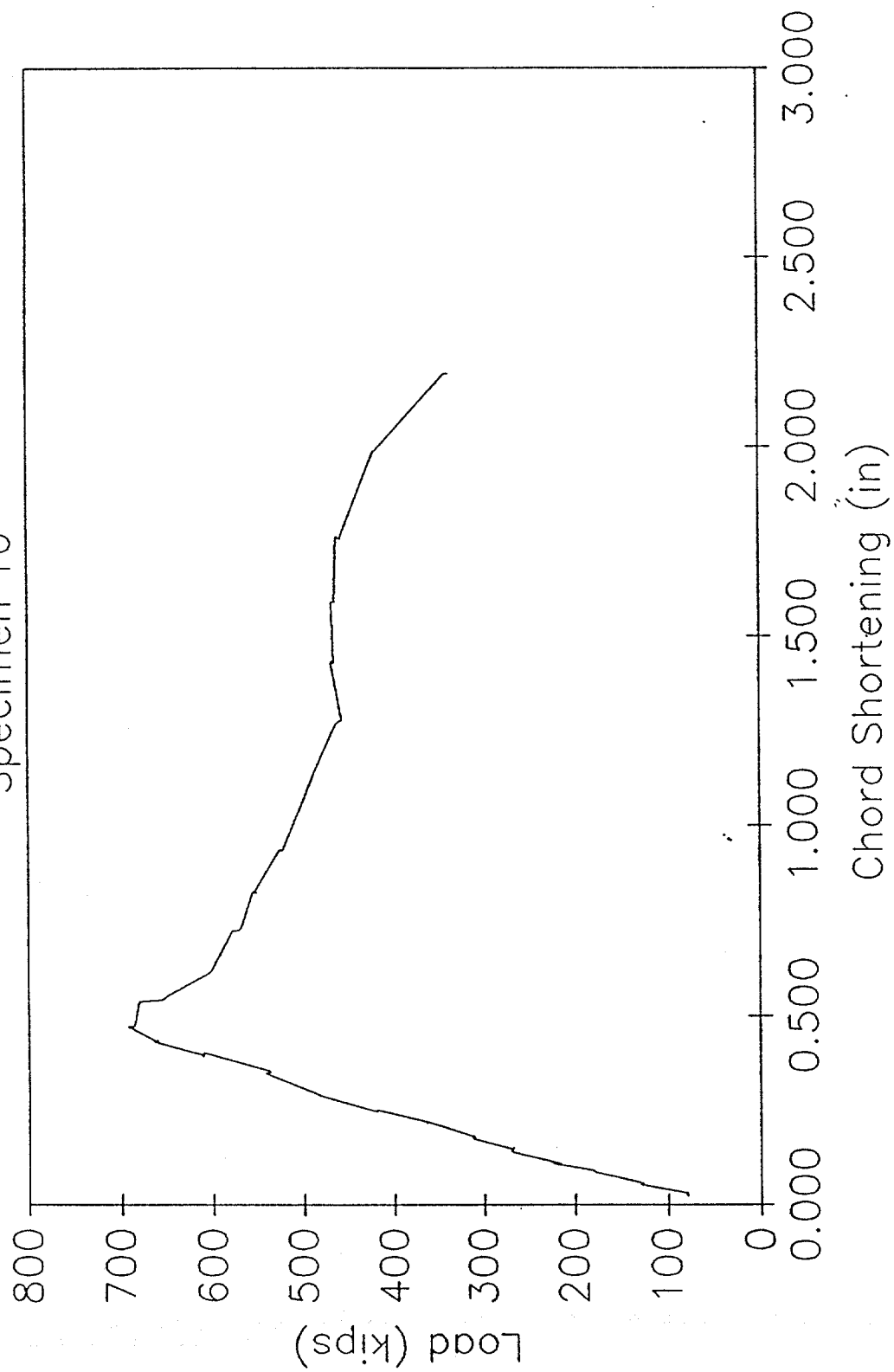


LOAD AND DEFLECTION vs LOAD STEP

Specimen 10

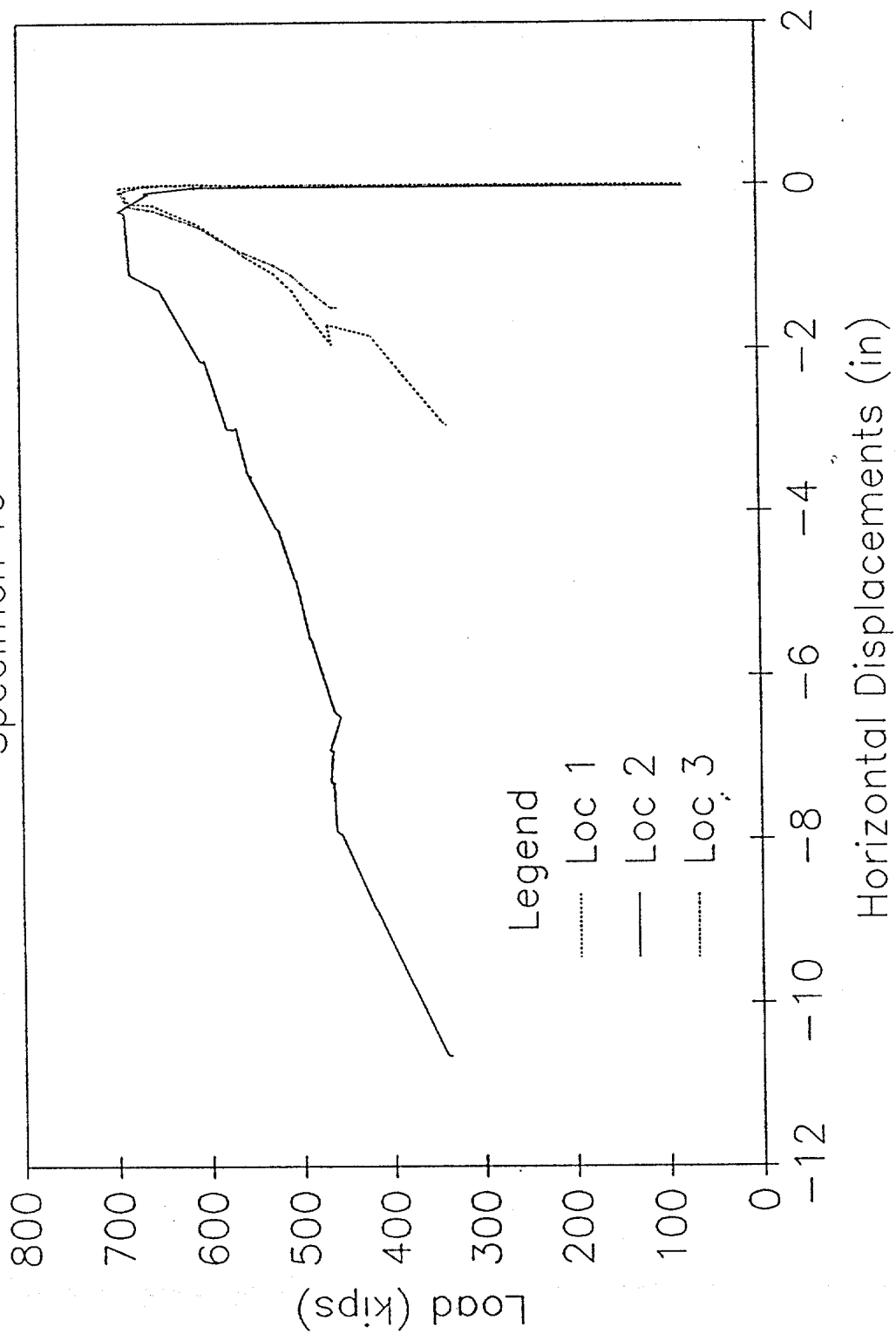


LOAD vs CHORD SHORTENING
Specimen 10



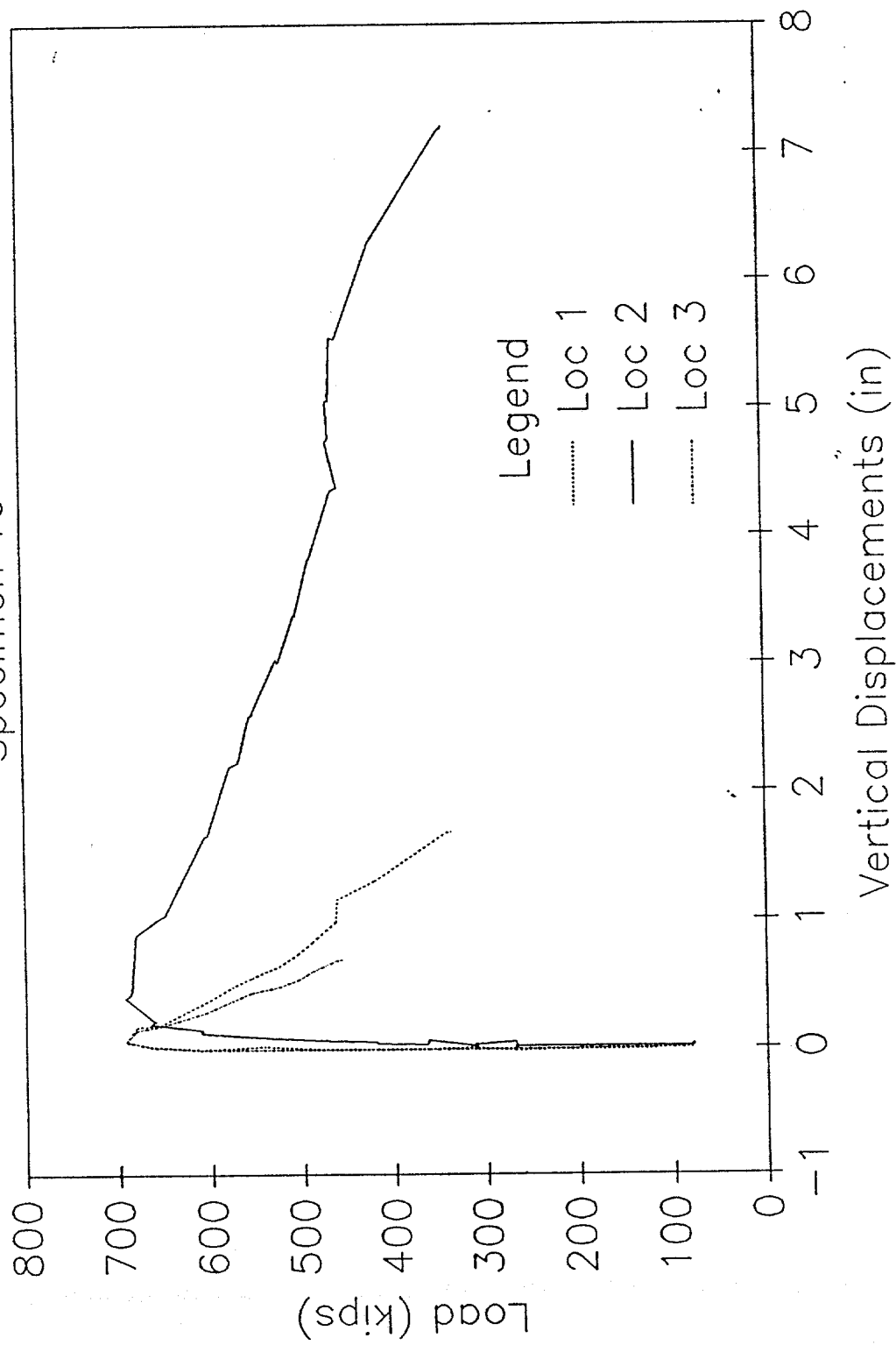
HORIZONTAL DISPLACEMENTS

Specimen 10

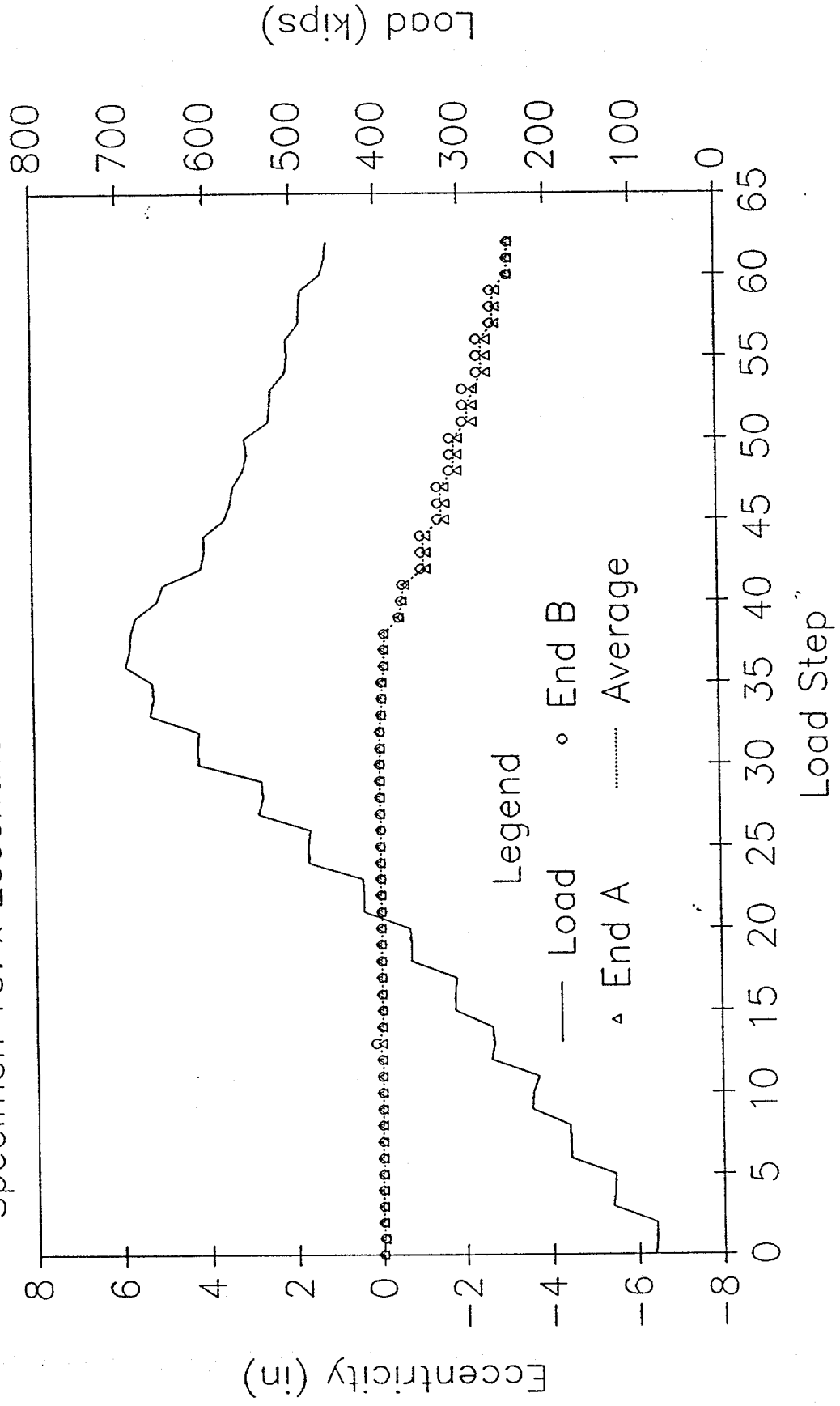


VERTICAL DISPLACEMENTS

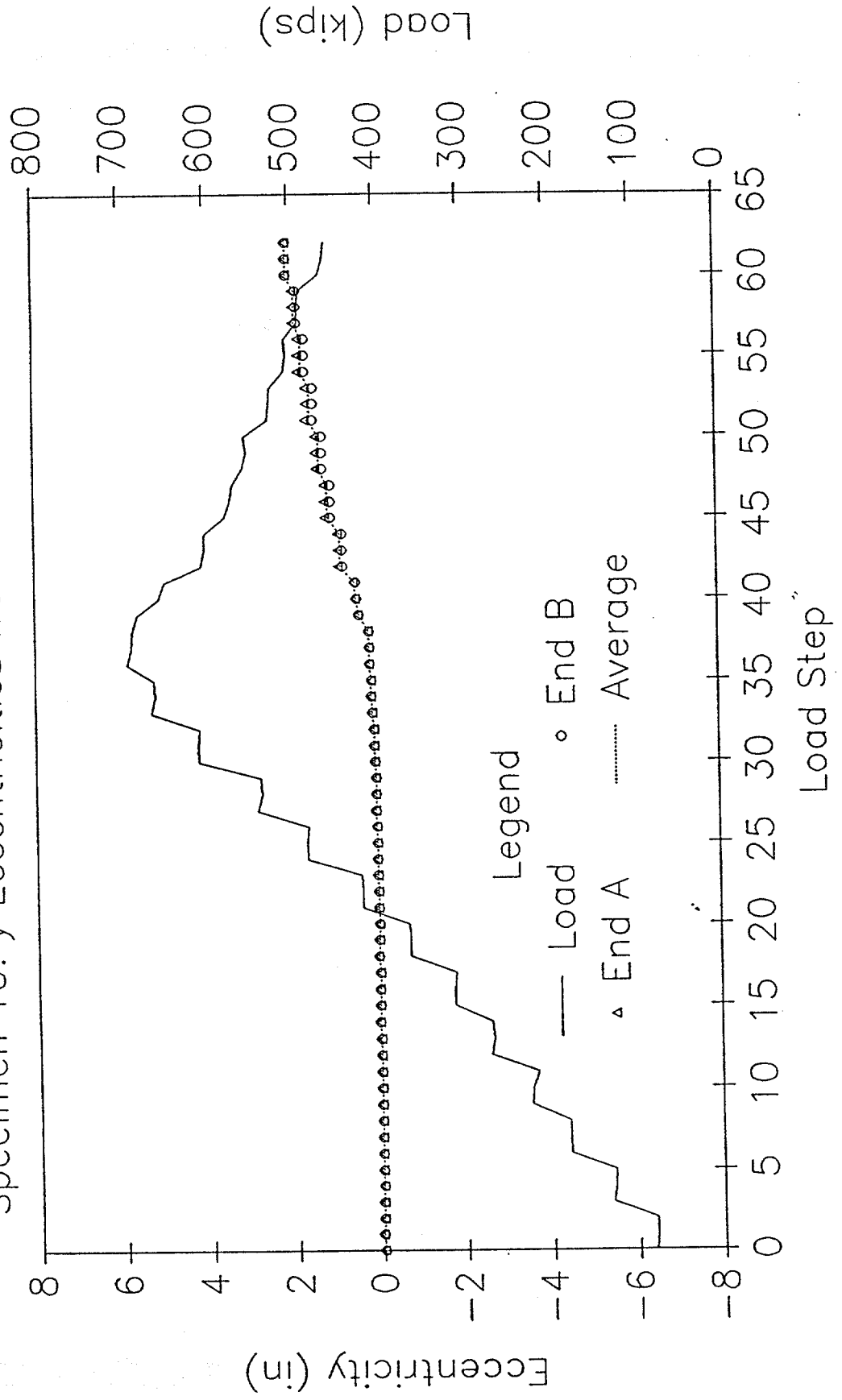
Specimen 10



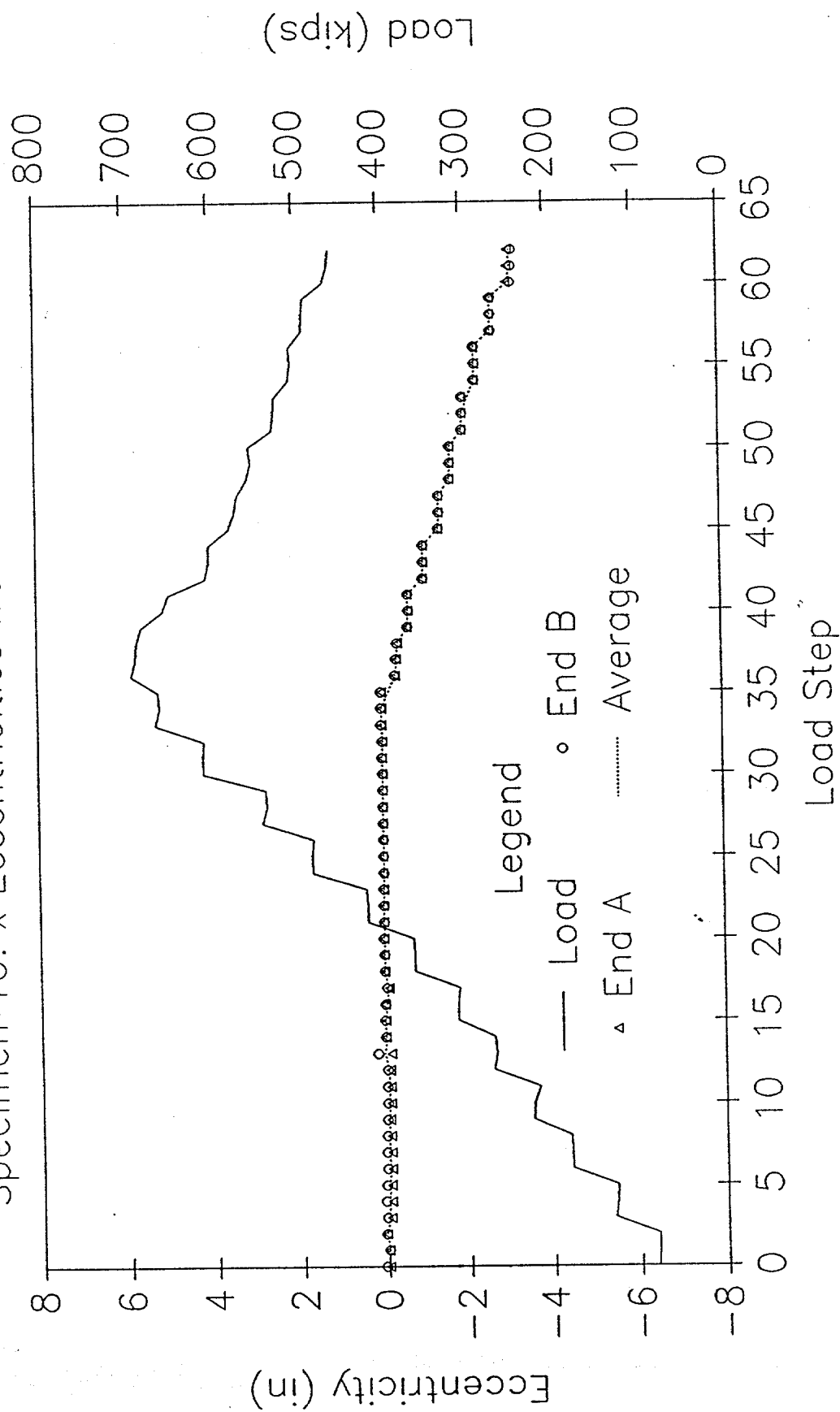
LOAD AND ECCENTRICITY vs LOAD STEP Specimen 10: x Eccentricities from Inflection Points



LOAD AND ECCENTRICITY vs LOAD STEP
Specimen 10: y Eccentricities from Inflection Points

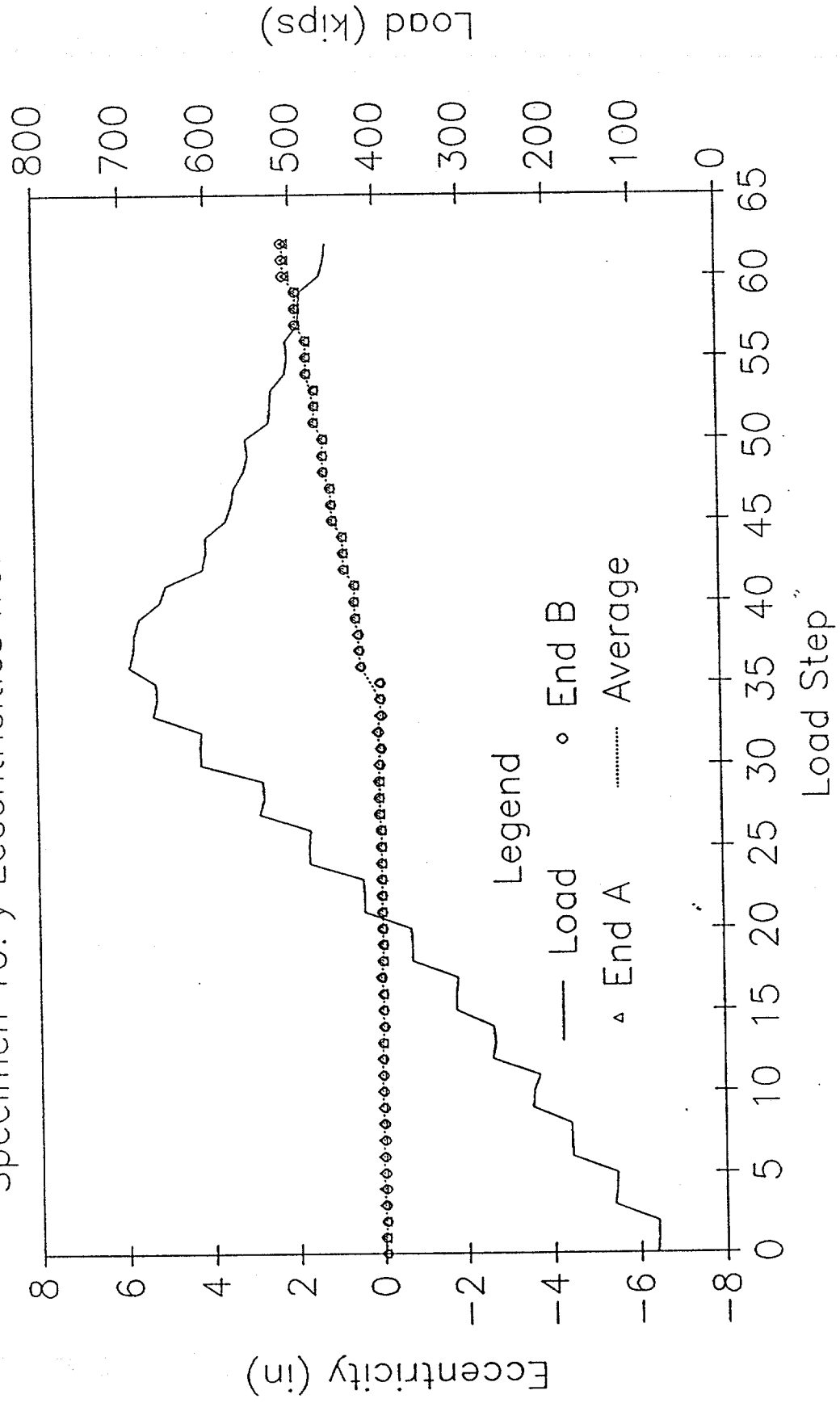


LOAD AND ECCENTRICITY vs LOAD STEP Specimen 10: x Eccentricities from End Moments



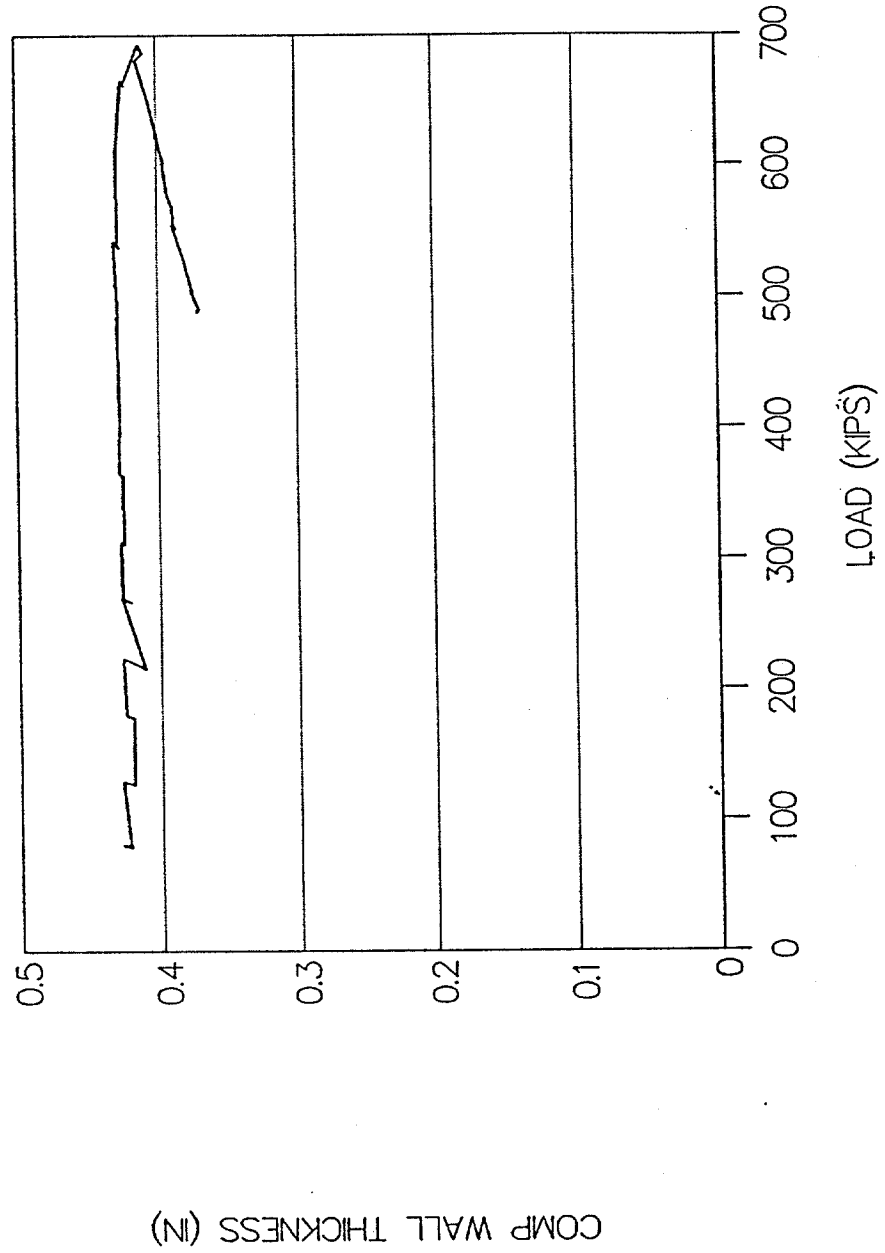
LOAD AND ECCENTRICITY vs LOAD STEP

Specimen 10: y Eccentricities from End Moments



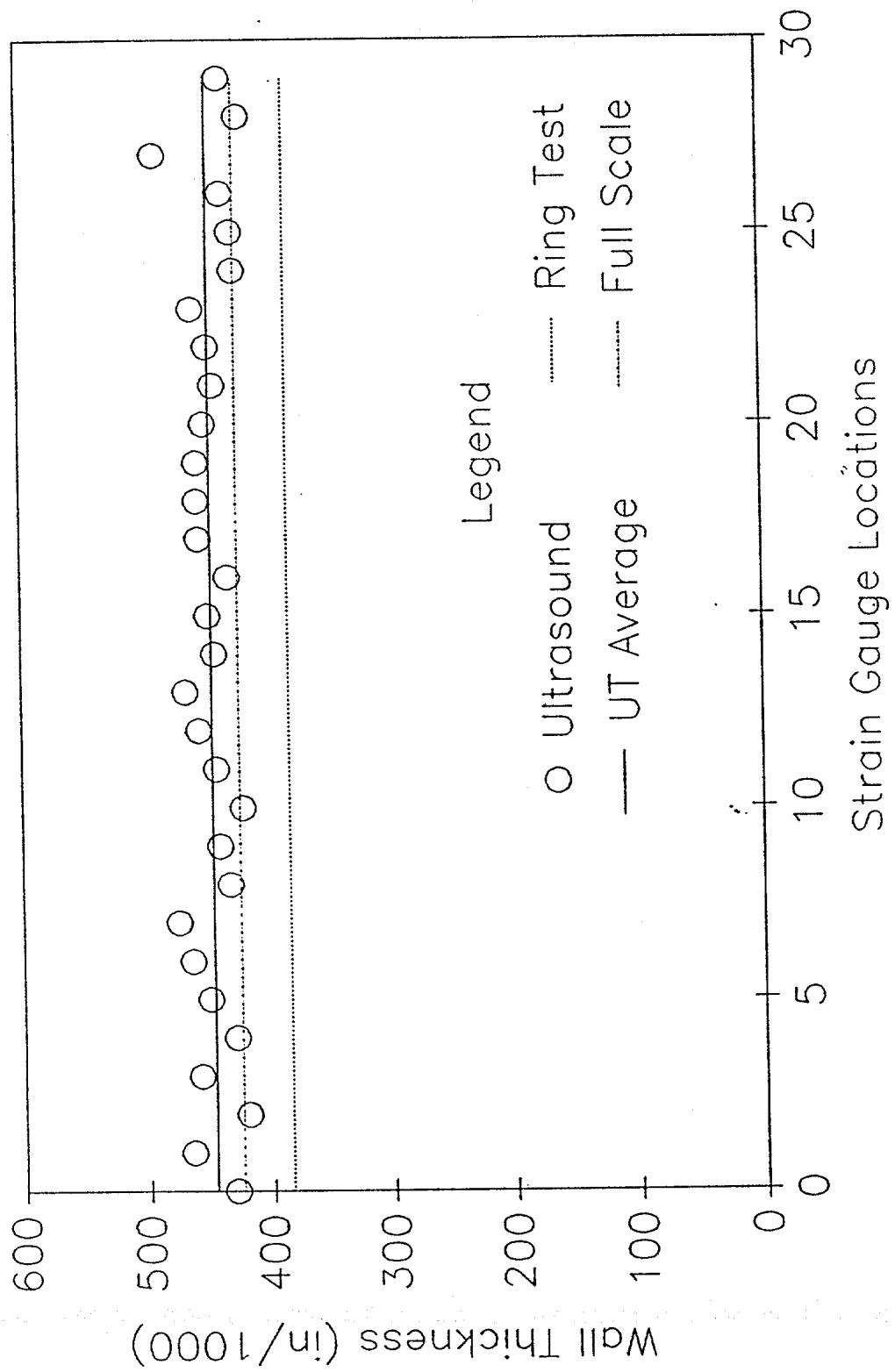
SPECIMEN 10--FULL SCALE TEST

COMPUTED WALL THICKNESS



SPECIMEN 10: WALL THICKNESS

Nominal Wall Thickness = 0.500 in



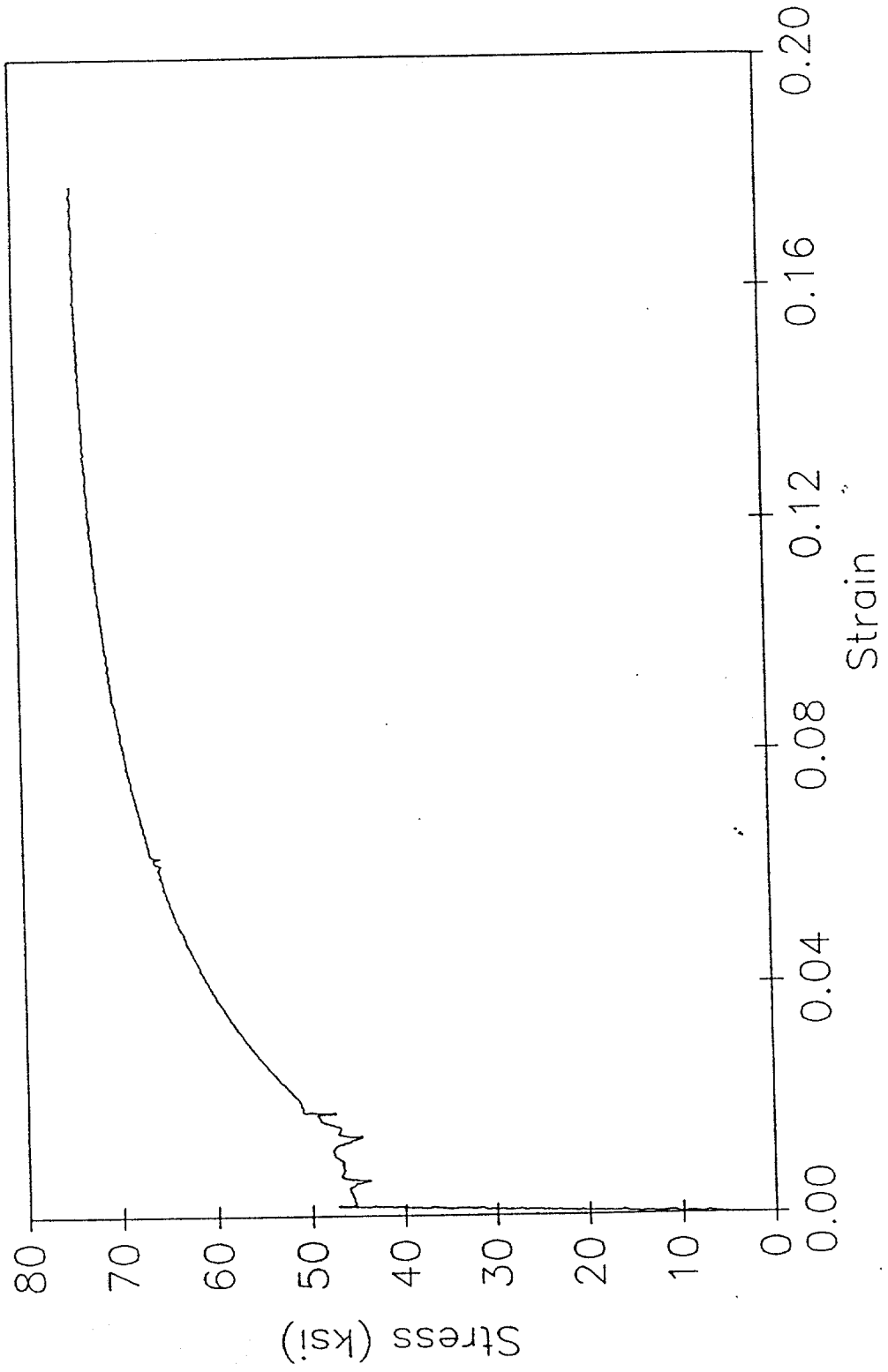
Ultrasound Data for Specimen 10
(All values in inches)

Gauge No.	UT Thickness	UT Average
0	0.430	
1	0.465	
2	0.420	
3	0.458	
4	0.429	
5	0.450	0.442
6	0.464	
7	0.475	
8	0.433	
9	0.441	
10	0.422	
11	0.443	0.446
12	0.457	
13	0.468	
14	0.444	
15	0.449	
16	0.433	
17	0.456	0.451
18	0.457	
19	0.457	
20	0.451	
21	0.443	
22	0.448	
23	0.460	0.453
24	0.426	
25	0.428	
26	0.435	
27	0.489	
28	0.421	
29	0.436	0.439

Overall Average = 0.446

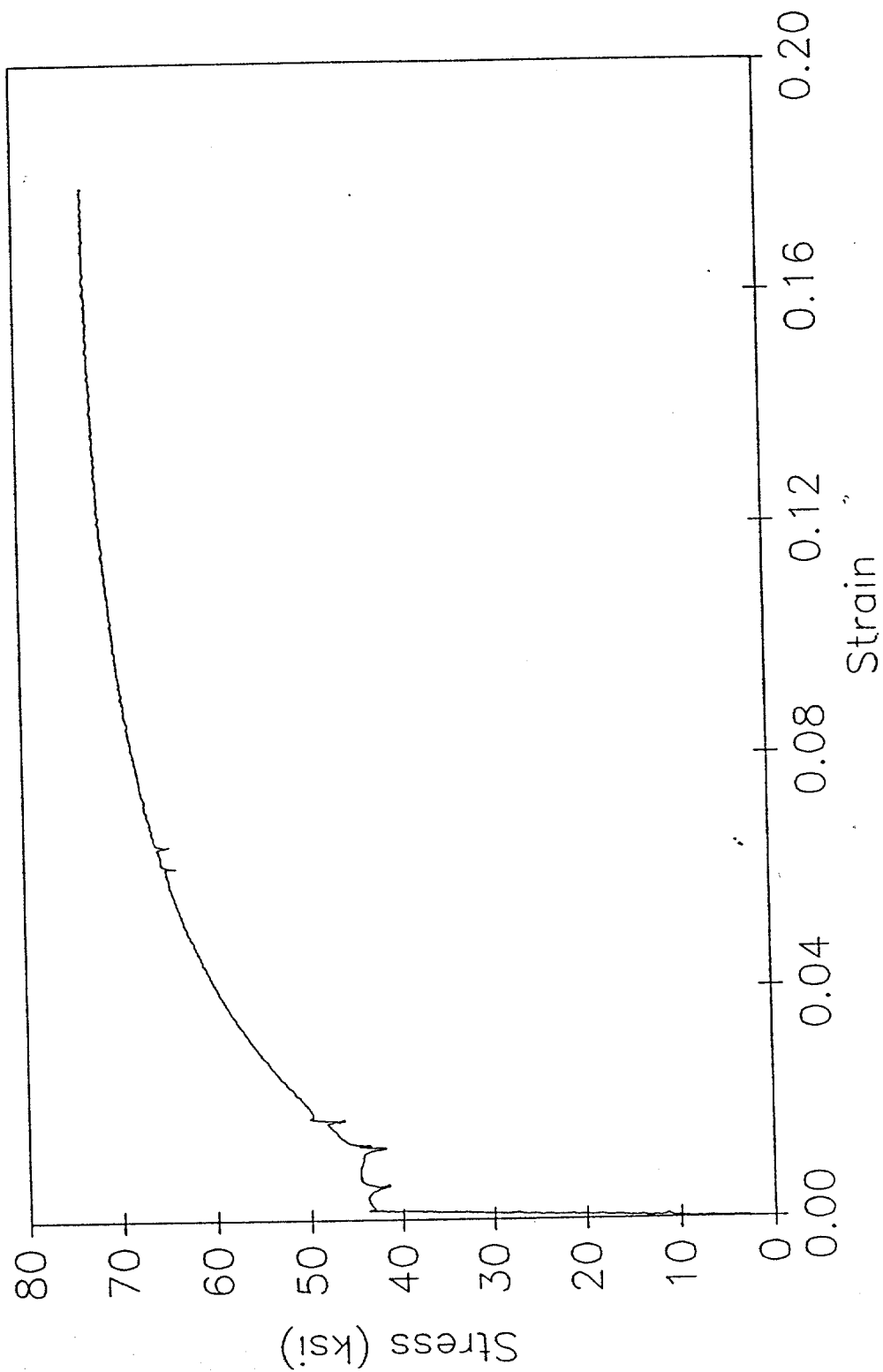
TENSILE SPECIMEN 10-1

Stress vs Strain



TENSILE SPECIMEN 10-2

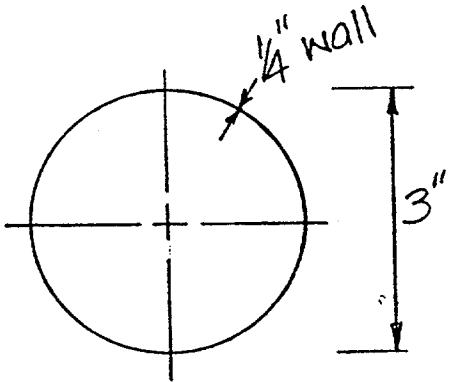
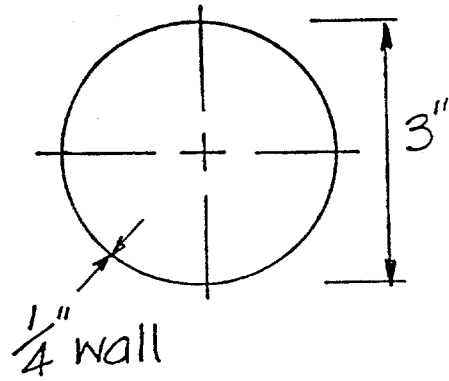
Stress vs Strain



SPECIMEN 11

DAMAGE SUMMARY

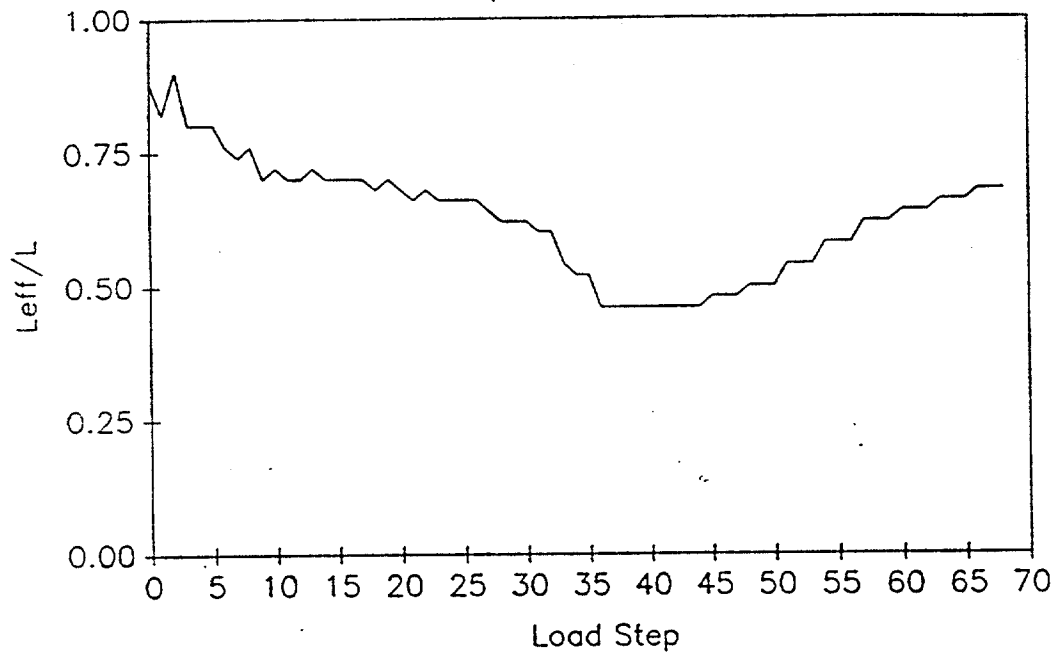
Specimen No. 11

DISTANCE FROM END "B"	*DISTANCE FROM CHALK LINE		DESCRIPTION OF DAMAGE
	LEFT	RIGHT	
1. 10'-1"			3/4" circumferential butt weld
2. 12'-6"		10"	3" diameter, round, welded bracing attachment (cut-off) 
3. 17'-5 1/2"		7 1/4"	3" diameter, round, welded bracing attachment (cut-off) 

*Looking from end "A" towards end "B"

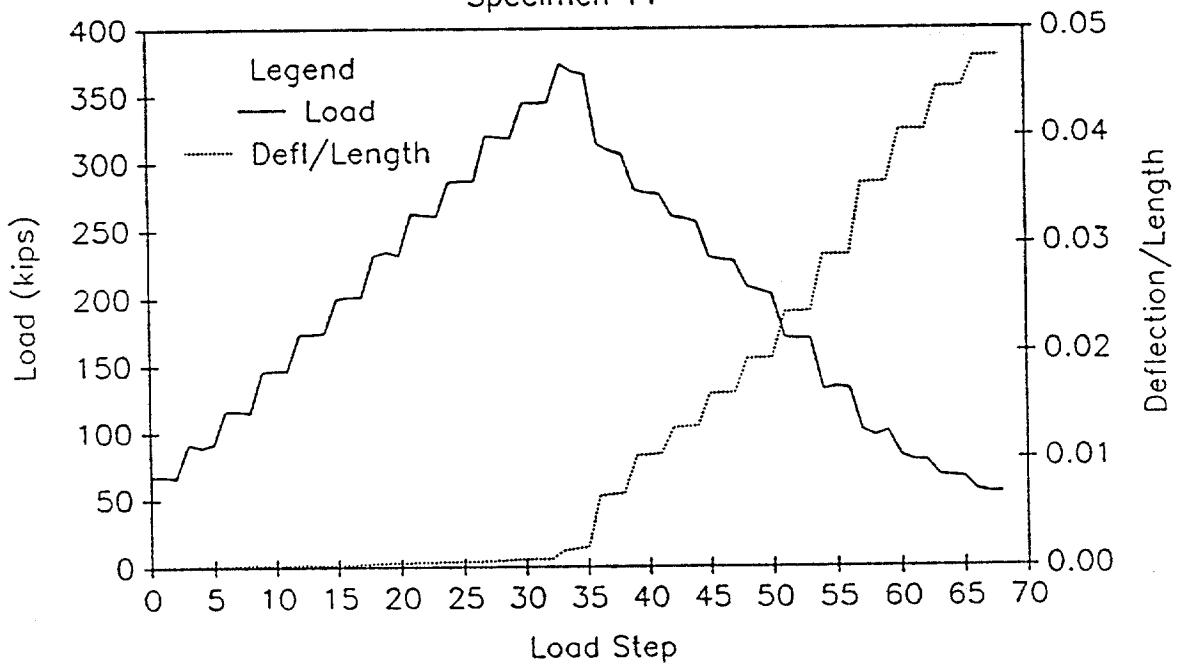
EFFECTIVE LENGTH vs LOAD STEP

Specimen 11



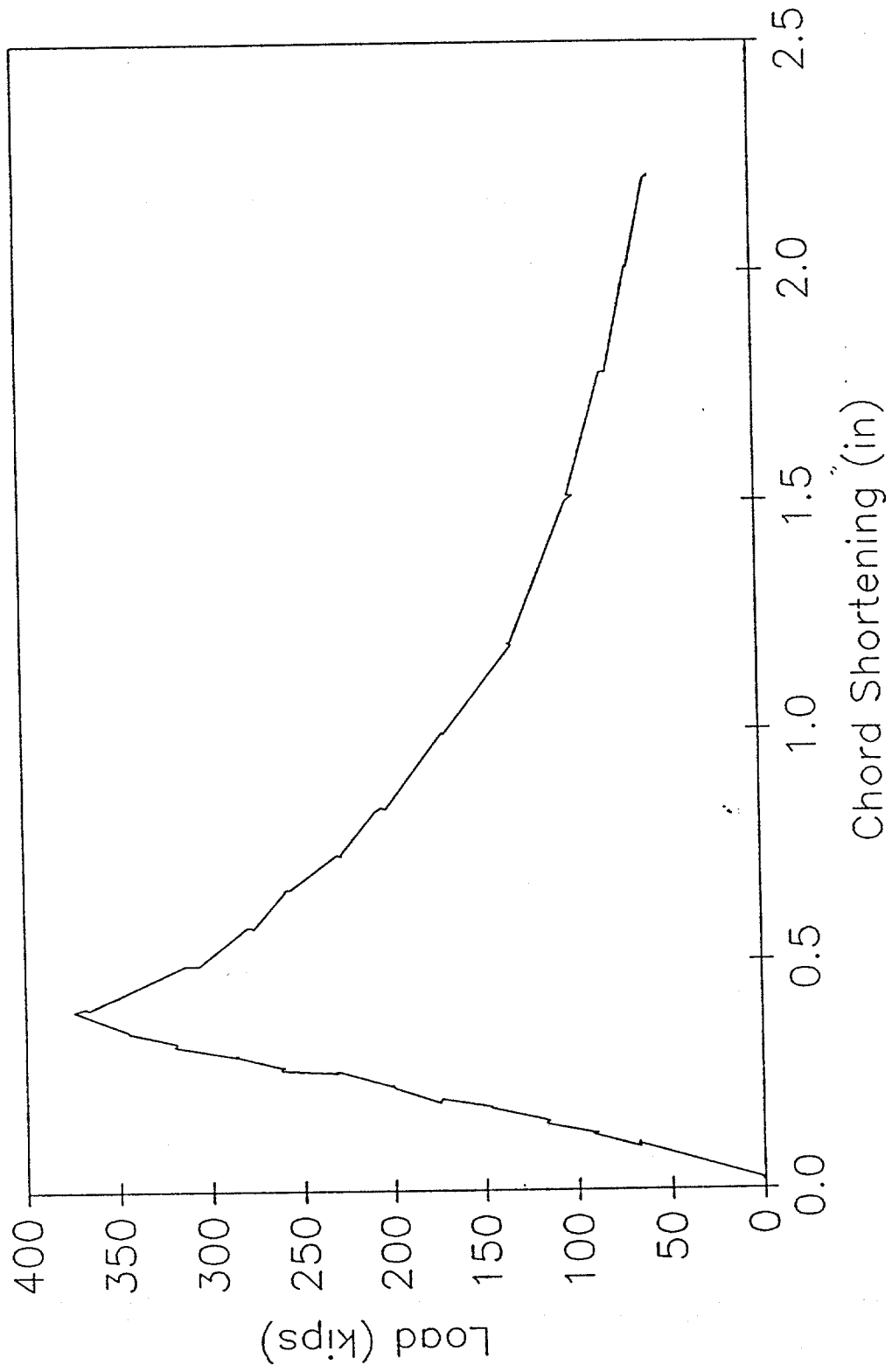
LOAD AND DEFLECTION vs LOAD STEP

Specimen 11



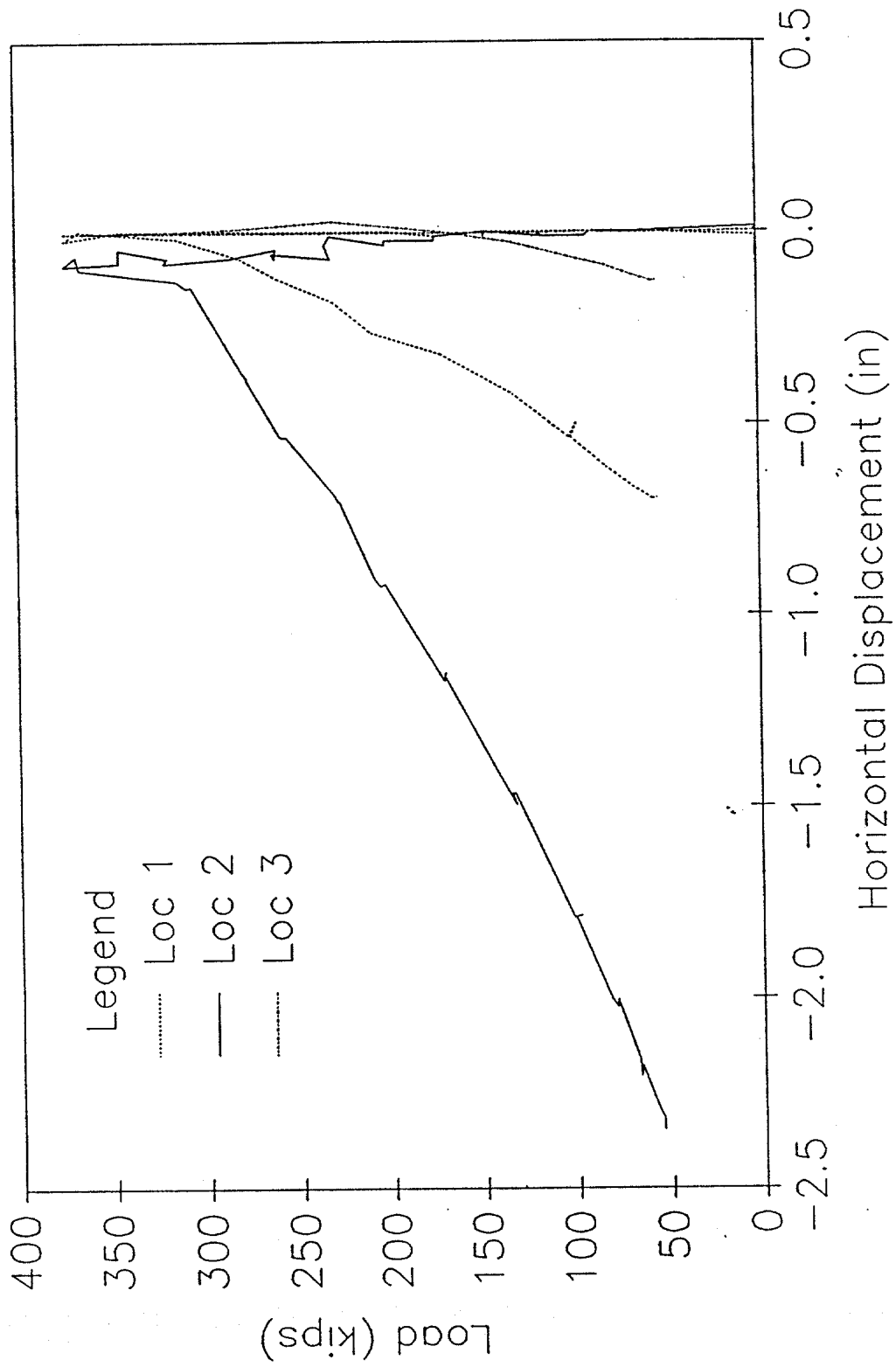
LOAD vs CHORD SHORTENING

Specimen 11



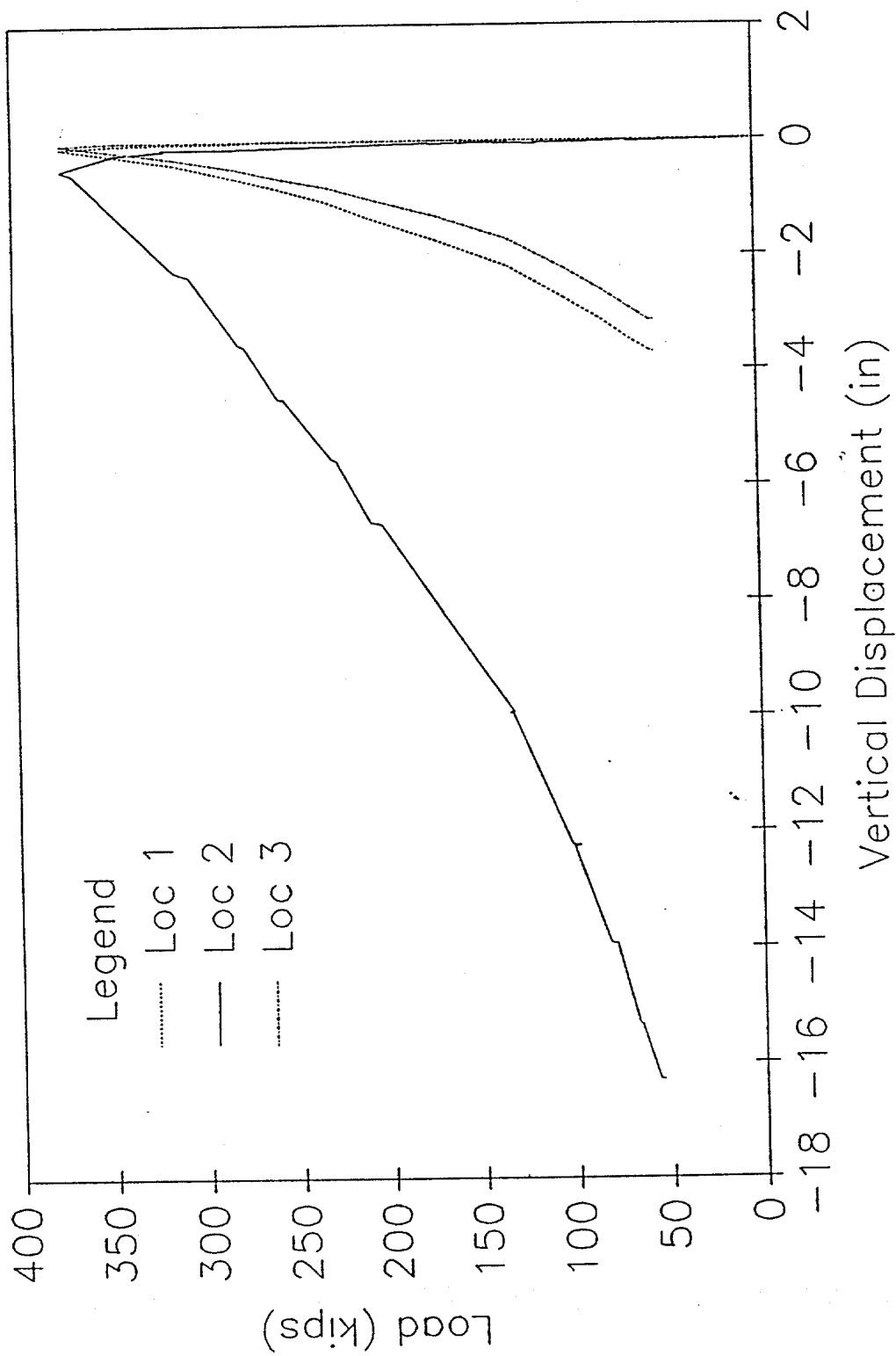
HORIZONTAL DISPLACEMENTS

Specimen 11



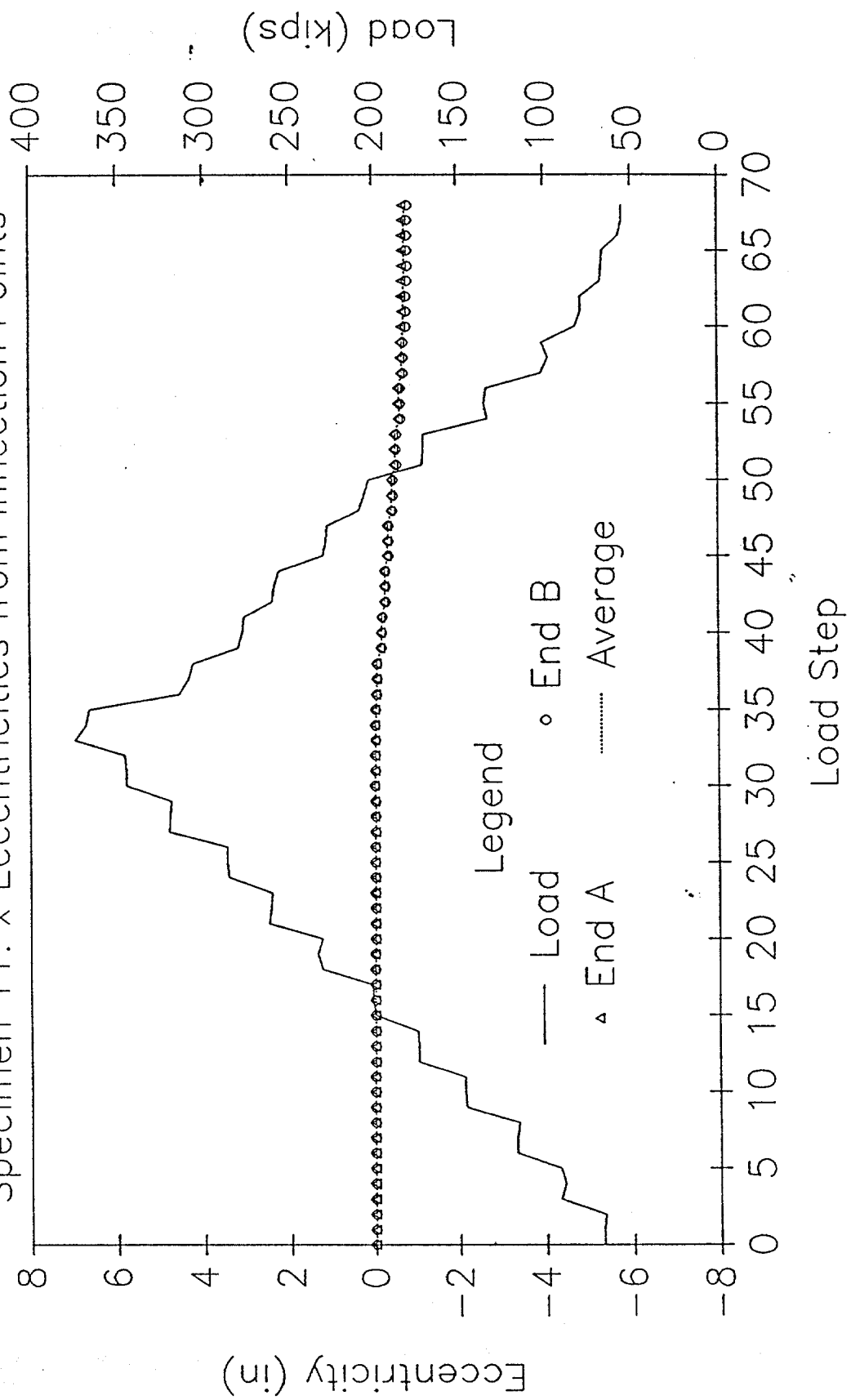
VERTICAL DISPLACEMENTS

Specimen 11



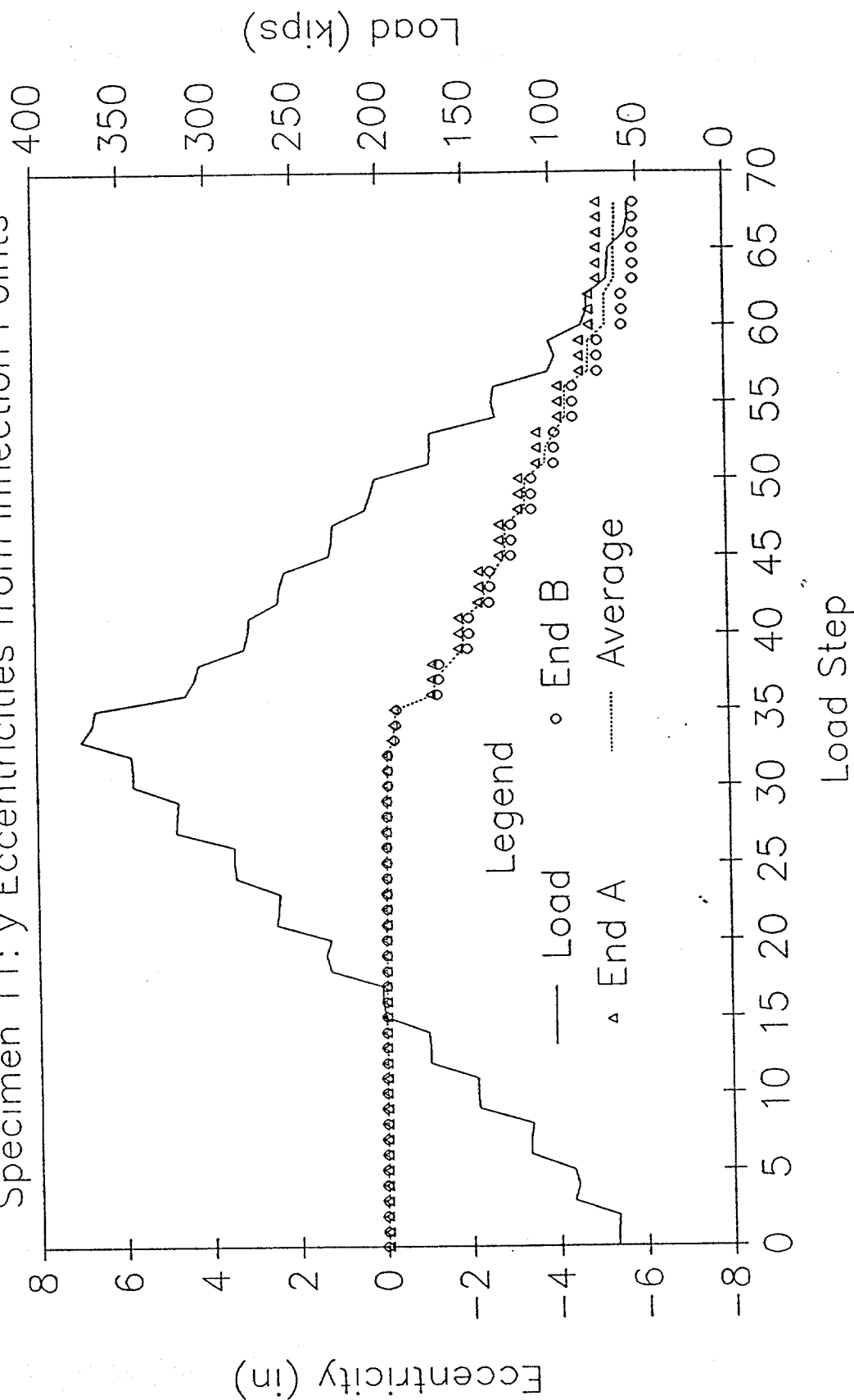
LOAD AND ECCENTRICITY vs LOAD STEP

Specimen 11: x Eccentricities from Inflection Points



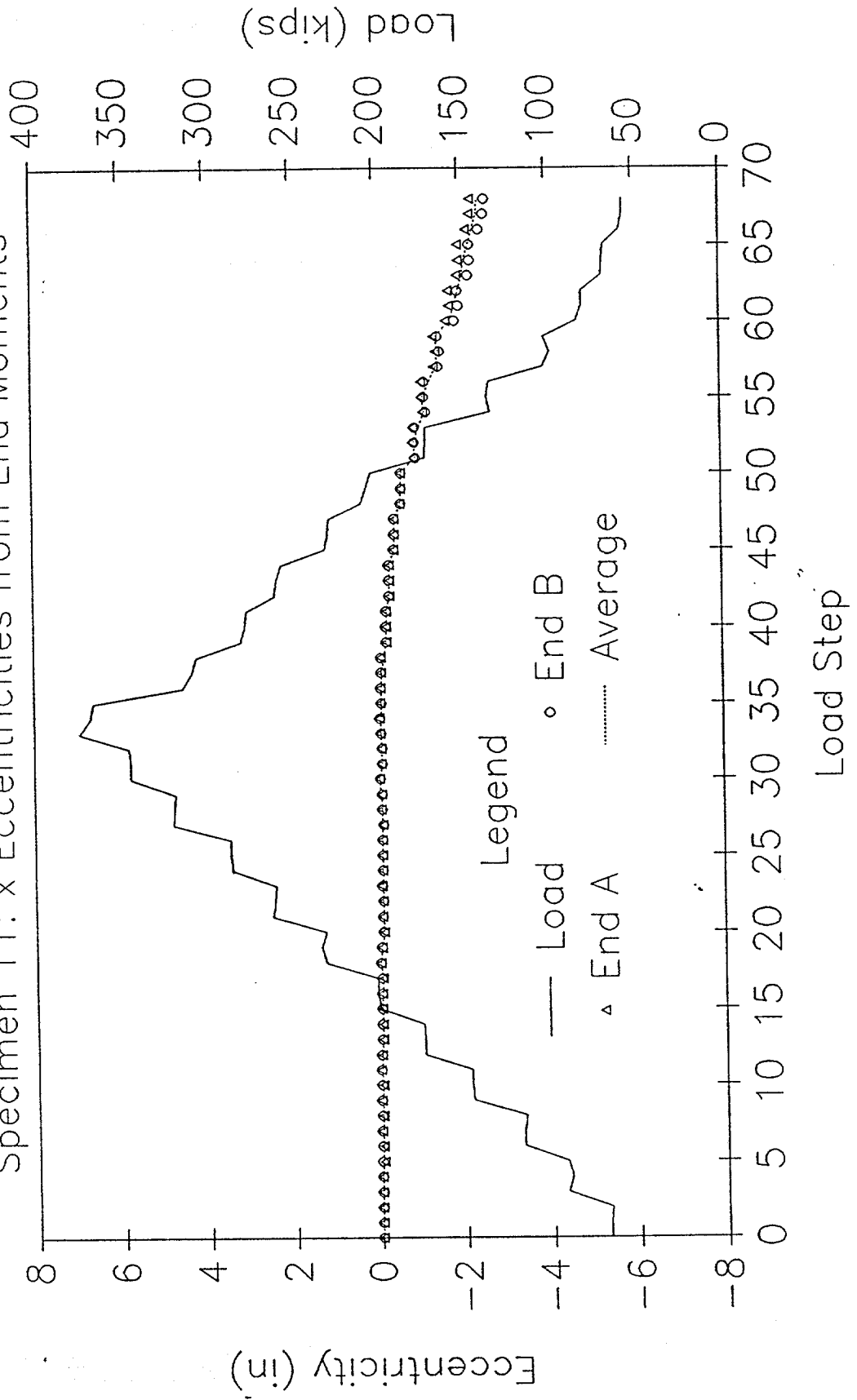
LOAD AND ECCENTRICITY vs LOAD STEP

Specimen 11: y Eccentricities from Inflection Points



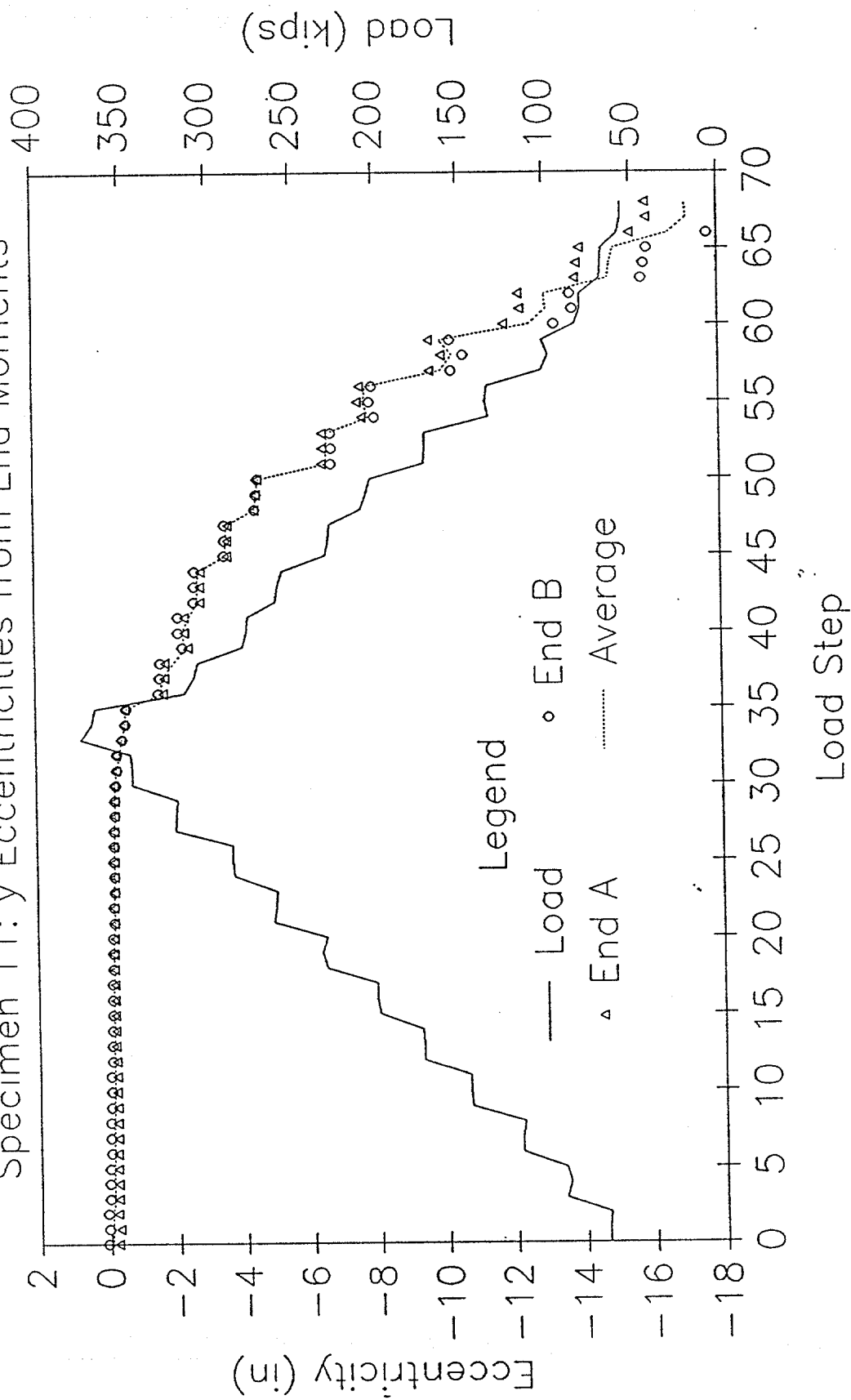
LOAD AND ECCENTRICITY vs LOAD STEP

Specimen 11: x Eccentricities from End Moments



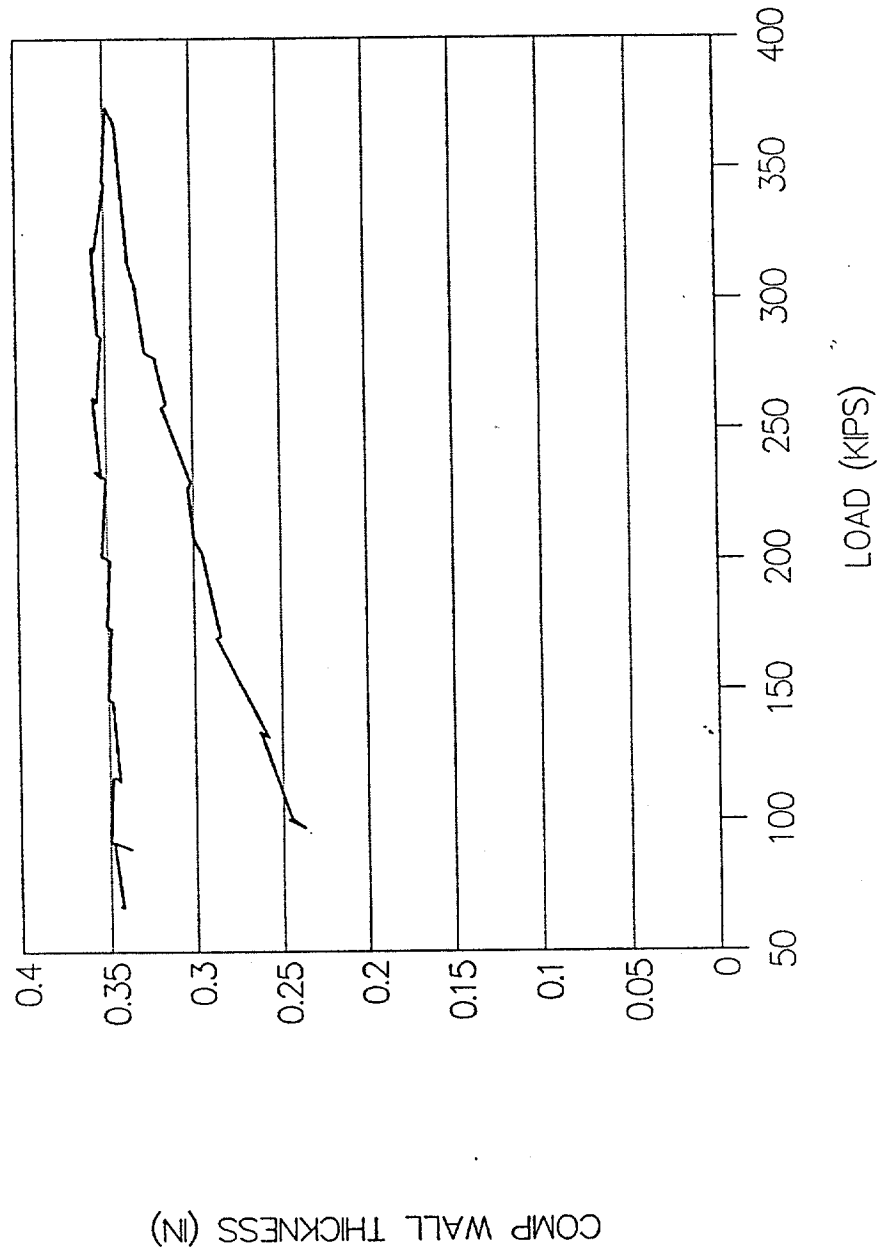
LOAD AND ECCENTRICITY vs LOAD STEP

Specimen 11: y Eccentricities from End Moments



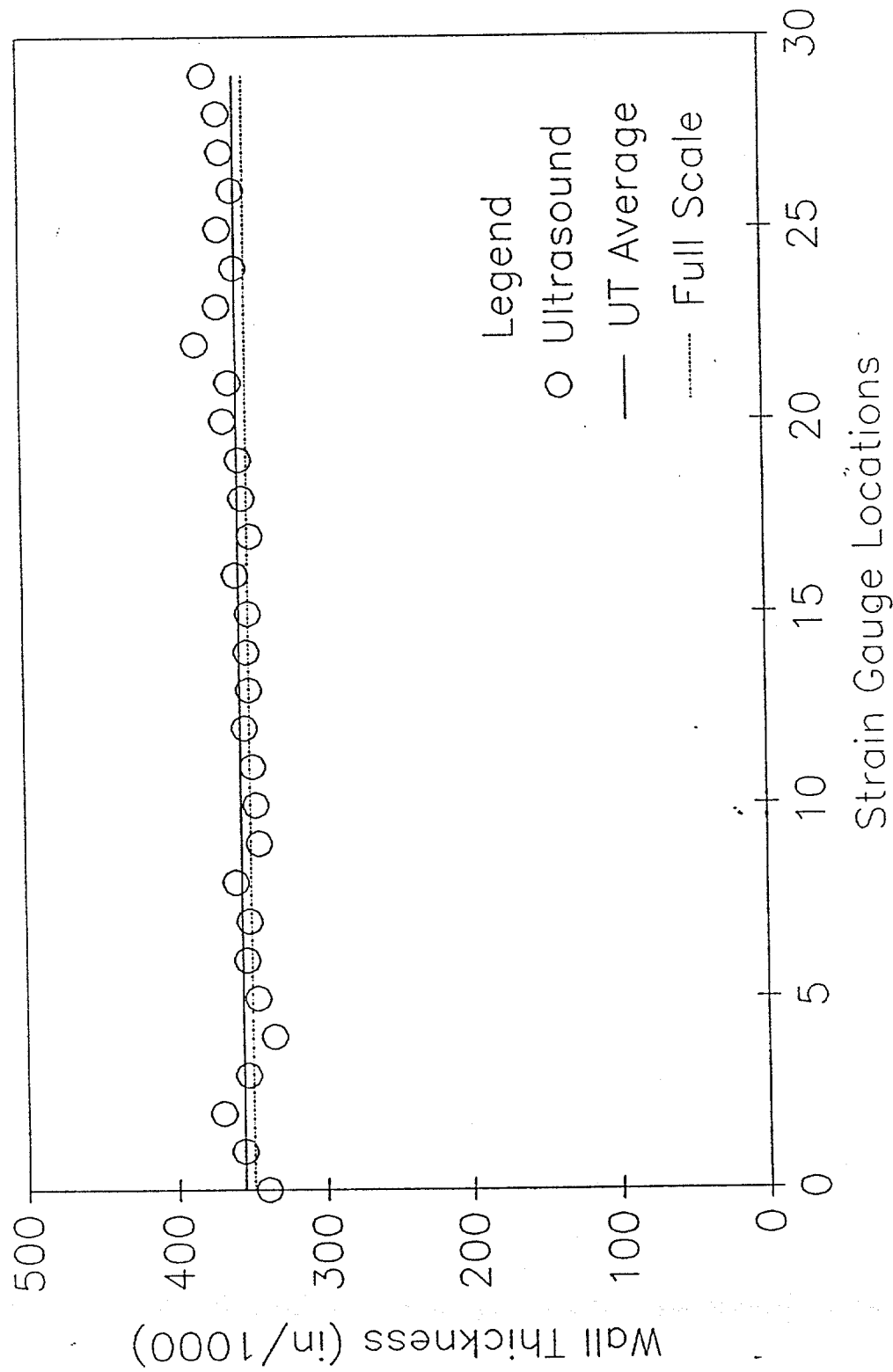
SPECIMEN NO 11-FULL SCALE TEST

COMPUTED WALL THICKNESS



SPECIMEN 11: WALL THICKNESS

Nominal Wall Thickness = 0.375 in



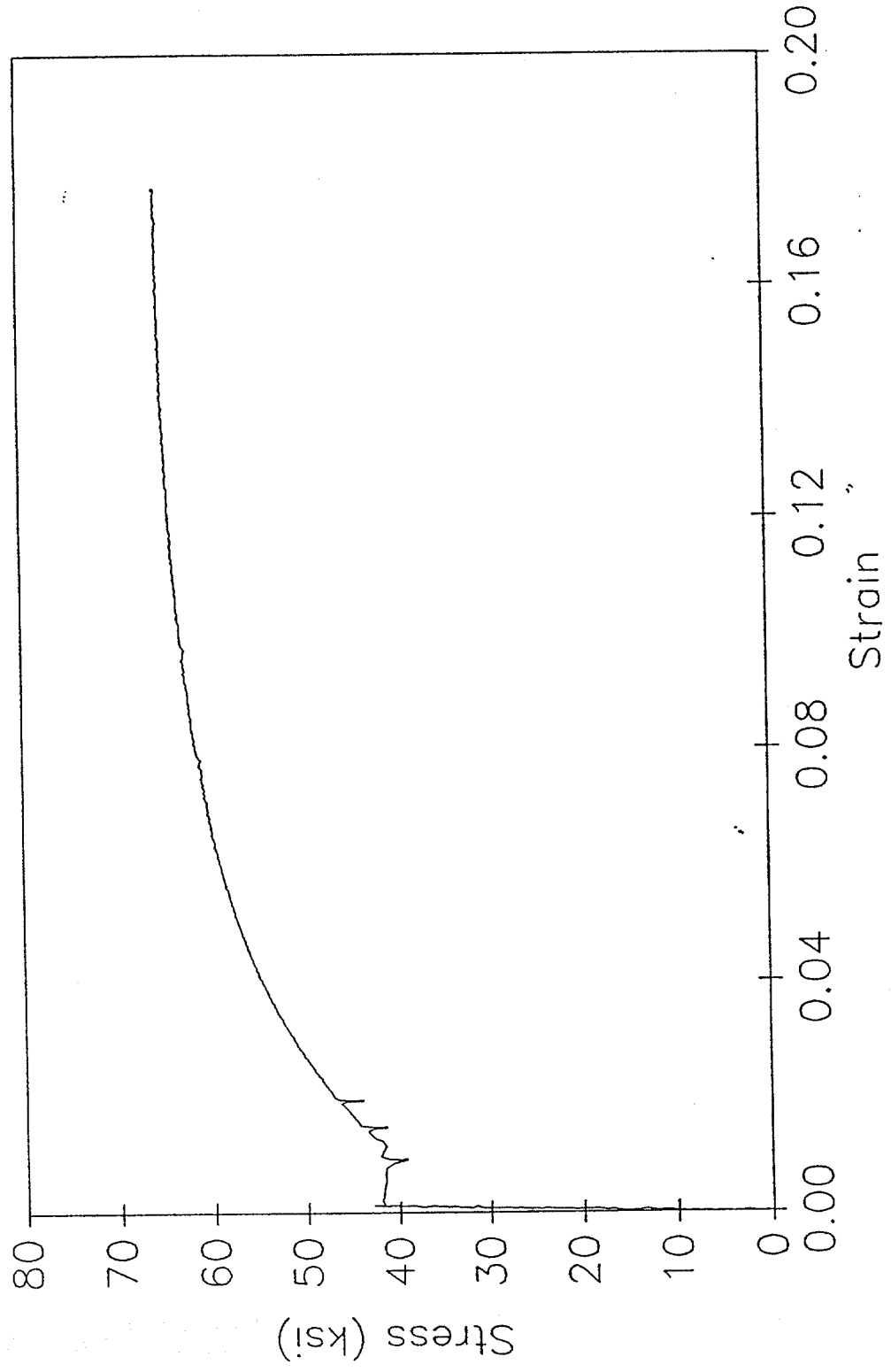
Ultrasound Data for Specimen 11
(All values in inches)

Gauge No.	UT Thickness	UT Average
0	0.340	
1	0.356	
2	0.370	
3	0.353	
4	0.335	
5	0.346	0.350
6	0.353	
7	0.351	
8	0.360	
9	0.344	
10	0.346	
11	0.348	0.350
12	0.353	
13	0.350	
14	0.351	
15	0.350	
16	0.358	
17	0.348	0.352
18	0.353	
19	0.355	
20	0.365	
21	0.361	
22	0.383	
23	0.368	0.364
24	0.357	
25	0.367	
26	0.358	
27	0.365	
28	0.367	
29	0.376	0.365

Overall Average = 0.356

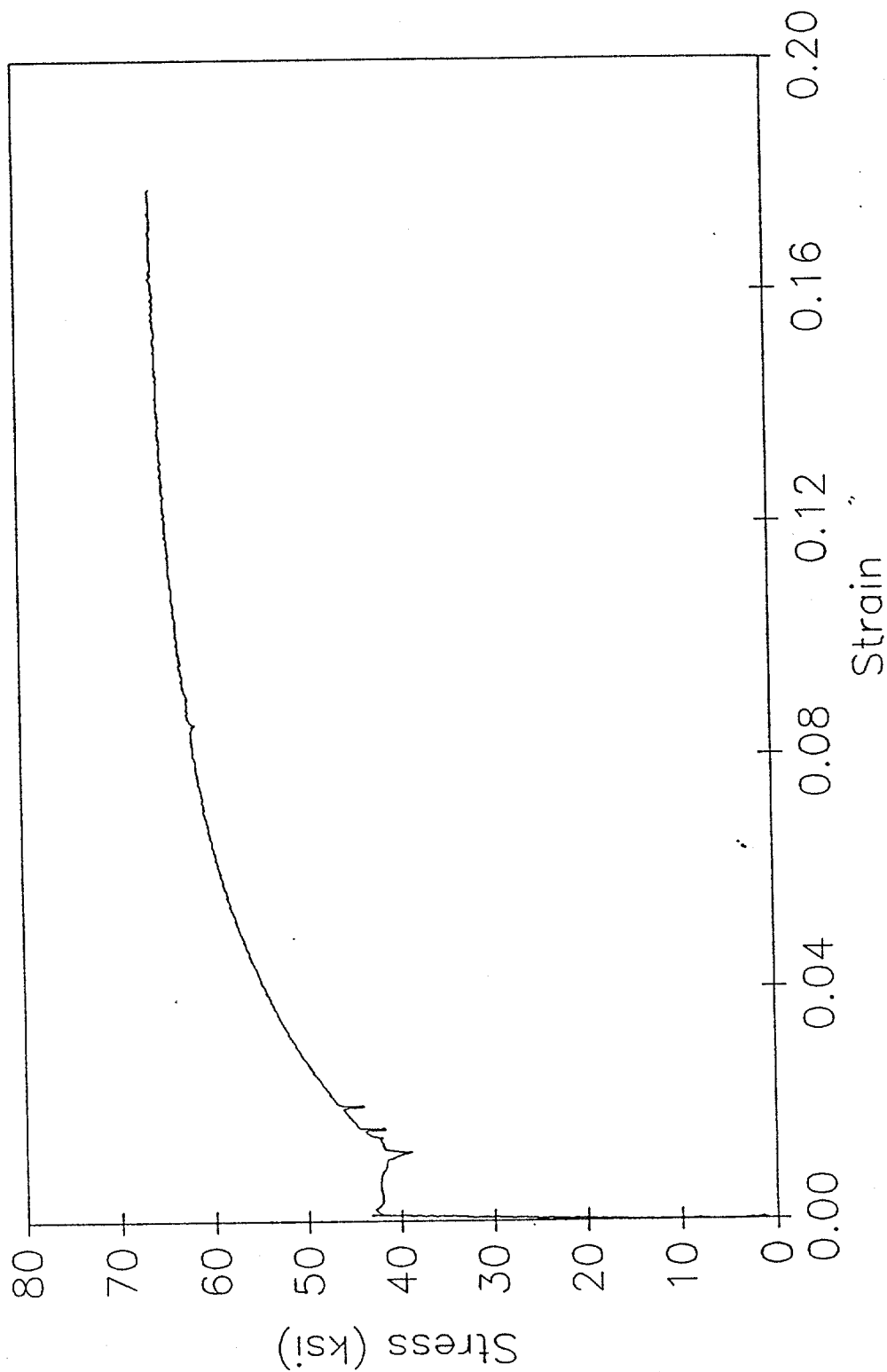
TENSILE SPECIMEN 11-1

Stress vs Strain



TENSILE SPECIMEN 11-2

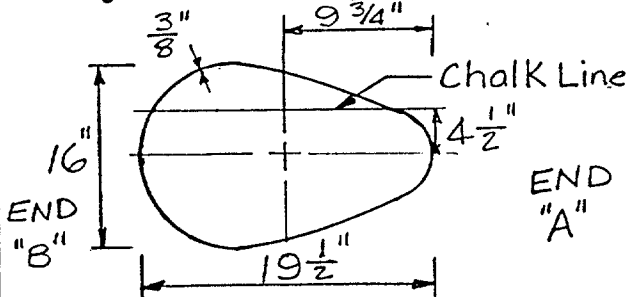
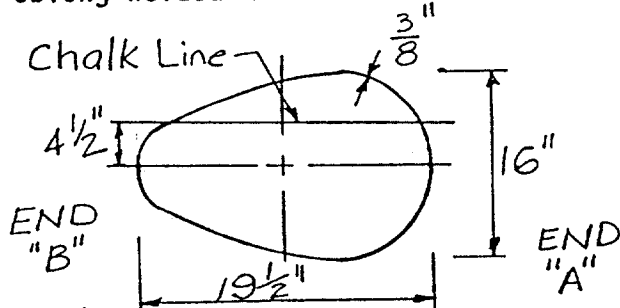
Stress vs Strain



SPECIMEN 12

DAMAGE SUMMARY

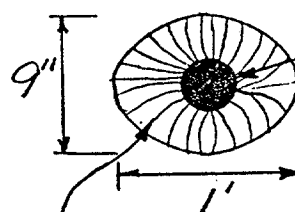
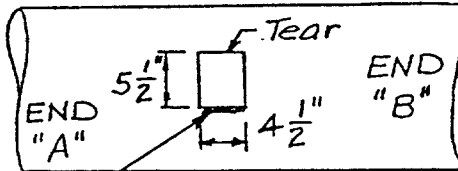
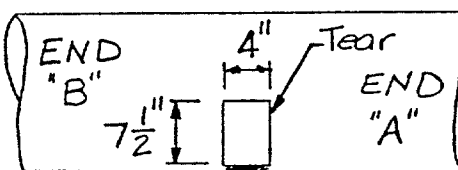
Specimen No. 12

DISTANCE FROM END "A"	*DISTANCE FROM CHALK LINE		DESCRIPTION OF DAMAGE
	LEFT	RIGHT	
1. 5'-9 1/2" (to center)		1'-4"	C-section welded to pipe (rectangular) 6" X 3"
2. 10'-5" (to center)		5 1/2"	7" diameter (round) bracing connection, 5/16" wall thickness
3. 10'-5" (to center)	1'-3"		7" diameter (round) bracing connection, 5/16" wall thickness
4. 10'-9" (to center)		1'-3 1/4"	C-section welded to pipe (rectangular) 6" X 3"
5. 17'-11" (to center)		5 1/2"	7" diameter (round) bracing connection, 5/16" wall thickness
6. 17'-11" (to center)	1'-2 1/4"		7" diameter (round) bracing connection, 5/16" wall thickness
7. 18'-5"	4 1/2"		Oblong welded bracing attachment 
8. 20'-7"	4 1/2"		Oblong welded attachment 

*Looking from end "A" towards end "B"

DAMAGE SUMMARY

Specimen No. 12

DISTANCE FROM END "A"	*DISTANCE FROM CHALK LINE		DESCRIPTION OF DAMAGE
	LEFT	RIGHT	
9. 20'-11" (to center)		1'-4"	<p>4" diameter circular <u>hole</u></p>  <p>4" diameter hole</p> <p>Elliptic dent with center same as hole-3" deep at hole's edge</p>
10. 21'-3 1/4" (to center)		5 1/2"	7" diameter (round) bracing connection, 5/16" wall thickness
11. 21'-3 1/4" (to center)	1'-3"		7" diameter (round) bracing connection, 5/16" wall thickness
12. 22'-1 1/2" (to center)		6"	<p>Rectangular <u>tear</u></p>  <p>4" long <u>dent</u> on bottom of tear, 2 1/4" deep at holes edge</p>
13. 25'-1" (to center)	1'-4"		<p>Rectangular <u>tear</u></p>  <p>On bottom of pipe--<u>dent</u>, 6" long X 10" wide, on bottom of tear, 1 3/4" deep at holes edge</p>

*Looking from end "A" towards end "B"

DAMAGE SUMMARY

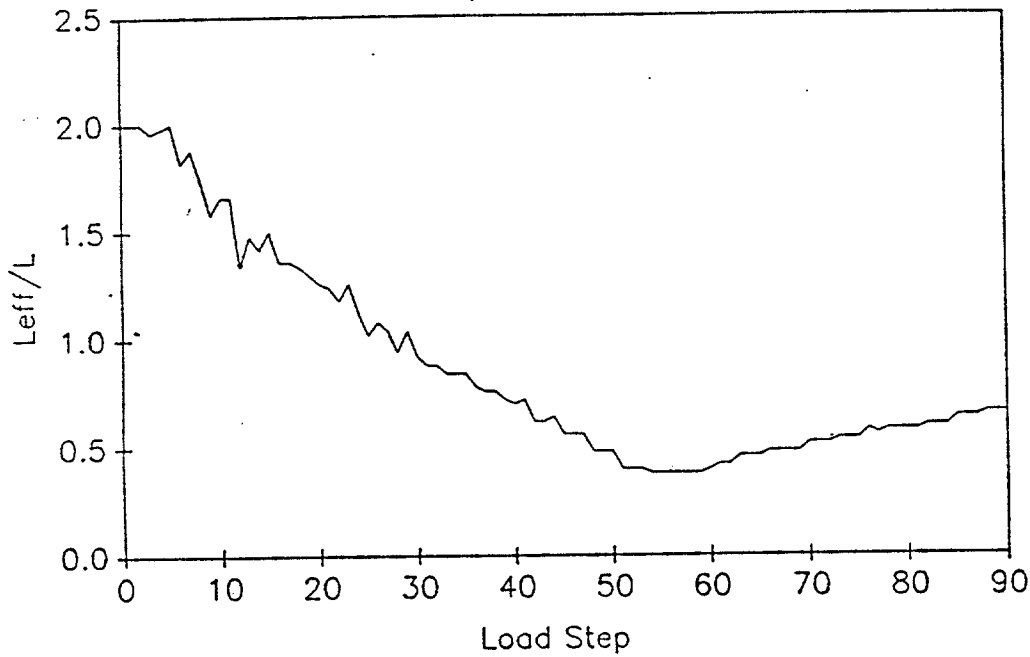
Specimen No. 12

DISTANCE FROM END "A"	*DISTANCE FROM CHALK LINE		DESCRIPTION OF DAMAGE
	LEFT	RIGHT	
14. 28'-9" (to center)		5"	7' diameter (round) bracing connection, 5/16" wall thickness
15. 28'-9" (to center)	1'-3"		7" diameter (round) bracing connection, 5/16" wall thickness
16. 29'-10 1/2" (to center)		1'-3"	C-section welded to pipe (rectangular) 6" X 3"
17. 29'-8" (to center)	1'-3 1/2"		10" diameter (round) old bracing connection, 3/8" wall thickness
18. 26'-9 1/4" (to center)			circumferential butt weld, 5/8" thick
19. 30'-10" \center of weld/	5 1/2"		20" long, longitudinal weld, 5/8" thick
20. 35'-0"		1'-2 3/4"	C-section welded to pipe (rectangular) 6" X 3"

*Looking from end "A" towards end "B"

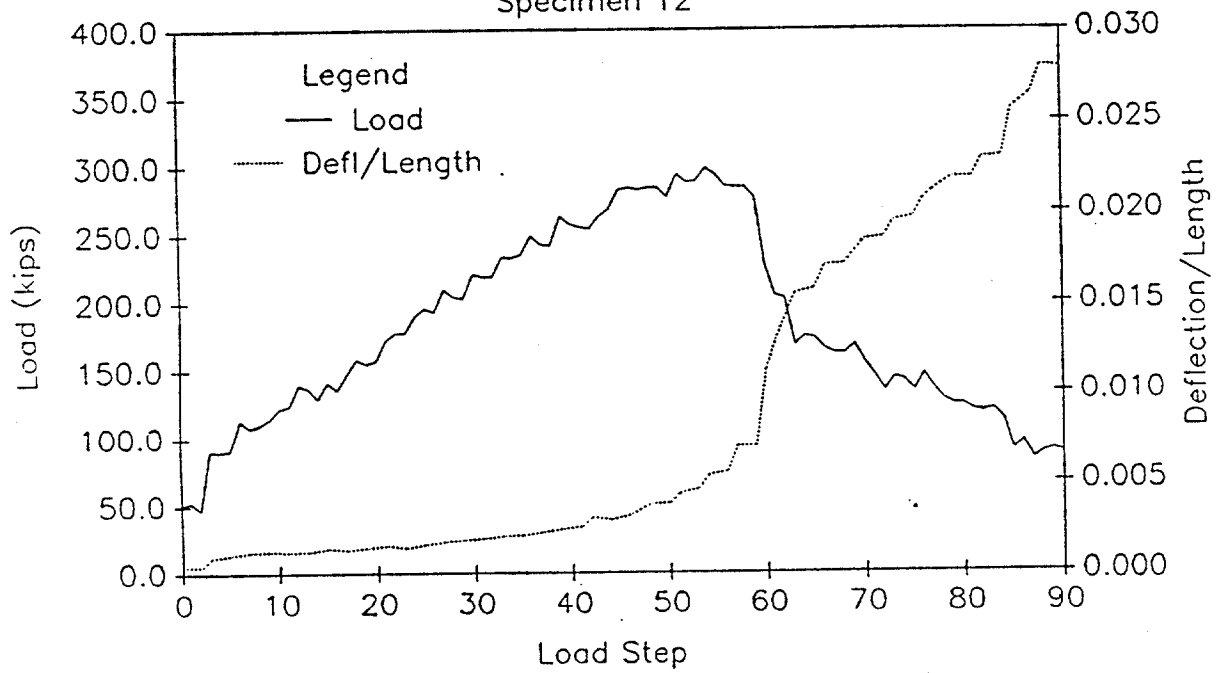
EFFECTIVE LENGTH vs LOAD STEP

Specimen 12



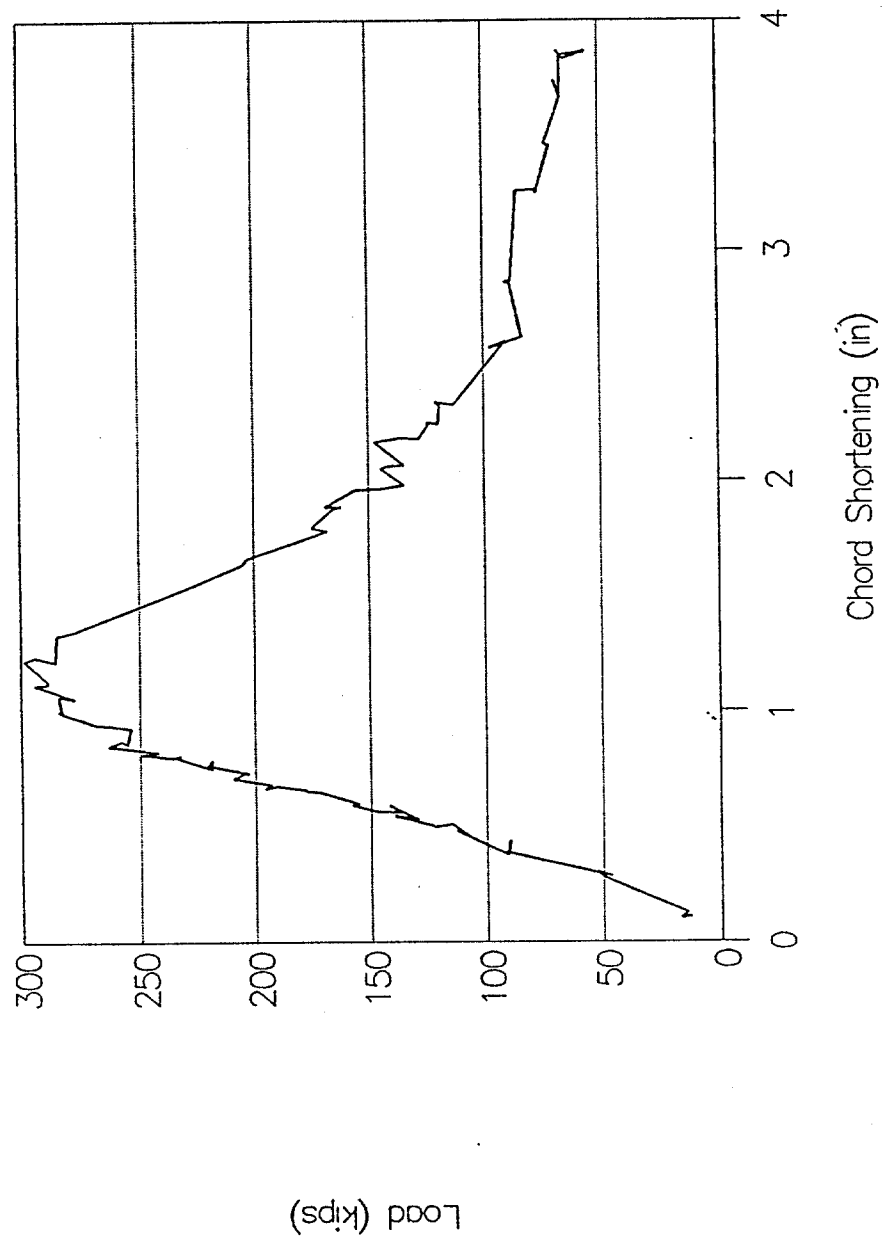
LOAD AND DEFLECTION vs LOAD STEP

Specimen 12

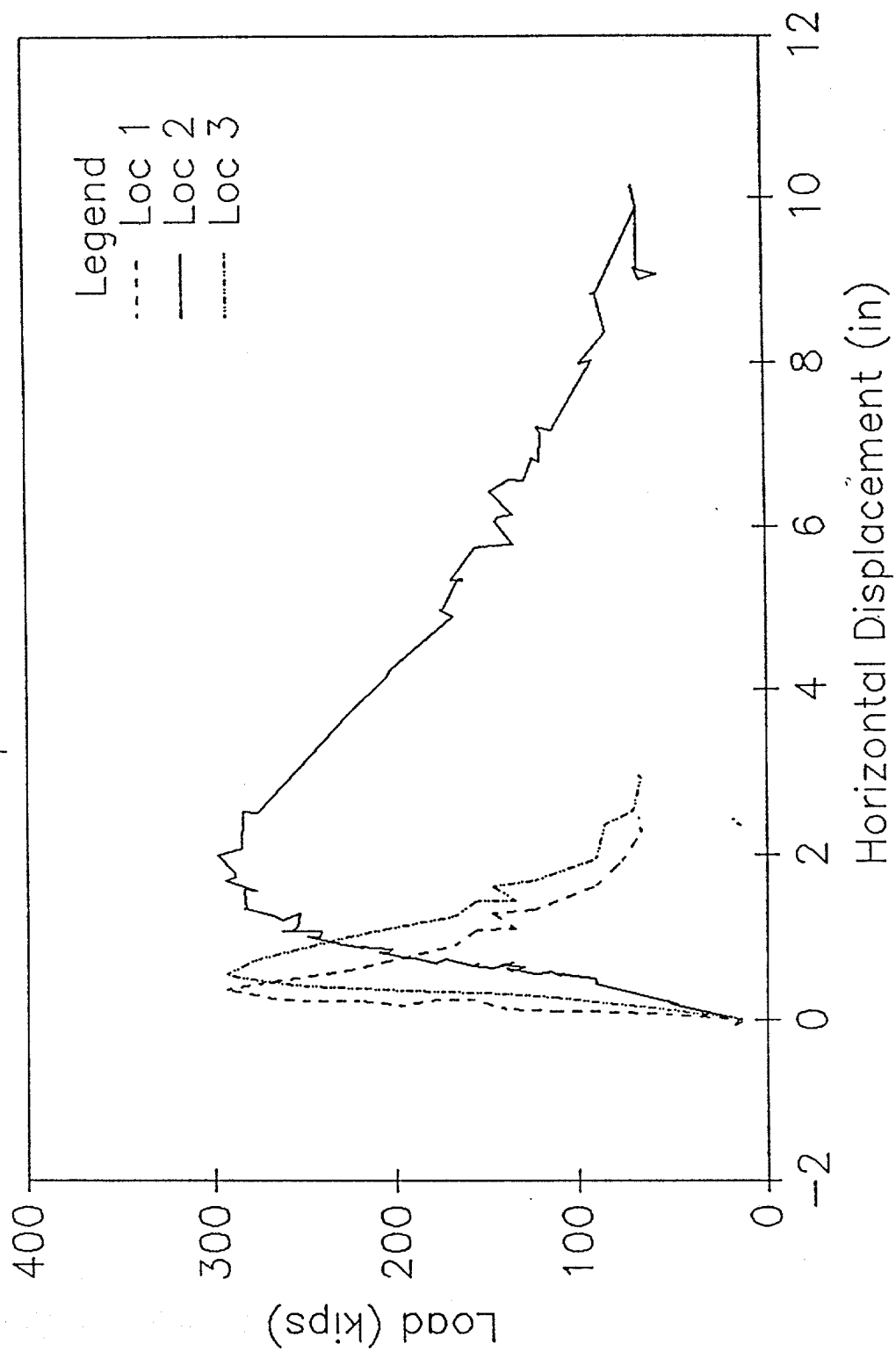


Chord Shortening

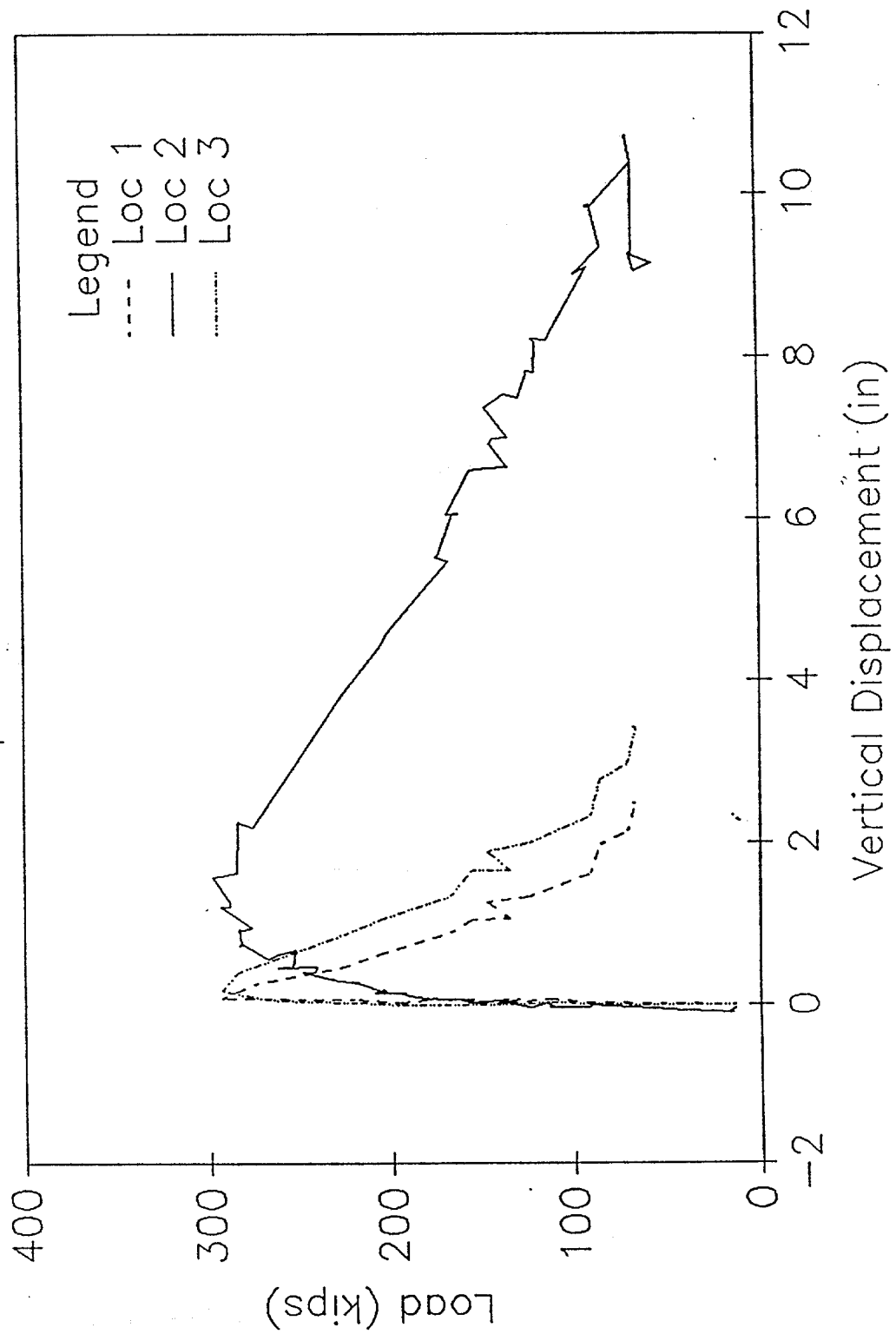
Specimen 12



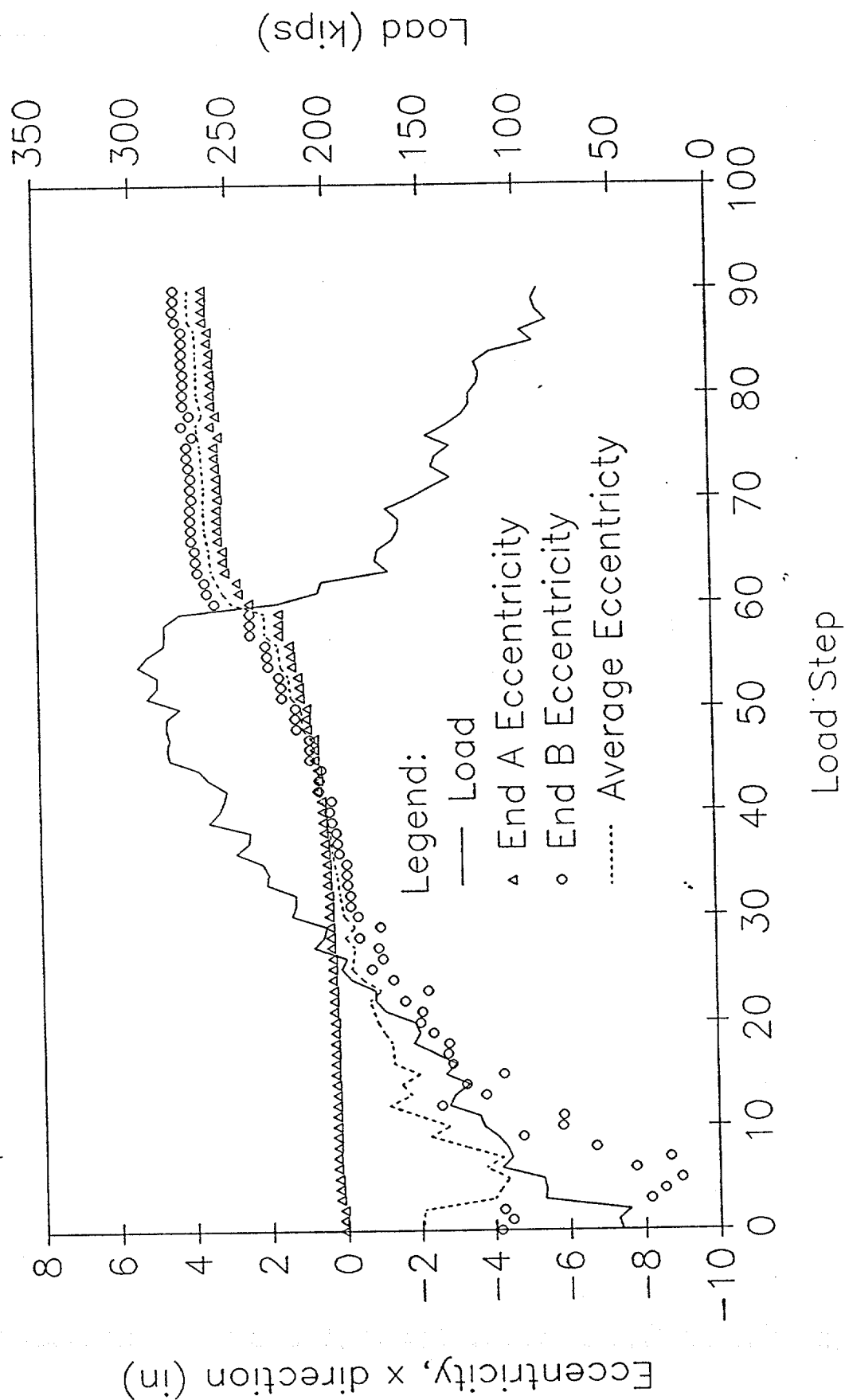
Horizontal Displacements Specimen 12



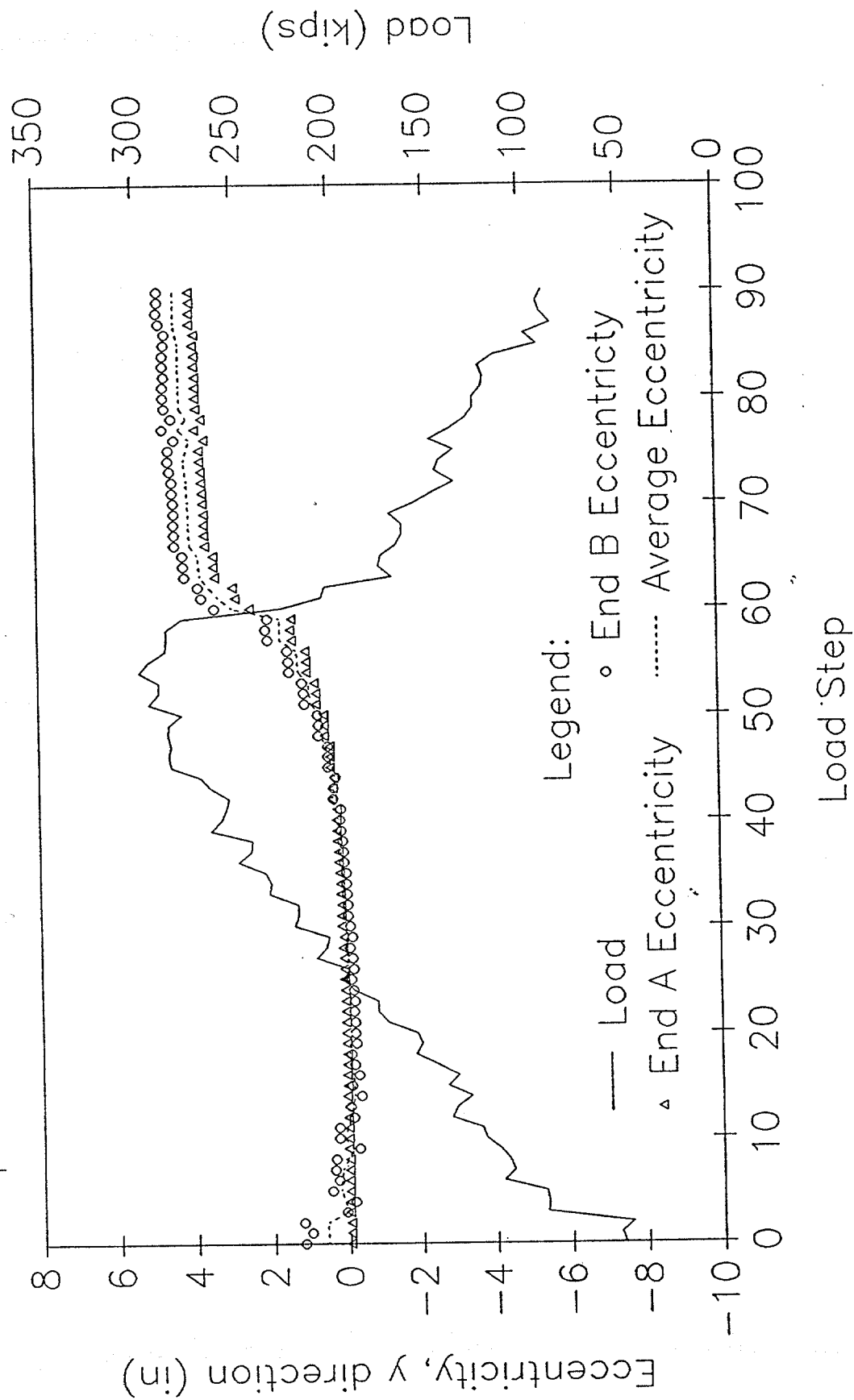
Vertical Displacements
Specimen 12



LOAD AND ECCENTRICITY vs LOAD STEP
Specimen 12: Eccentricities from Inflection Points

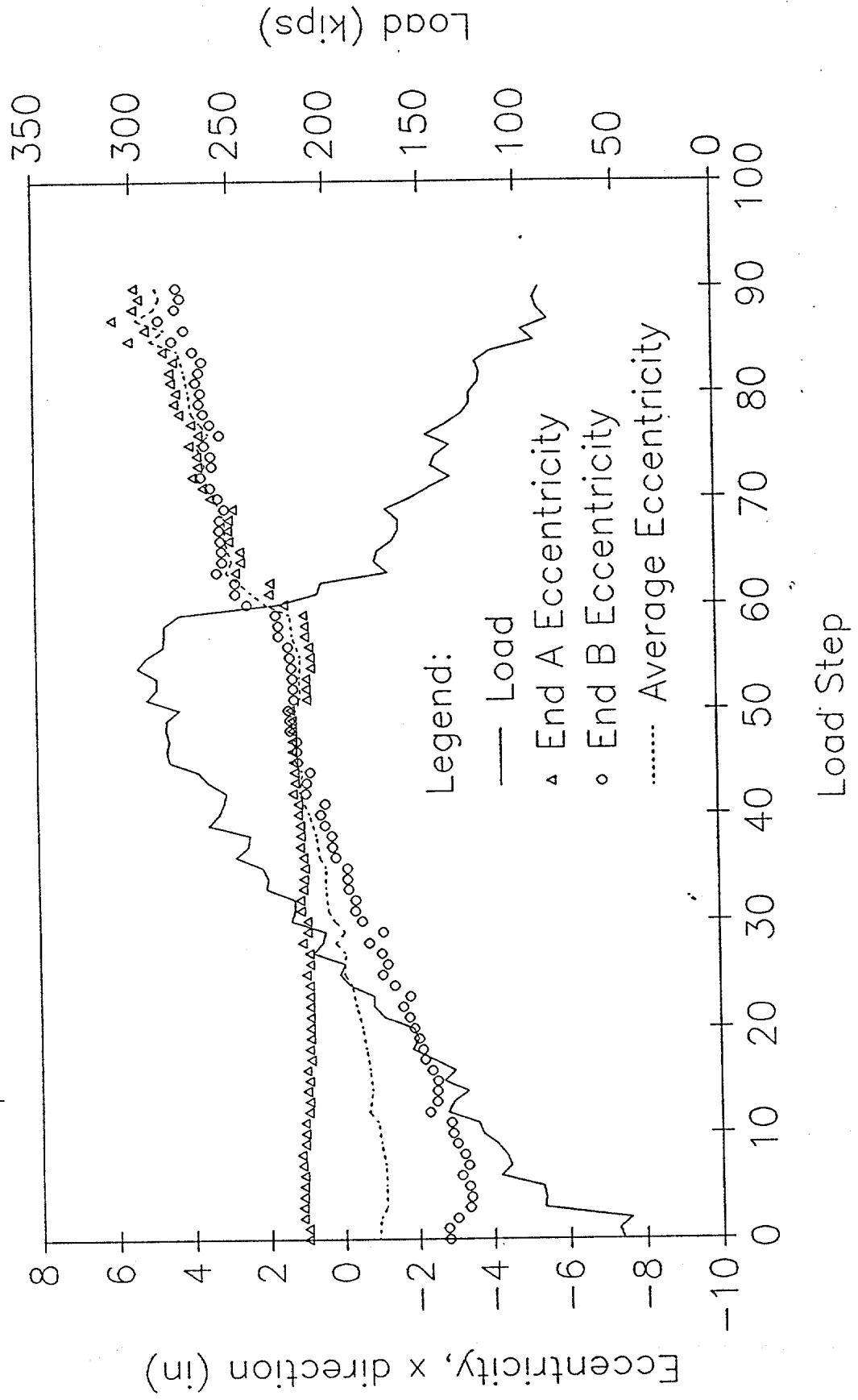


LOAD AND ECCENTRICITY vs LOAD STEP Specimen 12: Eccentricities from Inflection Points



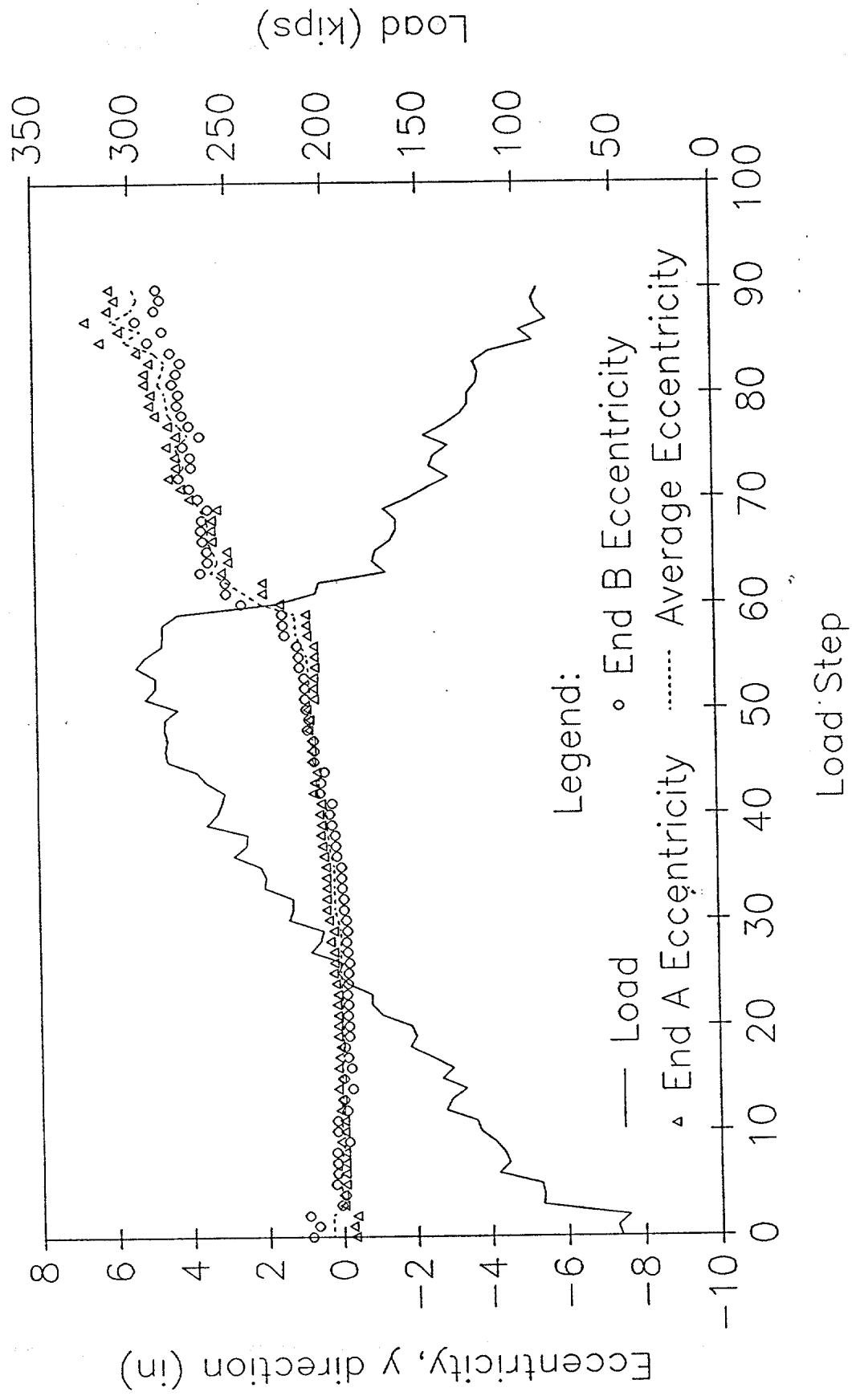
LOAD AND ECCENTRICITY vs LOAD STEP

Specimen 12: Eccentricities from Moments



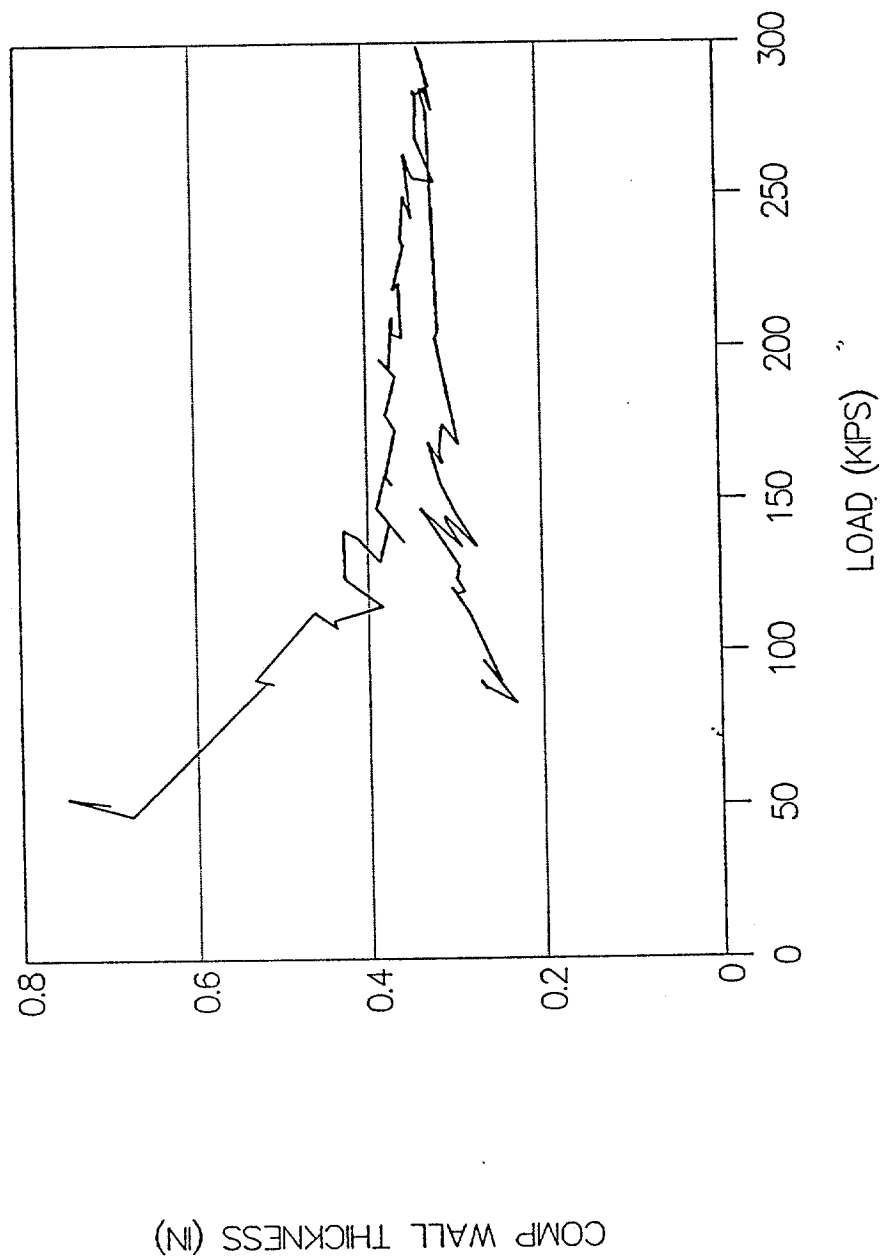
LOAD AND ECCENTRICITY vs LOAD STEP

Specimen 12: Eccentricities from Moments

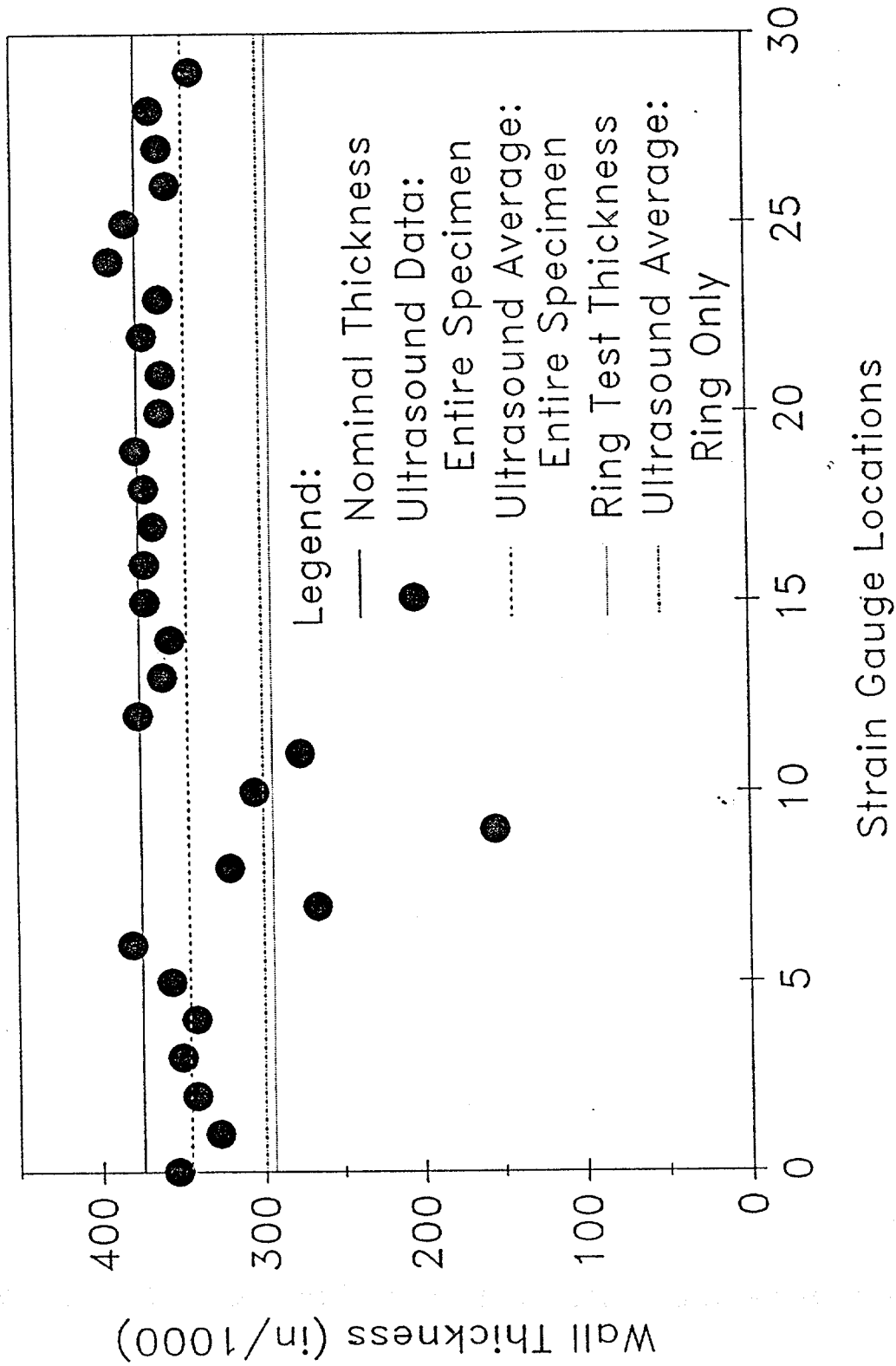


SPECIMEN NO 12-FULL SCALE TEST

COMPUTED WALL THICKNESS



Specimen 12: Wall Thickness Nominal Thickness = 0.375 in



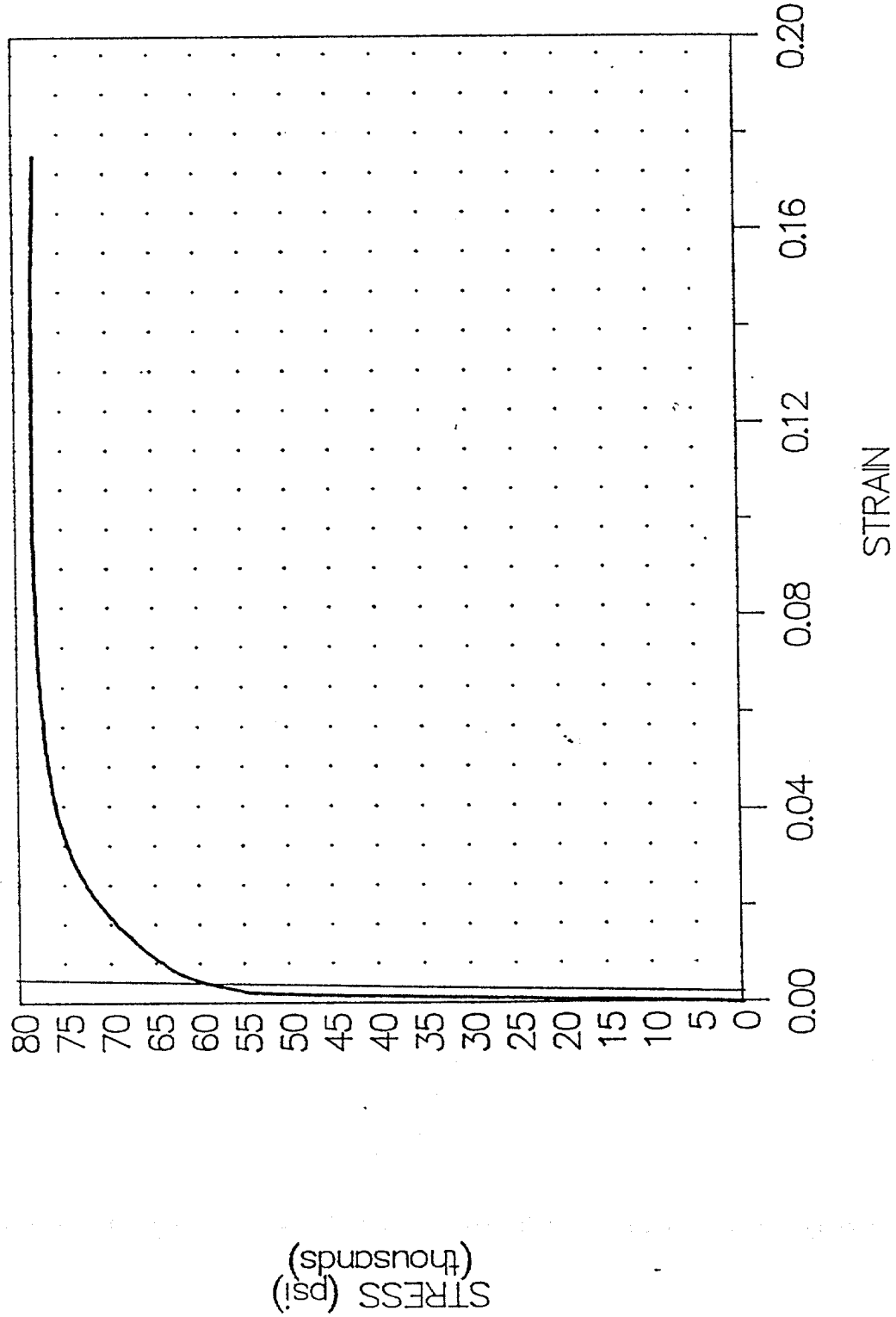
Ultrasound Data for Specimen 12
(All data in inches)

Gauge No.	UT Thickness	UT Average
0	0.354	
1	0.328	
2	0.342	
3	0.351	
4	0.342	
5	0.357	0.346
6	0.381	
7	0.266	
8	0.321	
9	0.155	
10	0.305	
11	0.276	0.284
12	0.376	
13	0.361	
14	0.356	
15	0.371	
16	0.371	
17	0.366	0.367
18	0.371	
19	0.376	
20	0.361	
21	0.360	
22	0.371	
23	0.361	0.367
24	0.391	
25	0.381	
26	0.356	
27	0.361	
28	0.366	
29	0.341	0.366

Overall Average = 0.346

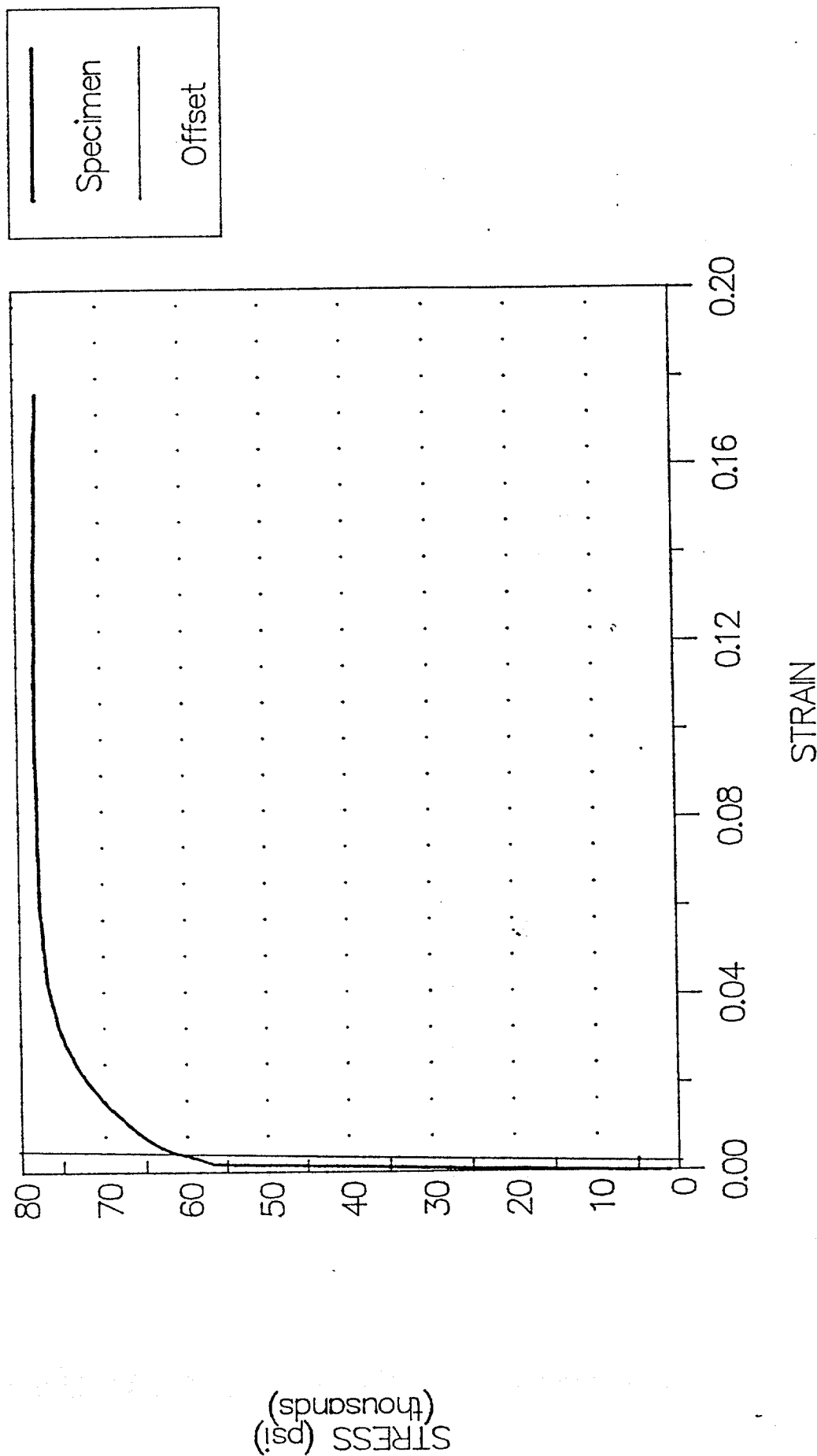
TENSILE SPECIMEN 12-1

Stress vs Strain



TENSILE SPECIMEN 12-2

Stress vs Strain



SPECIMEN 13

DAMAGE SUMMARY

Specimen No. 13
12/20/89

DISTANCE FROM END "B"	*DISTANCE FROM CHALK LINE		DESCRIPTION OF DAMAGE
	LEFT	RIGHT	
1. 7'-9"	0'-6"		Dent. See additional sheets.
2. 8'-6"		0'-1"	Dent. See additional sheets.
3. 10'-9"	0'-4"		Dent. See additional sheets.
4. 17'-8"	0'-6 1/2"		Dent. See additional sheets.

WIDESPREAD CORROSION OVER ENTIRE SPECIMEN.

*Looking from end "A" towards end "B"

Out-of-Straightness Measurements
for Specimen 13

The specimen was initially curved in the yz-plane and in the xz-plane. The following measurements are in the x-direction.

Distance from End B (ft)	Distance from stringline to top of pipe (in)	Out-of straightness in x direction (in)
0	4.25	0
1	4.25	0
2	4.0	0.25
3	4.0	0.25
4	4.0	0.25
5	3.75	0.5
6	3.75	0.5
7	3.625	0.625
8	3.25	1
9	3.125	1.125
10	3.125	1.125
11	3.0	1.25
12	2.75	1.5
13	2.625	1.625
14	2.5	1.75
15	2.5	1.75
16	2.0	2.25
17	1.75	2.5
18	1.75	2.5
19	2.0	2.25
20	2.5	1.75
21	3.0	1.25
22	3.375	0.875
23	3.75	0.5
24.125	4.25	0

Out-of-Straightness Measurements
for Specimen 13

The specimen was initially curved in the yz-plane and in the xz-plane. The following measurements are in the y-direction.

Distance from End B (ft)	Distance from stringline to top of pipe (in)	Out-of straightness in y direction (in)
0	3.875	0
1	4.75	-0.875
2	5.25	-1.375
3	5.75	-1.875
4	6.5	-2.625
5	7.25	-3.375
6	8.0	-4.125
7	8.875	-5
8	10.25	-6.375
8.5	12.0	-8.125
9	11.0	-7.125
10	10.125	-6.25
11	9.5	-5.625
12	9.125	-5.25
13	8.875	-5
14	8.5	-4.625
15	8.25	-4.375
16	8.0	-4.125
17	7.5	-3.625
18	7.25	-3.375
19	6.625	-2.75
20	6.375	-2.5
21	5.75	-1.875
22	5.0	-1.125
23	4.375	-0.5
24.125	3.875	0

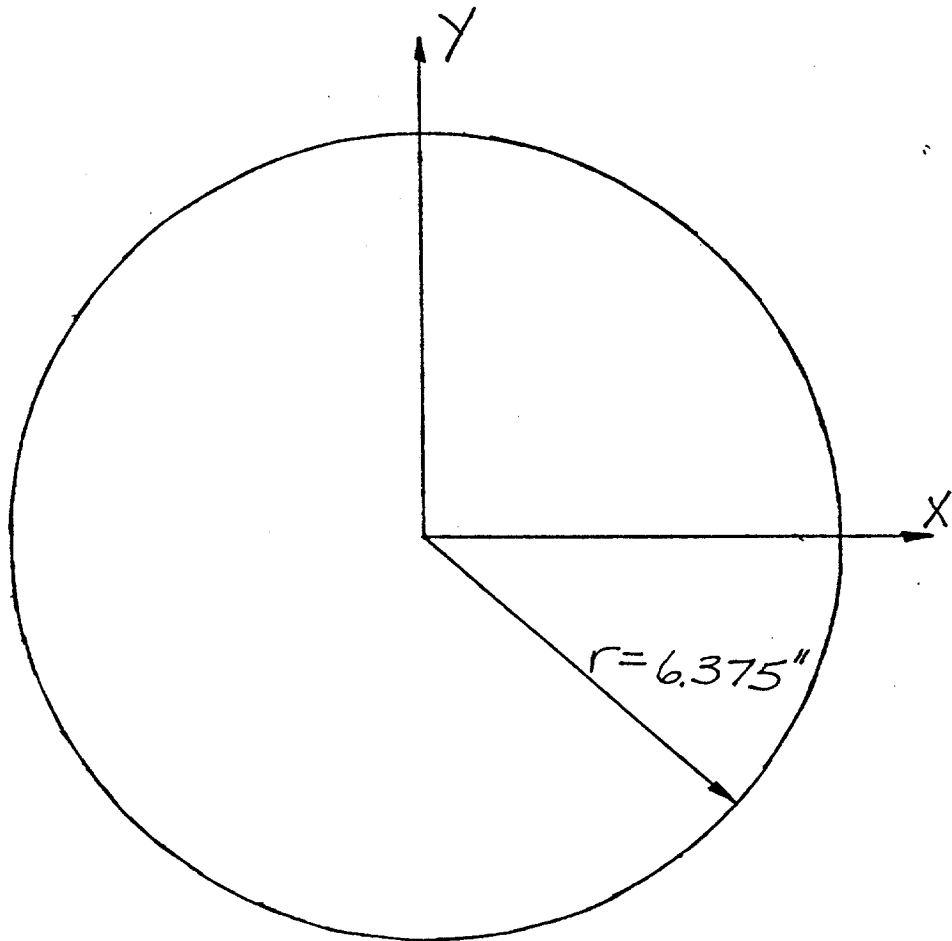
DENT CROSS SECTION

Specimen No. 13

Damage No. 1

Distance from End B 6'-9"

Scale 1" = 3"



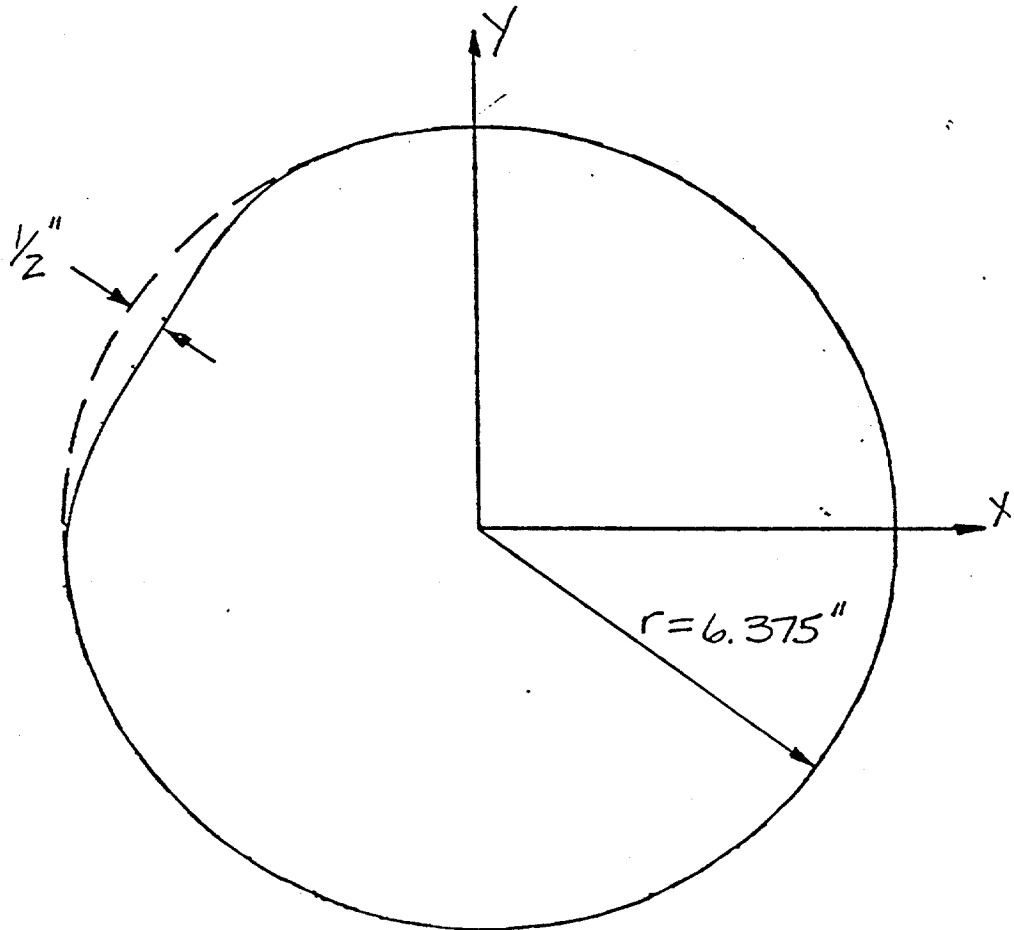
DENT CROSS SECTION

Specimen No. 13

Damage No. 1

Distance from End B 7'-0"

Scale 1" = 3"



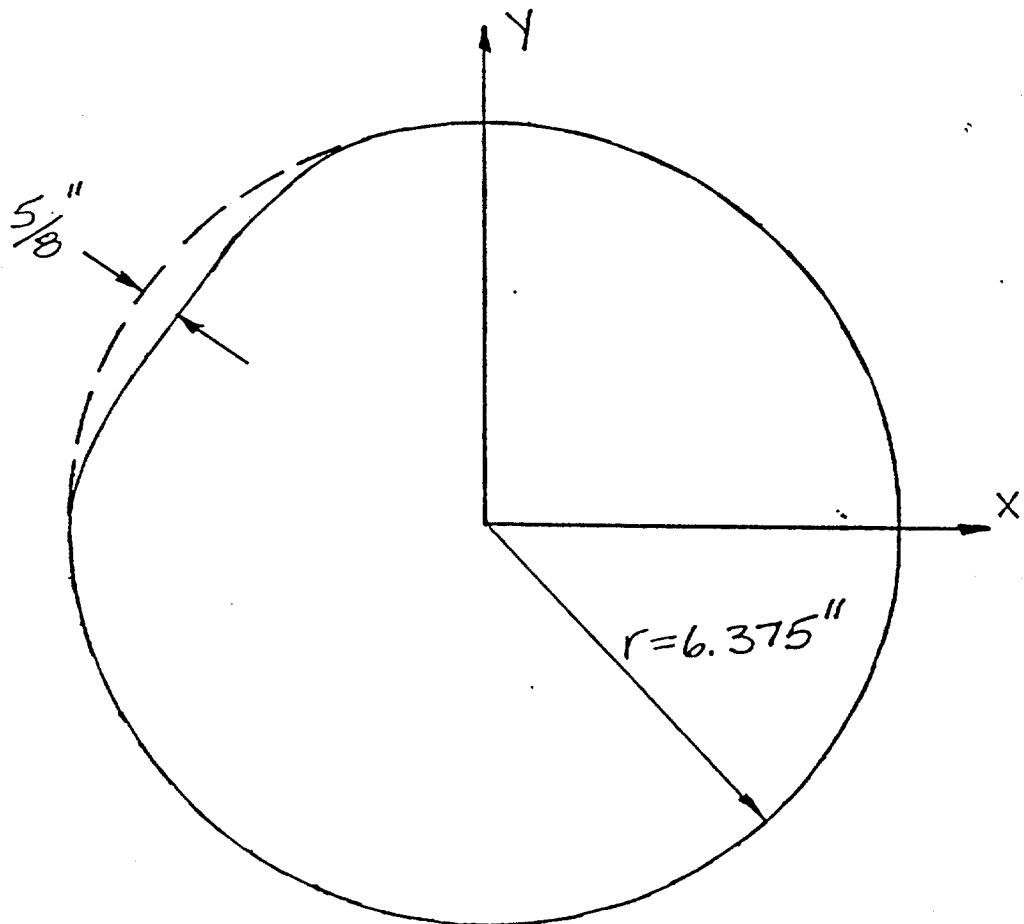
DENT CROSS SECTION

Specimen No. 13

Damage No. 1

Distance from End B 7'-3"

Scale 1"=3"



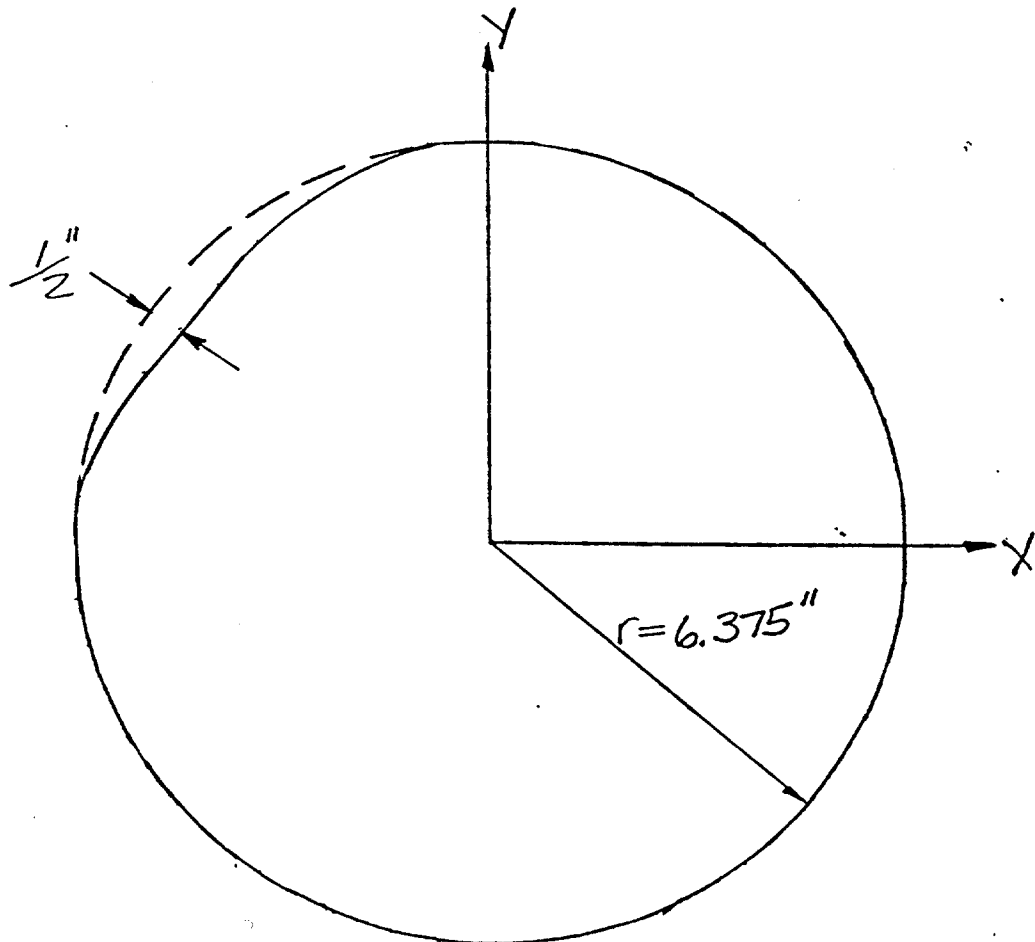
DENT CROSS SECTION

Specimen No. 13

Damage No. 1

Distance from End B 7'-6"

Scale 1"=3"



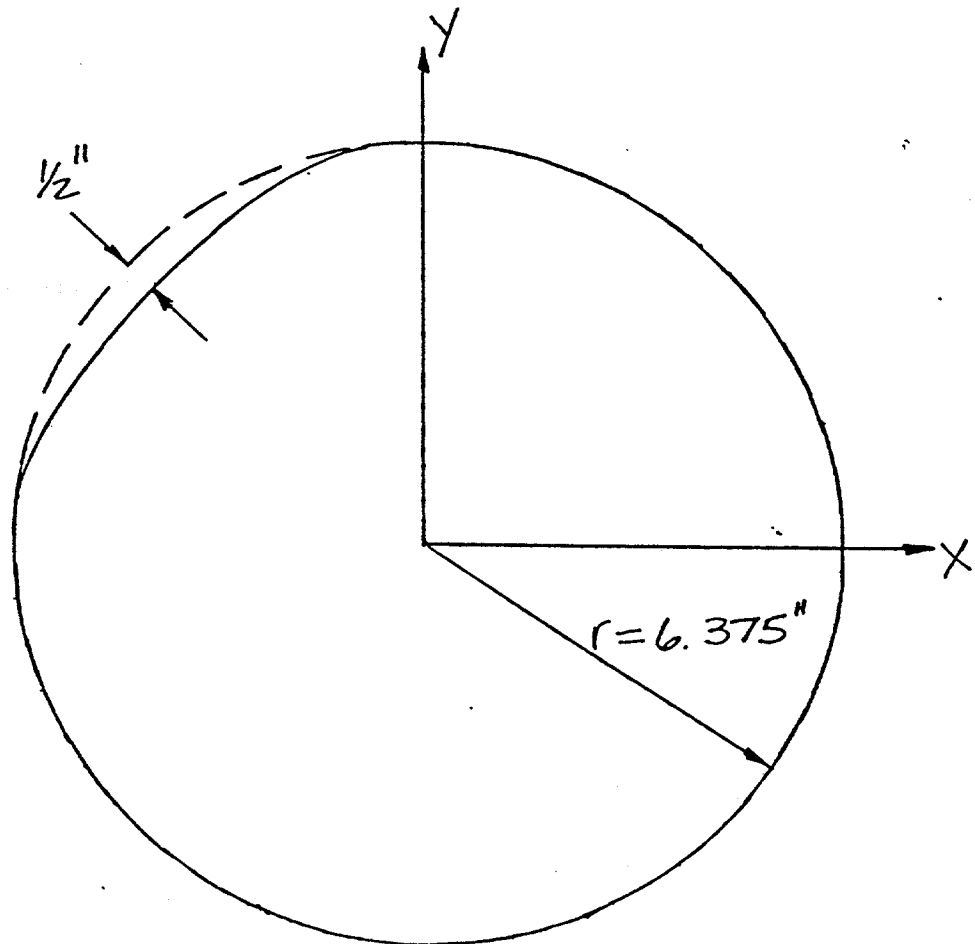
DENT CROSS SECTION

Specimen No. 13

Damage No. 1

Distance from End B 7'-9"

Scale 1"=3"



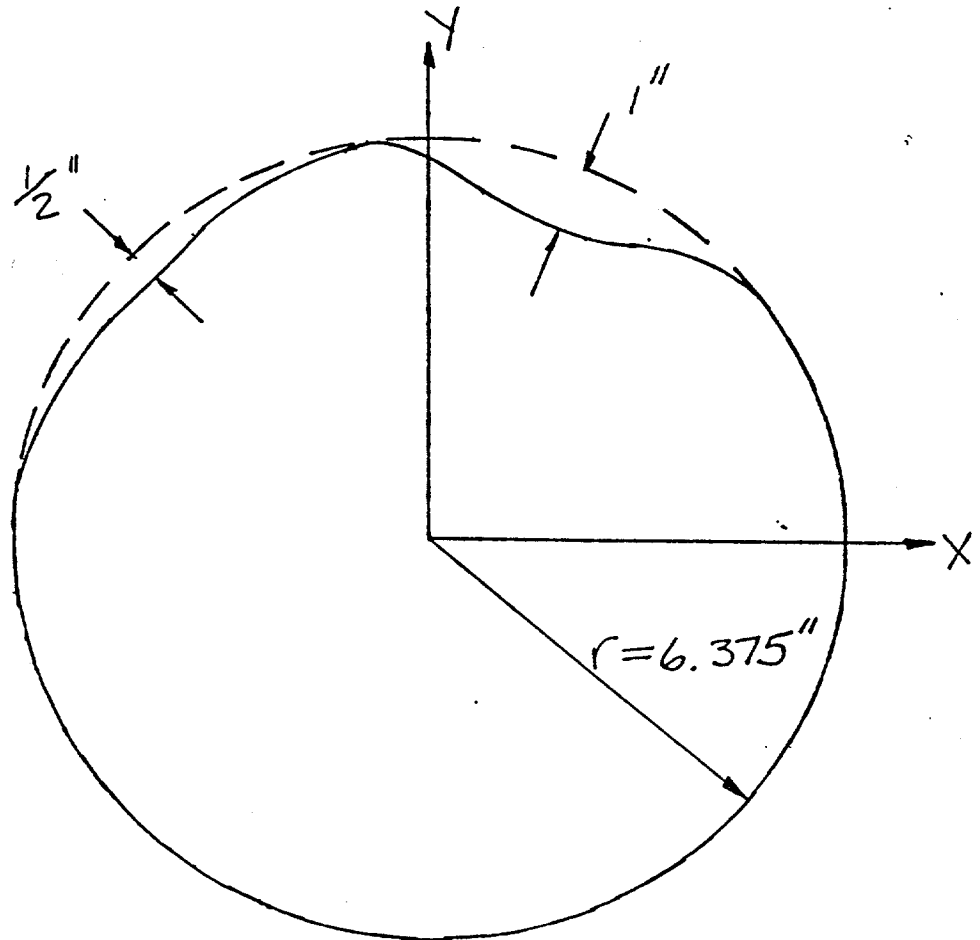
DENT CROSS SECTION

Specimen No. 13

Damage No. 142

Distance from End B 8'-0"

Scale 1"=3"



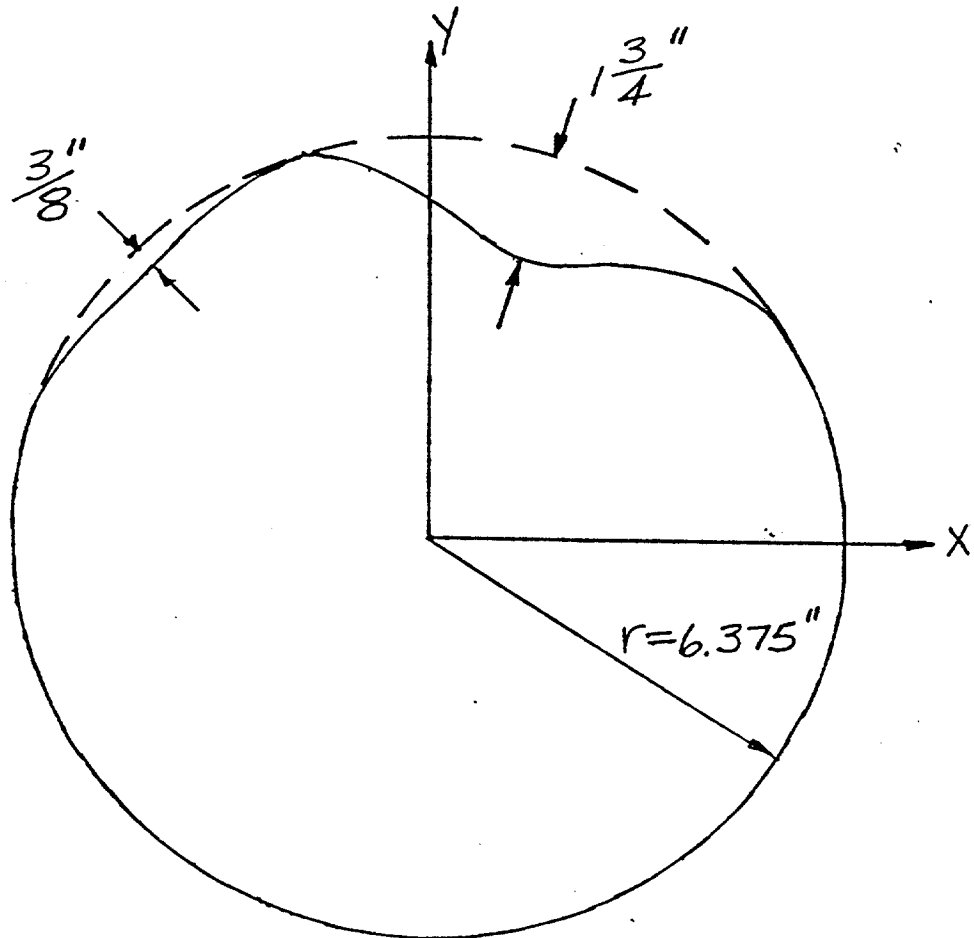
DENT CROSS SECTION

Specimen No. 13

Damage No. 142

Distance from End B 8'-3"

Scale 1"=3"



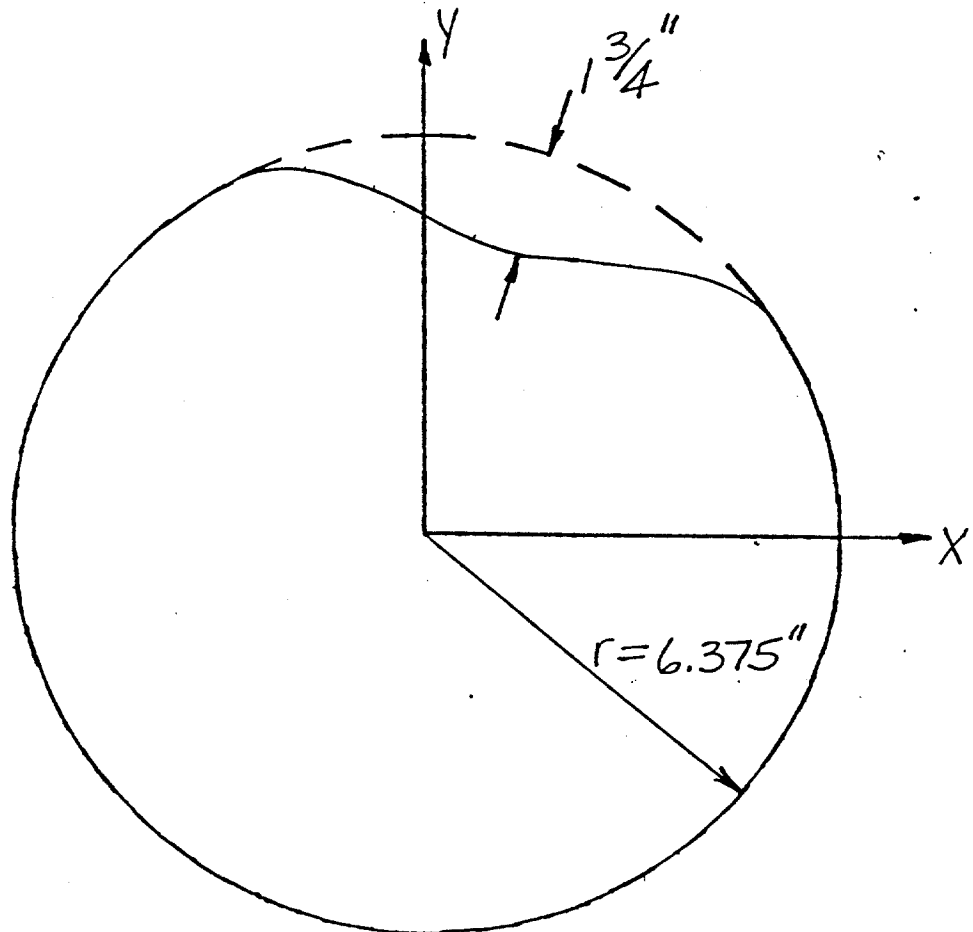
DENT CROSS SECTION

Specimen No. 13

Damage No. 2

Distance from End B 8'-6"

Scale 1"=3"



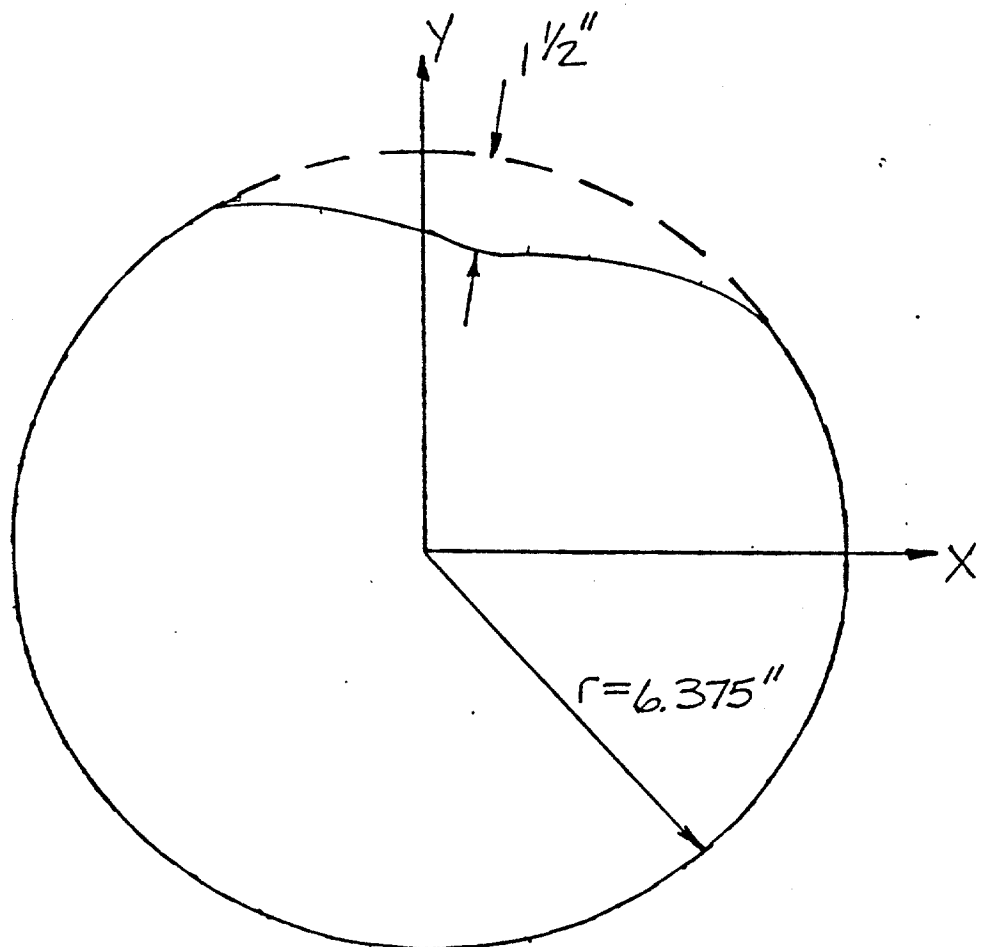
DENT CROSS SECTION

Specimen No. 13

Damage No. 2

Distance from End B 8'-9"

Scale 1"=3"



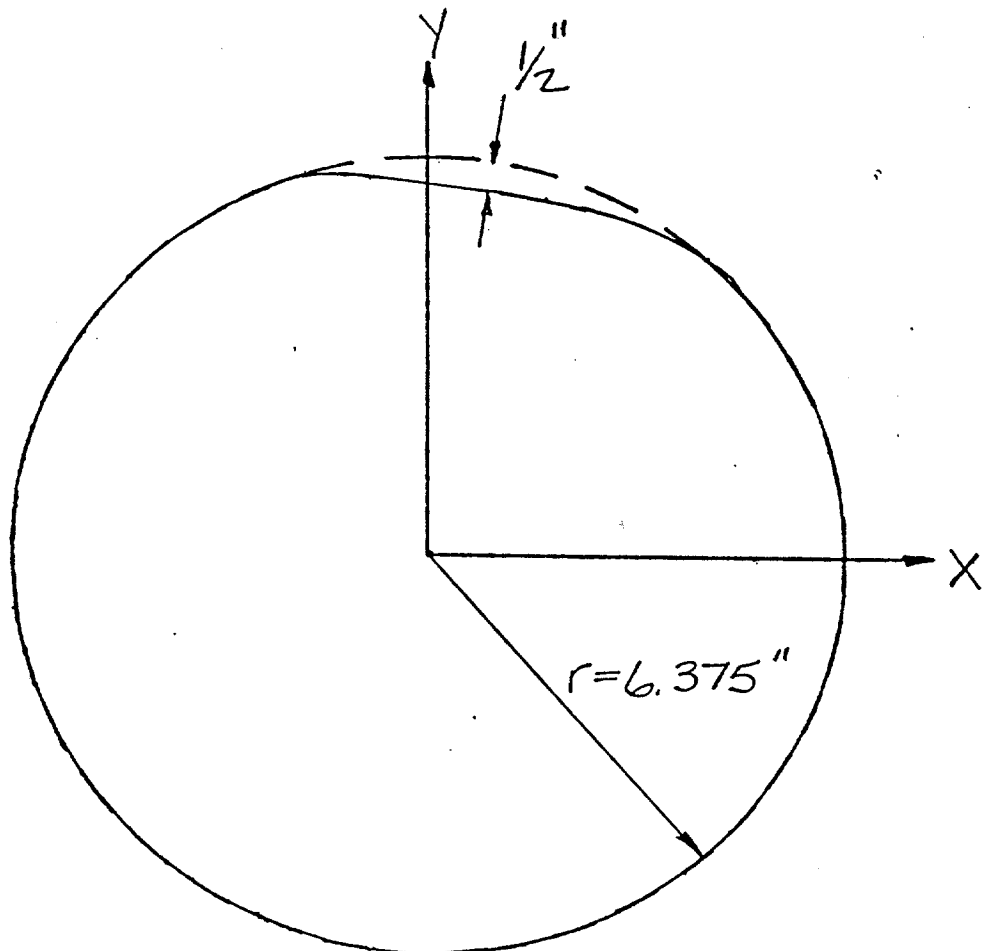
DENT CROSS SECTION

Specimen No. 13

Damage No. 2

Distance from End B 9'-0"

Scale 1" = 3"



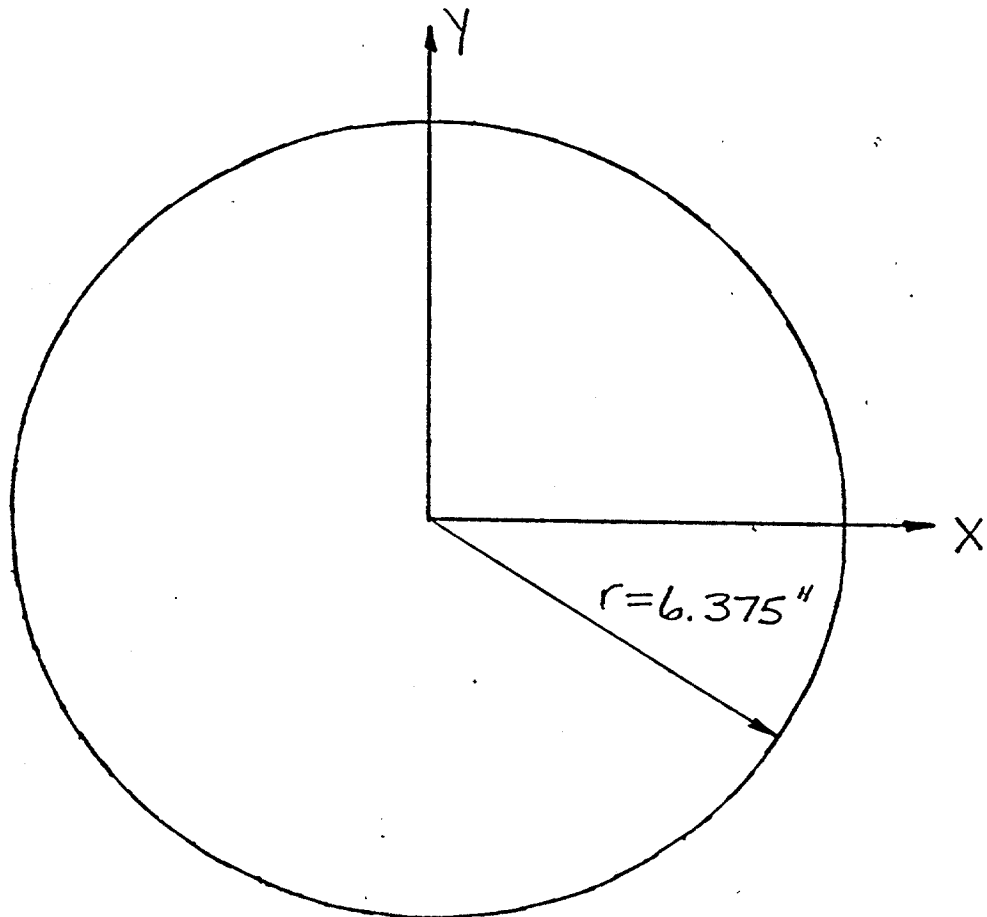
DENT CROSS SECTION

Specimen No. 13

Damage No. 2

Distance from End B 9'-3"

Scale 1"=3"



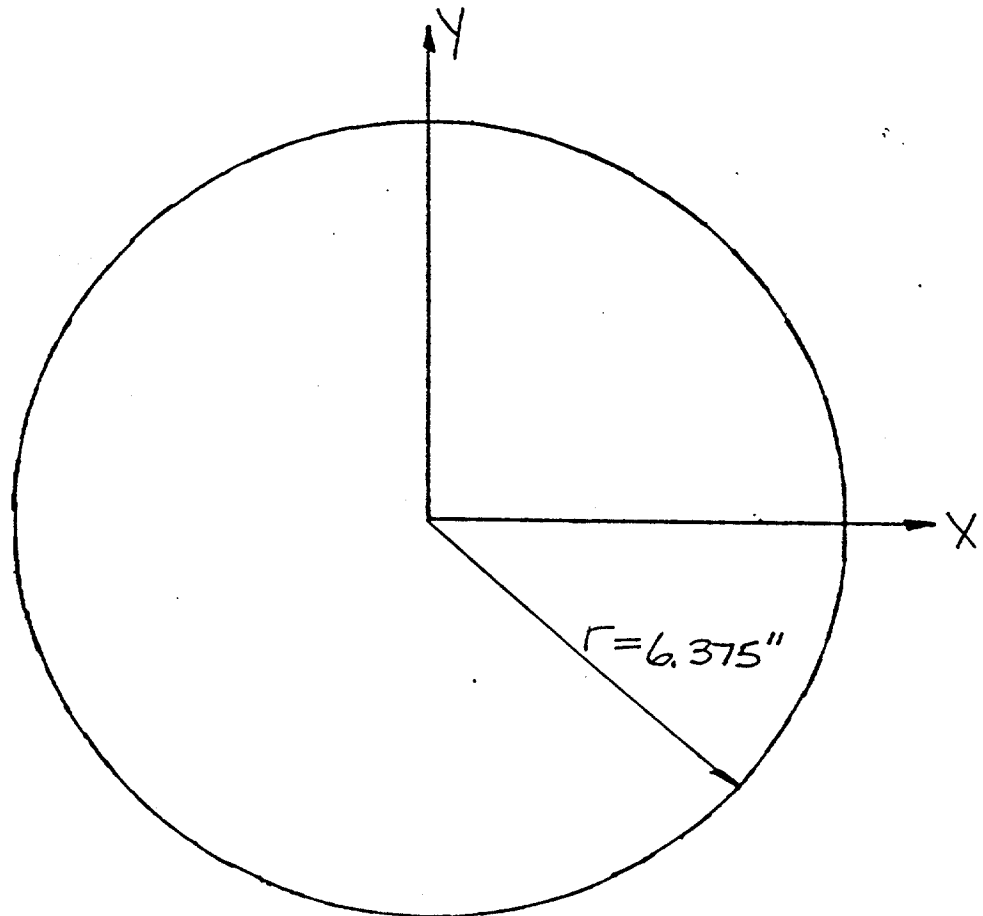
DENT CROSS SECTION

Specimen No. 13

Damage No. 3

Distance from End B 10'-0"

Scale 1"=3"



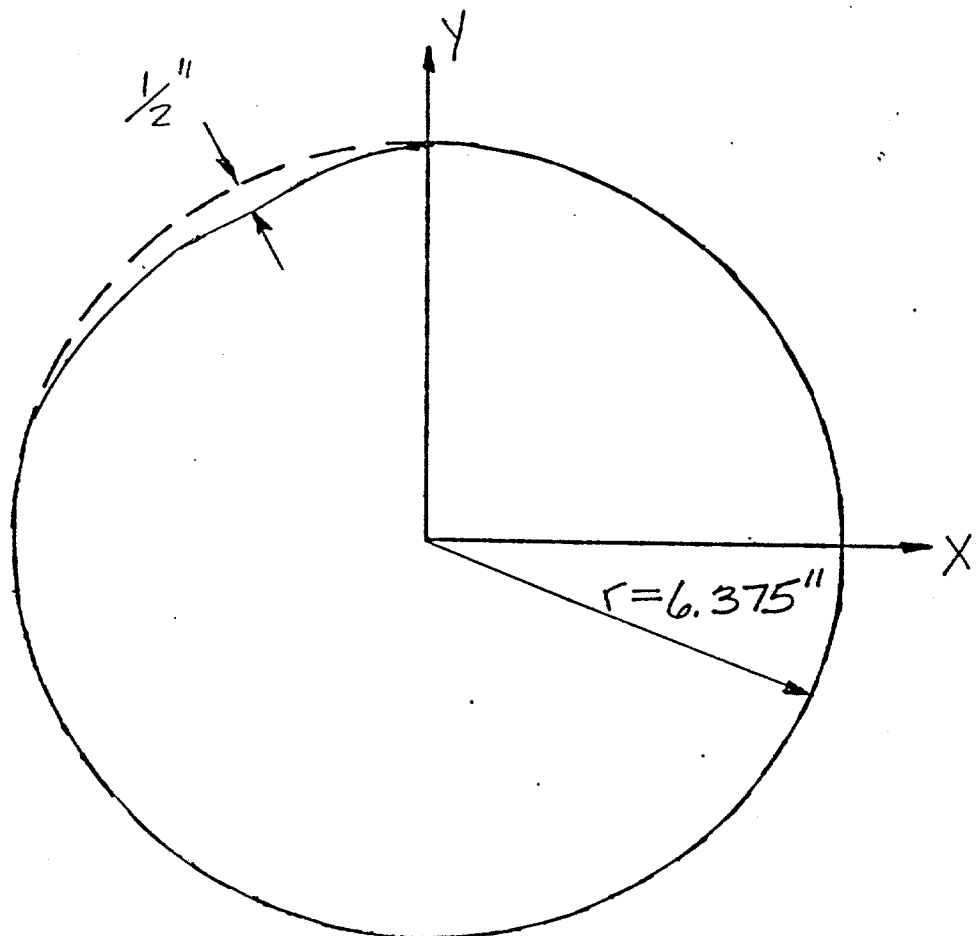
DENT CROSS SECTION

Specimen No. 13

Damage No. 3

Distance from End B 10'-3"

Scale 1"=3"



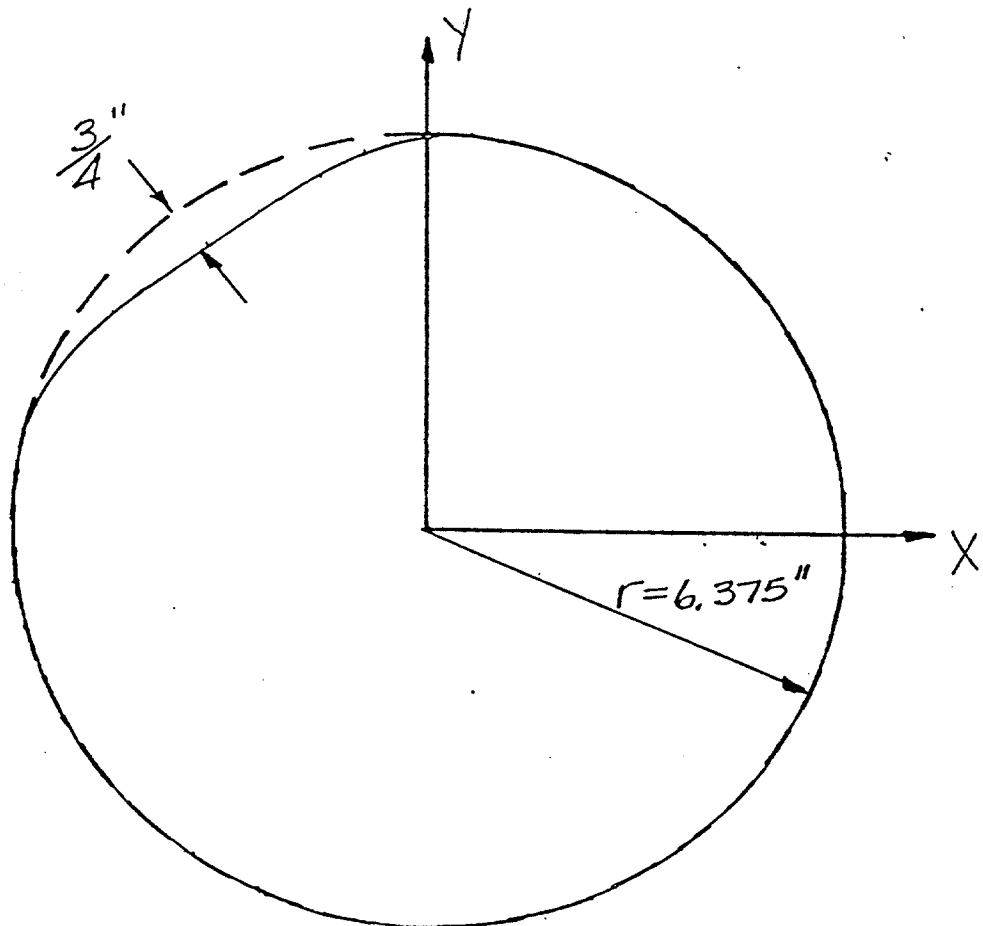
DENT CROSS SECTION

Specimen No. 13

Damage No. 3

Distance from End B 10'-6"

Scale 1"=3"



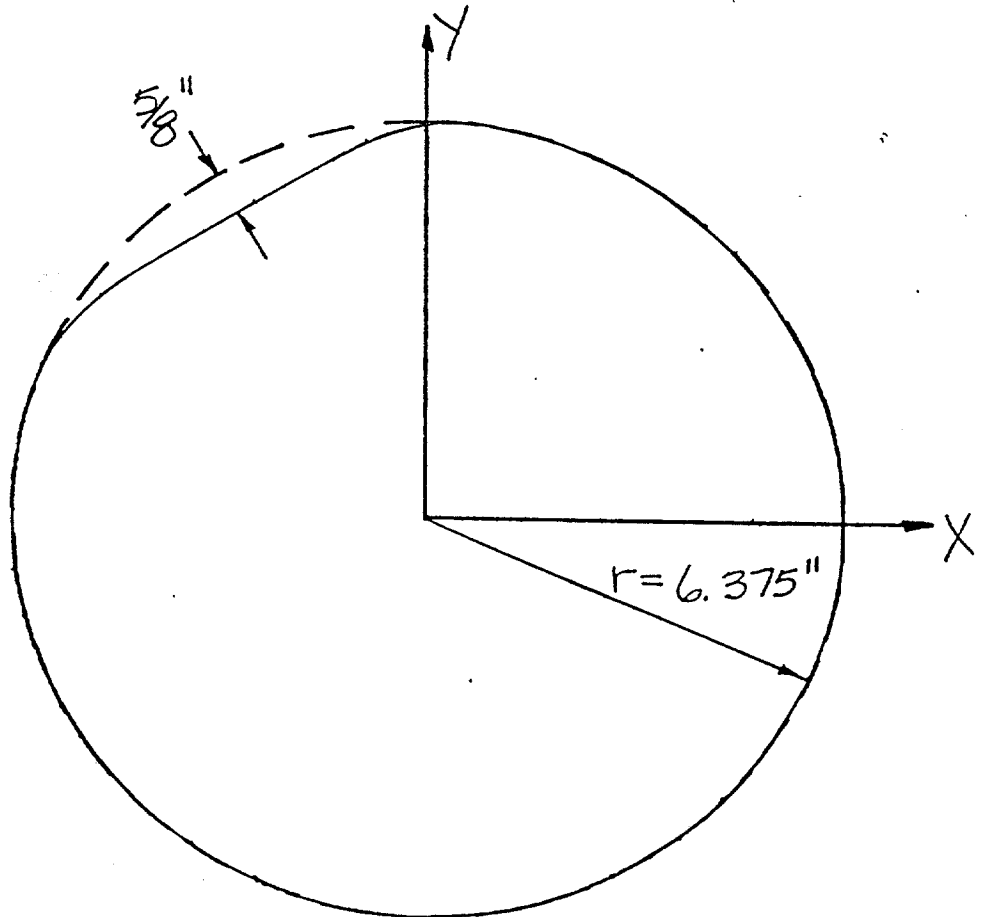
DENT CROSS SECTION

Specimen No. 13

Damage No. 3

Distance from End B 10'-9"

Scale 1"=3"



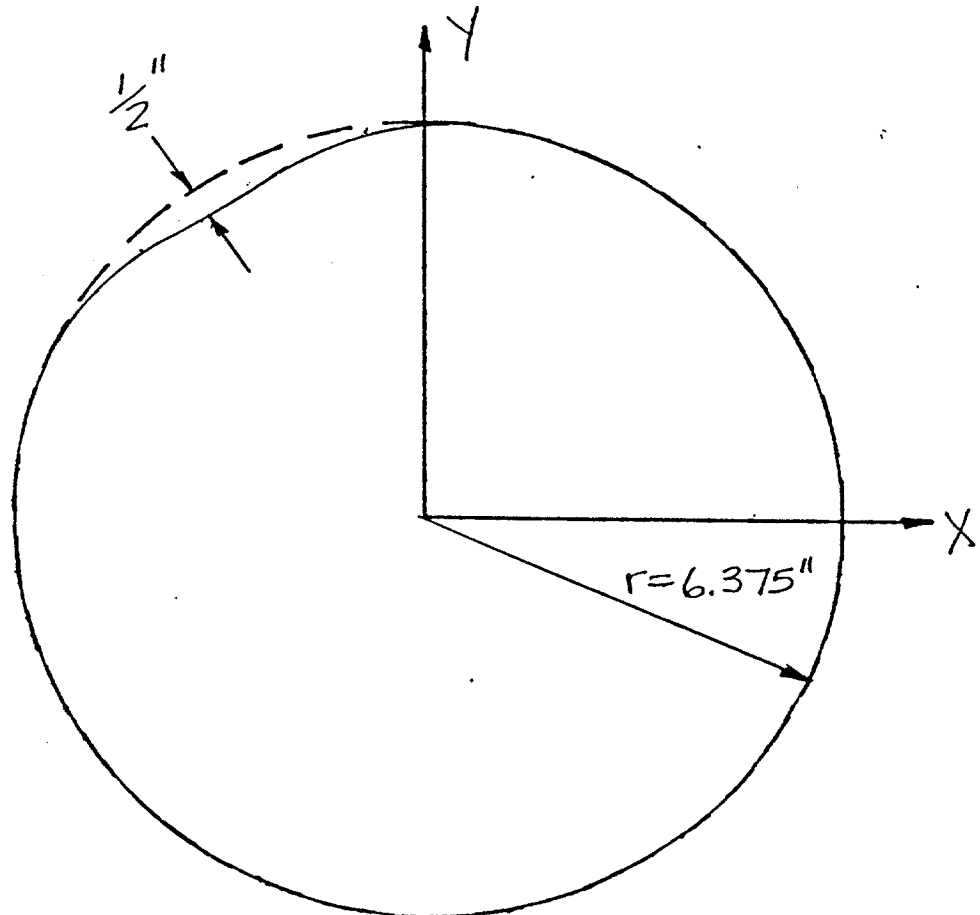
DENT CROSS SECTION

Specimen No. 13

Damage No. 3

Distance from End B 11'-0"

Scale 1" = 3"



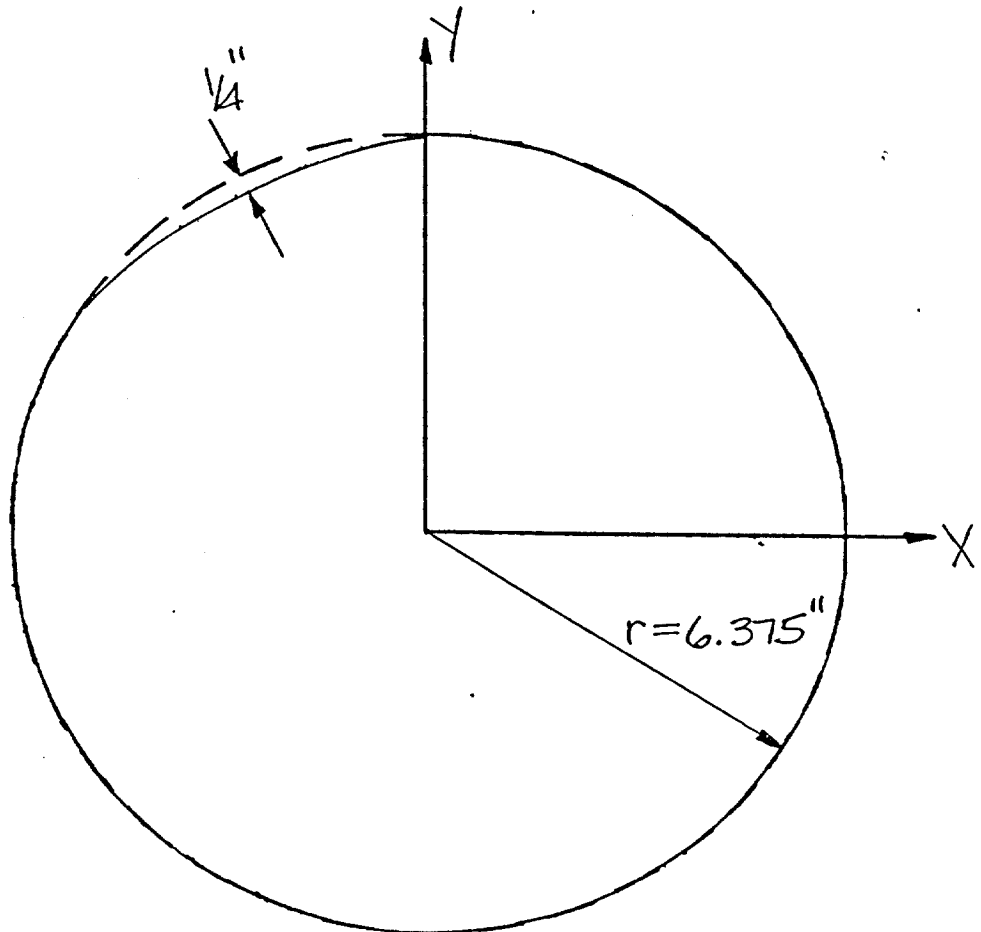
DENT CROSS SECTION

Specimen No. 13

Damage No. 3

Distance from End B 11'-3"

Scale 1"=3"



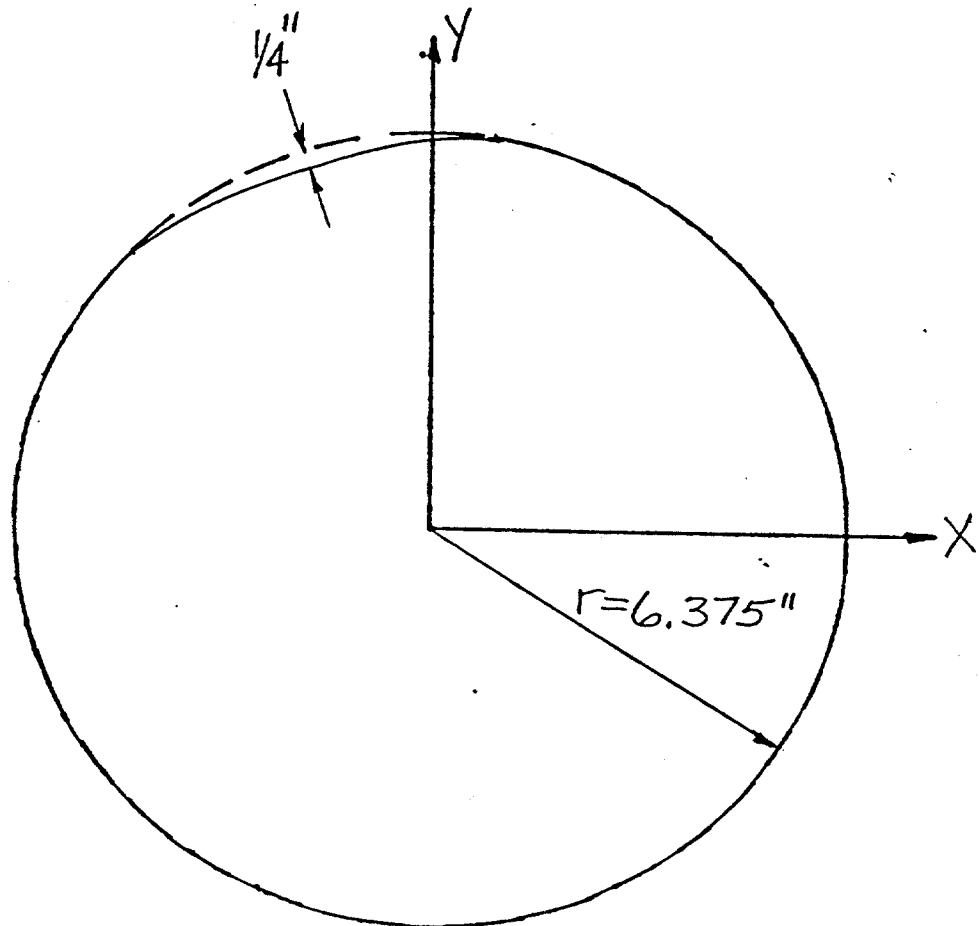
DENT CROSS SECTION

Specimen No. 14

Damage No. 244

Distance from End B 1'-8"

Scale 1"=3"



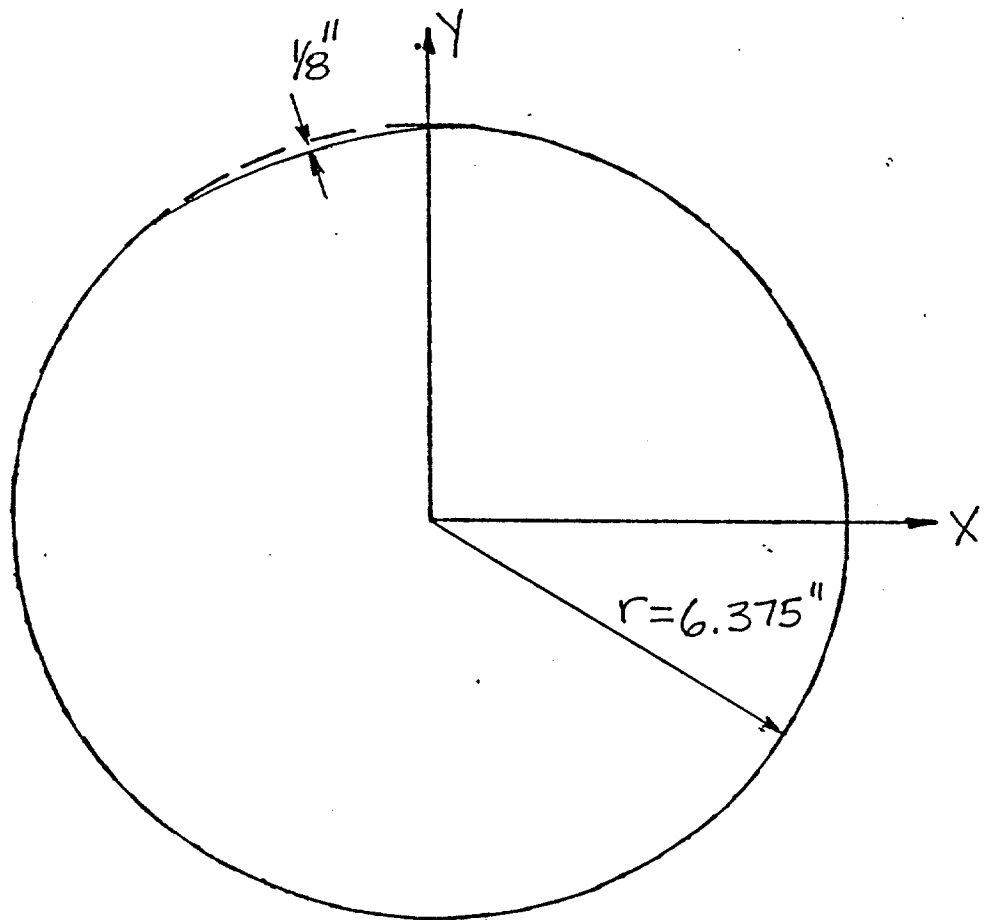
DENT CROSS SECTION

Specimen No. 14

Damage No. 4

Distance from End B 1'-10"

Scale 1"=3"



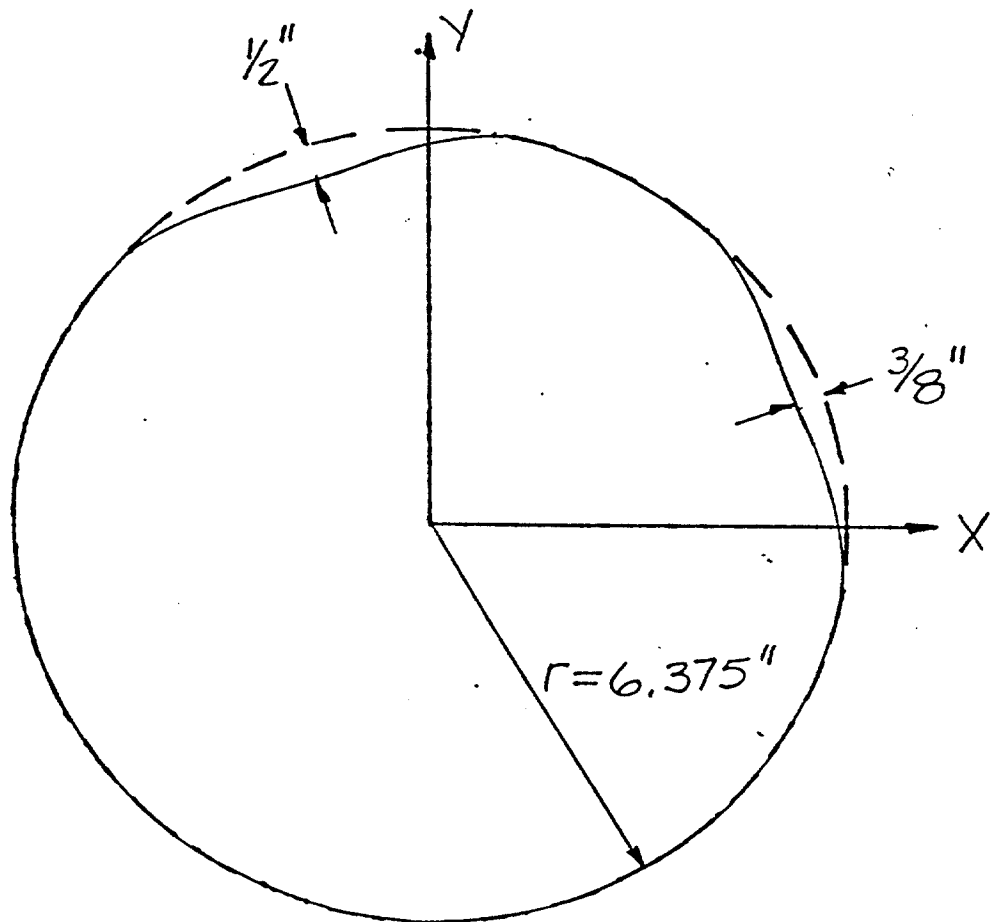
DENT CROSS SECTION

Specimen No. 14

Damage No. 243

Distance from End B 1'-4"

Scale 1"=3"



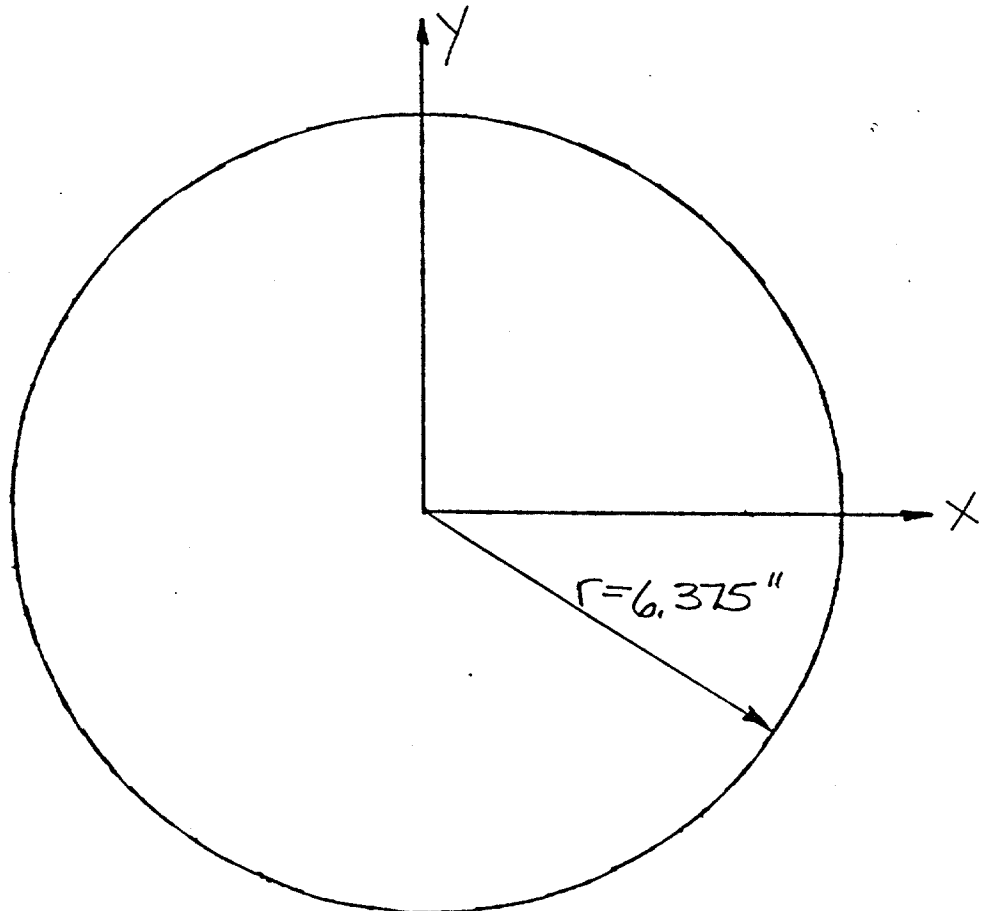
DENT CROSS SECTION

Specimen No. 13

Damage No. 3

Distance from End B 11'-6"

Scale 1"=3"



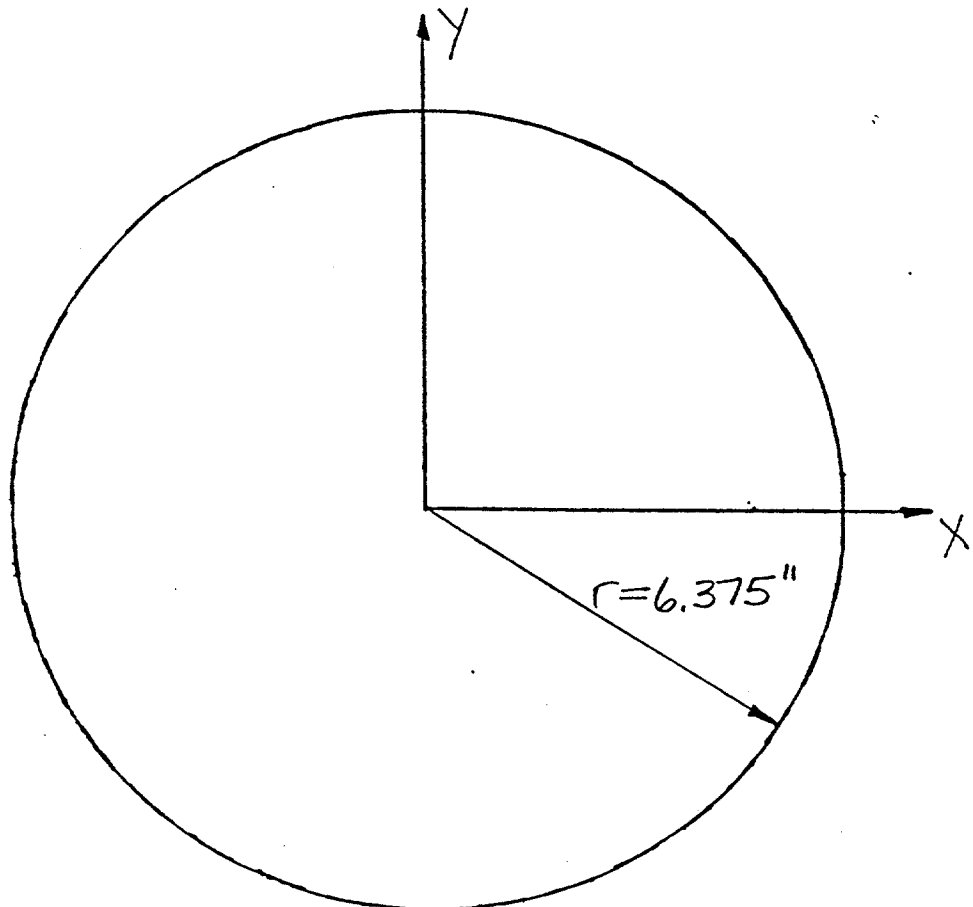
DENT CROSS SECTION

Specimen No. 13

Damage No. 4

Distance from End B 17'-0"

Scale 1"=3"



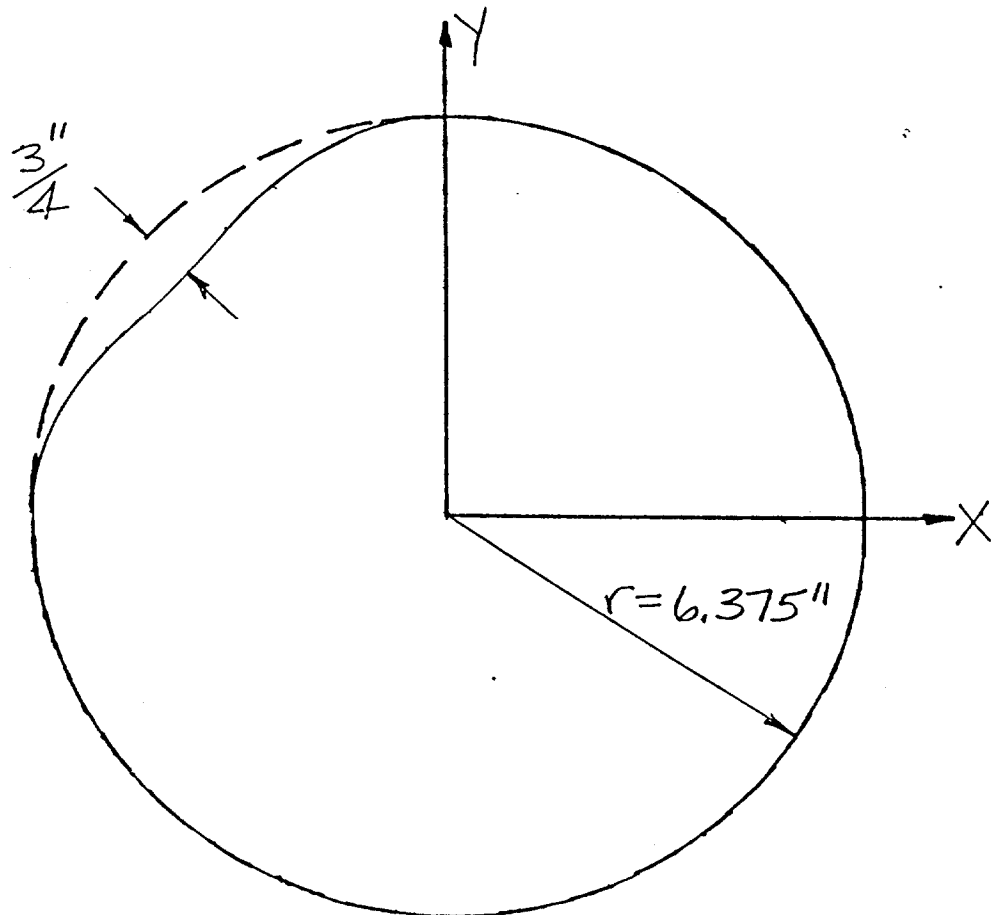
DENT CROSS SECTION

Specimen No. 13

Damage No. 4

Distance from End B 17'-3"

Scale 1"=3"



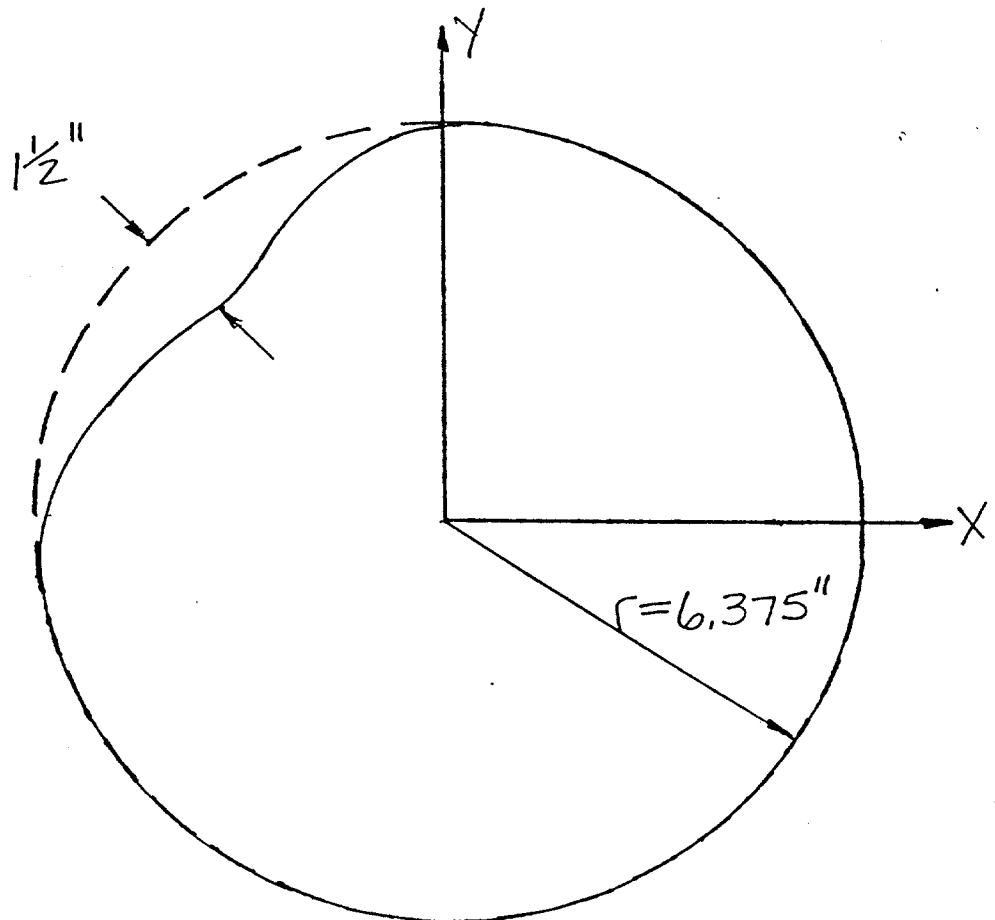
DENT CROSS SECTION

Specimen No. 13

Damage No. 4

Distance from End B 17'-6"

Scale 1"=3"



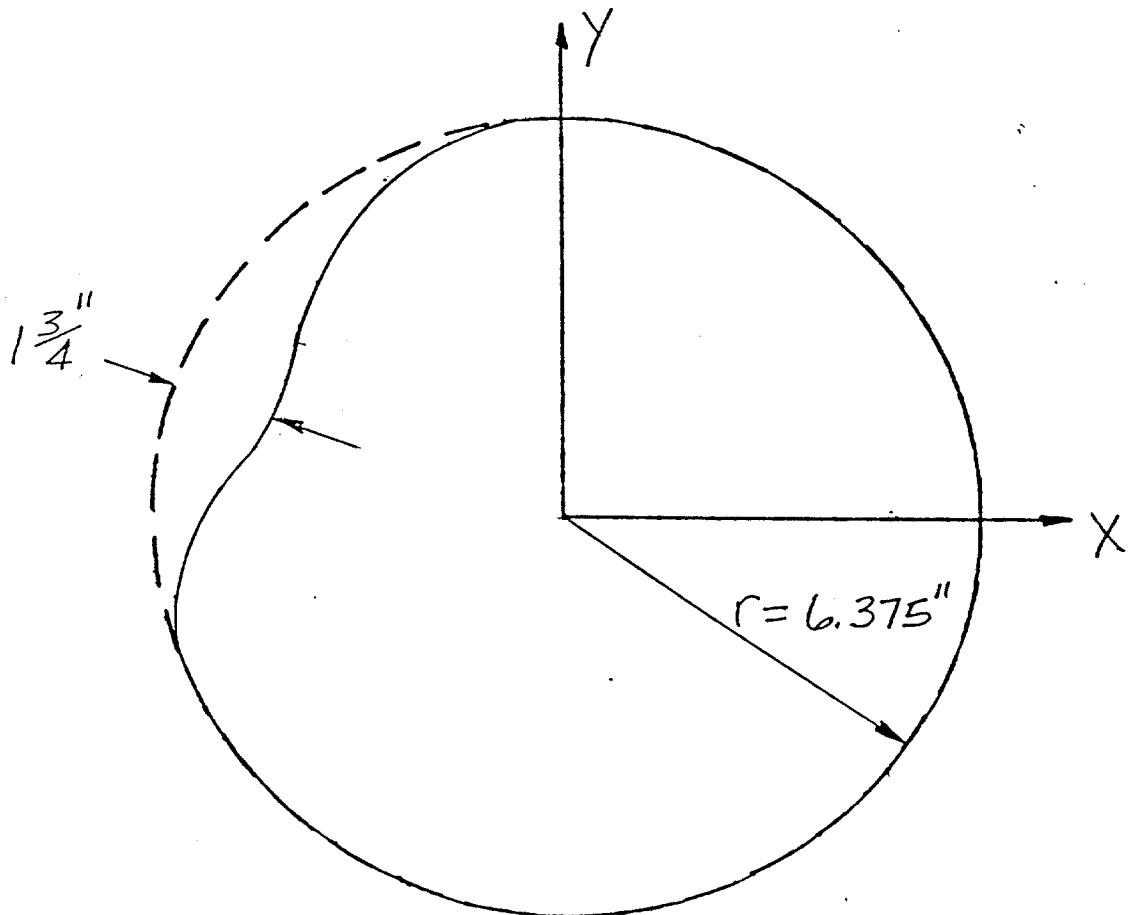
DENT CROSS SECTION

Specimen No. 13

Damage No. 4

Distance from End B 17'-9"

Scale 1"=3"



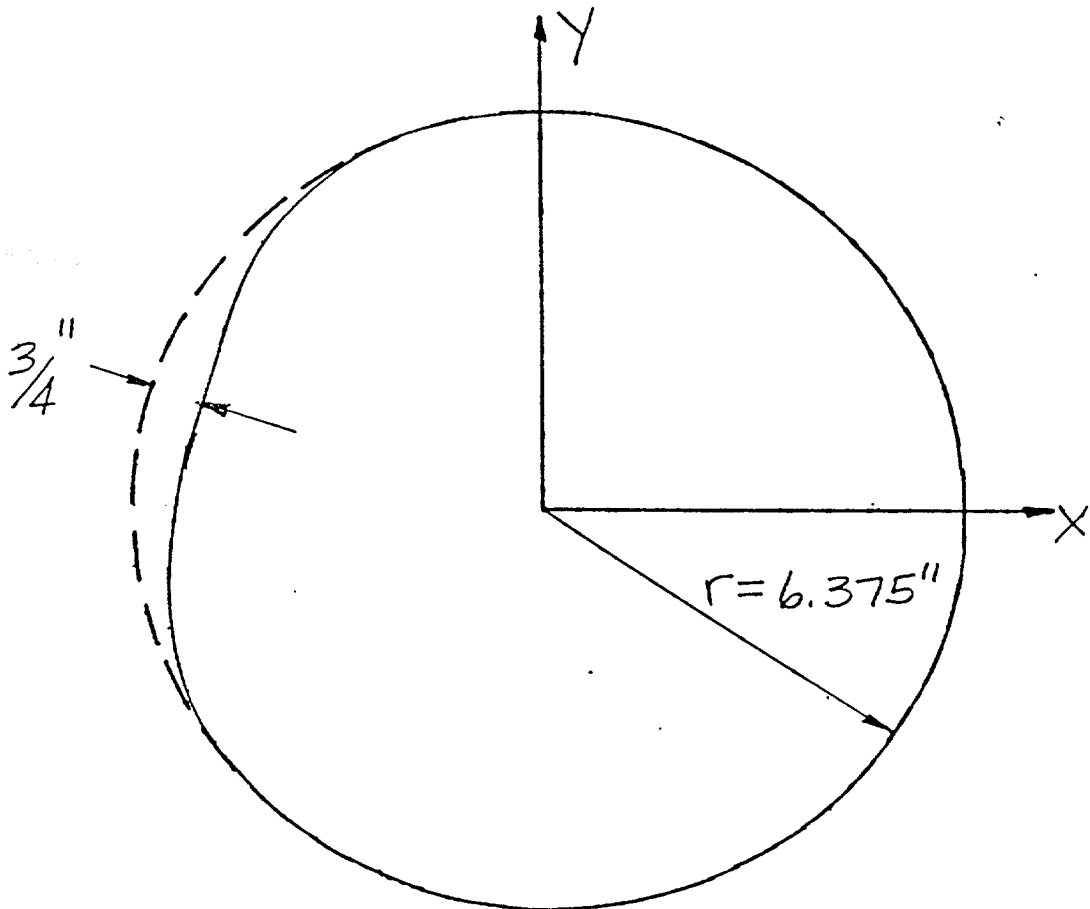
DENT CROSS SECTION

Specimen No. 13

Damage No. 4

Distance from End B 18'-0"

Scale 1" = 3"



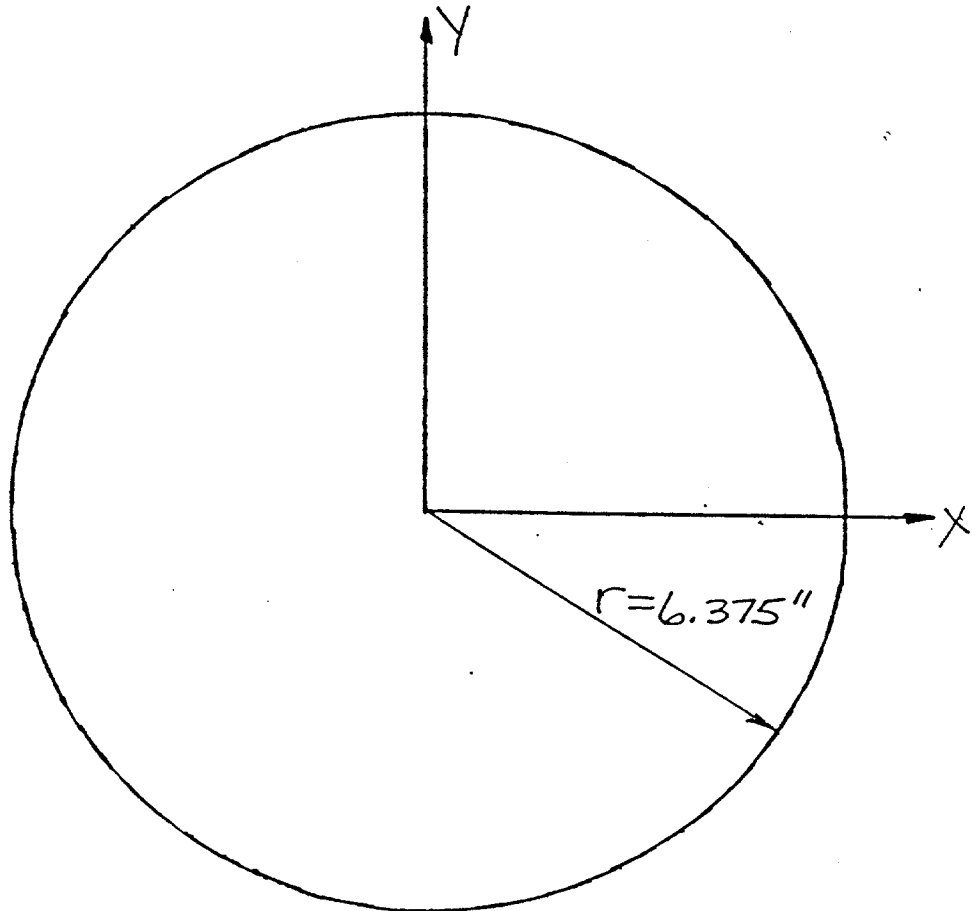
DENT CROSS SECTION

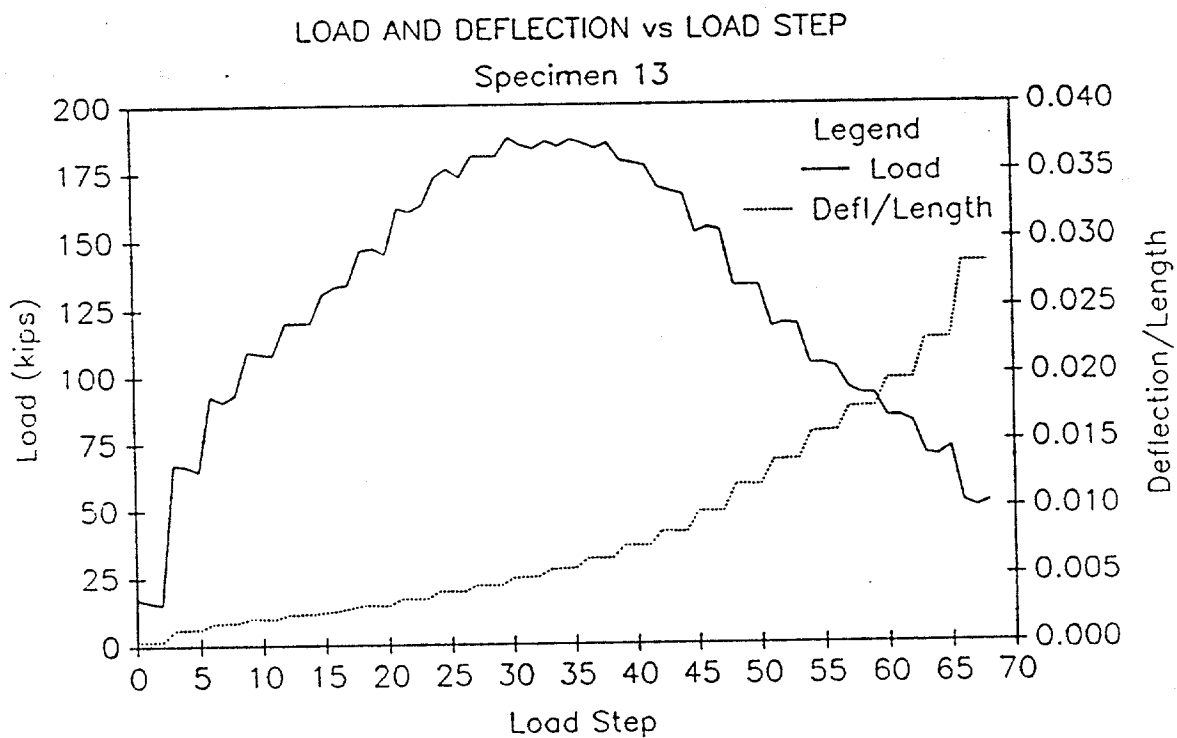
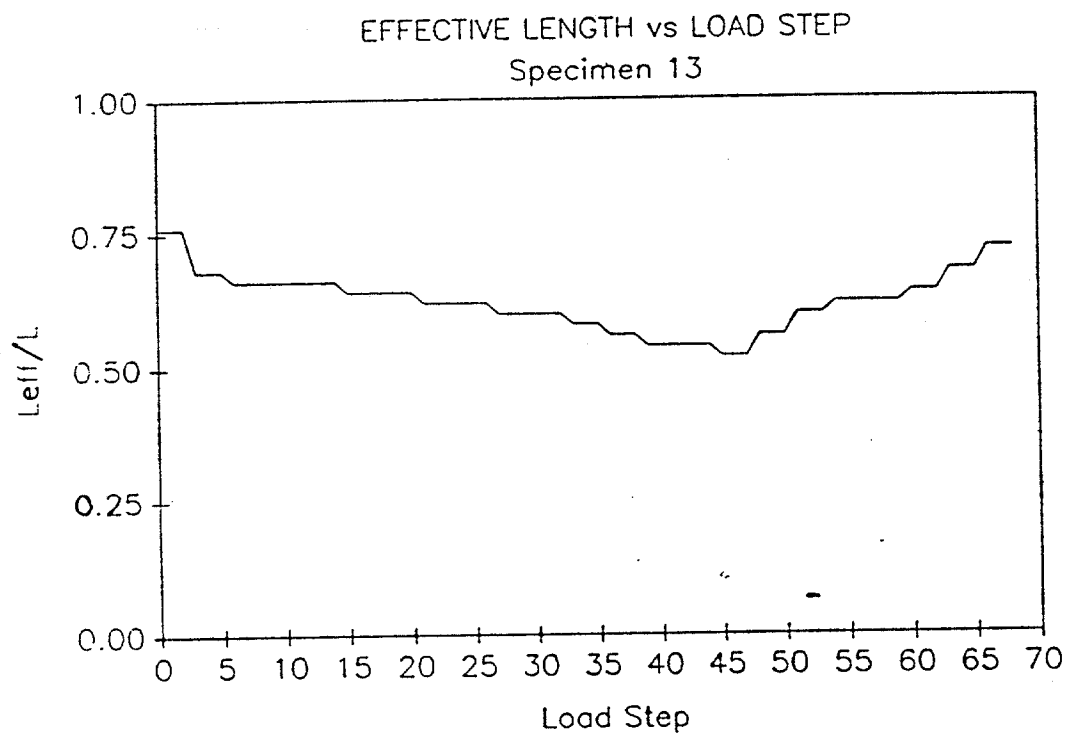
Specimen No. 13

Damage No. 4

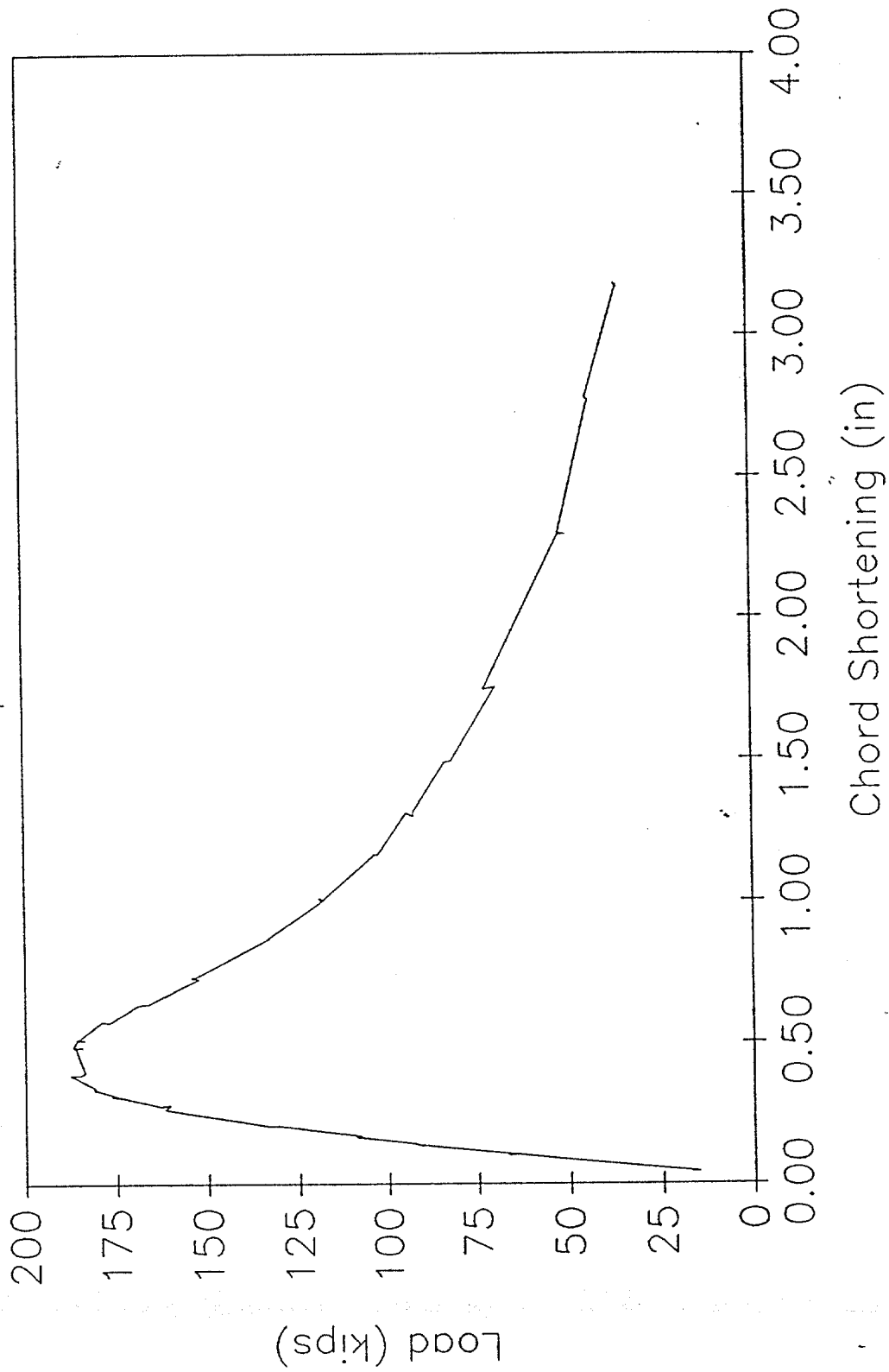
Distance from End B 18'-3"

Scale 1"=3"



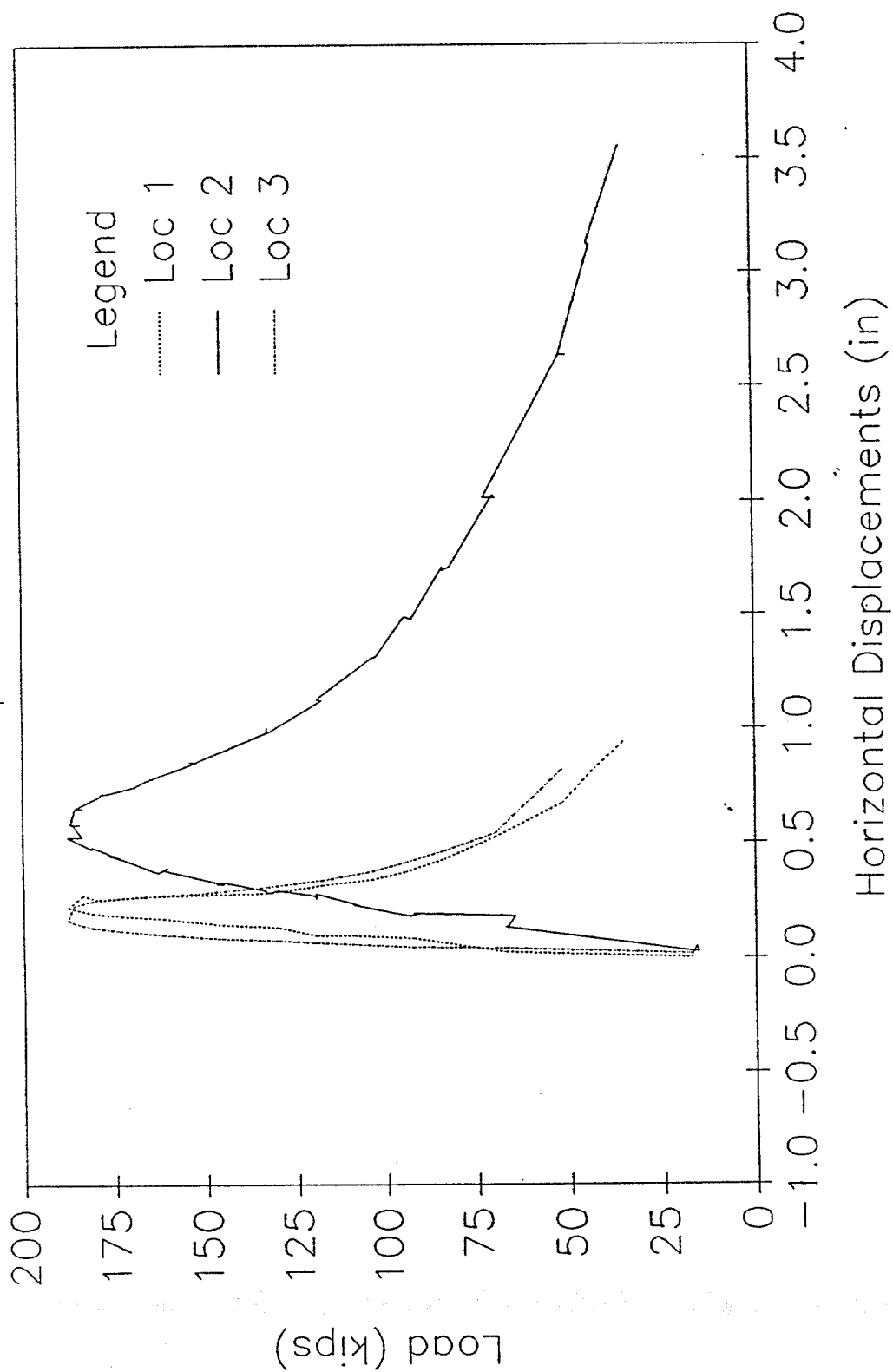


LOAD vs CHORD SHORTENING
Specimen 13



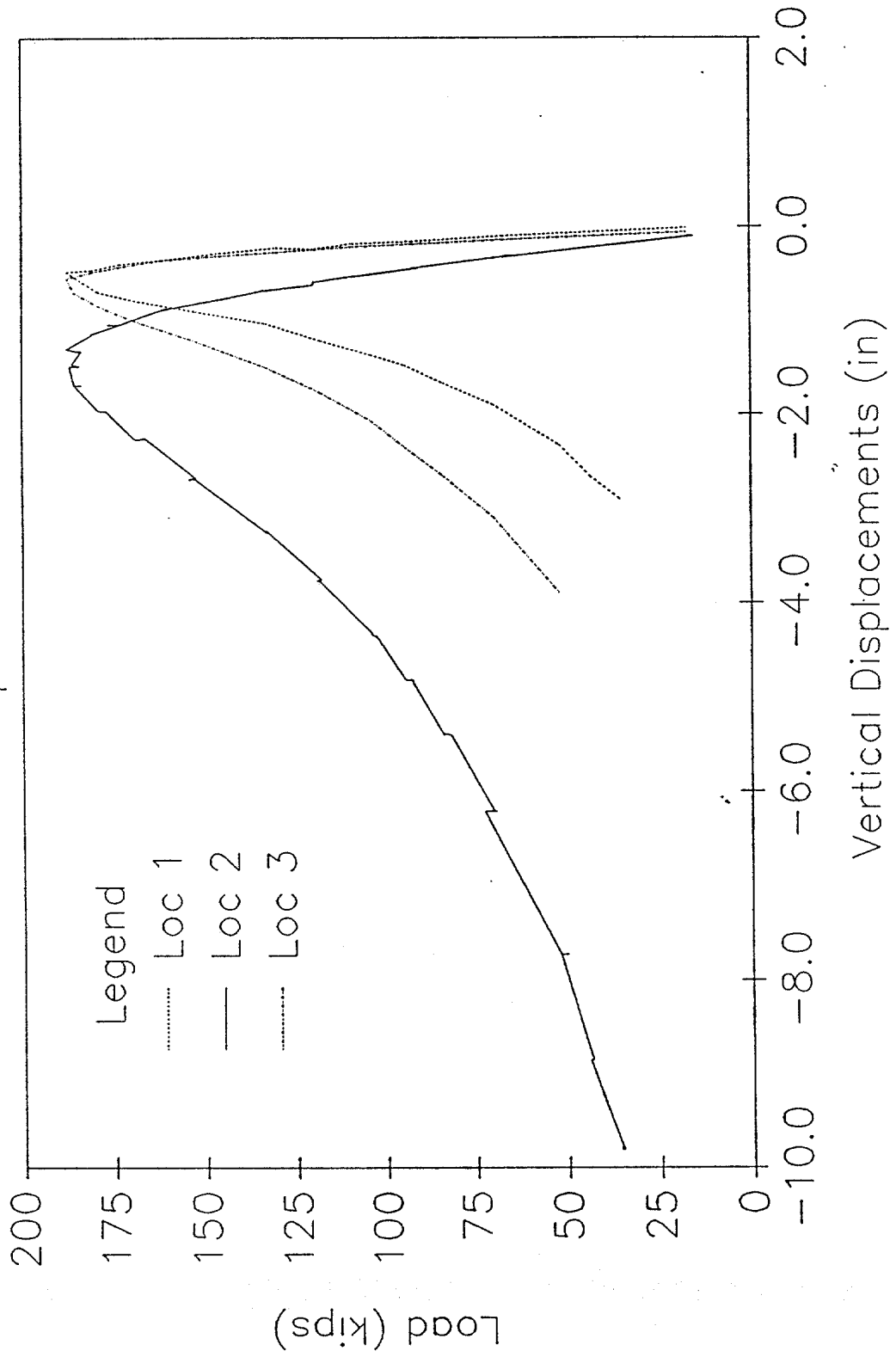
HORIZONTAL DISPLACEMENTS

Specimen 13



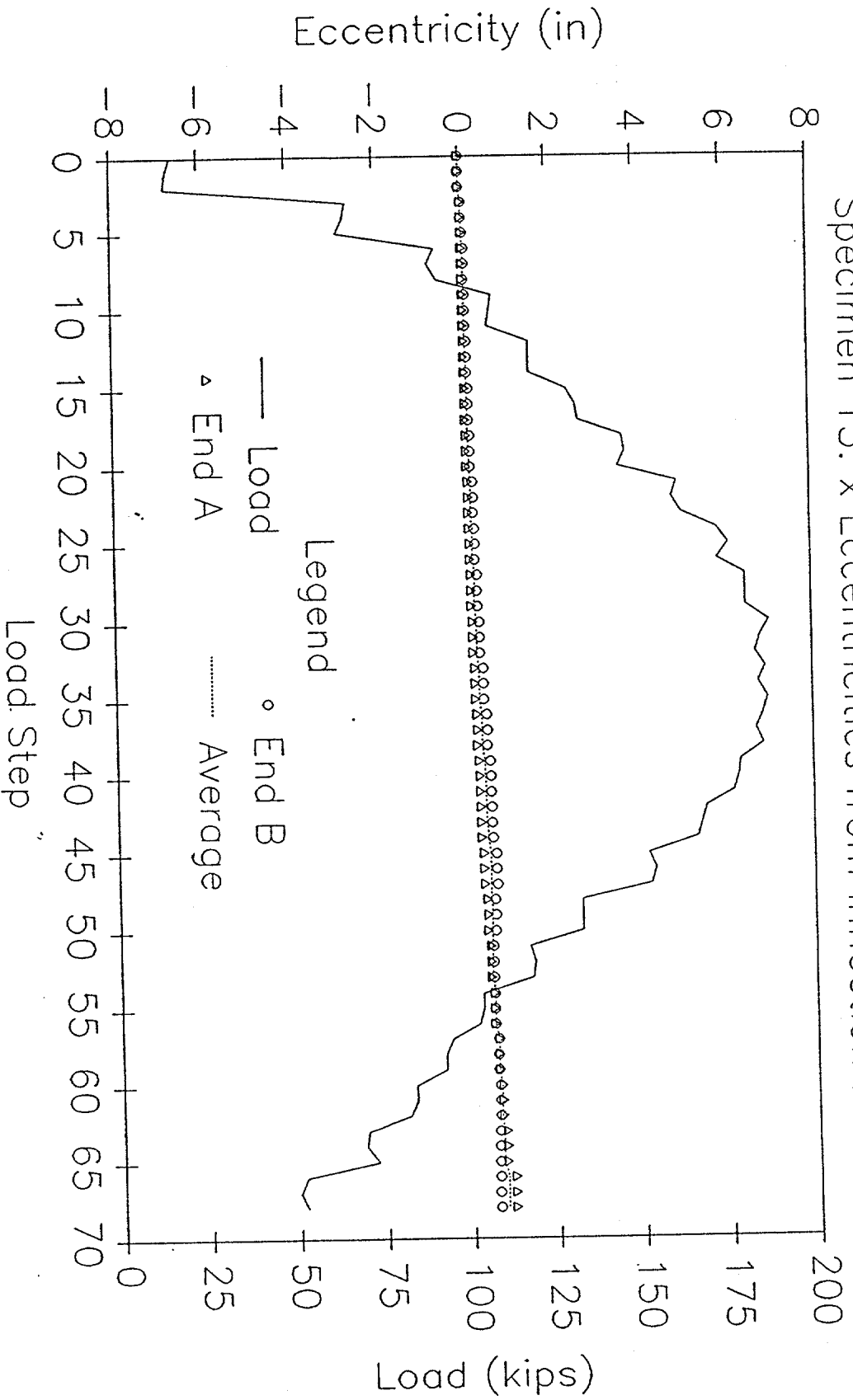
VERTICAL DISPLACEMENTS

Specimen 13



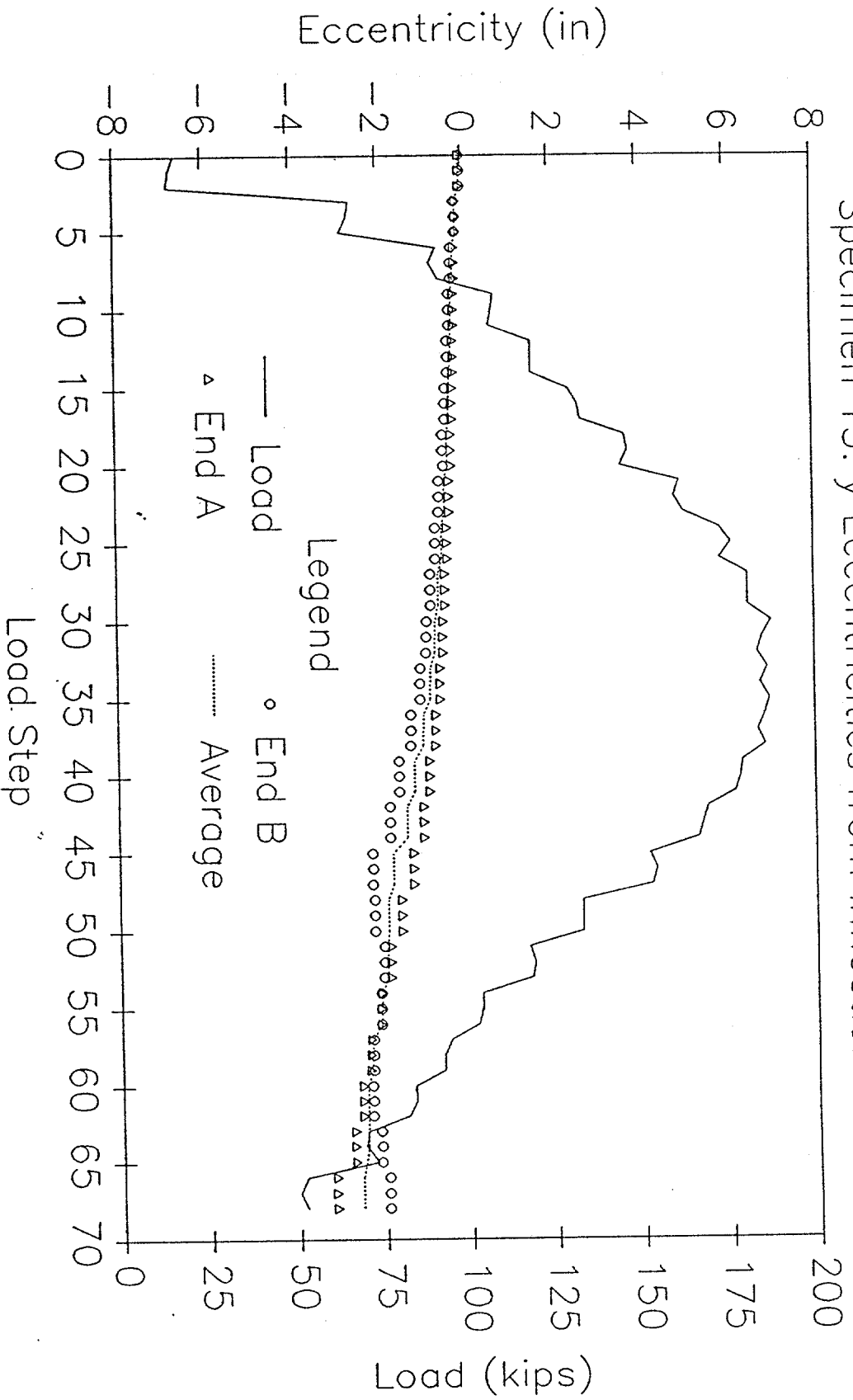
LOAD AND ECCENTRICITY vs LOAD STEP

Specimen 13: x Eccentricities from Inflection Points



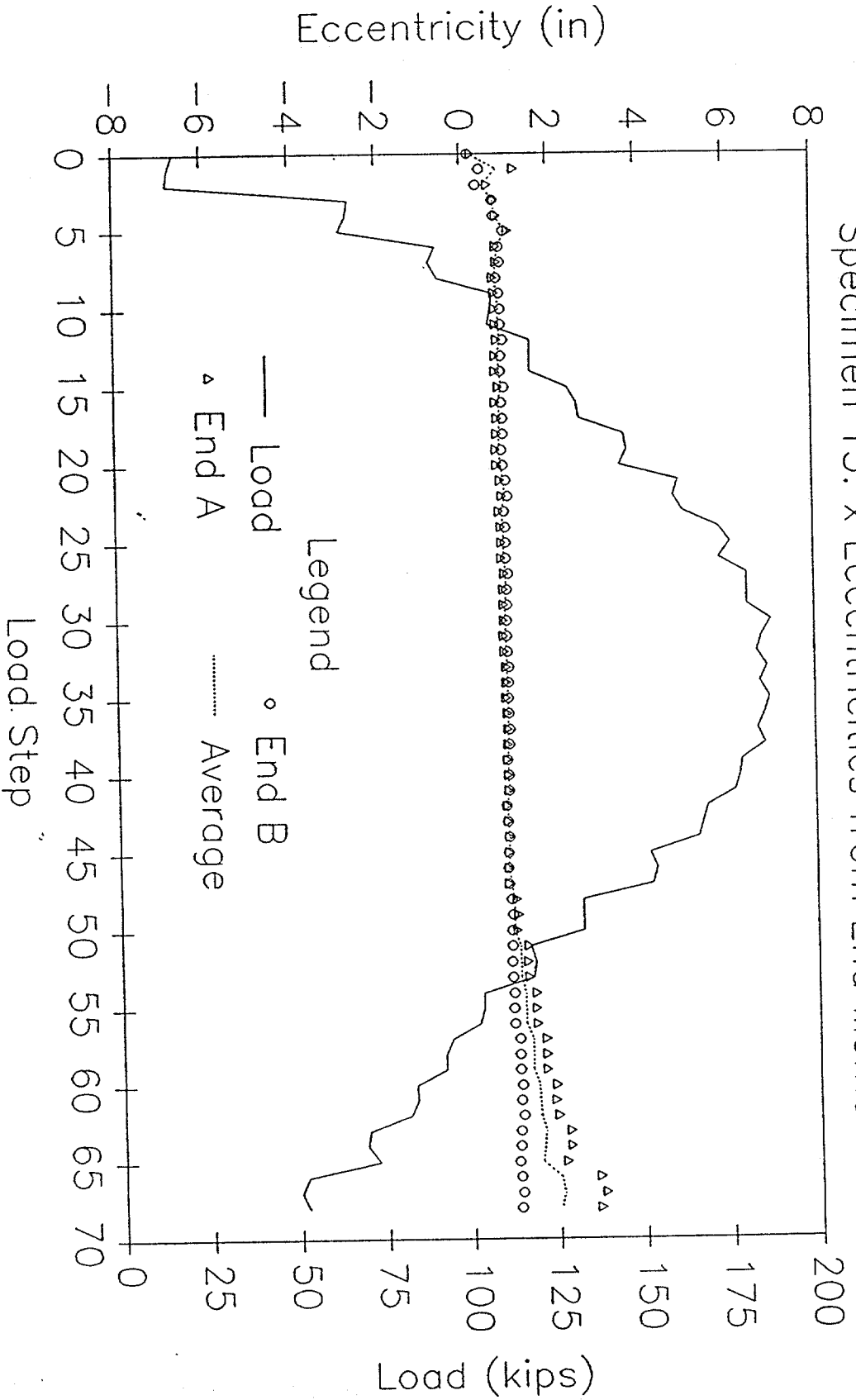
LOAD AND ECCENTRICITY vs LOAD STEP

Specimen 13: y Eccentricities from Inflection Points



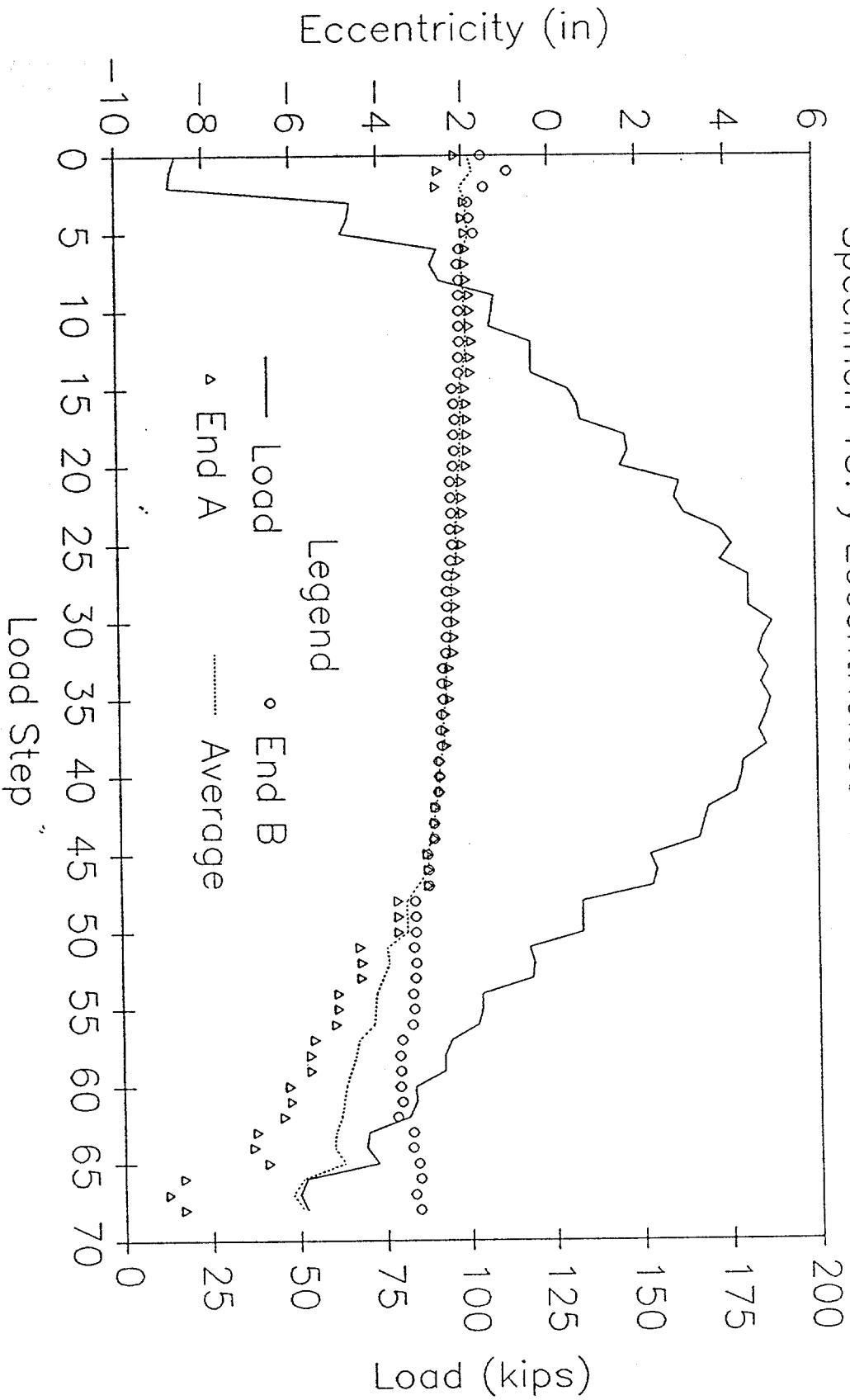
LOAD AND ECCENTRICITY vs LOAD STEP

Specimen 13: x Eccentricities from End Moments



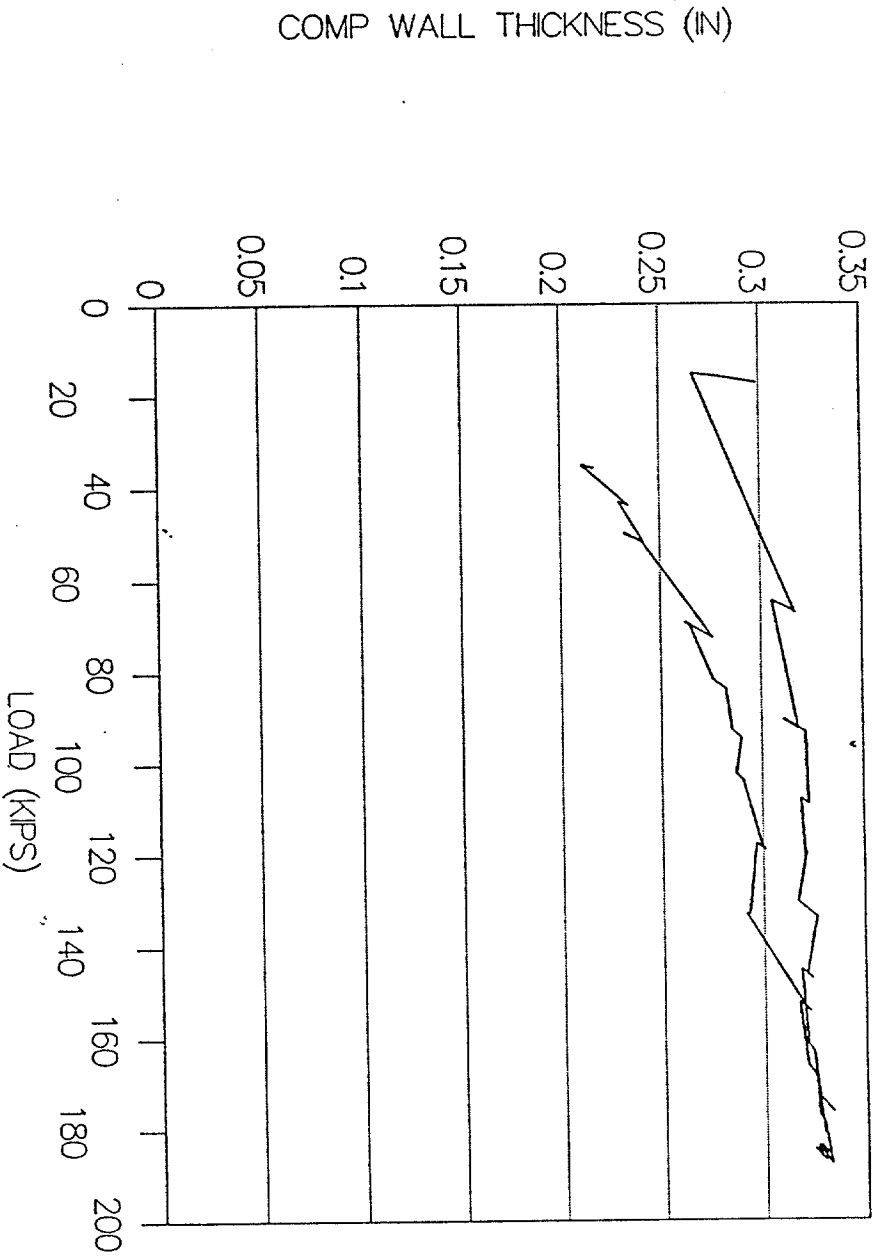
LOAD AND ECCENTRICITY vs LOAD STEP

Specimen 13: y Eccentricities from End Moments



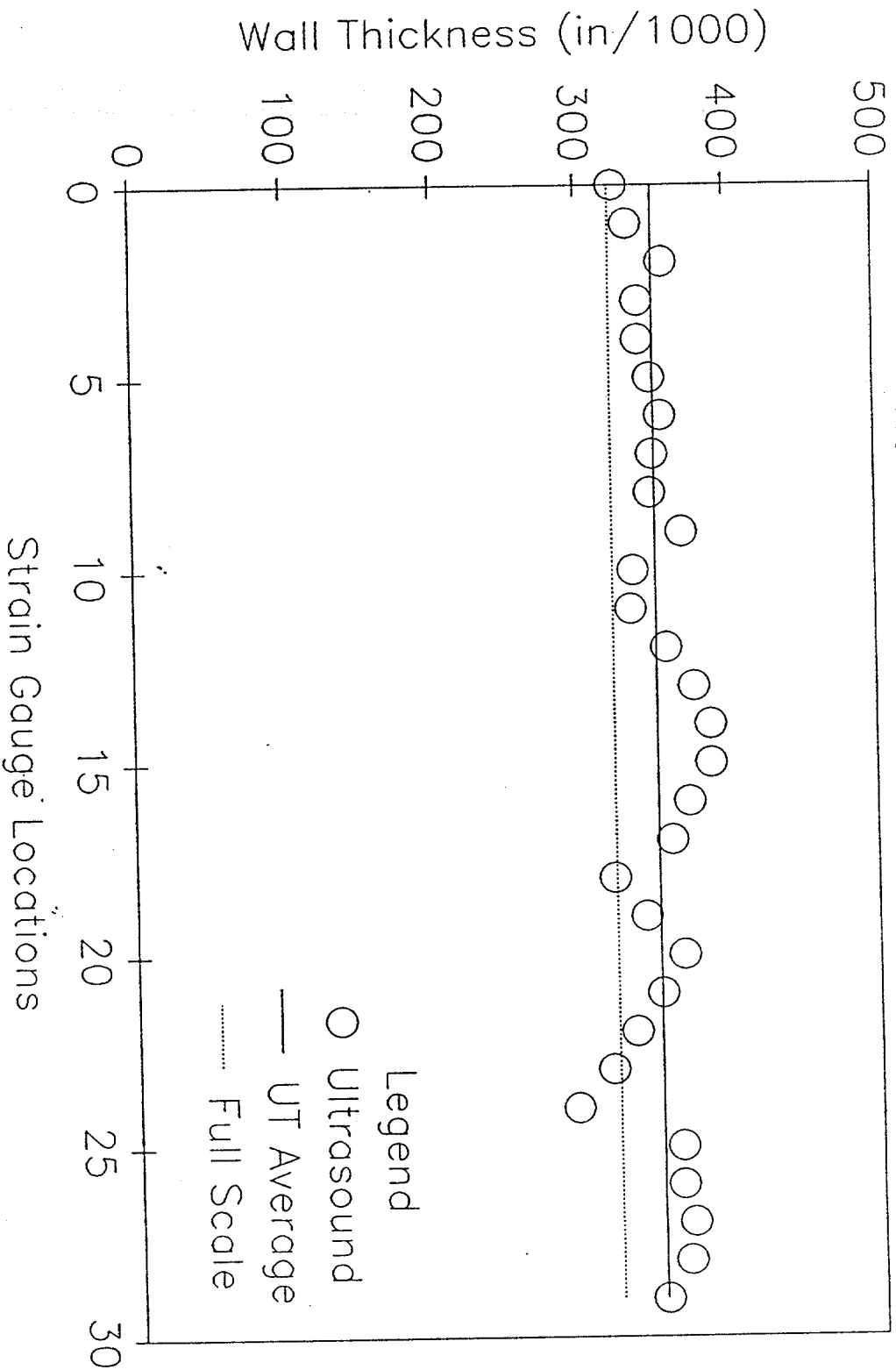
SPECIMEN 13-FULL SCALE TEST

COMPUTED WALL THICKNESS



SPECIMEN 13: WALL THICKNESS

Nominal Wall Thickness = 0.375 in

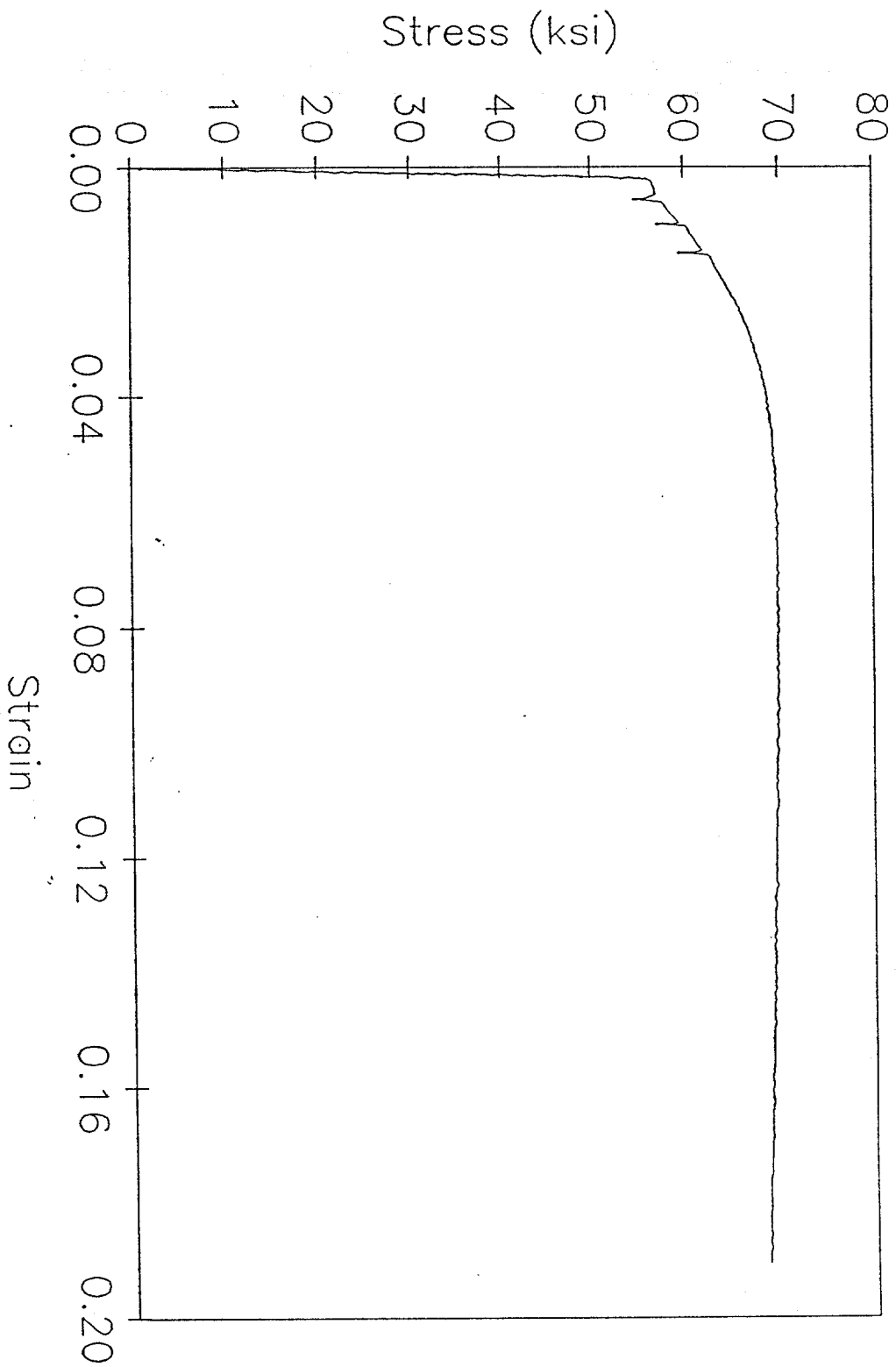


Ultrasonnd Data for Specimen 13
(All values in inches)

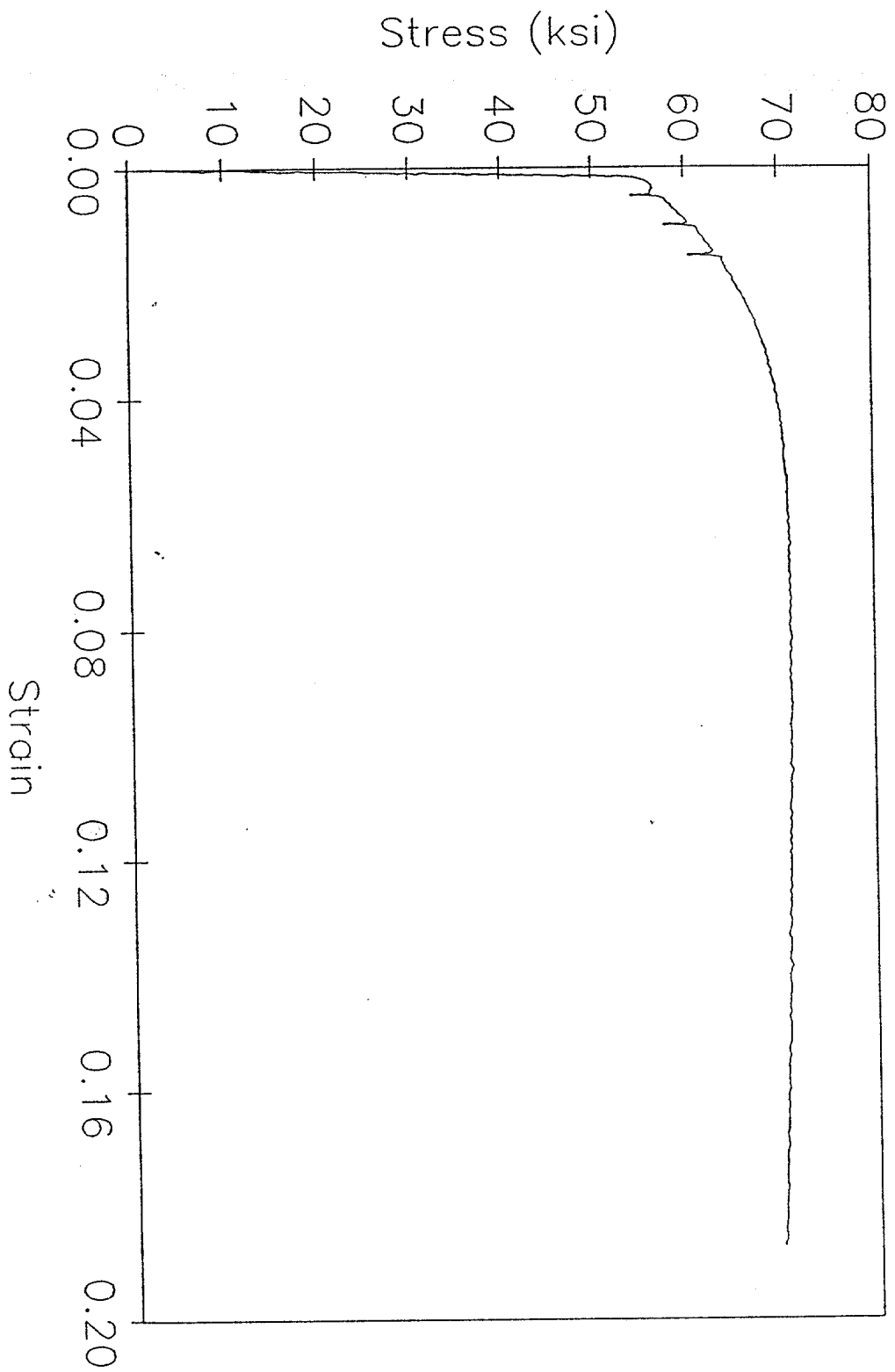
Gauge UT
No. Thickness Average

0	0.326	
1	0.335	
2	0.359	
3	0.342	
4	0.342	
5	0.350	0.342
6	0.357	
7	0.351	
8	0.349	
9	0.370	
10	0.337	
11	0.335	0.350
12	0.359	
13	0.377	
14	0.388	
15	0.388	
16	0.373	
17	0.361	0.374
18	0.322	
19	0.343	
20	0.368	
21	0.353	
22	0.335	
23	0.319	0.340
24	0.295	
25	0.365	
26	0.365	
27	0.372	
28	0.369	
29	0.353	0.353
Overall Average = 0.352		

TENSILE SPECIMEN 13-1
Stress vs Strain



TENSILE SPECIMEN 13-2
Stress vs Strain



SPECIMEN 14

DAMAGE SUMMARY

Specimen No. 14
3-3-90

DISTANCE FROM END "B"	*DISTANCE FROM CHALK LINE		DESCRIPTION OF DAMAGE
	LEFT	RIGHT	
1. 1'-1 1/4"		12"	1/2" ϕ corrosion hole
2. 1'-4"		8"	Dent - See additional sheets
3. 1'-4"	2"		Dent - See additional sheets
4. 1'-8"	2"		Dent - See additional sheets
5. 4'-1"	5 1/2"		3" x 1/4" cut-off attachment
6. 4'-0"		13"	6" (long) x 3/8" (wide) cut-off attachment (Runs circumferentially)
7. 4'-9"		8"	Heavily corroded area, 2 small holes = 1" ϕ , 3/4" ϕ
8. 4'-11"			3/4" circumferential butt weld
9. 5'-3"			3/4" circumferential butt weld
10. 10'-10"	17"		3" x 1/4" cut-off attachment

*Looking from end "A" towards end "B"

SEE ADDITIONAL SHEETS FOR OUT-OF-STRAIGHTNESS MEASUREMENTS
WIDESPREAD HEAVY CORROSION

Out-of-Straightness Measurements
for Specimen 14

The specimen was initially curved in the yz-plane and in the xz-plane. The following measurements are in the x-direction.

Distance from End B (ft)	Distance from stringline to top of pipe (in)	Out-of straightness in x direction (in)
0	3.75	0
1	3.875	-0.125
2	3.875	-0.125
3	4.0	-0.25
4	4.125	-0.375
5	4.25	-0.5
6	4.0	-0.25
7	4.0	-0.25
8	3.875	-0.125
9	3.875	-0.125
10	3.875	-0.125
11	3.8125	-0.0625
12	3.8125	-0.0625
13	3.75	0
14	3.75	0
15	3.75	0
16	3.75	0
16.75	3.75	0

Out-of-Straightness Measurements
for Specimen 14

The specimen was initially curved in the yz-plane and in the xz-plane. The following measurements are in the y-direction.

Distance from End B (ft)	Distance from stringline to top of pipe (in)	Out-of straightness in y direction (in)
0	3.875	0
1	4.375	-0.5
2	5.125	-1.25
3	5.5	-1.625
4	6.0	-2.125
5	6.75	-2.875
6	6.875	-3
7	6.5	-2.625
8	6.25	-2.375
9	5.875	-2
10	5.625	-1.75
11	5.375	-1.5
12	5.125	-1.25
13	4.75	-0.875
14	4.5	-0.625
15	4.25	-0.375
16	4.0	-0.125
16.75	3.875	0

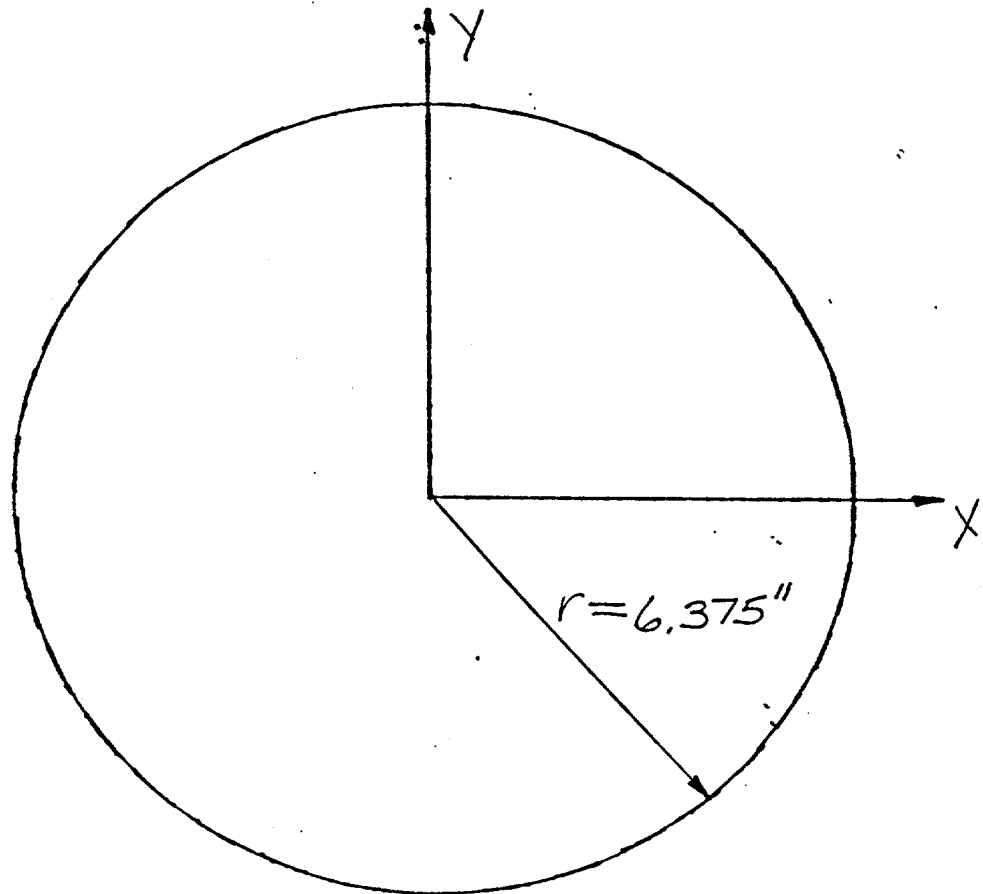
DENT CROSS SECTION

Specimen No. 14

Damage No. 3

Distance from End B 1'-0"

Scale 1" = 3"



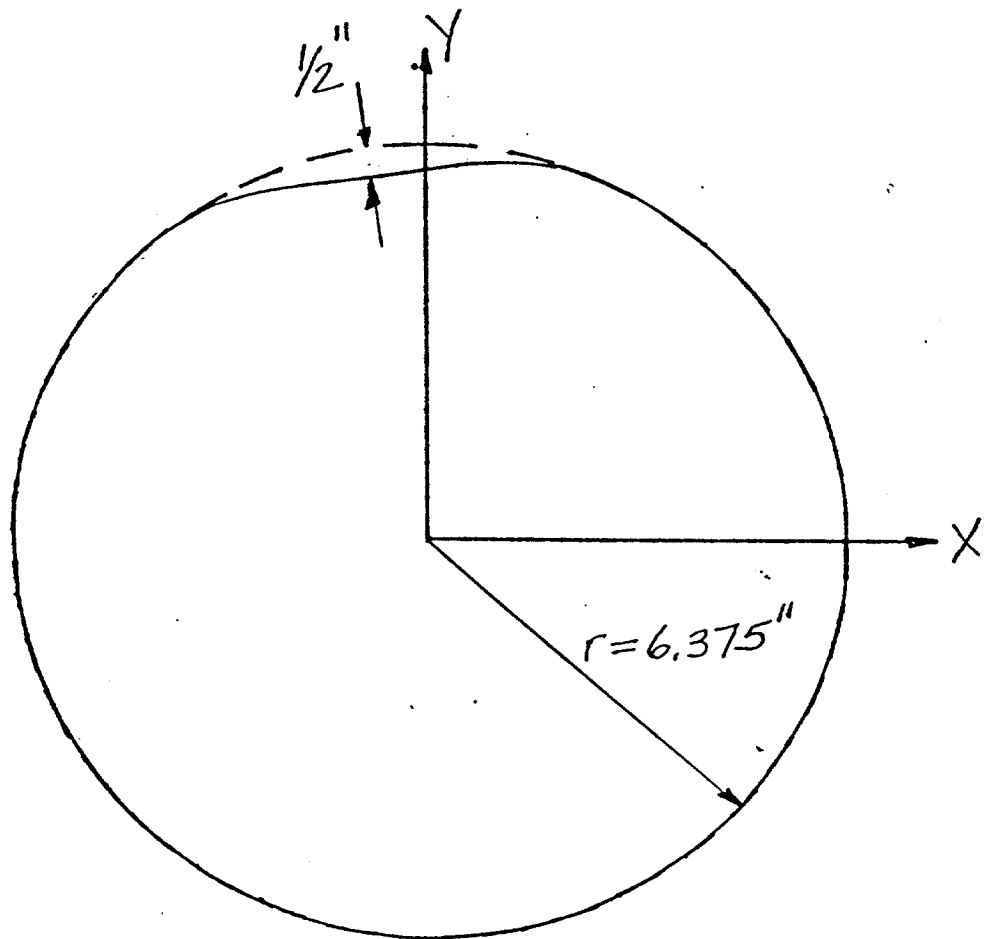
DENT CROSS SECTION

Specimen No. 14

Damage No. 243

Distance from End B 1'-2"

Scale 1" = 3"



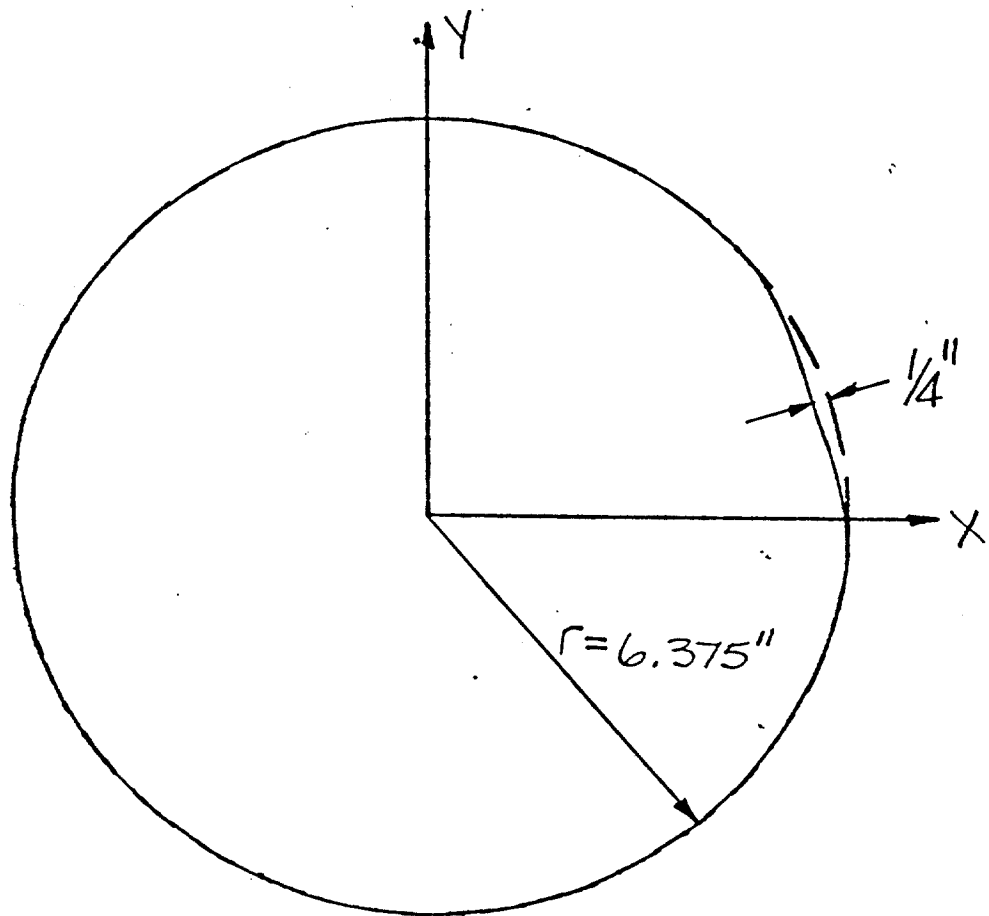
DENT CROSS SECTION

Specimen No. 14

Damage No. 2,3,44

Distance from End B 1'-6"

Scale 1"=3"



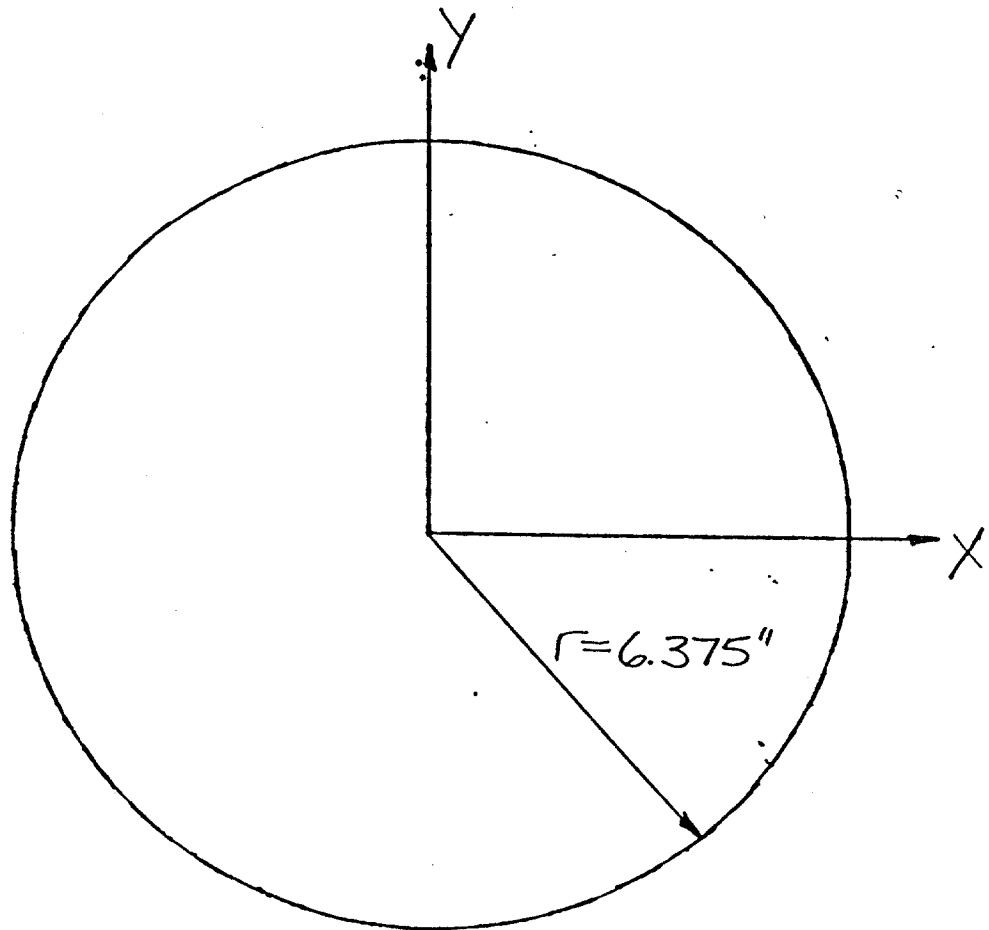
DENT CROSS SECTION

Specimen No. 14

Damage No. 4

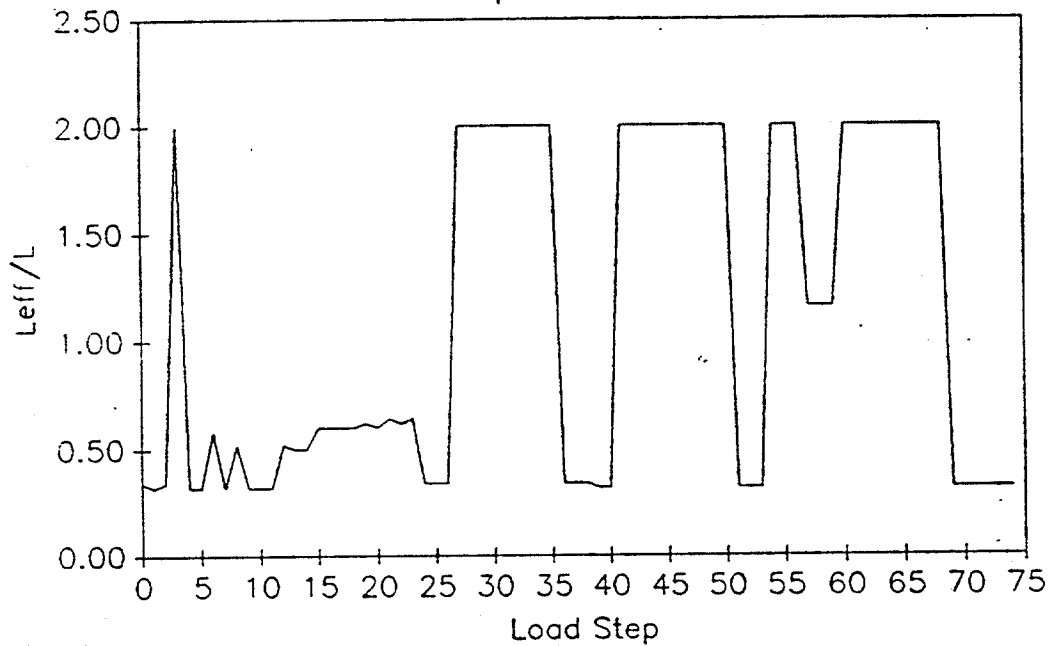
Distance from End B 2'-0"

Scale 1"=3"



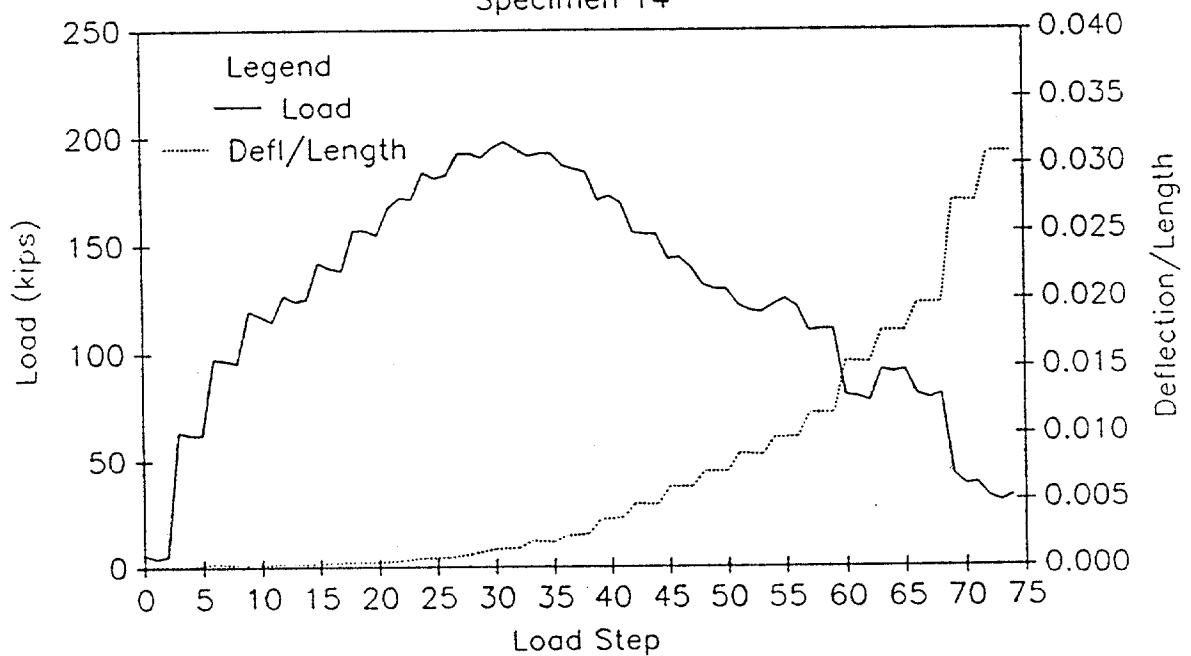
EFFECTIVE LENGTH vs LOAD STEP

Specimen 14

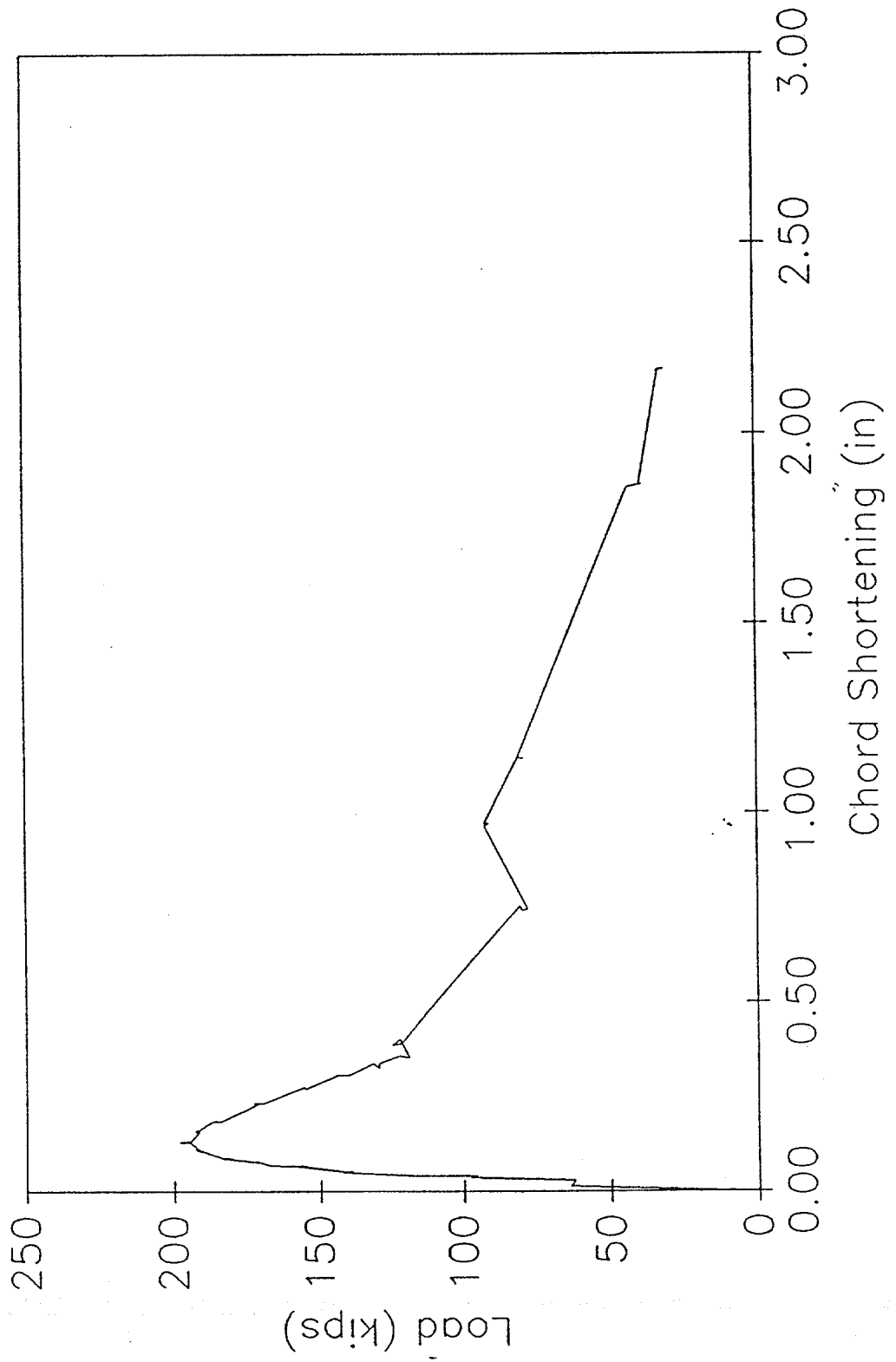


LOAD AND DEFLECTION vs LOAD STEP

Specimen 14

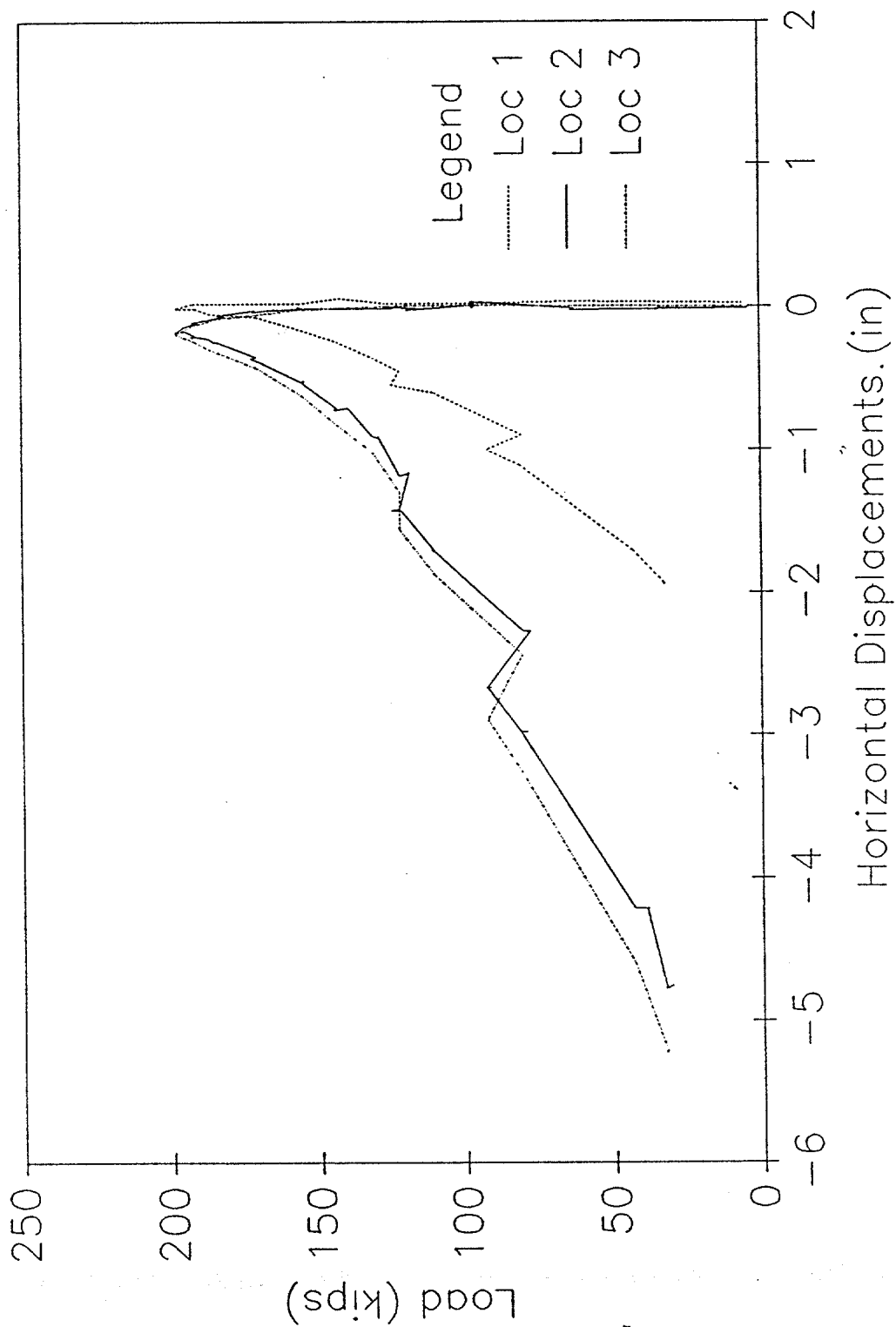


LOAD vs CHORD SHORTENING
Specimen 14



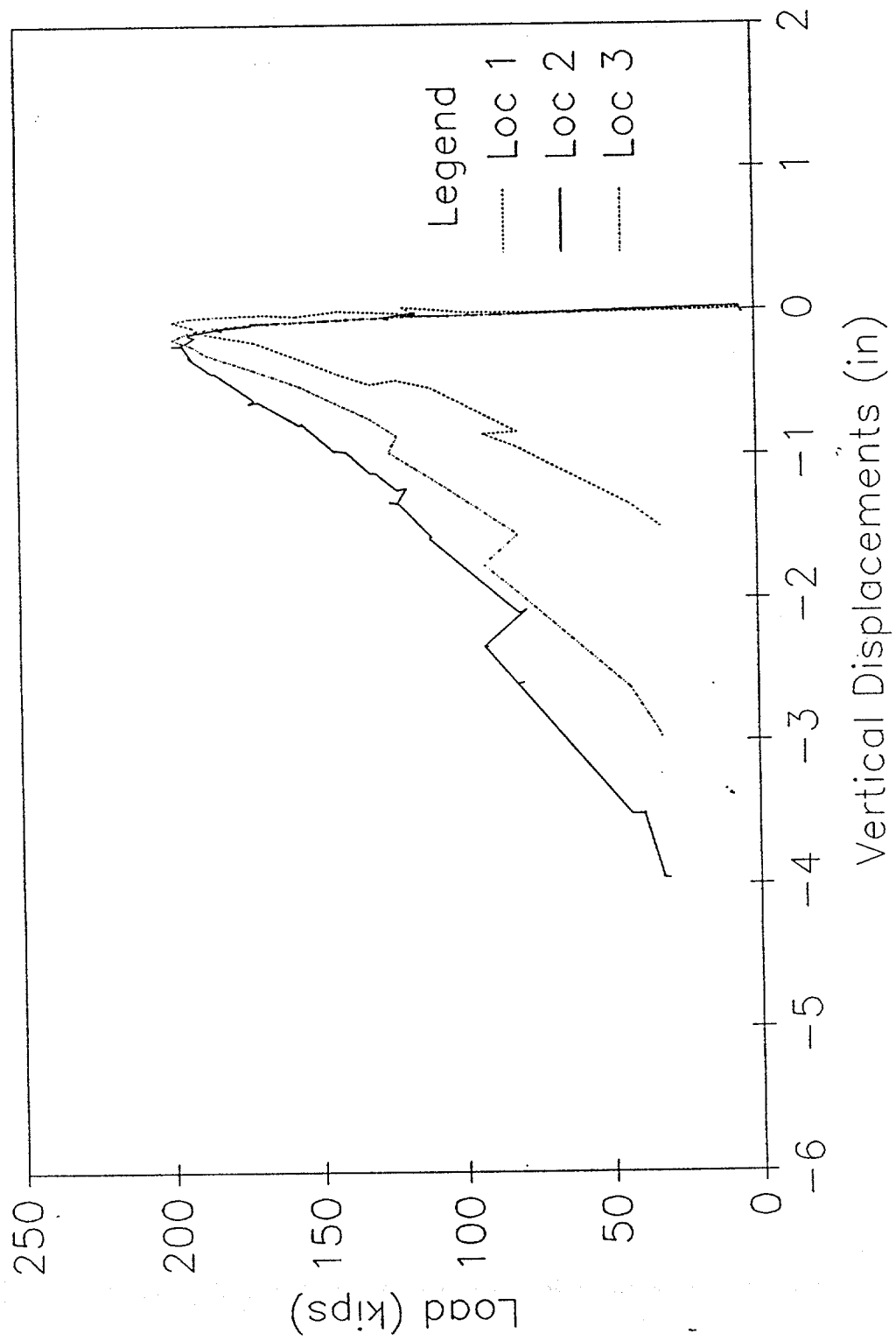
HORIZONTAL DISPLACEMENTS

Specimen 14



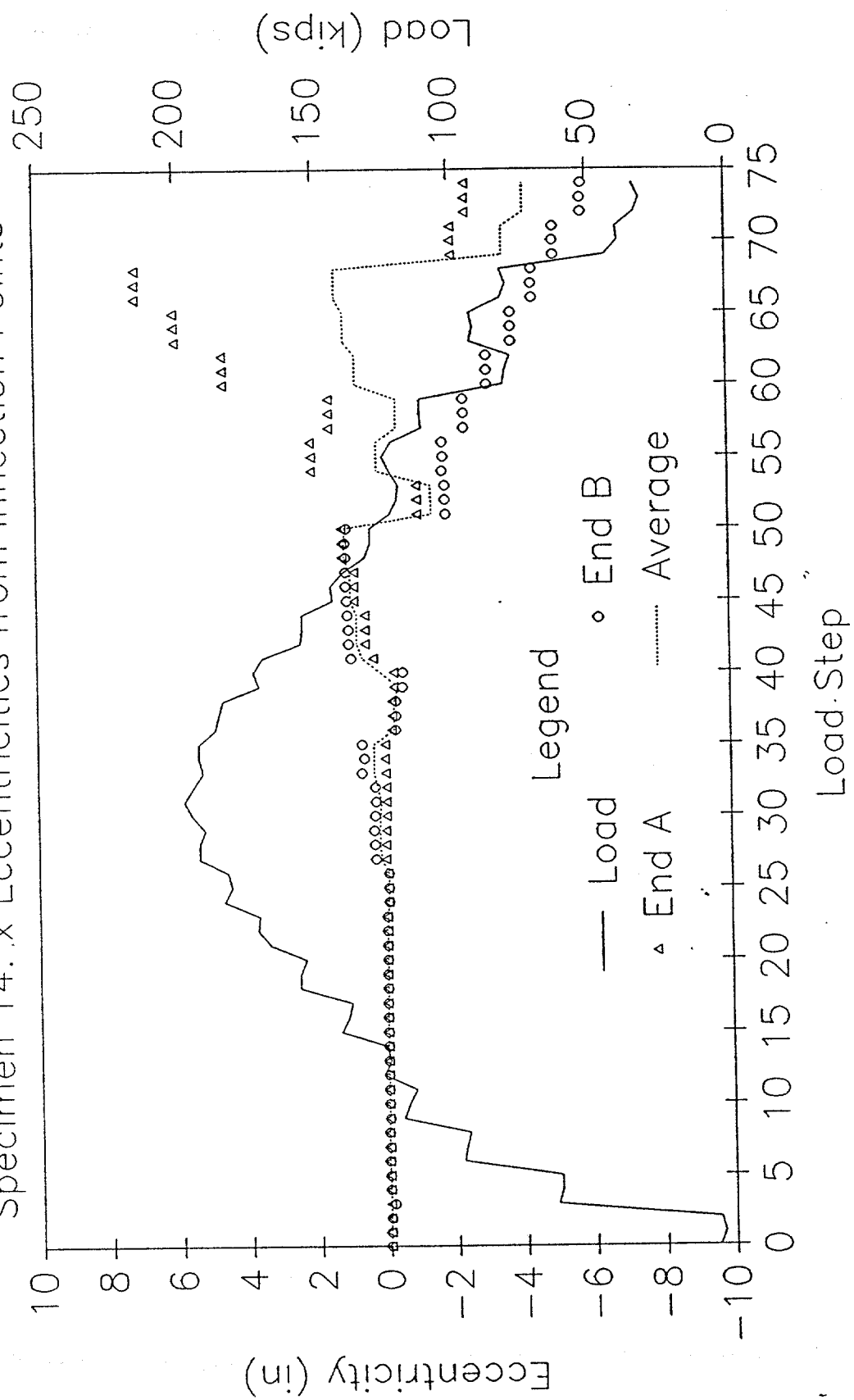
VERTICAL DISPLACEMENTS

Specimen 14



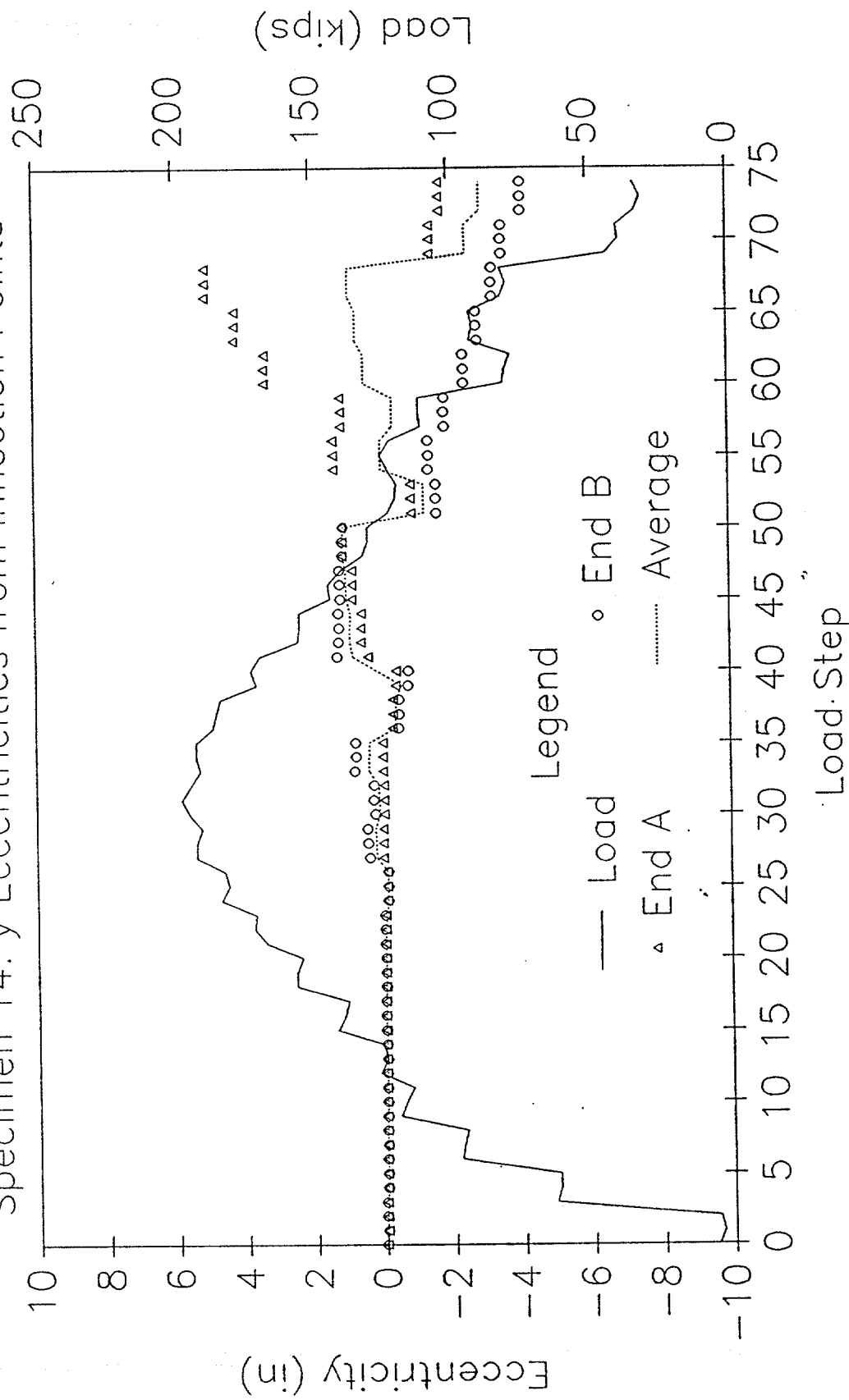
LOAD AND ECCENTRICITY vs LOAD STEP

Specimen 14: x Eccentricities from Inflection Points



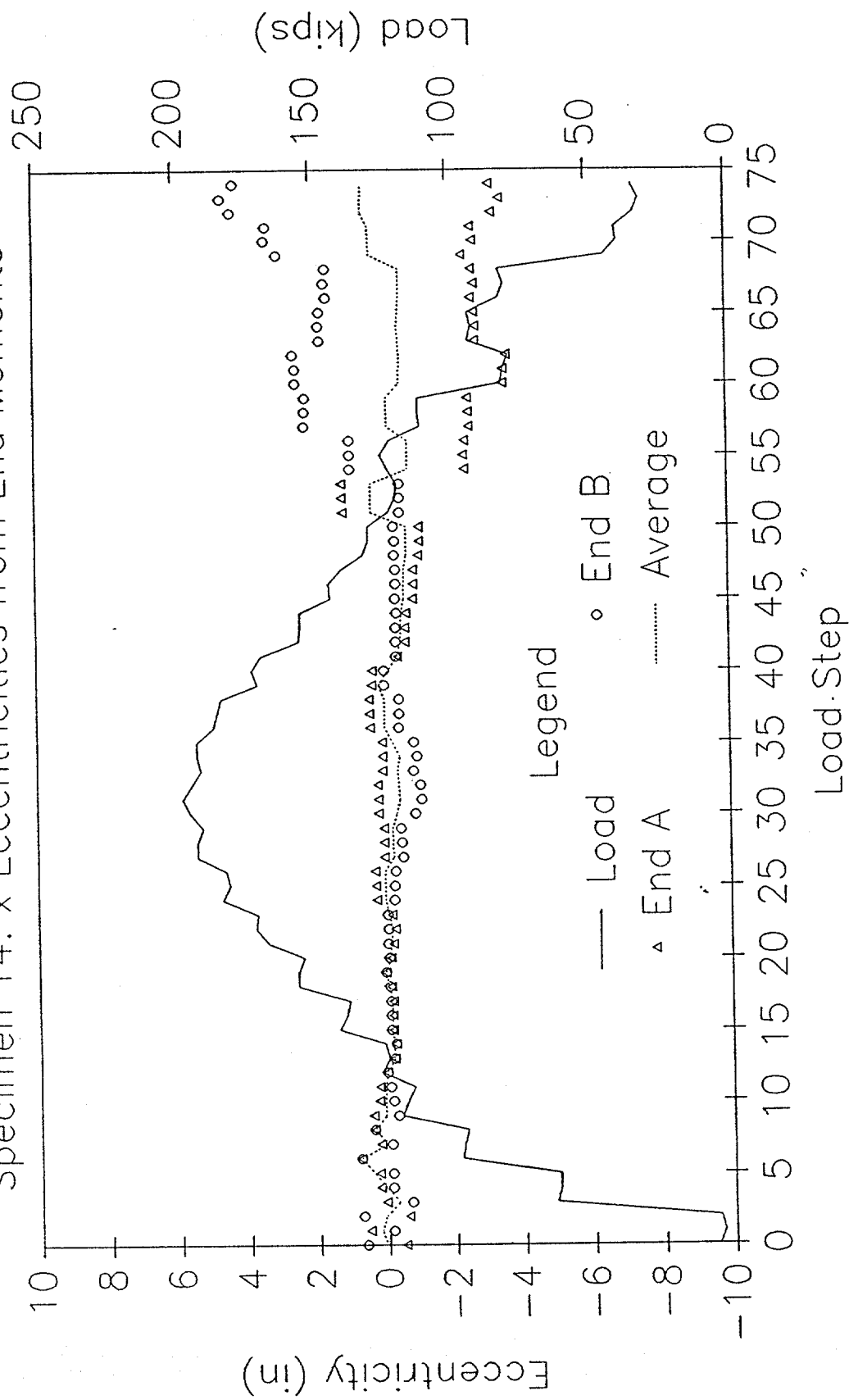
LOAD AND ECCENTRICITY vs LOAD STEP

Specimen 14: y Eccentricities from Inflection Points



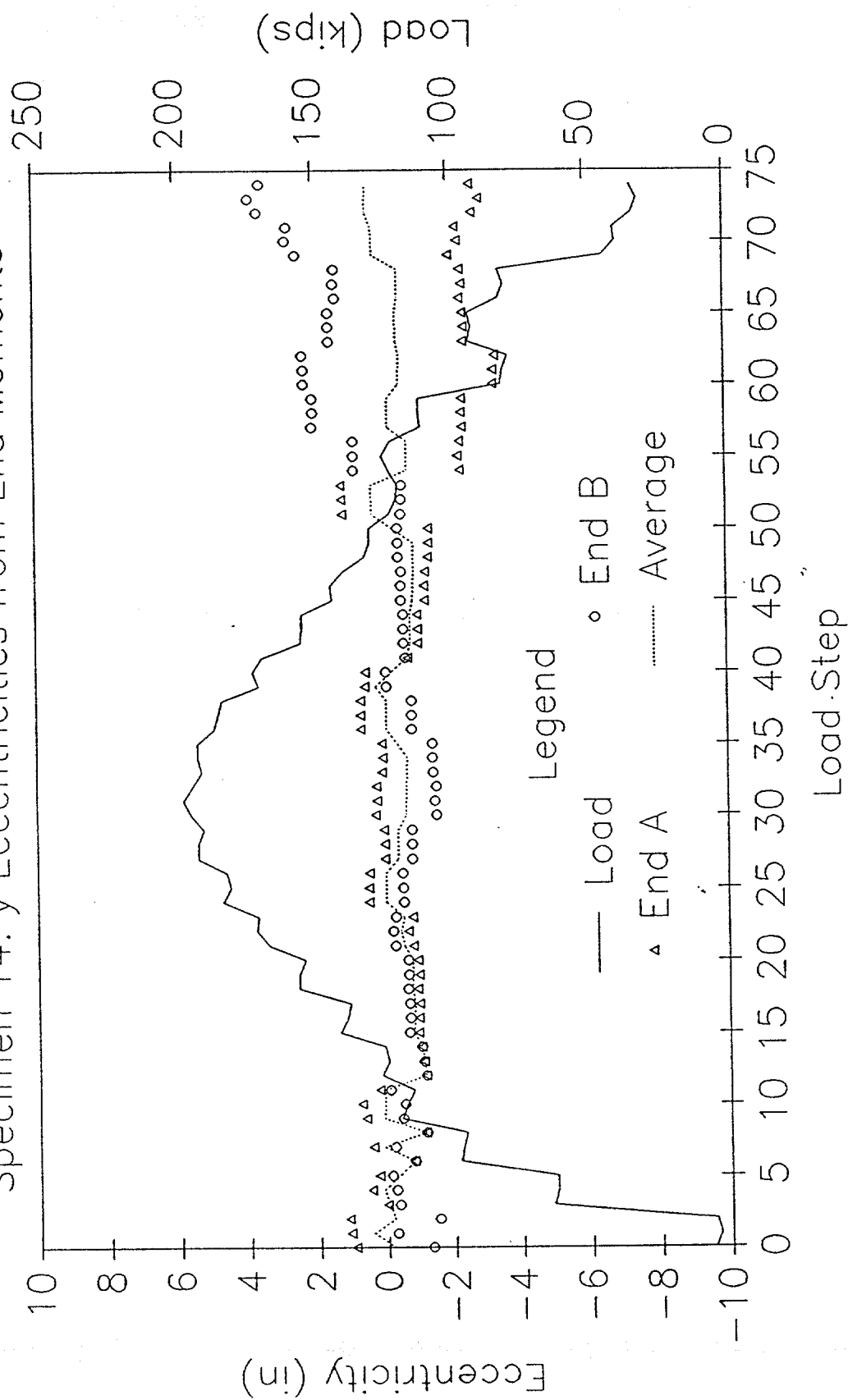
LOAD AND ECCENTRICITY vs LOAD STEP

Specimen 14: x Eccentricities from End Moments



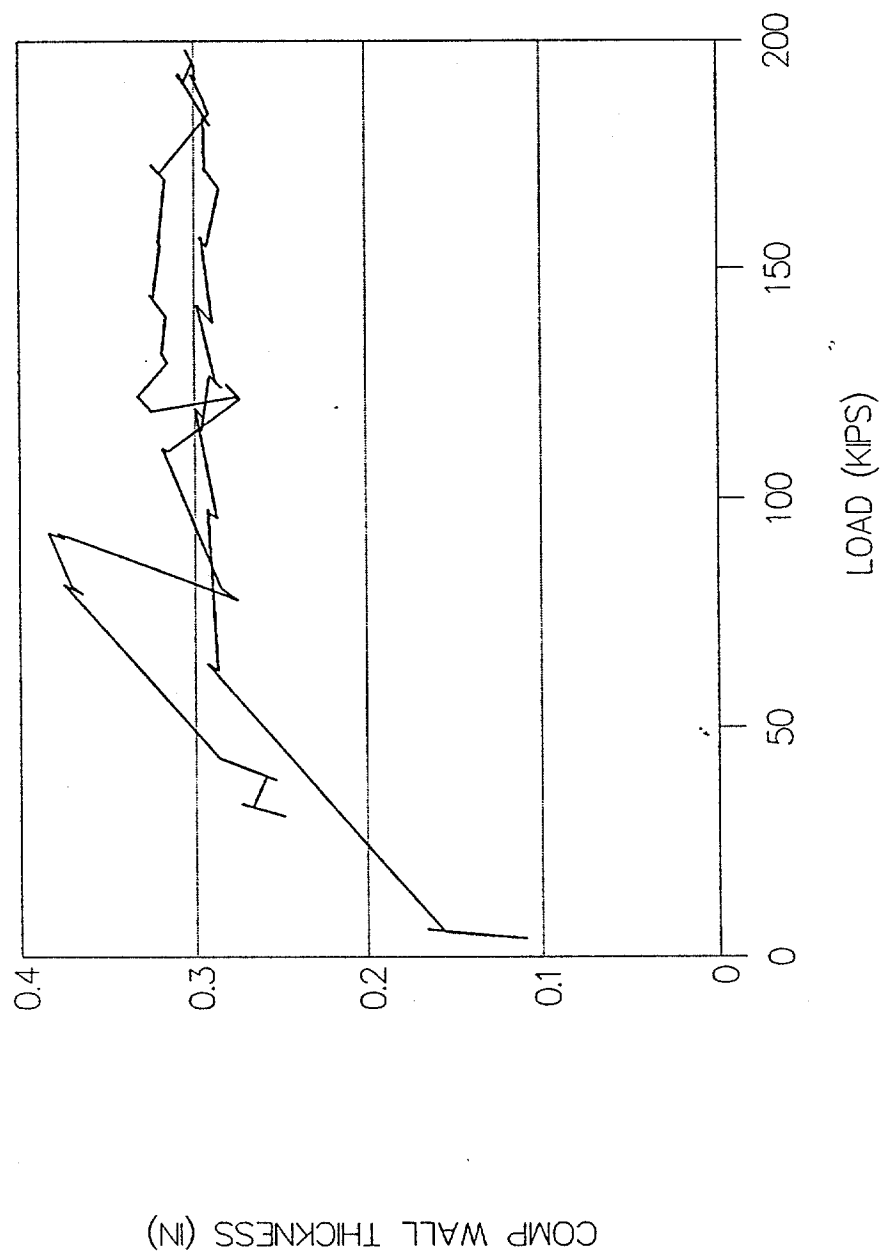
LOAD AND ECCENTRICITY vs LOAD STEP

Specimen 14: y Eccentricities from End Moments



SPECIMEN 14-FULL SCALE TEST

COMPUTED WALL THICKNESS



Ultrasound Data for Specimen 14
(All values in inches)

Gauge No.	UT Thickness	UT Average
0	0.303	
1	0.356	
2	0.358	
3	0.391	
4	0.263	
5	0.226	0.316
6	0.327	
7	0.389	
8	0.410	
9	0.290	
10	0.301	
11	0.308	0.337
12	0.379	
13	0.397	
14	0.355	
15	0.363	
16	0.364	
17	0.352	0.368
18	0.389	
19	0.455	
20	0.402	
21	0.323	
22	0.360	
23	0.429	0.393
24	0.347	
25	0.242	
26	0.393	
27	0.257	
28	0.236	
29	0.197	0.279

Overall Average = 0.339

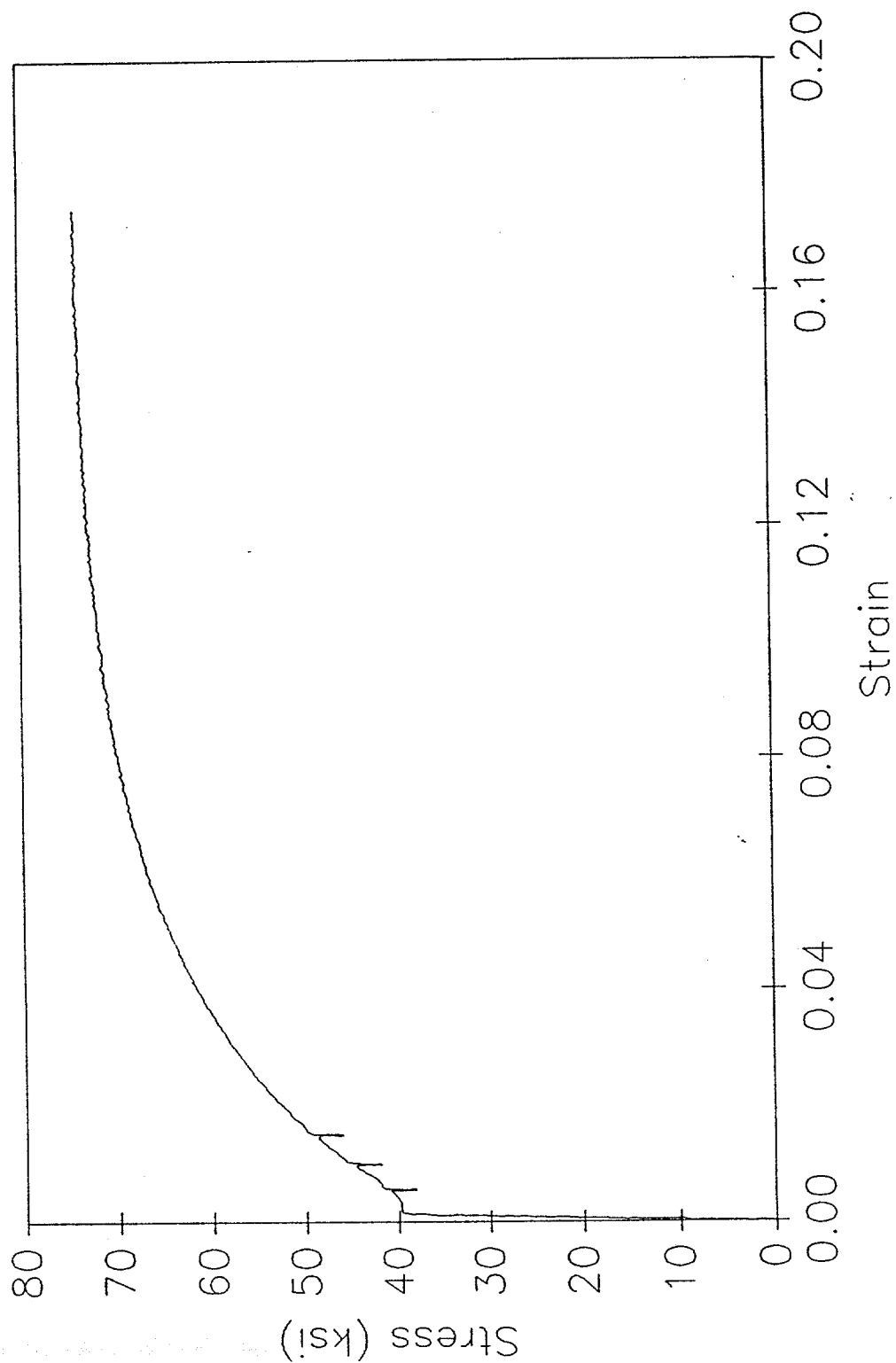
Random Readings near Buckling Point

No.	Reading
1	0.247
2	0.211
3	0.208
4	0.235
5	0.203
6	0.212

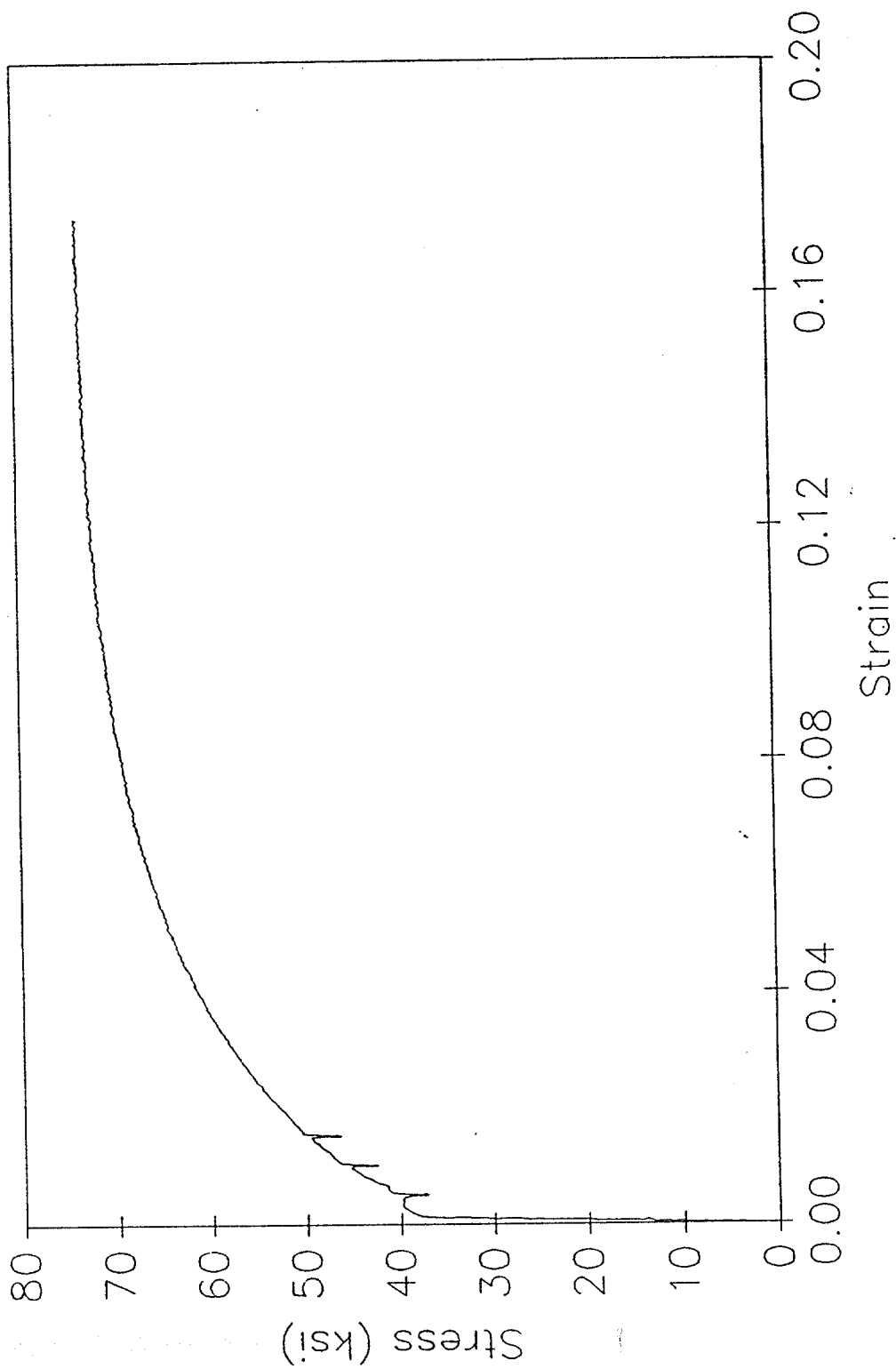
Random Average = 0.219

TENSILE SPECIMEN 14-1

Stress vs Strain



TENSILE SPECIMEN 14-2
Stress vs Strain



SPECIMEN 16

DAMAGE SUMMARY

Specimen No. 16

DISTANCE FROM END "B"	*DISTANCE FROM CHALK LINE		DESCRIPTION OF DAMAGE
	LEFT	RIGHT	
1. 1'-6"		9"	Rectangular welded attachment (cut-off) 5" long x 3/4" wide (oriented longitudinally)
2. 4'-6"	0"		Rectangular welded attachment (cut-off) 5" long X 3/4" wide (oriented longitudinally)
3. 6'-8"	0"		Rectangular welded attachment (cut-off) 5" long X 3/4" wide (oriented longitudinally)
4. 4'-6"	20"		Rectangular welded attachment (cut-off) 5" long X 3/4" wide (oriented longitudinally)
5. 4'-7"			1/2" thick collar welded to pipe Widest point longitudinally = 24" Smallest point longitudinally = 18" (See additional page for sketch and more information)
6. 8'-8"		10"	Dent - 3" X 3" with 1/8" depth at center (See additional pages for cross sections)
7. 9'-5"	1/2"		Dent - 8" long by 3 1/2" wide, 1/4" depth at center (See additional pages for cross sections)
8. 13'-1"	0"		Dent - 6" X 6" - 1/4" depth at center (See additional pages for cross sections)
9. 13'-10"		7"	Dent - 4" long X 5" wide - 1/4" depth at center (See additional pages for cross sections)
10. 20'-5 1/2"	0"		T-section welded to pipe (cut-off) - 14'-9" long (See additional page for sketch)
11. 17'-3 1/2"	0"		5/8" hole (torch hole)
12. 18'-3 1/2"			1/4" circumferential butt weld
13. 27'-9"		10"	1" diameter hole

The specimen is curved in the x- and y- directions. See additional pages for initial out-of-straightness information.

*Looking from end "A" towards end "B"

Out-of-Straightness Measurements for Specimen 16

The specimen was initially curved in the yz-plane and in the xz-plane. The following measurements are in the x-direction.

Distance from End B (ft)	Distance from stringline to top of pipe (in)	Out-of- straightness in x direction (in)
0	2.125	2.125
1	2.5	2.125
2	3.25	2.125
3	3.75	2.125
4	3.875	2.125
5	4	2.125
6	3.875	2.125
7	3.75	2.125
8	3.625	2.125
9	3.375	2.125
10	3.125	2.125
11	3.125	2.125
12	3	2.125
13	2.75	2.125
14	2.625	2.125
15	2.75	2.125
16	2.625	2.125
17	2.625	2.125
18	2.5	2.125
19	2.375	2.125
20	2.375	2.125
21	2.25	2.125
22	2.25	2.125
23	2.25	2.125
24	2.125	2.125
25	2.125	2.125
26	2.125	2.125
27	2.125	2.125
28	2.125	2.125
28.667	2.125	2.125

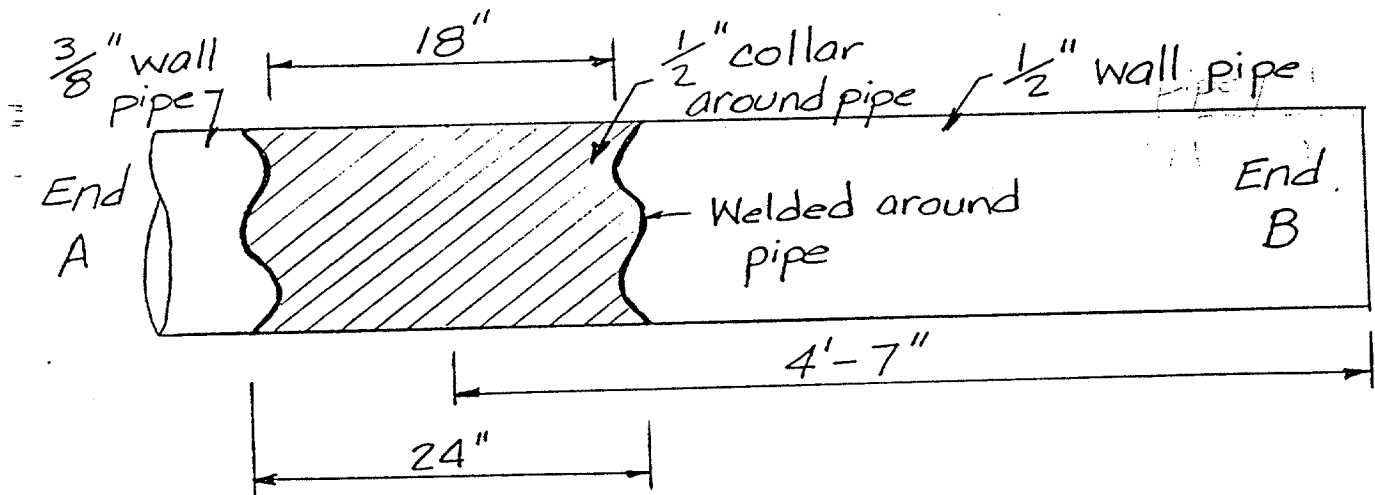
Out-of-Straightness Measurements
for Specimen 16

The specimen was initially curved in the yz-plane and in the xz-plane. The following measurements are in the y-direction.

Distance from End B (ft)	Distance from stringline to top of pipe (in)	Out-of- straightness in y direction (in)
0	2.5	0
1	3.25	-0.75
2	3.625	-1.125
3	4.875	-2.375
4	5.5	-3
5	6.375	-3.875
6	7	-4.5
7	7.375	-4.875
8	7.875	-5.375
9	8.5	-6
10	8.625	-6.125
11	8.75	-6.25
12	8.875	-6.375
13	9.125	-6.625
14	9	-6.5
15	8.4375	-5.9375
16	8.125	-5.625
17	7.375	-4.875
18	7.25	-4.75
19	6.875	-4.375
20	6.375	-3.875
21	6	-3.5
22	5.625	-3.125
23	5.25	-2.75
24	4.875	-2.375
25	4.375	-1.875
26	3.875	-1.375
27	3.75	-1.25
28	2.75	-0.25
28.667	2.5	0

Specimen No. 16

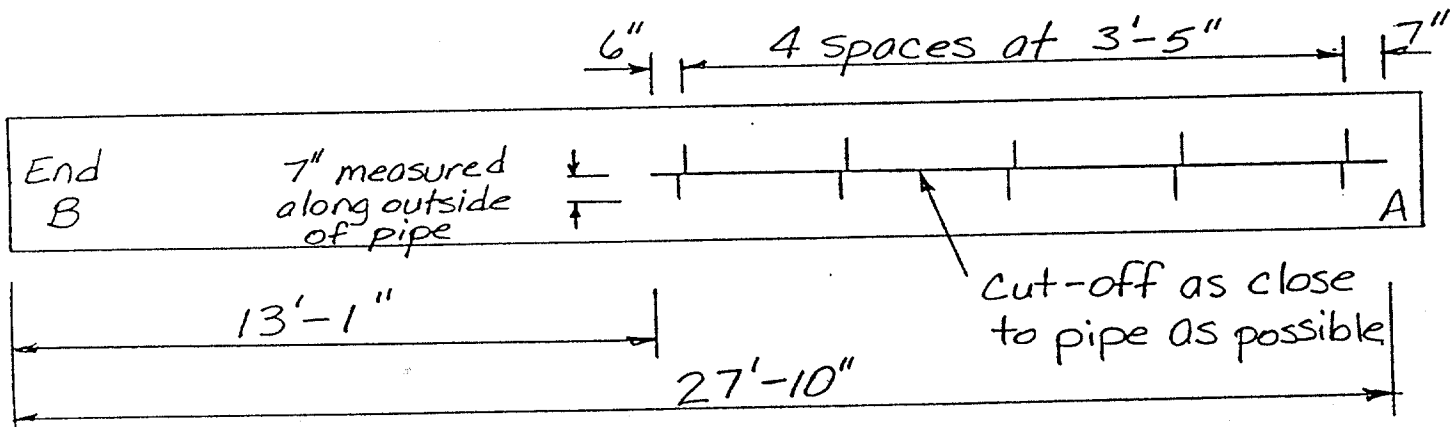
Damage No. 5



The length of pipe ($\frac{3}{8}$ \" or $\frac{1}{2}$ \") under the collar is unknown. We assume that $\frac{1}{2}$ \" wall pipe extends under half the collar (to 4'-7\") and that the rest of the pipe is $\frac{3}{8}$ \" thick.

Damage No. 10

Top View



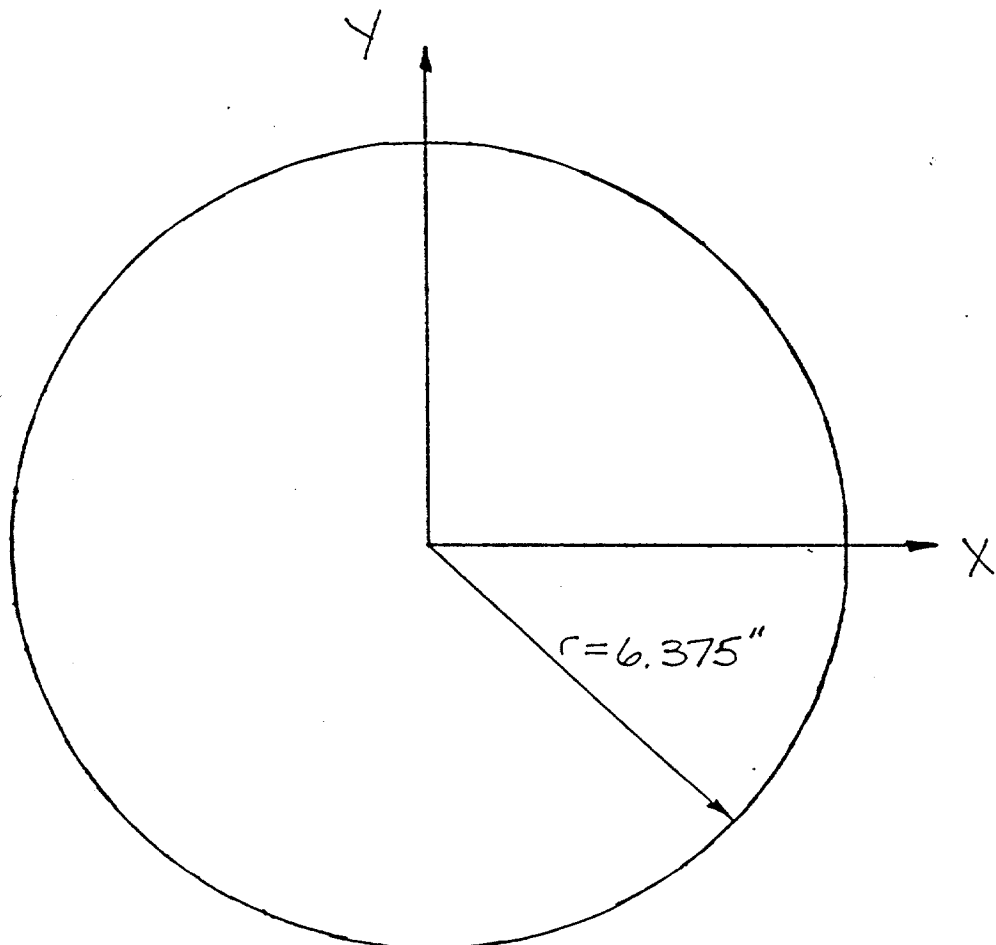
DENT CROSS SECTION

Specimen No. 16

Damage No. 6

Distance from End B 8'-7"

Scale 1"=3"



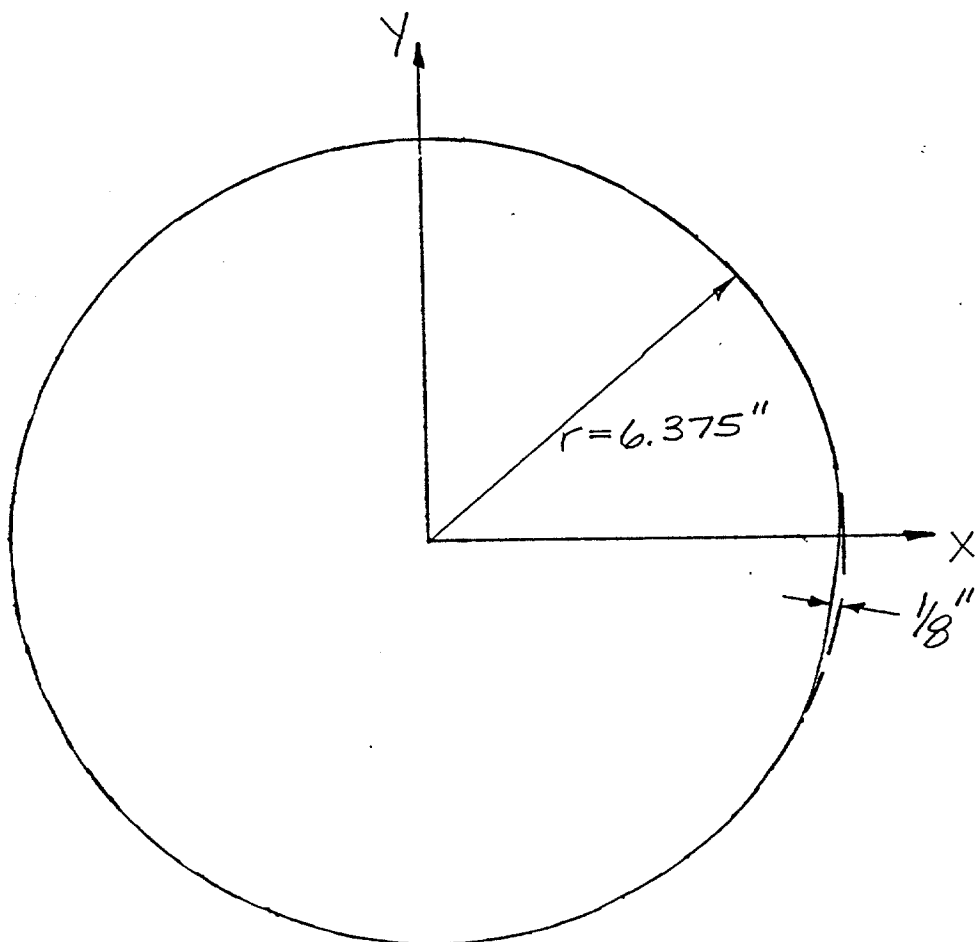
DENT CROSS SECTION

Specimen No. 16

Damage No. 6

Distance from End B 8'-8"

Scale 1" = 3"



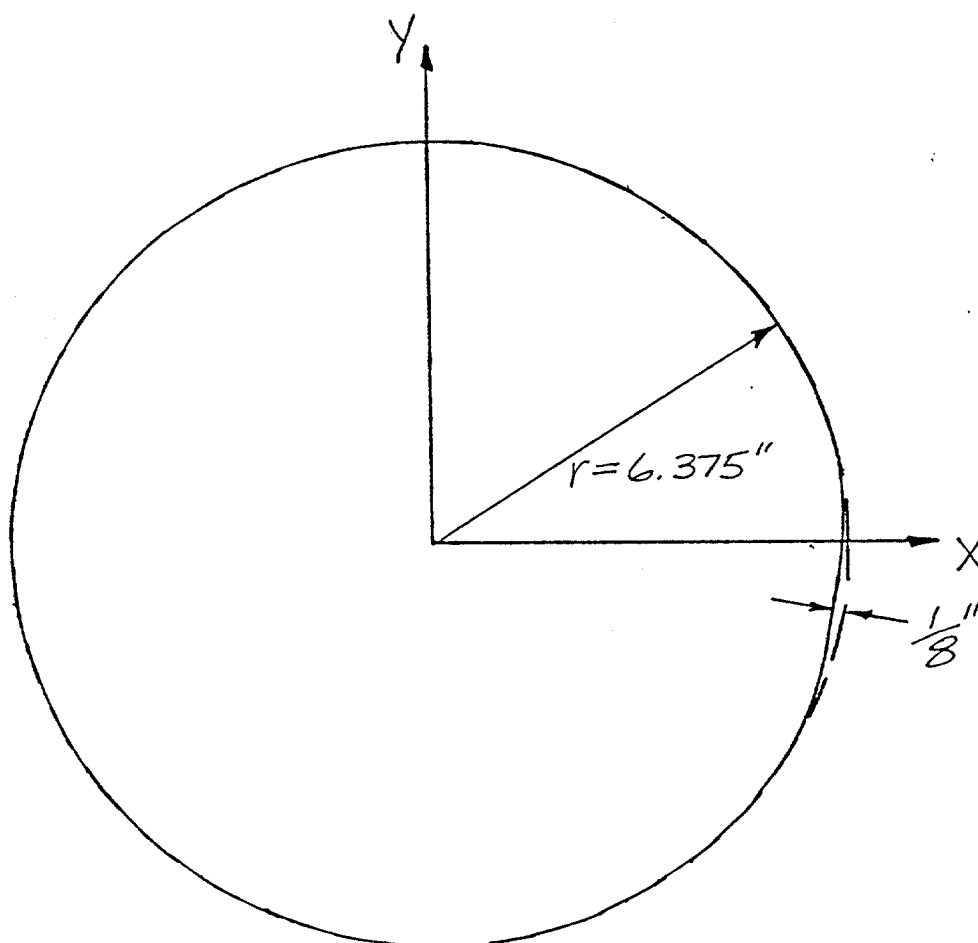
DENT CROSS SECTION

Specimen No. 16

Damage No. 6

Distance from End B 8'-9"

Scale 1"=3"



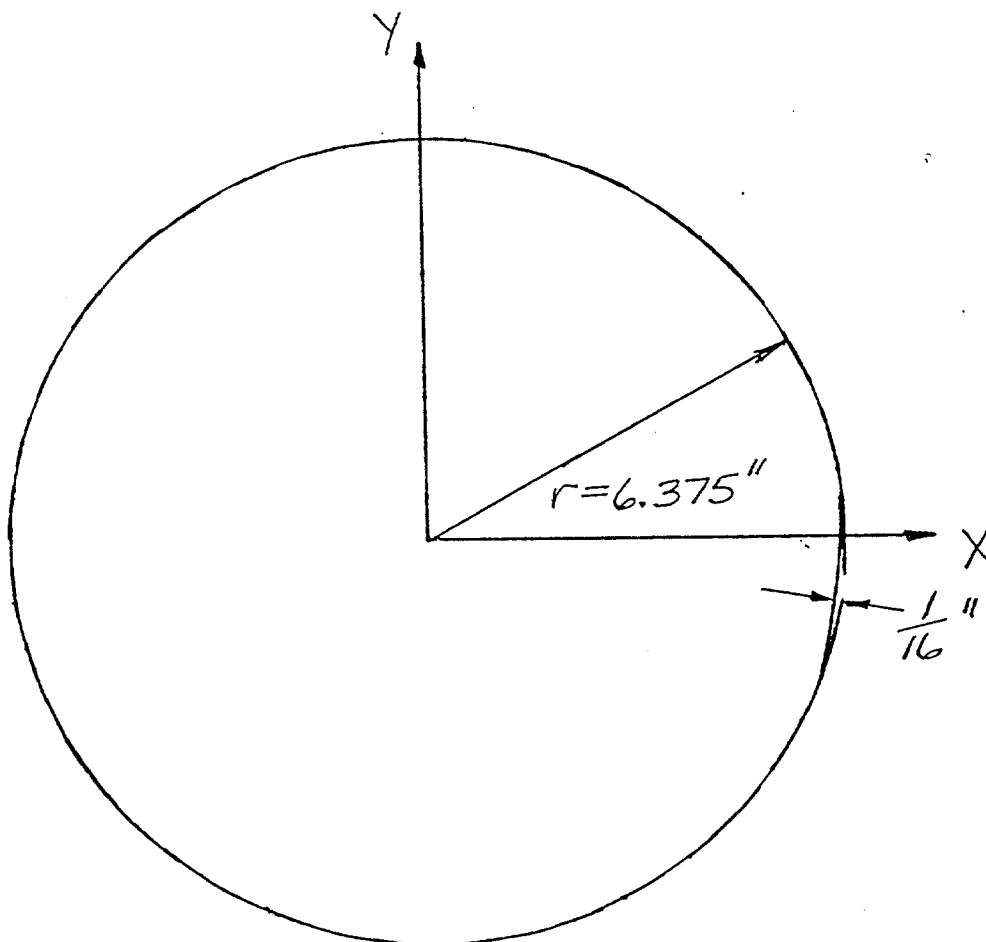
DENT CROSS SECTION

Specimen No. 16

Damage No. 647

Distance from End B 8'-10"

Scale 1" = 3"



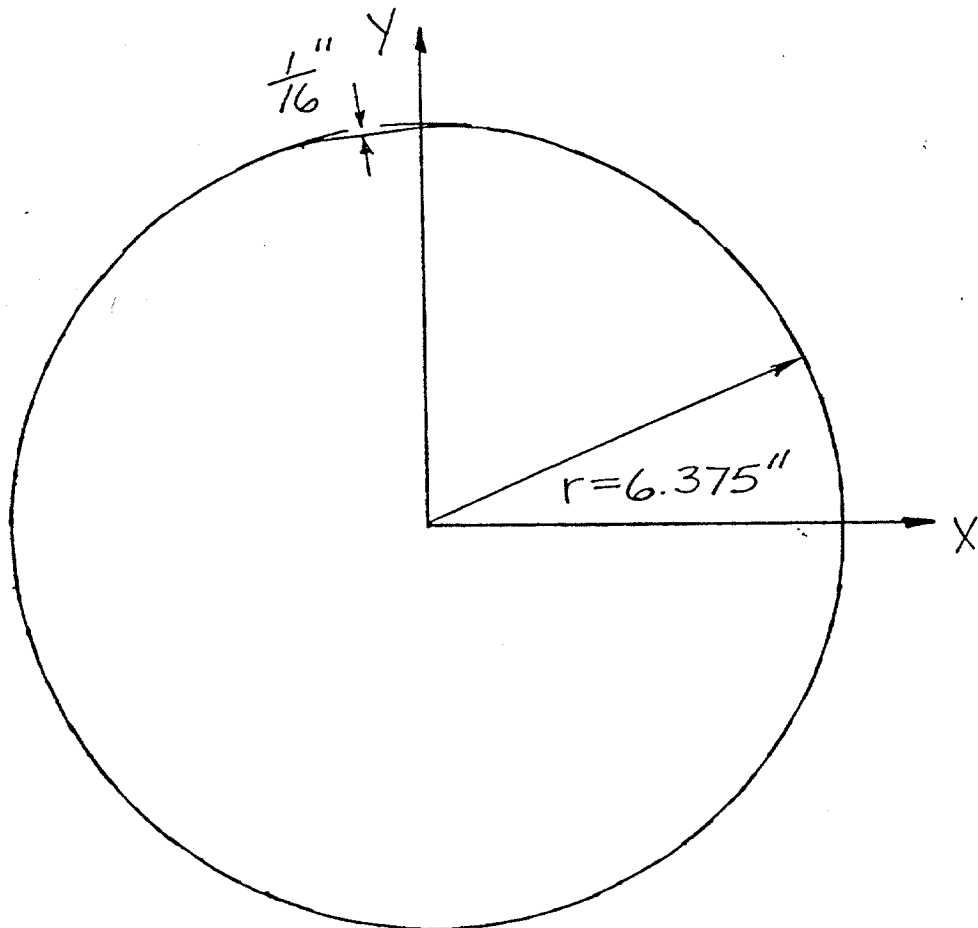
DENT CROSS SECTION

Specimen No. 16

Damage No. 647

Distance from End B B'-11"

Scale 1" = 3"



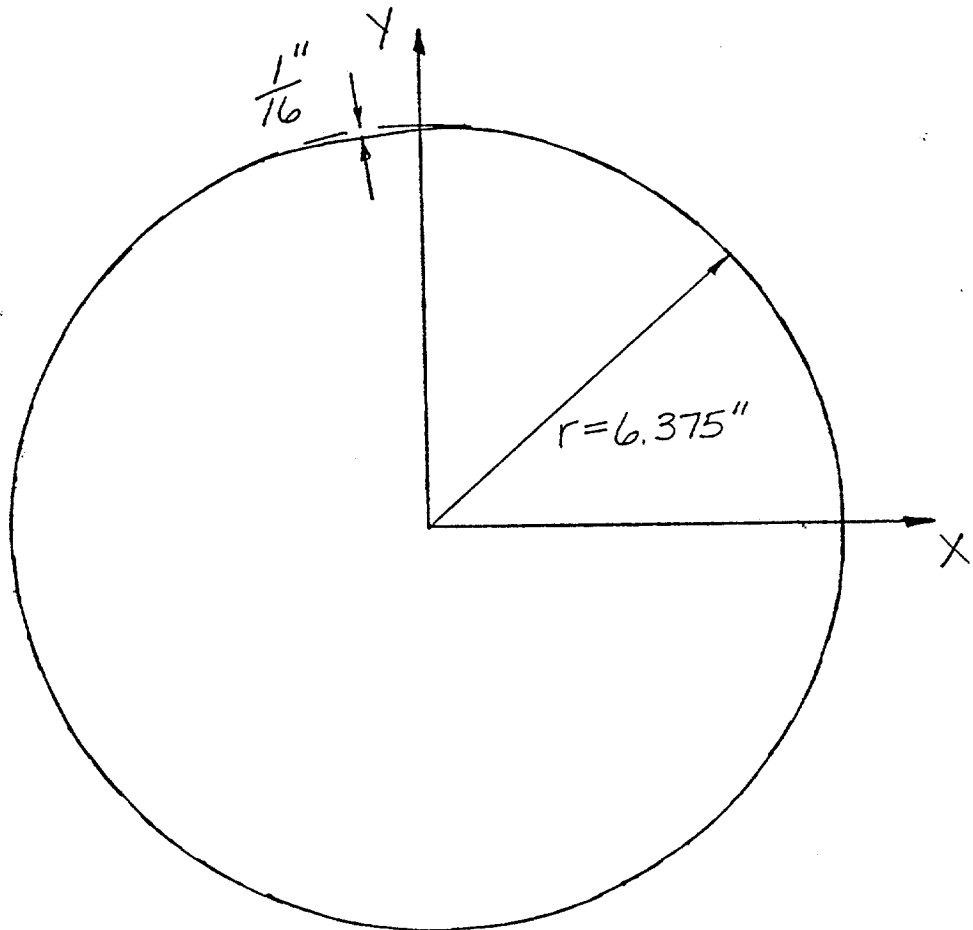
DENT CROSS SECTION

Specimen No. 16

Damage No. 7

Distance from End B 9'-0"

Scale 1"=3"



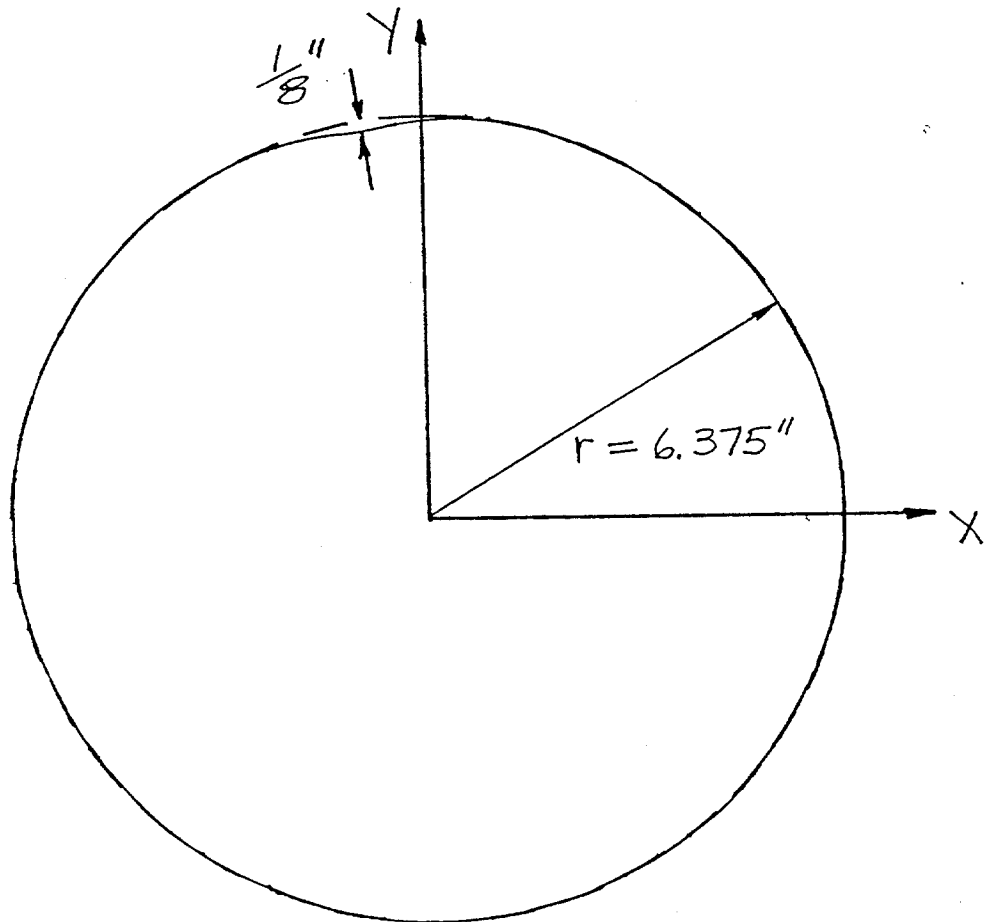
DENT CROSS SECTION

Specimen No. 16

Damage No. 7

Distance from End B 9'-1"

Scale 1"=3"



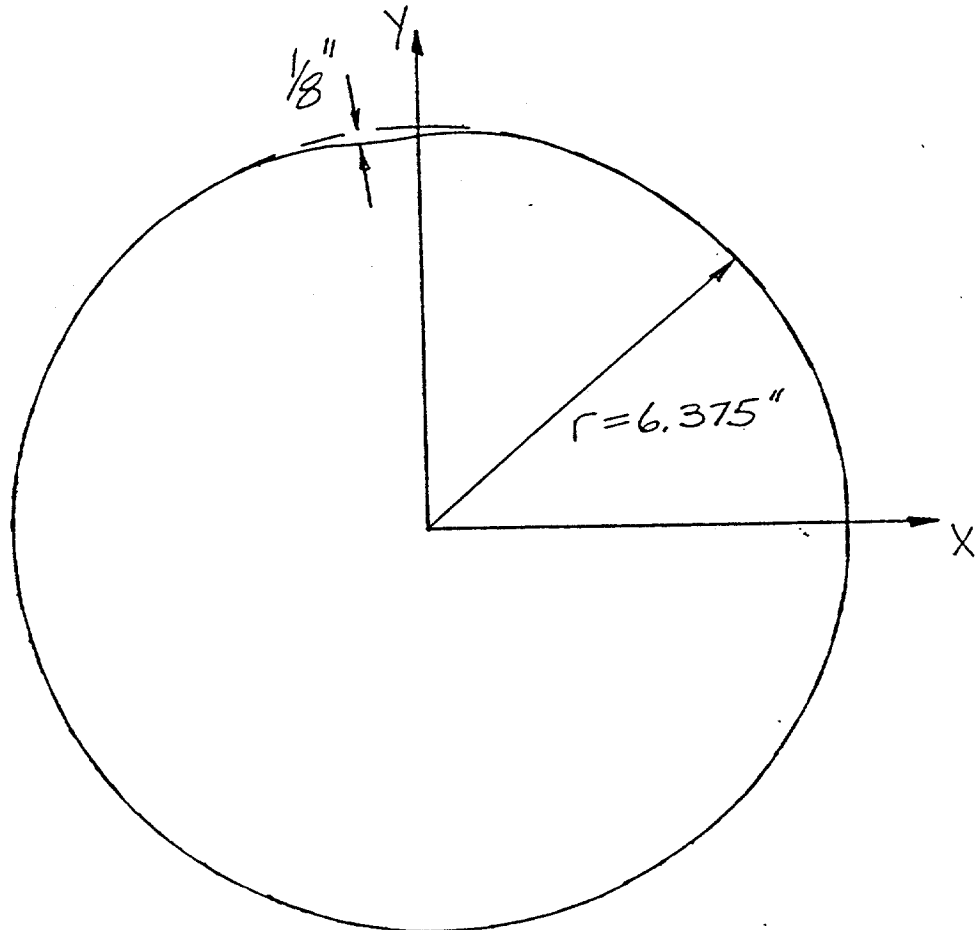
DENT CROSS SECTION

Specimen No. 16

Damage No. 7

Distance from End B 9'-2"

Scale 1" = 3"



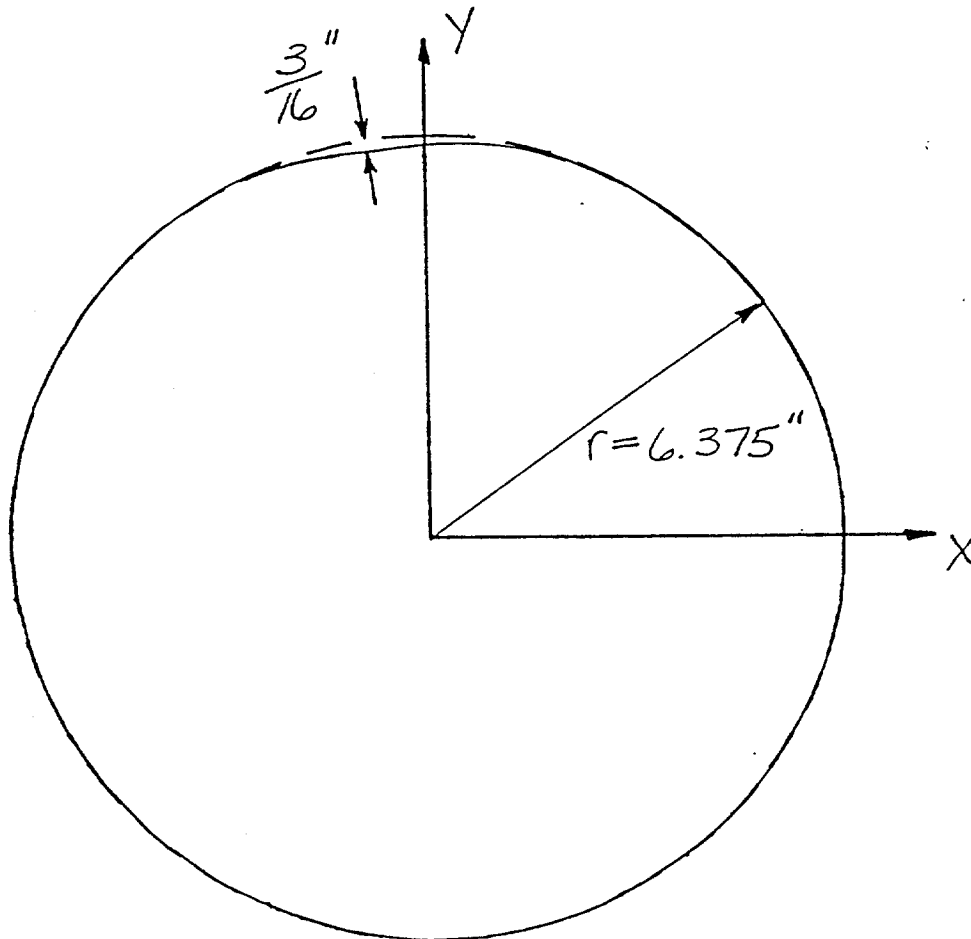
DENT CROSS SECTION

Specimen No. 16

Damage No. 7

Distance from End B 9'-3"

Scale 1" = 3"



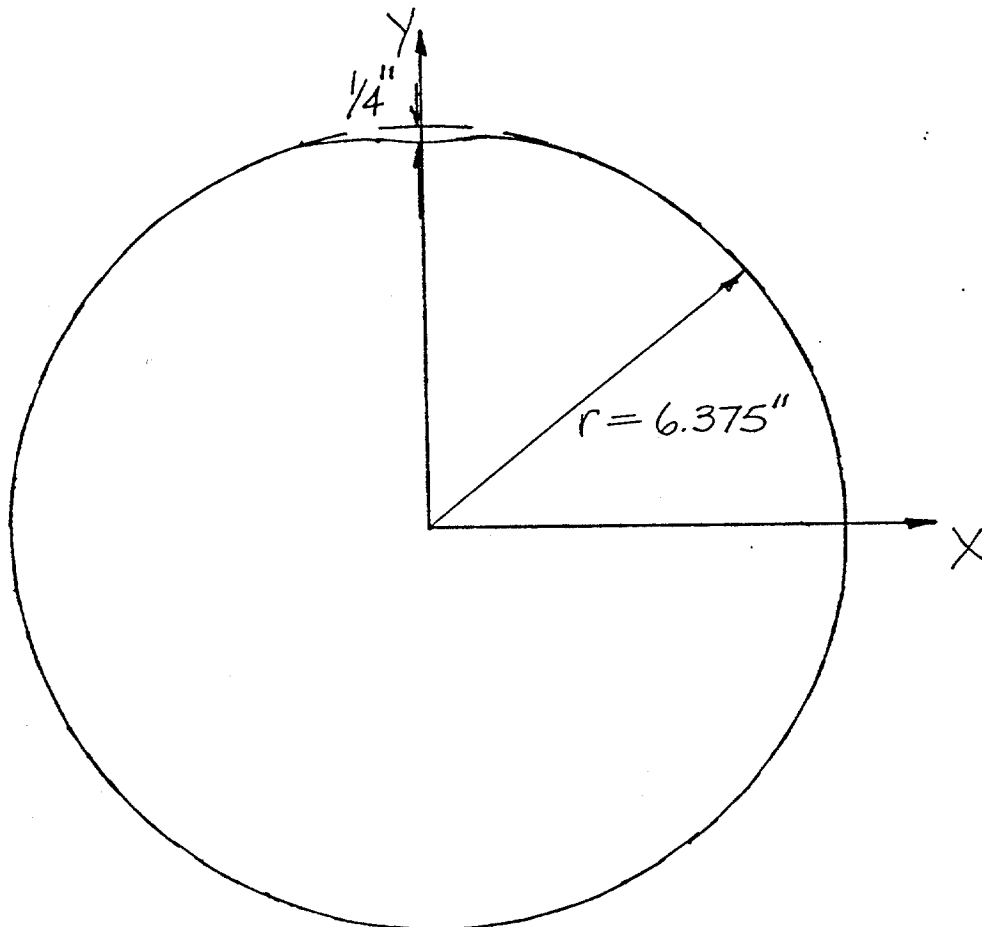
DENT CROSS SECTION

Specimen No. 16

Damage No. 7

Distance from End B 9'-4"

Scale 1"=3"



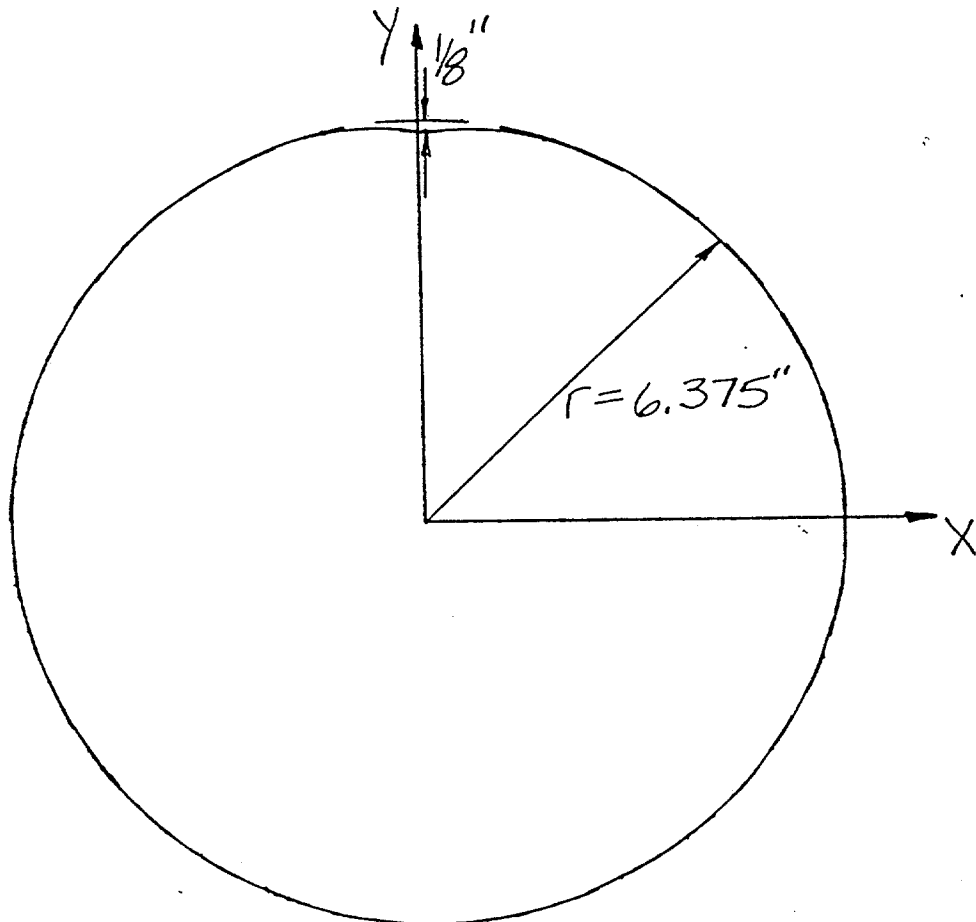
DENT CROSS SECTION

Specimen No. 16

Damage No. 7

Distance from End B 9'-5", 9'-6", 49'-7"

Scale 1"=3"



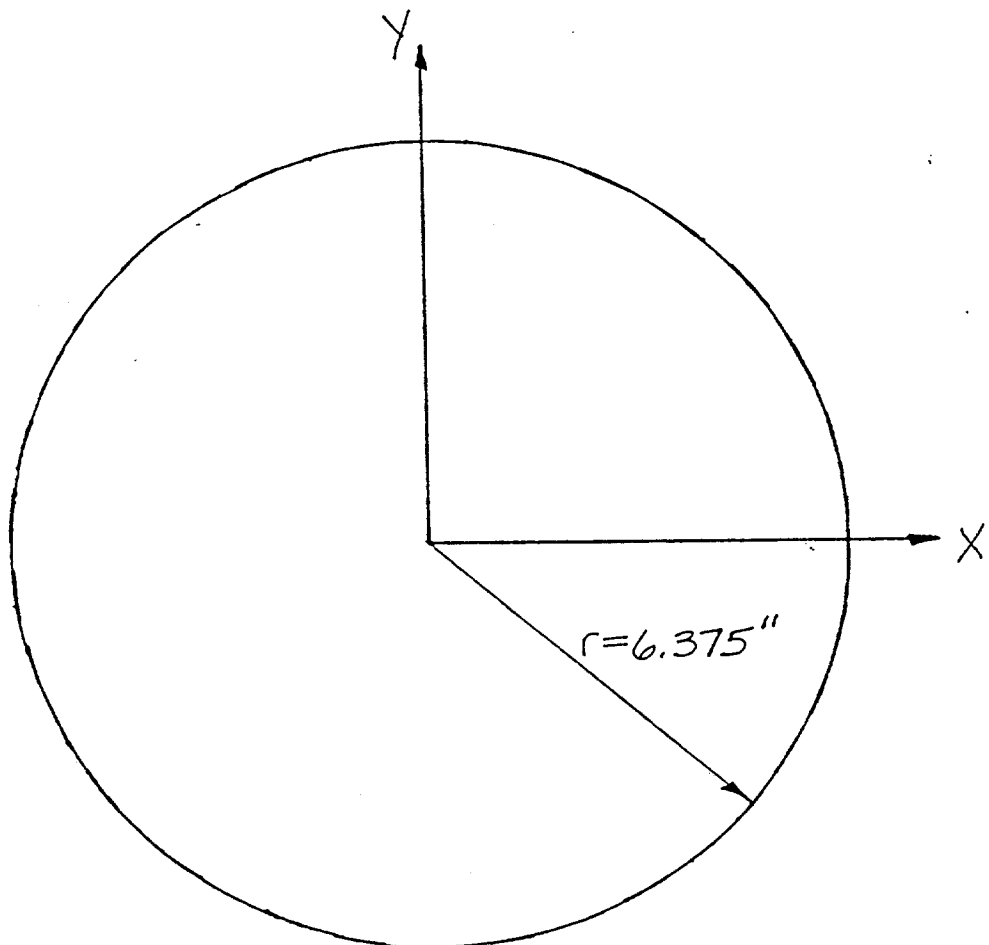
DENT CROSS SECTION

Specimen No. 16

Damage No. 7

Distance from End B 9'-8"

Scale 1"=3"



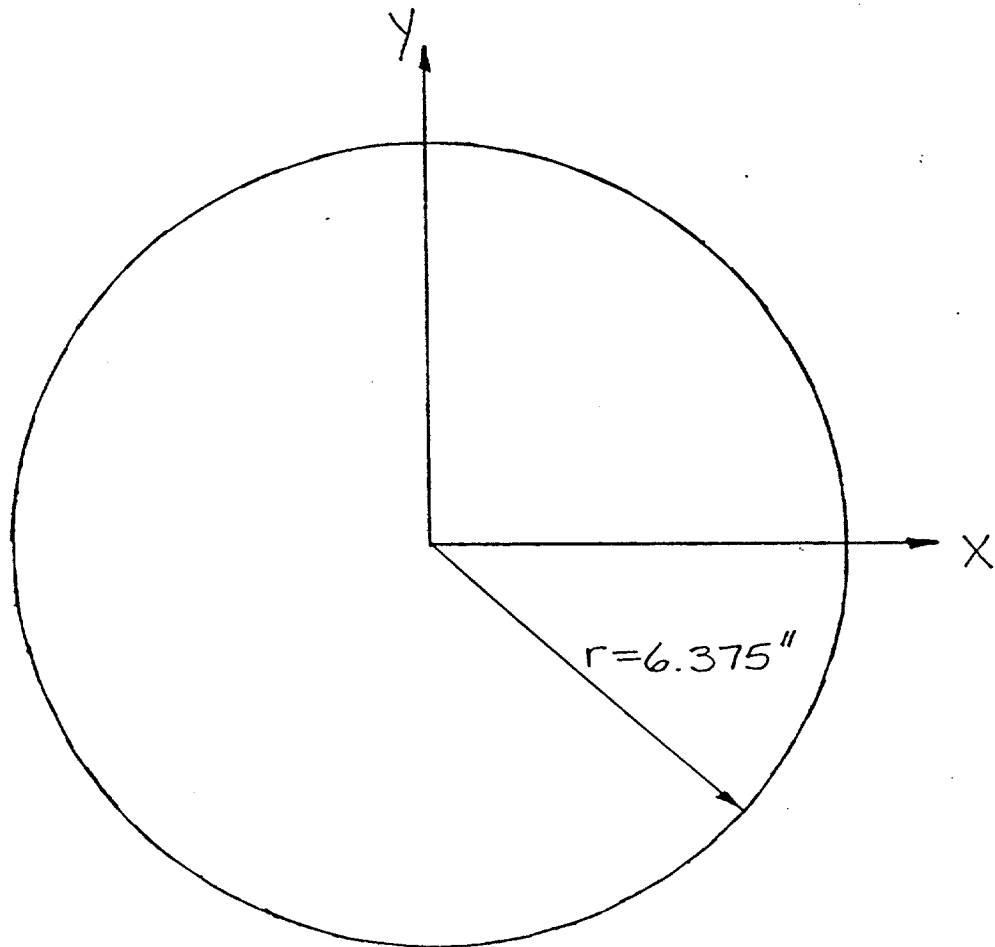
DENT CROSS SECTION

Specimen No. 16

Damage No. 8

Distance from End B 12'-10"

Scale 1"=3"



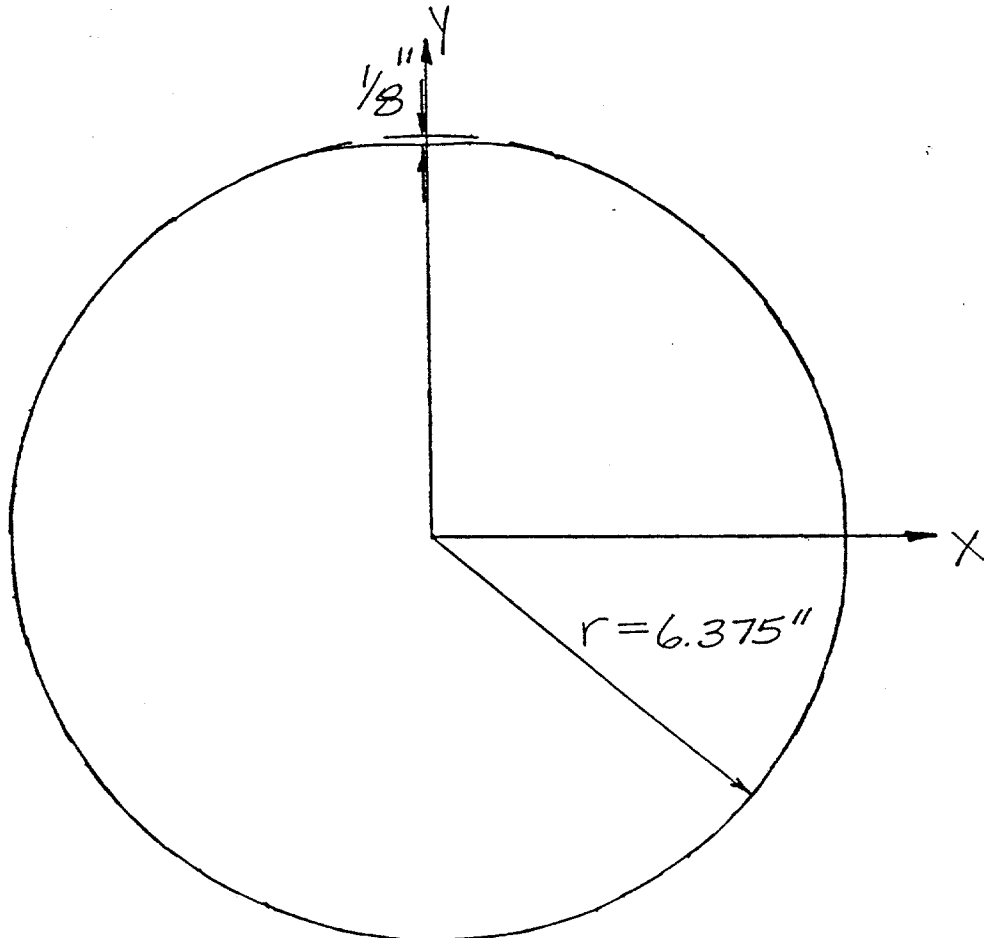
DENT CROSS SECTION

Specimen No. 16

Damage No. 8

Distance from End B 12'-11"

Scale 1"=3"



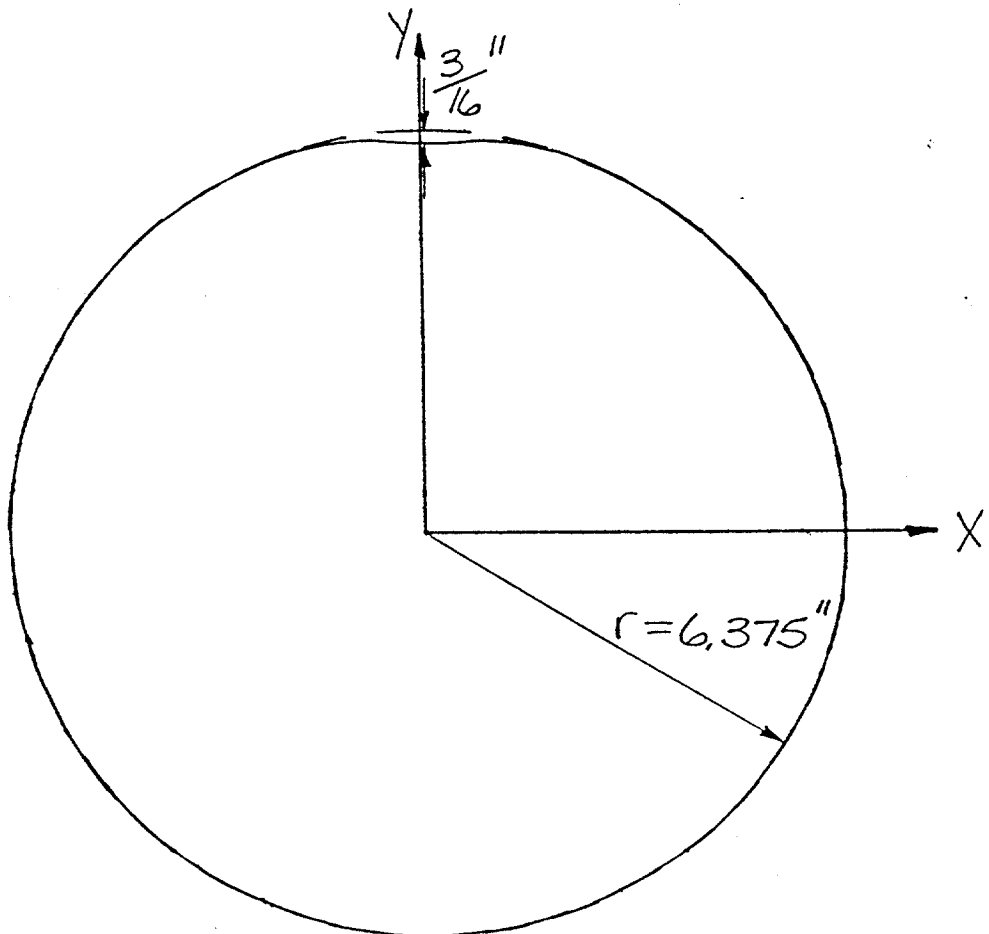
DENT CROSS SECTION

Specimen No. 16

Damage No. 8

Distance from End B 13'-0"

Scale 1" = 3"



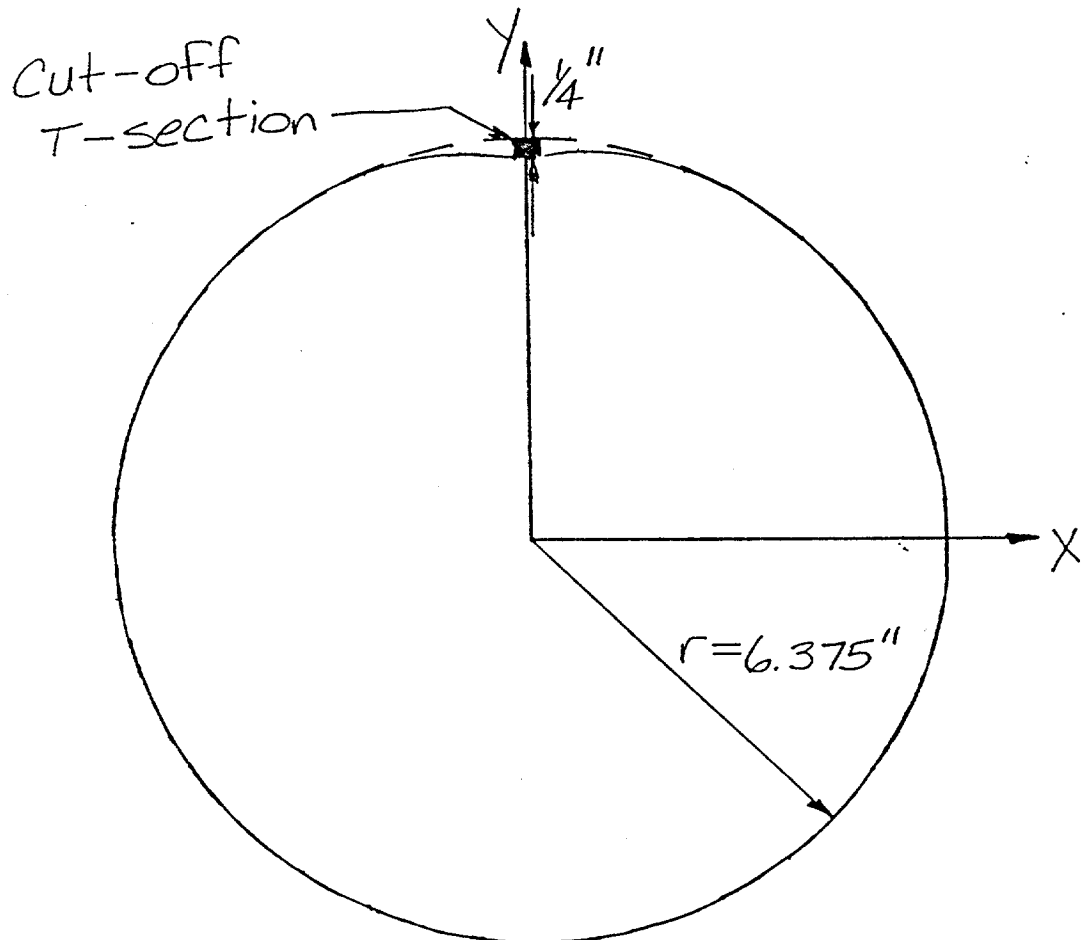
DENT CROSS SECTION

Specimen No. 16

Damage No. 8

Distance from End B 13'-1"

Scale 1"=3"



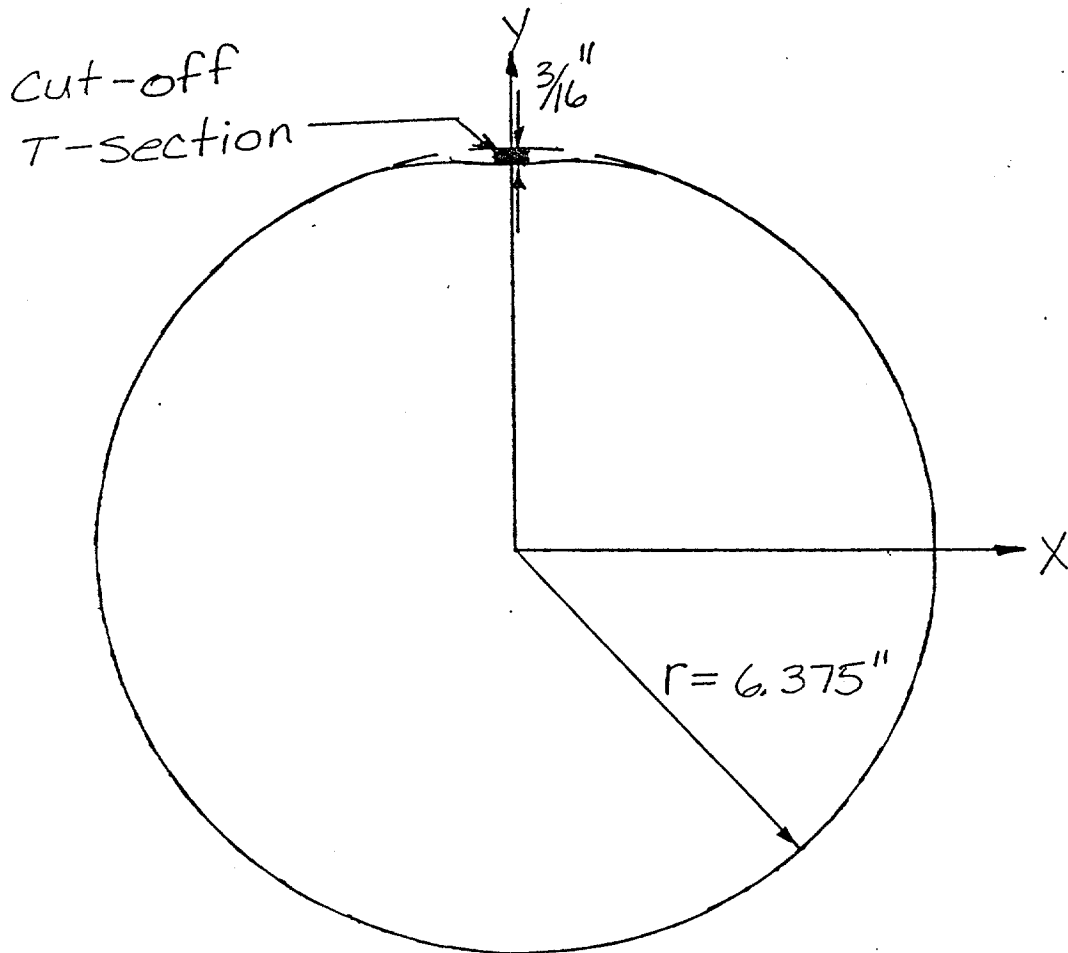
DENT CROSS SECTION

Specimen No. 16

Damage No. 8

Distance from End B 13'-2"

Scale 1"=3"



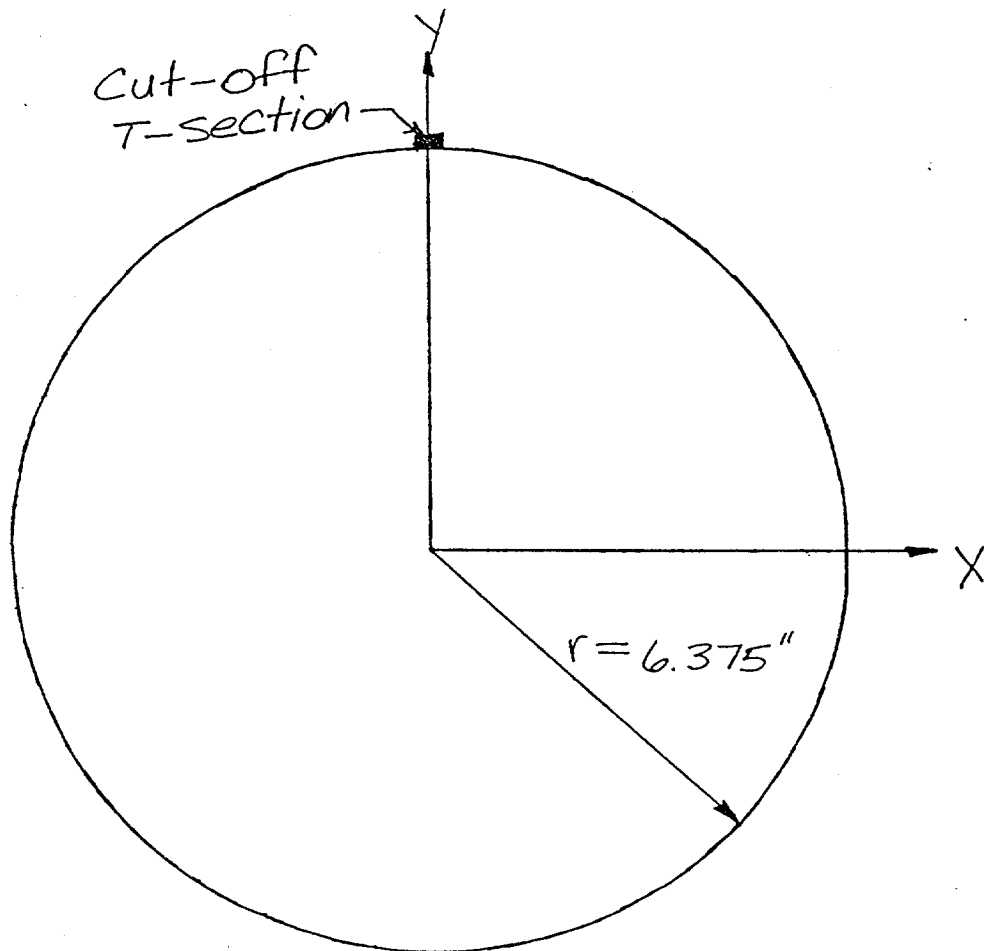
DENT CROSS SECTION

Specimen No. 16

Damage No. 8

Distance from End B 13'-3"

Scale 1"=3"



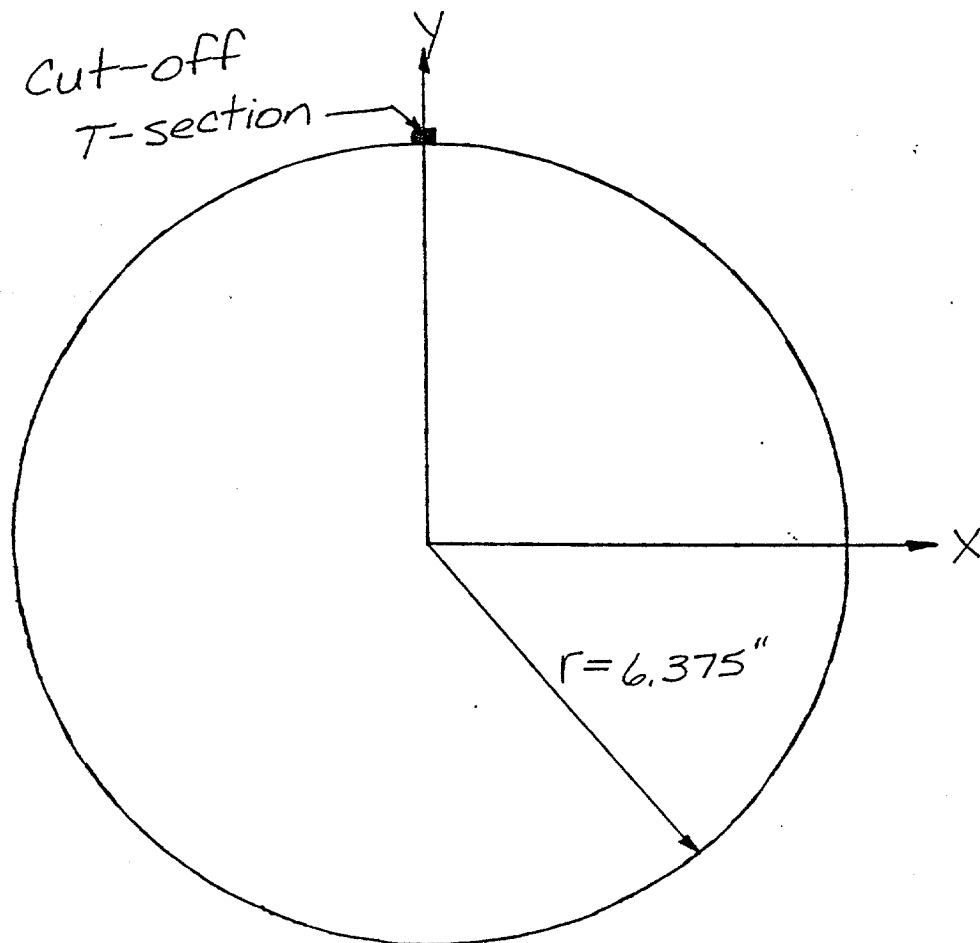
DENT CROSS SECTION

Specimen No. 16

Damage No. 9

Distance from End B 13'-8"

Scale 1"=3"



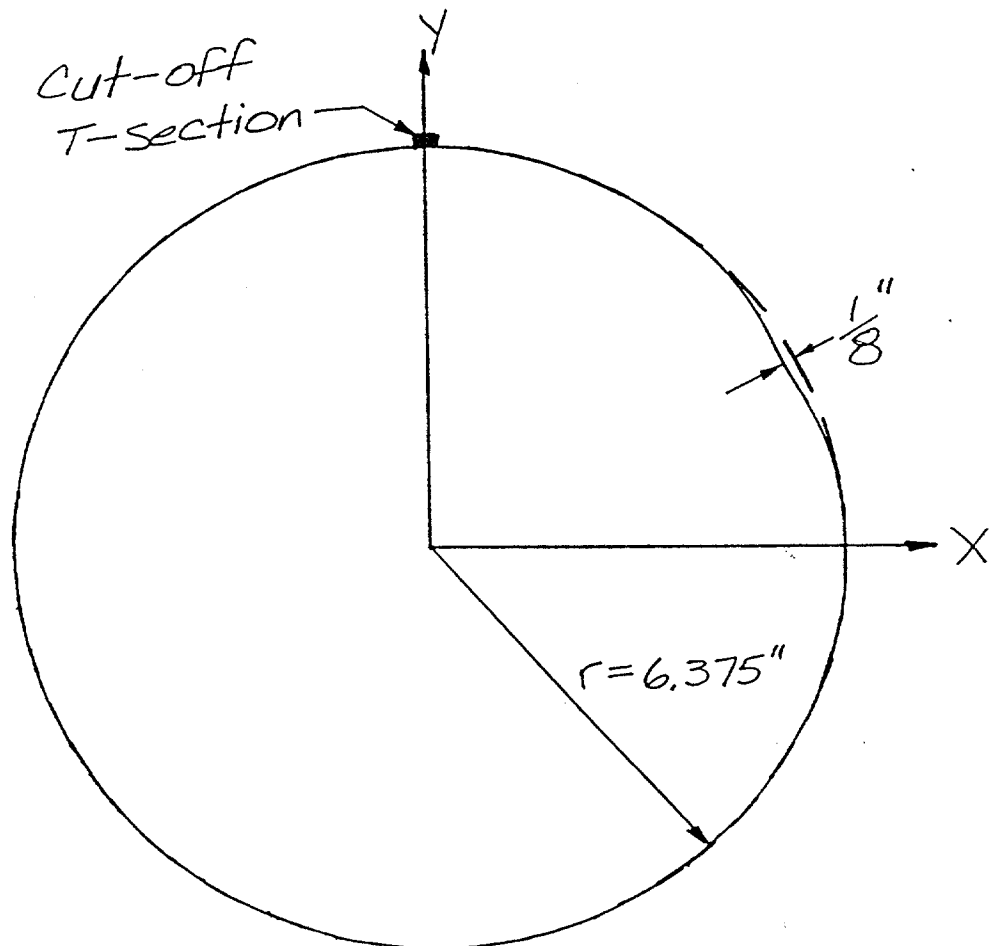
DENT CROSS SECTION

Specimen No. 16

Damage No. 9

Distance from End B 13'-9"

Scale 1"=3"



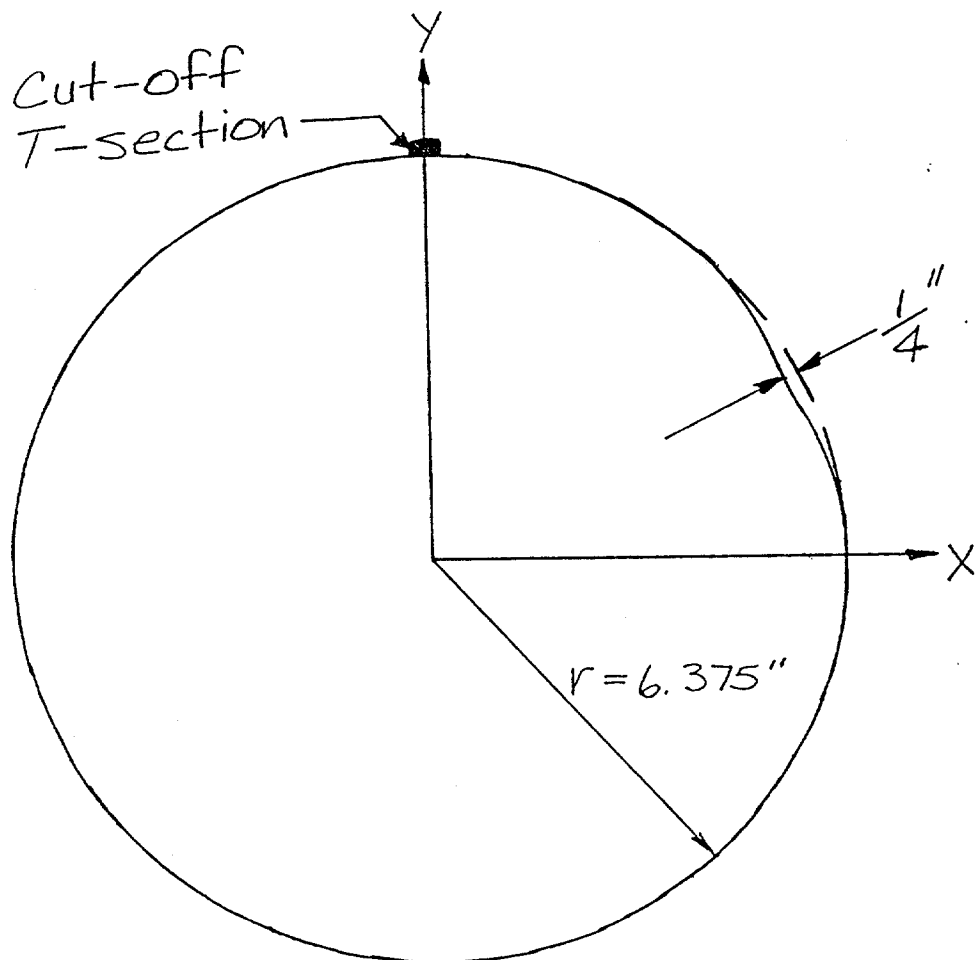
DENT CROSS SECTION

Specimen No. 16

Damage No. 9

Distance from End B 13'-10"

Scale 1"=3"



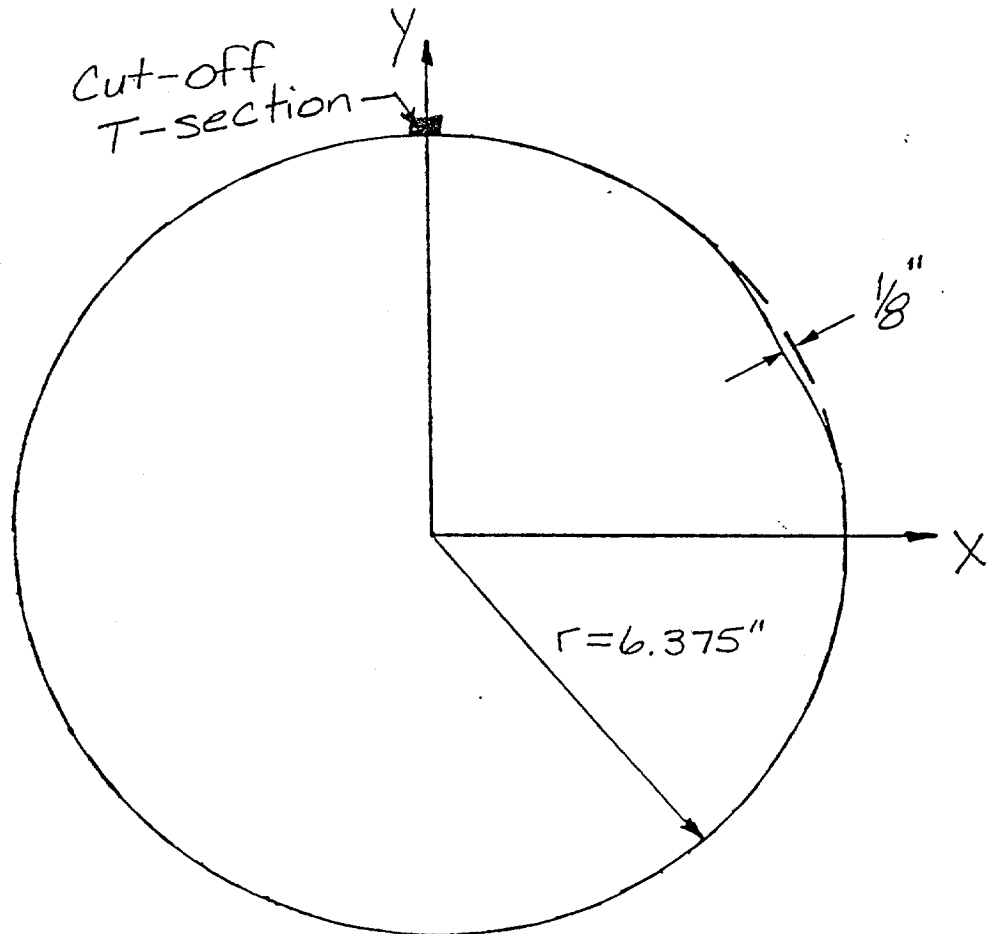
DENT CROSS SECTION

Specimen No. 16

Damage No. 9

Distance from End B 13'-11"

Scale 1"=3"



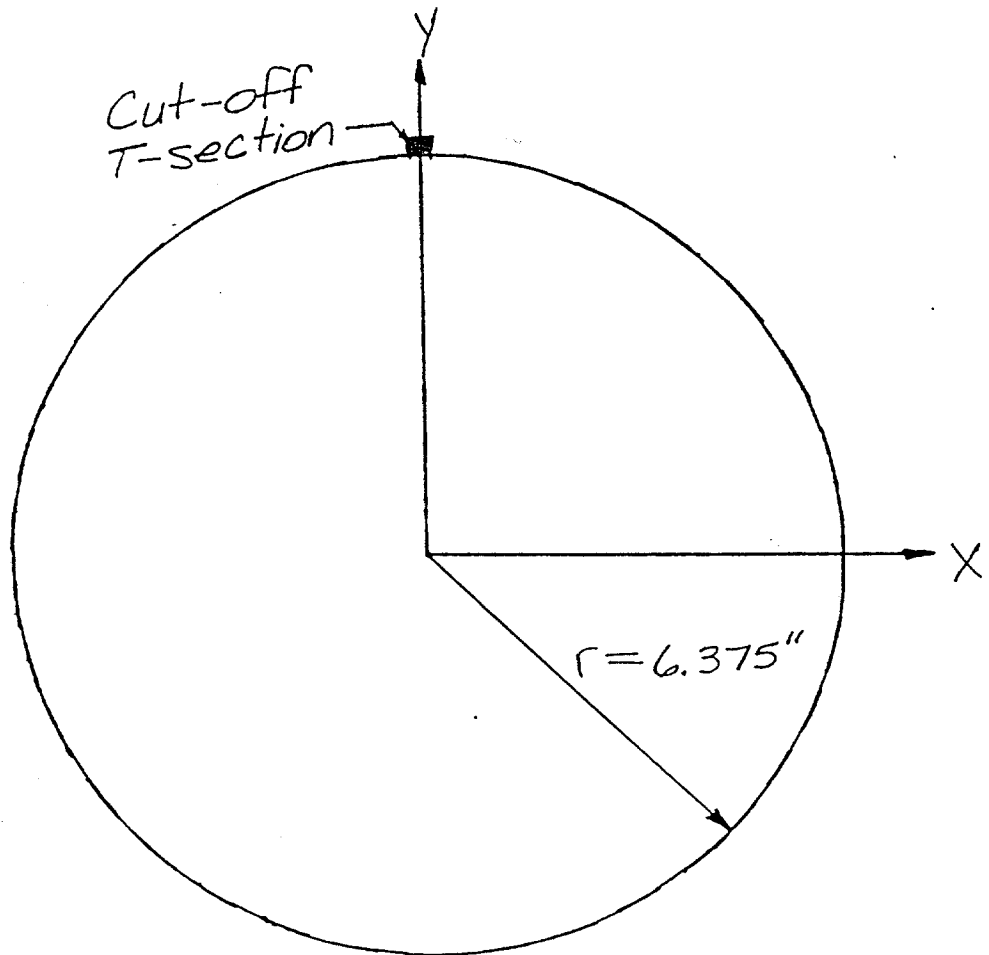
DENT CROSS SECTION

Specimen No. 16

Damage No. 9

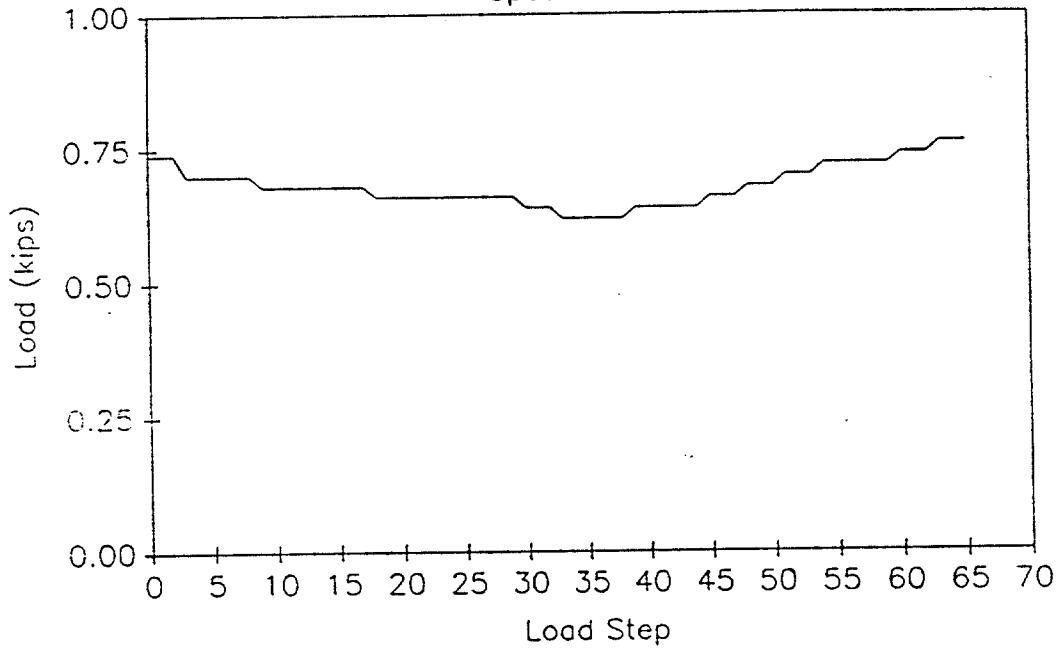
Distance from End B 14'-0"

Scale 1"=3"



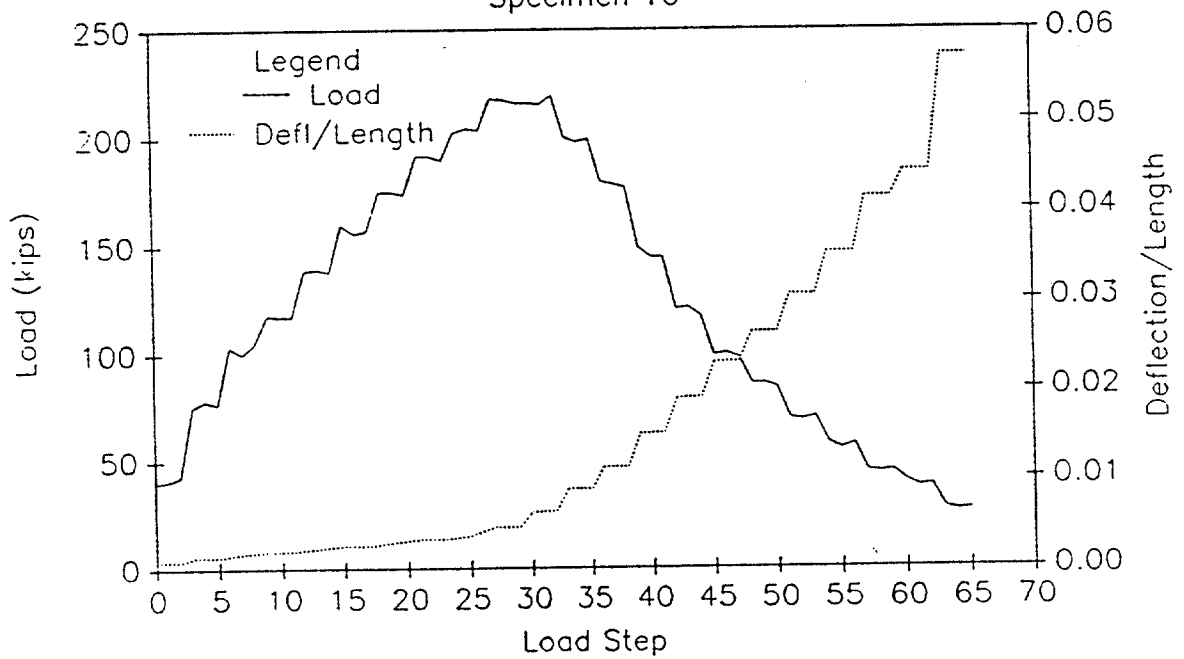
EFFECTIVE LENGTH vs LOAD STEP

Specimen 16

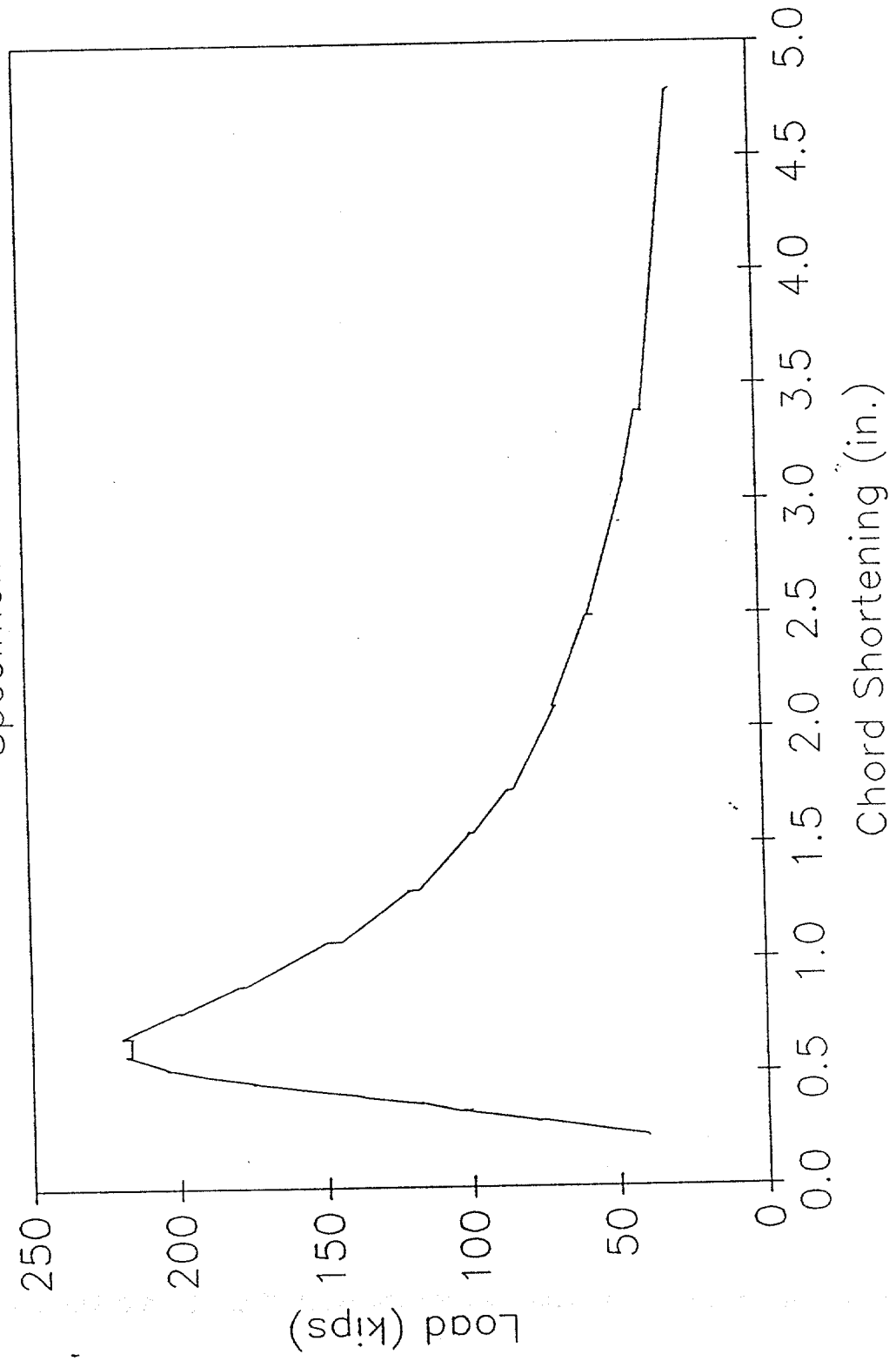


LOAD AND DEFLECTION vs LOAD STEP

Specimen 16

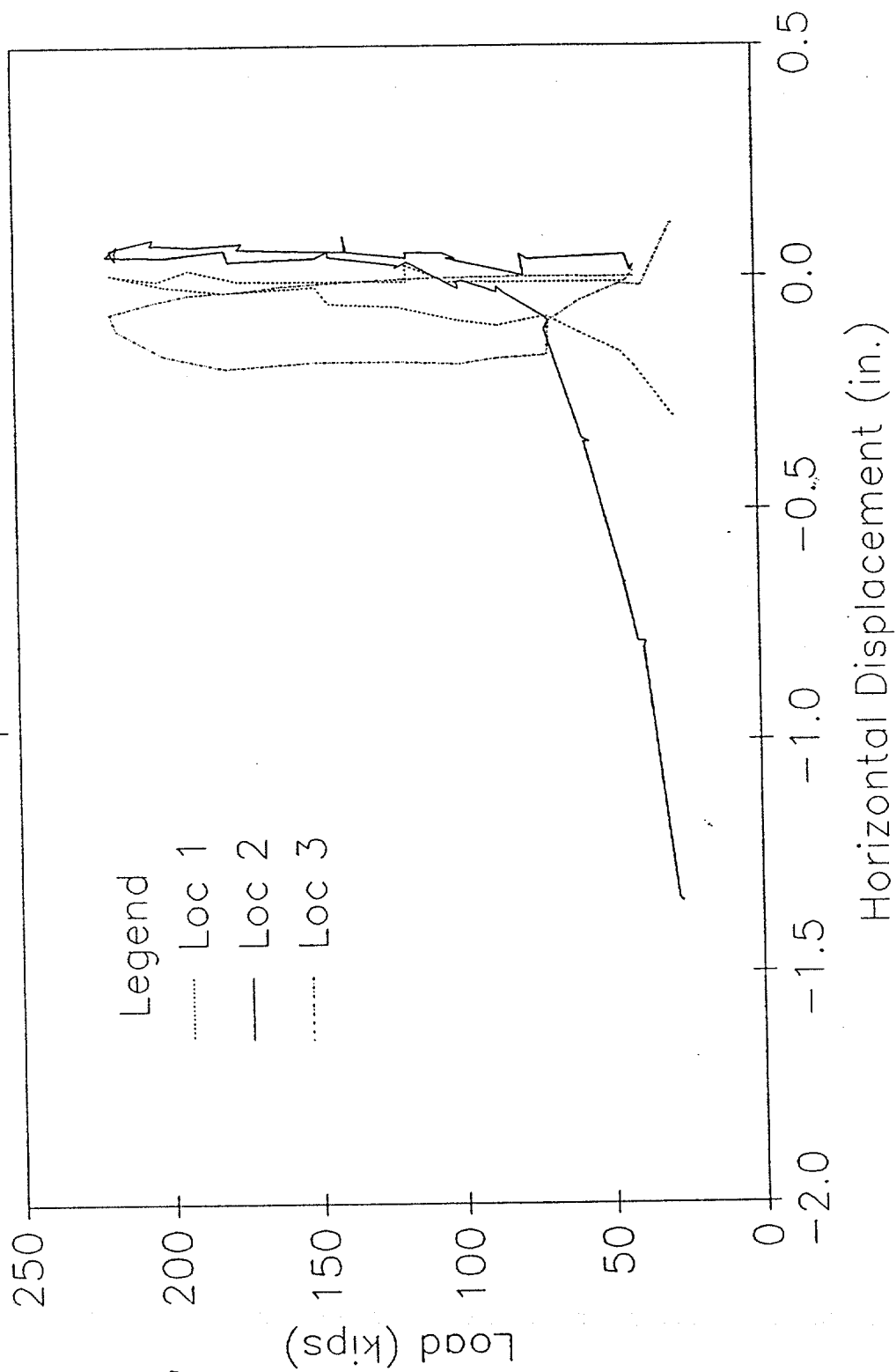


LOAD vs CHORD SHORTENING
Specimen 16



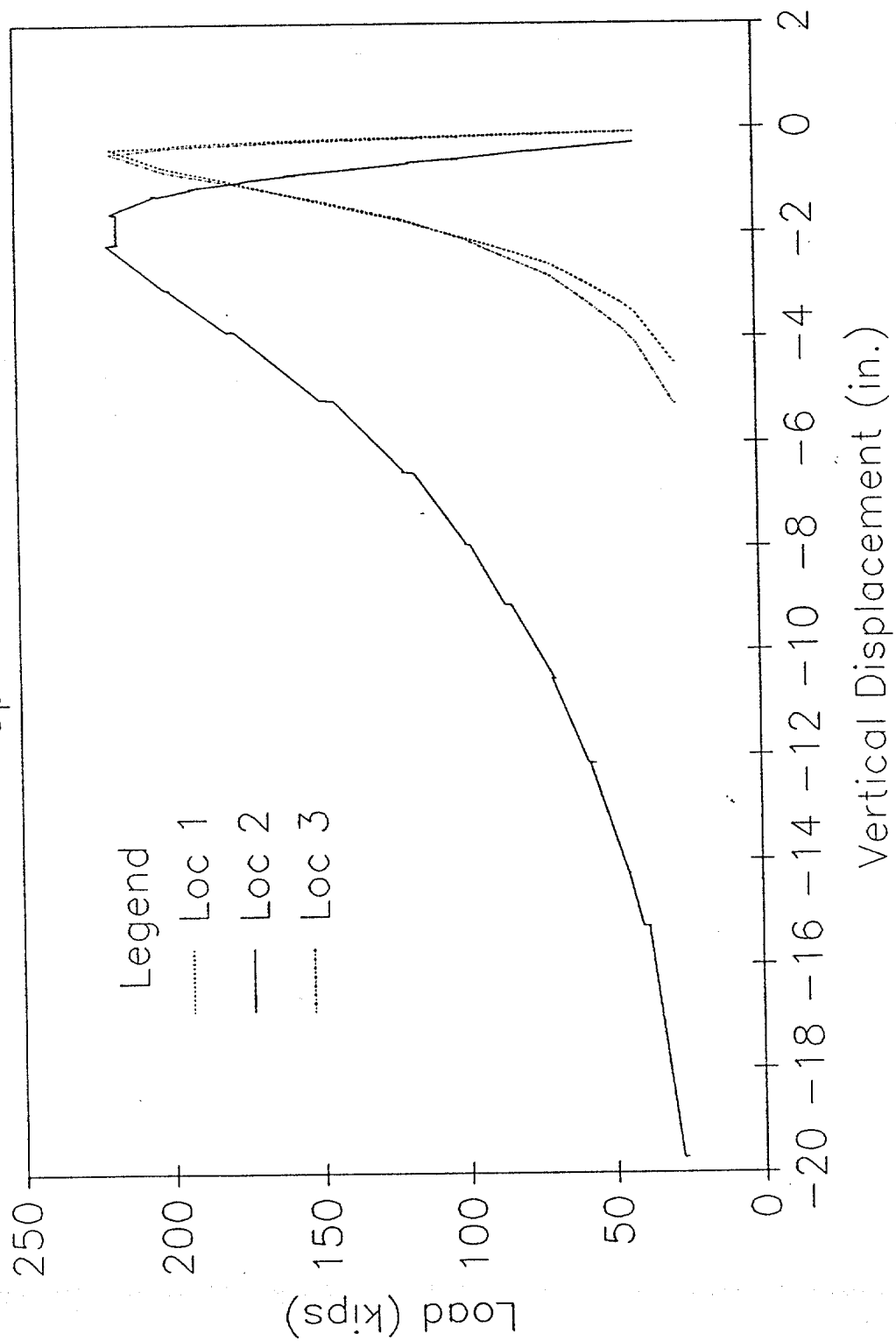
HORIZONTAL DISPLACEMENTS

Specimen 16



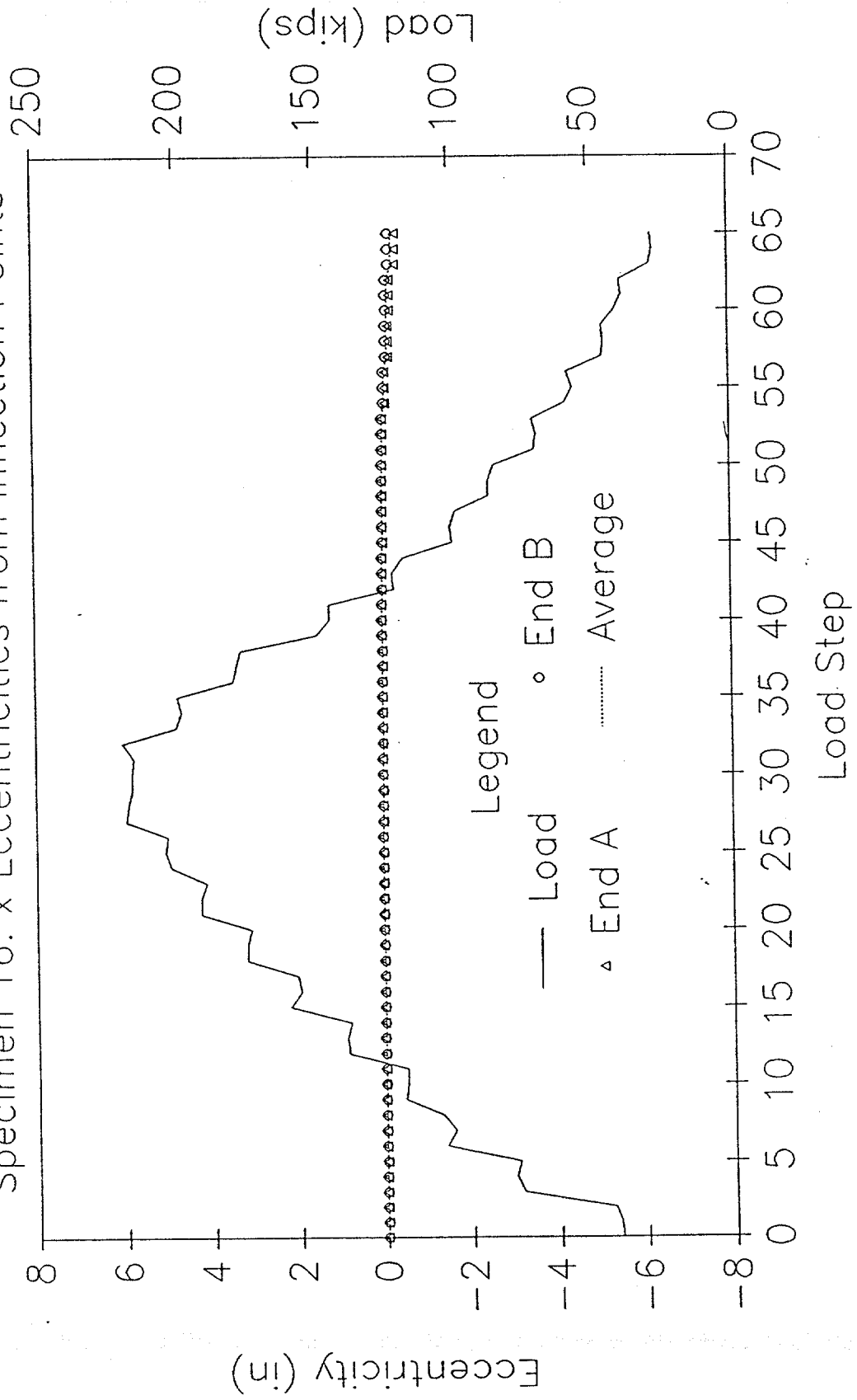
VERTICAL DISPLACEMENTS

Specimen 16



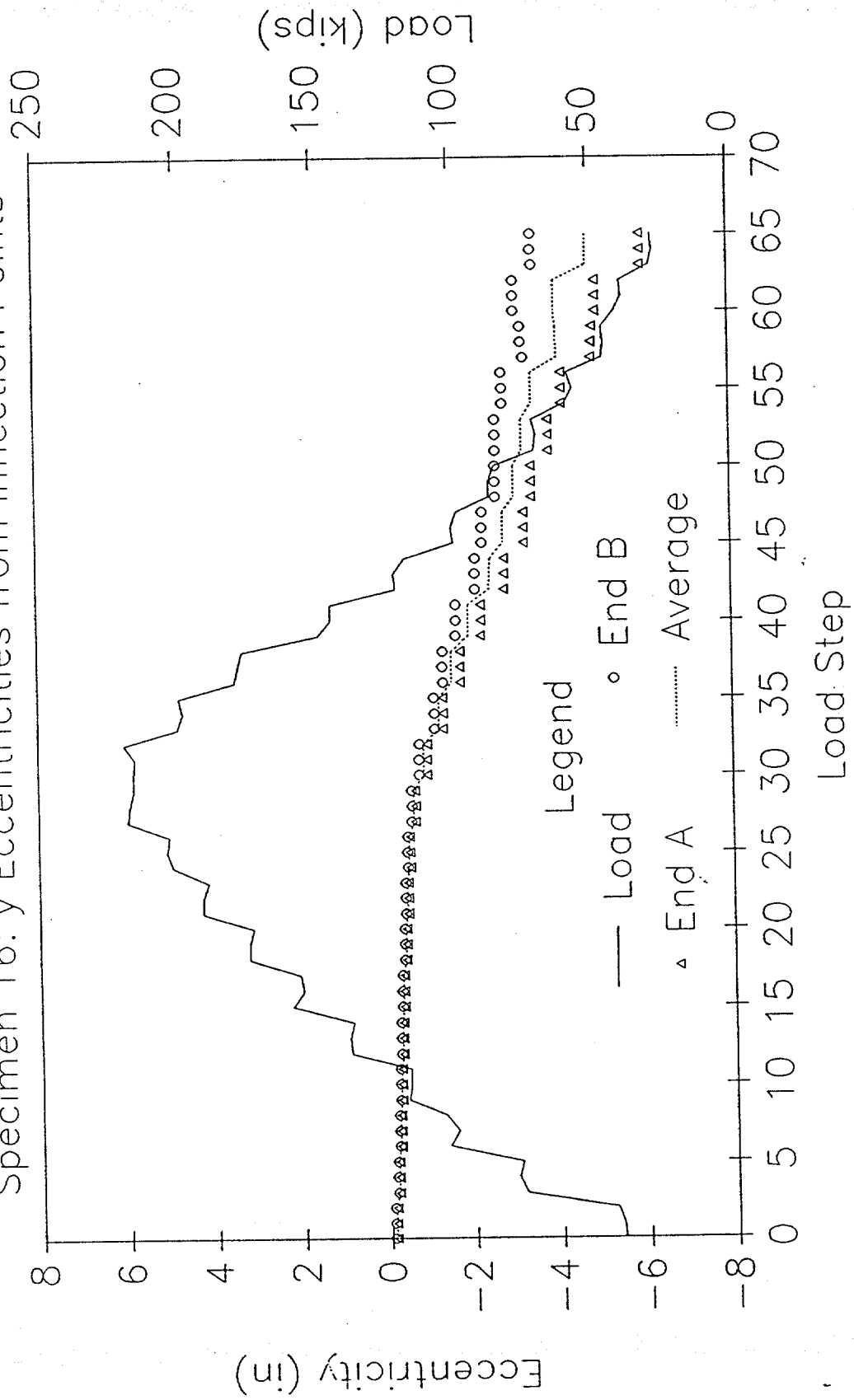
LOAD AND ECCENTRICITY vs LOAD STEP

Specimen 16: x Eccentricities from Inflection Points



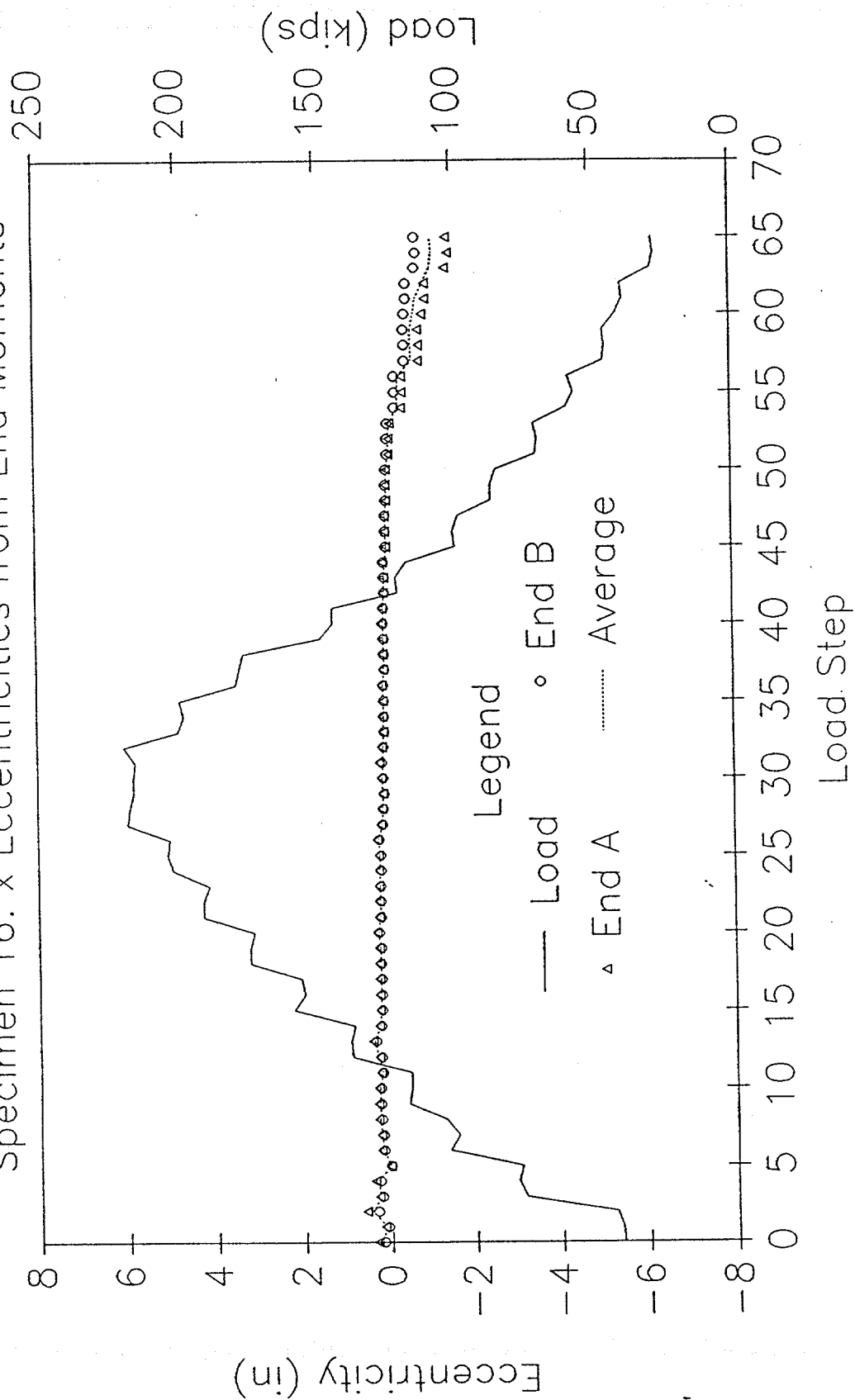
LOAD AND ECCENTRICITY vs LOAD STEP

Specimen 16: y Eccentricities from Inflection Points



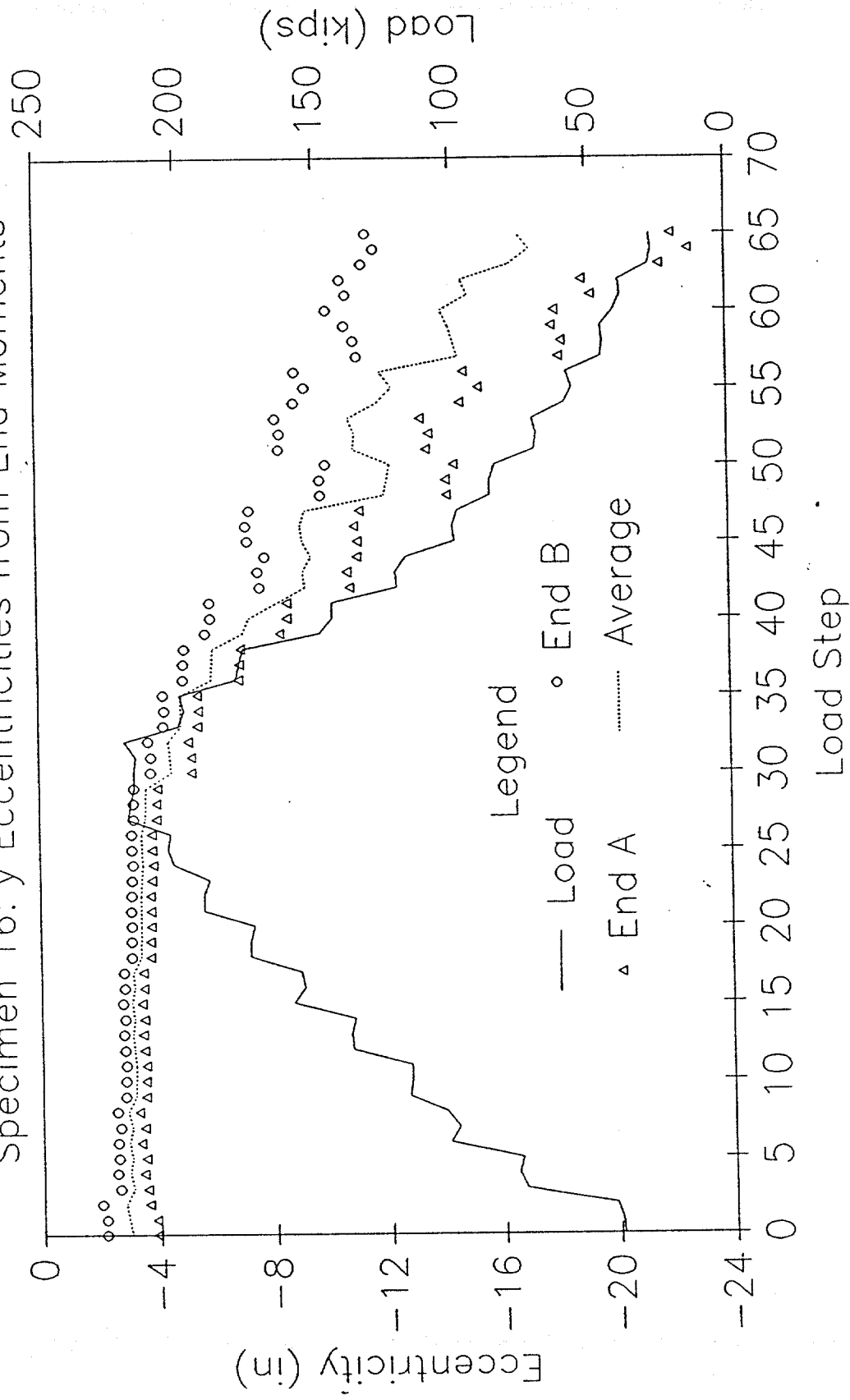
LOAD AND ECCENTRICITY vs LOAD STEP

Specimen 16: x Eccentricities from End Moments



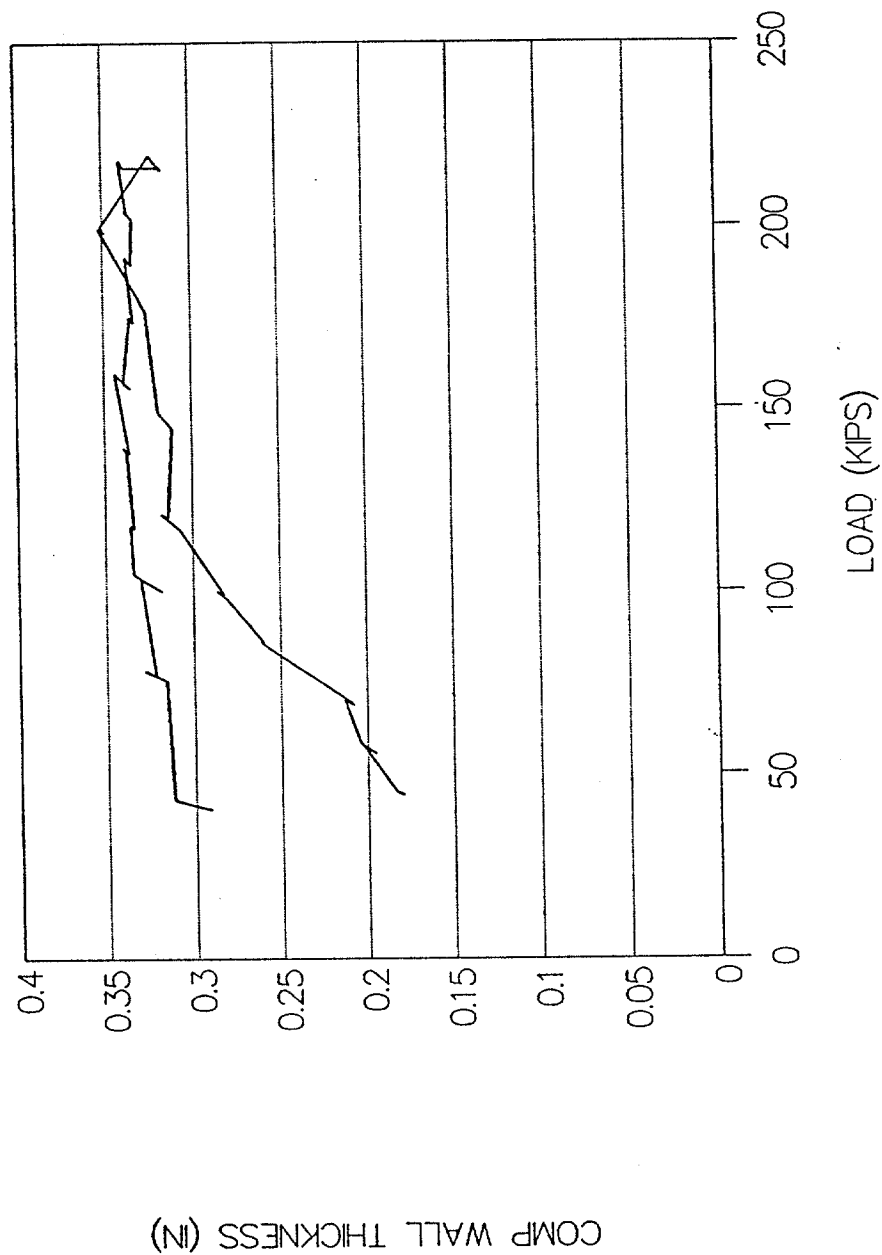
LOAD AND ECCENTRICITY vs LOAD STEP

Specimen 16: y Eccentricities from End Moments



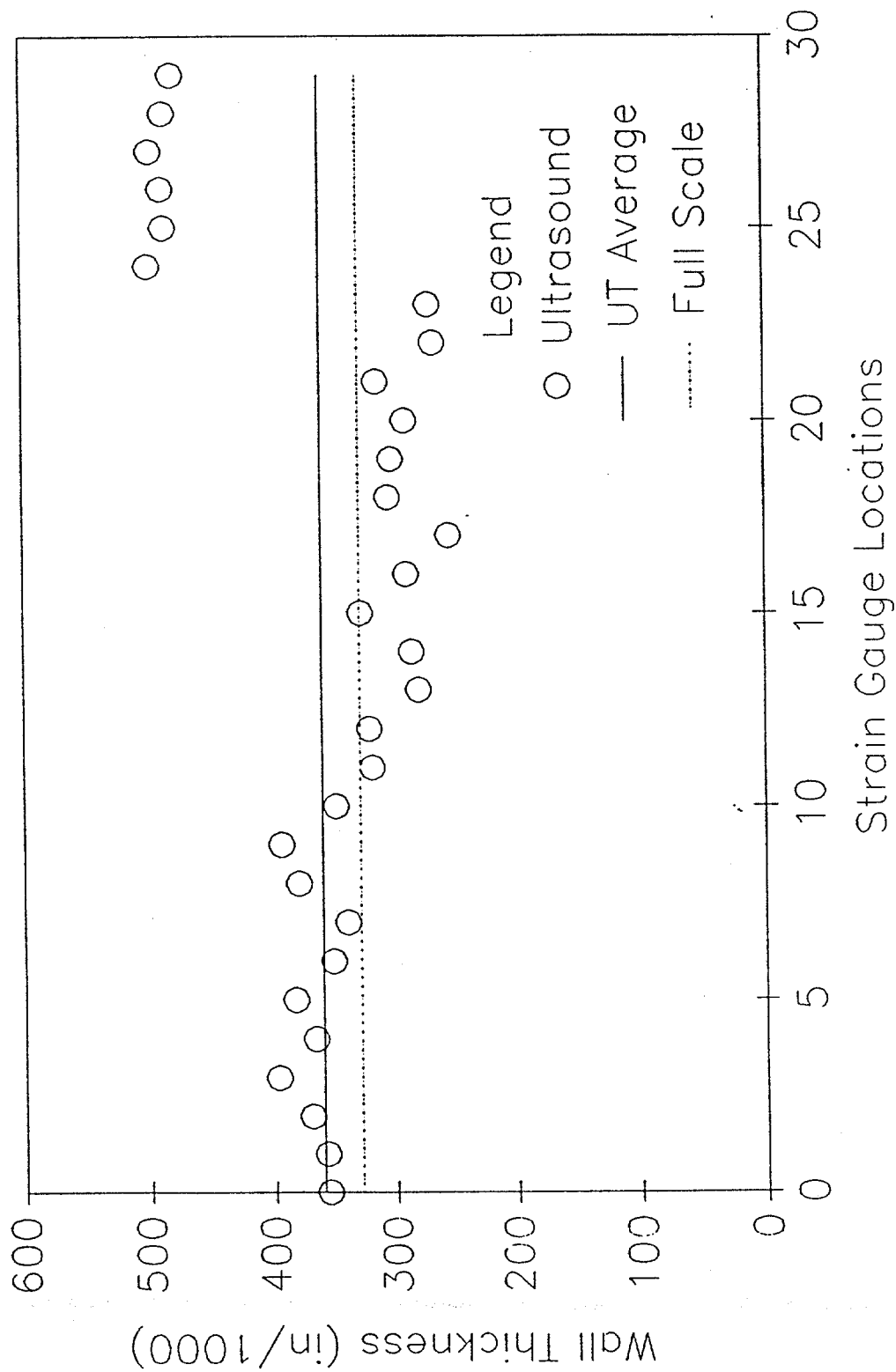
SPECIMEN 16-FULL SCALE TEST

COMPUTED WALL THICKNESS



SPECIMEN 16: Wall Thickness

Nominal Wall Thickness = 0.375 in

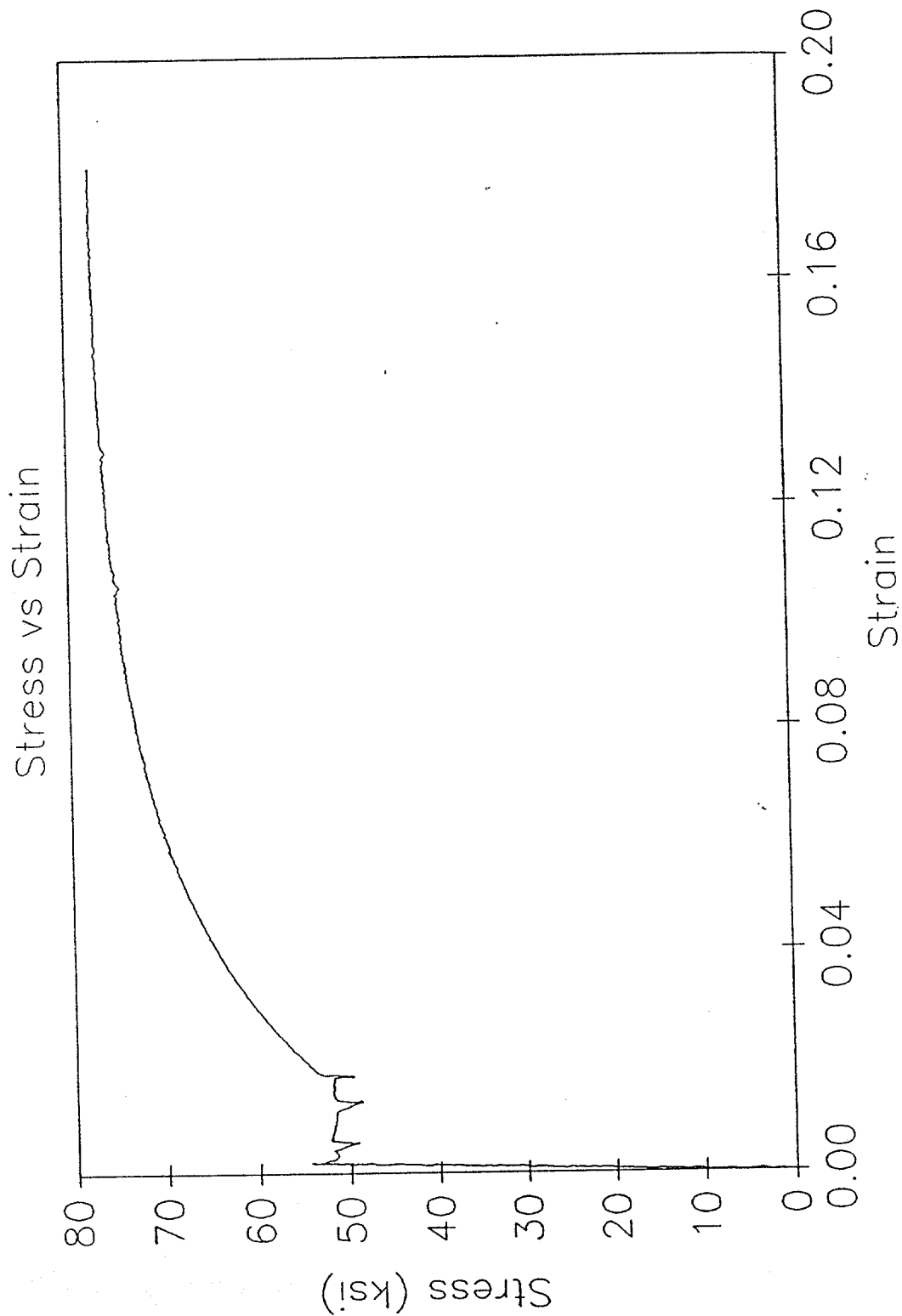


Ultrasound Data for Specimen 16
(All values in inches)

Gauge No.	UT Thickness	UT Average
0	0.356	
1	0.358	
2	0.370	
3	0.397	
4	0.367	
5	0.383	0.372
6	0.352	
7	0.340	
8	0.380	
9	0.394	
10	0.349	
11	0.319	0.356
12	0.321	
13	0.280	
14	0.286	
15	0.328	
16	0.290	
17	0.255	0.293
18	0.305	
19	0.302	
20	0.291	
21	0.314	
22	0.267	
23	0.271	0.292
24	0.499	
25	0.486	
26	0.488	
27	0.497	
28	0.486	
29	0.479	0.489

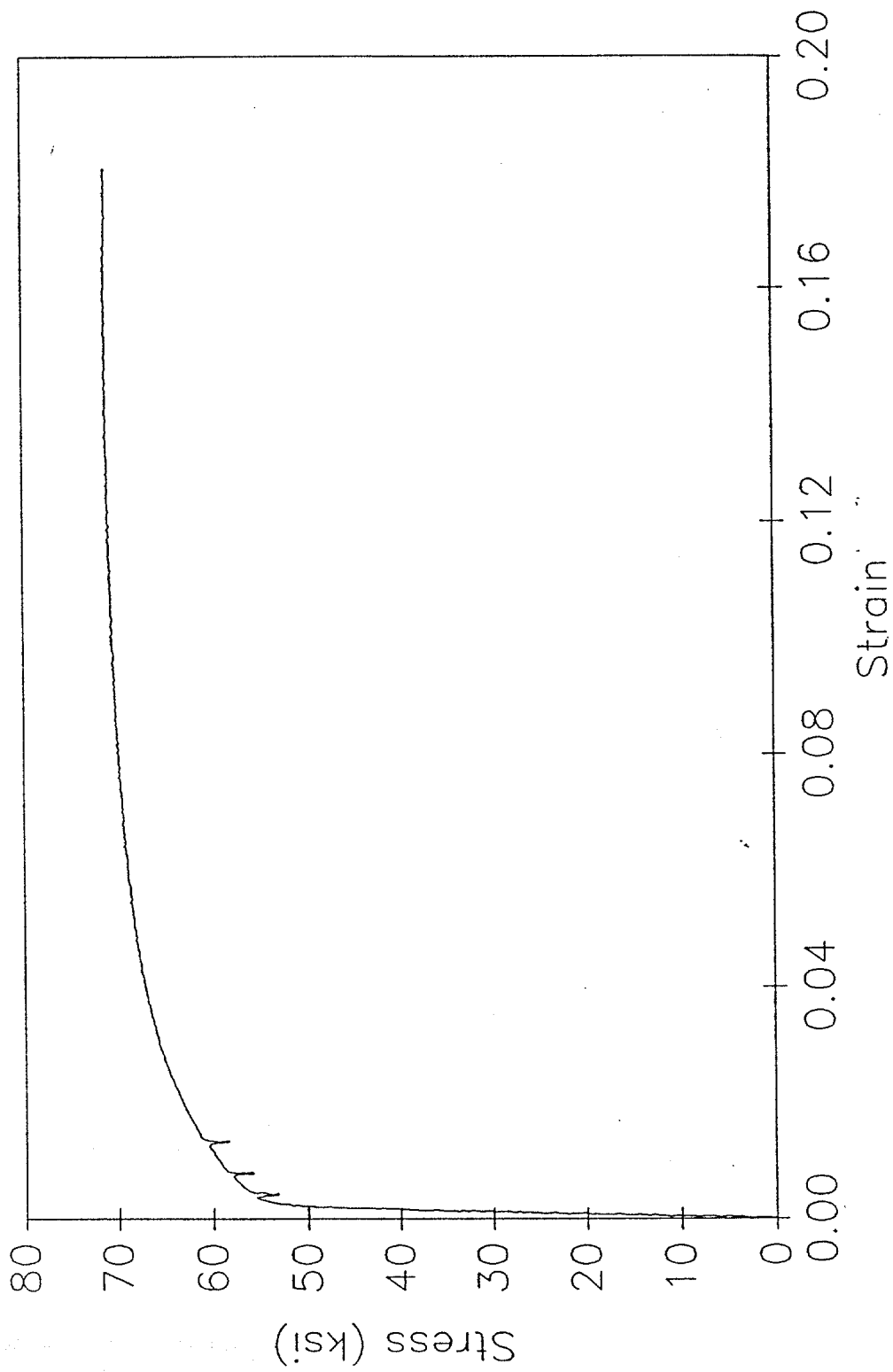
Overall Average = 0.360

TENSILE SPECIMEN 16-1



TENSILE SPECIMEN 16-2

Stress vs Strain



SPECIMEN 17

DAMAGE SUMMARY

Specimen No. 17

DISTANCE FROM END "B"	*DISTANCE FROM CHALK LINE		DESCRIPTION OF DAMAGE
	LEFT	RIGHT	
1. 4'-8 3/4"			3/4" circumferential butt weld
2. 19'-1"		2" (center)	8" diameter dent (Round) (See additional pages for cross sections)

The specimen is curved. See additional page for initial out-of-straightness information.

*Looking from end "A" towards end "B"

Out-of-Straightness Measurements for Specimen 17

The specimen was initially curved in the yz-plane and straight in the xz-plane. The following measurements are in the y-direction.

	Distance from End B (ft)	Distance from stringline to top of pipe (in)	Out-of- straightness in y direction (in)
	0	3.875	0
	1	4	-0.125
	2	4.25	-0.375
	3	4.5	-0.625
	4	4.75	-0.875
	5	5	-1.125
	6	5.1875	-1.3125
	7	5.375	-1.5
	8	5.5	-1.625
	9	5.6875	-1.8125
	10	5.875	-2
	11	6.0625	-2.1875
	12	6.25	-2.375
	13	6.4375	-2.5625
	14	6.625	-2.75
	15	6.75	-2.875
	16	6.9375	-3.0625
	17	7.125	-3.25
	18	7.375	-3.5
Begin dent	18.583	7.625	-3.75
	19	8.5	-4.625
Dent center	19.083	8.625	-4.75
End dent	19.5	7.625	-3.75
	20	7.375	-3.5
	21	6.875	-3
	22	6.5	-2.625
	23	6.25	-2.375
	24	5.9375	-2.0625
	25	5.625	-1.75
	26	5.3125	-1.4375
	27	4.9375	-1.0625
	28	4.625	-0.75
	29	4.375	-0.5
	30	4	-0.125
	31	3.875	0
	31.167	3.875	0

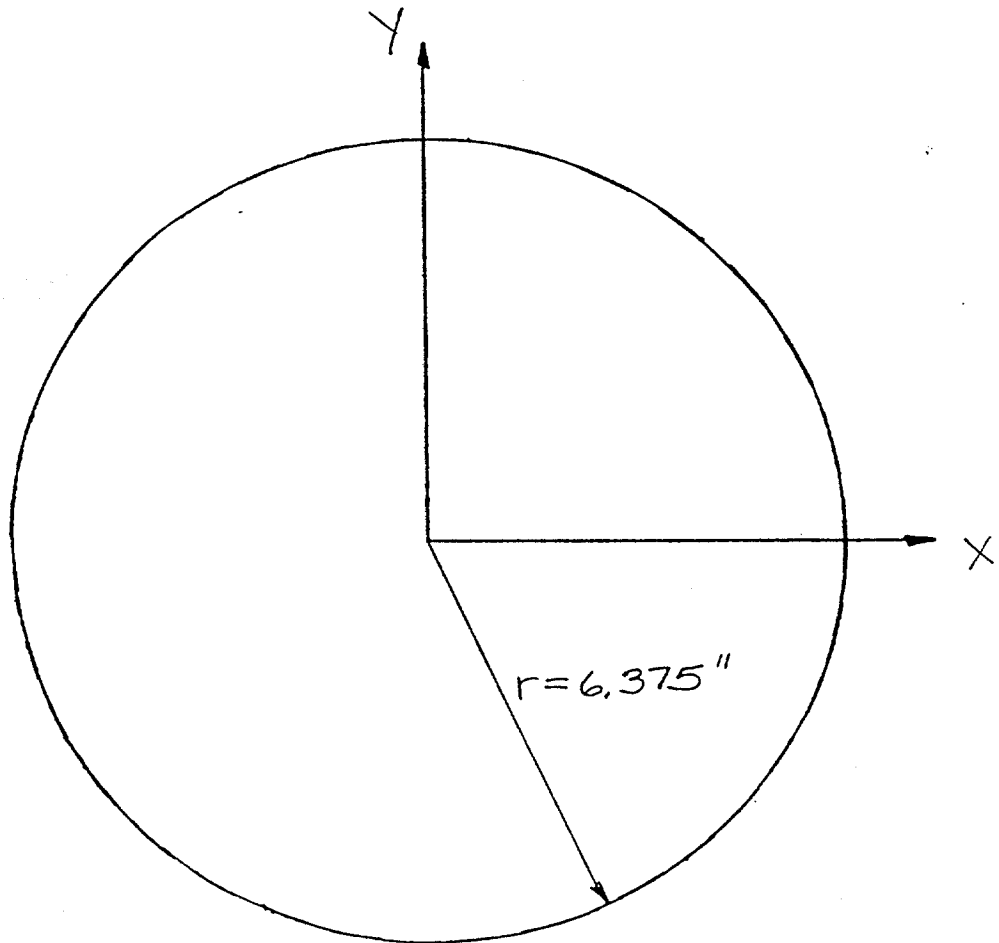
DENT CROSS SECTION

Specimen No. 17

Damage No. 2

Distance from End B 18'-9"

Scale 1" = 3"



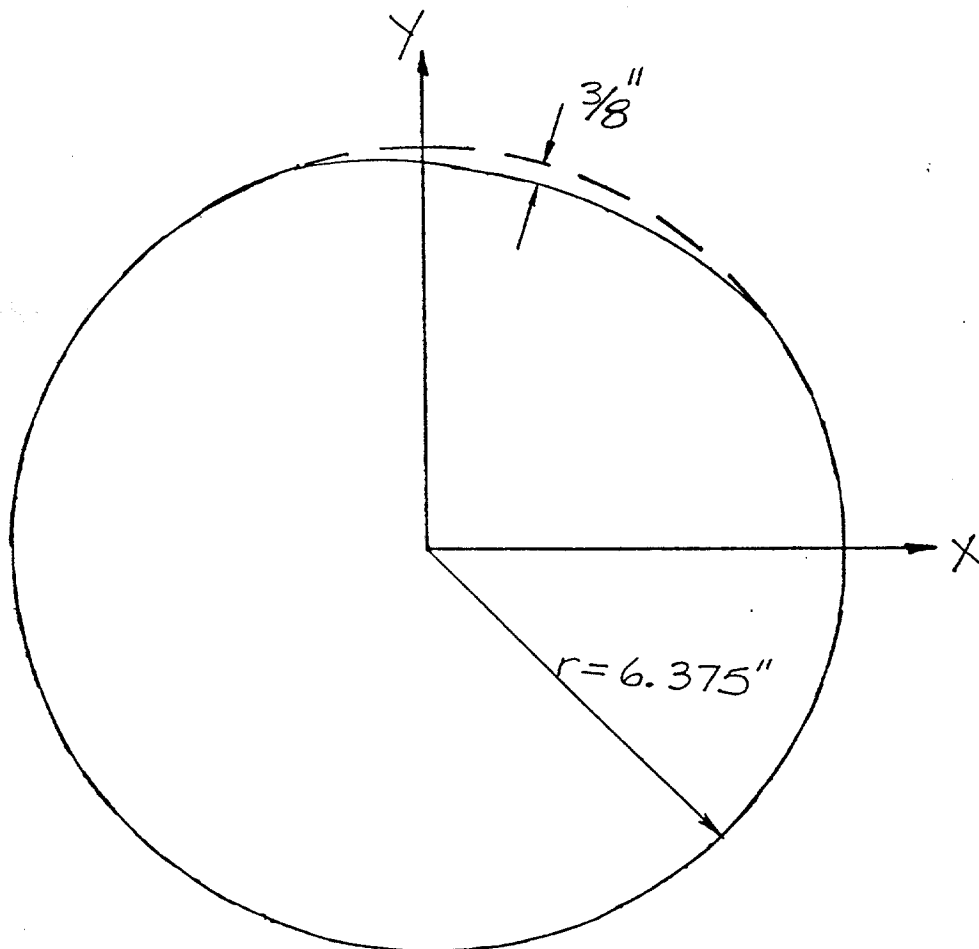
DENT CROSS SECTION

Specimen No. 17

Damage No. 2

Distance from End B 18'-10"

Scale 1" = 3"



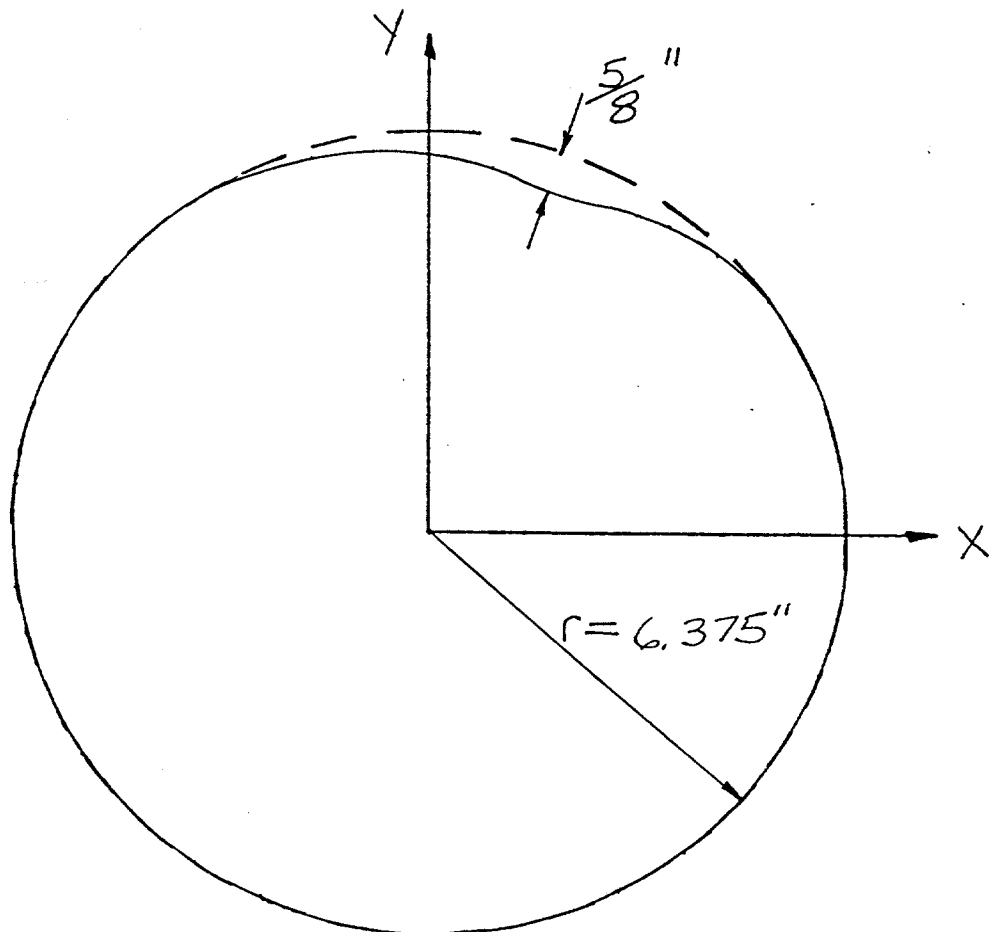
DENT CROSS SECTION

Specimen No. 17

Damage No. 2

Distance from End B 18'-11"

Scale 1" = 3"



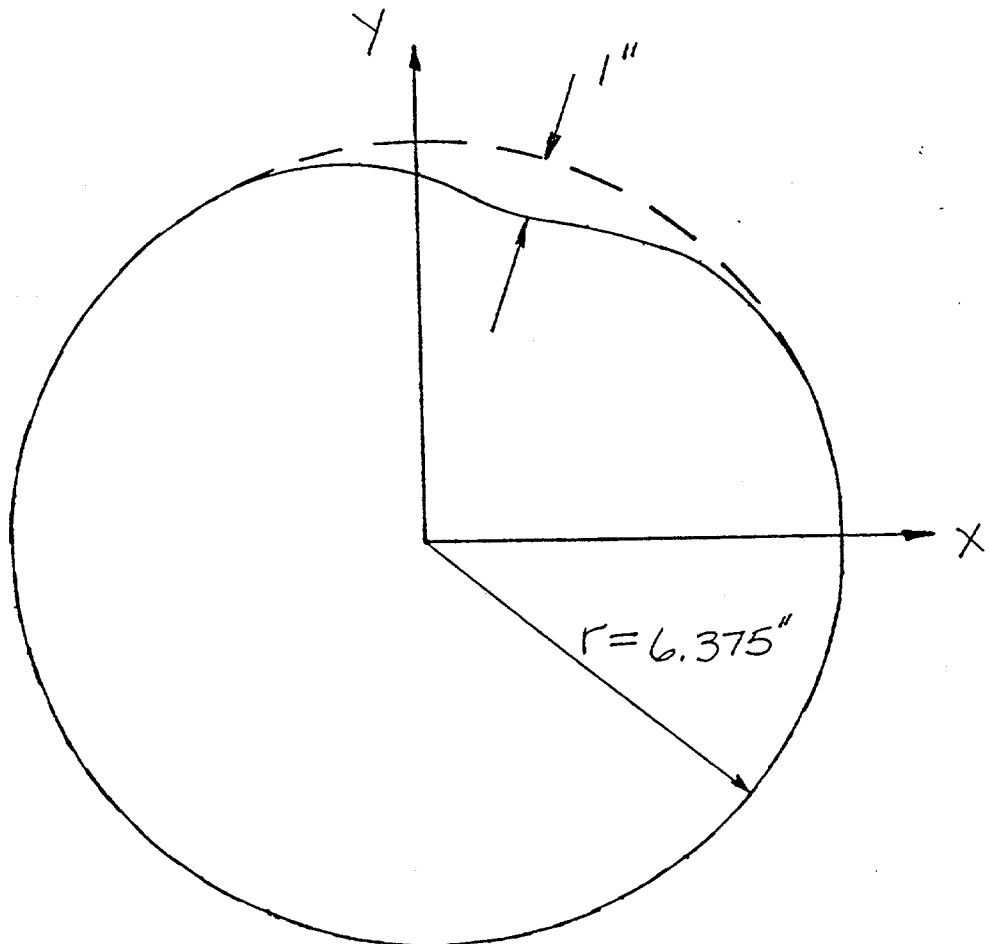
DENT CROSS SECTION

Specimen No. 17

Damage No. 2

Distance from End B 19'-0"

Scale 1"=3"



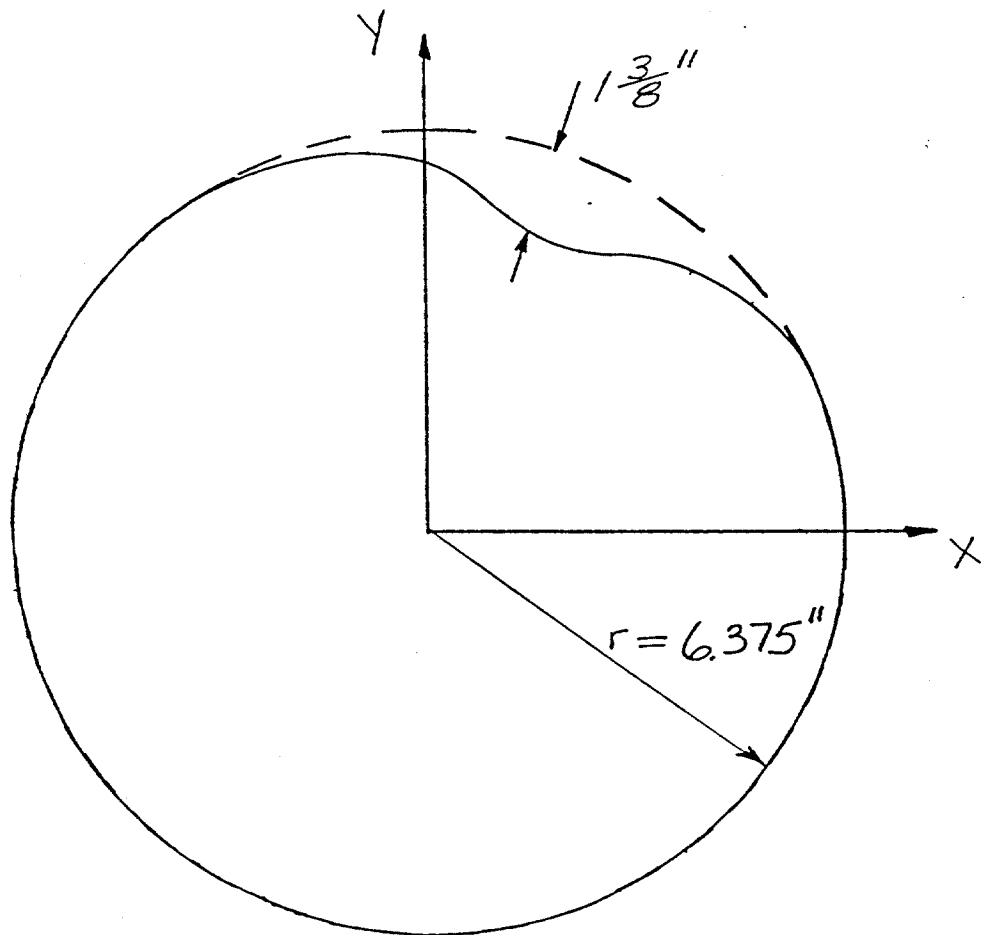
DENT CROSS SECTION

Specimen No. 17

Damage No. 2

Distance from End B 19'-1"

Scale 1" = 3"



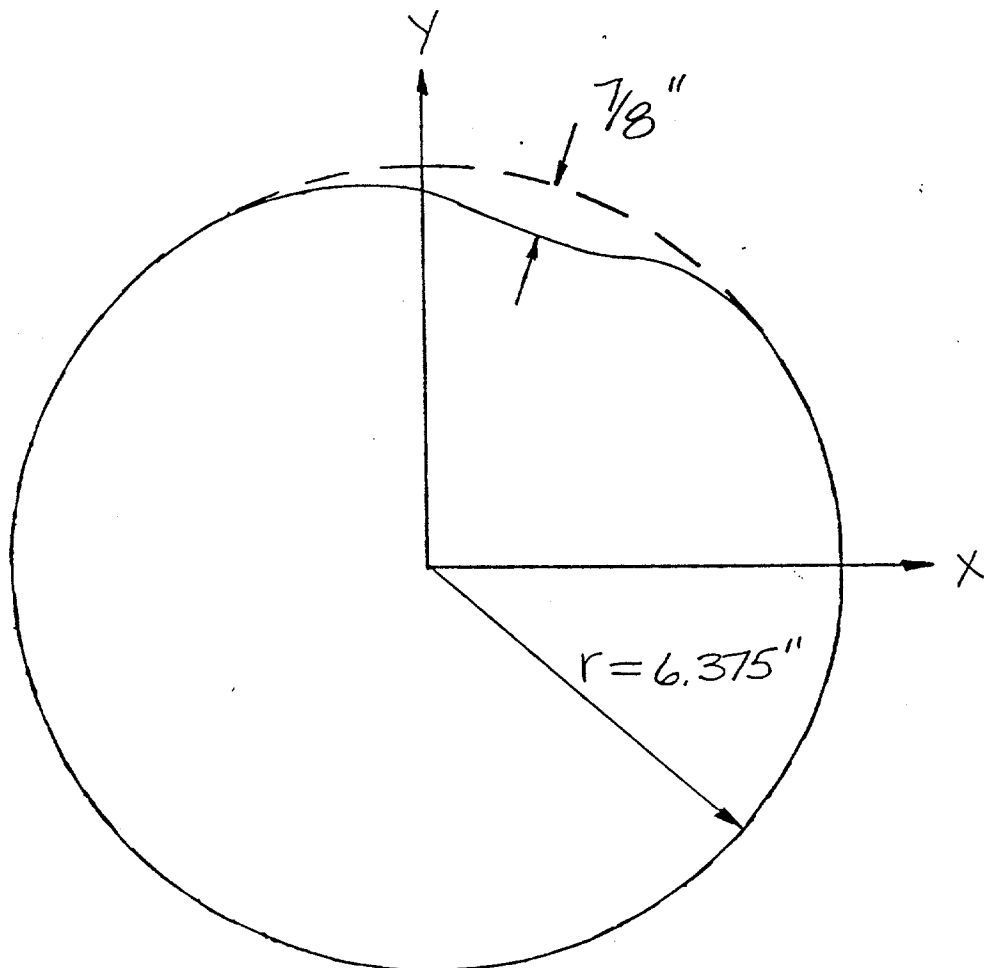
DENT CROSS SECTION

Specimen No. 17

Damage No. 2

Distance from End B 19'-2"

Scale 1" = 3"



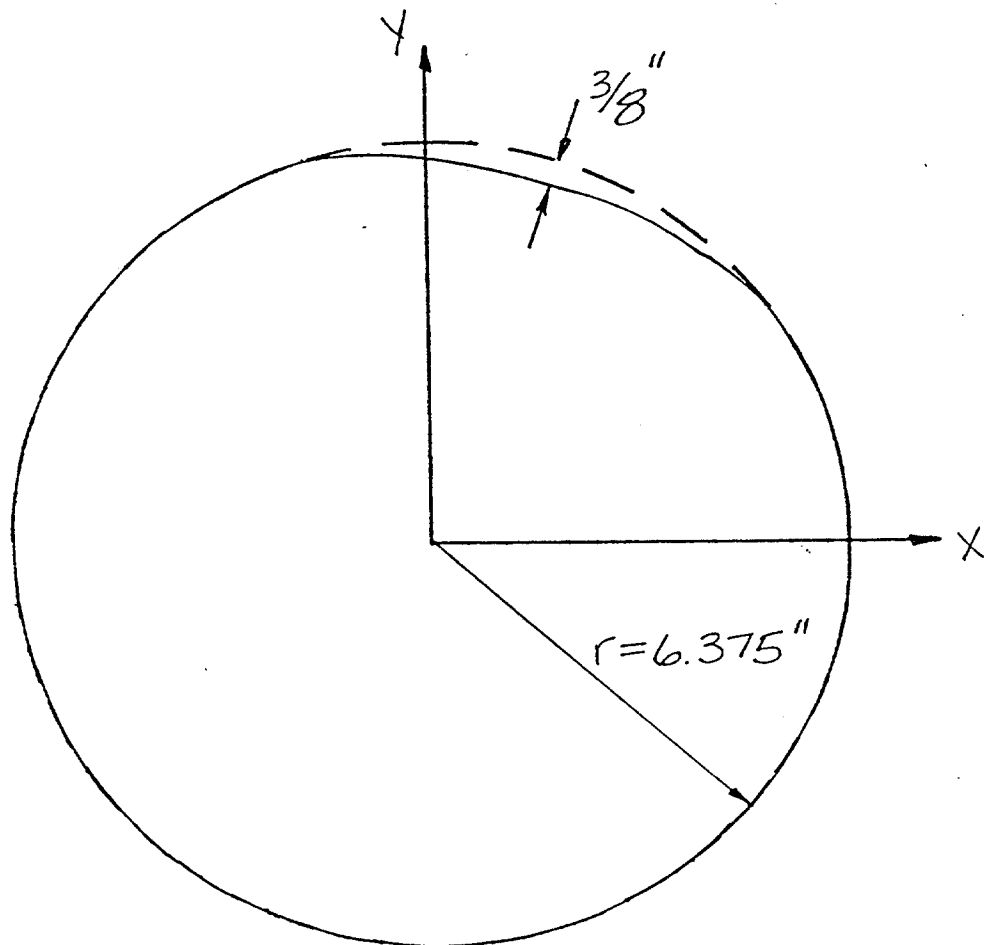
DENT CROSS SECTION

Specimen No. 17

Damage No. 2

Distance from End B 19'-3"

Scale 1"=3'



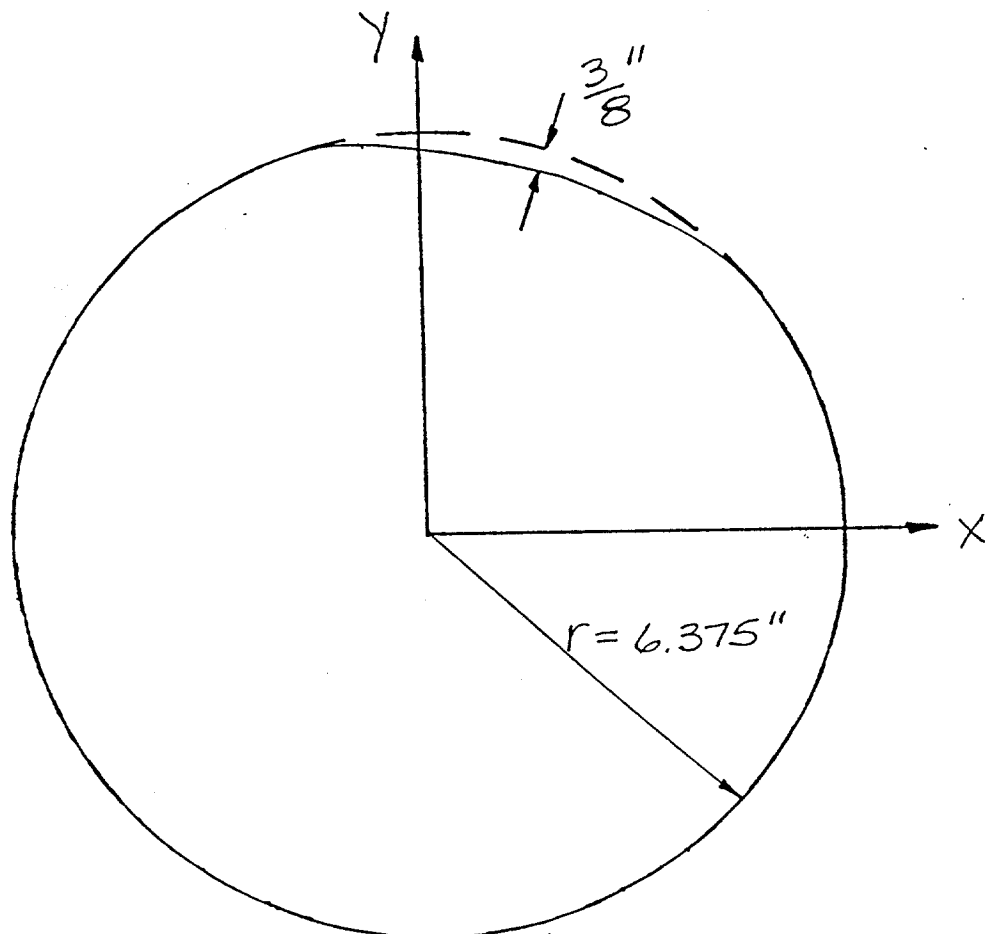
DENT CROSS SECTION

Specimen No. 17

Damage No. 2

Distance from End B 19'-4"

Scale 1"=3'



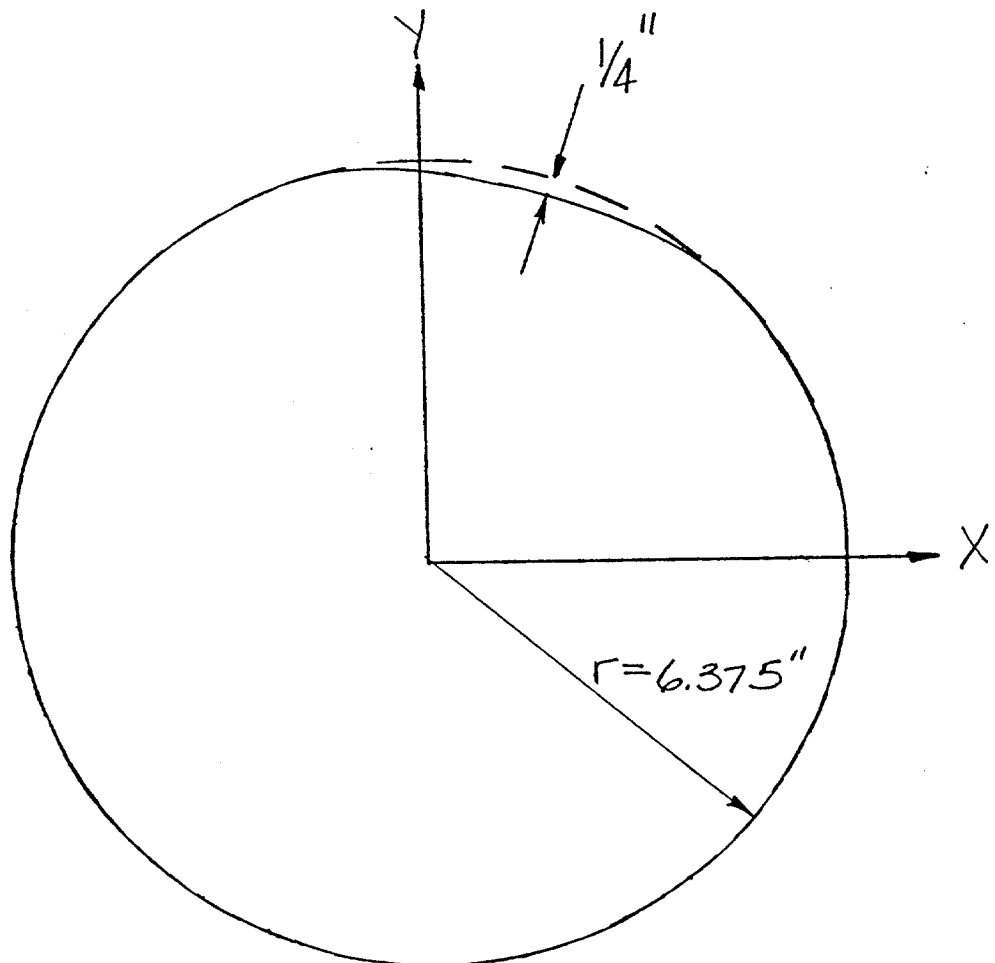
DENT CROSS SECTION

Specimen No. 17

Damage No. 2

Distance from End B 19'-5"

Scale 1"=3"



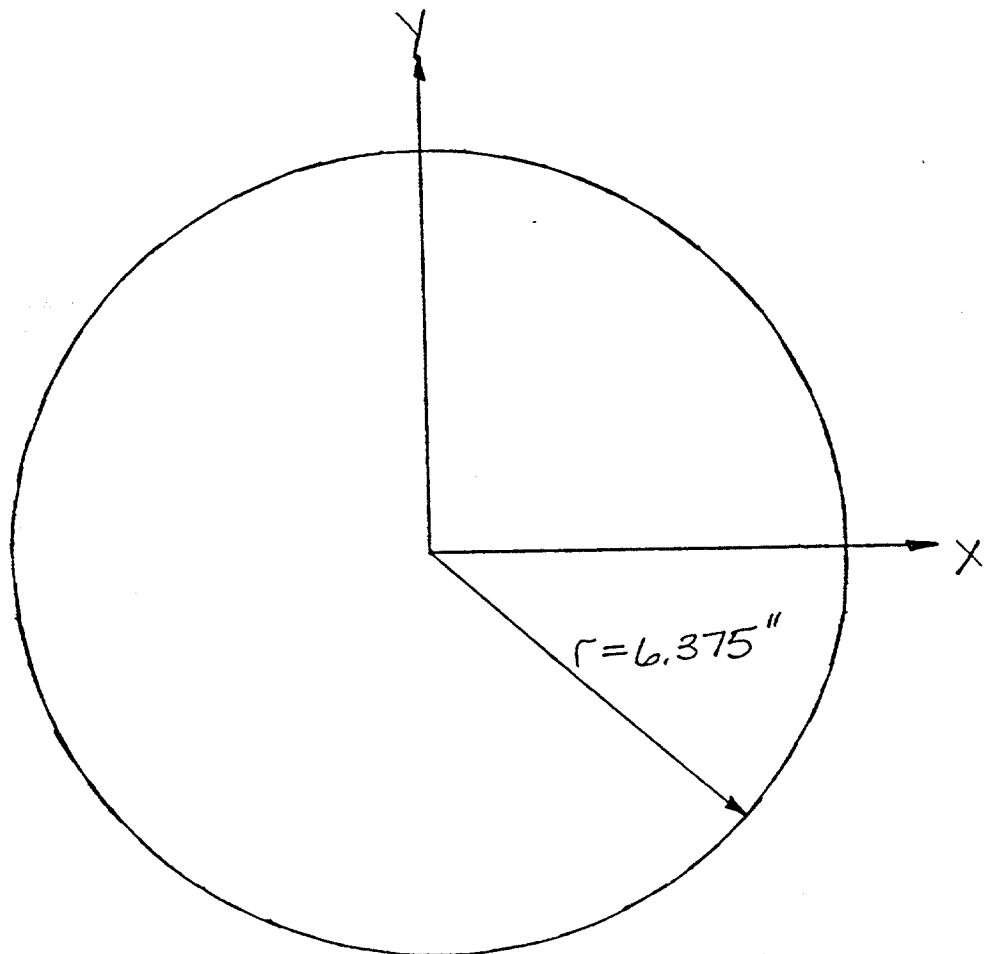
DENT CROSS SECTION

Specimen No. 17

Damage No. 2

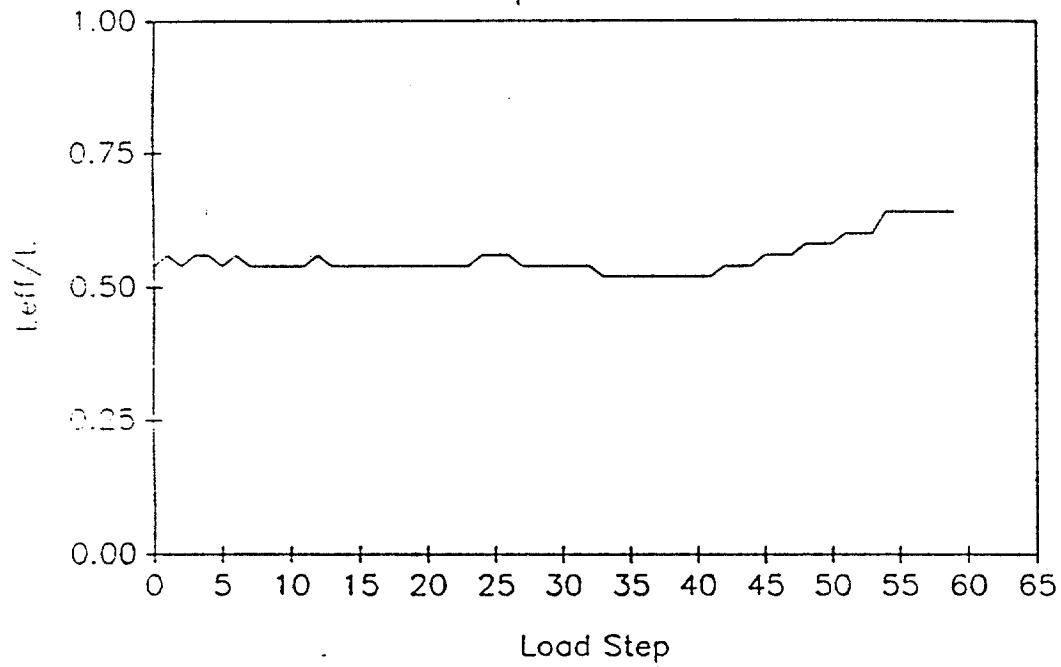
Distance from End B 19'-6"

Scale 1" = 3"



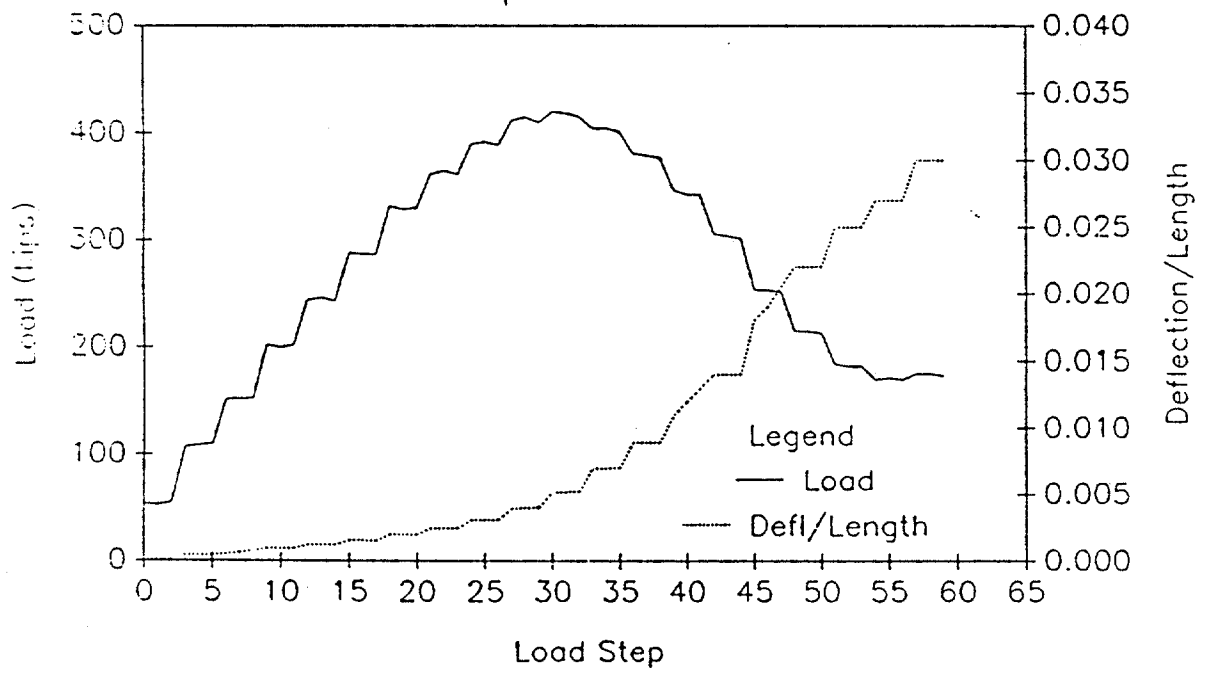
EFFECTIVE LENGTH vs LOAD STEP

Specimen 17



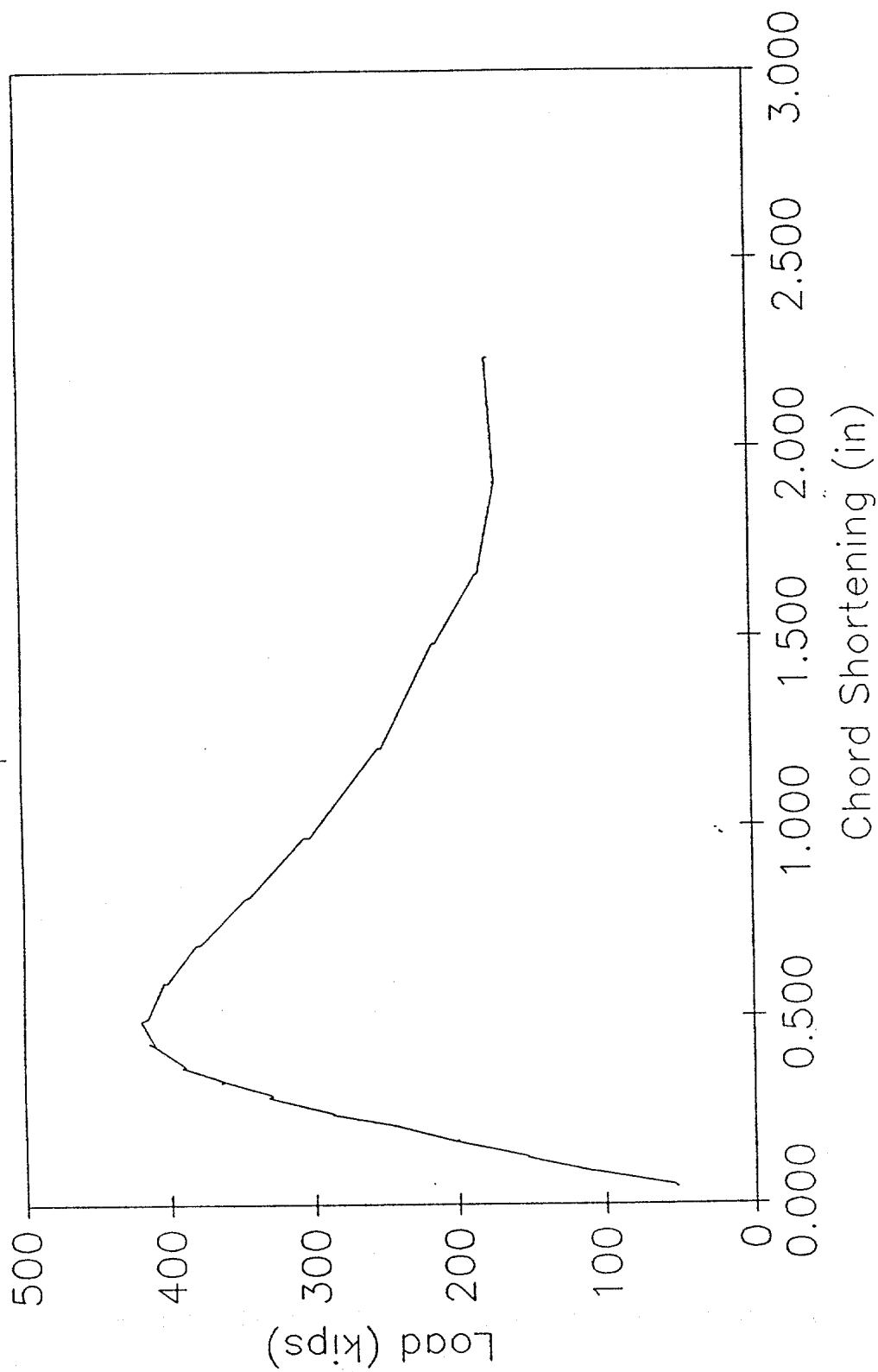
LOAD AND DEFLECTION vs LOAD STEP

Specimen 17



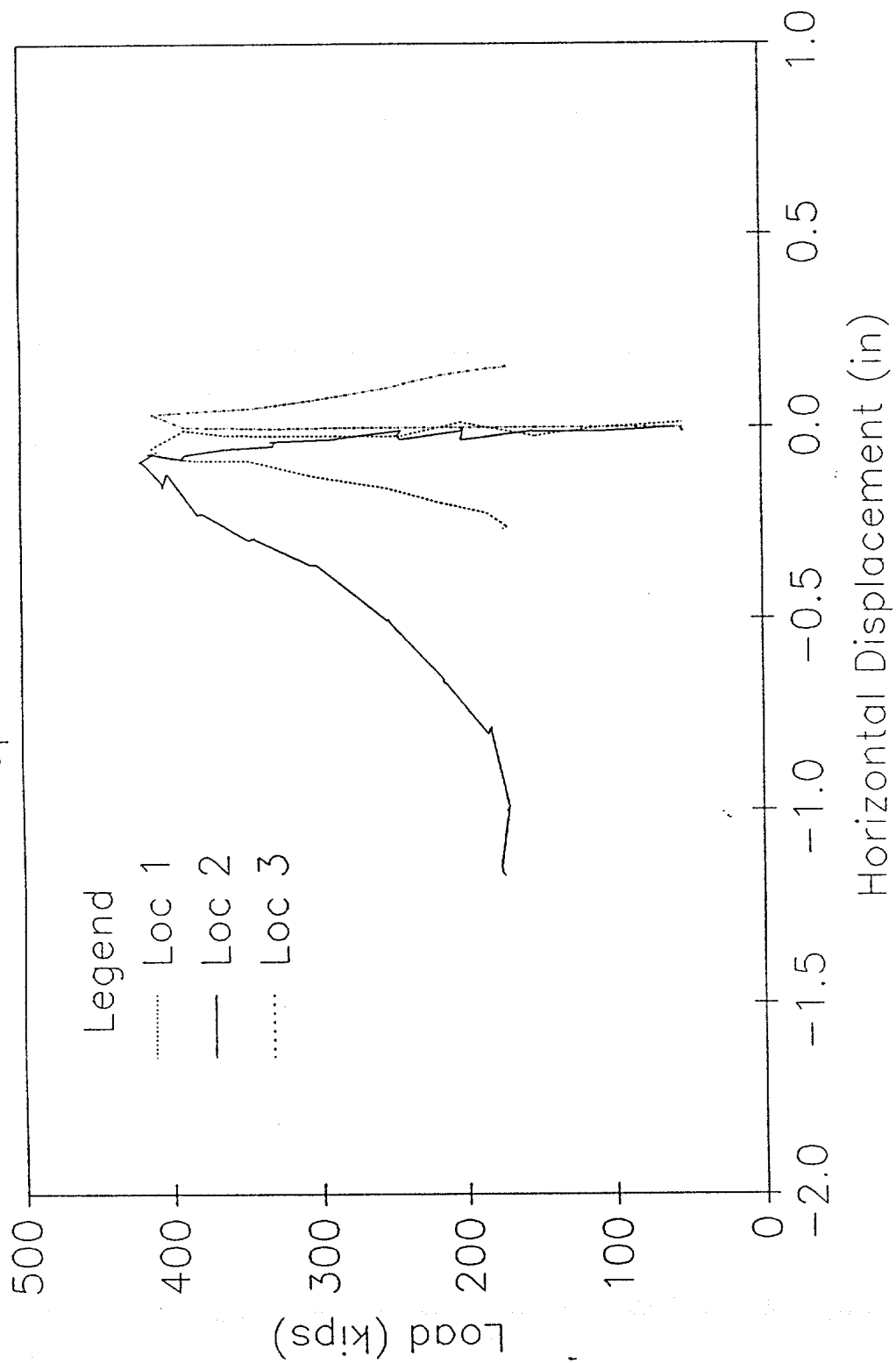
LOAD vs CHORD SHORTENING

Specimen 17



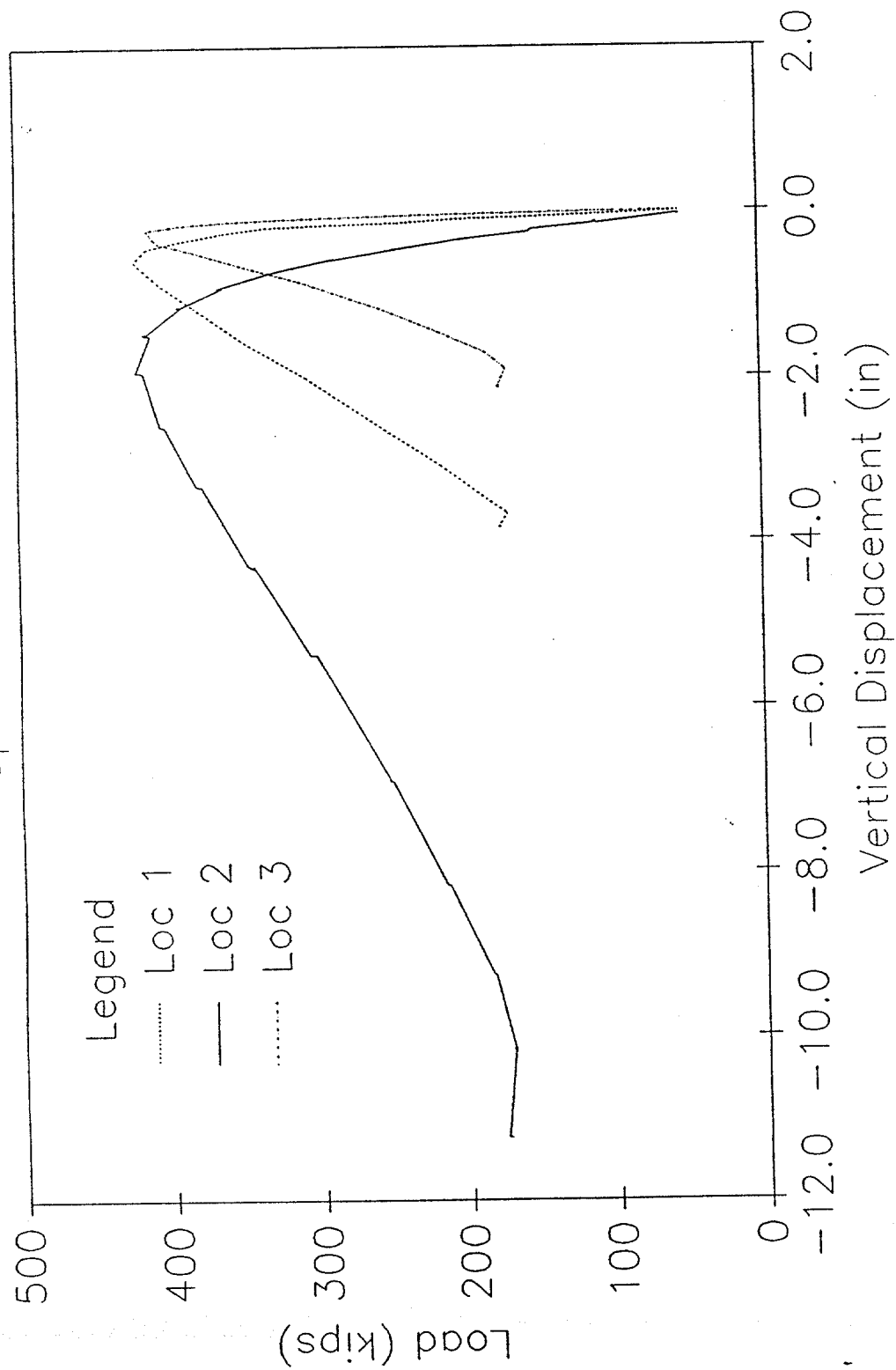
HORIZONTAL DISPLACEMENTS

Specimen 17



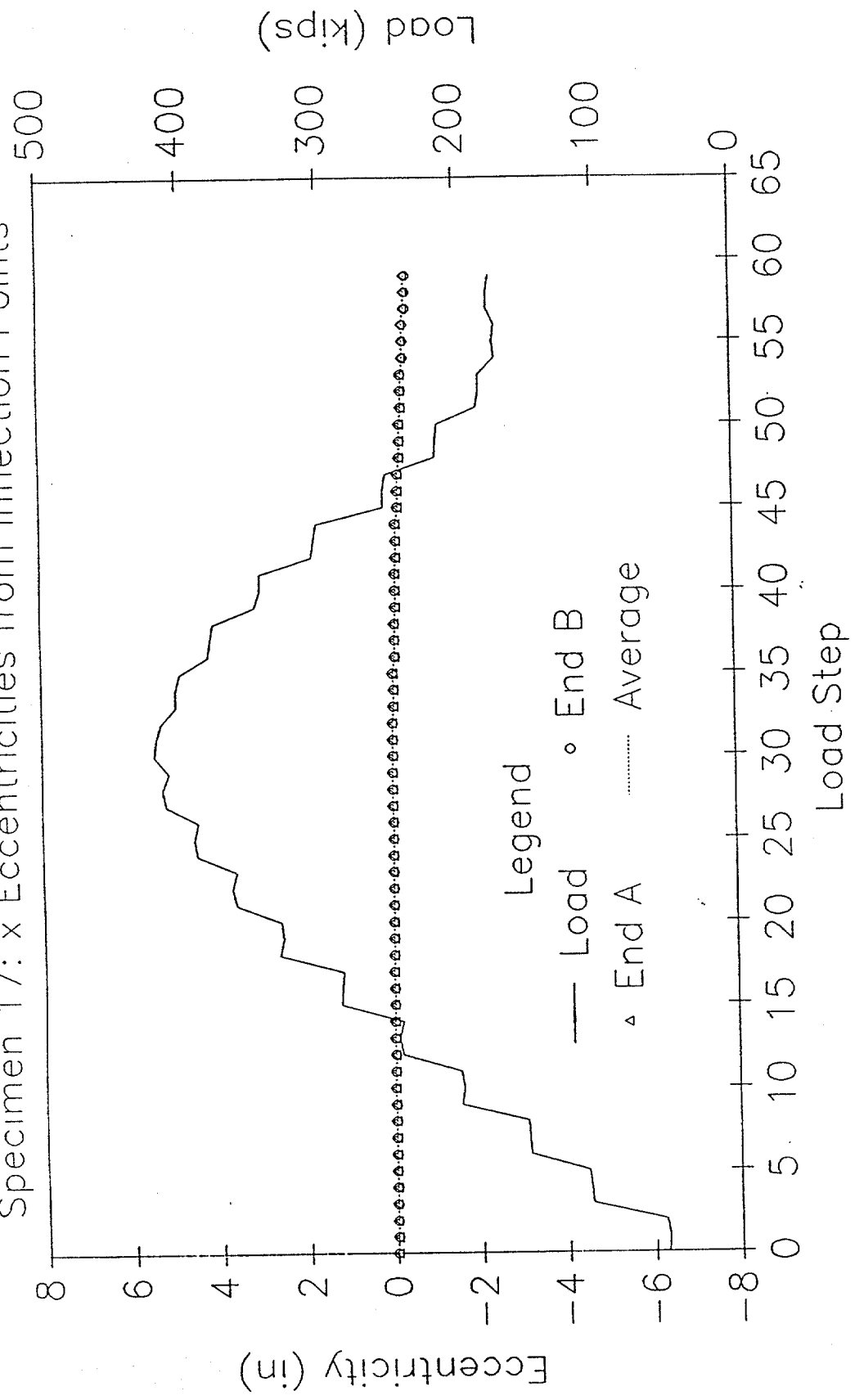
VERTICAL DISPLACEMENTS

Specimen 17



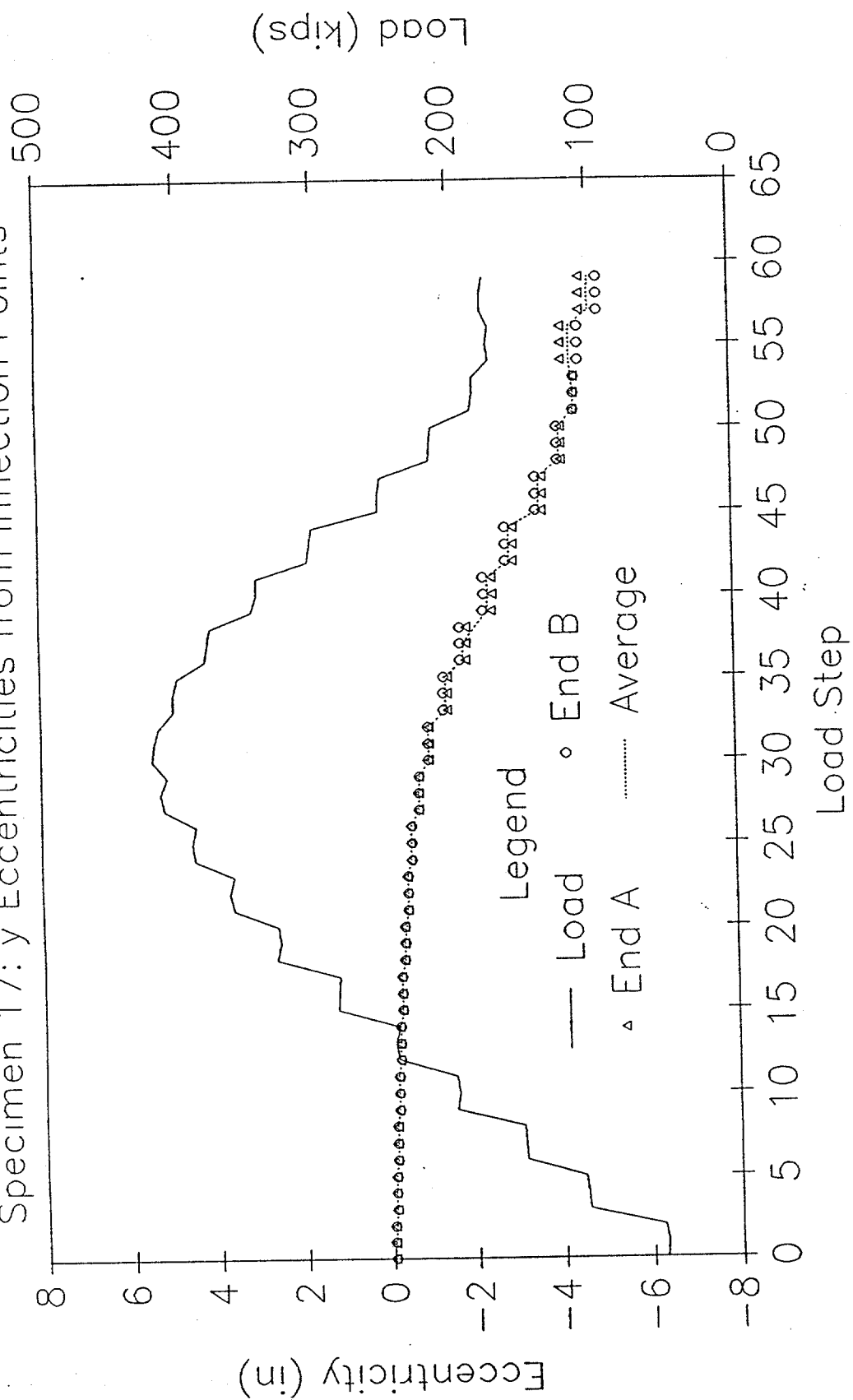
LOAD AND ECCENTRICITY vs LOAD STEP

Specimen 17: x Eccentricities from Inflection Points



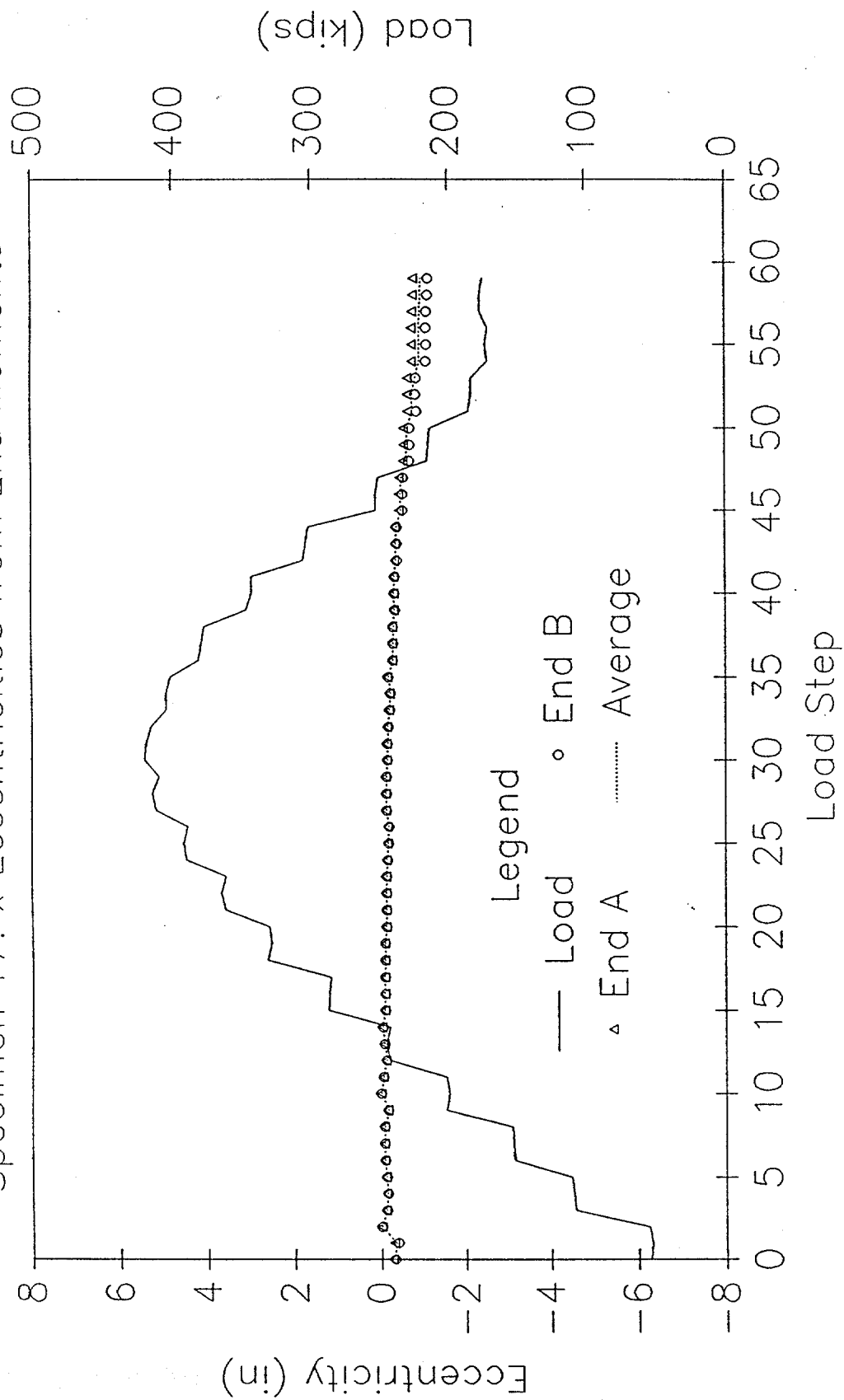
LOAD AND ECCENTRICITY vs LOAD STEP

Specimen 17: y Eccentricities from Inflection Points



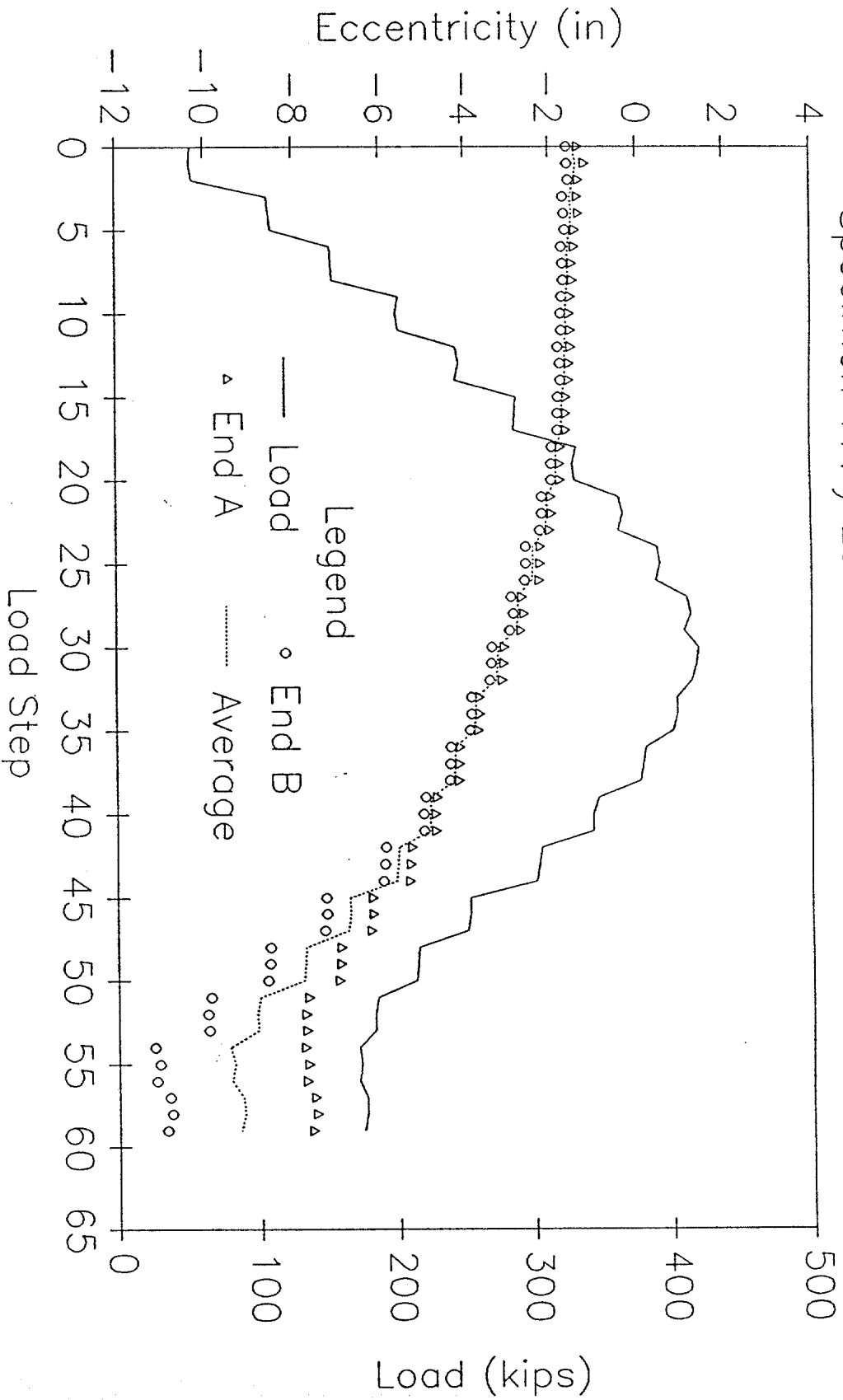
LOAD AND ECCENTRICITY vs LOAD STEP

Specimen 17: x Eccentricities from End Moments

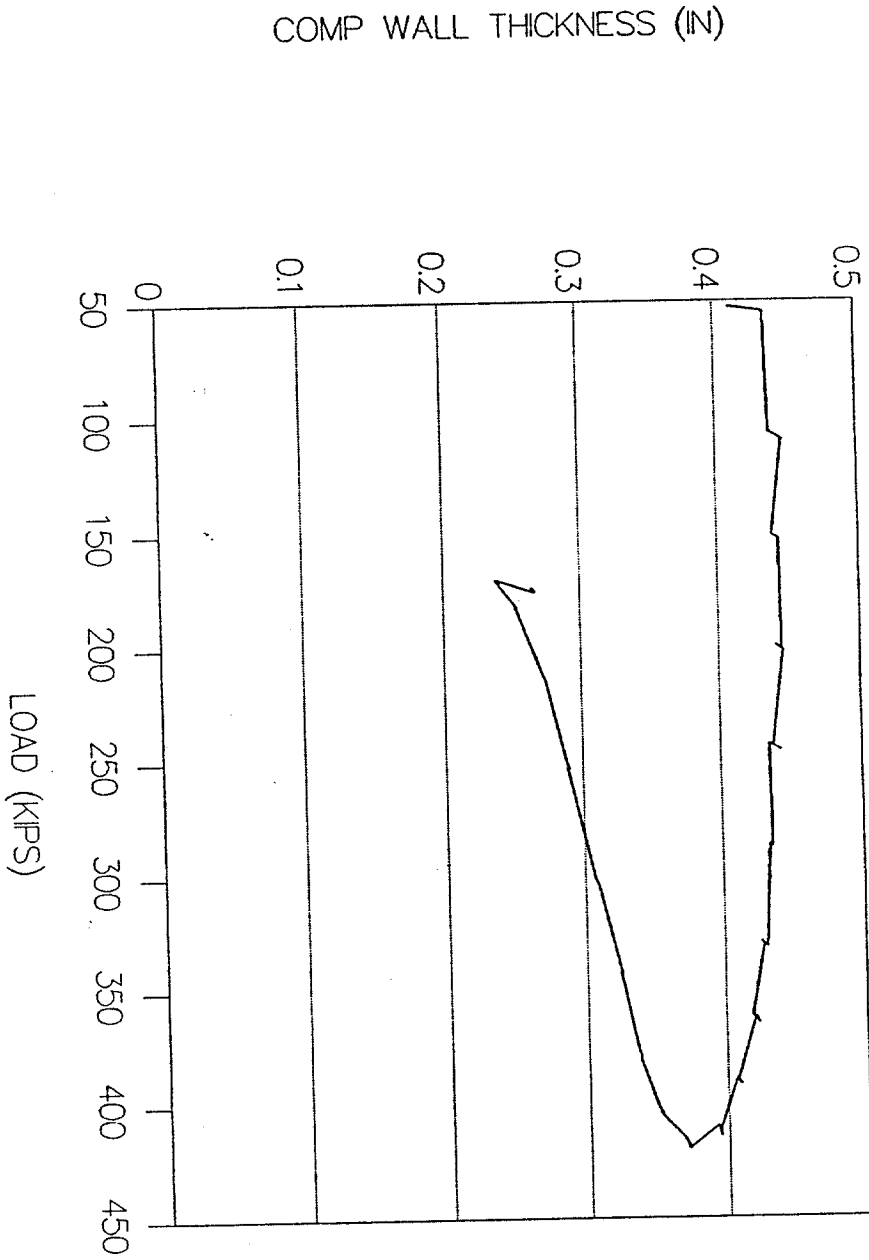


LOAD AND ECCENTRICITY vs LOAD STEP

Specimen 17: y Eccentricities from End Moments

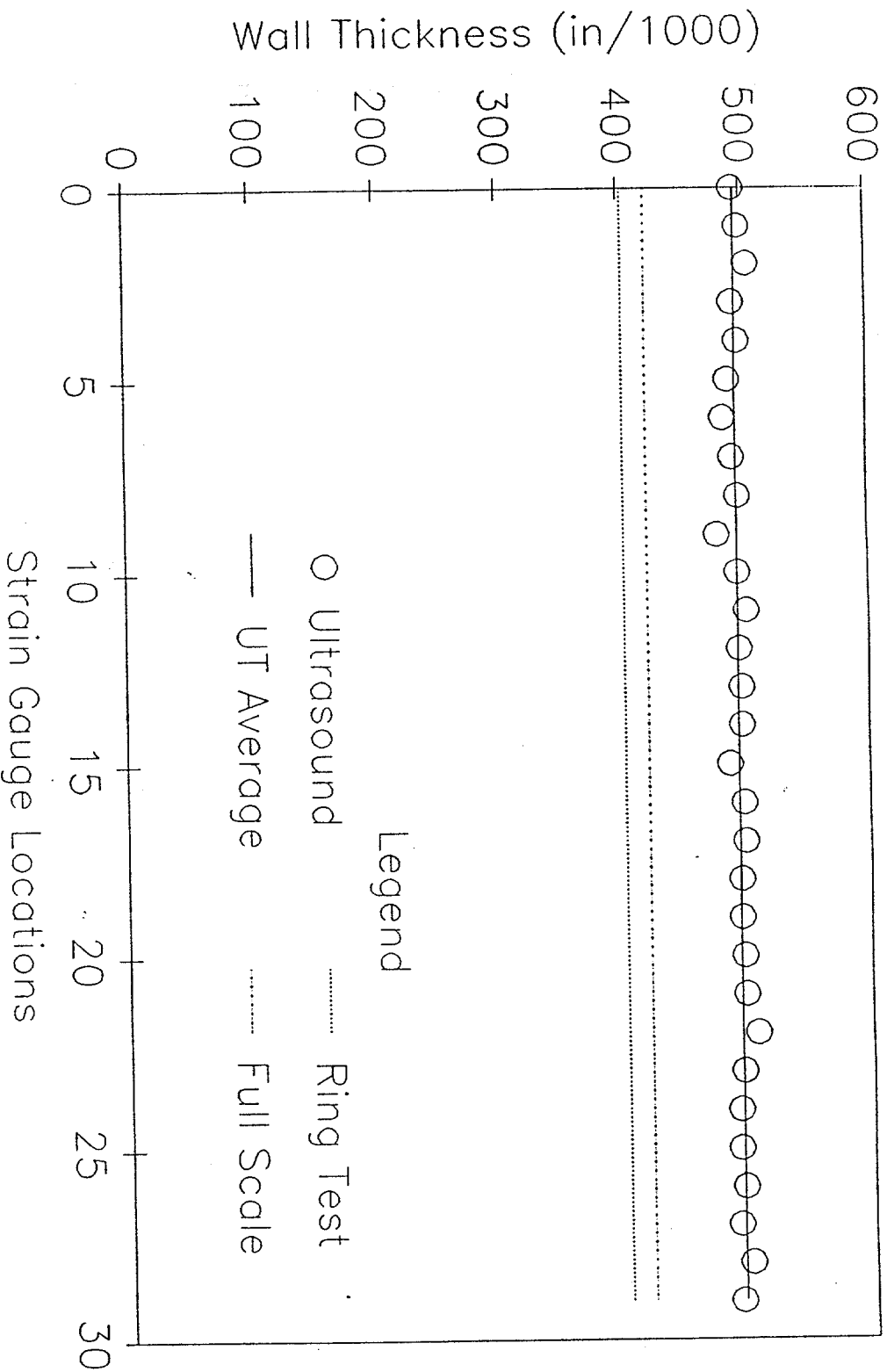


SPECIMEN NO 17-FULL SCALE TEST COMPUTED WALL THICKNESS



SPECIMEN 17: WALL THICKNESS

Nominal Wall Thickness = 0.500 in

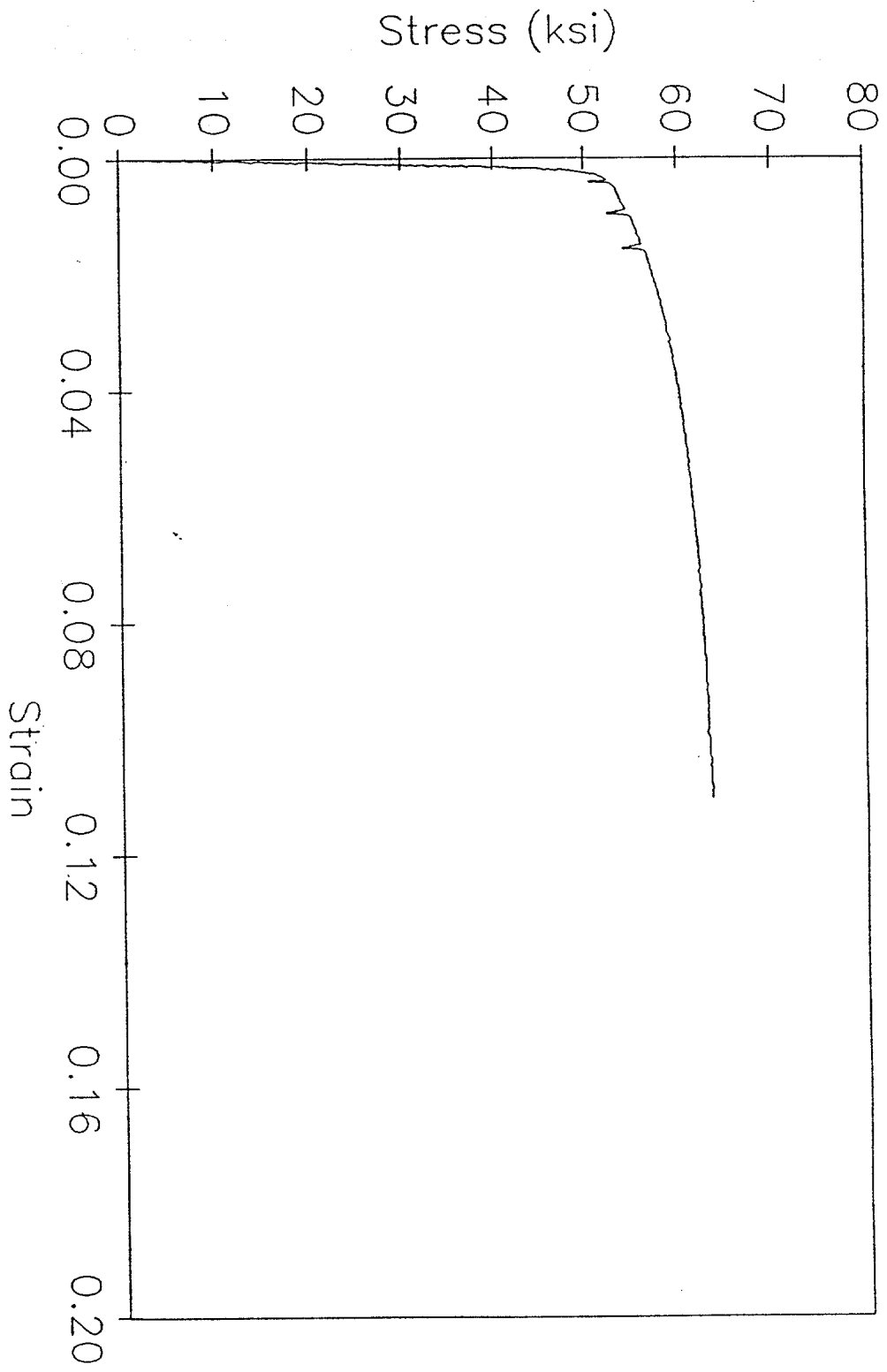


Ultrasonnd Data for Specimen 17
(All values in inches)

Gauge	No.	Thickness	Average
UT	0	0.494	UT
UT	1	0.498	UT
UT	2	0.505	UT
UT	3	0.493	UT
UT	4	0.497	UT
UT	5	0.489	UT
UT	6	0.485	UT
UT	7	0.492	UT
UT	8	0.496	UT
UT	9	0.479	UT
UT	10	0.495	UT
UT	11	0.502	UT
UT	12	0.496	UT
UT	13	0.498	UT
UT	14	0.498	UT
UT	15	0.488	UT
UT	16	0.499	UT
UT	17	0.500	UT
UT	18	0.496	UT
UT	19	0.496	UT
UT	20	0.498	UT
UT	21	0.499	UT
UT	22	0.508	UT
UT	23	0.496	UT
UT	24	0.493	UT
UT	25	0.493	UT
UT	26	0.496	UT
UT	27	0.492	UT
UT	28	0.501	UT
UT	29	0.493	UT
Overall Average	=	0.496	

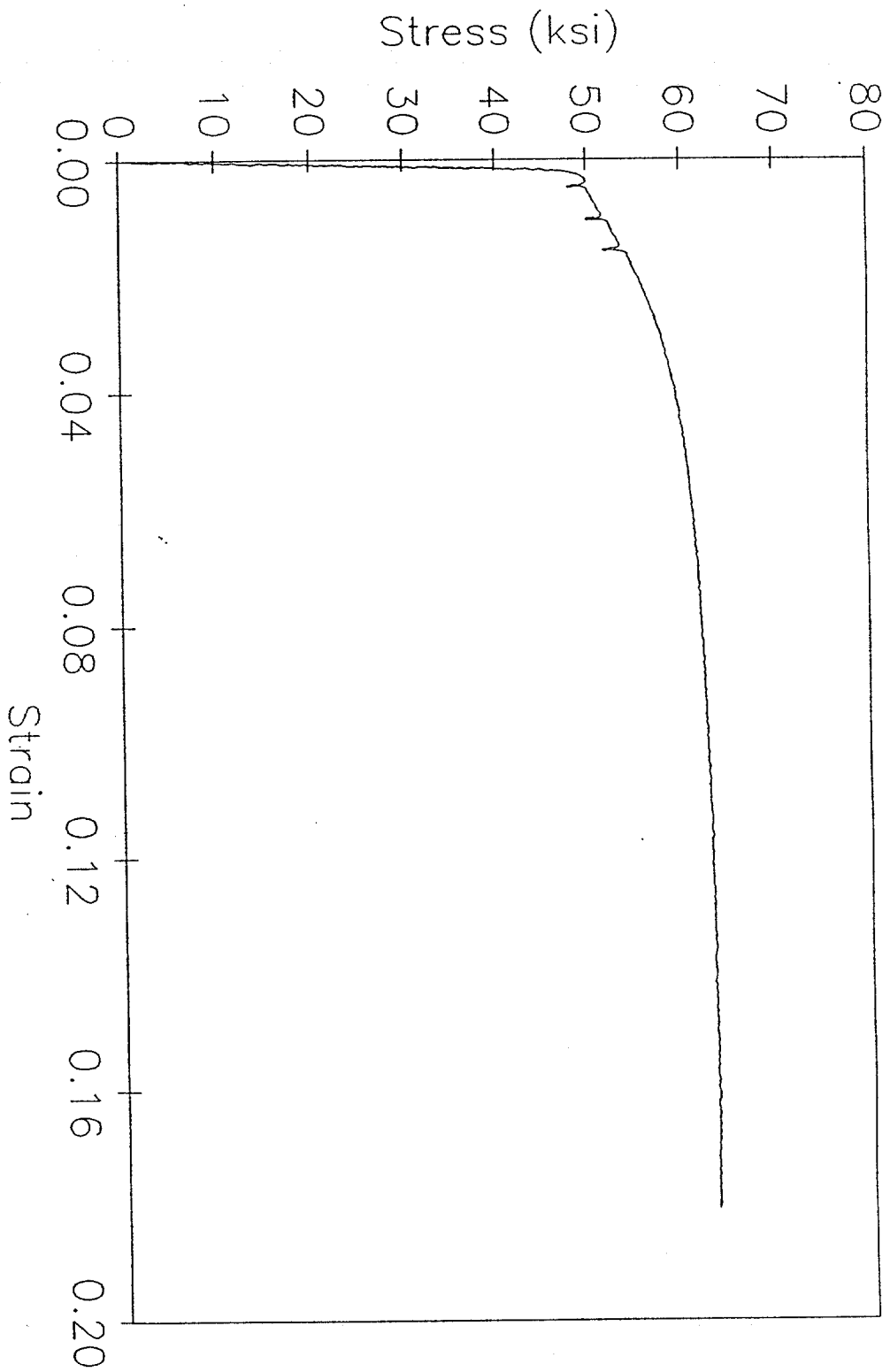
TENSILE SPECIMEN 17-1

Stress vs Strain



TENSILE SPECIMEN 17-2

Stress vs Strain



SPECIMEN 18

DAMAGE SUMMARY

Specimen No. 18
2-28-90

DISTANCE FROM END "B"	*DISTANCE FROM CHALK LINE		DESCRIPTION OF DAMAGE
	LEFT	RIGHT	
1. 5'-1"	2"		Dent - 6" long x 4" wide 1/4" deep at center
2. 5'-4 1/2"		5"	Dent - 4" long x 8" wide 3/8" deep at center
3. 9'-11"	3"		Dent - 2" long x 2" wide 1/8" deep at center
4. 11'-2"		4"	Dent - 5" long x 6" wide 1/4" deep at center
5. 11'-3"	1"		Dent - 2" long x 2" wide 1/8" deep at center
6. 12'-10 1/2"	1"		Dent - 2" long x 2" wide 1/4" deep at center
7. 11'-10"		5"	Dent - 4" long x 2" wide 1/8" deep at center
8. 8'-8 1/2"			1/2" circumferential butt weld

*Looking from end "A" towards end "B"

WIDESPREAD MODERATE TO HEAVY CORROSION

SEE ADDITIONAL SHEETS FOR DENT PROFILES AND OUT-OF-STRAIGHTNESS

Out-of-Straightness Measurements
for Specimen 18

The specimen was initially curved in the yz-plane.
The following measurements are in the y-direction.

Distance from End B (ft)	Distance from stringline to top of pipe (in)	Out-of straightness in y direction (in)
0	3.625	0
1	3.75	-0.125
2	4.0	-0.375
3	4.125	-0.5
4	4.1875	-0.5625
5	4.375	-0.75
6	4.375	-0.75
7	4.375	-0.75
8	4.375	-0.75
9	4.5	-0.875
10	4.375	-0.75
11	4.375	-0.75
12	4.3125	-0.6875
13	4.25	-0.625
14	4.125	-0.5
15	4.0	-0.375
16	3.875	-0.25
17	3.625	0

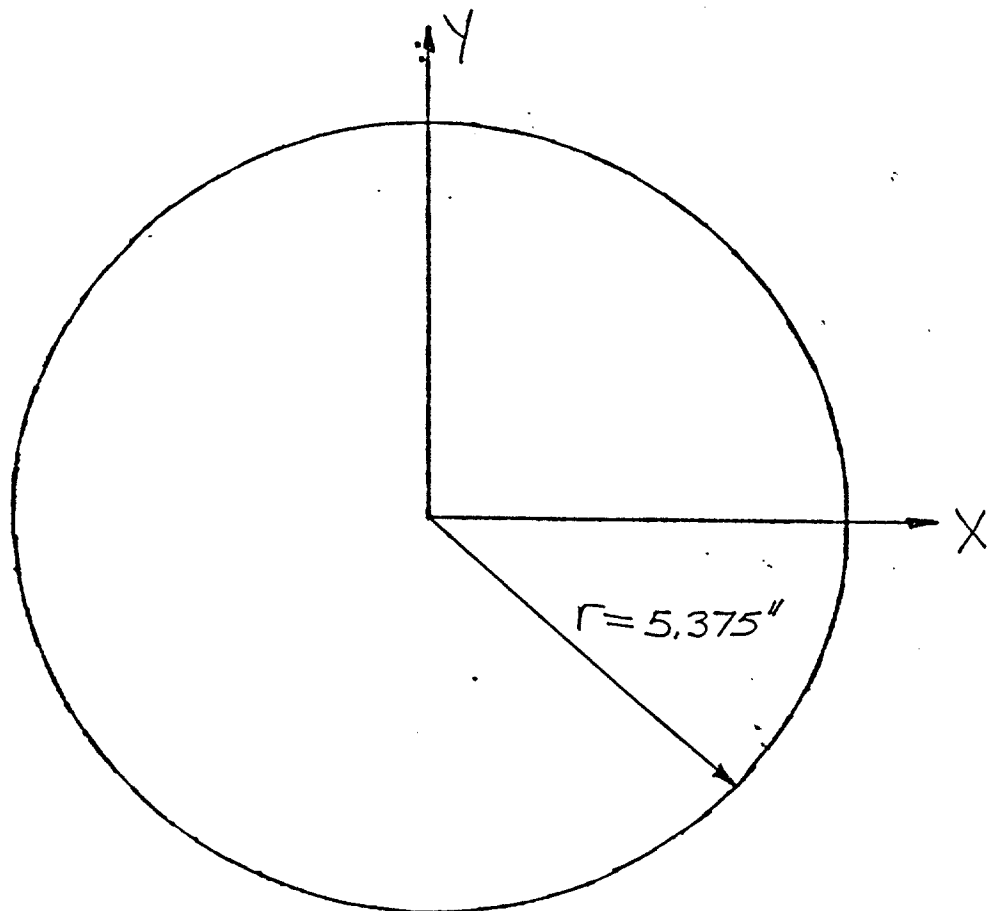
DENT CROSS SECTION

Specimen No. 18

Damage No. 1

Distance from End B 4'-9"

Scale 1" = 2.53"



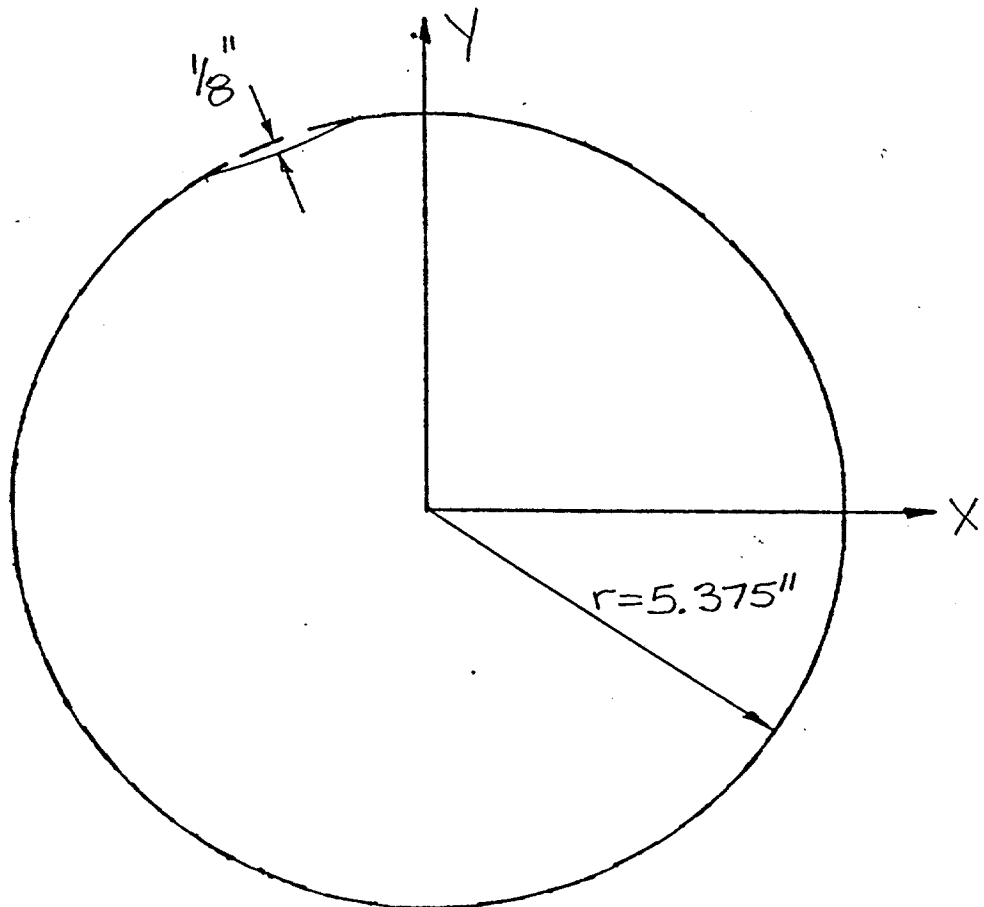
DENT CROSS SECTION

Specimen No. 18

Damage No. 1

Distance from End B 4'-11"

Scale 1" = 2.53"



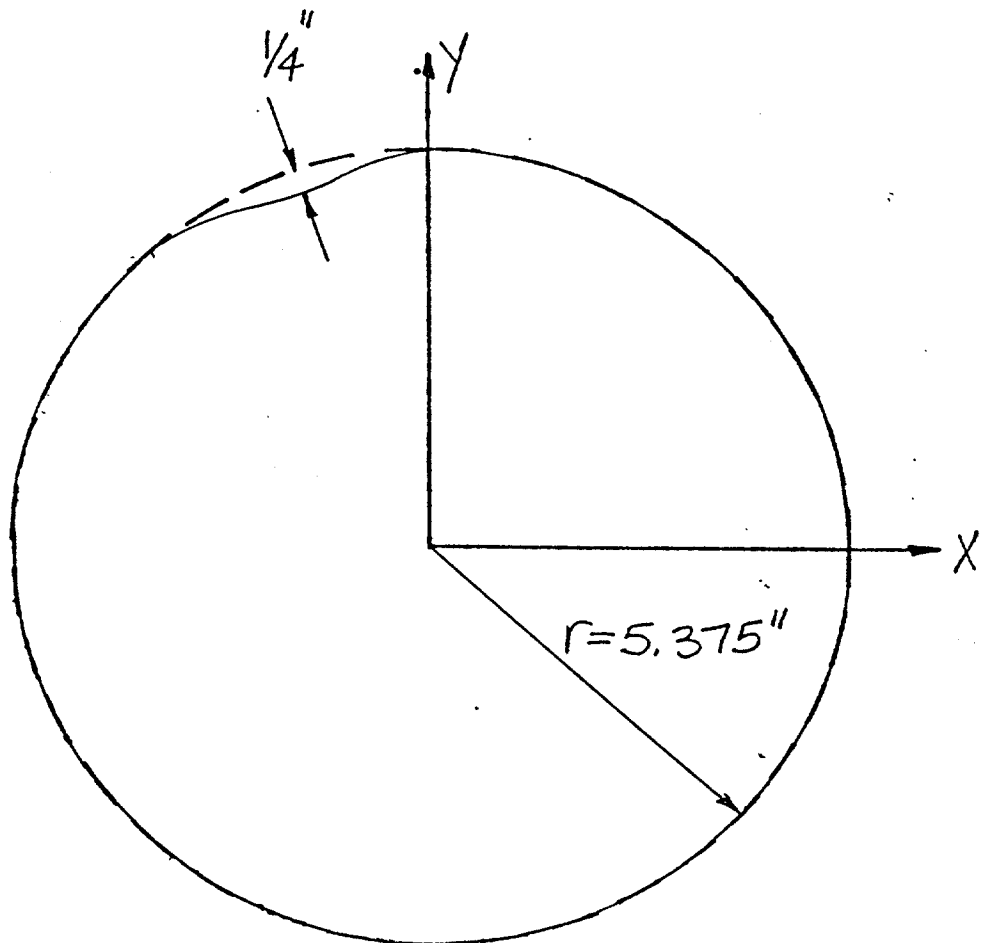
DENT CROSS SECTION

Specimen No. 18

Damage No. 142

Distance from End B 5'-1"

Scale 1" = 2.53"



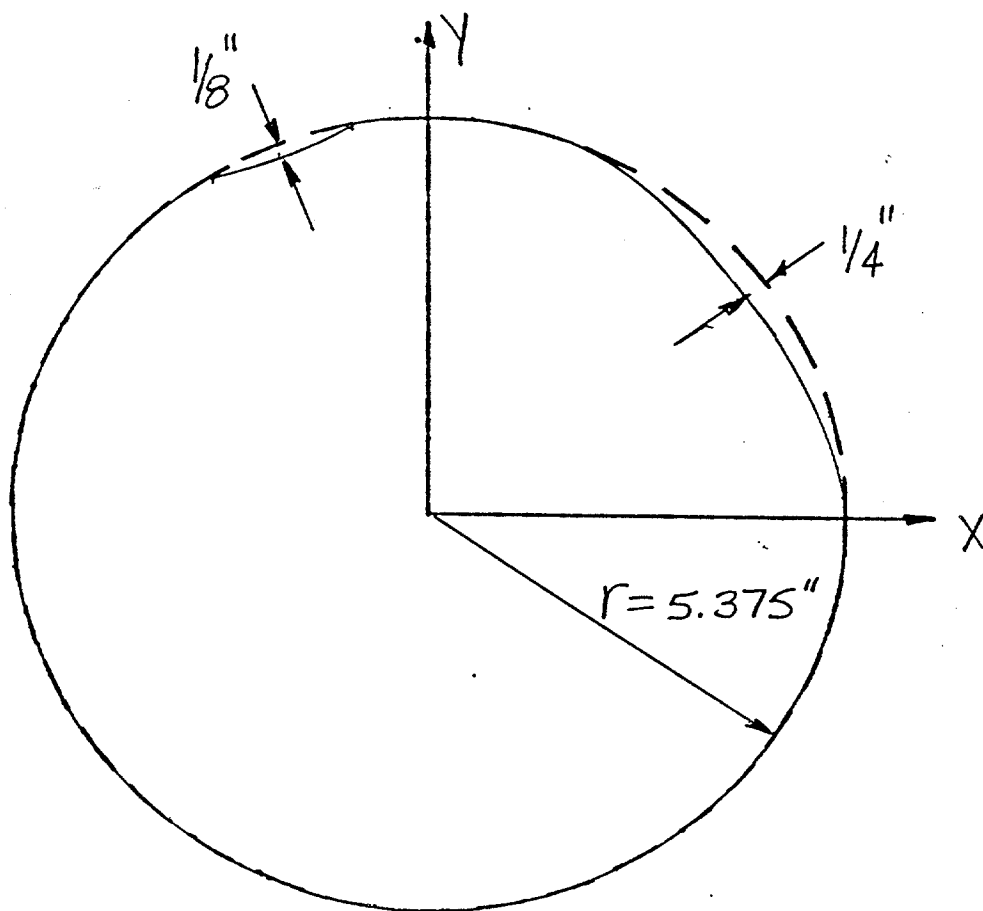
DENT CROSS SECTION

Specimen No. 18

Damage No. 142

Distance from End B 5'-3"

Scale 1" = 2.53"



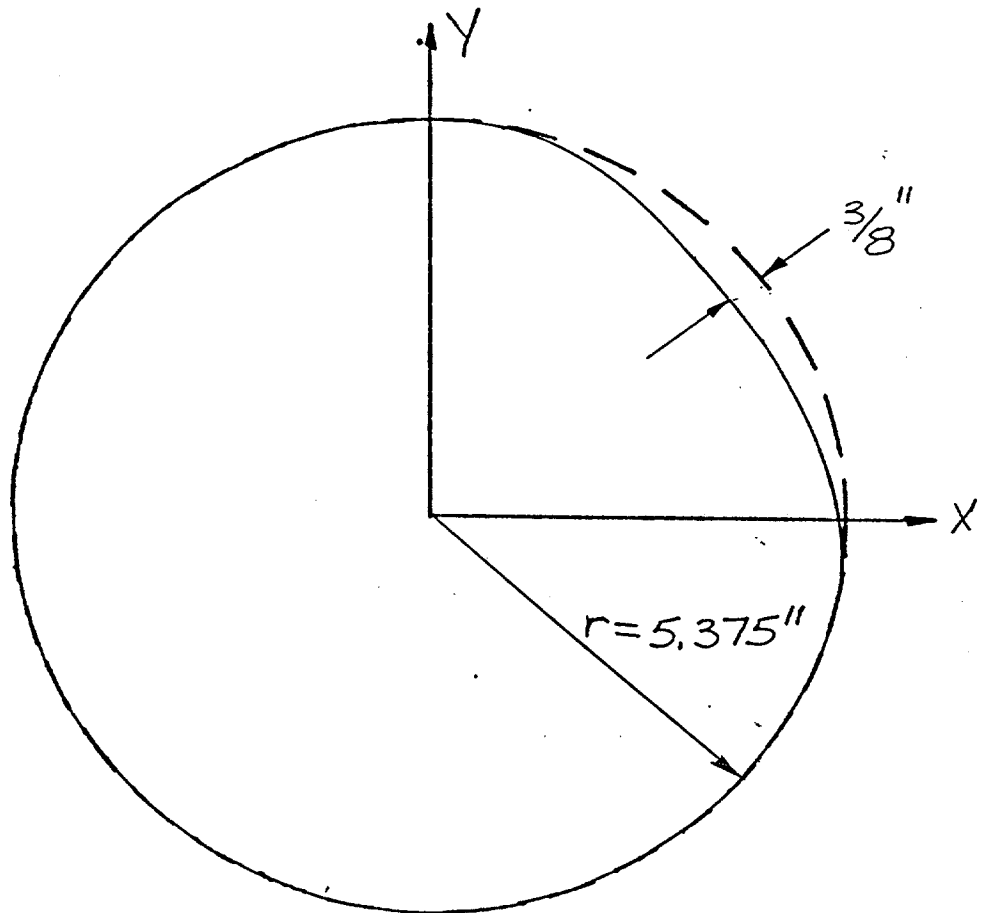
DENT CROSS SECTION

Specimen No. 18

Damage No. 142

Distance from End B 5'-4 1/2"

Scale 1"=2.53"



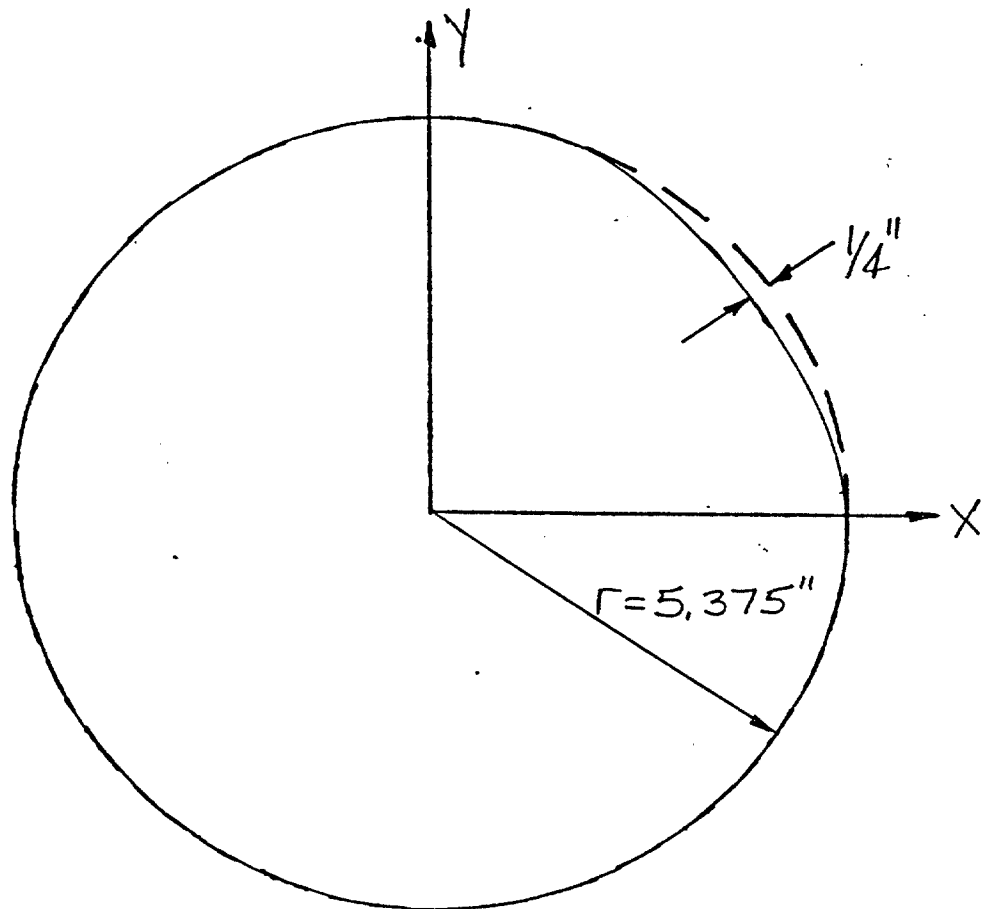
DENT CROSS SECTION

Specimen No. 18

Damage No. 2

Distance from End B 5'-6"

Scale 1" = 2.53"



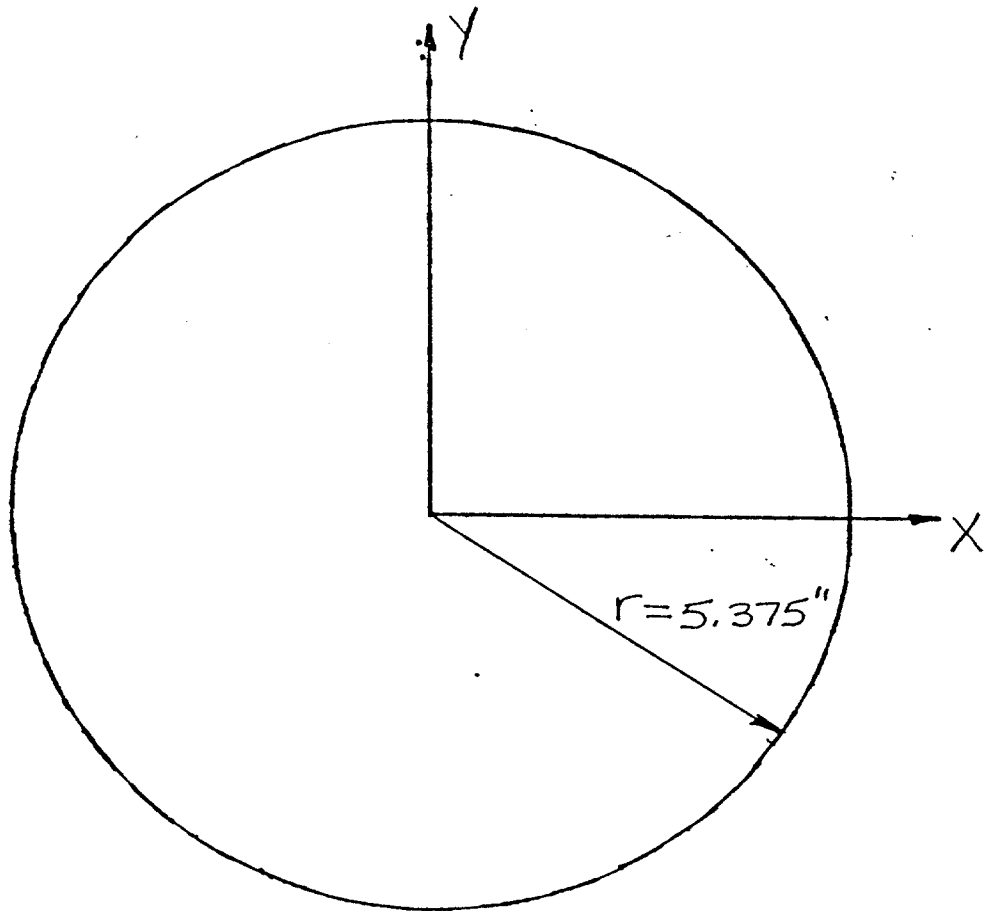
DENT CROSS SECTION

Specimen No. 18

Damage No. 2

Distance from End B 5'-7"

Scale 1"=2.53"



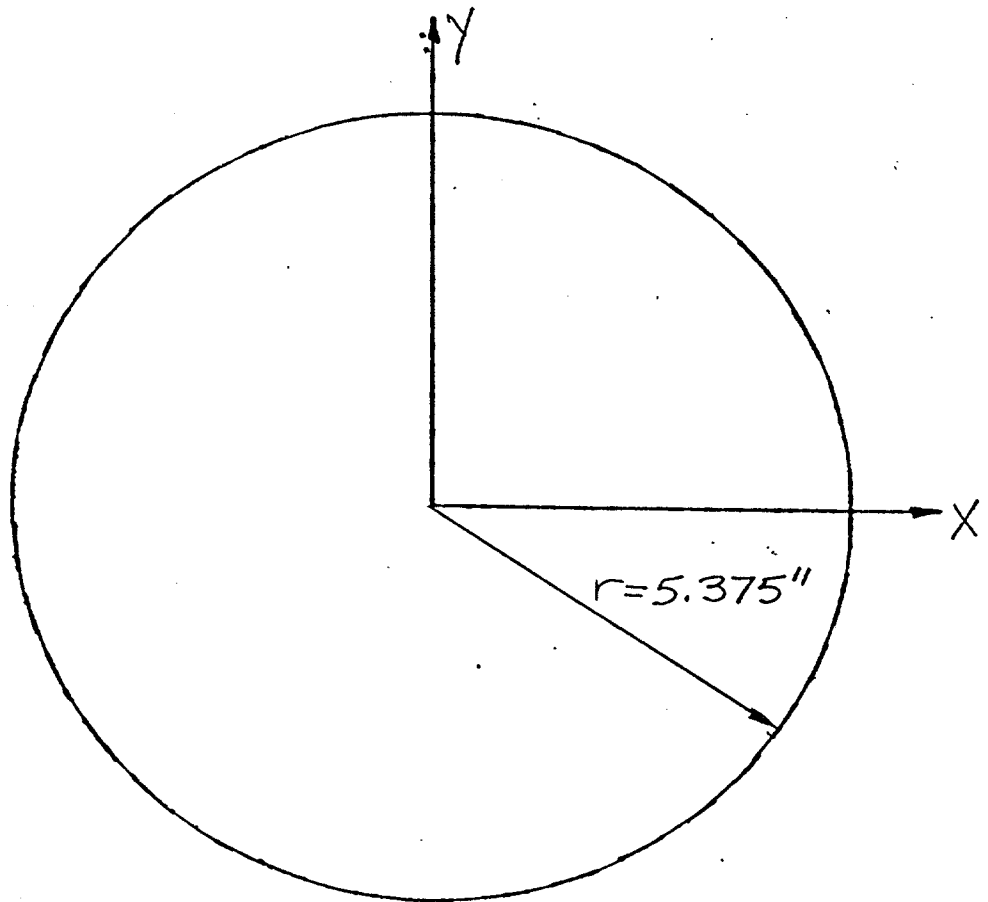
DENT CROSS SECTION

Specimen No. 18

Damage No. 3

Distance from End B 9'-10"

Scale 1"=2.53"



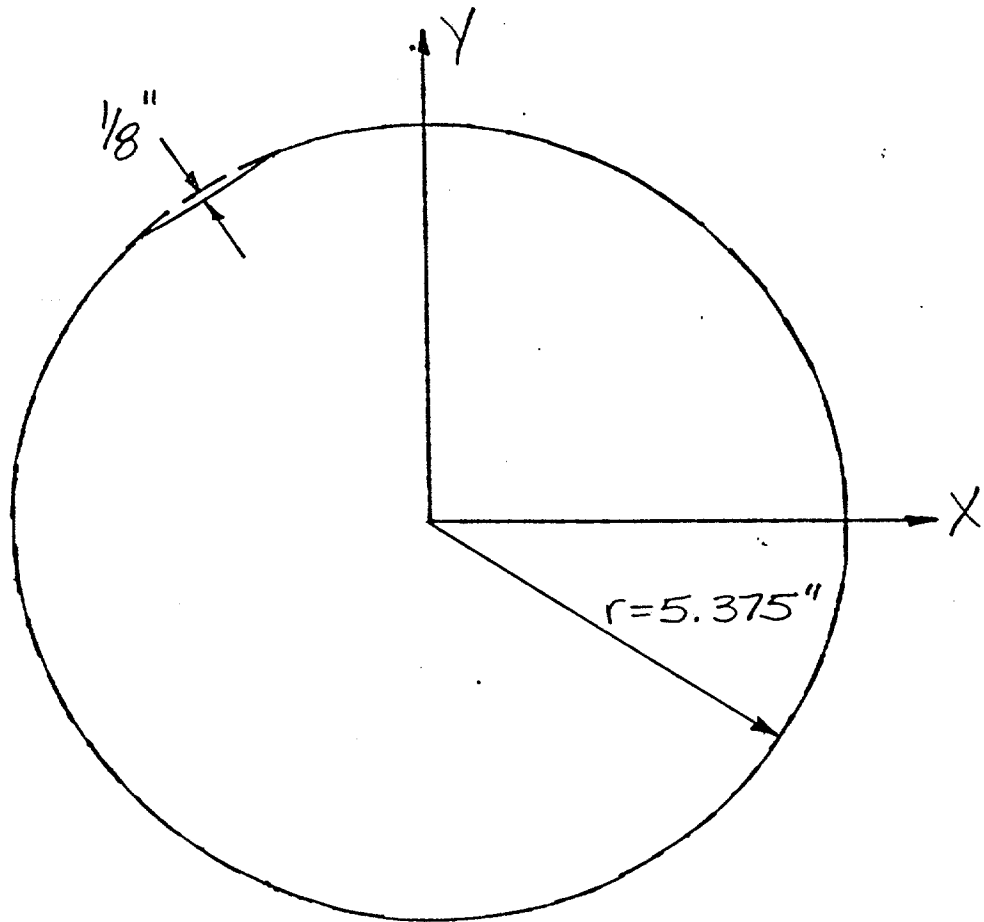
DENT CROSS SECTION

Specimen No. 18

Damage No. 3

Distance from End B 9'-11"

Scale 1"=2.53"



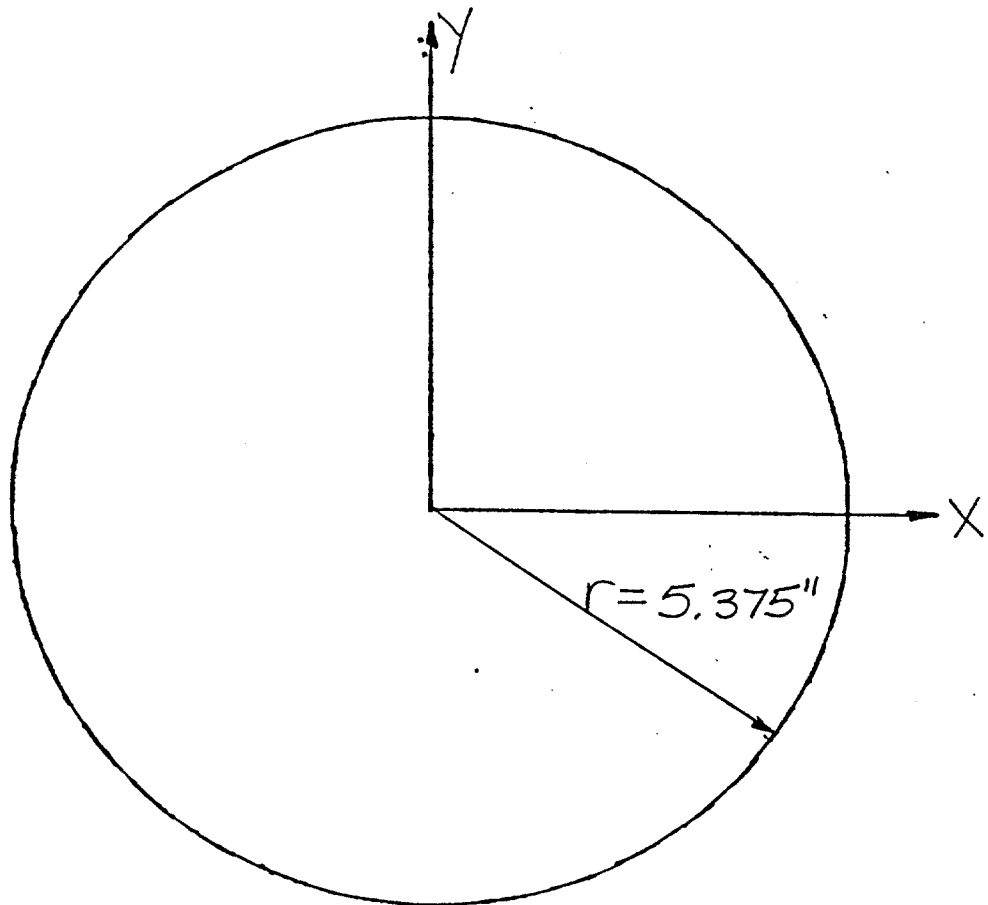
DENT CROSS SECTION

Specimen No. 18

Damage No. 3

Distance from End B 10'-0"

Scale 1"=2.53"



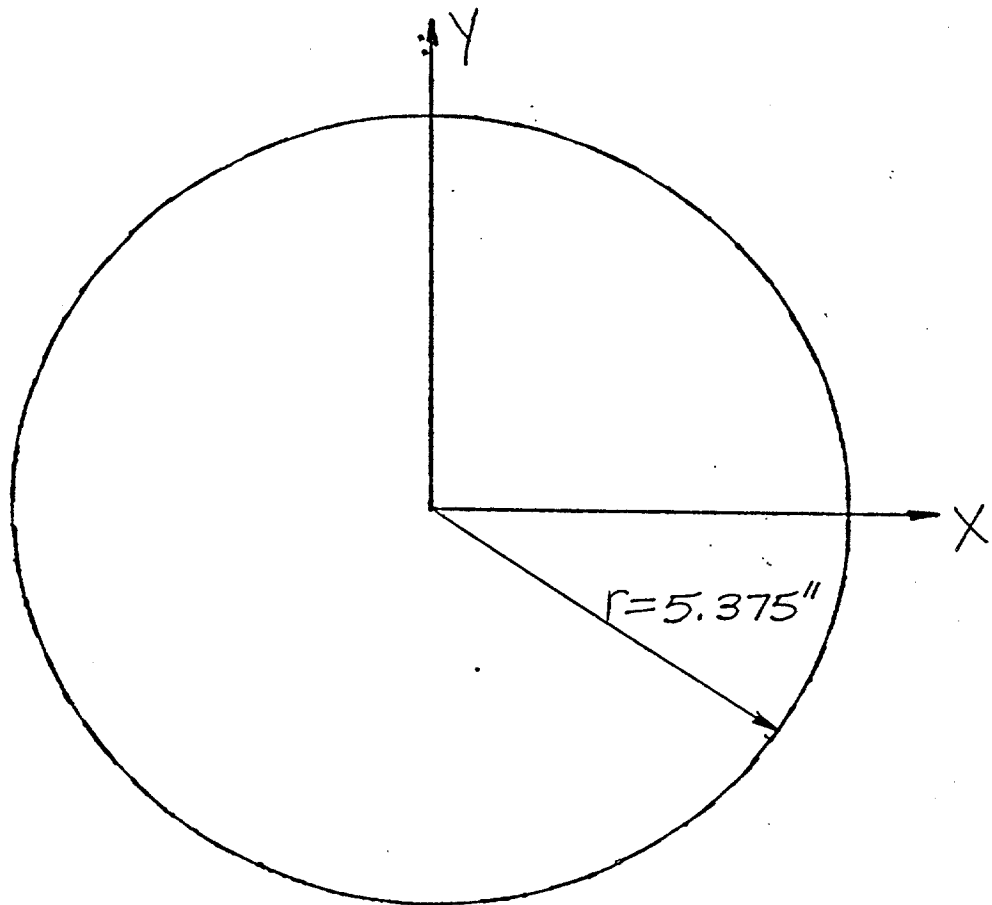
DENT CROSS SECTION

Specimen No. 18

Damage No. 4

Distance from End B 10'-11"

Scale 1"=2.53"



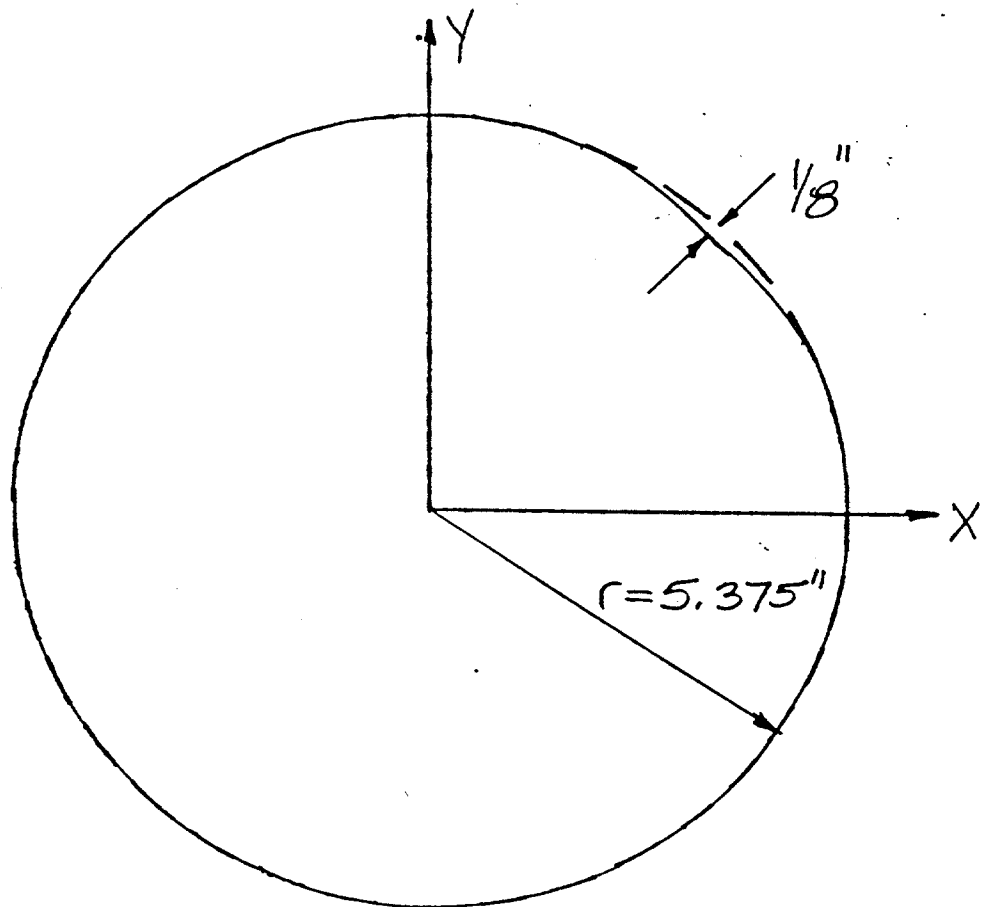
DENT CROSS SECTION

Specimen No. 18

Damage No. 4

Distance from End B 11'-0"

Scale 1"=2.53"



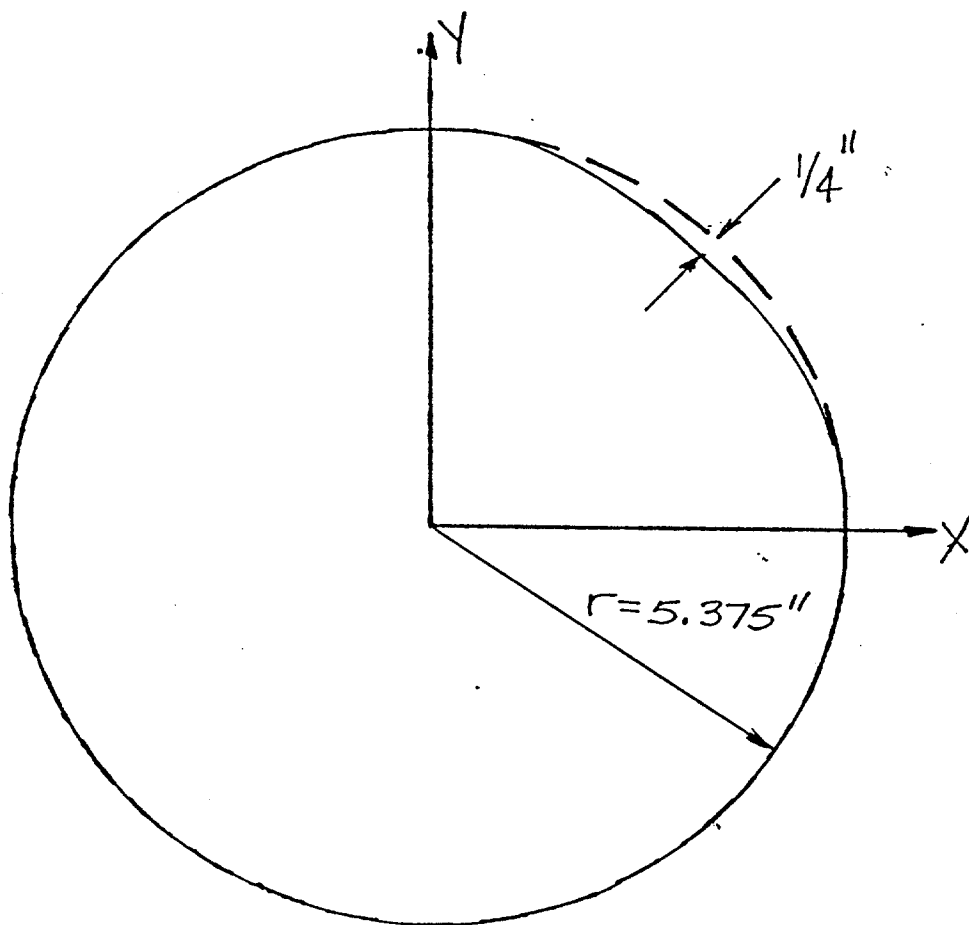
DENT CROSS SECTION

Specimen No. 18

Damage No. 445

Distance from End B 11-2"

Scale 1"=2.53"



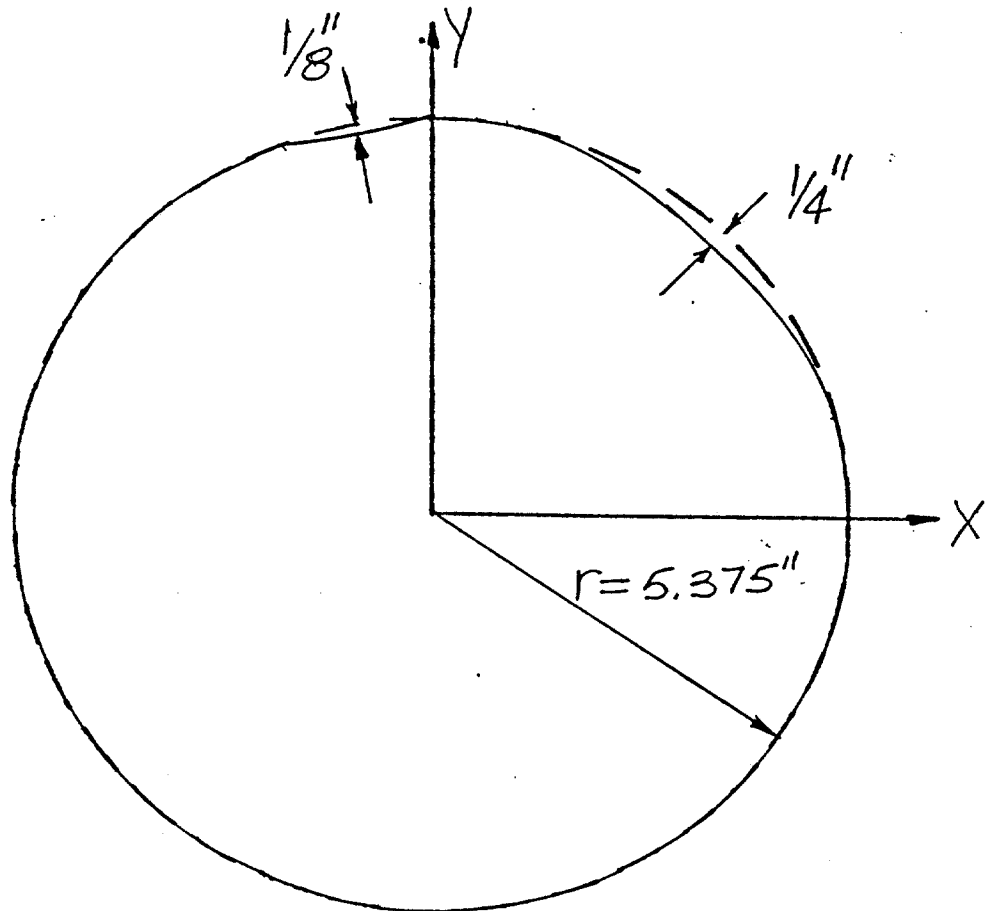
DENT CROSS SECTION

Specimen No. 18

Damage No. 445

Distance from End B 11'-3"

Scale 1"=2.53"



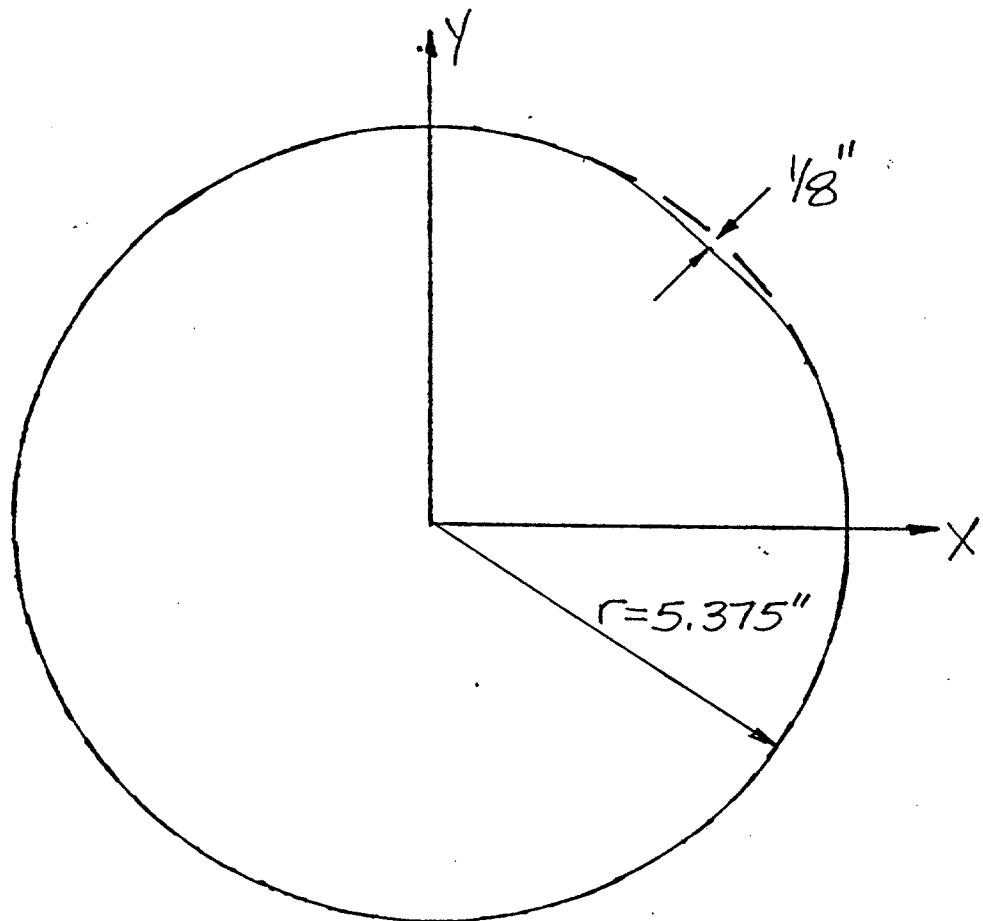
DENT CROSS SECTION

Specimen No. 18

Damage No. 445

Distance from End B 11'-4"

Scale 1"=2.53"



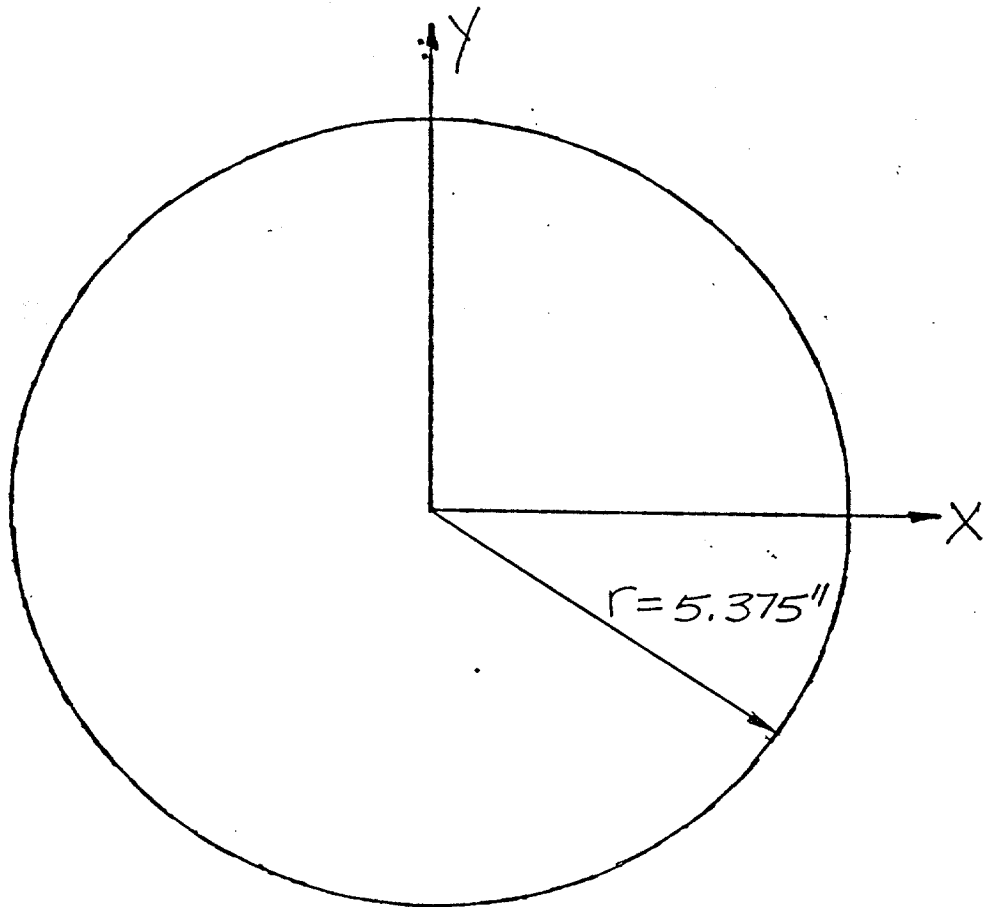
DENT CROSS SECTION

Specimen No. 18

Damage No. 4

Distance from End B 11'-5"

Scale 1"=2.53"



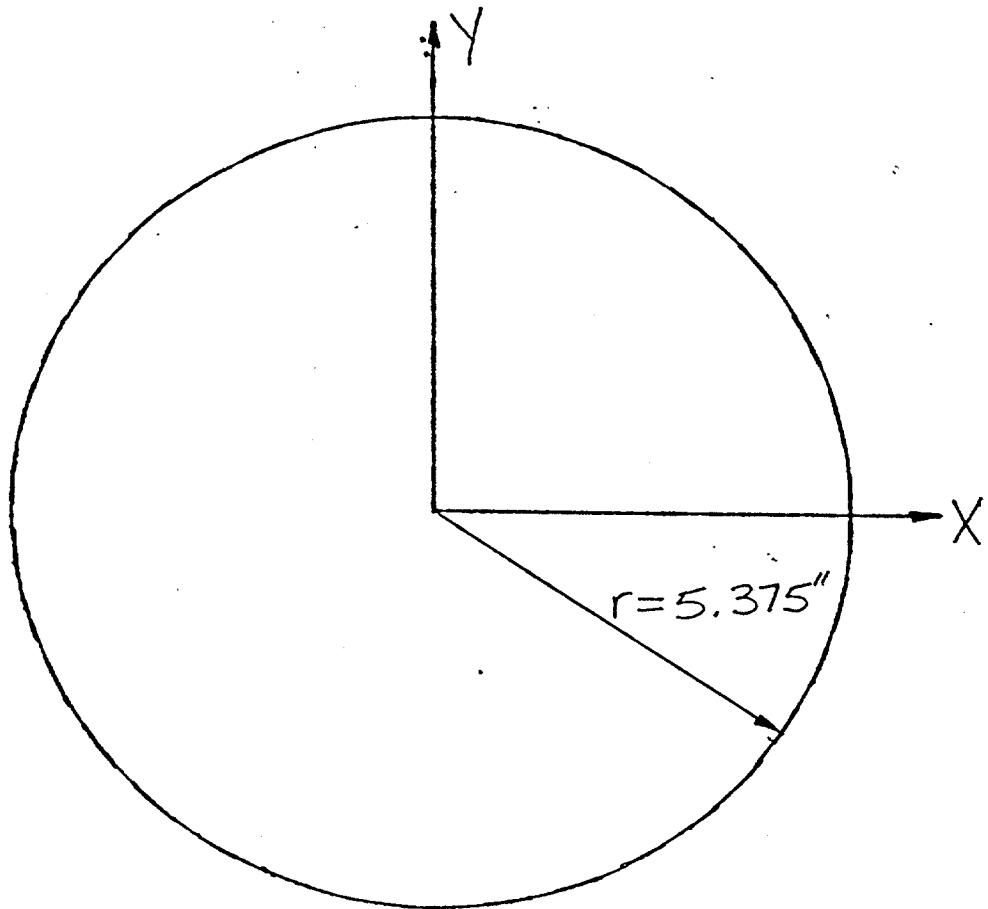
DENT CROSS SECTION

Specimen No. 18

Damage No. 6

Distance from End B 12'-9"

Scale 1" = 2.53"



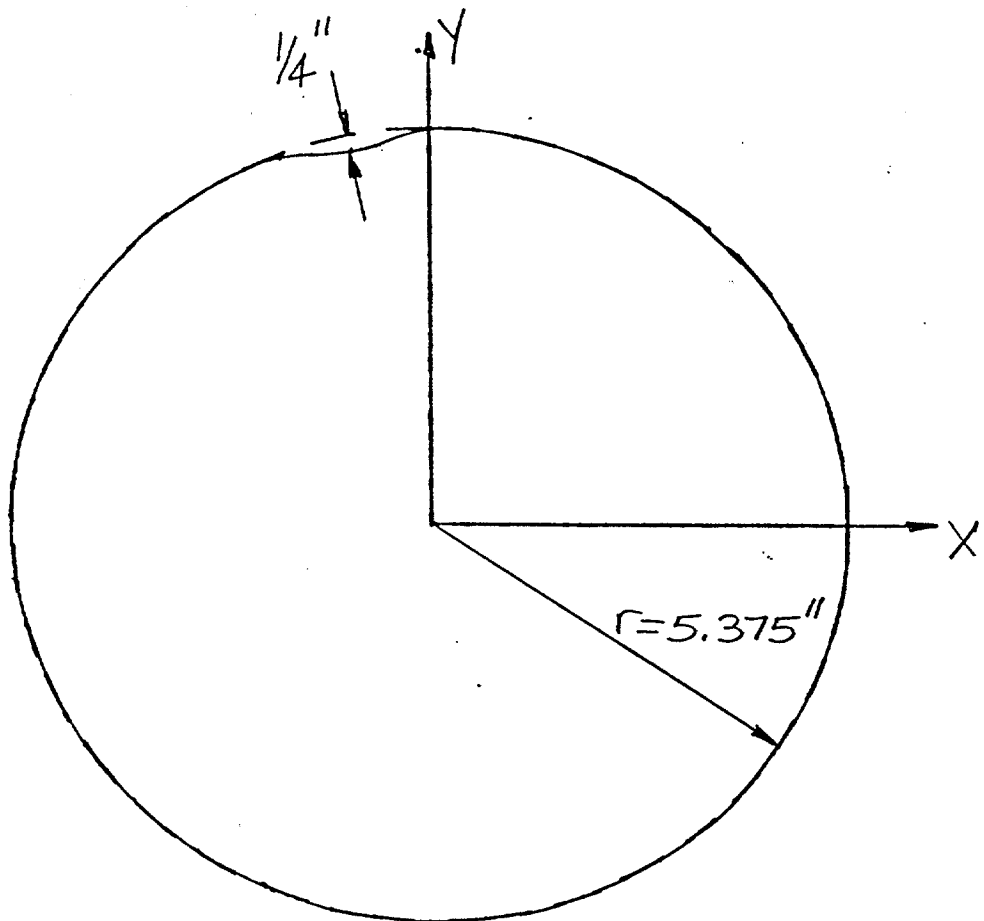
DENT CROSS SECTION

Specimen No. 18

Damage No. 6

Distance from End B 12'-10 1/2"

Scale 1" = 2.53"



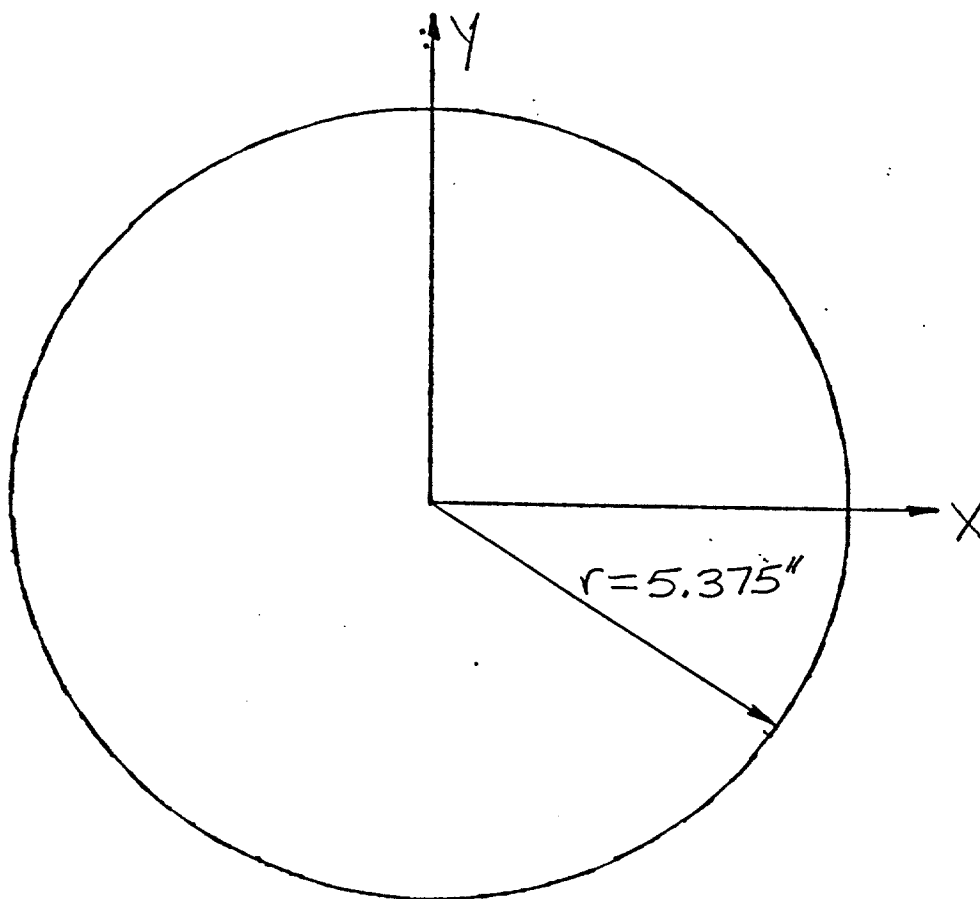
DENT CROSS SECTION

Specimen No. 18

Damage No. 6

Distance from End B 13'-0"

Scale 1"=2.53"



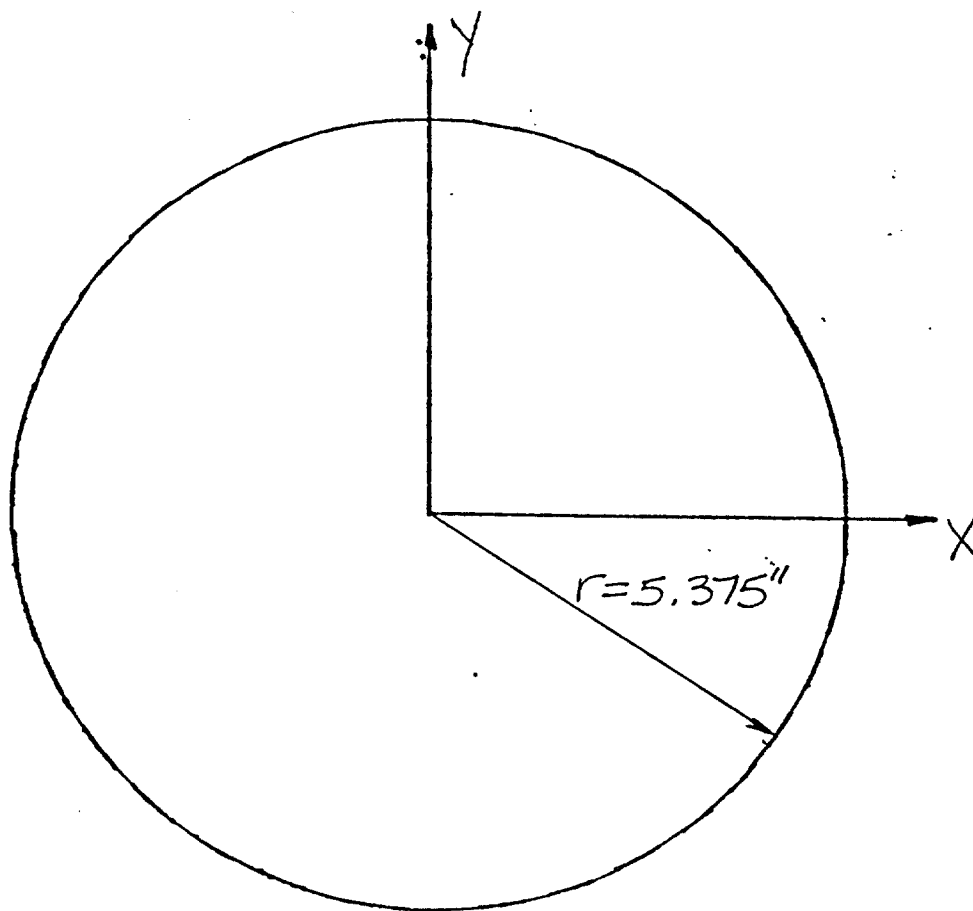
DENT CROSS SECTION

Specimen No. 18

Damage No. 7

Distance from End B 11'-7"

Scale 1"=2.53"



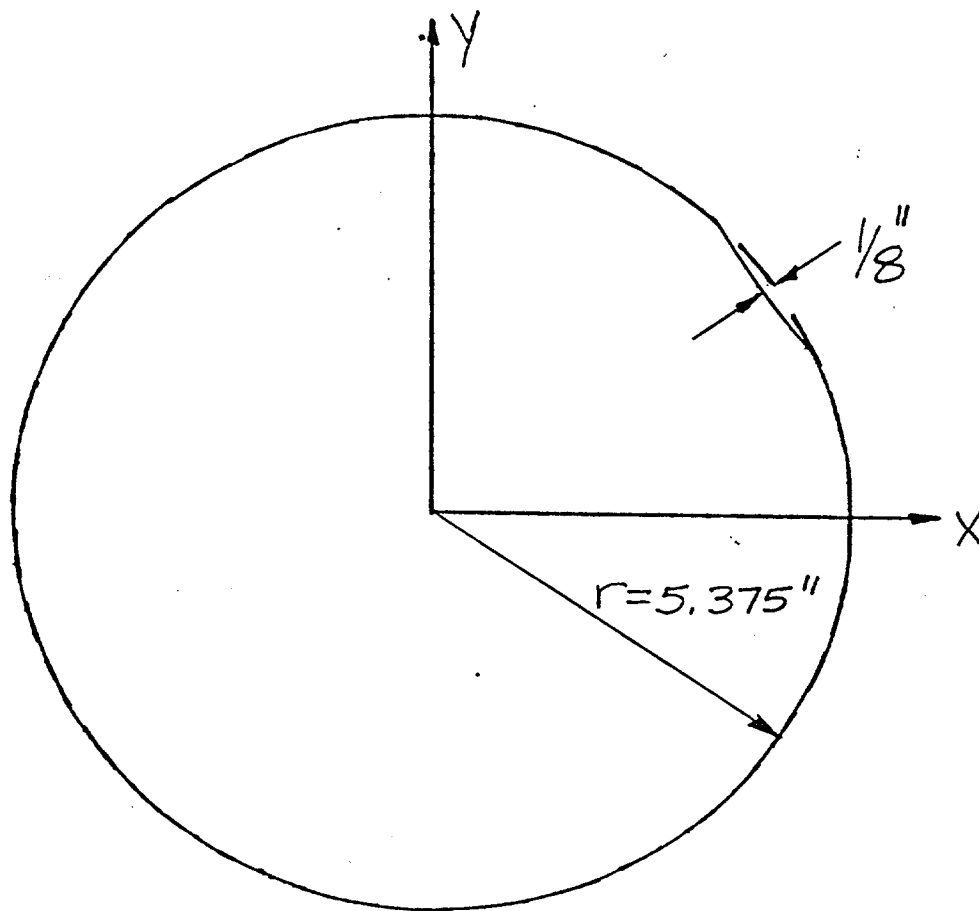
DENT CROSS SECTION

Specimen No. 18

Damage No. 7

Distance from End B 11'-9"

Scale 1" = 2.53"



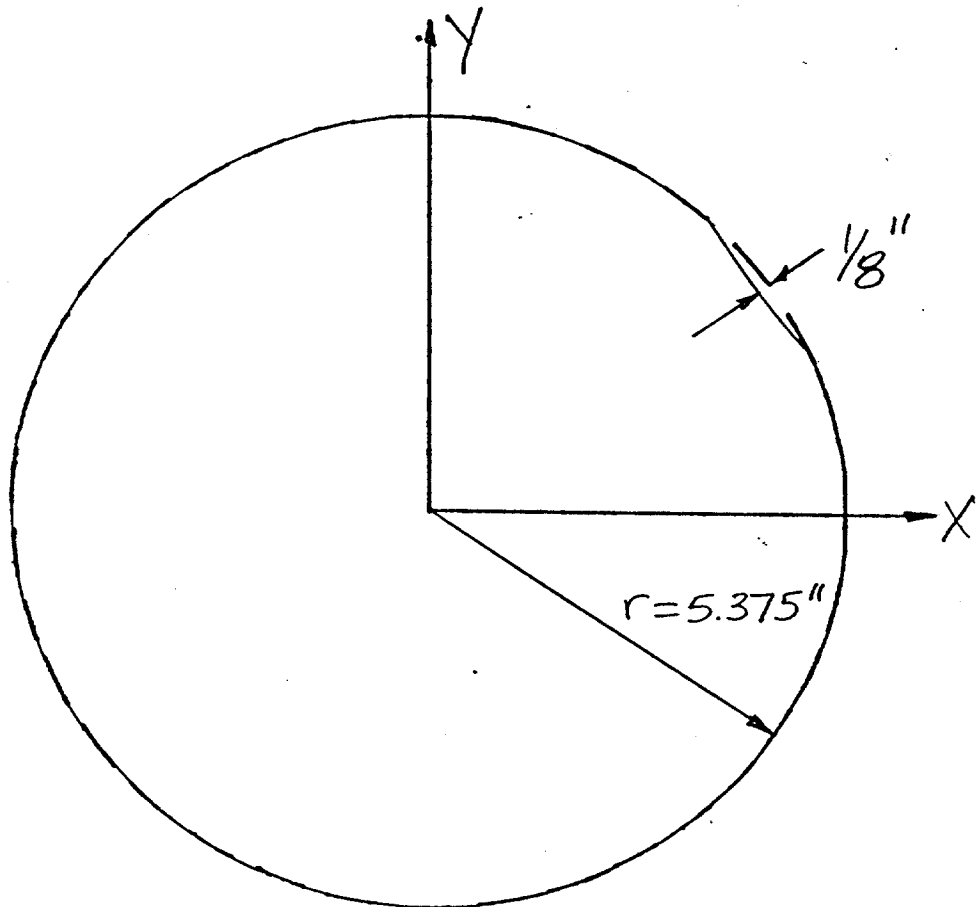
DENT CROSS SECTION

Specimen No. 18

Damage No. 7

Distance from End B 11'-10"

Scale 1"=2.53"



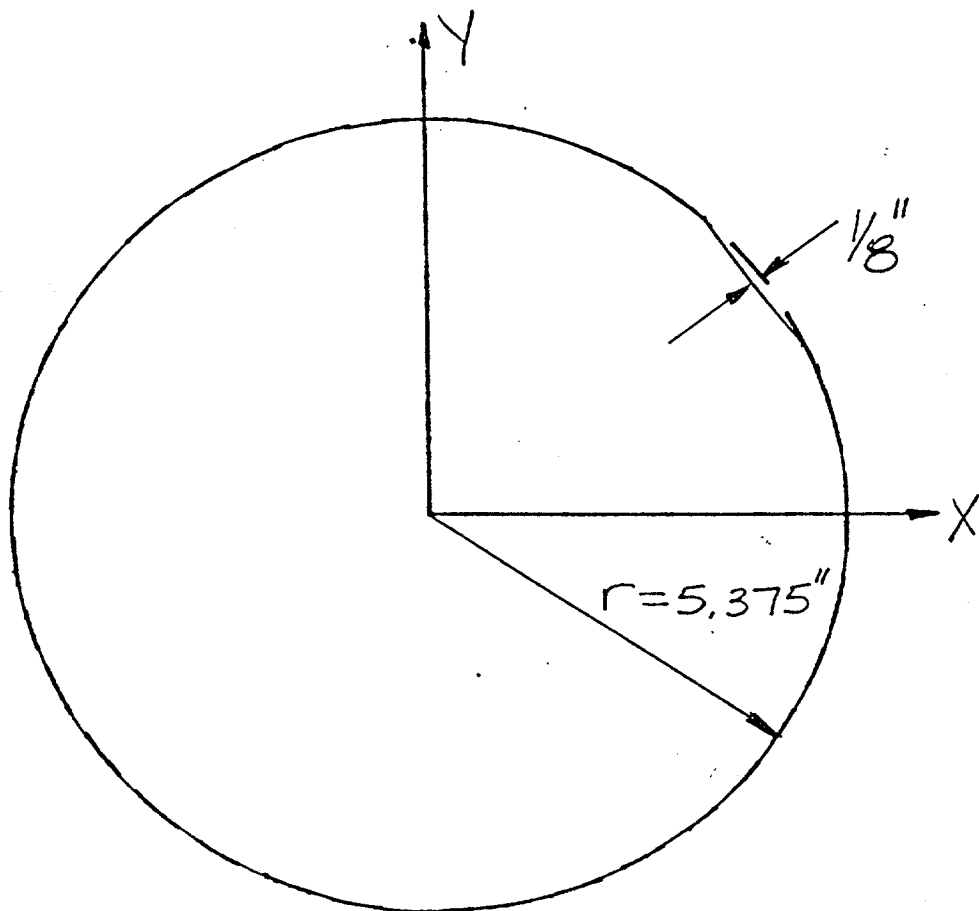
DENT CROSS SECTION

Specimen No. 18

Damage No. 7

Distance from End B 11'-11"

Scale 1"=2.53"



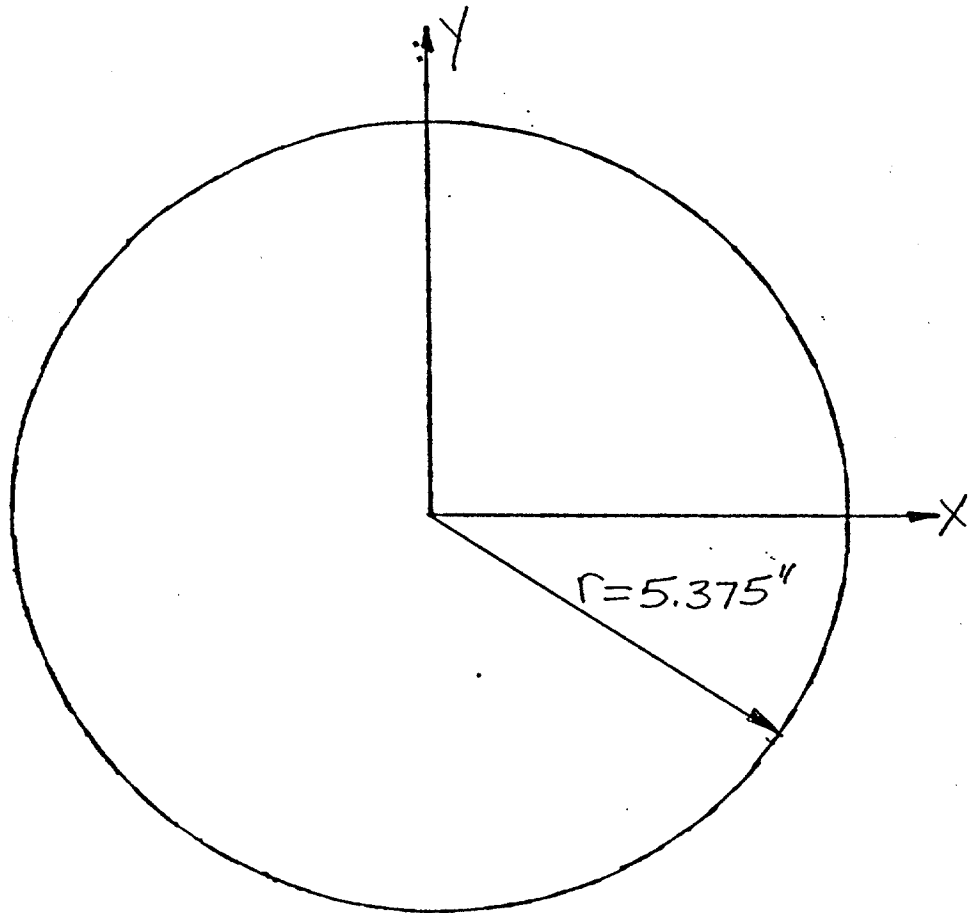
DENT CROSS SECTION

Specimen No. 18

Damage No. 7

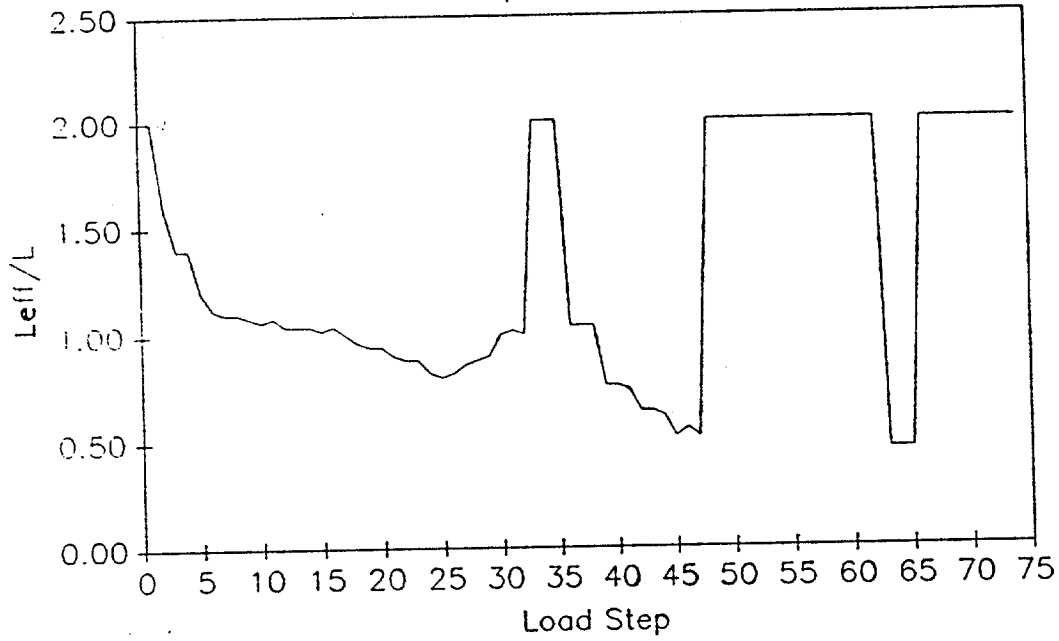
Distance from End B 12'-0"

Scale 1"=2.53"



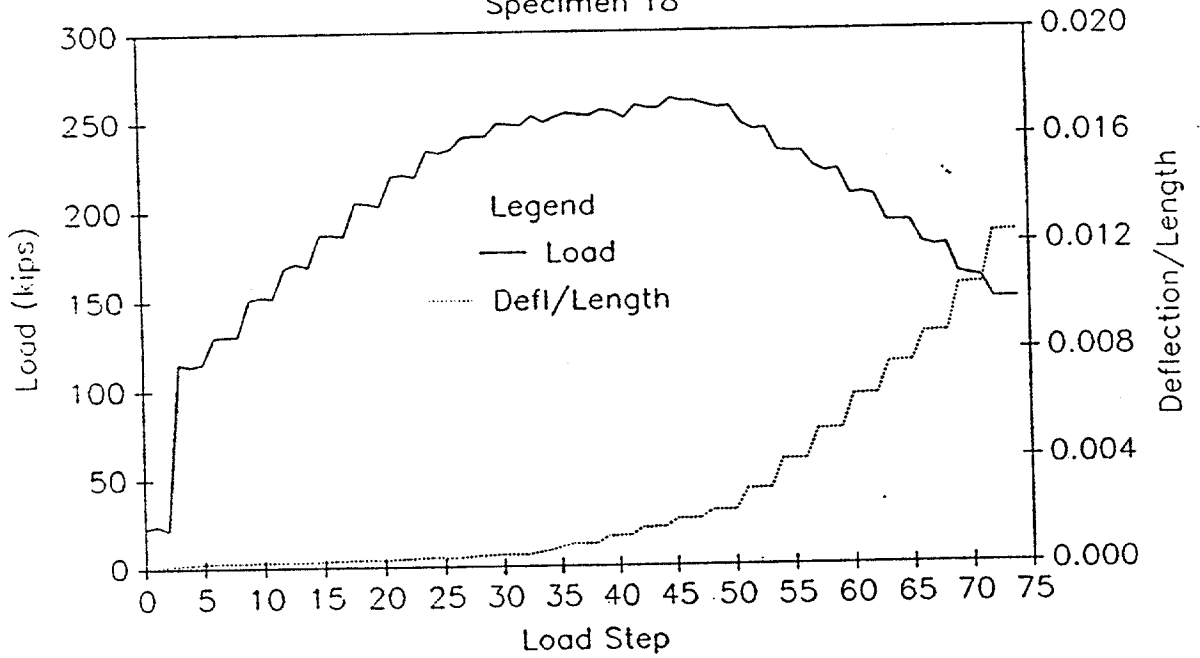
EFFECTIVE LENGTH vs LOAD STEP

Specimen 18

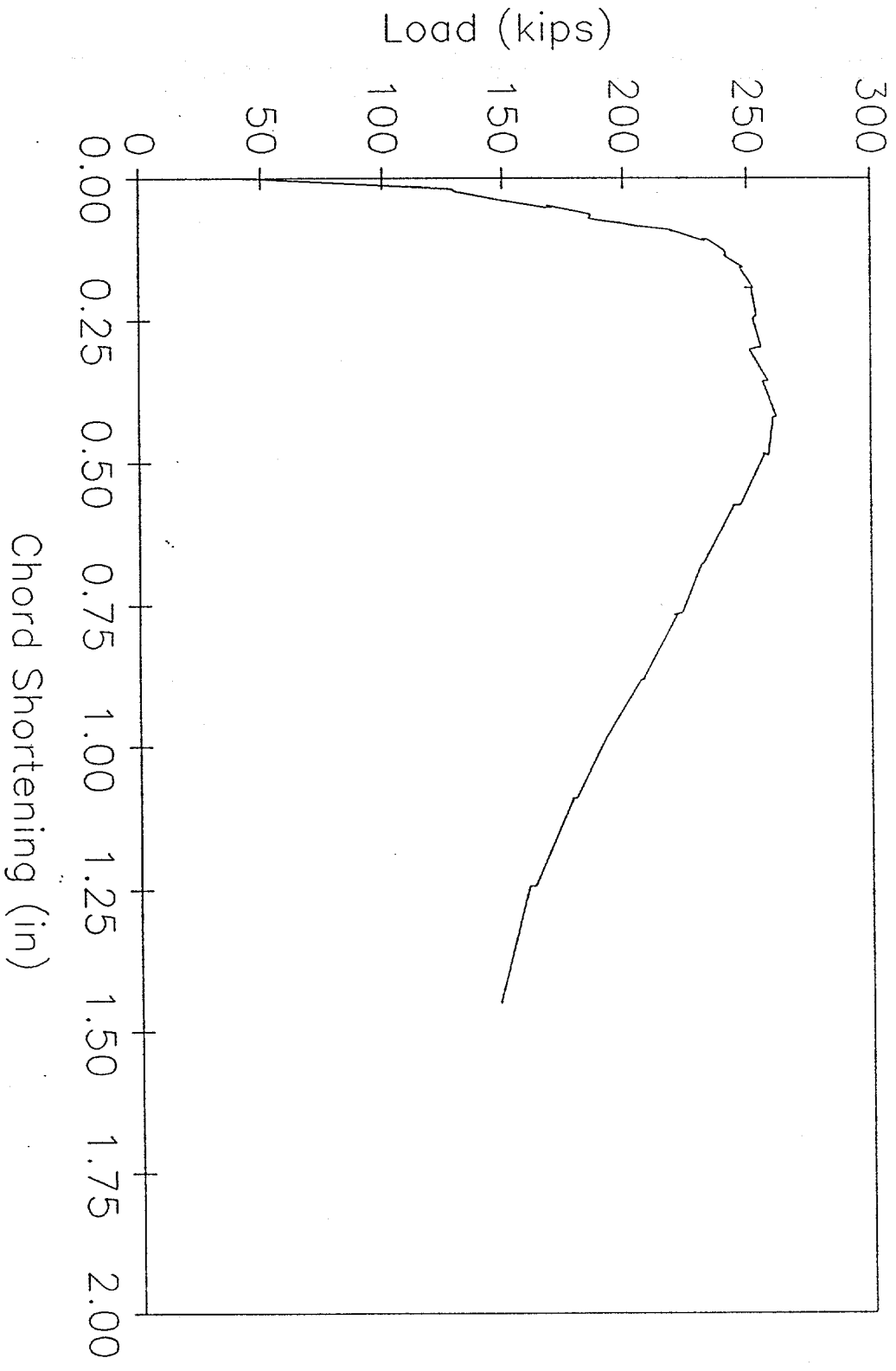


LOAD AND DEFLECTION vs LOAD STEP

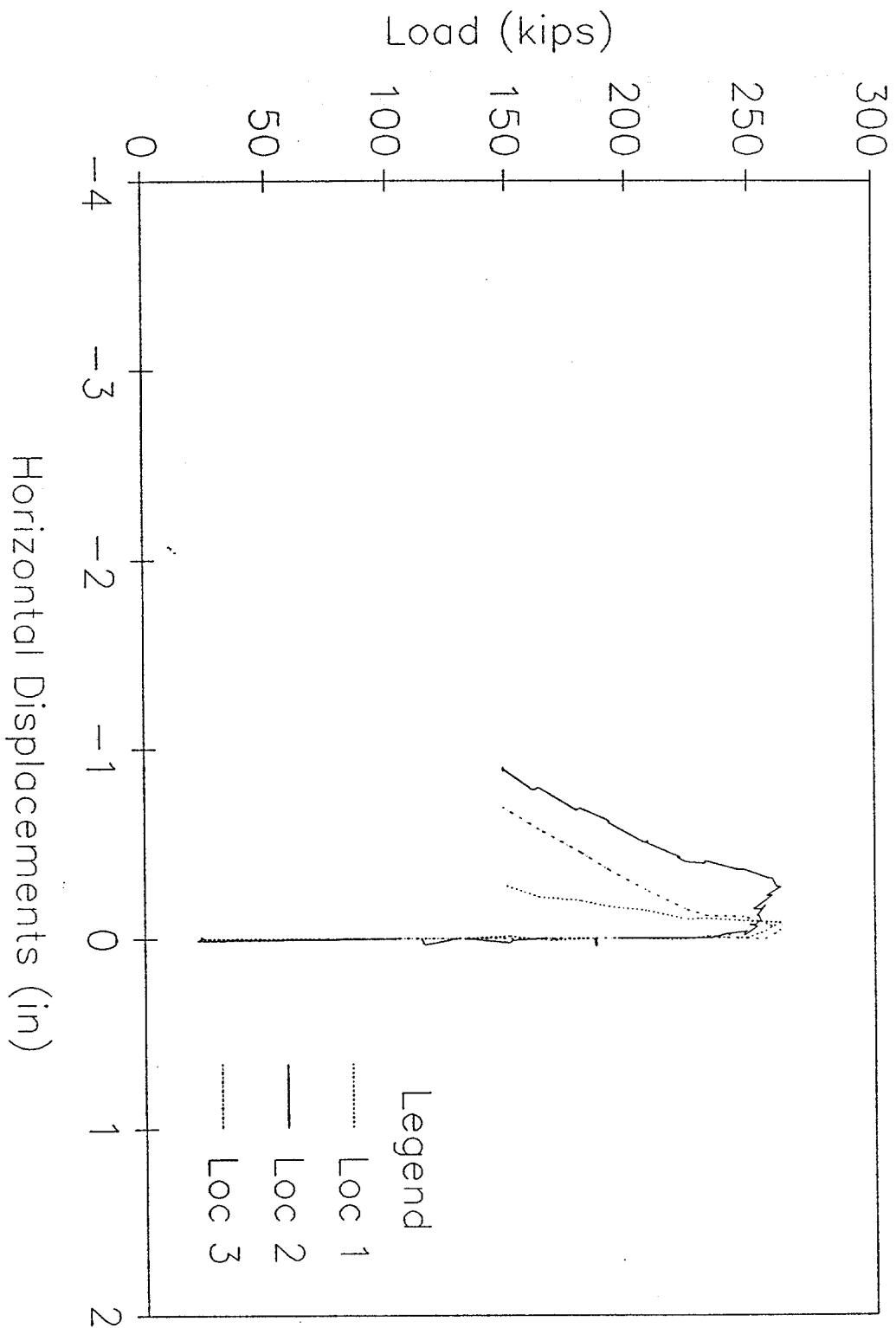
Specimen 18



LOAD vs CHORD SHORTENING
Specimen 18

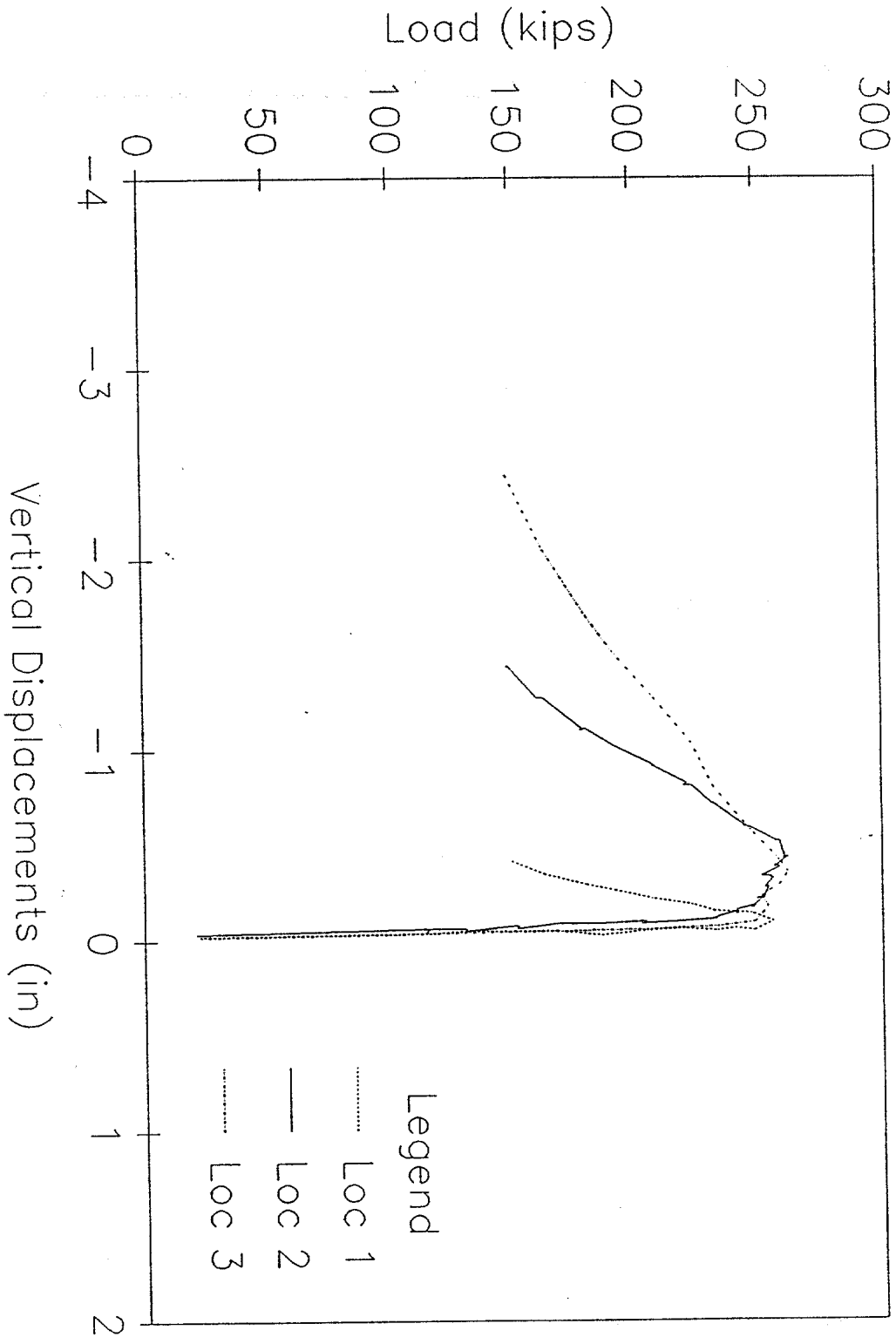


HORIZONTAL DISPLACEMENTS Specimen 18



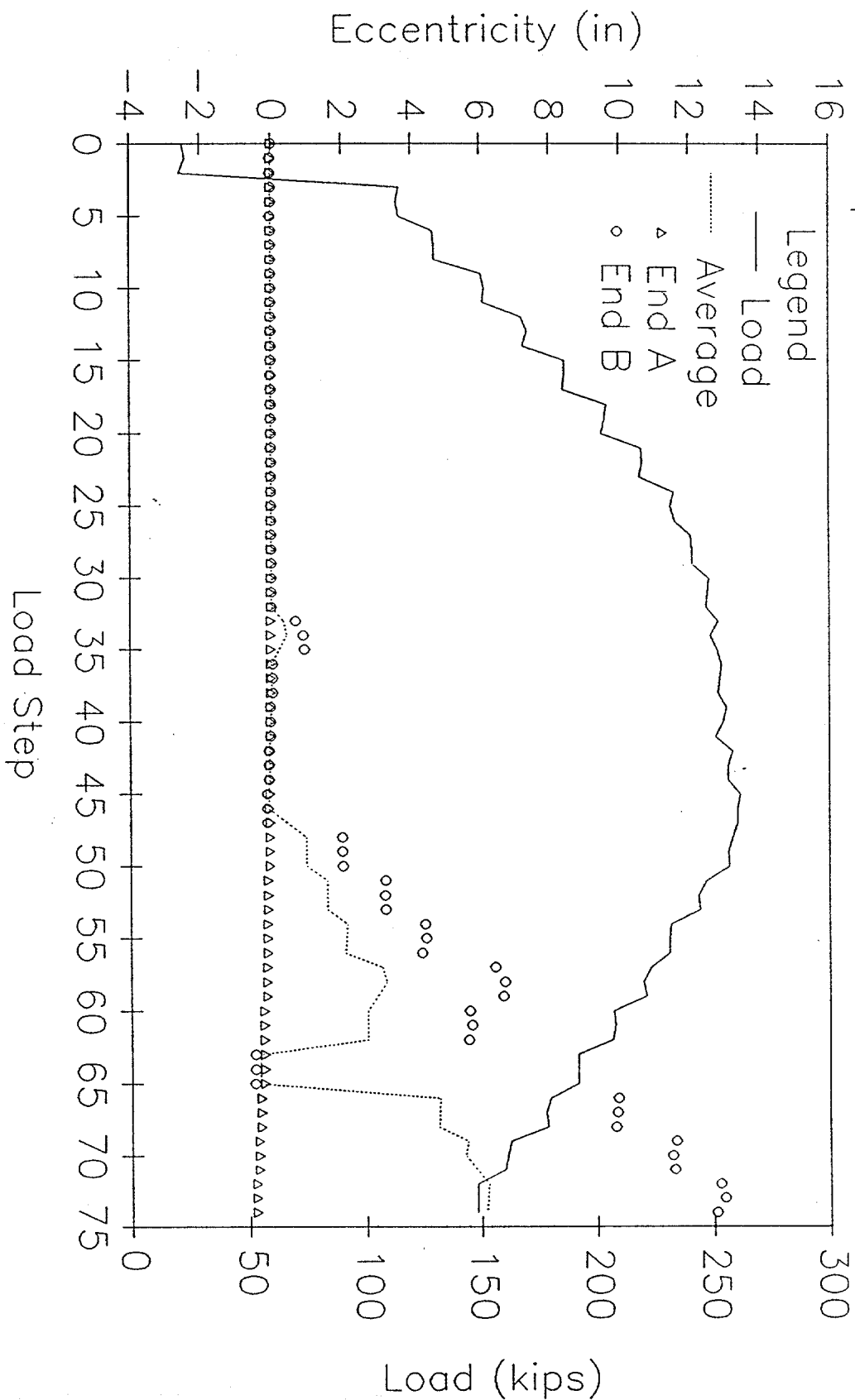
VERTICAL DISPLACEMENTS

Specimen 18



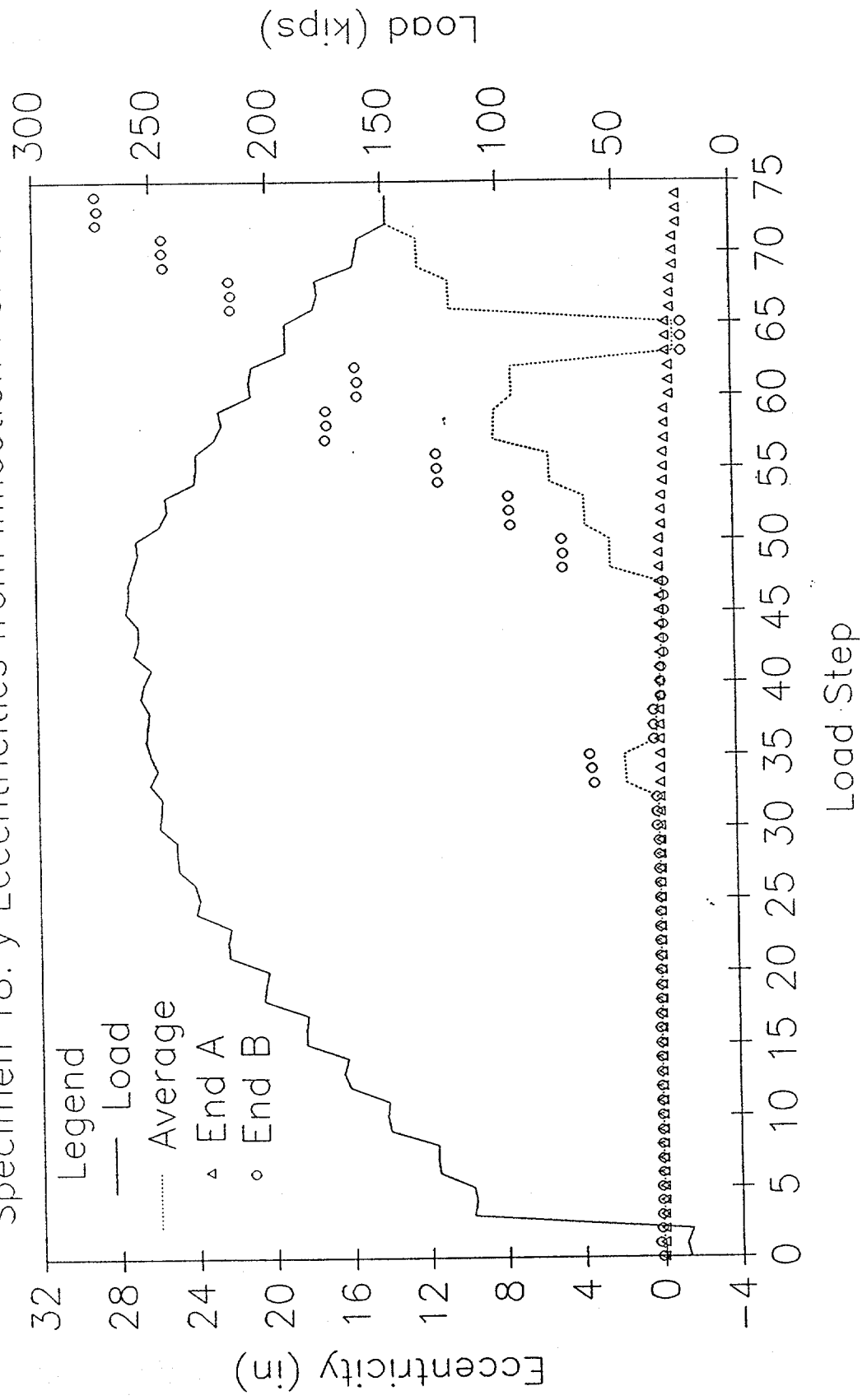
LOAD AND ECCENTRICITY vs LOAD STEP

Specimen 18: x Eccentricities from Inflection Points



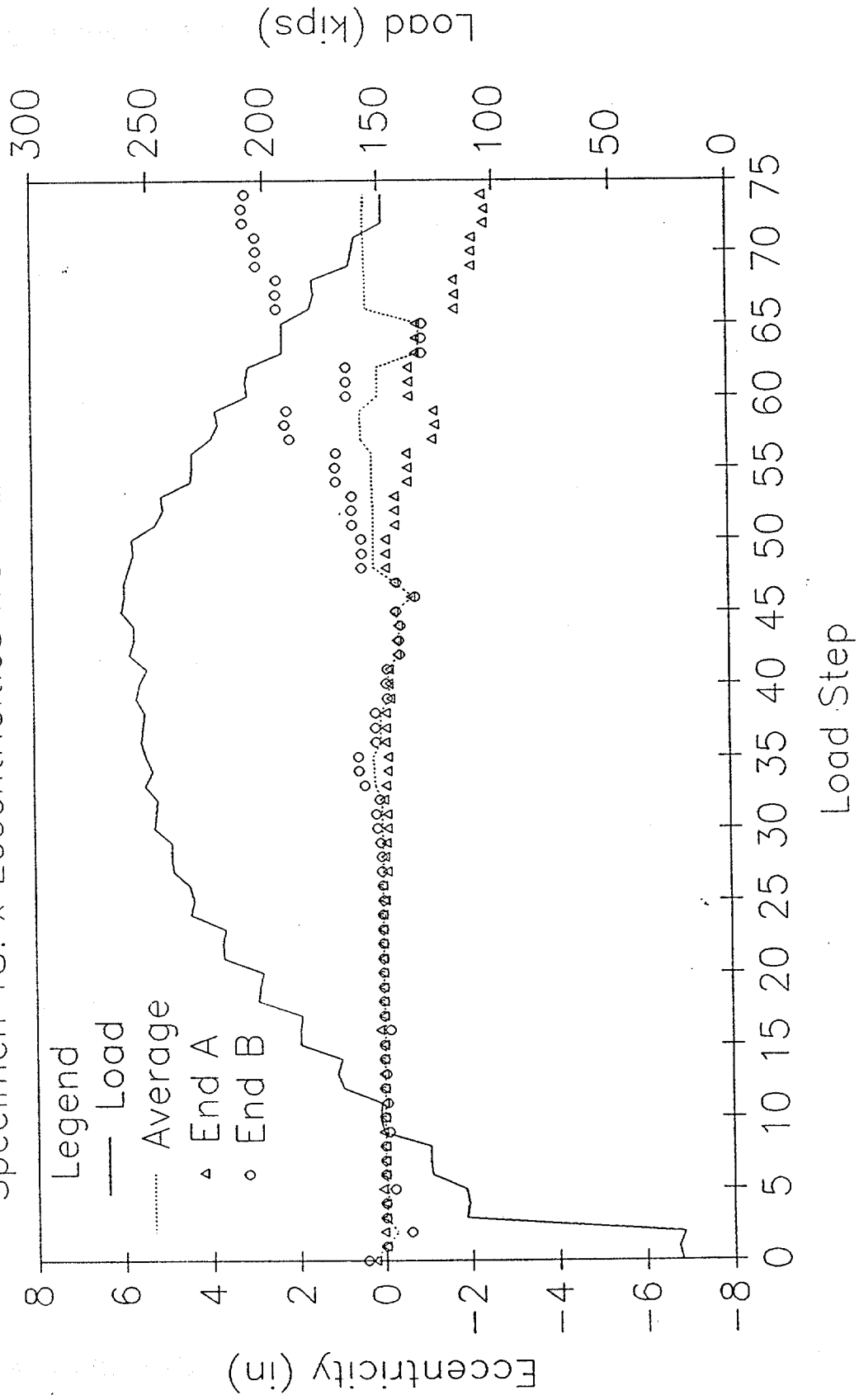
LOAD AND ECCENTRICITY vs LOAD STEP

Specimen 18: y Eccentricities from Inflection Points



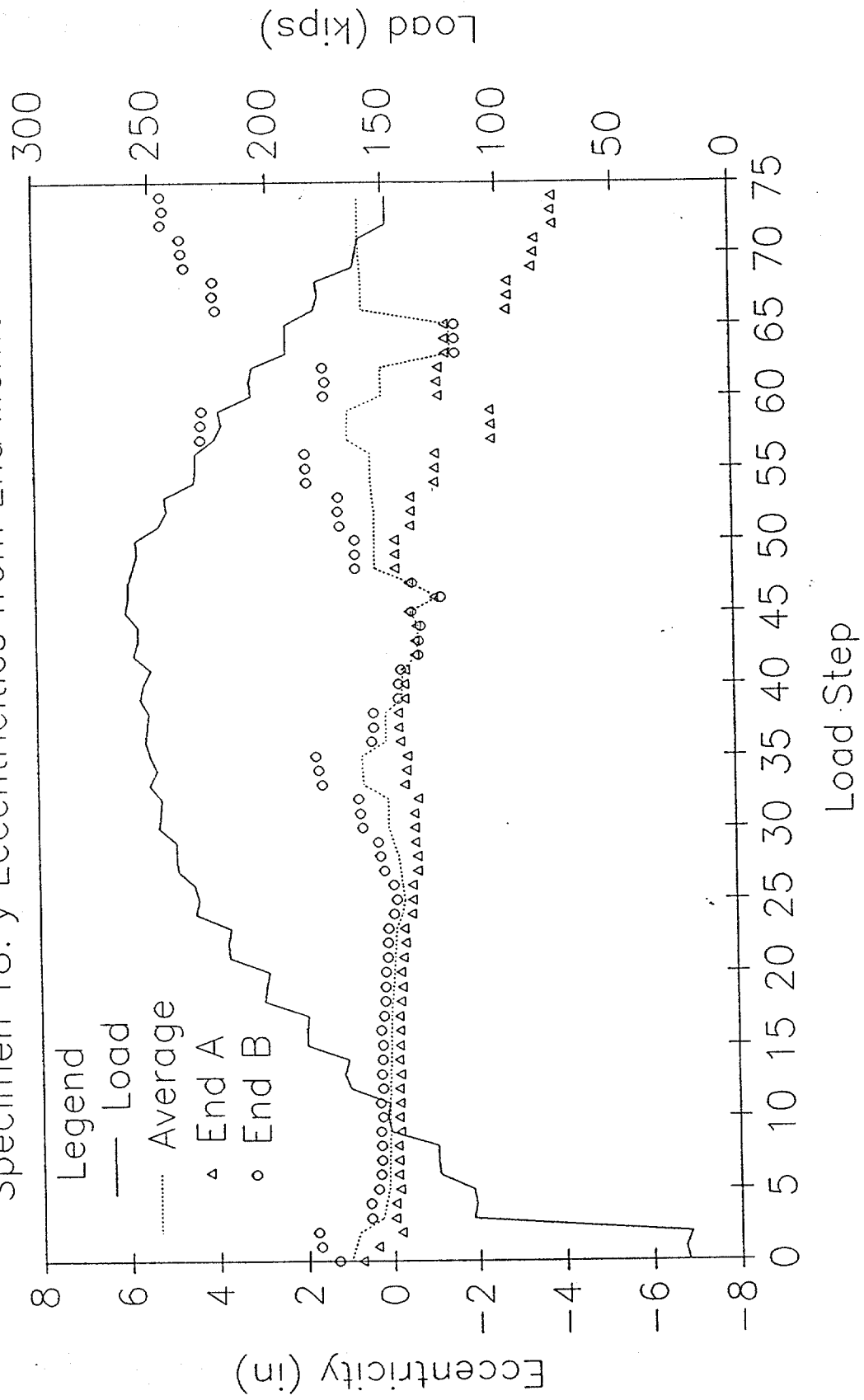
LOAD AND ECCENTRICITY vs LOAD STEP

Specimen 18: x Eccentricities from End Moments



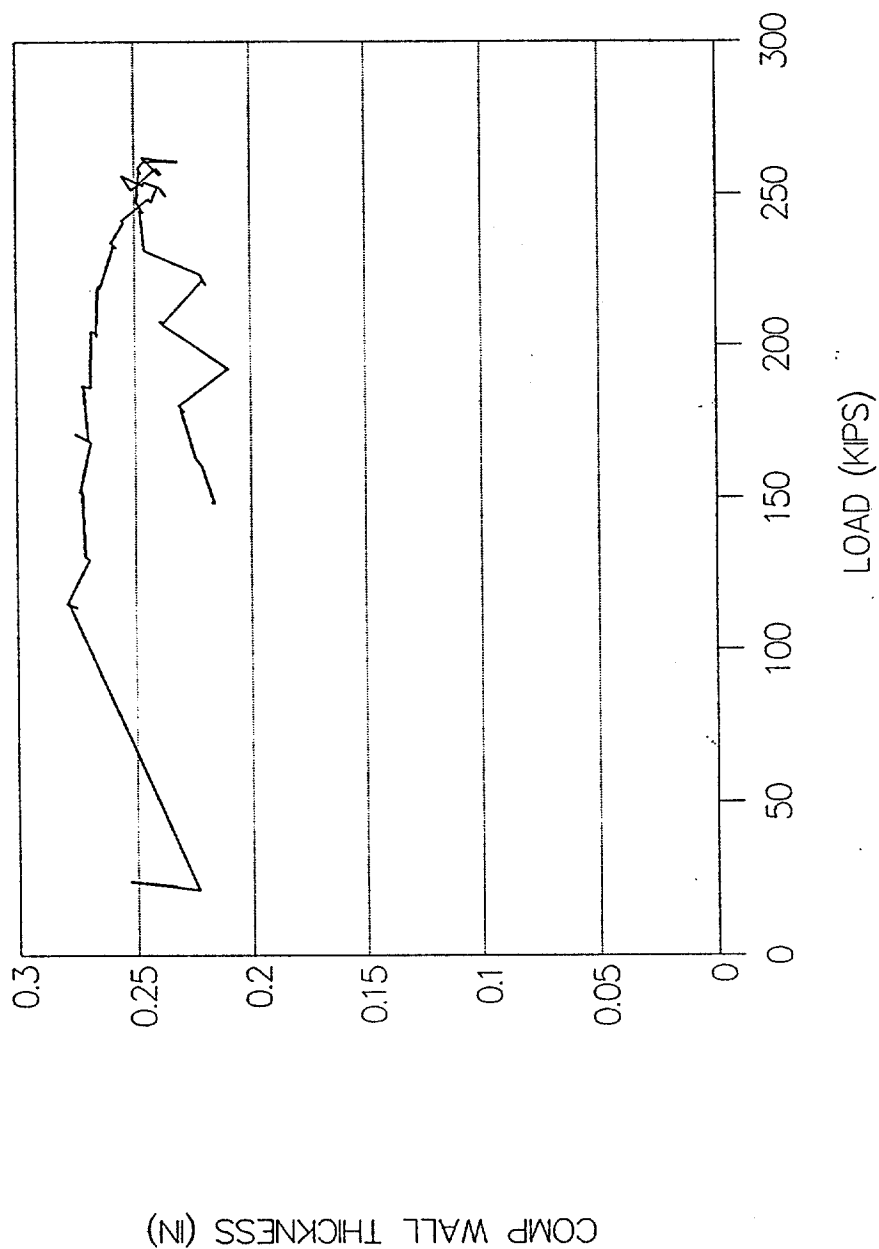
LOAD AND ECCENTRICITY vs LOAD STEP

Specimen 18: y Eccentricities from End Moments



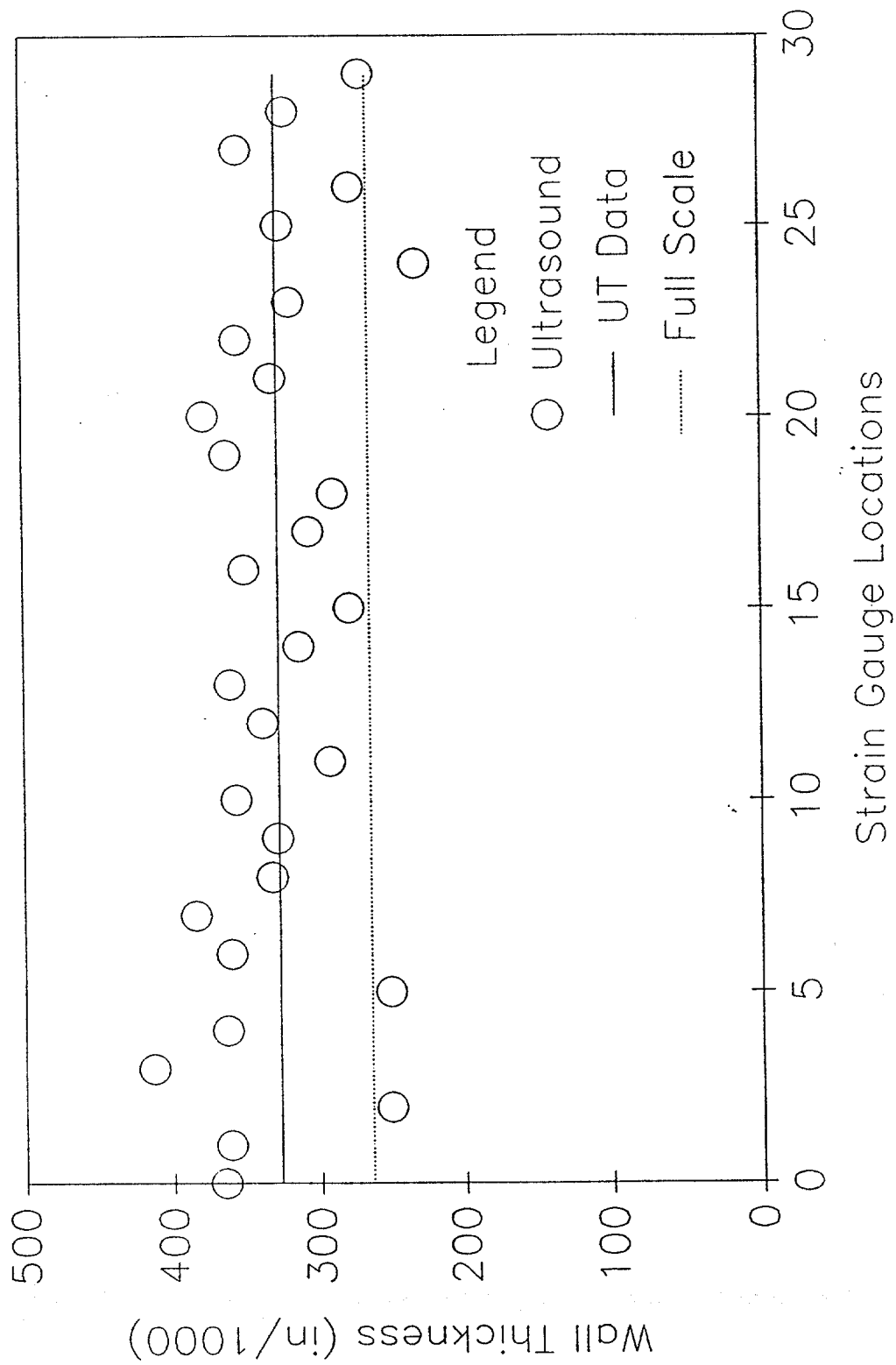
SPECIMEN 18-FULL SCALE TEST

COMPUTED WALL THICKNESS



SPECIMEN 18: WALL THICKNESS

Nominal Wall Thickness = 0.375 in



Ultrasound Data for Specimen 18
(All values in inches)

Gauge No.	UT Thickness	UT Average
0	0.365	
1	0.361	
2	0.251	
3	0.413	
4	0.363	
5	0.251	0.334
6	0.360	
7	0.384	
8	0.332	
9	0.328	
10	0.356	
11	0.292	0.342
12	0.338	
13	0.360	
14	0.313	
15	0.278	
16	0.350	
17	0.306	0.324
18	0.289	
19	0.362	
20	0.377	
21	0.331	
22	0.354	
23	0.318	0.339
24	0.231	
25	0.325	
26	0.276	
27	0.353	
28	0.321	
29	0.269	0.296

Overall Average = 0.327

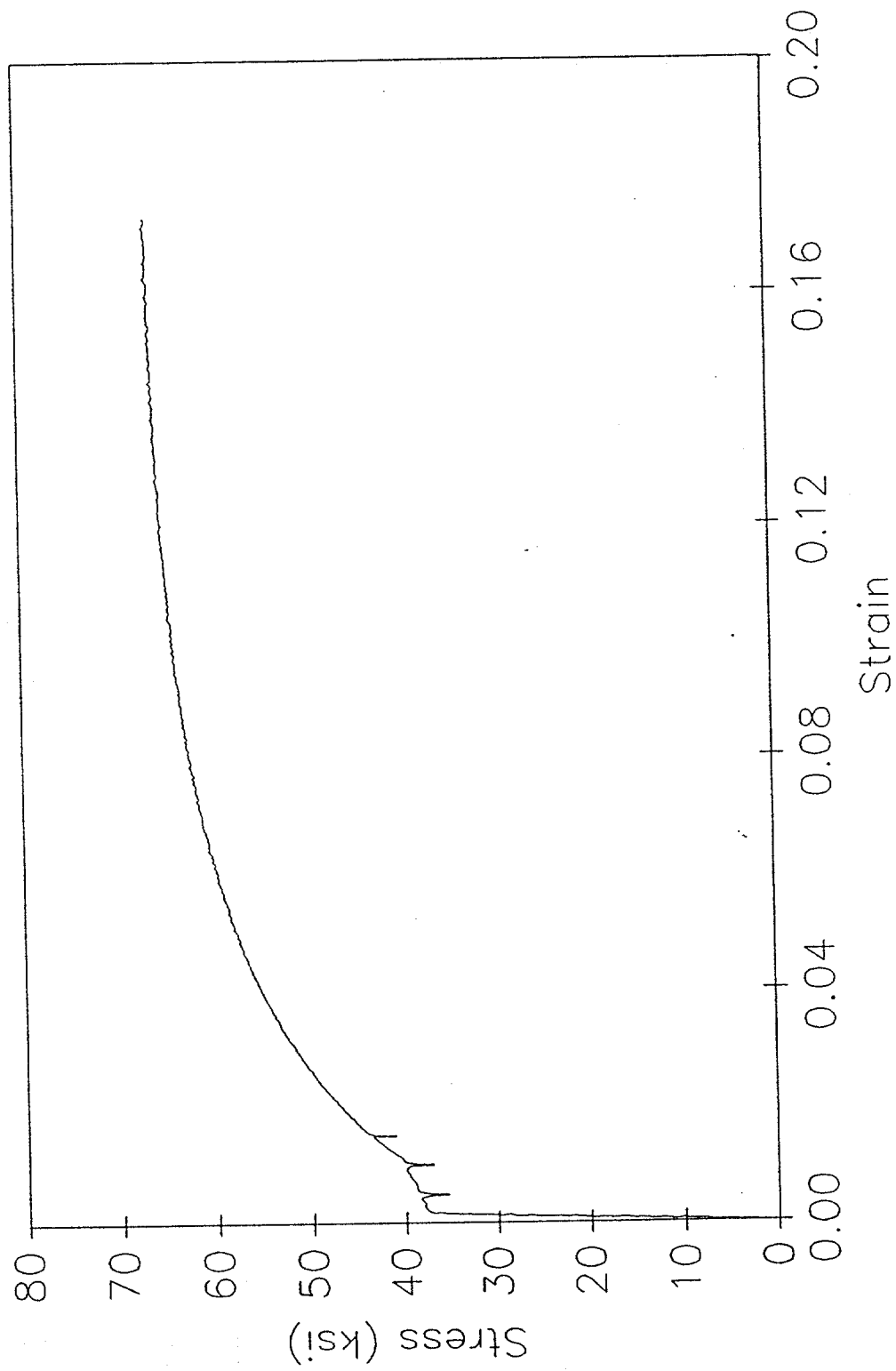
Random Readings near Buckling Point

No.	Reading
1	0.230
2	0.278
3	0.244
4	0.298
5	0.256

Random Average = 0.261

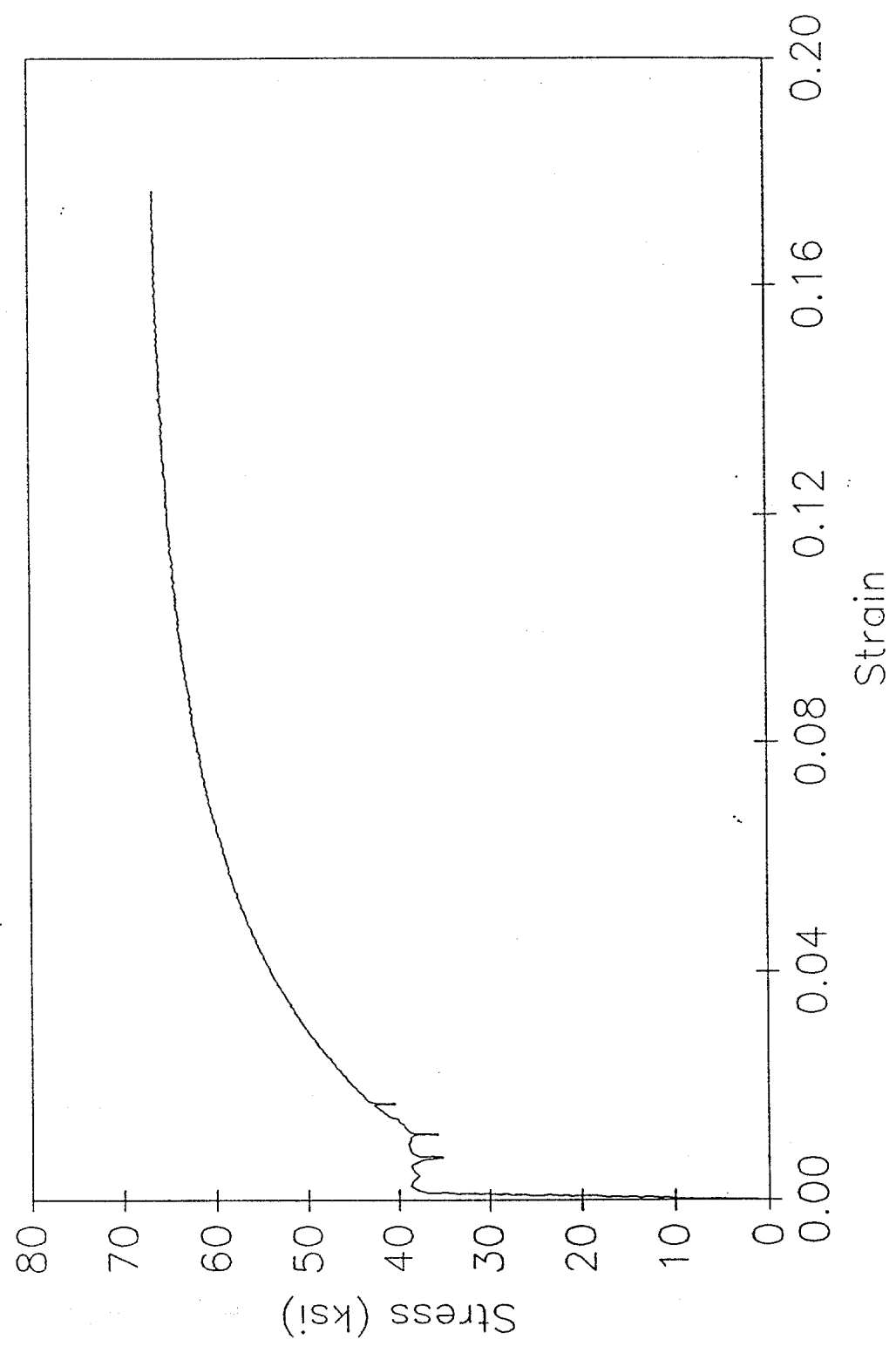
TENSILE SPECIMEN 18-1

Stress vs Strain



TENSILE SPECIMEN 18-2

Stress vs Strain



SPECIMEN 19

DAMAGE SUMMARY

Specimen No. 19

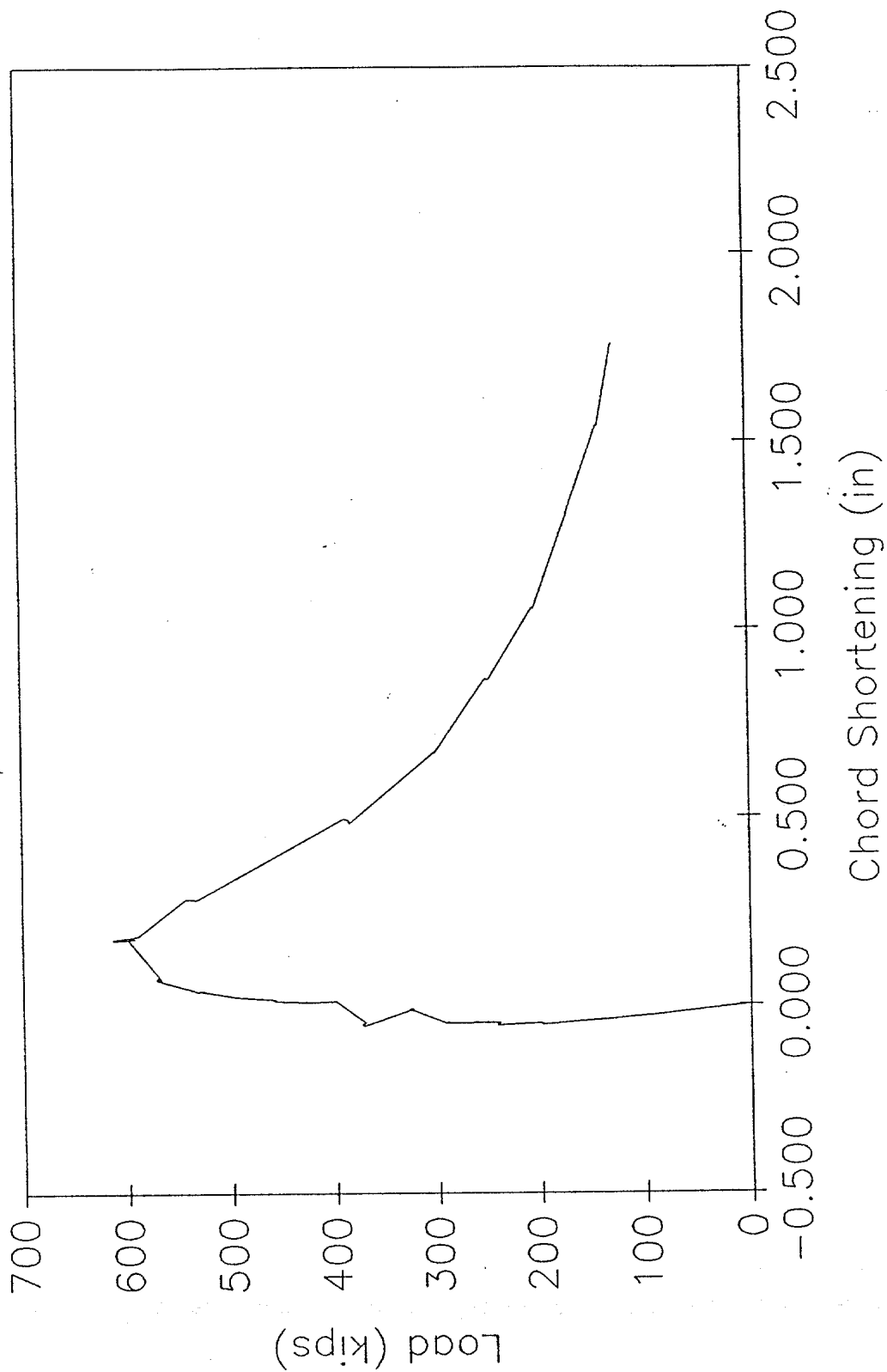
DISTANCE FROM END "B"	*DISTANCE FROM CHALK LINE		DESCRIPTION OF DAMAGE
	LEFT	RIGHT	
1. 34'-3"	4"		70" split in seam (longitudinal crack)

Specimen is corroded!

*Looking from end "A" towards end "B"

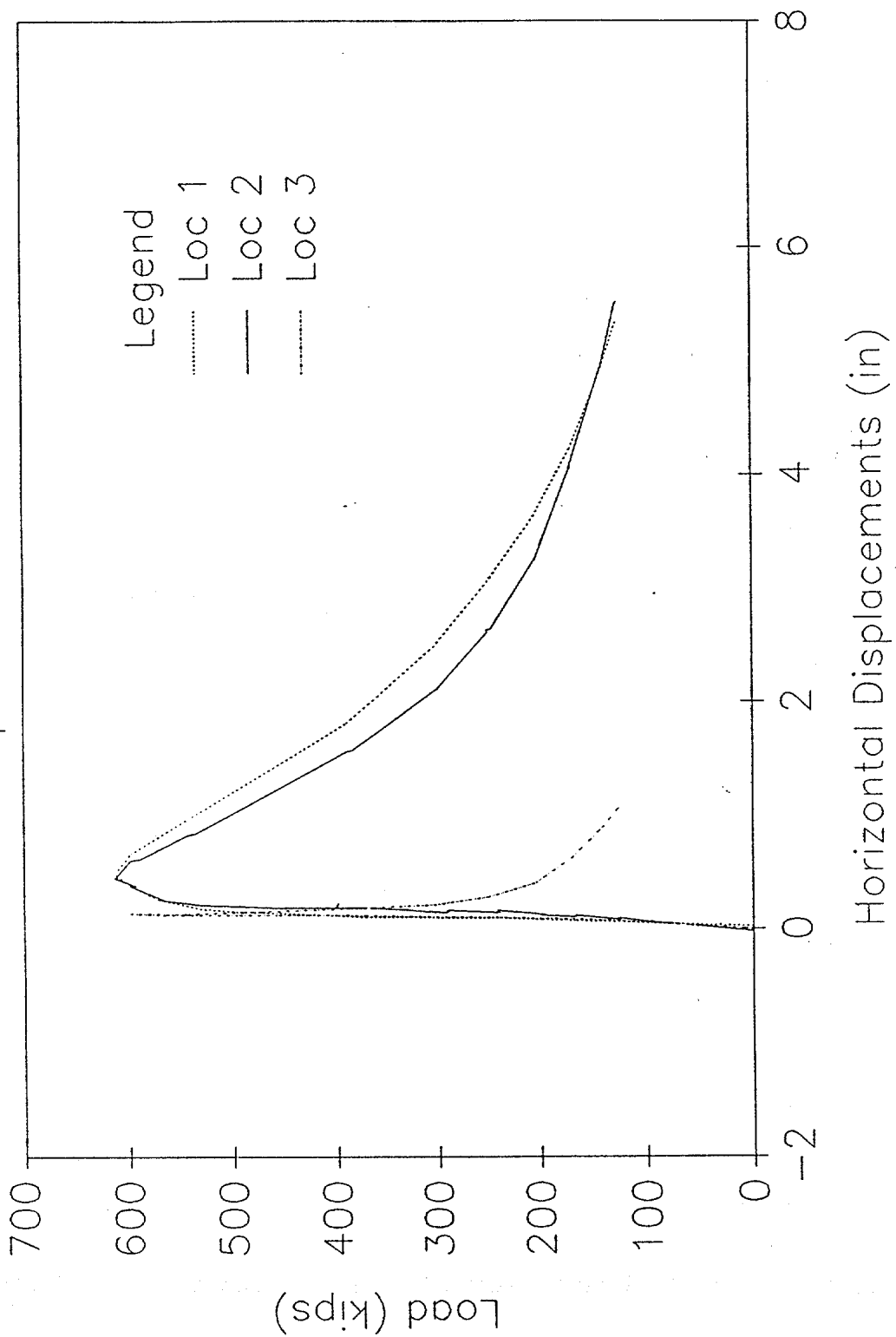
LOAD vs CHORD SHORTENING

Specimen 19



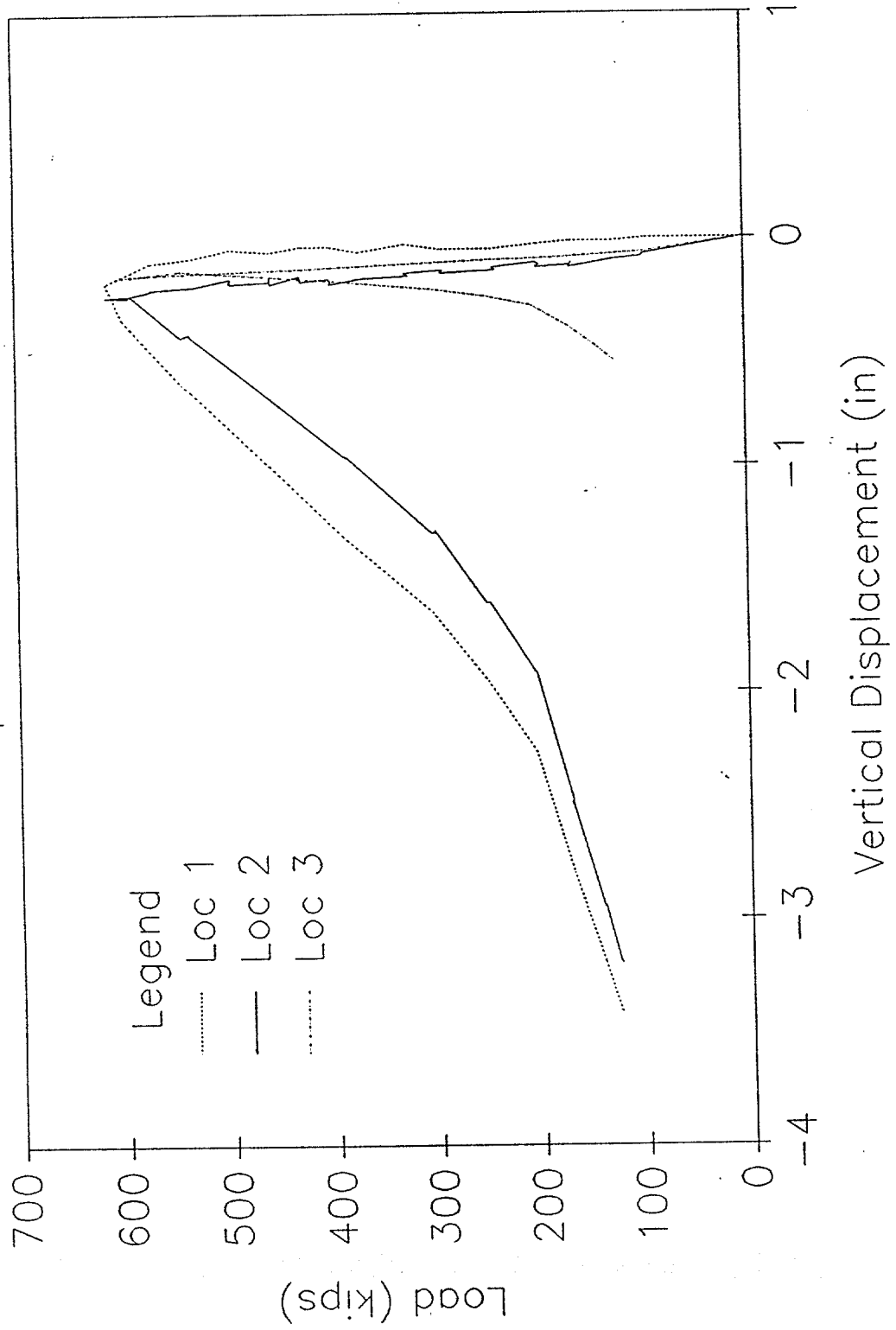
HORIZONTAL DISPLACEMENTS

Specimen 19



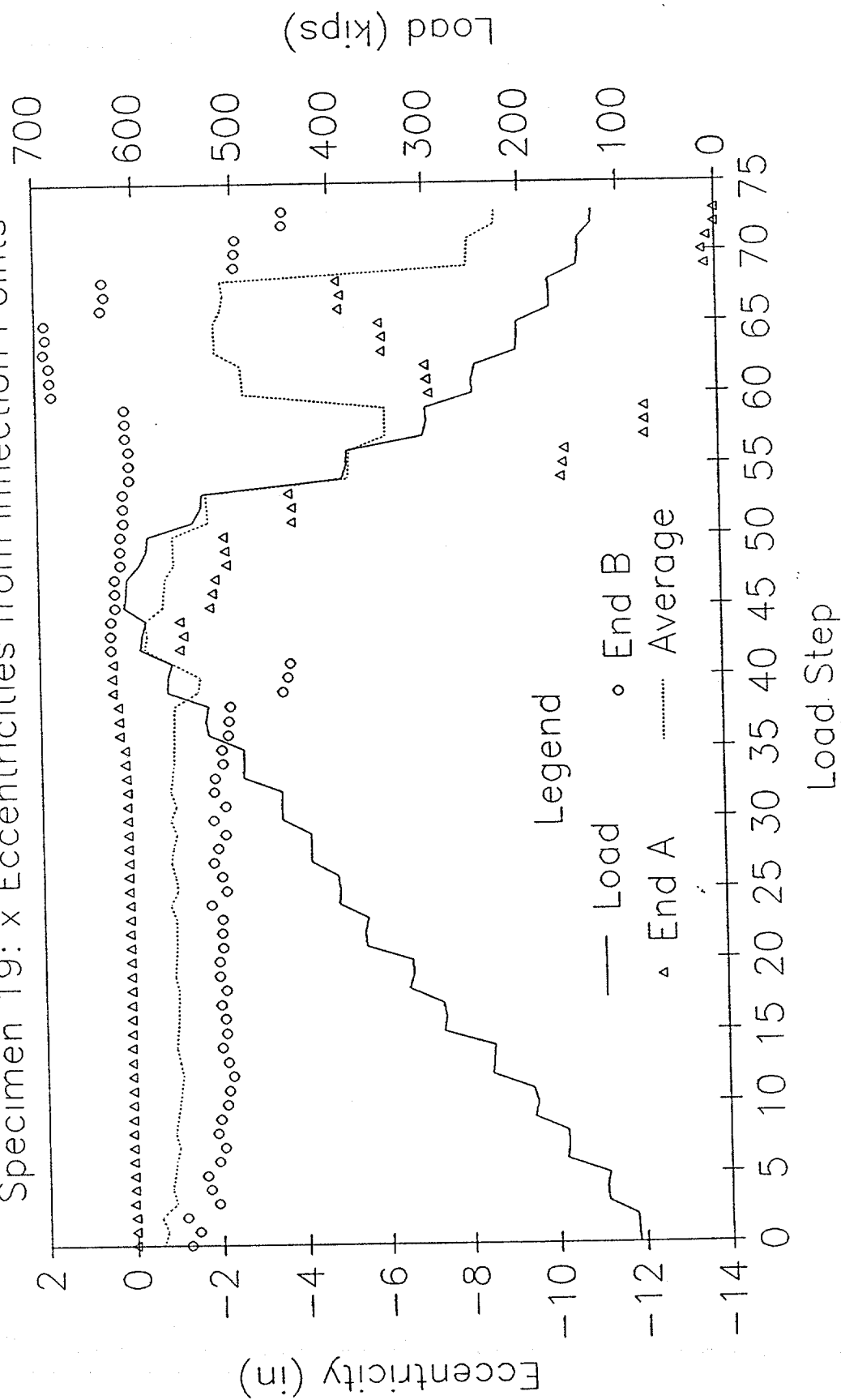
VERTICAL DISPLACEMENTS

Specimen 19



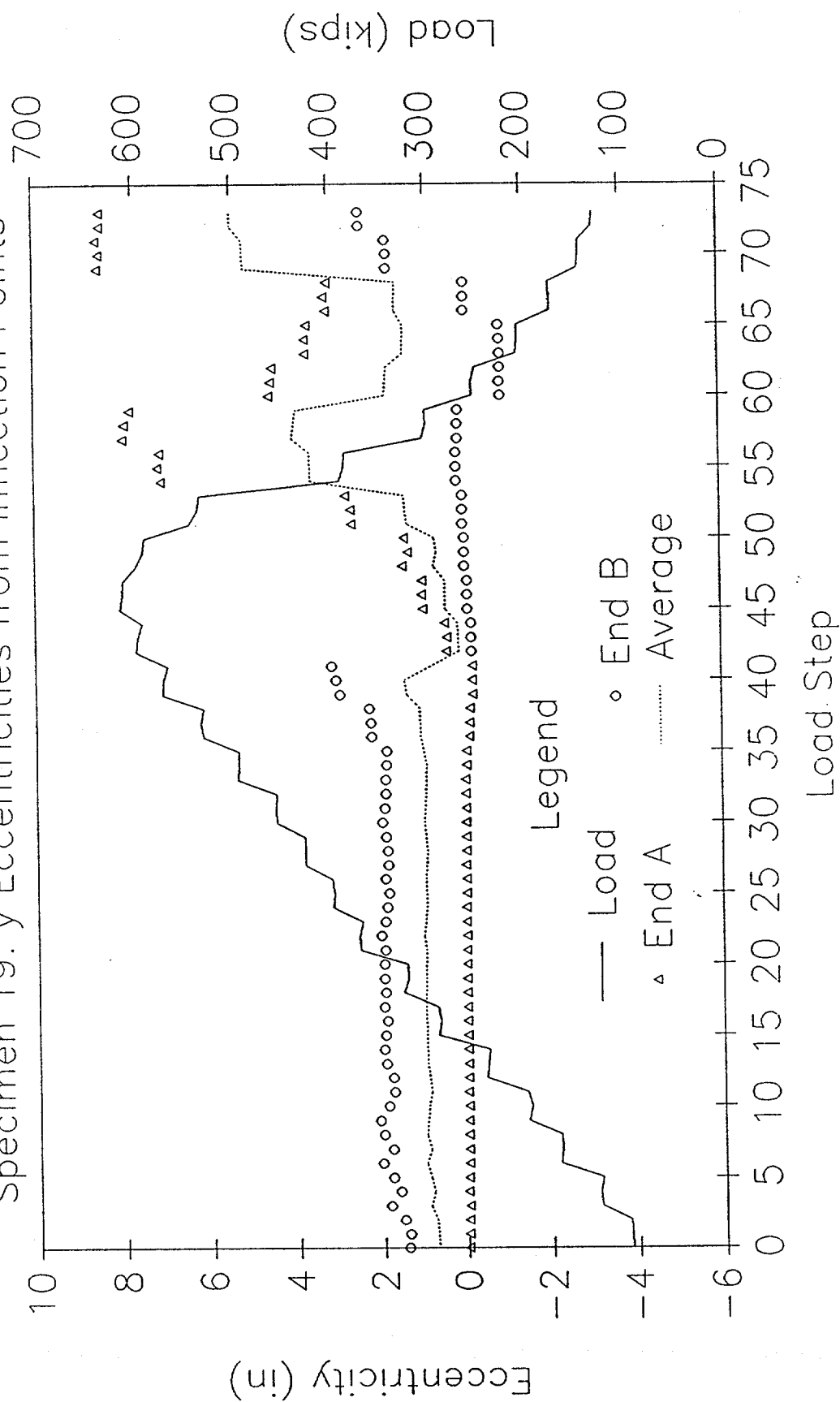
LOAD AND ECCENTRICITY vs LOAD STEP

Specimen 19: x Eccentricities from Inflection Points



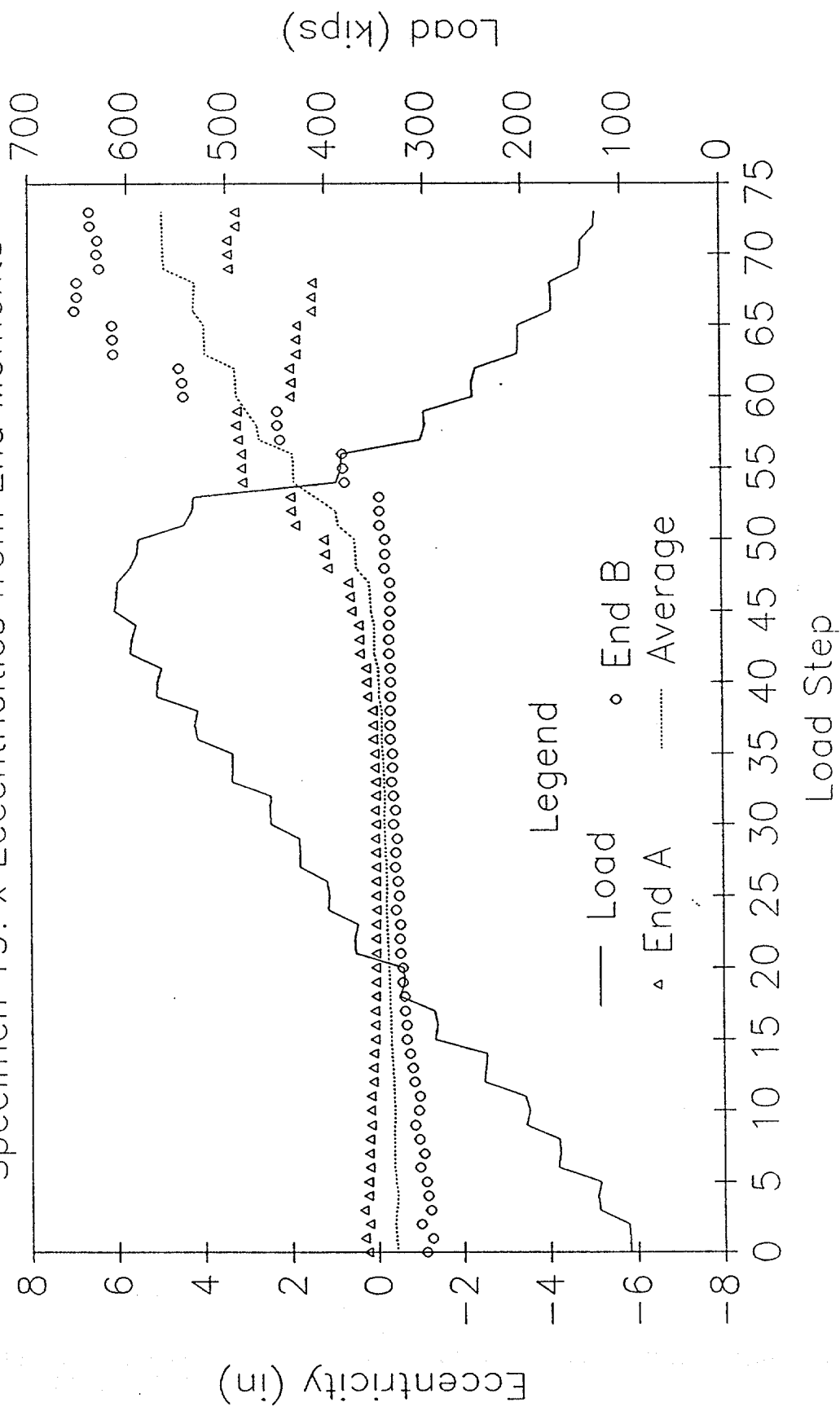
LOAD AND ECCENTRICITY vs LOAD STEP

Specimen 19: y Eccentricities from Inflection Points



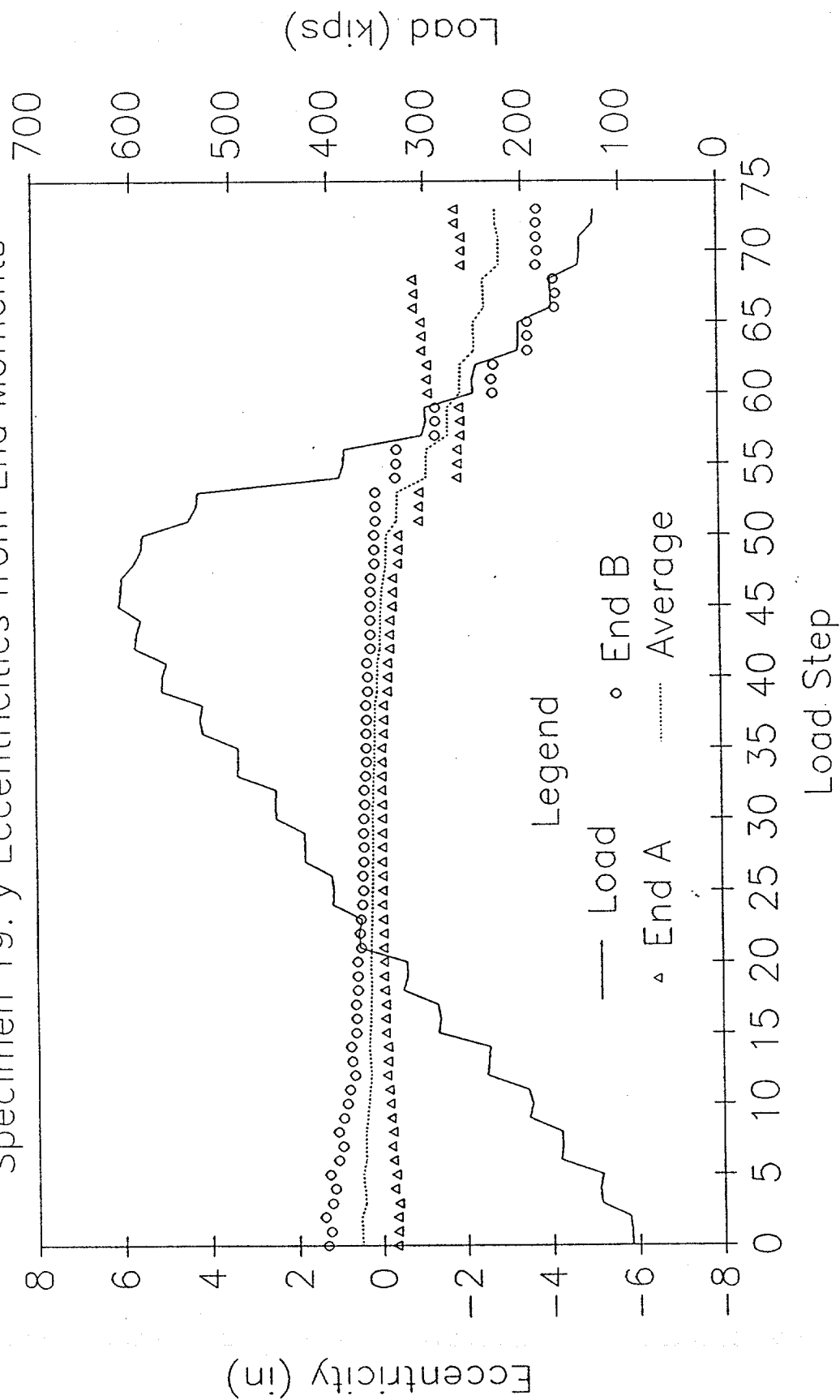
LOAD AND ECCENTRICITY vs LOAD STEP

Specimen 19: x Eccentricities from End Moments



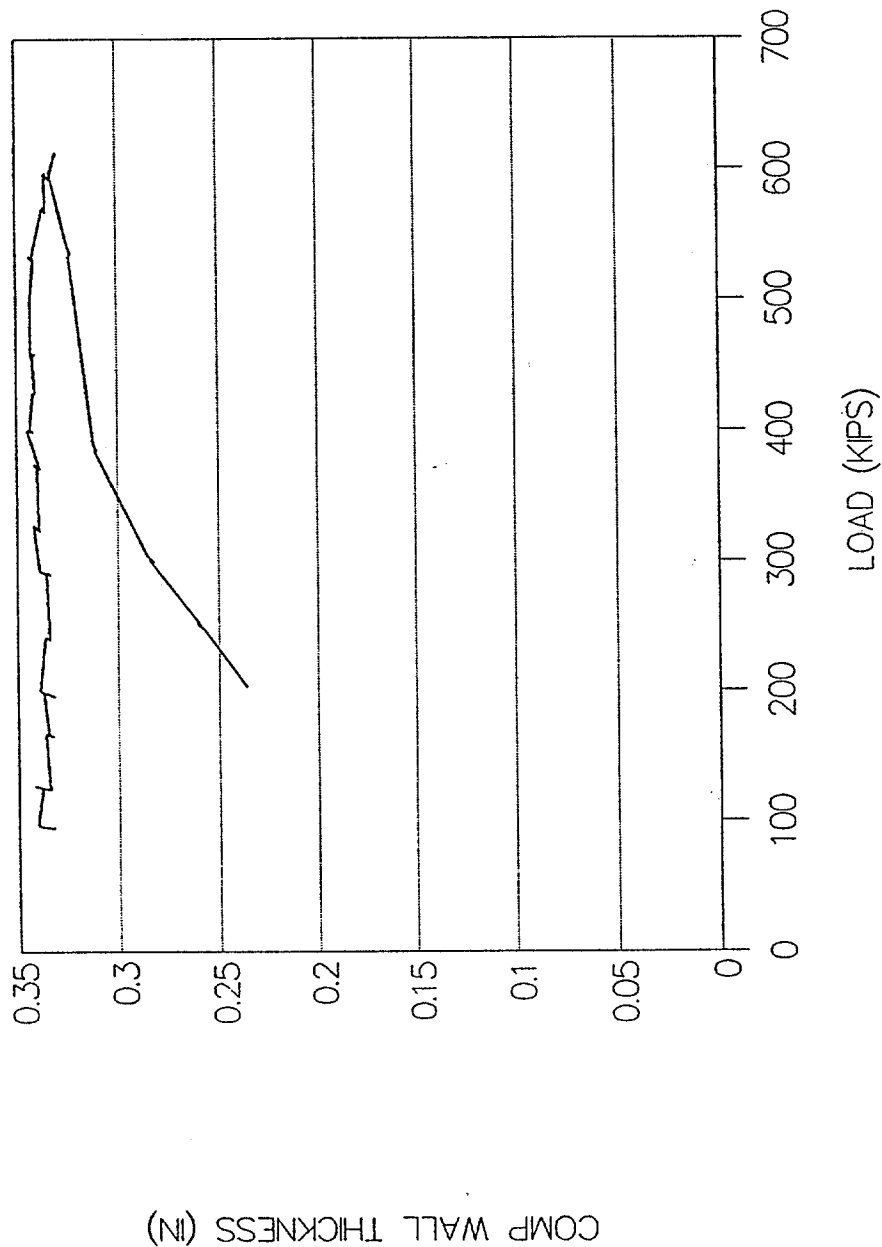
LOAD AND ECCENTRICITY vs LOAD STEP

Specimen 19: y Eccentricities from End Moments



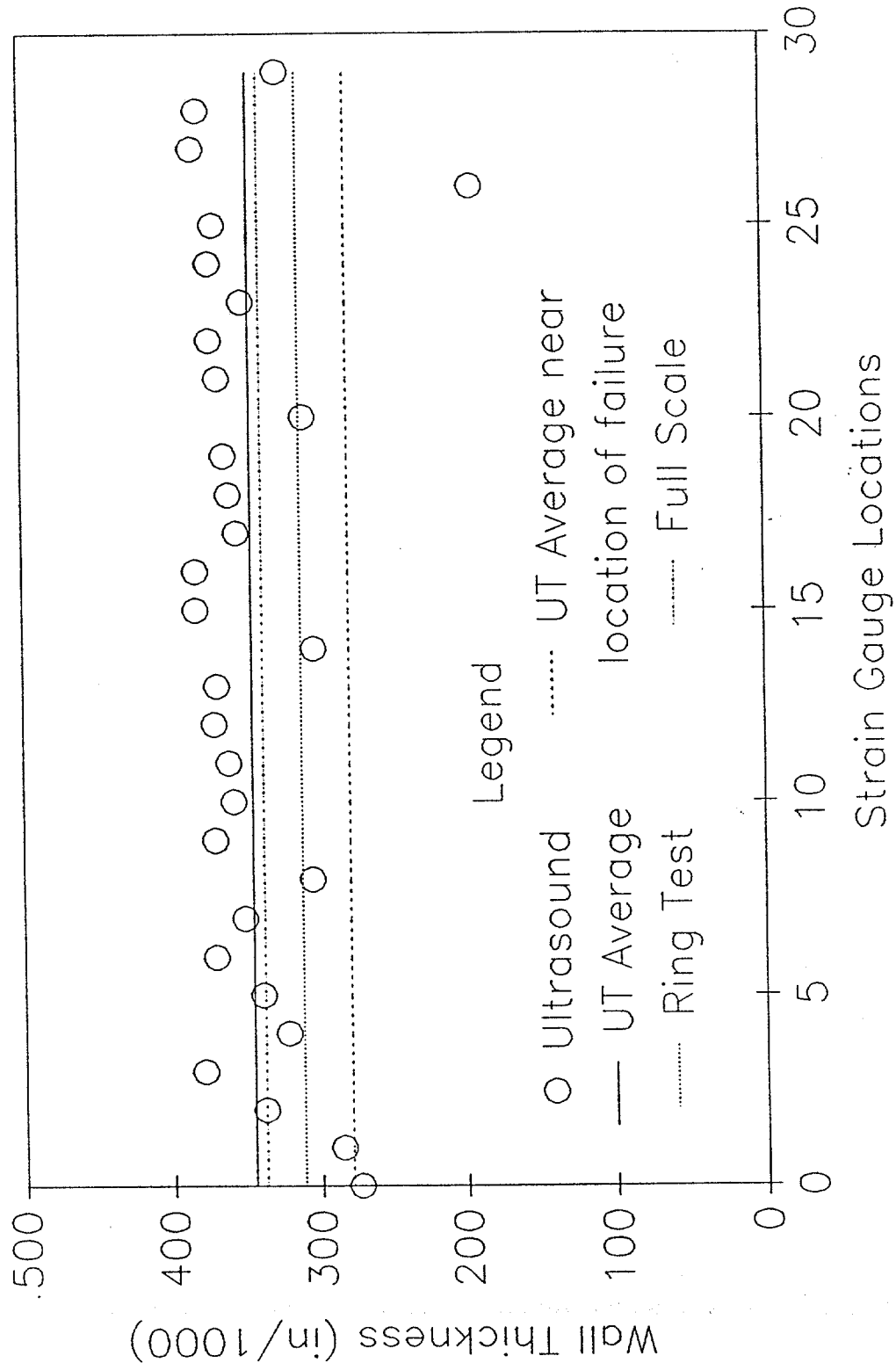
SPECIMEN NO 19-FULL SCALE TEST

COMPUTED WALL THICKNESS



SPECIMEN 19: WALL THICKNESS

Nominal Wall Thickness = 0.375 in



Ultrasound Data for Specimen 19
(All values in inches)

Gauge No.	UT Thickness	UT Average
0	0.273	
1	0.285	
2	0.338	
3	0.379	
4	0.322	
5	0.339	0.323
6	0.371	
7	0.351	
8	0.305	
9	0.371	
10	0.358	
11	0.361	0.353
12	0.371	
13	0.369	
14	0.303	
15	0.383	
16	0.383	
17	0.355	0.361
18	0.360	
19	0.363	
20	0.309	
21	0.367	
22	0.372	
23	0.350	0.353
24	0.372	
25	0.369	
26	0.193	
27	0.383	
28	0.379	
29	0.325	0.337

Overall Average = 0.345

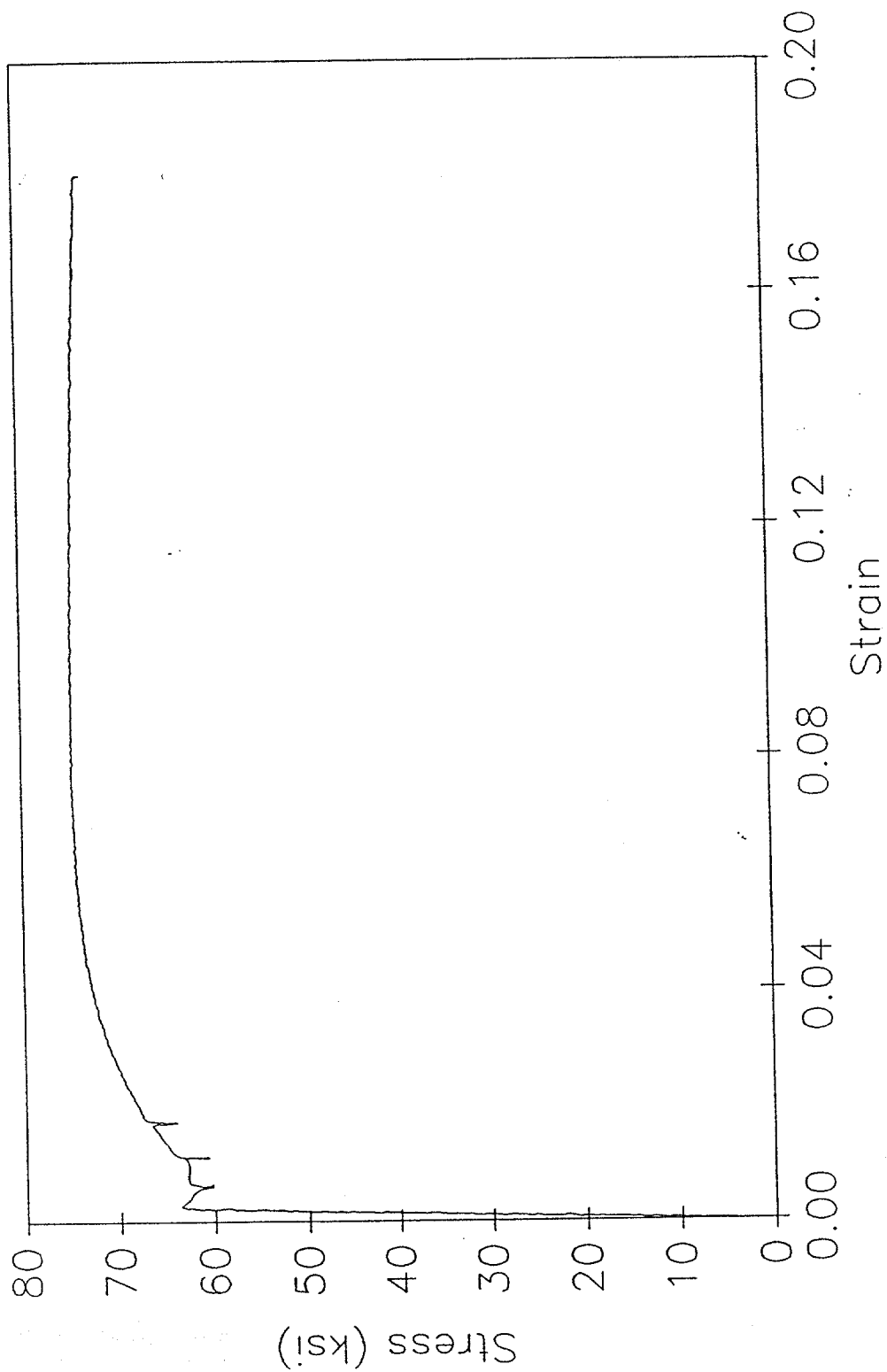
Random Readings near Buckling Point

No.	Reading
1	0.305
2	0.277
3	0.285
4	0.298
5	0.287
6	0.288
7	0.206
8	0.284

Random Average = 0.279

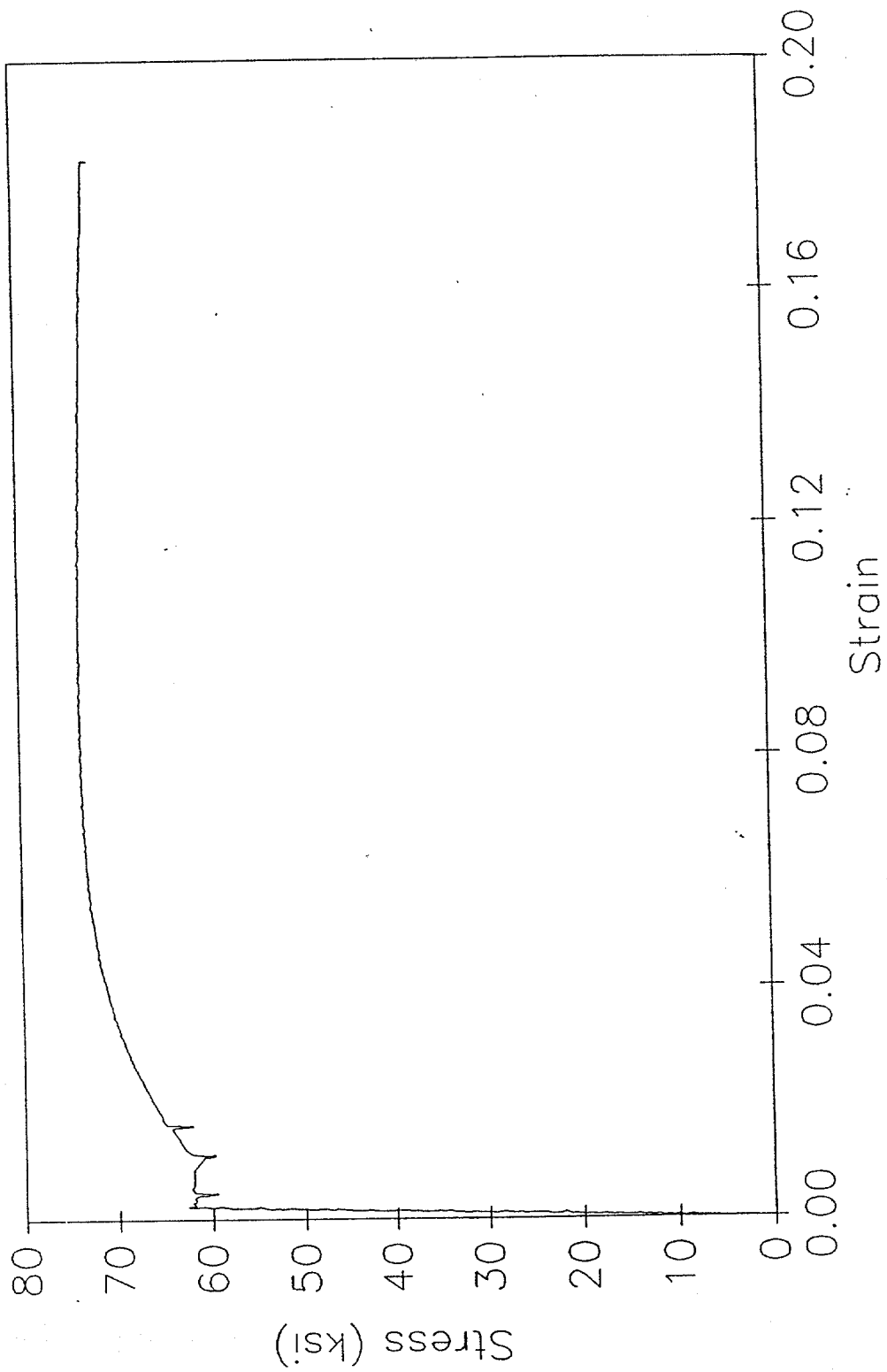
TENSILE SPECIMEN 19--1

Stress vs Strain



TENSILE SPECIMEN 19-2

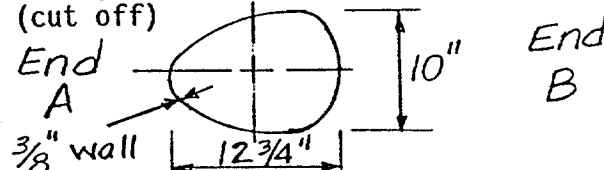
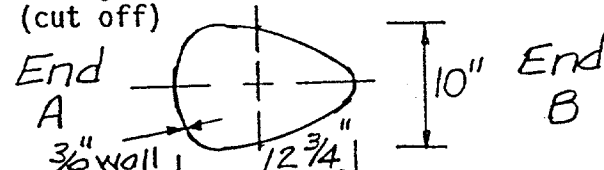
Stress vs Strain



SPECIMEN 20

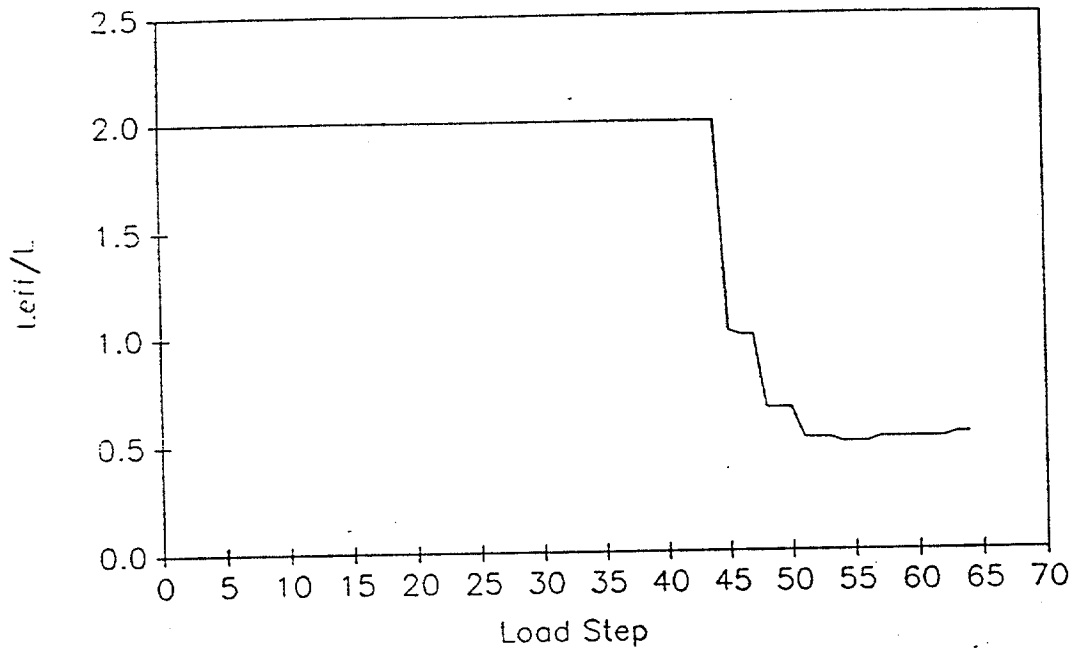
DAMAGE SUMMARY

Specimen No. 20

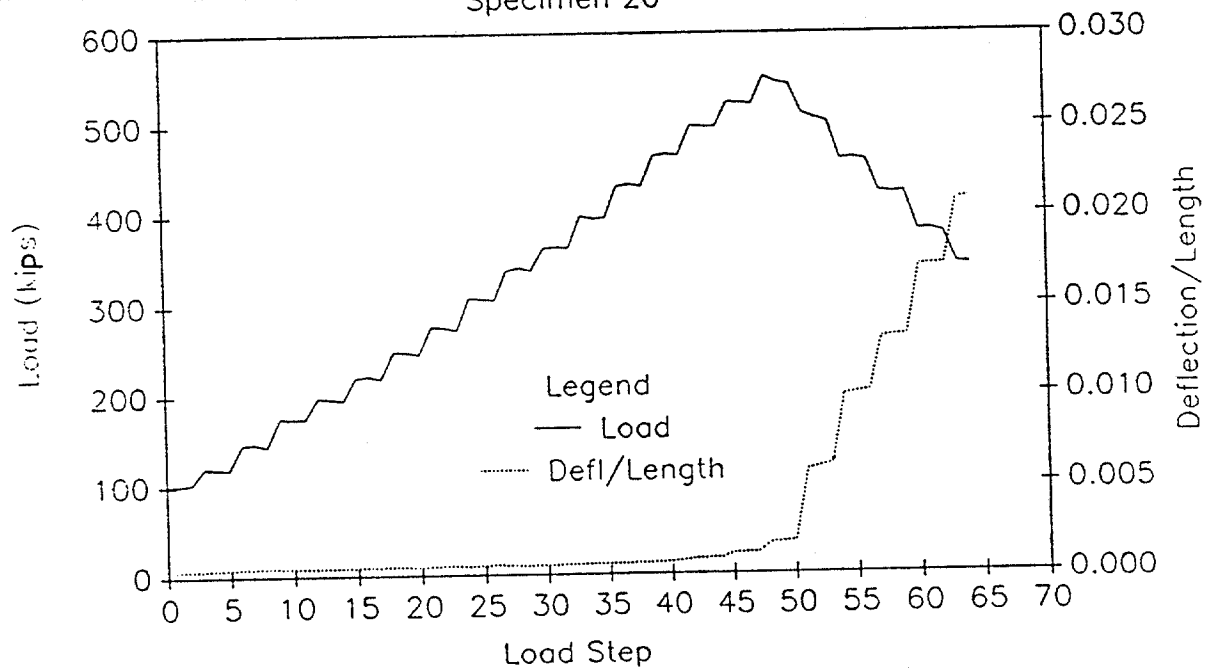
DISTANCE FROM END "B"	*DISTANCE FROM CHALK LINE		DESCRIPTION OF DAMAGE
	LEFT	RIGHT	
1. 18'-10"		13"	<p>Oblong welded bracing attachment (cut off)</p> 
2. 17'-5"		13"	<p>Oblong welded bracing attachment (cut off)</p> 
3. 10'-10 3/4"	17"		2" dia., 1/4" wall, round bracing attachment (cut off)
4. 25'-6 5/8"	17 1/4"		2" dia., 1/4" wall, round bracing attachment (cut off)

* Looking from end "A" towards end "B"

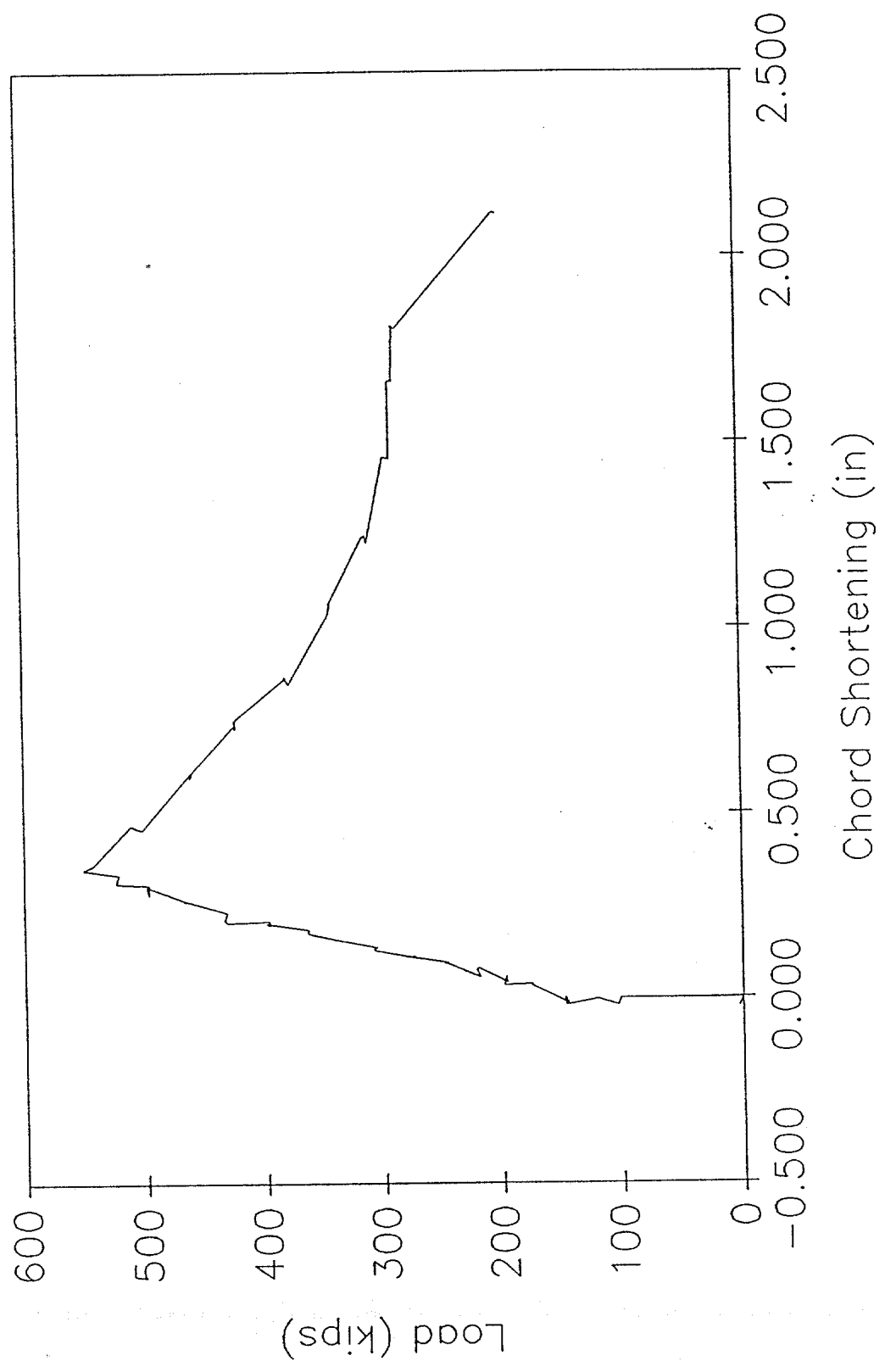
EFFECTIVE LENGTH vs LOAD STEP
Specimen 20



LOAD AND DEFLECTION vs LOAD STEP
Specimen 20

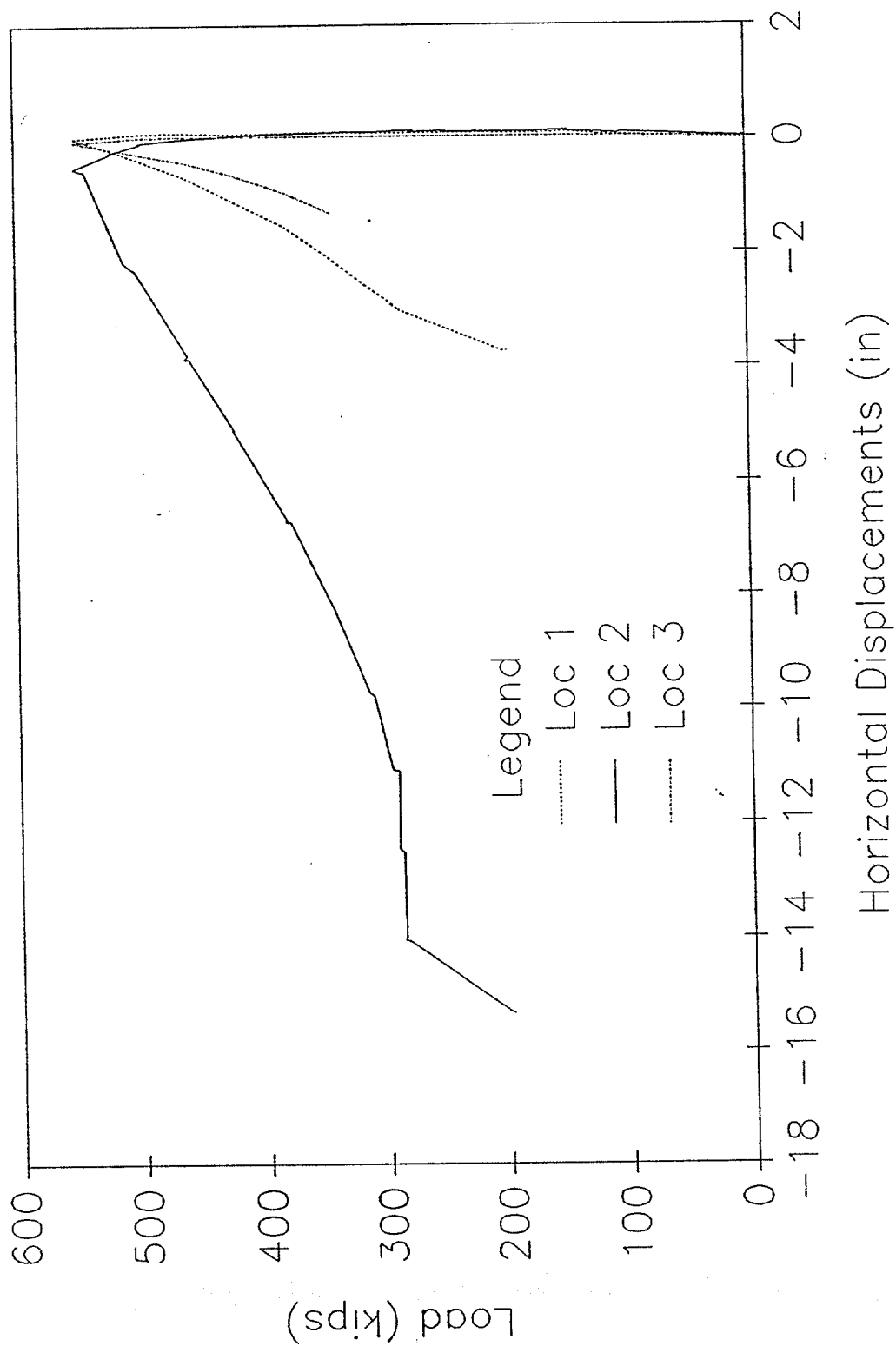


LOAD vs CHORD SHORTENING
Specimen 20



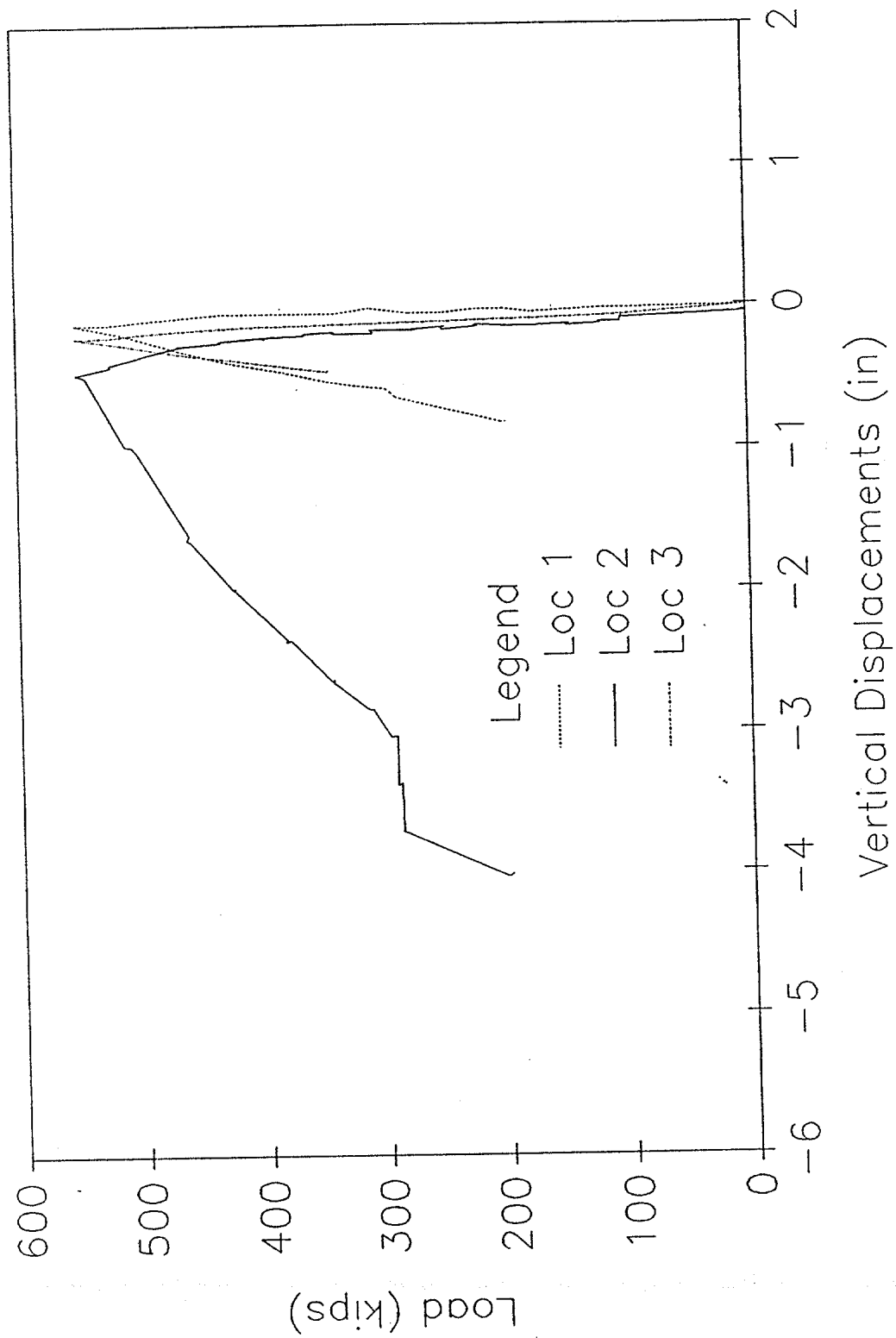
HORIZONTAL DISPLACEMENTS

Specimen 20



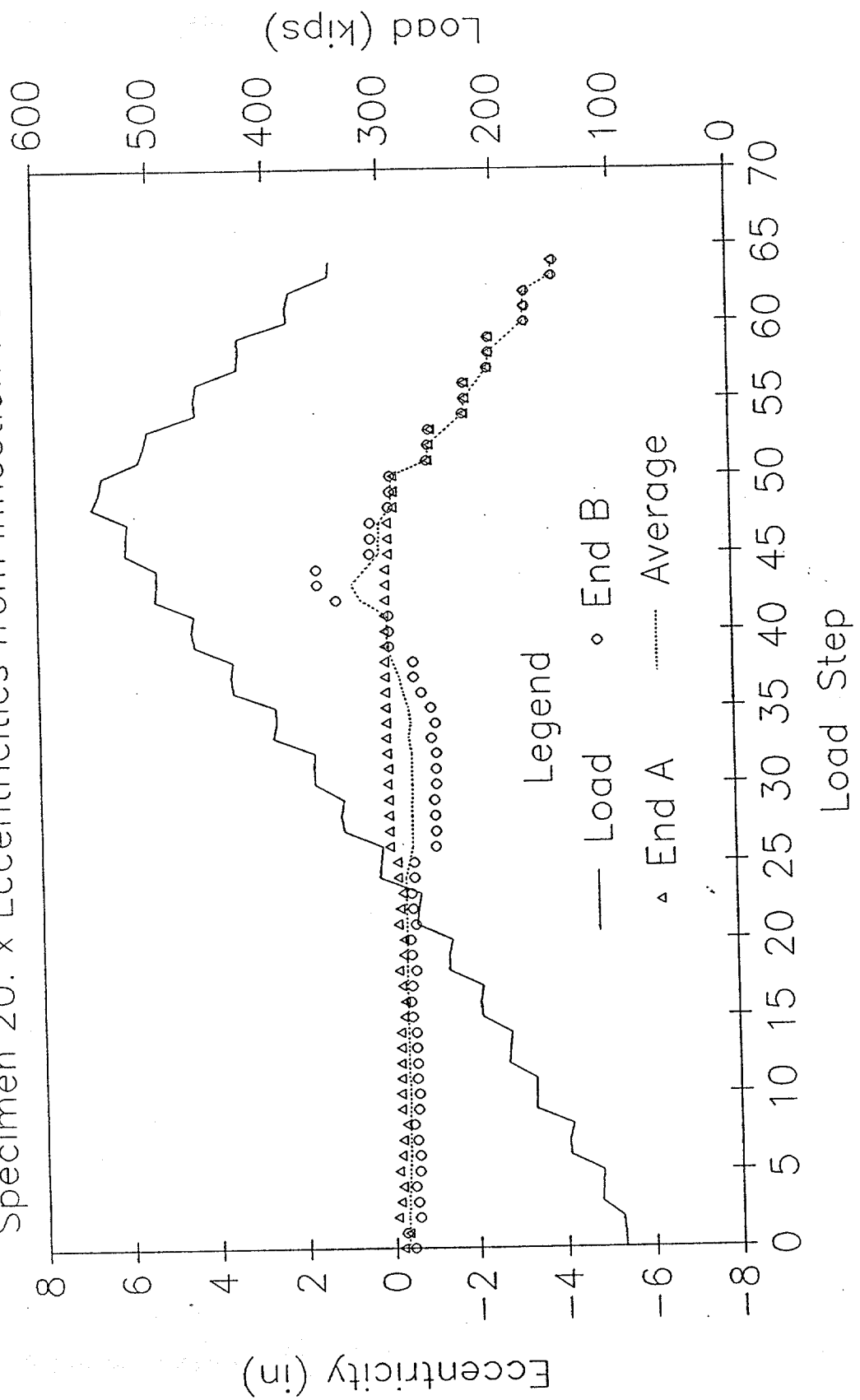
VERTICAL DISPLACEMENTS

Specimen 20



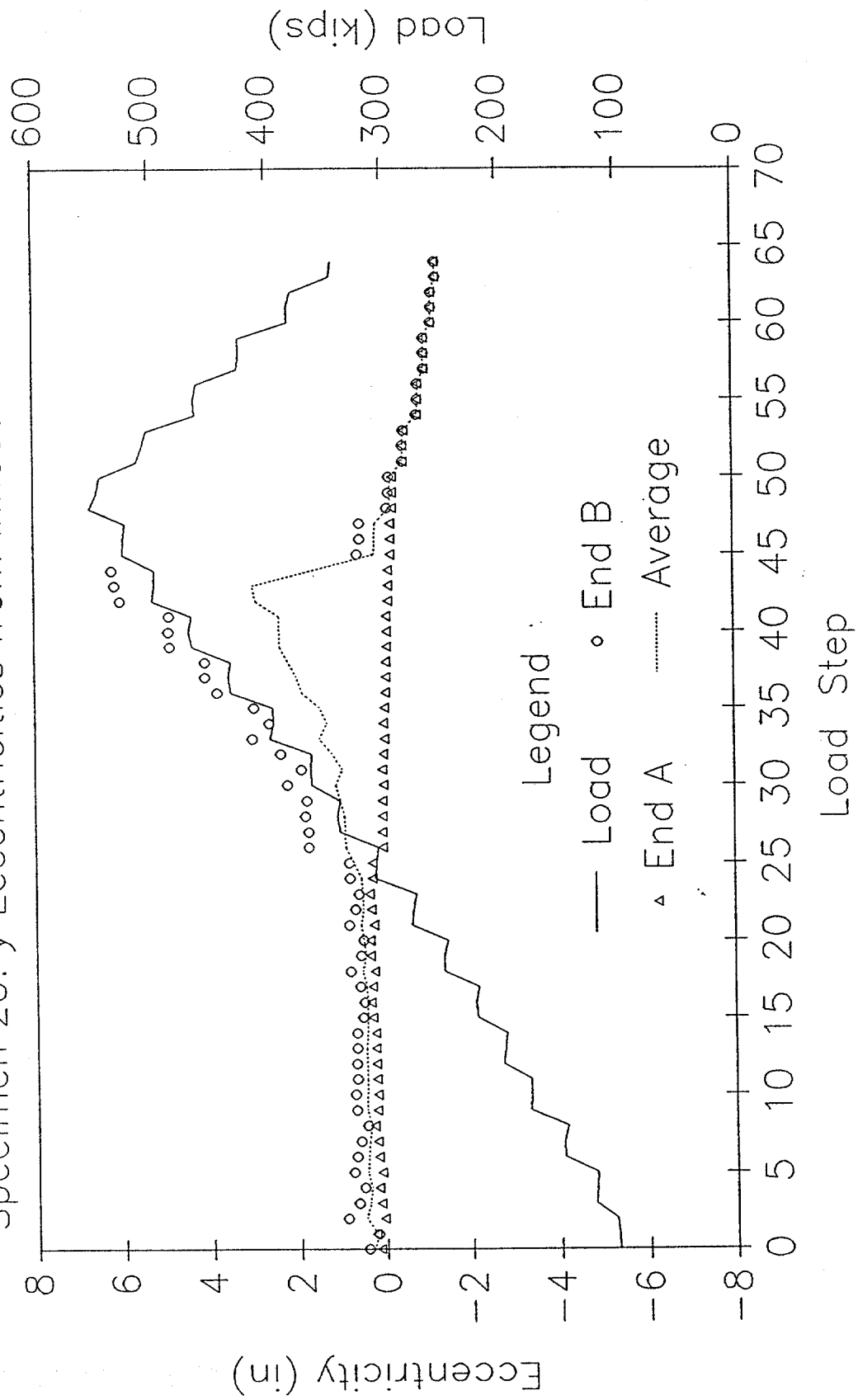
LOAD AND ECCENTRICITY vs LOAD STEP

Specimen 20: x Eccentricities from Inflection Points



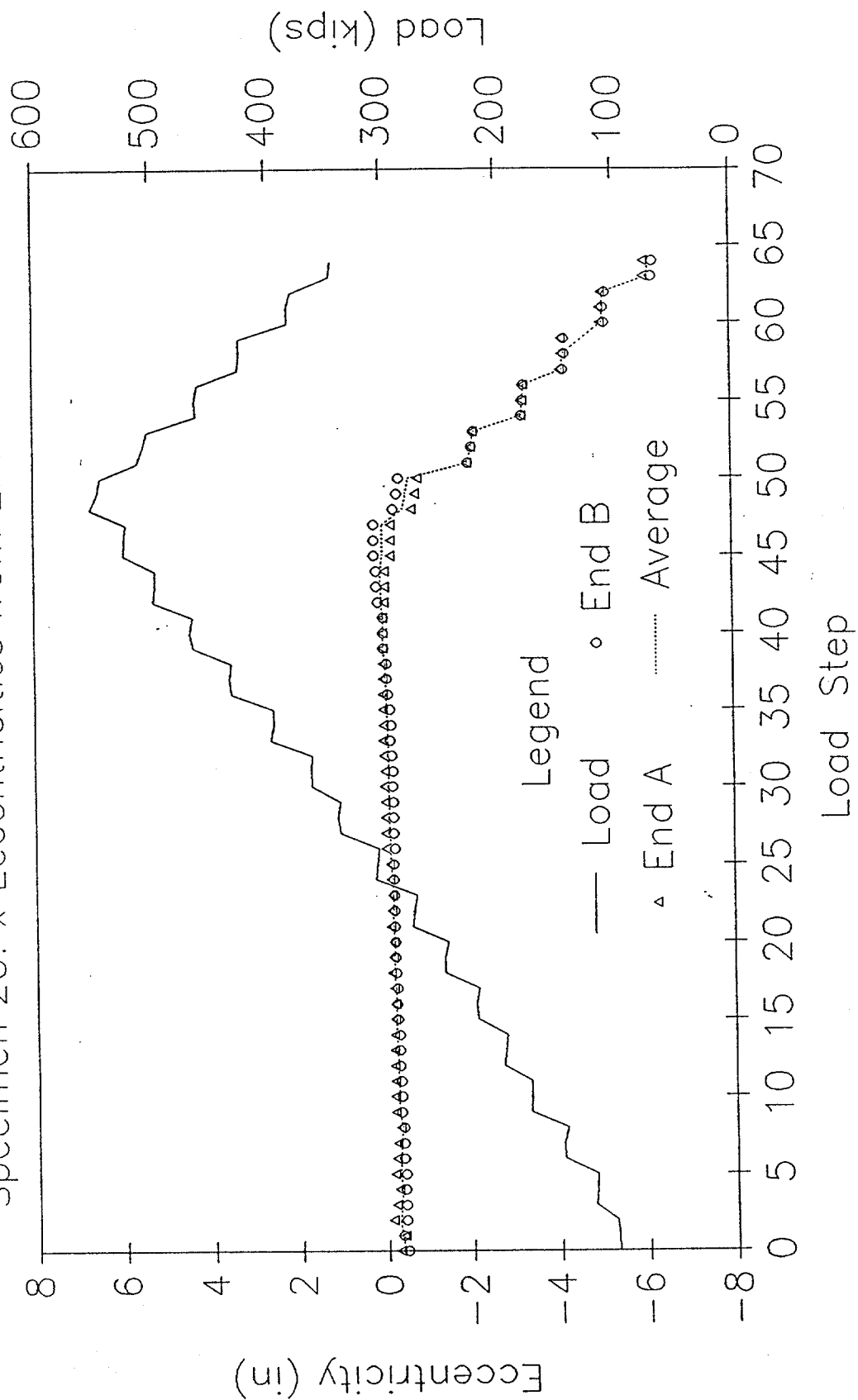
LOAD AND ECCENTRICITY vs LOAD STEP

Specimen 20: y Eccentricities from Inflection Points



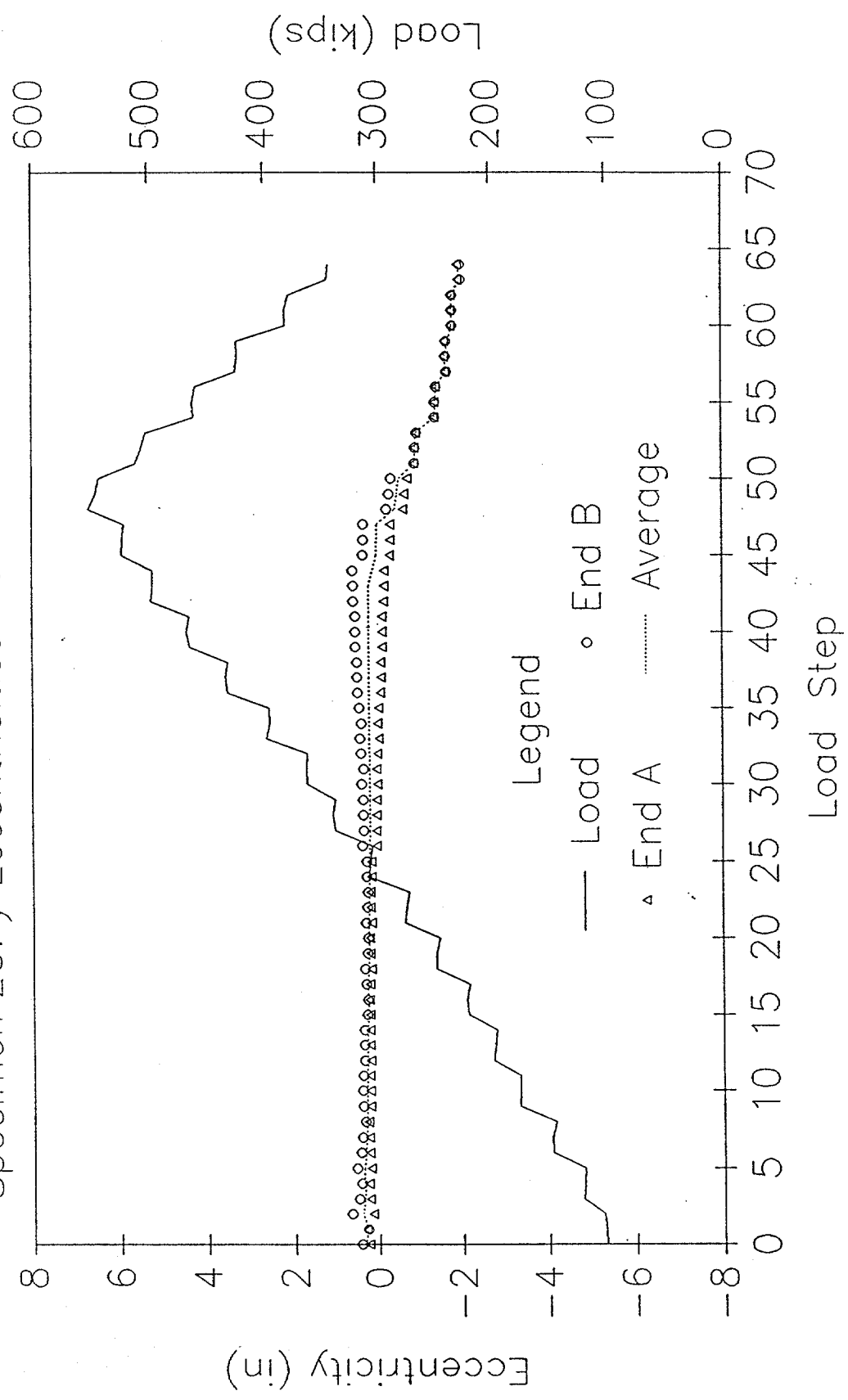
LOAD AND ECCENTRICITY vs LOAD STEP

Specimen 20: x Eccentricities from End Moments



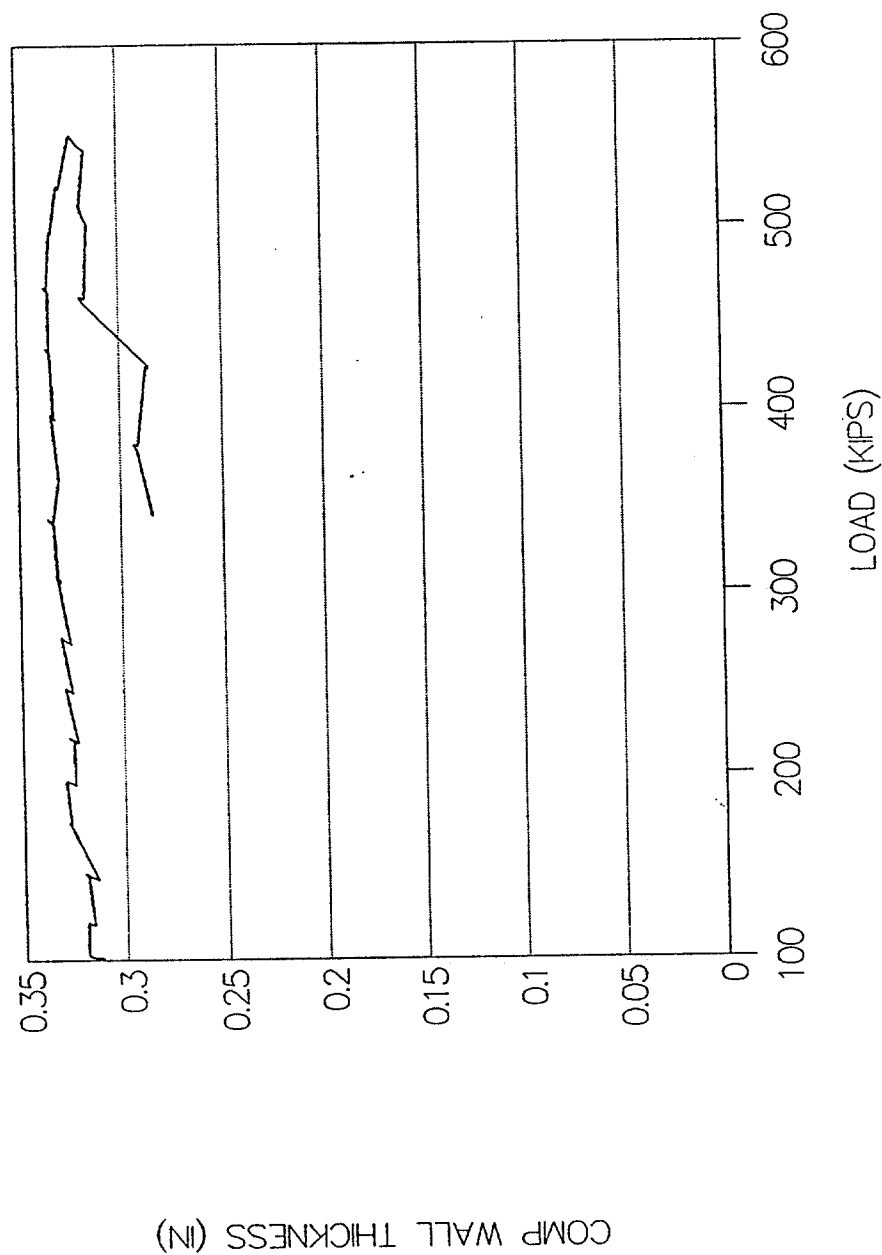
LOAD AND ECCENTRICITY vs LOAD STEP

Specimen 20: y Eccentricities from End Moments



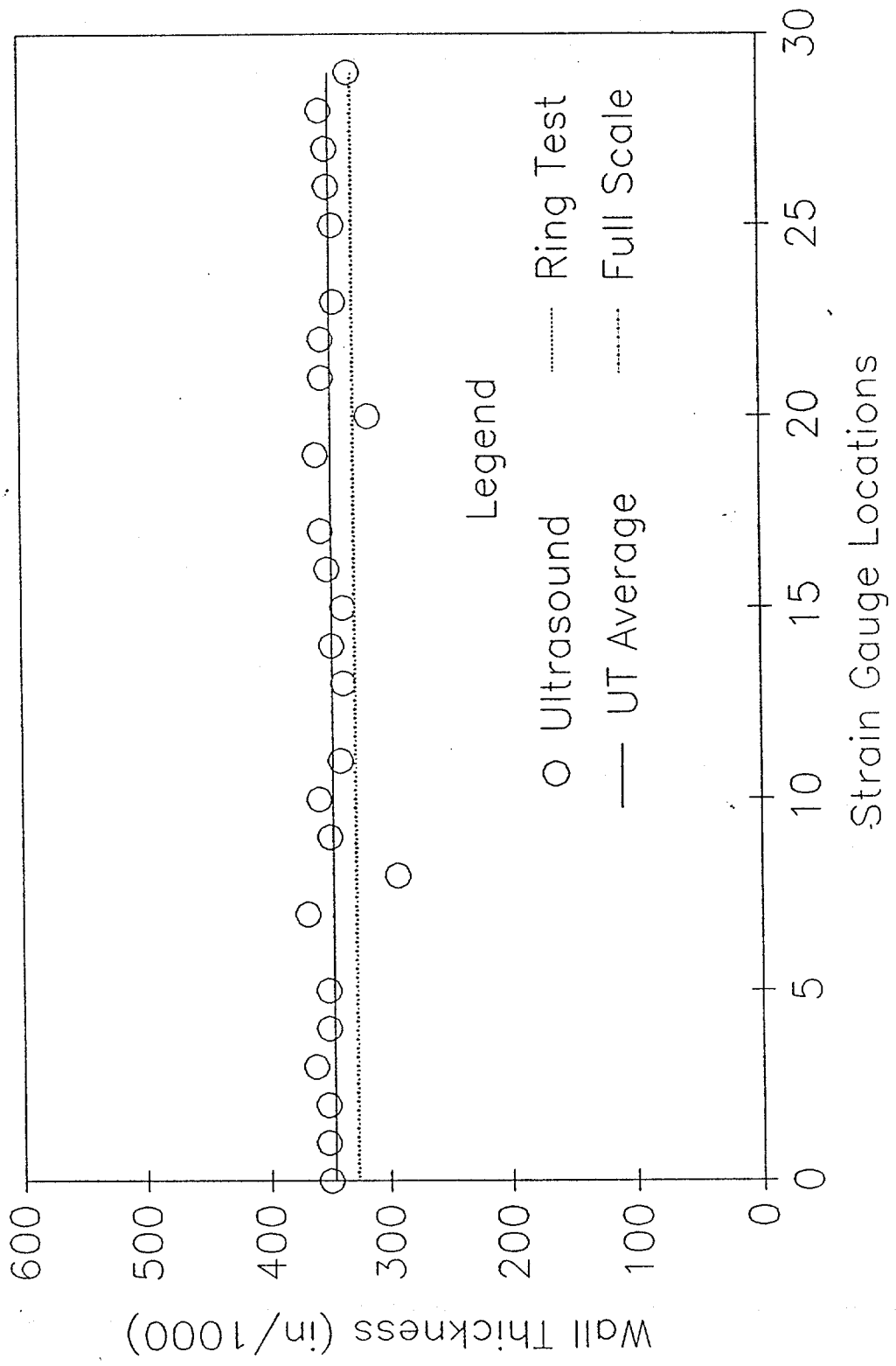
SPECIMEN NO 20--FULL SCALE TEST

COMPUTED WALL THICKNESS



SPECIMEN 20: WALL THICKNESS

Nominal Wall Thickness = 0.375 in



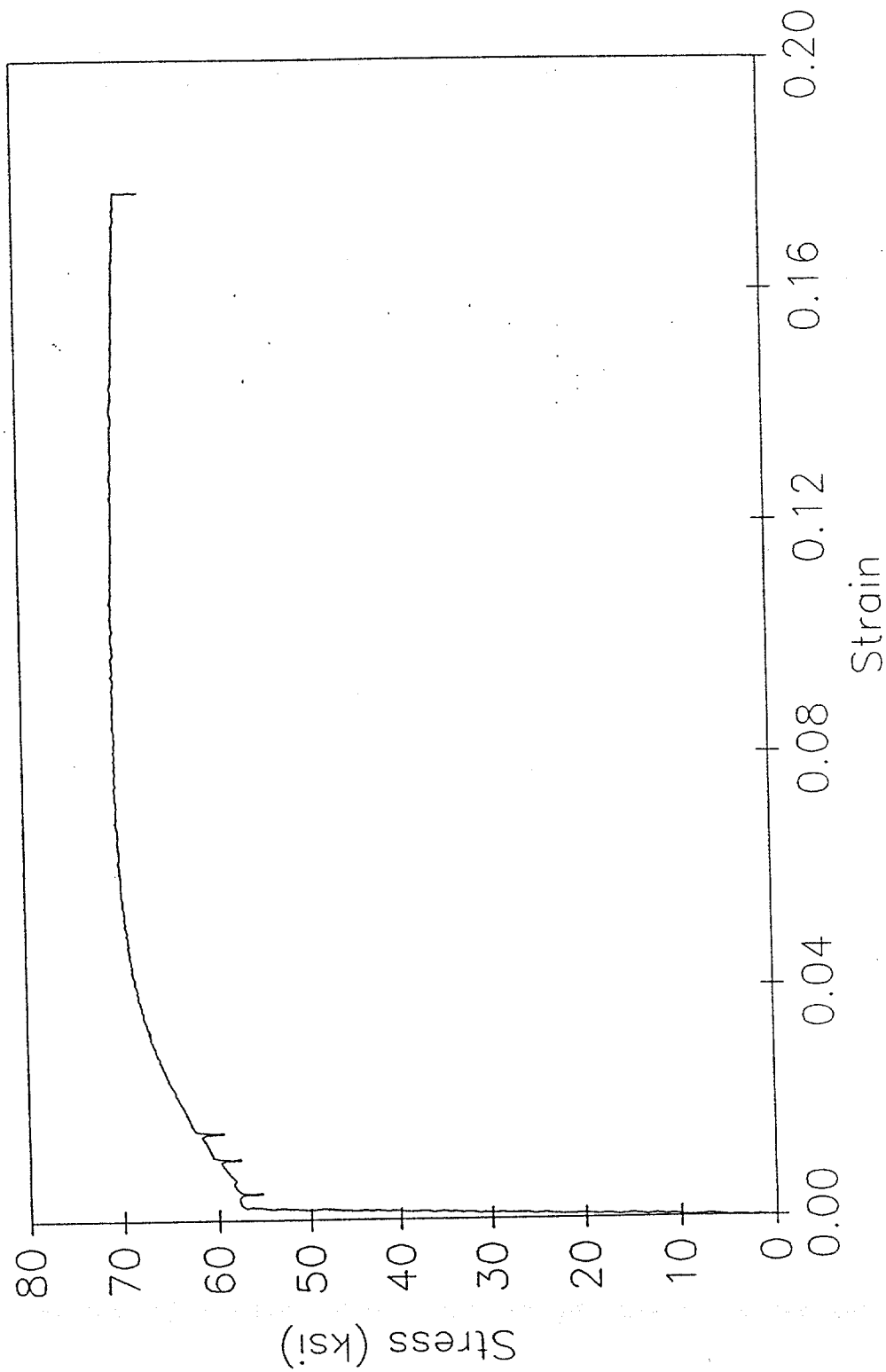
Ultrasound Data for Specimen 20
(All values in inches)

Gauge No.	UT Thickness	UT Average
0	0.350	
1	0.352	
2	0.352	
3	0.362	
4	0.351	
5	0.351	0.353
6	0.368	
7	0.293	
8	0.349	
9	0.358	
10	0.340	0.342
11	0.337	
12	0.347	
13	0.337	
14	0.350	
15	0.355	0.345
16	0.359	
17	0.315	
18	0.354	
19	0.354	
20	0.343	0.345
21	0.344	
22	0.348	
23	0.349	
24	0.354	
25	0.330	0.345

Overall Average = 0.346

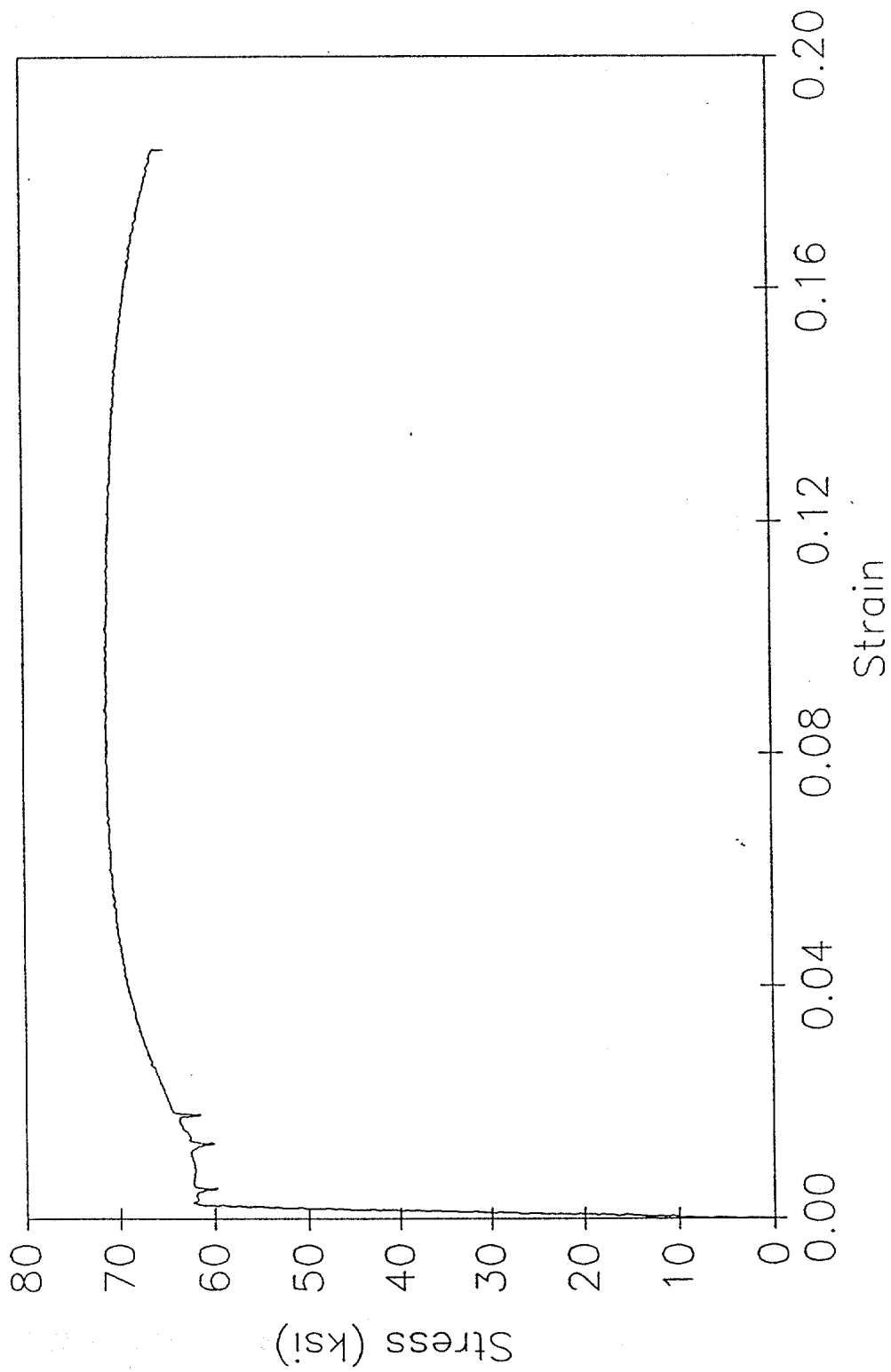
TENSILE SPECIMEN 20-1

Stress vs Strain



TENSILE SPECIMEN 20-2

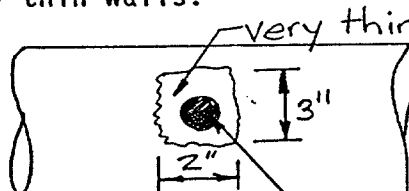
Stress vs Strain



SPECIMEN 21

DAMAGE SUMMARY

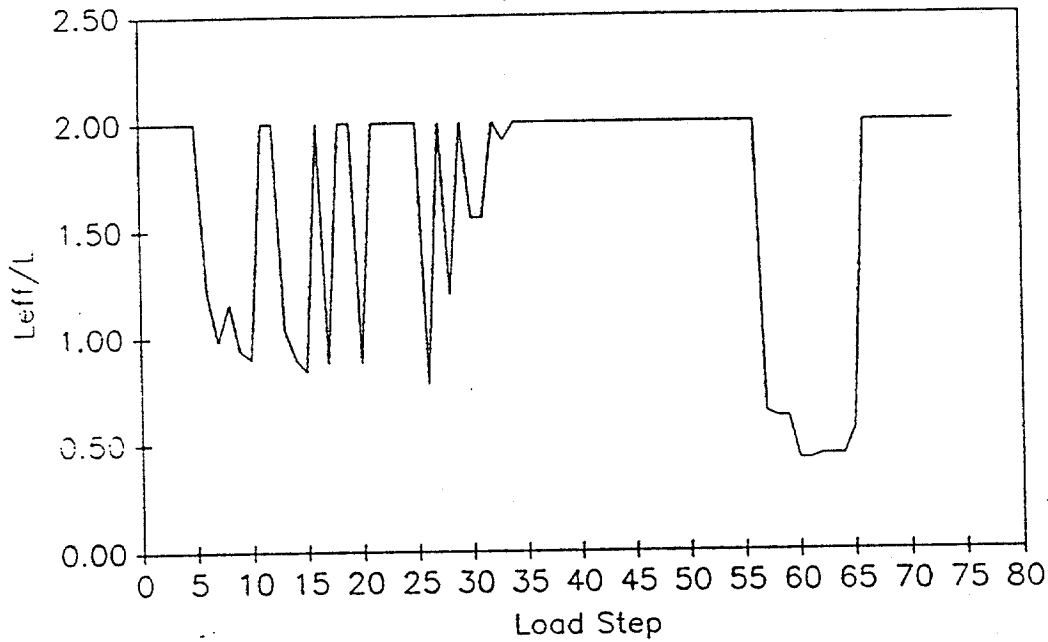
Specimen No. 21
1/8/90

DISTANCE FROM END "B"	*DISTANCE FROM CHALK LINE		DESCRIPTION OF DAMAGE
	LEFT	RIGHT	
1. From 8 1/2" to 1'-9 1/2"	5 1/4"		Longitudinal crack in pipe (About 1/8" opening at surface)
2. From 1'-10 1/2" to 3'-1"	5 1/4"		Longitudinal crack in pipe (small)
3. From 8'-8" to 10'-11"	5 1/4"		Longitudinal crack in pipe (About 1/8" opening at surface)
4. From 11'-3" to 14'-11 1/2"	5 1/4"		Longitudinal crack through pipe (About 1/8" split through the pipe surface)
5. From 15'-5" to 19'-10"	5 1/4"		Longitudinal crack through pipe (About 1/8" split through the pipe surface)
6. 19'-11 1/4"			1/2" circumferential butt weld
7. 20'-3"	10"		1" diameter corrosion hole with a surrounding 2" x 3" area with very thin walls. 

*Looking from end "A" towards end "B"

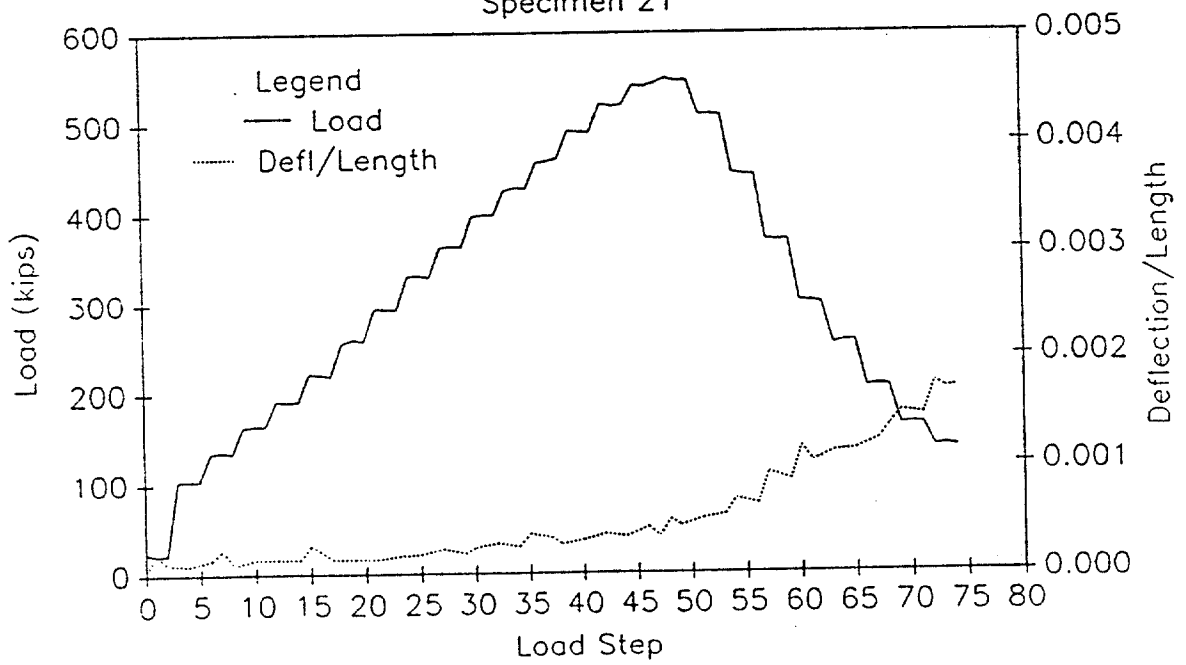
EFFECTIVE LENGTH vs LOAD STEP

Specimen 21



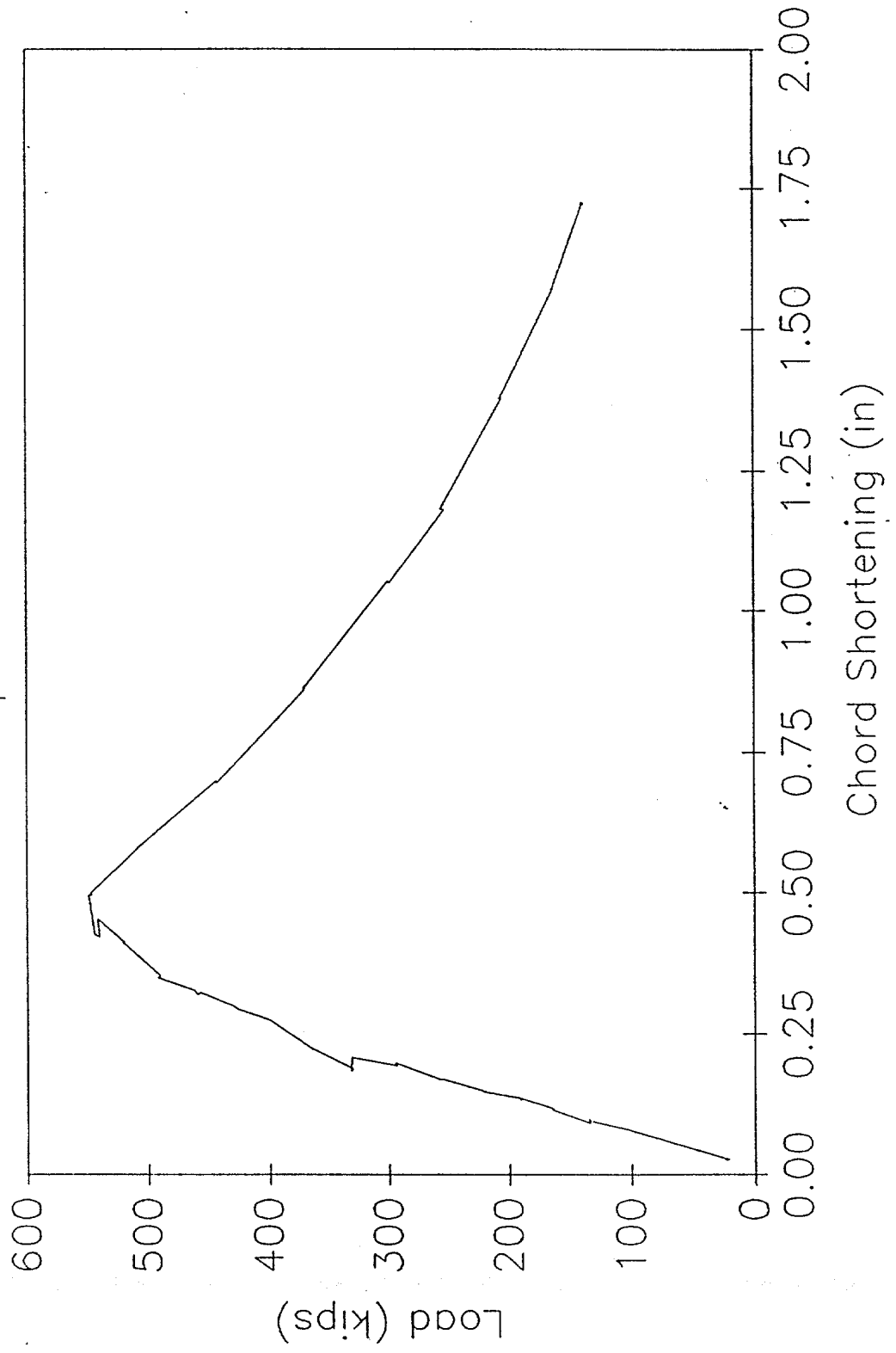
LOAD AND DEFLECTION vs LOAD STEP

Specimen 21



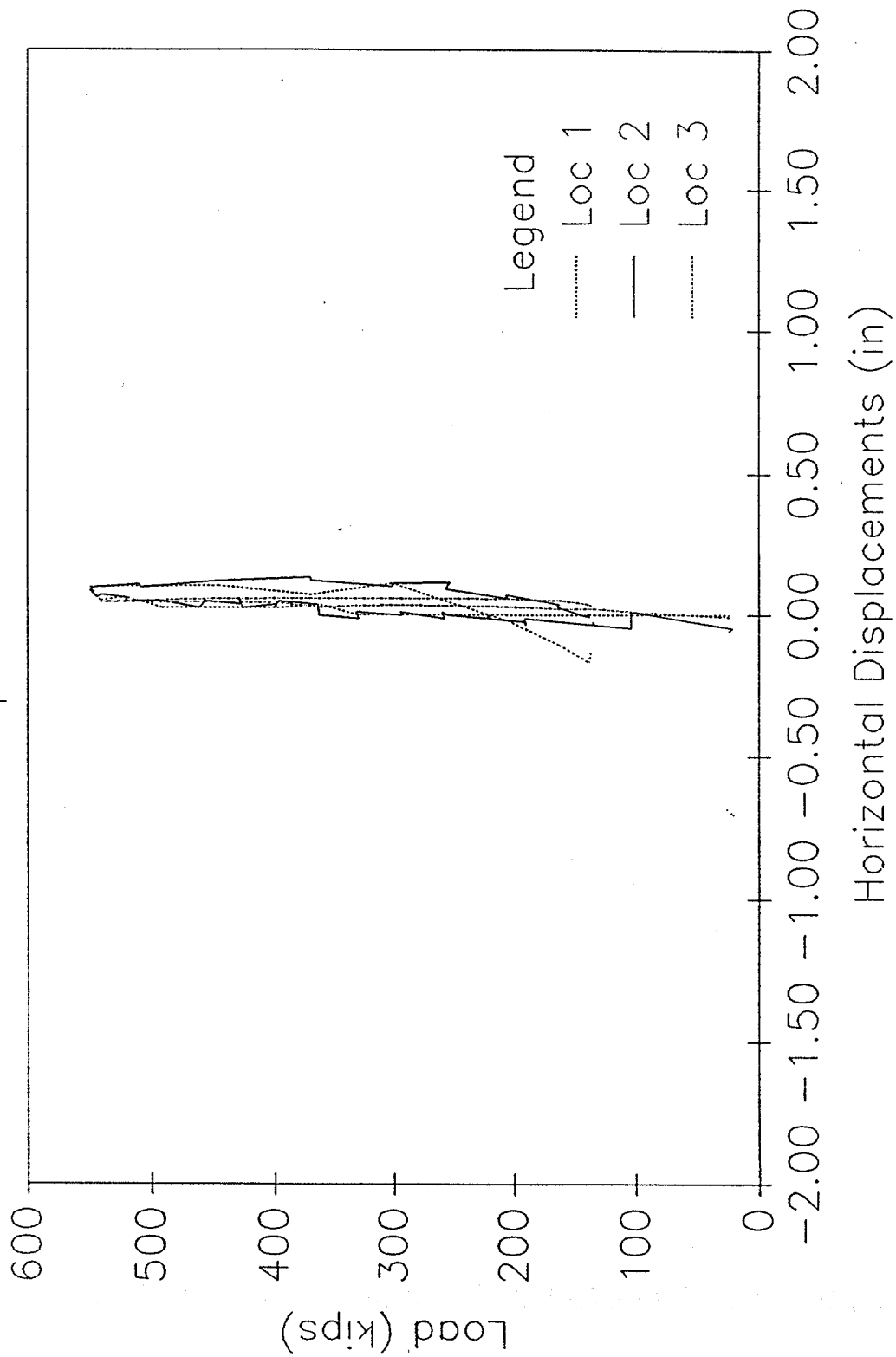
LOAD vs CHORD SHORTENING

Specimen 21



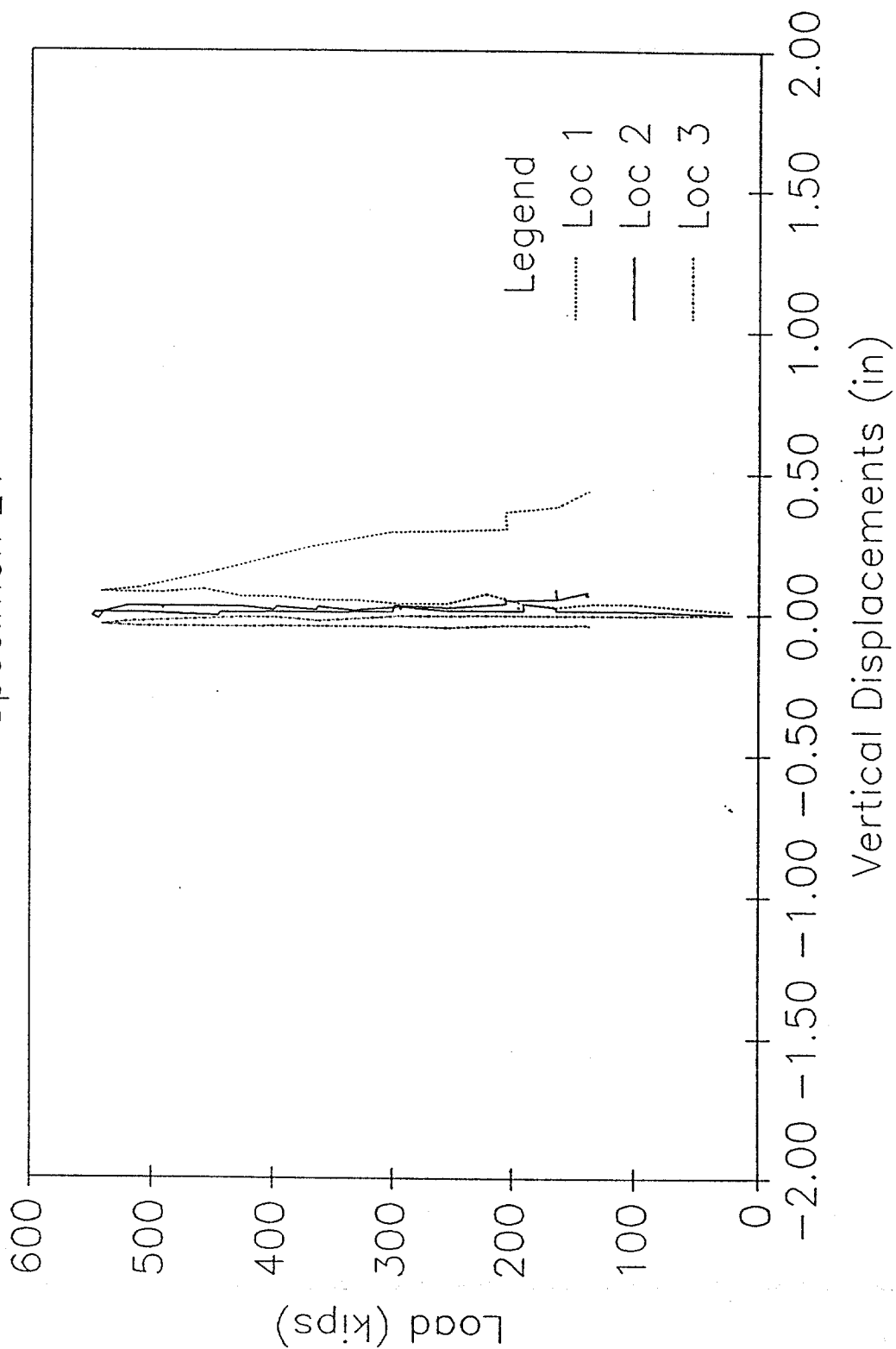
HORIZONTAL DISPLACEMENTS

Specimen 21



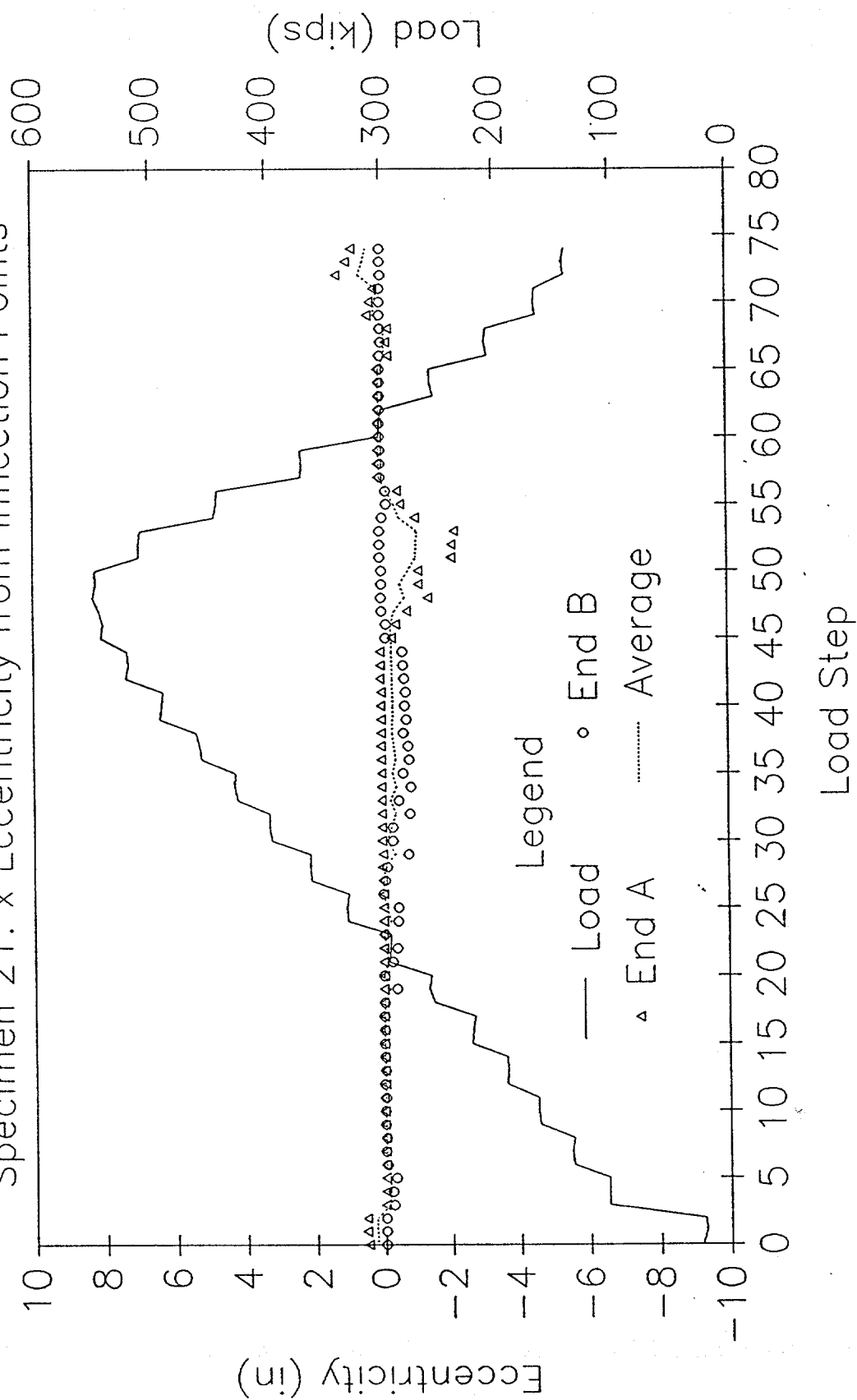
VERTICAL DISPLACEMENTS

Specimen 21



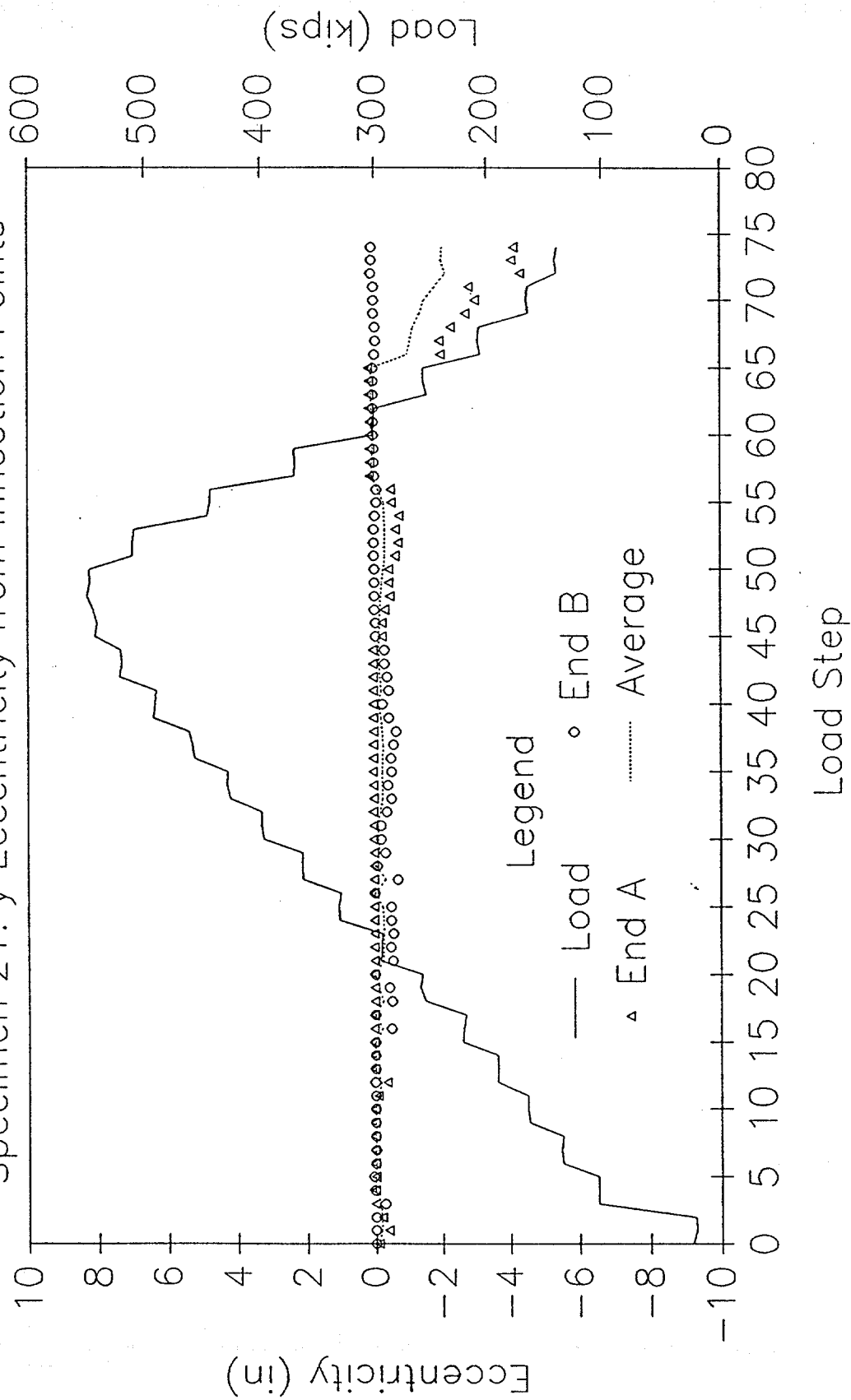
LOAD AND ECCENTRICITY vs LOAD STEP

Specimen 21: x Eccentricity from Inflection Points



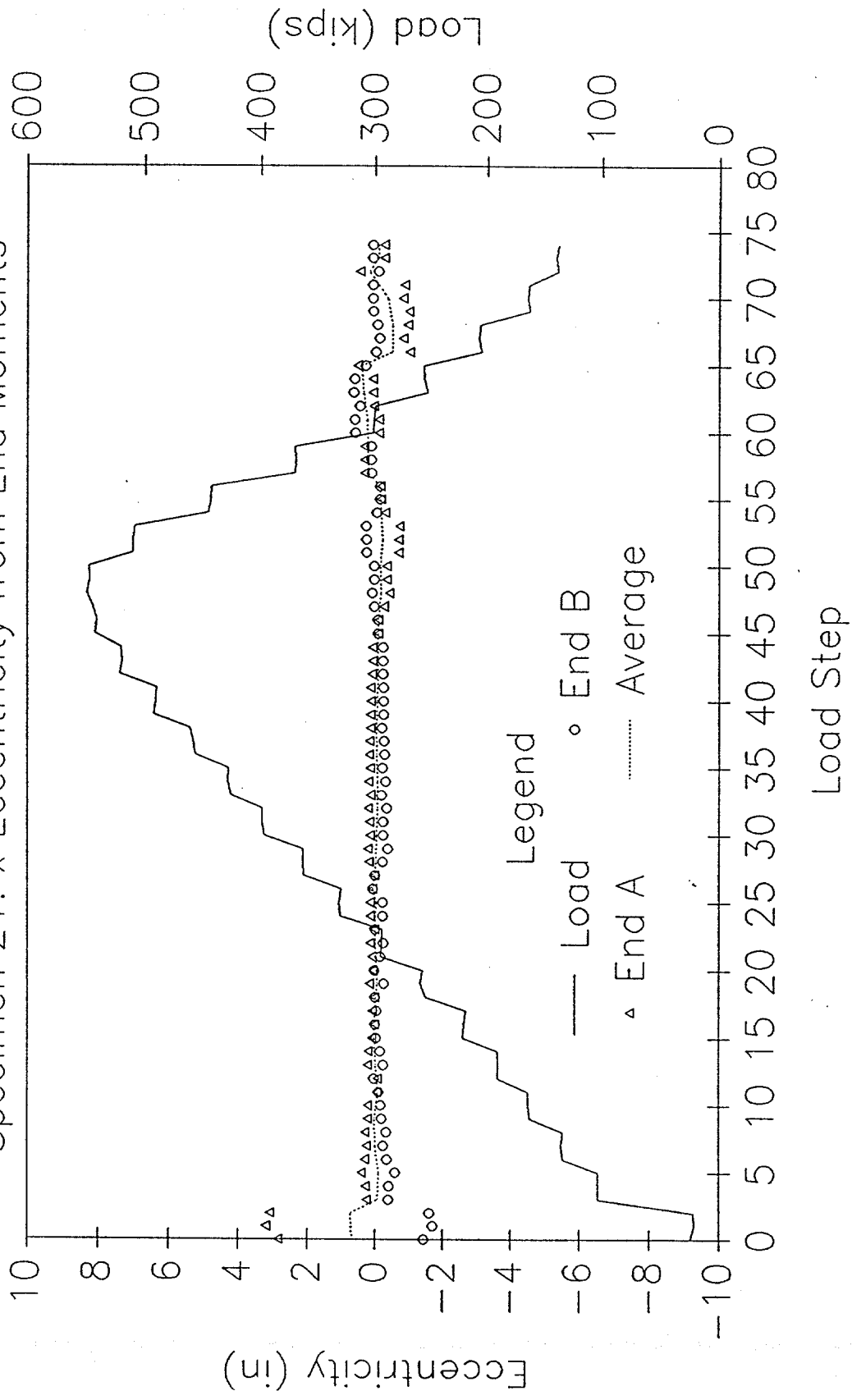
LOAD AND ECCENTRICITY vs LOAD STEP

Specimen 21: y Eccentricity from Inflection Points



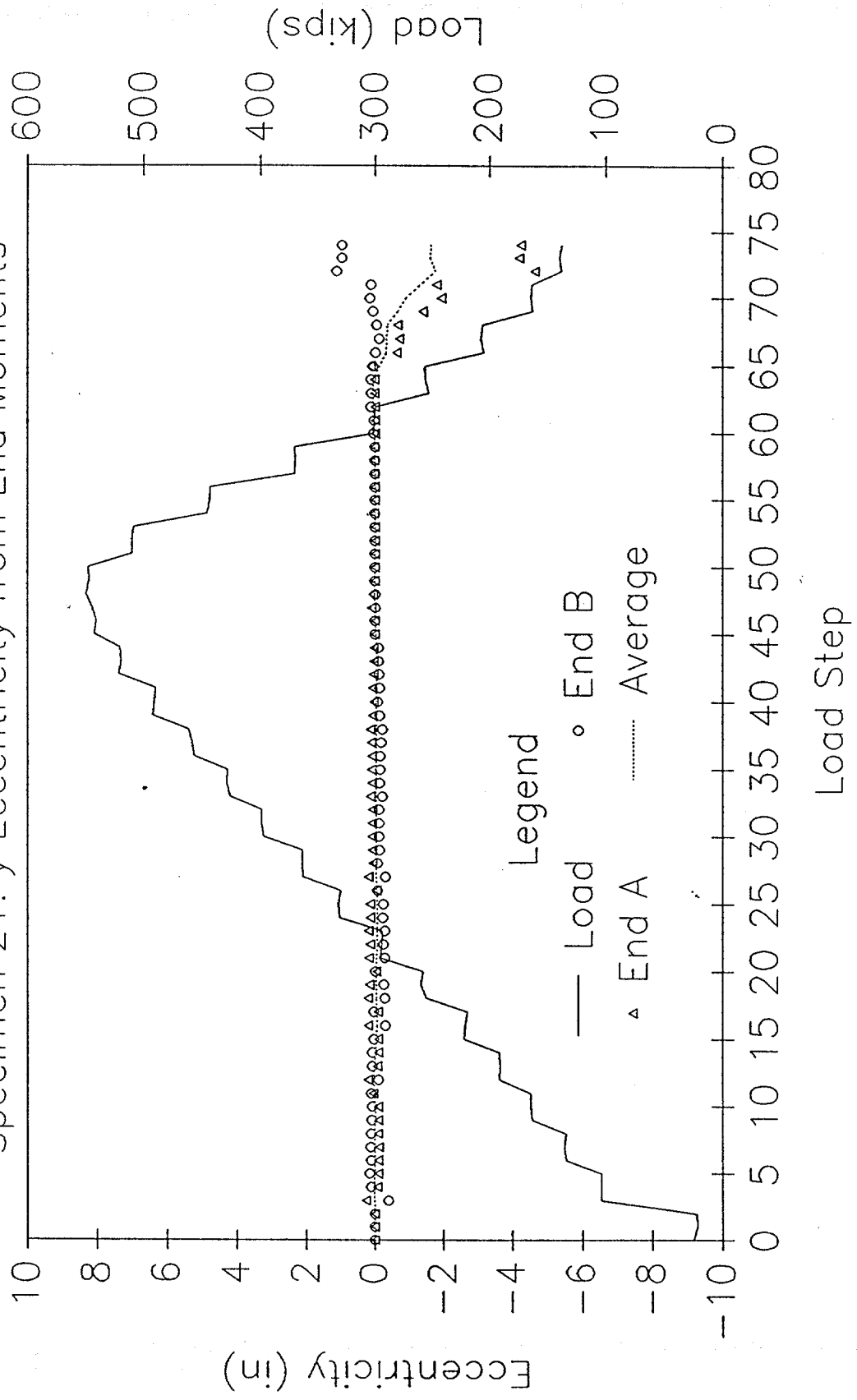
LOAD AND ECCENTRICITY vs LOAD STEP

Specimen 21: x Eccentricity from End Moments



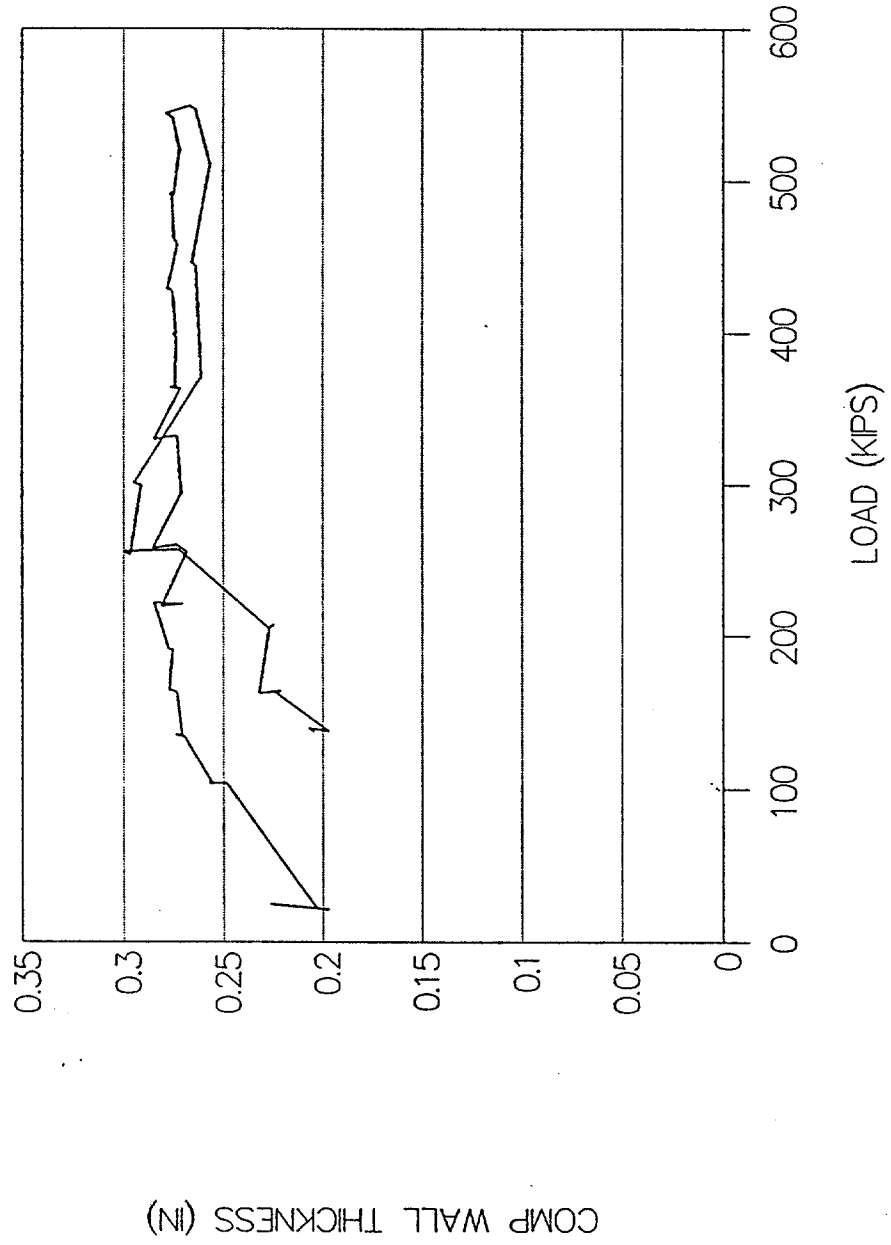
LOAD AND ECCENTRICITY vs LOAD STEP

Specimen 21: y Eccentricity from End Moments



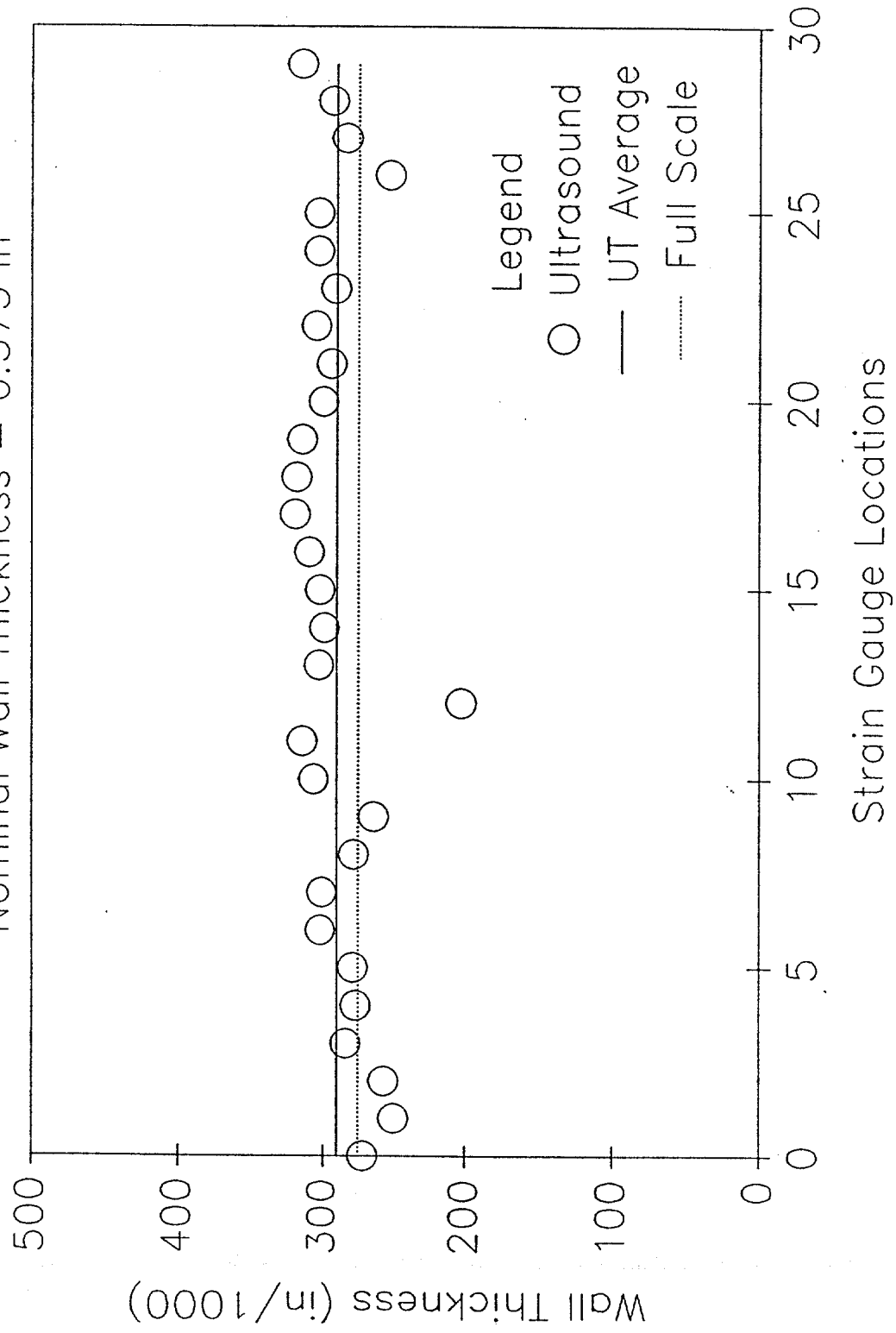
SPECIMEN 21-FULL SCALE TEST

COMPUTED WALL THICKNESS



SPECIMEN 21: WALL THICKNESS

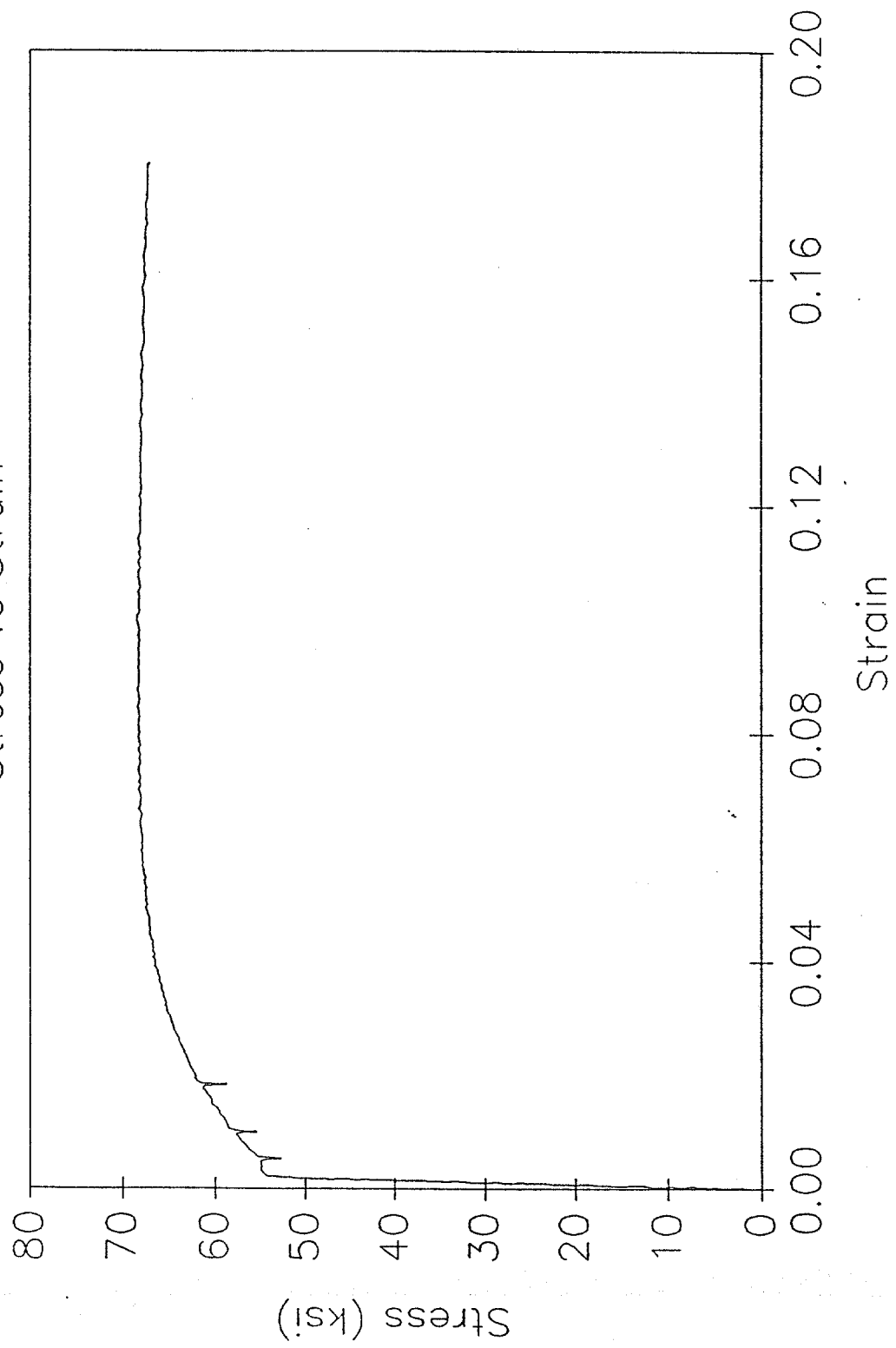
Nominal Wall Thickness = 0.375 in



Ultrasound Data for Specimen 21
(All values in inches)

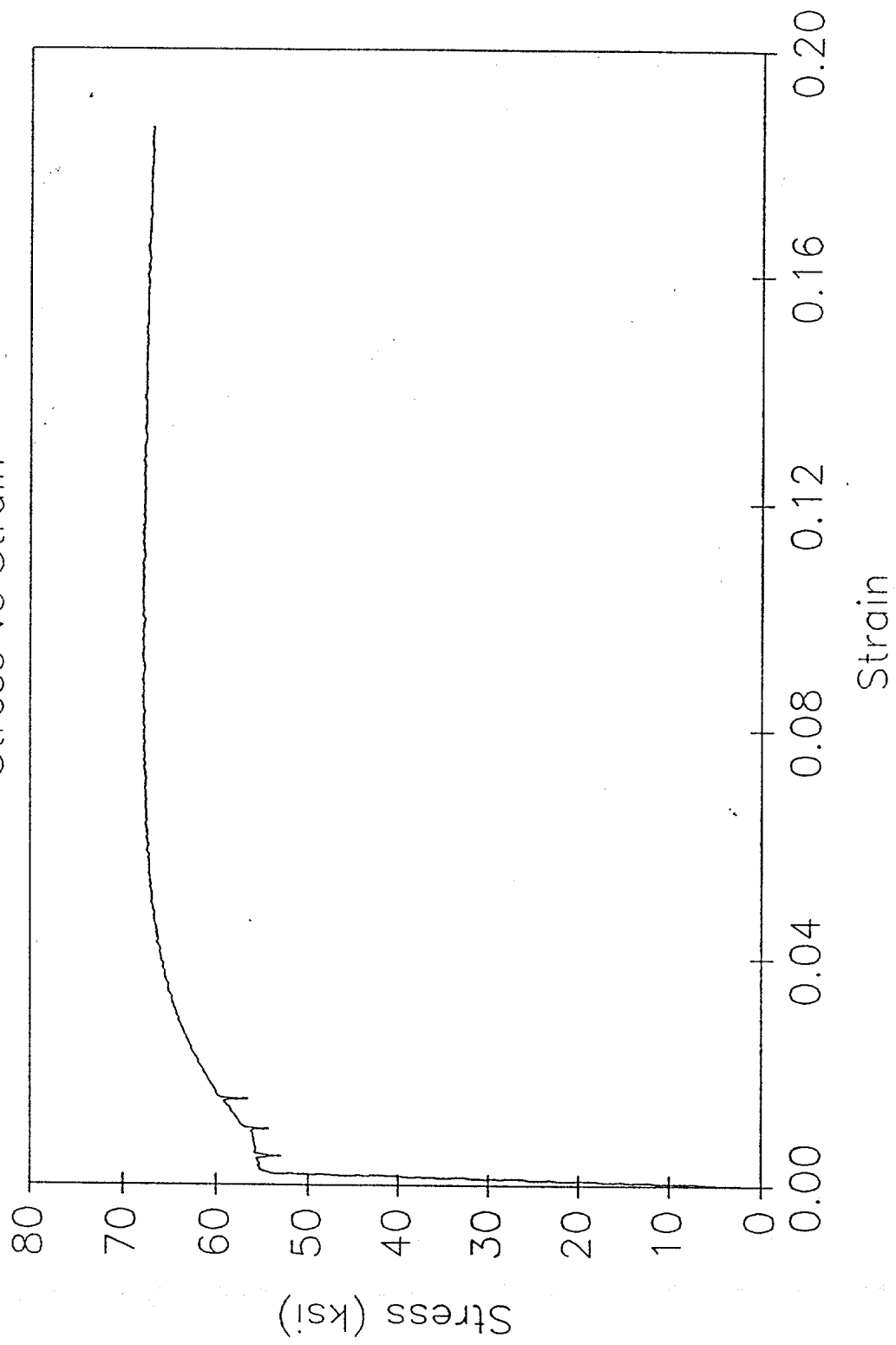
Gauge No.	UT Thickness	UT Average
0	0.272	
1	0.250	
2	0.257	
3	0.284	
4	0.277	
5	0.279	0.270
6	0.302	
7	0.301	
8	0.278	
9	0.264	
10	0.307	
11	0.315	0.294
12	0.203	
13	0.303	
14	0.299	
15	0.302	
16	0.310	
17	0.320	0.290
18	0.319	
19	0.315	
20	0.300	
21	0.294	
22	0.305	
23	0.291	0.304
24	0.303	
25	0.303	
26	0.253	
27	0.283	
28	0.293	
29	0.315	0.292
Overall Average =		0.290

TENSILE SPECIMEN 21-1
Stress vs Strain



TENSILE SPECIMEN 21-2

Stress vs Strain



APPENDIX B

COMPUTER CODE FOR DISPLACE PROGRAM

PROGRAM DISP

```

*****
* Scott Moehlman *
* PMB - Program *
* June 20, 1989 *
*****

```

PROGRAM DESCRIPTION

THIS IS A PROGRAM TO COMPUTE CHORD SHORTENING, LOAD, AND
RESULTANT HORIZONTAL AND VERTICAL DISPLACEMENTS.

DESCRIPTION OF THE VARIABLES

```

. A(I,J) = .....RESULTANT HORIZONTAL DISPLACEMENT
. BO      = .....DISTANCE FROM WEB TO STRAIN GAUGE
. B(I,J)  = .....RESULTANT VERTICAL DISPLACEMENT
. C(J)    = .....ORIGINAL HORIZONTAL DISPLACEMENT
. CAL(I)  = .....CALIBRATION FACTORS
. CS(I)   = .....CHORD SHORTENING AT TIME I
. CSX(I,J) = .....CHANGE IN X DUE TO CHORD SHORTENING
. CSY(I,J) = .....CHANGE IN Y DUE TO CHORD SHORTENING
. D(I,J)  = .....CHANGE IN "HORIZONTAL" DISPLACEMENT
. DGA(I)  = .....CHORD SHORTENING D.G. CORR. AT A
. DGB(I)  = .....CHORD SHORTENING D.G. CORR. AT B
. E(J)    = .....ORIGINAL VERTICAL DISPLACEMENT
. F(I,J)  = .....CHANGE IN "VERTICAL" DISPLACEMENT
. HO      = .....DISTANCE FROM WEB CENTER TO GAUGE
. INERX   = .....MOMENT OF INERTIA ABOUT X-AXIS
. INERY   = .....MOMENT OF INERTIA ABOUT Y-AXIS
. L(I)    = .....DISTANCE TO HORIZ AND VERT POTS
. LD(I,J) = .....INPUTTED LOADS FROM LOAD FRAME
. LENGTH  = .....ORIGINAL LENGTH OF PIPE
. LOAD(I) = .....TOTAL APPLIED LOAD AT TIME I
. MOD     = .....MODULUS OF ELASTICITY OF LOAD FRAME
. N       = .....NUMBER OF DATA STEPS
. SP(I,J) = .....LONGITUDINAL STRINGPOT READINGS
. TIME(I) = .....TIME AT READING I
. TITLE   = .....DESCRIPTION OF PIPE
. U(I)    = .....LOCATION OF HORIZONTAL LOAD RESULT
. V(I)    = .....LOCATION OF VERTICAL LOAD RESULTANT
. W(I)    = .....DISTANCE FROM CENTER OF FRAME TO LEG.
. X(I,J)  = .....HORIZONTAL POT READINGS
. Y(I,J)  = .....VERTICAL POT READINGS

```

VARIABLE DECLARATIONS

```

IMPLICIT REAL (A-H,O-Z)
REAL A(150,3),B(150,3),C(3),D(150,3),E(3),BO,HO,CAL(9),
1 F(150,3),SP(150,3),TIME(150),X(150,3),Y(150,3),CS(150),
1 LOAD(150),LENGTH,L(3),CSY(150,3),CSX(150,3),LD(150,9),
1 MOD,INERX,INERY,U(150),V(150),W(3),DGA(150),DGB(150)
INTEGER N
CHARACTER TITLE*30

```

```
C
C -----
C INPUT DATA WITH SUBROUTINE DATAIN
C -----
C
C CALL DATAIN(LENGTH,L,TIME,TITLE,SP,X,Y,LD,C,E,CAL,MOD,
1 INERX,INERY,BO,HO,W,DGA,DGB,N)
C
C -----
C WRITE INPUT DATA TO FILE "SPEC#.INP
C -----
C
C -----
C OPEN FILE FOR OUTPUT
C -----
C
C OPEN (UNIT=7, FILE='SPEC.INP', STATUS='UNKNOWN')
C
C DO 100 I = 1,N
C   WRITE (7,1000) TIME(I),SP(I,1),SP(I,2),SP(I,3)
100 CONTINUE
C   WRITE (7,950)
C   DO 110 I = 1,N
C     WRITE (7,1010) X(I,1),Y(I,1),X(I,2),Y(I,2),X(I,3),
1 Y(I,3)
110 CONTINUE
C   WRITE (7,950)
C   DO 120 I = 1,N
C     WRITE (7,1020) LD(I,1),LD(I,2),LD(I,3),LD(I,4),LD(I,5)
120 CONTINUE
C   WRITE (7,950)
C   DO 130 I = 1,N
C     WRITE (7,1030) LD(I,6),LD(I,7),LD(I,8),LD(I,9)
130 CONTINUE
C
C -----
C COMPUTE CHORD SHORTENING, LOAD, AND CORRECTED READINGS
C -----
C
C CALL CHORDS(LENGTH,L,LD,TIME,SP,X,Y,LOAD,CS,CSX,CSY,C,
1 D,E,F,DGA,DGB,N)
C
C -----
C COMPUTE LOAD RESULTANT
C -----
C
C CALL LOCAT(LD,CAL,MOD,INERX,INERY,BO,HO,U,V,W,
1 TIME,LOAD,CS,TITLE,N)
C
C -----
C COMPUTE "RESULTANT" HORIZONTAL AND
C VERTICAL DISPLACEMENTS
C -----
C
C CALL RESULT(A,B,C,D,E,F,N)
```



```

C
C
C -----
C   FORMAT STATEMENTS
C -----
C
  950 FORMAT (' ')
 1000 FORMAT (' ',F9.2,',',F9.5,',',F9.5,',',F9.5)
 1010 FORMAT (' ',F9.5,',',F9.5,',',F9.5,',',F9.5,',',F9.5,
1      ', ',F9.5)
 1020 FORMAT (' ',F9.5,',',F9.5,',',F9.5,',',F9.5,',',F9.5)
 1030 FORMAT (' ',F9.5,',',F9.5,',',F9.5,',',F9.5)
      END

C
C
C =====
C   SUBROUTINE DATAIN
C =====
C
  SUBROUTINE DATAIN(LENGTH,L,TIME,TITLE,SP,X,Y,LD,C,E,
1  CAL,MOD,INERX,INERY,BO,HO,W,DGA,DGB,N)

C
C   PURPOSE: INPUT PROBLEM DATA
C
C   DECLARE VARIABLES
  IMPLICIT REAL (A-H,O-Z)
  REAL SP(150,3),TIME(150),X(150,3),Y(150,3),CAL(9),MOD,
1  LENGTH,L(3),LD(150,9),C(3),E(3),INERX,INERY,BO,HO,
1  W(3),DGA(150),DGB(150)
  INTEGER N
  CHARACTER TITLE*30

C
C
C -----
C   OPEN FILES FOR INPUT
C -----
C
  OPEN (UNIT=1, FILE='LSP.DAT', STATUS='OLD')
  OPEN (UNIT=2, FILE='HVP.DAT', STATUS='OLD')

C
C   READ IN PROBLEM TITLE, PIPE LENGTH, DISTANCE TO HORIZ AND
C   VERT POTS, AND INITIAL POT EXTENSION.
C
  READ (1,*) TITLE
  READ (1,*) N
  READ (1,*) LENGTH, L(1), L(2), L(3)
  READ (1,*) C(1), E(1), C(2), E(2), C(3), E(3)
  READ (1,*) MOD,INERX,INERY,BO,HO
  READ (1,*) W(1),W(2),W(3)

C
C   READ IN CALIBRATION FACTORS
C
  DO 5 J = 1,9
    READ (1,*) CAL(J)
5  CONTINUE
C

```

```

C   READ TIME, POT DISPLACEMENTS, AND LOADS.
C
  DO 10 I = 1,N
    READ (1,*) TIME(I),SP(I,1),SP(I,2),SP(I,3),DGA(I),
1    DGB(I)
    READ (2,*) X(I,1),Y(I,1),X(I,2),Y(I,2),X(I,3),Y(I,3)
10 CONTINUE
    CLOSE (UNIT=1)
    CLOSE (UNIT=2)

C
C   -----
C   OPEN FILES FOR INPUT
C   -----
C
  OPEN (UNIT=3, FILE='LOAD1.DAT', STATUS='OLD')
  OPEN (UNIT=4, FILE='LOAD2.DAT', STATUS='OLD')

C
  DO 15 I =1,N
    READ (3,*) LD(I,1),LD(I,2),LD(I,3),LD(I,4),LD(I,5)
    READ (4,*) LD(I,6),LD(I,7),LD(I,8),LD(I,9)
15 CONTINUE
    CLOSE (UNIT=3)
    CLOSE (UNIT=4)
    RETURN
  END

C
C   =====
C   SUBROUTINE CHORDS
C   =====
C
  SUBROUTINE CHORDS(LENGTH,L,LD,TIME,SP,X,Y,LOAD,
1  CS,CSX,CSY,C,D,E,F,DGA,DGB,N)

C
C   PURPOSE: COMPUTE CHORD SHORTENING, LOAD, AND HORIZ.
C   AND VERT READINGS MINUS CHORD SHORTENING EFFECTS.
C
C   DECLARE VARIABLES
C   IMPLICIT REAL (A-H,O-Z)
C   REAL LENGTH,L(3),LD(150,9),TIME(150),
1  SP(150,3),X(150,3),Y(150,3),LOAD(150),CS(150),
1  CSX(150,3),CSY(150,3),C(3),D(150,3),E(3),F(150,3),
1  THETA(2,3),R(3),DGA(150),DGB(150)
C   INTEGER N

C
C   -----
C   COMPUTE CHORD SHORTENING, LOAD, AND CHORD
C   SHORTENING EFFECTS AT TIME I.
C   -----
C
  DO 20 I = 1,N
    CS(I) = (-(SP(I,1)+SP(I,2)+SP(I,3))/3)-DGA(I)-DGB(I)
    LOAD(I) = (LD(I,1)+LD(I,3)+LD(I,4)+LD(I,6)+LD(I,7)
1    +LD(I,9))/2
20 CONTINUE

```

```

C      DO 30 I = 1,N
C          DO 30 J = 1,3
C              R(J) = CS(I)*(LENGTH-L(J))/LENGTH
C
C              THETA(1,J) = ATAN(R(J)/C(J))
C              THETA(2,J) = ATAN(R(J)/E(J))
C
C              CSX(I,J) = C(J)*((1/COS(THETA(1,J)))-1)
C              CSY(I,J) = E(J)*((1/COS(THETA(2,J)))-1)
C
C              D(I,J) = X(I,J) - CSX(I,J)
C              F(I,J) = Y(I,J) - CSY(I,J)
30      CONTINUE
      RETURN
      END
C
C
C      =====
C      SUBROUTINE LOCAT
C      =====
C
C      SUBROUTINE LOCAT(LD,CAL,MOD,INERX,INERY,BO,HO,U,V,W,
1      TIME,LOAD,CS,TITLE,N)
C
C      PURPOSE:  TO COMPUTE THE LINE OF ACTION OF THE LOAD
C
C      DECLARE VARIABLES
C      IMPLICIT REAL (A-H,O-Z)
C      REAL LD(150,9),CAL(9),MOD,INERX,INERY,BO,HO,U(150),P(3),
1      V(150),THEE(3),S(3),ALPHA(3),BETA(3),W(3),EX(3),EY(3),
1      TIME(150),LOAD(150),CS(150)
C      INTEGER N
C      CHARACTER TITLE*30
C
C      -----
C      OPEN FILES FOR OUTPUT
C      -----
C
C      OPEN (UNIT=8, FILE='SPEC1.OUT', STATUS='UNKNOWN')
C
C      WRITE (8,*) TITLE
C      WRITE (8,2010)
C
C      COMPUTE THE LOCATION OF THE LOAD RESULTANT
C
C      DO 60 I = 1,N
C
C      COMPUTE THE RESULTANT LOCATION FOR EACH LEG
C
C      IF (LD(I,6)+LD(I,4).EQ.0) THEN
C          EX(1) = 0
C          EY(1) = 0
C      ELSE
C          EX(1) = -(LD(I,5)/(CAL(5)*30.6)-LD(I,6)/(CAL(6)

```

```

1      *30.6)) *INERY / (BO * (LD(I,6) + LD(I,4)))
      EY(1) = (LD(I,5) / (CAL(5) * 30.6) - LD(I,4) / (CAL(4)
1      *30.6)) *INERX / (HO * (LD(I,6) + LD(I,4)))
      ENDIF
      IF (LD(I,1) + LD(I,3) .EQ. 0) THEN
          EX(2) = 0
          EY(2) = 0
      ELSE
          EX(2) = -(LD(I,2) / (CAL(2) * 30.6) - LD(I,3) / (CAL(3)
1      *30.6)) *INERY / (BO * (LD(I,1) + LD(I,3)))
          EY(2) = (LD(I,2) / (CAL(2) * 30.6) - LD(I,1) / (CAL(1)
1      *30.6)) *INERX / (HO * (LD(I,1) + LD(I,3)))
      ENDIF
      IF (LD(I,7) + LD(I,9) .EQ. 0) THEN
          EX(3) = 0
          EY(3) = 0
      ELSE
          EX(3) = -(LD(I,7) / (CAL(7) * 30.6) - LD(I,8) / (CAL(8)
1      *30.6)) *INERY / (BO * (LD(I,7) + LD(I,9)))
          EY(3) = -(LD(I,8) / (CAL(8) * 30.6) - LD(I,9) / (CAL(9)
1      *30.6)) *INERX / (HO * (LD(I,7) + LD(I,9)))
      ENDIF

```

C
C
C

DETERMINE THE ANGLE THEE FOR LEGS 2 AND 3

```

      THEE(2) = ATAN(EY(2) / (W(2) - EX(2)))
      THEE(3) = ATAN(EY(3) / (W(3) + EX(3)))

```

C
C
C
C

FIND THE DISTANCE FROM THE RESULTANTS IN LEGS
2 AND 3 TO THE CENTER OF THE LOAD FRAME

```

      S(2) = W(2) - EX(2) / COS(THEE(2))
      S(3) = W(3) + EX(3) / COS(THEE(3))

```

C
C
C
C

COMPUTE X AND Y COMPONENTS OF DISTANCE TO CENTER
ALPHA(1) = X(1) AND BETA(1) = Y(1)

```

      ALPHA(1) = EY(1)
      BETA(1) = W(1) - EX(1)
      ALPHA(2) = -S(2) * COS(.5236 - THEE(2))
      BETA(2) = -S(2) * SIN(.5236 - THEE(2))
      ALPHA(3) = S(3) * COS(.5236 - THEE(3))
      BETA(3) = -S(3) * SIN(.5236 - THEE(3))

```

C
C
C

COMPUTE THE LOAD IN EACH LEG

```

      P(1) = (LD(I,4) + LD(I,6)) / 2
      P(2) = (LD(I,1) + LD(I,3)) / 2
      P(3) = (LD(I,7) + LD(I,9)) / 2

```

C
C
C

DETERMINE THE RESULTANT LOAD LOCATION

```

1      U(I) = (P(1) * ALPHA(1) + P(2) * ALPHA(2) + P(3) * ALPHA(3)) /
      (P(1) + P(2) + P(3))
1      V(I) = (P(1) * BETA(1) + P(2) * BETA(2) + P(3) * BETA(3)) /

```

```

C      1      (P(1)+P(2)+P(3))
C
C      -----
C      WRITE OUTPUT TO FILE
C      -----
C
C      WRITE (8,2020) TIME(I),LOAD(I),U(I),V(I),CS(I)
C
C      60 CONTINUE
C
C      2010 FORMAT (' ','TIME',' ',' ','LOAD',' ',' ','Xr',' ',' ',
1      'Yr',' ',' ','CHORD SH')
C      2020 FORMAT (' ',F9.2,' ',F9.4,' ',F9.5,' ',F9.5,' ',F9.5)
C
C      RETURN
C      END
C
C      =====
C      SUBROUTINE RESULT
C      =====
C
C      SUBROUTINE RESULT(A,B,C,D,E,F,N)
C
C      PURPOSE: COMPUTE RESULTANT HORIZONTAL AND VERTICAL
C      DISPLACEMENTS
C
C      DECLARE VARIABLES
C      IMPLICIT REAL (A-H,O-Z)
C      REAL A(150,3),B(150,3),C(3),D(150,3),E(3),
1      F(150,3),P(150,3),Q(150,3),Z(150,3),K(2)
C      INTEGER N
C
C      COMPUTE THE RESULTANT HORIZONTAL AND VERTICAL DISPLACEMENTS
C
C      -----
C      OPEN FILES FOR OUTPUT
C      -----
C
C      OPEN (UNIT=9, FILE='SPEC2.OUT', STATUS='UNKNOWN')
C
C      WRITE (9,2025)
C      WRITE (9,2030)
C
C      DO 51 I = 1, N
C      K(1) = 0
C      K(2) = 0
C      DO 50 J = 1,3
C      P(I,J) = -F(I,J)**4-4*E(J)*F(I,J)**3+(-4*E(J)**2
1      +2*D(I,J)**2+4*C(J)*D(I,J)+4*C(J)**2)*F(I,J)**2+(4*D(I,J)**2
1      +8*C(J)*D(I,J)+8*C(J)**2)*E(J)*F(I,J)+(4*D(I,J)**2
1      +8*C(J)*D(I,J)+4*C(J)**2)*E(J)**2-D(I,J)**4-4*C(J)*D(I,J)**3
1      -4*C(J)**2*D(I,J)**2
C
C      Q(I,J) = -F(I,J)**2-2*E(J)*F(I,J)+2*D(I,J)*F(I,J)

```

```

1 +2*C(J)*F(I,J)+2*D(I,J)*E(J)+2*C(J)*E(J)-D(I,J)**2-2*C(J)
1 *D(I,J)
C
Z(I,J) = F(I,J)**2+2*E(J)*F(I,J)+2*D(I,J)*F(I,J)+2*C(J)
1 *F(I,J)+2*D(I,J)*E(J)+2*C(J)*E(J)+D(I,J)**2+2*C(J)*D(I,J)
C
IF (P(I,J).LT.0) THEN
A(I,J) = -((-C(J)*F(I,J)**2-2*C(J)*E(J)*F(I,J)
1 -2*C(J)*E(J)**2+C(J)*D(I,J)**2+2*C(J)**2*D(I,J))/(2*E(J)**2
1 +2*C(J)**2))
K(1) = 1
ELSE
A(I,J) = -((E(J)*SQRT(-F(I,J)**4-4*E(J)*F(I,J)**3+(-4*E(J)**2
1 +2*D(I,J)**2+4*C(J)*D(I,J)+4*C(J)**2)*F(I,J)**2+(4*D(I,J)**2
1 +8*C(J)*D(I,J)+8*C(J)**2)*E(J)*F(I,J)+(4*D(I,J)**2
1 +8*C(J)*D(I,J)+4*C(J)**2)*E(J)**2-D(I,J)**4-4*C(J)*D(I,J)**3
1 -4*C(J)**2*D(I,J)**2)-C(J)*F(I,J)**2-2*C(J)*E(J)*F(I,J)
1 -2*C(J)*E(J)**2+C(J)*D(I,J)**2+2*C(J)**2*D(I,J))/(2*E(J)**2
1 +2*C(J)**2))
ENDIF
C
IF (Q(I,J).LT.0.OR.Z(I,J).LT.0) THEN
B(I,J) = -((E(J)*F(I,J)**2+2*E(J)**2*F(I,J)+(-D(I,J)**2-2*C(J)
1 *D(I,J)-2*C(J)**2)*E(J))/(2*E(J)**2+2*C(J)**2))
K(2) = 1
ELSE
B(I,J) = -((C(J)*SQRT(-F(I,J)**2-2*E(J)*F(I,J)+2*D(I,J)*F(I,J)
1 +2*C(J)*F(I,J)+2*D(I,J)*E(J)+2*C(J)*E(J)-D(I,J)**2-2*C(J)
1 *D(I,J))*SQRT(F(I,J)**2+2*E(J)*F(I,J)+2*D(I,J)*F(I,J)+2*C(J)
1 *F(I,J)+2*D(I,J)*E(J)+2*C(J)*E(J)+D(I,J)**2+2*C(J)*D(I,J))
1 +E(J)*F(I,J)**2+2*E(J)**2*F(I,J)+(-D(I,J)**2-2*C(J)*D(I,J)
1 -2*C(J)**2)*E(J))/(2*E(J)**2+2*C(J)**2))
ENDIF
C
50 CONTINUE
C
C -----
C WRITE OUTPUT TO FILE
C -----
C
IF (K(1).EQ.1.OR.K(2).EQ.1) THEN
WRITE (9,2040) A(I,1),B(I,1),A(I,2),B(I,2),A(I,3)
1 ,B(I,3)
ELSE
WRITE (9,2050) A(I,1),B(I,1),A(I,2),B(I,2),A(I,3)
1 ,B(I,3)
ENDIF
51 CONTINUE
2025 FORMAT (' ')
2030 FORMAT (' ','"HORIZ 1"',',',',',"VERT 1"',',',',',"HORIZ 2"
1 ',',',',"VERT 2"',',',',',"HORIZ 3"',',',',',"VERT 3"')
2040 FORMAT (' ',F9.5,',',',',F9.5,',',',',F9.5,',',',',F9.5,
1 ',',',',F9.5,',',',','*')
2050 FORMAT (' ',F9.5,',',',',F9.5,',',',',F9.5,',',',',F9.5,
1 ',',',',F9.5)

```

RETURN
END

APPENDIX C

DERIVATION OF FORMULATION FOR COMPUTED STRAIN AND DISPLACEMENT FROM MEASURED STRAIN AND DISPLACEMENT DATA

At any location on the test specimen, the strain may be expressed as a function of the specimen curvatures and the coordinates of the location. This relationship may be written as:

$$\epsilon = -yk_x(z) - xk_y(z) + C \quad (C-1)$$

where: ϵ = total strain at a point in the specimen

x, y, z = coordinates of point

$$k_x = \text{curvature about the specimen x-axis} = \frac{d^2y}{dz^2}$$

$$k_y = \text{curvature about the specimen y-axis} = \frac{d^2x}{dz^2}$$

C = strain due to axial load, constant for a given axial load, P .

The curvature for a buckled member can be written as:

$$k_x = A \cos \left[\frac{\pi}{L_e} \left(z - \frac{L}{2} \right) \right] + B \sin \left[\frac{\pi}{L_e} \left(z - \frac{L}{2} \right) \right] \quad (C-2)$$

where: A, B = constants

L = length of specimen

L_e = distance between inflection points (locations of zero moment).

The "effective length" of a buckled member can then be computed as the distance between inflection points divided by the length of the column, or (L_e/L) . The y-axis curvature was related to the x-axis curvature using the relationship:

$$k_y(z) = rk_x(z) \quad (C-3)$$

$$\text{where: } r = \frac{\Delta x(2)}{\Delta y(2)}$$

and $\Delta x(2)$ = measured x displacement at or near midspan

$\Delta y(2)$ = measured y displacement at or near
midspan.

The constants A, B, C and L_o were determined to provide the least-square error to the 30 measured strains (ϵ_m).

Substituting Eq. C-3 into Eq. C-1 results in:

$$\epsilon = -(y + rx)k_x(z) + C. \quad (C-4)$$

Eq. C-2 can also be written as:

$$k_x = A \cos \psi + B \sin \psi \quad (C-5)$$

$$\text{where } \psi = \frac{\pi}{L_o} \left(z - \frac{L}{2} \right).$$

Substituting Eq. C-5 into Eq. C-4 results in an expression for computing the total strain:

$$\epsilon = -(y + rx)(A \cos \psi + B \sin \psi) + C. \quad (C-6)$$

Subtracting the calculated strain, ϵ , from the measured strain, ϵ_m , at each gage location results in the fit error, $EFIT$, or:

$$EFIT = \epsilon_m - \epsilon. \quad (C-7)$$

The total error of the data fit was computed by summing the square of the errors of all individual measurements:

$$\xi = \sum_{i=1,n} [EFIT(i)]^2 \quad (C-8)$$

where: n = number of measured strains.

Eq. C-8 is an expression of the error, ξ , which was minimized to obtain the best fit to the measured strains. Typically $n = 30$, however strain readings from gages in a yielded region, i.e. - gages with $|\epsilon_m| > 3000$, and readings which were statistical outliers were excluded from the data fit. To determine the statistical outliers, the strain error for each gage with $\epsilon_m < 3000$ was computed at each data step. The average and the

standard deviation of these strain errors were also calculated at each data step. Any gage with a strain error greater than 2 standard deviations from the average strain error was considered a statistical outlier and was eliminated from the data for that load step.

The constants A, B, C and L_e were determined to calculate the strain at a given location at each load step. To obtain the best fit for the measured strains, L_e was varied from $0.32L$ to $2.00L$. This corresponds to an effective length between 0.32 and 2.00 which were believed to be acceptable lower and upper bound values for the end conditions in this study. For each value of L_e , the constants A, B and C were computed that resulted in the least-square error. This error was then compared to the error for the other values of L_e . The L_e that resulted in the minimum least-square error was determined to be the effective length of the specimen for that load step. Values for L_e were determined at all data steps.

In order to obtain the least-square error, the partial derivative of the error, ξ , was taken with respect to the constants A, B , and C and set equal to zero. This results in three equations:

$$\frac{\partial \xi}{\partial A} = 2 \sum EFIT * \frac{\partial(-\epsilon)}{\partial A} = 0$$

$$\frac{\partial \xi}{\partial A} = 2 \sum EFIT * (y + rx) \cos \psi = 0 \quad (C-9)$$

$$\frac{\partial \xi}{\partial B} = 2 \sum EFIT * \frac{\partial(-\epsilon)}{\partial B} = 0$$

$$\frac{\partial \xi}{\partial B} = 2 \sum EFIT * (y + rx) \sin \psi = 0 \quad (C-10)$$

$$\frac{\partial \xi}{\partial C} = 2 \sum EFIT * \frac{\partial(-\epsilon)}{\partial C} = 0$$

$$\frac{\partial \xi}{\partial C} = 2 \sum EFIT * (-1) = 0 \quad (C-11)$$

which can be solved simultaneously to obtain A, B, and C. Substituting Eq. C-6 into Eq. C-7 results in an expression for EFIT:

$$EFIT = \epsilon_m + (y + rx)(A \cos \psi + B \sin \psi) - C. \quad (C-12)$$

Substituting Eq. C-12 into Eq. C-9 gives:

$$m_{11}A + m_{12}B + m_{13}C = a_1 \quad (C-13)$$

$$\text{where: } m_{11} = \sum (y_i + rx_i)^2 \cos^2 \psi_i$$

$$m_{12} = \sum (y_i + rx_i)^2 \sin \psi_i \cos \psi_i$$

$$m_{13} = - \sum (y_i + rx_i) \cos \psi_i$$

$$a_1 = - \sum \epsilon_{m_i} (y_i + rx_i) \cos \psi_i.$$

Similarly, substituting Eq. C-12 into Eq. C-10 gives:

$$m_{21}A + m_{22}B + m_{23}C = a_2 \quad (C-14)$$

$$\text{where: } m_{21} = m_{12}$$

$$m_{22} = \sum (y_i + rx_i)^2 \sin^2 \psi_i$$

$$m_{23} = - \sum (y_i + rx_i) \sin \psi_i$$

$$a_2 = - \sum \epsilon_{m_i} (y_i + rx_i) \sin \psi_i.$$

Finally, substituting Eq. C-12 into Eq. C-11 gives:

$$m_{31}A + m_{32}B + m_{33}C = a_3 \quad (C-15)$$

$$\text{where: } m_{31} = m_{13}$$

$$m_{32} = m_{23}$$

$$m_{33} = n$$

$$a_3 = \sum \epsilon_{m_i}.$$

Writing Eqs. C-13, C-14, and C-15 in matrix form:

$$\begin{bmatrix} m_{11} & m_{12} & m_{13} \\ m_{12} & m_{22} & m_{23} \\ m_{13} & m_{23} & m_{33} \end{bmatrix} \begin{Bmatrix} A \\ B \\ C \end{Bmatrix} = \begin{Bmatrix} a_1 \\ a_2 \\ a_3 \end{Bmatrix} \quad (C-16)$$

Applying Cramer's Rule to Eq. C-16 the unknown constants are obtained by:

$$\det = m_{11}m_{22}m_{33} + 2m_{12}m_{13}m_{23} - m_{13}^2m_{22} - m_{12}^2m_{33} - m_{23}^2m_{11}$$

$$A = \frac{1}{\det} [a_1m_{22}m_{33} + a_2m_{13}m_{23} + a_3m_{12}m_{23} - a_1m_{23}^2 - a_2m_{12}m_{33} - a_3m_{22}m_{13}]$$

$$B = \frac{1}{\det} [a_1m_{13}m_{23} + a_2m_{11}m_{33} + a_3m_{12}m_{13} - a_1m_{12}m_{33} - a_2m_{13}^2 - a_3m_{23}m_{11}]$$

$$C = \frac{1}{\det} [a_1m_{12}m_{23} + a_2m_{12}m_{13} + a_3m_{11}m_{22} - a_1m_{13}m_{22} - a_2m_{23}m_{11} - a_3m_{12}^2]$$

If the strain gages are evenly spaced around the circumference of the specimen and if all gages are included, then $m_{13} = m_{23} = 0$ so that $C = a_3/n$.

The curvature about the x and y-axis was calculated using Eq. C-5 and C-3.

The expression for curvature was integrated twice to determine the deflection of the specimen due to bending. Integrating Eq. C-2 twice and applying the boundary conditions, $f(0) = 0$ and $f(L) = 0$, results in:

$$f(z) = \frac{-L_e^2}{\pi^2} \left\{ k_x(z) - A \cos \left[\frac{\pi}{L_e} \left(\frac{L}{2} \right) \right] + B \sin \left[\frac{\pi}{L_e} \left(\frac{L}{2} \right) \left(\frac{\frac{L}{2} - z}{\frac{L}{2}} \right) \right] \right\} \quad (C-17)$$

where: $f(z)$ = y-deflection at location z from origin of coordinate system.

It was observed during the full scale testing that a hinge often forms at some location along the specimen.

Thus, a rigid body component was included in the total deflection expression. The total deflection at any location on the specimen was then calculated as:

$$\Delta x(z) = rf(z) + \beta_x g(z) \quad (C-18)$$

and

$$\Delta y(z) = f(z) + \beta_y g(z) \quad (C-19)$$

where: β_x and β_y = constants equal to the rigid body deflections at the point of hinging in x and y-directions, respectively
 $g(z)$ = function relating the hinging location and any location on the specimen

$$g(z) = \begin{cases} \frac{z}{z_b} & \text{for } z \leq z_b \\ \frac{L - z}{L - z_b} & \text{for } z \geq z_b \end{cases}$$

z_b = location of hinge.

The rigid body deflection constants, β_x and β_y , were determined to produce calculated displacements with a least-square error to the measured displacements. This was done by computing an error term for the calculated displacements, setting the derivatives of the error term with respect to β_x and β_y to zero, and solving the resulting equations.

Taking z_j to be the location of a measured displacement, then:

$$f_j = f(z_j)$$

$$g_j = g(z_j).$$

If the measured displacements at z_j are denoted by Δx_j

and Δy_j , the error term for the displacement in the x direction, *EDISP*, becomes:

$$EDISP = rf_j + \beta_x g_j - \Delta x_j. \quad (C-20)$$

The total error for the x-displacements, ζ , was calculated as the sum of the squares of the individual *EDISP* errors, so that:

$$\zeta = \sum_{j=1,m} (rf_j + \beta_x g_j - \Delta x_j)^2 \quad (C-21)$$

where: m = number of locations where x-displacement was measured

= 3.

Taking the partial derivative of Eq. C-21 with respect to β_x :

$$\frac{\partial \zeta}{\partial \beta_x} = 2 \sum (rf_j + \beta_x g_j - \Delta x_j) g_j. \quad (C-22)$$

To minimize the x-displacement error, set Eq. C-22 equal to zero and solve for β_x so that:

$$\beta_x = \frac{\sum (\Delta x_j - rf_j) g_j}{\sum g_j^2}. \quad (C-23)$$

Similarly, the error was minimized for the y-displacements by taking the partial derivative of ζ with respect to β_y and setting it equal to zero, where:

$$\zeta = \sum_{j=1,m} (f_j + \beta_y g_j - \Delta y_j)^2. \quad (C-24)$$

The resulting equation is:

$$\beta_y = \frac{\sum (\Delta y_j - f_j) g_j}{\sum g_j^2}. \quad (C-25)$$

A FORTRAN computer code, CURVE, was written to perform the analysis described in this appendix and is listed on the following pages. In addition to determining the effective length of the specimen, the x-

and y-eccentricity of the applied load was also computed. This was accomplished by computing the x and y-displacements at the two inflection locations. Since the moment must be zero at an inflection location, the line of action of the load must pass through the centroid of the cross-section at that location. Therefore, the x- and y- displacements at the inflection locations must be equal to the x- and y- eccentricity of the applied load.

PROGRAM CURVE

PURPOSE: THIS PROGRAM ATTEMPTS TO FIND THE EFFECTIVE LENGTH OF THE PIPE. IN ORDER TO DO THIS, IT FITS A COSINE WAVE, A SINE WAVE, AND A LINEAR TERM TO THE CURVATURE OF THE SPECIMEN BY USING THE STRAIN GAUGE DATA AND A LEAST SQUARES METHOD.

VARIABLE LIBRARY

A = THE COEFFICIENT OF THE COSINE WAVE TERM
 A_{ij} = THE A_{ij} COEFFICIENT OF THE CURVE FITTING MATRIX
 A_{ji} = THE A_{ji} COEFFICIENT OF THE CURVE FITTING MATRIX
 AMIN = THE A ASSOCIATED WITH ERRMIN
 B = THE COEFFICIENT OF THE SINE WAVE TERM
 BETAX = THE COEFFICIENT FOR THE LINEAR TERM OF THE X DISPLACEMENTS
 BETAY = THE COEFFICIENT FOR THE LINEAR TERM OF THE Y DISPLACEMENTS
 BMIN = THE B ASSOCIATED WITH ERRMIN
 BUKLPT = THE POINT OF THE HINGE IN THE PIPE WHEN IT BUCKLES
 C = THE COEFFICIENT OF THE AXIAL STRAIN TERM
 CMIN = THE C ASSOCIATED WITH ERRMIN
 COORD(I,1) = THE X COORDINATE OF STRAIN GAUGE I
 COORD(I,2) = THE Y COORDINATE OF STRAIN GAUGE I
 COORD(I,3) = THE Z COORDINATE OF STRAIN GAUGE I
 DEN = THE DENOMINATOR OF THE EXPRESSION USED TO CALCULATE BETAX AND BETAY
 DET = THE DETERMINANT OF THE CURVE FITTING MATRIX
 DOAGIN = LOGICAL VARIABLE USED TO DETERMINE IF A, B, AND C SHOULD BE RE-COMPUTED WITH OUTLYING STRAIN GAUGE READINGS ELIMINATED FROM A TIME STEP
 DUM1 = A DUMMY VARIABLE THAT TAKES ON DIFFERENT VALUES IN DIFFERENT PARTS OF THE PROGRAM
 DUM2 = A DUMMY VARIABLE THAT TAKES ON DIFFERENT VALUES IN DIFFERENT PARTS OF THE PROGRAM
 DX(NN,I) = THE MEASURED X DISPLACEMENT AT LOCATION I AND LOAD STEP NN
 DY(NN,I) = THE MEASURED Y DISPLACEMENT AT LOCATION I AND LOAD STEP NN
 ERRMIN = THE MINIMUM ERROR OF FIT FOUND FOR THE CURVATURE
 ERRX = THE SQUARED ERROR OF THE COMPUTED X DISPLACEMENTS
 ERRY = THE SQUARED ERROR OF THE COMPUTED Y DISPLACEMENTS
 EX = THE ROOT MEAN SQUARED ERROR OF THE COMPUTED X DISPLACEMENTS
 EY = THE ROOT MEAN SQUARED ERROR OF THE COMPUTED Y DISPLACEMENTS
 F(I) = THE TRANSCENDENTAL FUNCTION USED IN COMPUTING DISPLACEMENTS
 FIRST = LOGICAL VARIABLE USED TO PREVENT MORE THAN ONE SET OF OUTLYING STRAIN GAUGE READINGS FROM BEING ELIMINATED IN A LOAD STEP
 GEC = THE LINEAR FUNCTION USED IN COMPUTING DISPLACEMENTS AT INFLECTION POINTS
 G(I) = THE LINEAR FUNCTION USED IN COMPUTING DISPLACEMENTS
 H(I) = THE COMPUTED HORIZONTAL DISPLACEMENT AT LOCATION I
 I = A LOOP COUNTER
 J = A LOOP COUNTER
 JJ = A LOOP COUNTER
 K = A LOOP COUNTER
 KK = A LOOP COUNTER
 L = THE LENGTH OF THE PIPE
 LEFF = THE EFFECTIVE LENGTH OF THE PIPE
 LMIN = THE L ASSOCIATED WITH ERRMIN
 MSR = THE SUM OF THE SQUARED X AND Y DISPLACEMENTS

```

C      MSS = MEAN SQUARED STRAIN
C      NDS = THE NUMBER OF DATA STEPS
C      NN = A LOOP COUNTER
C      NUMX = THE NUMERATOR OF THE EXPRESSION USED TO CALCULATE BETAX
C      NUMY = THE NUMERATOR OF THE EXPRESSION USED TO CALCULATE BETAY
C      PI = 3.141592654
C      PSI = THE ARGUMENT OF THE SINE AND COSINE TERMS
C      R = THE RATIO BETWEEN THE Y CURVATURES AND THE X CURVATURES
C      RHSI = THE RIGHT HAND SIDE OF EQUATION I
C      RMIN = THE R ASSOCIATED WITH ERRMIN
C      RMS = ROOT MEAN SQUARED ERROR
C      SDEV = STANDARD DEVIATION OF THE NORMALIZED STRAIN GAUGE READING ERRORS
C              FOR A LOAD STEP
C      STRAIN(I) = THE MEASURED STRAIN OF GAUGE I
C      STRER = AVERAGE NORMALIZED STRAIN GAUGE READING ERROR FOR A LOAD STEP
C      STRER(I) = NORMALIZED STRAIN GAUGE READING ERROR FOR GAUGE I
C      V(I) = THE COMPUTED VERTICAL DISPLACEMENT AT LOCATION I
C      XECI = THE COMPUTED X ECCENTRICITY OF THE LOAD AT LOCATION I
C      XEFF = THE LOCATION OF THE INFLECTION POINT RELATIVE TO THE ORIGIN
C              OF THE COORDINATE SYSTEM
C      XEFF1 = THE LOCATION OF THE INFLECTION POINT CLOSEST TO THE ORIGIN OF THE
C              COORDINATE SYSTEM
C      XEFF2 = THE LOCATION OF THE INFLECTION POINT FURTHEST FROM THE ORIGIN OF
C              THE COORDINATE SYSTEM
C      YECI = THE COMPUTED Y ECCENTRICITY OF THE LOAD AT LOCATION I
C      Z(I) = THE Z COORDINATE OF THE VERTICAL AND HORIZONTAL DISPLACEMENT
C              MEASUREMENTS AT LOCATION I
C
C      IMPLICIT NONE
C      INTEGER I, J, K, NDS, NN, JJ, KK
C      REAL COORD(0:29,3), A11, A12, A22, RHS1, RHS2, STRAIN(0:29), LEFF,
+      L, PI, DUM1, A, B, R, PSI, ERRMIN, RMS, AMIN, BMIN, STRER,
+      RMIN, MSS, LMIN, C, CMIN, RHS3, A13, A23, A33, DET, G(3),
+      BUKLPT, Z(3), DX(150,3), DY(150,3), F(3), BETAX, BETAY, NUMX,
+      NUMY, DEN, DUM2, MSR, ERRX, ERRY, EX, EY, V(3), H(3), SDEV,
+      GEC, XEFF1, XEFF2, XEC1, XEC2, YEC1, YEC2, XEFF, STRERR(0:29)
C      LOGICAL DOAGIN, FIRST
C
C      OPEN(UNIT=10,FILE='RING1.STR',STATUS='OLD')
C      OPEN(UNIT=20,FILE='RING2.STR',STATUS='OLD')
C      OPEN(UNIT=30,FILE='RING3.STR',STATUS='OLD')
C      OPEN(UNIT=40,FILE='RING4.STR',STATUS='OLD')
C      OPEN(UNIT=50,FILE='RING5.STR',STATUS='OLD')
C      OPEN(UNIT=60,FILE='SGLOC.OUT',STATUS='OLD')
C      OPEN(UNIT=70,FILE='CURVE.OUT',STATUS='NEW')
C
C      PI = 3.141592654
C
C      READ IN GAUGE LOCATIONS, L, AND NUMBER OF DATA STEPS
C
C      READ(60,*) ((COORD(I,J),J=1,3),I=0,29), L ,NDS
C
C      CLOSE(UNIT=60)
C      OPEN(UNIT=80,FILE='HVDISP.INP',STATUS='OLD')
C

```

```

C READ IN THE Z DISTANCES TO THE STRINGPOTS AND THE BUCKLED POINT
C READ ALL THE HORIZONTAL AND VERTICAL DISPLACEMENTS
C
  READ(80,*) BUKLPT
  READ(80,*) (Z(I),I=1,3)
  DO 125 I = 1,NDS
    READ(80,*) DX(I,1),DY(I,1),DX(I,2),DY(I,2),DX(I,3),DY(I,3)
125 CONTINUE
  CLOSE(UNIT=80)
C COMPUTE THE FUNCTION G(I) FOR USE IN COMPUTING DISPLACEMENTS
C
  DO 120 I = 1,3
    IF (Z(I).LT.BUKLPT)THEN
      G(I) = Z(I)/BUKLPT
    ELSE
      G(I) = (L-Z(I))/(L-BUKLPT)
    ENDIF
120 CONTINUE
C
C READ IN THE STRAINS AND HORIZONTAL AND VERTICAL DISPLACEMENTS
C
  DO 1000 NN = 1, NDS
    JJ=NN-1
    PRINT 110, JJ, NDS-1
110 FORMAT(' ', 'TIMESTEP', I3, ' OF ', I3)
    READ(10,*) (STRAIN(I),I=0,5)
    READ(20,*) (STRAIN(I),I=6,11)
    READ(30,*) (STRAIN(I),I=12,17)
    READ(40,*) (STRAIN(I),I=18,23)
    READ(50,*) (STRAIN(I),I=24,29)
C
C DIVIDE THE INPUTTED STRAINS BY 10**6
C
  DO 150 I = 0,29
    STRAIN(I) = STRAIN(I)/10**6
150 CONTINUE
C
C ITERATE FROM LEFF = 0.5*L TO 2.0L
C
  FIRST = .TRUE.
  5 ERRMIN = 100.0
  LMIN = L
  AMIN = 0.0
  BMIN = 0.0
  CMIN = 0.0
  RMIN = 0.0
  KK=0
C
C CALCULATE MSS
C
  MSS = 0.0
  DO 20 I=0,29
    IF (ABS(STRAIN(I)).GT.0.003) THEN
      GO TO 20
    ELSE

```

```

        MSS = MSS+STRAIN(I)**2
    END IF
20 CONTINUE
C
    DO 35 J=0,84
        KK=KK+1
        LEFF = (0.32+FLOAT(J)/50.0)*L
C
C FIND BEST A, B, AND C
C
        R=DX(NN,2)/DY(NN,2)
C
C THE FOLLOWING LOOP FINDS THE VALUES OF A, B, AND C
C
        A11 = 0.0
        A12 = 0.0
        A13 = 0.0
        A22 = 0.0
        A23 = 0.0
        A33 = 0.0
        RHS1 = 0.0
        RHS2 = 0.0
        RHS3 = 0.0
        DO 10 I=0,29
            IF (ABS(STRAIN(I)).GT.0.003) THEN
                GO TO 10
            ELSE
                PSI = PI/LEFF*(COORD(I,3)-L/2.0)
                DUM1 = COORD(I,2)+R*COORD(I,1)
                A11 = A11+(COS(PSI)*DUM1)**2
                A12 = A12+SIN(PSI)*COS(PSI)*DUM1**2
                A13 = A13-DUM1*COS(PSI)
                A22 = A22+(SIN(PSI)*DUM1)**2
                A23 = A23-DUM1*SIN(PSI)
                A33 = A33+1
                RHS1 = RHS1-STRAIN(I)*COS(PSI)*DUM1
                RHS2 = RHS2-STRAIN(I)*SIN(PSI)*DUM1
                RHS3 = RHS3+STRAIN(I)
            END IF
10 CONTINUE
C
C CRAMER'S RULE TO FIND A, B AND C (NOTE: A12 = A21, A23=A32, A13=A31)
C
        DET = A11*A22*A33+2*A12*A13*A23-A22*A13**2
        + -A33*A12**2-A11*A23**2
        A = (RHS1*A22*A33+RHS2*A13*A23+RHS3*A12*A23
        + -RHS1*A23**2-RHS2*A12*A33-RHS3*A22*A13)/DET
        B = (RHS1*A13*A23+RHS2*A11*A33+RHS3*A12*A13
        + -RHS1*A12*A33-RHS2*A13**2-RHS3*A23*A11)/DET
        C = (RHS1*A12*A23+RHS2*A12*A13+RHS3*A11*A22
        + -RHS1*A13*A22-RHS2*A23*A11-RHS3*A12**2)/DET
C
C FIND ERROR OF FIT FOR A, B, AND R
C
        RMS = 0.0

```

```

DO 30 I=0,29
  IF (ABS(STRAIN(I)).GT.0.003) THEN
    GO TO 30
  ELSE
    PSI = PI/LEFF*(COORD(I,3)-L/2.0)
    RMS = RMS+(STRAIN(I)-C+(A*COS(PSI)+B*SIN(PSI))
      + *(COORD(I,2)+R*COORD(I,1)))**2
    END IF
30  CONTINUE
    RMS = SQRT(RMS/MSS)*100.0
    IF (RMS.LT.ERRMIN) THEN
      ERRMIN = RMS
      LMIN = LEFF
      AMIN = A
      BMIN = B
      CMIN = C
    END IF
35  CONTINUE
    LEFF = LMIN
    A = AMIN
    B = BMIN
    C = CMIN
C
C  DETERMINE IF ANY OF THE GAUGES SHOULD BE THROWN OUT
C
  IF (FIRST) THEN
    FIRST = .FALSE.
    STRER = 0.0
    RMS = 0.0
    KK = 30
  DO 50 I=0,29
    IF (ABS(STRAIN(I)).GT.0.003) THEN
      KK = KK-1
      GO TO 50
    ELSE
      PSI = PI/LEFF*(COORD(I,3)-L/2.0)
      STRERR(I) = STRAIN(I)-C+(A*COS(PSI)+B*SIN(PSI))
      + *(COORD(I,2)+R*COORD(I,1))
      STRER = STRER+STRERR(I)
    END IF
  50  CONTINUE
    RMS = SQRT(MSS/KK)
    STRER = STRER/KK/RMS
C
C  CALCULATE THE STANDARD DEVIATION OF THE ERRORS
C
    SDEV = 0.0
    DO 60 I=0,29
      IF (ABS(STRAIN(I)).GT.0.003) THEN
        GO TO 60
      ELSE
        SDEV = SDEV+(STRERR(I)/RMS-STRER)**2
      END IF
    60  CONTINUE
    SDEV = SQRT(SDEV/(KK-1))

```

```

C
C  THROW OUT POINTS OVER TWO STANDARD DEVIATIONS OF ERROR FROM THE AVERAGE
C  ERROR
C
      DOAGIN = .FALSE.
      DO 70 I=0,29
        IF (ABS(STRAIN(I)).GT.0.003) THEN
          GO TO 70
        ELSE IF (ABS(STRERR(I)/RMS-STRER).GT.2.0*SDEV) THEN
          STRAIN(I) = 0.0031
          DOAGIN = .TRUE.
        END IF
      70 CONTINUE
C
C  RECALCULATE A, B, AND C IF ONE OF THE GAUGES WAS THROWN OUT
C
      IF (DOAGIN) THEN
        GO TO 5
      END IF
      END IF
C
C  COMPUTE THE COEFFICIENTS OF THE LINEAR PORTION OF THE DISPLACED SHAPE
C
      NUMX = 0.0
      NUMY = 0.0
      DEN = 0.0
      DUM1 = PI/2.0*L/LEFF
      DO 130 I = 1,3
        PSI = PI/LEFF*(Z(I)-L/2.0)
        DUM2 = (L/2.0-Z(I))/(L/2.0)
        F(I) = -(A*(COS(PSI)-COS(DUM1))+B*(SIN(PSI)+DUM2
+          *SIN(DUM1)))*(LEFF/PI)**2
        NUMX = NUMX+(DX(NN,I)-R*F(I))*G(I)
        NUMY = NUMY+(DY(NN,I)-F(I))*G(I)
        DEN = DEN+(G(I)**2)
      130 CONTINUE
      BETAX = NUMX/DEN
      BETAY = NUMY/DEN
C
C  COMPUTE X AND Y DISPLACEMENT ERRORS
C
      MSR = 0.0
      ERRX = 0.0
      ERRY = 0.0
      DO 170 I = 1,3
        H(I) = R*F(I) + BETAX*G(I)
        V(I) = F(I) + BETAY*G(I)
        MSR = MSR+DX(NN,I)**2+DY(NN,I)**2
        ERRX = ERRX+(H(I)-DX(NN,I))**2
        ERRY = ERRY+(V(I)-DY(NN,I))**2
      170 CONTINUE
      EX = 100.0*SQRT(ERRX/MSR)
      EY = 100.0*SQRT(ERRY/MSR)
C
C  COMPUTE THE POINTS OF INFLECTION AND ECCENTRICITIES BASED ON CURVATURE

```

C

```

XEFF = L/2.0-LEFF/PI*ATAN(A/B)
IF(XEFF.GT.L/2.0) THEN
  XEFF2 = XEFF
  XEFF1 = XEFF2-LEFF
ELSE
  XEFF1 = XEFF
  XEFF2 = XEFF1+LEFF
END IF
IF(XEFF1.LT.BUKLPT) THEN
  GEC = XEFF1/BUKLPT
ELSE
  GEC = (L-XEFF1)/(L-BUKLPT)
END IF
DUM1 = PI/LEFF*(XEFF1-L/2.0)
DUM2 = PI/2.0*L/LEFF
XEC1 = BETAX*GEC-(A*(COS(DUM1)-COS(DUM2))+B*(SIN(DUM1)-2.0/L*
+ (XEFF1-L/2.0)*SIN(DUM2)))*R*((LEFF/PI)**2)
YEC1 = BETAY*GEC-(A*(COS(DUM1)-COS(DUM2))+B*(SIN(DUM1)-2.0/L*
+ (XEFF1-L/2.0)*SIN(DUM2)))*((LEFF/PI)**2)
IF(XEFF2.LT.BUKLPT) THEN
  GEC = XEFF2/BUKLPT
ELSE
  GEC = (L-XEFF2)/(L-BUKLPT)
END IF
DUM1 = PI/LEFF*(XEFF2-L/2.0)
XEC2 = BETAX*GEC-(A*(COS(DUM1)-COS(DUM2))+B*(SIN(DUM1)-2.0/L*
+ (XEFF2-L/2.0)*SIN(DUM2)))*R*((LEFF/PI)**2)
YEC2 = BETAY*GEC-(A*(COS(DUM1)-COS(DUM2))+B*(SIN(DUM1)-2.0/L*
+ (XEFF2-L/2.0)*SIN(DUM2)))*((LEFF/PI)**2)

```

C

C PRINT OUT FINAL RESULTS

C

WRITE(70,100) JJ

100 FORMAT(' '// 'STEP NO. = ',I3)

C

C PRINT OUT THE GAUGES THROWN OUT

C

DO 250 I=0,29

IF (STRAIN(I).EQ.0.0031) THEN

WRITE(70,230) I

230 FORMAT(' ', 'GAUGE NO. ', I2, ' ELIMINATED DUE TO DEVIATION',

+ ' ERROR')

ELSE IF (ABS(STRAIN(I)).GT.0.003) THEN

WRITE(70,240) I

240 FORMAT(' ', 'GAUGE NO. ', I2, ' ELIMINATED DUE TO MAX READING')

END IF

250 CONTINUE

PRINT 36, LEFF/L, A, B, C, R, ERRMIN

PRINT 300

300 FORMAT(/)

WRITE(70,36) LEFF/L, A, B, C, R, ERRMIN

36 FORMAT('LEFF/L = ', F4.2, 3X, 'A = ', G12.5, 3X, 'B = ', G12.5, 3X,

+ 'C = ', G12.5, '/', 'R = ', G12.5, 3X, 'STRAIN ERROR = ', F6.2, '%')

WRITE(70,160) BETAX, BETAY

```

160 FORMAT(' ', 'BETAX = ', G12.5, 3X, 'BETAY = ', G12.5)
    DO 200 I = 1, 3
        WRITE(70, 190) I, H(I), I, V(I)
190 FORMAT(' ', 'X', I1, ' = ', G12.5, 3X, 'Y', I1, ' = ', G12.5)
200 CONTINUE
        WRITE(70, 180) EX, EY
180 FORMAT(' ', 'X DISP ERROR = ', F6.2, ' ', 3X, 'Y DISP ERROR = ',
    +      F6.2, ' ')
        WRITE(70, 210) XEFF1/L, XEC1, YEC1, XEFF2/L, XEC2, YEC2
210 FORMAT(' ', 'ZEFF1/L = ', F9.4, 3X, 'XEC1 = ', F9.4, 3X, 'YEC1 = ', F9.4,
    +      ' ', 'ZEFF2/L = ', F9.4, 3X, 'XEC2 = ', F9.4, 3X, 'YEC2 = ', F9.4)
1000 CONTINUE
C
C CLOSE FILES AND LEAVE
C
    DO 40 I=10, 50, 10
        CLOSE(UNIT=I)
40 CONTINUE
    CLOSE(UNIT=70)
END

```


APPENDIX D

APPLIED LOAD ECCENTRICITY AS COMPUTED FROM
END MOMENTS

In the experimental program, the line of action of the applied compressive load was located as near to the centroid of the cross-section as possible. Since the ends of the specimens were not attached to the load frame, it was possible for the ends to rotate if the specimen failed in an overall buckling mode. If the ends rotated, the compressive load was no longer applied through the centroid of the cross-section, but rather, was applied eccentrically. The eccentricity of loading was determined by computing the displacements at the inflection points of the buckled specimen as described in Appendix C. In addition, the load eccentricity may also be calculated using the end moments as computed from the curvature of the buckled specimen. This appendix contains a detailed description of this method for computing the load eccentricity.

An eccentric compressive load induces an applied bending moment at the ends of the specimen. This applied bending moment is:

$$M = Pe \quad (D-1)$$

where: P = applied compressive load

e = eccentricity of applied load.

From fundamental mechanics, the bending moment can be expressed in terms of the curvature at any location along a member by:

$$M_i = k_i EI_i \quad (D-2)$$

where: M_i = bending moment with respect to the i-axis

k_i = specimen curvature with respect to the i-axis

E = modulus of elasticity (29,500 ksi)

I_i = moment of inertia with respect to the i-axis.

Substituting Eq. D-2 into Eq. D-1 results in:

$$Pe_j = k_i EI_i. \quad (D-3)$$

Solving Eq. D-3 for eccentricity results in:

$$e_j = EI_i \frac{k_i}{P} \quad (D-4)$$

where: j axis is perpendicular to the i axis.

The modulus of elasticity and moment of inertia were assumed constant along the length of each specimen for all load steps. The moment of inertia was computed based on nominal section properties while the applied compressive load was computed from the measured data at each load step. The curvature at each end of the specimen was determined by substituting $z = 0$ and $z = L$ into Eq. C-3 and C-5 of Appendix C. Using Eq. D-4, the eccentricity in the x and y directions at each end of the specimen was then computed for each load step.

The computer program ECC was written and utilized to perform these calculations. A listing of this program can be found on the following pages.

PROGRAM ECC

```

C
C PURPOSE: THIS PROGRAM CALCULATES THE END ECCENTRICITIES OF THE PIPE AND
C AVERAGES THEM.
C
C VARIABLE LIBRARY
C
C   A = THE COEFFICIENT OF THE COSINE TERM USED TO FIT THE DISPLACED
C       SHAPE IN CURVE.FOR
C   B = THE COEFFICIENT OF THE SINE TERM USED TO FIT THE DISPLACED
C       SHAPE IN CURVE.FOR
C   EI = YOUNG'S MODULUS TIMES THE MOMENT OF INERTIA
C   EX1 = THE X-ECCENTRICITY AT Z = 0
C   EX2 = THE X-ECCENTRICITY AT Z = L
C   EY1 = THE Y-ECCENTRICITY AT Z = 0
C   EY2 = THE Y-ECCENTRICITY AT Z = L
C   I = A LOOP COUNTER
C   KE = THE LENGTH OF THE PIPE DIVIDED BY THE EFFECTIVE LENGTH OF THE
C       PIPE
C   NOSTEP = THE NUMBER OF TIME STEPS
C   P = LOAD
C   PI = 3.141592654
C   R = Y-CURVATURE/X-CURVATURE
C
C TYPE DECLARATIONS
C
C   IMPLICIT NONE
C   INTEGER I, NOSTEP
C   REAL A, B, EI, EX1, EX2, EY1, EY2, KE, P, PI, R
C
C OPEN INPUT AND OUTPUT FILES
C
C   OPEN(UNIT=10,FILE='ECC.INP',STATUS='OLD')
C   OPEN(UNIT=20,FILE='ECC.OUT',STATUS='NEW')
C   OPEN(UNIT=30,FILE='ECC.PLT',STATUS='NEW')
C
C READ IN THE NUMBER OF TIME STEPS AND EI
C
C   READ(10,*) NOSTEP, EI
C
C CALCULATE THE ECCENTRICITIES AND WRITE THEM TO THE OUTPUT FILE
C
C   PI = 3.141592654
C   DO 30 I=0,NOSTEP
C     READ(10,*) KE, A, B, R, P
C     EY1 = EI/P*(A*COS(PI/(2.0*KE))-B*SIN(PI/(2.0*KE)))
C     EY2 = EI/P*(A*COS(PI/(2.0*KE))+B*SIN(PI/(2.0*KE)))
C     EX1 = EY1*R
C     EX2 = EY2*R
C     WRITE(20,25) I,EX1,EY1,EX2,EY2,(EX1+EX2)/2.0,(EY1+EY2)/2.0
C     WRITE(30,20) EX1, EX2, (EX1+EX2)/2.0, EY1, EY2, (EY1+EY2)/2.0
C 30 CONTINUE
C
C FORMAT STATEMENTS
C

```

```
20 FORMAT(' ',6(G12.5,1X))
25 FORMAT(' ', 'STEP NO.',I3/'EX1 = ',G12.5,3X,'EY1 = ',G12.5/'EX2 = '
    +,G12.5,3X,'EY2 = ',G12.5/'AVERAGE EX = ',G12.5,3X,'AVERAGE EY = ',
    +G12.5/)
```

```
C
C CLOSE FILES AND LEAVE
C
```

```
    CLOSE(UNIT=10)
    CLOSE(UNIT=20)
    CLOSE(UNIT=30)
END
```

APPENDIX E

FORMULATION FOR COMPUTING FULL SCALE
EFFECTIVE WALL THICKNESS

The average axial strain in a linearly, elastic member subjected to a compressive axial load can be written as:

$$\epsilon_{avg} = \left(\frac{P}{A E} \right) \quad (E-1)$$

where:

P = axial load,

A = cross-sectional area,

E = modulus of elasticity (for steel, 29,500 ksi).

Equating this expression to the axial strain coefficient from the CURVE algorithm:

$$C = \epsilon_{avg} = \left(\frac{P}{A_{eff} E} \right) \quad (E-2)$$

where:

C = axial strain coefficient from CURVE algorithm
(see Appendix C) at a given load step,

P = measured load at a given load step,

A_{eff} = effective cross-sectional area of the member
at a given load step.

Solving Eq. E-2, for the effective area at a given load step:

$$A_{eff} = \left(\frac{P}{C E} \right) = \frac{\pi}{4} (d_o^2 - d_i^2) \quad (E-3)$$

where:

d_o = measured nominal outside diameter,

d_i = computed inside diameter at a given load

step.

Solving for the computed inside diameter at a given load step:

$$d_i = \left(d_o^2 - \frac{4}{\pi} A_{eff} \right) = \left[d_o^2 - \frac{4}{\pi} \left(\frac{P}{C E} \right) \right]^{1/2} \quad (E-4)$$

Substituting the effective wall thickness:

$$t_{eff} = \frac{d_o - d_i}{2}$$

into Eq. E-4, results in an expression for the effective wall thickness for a given load step:

$$t_{eff} = \frac{d_o - \left[d_o^2 - \frac{4}{\pi} \left(\frac{P}{C E} \right)^{1/2} \right]}{2} \quad (E-5)$$

DOCUMENTATION OF INFORMATION PRESENTED ON COMPUTER DISKS

Computer Code, Input Files, and Output Files

Computer Code

The measured data was reduced using 5 computer codes written specifically for this study. The fortran code (uncompiled) is on this disk for each program with the file extension (.FOR). In order to run the programs, the code must be compiled to create an executable (.EXE) file. It should be noted that these programs have been upgraded to facilitate data input since they were first written. As a result, some of the input files may have to be slightly modified before they will run in the current format. For instance, all input to the DISPLAC program first had the specimen number in the filename, i.e. LSP01.DAT. Using this method, the computer code must be changed to read filenames with the correct specimen number and recompiled for every specimen. Therefore, the code was changed to input data from filenames without the specimen number identification, i.e. LSP.DAT.

The possible adjustments which may be needed to run each program are presented in this section. Changes to filenames or computer codes should be made using a non-document type of word processing editor.

PROGRAM SGL.FOR

This program converts the longitudinal and circumferential strain gage location measurements to x,y, and z coordinates corresponding to the full scale test sign convention. Input is from the file SGLOC.INP and output is to the file SGLOC.OUT. Example input and output files are shown on the following pages.

Input necessary for this program includes specimen number, diameter, length, and strain gage locations as measured prior to full scale testing. The SGLOC.INP files listed on the accompanying specimen disks should be ready to input into SGL.FOR. The output file is to be used in the program CURVE.FOR. Please note that the number of data steps must be added to this file prior to running the CURVE program.

Please note: Information typed in boldface is for explanation only and not included in files.

Example SGLOC.INP file:

01, 9.0, 235.25	Specimen No., diameter, length
5.25	- Gage 0
12.5	- Gage 1
24.5	
-22.75	
-13.375	
-3.5	- Etc. -
13.625	
24.375	
-22.5	
-13.25	
-2.375	
5.5	
15.0	
24.375	
-22.75	
-14.625	
-5.25	
5.5	
12.75	
26.75	
-22.875	
-13.75	
-3.75	
5.625	
14.875	
24.125	
-23.375	
-13.875	
-4.625	- Gage 29
195.875	- Distance to gages 0,1,2,3,4 and 5 from end B
156.75	
117.625	- Etc.
82.75	
44.8758	- Distance to gages 24,25,26,27,28 and 29 from end B

Note: All measurements in inches.

Example SGLOC.OUT file:

x	y	z	coordinates
4.9573	7.5117	195.8750	
8.8515	1.6282	195.8750	
3.6647	-8.2201	195.8750	
-5.1839	-7.3571	195.8750	
-8.9677	.7613	195.8750	
-3.4124	8.3280	195.8750	
5.1640	7.3711	156.7500	
8.9854	.5119	156.7500	
3.7785	-8.1684	156.7500	
-5.3862	-7.2103	156.7500	
-8.9563	.8857	156.7500	
-2.3475	8.6884	156.7500	
5.1640	7.3711	117.6250	
8.9587	-.8615	117.6250	
3.7785	-8.1684	117.6250	
-5.1839	-7.3571	117.6250	
-8.9868	-.4876	117.6250	
-4.9573	7.5117	117.6250	
5.1640	7.3711	82.7500	
8.8933	1.3817	82.7500	
1.5171	-8.8712	82.7500	
-5.0812	-7.4284	82.7500	
-8.9917	.3870	82.7500	
-3.6424	8.2300	82.7500	
5.2659	7.2987	44.8758	
8.9698	-.7370	44.8758	
4.0039	-8.0603	44.8758	
-4.6609	-7.6991	44.8758	
-8.9962	.2621	44.8758	
-4.4241	7.8376	44.8758	

235.2500 Length, inches.

75 Number of data steps, not include in SGL output.

Must be added before input to CURVE

PROGRAM DISPLAC.FOR

This program computes the resultant load, the chord shortening, the horizontal displacements, and the vertical displacements at each data step. The measured data is read from 4 files. These are LSP##.DAT, HVP##.DAT, LOAD##1.DAT, AND LOAD##2.DAT. For each specimen, the corresponding specimen number replaces ##, i.e. LSP01.DAT. The output is broken into two files. The first file, SPEC##1.OUT, contains the load and chord shortening information. In addition, the time and resultant load location is given. The second file, SPEC##2.OUT, contains the horizontal and vertical displacements measured at six locations.

Sample input and output files are given on the following pages. For some of the specimens, it may be necessary to add the number of load steps to the LSP##.DAT file. In addition, the specimen numbers must be removed from all the input filenames. For example, LSP01.DAT must be changed to LSP.DAT. The output filenames will not have specimen numbers included either, i.e. SPEC1.OUT. If the specimen numbers are desired for inventory purposes, the filename can be changed. See note below.

Some of the output files on the disks may or may not have the headers shown in the example files. This is because the headers are removed when the files are input into other programs to create plot files. However, none of the information is missing.

Note: To change a filename:

- 1) At DOS prompt, type `rename filename.ext filename.ext`

Example:

```
C:\> rename LSP01.DAT LSP.DAT
```

Please note: Information typed in boldface is for explanation only and not included in files.

Input Files

Example LSP.DAT file:

'"SPECIMEN 02 - 2/2/90"' Title

81 Number of data steps - may need to be added

22.125 3.958 10.8125 18.167 Specimen length,
distance to Loc 1, 2, and 3 of horizontal and vertical displacement
measurements from end A in ft., respectively.

22.5 19.25 23 19.5 12.5 9.25 Initial
pivot distances for pots 33, 34, 35, 36, 37, and 38 respectively in
inches.

30770 3100 259 4.38 11.28
E, Ix, and Iy of load frame and x and y coordinates of gages on
load frame

36 36 36
Distance from centroid of headstock/tailstock to load frame legs in
inches.

1.330093 Calibration factor for data channel 40.

1.325489 Calibration factor for data channel 41.

1.325999

1.322437 - Etc.

1.327159

1.333791

1.324886

1.323037

1.328089

Calibration factor for data channel 48

TIME	30	Data channel No		Chord Shortening Correction	
		31	32	End A	End B
124	0	-0.02359	-0.03524	0	0
142	-0.01181	-0.02359	-0.03524	0	0
160	-0.01181	-0.02359	-0.03524	0	0
270	-0.09449	-0.09434	-0.10571	0.0155	0.0155
287	-0.08267	-0.09434	-0.10571	0.0155	0.0155

Example HVP.DAT file:

Data Channel No.					
33	34	35	36	37	38
-0.02368	0.011815	-0.01179	0	-0.0059	0.011843
0	0.011815	0	0	-0.00295	0.014804
-0.02368	0.011815	-0.01179	0.011822	-0.0059	0.014804
-0.01184	0.035446	-0.02358	0.047287	-0.02654	0.041451
-0.01184	0.035446	-0.02358	0.047287	-0.02359	0.041451

Example LOAD1.DAT file:

Data Channel No.					
40	41	42	43	44	
7.996836	5.323548	9.278746	6.61195	9.310329	
6.66403	3.992661	7.95321	5.28956	7.980282	
7.996836	3.992661	9.278746	5.28956	7.980282	
35.98576	38.59572	53.0214	44.96126	46.55165	
38.65138	37.26483	47.71926	44.96126	46.55165	

Example LOAD2.DAT file:

Data Channel No.				
45	46	47	48	
6.66966	5.302696	6.60757	6.64324	
9.337524	3.977022	3.964542	6.64324	
6.66966	3.977022	5.286056	6.64324	
38.68403	34.46753	39.64542	38.53079	
38.68403	35.7932	39.64542	38.53079	

Output Files

Example SPEC1.OUT file:

"SPECIMEN 01 - 2/15/90" Title
 "TIME", "LOAD", "Xr", "Yr", "CHORD SH" Headers - may be removed

Time	Load (kips)	Resultant Location x, (in) y, (in)		Chord Shortening (in.)
374.00,	21.2516,	-3.11270,	-1.35214,	-.00393
394.00,	19.9323,	-2.10154,	1.84687,	.00000
415.00,	19.9275,	-4.08448,	-2.05613,	-.00394
508.00,	122.8254,	-1.94773,	.49377,	.07070
530.00,	122.1700,	-1.42502,	.48950,	.07070

Example SPEC2.OUT file:

"HORIZ 1", "VERT 1", "HORIZ 2", "VERT 2", "HORIZ 3", "VERT 3"
 Header - may be removed

		Deflections			
Horiz.	Vert.	Horiz	Vert.	Horiz.	Vert.
1	1	2	2	3	3
(in.)	(in.)	(in.)	(in.)	(in.)	(in.)

1 - Deflections measured near End A
 2 - Deflections measured near midspan
 3 - Deflections measured near End B

.02368,	-.01180,	.01179,	-.01182,	.00591,	-.01184
.00000,	-.01182,	.01179,	-.01182,	.00296,	-.01480
.02368,	-.01180,	.01179,	-.01182,	.00591,	-.01480
.01194,	-.03536,	.02365,	-.04724,	.02661,	-.04141
.01194,	-.03536,	.02365,	-.04724,	.02366,	-.04141

PROGRAM CURVE.FOR

This program is a least squares algorithm which obtains the "best fit" for the strain gage and displacement data.

Input needed for this program includes the measured strains, the gage locations, and the measured displacements. The specimen strain gage readings are input in the RING#.STR files. The gage locations are read from the SGLOC.OUT file, and the displacements are input in the HVDISP.INP file.

The SGLOC.OUT file was previously presented. Remember, the number of data steps must be added to this file.

Example of the other input files are given on the following pages along with an example output page. The output is in the file CURVE.OUT and includes the effective length, information on deleted gages, eccentricities, and the error of fit.

The HVDISP.INP file is made by deleting the header on the SPEC2.OUT file and adding the information required for CURVE.

Please note: Information typed in **boldface** is for explanation only and not included in files.

Input Files

Example HVDISP.INP file:

36.0 **Distance to buckling point from end B, inches.**

191.75 121.0 41.0 **Distance from end B to locations**
1, 2, and 3 of horizontal and vertical measurements, respectively,
inches.

Remainder of file - same as SPEC2.OUT

.02368,	-.01180,	.01179,	-.01182,	.00591,	-.01184
.00000,	-.01182,	.01179,	-.01182,	.00296,	-.01480
.02368,	-.01180,	.01179,	-.01182,	.00591,	-.01480
.01194,	-.03536,	.02365,	-.04724,	.02661,	-.04141
.01194,	-.03536,	.02365,	-.04724,	.02366,	-.04141

Example RING1.STR file:

Data Channel No.					
0	1	2	3	4	5
-49.9495	-34.2368	-27.9085	-37.5443	-56.2146	-62.6567
-49.9495	-29.5681	-21.7066	-37.5443	-49.9686	-59.5239
-48.3886	-31.1244	-27.9085	-37.5443	-56.2146	-59.5239
-274.722	-230.32	-212.415	-212.751	-251.404	-303.885
-274.722	-231.876	-210.864	-214.315	-246.72	-300.752

Example RING2.STR file:

Data Channel No.					
6	7	8	9	10	11
-62.3394	-46.8879	-27.9838	-52.0146	-68.7857	-70.2122
-60.7809	-45.325	-26.4292	-50.4384	-65.6591	-67.0917
-59.2224	-45.325	-26.4292	-50.4384	-67.2224	-68.6519
-349.101	-300.083	-234.753	-296.326	-320.479	-344.82
-349.101	-298.52	-234.753	-297.902	-318.915	-349.501

Example RING3.STR file:

Data Channel No.					
12	13	14	15	16	17
-72.1206	-61.9974	-23.3142	-23.3311	-42.1872	-76.4513
-68.9849	-61.9974	-20.2056	-21.7757	-42.1872	-76.4513
-70.5528	-58.8976	-23.3142	-23.3311	-40.6247	-73.3309
-370.01	-644.773	-191.176	-217.757	-267.185	-357.293
-370.01	-644.773	-191.176	-217.757	-262.498	-354.172

Example RING4.STR file:

Data Channel No.					
18	19	20	21	22	23
-113.846	-57.9497	-15.5706	-18.6875	-26.4798	-76.0709
-110.727	-61.0821	-18.6847	-12.4583	-26.4798	-74.5185
-112.287	-57.9497	-15.5706	-17.1302	-26.4798	-72.966
-536.481	-296.013	-174.391	-144.828	-185.359	-357.068
-538.041	-296.013	-175.948	-144.828	-183.801	-353.963

Example RING5.STR file:

Data Channel No.					
24	25	26	27	28	29
-95.3012	-73.4097	-17.0815	-4.66893	-37.357	-66.8473
-93.7389	-73.4097	-17.0815	-6.22524	-37.357	-65.2927
-92.1766	-71.8478	-18.6344	-4.66893	-35.8004	-65.2927
-381.205	-362.363	-186.344	-174.307	-287.96	-317.136
-378.08	-363.925	-186.344	-174.307	-286.404	-318.691

Output File

Example CURVE01.OUT file:

STEP NO. = 0
GAUGE NO. 18 ELIMINATED DUE TO DEVIATION ERROR
LEFF/L = 2.00 A = .13598E-05 B = .56479E-06 C =
-.47634E-04
R = -.99746 STRAIN ERROR = 36.98%
BETAX = .51318E-02 BETAY = -.75262E-02
X1 = .67513E-02 Y1 = -.72883E-02
X2 = .11874E-01 Y2 = -.13269E-01
X3 = .96517E-02 Y3 = -.11998E-01
X DISP ERROR = 51.04% Y DISP ERROR = 13.96%
ZEFF1/L = -.2494 XEC1 = -.0165 YEC1 = .0204
ZEFF2/L = 1.7506 XEC2 = -.0484 YEC2 = .0506

STEP NO. = 1
GAUGE NO. 18 ELIMINATED DUE TO DEVIATION ERROR
LEFF/L = 2.00 A = .13244E-05 B = .66165E-06 C =
-.46125E-04
R = -.99746 STRAIN ERROR = 38.13%
BETAX = -.67983E-03 BETAY = -.99569E-02
X1 = .54093E-02 Y1 = -.77457E-02
X2 = .83146E-02 Y2 = -.14436E-01
X3 = .37927E-02 Y3 = -.14174E-01
X DISP ERROR = 25.50% Y DISP ERROR = 19.21%
ZEFF1/L = -.2051 XEC1 = -.0053 YEC1 = .0196
ZEFF2/L = 1.7949 XEC2 = -.0474 YEC2 = .0575

STEP NO. = 2
GAUGE NO. 18 ELIMINATED DUE TO DEVIATION ERROR
LEFF/L = 2.00 A = .13020E-05 B = .64230E-06 C =
-.46288E-04
R = -.99746 STRAIN ERROR = 36.75%
BETAX = .55156E-02 BETAY = -.10086E-01
X1 = .66624E-02 Y1 = -.76741E-02
X2 = .11719E-01 Y2 = -.14362E-01
X3 = .97625E-02 Y3 = -.14229E-01
X DISP ERROR = 49.70% Y DISP ERROR = 13.90%
ZEFF1/L = -.2082 XEC1 = -.0137 YEC1 = .0199
ZEFF2/L = 1.7918 XEC2 = -.0520 YEC2 = .0564

Definintion of output variables for CURVE.OUT.

LEFF/L is the effective length for which the "best-fit" of the data was determined.

A, B, C are constants of the function assumed to fit the curvatures. See Appendix C.

R is the ratio of the measured horizontal to vertical displacements at midspan.

STRAIN ERROR is the root mean square (RMS) error of the strain fit.

BETAX, BETAY are constants of the rigid-body displacement function.

X1 is the computed horizontal displacement at location 1.

Y1 is the computed vertical displacement at location 1.

X2 is the computed horizontal displacement at location 2.

Y2 is the computed vertical displacement at location 2.

X3 is the computed horizontal displacement at location 3.

Y3 is the computed vertical displacement at location 3.

X DISP ERROR is the RMS error of the horizontal displacements.

Y DISP ERROR is the RMS error of the vertical displacements.

ZEFF1/L, ZEFF2/L are the location of the inflection points.

XEC1 is eccentricity from inflection points at end B in the x-direction.

YEC1 is eccentricity from inflection points at end B in the y-direction.

XEC2 is eccentricity from inflection points at end A in the x-direction.

YEC2 is eccentricity from inflection points at end B in the y-direction.

PROGRAM CHANGE.FOR

This program arranges the output of CURVE into files for plotting. Input is from the files SPEC1.OUT and CURVE.OUT. The output is written to 5 files.

The applied load is read from the SPEC1.OUT file. Before running CHANGE, the title and header lines must be removed from this file.

The effective length, eccentricities from inflection points, etc. are input from CURVE.OUT. The number of data steps, location of buckling point from end B in inches, and length of the specimen in inches must be added to the beginning of this file.

The input files for this program have been previously presented. The output files are presented on the following pages.

Please note: Information typed in **boldface** is for explanation only and not included in files.

Output files

Example CHANGE.OUT file:

Load	Effective Length	Average		C
		XEC	YEC	
0	2.00	-.0324	.0355	-.47634E-04
1	2.00	-.0264	.0386	-.46125E-04
2	2.00	-.0329	.0382	-.46288E-04
3	1.18	-.0134	.0232	-.27068E-03
4	1.18	-.0123	.0233	-.27013E-03

Note: C is coefficient representing P/A term in curve fit.

Example ECC.INP file:

74, 17437034 Number of steps, EI

Leff	A	B	R	Load (kips)
2.00	.13598E-05	.56479E-06	-.99746	21.2516
2.00	.13244E-05	.66165E-06	-.99746	19.9323
2.00	.13020E-05	.64230E-06	-.99746	19.9275
1.18	.79026E-05	-.15513E-05	-.50064	122.8254

Note: A and B coefficients of curve fit. R is ratio of midspan displacements.

Example LOAD.PLT file:

Load Step	Load (kips)
0	21.2516
1	19.9323
2	19.9275
3	122.8254
4	122.1700

Example BETA.PLT file:

Curvature Displacement (in.)	Rigid body Displacement (in.)	Total Displacement (in.)
.54990E-07	.91093E-02	.91093E-02
.64418E-07	.99801E-02	.99801E-02
.62534E-07	.11496E-01	.11496E-01
.17251E-05	.15841E-01	.15843E-01
.17008E-05	.15316E-01	.15318E-01

Example ECCIP.PLT file:

XECC end B (in.)	XECC end A (in.)	XECC Ave. (in.)	YECC end B (in.)	YECC end A (in.)	YECC Ave. (in.)
-.165E-01	-.484E-01	-.3245E-01	.204E-01	.506E-01	.355E-01
-.530E-02	-.474E-01	-.2635E-01	.196E-01	.575E-01	.3855E-01
-.137E-01	-.520E-01	-.3285E-01	.196E-01	.564E-01	.3815E-01
-.254E-01	-.140E-02	-.1340E-01	.436E-01	.270E-02	.2315E-01
-.232E-01	-.140E-02	-.1230E-01	.438E-01	.270E-02	.2325E-01

PROGRAM ECC.FOR

This program computes the end eccentricities from the end moments calculated by the CURVE algorithm. Input is from the file ECC.INP generated by the CHANGE program. The number of data steps and EI must be added to the ECC.INP file.

The input file has already been presented. Two output files are created by this program. ECC.OUT gives the eccentricities in a stepwise form while ECC.PLT lists the eccentricities in tabular form for plotting purposes.

Example output files are given on the following page.

Please note: Information typed in **boldface** is for explanation only and not included in files.

ECC.OUT

STEP NO. 0
EX1 = -.46008 EY1 = .46125
EX2 = -1.1138 EY2 = 1.1166
AVERAGE EX = -.78693 AVERAGE EY = .78893

STEP NO. 1
EX1 = -.40893 EY1 = .40997
EX2 = -1.2254 EY2 = 1.2285
AVERAGE EX = -.81717 AVERAGE EY = .81926

STEP NO. 2
EX1 = -.40714 EY1 = .40818
EX2 = -1.2000 EY2 = 1.2030
AVERAGE EX = -.80355 AVERAGE EY = .80559

STEP NO. 3
EX1 = -.24041 EY1 = .48020
EX2 = -.26192E-01 EY2 = .52317E-01
AVERAGE EX = -.13330 AVERAGE EY = .26626

STEP NO. 4
EX1 = -.23811 EY1 = .47560
EX2 = -.26144E-01 EY2 = .52221E-01
AVERAGE EX = -.13212 AVERAGE EY = .26391

Note: EX1 is the eccentricity in the x-direction at end B in inches.

EY1 is the eccentricity in the y-direction at end A in inches.

Example ECC.PLT file:

XECC end B (in.)	XECC end A (in.)	XECC Ave. (in.)	YECC end B (in.)	YECC end A (in.)	YECC Ave. (in.)
-.46008	-1.1138	-.78693	.46125	1.1166	.78893
-.40893	-1.2254	-.81717	.40997	1.2285	.81926
-.40714	-1.2000	-.80355	.40818	1.2030	.80559
-.24041	-.26192E-01	-.13330	.48020	.52317E-01	.26626
-.23811	-.26144E-01	-.13212	.47560	.52221E-01	.26391

Input and Output Files

The input and output files for each specimen are saved on computer disks. Data from two specimens is saved on each of ten disks. Each specimen as a directory on the disk. All specimen data is saved in this directory. The data may be accessed using a word processing package or imported into a spreadsheet.

Note: To change directories, at the prompt type `cd\dirname`.

Example:

```
A:\> cd\spec01
```